SHOUT
SHARE
IT

MBL

Volume 202

Number 1

THE BIOLOGICAL BULLETIN

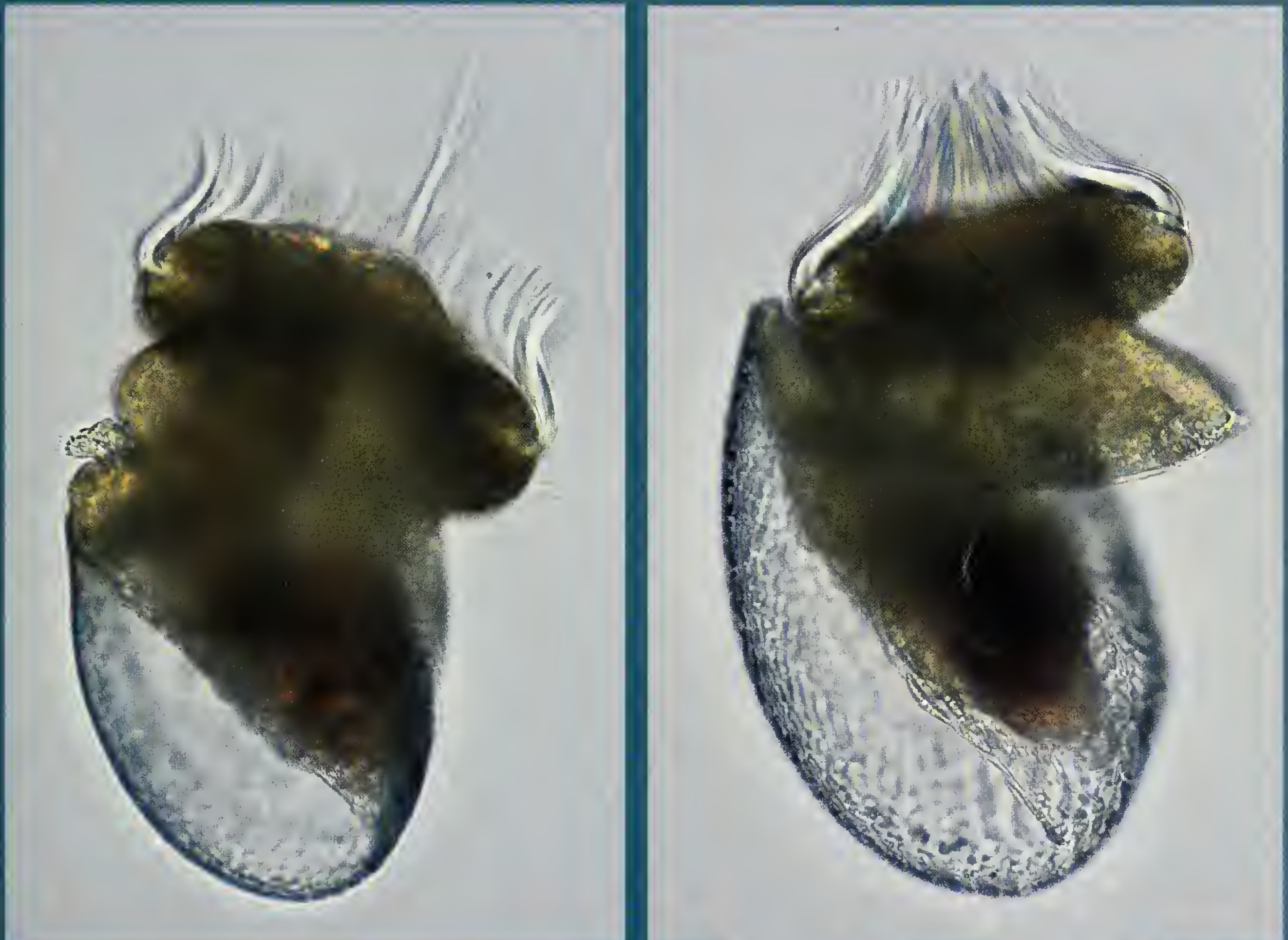

FEBRUARY 2002

Published by the Marine Biological Laboratory

http://www.biolbull.org

THE BIOLOGICAL BULLETIN
ONLINE

The Marine Biological Laboratory is pleased to announce that the full text of *The Biological Bulletin* is available online at

http://www.biolbull.org

The Biological Bulletin publishes outstanding experimental research on the full range of biological topics and organisms, from the fields of Neurobiology, Behavior, Physiology, Ecology, Evolution, Development and Reproduction, Cell Biology, Biomechanics, Symbiosis, and Systematics.

Published since 1897 by the Marine Biological Laboratory (MBL) in Woods Hole, Massachusetts, *The Biological Bulletin* is one of America's oldest peer-reviewed scientific journals.

The journal is aimed at a general readership, and especially invites articles about those novel phenomena and contexts characteristic of intersecting fields.

The Biological Bulletin Online contains the full content of each issue of the journal, including all figures and tables, beginning with the February 2001 issue (Volume 200, Number 1). The full text is searchable by keyword, and the cited references include hyperlinks to Medline. PDF files are available beginning in February 2000 (Volume 198, Number 1), some abstracts are available beginning with the October 1976 issue (Volume 151, Number 2), and some Tables of Contents are online beginning with the October 1965 issue (Volume 129, Number 2).

Each issue will be placed online approximately on the date it is mailed to subscribers; therefore the online site will be available prior to receipt of your paper copy. Online readers may want to sign up for the eTOC (electronic Table of Contents) service, which will deliver each new issue's table of contents *via* e-mail. The web site also provides access to information about the journal (such as Instructions to Authors, the Editorial Board, and subscription information), as well as access to the Marine Biological Laboratory's web site and other publications.

There is currently a free trial period for access to *The Biological Bulletin*. Once the free trial period ends on January 31, 2002, individuals and institutions who are subscribers to the journal in print or are members of the Marine Biological Laboratory Corporation will be able to activate an online subscription. All other access (*e.g.*, to Abstracts, eTOCs, searching, Instructions to Authors) will remain freely available. Online access will be included in the print subscription price.

---

http://www.biolbull.org

OLYMPUS
LUMPlanFl
20x/0.95 W
∞/0
The objective is not to touch the objective.

The BX51WI. A single 20x water immersion objective. A high N.A. of 0.95. A W.D. of 2.0mm. An intermediate magnification changer. Switch between low and high magnifications. Objective is untouched. Vibrations eliminated. Electrodes unmoved. It's a new movement in microscopy. **How Original. How Olympus.** Visit us at olympusamerica.com or call 1-800-446-5967.

OLYMPUS®
FOCUS ON LIFE

Cover

The images on the cover are a pair of veliger larvae. They developed from fertilized eggs of *Tectura scutum*, a patellogastropod (true limpet), were maintained at 12 °C, and were photographed at two different stages during their pelagic development. The larva on the left, at 46 hours after fertilization, has neither undergone ontogenetic torsion nor completed the secretion of its protoconch (embryonic shell). The one on the right, at 62 hours after fertilization, has completed both torsion and the secretion of its pre-metamorphic shell. Nonfeeding larvae of *T. scutum* become competent to metamorphose about 7 days after fertilization [see Fig. 1B (Page, 2002), p. 10 this issue].

The apical epidermis of the left-hand larva, located within the ring of locomotory cilia, bears a long apical ciliary tuft. The cells generating this tuft are intimately associated with the neurons of a putative larval sensory structure, the apical ganglion. Shortly after ontogenetic torsion, the long apical ciliary tuft is lost (right-hand larva), and the three large cells that gave rise to it also disappear from the apical epidermis.

Larvae with very long apical ciliary tufts are characteristic of patellogastropods, but this is the only gastropod clade in which such an apical structure appears. But because similar structures do arise from the apical pole of larvae in many other molluscan classes, and because current phylogenies designate patellogastropods as the most basal lineage of extant gastropods, the long apical ciliary tuft is probably a plesiomorphic trait for gastropods.

Rather than an apical tuft, the larvae of other gastropod clades bear, on either side of the midline of the apical surface, a pair of multiciliated cells, each of which generates a relatively short ciliary tuft. In this issue of *The Biological Bulletin* (pp. 6–22), Louise R. Page describes—through electron microscopy and serotonin immunohistochemistry—the structure of the apical sensory organ (*i.e.*, the neurons plus ciliogenic cells) in the larvae of *T. scutum*. She reports that these larvae have, not only an apical tuft of very long cilia, but also lateral, multiciliated cells that produce two shorter tufts. These short tufts are probably homologs of those in the larvae of other gastropods. The embryonic derivation of the apical sensory organs appears to be broadly similar among all molluscs, but a clear understanding of the developmental evolution of this structure awaits further comparative data.

(*Credits*: Photos by L. R. Page, University of Victoria, British Columbia, Canada; other graphics by Beth Liles, MBL.)

THE
BIOLOGICAL BULLETIN

FEBRUARY 2002

Marine Biological Laboratory
Woods Hole Oceanographic Institution
Library

FEB 20 2002

Woods Hole, MA 02543

Editor	Michael J. Greenberg	The Whitney Laboratory, University of Florida
Associate Editors	Louis E. Burnett	Grice Marine Biological Laboratory, College of Charleston
	R. Andrew Cameron	California Institute of Technology
	Charles D. Derby	Georgia State University
	Michael LaBarbera	University of Chicago
Section Editor	Shinya Inoué, *Imaging and Microscopy*	Marine Biological Laboratory
Online Editors	James A. Blake, *Keys to Marine Invertebrates of the Woods Hole Region*	ENSR Marine & Coastal Center, Woods Hole
	William D. Cohen, *Marine Models Electronic Record and Compendia*	Hunter College, City University of New York
Editorial Board	Peter B. Armstrong	University of California, Davis
	Ernest S. Chang	Bodega Marine Lab., University of California, Davis
	Thomas H. Dietz	Louisiana State University
	Richard B. Emlet	Oregon Institute of Marine Biology, Univ. of Oregon
	David Epel	Hopkins Marine Station, Stanford University
	Kenneth M. Halanych	Woods Hole Oceanographic Institution
	Gregory Hinkle	Cereon Genomics, Cambridge, Massachusetts
	Nancy Knowlton	Scripps Inst. Oceanography & Smithsonian Tropical Res. Inst.
	Makoto Kobayashi	Hiroshima University of Economics, Japan
	Esther M. Leise	University of North Carolina Greensboro
	Donal T. Manahan	University of Southern California
	Margaret McFall-Ngai	Kewalo Marine Laboratory, University of Hawaii
	Mark W. Miller	Institute of Neurobiology, University of Puerto Rico
	Tatsuo Motokawa	Tokyo Institute of Technology, Japan
	Yoshitaka Nagahama	National Institute for Basic Biology, Japan
	Sherry D. Painter	Marine Biomed. Inst., Univ. of Texas Medical Branch
	J. Herbert Waite	University of California, Santa Barbara
	Richard K. Zimmer	University of California, Los Angeles
Editorial Office	Pamela Clapp Hinkle	Managing Editor
	Victoria R. Gibson	Staff Editor
	Carol Schachinger	Editorial Associate
	Wendy Child	Subscription & Advertising Secretary

Published by
MARINE BIOLOGICAL LABORATORY
WOODS HOLE, MASSACHUSETTS

http://www.biolbull.org

Scientists Choose Microway® Athlon® Clusters

For Expert Integration, Superior Tech Support and Great Pricing

AT&T, BU, Cessna, Eos Biotechnology, Harvard, JPL, LANL, LLNL, Lucent, Marine Biological Laboratory, Millennium Pharmaceuticals, MIT, Mount Sinai Medical School, NASA, NIH, NIST, NRL, Pfizer, Raytheon, Rockefeller University, Sandia, Seagate, Stanford, University of Wisconsin, and Universities Worldwide Choose Microway Linux and UNIX Solutions.

- **New: Dual AMD Athlon™ MP 2000+ 1.66 GHz**
- **Intel 2.2 GHz Dual Xeon or 1.26 GHz Dual Pentium III**
- **New: 833 MHz, 8 or 16 MB DDR Cache, Dual Alpha 21264DP Clusters and Towers**
- **Myrinet, High Speed Low Latency Interconnects**
- **RAID and Fibre Channel Storage Solutions**

Microway® Screamer™ Dual Alpha 21264DP 833 MHz, 8MB Cache in RuggedRack™ Chassis with RRR™ Redundant Power Supply

Microway has earned an excellent reputation since 1982. If you need a quality product that is fine tuned and built to last, from a company that will be around to support you for years to come, Microway is The Number One Choice.

Microway has delivered high-performance computing solutions since 1982, when our pioneering software made it possible to use an 8087 in the IBM-PC. In 1987 we created the world's first PC parallel processing systems. Since then, our QuadPuter™ architecture has migrated from Transputers to i860s and finally to Alphas in 1995. We now integrate high end Beowulf Clusters for government agencies, biotechs, and universities worldwide. Over the past three years, we delivered over 300 clusters that utilized MPI running on Linux. As a software developer and hardware manufacturer, we know the value of extensive testing and validation. We are experts at configuring and validating the low latency interconnects we employ in our clusters. Our technical support is legendary — the systems we sell arrive at your site and WORK! Los Alamos chose Microway to maintain and upgrade its 144 node Alpha Avalon Cluster because of our reputation.

Microway clusters are delivered fully functional with all Linux and Myrinet software installed and configured for immediate deployment at customers' sites. The competence level of our integration and service teams far surpasses that of most competitors.

Large clusters we have sold include 400+ nodes at the University of Wisconsin, 250+ nodes at Rockefeller University, 210 nodes at University of Maine, 160+ nodes at AT&T Research, and 150+ nodes at Harvard University.

Microway offers 1U and 2U dual Athlon/Pentium enclosures, plus Alpha configurations in 3U, 4U RuggedRack,™ and full tower. Our 264DP includes dual 21264's with up to 4 GB of memory in our custom 4U RuggedRack, which features front accessible redundant power supplies and hard disks. This rugged configuration was chosen by the U.S. Navy for onboard use.

AMD
Athlon
MP

Harness Dual Athlon Power with a Microway Scalable 25 Node 50 Processor Cluster Using 1.66 GHz Dual AMD Athlon MP 2000+ and Myrinet Interconnect. Yields Peak Throughput of 166 Gigaflops.

> "Our committee chose **Microway** over other vendors because of their reputation in the HPC community for delivering high quality, fully integrated clusters. Our decision was based also on their extensive technical expertise with Myrinet, demonstrated financial stability and ability to quickly deliver the solution we required. The University of Maine has established this cluster as part of the Target Technology Center-an integrated R&D, business incubator, and economic development initiative to spur Information Technology growth in Maine."
>
> *– Jake Ward, Director of the Department of Industrial Cooperation, University of Maine at Orono*

Find out why over 75% of Microway's sales come from repeat customers. Please call 508-746-7341 for a technical salesperson who speaks your language!

Visit us at www.microway.com

Microway
Technology you can count on™

Research Park Box 79, Kingston, MA 02364 • 508-746-7341 • info@microway.com

CONTENTS

VOLUME 202, NO. 1: FEBRUARY 2002

SYSTEMATICS OF SEA MONSTERS

Carr, S. M., H. D. Marshall, K. A. Johnstone, L. M. Pynn, and G. B. Stenson
How to tell a sea monster: molecular discrimination of large marine animals of the North Atlantic 1

DEVELOPMENT AND REPRODUCTION

Page, Louise R.
Apical sensory organ in larvae of the patellogastropod *Tectura scutum* 6

Masseau, Isabelle, Pierre Bannon, Michel Anctil, and François Dubé
Localization and quantification of gonad serotonin during gametogenesis of the surf clam *Spisula solidissima* 23

Williams, Mark Elliott, and Matthew Graeme Bentley
Fertilization success in marine invertebrates: the influence of gamete age 34

Gross, Paul S., and Robert E. Knowlton
Morphological variations among larval-postlarval intermediates produced by eyestalk ablation in the snapping shrimp *Alpheus heterochaelis* Say 43

NEUROBIOLOGY AND BEHAVIOR

Stuart, Ann E., Harold E. Mekeel, and Elizabeth Kempter
Uptake of the neurotransmitter histamine into the eyes of larvae of the barnacle (*Balanus amphitrite*) 53

CELL BIOLOGY

Compère, Philippe, Marie-France Jaspar-Versali, and Gerhard Goffinet
Glycoproteins from the cuticle of the Atlantic shore crab *Carcinus maenas*: I. Electrophoresis and western-blot analysis by use of lectins 61

SYMBIOSIS AND PARASITOLOGY

Belda-Baillie, Carman A., Brett K. Baillie, and Tadashi Maruyama
Specificity of a model cnidarian-dinoflagellate symbiosis 74

ECOLOGY AND EVOLUTION

Hill, Malcolm S., and April L. Hill
Morphological plasticity in the tropical sponge *Anthosigmella varians*: responses to predators and wave energy 86

THE BIOLOGICAL BULLETIN

THE BIOLOGICAL BULLETIN is published six times a year by the Marine Biological Laboratory, 7 MBL Street, Woods Hole, Massachusetts 02543.

Subscriptions and similar matter should be addressed to Subscription Administrator, THE BIOLOGICAL BULLETIN, Marine Biological Laboratory, 7 MBL Street, Woods Hole, Massachusetts 02543. Subscription per year (six issues, two volumes): $260 for libraries; $105 for individuals. Subscription per volume (three issues): $130 for libraries; $52.50 for individuals. Back and single issues (subject to availability): $45 for libraries; $20 for individuals.

Communications relative to manuscripts should be sent to Michael J. Greenberg, Editor-in-Chief, or Pamela Clapp Hinkle, Managing Editor, at the Marine Biological Laboratory, 7 MBL Street, Woods Hole, Massachusetts 02543. Telephone: (508) 289-7428. FAX: 508-289-7922. E-mail: pclapp@mbl.edu.

http://www.biobull.org

THE BIOLOGICAL BULLETIN is indexed in bibliographic services including *Index Medicus* and MEDLINE, *Chemical Abstracts, Current Contents, Elsevier BIOBASE/Current Awareness in Biological Sciences,* and *Geo Abstracts.*

Printed on acid free paper,
effective with Volume 180, Issue 1, 1991.

POSTMASTER: Send address changes to THE BIOLOGICAL BULLETIN, Marine Biological Laboratory,
7 MBL Street, Woods Hole, MA 02543.

Copyright © 2002, by the Marine Biological Laboratory

Periodicals postage paid at Woods Hole, MA, and additional mailing offices.
ISSN 0006-3185

INSTRUCTIONS TO AUTHORS

The Biological Bulletin accepts outstanding original research reports of general interest to biologists throughout the world. Papers are usually of intermediate length (10–40 manuscript pages). A limited number of solicited review papers may be accepted after formal review. A paper will usually appear within four months after its acceptance.

Very short, especially topical papers (less than 9 manuscript pages including tables, figures, and bibliography) will be published in a separate section entitled "Research Notes." A Research Note in *The Biological Bulletin* follows the format of similar notes in *Nature.* It should open with a summary paragraph of 150 to 200 words comprising the introduction and the conclusions. The rest of the text should continue on without subheadings, and there should be no more than 30 references. References should be referred to in the text by number, and listed in the Literature Cited section in the order that they appear in the text. Unlike references in *Nature,* references in the Research Notes section should conform in punctuation and arrangement to the style of recent issues of *The Biological Bulletin.* Materials and Methods should be incorporated into appropriate figure legends. See the article by Lohmann *et al.* (October 1990, Vol. **179:** 214–218) for sample style. A Research Note will usually appear within two months after its acceptance.

The Editorial Board requests that regular manuscripts conform to the requirements set below; those manuscripts that do not conform will be returned to authors for correction before review.

1. ***Manuscripts.*** Manuscripts, including figures, should be submitted in quadruplicate, with the originals clearly marked. (Xerox copies of photographs are not acceptable for review purposes.) If possible, please include an electronic copy of the text of the manuscript. Label the disk with the name of the first author and the name and version of the wordprocessing software used to create the file. If the file was not created in some version of Microsoft Word, save the text in rich text format (rtf). The submission letter accompanying the manuscript should include a telephone number, a FAX number, and (if possible) an E-mail address for the corresponding author. The original manuscript must be typed in no smaller than 12 pitch or 10 point, using double spacing (*including* figure legends, footnotes, bibliography, etc.) on one side of 16- or 20-lb. bond paper, 8 by 11 inches. Please, no right justification. Manuscripts should be proofread carefully and errors corrected legibly in black ink. Pages should be numbered consecutively. Margins on all sides should be at least 1 inch (2.5 cm). Manuscripts should conform to the *Council of Biology Editors Style Manual,* 5th Edition (Council of Biology Editors, 1983) and to American spelling. Unusual abbreviations should be kept to a minimum and should be spelled out on first reference as well as defined in a footnote on the title page. Manuscripts should be divided into the following components: Title page, Abstract (of no more than 200 words), Introduction, Materials and Methods, Results, Discussion, Acknowledgments, Literature Cited, Tables, and Figure Legends. In addition, authors should supply a list of words and phrases under which the article should be indexed.

2. ***Title page.*** The title page consists of a condensed title or running head of no more than 35 letters and spaces, the manuscript title, authors' names and appropriate addresses, and footnotes listing present addresses, acknowledgments or contribution numbers, and explanation of unusual abbreviations.

3. ***Figures.*** The dimensions of the printed page, 7 by 9 inches, should be kept in mind in preparing figures for publication. We recommend that figures be about 1 times the linear dimensions of the final printing desired, and that the ratio of the largest to the smallest letter or number and of the thickest to the thinnest line not exceed 1:1.5. Explanatory matter generally should be included in legends, although axes should always be identified on the illustration itself. Figures should be prepared for reproduction as either line cuts or halftones. Figures to be reproduced as line cuts should be unmounted glossy photographic reproductions or drawn in black ink on white paper, good-quality tracing cloth or plastic, or blue-lined coordinate paper. Those to be reproduced as halftones should be mounted on board, with both designating numbers or letters and scale bars affixed directly to the figures. All figures should be numbered in consecutive order, with no distinction between text and plate figures and cited, in order, in the text. The author's name and an arrow indicating orientation should appear on the reverse side of all figures.

Digital art: The Biological Bulletin will accept figures submitted in electronic form; however, digital art must conform to the following guidelines. Authors who create digital images are wholly responsible for the quality of their material, including color and halftone accuracy.

Format. Acceptable graphic formats are TIFF and EPS. Color submissions must be in EPS format, saved in CMKY mode.

Software. Preferred software is Adobe Illustrator or Adobe Photoshop for the Mac and Adobe Photoshop for Windows. Specific instructions for artwork created with various software programs are available on the Web at the Digital Art Information Site maintained by Cadmus Professional Communications at http://cpc.cadmus.com/dal/

Resolution. The minimum requirements for resolution are 1200 DPI for line art and 300 for halftones.

Size. All digital artwork must be submitted at its actual printed size so that no scaling is necessary.

Multipanel figures. Figures consisting of individual parts (*e.g.*, panels A, B, C) must be assembled into final format and submitted as one file.

Hard copy. Files must be accompanied by hard copy for use in case the electronic version is unusable.

Disk identification. Disks must be clearly labeled with the following information: author name and manuscript number; format (PC or Macintosh); name and version of software used.

Color: The Biological Bulletin will publish color figures and plates, but must bill authors for the actual additional cost of printing in color. The process is expensive, so authors with more than one color image should—consistent with editorial concerns, especially citation of figures in order—combine them into a single plate to reduce the expense. On request, when supplied with a copy of a color illustration, the editorial staff will provide a pre-publication estimate of the printing cost.

4. ***Tables, footnotes, figure legends, etc.*** Authors should follow the style in a recent issue of *The Biological Bulletin* in preparing table headings, figure legends, and the like. Because of the high cost of setting tabular material in type, authors are asked to limit such material as much as possible. Tables, with their headings and footnotes, should be typed on separate sheets, numbered with consecutive Roman numerals, and placed after the Literature Cited. Figure legends should contain enough information to make the figure intelligible separate from the text. Legends should be typed double spaced, with consecutive Arabic numbers, on a separate sheet at the end of the paper. Footnotes should be limited to authors' current addresses, acknowledgments or contribution numbers, and explanation of unusual abbreviations. All such footnotes should appear on the title page. Footnotes are not normally permitted in the body of the text.

5. ***Literature cited.*** In the text, literature should be cited by the Harvard system, with papers by more than two authors cited as Jones *et al.*, 1980. Personal communications and material in preparation or in press should be cited in the text only, with author's initials and institutions, unless the material has been formally accepted and a volume number can be supplied. The list of references following the text should be headed Literature Cited, and must be typed double spaced on separate pages, conforming in punctuation and arrangement to the style of recent issues of *The Biological Bulletin*. Citations should include complete titles and inclusive pagination. Journal abbreviations should normally follow those of the U. S. A. Standards Institute (USASI), as adopted by Biological Abstracts and Chemical Abstracts, with the minor differences set out below. The most generally useful list of biological journal titles is that published each year by Biological Abstracts (biosis List of Serials; the most recent issue). Foreign authors, and others who are accustomed to using The World List of Scientific Periodicals, may find a booklet published by the Biological Council of the U.K. (obtainable from the Institute of Biology, 41 Queen's Gate, London, S.W.7, England, U.K.) useful, since it sets out the World List abbreviations for most biological journals with notes of the USASI abbreviations where these differ. Chemical Abstracts publishes quarterly supplements of additional abbreviations. The following points of reference style for The Biological Bulletin differ from USASI (or modified World List) usage:

A. Journal abbreviations, and book titles, all underlined (for *italics*)

B. All components of abbreviations with initial capitals (not as European usage in World List *e.g., J. Cell. Comp. Physiol.* NOT *J. cell. comp. Physiol.*)

C. *All* abbreviated components must be followed by a period, whole word components *must not* (*i.e., J. Cancer Res.*)

D. Space between all components (*e.g., J. Cell. Comp. Physiol.*, not *J.Cell.Comp.Physiol.*)

E. Unusual words in journal titles should be spelled out in full, rather than employing new abbreviations invented by the author. For example, use *Rit Vísindafjélags Íslendinga* without abbreviation.

F. All single word journal titles in full (*e.g., Veliger, Ecology, Brain*).

G. The order of abbreviated components should be the same as the word order of the complete title (*i.e.*, *Proc.* and *Trans.* placed where they appear, not transposed as in some BIOLOGICAL ABSTRACTS listings).

H. A few well-known international journals in their preferred forms rather than WORLD LIST or USASI usage (*e.g.*, *Nature*, *Science*, *Evolution* NOT *Nature, Lond.*, *Science, N.Y.*; *Evolution, Lancaster, Pa.*)

6. ***Reprints, page proofs, and charges.*** Authors may purchase reprints in lots of 100. Forms for placing reprint orders are sent with page proofs. Reprints normally will be delivered about 2 to 3 months after the issue date. Authors (or delegates for foreign authors) will receive page proofs of articles shortly before publication. They will be charged the current cost of printers' time for corrections to these (other than corrections of printers' or editors' errors). Other than these charges for authors' alterations, *The Biological Bulletin* does not have page charges.

Reference: *Biol. Bull.* **202:** 1–5. (February 2002)

How To Tell a Sea Monster: Molecular Discrimination of Large Marine Animals of the North Atlantic

S. M. CARR[1,*], H. D. MARSHALL[1], K. A. JOHNSTONE[1], L. M. PYNN[1], AND G. B. STENSON[2]

[1]*Genetics, Evolution, and Molecular Systematics Laboratory, Department of Biology, Memorial University of Newfoundland, St. John's, Newfoundland A1B 3X9, Canada; and* [2]*Marine Mammals Section, Science, Oceans, and Environment Branch, Department of Fisheries and Oceans, PO Box 5667, St. John's, Newfoundland A1C 5X1, Canada*

> *"Either we do know all the varieties of beings which people our planet, or we do not. If we do not know them all—if Nature has still secrets in the deeps for us, nothing is more conformable to reason than to admit the existence of fishes, or cetaceans of other kinds, or even of new species . . . which an accident of some sort has brought at long intervals to the upper level of the ocean."*
>
> —*Jules Verne,* Twenty Thousand Leagues Under the Sea, *1870*

Abstract. Remains of large marine animals that wash onshore can be difficult to identify due to decomposition and loss of external body parts, and in consequence may be dubbed "sea monsters." DNA that survives in such carcasses can provide a basis of identification. One such creature washed ashore at St. Bernard's, Fortune Bay, Newfoundland, in August 2001. DNA was extracted from the carcass and enzymatically amplified by the polymerase chain reaction (PCR): the mitochondrial NADH2 DNA sequence was identified as that of a sperm whale (*Physeter catodon*). Amplification and sequencing of cryptozoological DNA with "universal" PCR primers with broad specificity to vertebrate taxa and comparison with species in the GenBank taxonomic database is an effective means of discriminating otherwise unidentifiable large marine creatures.

Introduction

At least since the *Iliad*, the possible occurrence of unusually large, exotic marine creatures has exerted a powerful hold on the human imagination. Professor A. C. Oudemans' 1892 book *The Great Sea Serpent* described more than 200 reports of unknown marine creatures (Ley, 1959). Ellis (1994) gives a contemporary list. Even in the first year of a new century when the complete human genome has become known (International Human Genome Sequencing Consortium, 2001), the possibility that entirely new, previously unknown species may unexpectedly present themselves remains tantalizing. Discovery in the last century of the first coelacanth (*Latimeria*), the "megamouth" shark (*Megachasma*) and, most recently, a second species of coelacanth in the waters off Sulawesi in Indonesia (Holder *et al.*, 1999) keeps us alert to the possibility of "new varieties of beings" in the deeps. Modern methods of phylogenetic systematics, based on detailed morphological and molecular analyses, have made it possible to place such discoveries in their evolutionary context.

Morphological analysis of putative new species may be hampered by incomplete or poorly preserved material; in such cases, molecular biology may hold the key to natural history. Enzymatic amplification by the polymerase chain reaction (PCR) (Saiki *et al.*, 1988) of the minute amounts of DNA persisting in ancient or forensic biological material has been shown to be an effective means of individual and species identification (Herrmann and Hummell, 1994). The extra-nuclear mitochondrial (mt) DNA genome has been particularly valuable, as more than a decade of molecular systematic work has provided an extensive database ("GenBank") of molecular "type" sequences for many species of

---

Received 19 September 2001; accepted 13 November 2001.

* To whom correspondence should be addressed. E-mail: scarr@mun.ca

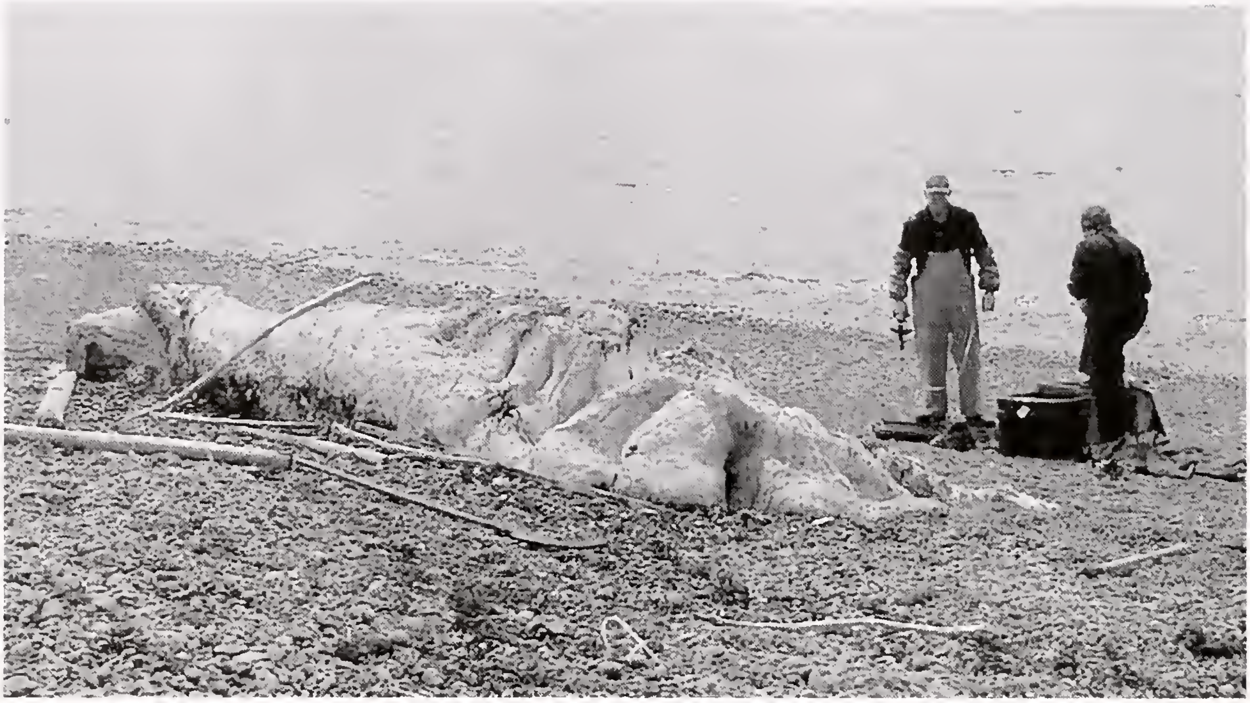

Figure 1. "Sea monster" discovered at St. Bernard's, Fortune Bay, Newfoundland, 2 August 2001. The maximum length of the carcass is 5.6 m. The transverse cuts were made during dissection. Note the lobes at the right-hand end on the side facing the camera.

marine sharks, fish, and mammals (Wheeler *et al.*, 2000; Benson *et al.*, 2000). Routine species identification of subfossil material hundreds or thousands of years old (Hofreiter *et al.*, 2001) is possible, as is forensic determination of questioned species in commercial products such as salted or dried fish (S. M. Carr and H. D. Marshall, unpubl. obs.), or processed whale meat (Baker *et al.*, 1996) including that from endangered species (Palumbi and Cipriano, 1998). We report here what appears to be the first successful use of PCR-based recovery of DNA to identify a "sea monster."

On 2 August 2001, residents of the community of St. Bernard's, Fortune Bay, on the south coast of the island of Newfoundland, were confronted with an enormous, whitish mass of rotting flesh that had washed up on a local beach overnight. They contacted the Department of Fisheries and Oceans in St. John's, who sent experts to examine the carcass (Fig. 1). The remains were about 5.6 m long and 5.0 m wide. Neither head nor tail was present: the carcass consisted primarily of bleached tissue. The surface was rough and fringed with material initially characterized as "hair," which upon closer inspection appeared to consist of abraded tissue mixed with seaweed and sand. There were seven or eight lobes or slits that extended roughly one-third the length of one side from one end; the last two slits did not extend to the outer margin. No lobes were present on the opposite side, but tissue had evidently been lost from that side. The remainder of the mass tapered slightly. No soft tissue or bones were present; dissection of the side opposite the lobes revealed a small amount of cartilage. The surface layer retained a structure consistent with muscle, but the interior had decomposed to an amorphous mass. Definite identification was impossible due to the state of decomposition and the absence of any remaining external features. The size and general morphology were consistent with either a large shark, such as a basking shark (*Cetorhinus maximus*), or one of the several species of large cetaceans present in Newfoundland waters. The possibility of a giant squid (*Architeuthis dux*) was excluded due to general morphology (Aldrich, 1991).

Materials and Methods

Scientists from the Department of Fisheries and Oceans removed a number of pieces of tissue from just under the exterior of the carcass. DNA was extracted in duplicate from four pieces of tissue by a protease-based method with a QIAamp® DNA Mini Kit (Qiagen, Inc.), according to the manufacturer's instructions.

On the basis of the availability in GenBank of sequences for the mitochondrial (mt) DNA NADH subunit 2 gene (hereinafter NADH2) for a variety of shark (Naylor *et al.*, 1999) and whale species, we performed a series of polymerase chain reaction (PCR) experiments with two forward and reverse primer pairs that amplify a 1103-bp region that includes the complete NADH2 gene as two overlapping regions of 564 and 711 bp, respectively:

p8F: 5′ aagctatcgggcccatacce 3′ and
p8R: 5′ ttagtcctcctcagcctcc 3′

p9F: 5′ cataatcctactcacatgac 3′ and
p9R: 5′ cttacttagggctttgaagg 3′

PCR reactions were carried out as a two-step procedure designed to enhance amplification of dilute DNA or of DNA with a poor match between template and primer. In this strategy, an initial set of PCR cycles with dilute primers (2.5% of usual concentration) generates a small quantity of amplified template with ends that have an exact match to the primers. A second phase follows, with primers at standard concentration to produce sufficient template for sequence analysis. In the first stage of the procedure, we prepared 25-μl reactions containing 1X PCR reaction buffer and 1 U of *Taq* polymerase (Roche Molecular Biochemicals, Inc.), 10 n*M* of each primer (Cortec DNA Service Laboratories, Inc.), 100 μ*M* of each deoxynucleoside triphosphate (dNTP; Amersham Pharmacia Biotech), and 2 μl of template DNA. Following an initial incubation at 93 °C for 3 min, samples were taken through 23 cycles, each comprising denaturation at 93 °C for 45 s, annealing at 45 °C for 45 s, a ramp from 45 °C to 55 °C over 45 s, and extension at 72 °C for 1 min. The last cycle was followed by a further extension at 72 °C for 10 min. In the second stage, a second 25-μl reaction volume was added to each reaction tube, containing 1X PCR reaction buffer, 1 U *Taq* polymerase, 800 n*M* each primer (so as to bring the final concentration of each to 400 n*M* in a 50-μl volume), and 100 μ*M* of each dNTP. Samples were taken through an additional 45 cycles of PCR, as described above. All thermal manipulations were achieved using the GeneAmp PCR System 9600 (Perkin-Elmer).

PCR product sizes were verified by electrophoresis of 5 μl of the product through 2% agarose in 1X TBE buffer followed by ethidium bromide staining. Excess primer and nucleotides were removed from the PCR products using a QIAquick® PCR Purification Kit (Qiagen, Inc.).

DNA sequencing was accomplished by fluorescent dye-terminator chemistry carried out on an Applied Biosystems 3700 Automated DNA sequencer (Qiagen Genomics Sequencing Service, Qiagen Genomics Inc.) with the same primers that were used for amplification.

Results

No special difficulties were encountered in DNA extraction. Agarose electrophoresis of small portions of the extracted product indicated the presence of high molecular weight DNA in all but one of the tissue samples. Amplification with the two pairs of NADH2 primers was successful in about one-half of trials, and produced amplification products of the expected size. Inspection of electrophoretic separations indicated clean but weak amplification. Products from three replicate amplifications of each region were pooled for DNA sequencing.

A complete NADH2 sequence was obtained by assembly of the overlapping forward and reverse sequences of the two amplified regions. A BLAST search against the complete GenBank database indicated that the composite sequence had a 99.6% (1040 out of 1044 bp) match with the published NADH2 sequence for a sperm whale (*Physeter catodon*) (Árnason *et al.*, 2000: GenBank accession NC002503). The four nucleotide differences included one second codon position C ↔ T transition difference that would be expected to result in a threonine ↔ methionine amino acid difference between the GenBank type and Fortune Bay sequences, respectively. The magnitude of the differences is consistent with expected intraspecific variation. The DNA sequence was submitted to GenBank and assigned the accession number AF414121.

Discussion and Conclusions

The Fortune Bay "sea monster" is the carcass of a sperm whale (*Physeter catodon*). Sperm whales are the largest of the toothed whales (Odontoceti), they are not uncommon in the waters off the southern shore of the island of Newfoundland (Leatherwood *et al.*, 1976), and strandings of more or less intact whales are not infrequent (G. B. Stenson, unpubl. data). The carcass appears to be a mass of decomposing muscle tissue that has separated from the vertebral column and ribs. The peripheral lobes, which might be mistaken for a set of chondrichthian gill arches, are consistent with intercostal flesh. The feathery or hairy appearance is apparently abraded tissue. Exact postmortem age of the carcass is impossible to determine, but it is likely to have been in the water a long time.

Accounts and pictures in the popular press indicate that carcasses resembling the one found in Fortune Bay have washed up in several oceans of the world; some of these have attracted international media attention. Verrill (1897) initially described a large, whitish carcass that appeared in St. Augustine, Florida, as a new species of giant octopus, though he later withdrew this identification. Original newspaper reports in 1962 of a Tasmanian creature dubbed the "Globster" described it in the following terms: "It was initially covered with fine hair. . . . There were five or six gill-like hairless slits on each side of the fore part. There were four large hanging lobes in the front, and between the center pair was a smooth, gullet-like orifice. The margin of the hind part had cushion like protuberances . . . and each of these carried a single row of spines, sharp, and hard, about as thick as a pencil and quill-like. . . [It had] a resilient flesh which appeared to be composed of numerous tendon-like threads welded together in a fatty substance. . . ." (quoted in Ellis, 1994). There was no bone. A later scientific investigation reported the carcass as 8 feet long, 3 feet wide, 10

Table 1

Large marine animals of the North Atlantic

Name and taxonomy	Max. size (meters)	GenBank accession NADH2	GenBank accession Cyt *b*
Elasmobranchii (sharks)[1]			
thresher shark (*Alopias vulpinus*)	6	U91432	U91442
white shark (*Carcharodon carcharias*)	8	U91426	L08031
basking shark (*Cetorhinus maximus*)	13	U91429	U91439
whale shark (*Rhincodon typus*)[2]	18	—	—
Greenland shark (*Somniosus microcephalus*)	7	—	—
Mysticeti (baleen whales)[3]			
bowhead whale (*Balaena mysticetus*)	20	—	X75588
Minke whale (*Balaenoptera acutorostrata*)	10	X87775	X75753
Sei whale (*Balaenoptera borealis*)	19	—	X75582
blue whale (*Balaenoptera musculus*)	26	NC001601[5]	
finback whale (*Balaenoptera physalus*)	27	NC001321[5]	
beluga (*Delphinapterus leucas*)	6	—	X92531
northern right whale (*Eubalaena glacialis*)	16	—	—
humpback whale (*Megaptera novaeangliae*)	16	—	X75584
Odontoceti (toothed whales)[3]			
Atlantic pilot whale (*Globicephala melaena*)	6	—	AF084056
killer whale (*Orcinus orca*)	9	—	X92532
sperm whale (*Physeter catodon*)	21	NC002503[5]	
Cephalopoda (squids & relatives)			
giant squid (*Architeuthis dux*)[4]	18	—	—

[1] Size data from Scott and Scott (1988).

[2] Not known to occur in Canadian Atlantic waters.

[3] Size data from Leatherwood *et al.* (1976).

[4] Aldrich (1991).

[5] Both sequences contained in the accession for the complete mtDNA genome.

inches thick, and without spines. A 1988 report from Bermuda described a "Glob," "2 1/2 to 3 feet thick . . . very white and fibrous with five 'arms or legs,' rather like a disfigured star. . . . It had no bones, cartilage, visible openings, or odor. . . ." (quoted in Ellis, 1994). In 1990, another carcass washed ashore in the Hebrides Islands, Scotland: "It had what appeared to be a head at one end, a curved back and seemed to be covered with eaten-away flesh or even a furry skin and was 12 feet long [and] it had all these shapes like fins along its back. . . ." (L. Phitts to S. McLean, Hancock Museum, Newcastle, UK; pers. comm. to S. M. Carr). Definitive species identification of any of these carcasses has been impossible. Pierce *et al.* (1995) concluded on the basis of ultrastructure and amino acid analysis that the Bermuda carcass was the remains of a vertebrate, and that Verrill's "giant octopus" was actually whale blubber.

In common with the Fortune Bay carcass, these and other reports (see Ellis, 1994) describe oblong whitish carcasses, several meters in length, bordered at one end with fleshy lobes, fringed with feathery white material resembling hair, and without apparent bone or cartilage. In contrast with other reports, we did not find the surface especially difficult to cut, and close examination revealed the presence of cartilage. We suggest that these and other similar remains are likely of cetacean origin. Given the variation in size of the various carcasses, it would be of interest to know the species diversity among such remains. Dead basking sharks present a somewhat different appearance. Decomposition of beached carcasses is accompanied by erosion of the caudal fin and sloughing of the head, leaving a long bony "tail" and a small chondrocranium "head" (Scott and Scott, 1988). A 1977 discovery in the nets of a Japanese fishing trawler was initially described as a "plesiosaur," but detailed morphological examination strongly suggests chondrichthian origins (Kuban, 1997). In future, discrimination of such carcasses should be possible by the means described here.

Because mtDNA is present in high copy number (~1% of total DNA) in vertebrate cells, any particular mitochondrial gene is far more likely to survive postmortem degradation, enzymatic breakdown, and mechanical damage than is any typical single-copy nuclear sequence (Hermann and Hummel, 1994). Here, adventitious "pickling" by prolonged immersion in cold seawater has left enough intact DNA for positive identification. Hofreiter *et al.* (2001) caution that care must be taken to avoid contaminating the minute amounts of DNA present in forensic material with exogenous species: in this case, no (other) sperm whale tissue was present in the laboratory, and appropriate experimental controls were always negative.

When anatomical identification is not possible and DNA can be recovered, effective identification of unknown marine creatures begins with PCR amplification with "universal" primers designed to be homologous to gene regions that are evolutionarily conserved across a diversity of taxa (Kocher *et al.*, 1989; Palumbi, 1996). The resultant DNA sequence can then be compared against the complete GenBank database of the National Center for Biotechnology Information (NCBI) [http://www.ncbi.nlm.nih.gov] by means of a BLAST search (Altschul *et al.*, 1997). This involves a simple "cut and paste" submission of the sequence data over the Internet: an answer is usually obtained within minutes (here, in under 30 seconds). The search returns a set of matches, ranked in order of degree of sequence similarity. In this case, an essentially exact match was obtained, which indicates a positive species identification.

Were a more inexact match to be obtained, phylogenetic analysis would be necessary to ascertain or at least narrow species affinities among the usual suspects. The GenBank taxonomy database currently comprises DNA sequences from more than 50,000 species, of which more than 9600 are vertebrate species, including 110 Elasmobranchii and 80 Cetacea. Reference sequences for the mitochondrial NADH2 gene, the cytochrome *b* gene, or both are available from 3 of the 4 species of sharks and 10 of the 11 species of whales that are found in Atlantic Canadian waters and exceed 6 m in length (Table 1). Failure to obtain positive identification through GenBank does not necessarily indicate an unknown species, but may instead indicate a previously recognized species for which genetic data, or data from a particular locus, are as yet unknown. Continuing studies in marine biology and molecular systematics will improve the range and depth of our knowledge of the genetics of these species, and should provide exact tests for future cryptozoological specimens.

Acknowledgments

We thank the people of St. Bernard's for drawing our attention to this interesting specimen; Mr. W. Peney, Mr. H. Whitney, Mr. W. King, and Mr. W. Mayo for their assistance in obtaining specimen material; Mr. Scott Federhen for help with GenBank; Mr. Steve McLean at the Hancock Museum for discussion of the Hebrides carcass; Dr. Sidney K. Pierce for discussion of the Bermuda carcass; Mr. Edward Ormondroyd for his thoughts on sea monsters; and Dr. Christoph Koenig at Qiagen for indulging our e-mails and phone calls. We thank Dr. Pierce, Ms. Dale Parmiter, and two anonymous reviewers for helpful comments on earlier drafts of this manuscript. Ms. Johnstone and Ms. Pynn were supported by the Women in Science and Engineering (WISE) program. This work was performed as part of the Strategic Alliance agreement between the Department of Fisheries and Oceans and Memorial University of Newfoundland, which includes investigation of the genetics and genomics of marine organisms.

Literature Cited

Aldrich, F. A. 1991. Some aspects of the systematics and biology of squid of the genus *Architeuthis* based on a study of specimens from Newfoundland waters. *Bull. Mar. Sci.* **49**: 457–481.

Altschul, S. F., T. L. Madden, A. A. Schäffer, J. Zhang, Z. Zhang, W. Miller, and David J. Lipman. 1997. Gapped BLAST and PSI-BLAST: a new generation of protein database search programs. *Nucleic Acids Res.* **25**: 3389–3402.

Árnason, Ú., A. Gullberg, S. Gretarsdottir, B. Ursing, and A. Janke. 2000. The mitochondrial genome of the sperm whale and a new molecular reference for estimating eutherian divergence dates. *J. Mol. Evol.* **50**: 569–578.

Baker, C. S., F. Cipriano, and S. R. Palumbi. 1996. Molecular genetic identification of whale and dolphin products from commercial markets in Korea and Japan. *Mol. Ecol.* **5**: 671–685.

Benson, D. A., I. Karsch-Mizrachi, D. J. Lipman, J. Ostell, B. A. Rapp, and D. L. Wheeler. 2000. GenBank. *Nuc. Acids Res.* **28**:15–18.

Ellis, R. 1994. *Monsters of the Sea.* Knopf, New York.

Hermann, B., and S. Hummel, eds. 1994. *Ancient DNA.* Springer-Verlag, New York.

Hofreiter, M. D., D. Serre, H. N. Poinar, M. Kuch, and S. Pääbo. 2001. Ancient DNA. *Nature Rev. Genetics* **2**. 353 –359.

Holder, M.T., M. V. Erdmann, T.P. Wilcox, R. L. Caldwell and D. M. Hillis. 1999. Two living species of coelacanths. *Proc. Nat. Acad. Sci. USA* **96**: 12616–12620.

International Human Genome Sequencing Consortium. 2001. Initial sequencing and analysis of the human genome. *Nature* **409**: 860–921.

Kocher, T. D., W. K. Thomas, A. Meyer, S. V. Edwards, S. Pääbo, F. X. Villablanca, and A. C. Wilson. 1989. Dynamics of mitochondrial DNA evolution in animals: amplification and sequencing with conserved primers. *Proc. Nat. Acad. Sci. USA***86**: 6196–6200.

Kuban, G. J. 1997. Sea-monster or shark? An analysis of a supposed plesiosaur carcass netted in 1977. *Reports of the National Center for Science Education* **17**: 16–28.

Leatherwood, S., D. K Caldwell, and H. E. Winn. 1976. Whales, dolphins and porpoises of the Western North Atlantic. A guide to their identification. *NOAA Technical Report* NMFS CIRC-396, 176 pp.

Ley, W. 1959. *Exotic Zoology.* Knopf. New York.

Naylor, G. J. P., A. P. Martin, E. K. Mattison, and W. M. Brown. 1999. Interrelationships of Lamniform sharks: testing phylogenetic hypotheses with sequence data. Pp. 199–218 in *Molecular Systematics of Fishes.* T. D. Kocher and C. A. Stepien, eds. Academic Press, New York.

Palumbi, S. R. 1996. Nucleic acids II: the polymerase chain reaction. Pp. 205–247 *in Molecular Systematics.* D. M. Hillis, C. Moritz, and B. K. Mable, eds. Sinauer, Sunderland, MA.

Palumbi, S. R., and F. Cipriano. 1998. Species identification using genetic tools: the value of nuclear and mitochondrial gene sequences in whale conservation. *J. Hered.* **89**: 459–464.

Pierce, S. K., G. N. Smith, Jr., T. K. Maugel, and E. Clark. 1995. On the Giant Octopus (*Octopus giganteus*) and the Bermuda Blob: homage to A.E. Verrill. *Biol. Bull.* **188**: 219–230.

Saiki, R. K., D. H. Gelfand, S. Stoffel, S. J. Scharf, R. Higuchi, G. T. Horn, K. B. Mullis, and H. A. Ehrilich. 1988. Primer-directed enzymatic amplification of DNA with a thermostable DNA polymerase. *Science* **239**: 487–491.

Scott, W. B., and M. G. Scott. 1988. *Atlantic Fishes of Canada.* Univ. Toronto Press.

Verrill, A. E. 1897. The supposed great Octopus of Florida: certainly not a cephalopod. *Amer. J. Sci.*, 4th series, **3**: 355.

Wheeler, D. L., C. Chappey, A. E. Lash, D. D. Leipe, T. L. Madden, G. D. Schuler, T. A. Tatusova, and B. A. Rapp. 2000. Database resources of the National Center for Biotechnology Information. *Nucleic Acids Res.* **28**: 10–14.

Reference: *Biol. Bull.* **202:** 6–22. (February 2002)

Apical Sensory Organ in Larvae of the Patellogastropod *Tectura scutum*

LOUISE R. PAGE

Department of Biology, University of Victoria, P.O. Box 3020 STN CSC,
Victoria, British Columbia, Canada V8W 3N5

Abstract. The apical sensory organ in veliger larvae of a patellogastropod, a basal clade of gastropod molluscs, was studied using ultrastructural and immunohistochemical techniques. Immediately before veligers of *Tectura scutum* undergo ontogenetic torsion, the apical sensory organ consists of three large cells that generate a very long apical ciliary tuft, two cells that generate a bilateral pair of shorter ciliary tufts, and a neural ganglion (apical ganglion). Putative sensory neurons forming the ganglion give rise to dendrites that extend to the apical surface of the larva and to basal neurites that contribute to a neuropil. The ganglion includes only one ampullary neuron, a distinctive neuronal type found in the apical ganglion of other gastropod veligers. Serotonin immunoreactivity is expressed by a medial and two lateral neurons, all having an apical dendrite, and also by neurites within the neuropil and by peripheral neurites that run beneath the ciliated prototrochal cells that power larval swimming. The three cells generating the long apical ciliary tuft are lost soon after ontogenetic torsion, and the medial serotonergic cell stops expressing serotonin antigenicity in late-stage veligers. The lateral ciliary tuft cells of *T. scutum* may be homologs of lateral ciliary tuft cells in planktotrophic opisthobranch veligers. A tripartite arrangement of sensory dendrites, as described previously for veligers of other gastropod clades, can be recognized in *T. scutum* after loss of the apical ciliary tuft cells.

Introduction

The apical sensory organ of larval gastropods has potential value for studies on patterns and mechanisms of evolutionary change during development. Existing evidence, albeit fragmentary, suggests that at least some cellular components of the apical sensory organ in veliger larvae of gastropods and in larvae of other molluscs are segregated early in embryogenesis and have a similar pattern of embryonic cell lineage (see Raven, 1966; Camey and Verdonk, 1970; Cather, 1973; van Dongen and Geilenkirchen, 1974; Verdonk and van den Biggelaar, 1983; Dohmen, 1992; Dictus and Damen, 1997). Studies on planktotrophic gastropod veligers have shown that the apical sensory organ is a discrete morphological unit consisting of a small neural ganglion (apical ganglion) and, in most species examined to date, a bilateral pair of ciliary tufts (Kempf *et al.*, 1997; Marois and Carew, 1997a; Page and Parries, 2000). These morphological data suggest that the apical ganglion includes sensory neurons and peripheral neurites extending from the ganglion innervate muscles and prototrochal cilia of the velum. Furthermore, recent experimental research on veligers of the nudibranch gastropod *Phestilla sibogae* has justified the long-held belief that the apical sensory organ detects the exogenous cue for induction of larval metamorphosis (Hadfield *et al.*, 2000).

Although the larval apical sensory organ of gastropods should be amenable to investigations of the developmental constraints and novelties that have interacted to produce evolutionary differences in final morphology, the solid platform of comparative data that such studies require is currently incomplete. To date, detailed morphological information is available on the apical sensory organ of planktotrophic veligers of caenogastropods (Uthe, 1995; Page and Parries, 2000) and heterobranchs (Bonar, 1978; Chia and Koss, 1984; Kempf *et al.*, 1997; Marois and Carew, 1997a, b, c;). However, these two sister groups constitute the most derived clade of extant gastropods, the Apogastropoda (Haszprunar, 1988; Ponder and Lindberg, 1997). Very little is known about the morphology of the apical sensory organ in basal clades of gastropods. There-

Received 24 May 2001; accepted 1 October 2001.
E-mail: lpage@uvvm.uvic.ca

fore, we cannot know which, if any, features of the apical sensory organ in larval apogastropods are broadly conserved throughout this molluscan class, much less speculate about the polarity of evolutionary change in the case of differences or the nature of modified developmental mechanisms.

The apical sensory organ of larval molluscs (see Kempf *et al.*, 1997, for a survey of other terms applied to this structure) may have homologs within the larval body plans of other spiralian phyla (Nielsen, 1995). Pioneering ultrastructural work by Lacalli (1981, 1984) showed that the apical organ of *Spirobranchus* trochophores (Polychaeta) is a structurally integrated unit consisting of neuronal cells in addition to cells generating a single long tuft of cilia. Neurites extending from the neurons intermingle within a plexus or neuropil so that a simple type of ganglion is formed. In veliger larvae of derived gastropod groups, the ganglionic component of the apical sensory organ consists of sensory and nonsensory neurons clustered over a neuropil (Kempf *et al.*, 1997; Marois and Carew, 1997a; Page and Parries, 2000). Dendrites extending from the sensory neurons are organized into three bundles (a medial and two lateral bundles) that penetrate the overlying epithelium (see also Chia and Koss, 1984). A subgroup of the sensory neurons, called ampullary neurons, have a deep invagination of the peripheral, dendritic membrane that is filled with cilia arising from the wall of the invagination. In addition, antibodies against serotonin label (1) three to six neuronal somata within the apical ganglion (the number is constant within each species that has been studied), (2) neurites within the neuropil of this ganglion, and (3) peripheral neurites that extend from the neuropil to muscle fibers and prototrochal ciliated cells of the larval velum (Kempf *et al.*, 1997; Marois and Carew, 1997a; Page and Parries, 2000).

A major enigma regarding the comparative structure of the apical sensory organ among gastropod larvae relates to the distinctive long ciliary tuft that is a characteristic component of this larval structure in many other spiralians, including at least some members of the molluscan classes: Scaphopoda, Polyplacophora, Aplacophora, and Bivalvia (see reviews by Raven, 1966; Verdonk and van den Biggelaar, 1983). Among gastropods, a long cohesive tuft of non-vibratile cilia arising from the center of the larval apical epidermis has been reported only for members of the Patellogastropoda (Smith, 1935; Dictus and Damen, 1997; Wanninger *et al.*, 1999, 2000), which is currently viewed as the most basal clade of extant gastropods (Haszprunar, 1988; Ponder and Lindberg, 1997). The homolog of the patellogastropod apical tuft in other gastropod groups is unclear. Some authors (Conklin, 1897; Cather, 1973) have suggested that the apical tuft in caenogastropods is represented in prehatching embryos by four apical cells bearing short, motile cilia. However, the fate of these cells in hatching larvae was not determined. More recently, ultrastructural studies on posthatching planktotrophic veligers of both caenogastropods and heterobranchs identified a potential homolog of the patellogastropod apical tuft in the form of two relatively short ciliary tufts that flank the midline at the ventral margin of the apical sensory organ (Chia and Koss, 1984; Kempf *et al.*, 1997; Page and Parries, 2000). As yet, the embryonic derivation of the cells generating these bilateral ciliary tufts in posthatching veliger larvae of caenogastropods and heterobranchs has not been determined.

I investigated the ultrastructure and serotonin immunoreactivity of the apical sensory organ in the patellogastropod *Tectura scutum* (Rathke 1833) with the goal of identifying similarities and differences relative to the apical sensory organ of planktotrophic apogastropod larvae. Overall development of posthatching larvae of *T. scutum* is similar to that described previously for two other patellogastropod species belonging to the genus *Patella* (Smith, 1935; Wanninger *et al.*, 1999, 2000).

Materials and Methods

Source of adults, fertilization of gametes, and culture of embryos and larvae

Adults of *Tectura scutum* were collected during late August and early September from the intertidal zone of rocky shores along the southwestern perimeter of Vancouver Island, Pacific coast of Canada. Adults were isolated into separate bowls of seawater at 12 °C, and 10% to 25% of these animals spawned eggs or sperm beginning at 15½ to 16 h after the time of lower low tide. Freshly spawned eggs were transferred to 1 liter of filtered (0.45 μm) seawater (FSW) so as to cover the bottom of the beaker with a sparse monolayer of eggs. One milliliter of concentrated sperm was mixed into 500 ml of FSW, and 1 to 2 ml of this sperm suspension was added to the eggs and stirred gently for ½ h. Seawater over settled eggs was decanted and replaced with fresh FSW. About 100 fertilized eggs were transferred into culture beakers containing 500 ml FSW at 12 °C. Culture water was changed daily by gently pouring cultures through a 49-μm sieve immersed in a small bowl of seawater. The sieve was constructed by replacing the bottom of a small plastic beaker with Nitex cloth attached by silicon glue. Larvae retained by the sieve were then pipetted into beakers of fresh FSW. To obtain normal development without adding antibiotics, it was important to culture embryos and larvae at very low density. Adult limpets were subsequently returned to the site of collection. Results reported here are based on five batches of larvae reared over three separate years.

Tissue preparation for scanning and transmission electron microscopy (SEM and TEM)

Larvae were pipetted into 8-ml vials and anesthetized by initial incubation for 2 h at 12°C in several changes of artificial seawater having augmented Mg^{++} and reduced Ca^{++} concentrations (225 mM NaCl, 5 mM KCl, 102 mM $MgCl_2$, 1 mM $CaCl_2$ in distilled water). The volume of fluid was then reduced to 1.5 ml, and a small piece of menthol crystal (7–10 mg) was floated on the fluid surface. After 45 min, the menthol and artificial seawater was replaced with two changes of primary fixative at room temperature.

Primary fixative consisted of 2.5% glutaraldehyde in 0.2 M Millonig's phosphate buffer (pH 7.6) and 0.14 M sodium chloride. Larvae were stored in this fixative at 8 ° to 10 °C for several days to one month before further processing. Subsequent processing steps were done at room temperature. Larval shells were decalcified in a 1:1 mixture of primary fixative and 10% ethylenediaminotetraacetic acid (disodium salt) for 1 h (Bonar and Hadfield, 1974). Specimens were then rinsed three or four times in 2.5% sodium bicarbonate (pH 7.2) and transferred to a 1:1 mix of 4% OsO_4 and 2.5% sodium bicarbonate for 1 h. A graded ethanol series was used to dehydrate fixed specimens, which were then transferred through three changes of propylene oxide and infiltrated and embedded in TAAB 812 epoxy resin (Marivac, Halifax, NS, Canada). The foregoing procedures, from anesthesia of the larvae to infiltration with epoxy resin, were done on specimens contained within squat, wide-mouth vials of 8-ml capacity. Specimens within the vials could be viewed with a stereomicroscope placed on the sill of a fume hood so that solutions could be removed from the vials using a bent pipette without accidentally removing larvae.

Thin sections were cut with a diamond knife and lifted onto 150-mesh copper grids. Central portions of each section were teased over openings in the grid mesh using an eyebrow hair mounted on an orange stick. Dried sections were stained in aqueous 2% uranyl acetate for 1.5 h and in 0.2% lead citrate for 6–7 min and were photographed with a Hitachi 7000 transmission electron microscope operated at 50 kV accelerating voltage.

For SEM, larvae were processed as described above except that specimens in 100% alcohol were transferred into modified Beam capsules for critical point drying from liquid carbon dioxide. The bottom of each Beam capsule was removed, and the top and bottom were covered with a small piece of Nitex cloth of 49-μm mesh size. The Nitex was held in place by sandwiching it between the Beam capsule itself and a Beam capsule lid from which a large hole had been cut. Specimens dried at critical point were transferred to double-sided sticky tape on an SEM stub, sputter-coated with gold, and photographed with a Hitachi 6500N scanning electron microscope operated at 8 to 15 kV accelerating voltage.

Immunohistochemistry

Anesthetized larvae were fixed in a solution consisting of 20 ml 8% paraformaldehyde (freshly prepared from powder according to instructions given in Hayat, 1970), 10 ml of 0.2 M Millonig's phosphate buffer (pH 7.6) and 10 ml of 0.14 M sodium chloride (final paraformaldehyde concentration was 4%). Specimens were fixed at 6 °C for 3 h, rinsed six times over an hour in phosphate-buffered saline (PBS) at pH 7.4 containing 0.1% sodium azide, and stored in the final rinse for 12 h to 4 days before further processing. All subsequent incubations were done at 6 °C on an orbital shaker. Fixed larvae were blocked for 4 h in PBS containing 0.1% Triton-X 100, 0.1% sodium azide, and 0.1% heat-inactivated goat serum, then incubated for 24 h in a rabbit polyclonal IgG against 5-hydroxytryptamine (serotonin) conjugated to paraformaldehyde (DiaSorin, Stillwater, MN; formerly Incstar) at a dilution of 1:1000 in blocking medium. This was followed by six to eight rinses in PBS + 0.1% Triton-X 100 + 0.1% sodium azide over 10 h.

To obtain a fluorescent label of primary antibody location, specimens were incubated in goat anti-rabbit secondary antibodies coupled to the fluorphore Alexa 488 (Molecular Probes, Eugene, OR) at a dilution of 1:250 in blocking medium for 24 h. These were then rinsed 6–8 times in PBS + 0.1% sodium azide and examined with a Zeiss Axioskop compound microscope or a Zeiss LSM 410 confocal laser scanning microscope using filter sets appropriate for fluorescein isothiocynate fluorescence.

To obtain a label of primary antibody location for visualization in sections examined by light or transmission electron microscopy, the secondary antibody was a biotinylated goat anti-rabbit IgG (Histostain kit, Zymed, San Fransisco, CA). After rinsing in PBS + 0.1% Triton-X 100 (no azide), specimens were transferred to a conjugate of streptavidin-horseradish peroxidase (Histostain kit) for 12 h. Specimens were then rinsed six to eight times over 10 h in PBS + Triton-X 100, followed by incubation for 30 min in diaminobenzidine (solution provided in kit marketed by DAKO Diagnostics, Mississauga, ON, Canada) diluted into PBS. Specimens were then transferred to diaminobenzidine diluted into the buffered substrate (containing hydrogen peroxide) supplied in the DAKO kit. After 30 to 40 min, the reaction was stopped by rinsing in PBS + 0.1% sodium azide. Specimens were postfixed in a 1:1 mix of 4% OsO_4 and 2.5% sodium bicarbonate, processed into epoxy resin, and sectioned for light or transmission electron microscopy as described above. Sections for light microscopy were cut at 1-μm thickness and stained with methylene blue and azure II in borax (Richardson *et al.*, 1960). Sections for TEM were cut at 80 nm and stained for 45 min in aqueous 2% uranyl acetate and 5 min in 0.2% lead citrate.

Images obtained from the transmission electron microscope were recorded on film. Digital images obtained from the scanning and confocal laser scanning microscopes were imported into Adobe Photoshop and adjusted for contrast, brightness, and image sharpness.

My analysis of the ultrastructure and serotonin immunoreactivity of the ganglion and associated ciliary structures of the larval apical sensory organ of *T. scutum* concentrated on larvae that were fixed at three stages: 52 h postfertilization (at the onset of ontogenetic torsion), 90 h postfertilization (30 h after completion of ontogenetic torsion), and 7 days postfertilization (onset of metamorphic competence). Several other stages were examined less thoroughly by either electron microscopy or immunohistochemistry.

Results

Overview of larval development and the apical sensory organ

Larvae of *Tectura scutum* hatch from the egg investments beginning at 12 to 15 h postfertilization (12 °C) and swim by means of long cilia of the prototroch, or pre-oral ciliary band. These trochophore-like hatching larvae are converted to the veliger larval form by secretion of the larval shell and swelling of the foot rudiment over the next 1½ days of development (Fig. 1A). Ontogenetic torsion, a morphogenetic movement involving a 180° rotation of the cephalopodium relative to the shell, mantle, and differentiating viscera, occurs between 52 and 58 h postfertilization. The foot enlarges considerably over the following days (Fig. 1B) so that larvae are capable of both swimming and pedal crawling by 7 days posthatching. Many larvae at this age undergo metamorphosis when added to small bowls containing seawater and pebbles collected from rocky shores inhabited by adults. Metamorphosed individuals lack prototrochal ciliated cells and resume shell secretion to begin the distinctive postmetamorphic teleoconch.

As veligers of *T. scutum* approach the onset of ontogenetic torsion, they have an apical sensory organ that consists of two components: neurons organized as a simple ganglion (the apical ganglion) and two types of distinctive ciliary structures. The most obvious ciliary structure in pretorsional veligers is a tuft of very long, nonmotile cilia that arises from the center of the apical epidermis (Fig. 1A, C, D). This long, apical ciliary tuft is flanked by two low papillae (Fig. 1C), each of which is the protruding, multiciliated apex of a single cell (lateral ciliary tuft cells). The centrally located, apical ciliary tuft is lost soon after ontogenetic torsion is completed, and a pair of cephalic tentacles subsequently grow from the apical surface of the veliger (Fig. 1B). Neurons of the apical ganglion give rise to cytoplasmic extensions, which are putative dendrites, that terminate at the exposed apical surface. The sketches in Figure 2 were traced from transmission electron micrographs of sections cut parallel to the apical surface of larvae at 52 and 90 h postfertilization, such as those shown in Figures 3A and 4. The tracings show positional relationships between cells giving rise to the distinctive ciliary structures of the apical sensory organ (the apical and lateral ciliary tuft cells) and six clusters of sensory dendrites arising from neurons of the apical ganglion. The position of a small pit within the apical epidermis is also indicated in these diagrams, although the pit is obscured by cilia in the scanning electron micrograph shown in Figure 1C. Details of these components are described below.

Ciliary structures of the apical sensory organ

Scanning electron micrographs of veligers at the onset of ontogenetic torsion (52 h post-fertilization) show that the apical surface within the ring of prototrochal ciliated cells is dominated by a field of cilia in the shape of a plus (+) symbol (Fig. 1C). The two axes of the plus are oriented along the dorsal-ventral and left-right axes of the larva, and the apical ciliary tuft arises from the center of the plus-shaped ciliary field (Fig. 1C). Cilia of the apical tuft form a cohesive bundle that is about 80 μm long and extends perpendicular to the planar surface of the apical epidermis (Fig. 1A). The tuft does not show rhythmic undulations and is lost within 4 to 8 h after larvae complete ontogenetic torsion. Many cilia within the left and right arms of the plus-shaped ciliary field extend from the low papillae that are the apices of the lateral ciliary tuft cells (Fig. 1C). Unlike the apical ciliary tuft, the lateral ciliary tufts are retained until larval metamorphosis.

Transmission electron microscopy shows that cilia of the apical tuft arise from three large cells (Figs. 2A, 3A) and are supported by very long and robust ciliary rootlets (Figs. 1D, 3D). These three multiciliated cells also contain longitudinal arrays of microtubules (Fig. 3D), which may provide further structural support for the cells. As shown in Figures 2A and 3A, the apical tuft cells constitute three of the four apical pole cells of pretorsional veligers of *T. scutum*. The fourth cell, which occupies the ventral position for this tetrad, is the ampullary sensory neuron, a distinctive type of apical ganglion neuron that is described below. Loss of the apical ciliary tuft following ontogenetic torsion appears to be due to degeneration of the three apical tuft cells, rather than simple shedding of cilia from cells that remain intact. Figure 4 (asterisk) shows a remnant of an apical tuft cell in a larva fixed at 90 h postfertilization (about 30 h after completing ontogenetic torsion).

Figure 5A shows the protruding apices of the two lateral ciliary tuft cells in a larva fixed at 90 h postfertilization, which is after the three large cells that produce the apical ciliary tuft have disappeared. In younger larvae (immediately prior to ontogenetic torsion), the central group of apical ciliary tuft cells lies between the two lateral tuft cells (Figs. 2A, 3A). Each lateral tuft cell consists of an expanded, multiciliated apex, a narrow middle zone, and a basal perinuclear region that lies at the ventrolateral margins of the apical ganglion on the left and right sides (Fig. 5C). The apparent "shrinkage" of the lateral ciliary tuft cells in the tracing shown in Figure 2B, relative to those shown in

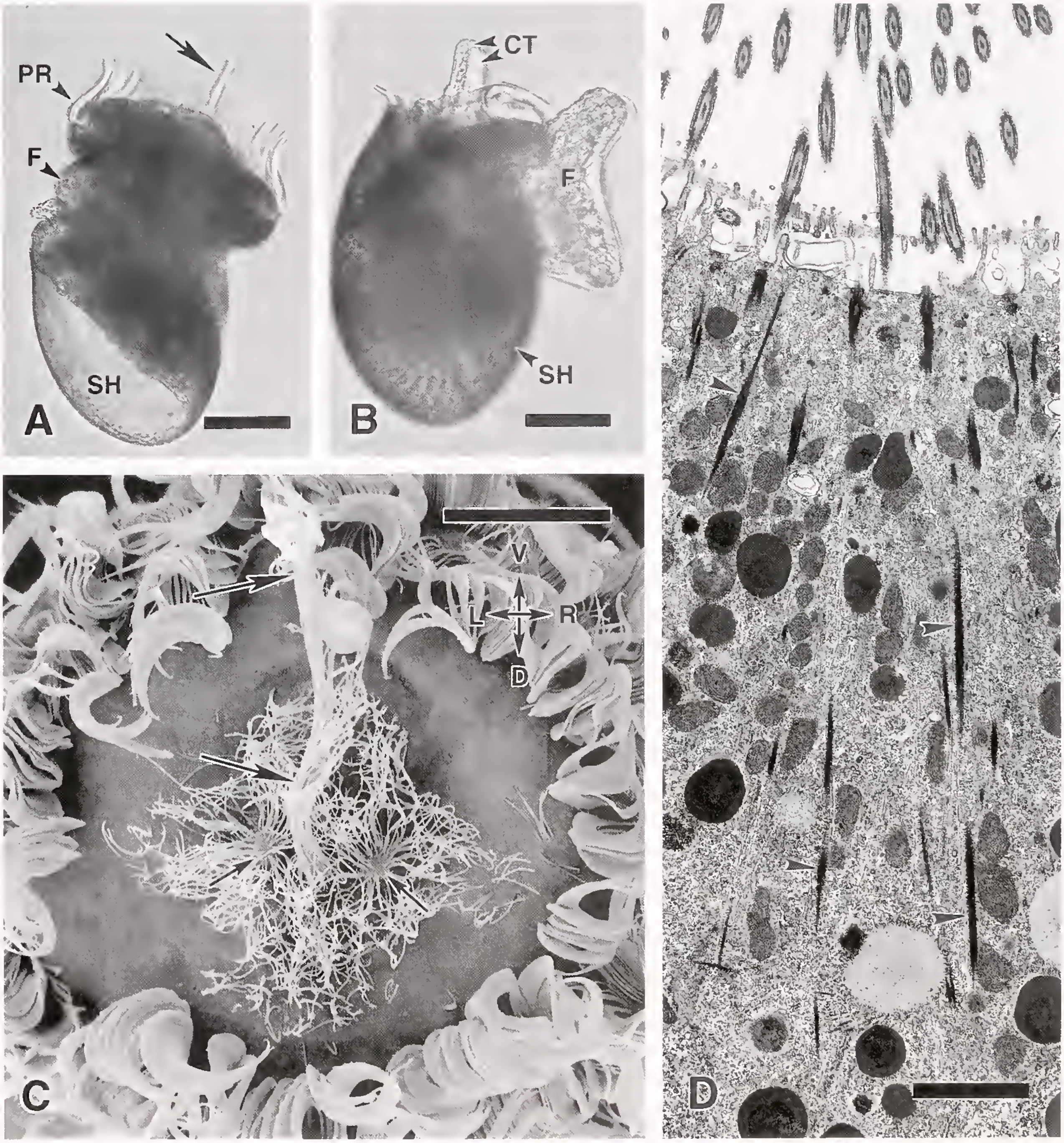

Figure 1. Early and late veliger larvae of *Tectura scutum* showing structures extending from the apical surface. (A) Light micrograph of a live veliger at 46 h postfertilization, prior to ontogenetic torsion; note cilia of the prototroch and the long apical ciliary tuft (arrow). Scale, 50 μm. (B) Light micrograph of a partially retracted veliger at 7 days postfertilization; note the pair of cephalic tentacles and enlarged foot. Scale, 50 μm. (C) Scanning electron micrograph of the apical surface at 52 h postfertilization showing the peripheral ring of prototrochal cilia and the central, plus-shaped ciliary field. The long apical ciliary tuft (large arrows) is flanked by small papillae bearing the lateral ciliary tufts (small arrows). Scale, 20 μm. (D) Transmission electron micrograph showing an apical ciliary tuft cell in longitudinal section from a larva at 48 h postfertilization; note very long ciliary rootlets (arrowheads). Scale, 2 μm. Abbreviations: CT, cephalic tentacles; F, foot; PR, prototroch; SH, shell. Orientation arrows: D, dorsal; L, left; R, right; V, ventral.

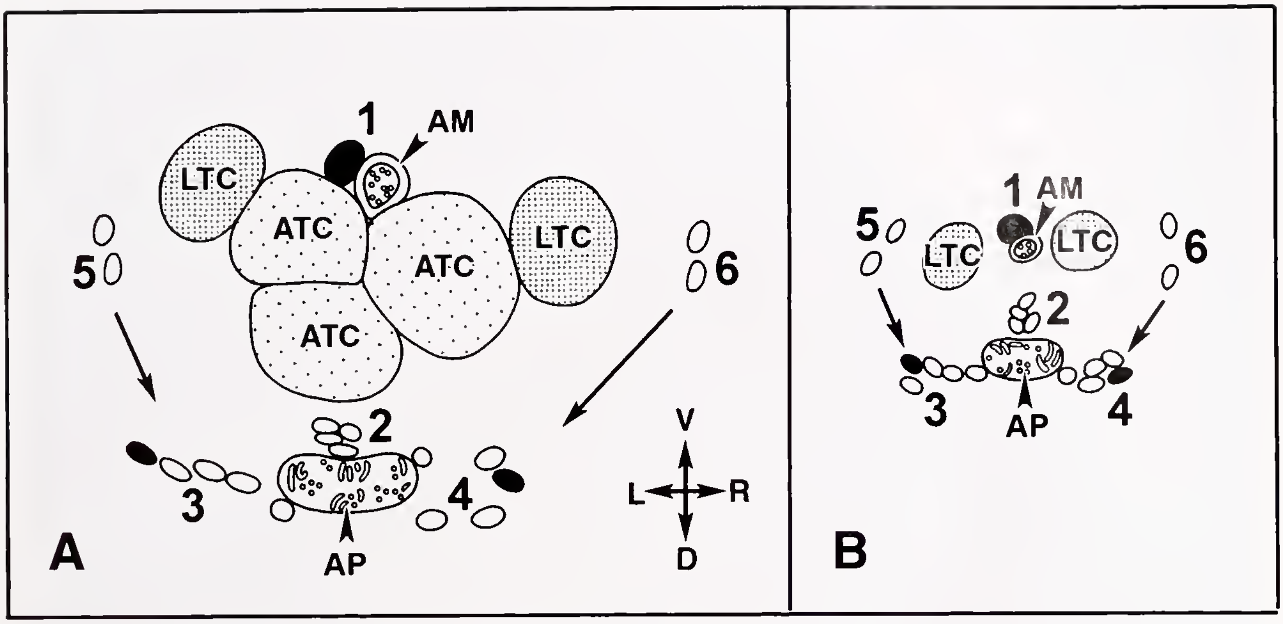

Figure 2. Relative positions of components of the apical sensory organ in veligers of *Tectura scutum* at 52 h postfertilization (A) and 90 h postfertilization (B). Sketches are traced from transmission electron micrographs of sections cut parallel to the apical surface of the larva at a level close to the epithelial surface (same enlargement for both sketches). Numbers refer to groups of dendrites (see text). Arrows indicate that dendrites in groups 5 and 6 join those of groups 3 and 4, respectively, at a deeper level. Filled profiles are dendrites of serotonin-immunoreactive neurons; unfilled profiles are dendrites from other sensory neurons of the apical ganglion. Abbreviations: AM, dendrite of ampullary neuron; AP, apical pit; ATC, apical tuft cell; LTC, lateral tuft cell. Orientation arrows, D, dorsal; L, left; R, right; V, ventral.

Figure 2A, is largely due to the fact that the middle zone of these cells becomes progressively longer and narrower between 52 and 90 h postfertilization. Cilia arising from the lateral ciliary tuft cells are anchored by forked, striated rootlets that are much shorter than the ciliary rootlets extending from the basal bodies of apical tuft cilia.

Apical ganglion

The larval apical ganglion of *T. scutum* is a cluster of neurons located immediately beneath the dorsal half of the apical epidermal disc. Most and possibly all of the apical ganglion neurons give rise to distal cytoplasmic extensions (putative dendrites) that extend to the exposed epidermal surface of the larva within the plus-shaped apical ciliary field. Two to four cilia arise from the distal terminals of these dendrites. The sketch in Figure 2A shows the positions of the dendritic terminals, relative to the apical and lateral ciliary tuft cells and the apical pit, in veligers at the onset of ontogenetic torsion. The sensory dendrites at the exposed surface of the apical epithelium are clustered into six groups: two medial groups and two pairs of lateral groups. Group 1 consists of two dendrites located ventromedially; one of these is the ampullary sensory neuron (Fig. 3A). Group 2 consists of five dendrites that occupy a central location between the large apical tuft cells and the apical pit. After loss of the three apical tuft cells, dendritic groups 1 and 2 come to lie in close proximity (Fig. 4). Dendritic groups 3 and 4 are located to the left and right, respectively, of the apical pit. Dendritic groups 5 and 6, each consisting of at least two dendrites, are located to the left and right, respectively, of the lateral ciliary tuft cells. After loss of the three large apical tuft cells, the dendrites and the lateral tuft cells shift centrally, but they nevertheless retain the same positional interrelationships (compare Fig. 2A to 2B and Figs. 3A to 4).

The ampullary sensory neuron within dendritic group 1 is a neuronal type that has been identified within the apical ganglion of all other gastropod larvae studied to date (reviewed by Page and Parries, 2000). The distal, dendritic membrane of this neuron is deeply invaginated and gives rise to many cilia that fill the inpocketing (Figs. 3A, 4, 5A). In larvae of *T. scutum*, the invaginated pocket of the ampullary neuron does not penetrate to the level of the basal, perinuclear cytoplasm, and cilia within the pocket have a 9+2 arrangement of axonemal microtubules (Fig. 3C). The ampullary neuron within dendritic group 1 is the only sensory neuron of this type within the larval apical ganglion of *T. scutum*. The second dendrite of the two which comprise dendritic group 1 extends along the left, anterolateral side of the ampullary neuron (Figs. 3A, B, 4). As described below,

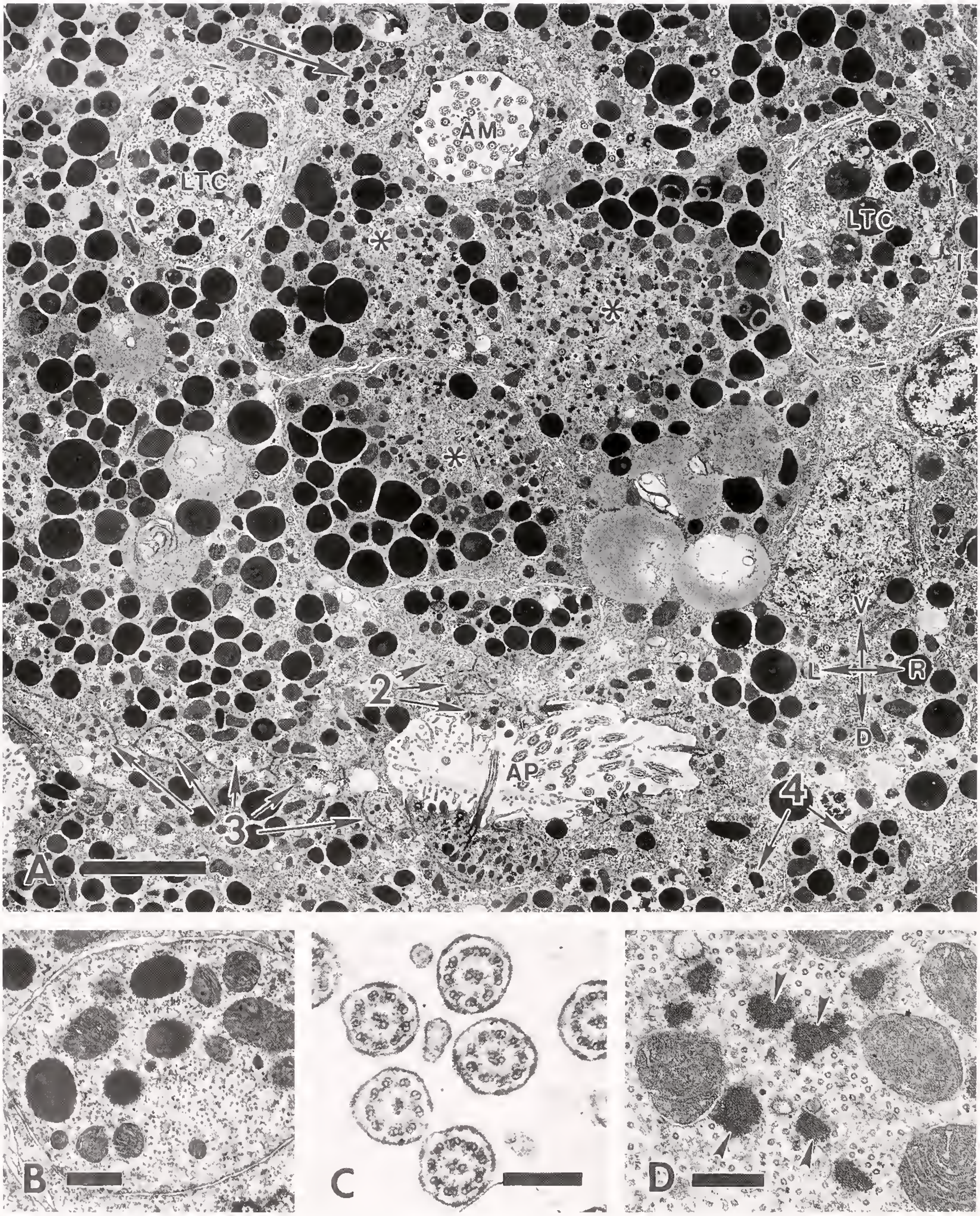

Figure 3. Transmission electron micrographs of a section cut parallel to the apical surface of a *Tectura scutum* veliger at 52 h postfertilization (onset of ontogenetic torsion) showing cellular components of the apical sensory organ. (A) Low-magnification view showing the three large cells (asterisks) that generate the apical ciliary tuft; these are bordered by the apices of lateral ciliary tuft cells (outlined by dashed lines) and dendrites

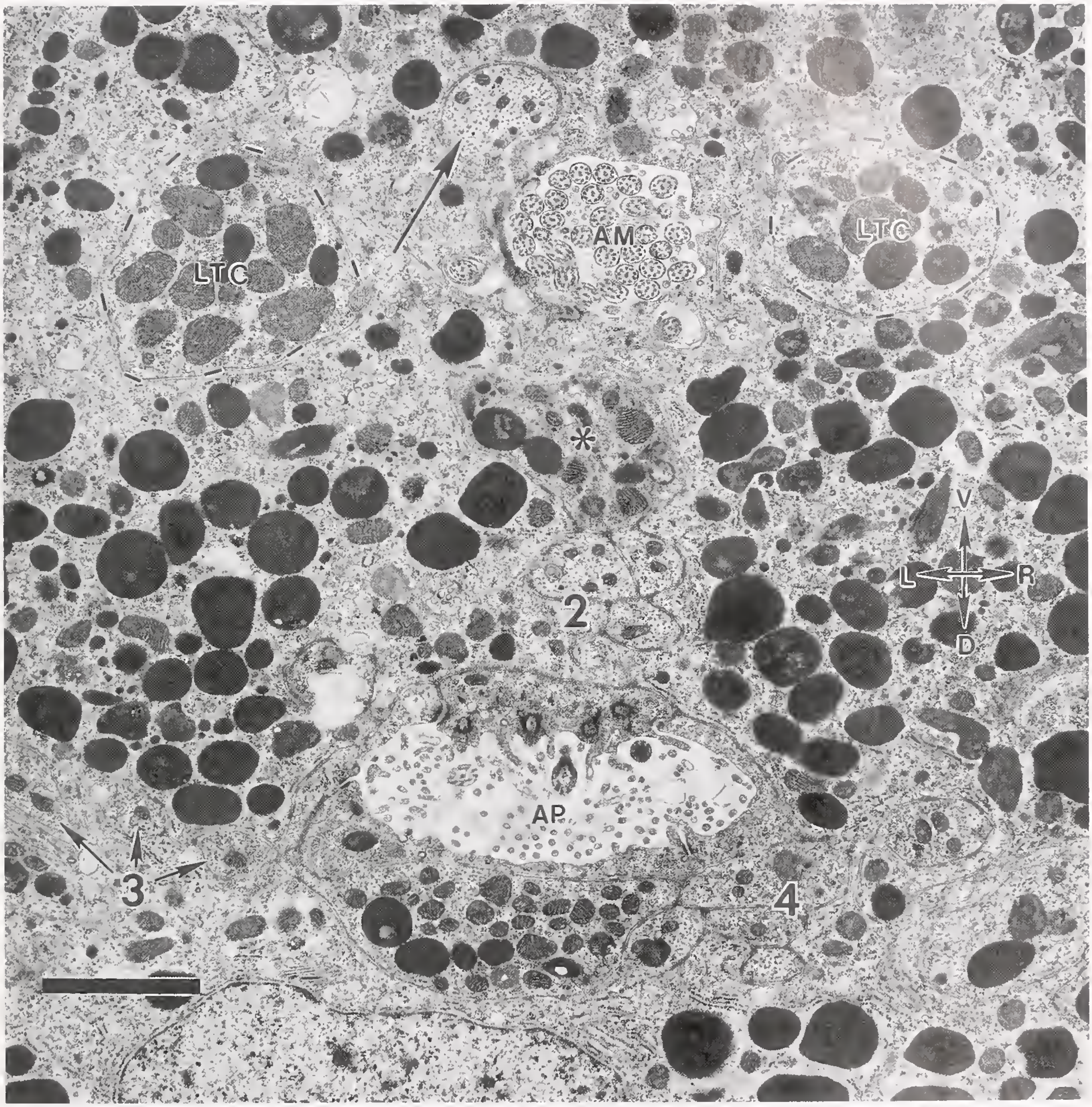

Figure 4. Transmission electron micrograph of a section cut parallel to the apical surface of a *Tectura scutum* veliger at 90 h postfertilization. Note the remnant of an apical tuft cell (asterisk). Arrow indicates dendrite of the non-ampullary neuron of dendritic group 1; dendritic groups 2, 3, and 4 are adjacent to the apical pit; dashed lines outline the lateral ciliary tuft cells. Scale, 2 μm. Abbreviations: AM, ampullary neuron; AP, apical pit; LTC, lateral tuft cells. Orientation arrows: D, dorsal; L, left; R, right; V, ventral.

---

of the ampullary and non-ampullary (arrow) sensory neurons belonging to dendritic group 1. The section also passes through the apical pit and adjacent dendrites belonging to groups 2, 3, and 4. Scale, 4 μm. (B) Enlargement of the non-ampullary sensory dendrite of dendritic group 1. Scale, 0.5 μm. (C) Detail of cilia within the invaginated pocket of the ampullary neuron; note the 9 + 2 arrangement of axonemal microtubules. Scale, 0.3 μm. (D) Detail of cytoplasm from an apical tuft cell showing robust ciliary rootlets (arrowheads) and small circular profiles of longitudinally aligned microtubules. Scale, 0.3 μm. Abbreviations: AM, ampullary neuron; AP, apical pit; LTC, lateral tuft cells. Orientation arrows: D, dorsal; L, left; R, right; V, ventral.

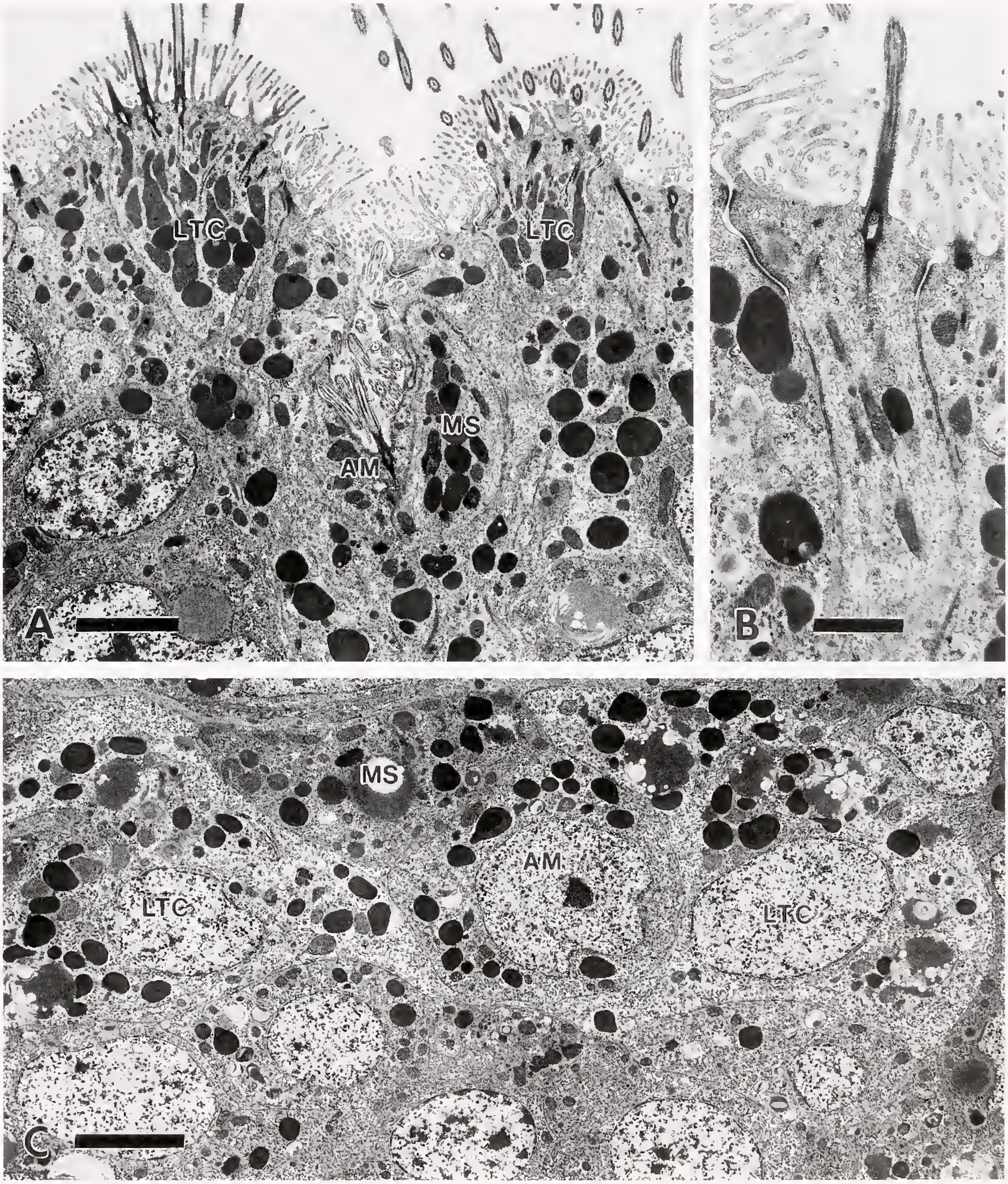

Figure 5. Ciliary and neuronal elements within the ventral portion of the apical sensory organ of *Tectura scutum* at 90 h postfertilization (apical tuft cells are absent at this stage). (A) Transmission electron micrograph (TEM) of a frontal section showing apices of the lateral ciliary tuft cells flanking distal dendrites of the ampullary and non-ampullary neuron (medial serotonergic neuron) of dendritic cluster 1. Scale, 3 μm. (B) TEM of a slightly more ventral section showing a cilium arising from the distal dendrite of the medial serotonergic neuron. Scale, 1 μm. (C) TEM of a section cut parallel to the apical surface at the level of the cell bodies of the apical ganglion. The medial serotonergic neuron, ampullary neuron, and lateral ciliary tuft cells are identified; other neuronal somata of the apical ganglion lie dorsal to these identified cells. Scale, 3 μm. Abbreviations: AM, ampullary neuron; LTC, lateral ciliary tuft cells; MS, medial serotonergic neuron.

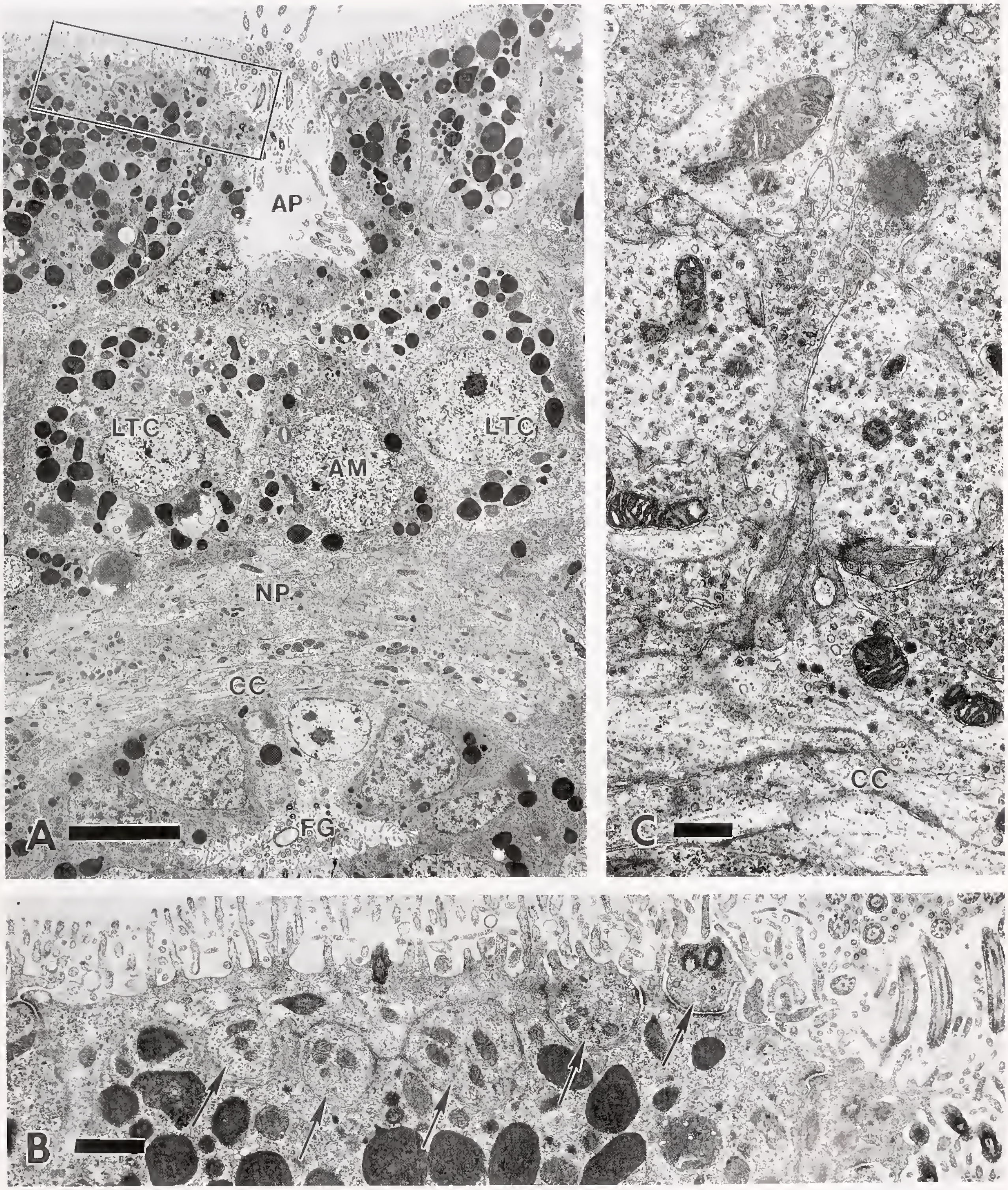

Figure 6. (A) Transmission electron micrograph of a longitudinal section through the apical sensory organ of *Tectura scutum* at 90 h postfertilization showing the apical pit and basal perinuclear regions of the ampullary neuron and lateral tuft cells; neuropil of the apical ganglion overlies the cerebral commissure. Boxed area is enlarged in (B). Scale, 5 μm. (B) Profiles of distal dendrites (arrows) located on one side of the apical pit. Scale, 1 μm. (C) Detail of sectioned neurites within the neuropil of the apical ganglion showing large swellings filled with electron-dense vesicles; a portion of the cerebral commissure is also shown. Scale, 0.5 μm. Abbreviations: AM, ampullary neuron; AP, apical pit; CC, cerebral commissure; FG, foregut; LTC, lateral tuft cells; NP, neuropil.

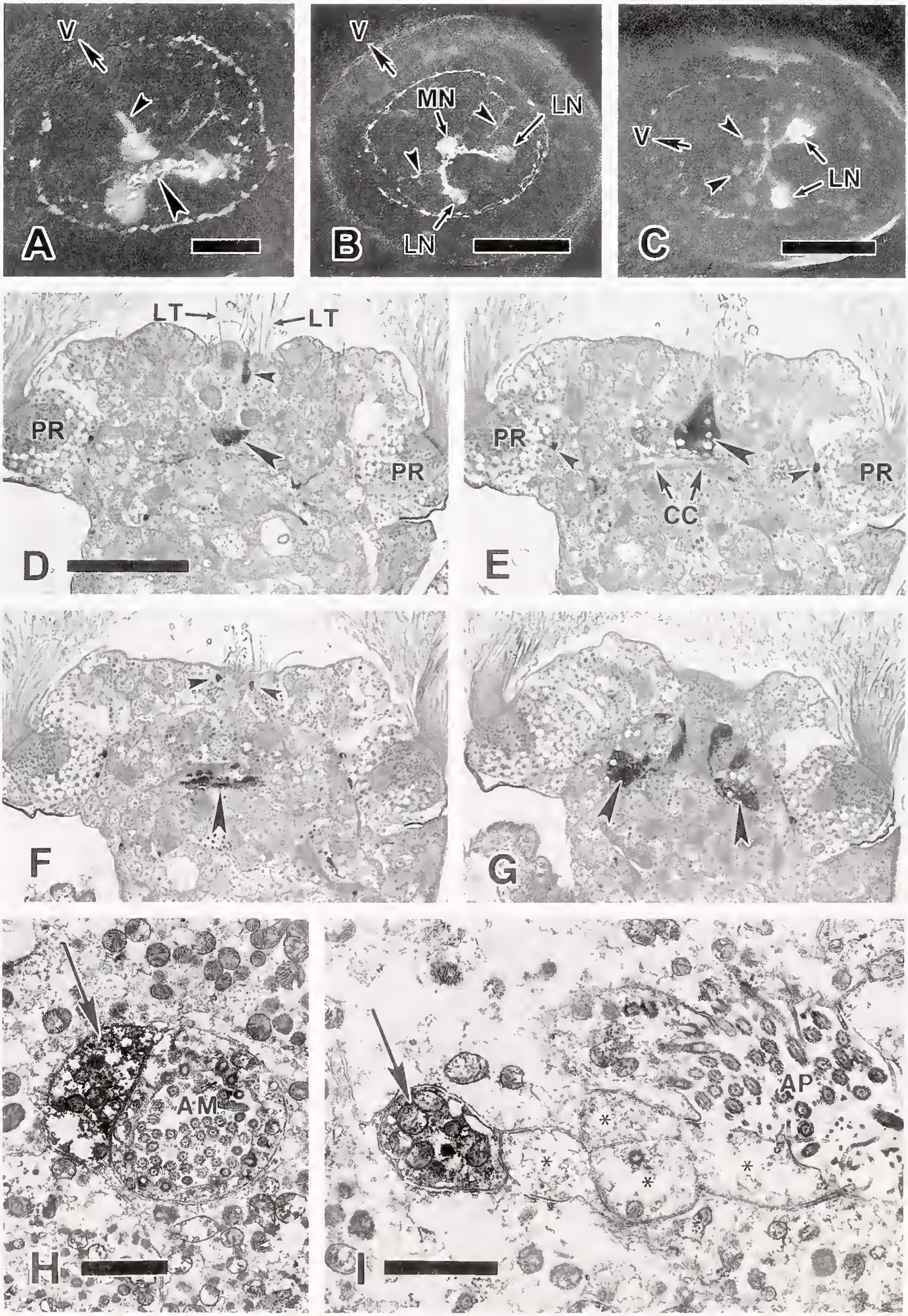
V
A
V
MN
LN
LN
B
LN
V
LN
C
LT
LT
PR
PR
D
PR
PR
CC
E
F
G
AM
H
AP
I

this neuron corresponds to a medially located neuron expressing serotonin immunoreactivity and is therefore identified as the medial serotonergic neuron (MS) in Figure 5A, C. One of several cilia arising from this dendrite is shown in Figure 5B. The subepithelial cell bodies of the two sensory neurons of dendritic group 1 are sandwiched between the large, subepithelial cell bodies of the lateral tuft cells (Figs. 5C, 6A).

The largest number of dendrites within the larval apical ganglion of *T. scutum* are associated with the rim of the apical pit. Dendritic group 2 is located immediately ventral to the pit (Figs. 3A, 4), whereas groups 3 and 4 are located to the left and right, respectively, of the pit (Figs. 3A, 4, 6A, B). The apices of dendrites within groups 5 and 6 are located to either side of the ciliary tuft cells (Fig. 2A, B), but they deflect mediodorsally as they descend through the apical epidermis so as to join the ipsilateral group of dendrites on either side of the apical pit (Fig. 2A, B).

Neuropil of the apical ganglion

Neuronal cell bodies of the apical ganglion overlie a tangled collection of interdigitating neurites. Neurites of this ganglionic neuropil are characterized by large swellings stuffed with electron-dense vesicles (Fig. 6C). The neuropil overlies the cerebral commissure, a tract of neurites connecting between the two developing cerebral ganglia (Fig. 6A), but two stubby horns of the neuropil project dorsolaterally. The neuropil is ultrastructurally distinct from the cerebral commissure because neurites of the commissure tend to have parallel trajectories as they extend between the two cerebral ganglia and commissural neurites lack large swellings filled with masses of electron-dense vesicles.

Serotonin immunoreactivity within the apical ganglion and peripheral neurites

Three apical neurons, a medial neuron located centrally beneath the apical disc and two neurons located dorsolateral to the medial neuron, are recognized by antibodies against serotonin in veligers fixed at 52 h and 90 h postfertilization (Fig. 7A, B), and at 5 days postfertilization. A neurite from each lateral neuron extends ventrally to a concentration of neurites located beneath the medial, serotonin-immunoreactive neuron. The fluorescent label identifies large varicosities within the central concentration of neurites (Fig. 7A). Peripheral neurites extend laterally from each side of the central concentration of neurites and continue along the base of the large, prototrochal ciliated cells that encircle the apical disc (Fig. 7A, B). These peripheral neurites have a beaded appearance.

Immunolabeled larvae that were sectioned after processing for diaminobenzidine (DAB) reaction product show that the medial serotonin-immunoreactive neuron is the non-ampullary sensory neuron that contributes one of the two dendrites belonging to dendritic group 1 (Fig. 7D, E, H). The lateral neurons have dendrites belonging to dendritic groups 3 and 4, which lie on either side of the apical pit (Fig. 7F, I). Although the stout dendrite of the medial neuron can often be seen in fluorescently labeled larvae (Fig. 7B), the slender dendrites of the lateral neurons are difficult to ascertain without sections prepared from DAB-

Figure 7. Serotonin immunoreactivity within apical ganglion neurons and peripheral neurites of *Tectura scutum* veligers. (A-C) Confocal scanning laser micrographs of fluorescently labeled whole larvae in apical view; arrows labeled "V" indicate ventral side. (A) Larva at 90 h postfertilization (velar margin slightly contracted) showing label within the neuropil (large arrowhead) and the stout dendrite (small arrowhead) arising from the medial serotonergic neuron. Scale, 20 μm. (B) Larva at 90 h postfertilization showing label within a medial and two lateral neurons, and peripheral tracts on either side (arrowheads) projecting to a circular tract running beneath the prototrochal cells. Scale, 40 μm. (C) Apical view of a larva at 7 days postfertilization showing label within the two lateral serotonergic neurons but not in the medial neuron; arrowheads indicate small labeled neurons within the developing cerebral ganglia. Scale, 40 μm. (D-G) Frontal sections (1-μm thickness) through the head of a *T. scutum* larva at 90 h postfertilization labeled with DAB reaction product (dark deposit in cells). Sections proceed from ventral to dorsal side of the apical sensory organ. Scale, 30 um. (D) Section passing through the ventral margin of the apical sensory organ showing the lateral ciliary tufts and the distal dendrite (small arrowhead) and portion of the basal soma (large arrowhead) of the medial serotonergic neuron. (E) Soma of the medial serotonergic neuron (large arrowhead); also note label within neurites at the base of the large prototrochal cells (small arrowheads) and absence of label within the cerebral commissure. (F) Label within the neuropil (large arrowhead) of the apical ganglion; also note label within distal dendrites (small arrowheads) of two lateral serotonergic neurons. (G). Section through the somata of two lateral serotonergic neurons showing their irregular shape. (H-I) Transmission electron micrographs of sections cut parallel to the apical surface of a DAB-labeled *T. scutum* larva at 52 h postfertilization. (H) Dendritic profiles of the ampullary neuron and non-ampullary neuron (arrow) within dendritic group 1; DAB label within the latter profile identifies it as the medial serotonergic neuron. Scale, 2 μm. (I) Dendritic profiles (asterisks) located to the immediate left of the apical pit; the most peripheral profile contains DAB label (large arrow). Scale, 2 μm. Abbreviations: AM, ampullary neuron; AP, apical pit; CC, cerebral commissure; LN, lateral serotonergic neuron; LT, lateral ciliary tuft; MN, medial serotonergic neuron; PR, prototrochal cell.

labeled specimens. Sections of DAB-labeled specimens also reveal that the cell bodies of the lateral neurons have a very irregular outline (Fig. 7G). The central concentration of varicose neurites identified in fluorescent images corresponds to the neuropil of the apical ganglion (Fig. 7F).

In metamorphically competent larvae (7 days postfertilization), antibodies against serotonin continue to label the two lateral neurons and the peripheral ring of neurites underlying the prototrochal ciliated cells, but a medial neuron does not label (Fig. 7C). However, smaller neurons within the cerebral ganglia begin to express serotonin antigenicity at 7 days postfertilization (Fig. 7C). Despite loss of serotonin antigenicity within the medial neuron in late-stage larvae, this neuron can still be identified in sections of 7-day larvae examined by transmission electron microscopy (Fig. 8). Positive identification of this neuron is facilitated by the fact that its dendrite has a stereotypical location relative to that of the distinctive ampullary neuron and the lateral ciliary tuft cells (Fig. 2B).

Discussion

A goal for this study was to compare the apical sensory organ in a patellogastropod veliger to that of apogastropod veligers (caenogastropods and heterobranchs) in order to identify conserved and variant aspects of this larval neural structure among gastropod molluscs. However, uncertainty about the cellular constituents that are properly included within the structural entity that has been called the "apical organ," the "apical sensory organ," and the "cephalic sensory organ" (see Kempf *et al.*, 1997) can complicate comparisons among larval gastropods and among larval spiralians in general. As previously stated, I use the term "apical sensory organ" to refer to the cellular complex that includes both the apical ganglion and cells bearing prominent ciliary structures at the larval apex. It is unclear if, among gastropod veligers, the distinctive apical ciliated cells are a type of sensory neuron (Chia and Koss, 1984; Marois and Carew, 1997a; Kempf *et al.*, 1997; Page and Parries, 2000). Additional work is needed to resolve this issue.

A second complicating factor for comparisons of the apical sensory organ among gastropod larvae derives from differences in life history. For most patellogastropods, fertilization is external, and a trochophore-like larvae hatches from the egg investments after prototrochal cilia have differentiated but before most other components of the veliger larval form have developed (Smith, 1935; Wanninger *et al.*, 1999, 2000; present study). The shell, foot, retractor muscles, and gut emerge rapidly over the course of a relatively short, nonfeeding larval phase. By contrast, the ancestral pattern for the Apogastropoda, which is retained by many extant species, involves internal fertilization and deposition of encapsulated eggs that eventually hatch as feeding veliger larvae with well-formed shell, foot, larval retractor muscle, and gut. After hatching, planktotrophic apogastropod veligers typically undergo further growth and development during a planktonic life lasting weeks or months before metamorphic competence is achieved. Life-history differences between patellogastropods and apogastropods mean that differences in apical organ structure between a single developmental stage from each group may be merely maturational differences in a common developmental program for both.

In an effort to distinguish truly novel features for the apical sensory organ in veliger larvae of *T. scutum* together with features shared with planktotrophic apogastropod veligers, as described in greatest detail by Chia and Koss (1984), Kempf *et al.* (1997), Marois and Carew (1997a), and Page and Parries (2000), I examined a range of larval stages for this patellogastropod. The similarities include a bilateral pair of lateral ciliary tuft cells, neurons clustered over a neuropil to form a simple ganglion, a tripartite distribution of neuronal dendrites extending from the ganglion to the apical surface, and a tripartite distribution of serotonin-immunoreactive neurons with peripheral neurites extending to the base of the ciliated prototrochal cells. Features of the apical sensory organ of *T. scutum* that have not been previously identified among apogastropod veligers include a centrally located tuft of very long apical cilia that is lost early in larval development, the presence of only a single ampullary neuron, and the loss of serotonin immunoreactivity by the medial serotonergic neuron during late larval development. These comparisons are discussed further below.

Apical and lateral ciliary tufts: identifying homologs in other gastropods

Apical ciliary structures in veliger larvae of apogastropods have been difficult to reconcile with the condition in larvae of patellogastropods and of many other molluscan classes, where a long apical tuft of nonmotile cilia is produced by some or all of the apical rosette micromeres of the embryo (see Raven, 1966; van Dongen and Geilenkirchen, 1974; Verdonk and van den Biggelaar, 1983; Dohmen, 1992; Dictus and Damen, 1997). Observations on multiple larval stages of *T. scutum* help to resolve this uncertainty because larvae of this species have both a centrally located, very long apical ciliary tuft as well as two lateral tufts that flank the midline and consist of shorter cilia.

The lateral ciliary tuft cells in *T. scutum* are strikingly similar in both position and morphology to the bilateral multiciliated cells reported previously for planktotrophic opisthobranch larvae (Heterobranchia) (Chia and Koss, 1984; Kempf *et al.*, 1997; Marois and Carew, 1997a). In both groups, the cells have expanded, multiciliated apices and a narrow, stalk-like middle zone that connects with a basal, perinuclear region. The perinuclear regions of the

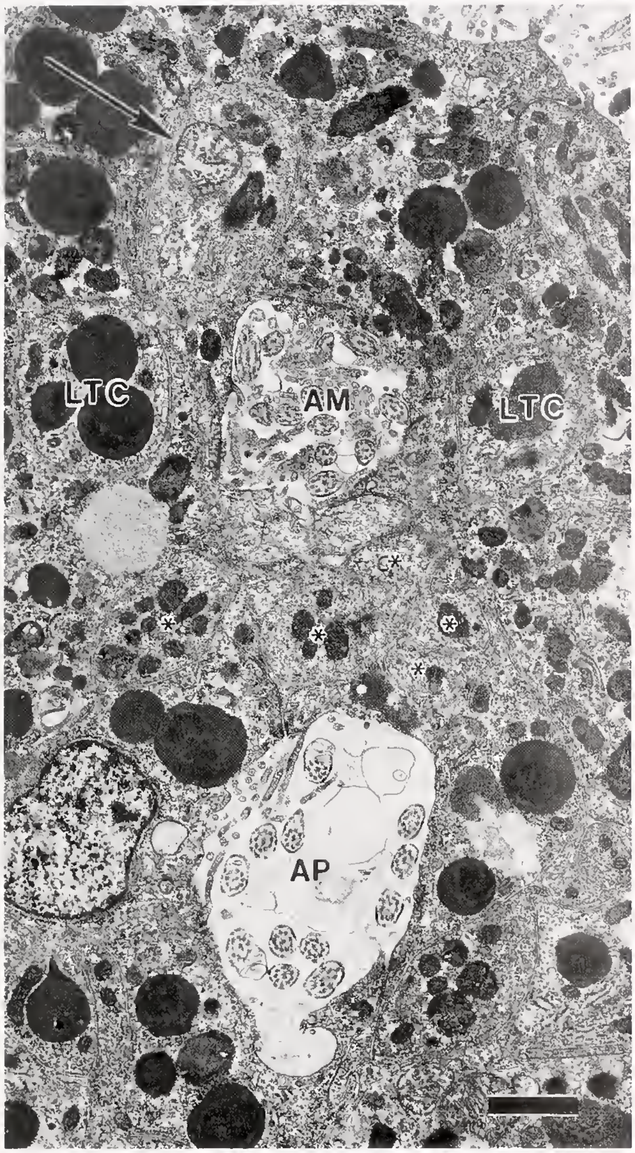

Figure 8. Transmission electron micrograph of a section cut parallel to the apical surface of a *Tectura scutum* larvae at 7 days postfertilization (metamorphic competence). Large arrow indicates dendrite of medial sensory neuron, which persists despite loss of serotonin immunoreactivity at this stage. Asterisks indicate dendrites within dendritic group 2. Scale, 1 μm. Abbreviations: AM, ampullary neuron; AP, apical pit; LTC, lateral ciliary tuft cell.

lateral ciliary tuft cells are intimately associated with neuronal somata along the ventral side of the apical ganglion. Furthermore, the expanded apices of the lateral ciliary tuft cells flank the dendrites of the medial serotonergic neuron and the medial ampullary neuron in planktotrophic veligers of several nudibranch larvae (Kempf *et al.*, 1997) and in veligers of *T. scutum* after disappearance of the three large cells that generate the long, centrally located apical ciliary tuft (Figs. 2B, 4, 5A).

The lateral ciliary tuft cells within the apical epidermis of caenogastropod larvae show fewer similarities to those of *T. scutum* and opisthobranch larvae. In two caenogastropods where lateral ciliary tufts have been identified (*Lacuna vincta* and *Euspira lewisii*; Page and Parries, 2000), the multiciliated cells have a cuboidal shape and are entirely contained within the thickness of the apical epidermis (Page and Parries, 2000). These multiciliated cells lie ventral to the apical ganglion, but they are not intimately associated with any of the neuronal elements of the ganglion.

In Smith's (1935) description of larvae belonging to the patellogastropod *Patella vulgata*, he used the term "refractile bodies" for what are probably the protruding, multiciliated apices of lateral ciliary tuft cells. However, contrary to observations reported here for *T. scutum*, Smith (1935) suggested that the centrally located, long apical tuft of *P. vulgata* (another patellogastropod) persists up to metamorphosis, whereas the flanking ciliated cells (refractile bodies) degenerate early in larval development. This discrepancy between reports on *T. scutum* and *P. vulgata* may represent a real difference between larvae of these two patellogastropods. However, Smith (1935) was restricted to observations using light microscopy; his observations on the fate of apical ciliary structures in *P. vulgata* larvae should be confirmed using electron microscopical techniques.

Larvae of many bivalve species possess a single long apical ciliary tuft that is often lost during later development (Cragg, 1996). Ultrastructural observations by Tardy and Dongard (1993) show that the apical ciliary tuft ("frontal cirri") of the bivalve *Ruditapes philippinarum*, like that of *T. scutum*, is generated by three large apical cells containing very long ciliary rootlets. The apical tuft of *R. philippinarum* persists until metamorphosis.

Results of the present study on *T. scutum*, when combined with previous observations on the apical sensory organ of other gastropods and other molluscs, suggest that a single, centrally placed tuft of very long apical cilia and a bilateral pair of shorter ciliary tufts are both plesiomorphic traits of the apical sensory organ among gastropod veligers. As discussed above, veligers of both basal and derived clades of gastropods appear to possess a bilateral pair of short ciliary tufts. Furthermore, larvae of the most basal clade of gastropods, the Patellogastropoda, together with larvae of many nongastropod molluscs, have a centrally placed tuft of long apical cilia that arises from descendants of the apical rosette micromeres. Under this hypothesis, evolutionary descendants of the apical rosette micromeres in posthatching apogastropod veligers have lost the long apical tuft phenotype. Homologous cells in developing apogastropods may degenerate prior to hatching or may have been co-opted in prehatching stages to serve a derived function associated with encapsulation. Many caenogastropod embryos develop a crown of motile cilia that is lost shortly before or after hatching, and descendants of the apical rosette micromeres may contribute to this ciliary crown (Conklin, 1897; Cather, 1973). Beating of these crown cilia may supplement the beating of prototrochal cilia to help prevent buildup of an anoxic boundary layer around closely packed embryos (Hunter and Vogel, 1986; alternative view given by Strathmann and Strathmann, 1995). This hypothesis about derived states of the apical tuft cells in apogastropod embryos should be explored using cell lineage tracers in conjunction with ultrastructural analysis.

Larval apical ganglion of T. scutum *(Patellogastropoda): comparisons to apogastropods*

Existing information suggests that the apical ganglion of planktotrophic larvae of caenogastropods and opisthobranch members of the Heterobranchia includes neurons with and without an apical dendrite and that the ganglion provides innervation of prototrochal cilia and muscles of the larval velum (Kempf *et al.*, 1997; Marois and Carew, 1997a, c; Page and Parries, 2000; Hadfield *et al.*, 2000; Hay-Schmidt, 2000). Neuronal elements of the apical sensory organ of *T. scutum* are also organized as a simple ganglion, with neuronal somata overlying a neuropil. Many neurons of the apical ganglion in *T. scutum* have a distal dendrite and are presumably sensory, but the possible presence of neurons lacking an apical dendrite was not ascertained for *T. scutum* because neurons without an apical dendrite were not recognized by antibodies against serotonin.

Ampullary neurons represent a morphologically distinctive class of sensory neurons within the apical ganglion of apogastropod larvae and have also been reported in a larval bivalve (Tardy and Dongard, 1993). However, apogastropods have a minimum of four ampullary neurons within the larval apical ganglion (see Chia and Koss, 1984; Marois and Carew, 1997a, c; Kempf *et al.*, 1997; Page and Parries, 2000), whereas larvae of *T. scutum* have only one neuron of this distinctive type. Cilia within the invaginated pocket of ampullary neurons have a 9 + 2 arrangement of axonemal microtubules in veligers of *T. scutum* (present study), which is also true of larval opisthobranchs (Bonar, 1978; Chia and Koss, 1984; Kempf *et al.*, 1997; Marois and Carew, 1997a) and larvae of the bivalve *Rhuditapes philippinarum* (Tardy and Dongard, 1993). The ciliary axonemes of ampullary neurons in caenogastropods show differences from the 9+2 pattern (Uthe, 1995; Page and Parries, 2000).

Dendrites arising from sensory neurons of the apical ganglion in planktotrophic larvae of caenogastropods and opisthobranch heterobranchs are organized into three bundles: a medial bundle and two lateral bundles (Chia and Koss, 1984; Kempf *et al.*, 1997; Marois and Carew, 1997a). This tripartite organization is not readily apparent in pretorsional veligers of *T. scutum*. However, after the three large cells that produce the apical ciliary tuft disappear, the dendritic components in the apical epidermis shift centrally and a three-part disposition of dendrites becomes easier to recognize, when compared to the condition in posthatching opisthobranch veligers. I suggest that dendritic groups 1 and 2 in *T. scutum*, which collectively include the ampullary neuron and medial serotonergic neuron, correspond to the medial dendritic grouping in opisthobranch veligers, which also includes a single ampullary and serotonergic sensory neuron (Kempf *et al.*, 1997; Marois and Carew, 1997a). I further suggest that the dendritic groups 3 and 5 on the left side of the apical pit and groups 4 and 6 on the right side of the apical pit correspond to the left and right lateral dendritic groups within the apical ganglion of opisthobranch veligers. In opisthobranchs (*Aplysia californica* and several nudibranchs) and in *T. scutum*, each lateral group of dendrites includes a single dendrite arising from a serotonergic sensory neuron.

Comparative patterns of serotonin immunoreactive neurons in larval gastropods

Among gastropod larvae studied to date, larvae of *T. scutum* are not unusual in having a tripartite distribution of neurons showing serotonin immunoreactivity (see Marois and Carew, 1997a, b, c; Kempf *et al.*, 1997; Page and Parries, 2000). However, two aspects of the serotonin-immunoreactive neurons in *T. scutum* are unprecedented. First, all three serotonergic neurons within the apical ganglion of *T. scutum* have a distal cytoplasmic extension ("dendrite") that runs to the external surface of the apical epidermis. Therefore, these are all putative sensory neurons. In apogastropod veligers studied to date, at least some of the serotonin-immunoreactive neurons within the apical ganglion lack distal dendrites. Second, one of the three serotonergic neurons in *T. scutum* (the non-ampullary neuron within dendritic group 1) appears to arrest expression of serotonin in metamorphically competent larvae. Nevertheless, the possibility that the medial serotonergic neuron is lost entirely and replaced by a new neuron that lacks serotonin antigenicity cannot be ruled out.

Assuming that neurites of the medial neuron also lose serotonin antigenicity in metamorphically competent larvae (or these neurites are lost entirely), persistence of serotonin immunoreactivity within neurites along the base of the prototrochal ciliary cells implies that the prototrochal neurites originate from the lateral serotonergic neurons of the apical ganglion. If this is the case, then the lateral neurons may function as both sensory and motor neurons. Hay-Schmidt (2000) has speculated that lateral serotonin-immunoreactive neurons within the apical ganglion of diverse spiralian larvae always innervate the larval ciliary band.

A similar case of developmental arrest of neurotransmitter synthesis without destruction of the neuron has been reported by Diefenbach *et al.* (1998) for a pair of apically located sensory neurons (ENC1) within encapsulated embryos of the pulmonate *Helisoma trivolvis* (Heterobranchia). This species lacks a free-living larval stage, and development is highly modified relative to heterobranchs with a planktotrophic larva. Early expression of serotonin immunoreactivity by the ENC1 neuronal pair is lost during later embryogenesis.

Transient expression of serotonin by an apical ganglion neuron in *T. scutum* may occur because of ontogenetic change in a larval behavior, possibly associated with settlement and metamorphosis, which removes the functional requirement for this neurotransmitter. Hadfield *et al.* (2000) have recently described evidence for apical ganglion involvement in reception of the metamorphic cue in an opisthobranch. However, a second possibility relates to the established role of serotonin in regulating aspects of molluscan neurogenesis (Haydon *et al.*, 1984, 1987; Murrain *et al.*, 1990; Zhu *et al.*, 1994; Diefenbach *et al.*, 1995). Temporary developmental expression of serotonin by an apical ganglion neuron might reflect a transient role for this transmitter in establishing neurite trajectories or neurite branching patterns within the larval or prospective, postmetamorphic nervous system. The notion that neurites extending from the apical ganglion may help organize later formed components of the nervous system has been suggested previously by Lacalli (1981, 1984), on the basis of studies of several species of polychaete trochophores.

Acknowledgments

I am grateful to Dr. M. G. Hadfield, University of Hawaii, for advice about the spawning behavior of *Tectura scutum*. This work was supported by a research grant from the Natural Sciences and Engineering Research Council of Canada.

Literature Cited

Bonar, D. B. 1978. Ultrastructure of a cephalic sensory organ in larvae of the gastropod *Phestilla sibogae* (Aeolidacea, Nudibranchia). *Tissue Cell* **10:** 153–165.

Bonar, D. B., and M. G. Hadfield. 1974. Metamorphosis of the marine gastropod *Phestilla sibogae* Bergh (Nudibranchia: Aeolidacea). I. Light and electron microscopic analysis of larval and metamorphic stages. *J. Exp. Mar. Biol. Ecol.* **16:** 227–255.

Camey, T., and N. H. Verdonk. 1970. The early development of the snail *Biomphalaria glabrata* (Say) and the origin of the head organs. *Neth. J. Zool.* **20:** 93–121.

Cather, J. N. 1973. Regulation of apical cilia development by the polar lobe of *Ilyanassa* (Gastropoda: Nassariidae). *Malacologia* **12:** 213–223.

Chia, F. S., and R. Koss. 1984. Fine structure of the cephalic sensory organ in the larva of the nudibranch *Rostanga pulchra* (Mollusca, Opisthobranchia, Nudibranchia). *Zoomorphology* **104:** 131–139.

Conklin, E. G. 1897. The embryology of *Crepidula*. *J. Morphol.* **13:** 1–226.

Cragg, S. M. 1996. The phylogenetic significance of some anatomical features of bivalve veliger larvae. Pp. 91–121 in *Origin and Evolutionary Radiation of the Mollusca*, J. D. Taylor, ed. Oxford University Press, Oxford.

Dictus, W. J. A. G., and P. Damen. 1997. Cell-lineage and clonal-contribution map of the trochophore larva of *Patella vulgata* (Mollusca). *Mech. Dev.* **62:** 213–226.

Diefenbach, T. J., B. D. Sloley, and J. I. Goldberg. 1995. Neurite branch development of an identified serotonergic neuron from embryonic *Helisoma*: evidence for autoregulation by serotonin. *Dev. Biol.* **167:** 282–293.

Diefenbach, T. J., R. Koss, and J. I. Goldberg. 1998. Early development of an identified serotonergic neuron in *Helisoma trivolvis* embryos: serotonin expression, de-expression, and uptake. *J. Neurobiol.* **34:** 361–376.

Dohmen, M. R. 1992. Cell lineage in molluscan development. *Microsc. Res. Tech.* **22:** 75–102.

Hadfield, M. G., E. A. Meleshkevitch, and D. Y. Boudko. 2000. The apical sensory organ of a gastropod veliger is a receptor for settlement cues. *Biol. Bull.* **198:** 67–76.

Haszprunar, G. 1988. On the origin and evolution of major gastropod groups, with special reference to the Streptoneura. *J. Molluscan Stud.* **54:** 367–441.

Hay-Schmidt, A. 2000. The evolution of the serotonergic nervous system. *Proc. R. Soc. Lond. B* **267:** 1071–1079.

Hayat, M. A. 1970. *Principles and Techniques of Electron Microscopy*, vol. 1. Van Nostrand Reinhold, New York. P. 341.

Haydon, P. G., D. P. McCobb, and S. B. Kater. 1984. Serotonin selectively inhibits growth cone motility and synaptogenesis of specific identified neurons. *Science* **226:** 561–564.

Haydon, P. G., D. P. McCobb, and S. B. Kater. 1987. The regulation of neurite outgrowth, growth cone motility, and electrical synaptogenesis by serotonin. *J. Neurobiol.* **18:** 197–215.

Hunter, T., and S. Vogel. 1986. Spinning embryos enhance diffusion through gelatinous egg masses. *J. Exp. Mar. Biol. Ecol.* **96:** 303–308.

Kempf, S. C., L. R. Page, and A. Pires. 1997. Development of serotonin-like immunoreactivity in the embryos and larvae of nudibranch mollusks with emphasis on the structure and possible function of the apical sensory organ. *J. Comp. Neurol.* **386:** 507–528.

Lacalli, T. C. 1981. Structure and development of the apical organ in trochophores of *Spirobranchus polycerus*, *Phyllodoce maculata* and *Phyllodoce mucosa* (Polychaeta). *Proc. R. Soc. Lond. B* **212:** 381–402.

Lacalli, T. C. 1984. Structure and organization of the nervous system in the trochophore larva of *Spirobranchus*. *Philos. Trans. R. Soc. Lond. B* **306:** 79–135.

Marois, R., and T. J. Carew. 1997a. Fine structure of the apical ganglion and its serotonergic cells in the larva of *Aplysia californica*. *Biol. Bull.* **192:** 388–398.

Marois, R., and T. J. Carew. 1997b. Ontogeny of serotonergic neurons in *Aplysia californica*. *J. Comp. Neurol.* **386:** 477–490.

Marois, R., and T. J. Carew. 1997c. Projection patterns and target tissues of the serotonergic cells in larval *Aplysia californica*. *J. Comp. Neurol.* **386:** 491–506.

Murrain, M., A. D. Murphy, L. R. Mills, and S. B. Kater. 1990. Neuron-specific modulation by serotonin of regenerative outgrowth and intracellular calcium within the CNS of *Helisoma trivolvis*. *J. Neurobiol.* **21:** 611–618.

Nielsen, C. 1995. *Animal Evolution: Interrelations of Living Phyla*. Oxford University Press, Oxford.

Page, L. R., and S. C. Parries. 2000. Comparative study of the apical ganglion in planktotrophic caenogastropod larvae: ultrastructure and immunoreactivity to serotonin. *J. Comp. Neurol.* **418:** 383–401.

Ponder, W. F., and D. R. Lindberg. 1997. Toward a phylogeny of gastropod mollusks: an analysis using morphological characters. *Zool. J. Linn. Soc.* **119:** 83–265.

Raven, C. P. 1966. *Morphogenesis: the Analysis of Molluscan Development*, 2nd ed. Pergamon Press, Oxford.

Richardson, K. C., L. Jarrett, and E. H. Finke. 1960. Embedding in epoxy resins for ultrathin sectioning in electron microsopy. *Stain Technol.* **35:** 313–323.

Smith, F. G. W. 1935. The development of *Patella vulgata. Philos. Trans. R. Soc. Lond. B* **225:** 95–125.

Strathmann, R. R., and M. R. Strathmann. 1995. Oxygen supply and limits on aggregation of embryos. *J. Mar. Biol. Assoc. UK.* **75:** 413–428.

Tardy, J., and S. Dongard. 1993. Le complexe apical de la véligère de *Ruditapes philippinarum* (Adams et Reeve, 1850) Mollusque Bivalve Vénéride. *C.R. Acad. Sci. Paris Ser. III* **316:** 177–184.

Uthe, D. 1995. Fine structure of the cephalic sensory organ in veliger larvae of *Littorina littorea* (L.) (Mesogastropoda, Littorinidae). *Hydrobiologia* **309:** 45–52.

van Dongen, C. A. M., and W. L. M. Geilenkirchen. 1974. The development of *Dentalium* with special reference to the significance of the polar lobe. Division chronology and development of the cell pattern in *Dentalium dentale* (Scaphopoda). *Proc. K. Ned. Akad. Wet. Ser. C* **77:** 57–100.

Verdonk, N. H., and J. A. M. van den Biggelaar. 1983. Early development and the formation of the germ layers. Pp. 91–121 in *The Mollusca, Vol. 3, Development*, N. H. Verdonk, J. A. M. van den Biggelaar, and A. S. Tompa, eds. Academic Press, New York.

Wanninger, A., B. Ruthensteiner, S. Lobenwein, W. Salvenmoser, W. J. A. G. Dictus, and G. Haszprunar. 1999. Development of the musculature in the limpet *Patella* (Mollusca, Patellogastropoda). *Dev. Genes Evol.* **209:** 226–238.

Wanninger, A., B. Ruthensteiner, and G. Haszprunar. 2000. Torsion in *Patella caerulea* (Mollusca, Patellogastropoda): ontogenetic process, timing, and mechanisms. *Invertebr. Biol.* **119:** 177–187.

Zhu, H., F. Wu, and S. Schacher. 1994. *Aplysia* cell adhesion molecules and serotonin regulate sensory cell-motor cell interactions during early stages of synapse formation *in vitro. J. Neurosci.* **14:** 6886–6900.

Reference: *Biol. Bull.* **202:** 23–33. (February 2002)

Localization and Quantification of Gonad Serotonin During Gametogenesis of the Surf Clam, *Spisula solidissima*

ISABELLE MASSEAU[1,2], PIERRE BANNON[2], MICHEL ANCTIL[1], AND FRANÇOIS DUBÉ[2,*]

[1]*Département des sciences biologiques, Université de Montréal, Montréal, Québec, Canada H3C 3J7; and* [2]*Département d'Obstétrique-Gynécologie, Université de Montréal, Centre de recherche du CHUM, Hôpital Saint-Luc, Montréal, Québec, Canada H2X 1P1*

Abstract. In the surf clam, *Spisula solidissima*, serotonin was reported to induce spawning when injected into the gonads. At nanomolar concentrations, it facilitates the fertilizability of oocyte by sperm, at micromolar concentration, it triggers the meiotic maturation of prophase 1-arrested oocytes, thus mimicking the effect of sperm. To further understand the role of serotonin in the gametogenic and spawning processes, we used both immunohistochemistry and high-pressure liquid chromatography linked with electrochemical detection to detect serotonin in the gonads of the surf clam. We found serotonin-containing varicose fibers covering the surface of the germinal epithelium in both sexes. The area occupied by the serotonergic innervation field encircling gonad acini varied according to the gonadal stages (active phase, ripe phase, partially spawned phase, spent phase). We also found large variations in the serotonin concentration between specimens during the gametogenic cycle. The serotonin concentration was correlated with gonad growth: it decreased in the ripe phase in comparison with the previous phase, the active phase. We attribute the decrease to the increase of total gonad mass in this stage. In contrast, as spawning begins, the total gonad mass declines while the gonad serotonin concentration increases to a level similar to that found in active phase. The finding that prior to spawning, serotonin is present in the gonads within fibers exhibiting distinct varicosities suggests that it is implicated in spawning.

Introduction

Serotonin (5-hydroxytryptamine, 5-HT) has been implicated in the spawning process of bivalve molluscs since the pioneer work of Matsutani and Nomura (1982), who first reported that serotonin induces the release of gametes in the scallop *Patinopecten yessoensis*. Subsequently, serotonin was found to trigger spawning in several other pelecypods such as the bay scallop *Argopecten irradians*, the hard clam *Mercenaria mercenaria*, the ocean quahog *Arctica islandica*, the ribbed mussel *Geukensia demissa* (Gibbons and Castagna, 1984), the zebra mussel *Dreissena polymorpha* (Ram *et al.*, 1992), the doughboy scallop *Chlamys asperrima* (O'Connor and Heasman, 1995), the pismo clam *Tivela stultorum* (Alvarado-Alvarez *et al.*, 1996), the hen clam *Mactra chinensis* (Fong *et al.*, 1996), and particularly the surf clam, *Spisula solidissima* (Gibbons and Castagna, 1984; Hirai *et al.*, 1988). In this latter species (*Spisula solidissima*), serotonin, at high concentration (1–10 μM), also reinitiates the meiotic maturation of isolated prophase 1-arrested oocytes (Hirai *et al.*, 1988), whereas at lower concentration (<500 nM) it enhances the fertilizability of oocytes by sperm (Juneja *et al.*, 1993; Clotteau and Dubé, unpubl. data). This suggests that serotonin might be present in the gonad, where it would play a physiological role during the spawning process. Furthermore, this hypothesis is supported by radioligand binding studies revealing the presence of a new subtype of serotonin receptor on *Spisula* oocytes (Krantic *et al.*, 1991, 1993). In agreement with the possibility that endogenous serotonin is a central neurochemical involved in surf clam reproduction, its presence in the animal's central nervous system (CNS) was reported long ago (Welsh and Moorhead, 1960), and a serotonin-like

Received 11 May 2001; accepted 21 November 2001.

* To whom correspondence should be addressed. E-mail: francois.dube@umontreal.ca

substance was detected in its body fluids (Kadam and Koide, 1989). However, to date, no studies have reported the presence of serotonin in surf clam gonads.

In other molluscs, immunohistochemical and biochemical studies report that serotonin is present in the ganglia of *Mytilus edulis* (Welsh and Moorhead, 1960; York and Twarog, 1973; Stefano and Catapane, 1977), *Artica islandica, Venus mercenaria, Ensis directus, Mya arenaria* (Welsh and Moorhead, 1960), and *Mytilus galloprovincialis* (Vitellaro-Zuccarello *et al.*, 1991). In other species, serotonin was detected both in ganglia and gonads of *Patinopecten yessoensis* (Matsutani and Nomura, 1986), *Dreissena polymorpha* (Ram *et al.*, 1992), *Pecten maximus* (Paulet *et al.*, 1993), *Argopecten purpuratus* (Martinez and Rivera, 1994; Martinez *et al.*, 1996), and *Placopecten magellanicus* (Croll *et al.*, 1995; Pani and Croll, 1995). Therefore, it has been suggested that serotonin would be axonally transported from the CNS towards the gonads, where several serotonin-immunoreactive fiberlike projections have been observed surrounding male and female acini (Matsutani and Nomura, 1986; Ram *et al.*, 1992; Paulet *et al.*, 1993; Croll *et al.*, 1995). On the other hand, Ram *et al.* (1993) observed that female responsiveness (spawning) to serotonin varies during the gametogenic cycle of zebra mussels. In those experiments, serotonin failed to induce spawning of ripe females, even though—a few weeks later—those same ripe females (or even less mature ones) might spawn upon injection of serotonin. These results suggest that endogenous serotonin might be modified in the gonad, prior to spawning (Ram *et al.*, 1993). Variations in serotonin localization have been described in the scallop *Placopecten magellanicus*, in which serotonin-immunoreactive fibers were abundant surrounding gonad acini only a few weeks subsequent to spawning, whereas in spring, before spawning, they were only occasionally detected around the germinal acini (Croll *et al.*, 1995). Furthermore, in the ganglia of *Mytilus edulis* and the scallop *Pecten maximus* and in both the ganglia and the gonads of the hermaphrodite *Argopecten purpuratus*, variations of serotonin content correlated with modifications occurring during the gametogenic cycle (York and Twarog, 1973; Stefano and Catapane, 1977; Paulet *et al.*, 1993; Martinez and Rivera, 1994).

The precise involvement of serotonin in the control of spawning in bivalves remains unclear. The surf clam, *Spisula solidissima*, offers a good model for studying how serotonin is implicated in spawning, since the effects of exogenous serotonin on its spawning (Gibbons and Castagna, 1984), oocyte maturation (Hirai *et al.*, 1988), and fertilizability (Juneja *et al.*, 1993) are well documented. In addition, this species has a well-known gametogenic cycle that has been described extensively by Ropes (1968). Finally, this pelecypod is dioecious, allowing both sexes to be studied individually.

The purpose of this study was to determine whether serotonin is present in the gonads of *S. solidissima* and to localize and quantify it through the gametogenic cycle. The distribution of serotonin in surf clam gonads was determined by immunohistochemistry and by high-pressure liquid chromatography with electrochemical detection (HPLC/ED). The results indicate the presence of serotonin within fiberlike projections that surround both male and female germinal acini. These serotonin-containing fibers are present throughout the gametogenic cycle, which—despite some variations in their distribution and in gonad serotonin concentration during this period—indicates that serotonin might be involved extensively throughout the gametogenic cycle of the surf clam.

Materials and Methods

Handling of specimens

Surf clams (*Spisula solidissima*, 80–100 mm) were collected at Iles-de-la-Madeleine (Québec, Canada) from April to September and shipped to the Centre Hospitalier de l'Université de Montréal (Montréal, Canada) where they were kept in an aquarium at 8 °C. Surf clams were used within 2 days for both immunolocalization and quantification of serotonin assessed in gonads from 69 collected animals.

Immunohistochemistry

Pieces of gonad were excised and fixed overnight at 4 °C in a solution of 4% paraformaldehyde in 0.1 *M* phosphate buffer (pH 7.4) containing 2.4% NaCl. They were washed thrice, 15 min each, in phosphate buffered saline (PBS), and transferred to a solution of 15% sucrose in PBS for 20 min in preparation for subsequent freezing. They were then immersed in PBS containing 30% sucrose until gonadal tissues settled on the bottom of the dish. Specimens were embedded with O.C.T. compound (Miles), frozen in chilled 2-methyl butane, and stored at −80 °C until used. Cryostat sections, about 30 μm in thickness, were placed alternately on different glass slides coated with 1 mg/ml L-polylysine (Sigma) for dual procedures of immunohistochemistry and histology.

After they were left to dry for 2 h, tissue sections were given three 15-min washes in PBS at room temperature. They were incubated in 1% normal goat serum (Jackson ImmunoResearch Laboratory) containing 0.3% Triton X-100 in PBS for 20 min. This was followed by incubation with a rabbit anti-serotonin antibody (Incstar, diluted 1:1750) and 0.2% Triton X-100 in PBS for 20–24 h at 4 °C. After three rinses, of 15 min each, in PBS, the tissue sections were incubated with Cy3-conjugated goat anti-rabbit IgG (Jackson ImmunoResearch, diluted 1:100 in PBS) for 1 h at room temperature. All subsequent procedures were performed at room temperature. After another rinse in PBS, sections were incubated, for 1 h, with 1 μg/ml Hoechst 33258 (Sigma) for DNA staining. They were again washed three times, 10 min each, in PBS. Sections were mounted with Aquamount. Preparations were viewed and photographed using a Leitz Dialux EB epifluorescence microscope with two filter sets: for 5-HT detection, an excitation filter of 515–560 nm and an emission filter of 580 nm; for Hoechst detection, an excitation filter of 340–380 nm and an emission filter of 430 nm. The specificity of the anti-serotonin antibody was assessed by pre-absorbing 1 ml of diluted antibody with 200 μg of serotonin/bovine serum albumin conjugate (Incstar) over 16–24 h with gentle agitation at 4 °C.

To determine the gonadal stages of surf clams, frozen tissue sections on gelatin-coated slides were processed for standard hematoxylin and eosin staining. Sections were then viewed using a Zeiss Axiomat microscope, and the four gonadal stages as defined by Ropes (1968)—active phase, ripe phase, partially spawned phase, and spent phase—were determined (for more details see Results section). Light photomicrographs (shown in Fig. 1) were taken from standard hematoxylin-and-eosin-stained paraffin gonad sections of 10 μm in thickness that came from the entire visceral mass preserved in Bouin's fixative.

Measurement of serotonin content

After small portions of gonadal tissues were collected for immunohistochemistry, the serotonin content of the remaining gonad was measured by HPLC. Some gonads were cut in half prior to further processing. After dissection, gonads or gonad halves were individually put in preweighed Eppendorf tubes containing 0.6–1.0 ml of ice-cold 0.1 *N* perchloric acid, weighed again, and homogenized with a Kinematica polytron. The homogenate was centrifuged at 16,000 × *g* for 15 min at 4 °C, and the supernatant was stored at −80 °C until processed. As a measure of serotonin recovery, a known amount of serotonin creatinine sulfate (Sigma) was added to half-gonad specimens, and the results were compared with the values for the matching halves that received no exogenous serotonin.

The HPLC system consisted of a Waters pump (model 590), equipped with a Waters automatic injection system (model 710B). A Waters M460 electrochemical detector with a potential of +0.85V applied across the electrode was used for amine detection. Chromatographic separations were carried out on a Supelcosil LC-18-DB reverse-phase column (Supelco, 150 × 4.6 mm i.d.) packed with 5-μm particles and equipped with a guard column (Supelguard LC-18-DB, 20 × 4.6 mm i.d.). Both columns were maintained at 40 °C while the rest of the system was run at ambient temperature (22 °C).

The mobile phase consisted of 300 m*M* phosphate buffer containing 4 m*M* 1-heptane sulfonic acid (Sigma), 0.2 g/l Na_2 EDTA (Fisher), and 5% acetonitrile (Baxter, Burdick and Jackson). The pH was adjusted to 2.5 with 85% *o*-phosphoric acid (Fisher). This solution was prepared with distilled and deionized water and purified by a Norganic cartridge (Millipore) to remove any organic substances. The mobile phase was filtered through Millipore membrane filters of 0.45-μm porosity under vacuum. The mobile phase was degassed with helium and pumped at a rate of 1.3 ml/min, producing a background pressure of about 1000 psi. All reagent chemicals used were of HPLC grade.

The stock solutions of serotonin, 5-hydroxytryptophan, dopamine, and of the internal standard 3,4-dihydroxybenzylamine (DHBA), all from Fisher Scientific, were prepared in 0.1 *N* perchloric acid at a concentration of 1 m*M* and stored at 4 °C. The working standard solutions were prepared by diluting the stock solutions in 0.1 *N* perchloric acid. The standard retention times were 3.3 min for DHBA and 10.3 min for serotonin.

For each run, three serotonin and DHBA standards were processed to identify their retention times and confirm the serotonin elution peak from samples. This was followed by extracts containing the same amount of the DHBA standard. In all cases, 25 μl of samples and standards were injected in the column. The signal from the electrochemical detector was fed directly to a Waters data module 740 acquisition system. The serotonin content was determined by comparing serotonin/DHBA peak height ratios of unknown sample chromatograms with those of chromatograms from serotonin standards.

Statistical procedures

The data (nanograms of serotonin per gram of gonad wet weight) of combined male and female surf clams were tested for normality ($P < 0.01$) and heteroscedasticity ($P < 0.001$). Since data were not normally distributed, and because of the small sample size, a nonparametric test was used. No such test exists for two-way analysis of variance (ANOVA). Therefore, all data were rank-transformed before computing a two-way ANOVA (Shirley, 1987). Pairwise comparisons were done using the Student-Newman-Keuls test. The accepted level of statistical significance was $P < 0.05$.

Next, female and male gonad serotonin concentrations (ng/g of gonad wet weight) were analyzed separately. As for the combined data, they were both tested for normality (female: $P > 0.05$; male: $P < 0.01$) and heteroscedasticity (female: $P < 0.001$ male: $P > 0.05$). Since data from each sex were not normally distributed and comparison with combined data was necessary, all data were rank-transformed, and a one-way ANOVA was performed for each sex. Pairwise comparisons were done using the Student-

Newman-Keuls test. The accepted level of statistical significance was $P < 0.05$.

The same statistical procedures were used for the analysis of gonad wet weight (g) of combined female and male surf clams. A two-way ANOVA was performed on rank-transformed data since they were not normally distributed (normality: $P > 0.01$ and heteroscedasticity: $P < 0.001$) and because of the small sample size. Subsequently, a one-way ANOVA was done on rank-transformed data from each sex separately since they were not normally distributed (normality: female, $P < 0.01$; male, $P > 0.2$; heteroscedasticity: female, $P < 0.01$; male, $P < 0.01$). Pairwise comparisons were performed as above.

Results

Surf clams used for immunohistochemistry and HPLC were first examined to determine their gonadal stages. As shown in Figure 1, we used specimens of every stage of the gametogenic cycle. Males in active phase (stage 1) of their gametogenic cycle are easily distinguishable by the granular aspect of their acini (Fig. 1A). In this phase, spermatogonia proliferate from alveolar walls, and early spermatocytes begin to occupy the lumen of acini, forming radial columns. In the ripe phase (stage 2), acini exhibit, instead of a granular aspect, a braided shape as a result of sperm tails orienting toward the lumen of acini (Fig. 1B). When a lumen appears in the center of acini with some sperm tails still visible, spawning has begun and specimens are classified as partially spawned males (stage 3, Fig. 1C). At the end of the gametogenic cycle, when males have released all of their gametes, acini are almost devoid of mature cells, with some spermatogonia proliferating in alveolar walls (stage 4, Fig. 1D). The female gametogenic cycle follows almost the same pattern as the male. In females in active phase (stage 1), oogonia and early oocytes appear in the periphery of acini, the latter being attached to the wall by a stalk (Fig. 1E). Afterwards, ripe females (stage 2) are easily recognizable by their large mature oocytes filling the lumen space of acini and by their thin alveolar wall (Fig. 1F). When spawning has begun, less mature oocytes are observed in the lumen of acini (stage 3, Fig. 1G). Finally, females in the last phase (stage 4) of their gametogenic cycle have already released almost all ripe oocytes, and oogenesis has already begun in the alveolar walls (Fig 1H).

Serotonin content

The specimens identified by their gametogenic stage were used to measure gonad serotonin content by HPLC/ED. This analysis revealed the presence of a compound co-eluting with serotonin. The chromatogram in Figure 2 illustrates the serotonin elution peak for both the standard and a typical sample. From around 10.3 min of elution time onward, the serotonin elution peak is the only one present in all gonad extracts tested. We also found traces of compounds co-eluting with dopamine and 5-hydroxytryptophan in most of the gonad extracts (not shown). Small elution peaks of unknown origin were common in the extract chromatograms.

Serotonin was detected in all gonad extracts tested. We found large variations in gonad serotonin content among specimens, from 7.5 to 2117 ng/g of gonad (wet weight). To determine if these fluctuations were related to sex or gonadal stage, we used a two-way ANOVA on data transformed on ranks. We found that these variations of gonad serotonin concentration (ng/g) are observed in both male and female gonads and that for each gonadal stage serotonin concentrations were not significantly different between males and females. Since no difference between sexes was found, we tested the hypothesis that the variations in serotonin concentration might be related to the gametogenic stage of the gonad. Analysis of data from combined sexes revealed a significant difference ($P < 0.002$) of serotonin concentration (ng/g) between the different gonadal stages. In fact, all pairwise multiple comparisons (Student-Newman-Keuls Method) indicate that the serotonin concentration in ripe phase (stage 2) differs greatly from the concentrations in the active (stage 1, $P < 0.01$) and spent phases (stage 4, $P < 0.01$, Fig. 3). A high gonad serotonin concentration is seen in active phase (stage 1), followed by an abrupt decline in ripe phase (stage 2), just before spawning. The gonad serotonin concentration seems to increase again after spawning (stage 3), but this increase is not statistically significant (Fig. 3). A significantly higher gonad serotonin concentration is reached only when gametes have all been expelled from clams in the spent phase (stage 4, Fig. 3). Next, female and male clams were considered separately using one-way ANOVA with rank-transformed data to test whether the relationship between the gonadal stage and the serotonin concentration was similar in both sexes. For female clams, a significant difference in serotonin concentrations ($P < 0.002$) between the gonadal stages (Fig. 4) mirrors observations with sexes combined (Fig. 3). In contrast, no significant difference emerged from analysis of male gonad serotonin concentrations (Fig. 4).

Another two-way ANOVA was performed to determine if the significant relation between gonadal stage and serotonin concentration was associated with variations of gonad weight during the gametogenic cycle. When the average total gonad weights were analyzed, no significant differences were noted between sexes, regardless of whether all specimens were combined or those from a specific gonadal stage were considered. In contrast, a significant difference ($P < 0.001$) was noted when the total gonad weights, both sexes combined, were compared for each gonadal stage (Fig. 5). All pairwise multiple comparisons (Student-Newman-Keuls Method) indicate that gonad weight increases significantly as the clams ripen between the active phase

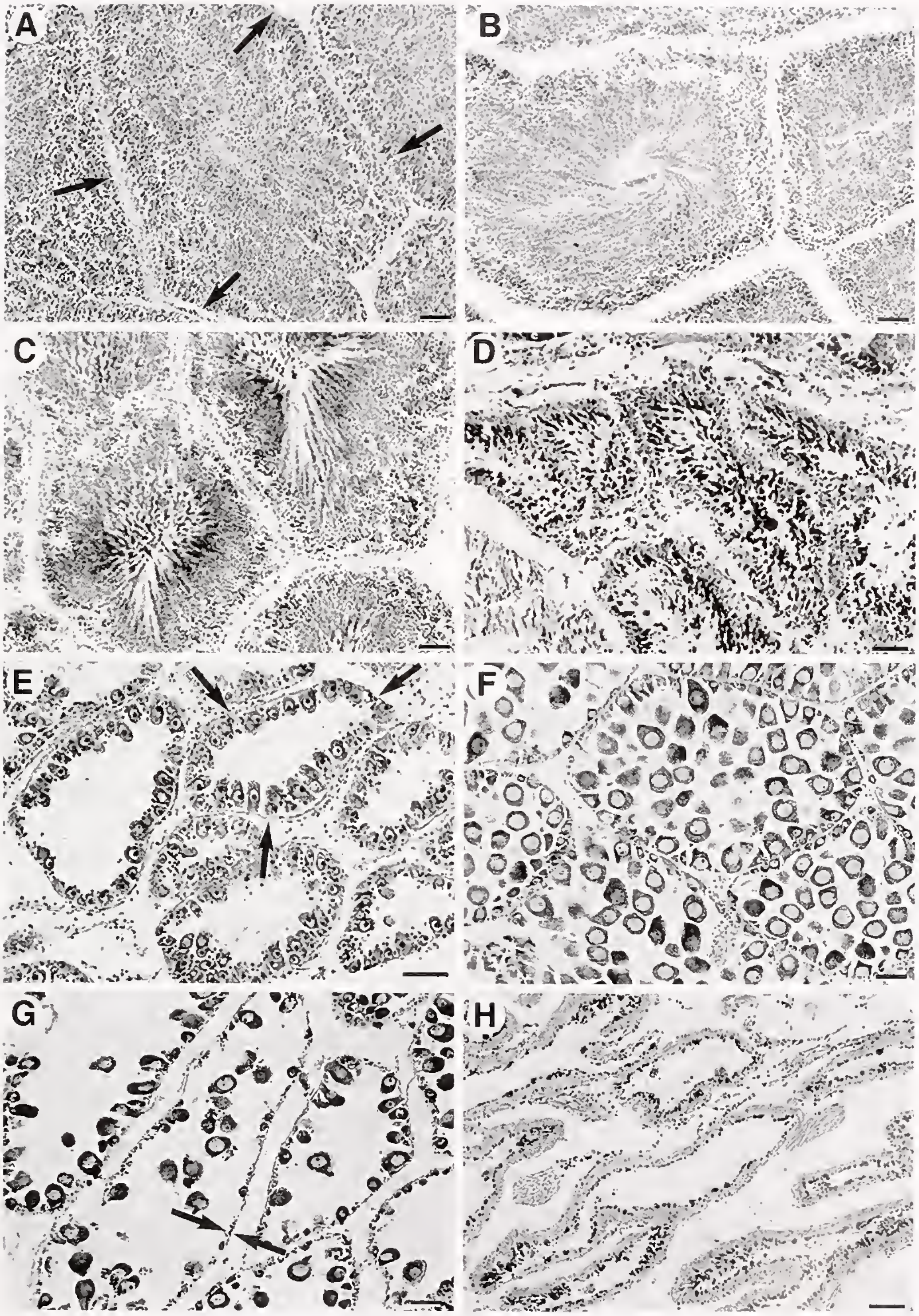

Figure 1. Sections of gonads at the different stages of surf clam gametogenic cycle: A-D, males; E-H, females. The various stages depicted are active phase (stage 1; A, E), ripe phase (stage 2; B, F), partially spawned phase (stage 3; C, G), and spent phase (stage 4; D, H). Note typical male (A) and female (E) acini that are surrounded by arrows. Also, note the thin alveolar wall (*between arrows*) in female partially spawned phase (G). Scale bars: 100 μm.

(stage 1) and the ripe phase (stage 2, $P < 0.001$, Fig. 5). This is followed by an apparent, but statistically insignificant, decrease as the clams begin to spawn (stage 3, Fig. 5). When the clams have released all their gametes, a significant decrease is noted between the ripe phase (stage 2) or the partially spawned phase (stage 3) and the spent phase

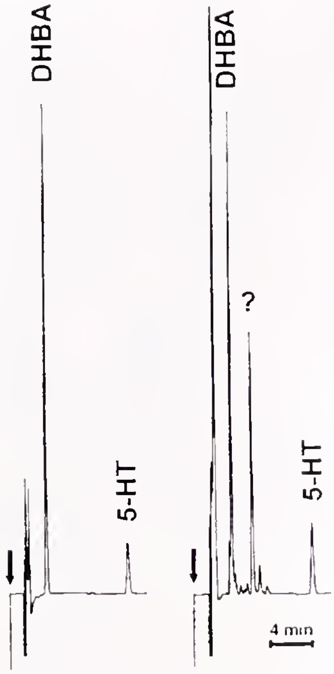

Figure 2. HPLC-ED detection of serotonin in surf clam tissue extracts. Left trace: Detection of standards following injection (*arrow*) of 4.4 ng of serotonin (5-HT) and 3.5 ng of 3,4-dihydroxybenzylamine (DHBA). Right trace: Chromatogram of surf clam gonad extract run consecutively to the standard. DHBA was used as an internal standard (see Materials and Methods). Note in the right trace that an unidentified peak (?) is shown that does not correspond to any other serotonin-related or catecholaminergic compounds tested, *e.g.*, 5-hydroxy-3-indoleacetic acid, *N*-acetyl-serotonin, epinephrine, norepinephrine.

(stage 4, $P < 0.001$, Fig. 5). Using one-way ANOVA on ranked data, we found the same relation between gonad weight and gonadal stage in males and females analyzed separately (not shown).

Localization of serotonin immunoreactivity

In agreement with the detection of serotonin in gonads by HPLC/ED, serotonin-immunoreactive (5-HT-IR) fibers were detected in surf clam gonads of both sexes. Control sections (treated as described in Materials and Methods) were devoid of any staining in gonads (not shown). 5-HT-IR fibers were observed in specimens from all gametogenic stages. Transverse sections of acini show 5-HT-IR fibers located at the periphery of each acinus, with variations in their distribution among the gametogenic stages as shown for females (Figs. 6 and 7). Thus, in active-phase females (Fig. 6A), 5-HT-IR fibers surrounded each acinus, where they formed a thin discontinuous innervation field. At low magnification, little difference in 5-HT-IR staining was apparent between active-phase and ripe-phase females (Fig. 6A, B), even though the alveolar wall was much thicker in the former (compare Fig. 7A and B). However, in ripe females, the staining around acini was more frequently interrupted (Fig. 6B), and it was concentrated in varicosities within 5-HT-IR fibers (Fig. 7B). It was also noted that staining was observed neither on or in oocytes present in gonad sections (Fig. 7B) nor in isolated oocytes (not shown). In the subsequent stage, when spawning had begun and acini contained fewer ripe oocytes in their lumen, different patterns of 5-HT-IR fibers could be seen (Figs. 6C,

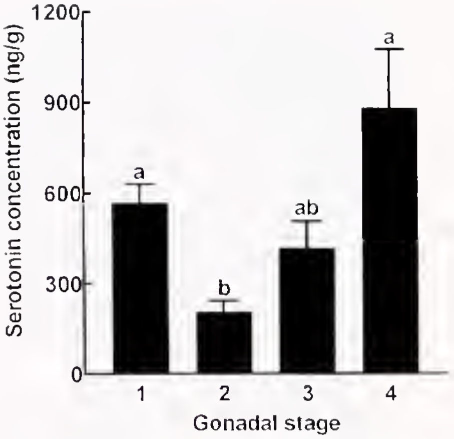

Figure 3. Average serotonin concentration in surf clam gonads during the gametogenic cycle. Data from both sexes are combined. The gametogenic cycle was divided into four stages: (1) active phase, (2) ripe phase, (3) partially spawned phase, and (4) spent phase. The letters a and b indicate relationships among the stages. The two stages (1 and 4) marked "a" are not different from each other, but they are significantly different from the stage (2) marked "b". The stage (3) marked "ab" is not significantly different from any of the three other stages. Vertical error bars correspond to the standard error of the means (SEM).

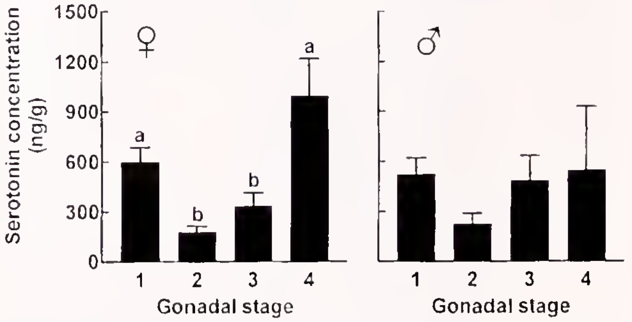

Figure 4. Average serotonin concentration in surf clam gonads during female and male gametogenic cycle. The gametogenic cycle was divided into four stages: (1) active phase, (2) ripe phase, (3) partially spawned phase, and (4) spent phase, for both females (♀) and males (♂). The only significant differences were found in females between gonadal stages 1 and 2, 1 and 3, 2 and 4, and 3 and 4. The letters a and b indicate relationships among the stages. The two stages marked "a" are not different from each other, but they are significantly different from the other two stages marked "b". In males, none of the stages were significantly different one from another. Vertical error bars correspond to the standard error of the means (SEM).

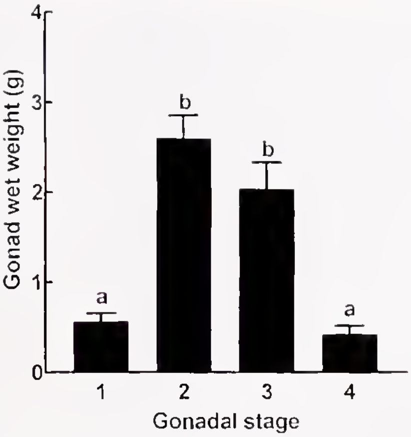

Figure 5. Average gonad wet weight in surf clam gonads during the gametogenic cycle. Data from both sexes are combined. The gametogenic cycle was divided into four stages: (1) active phase, (2) ripe phase, (3) partially spawned phase, and (4) spent phase. The letters a and b indicate relationships among the stages. The two stages (1 and 4) marked "a" are not different from each other, but they are significantly different from the other two stages (2 and 3) marked "b". Vertical error bars correspond to the standard error of the means (SEM).

7C). Staining depended on the spawning condition of the acinus. Acini that were still full of oocytes showed the same immunoreactive staining as ripe females (Fig. 6C), whereas acini that had begun to expel some oocytes showed an uninterrupted staining all around the acinus (Fig. 7C). Also, in contrast to ripe-stage gonads exhibiting generally a single 5-HT-IR fiber running parallel to the acinus (Fig. 7B), acini devoid of most of their oocytes in partially spawned gonads had more numerous fibers in diverse orientations (Fig. 7C). As the spent phase was reached, almost all mature oocytes have been expelled, and gonadal tissues began to disrupt. At this stage, some acini remained recognizable, whereas others were completely disrupted or apparently shrunken (Fig. 6D). In nondisrupted acini, as well as in disrupted acini constituting the major part of the gonad, the meshwork of 5-HT-IR fibers appeared more disorganized and spread over a larger area than in other stages (Fig. 6D). In addition, these fibers displayed no specific orientation plan, sometimes being parallel to the alveolar wall and sometimes perpendicular or at any other angle (Fig. 7D).

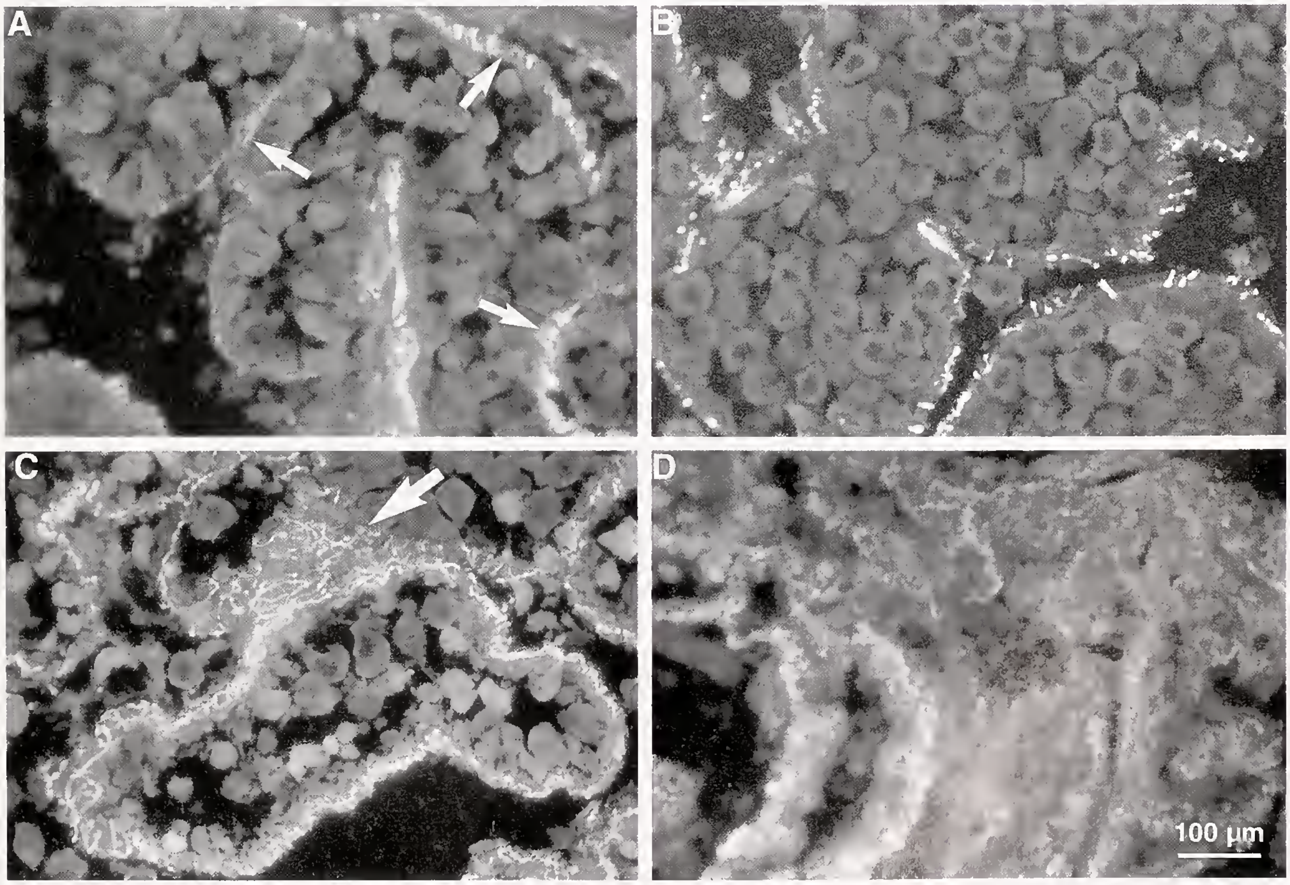

Figure 6. Localization of serotonin immunoreactivity in surf clam female gonads during the gametogenic cycle. The gametogenic cycle was divided into four stages: (A) active phase, (B) ripe phase, (C) partially spawned phase, and (D) spent phase. Note in A the localization of staining indicated by arrows surrounding active-phase acini. Note in C a meshwork of serotonin-immunoreactive fibers in a tangential gonad section (*arrow*).

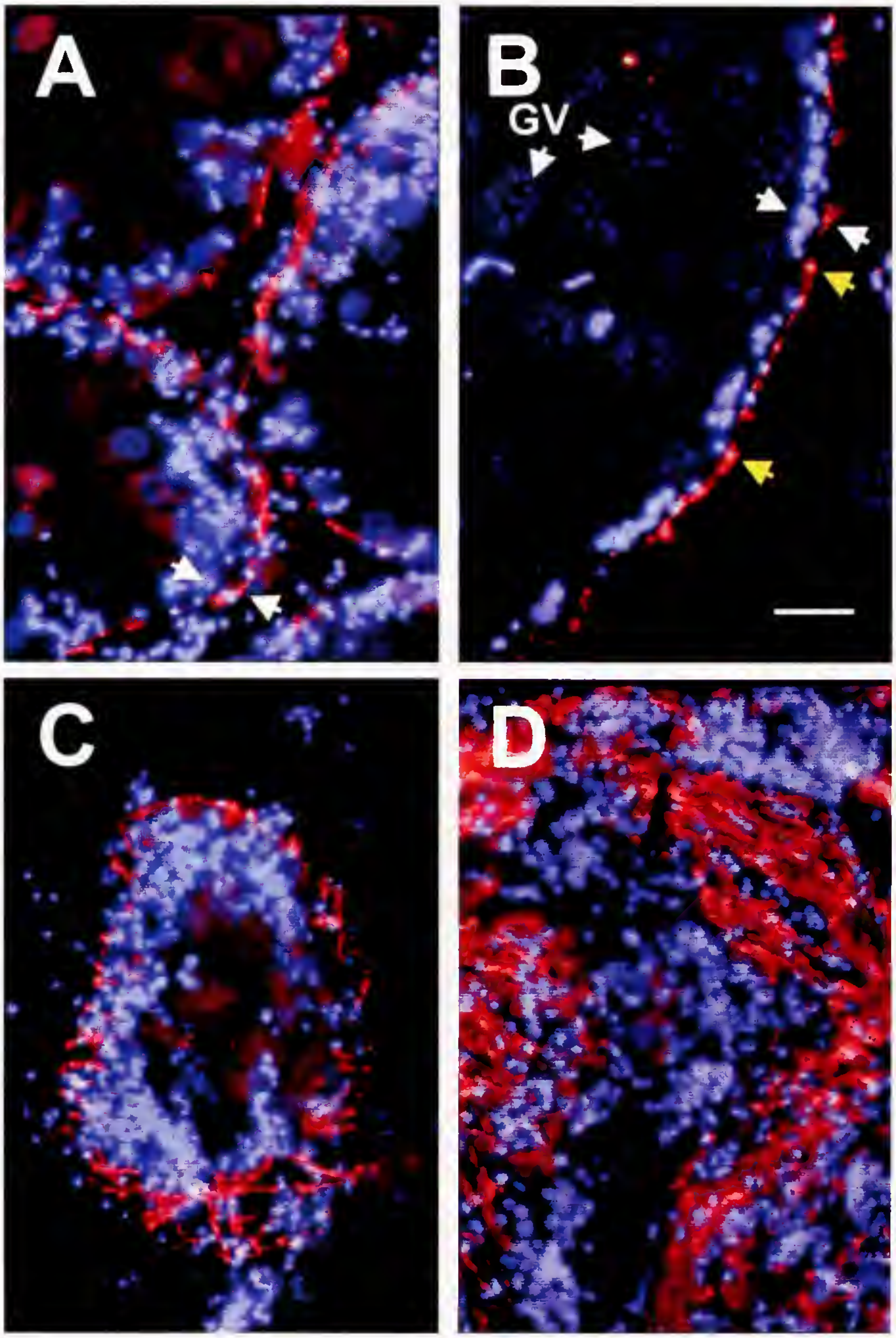

Figure 7. Epifluorescence micrographs of serotonin immunoreactivity and DNA staining (Hoechst 33258) in surf clam female gonads during the gametogenic cycle. Serotonin-immunoreactive elements are stained in red and DNA in blue. The gametogenic cycle was divided into four stages: (A) active phase, (B) ripe phase, (C) partially spawned phase, and (D) spent phase. Note in A and B the width of the alveolar wall (*between white arrows*). Also, note in B the two varicosities of serotonin-immunoreactive projection (*yellow arrows*). GV: germinal vesicle of ripe oocytes. Scale bar, 50 μm.

During the male gametogenic cycle (Fig. 8), the distribution of 5-HT-IR fibers was similar to that of females. In active-phase males (Fig. 8A), granular acini were surrounded by a few 5-HT-IR fibers that formed a thin innervation field. As they reached the ripe phase (Fig. 8B), male acini displayed an interrupted staining pattern resulting mostly from varicosities within one 5-HT-IR fiber. In males that had already begun to spawn (Fig. 8C), several 5-HT-IR fibers occupied a larger innervation field around the acinus than in ripe-phase gonads. After sperm had been completely

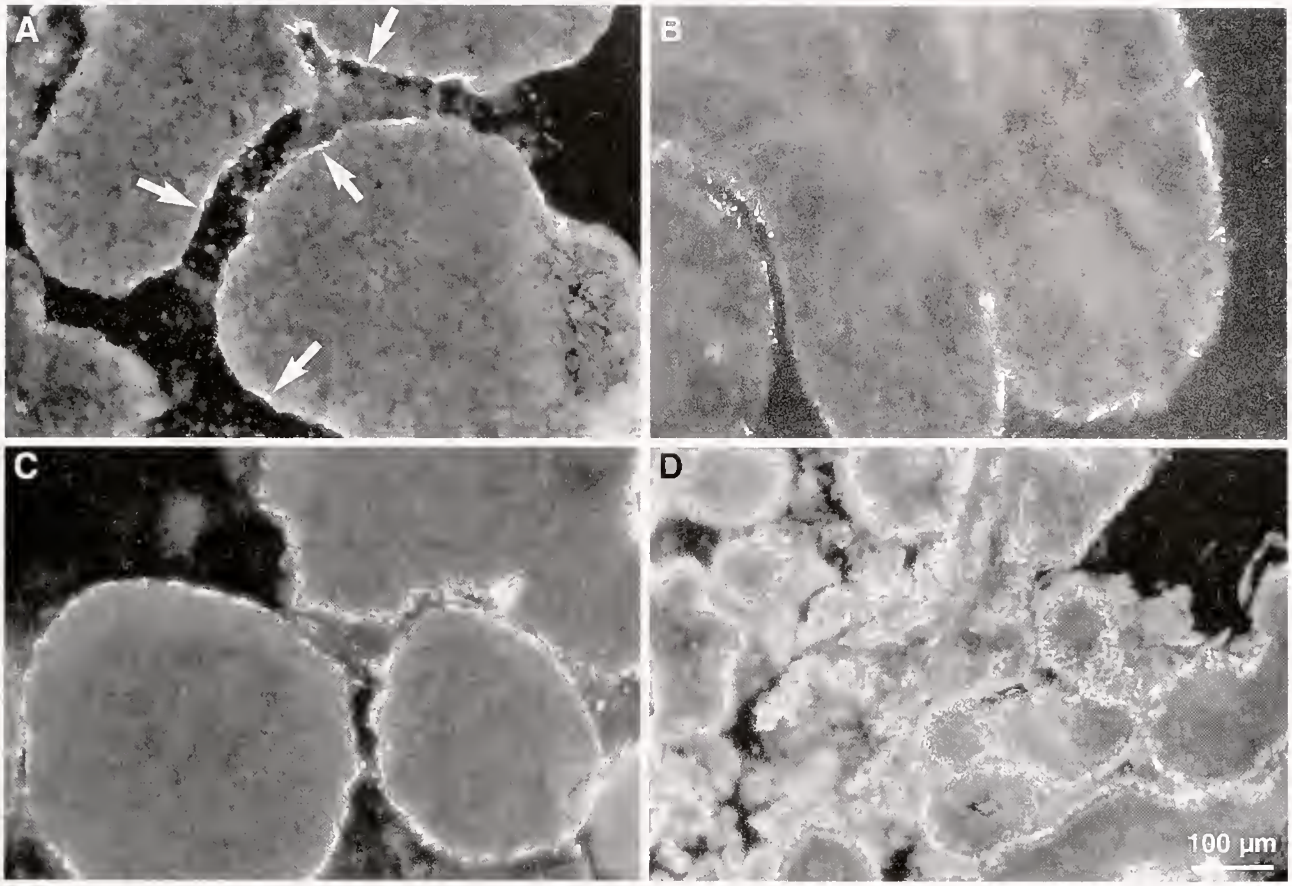

Figure 8. Localization of serotonin immunoreactivity in surf clam male gonads during the gametogenic cycle. The gametogenic cycle was divided into four stages: (A) active phase, (B) ripe phase, (C) partially spawned phase, and (D) spent phase. Note in A the localization of reactive fibers surrounding two acini (*arrows*).

expelled from acini (Fig. 8D), the immunoreactive field around recognizable acini was expanded as in females.

Discussion

The present study provides immunohistochemical and biochemical evidence for the presence of serotonin within the gonad of the surf clam, *Spisula solidissima.* Although serotonin has been reported from the gonads of some other bivalves, our work is the first to report changes in the pattern of gonadal serotonin innervation during the various stages of the gametogenic cycle. During the active phase (stage 1) when clam gonads contain small but recognizable gametes, some serotonin-containing fibers are detected covering the surface of the germinal acini, an observation also reported for scallops at a similar stage (Croll *et al.*, 1995). However, later in the season, in ripe gonads (stage 2), these varicose fibers conserve a similar shape and can be easily detected, but they appear less numerous along the germinal acini than in the previous phase, an observation never reported for other bivalves. Concurrently, the gonadal serotonin concentration (measured as nanograms of serotonin per gram of gonadal tissue) is, at this phase (ripe phase), significantly lower than in the active phase. This was also observed for the female gonad portion of the hermaphrodite *Argopecten purpuratus,* in which the serotonin concentration decreases during the 2 weeks before the second annual spawning (Martinez and Rivera, 1994). When spawning has begun, and the total mass of gonads starts decreasing, a more extensive network of conspicuous serotonin-containing fibers is detected around the germinal epithelium. Croll *et al.* (1995) made similar qualitative observations with scallops, that were not, however, supported by any parallel significant changes in serotonin levels. When surf clams have completed spawning (stage four, spent phase) and almost all mature gametes have been expelled, leaving nearly empty, shrunken, and lower-mass gonad, numerous serotonin-containing fibers encircle the acini, as also reported for the scallop *Placopecten magellanicus* of the same gonadal stage (Croll *et al.*, 1995). This observation is supported by a significantly higher serotonin concentration in comparison with values obtained from ripe clams (stage 2). Thus, unlike *Argopecten purpuratus* (Martinez and Rivera, 1994), in which the serotonin concentration decreases after spawning, clams show an increase in serotonin, and the concentration presumably remains high until the subsequent ripe stage.

In contrast, even though similar qualitative changes could be observed in the serotonergic innervation in male gonads during the gametogenic cycle, these observations are not paralleled by significant changes in serotonin concentrations between the various gametogenic stages. This may be partly due to the great variations in serotonin concentrations between individual specimens and the small sample size for the fourth phase (spent phase) of the gametogenic cycle. Indeed, since overall immunohistochemical observations are similar in male and female surf clams and the male gonad mass varies in the same manner as the female, we would expect a similar regulation of the gonadal serotonergic network in both sexes. Indeed, the gonadal serotonin concentrations are largely at comparable levels in both male and female surf clams and their responsiveness to injected serotonin is similar, thus suggesting that gonadal serotonin has equivalent roles in the reproductive processes in both sexes.

Overall, we find that gonadal serotonin concentration is correlated with total gonad mass. Indeed, the significant decrease in serotonin concentration during the ripe phase (Fig. 3) most probably reflects the major increase in the total mass of gonads when they are ripe (Fig. 5). Since this increase in total gonadal mass is mostly due to multiplication and growth of gametes, which are devoid of serotonin, this results in a lower serotonin concentration when expressed in nanograms per gram of gonadal tissue. In contrast, when spawning is complete and the total gonad mass is low, the serotonin concentration is high. Therefore, the total serotonin content within gonads appears to remain rather stable at substantial levels throughout the gametogenic cycle. In *Spisula*, since endogenous serotonin is present in the ripe-phase gonad, and since exogenous serotonin induces the release of gametes, serotonin is believed to be directly involved in the spawning process. Our observations of a stable gonadal serotonin content throughout gametogenesis suggest that the gonadal serotonin release that presumably induces spawning might be restricted in time, with normal levels being rapidly reestablished. In addition to inducing spawning, this release of serotonin in the gonads could also enhance the fertilizability of oocyte by sperm *in vivo*, as reported *in vitro* for isolated *Spisula* oocytes (Juneja *et al.*, 1993). In conclusion, our present work clarifies the localization and pattern of serotonin and its quantitative fluctuations during the gametogenic cycle. This opens new avenues for further investigations on issues such as the neuronal regulation of serotonin release and the nature of the gonadal serotonin receptors involved in the reproductive process.

Acknowledgments

We thank Ghislain Cummings for the collection and shipping of specimens. We are also grateful to Louise Pelletier and Gilles Clotteau for their technical support and to Dr. F.-J. Lapointe for statistical advice. This research was supported by an NSERC grant to F.D. and a FCAR team grant to M.A. and F.D.

Literature Cited

Alvarado-Alvarez, R., M. C. Gould, and J. L. Stephano. 1996. Spawning, *in vitro* maturation, and changes in oocyte electrophysiology induced by serotonin in *Tivela stultorum*. Biol. Bull. **190:** 322–328.

Croll, R. P., C. K. L. Too, A. K. Pani, and J. Nason. 1995. Distribution of serotonin in the sea scallop *Placopecten magellanicus*. *Invertebr. Reprod. Dev.* **28:** 125–135.

Fong, P. P., R. Deguchi, and K. Kyozuka. 1996. Serotonergic ligands induce spawning but not oocyte maturation in the bivalve *Mactra chinensis* from Central Japan. *Biol. Bull.* **191:** 27–32.

Gibbons, M. C., and M. Castagna. 1984. Serotonin as an inducer of spawning in six bivalve species. *Aquaculture* **40:** 189–191.

Hirai, S., T. Kishimoto, A. L. Kadam, H. Kanatani, and S. S. Koide. 1988. Induction of spawning and oocyte maturation by 5-hydroxytryptamine in the surf clam. *J. Exp. Zool.* **245:** 318–321.

Juneja, R., S. J. Segal, and S. S. Koide. 1993. Promotion of fertilizability of *Spisula* oocytes with 5-hydroxytryptamine. *Invertebr. Reprod. Dev.* **24:** 103–106.

Kadam, A. L., and S. S. Koide. 1989. Characterization of a factor with oocyte maturation inducing activity in *Spisula. Biol. Bull.* **176:** 8–13.

Krantic, S., F. Dubé, R. Quirion, and P. Guerrier. 1991. Pharmacology of the serotonin-induced meiosis reinitiation in *Spisula solidissima* oocytes. *Dev. Biol.* **146:** 491–498.

Krantic, S., F. Dubé, and P. Guerrier. 1993. Evidence for a new subtype of serotonin receptor in oocytes of the surf clam *Spisula solidissima. Gen. Comp. Endocrinol.* **90:** 125–131.

Martinez, G., and A. Rivera. 1994. Role of monoamines in the reproductive process of *Argopecten purpuratus. Invertebr. Reprod. Dev.* **25:** 167–174

Martinez, G., F. Saleh, L. Mettifogo, E. Campos, and N. Inestrosa. 1996. Monoamines and the release of gametes by the scallop *Argopecten purpuratus. J. Exp. Zool.* **274:** 365–372.

Matsutani, T., and T. Nomura. 1982. Induction of spawning by serotonin in the scallop, *Patinopecten yessoensis* (Jay). *Mar. Biol. Lett.* **3:** 353–358.

Matsutani, T., and T. Nomura. 1986. Serotonin-like immunoreactivity in the central nervous system and gonad of the scallop, *Patinopecten yessoensis. Cell Tissue Res.* **244:** 515–517.

O'Connor, W. A., and M. P. Heasman. 1995. Spawning induction and fertilization in the doughboy scallop *Chlamys (Mimachlamys) asperrima. Aquaculture* **136:** 117–129.

Pani, A. K., and R. P. Croll. 1995. Distribution of catecholamines, indoleamines, and their precursors and metabolites in the scallop, *Placopecten magellanicus* (Bivalvia, Pectinidae). *Cell. Mol. Neurobiol.* **15:** 371–386.

Paulet, Y.-M., A. Donval, and F. Bekhadra. 1993. Monoamines and reproduction in *Pecten maximus*, a preliminary approach. *Invertebr. Reprod. Dev.* **23:** 89–94.

Ram, J. L., R. P. Croll, S. J. Nichols, and D. Wall. 1992. The zebra mussel (*Dreissena polymorpha*), a new pest in North America: reproductive mechanisms as possible targets of control strategies. *Invertebr. Reprod. Dev.* **22:** 77–86.

Ram, J. L., G. W. Crawford, J. U. Walker, J. J. Mojares, N. Patel, P. P.

Fong, and K. Kyozuka. 1993. Spawning in the zebra mussel (*Dreissena polymorpha*): activation by internal or external application of serotonin. *J. Exp. Zool.* **265:** 587–598.

Ropes, J. W. 1968. Reproductive cycle of the surf clam, *Spisula solidissima,* in offshore New Jersey. *Biol. Bull.* **135:** 349–365.

Shirley, E. 1987. Applications of ranking methods to multiple comparison procedures and factorial experiments. *Appl. Statistics* **36:** 205–213.

Stefano, G. B., and E. J. Catapane. 1977. Seasonal monoamine changes in the central nervous system of *Mytilus edulis* (Bivalvia). *Experientia* **33:** 1341–1342.

Vitellaro-Zuccarello, L., S. De Biasi, P. Bernardi, and A. Oggioni. 1991. Distribution of serotonin-, gamma-aminobutyric acid- and substance P-like immunoreactivity in the central and peripheral nervous system of *Mytilus galloprovincialis. Tissue Cell* **23:** 261–270.

Welsh, J. H., and M. Moorhead. 1960. The quantitative distribution of 5-hydroxytryptamine in the invertebrates, especially in their nervous systems. *J. Neurochem.* **6:** 146–169.

York, B., and B. M. Twarog. 1973. Evidence for the release of serotonin by relaxing nerves in molluscan muscle. *Comp. Biochem. Physiol.* **44A:** 423–430.

Reference: *Biol. Bull.* **202:** 34–42. (February 2002)

Fertilization Success in Marine Invertebrates: The Influence of Gamete Age

MARK ELLIOTT WILLIAMS AND MATTHEW GRAEME BENTLEY*

Gatty Marine Laboratory, The University, St Andrews, Fife, KY16 8LB UK

Abstract. Gamete age has been postulated to be unimportant to the fertilization ecology of marine invertebrates. However, recent research suggests that, for some species at least, it may have a direct impact upon fertilization success. We present comparative data on the influence of gamete age on fertilization and development success in several marine invertebrates: the polychaetes *Arenicola marina* and *Nereis virens* and the asteroid echinoderm *Asterias rubens*. Oocytes are much longer lived in the polychaetes than in the echinoderm, with *A. marina* oocytes still capable of fertilizing and developing normally 96 h post-spawning. Developmental abnormalities and failure to reach blastula tend to occur well before the fertilizable life of the oocytes has expired. Sperm are similarly longer lived in the polychaetes; however, fertilizing capacity is markedly reduced following incubation in conspecific egg-conditioned seawater. These results are discussed in terms of the fertilization strategies of the three species. We further suggest that, for *A. marina* at least, longer-lived sperm and eggs are central to the fertilization strategy of this species.

Introduction

Whether the length of time that sperm and eggs are viable following spawning affects the reproductive success of broadcast spawning species is a subject for debate. The view of workers such as Levitan *et al.* (1991) is that dilution of gametes below fertilizable concentrations occurs well before the viable life of the gametes has expired, leading to the hypothesis that gamete longevity is not important to the fertilization ecology of free-spawning species. Yund (2000) suggests, however, that adaptations to reduce sperm limitation may lead to high levels of fertilization success, although sperm dilution effects remain undoubtedly important for certain shallow subtidal free-spawning echinoderms and molluscs. Circumstances in which gamete longevity is combined with reduced gamete dilution due to the viscous nature of the fluids in which gametes are released may increase fertilization levels in free-spawning species. This has been demonstrated recently in *Strongylocentrotus droebachiensis* using laboratory investigations (Meidel and Yund, 2001). A different situation exists in the brooding starfish *Leptasterias polaris*, in which sperm deposited on the substratum are not dispersed, but remain quiescent until activated by female spawning (Hamel and Mercier, 1995). In such cases, longer-lived sperm would be a distinct advantage. Sperm longevity is also important in some internally fertilizing ascidians where females filter large volumes of seawater, which can result in the collection and concentration of diluted sperm to effect a high level of fertilization many hours after male spawning (Bishop, 1998).

This study investigates egg and sperm longevity of the polychaetes *Arenicola marina* and *Nereis virens* and the asteroid *Asterias rubens*, which are all species that have seasonal reproduction. *Arenicola marina* and *Asterias rubens* are annual iteroparous species, while *N. virens* is semelparous. The findings will be discussed in an ecological context. The mediation of sperm activity by egg compounds will also be examined to a certain extent for *Arenicola marina* and *Asterias rubens*.

In most populations of the lugworm *Arenicola marina*, spawning is epidemic, cued by environmental and endogenous factors (Bentley and Pacey, 1992; Watson and Bentley, 1998; Watson *et al.*, 2000), and takes place over only a few days in late autumn in most localities (Williams *et al.*, 1997). Male and female lugworms exhibit different spawning strategies. Females spawn their oocytes into the U-

Received 18 February 2000; accepted 18 September 2001.

* To whom correspondence should be addressed. Current address: Department of Marine Sciences and Coastal Management, University of Newcastle, Ridley Building, Claremont Road, Newcastle upon Tyne, NE1 7RU UK. E-mail: m.g.bentley@ncl.ac.uk

shaped burrow, which is irrigated on the flood tide, drawing sperm-enriched water into the fertilization site. Males release sperm puddles onto the surface of the sediment at low water, ejecting small streams of sperm from the tail shaft of the burrow. The sperm coalesce to form a dense puddle with a highly cohesive, oily consistency. In this state the sperm are quiescent (Pacey *et al.*, 1994a). On the flood tide, the sperm puddles are dispersed across the beach, affording females the opportunity to "collect" sperm for fertilization. Field studies of fertilization success indicate that it is highly variable, between 0% and 100% (Williams *et al.*, 1997).

The king ragworm, *Nereis virens*, spawns only once at age 2–5 years, during periods of spring tides in early spring along the East Coast of Scotland. Sperm develop as tetrads, and ripe males are characterized by having free-swimming sperm within the coelomic cavity. Spawning is characterized by swarming, when ripe males leave the sediment and swim actively in the water column releasing gametes (Bass and Brafield, 1972), and the female remains in the substratum depositing her eggs on the surface of the sediment.

Asterias rubens generally spawns during spring in northern European waters, although more northerly populations spawn in the late spring or early summer (Nichols and Barker, 1984). Oocyte maturation and spawning is initiated by 1-methyl adenine (Kanatani, 1979). During spawning, *A. rubens* adopts a spawning posture typical of many asteroids. Waves of contraction pass along the arms of the starfish and the central disc is raised several centimeters off the substratum so that the starfish is supported on the tips of its arms.

Materials and Methods

Collection and maintenance of experimental animals

Mature specimens of *Arenicola marina* were collected by digging from an intertidal sandflat at Red Wharf Bay, Anglesey, North Wales (53°18.6′N 4°12.0′W). This population spawns epidemically during spring tides in early December, and ripe individuals (responsive to endocrine manipulation to stimulate spawning) were available from mid-November. In the laboratory, worms were sexed and housed individually in polyethylene pots with fresh filtered seawater in a controlled temperature room under ambient temperature and illumination. The worms were left for at least 24 h before use in experiments to allow gut contents to be voided, and the water was changed daily.

Gravid individuals of *Nereis virens* were provided by Seabait Ltd. (Ashington, Northumberland) and collected by digging from a designated broodstock bed during late February and March. In the laboratory, the animals were stored in polyethylene pots with a layer of gravel and 0.5-mm diameter holes drilled into the walls and lid. The pots were then placed into single-sex, flow-through tanks and maintained at 5°C with ambient illumination. Using farmed animals rather than field-collected specimens provides animals at a known stage of reproductive development. Animals at the peak of gamete development (100% fertilization and development to blastula, free sperm in coelomic cavity, and some spontaneous spawning) were selected for use in experiments.

Specimens of *Asterias rubens* were collected from fishing creels set at a number of sites around the East Coast of Fife, Scotland. They were stored in large tanks (1 m × 3 m × 1 m) with a continuous flow-through of fresh seawater and maintained under conditions of ambient temperature and illumination. Starfish were used within a week of collection.

Spawning induction and collection of gametes

Arenicola marina. Mature oocytes were collected from animals induced to spawn by injection of homogenized prostomia from mature females, as described by Pacey and Bentley (1992). Each recipient female was injected with one prostomial equivalent of homogenate and placed into fresh seawater to spawn. Upon spawning, excess water was decanted, and the eggs were washed twice by resuspending in 100 ml sterile filtered seawater (SFSW). They were then allowed to settle out, and a sample was transferred to microcentrifuge tubes. The density of settled eggs in the tubes was determined by counting microliter volumes under a compound microscope.

Sperm maturation through the injection of 8,11,14-eicosatrienoic acid. To induce spawning, each gravid male was injected with the sperm maturation factor 8,11,14-eicosatrienoic acid (Sigma), using an optimal concentration of 13 $\mu g \cdot g^{-1}$ body mass (for full details see Pacey and Bentley, 1992). A 200-μl Gilson pipette was used to collect sperm dry (*i.e.*, undiluted) as it emerged from the nephromixia. The sperm samples were placed into microcentrifuge tubes and left for a few minutes to allow them to coalesce to maximal concentration; the excess water was then pipetted off.

In vitro *maturation of coelomic sperm.* Sperm were activated *in vitro* by incubation in appropriate concentrations of 8,11,14-eicosatrienoic acid (Pacey and Bentley, 1992). Samples, about 200 μl in volume, of coelomic fluid were withdrawn from the coelomic cavity of gravid males and placed in microcentrifuge tubes. This allowed multiple sampling from each male. Coelomic samples were incubated with equivalent volumes of 1×10^{-4} M 8,11,14-eicosatrienoic acid. They were then shaken by hand and left for 30 min at 8°C to mature. The mature sperm typically coalesced into oily droplets at the bottom of the tube, and the excess fluid was removed. Mature sperm had the same fertilizing capacity as normally spawned sperm. This technique was used when large numbers of small samples of sperm were required and when only the eggs were the subject of investigation.

Nereis virens. Samples of oocytes were withdrawn from the coelomic cavity with a disposable 1-ml syringe. The oocyte sample was expelled into about 100 ml SFSW and allowed to settle before being washed again in the same volume. Samples of eggs were then transferred to microcentrifuge tubes, and the density of settled eggs was determined. Coelomic sperm were withdrawn using a syringe and stored dry (*i.e.*, undiluted) in microcentrifuge tubes at 8°C until required.

Asterias rubens. Mature oocytes were collected following injection of 1-methyl adenine (1-MeAde) into ripe individuals of *Asterias rubens*. Fresh starfish were collected from the aquarium and placed in about 100 ml SFSW in glass bowls. One to two ml of 10^{-4} *M* 1-MeAde (prepared in seawater) was injected through the aboral surface of one of the arms. This gave an approximate concentration in the animals of 1×10^{-6} *M* 1-MeAde. Mature oocytes were collected from the bowl, washed twice in SFSW, and transferred to a beaker with about 100 ml SFSW. Settled egg density was determined as described above.

Asterias rubens sperm were also collected by dissection of gonadal tissue. Pieces of excised testis were placed in a small petri dish containing 10 ml SFSW. Gentle probing with a pipette tip led to the extrusion of sperm from the tissue, which was collected dry using a 200-μl Gilson pipette. This technique was used only when eggs were under test. Sperm collected following spawning induction were used during investigations of sperm performance.

Oocyte age

Mature oocytes were harvested as described above. Approximately 10^6 eggs from each female were transferred to separate autoclaved beakers containing 1 l of SFSW. Sampling 1 ml of the mixed egg suspensions yielded between 500 and 1000 eggs. The beakers were then stored at 8°C for the duration of the experiment, and the water was carefully changed every 4–8 h with fresh SFSW to maintain oxygen tensions. For *Arenicola marina* and *Asterias rubens*, eggs from five females were used; for *Nereis virens*, eggs from three females were used.

Fertilization assay

To discern any decline in fertilization success, it was necessary to fertilize the eggs with the minimum quantity of sperm required to achieve 100% fertilization. The fertilization assay was conducted by pipetting 1 ml of 5×10^5 sperm · ml^{-1} directly over the eggs in the fertilization chamber. This gave an overall sperm concentration in the 20-ml volume of 2.5×10^4 sperm · ml^{-1}, and 100% fertilization was recorded; incidences of abnormal development at time 0 (possibly attributable to polyspermy) were rare. Any fall in fertilization success (and hence gamete fitness) was therefore immediately apparent.

Egg longevity

For *Arenicola marina*, fresh sperm suspension was prepared *in vitro* from at least five males at each time point. The suspension was examined under the microscope to ensure the presence of free-swimming sperm; concentrations were determined using a hemocytometer. Suspensions from each of the males were then pooled to give a final concentration of 10 ml of 5×10^5 sperm · ml^{-1}. For males of *Asterias rubens*, small pieces of testis were excised from one arm of each of five males, and sperm were extracted as described above. Each of the five pairs of testes was sampled only once. After collection, the sperm were treated as for *Arenicola marina*. Sperm were collected from *Nereis virens* males directly from the coelomic cavity as described above, and stock solutions of 10 ml of 5×10^5 sperm · ml^{-1} were pooled from at least three males. The fertilizing capacity of the ragworm sperm was tested. Use of these techniques permitted each male to be used several times during the experiment.

Eggs from each species under test were withdrawn from five females as described earlier. Fertilizations were conducted in sterile 25-ml petri dishes. Three replicate fertilizations were conducted for each of the five females at all of the time points used. At each time point, 500–1000 oocytes were pipetted in 1 ml of seawater from the storage beakers into the appropriate petri dish that contained 18 ml SFSW. One milliliter of pooled sperm suspension was then added to the petri dish to give a final volume of 20 ml and a final sperm concentration of approximately 2.5×10^4 sperm · ml^{-1}; the petri dishes were then left for 24 h at 8°C. Fertilization success was assessed by examining 150 eggs from each of the dishes. Oocytes were recorded as fertilized with normal development, fertilized with abnormal development, or unfertilized. Abnormal development was defined as embryos failing to develop or degenerating. Allowing such eggs to continue to develop revealed only further degeneration.

Sperm longevity at 10^5 sperm · ml^{-1} and 10^9 sperm · ml^{-1}

Gamete handling. Fresh sperm were collected dry from each of five male *Arenicola marina*, five *Asterias rubens*, and three *Nereis virens*; and stock suspensions of 20 ml 5×10^9 sperm · ml^{-1} were prepared in autoclaved glass petri dishes. Aliquots of each of the sperm suspensions were taken and serially diluted to provide 200 ml of sperm suspension at a concentration of 5×10^5 sperm · ml^{-1}. These were then stored at 8–10°C for the duration of the experiment. Oocytes were collected from at least three females of each of the species and treated as described above. Fresh oocytes were collected from *Arenicola marina* every 24 h, and from *Asterias rubens* and *Nereis virens* at each fertilization point.

Fertilizations were conducted in sterile 25-ml petri dishes. At each time point, 18 ml of SFSW was pipetted into the fertilization dishes together with 1 ml containing approximately 500–1000 fresh oocytes. One milliliter of the 5×10^5 sperm · ml^{-1} suspension was pipetted into the appropriate petri dish over the oocytes to give a final concentration of 2.5×10^4 sperm · ml^{-1}. One-hundred microliter samples of the 5×10^9 sperm · ml^{-1} suspensions were taken and serially diluted to a concentration of 5×10^5 sperm · ml^{-1}, 1 ml of which was pipetted into the appropriate petri dishes. Three replicate fertilizations were performed for each male and treatment used. The fertilization dishes were then left at 8–10°C for at least 18 h. Fertilization success was scored by sampling 150 eggs from each petri dish for evidence of cleavage.

Effect of egg-derived compounds upon sperm longevity. Eggs were collected from *Arenicola marina* and *Asterias rubens* 12 h before the beginning of the experiment from each of five females by injection of appropriate spawning hormones, as described above. The oocytes were gently washed twice in SFSW, pooled, and their density determined. Approximately 3×10^6 eggs were then carefully pipetted into an autoclaved beaker containing 300 ml of SFSW. The suspension was incubated for 12 h at 8°C, and then the upper 200 ml of water was slowly decanted from the eggs and passed through a 60-μm Nitex mesh. No eggs were observed on the mesh. The water was filtered to 0.2 μm. The filtrate was used subsequently to observe possible effects of egg-derived compounds on sperm longevity (see below). Eggs from *Asterias rubens* were used for only 3–4 h before being replaced by fresh samples. However, oocytes collected from *Arenicola marina* were used throughout the experiment and were stored as described above. The egg concentration was determined and the volume of water containing 500–1000 eggs calculated.

Sperm were collected dry from each of five males, and fertilization assays were conducted as above. Appropriate aliquots of sperm from each male were then taken and pipetted individually into five crystallizing dishes containing 40 ml of the egg water (filtrate), to give a final concentration of 5×10^5 sperm · ml^{-1}. As a control, further aliquots of sperm were taken from each sample and pipetted into crystallizing dishes with 40 ml of 0.2-μm-filtered seawater that had been left for 12 h at 8°C.

Results

Oocyte age

The percent fertilization and developmental success of oocytes from *Arenicola marina* aged over 5 days are shown in Figure 1A. Fertilization success remained around 100% for up to 72 h but then began to fall rapidly, with only a quarter of oocytes being fertilized at 96 h and almost none at 120 h. Developmental capacity was not diminished to any great extent until 96 hours post-spawning (Fig. 2B). This increase in abnormal development before blastula coincided with the greatest drop in fertilization success.

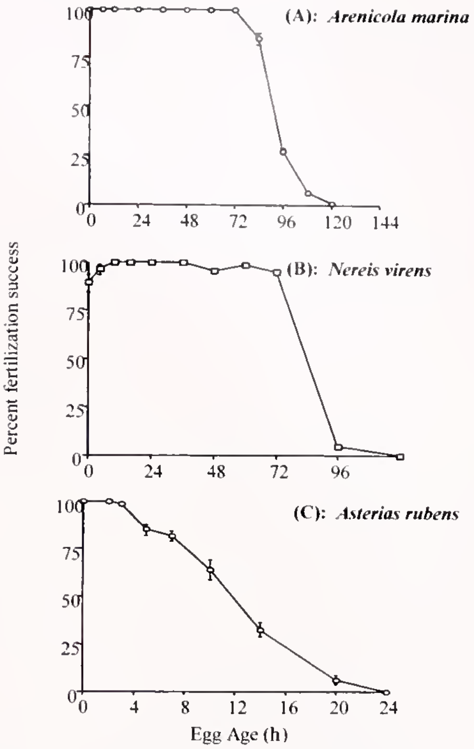

Figure 1. Oocyte fertilization success at a number of time intervals following spawning in *Arenicola marina* (A), *Nereis virens* (B), and *Asterias rubens* (C). Note the difference in timescale over which oocytes were viable for each of the species. Standard errors were calculated from the arcsine-transformed percentage data and back-transformed for presentation.

Most oocytes of *Nereis virens* could be fertilized for at least 72 h after extraction from the coelomic cavity (Fig. 1B); however, the developmental capacity decreased throughout this period so that from 60 h on, only about 10% of the oocytes developed to blastula (Fig. 2B). In contrast to the polychaetes, *Asterias rubens* showed 100% fertilization of oocytes for only the first 4 h after spawning (Fig. 1C). Thereafter, fertilization success fell to zero by 24 h. Cases of abnormal development rose gradually with increasing age (Fig. 2C).

Sperm age

Arenicola marina sperm stored at 10^5 sperm · ml^{-1} retained a high fertilization capacity up to 60 h post-spawning, before dropping to almost zero at 86 h (Fig. 3A). The same graph shows the fertilization success of sperm stored at 10^9 sperm · ml^{-1}. Success remained high throughout the experiment and continued beyond the time shown in the figure. When examined, sperm stored at 10^9 sperm · ml^{-1} had

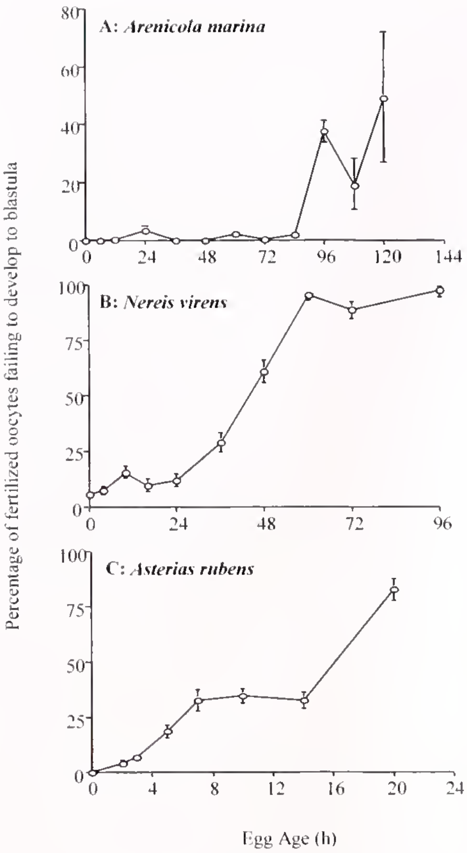

Figure 2. Percentage of oocytes failing to develop to blastula when fertilized at several time intervals following spawning, from *Arenicola marina* (A), *Nereis virens* (B), and *Asterias rubens* (C). Note the difference in timescale over which oocytes were viable for each of the species. Standard errors were calculated from the arcsine-transformed percentage data and back-transformed for presentation.

coalesced into oily droplets at the bottom of the petri dish, and in this state it was quiescent.

Nereis virens sperm stored at the higher concentration was similarly long lived. However, sperm stored at 10^5 sperm · ml^{-1} rapidly lost the ability to fertilize, falling to almost zero after 24 h (Fig. 3B). In contrast, the fertilizing capacity of *Asterias rubens* sperm stored at 10^9 sperm · ml^{-1} and 10^5 sperm · ml^{-1} was found to be similar (Fig. 3C). At each of the time points, success was slightly greater for the sperm stored at the higher concentration, but both successes fell to approximately zero after 26 h.

Sperm stored in egg water

It is apparent that egg water had a marked effect upon the fertilizing capacity of sperm for both *Arenicola marina* (Fig. 4A) and *Asterias rubens* (Fig. 4B). The fertilization capacity of *Arenicola marina* sperm stored in egg water fell to zero after 28 h, whereas that stored in SFSW remained at 100% (data were the same as in Fig. 3A). The fall in fertilization success of *Asterias rubens* sperm was even more dramatic, dropping to zero after 8 h. The fertilization success of sperm stored in SFSW is comparable to the data presented in Fig. 3C.

Discussion

The longevity of unfertilized oocytes has a marked impact upon fertilization success. This paper demonstrates that there is a finite period following spawning in which the oocyte is capable of being fertilized and subsequently developing to at least the blastula stage. The choice of blastula/early gastrula stage as a cut-off point in the experiments was an arbitrary decision based on the likelihood that artifacts associated with nurturing large batches of larvae might influence the results. Further development may have been

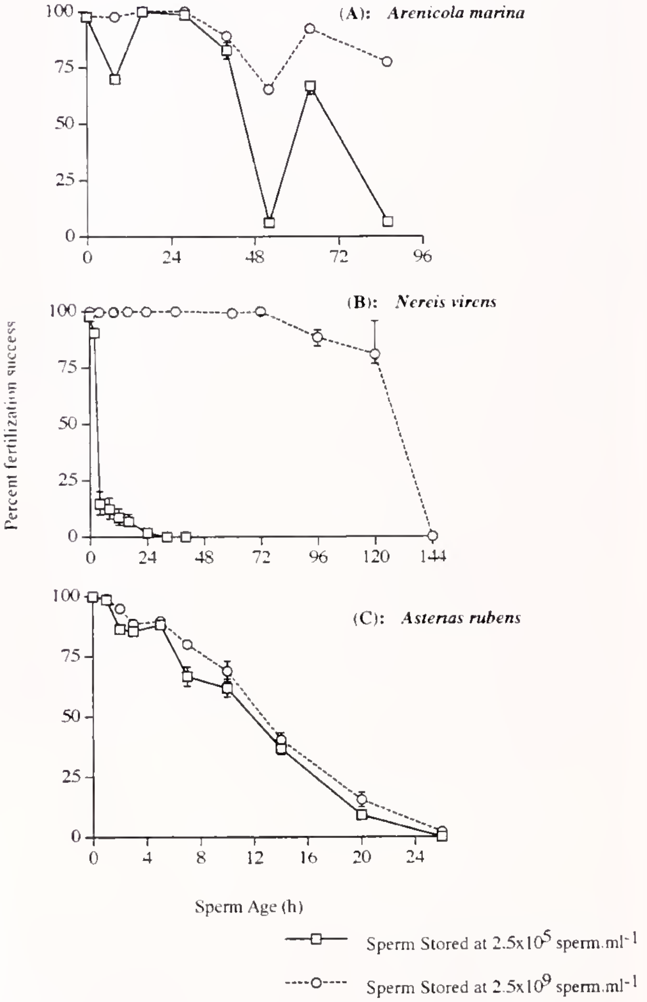

Figure 3. Fertilizing capacity of sperm from *Arenicola marina* (A), *Nereis virens* (B), and *Asterias rubens* (C) stored and aged at two concentrations. Note the difference in timescale over which oocytes were viable for each of the species. Standard errors were calculated from the arcsine-transformed percentage data and back-transformed for presentation.

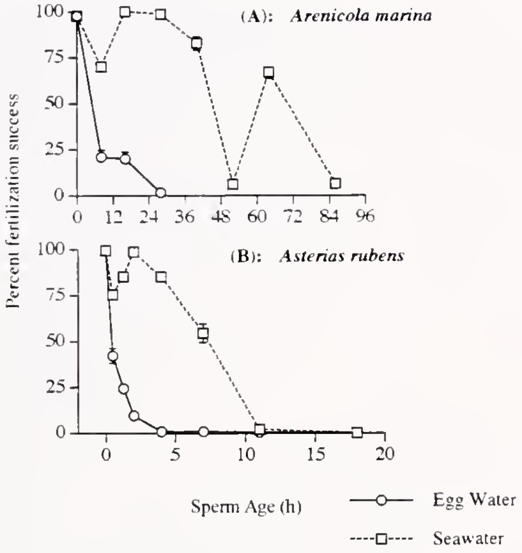

Figure 4. Fertilizing capacity of dilute sperm from *Arenicola marina* (A) and *Asterias rubens* (B) stored either in seawater or in conspecific-egg–conditioned seawater. Note the difference in timescale over which oocytes were viable for each of the species. Standard errors were calculated from the arcsine-transformed percentage data and back-transformed for presentation.

impeded for some embryos as a consequence of oxygen tensions or biotic factors (*e.g.*, infection). The blastula/early gastrula stage, which lasts for a number of hours, also allowed the success (or otherwise) of early embryonic development to be examined and scored without the need for fixation of the samples.

Very few data exist on the longevity of unfertilized gametes among marine invertebrates. That there is a limited life span of gametes was recognized by several early workers (*i.e.*, Lillie, 1915). Recent work has quantified the length of time that gametes are viable, but as Benzie and Dixon (1994) point out, this has not been discussed in an ecological context. It is generally reported that sperm become senescent more rapidly than eggs in free-spawning invertebrates, their longevity being measured from minutes to 1 or 2 hours (see Levitan, 1995; Table 1). This extends across a range of invertebrate groups including chelicerates (Brown and Knouse, 1973), echinoids (Pennington, 1985; Levitan *et al.*, 1991), asteroids (Benzie and Dixon, 1994), bivalve molluscs (André and Lindegarth, 1995), and hydroids (Yund, 1990).

Oocyte longevity

There are marked differences in the oocyte longevity of the species studied here. *Arenicola marina* oocytes remain fertilizable and capable of developing to blastula for more than 96 h (Figs. 1 and 2). Oocytes from *Nereis virens* remain fertilizable for a similar length of time, but the probability of producing viable offspring decreases to almost zero after 48 h. In contrast, the fertilization capacity of *Asterias rubens* oocytes falls to zero after 24 h, while cases of abnormal development rise steadily throughout. Although there was no evidence for treatment effects on fertilization rates in this study, it is possible that absolute fertilization rates differ from those given. Most of the comprehensive studies of the effect of gamete age upon fertilization success fail to record the length of time that eggs are viable. They simply state that the fall in fertilization success is attributable to a drop in sperm viability and that eggs remain fertilizable for a short time after the sperm has senesced. The oocyte longevity of *A. rubens* is comparable to the qualitative observation by Benzie and Dixon (1994) that oocytes of the starfish *Acanthaster planci* are fertilizable for "a few hours." André and Lindegarth (1995) investigated the independent effect of egg age for the bivalve *Cerastoderma edule*. They reported that eggs could give rise to normally developing embryos for less than 5 h post-spawning.

Arenicola marina oocytes have a remarkable longevity compared to those of the free-spawning species mentioned above and are comparable to the eggs of the ascidian *Ascidia mentula*, where fertilization and development proceeds normally for 96 h after extraction (Havenhand, 1991). Such longevity is not reported elsewhere for externally fertilizing marine invertebrates, and little is known of the factors that determine longevity of oocytes. Internal energy

Table 1

Lengths of time that dilute sperm remain viable at concentrations comparable to those in this paper in some of the species for which sperm longevity has been extensively studied

Species	Viable time (h)	Temp (°C)	Reference
Arenicola marina	70+	10	This study
Nereis virens	24	10	This study
Cerastoderma edule (bivalve mollusc)	5	20	André and Lindegarth, 1995
Asterias rubens	24	10	This study
Acanthaster planci (asteroid echinoderm)	5	28	Benzie and Dixon, 1994
Strongylocentrotus droebachiensis (echinoid echinoderm)	2	14	Pennington, 1985
Strongylocentrotus franciscanus (echinoid echinoderm)	2.5	12	Levitan *et al.*, 1991

stores will most likely be involved, and the oocytes of both *Arenicola marina* and *Nereis virens* are considerably larger than those of *Asterias rubens*. Following extrusion from the body cavity, the oocytes will be exposed to a range of pathogenic bacteria and toxic compounds. Toomey and Epel (1993) describe embryos of the infaunal echiuran *Urechis caupo* as having a well-developed system for removing toxic compounds that is absent in free-spawned sea urchin embryos. In addition, antibiotic and antifungal resistance is described for the mollusc *Aplysia kurodai* (Iijima *et al.*, 1995). It is likely that the oocytes of *Arenicola marina* will have well-developed defense mechanisms to enable them to remain viable over a longer period of time in the sediment.

Sperm longevity

The results presented here for the polychaetes (Fig. 3A, B) are in accordance with a number of studies on echinoderms (Chia and Bickell, 1983; Levitan *et al.*, 1991; Benzie and Dixon, 1994). The longevity of a sperm suspension is related to sperm concentration; this has been attributed to the rate of consumption of oxygen. The fact that concentrated sperm respire at a lower rate than dilute sperm—termed the respiratory dilution effect (Chia and Bickell, 1983)—has been clearly demonstrated for the echinoid *Strongylocentrotus franciscanus* (Levitan *et al.*, 1991) and the asteroid *Acanthaster planci* (Benzie and Dixon, 1994). *Asterias rubens* sperm was only slightly longer lived at the higher sperm concentration (Fig. 3C). Despite not being assessed over a wide range of concentrations, the dilute (10^5 sperm · ml^{-1}) sperm samples for all the species studied here were considerably longer lived than those of some of the species studied elsewhere at comparable concentrations (see Table 1). The sperm longevity of the species presented in this table is less than 5 h, whereas sperm from *Arenicola marina* remains viable for more than 72 h (though at a reduced fertilization success after 48 h). Further, the quiescence of concentrated *A. marina* sperm was shown by Pacey and Bentley (1992).

Following release from the male, sperm from many species require an activation step, which in free-spawning invertebrates is provided by dilution in seawater. Dilution raises the pH of the sperm to that of seawater; this has been shown to activate the spermatozoa of *Arenicola marina* (Pacey *et al.*, 1994a). Dilution also leads to a raised respiration rate and a more active swimming behavior. There is a finite "respiratory life" of a spermatozoon, with those stored at low density having a shorter half-life than more concentrated sperm (Chia and Bickell, 1983). Studies on the swimming behavior of *A. marina* sperm have shown that it has intermittent periods of quiescence, which may be modulated by light radiation (Pacey *et al.*, 1994b). This has also been described for tunicates (Brokaw, 1984) and some sea urchins (Gibbons, 1980). Bishop (1998) attributes the longevity of ascidian sperm to its intermittent swimming behavior, which results in the conservation of energy stores; such a mechanism could conceivably facilitate the sperm longevity of *A. marina*. Temperature may also influence sperm longevity by changing respiration rate. In the experiments here, sperm was stored at 8°C, which was close to ambient for the time of year but cooler than the temperatures used in the studies presented in Table 1.

Havenhand (1991) showed that sperm from a solitary ascidian (*Ascidia mentula*) can successfully fertilize oocytes for up to 48 h after release and that eggs are similarly longer lived. This longevity was subsequently confirmed for three other ascidian species (Bolton and Havenhand, 1996; Bishop, 1998). The situation in these ascidians is slightly different from that of other free-spawning invertebrates in that the female retains the eggs and fertilization is facilitated by the female collecting the sperm and brooding the eggs. A high fertilization success occurs at sperm densities that are low (around 10 sperm · ml^{-1}), which is in contrast to the results of studies by Levitan *et al.* (1991) and Benzie and Dixon (1994) on echinoderms.

One factor that should be considered when comparing species that have slightly different fertilization strategies is that the term "dilute sperm" is a relative one and that it is functional dilution level that is important. For example, some free-spawning echinoderms require hundreds of thousands of sperm per milliliter in the surrounding water to effect a reasonable fertilization success (Levitan *et al.*, 1991). Conversely, some (male only) free-spawning ascidians capture sufficient sperm from the surrounding water to fertilize eggs at concentrations measured in the tens of sperm per milliliter, long after male spawning has ceased (Bishop, 1998). Comparisons of the impact of dilution on longevity between these species would therefore be tenuous, since the fertilization strategy is clearly different. Within the species used in this study, it is interesting that sperm at the lower concentration are longer lived in *Arenicola marina* than in the others, as this species has a fertilization strategy more akin to the ascidian than are the strategies of the other two species.

Impact of egg-conditioned water on sperm activity

For many years before the phenomenon was unequivocally demonstrated, investigators suspected that chemical attraction and subsequent taxis of a sperm towards an egg occurred in animal phyla. It has, however, been known for over a century in plants, and much is known of the nature of the chemical attractants, in the marine brown algae particularly (Maier and Müller, 1986). Chemotaxis in marine invertebrates was first shown by Dan (1950), in a medusoid cnidarian; extensive work by Miller during the 1960s and 1970s demonstrated chemotaxis in a number of other species of Cnidaria (Miller, 1970; 1978). It has since been demonstrated in a number of phyla including molluscs (Miller, 1977; Miller *et al.*, 1994), arthropods (*Limulus* sp., Clapper and Brown, 1980), echinoderms (Miller, 1985), and tunicates (Miller, 1975). Whether such chemotaxis exists in annelids is inconclusive at present.

Chemicals derived from the egg can have three types of effect upon the swimming of the sperm. First, they can initiate swimming (*e.g.*, *Limulus* sp., Clapper and Brown, 1980); second, they can increase swimming velocity; and finally, they can cause the sperm to swim in a directed manner towards the egg (see Miller, 1984, for review of sperm swimming behavior). The outcome of these behaviors is simply to increase the probability of sperm-egg interaction. It is believed that the principal effect of a sperm attractant that is released from the spawned egg is to create a larger surface area for the egg, thus making "larger targets" for passing sperm (see Cosson, 1990). However, the distance over which the attractants are effective will be limited by the constraints of sperm swimming capacity and by hydrodynamic effects.

Incubation of *Arenicola marina* sperm and *Asterias rubens* sperm in egg-conditioned water dramatically reduced their respective half lives. The fertilizing capacity of *Arenicola marina* sperm dropped to zero after little more than a day, and *Asterias rubens* sperm produced almost no fertilization after 4 h. These results are similar to data obtained by Bolton and Havenhand (1996) for the solitary ascidians *Ciona intestinalis* and *Ascidiella aspersa*, whose sperm is usually active for more than 12 h. It seems likely that the egg-derived compounds studied here act by raising the activity and respiration levels of the sperm, in a mechanism similar to that described by Suzuki and Garbers (1984). Bolton and Havenhand (1996) noted that ascidian sperm incubated in egg water swam more often than those incubated in seawater. We found some preliminary evidence to support the hypothesis that egg compounds increase the rate of sperm respiration in *Arenicola marina*, but limitations of the experimental equipment prevented a more rigorous investigation of this hypothesis.

Ecological considerations

Oocyte longevity is probably related to the mode of reproduction of a species. Data gathered from the field indicate that the oocytes of *Arenicola marina* may be spawned early in the spawning period (Williams *et al.*, 1997). Fertilization success is limited by sperm puddle density, and not all oocytes are fertilized after one exposure to sperm. Consequently, longer-lived oocytes confer an advantage by being capable of fertilizing and developing up to 5 days after spawning. We propose that the fertilization strategy of *A. marina* is that the female releases her eggs at the beginning of the spawning period, and that overall fertilization success is the result of an accumulation of fertilizations over the 4- to 5-day spawning period (see Williams *et al.*, 1997). In comparison, the eggs and sperm of *Nereis virens* and *Asterias rubens* are more likely to be dispersed by water currents before their longevity has expired, according to Levitan (1995). However, the dilution of gametes beyond fertilizable concentrations in the field has been examined for only a few species of echinoderm, and the theory that dilution is more important than longevity may be found not to hold true for a wider range of free-spawning species. Thomas has demonstrated that the viscosity of egg and sperm fluids in several free-spawning echinoderms (Thomas, 1994a) and polychaetes (Thomas, 1994b) is such that dilution is delayed and gamete longevity may still be important.

The longevity of *Arenicola marina* sperm at low densities may also be an adaptation to the fertilization strategy of this species. Sperm are released onto the surface of the sediment at low water, where they coalesce into dense puddles. It may be several hours before they are dispersed by the tide, so the lack of activity in high concentration, which is further enhanced by light (Pacey *et al.*, 1994b), prevents the spermatozoa from expending too much energy while they are remote from the eggs. After the sperm are diluted and carried into the female burrow, there may be a further delay before they encounter an egg, because the rate of irrigation of the female burrow is low. Consequently, interaction between sperm and egg in *Arenicola marina* may occur many hours after either has been spawned, in contrast to most other free-spawning invertebrates.

Egg-derived compounds could play an important role in the fertilization success—and thus the fertilization strategy—of *Arenicola marina*. Stimulatory compounds from the eggs would ensure that sperm were most active when close to an oocyte. Thus, there is a twofold process. The hydrodynamic factors bring the sperm and eggs into brief contact, and the chemicals emanating from the egg stimulate the sperm to respond. The lack of turbulent mixing in the female burrow of *Arenicola marina* and the comparatively long viable life of the sperm may mean that compounds released by the egg that enhance sperm swimming are of particular importance in increasing the probability of encounters between sperm and egg.

Acknowledgments

The authors are grateful for the financial support of the Natural Environment Research Council (grant GR3/10521 and DEMA grant GST/02/2164 to MGB, NERC studentship to MEW). We are also grateful to Dr. G.J. Watson and Dr. L.A. Paterson for assistance in field collections, and to Peter Cowin of Seabait Ltd. for providing *Nereis virens*. This manuscript benefited from the comments of Dr. Phil Yund and an anonymous reviewer.

Literature Cited

André, C. and M. Lindegarth. 1995. Fertilization efficiency and gamete viability of a sessile, free-spawning bivalve, *Cerastoderma edule*. *Ophelia* **43:** 215–227.

Bass, N. R., and A. E. Brafield. 1972. The life cycle of the polychaete *Nereis virens*. *J. Mar. Biol. Assoc. UK* **52:** 701–726.

Bentley, M. G., and A. A. Pacey. 1992. Physiological and environmental control of reproduction in polychaetes. Pp. 443–481 in *Oceanography and Marine Biology: An Annual Review*, Vol. 30. M. Barnes, A. D. Ansell, and R. N. Gibson, eds. UCL Press, London.

Benzie, J. A. H., and P. Dixon. 1994. The effects of sperm concentration, sperm:egg ratio, and gamete age on fertilization success in crown-of-thorns starfish (*Acanthaster planci*) in the laboratory. *Biol. Bull.* **186:** 139–152.

Bishop, J. D. D. 1998. Fertilization in the sea: are the hazards of broadcast spawning avoided when free-spawned sperm fertilize retained eggs? *Proc. R. Soc. Lond. B* **265:** 725–731.

Bolton T. F., and J. N. Havenhand. 1996. Chemical mediation of sperm activity and longevity in the solitary ascidians *Ciona intestinalis* and *Ascidiella aspersa*. *Biol. Bull.* **190:** 329–335.

Brokaw, C. J. 1984. Cyclic AMP-dependent activation of sea urchin and tunicate sperm motility. *Ann. N. Y. Acad. Sci.* **438:** 132–141.

Brown, G. G., and J. R. Knouse. 1973. Effects of sperm concentration, sperm aging, and other variables on fertilization in the horseshoe crab, *Limulus polyphemus* L. *Biol. Bull.* **144:** 462–470.

Chia, F. S., and L. R. Bickell. 1983. Echinodermata. Pp. 545–619 in *Reproductive Biology of Marine Invertebrates Vol. II: Spermatogenesis and Sperm Function*, K. G. and R. G. Adiyodi, eds. Wiley and Sons, New York.

Clapper, D. L., and G. G. Brown. 1980. Sperm motility in the horseshoe crab, *Limulus polyphemus*. I. Sperm behavior near eggs and motility initiation by egg extracts. *Dev. Biol.* **76:** 341–349.

Cosson, M. P. 1990. Sperm chemotaxis. Pp. 103–135 in *Controls of Sperm Motility: Biological and Clinical Aspects*, C. Gagnon, ed. CRC Press, Boca Raton, FL.

Dan, J. C. 1950. Fertilization in the medusan, *Spirocodon saltatrix*. *Biol. Bull.* **99:** 412–415.

Gibbons, B. H. 1980. Intermittent swimming in live sea urchin sperm. *J. Cell. Biol.* **84:** 1–12.

Hamel, J.-F., and A. Mercier. 1995. Prespawning behavior, spawning, and development of the brooding starfish *Leptasterias polaris*. *Biol. Bull.* **188:** 32–45.

Havenhand, J. N. 1991. Fertilization and the potential for dispersal of gametes and larvae in the solitary ascidian *Ascidia mentula* Müller. *Ophelia* **33:** 1–15.

Iijima, R., J. Kisugi, and M. Yamazaki. 1995. Antifungal activity of aplysianin-e, a cytotoxic protein of sea-hare (*Aplysia kurodai*) eggs. *Dev. Comp. Immunol.* **19:** 13–19.

Kanatani, H. 1979. Hormones in echinoderms. Pp. 273–307 in *Hormones and Evolution*, Vol. 1, E. J. W Barrington, ed. Academic Press, London.

Levitan, D. R. 1995. The ecology of fertilization in free-spawning invertebrates. Pp. 123–156 in *Ecology of Marine Invertebrate Larvae*, L. McEdward, ed. CRC Press, Boca Raton, FL.

Levitan, D. R., M. A. Sewell, and F.-S. Chia. 1991. Kinetics of fertilization in the sea urchin *Strongylocentrotus franciscanus*: interaction of gamete dilution, age, and contact time. *Biol. Bull.* **181:** 371–378.

Lillie, F. R. 1915. Studies on fertilization. VII: Analysis of variations in the fertilizing power of sperm suspensions of *Arbacia*. *Biol. Bull.* **28:** 229–251.

Maier, I., and D. G. Müller. 1986. Sexual pheromones in algae. *Biol. Bull.* **170:** 145–175.

Meidel, S. K. and P. O. Yund. 2001. Egg longevity and time-integrated fertilization in a temperate sea urchin (*Strongylocentrotus droebachiensis*). *Biol. Bull.* **201:** 84–94.

Miller, R. L. 1970. Sperm migration prior to fertilization in the hydroid *Gonathyrea loveni*. *J. Exp. Zool.* **175:** 493–504.

Miller, R. L. 1975. Chemotaxis in the spermatozoa of *Ciona intestinalis*. *Nature* **254:** 244–245.

Miller, R. L. 1977. Chemotactic behaviour of the sperm of chitons (Mollusca: Polyplacophora). *J. Exp. Zool.* **202:** 203.

Miller, R. L. 1978. Site-specific sperm agglutination and the timed release of a sperm chemoattractant by the egg of the leptomedusan, *Orthopyxis caliculata*. *J. Exp. Zool.* **205:** 385.

Miller, R. L. 1984. Sperm chemo-orientation in the metazoa. Pp. 275–357 in *Biology of Fertilization*, C. B. Metz and A. Monroy, eds. Academic Press, New York.

Miller, R. L. 1985. Demonstration of sperm chemotaxis in the Echinodermata: Asteroidea, Holothuroidea and Ophiuroidea. *J. Exp. Zool.* **234:** 383–414.

Miller, R. L., J. J. Mosares, and J. L. Ram. 1994. Species-specific sperm attraction in the zebra mussel, *Dreissena polymorpha* and the quagga mussel, *Dreissena bugensis*. *Can. J. Zool.* **72:** 1764–1770.

Nichols, D., and M. F. Barker. 1984. A comparative study of reproductive and nutritional periodicities in two populations of *Asterias rubens* (Echinodermata: Asteroidea) from the English Channel. *J. Mar. Biol. Assoc. UK.* **64:** 471–484.

Pacey, A. A., and M. G. Bentley. 1992. The fatty acid 8, 11, 14 eicosatrienoic acid induces spawning in the male lugworm *Arenicola marina*. *J. Exp. Biol.* **173:** 165–179.

Pacey, A. A., J. C. Cosson, and M. G. Bentley. 1994a. The acquisition of forward motility in the spermatozoa of the polychaete *Arenicola marina*. *J. Exp. Biol.* **195:** 259–280.

Pacey, A. A., J. C. Cosson, and M. G. Bentley. 1994b. Intermittent swimming in the spermatozoa of the lugworm *Arenicola marina* (L.) (Annelida, Polychaeta). *Cell Motil. Cytoskel et.* **29:** 186–194.

Pennington, J. T. 1985. The ecology of fertilization of echinoid eggs: the consequences of sperm dilution, adult aggregation, and synchronous spawning. *Biol. Bull.* **169:** 417–430.

Suzuki, N., and D. L. Garbers. 1984. Stimulation of sperm respiration rates by speract and resact at alkaline extracellular pH. *Biol. Reprod.* **30:** 1167–1174.

Thomas, F. I. M. 1994a. Physical properties of gametes in three sea urchin species. *J. Exp. Biol.* **194:** 263–284.

Thomas, F. I. M. 1994b. Transport and mixing of gametes in three free-spawning polychaete annelids, *Phugmatopoma californica* (Fewkes), *Sabellaria cementarium* (Moore) and *Schizobranchia insignis* (Bush). *J. Exp. Mar. Biol. Ecol.* **179:** 11–27.

Toomey, B. H., and D. Epel. 1993. Multixenobiotic resistance in *Urechis caupo* embryos: protection from environmental toxins. *Biol. Bull.* **185:** 355–364.

Watson, G. J., and M. G. Bentley. 1998. Action of CMF (Coelomic Maturation Factor) on oocytes of the polychaete *Arenicola marina* (L.). *J. Exp. Zool.* **281:** 65–71.

Watson, G. J., M. E., Williams, and M. G. Bentley. 2000. Can synchronous spawning be predicted from environmental parameters? A case study of the lugworm *Arenicola marina*. *Mar. Biol.* **136:** 1003–1017.

Williams, M. E., M. G. Bentley, and J. D. Hardege. 1997. Assessment of field fertilization success in the infaunal polychaete *Arenicola marina* (L.). *Invertebr. Reprod. Dev.* **31:** 189–197.

Yund, P. O. 1990. An *in situ* measurement of sperm dispersal in a colonial marine hydroid. *J. Exp. Zool.* **253:** 102–106.

Yund, P. O. 2000. How severe is sperm limitation in natural populations of marine free-spawners? *Trends Ecol. Evol.* **15:** 10–13.

Reference: *Biol. Bull.* **202:** 43–52. (February 2002)

Morphological Variations Among Larval-Postlarval Intermediates Produced by Eyestalk Ablation in the Snapping Shrimp *Alpheus heterochaelis* Say

PAUL S. GROSS[1,*] AND ROBERT E. KNOWLTON[2]

[1]*Department of Biochemistry and Molecular Biology, Medical University of South Carolina, Charleston, South Carolina 29425; and* [2]*Department of Biological Sciences, George Washington University, Washington, DC 20052*

Abstract. The eyestalk of many crustaceans contains the X-organ, the presumptive site of production and release of many protein and peptide hormones into the hemolymph. Removal of the eyestalk deprives the animal of these hormones and is known to affect many physiological processes in the adult and developing larva. In the snapping shrimp *Alpheus heterochaelis* Say, eyestalk ablation performed early in larval development has profound effects on morphogenesis, causing the appearance of supernumerary larval stages, accompanied by retardation and even complete arrest of morphogenesis. In this study, we examined the effects on morphogenesis of bilateral eyestalk removal at carefully controlled intervals. We found that the crucial point for this operation—the point at which the animal attains the ability to metamorphose fully—is just before the onset of ecdysis to the third instar. Additionally, the pattern of development and morphogenesis among body segments follows a discernible double gradient pattern along the anterior-posterior axis in which the extremities of the animal attain the potential for morphogenetic advance prior to the central thorax. This pattern of morphogenesis, punctuated by ecdysis, is a continuous rather than a stepwise or compartmentalized phenomenon.

Introduction

In decapod Crustacea, larval morphogenesis generally consists of small increments of structural change (from the initial hatching morphology) manifested as several zoeal instars, culminating in a distinct change (metamorphosis) to a "postlarva" or "megalops" that more closely resembles the adult form (Williamson, 1982; Felder *et al.*, 1985). The metamorphic molt is usually of sufficient magnitude for the postlarva to assume the life habit of the adult, but some larval features may be retained until the next molt, to a juvenile form that is similar to the adult except for size.

Morphogenesis and molting history can be affected by environmental factors such as diet, temperature, and photoperiod (reviewed in Knowlton, 1974), and by hormonal cues. An "X-organ–sinus gland complex," located in each of the paired eyestalks just medial to each optic complex, has long been known as a source of many hormones that can affect various physiological processes either directly or indirectly in adult decapods (reviewed in Carlisle and Knowles, 1959; Passano, 1960, 1961; Welsh, 1960; Kelly, 1967; Jenkin, 1970; Kleinholz, 1976; Cooke and Sullivan, 1982; and Fingerman, 1987). This complex also plays a role in control of larval development (reviewed in Christiansen, 1988; Charmantier and Charmantier, 1998). Eyestalk ablation has been shown to produce supernumerary larval stages, larval-postlarval intermediates, or both in various crustaceans such as *Rhithropanopeus harrisii* (Costlow, 1966) and *Homarus americanus* (Charmantier *et al.*, 1985; Charmantier and Aiken, 1987).

Larvae of the snapping shrimp *Alpheus heterochaelis* Say from coastal North Carolina (described by Knowlton, 1973) exhibit some unique developmental features. The larval phase is abbreviated, lasting only 4–5 days when reared at 22–25°C and consisting of three larval (zoeal) and one postlarval stage. The larvae hatch with a large amount of stored yolk and oil, which they apparently use as the sole source of energy throughout the larval period. Exogenous

Received 12 June 2001; accepted 27 November 2001.

* To whom correspondence should be addressed. E-mail: grossp@musc.edu

feeding does not begin until the postlarval stage when the mouthparts develop into functional feeding organs (Gross and Knowlton, 1991).

Eyestalkless *A. heterochaelis* larvae have been observed to form larval-postlarval intermediates consistently as long as eyestalk removal is performed prior to the midpoint of larval Stage III (Knowlton, 1988, 1994). An array of different morphologies was discerned, depending on the time (during the second and third larval instars) that the eyestalk extirpation was performed. Knowlton (1994) described four types of larval intermediates, designated stages IVA through IVD, each possessing more developmentally advanced features and occurring between stage III and the postlarva. In his study, operations were performed once a day at the same time of day over the 4- to 5-day larval period. In the present study, this protocol was refined by increasing the number of time points at which operations were performed to seven (*i.e.*, at 2 h, at 20 h, and at subsequent 10-h intervals over the duration of larval development), utilizing more animals at each time point, and maintaining the animals over several instars (molts). Two series of experiments, each involving larvae hatched from eggs borne by four different females, were executed. Specific objectives of these experiments were (1) to ascertain whether morphogenesis occurs in discrete steps or is continuous and (2) to establish if extirpation at various times results in developmental arrest (either complete or delayed), and whether there is a critical threshold time after which development to the postlarval stage is determined.

Materials and Methods

Collection and maintenance of adults

Ovigerous adult female specimens of *Alpheus heterochaelis* were collected periodically during the summer months at three sites ("Duncan's Green," "Research Cove," and Radio Island) in Beaufort, North Carolina. Each shrimp was maintained individually in a 2-l aquarium containing 1.5 l of aerated (by pump and stone) seawater and an oyster shell "house" for the shrimp to hide under. The animals were maintained on a cycle of 14 h daylight and 10 h darkness and were fed Tetramin large flake fish food *ad libitum*. Gravid females were assessed daily for brood maturity. To establish the absolute age of any brood, only larvae for which the hatching event was actually observed were used.

Rearing of larvae

Seawater used in all experimental procedures was prepared as described in Gross and Knowlton (1997). Hatched zoea larvae were maintained in UV-treated seawater, which was further filter sterilized through a 0.45-μm filter to which the following chemicals were added: 50 ng/ml amphotericin B, an antifungal agent, plus 50 μg/ml each of the antibiotics streptomycin sulfate and ampicillin (ICN Biochemicals, Costa Mesa, CA). Larvae were maintained in 10 ml of processed seawater, changed daily, in an incubator at a constant 25°C to provide optimum development and a "standard" 4-day larval development pattern for control animals (Knowlton, 1973). When animals reached the postlarval and juvenile condition, they were fed freshly hatched *Artemia salina* (brine shrimp) nauplii *ad libitum*. General laboratory procedures are given in Gross and Knowlton (1997, 1999).

Protocol of operations

Immediately after all larvae in a particular brood had molted to larval stage II (about 2–3 h post-hatching), a subset of the brood, designated t_2 (for 2 h post-hatching) was subjected to eyestalk extirpation. A second population was ablated 18 h after t_2 and designated t_{20}. Eyestalk ablations were then performed at 10-h intervals after t_{20} up to 70 h, with groups being designated accordingly. In a previous study, it was found that larvae ablated at 10 h post-hatching (t_{10}) closely resembled those of the t_{20} group (data not shown; Gross and Knowlton, 1991). Typically, eyestalk ablations at t_2 and t_{20} occurred during Stage II and all other ablations during larval stage III, with t_{30} occurring almost immediately after the molt to stage III. A number of larvae in each brood were retained as unoperated controls. The control group and each group of larvae designated for surgery at a particular time point had roughly equal numbers of animals.

Analysis of intermediate morphologies

In the first series of experiments, a total of 274 larvae from four broods were used. After the final set of operations at t_{70}, each larva was individually monitored as it molted to the intermediate form (stage IV of Knowlton, 1994) or postlarva (in controls). Data pertaining to size differences are given in Gross and Knowlton (1999). At this time, the animal was preserved in 70% ethanol (EtOH). Each larva was then cleared in 5% KOH, stained using carmine-borax/35% EtOH, and placed in 100% glycerol by serial transfer, in preparation for structural examination and measurement (Guyer, 1906; Gross, 1995). Glycerin was chosen as the final medium because it maintains the clarity of the stained specimen; it is significantly more viscous than water, giving the specimen a greater internal rigidity; and it causes the otherwise brittle exoskeleton to become pliable, allowing the appendages to be moved and posed easily during analysis of larval characteristics. Both dissecting and compound microscopes were used to analyze morphological features of the fourth and fifth instar intermediate forms with respect to time of ablation, and were related to analogous morphological characters found in control postlarvae and juveniles.

In the second series of experiments, a separate set of 629 larvae was used. The procedure was similar to that already outlined except that the larvae were not sacrificed but were allowed to continue development through subsequent instars (molts). For consistency, operations on larvae were performed at the same time points. As they developed, live animals were examined for morphological diagnostic characteristics (along with instar duration and mortality; see Gross and Knowlton, 1997). Each larva was assigned a substage or "form" designation based on the system proposed by Knowlton (1994). Two behavioral characters were also recorded after each molting: (1) the orientation of the larva—dorsal side up (walking posture), consistent with an adult benthic life habit, or dorsal side down (swimming behavior), exhibited by pelagic larva; and (2) consumption of *Artemia salina* nauplii, as evidenced by food (opacity) in the stomach.

Results

Analysis of fourth instar (stage IV intermediate) morphology

The range of intermediates between stage III (third instar) and the postlarva (normally fourth instar) produced by bilateral eyestalk extirpation in these experiments is consistent with the four broad categories (*i.e.*, IVA-IVD) established by Knowlton (1994), but upon closer examination of individual specimen morphologies, some modifications of these broad categories are indicated. With more frequent ablation and monitoring, 10 forms were discerned, whose major structural features are summarized in Table 1.

Stage IVA, as described by Knowlton (1994), differs from stage III (see Knowlton, 1973) only with respect to abdominal development, and two distinct subtypes of the IVA form were discerned. In general, Stage IVA_1 is typified by very little morphological change. Stage IVA_1 animals were "more postlarval" with respect to the tail region (*e.g.*, formation of uropodal endopodite and acquisition of the postlarval number of terminal setae on the telson). However, the telson of each IVA_1 larva retained its stage III shape, with the uropodal exopodite being underdeveloped, lacking both the spine located on the outer margin and the distal-most joint, and the endopodite being smaller than that of a normal postlarva in most cases (69.6% of those examined). Stage IVA_2 animals often possessed pleopods about normal postlarval size and bearing long plumose setae (as in the postlarva); less often (in 31.6% of those examined), the uropodal endopodite was reduced. The IVA_1 form was encountered exclusively among larvae ablated at t_2, whereas the IVA_2 form was encountered primarily among t_{20} larvae (Table 2).

Table 1

Recognition characters of expanded intermediate morphogenetic categories (forms)

Form	Additional key features
A_1	Pleopods asetose (or with very short setae)
A_2	Pleopods setose (=Knowlton's stage IVA)
A/B	Antennal flagellum with 5 segments Antennule flagella as in stage IVA
B	Antennal flagellum with 9–16 segments, protopod with basicerite Antennular inner and outer flagellum segmented, peduncle with stylocerite (=Knowlton's stage IVB)
B/C	Exopods of pereiopods 1–4 setose Exopod of pereiopod 4 shortened
C_1	Telson lacks pair of dorsal spines
C_2	Exopods of pereiopods 1–4 shorter but setose Endopods of pereiopods 1–5 with more claw-like dactyls (=Knowlton's stage IVC)
C/D	Exopods of pereiopods 1–3 setose and shortened Exopod of pereiopod 4 asetose, nearly vestigial
D	Exopods of pereiopods 1–2 shorter but setose Exopods of pereiopods 3–4 asetose, nearly vestigial (=Knowlton's stage IVD)
D/PL	Exopod of pereiopod 1 setose, nearly vestigial Exopods of pereiopods 2–4 asetose, vestigial
E	Exopods of pereiopods 1–4 asetose, vestigial (as in postlarva) Telson with two pairs of spines on dorsal surface (as in juvenile)
F	Exopods of pereiopods 1–3 vestigial (absent on 4) Telson with two pairs of spines on dorsal surface (as in juvenile)
G	Exopods of pereiopods 1–2 vestigial (absent on 3 and 4) Telson with two pairs of spines on dorsal surface (as in juvenile)

Stage IVB, as described by Knowlton (1994), incorporates the abdominal development seen in the IVA_2 form with an array of morphogenetic advances in the head region, but development in the thoracic region is not yet seen. Much variation in form was noted among IVB larvae, especially with regard to the development of head appendages. A few larvae had the full (*i.e.*, normal postlarval) complement of 4 segments on the outer flagellum of the antennule, but typically only 1–2 segments were present. Conversely, the inner flagellum of the antennule usually was postlarval in form (possessing 3 segments), but a few larvae had 1–2 segments added. A wide range of antennal flagellum segments (1–22) was displayed by animals in this form, but even when a full complement of segments was present (22–26), the overall length of the antennal flagellum was significantly different ($F = 77.30$, $P < 0.05$) than in the normal postlarva. Although the third and final segment of the antennular peduncle was usually present, the basicerite was rarely added and the statocyst never found among stage IVB animals. This form was most often produced when eyestalks were removed late in stage II (t_{20}) and early in stage III (t_{30}), but many other intermediate forms were also produced as a result of eyestalk ablation during this period (Table 2). Some larvae, primarily in the t_{20} group IVA/B, showed very little advance over the IVA_2 form but did have 1–2 segments added to the antennal flagellum (Table 1). The A/B designation indicates that these larvae were not quite equivalent to either the IVA_2 or IVB forms.

Table 2

Distribution of fourth instar forms at each operative time point (percent of total survivors per operative time point)

Fourth instar form	Operation time (in hours)							
	t_2	t_{20}	t_{30}	t_{40}	t_{50}	t_{60}	t_{70}	Control
A_1	83.7 (72)							
A_2	12.8 (11)	40.3 (27)						
A/B	1.2 (1)	20.9 (14)	2.5 (2)					
B	2.3 (2)	37.3 (25)	38.0 (30)	9.9 (8)				
B/C			2.5 (2)					
C_1			13.9 (11)	4.9 (4)				
C_2		1.5 (1)	22.8 (18)	14.8 (12)				
C/D			3.8 (3)	1.2 (1)				
D			12.7 (10)	38.3 (31)	10.6 (9)	3.5 (3)		
D/PL				1.2 (1)	4.7 (4)	2.3 (2)	2.3 (2)	
PL			3.8 (3)	29.6 (24)	84.7 (72)	91.2 (81)	97.7 (85)	100 (151)

Data in parentheses are actual number of animals (*n*) assigned to the category. Designations A_1 to D/PL indicate fourth instar forms that are intermediate between larva and postlarva (PL).

In Knowlton's (1994) stage IVC, the head and abdominal regions are morphologically postlarval, but the thoracic appendages are only partially developed toward the postlarval form. Like the previous intermediate forms, the IVC form generally swims ventral side up and is incapable of feeding. In the present study, three additional IVC types, based on the degree of morphological advance in the thorax and abdomen, were distinguished (Table 1).

Stage IVB/C larvae, found only among animals ablated at t_{30} (Table 2), exhibited most of the characteristics of Knowlton's stage IVC, but only the exopod of pereiopod 4 showed reduction in size and loss of swimming function. Animals designated stage IVC_1 lacked the pair of spines on the dorsal side of the telson about three-quarters of the length distal from the joint connecting the telson to the sixth abdominal somite (as in the postlarva), whereas those designated stage IVC_2 possessed these spines. In addition, the IVC_1 form was more commonly found in animals from the t_{30} group (relative to the t_{40} group). The IVC_2 form was more common than the IVC_1 form among larvae ablated at t_{40} (Table 2).

Some characteristics were shared by all larvae classified as stage IVC. For example, although the uropodal exopodite is jointed in the postlarva, it was never jointed in animals classified as stage IVC; however, the typical postlarval spine located on the outer margin was always acquired. The antennal flagellum was essentially postlarval in its length and number of segments. In some animals, the inner and outer antennular flagella had 3 segments instead of the postlarval 4. The antennular peduncle was always 3-segmented and the basicerite was usually present, but the statocyst was never completely formed.

The thoracic appendages of the stage IVC form (both IVC_1 and IVC_2) were in many ways still similar to those of earlier intermediate forms, and morphogenetic advance was more pronounced in posterior thoracic appendages than in the anterior ones. The exopods of pereiopods 1 and 2 exhibited almost no change relative to stage III. However, those of pereiopods 3 and 4 were dramatically shortened (but not to the extent seen in the normal postlarva) and curled in appearance, with 4–6 misshapen setae on each terminus. Pereiopod 5, which lacks a swimming exopod throughout development, remained 7-segmented, but its dactyl was blunter than the very long styliform appendage associated with Stage III. All joints on this appendage appeared to be functional, with the joint between the merus and carpus modified to form a knee-like joint more suited to walking. The endopods of pereiopods 3 and 4 underwent proportionately more morphological change (compared with those of pereiopods 1 and 2). In most animals, they had the full complement of 7 segments (sometimes 6), with the styliform dactyl being replaced by a blunter form; joints on these appendages were always functional. The endopod of pereiopod 2 displayed the most segments (8–10), but development was incomplete as the joints were not articulating. New segments were usually added to the endopod of pereiopod 1, but the joints of this appendage were never fully articulated at this stage.

Individuals assessed as stage IVD (Knowlton, 1994), as exemplified by larvae ablated at t_{30}–t_{60} (Table 2), possessed most of the characteristics of the postlarva while still retaining a few larval characteristics. In these animals, the telson was postlarval in shape, possessing the typical 4 + 4 terminal setation pattern and the characteristic pair of spines located on the dorsal surface. The uropods were fully developed, with the exopodite bearing both the outer spine and distal joint. The antennal flagellum was as long as that of the typical postlarva, with a full complement of segments (22–

26). Some specimens possessed 3-segmented inner and outer antennular flagella (rather than the usual 4 segments), but the peduncle was always 3-segmented, with basicerite and statocyst fully developed. These larvae exhibited complete transformation of pereiopods 3–5 to postlarval form. The endopod of pereiopod 1 was morphologically postlarval in this stage as well, always being composed of the full complement of 6 segments, with the elbow-like joint between merus and carpus, and completion of the joint between the propodus and dactyl to form a functional chela. The endopod of pereiopod 2 still showed some variability in segment number (9–10), but was functionally complete, with an articulated chela and an elbow-like joint between the merus and first carpal article. Exopods of pereiopods 3 and 4 were usually devoid of setation and nub-like (Table 1), as in the postlarva; in some specimens, however, these exopods were longer than that of a normal postlarva. Exopods of pereiopods 1 and 2 were not functional but had not attained the naked nub-like appearance of the postlarva. Stage IVD animals typically walked ventral side down, like the postlarva, consistent with the presence of a fully developed organ of balance (statocyst). They were usually capable of feeding (also like the postlarva), as evidenced by the presence of *Artemia salina* nauplii remains in the stomach.

A few animals (C/D in Table 2) ablated at t_{30} and t_{40} possessed setose exopods on pereiopods 1–3. Similarly, a significant proportion of those larvae ablated at t_{50}–t_{70} possessed setation only on the exopod of pereiopod 1 (D/PL). These larvae appeared to be similar to the postlarva in other respects, except that the second pereiopodal endopod occasionally had 9 segments rather than 10.

In summary, detailed examination of ablated larvae from each time point yielded in essence a continuum of stage IV morphologies between larval stage III and the normal postlarva, and larvae ablated at t_{30} and t_{40} showed the greatest variability in intermediate form morphology (Table 2).

Analysis of fifth instar morphology

Intermediate morphologies encountered at the fifth instar (*i.e.*, after four molts post-hatching), which is normally the molt to a juvenile form, are enumerated in Table 3 with the same nomenclature used to describe fourth instar forms. A stage V designation identifies fifth instar intermediates, which are still morphologically intermediate between larval stage III and postlarva, while E, F, and G designations are reserved for individuals with characteristics intermediate between the postlarva (PL) and juvenile (J).

At the fifth instar, some larvae continued to exhibit a lag in morphological advancement. Some larvae ablated at t_2 (IVA_1 in Table 2) did not exhibit any structural change after the molt to the fifth instar (Table 3) and were designated stage VA_1 since another molt had occurred. However, most (55.5%) IVA_1 larvae exhibited slight morphological advancement (*i.e.*, they were morphologically identical to stage IVA_2) and were designated stage VA_2. A significant proportion of animals (39.7%) advanced to either stage VA/B or VB (equivalent to IVA/B and IVB, respectively). All but one of the t_2 animals died during this instar, with only a single stage VB larva surviving to molt unchanged to a sixth instar. A similar trend of developmental arrest is seen among larvae ablated at t_{20}: 75.8% of animals exhibiting stage IVA_2, IVA/B, or IVB morphology at the fourth instar (Table 2) did not advance morphologically beyond stage VB at the fifth instar (Table 3). However, three larvae from the t_{20} group molted to postlarval form, surviving to molt to a morphologically normal juvenile by the sixth instar. It is interesting that three t_{20} larvae had morphological features spanning the gap between form D and the juvenile. These three larvae (designated VD/PL/J) possessed setose exopods on pereiopods 1 and 2 (as in form D) and had a telson morphology (*i.e.*, two pairs of dorsal spines) consistent with that of a juvenile.

Many (45.0%) of the larvae ablated at t_{30}, which as fourth instars formed a wide array of larval-postlarval intermediate forms (Table 2), molted to the juvenile form at the next molt; nine animals (15.0%) resembled normal postlarvae at the fifth instar (Table 3). A significant number of animals from this group exhibited characteristics, noted under E in Table 1, that were intermediate between the normal postlarva and juvenile. Some larvae ablated at t_{30} were found to possess the juvenile telson morphology with vestigial exopod nubs on pereiopods 1–3, or on 1–2 only (remaining pereiopods being uniramous); these intermediate forms were designated F and G, respectively (Table 3). Of the broad spectrum of intermediate stage IV types noted among larvae ablated at t_{40} (Table 2), the majority (70.5%) molted to juvenile at the fifth instar, but most of the others (E in Table 3) retained all pereiopod exopod rudiments on pereiopods 1–4. All larvae from the t_{50}–t_{70} groups molted to the juvenile form at the fifth instar.

All animals surviving to the sixth instar, which attained some semblance of postlarval morphology at the fifth instar, were found to exhibit morphology consistent with classification as juveniles. Comparing the distribution of larval intermediates found at the fifth (*vs.* fourth) instar, larvae ablated prior to the molt to stage III (t_2 and t_{20}) appeared, for the most part, to be incapable of completing development (metamorphosis). Conversely, those ablated after the molt to stage III (t_{30} through t_{70}) completed metamorphosis by the sixth instar. However, animals ablated at t_{30} (and to some extent at t_{40}) showed a definite lag in morphogenesis relative to larvae ablated at later times and were more prone to appear as postlarval-juvenile intermediates during the fifth instar.

Table 3

Distribution of fifth instar forms at each operative time point (percent of total survivors per operative time point)

Fifth instar form	Operation time (in hours)							
	t_2	t_{20}	t_{30}	t_{40}	t_{50}	t_{60}	t_{70}	Control
A_1	4.8 (3)							
A_2	55.5 (35)	18.2 (6)						
A/B	11.1 (7)	9.1 (3)						
B	28.6 (18)	48.5 (16)	3.3 (2)					
B/C		6.1 (2)	1.7 (1)					
C								
D								
D/PL/J		9.1 (3)						
PL		9.1 (3)	15.0 (9)					
E			25.0 (15)	27.9 (17)				
F			3.3 (2)					
G			6.7 (4)	1.6 (1)				
J			45.0 (27)	70.5 (43)	100 (63)	100 (63)	100 (53)	100 (127)

Data in parentheses are actual number of animals (n) assigned to the category. Designations A_1 to D/PL/J indicate fifth instar forms that are intermediate between larva and postlarva (PL), designations E-G indicate intermediate forms between postlarva and juvenile (J)

Discussion

Distribution of larval intermediate types in relation to time of ablation

Results of our study indicate that in *Alpheus heterochaelis*, time of eyestalk ablation governs the amount of morphogenetic advance, such that more advanced forms are produced from successively later ablations (Table 2–3). Further, the array of larval-postlarval intermediate forms caused by eyestalk extirpation is virtually continuous. These forms (Table 1) resulted from operations carried out at seven different time points (t_x), with much morphological variation being noted within each t_x group as well as among groups. The range of morphogenetic variability was least among animals ablated either very early or very late and was at a maximum among the t_{30} and t_{40} groups. Larvae ablated at the earliest time point (t_2) were morphogenetically least advanced, most animals exhibiting the IVA_1 form (Table 2). This intermediate type was found only among larvae ablated at t_2 and not among larvae ablated 10 h post-hatching (Gross and Knowlton, 1991). The t_{20} group included animals ranging in form from IVA_2 to IVB, but the IVA_2 form was never found among t_{30} larvae, whose individuals exhibited IVB-IVD forms (Table 2). Among t_{40} animals, occurrences of the IVB form were fewer, whereas intermediates exhibiting the IVD morphology were more common. Stage IVC (*i.e.*, IVC_1, IVC_2, or IVC/D) animals were distributed between t_{30} and t_{40} and were essentially restricted to these groups. Larvae ablated after t_{40} exhibited progressively fewer intermediate types, and incidences of complete transformation to the postlarval form became the norm.

Crucial points in morphogenesis

The crucial point at which the *A. heterochaelis* larva becomes capable of completing morphogenesis to the juvenile condition (normally the fifth instar) seems to occur around the time of ecdysis to stage III. None of the larvae in the t_2 group changed structurally beyond form B (Table 2), and most of the t_{20} animals died without morphological advance beyond form B/C (Table 3). A small number of animals from the t_{20} group did succeed in attaining a postlarval morphology, or a form close to it (VD/PL/J), at the fifth instar, but only two individuals survived to molt to a morphogenetically normal juvenile at the sixth instar. Thus, with few exceptions, larvae ablated before the molt to stage III were incapable of morphogenetic advance to the postlarval or juvenile form. Similarly, in *Homarus americanus* (which exhibits a pattern of larval development similar to *A. heterochaelis*), Charmantier and Aiken (1987) noted that the critical period for eyestalk removal leading to developmental arrest and the appearance of larval-postlarval (stage IVa) intermediates was in molting stage D_1 of larval stage II. Conversely, *A. heterochaelis* larvae that underwent eyestalk ablation during stage III could complete morphogenesis to a feeding juvenile or could attain an intermediate morphology between postlarva and juvenile (*i.e.*, forms E, F, and G) during the fifth instar. However, a few animals ablated close to the completion of ecdysis to stage III did not advance beyond form B. Thus, the "turning point" separating completion of metamorphosis from developmental arrest seems to be at the interface between stages II and III at or about the time of ecdysis, which is in agreement with the findings of Knowlton (1994).

Whereas Knowlton (1994) did not note any further morphological changes among larvae ablated during stage II (before attaining the IVA or IVB form), our more detailed analysis showed that by the fifth instar most larvae exhibited some change in morphology relative to their stage IV counterparts. The majority of t_2 animals advanced from form A_1 to the A_2, A/B, or B form, and most t_{20} animals surviving to a fifth instar also advanced slightly in form. Thus it appears that even though metamorphosis is blocked by ablation before the third instar, morphogenesis is not completely arrested. Even among larvae that can complete metamorphosis to the juvenile form, the effects of eyestalk ablation may only be overcome over multiple instars and elongation of the larval period (Gross and Knowlton, 1999). On the other hand, even though t_{30} and t_{40} larvae were able to complete metamorphosis to a morphologically normal juvenile by the sixth instar, there was a definite lag in morphogenesis.

Form D animals are substantially different and more advanced than those of form C since they possess fully functional (articulating) thoracic endopods (as in the postlarva) and are able to feed, orient themselves ventral side down, and walk. It is apparent that at about 35–40 h post-hatching the third instar larva attains the ability to make, after molting to the fourth instar, a more "complete" morphological conversion from a planktonic larval existence to a more adult benthic existence. Ablation after about 35 h post-hatching more frequently resulted in the stage IVD form or more advanced forms (up to and including normal postlarva—Table 2). Most t_{50} individuals exhibited morphology consistent with the postlarva (at the fourth instar). But morphogenesis was not "finalized" until late in the third instar, since larvae with form D features were seen even among t_{70} animals.

The nature of the morphogenetic continuum

Carlisle and Knowles (1959) postulated that factors located in the X-organ and released at the sinus gland control molting and that morphogenesis is a stepwise process which coincides with the molt cycle and may even be controlled by it. This does not appear to be the case for *A. heterochaelis* larvae, which, when their eyestalks are ablated at various times, display a continuum of intermediate morphologies independently of the molting cycle. If molting and morphogenesis were inextricably tied, then it would be reasonable to assume that premature molting would either fail to produce any morphogenetic advance or would yield a stepwise array of developmental intermediates. Knowlton (1994) observed a limited array of intermediates in experiments in which eyestalks were ablated only once per day. However, by increasing the number of time points for eyestalk ablation, a more continuous array of intermediates was produced that encompassed many more intermediate morphological forms. Our results argue against developmental patterns in higher Crustacea being "fixed" (Gurney, 1939), with all individuals showing exactly the same changes at each molt; or "compartmentalized" (Fraser, 1936), with individuals exhibiting morphological variation within a limited range (compartment). Indeed, they provide ample evidence that development in these crustaceans is continuous—a gradual process in which different body segments attain the potential for differentiation into their adult morphology at different times. Removal of the eyestalk at intervals makes this aspect of gradual morphogenetic change more apparent and shows that molting and morphogenesis are concurrent but independently controlled processes.

The axis of morphogenetic change

Eyestalk ablation at various times interrupts the normal process of morphogenesis at different points along the morphogenetic continuum (described above). Differentiation appears to take place at different rates in each segment in a "double gradient" pattern. This is well evidenced by the descriptive data collected from groups of animals at each ablation time point. The ability to differentiate at the next molt is attained in the tail region first, with uropodal endopods and pleopods gaining the ability to differentiate to postlarval form (and size) as early as 2 and 20 h post-hatching, respectively. Under eyestalk control, ability to differentiate is attained in the head region slightly later, since larvae ablated at t_{20} and t_{30} begin to exhibit morphogenetic advances (changes in form and size of appendages) in the head region at the fourth instar. The segment bearing pereiopod 5 gains the ability to metamorphose (*i.e.*, convert the styliform dactyl to a blunter form and shorten in overall length) at the fourth instar at about the same time as the head appendages (around t_{30}), reinforcing the idea that determination is advancing forward from the tail. Among eyestalkless animals, determination in the middle region (thorax) occurs later than in the head and tail region and is attained in exopods of the third and fourth pereiopods well before those of the first and second.

Differentiation in form (*e.g.*, adding segments to appendages) precedes the potential for functional changes (*e.g.*, formation of movable joints). Pereiopod 5 differentiates to postlarval length and segment number with the t_{30} group, but functional joints are not commonly found on this appendage at the fourth instar in these animals, whereas in the t_{40} group the fifth pereiopod is usually fully functional by the fourth instar. Among larvae ablated at t_{30}, the third and fourth pereiopodal endopods were equivalent to controls in length and segment number, but functional joints on these appendages were generally not seen until later (*e.g.*, among t_{40} or t_{50} animals). At the fourth instar, endopods of pereiopods 1 and 2 both become functional among larvae ablated around t_{40} (or t_{50}). They lag behind pereiopods 3–5 in onset of morphogenesis (reaching postlarval length and segment number) and attainment of functionality (articulating joints).

One can hypothesize that, under normal circumstances, the ability to metamorphose (at the molt to the fourth instar) is attained at different times by different body regions and even by specific segments within a body region of the *A. heterochaelis* larva. Factors in the eyestalk either control this process directly, or different body segments become receptive at different times to a factor or factors released by the eyestalk. Morphogenetic advance is not manifested until ecdysis, but the potential for morphogenesis toward the postlarval form starts early in the second instar, increasing gradually and continuously over the larval period. This potential for morphogenesis (differentiation at the next molt) is not the same along the posterior-anterior axis but instead may be visualized as a "double gradient" extending from the posterior and anterior ends toward the thorax. The trend is that the capacity to differentiate develops in the abdomen and abdominal appendages (uropods and pleopods) first, followed shortly thereafter by the head and its appendages, and lastly by the thorax. In the thorax, determination occurs earliest in the segments bearing pereiopod 5 and maxilliped 1, while the last segment to be determined bears the second pereiopod. Thus, the double gradient simultaneously extends forward from the fifth pereiopod and backward from the first maxilliped, converging on the second pereiopod.

Possible mechanisms of hormonal control

Several models could account for the production, through bilateral eyestalk ablation, of larval-postlarval intermediate forms and for the double gradient pattern of gradual determination. One explanation is that eyestalk removal deprives the developing larva of a critical regulatory principle or hormone that causes a given segment to transform from larval to postlarval morphology, and that this potential is realized gradually or at different times in different segments. The functional details of these mechanisms are still a matter of conjecture.

The simplest explanation for the appearance of larval-postlarval intermediate forms, advanced by Knowlton (1994), posits the existence of a morphogenetic hormone (MH) that is secreted by the eyestalk (presumably by the X-organ–sinus gland complex). This release would necessarily be gradual and begin early in stage II. Imam (1982) noted that certain tissues having a glandular appearance early in stage III differentiate in the larval eyestalk, only to degenerate in the postlarval eyestalk, surmising that these structures play a secretory role in the control of morphogenesis. A morphogenetic hormone would have to activate different segments at different times: either a segment could respond when the hormone reached a specific (and variable from segment to segment) concentration threshold in that segment, or it could respond only at a specific time in the morphogenetic continuum. If morphogenetic activation of certain segments does depend on a certain MH threshold, then removal of the eyestalk (which deprives the developing larva of any further production of this hormone) should produce morphogenetic arrest in those segments—presumably the more central thoracic ones—that were below threshold at the time of eyestalk removal. This condition should be permanent for those segments below threshold, since circulating titers of the morphogenetic factor would be below threshold level at the time of ablation. Clearly this is not the case since almost all larval-postlarval intermediates produced by means of bilateral eyestalk ablation during stage III are capable of metamorphosis to a normal form, given enough time.

If specific segments became responsive to MH at different times during the morphogenetic continuum, then in order for morphogenesis to continue in those segments that are activated later or at a slower rate, MH would have to be available in the circulation well after its source was removed. MH would thus have to be an extraordinarily long-lived factor, which is not typical for circulating hormones. Alternatively, MH may be released in small amounts during stage II (enough to instigate abdominal morphogenesis even after eyestalk ablation), but this release is either not adequate to activate other body regions or other body regions are unresponsive at this stage. After the molt to stage III, MH may be released in a quantity high enough to instigate morphogenesis in all body regions but in a quantity too low to control the timing of morphogenesis (since larvae ablated at t_{30} exhibit a wide variety of larval-postlarval intermediates but can eventually attain the normal juvenile form), especially in the thoracic region. That is, circulating titers of MH may control the timing of morphogenesis in each segment, but activation depends on a certain basal concentration of MH being released.

In insects, morphogenesis is not controlled by a hormone that instigates the process but by a metamorphosis-inhibiting factor (MIF) or juvenile hormone (JH) that inhibits its onset until a specific time (pupation). This hormone (JH) is maintained in high titers during the larval phase and drops precipitously at metamorphosis. If the control of metamorphosis were similar in the Crustacea, it seems more likely that the eyestalk produces some sort of regulatory factor, which controls morphogenesis through a second hormone.

Some inferential evidence for a crustacean juvenile hormone or metamorphosis-inhibiting factor does exist. Freeman and Costlow (1983) found that whole-body extracts of stage III *Rhithropanopeus harrisii* larvae inhibited resorption of the large dorsal spine (characteristic of the zoea) *in vitro*. Further, Laufer and Borst (1988) have advanced the idea that methyl farnesoate (MF), produced in the mandibular organ (MO), functions as a MIF; they established that control of its secretion is under the influence of tissues in the eyestalk. It has been shown conclusively that the X-organ–sinus gland complex secretes a mandibular organ inhibiting hormone (MOIH), which controls titers of MF by inhibiting its production within the MO (Liu and Laufer, 1996; Wainwright *et al.*, 1996; Liu *et al.*, 1997)

The results of the present research cannot conclusively distinguish between Knowlton's "MH hypothesis" and the existence of a MIF, and it may be that both systems exist in tandem. Knowlton (1994) asserted that in such a case it would be a balance between MIF and MH that controls the onset and timing of morphogenesis. But on the basis of this and other research (*e.g.*, Freeman and Costlow, 1983), it is possible that one or more factors, released from the eyestalk, inhibit MIF function or release from a second gland, and that different body segments have unique thresholds to MIF titers. The hypothesis that the eyestalk produces a regulatory hormone modulating the release of MIF would partially explain the double gradient pattern of morphogenetic potentiation in *A. heterochaelis* larvae if, as postulated by Borst *et al.* (1987), the mandibular organ is the source of MIF and that MIF is in fact MF. Simple proximity to this gland could be related to circulating titers of MIF. The extreme ends of the animal could be subjected to lower amounts of MIF naturally, by virtue of being the most distant from the mandibular organ, and thus would be released from inhibition earlier, while the central body segments would be proportionately more affected by MIF and released from inhibition later as titers of MIF dropped off under the influence of eyestalk secretion. Release of MIF and circulating titers may be controlled by a factor released from the X-organ–sinus gland complex in the intact animal. In eyestalkless animals, responsiveness to MIF may drop over time (even though circulating titers may not), or circulating titers of MIF may fall even without the influence of the factor or factors released by the eyestalk (though more gradually than in intact animals). This could produce the double gradient effect as each segment becomes progressively less responsive or titers fall below the unique threshold of each segment sequentially.

The idea that MF is the active JH in crustaceans is still very much in doubt, but some compelling evidence does exist. Exposure to MF has been shown to retard metamorphosis in *H. americanus* (Borst *et al.*, 1987), to retard early development in *Macrobrachium rosenbergii* (Abdu *et al.*, 1998a), and to have a juvenilizing effect on *Balanus amphitrite* larvae (Smith *et al.*, 2000). However, as pointed out by Abdu *et al.* (1998b), these effects could be due to nonspecific toxicity related to continuous exposure to MF. These same authors (Abdu *et al.*, 1998b) present a strong case that MF is the direct hormonal agent controlling metamorphosis; the arguments are particularly convincing when coupled with the identification of an eyestalk-related MOIH. In relation to these studies, the present work clearly indicates that MIF, be it MF or some other factor, controls metamorphosis directly and that the relationship between morphogenesis and molting is not one that affects molt timing but one that affects hormonal activation of the remodeling process itself.

Literature Cited

Abdu, U., P. Takac, G. Yehezkel, R. Chayoth, and A. Sagi. 1998a. Administration of methyl farnesoate through the *Artemia* vector, and its effect on *Macrobrachium rosenbergii* larvae. *Isr. J. Aquacult. Bamidgeh* **50:** 73–81.

Abdu, U., P. Takac, H. Laufer, and A. Sagi. 1998b. Effect of methyl farnesoate on late larval development and metamorphosis in the prawn *Macrobrachium rosenbergii*. (Decapoda, Palaemonidae): A juvenoid-like effect? *Biol. Bull.* **195:** 112–119.

Borst, D. W., H. Laufer, M. Landau, E. S. Chang, W. A. Hertz, F. C. Baker, and D. A. Schooley. 1987. Methyl farnesoate and its role in crustacean reproduction and development. *Insect Biochem.* **17:** 1123–1127.

Carlisle, D. B., and F. Knowles. 1959. *Endocrine Control in Crustaceans.* Cambridge University Press, London. 120 pp.

Charmantier, G., and D. E. Aiken. 1987. Intermediate larval and postlarval stages of *Homarus americanus* H. Milne Edwards, 1837 (Crustacea: Decapoda). *J. Crustac. Biol.* **7:** 525–535.

Charmantier, G., and M. Charmantier-Daures. 1998. Endocrine and neuroendocrine regulations in embryos and larvae of crustaceans. *Invertebr. Reprod. Dev.* **33:** 273–287.

Charmantier, G., M. Charmantier-Daures, and D. E. Aiken. 1985. Eyestalk involvement in the control of metamorphosis in *Homarus americanus. C. R. Acad. Sci. Paris* **300:** 271–276.

Christiansen, M. E. 1988. Hormones in decapod larvae. Pp. 47–68 in *Aspects of Decapod Crustacean Biology, Symposium of the Zoological Society of London*, A. A. Fincham and P. S. Rainbow, eds. Clarendon Press, Oxford.

Cooke, I. M., and R. E. Sullivan. 1982. Hormones and neurosecretion. Pp. 205–290 in *The Biology of Crustacea*, Vol. 3, D. E. Bliss, ed. Academic Press, New York.

Costlow, J. D., Jr. 1966. The effect of eyestalk extirpation on larval development of the mud crab, *Rhithropanopeus harrisii* Gould. *Gen. Comp. Endocrinol.* **7:** 255–274.

Felder, D. L., J. W. Martin, and J. W. Goy. 1985. Patterns in early postlarval development of decapods. Pp. 163–225 in *Larval Growth, Crustacean Issues*, Vol. 2. A. M. Wenner, ed. A. A. Balkema, Rotterdam.

Fingerman, M. 1987. The endocrine mechanisms of crustaceans. *J. Crustac. Biol.* **7:** 1–24.

Fraser, F. C., 1936. On the development and distribution of young stages of the krill (*Euphausia superba*). *Discovery Rep.* **16:** 40–48.

Freeman, J. A., and J. D. Costlow. 1983. Endocrine control of spine epidermis resorption during metamorphosis in crab larvae. *Roux Arch. Dev. Biol.* **192:** 362–365.

Gross, P. S. 1995. Intrinsic control of larval morphogenesis and molting in the caridean shrimp *Alpheus heterochaelis* Say. Ph.D. dissertation, George Washington University, Washington, DC. 137 pp.

Gross, P. S., and R. E. Knowlton. 1991. Fine structure of eyestalkless *Alpheus heterochaelis* zoeal-postlarval intermediate forms. *Am. Zool.* **31:** 23A.

Gross, P. S., and R. E. Knowlton. 1997. Effects of timed eyestalk ablation on molting in larvae of the snapping shrimp, *Alpheus heterochaelis* Say. *Invertebr. Reprod. Dev.* **32:** 119–126.

Gross, P. S., and R. E. Knowlton. 1999. Variation in larval size after eyestalk ablation in larvae of the snapping shrimp, *Alpheus heterochaelis* Say. *J. Crustac. Biol.* **19:** 8–13.

Gurney, R. 1939. *Larvae of Decapod Crustacea.* Ray Society, London. 306 pp.

Guyer, M. F. 1906. P. 227 in *Animal Micrology: Practical Exercises in Zoölogical Micro-technique.* University of Chicago Press, Chicago.

Imam, F. S. 1982. Formation, growth, and spatial relationship of eyestalk neuroendocrine stuctures in *Alpheus heterochaelis. Am. Zool.* **22:** 911A.

Jenkin, P. M. 1970. *Control of Growth and Metamorphosis, Part II. Animal Hormones: A Comparative Study.* Pergamon Press, Oxford. 310 pp.

Kelly, G. 1967. *Endocrine Coordination in Invertebrates: An Introduction To Neuroendocrine Regulation In Animals.* Pageant Press, New York. 210 pp.

Kleinholz, L. H. 1976. Crustacean neurosecretory hormones and physiological specificity. *Am. Zool.* **16:** 151–166.

Knowlton, R. E. 1973. Larval development of the snapping shrimp, *Alpheus heterochaelis* Say, reared in the laboratory. *J. Nat. Hist.* **7:** 273–306.

Knowlton, R. E. 1974. Larval developmental processes and controlling factors in Crustacea, with emphasis on Caridea. *Thalassia Jugosl.* **10:** 138–158.

Knowlton, R. E. 1988. Effects of eyestalk extirpation on larval and early postlarval stages of the snapping shrimp *Alpheus heterochaelis* Say. *Am. Zool.* **28:** 94A.

Knowlton, R. E. 1994. Effects of larval eyestalk extirpation on morphogenesis and molting in the snapping shrimp, *Alpheus heterochaelis* Say. *J. Exp. Zool.* **270:** 162–174.

Laufer, H., and D. W. Borst. 1988. Juvenile hormones in Crustacea. Pp. 305–313 in *Endocrinology of Selected Invertebrate Types,* H. Laufer and G. H. Downer, eds. Alan R. Liss, New York.

Liu, L., and H. Laufer. 1996. Isolation and characterization of sinus gland neuropeptides with both mandibular organ inhibiting and hyperglycemic effects from the spider crab *Libinia emarginata. Arch. Insect Biochem. Physiol.* **32:** 375–385.

Liu, L., H. Laufer, Y. J. Wang, and T. Hayes. 1997. A neurohormone regulating both methyl farnesoate synthesis and glucose metabolism in a crustacean. *Biochem. Biophys. Res. Commun.* **237:** 694–701.

Passano, L. M. 1960. Molting and its control. Pp. 473–535 in *The Physiology of Crustacea,* Vol. 1. T. H. Waterman, ed. Academic Press, New York.

Passano, L. M. 1961. The regulation of crustacean metamorphosis. *Am. Zool.* **1:** 89–95.

Smith, P. A., A. S. Clare, H. H. Rees, M. C. Prescott, G. Wainwright, and M. C. Thorndyke. 2000. Identification of methyl farnesoate in the cypris larva of the barnacle, *Balanus amphitrite,* and its role as a juvenile hormone. *Insect Biochem. Mol. Biol.* **30:** 885–890.

Wainwright, G., S. G. Webster, M. C. Wilkinson, J. S. Chung, and H. H. Rees. 1996. Structure and significance of mandibular organ-inhibiting hormone in the crab, *Cancer pagurus*—involvement in multihormonal regulation of growth and reproduction. *J. Biol. Chem.* **271:** 12749–12754.

Welsh, J. H. 1960. Neurohumors and neurosecretion. Pp. 281–311 in *The Physiology of Crustacea,* Vol. 2. T. H. Waterman, ed. Academic Press, New York.

Williamson, D. I. 1982. Larval morphology and diversity. Pp. 43–110 in *The Biology of Crustacea, Vol. 2. Embryology, Morphology, and Genetics,* L. G. Abele, ed. Academic Press, New York.

Reference: *Biol. Bull.* **202:** 53–60. (February 2002)

Uptake of the Neurotransmitter Histamine into the Eyes of Larvae of the Barnacle (*Balanus amphitrite*)

ANN E. STUART, HAROLD E. MEKEEL, AND ELIZABETH KEMPTER

Department of Cell and Molecular Physiology, University of North Carolina at Chapel Hill, Chapel Hill, North Carolina 27599-7545

Abstract. The photoreceptors of adult barnacles use histamine as their neurotransmitter and take up ^{3}H-histamine selectively from the extracellular medium. We assayed for the uptake of ^{3}H-histamine into the eyes of the free-swimming (nauplius) and settling (cyprid) larval stages of *Balanus amphitrite*. The extracellular space of nauplii proved permeable to dyes below about 800 molecular weight (MW), indicating that ^{3}H-histamine (MW 111) introduced into seawater would have access to internal structures. ^{3}H-Histamine was taken up into nauplii by a process with a K_D of 0.32 μM. Uptake was antagonized by chlorpromazine, which also blocks uptake of ^{3}H-histamine into adult photoreceptors. In autoradiographs of serial sections of nauplii and cyprids incubated in ^{3}H-histamine, the ocelli and compound eyes were labeled; other structures in the animal were not. No eyes or other structures were labeled with ^{3}H-serotonin, a related amine whose transporter commonly transports histamine as well. These experiments show that a histamine-specific transporter similar to that found in the adult is expressed in all of the eyes of barnacle larvae. In the ocelli, where photoreceptors and pigment cells may be distinguished in the light microscope, label was unexpectedly concentrated far more over the pigment cells than over the photoreceptors.

Introduction

The photoreceptors of a wide spectrum of arthropods, including various insects, crustaceans, and arachnids, synthesize histamine and use it as their neurotransmitter (reviewed by Stuart, 1999). In *Drosophila*, the photoreceptors of the compound eyes of adults are immunolabeled for histamine (Sarthy, 1991; Pollack and Hofbauer, 1991) but the photoreceptors of the third-stage larvae are not, suggesting that these cells use a different transmitter (Pollack and Hofbauer, 1991). Substantiating this difference between adult and larva is the finding that mutant flies lacking the synthetic enzyme for histamine are blind but their larvae are not (Melzig *et al.*, 1996). Indeed, it is likely that the larval photoreceptors employ acetylcholine as their neurotransmitter (Yasuyama *et al.*, 1995). This observation led us to ask whether the histaminergic neurotransmitter system is expressed in the larvae of another arthropod, the barnacle, where the visual system undergoes dramatic changes during the animal's life cycle (Thorson, 1964; Crisp and Ritz, 1973; Lang *et al.*, 1979).

Histaminergic photoreceptors take up ^{3}H-histamine, added to the extracellular medium, *via* a histamine-specific transporter (Stuart *et al.*, 1996; Melzig *et al.*, 1998; Battelle *et al.*, 1999; Borycz and Meinertzhagen, 2000) and are clearly labeled in autoradiographs. In the present study, we used autoradiography as well as biochemistry to assay for the uptake of ^{3}H-histamine into the eyes of barnacle larvae. We find that ^{3}H-histamine is taken up into both the simple and compound eyes but not into other cells in the animal. Thus the larvae have a histamine transporter as does the adult. Unexpectedly, label was more concentrated over the pigment cells surrounding the light-sensitive dendrites of the photoreceptors than over the photoreceptors themselves.

Materials and Methods

Animals and preparations

Nauplius and cyprid larvae of *Balanus amphitrite* were obtained from the laboratory of Dr. Daniel Rittschof at the Duke University Marine Laboratory, Beaufort, North Carolina, where they were collected after induced release from adult animals maintained in the laboratory (Rittschof *et al.*,

Received 28 June 2001; accepted 20 November 2001.
E-mail: stuart@med.unc.edu

1984). Nauplii used in experiments were in the first or second instars of larval development. Larvae were concentrated to approximately 2000–6000 nauplii/ml either by attraction to a spot of light or by cooling to 6°C to inhibit swimming. Nauplii swim actively at room temperature, the temperature at which experiments were carried out.

Assay of ^{3}H-histamine uptake by scintillation counting

Nauplius larvae were incubated in 100 μl of 0.2 μ*M* ^{3}H-histamine (Amersham; 36–55 Ci/mmol) for 15 min in Eppendorf tubes at room temperature in the light, as noted in the Results. At the end of the incubation, 1 ml of 12.5 m*M* Co^{2+}/2.5 m*M* Ca^{2+} saline was added to the tube to minimize release of any ^{3}H-histamine taken up (Stuart *et al.*, 1996). The contents of the tube were then filtered and washed with 10–20 ml of 12.5 m*M* Co^{2+}/2.5 m*M* Ca^{2+} saline using a Millipore 12-unit filtration device (Whatman GF/C filters). Radioactivity on each filter (in the nauplii) was then counted using Biofluor scintillate. In experiments in which ionic content was altered, nauplii were filtered onto Millipore 0.45-μm filter disks and rinsed with 1 ml of the altered ion solution. The disk containing the nauplii was then placed into the incubation saline.

Autoradiography

For autoradiography incubations, larvae were further concentrated as follows. The larvae were pipetted into the front chamber of a Millipore filter holder (modified by sawing off the projecting needle connector) and sucked onto the filter disk (Millipore 0.45 μm) within the unit by an attached syringe. In this fashion the larvae were concentrated onto the filter. This procedure did not kill the larvae; when the disk was then removed and touched to a drop of incubation medium, they swam normally. Larvae were incubated in 100 μl of 20 μ*M* ^{3}H-histamine (Amersham; 36–55 Ci/mmol) or 40 μ*M* ^{3}H-serotonin (Amersham or New England Nuclear; 18.2 or 24.7 Ci/mmol) for 15 min in Eppendorf tubes or in isolated drops on Parafilm at room temperature in the light. Triton X-100 (0.1%) or digitonin (0.25%) were included in incubations of cyprid larvae for autoradiography.

Following incubation, larvae were washed from the final filter disk into a glass scintillation vial and fixed overnight in glutaraldehyde (250 m*M*, E. M. Sciences) fixative modified from Hudspeth and Stuart (1977) to contain 0.2 *M* Na^+ cacodylate (pH 7.7) instead of phosphate buffer. Fixed larvae were postfixed in osmium tetroxide (1%) in cacodylate buffer (1 h, room temp), dehydrated, and immersed in Epon/propylene oxide (1:1) overnight. The vial was left uncapped in the hood and the propylene oxide allowed to evaporate. The larvae were then spread about on an aluminum foil weighing dish and covered with drops of fresh Epon for 1 h for the plastic to infiltrate the tissue. Individual larvae were then lifted from the dish with a sharpened orangewood applicator stick, placed in a new foil dish, covered with a thin layer of Epon, and embedded at 60°C overnight. Selected larvae were oriented as desired by re-embedding in either inverted Beem capsules or latex coffin molds.

Blocks were serially sectioned at 2 μm. Sections were dried on gelatin-coated slides, dipped in Kodak NTB-2 autoradiographic emulsion, exposed at 4°C for 5 days to 2 weeks, and developed in D-19 (Kodak).

Dye exclusion assays

Fluorescent dye exclusion assays were performed by placing live nauplii in saline containing 2% Lucifer yellow CH, Procion yellow MX-4R, Procion yellow H-5G, or Procion yellow H-5G covalently bound to a dextran of about 40,000 MW (all Sigma). Following 15 min in dye, the nauplii were filtered, suspended in O.C.T. compound mounting medium (Pelco International), placed in a plastic capsule, and immediately frozen in a beaker of isopentane (Kodak) precooled by dry ice. Nauplii were then sectioned at 10 μm on a cryostat, placed on Fisher Superfrost-plus charged slides, coverslipped with 2 drops of glycerol/N-propyl gallate, and viewed under a fluorescence microscope with XF22 filters (Omega).

Results

Barnacles (of the genus *Balanus*) have three stages to their life cycle: the free-swimming nauplius; the cyprid, specialized for settling; and the reproductive adult. The nauplius has one simple eye and swims towards light, presumably to disperse (Thorson, 1964; Sastry, 1983). The cyprid retains the simple eye but, in addition, suddenly develops a pair of compound eyes (Barnett *et al.*, 1979), presumably to guide the animal in settling appropriately. The sessile adult sheds the compound eyes (Walker and Lee, 1976), no longer needed, and retains the simple eye, which separates into the median and paired lateral eyes of the adult (Takenaka *et al.*, 1993) that mediate a defensive response to shadows.

Penetrability of larvae

The epidermis of early-stage nauplii is not well developed (Freeman, 1993), suggesting that substances introduced into seawater might diffuse into the animal's extracellular space and be accessible to internal structures such as the ocelli. To test the permeability of nauplii, we exposed them to dyes ranging in molecular weight from 289 to 40,000.

Simply observing living, dye-soaked nauplii through the light microscope suggested that lower molecular weight dyes penetrated into the animals, whereas a dye of higher molecular weight did not. The cutoff appeared to be at a molecular weight of about 800: neutral red (MW 289), toluidine blue (MW 306), neutral violet (MW 409), and ruthenium red (MW 786) stained the animal, whereas fast green (MW 809) did not. To make certain that the dyes were indeed inside the animal, nauplii were exposed to four fluorescent dyes of differing molecular weights, frozen quickly, and sectioned on a cryostat. Fluorescence was found throughout the sections of animals exposed to Lucifer yellow CH (MW 457.2) and Procion yellow MX-4R (Reactive orange 14) (MW 631.4), but not in sections of animals exposed to Procion yellow H-5G (Reactive yellow 2) (MW 873) or its dextran-bound derivative (MW ~40,000). We conclude that the naupliar epidermis does not present a significant barrier to compounds of molecular weight below about 800 and that substances such as ^{3}H-histamine (MW 111) might be expected to penetrate easily into the animal and be taken up by internal structures.

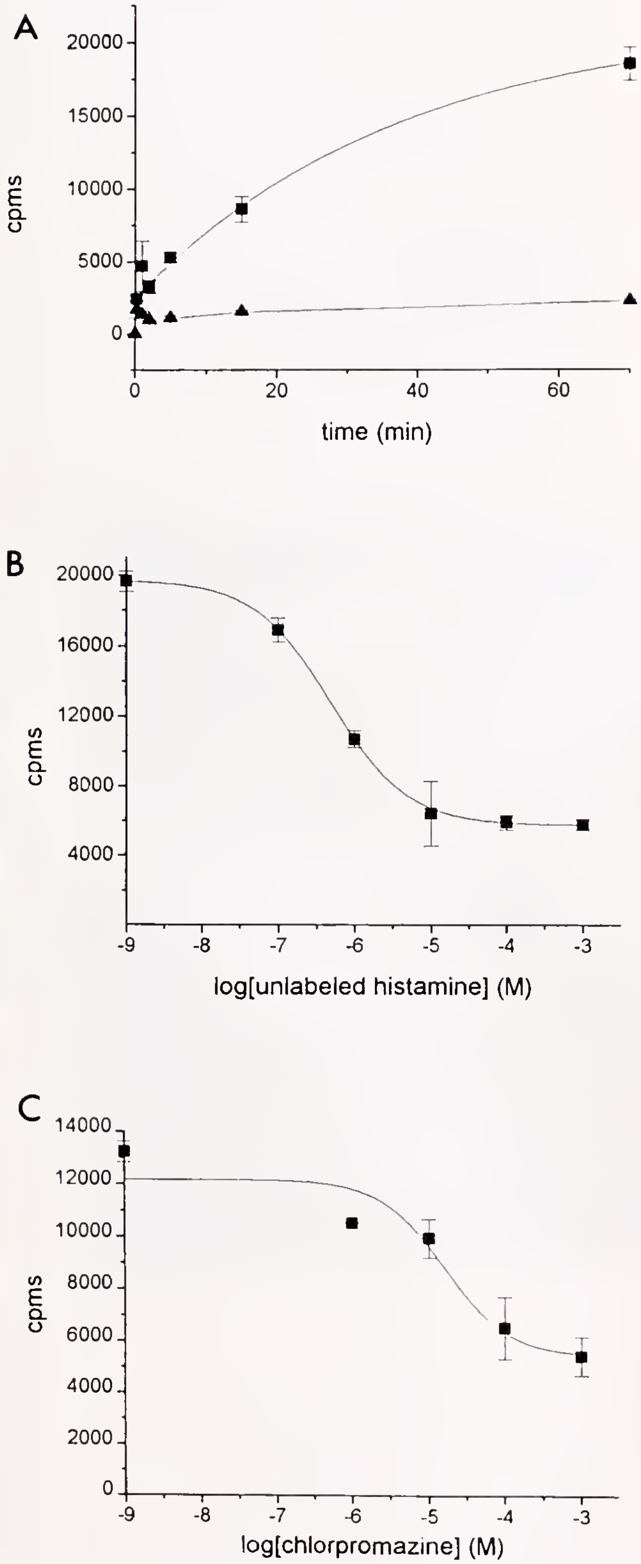

Biochemistry

When incubated with ^{3}H-histamine (0.2 μM), nauplii took up this compound in a time-dependent fashion (Fig. 1A). The time course of uptake could be fitted with an exponential association curve with a rate constant of 0.028/min. Inclusion of an excess (2 mM) of unlabeled histamine in the incubation medium blocked the uptake of labeled compound (Fig. 1A), indicating that uptake is a competitive process. From the dose/response curve describing this competition (Fig. 1B), a K_D of 0.32 μM was calculated for ^{3}H-histamine uptake, a value suggesting a high-affinity uptake mechanism.

Chlorpromazine, which antagonizes the uptake of ^{3}H-histamine into the photoreceptors of adult barnacles (Stuart *et al.*, 1996) and into snail neurons (Osborne *et al.*, 1979), also markedly decreased the uptake of ^{3}H-histamine into nauplii (Fig. 1C) (K_I = 21 μM). Block appeared to be incomplete, as is the case with adult photoreceptors (Stuart *et al.*, 1996), although block of uptake of ^{3}H-histamine by a high concentration of drug was not compared with competitive antagonism by cold histamine in the same assay. The maximum inhibition in the adult was about 70% (Stuart *et al.*, 1996) and in nauplii about 50%. The sensitivity of ^{3}H-histamine uptake to chlorpromazine in both the larvae and the adult suggests that it is mediated by a similar

Figure 1. Uptake of ^{3}H-histamine into nauplius larvae assayed by scintillation counting. (A) Time course of uptake. Two equal aliquots of larvae were incubated for each time point (0,1,5,15, or 70 min) in 0.2 μM ^{3}H-histamine without (■) or with (▲) 2 mM unlabeled histamine. Addition of unlabeled histamine to the incubation medium blocks the uptake of ^{3}H-histamine. (B) Competition of unlabeled histamine with ^{3}H-histamine for uptake into nauplii. The data were fit to a one-site competition algorithm with a K_D of 0.32 μM. (C) Chlorpromazine antagonizes the uptake of ^{3}H-histamine into nauplii. Aliquots of larvae were incubated with increasing concentrations of drug, as described in Materials and Methods. A simple competition fit to the points gives a K_I of 21 μM. In each experiment the symbol shows the average of the values for two samples, and the bar shows the range of these values; cpms = counts per minute.

transporter. Nauplii incubated either in 2 mM histamine or in 20 μM chlorpromazine (which would presumably have increased extracellular histamine by blocking uptake) stopped swimming towards the light and eventually sank to the bottom of the tube. The current notion of histamine's action in the visual pathway suggests that the presence of histamine in the cleft would lead to more movement, not less (see Discussion): thus these observations cannot easily be explained and may involve histamine's actions on neurons other than those of the visual system in the larva.

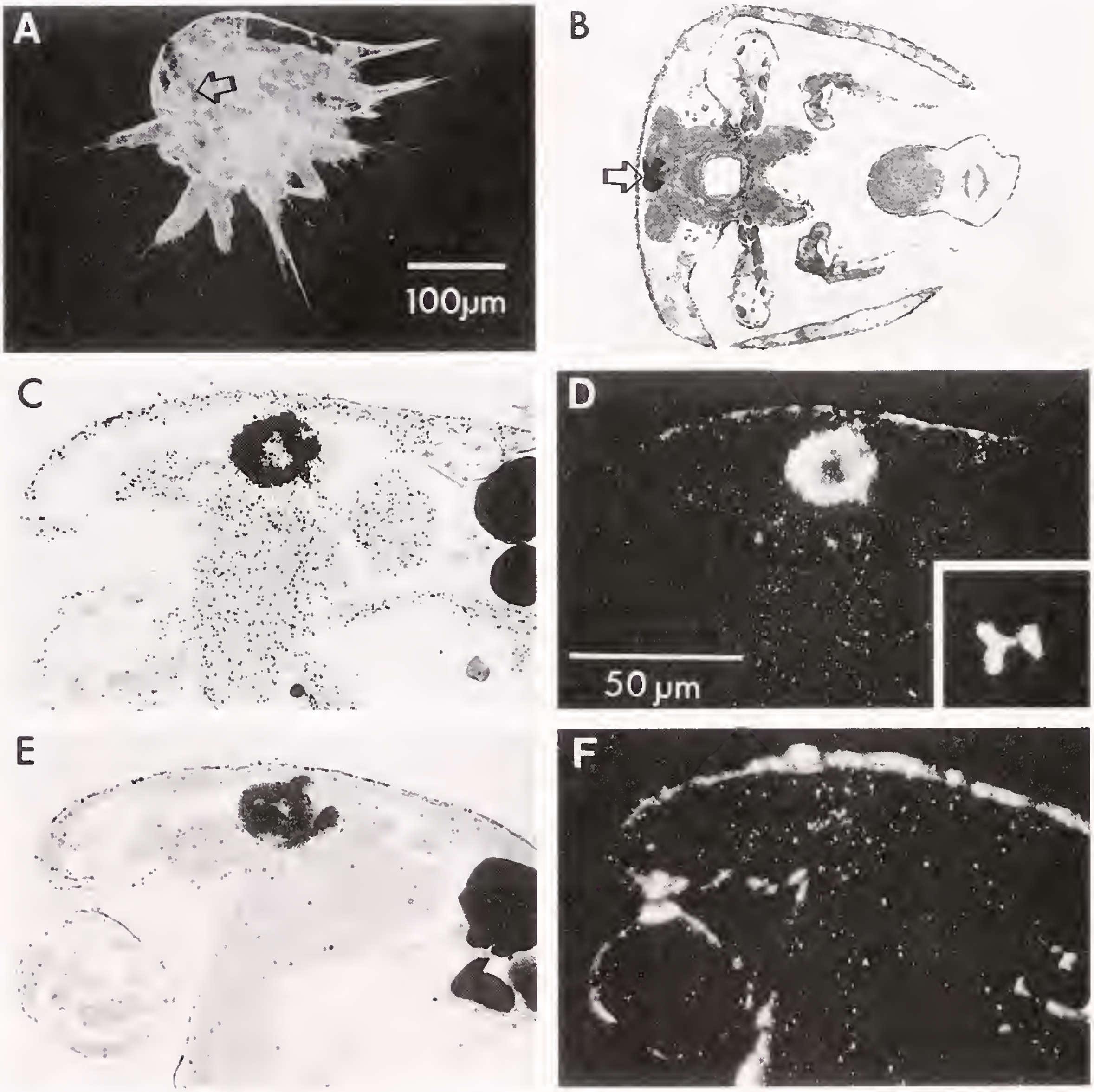

Figure 2. Uptake of ^{3}H-histamine into the ocellus of nauplius larvae as revealed by autoradiography. (A) A whole mount of a nauplius larva viewed from the side. (B) A section of a nauplius larva through the ocellus, viewed from the top. The pigmented ocellus (arrows in A and B) is obvious within this transparent animal and in sections. (C) Brightfield and (D) epipolarization illumination of an ocellus in a 2-μm section of a nauplius that had been incubated in ^{3}H-histamine. Accumulation of silver grains over the ocellus cannot be distinguished from pigment in brightfield illumination but is obvious in epipolarized light, which reflects from the silver grains but not from the pigment. The insert shows a section through another eye at a different orientation in which the pigment arms form two back-to-back cups around the photoreceptors; the right arm of the upper cup is incomplete. (E) Brightfield and (F) epipolarization illumination of a 2-μm section of a nauplius that had been incubated in ^{3}H-serotonin. There is no accumulation of grains over the ocellus. Scale bar in D applies to C–F.

Autoradiography of nauplius larvae

The single, median eye (the ocellus) of the nauplius (Fig. 2A, B, arrows) is a striking feature of this larval stage. The two pigment cells at the center of this simple eye give it a deep red color that allows it to be clearly seen, even under the dissecting microscope. The photoreceptors are subdivided by these pigment cells into three groups that "look" in three different directions. The pigment cells are shaped to form three cups, and within each cup are two to six photoreceptors, termed retinular cells (Kauri, 1962; Walley, 1969; Walker *et al.*, 1987; Clare and Walker, 1989). A comparison of the light intensity on each group of photoreceptors, made by higher-order cells, is presumably the mechanism that permits these free-swimming stages to determine from which direction the light is coming.

In sections viewed at high power with the light microscope, the pigment cells may be clearly differentiated from the photoreceptors enveloped by their processes (*e.g.*, Fig. 3B). A pigment cell cup may have been sectioned horizontally across the cup wall so that the pigment forms a ring (Fig. 2C, D). Alternatively, the section may reveal the cuplike shape of the cell (Fig. 3) as it envelopes the photoreceptor processes. The long, dark lines of the rhabdomes of the apposed photoreceptor neurons (Takenaka *et al.*, 1993) may be seen especially well in Figure 3B, forming a "V" within the arms of the pigment cells.

To determine whether the ocellus or other structures within the nauplius larva take up ^{3}H-histamine, serial sections through nauplii incubated in ^{3}H-histamine (20 μM) were exposed for autoradiography. Examination of these sections revealed that the label is concentrated over the ocellus but not over other parts of the animal (Fig. 2D). The ocelli of larvae incubated in an excess of unlabeled histamine (2 mM) added to the ^{3}H-histamine were not labeled above background (not shown). Unexpectedly, the regions within the pigment ring or cup, where the photoreceptors lie, are labeled only weakly compared to the labeling of the pigment cells (Figs. 2C, D; 3A). Brightfield photographs (Fig. 2C) do not allow one easily to distinguish silver grains from pigment, but in epipolarized light (Fig. 2D) the pigment does not reflect the light and the silver grains stand out clearly. The inset of Figure 2D shows a section through another eye in which two back-to-back, labeled pigment cell cups form an incomplete "H" as they extend arms around two groups of photoreceptors (Takenaka *et al.*, 1993).

Nauplii incubated in ^{3}H-serotonin (20 μM) did not show increased labeling over the ocellus or, indeed, over any structure (Fig. 2E, F; Fig. 3B). Adult *Balanus nubilus* photoreceptors are not labeled when incubated with ^{3}H-serotonin, but a small number of other neurons within the adult nervous system do show labeling (Stuart *et al.*, 1996). Further, serotonin has been detected in cyprid larvae and appears to be important in settlement (Yamamoto *et al.*, 1999). In the nauplius larva these neurons may not have developed as yet or may have been too small to detect, or their absence may reflect a species difference between the adult *Balanus nubilus* and the larval *Balanus amphitrite* nervous systems. The lack of labeling of the ocelli with ^{3}H-serotonin indicates that the uptake of ^{3}H-histamine into barnacle eyes is by a process selective for histamine in the nauplius larva, as it is in the adult.

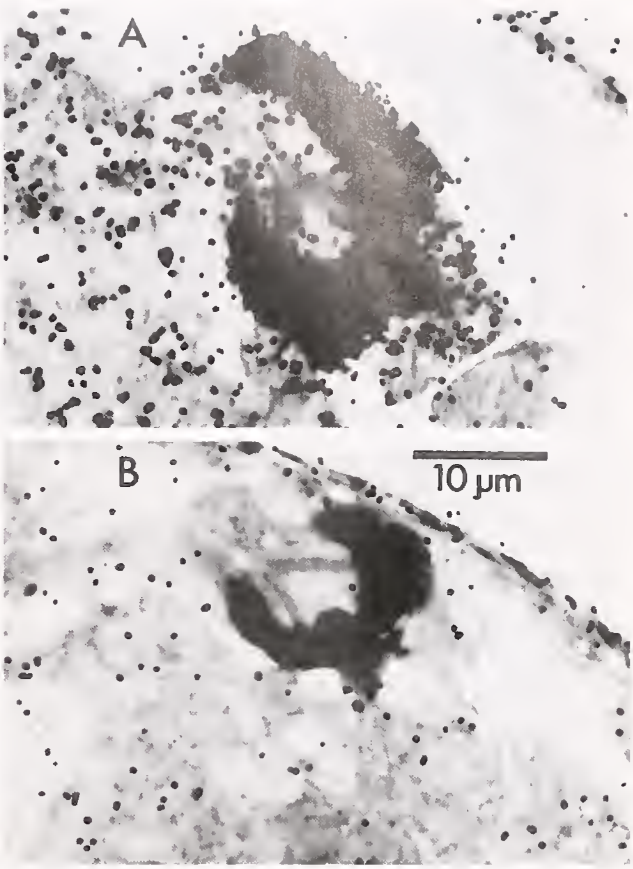

Figure 3. Autoradiographs of sections through ocelli of nauplii that had been incubated in (A) ^{3}H-histamine or (B) ^{3}H-serotonin. In both autoradiographs, the rhabdomes of the photoreceptors are visible as two gray lines forming a "V" (pointing to the upper left) within the arms of the pigment cells. In (A) grains are concentrated over the pigment cells (same animal as in Fig. 2C, D). Although the grains are difficult to distinguish from pigment in brightfield illumination, they clearly are not concentrated over the photoreceptors, whose processes lie within the pigment cell cup. In (B) there is no concentration of grains over either cell type (same animal as in Fig. 2E, F).

Autoradiography of cyprid larvae

A whole mount of a cyprid larva viewed from the side is depicted in Figure 4A, and a section through the eyes of a cyprid viewed from the top is seen in Figure 4B. The medially located ocellus (smaller arrows) and laterally located pair of compound eyes (larger arrows) may be clearly seen. Cyprids were incubated in ^{3}H-histamine (20 μM) and

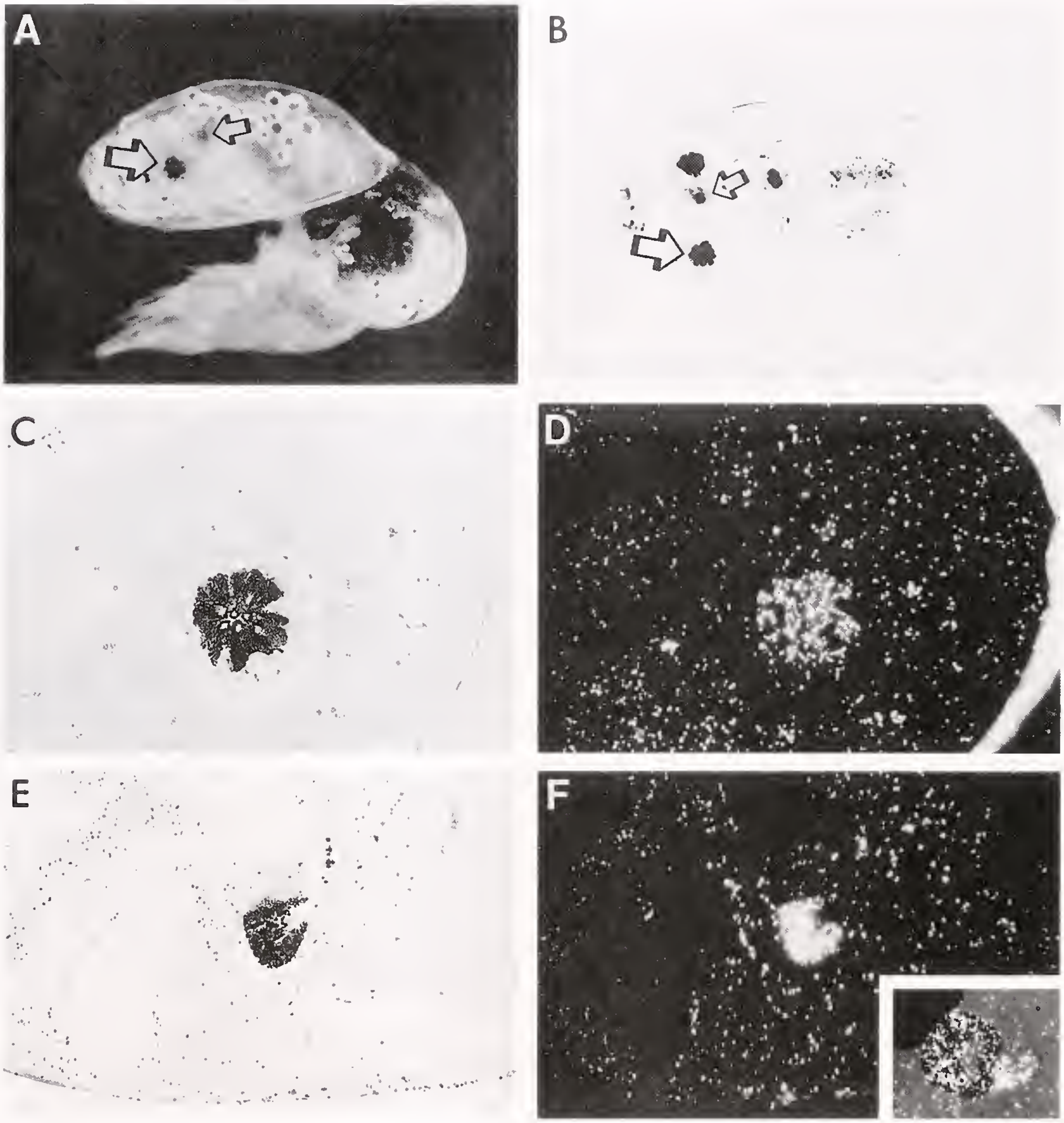

Figure 4. Uptake of ^{3}H-histamine into the compound eyes and ocellus of the cyprid larva as revealed by autoradiography. (A) Whole mount of a cyprid larva viewed from the side, and (B) a section through the three eyes of a cyprid viewed from the top. Compound eyes are labeled with larger arrows and the ocellus with a smaller arrow in A and B. (C) Brightfield and (D) epipolarization illumination of a compound eye in a 2-μm section of a cyprid that had been incubated in ^{3}H-histamine and Triton X-100, showing increased label over the eye compared to surrounding tissues. (E) Brightfield and (F) epipolarization illumination of the ocellus in the same animal shows a pattern of label over the pigment cells. (Inset) Phase contrast/epipolarization illumination of the ocellus from another animal.

processed for autoradiography. Unlike nauplii, cyprids have a thick cuticle overlying the epidermis, so would be expected to be poorly penetrated by substances added to the seawater. Indeed, when the larvae were incubated in ^{3}H-histamine alone, the eyes were labeled only faintly. Addition of the solubilizing agent Triton X-100 during the incubation increased the degree of labeling of both the compound eyes (Fig. 4C, D) and the median eye (Fig. 4E, F). The cuplike shape of the label within the median eye (Fig. 4E, F) again indicates that the pigment cells may be more heavily labeled than the photoreceptors. A section through the eye of another specimen, catching the pigment cup as a ring, indicates that grains might also be concentrated within and beside the cup (Fig. 4F, inset). It was not possible to determine which structures were labeled within the compound eye.

Discussion

We report here that all of the eyes of both the nauplius and cyprid larvae of balanoid barnacles are labeled when incubated in ^{3}H-histamine, but that other tissues in the animal are not. Uptake is blocked by chlorpromazine and is specific in that ^{3}H-serotonin is not taken up, as is also the case with uptake of ^{3}H-histamine into the adult median photoreceptors. Thus a histamine transporter similar to that of the adult appears to be expressed in the eyes of the larvae.

In the simple median eyes of both the nauplii and cyprid, autoradiographs showed label concentrated primarily over the pigment cells surrounding the photoreceptors rather than over the photoreceptor rhabdomeric processes enveloped by the pigment cells. But histamine uptake may take place only in the axons and terminals of these sensory neurons, as it does in the adult (Stuart *et al.*, 1996). In the larvae, the axons of the photoreceptors could not be reliably followed to settle this point. We also do not know if the heavy labeling of the pigment cells is specific to larvae, since in the adult there are no pigment cells associated with the commonly studied median eye. Adult lateral eyes of certain species retain pigment cells, but the uptake of ^{3}H-histamine has not been studied in those cases. It is not yet possible, then, to determine whether ^{3}H-histamine uptake in the larval eyes follows or differs from the adult pattern.

Although the behaviors of the nauplius larva and the adult barnacle with respect to light seem very different at first glance, they are actually similar and indeed might not require radical changes in circuitry (such as a different photoreceptor transmitter) during development. In both larvae and adults, changes in the ambient light affect the rhythmic motion of the animal's appendages, the cirri. In the larvae, this motion underlies swimming, whereas in the adult it is devoted to feeding.

In adult barnacles, rhythmic feeding by the cirri proceeds in the light, but the dimming of light halts rhythmic cirral motion and provokes the retraction of the cirri into the shell. The visual pathway is kept from interfering with the cirral rhythm as long as the light is not disturbed: histamine, continuously liberated by the illuminated photoreceptors, inhibits the postsynaptic cells, keeping the visual pathway silent. Dimming of the light (for example, by shadows of predators) interrupts the release of histamine, releases the second-order cells from inhibition, and initiates impulses in the visual pathway (Stuart and Oertel, 1978), leading to the cessation of these feeding movements. A complex behavior involving most of the animal's muscles is set in motion: the cirri stop their rhythmic motion, withdrawing into the shell, and the opercular plates are pulled closed to seal the animal within its fortress (Gwilliam, 1963).

In the nauplius larvae, the job of the cirri is to propel the animals toward light. The direction from which the light is coming is determined by the ocellus. The three divisions of the naupliar eye look in three different directions, and presumably the division in greatest light somehow causes the strongest movement of the animal in that particular direction. Thus the function of light in the nauplius and adult would seem similar in that light is accompanied by movement (feeding in the adult, swimming in the nauplius) and dimming or less light by the cessation or a decrease of movement. It might be that the neural circuits are similar at the two stages, although they accomplish very different behaviors depending on whether the animal is free-swimming or sessile.

Acknowledgments

We are grateful to Kirk McNaughton for his assistance with the cryostat technique, to Dr. Dan Rittschof and Marion McClary of the Duke University Marine Laboratory, Beaufort, North Carolina, for providing barnacle larvae, and to Jennifer R. Morgan for helpful comments on the manuscript. Supported by USPHS grant EY03347 to AES.

Literature Cited

Barnett, B. E., S. C. Edwards, and D. J Crisp. 1979. A field study of settlement behaviour in *Balanus balanoides* and *Elminius modestus* (Cirripedia: Crustacea) in relation to competition between them. *J. Mar. Biol. Assoc. UK* **59:** 575–580.

Battelle, B. A., B. G. Calman, and M. K. Hart. 1999. Cellular distributions and functions of histamine, octopamine, and serotonin in the peripheral visual system, brain, and circumesophageal ring of the horseshoe crab, *Limulus polyphemus. Microsc. Res. Tech.* **44:** 70–80.

Borycz, J., and I. A. Meinertzhagen. 2000. Histamine and histamine uptake in the heads of wild-type and mutant *Drosophila. Soc. Neurosci. Abstr.* 343.13.

Clare, A. S., and G. Walker. 1989. Morphology of the nervous system of barnacles: the median ocellus of *Balanus hameri* (= *Chirona hamen*) (Crustacea: Cirripedia). *J. Mar. Biol. Assoc. UK* **69:** 769–784.

Crisp, D. J., and D. A. Ritz. 1973. Responses of Cirripedia larvae to light. I. Experiments with white light. *Mar. Biol.* **23:** 327–335.

Freeman, J. A. 1993. The crustacean epidermis during larval development. Pp. 193–219 in *The Crustacean Integument: Morphology and Biochemistry*. M. N Horst and J. A. Freeman, eds. CRC Press, Boca Raton, FL.

Gwilliam, G. F. 1963. The mechanism of the shadow reflex in Cirripedia. I. Electrical activity in the supraesophageal ganglion and ocellar nerve. *Biol. Bull.* **125:** 470.

Hudspeth, A. J., and A. E. Stuart. 1977. Morphology and responses to light of the somata, axons and terminal regions of individual photoreceptors of the giant barnacle. *J. Physiol. (Lond)* **272:** 1–23.

Kauri, T. 1962. On the frontal filaments and nauplius eye in *Balanus. Crustaceana* **4:** 131–142.

Lang, W. H., R. B. Forward, Jr., and D. C. Miller. 1979. Behavioral responses of *Balanus improvisus* nauplii to light intensity and spectrum. *Biol. Bull.* **157:** 166–181.

Metzig, J., S. Buchner, F. Wiebel, R. Wolf, M. Burg, W. L. Pak, and E.

Buchner. 1996. Genetic depletion of histamine from the nervous system of *Drosophila* eliminates specific visual and mechanosensory behavior. *J. Comp. Physiol. A* **179:** 763–773.

Melzig, J., M. Burg, M. Gruhn, W. L. Pak, and E. Buchner. 1998. Selective histamine uptake rescues photo- and mechanoreceptor function of histidine decarboxylase-deficient *Drosophila* mutant. *J. Neurosci.* **18:** 7160–7166.

Osborne, N. N., K. D. Wolter, and V. Neuhoff. 1979. *In vitro* experiments on the accumulation and release of ^{14}C-histamine by snail (*Helix pomatia*) nervous tissue. *Biochem. Pharmacol.* **28:** 2799–2805.

Pollack, I., and A. Hofbauer. 1991. Histamine-like immunoreactivity in the visual system and brain of *Drosophila melanogaster. Cell Tissue Res.* **266:** 391–398.

Rittschof D., E. S. Branscomb, and J. D. Costlow. 1984. Settlement and behavior in relation to flow and surface in larval barnacles, *Balanus amphitrite. J. Exp. Mar. Biol. Ecol.* **82:** 131–146.

Sarthy, P. V. 1991. Histamine: a neurotransmitter candidate for *Drosophila* photoreceptors. *J. Neurochem.* **57:** 1757–1768.

Sastry, A. N. 1983. Pelagic larva ecology and development. Pp. 214–282 in *The Biology of Crustacea*, Vol. 7D. E. Bliss, ed. Academic Press, New York.

Stuart, A. E. 1999. From fruit flies to barnacles, histamine is the neurotransmitter of arthropod photoreceptors. *Neuron* **22:** 431–433.

Stuart, A. E., and D. Oertel. 1978. Neuronal properties underlying processing of visual information in the barnacle. *Nature* **275:** 287–290.

Stuart, A. E., J. R. Morgan, H. E. Mekeel, E. Kempter, and J. C. Callaway. 1996. Selective, activity-dependent uptake of histamine into an arthropod photoreceptor. *J. Neurosci.* **16:** 3178–3188.

Takenaka, M., A. Suzuki, T. Yamamoto, M. Yamamoto, and M. Yoshida. 1993. Remodeling of the nauplius eye into the adult ocelli during metamorphosis of the barnacle, *Balanus amphitrite hawaiiensis. Dev. Growth Differ.* **35:** 245–255.

Thorson, G. 1964. Light as an ecological factor in the dispersal and settlement of larvae of marine bottom invertebrates. *Ophelia* **1:** 167–208.

Walley, L. J. 1969. Studies on the larval structure and metamorphosis of *Balanus balanoides* (L.). *Philos. Trans. R. Soc. Lond. B* **256:** 237–280.

Walker, G., and V. E. Lee. 1976. Surface structures and sense organs of the cypris larva of *Balanus balanoides* as seen by scanning and transmission electron microscopy. *J. Zool.* **178:** 161–172.

Walker G., A. B. Yule, and J. A. Nott. 1987. Structure and function in balanomorph larvae. Pp. 307–327 in *Crustacean Issues Vol. 5: Barnacle Biology*, A. J. Southward, ed. A. A. Balkema, Rotterdam.

Yamamoto, H. K. Shimizu, A. Tachibana, and N. Fusetani. 1999. Roles of dopamine and serotonin in larval attachment of the barnacle, *Balanus amphitrite. J. Exp. Zool.* **284:** 746–758.

Yasuyama, K., T. Kitamoto, and P. M. Salvaterrra. 1995. Localization of choline acetyltransferase-expressing neurons in the larval visual system of *Drosophila melanogaster. Cell Tissue Res.* **282:** 193–202.

Reference: *Biol. Bull.* **202:** 61–73. (February 2002)

Glycoproteins from the Cuticle of the Atlantic Shore Crab *Carcinus maenas*: I. Electrophoresis and Western-Blot Analysis by Use of Lectins

PHILIPPE COMPÈRE[1,*], MARIE-FRANCE JASPAR-VERSALI[2], AND GERHARD GOFFINET[1]

[1]*Laboratoire de Biologie générale et de Morphologie ultrastructurale, Université de Liège, Institut de Zoologie (I1), 22, quai Ed. Van Beneden, B-4020 Liège, Belgium; and* [2]*Groupe de Recherche Chitine-Chitosane, Université de Liège, Département de Botanique (B22), Sart-Tilman, B-4000 Liège, Belgium*

Abstract. The protein and glycoprotein content of four different neutral or acidic solvent extracts (0.5 *M* KCl, 10% EDTA, 0.1 N HCl, or 2% acetic acid) from the mineralized exoskeleton of a decapod crustacean, the Atlantic shore crab *Carcinus maenas*, were characterized by quantitative analysis of proteins, SDS-PAGE analysis, and probing with lectins on blots. The lectins used were Conconavalin A, Jacalin, soybean agglutinin, *Maackia amurensis* agglutinin II, and *Sambucus nigra* agglutinin. The results show that many proteins can be obtained from the crab cuticle without strong denaturants in the extraction medium. Many of the extracted cuticle proteins appeared to be glycosylated, bearing *O*-linked oligosaccharides and *N*-linked mannose-rich glycans. *N*-acetyl-galactosamine and *N*-acetylneuraminic acids were revealed, for the first time, as terminal residues on *N*-linked mannose-rich structures of crab cuticle glycoproteins. Sialylated glycoproteins might thus be involved in organic-mineral interactions in the calcified crab exoskeleton. The amount and variety of glycoproteins extracted with the acidic solvents are obviously different from those extracted with neutral solvents. HCl proved to be the best of the tested extraction solvents and a valuable alternative to EDTA.

Introduction

Arthropods are characteristically invested by an exoskeleton, the cuticle. They grow by periodic molts, during which they synthesize a new cuticle and partly degrade the old one before it is shed at ecdysis (for reviews, see Stevenson, 1985; Roer and Dillaman, 1993; Goffinet and Jeuniaux, 1994). Covering different integumental regions, the cuticle acts as a protective barrier, an exchange surface, and a supporting skeleton. In decapod crustaceans, the solid cuticle of sclerites is composed of an outer thin epicuticle and three fibrous composite layers forming the procuticle (for reviews, see Neville, 1975, 1984, 1993; Goffinet and Jeuniaux, 1994; Compère, 1995). The framework of the procuticle layers consists of a helicoidal twisted plywood-like arrangement of chitin-protein microfibers (Neville, 1993). The two major procuticle layers (the pigmented layer and the principal layer) are stiffened by impregnation of the interfibrillar matrix with calcium salts, mainly calcite; the innermost layer (the membranous layer) is not mineralized and remains in contact with the epidermis throughout the anecdysial period (for reviews, see Stevenson, 1985; Roer and Dillaman, 1993; Goffinet and Jeuniaux, 1994).

The protein component of the arthropod cuticle is usually subdivided into proteins covalently bound and proteins noncovalently bound to chitin or another component (for review, see Hackman, 1984; O'Brien *et al.*, 1993). Noncovalently bound proteins are those extracted by various solvents, the differences in solubility reflecting differences in association with other cuticular components. Since most exoskeletal proteins seemed to resemble each other (Hackman and Goldberg, 1976), cuticular proteins were neglected for a long time (Willis, 1987), and those of the crustacean cuticle have not yet been characterized as extensively as those of the insect cuticle. From several recent investigations on the exoskeletal proteins of crustaceans (Skinner *et al.*, 1992; O'Brien *et al.*, 1993; Andersen, 1998, 1999; Coblentz *et al.*, 1998) and insects (Willis, 1987; Andersen *et*

Received 15 June 1999; accepted 21 November 2001.

* To whom correspondence should be addressed. E-mail: pcompere@ulg.ac.be

al., 1995; Jensen *et al.*, 1998; Andersen, 2000), these proteins have emerged as among the most important organic constituents of the cuticle, and they are largely responsible for its mechanical properties. They are structural components of the chitin-protein microfibers and are involved in the interactions between microfibers, the interfibrillar matrix, and also the mineral in calcified exoskeletons (Andersen, 1999, 2000; Coblentz *et al.*, 1998; Willis, 1999).

In the decapod crustacean cuticle, the amount of protein does not exceed 40% of the decalcified dry weight (Welinder, 1974). Electrophoretical analyses and amino acid sequencing studies carried out on several species (*Scylla serrata*, Hackman, 1974; *Astacus leptodactylus*, Vranckx and Durliat, 1980, 1986; *Pandalus borealis*, Andersen, 1991; *Gecarcinus lateralis*, O'Brien *et al.*, 1991; Skinner *et al.*, 1992; Kumari and Skinner, 1995; Kumari *et al.*, 1995; *Homarus americanus*, Kragh *et al.*, 1997; Nousiainen *et al.*, 1998; *Cancer pagurus*, Andersen, 1999) showed that most proteins extracted from the calcified cuticles have an acidic pI and are smaller than 31 kDa. On the other hand, many recent reports suggest that acidic macromolecules—and notably glycoproteins—play a role of prime importance in the promotion and inhibition of crystal growth during calcification of diverse extracellular matrices (teeth: Akita *et al.*, 1992; bones: Hunter and Goldberg, 1993; Hunter *et al.*, 1996; mollusc shells: Wheeler *et al.*, 1988; avian eggshell: Gaudron *et al.*, 1996; sea urchin test and spicules: Berman *et al.*, 1990; Harvey *et al.*, 1995; Albeck *et al.*, 1996; for reviews, see Addadi and Weiner, 1992; Sikes *et al.*, 1994; Marsh, 1994). Few authors were interested in studying such macromolecules in crustacean exoskeletons (*Callinectes sapidus*: Shafer *et al.*, 1994; 1995; Coblentz *et al.*, 1998; *G. lateralis*: Kumari and Skinner, 1995), but they extracted glycoproteins that bear mannose-rich structures and have a relatively high apparent molecular weight (MW). These authors suggested that cuticle glycoproteins are involved in the mineralization process. In addition, Shafer *et al.* (1995) revealed that the glycosylation of the cuticular proteins of the blue crab *C. sapidus* undergoes molt-related changes concurrent with the mineralization of the cuticle after ecdysis. More recently—confirming that matrix proteins from solid cuticle of the blue crab influence *in vitro* crystallization of calcium carbonate (Gunthorpe *et al.*, 1990)—Coblentz *et al.* (1998) electrophoretically separated several crystal-associated proteins (CAPs), probably glycosylated, from extracts of the cuticle of early post-ecdysial blue crabs. They showed that these CAPs bind to calcite crystals and delay their nucleation in *in vitro* crystallization assays.

Although many studies have been devoted to the cuticular proteins of marine, freshwater, and terrestrial brachyuran decapods, conflicting results have been obtained, and close comparisons are hazardous because different species were studied and different extraction conditions used (medium composition, duration, temperature). On the other hand, because the crustacean solid cuticle is calcified, calcium salts must be solubilized prior to the extraction of proteins—especially those that are bound to the mineral. Most authors have therefore used ethylenediamine tetraacetate (EDTA), which has the advantage of promoting decalcification at neutral pH, either in the extraction medium (O'Brien *et al.*, 1991; Kumari and Skinner, 1995; Shafer *et al.*, 1994, 1995; Coblentz *et al.*, 1998), or separately, prior to the extraction (Andersen, 1991, 1999; Kragh *et al.*, 1997; Nousiainen *et al.*, 1998). According to Albeck *et al.* (1993), EDTA probably affects the aggregation state and the Ca-binding properties of the proteins, hindering their subsequent analysis; moreover, EDTA is extremely difficult to remove completely by dialysis. To extract proteins from exoskeletons, therefore, these authors recommended the use of dilute HCl, which proved more efficient than EDTA as a solvent for solubilizing proteins in an intact state from molluscan shells and sea urchin tests.

The first and main purpose of the present work is to characterize the proteins extracted from the calcified cuticle of a European marine decapod, the Atlantic shore crab *Carcinus maenas*, by sodium dodecylsulfate-polyacrylamide gel electrophoresis (SDS-PAGE) and probing glycosylations on blots with various lectins. The second purpose is to compare four non-denaturing or weakly denaturing solvents (KCl, EDTA, HCl, and acetic acid) for their efficiency in solubilizing medium- and high-MW proteins and glycoproteins. The present work is also preparatory to a forthcoming paper, which tentatively aims to relate the present data to the distribution of polyanions and glycoproteins in the cuticle layers as determined by cytochemical techniques and gold-conjugated lectin probes.

Materials and Methods

Biological material and preparation of cuticle extracts

Large specimens of the Atlantic shore crab (*Carcinus maenas*), with a cephalothoracic shield exceeding 5 cm in width, were obtained from a local distributor. Anecdysial crabs were selected according to the criteria of Drach and Tchernigovtzeff (1967). The cuticle of the cephalothoracic shield was excised and carefully cleaned of adhering tissue remnants with a wet paper tissue. Samples (two sets of four) of isolated fresh cuticle, weighing 4 g each, were either crushed (first set) or ground to powder (second set), then extracted in the presence of a bactericide (10 m*M* NaN_3) and a protease inhibitor (1 m*M* phenylmethylsulfonylfluoride, PMSF) in one of four solvents: 0.5 *M* KCl at pH 7.0, 10% ethylenediamine tetraacetate (EDTA) at pH 7.0, 0.1 N HCl at pH 2.0, or 2% acetic acid (HAc) at pH 3.0. Extraction was carried out with stirring for 48 h at 4°C in 1 liter of solvent, which was renewed three times. The samples were enclosed in cellulose dialysis tubes (10,000 Da MW cutoff) filled with 10 ml of solvent. The extracts were centrifuged at 14,000 × *g* for 10 min, and the supernatants were dialyzed for 40 h at 4°C against 10 m*M* NH_4HCO_3 containing 2.5 m*M* NaN_3 and 1 m*M* PMSF.

Protein quantification assays

Before lyophilization, the protein contents of all dialyzed extracts were measured with the bicinchoninic acid protein assay (BCA protein assay reagent kit, Pierce no. 23225), using bovine serum albumin (BSA) as the standard (Smith *et al.*, 1985; Wiechelman *et al.*, 1988). In preliminary comparisons of different protein assays, UV absorption at 280 nm, Biuret's method, and the BCA method yielded relatively close and consistent protein concentrations for crab cuticle extracts, while Bradford's technique (1976) yielded values 5 to 10 times lower. The difference is probably due to the presence of many acidic proteins in the extracts, since the Coomassie blue is known to stain such proteins weakly. Bergers *et al.* (1993) also found Bradford's method less efficient for quantifying proteins extracted from a marine diatom.

Gel electrophoresis

SDS-polyacrylamide gel electrophoresis was carried out according to Laemmli (1970) in 15% polyacrylamide gels. Samples were solubilized by boiling for 5 min in 62.5 m*M* Tris-HCl buffer (pH 6.8, 2% SDS, 5% β-mercaptoethanol, 10% glycerol, 0.002% bromophenol blue). Each well was loaded with 10 μl of a sample containing 25 to 100 μg total proteins. Electrophoretical separations were performed for 70 min at 150 V with a Hoefer SE Mighty Small II apparatus in 25 m*M* Tris-HCl-buffer (pH 6.80, 0.192 *M* glycine, 0.1% SDS). The 10-kDa Protein Ladder (GibcoBRL) was used as the molecular weight (MW) standard. Gels were stained with either Coomassie Brilliant Blue R-250 (Dzandu *et al.*, 1984) or silver (Wray *et al.*, 1981).

Electroblotting

Proteins were electroblotted under semi-dry conditions onto polyvinylidene difluoride (PVDF) membranes (0.2 μm, Boehringer-Mannheim) for 75 min in a Multiphor II Novablot unit (Pharmacia Biotech). Transfer buffer consisted of 25 m*M* Tris-HCl, 192 m*M* glycine (pH 8.3) made up in 15% v/v aqueous methanol. Blotting was allowed to proceed for 1 h at constant current (40 mA). To ascertain the efficiency of protein transfer, the gels were stained with Coomassie blue. The pre-stained 14,300–200,000 MW Range (GibcoBRL) was used as the protein MW standard.

Lectin probing

The glycoproteins immobilized on the PVDF membranes were probed with biotinylated lectins secondarily labeled with the avidin-biotinylated HRP (horseradish peroxidase) complex (Vector no. A-2004). The procedure generally followed Rohringer and Holden (1985). The secondary label was then revealed by the diaminobenzidine (DAB) staining method (Hsu and Soban, 1982) using the Sigma Fast DAB peroxidase substrate tablet set (Sigma no. D-4418). The biotinylated lectins used were Concanavalin A (Con A, Sigma no. C-2272), Jacalin (Jac, Vector no. 1155), soybean agglutinin (SBA, Sigma no. L-3395), *Maackia amurensis* agglutinin II (MAA II, Vector no. B-1265), and *Sambucus nigra* agglutinin (SNA, Vector no. B-1305). Con A essentially binds to α-mannose and α-glucose residues (α-Man, α-Glc), but not to related sugar residues such as α,β-galactose (α,β-Gal) (Goldstein *et al.*, 1965a, b; Hayat, 1993). Jac preferentially binds to galactosyl (β-1,3)*N*-acetylgalactosamine (Gal(β-1,3)GalNAc) sequences in *O*-linked oligosaccharides (Hayat, 1993; Shafer *et al.*, 1994). SBA recognizes terminal α,β-*N*-acetylgalactosaminyl (α,β-GalNAc) and α,β-galactosaminyl (α,β-Gal) residues (Lotan *et al.*, 1973; Hayat, 1993). MAA II (Knibbs *et al.*, 1991) and SNA (Broekaert *et al.*, 1984) bind to *N*-acetylneuraminic residues (NeuNAc or sialic acids) preferentially in α(2,3) and α(2,6) linkages respectively.

The probing procedure was as follows. Nonspecific binding sites on the membranes were blocked overnight at 4°C with 0.5% gelatin from coldwater-fish skin (Sigma no. G-7765) in the specific lectin buffer. For all three lectins the incubation buffer was PBS-Tween (0.01 *M* Na-phosphate, 0.15 *M* NaCl, 0.05% NaN_3, 0.05% Tween 20) containing 0.1% fish gelatin. This buffer was adjusted to pH 6.8 for Con A and SBA, and to pH 7.5 for Jac, MAA II, and SNA. It was supplemented with 0.1 m*M* $CaCl_2$ and 0.1 m*M* $MnCl_2$ for Con A, and with 0.1 m*M* $CaCl_2$ for SNA and Jac. The membranes were incubated for 2 h at 20°C, either with 1 μg/ml lectin for Con A and Jac, or with 5 μg/ml lectin for SBA, MAA II, SNA. They were washed six times in PBS-Tween and incubated for 2 h at 20°C with 5 μg/ml avidin-biotin peroxidase complex in PBS-Tween at pH 7.5 with 0.1% fish gelatin. After washing in PBS-Tween, the blots were washed five times in TBS (0.05 *M* Tris, 0.15 NaCl pH 7.6) and allowed to react for from 30 s to 1 min with 0.5 mg/ml 3,3′-diaminobenzidine tetrahydrochloride and 1 μ*M* H_2O_2 in TBS. They were then washed three times in TBS and three times in Milli-Q water. To test the specificity of the binding, inhibition experiments (Glass *et al.*, 1981) were performed with 0.2 *M* methyl-α-D-mannopyranoside (MMP, Sigma no. M-6160) for Con A and 0.15 *M* *N*-acetylneuraminyllactose (sialyllactose, Sigma no. A-3307) for MAA II and SNA, as lectin-binding inhibitors in the incubation media.

To determine the linkage of the carbohydrate moieties of the glycoproteins observed on the gels, extracts were treated with the enzyme *N*-glycosidase F (from *F. meningoepticum*, EC 3.2.2.18 and 3.5.1.52) under denaturing conditions be-

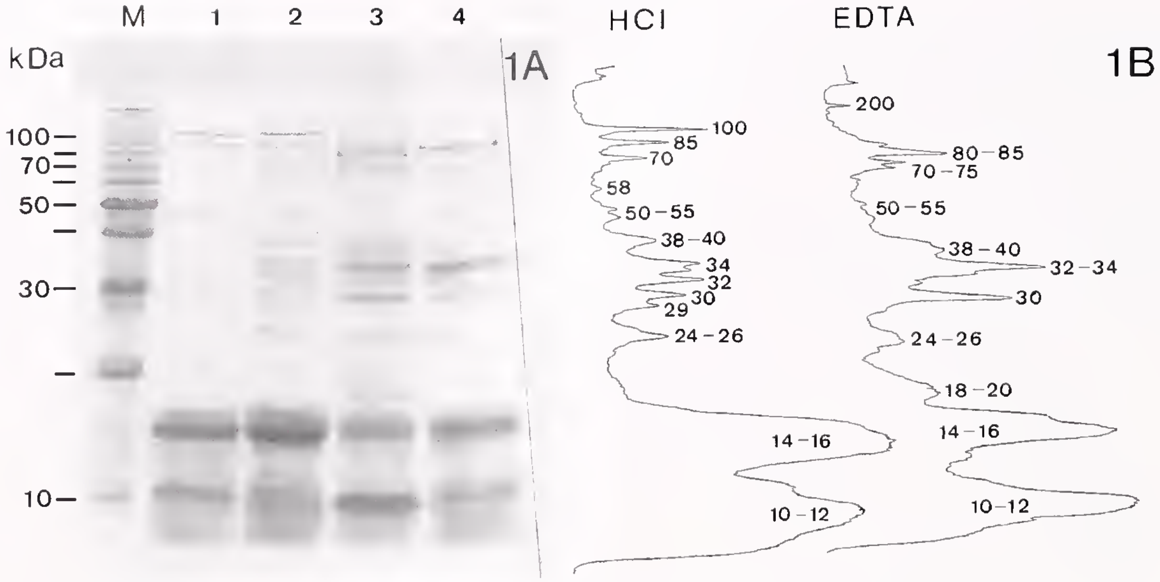

Figure 1. Proteins extracted from the cephalothoracic shield cuticle of anecdysial *Carcinus maenas.* Coomassie blue-stained SDS-polyacrylamide gel (15%), 50 μg protein/lane. Fig. 1A. Lane 1: 2% HAc-extract; Lane 2: 0.1 N HCl-extract; Lane 3: 10% EDTA-extract; Lane 4: 0.5 M KCl-extract; Lane M: Molecular Weight Marker 10 kDa Protein Ladder (GibcoBRL). Fig. 1B. Densitometric profiles of the HCl- and EDTA-extracts lanes (2 and 3).

fore SDS-PAGE, electroblotting, and lectin probing. *N*-glycosidase F specifically cleaves sugars that are *N*-linked to nonterminal asparagines of glycoproteins (Tarentino *et al.*, 1985; Maley *et al.*, 1989). Glycoproteins (100 μg) were denatured by boiling in the presence of 1% SDS (5 μl). *N*-glycosidase F buffer (45 μl; 20 mM Na-phosphate buffer pH 7.2, 10 mM NaN$_3$, 50 mM EDTA, 0.5% Nonidet P-40) was added, and the mixture was boiled again for 2 min. Protein deglycosylation (100 μg protein) was carried out by incubating for 20 h at 37°C in the presence of 2 units of *N*-glycosidase F (Boehringer-Mannheim).

Analysis of electrophoretical profiles

Banding profiles on SDS-polyacrylamide gels and Western blots were digitized and analyzed with a Bio-Rad densitometer (model GS-670) and with the Molecular Analyst/PC program for identification of corresponding protein bands, molecular weight determinations, and densitometric profile drawing.

Results

Gel electrophoresis

Prior to gel electrophoresis, the protein contents of the extracts were estimated by the BCA method. The EDTA extract displayed the lowest protein content, ranging from 3 to 4 mg/g of initial cuticle fresh weight (FW) whatever the sample treatment (crushed or reduced into powder). The values recorded for the other extracts were from 25% to 75% higher, ranging from 5 to 6 mg/g of initial cuticle FW in the HCl extract and from 6 to 7 in the HAc and KCl extracts.

Coomassie blue and silver staining yielded quite similar electrophoretical patterns (Figs. 1 and 2), although some bands appeared with one stain and not the other, and some bands differed as to their staining intensity (detailed below). The molecular weights corresponding with the band positions were estimated from the densitometric profiles (Figs. 1B and 2B). All extracts yielded protein bands mainly in three molecular weight ranges: a few bands in a high-MW range (55–100 kDa), many in a medium-MW range (20–50 kDa), and some very thick bands in a low-MW range (10–20 kDa). The KCl and EDTA extracts displayed very similar banding profiles, with thick bands in the low-MW range, major bands in the high- and medium-MW ranges at 30 kDa, 32–34 kDa, 70–75 kDa, and 80–85 kDa, and a narrow band at 200 kDa. When extraction was done in an acidic rather than a neutral solvent, the banding pattern was different. The HCl extract displayed most of the protein bands observed with neutral solvent extracts. The only exceptions were the 200-kDa band and a weak 38-kDa band on silver-stained gels. Moreover, the HCl extract exhibited several intense additional bands at 17 kDa, 24–26 kDa, and 100 kDa. Except for a 45-kDa band that appeared in the HAc extract lane on silver-stained gels only, the banding pattern of the HAc extract closely

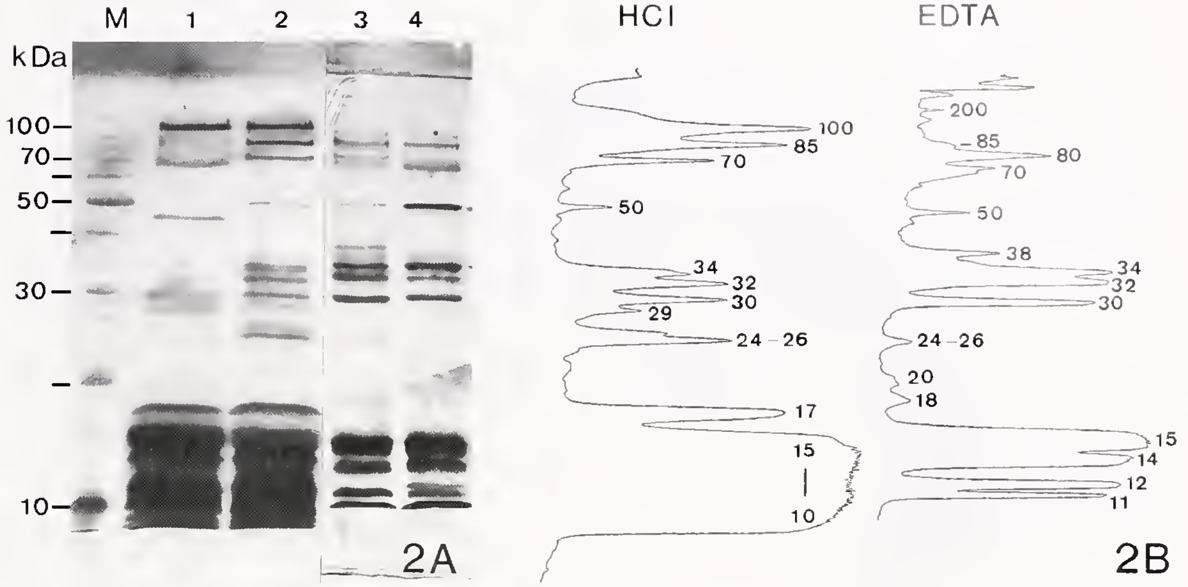

Figure 2. Proteins extracted from the cephalothoracic shield cuticle of anecdysial *Carcinus maenas*. Silver-stained SDS-polyacrylamide gels (15%), 50 μg protein/lane. Fig. 2A Lane 1: 2% HAc-extract; Lane 2: 0.1 N HCl-extract; Lane 3: 10% EDTA-extract; Lane 4: 0.5 *M* KCl-extract; Lanes M: Molecular Weight Marker 10 kDa Protein Ladder (GibcoBRL). Fig. 2B. Densitometric profiles of the HCl- and EDTA-extracts lanes (2 and 3).

resembled that of the HCl extract in the low-MW ranges, but in the high- and medium-MW ranges, many bands were missing or very faint.

As mentioned above, the staining intensity of a protein band could vary drastically with the gel staining method. The 17-kDa band of the HAc and HCl extracts, for instance, was stained only by silver (Fig. 2), and the 16-kDa band that was intensely stained by Coomassie blue whatever the extract (Fig. 1) was not revealed by silver staining (Fig. 2).

Reaction of extracted proteins with lectins

Lectin binding revealed that most of the proteins extracted by the described procedure are glycosylated. The labeling intensity varied, however, according to the protein band and the lectin used. Conspicuous differences were again observed between neutral- and acidic-solvent extracts.

Concanavalin A. Of the five lectins tested, Con A labeled the greatest number of protein bands (Fig. 3). Almost all the protein bands in the high- and medium-MW ranges bound Con A, suggesting that they are glycosylated, primarily with mannose. In these ranges, only a few differences were observed between the various extracts (*e.g.*, differences in the intensity of some high-MW bands between acidic- and neutral-solvent extracts). The bands exhibiting the strongest Con A binding were mostly those staining intensely with Coomassie blue or silver. The 200-kDa band appeared to be labeled in every extract lane, even when it did not appear, or was very faint, after Coomassie or silver staining.

In the low-MW range, few of the very thick protein bands appearing on Coomassie- or silver-stained gels reacted with Con A. Moreover, obvious differences appeared between extracts. Several positive bands appearing in the range of 10–15 kDa in the lanes loaded with acidic-solvent extracts were completely missing in the EDTA-extract lane. Only two of them appeared in the KCl-extract lane, and those were very faint. A 20-kDa band accompanied the 24–26-kDa bands in all lanes. This band was faint to undetectable on Coomassie- and silver-stained gels.

Con A binding was completely inhibited by methyl-α-D-mannopyranoside (MMP) (Fig. 3A, lanes 5 and 6), except for some of the most intensely labeled bands (30–34 kDa). When the extracted proteins were treated with *N*-glycosidase F prior to separation, transferred to a PVDF membrane, and probed with Con A (Fig. 3A, lanes 7 and 8), none of the low-MW protein bands were labeled, and the high-MW protein bands appeared much fainter. This confirms that mannose-rich carbohydrates are *N*-linked to these proteins.

Jacalin. Like Con A, Jac bound to most of the bands in the high- and medium-MW ranges and to some low-MW bands (see Fig. 4, HCl and EDTA extracts). The reacting bands from the HCl and EDTA extracts were about the same; the only differences were a more pronounced labeling of the 65-kDa band and additional 24–26-kDa bands from the HCl extract and of the 32- and 45-kDa bands from the EDTA extract. Labeling with Jac was somewhat less intense than with Con A. Almost all of the Jac-positive bands were

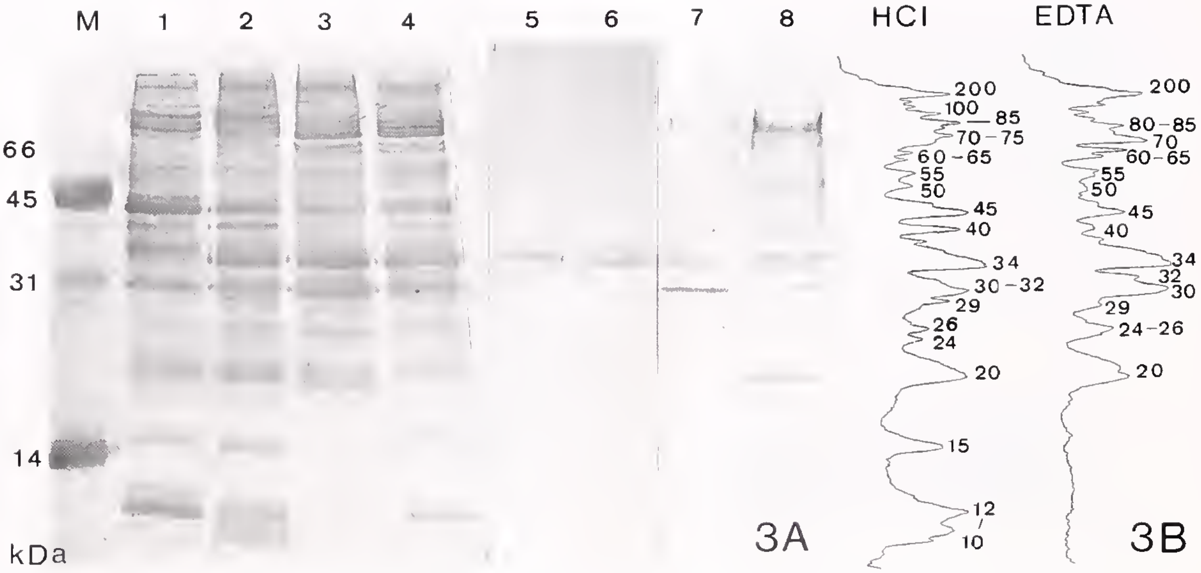

Figure 3. Glycoproteins of the *Carcinus maenas* cephalothoracic shield cuticle separated on SDS-polyacrylamide gels (15%, 25 μg protein/lane), electroblotted to PVDF, and probed with Con A (lanes M and 1 to 4) in the presence of MMP (lanes 5 and 6) and with previous deglycosylation by *N*-glycosidase F (lanes 7 and 8). Fig. 3A. Blotting membranes Lane M: pre-stained Molecular Weight Marker 14.300–200.000 Molecular Weight Range (GibcoBRL) with labeled 14.3-, 31- and 45-kDa bands; Lane 1: 2% HAc-extract; Lanes 2, 5, and 7: 0.1 N HCl-extract, Lanes 3, 6, and 8: 10% EDTA-extract; Lane 4: 0.5 *M* KCl-extract. Fig. 3B. Densitometric profiles of the HCl- and EDTA-extracts lanes (2 and 3).

ones previously found to react with Con A (*e.g.*, the bands at 29, 30–32, 34, 40, 45, 50, 55, and 100 kDa in both extracts; at 10, 15 and 22–24 kDa in the HCl extract; and at 80–85 kDa in the EDTA-extract), but several Con A-positive bands failed to react with Jac (*e.g.*, the bands at 12, 15, 20, 32, and 200 kDa in the HCl-extract lane; the bands at 20, 24–26, 70, and 200-kDa in the EDTA-extract lane).

Sambucus nigra *agglutinin and* Maackia amurensis *ag-*

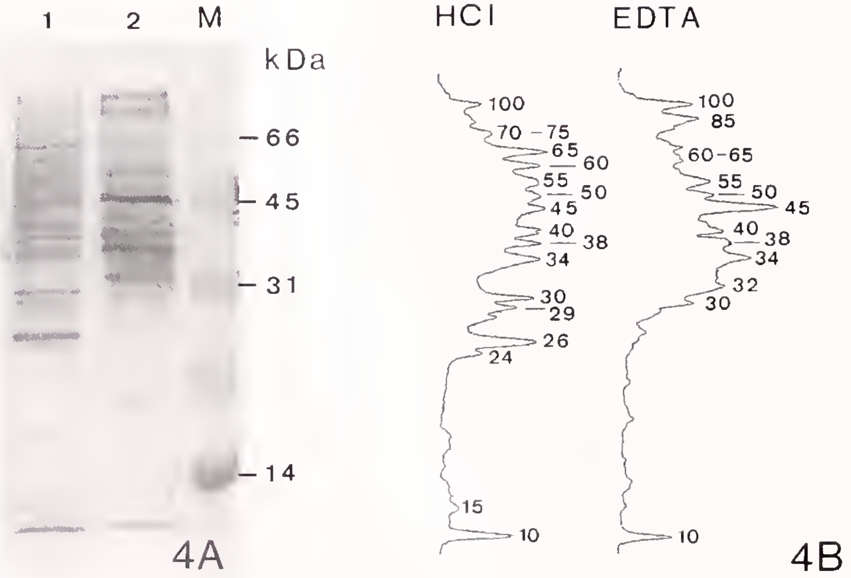

Figure 4. Glycoproteins of the *Carcinus maenas* cephalothoracic shield cuticle separated on 1D SDS-polyacrylamide gel (15%, 25 μg protein/lane), electroblotted to PVDF, and probed with Jac. Fig. 4A. Lane M: pre-stained Molecular Weight Marker 14,300–200,000 Molecular Weight Range (GibcoBRL) with labeled 14.3- and 45-kDa bands; Lane 1: 0.1 N HCl-extract; Lane 2: 10% EDTA-extract. Fig. 4B. Densitometric profiles.

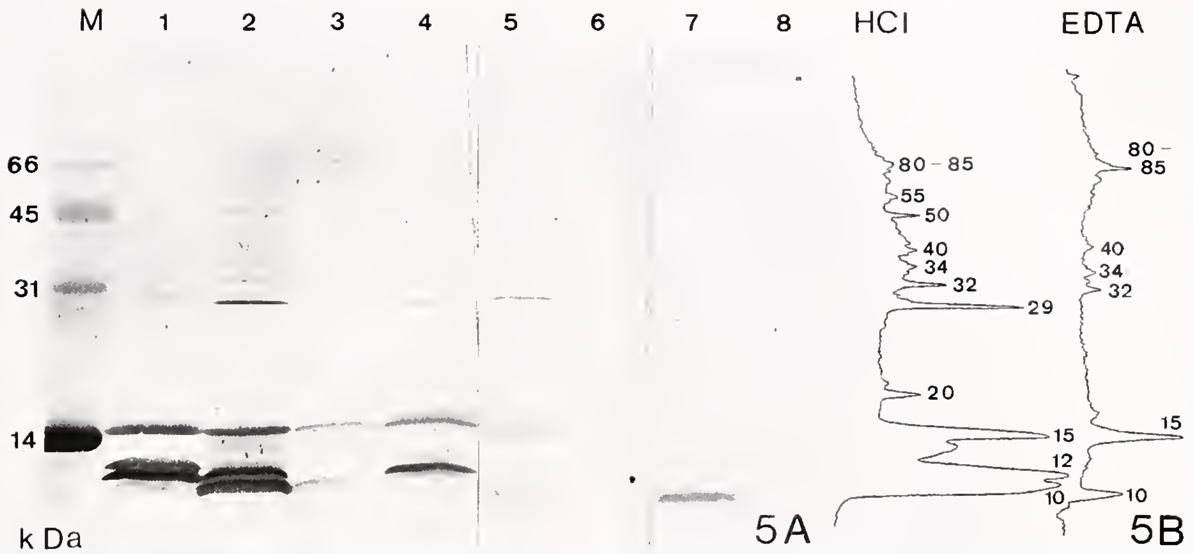

Figure 5. Glycoproteins of the *Carcinus maenas* cephalothoracic shield cuticle separated on 1D SDS-polyacrylamide gels (15%, 100 μg protein/lane), electroblotted to PVDF, and probed with MAA II (lanes M and 1 to 4), in the presence of sialyllactose (lanes 5 and 6) and with previous deglycosylation by *N*-glycosidase F (lanes 7 and 8). Fig. 5A. Lane M: pre-stained Molecular Weight Marker 14,300–200,000 Molecular Weight Range (GibcoBRL) with labeled 14.3- and 31-kDa; Lane 1: 2% HAc-extract; Lanes 2, 5, and 7: 0.1 N HCl-extract; Lanes 3, 6, and 8: 10% EDTA-extract; Lane 4: 0.5 *M* KCl-extract. Fig. 5B. Densitometric profiles of the HCl- and EDTA-extracts lanes (2 and 3).

glutin II. In contrast to Con A and Jac labeling, only a few bands were found to react with the sialic-acid-binding lectins MAA II and SNA (Figs. 5 and 6 respectively). The most intensely labeled bands appeared in the low-MW range (10–15 kDa) of the HCl and HAc extracts. Two positive bands (at 12–13 and 15 kDa) were also visible in the KCl

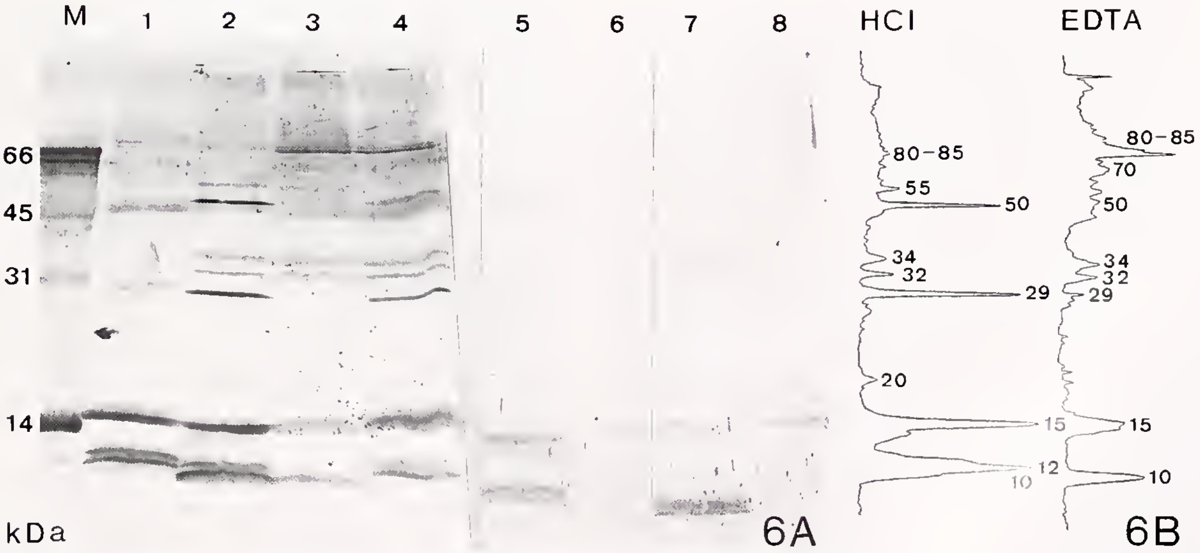

Figure 6. Glycoproteins of the *Carcinus maenas* cephalothoracic shield cuticle separated on 1D SDS-polyacrylamide gels (15%, 100 μg protein/lane), electroblotted to PVDF, and probed with SNA (lanes M and 1 to 4), in the presence of sialyllactose (lanes 5 and 6) and with previous deglycosylation by *N*-glycosidase F (lanes 7 and 8). Fig. 6A. Lane M: pre-stained Molecular Weight Marker 14,300–200,000 Molecular Weight Range (GibcoBRL) with labeled 14.3- and 66-kDa bands; Lane 1: 2% HAc-extract; Lanes 2, 5, and 7: 0.1 N HCl-extract; Lanes 3, 6, and 8: 10% EDTA-extract; Lane 4: 0.5 *M* KCl-extract. Fig. 6B. Densitometric profiles of the HCl- and EDTA-extracts lanes (2 and 3).

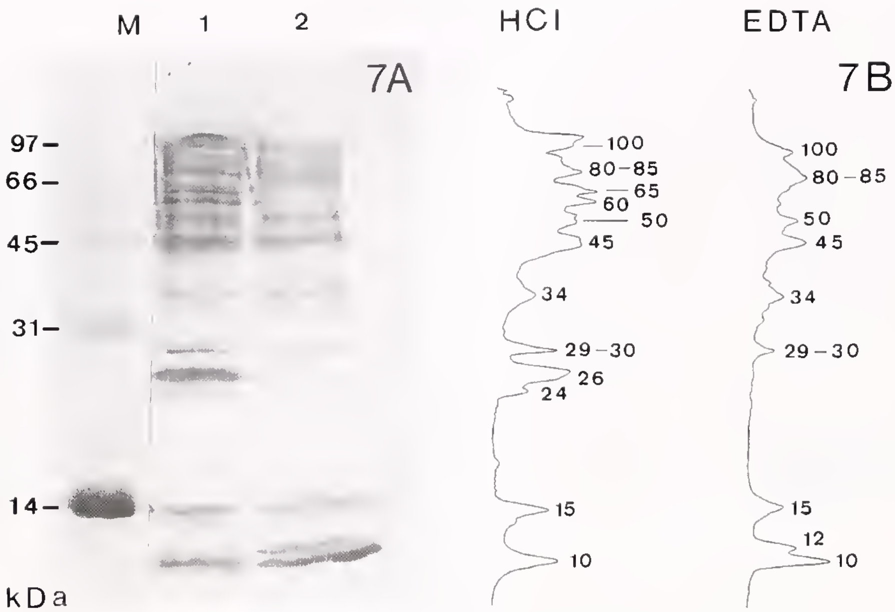

Figure 7. Glycoproteins of the *Carcinus maenas* cephalothoracic shield cuticle separated on 1D SDS-polyacrylamide gel (15%, 100 μg protein/lane), electroblotted to PVDF, and probed with SBA. Fig. 7A. Lane M: pre-stained Molecular Weight Marker 14,300–200,000 Molecular Weight Range (GibcoBRL) with labeled 14.3-kDa band; Lane 1: 0.1 N HCl-extract; Lane 2: 10% EDTA-extract. Fig. 7B. Densitometric profiles.

extract, but they were labeled much less intensely. They were missing or nearly undetectable in the EDTA-extract lane. In the high- and medium-MW ranges, some positive bands corresponded with ones showing a high affinity for Con A (*e.g.*, the bands at 32, 34, and 80–85 kDa in the KCl-, EDTA- and HCl-extract lanes). The HCl-extract lanes also exhibited additional, strongly positive 29- and 50-kDa bands that were missing in the EDTA-lane but present—though less intensely labeled—in the KCl-extract lane. These bands (29- and 50-kDa) reacted weakly with Con A and Jac. In the HAc-extract lane, labeling of the high- and medium-MW bands was very poor.

The intensity of SNA and MAA II labeling was significantly reduced when sialyllactose was present (Figs. 5 and 6, lanes 5 and 6), and labeling was almost completely absent when the extracts were previously deglycosylated with *N*-glycosidase F (Figs. 5 and 6, lanes 7 and 8). This suggests that the sialic acid residues detected belong to *N*-linked oligosaccharides.

Soybean agglutinin. As illustrated for the HCl and EDTA extracts (Fig. 7), SBA reacted with a few bands of high- and medium-MW. These were bands that also reacted with Con A, Jac, or both (*e.g.*, the bands at 29–30, 34, 45, 50, 80–85 and 100 kDa in both lanes). SBA also reacted with a few low-MW bands (in the 10–15 kDa range). The HCl extract displayed more labeled bands than the EDTA extract (additional bands at 24–26 and 60–65 kDa).

Discussion

We have electrophoretically characterized the proteins extracted from the calcified cuticle of the Atlantic shore crab *Carcinus maenas*. The results confirm previous findings on other decapod crustaceans that many extractable proteins appear to be glycosylated. This is the first report, however, of the presence of sialic acids in crustacean cuticle extracts. We also provide new information about the type of glycosylation and the sugar residues present. Our results raise physiological questions such as the location, origin, and role of these glycoproteins in the cuticle architecture, especially as regards their interactions with the organic matrix and calcium carbonate.

In addition, the results give evidence that the nature and the related extraction capacities of the solvent used are of prime importance for subsequent analyses of proteins and glycoproteins from the calcified crustacean cuticle.

Extraction efficiency of the solvents

Because much of the protein in the decapod exoskeleton is presumably associated with calcium salts, the dissolution of calcite is generally accepted as a prerequisite to the extraction of mineral-bound proteins (Gunthorpe *et al.*, 1990; O'Brien *et al.*, 1993). Thus, most of the procedures for extracting proteins from calcified cuticles have included either EDTA (0.4 *M*) together with guanidine thiocyanate (5 *M*) (O'Brien *et al.*, 1991; Kumari and Skinner, 1995; Kumari *et al.*, 1995), or have involved a separate decalcification step with 0.1 *M* EDTA (Andersen, 1991) or 10% acetic acid (Kragh *et al.*, 1997; Nousiainen *et al.*, 1998; Andersen, 1999) prior to extraction by 6 *M* urea in 0.1 % trifluoroacetic acid (TFA). But with these procedures, the extraction of proteins would be mainly due to the strong denaturants (guanidine thiocyanate and urea) in the solvent. In the present study, the amount of protein extracted from the *C. maenas* cuticle by the different solvents is only a small fraction (less than 10%) of the total protein content of the cuticle, which does not exceed 40% of the decalcified dry weight, or about 15% of the cuticle dry weight (Welinder, 1974). Nevertheless, the results show that many proteins, and especially glycoproteins, can be obtained from the calcified crab carapace without strong denaturants in the extraction medium, and even without decalcification. In addition to some very intense low-MW protein bands, the electrophoretical pattern of the extracts from the *C. maenas* cuticle exhibited many protein and glycoprotein bands in the medium- and high-MW ranges (from 30 kDa up to 200 kDa), as was the case for the banding patterns recorded from the 0.1 *M* EDTA extracts (Shafer *et al.*, 1994, 1995) and the EDTA/guanidine thiocyanate extracts (O'Brien *et al.*, 1991, 1993; Kumari and Skinner, 1995) of several decapod cuticles. In contrast, in the urea extracts of previously decalcified cuticle samples from three other decapods (*Pandalus borealis*: Andersen, 1991; *Homarus americanus*: Kragh *et al.*, 1997; Nousiainen *et al.*, 1998; *Cancer pagurus*: Andersen, 1999), the proteins were mostly of low MW, and none of them appeared to be glycosylated. The molecular weight calculated by these authors from the sequence agreed with the MW determined by mass spectrometry of the intact proteins, indicating that no residue is missing. As Kragh *et al.* (1997) already implied, this indicates that substantial amounts of proteins and glycoproteins were removed during the decalcification step prior to the urea extraction. A comparison of these urea extracts (Andersen, 1991, 1999; Kragh *et al.*, 1997; Nousiainen *et al.*, 1998) with the extracts obtained with decalcifying solvents alone (Shafer *et al.*, 1994, 1995; present results) indicates that proteins preferentially extracted in neutral or acid solvents without denaturants tend to be of high MW and glycosylated, whereas proteins extracted in strongly denaturing conditions tend to be of low MW and non-glycosylated. Their amino acid sequence suggested to Nousiainen *et al.* (1998) and Andersen (1999) that such low-MW, non-glycosylated proteins could indeed be strongly bound together or to the chitin-protein microfibers, perhaps by hydrophobic interactions that would not be broken by salts or acids.

On the other hand, the results presented here demonstrated differences between samples extracted with acidic solvents and those extracted with neutral solvents. These differences were particularly obvious when comparing the HCl and the EDTA extracts, especially the lectin-binding patterns. Besides displaying the lowest total protein content, the EDTA extract had a protein-banding pattern that did not differ much from that of the KCl extract obtained without dissolving the mineral. In comparison with the HCl extract, the EDTA extract was apparently missing several bands (*e.g.*, the 17- and 100-kDa bands observed on Coomassie blue- or silver-stained gels, the Con A-labeled bands at 10–15 and 20 kDa, the Jac-labeled bands at 24–26 kDa, the SBA-labeled bands at 24–26 kDa and 60–65 kDa). Particularly poorly represented in this extract were the sialylated glycoprotein bands of low and medium MW (*i.e.*, the SNA- or MAA II-positive bands at 10–12, 15, 20, 29, and 50 kDa), even though they were also present in the KCl extract. HCl (0.1 N) thus emerged as a more efficient solvent than EDTA (10%). HCl also appeared more efficient than 2% HAc, which also seems to extract different proteins than EDTA from the cuticle of newly molted blue crabs (Coblentz *et al.*, 1998). The present electrophoretical analyses and lectin-binding patterns clearly show that many of the high-MW bands present in the HCl extract are missing in the HAc extract. The better extraction efficiency of 0.1 N HCl (pH 2.0) compared to 2 % HAc (pH 3.0) is presumably due to pronounced electrostatic repulsion between net positive charges at the low pH. With 0.1 N HCl, of course, the risk that low pH might affect or break the extracted proteins cannot be neglected. For this reason, protein extraction by 0.1 N HCl should be performed in the cold. The greater extraction efficiency of HCl compared with EDTA agrees with the conclusion of Albeck *et al.* (1993), who concluded that HCl extracts approximately twice as much protein from a molluscan shell (*Atrina rigida*) or a sea urchin test (*Paracentrotus lividus*) as does EDTA. In addition, these authors obtained better fractionation by HPLC of extract from HCl extracts than from EDTA, as well as more acidic amino acids in the HCl-extracted proteins. They proposed that traces of EDTA, extremely difficult to remove, can remain bound to the strongly ionic macromolecules and may influence their charge, conformation, and aggregation state. This could affect protein quantification, migration on gels, and subsequent detection of Ca-binding capability. Other authors (Samata and Matsuda, 1986, in Albeck *et al.*, 1993) proposed that protein might be lost during decalcification by EDTA, either due to the breakdown and leakage through the dialysis membrane, or to the binding *via* EDTA to the dialysis membrane. Such effects of EDTA would explain both the low total protein content of our EDTA extract and its low content of glycoproteins, especially those bearing sialic acids. Extraction with Tris-EDTA may also be the reason why Shafer *et al.* (1994, 1995) failed to detect MAA II- and SNA-binding glycoproteins in extracts of blue crab sclerite cuticle. Although EDTA has the advantage of dissolving the mineral at neutral pH, and thus under conditions more likely to protect the proteins, our data support the recommendation of Albeck *et al.* (1993) that mild acidic solvents, especially dilute HCl, should be the extraction media for proteins from mineralized matrices.

Comparison of electrophoretical patterns

For the reasons discussed above, comparing the electrophoretical patterns obtained with cuticle protein extracts from *C. maenas* and other decapod species is limited to the results of studies in which EDTA-containing or mild acidic extraction media were used. Moreover, the apparent molecular weights of the band-forming proteins should be compared with special caution, because most of them are glycosylated. Glycosylation causes many proteins to run anomalously on SDS-polyacrylamide gels (Segrest and Jackson, 1972). As previously mentioned (O'Brien *et al.*, 1991; Kragh *et al.*, 1997), bands obtained on gels are likely to contain several proteins of similar MW, but different pI values, forming so-called "charge trains." Thus, determining whether the different types of glycans and residues identified on blots belong to a single glycoprotein or to several different ones of similar MW is impossible. Despite these limitations, comparing electrophoretical and western blot patterns of cuticular proteins in different decapod species may prove informative.

The prevalence of low-MW proteins (MW $<$ 31 kDa) appears to be a common feature in cuticle extracts from many arthropod species (Kumari and Skinner, 1993), including arachnids (Norup *et al.*, 1996). This generalization is supported by the present study. The electrophoretical patterns obtained here with *C. maenas* cuticle proteins, and the affinity of these proteins for lectins on blots, were in good agreement with previous results on other decapod species, such as *Gecarcinus lateralis* (O'Brien *et al.*, 1991, 1993; Skinner *et al.*, 1992; Kumari and Skinner, 1995) and *Callinectes sapidus* (Shafer *et al.*, 1994, 1995). This was especially true of the EDTA extract on Coomassie-stained gels and on blots probed with Con A. This suggests the presence of comparable cuticular proteins and glycoproteins in the sclerites of different crustaceans, at least among the brachyuran decapods. Remarkably, a band staining with Coomassie blue, but not with silver, was recorded at 16 kDa for *C. maenas* extracts, and at 15 kDa for *G. lateralis* extracts (O'Brien *et al.*, 1991). In *C. maenas* (present work), *Callinectes sapidus* (Shafer *et al.*, 1995), and *G. lateralis* (Kumari and Skinner, 1995) extracts, Con A recognized most of the high- and medium-MW protein bands. More precisely, major Con A-binding protein bands from *C. maenas* (*e.g.*, the bands at 20, 24–26, 30–32, 34, 45, and 50–55 kDa) coincided with those recorded from *G. lateralis* (the bands at 22, 26, 32, 34, 52, and 54 kDa). Kumari and Skinner (1995), moreover, found some low-MW, Con-A-positive bands in extracts of the procuticular layers (at 11.3, 10.2, and 9.7 kDa) similar to those observed in *C. maenas* extracts—notably the HCl extract.

Some of the above-mentioned bands in the medium-MW range might be formed by subunits of crustacyanin. Blue crustacyanin (β-form) is an oligomeric carotenoprotein that colors the carapace of decapods (Zagalsky *et al.*, 1970; Vranckx and Durliat, 1986). It is easily extracted from the cuticle by neutral and acidic solvents and dissociates irreversibly into purple subunits (40–50 kDa; α-form) or, upon removal of the carotenoid, into subunits of about 20 kDa. Thus, several bands obtained with *C. maenas* cuticle extracts in the medium-MW range probably contain or correspond to crustacyanin subunits. This may also be true of the 54-, 50-, 48-, 44- and 42-kDa bands observed by O'Brien *et al.* (1991) with *G. lateralis* cuticle extracts. These bands are considered by the authors to be formed of specific proteins from the epicuticle (so-called the "epicuticular quintet"), which are especially prominent in extracts of the cuticle of pigmented sclerites.

Cuticle-protein-associated glycans

Our observation that lectins (Con A, Jac, SBA, MAA II, and SNA) recognize various blotted protein bands obtained from *C. maenas* sclerite cuticle extracts, especially HCl extracts, suggests that the glycosylated proteins contain both *N*-linked mannose-rich glycans and *O*-linked oligosaccharides. These results agree with those obtained by lectin labeling of ultrathin sections (Compère and Goffinet, unpubl. data).

The affinity of many glycoprotein bands for Jac suggests the presence of *O*-linked glycans. Jac is known to bind to the Gal(β1,3)GalNAc sequences common in *O*-linked glycans. Shafer *et al.* (1994) likewise detected some Jac-positive protein bands in *Callinectes sapidus* extracts. Our results suggest that many *C. maenas* cuticular proteins of different molecular weights are *O*-glycosylated.

The presence of *N*-linked mannose-rich glycans is supported by the strong affinity for Con A of many glycoprotein bands on our blots and by the drastic reduction of Con A labeling after deglycosylation with *N*-glycosidase F. The presence of *N*-linked glycans in crab cuticular glycoproteins was previously suggested by Shafer *et al.* (1994, 1995), but not demonstrated. The present results agree with those of Kumari and Skinner (1995), who showed that Con A labeling of *Callinectes sapidus* and *G. lateralis* exoskeletal glycoproteins is sensitive to *N*-glycosidase F deglycosylation. Con A mainly recognizes both internal and terminal α(1,2)-linked mannosyl residues, and requires two successive residues of this type to bind tightly (Ogata *et al.*, 1975; Kobata and Endo, 1992). Con A is thus known to have an affinity for many monoantennary and biantennary complex-type *N*-linked oligosaccharides. In contrast to previous results, however, our experiments suggest that many of these *N*-linked glycans bear terminal GalNAc or NeuNAc residues. Terminal α,β -GalNAc residues are recognized by SBA.

The similar binding patterns of MAA II and SNA, which bind to sialic acids in $\alpha(2,3)$ and $\alpha(2,6)$ linkages with different affinities, suggest that both $\alpha(2,3)$- and $\alpha(2,6)$-linked sialic acids are about equally represented. That these GalNAc and NeuNAc residues are present on mannose-rich structures of *N*-linked glycans is supported by several arguments. First, glycoprotein bands reacting with SBA, SNA, and MAA II correspond to ones positive to Con A. Second, the affinity of the protein bands for the three lectins and Con A is reduced by *N*-glycosidase F treatment. Finally, a mannosidase treatment (performed on tissue thin sections) abolished labeling of the cuticle layers by Con A and the three lectins (SBA, SNA, and MAA II), and it must therefore have removed, not only the mannose residues but also the terminal GalNAc and NeuNAc residues linked to them (Compère and Goffinet, unpubl. data). Kumari and Skinner (1995), in contrast, found SBA to react with only a few glycoprotein bands obtained with *G. lateralis* extracts. Shafer *et al.* (1994) detected no MAA II- or SNA-positive bands on blots from *Callinectes sapidus* and came to the conclusion that sialylated residues were absent. We, on the contrary, have detected several MAA II- and SNA-positive protein bands, especially with the HCl extract of *C. maenas* cuticle, suggesting that sialic acids may well be present as terminal sugar residues in cuticular glycoproteins.

Prospects

Because many of the proteins extracted from the cuticle of decapod crustaceans are glycosylated, we must ask about the role of these glycosyl residues and the location of glycoproteins in the cuticle layers. Are the detected glycoproteins constituents of the chitin-protein microfibers or of the interfibrillar matrix? Glycans might contribute, for instance, to the architecture of the cuticle or be involved in organic-mineral interactions, as reported for other extracellular matrices (Wheeler *et al.*, 1988; Berman *et al.*, 1990; Akita *et al.*, 1992; Addadi and Weiner, 1992; Sikes *et al.*, 1994; Marsh, 1994; Hunter and Goldberg, 1993; Hunter *et al.*, 1996; Gaudron *et al.*, 1996). In the crustacean cuticle, this hypothesis is reinforced by the finding that several proteins of medium and high MW extracted from the cuticle of newly molted blue crabs bind to the surface of calcite crystals, as revealed by *in vitro* crystallization assays (Coblentz *et al.*, 1998). In a report on post-ecdysial changes in the glycoproteins of the *Callinectes sapidus* cuticle, and on the lack of affinity of these glycoproteins for lectins that recognize terminal sugar residues, Shafer *et al.* (1995) hypothesized that the *N*-linked glycans of cuticular glycoproteins could be terminally sulfated or phosphated and could be involved in mineralization. The sialylated glycoproteins discovered here in *C. maenas* cuticle extracts might also interact with mineral *via* the negatively charged carboxyl groups of their sialic acids.

From our perspective, it is paramount to localize the (glyco)proteins in the cuticle. The identity of the layers from which the proteins are extracted is a question that has been tackled only by O'Brien *et al.* (1991); these authors mechanically isolated the four layers of the *G. lateralis* cuticle and processed them separately. Although some layer-specific proteins were identified, this kind of experiment is limited because the different layers interdigitate and can never be completely separated. Moreover, microorganisms on the cuticle surface and cytoplasm in the setae ducts and dermal gland ducts introduce contaminants that increase the difficulty of the problem. Consequently, a promising approach may be the ultrastructural localization of glycosyl-residues in the decapod cuticle layers by lectin labeling. This is the focus of a forthcoming paper.

Acknowledgments

The authors are grateful to Dr. B. Focant for his helpful advice and for allowing the use of his equipment for densitometric profile analyses. They also wish to thank Mrs. Cl. Toussaint and Mrs. F. Clérisse for their excellent technical assistance in electrophoresis and Western blotting. This work was funded by the Belgian Fund for Joint Basic Research (FRFC, conventions n° 2.4512.95 and n° 2.4533.01F).

Literature Cited

Addadi, L., and S. Weiner. 1992. Control and design principles in biological mineralisation. *Angew. Chem. Int. Ed. Engl.* **31:** 153–169.

Akita, H., M. Fukae, S. Shimoda, and T. Aoba. 1992. Localization of glycosylated matrix proteins in secretory porcine enamel and their possible functional role in enamel mineralization. *Arch. Oral Biol.* **37:** 953–962.

Albeck, S., J. Aizenberg, L. Addadi, and S. Weiner. 1993. Interactions of various skeletal intracrystalline components with calcite crystals. *Am. Chem. Soc.* **115:** 11691–11697.

Albeck, S., S. Weiner, and L. Addadi. 1996. Polysaccharides of intracrystalline glycoproteins modulate calcite crystal growth *in vitro*. *Chem. Eur. J.* **2:** 278–284.

Andersen, S. O. 1991. Cuticular proteins from the shrimp, *Pandalus borealis*. *Comp. Biochem. Physiol. B* **99:** 453–458.

Andersen, S. O. 1998. Characterization of proteins from arthrodial membranes of the lobster, *Homarus americanus*. *Comp. Biochem. Physiol. A* **121:** 375–383.

Andersen, S. O. 1999. Exoskeletal proteins from the crab, *Cancer pagurus*. *Comp. Biochem. Physiol. A* **123:** 203–211.

Andersen, S. O. 2000. Studies on proteins in post-ecdysial nymphal cuticle of locust, *Locusta migratoria*, and cockroach, *Blaberus craniifer*. *Insect Biochem. Mol. Biol.* **30:** 569–577.

Andersen, S. O., P. Hojrup, and P. Roepstorff. 1995. Insect cuticular proteins. *Insect Biochem. Mol. Biol.* **25:** 153–176.

Bergers, J. A., A. E. Fisher, and P. J. Harrison. 1993. A comparison of Lowry, Bradford and Smith protein assays using different protein standards and protein isolated from marine diatom *Thalassiosira pseudonana*. *Mar. Biol.* **115:** 187–193.

Berman, A., S. Addadi, A. Kvik, L. Leiserowitz, M. Nelson, and S. Weiner. 1990. Intercalation of sea urchin proteins in calcite: study of a crystalline composite material. *Science* **250:** 664–667.

Bradford, M. M. 1976. A rapid and sensitive method for the quantitation of microgram quantities of protein utilizing the principle of protein-dye binding. *Anal. Biochem.* **72:** 248–254.

Broekaert, W. F., M. Nsimba-Lubaki, B. Peeters, and W. J. Peumans. 1984. A lectin from elder (*Sambucus nigra* L.) bark. *Biochem. J.* **221:** 163–169.

Coblentz, F. E., T. H. Shafer, and R. D. Roer. 1998. Cuticular proteins from the blue crab alter *in vitro* calcium carbonate mineralization. *Comp. Biochem. Physiol. B* **121:** 349–360.

Compère, P. 1995. Fine structure and morphogenesis of the sclerite epicuticle in the Atlantic shore crab *Carcinus maenas*. *Tissue Cell* **27:** 525–538.

Drach, P., and C. Tchernigovtzeff. 1967. Sur la méthode de détermination des stades d'intermue et son application générale aux Crustacés. *Vie Milieu Sér. A Biol. Mar.* **18:** 595–609.

Dzandu, J. K., M. E. Deh, D. L. Barriatt, and G. E. Wise. 1984. Detection of erythrocyte membrane proteins, sialoglycoproteins, and lipids in the same polyacrilamide gel using a double staining technique. *Proc. Natl. Acad. Sci. USA* **81:** 1733–1737.

Gaudron, J., M. Bain, S. Solomon, and Y. Nys. 1996. Soluble matrix of hen's eggshell extracts changes *in vitro* the rate of calcium precipitation and crystal morphology. *Br. Poult. Sci.* **37:** 853–866.

Glass, W. F., R. C. Briggs, and L. S. Hnilica. 1981. Use of lectins for detection of electrophoretically separated glycoproteins transferred onto nitrocellulose sheets. *Anal. Biochem.* **115:** 219–224.

Goffinet, G., and C. Jeuniaux. 1994. Le Tégument: Morphologie et Biochimie. Pp. 49–90 in *Traité de Zoologie, Tome VII: Crustacés, Fascicule 1: Morphologie, Physiologie, Reproduction, Embryologie*, P. P. Grassé, ed. Masson & Cie, Paris.

Goldstein, I. J., C. E. Hollerman, and E. E. Smith. 1965a. Protein carbohydrate interaction. I. Interaction of polysaccharides with concanavalin A. *Biochem. Biophys. Acta* **97:** 68–76.

Goldstein, I. J., C. E. Hollerman, and E. E. Smith. 1965b. Protein carbohydrate interaction. II. Inhibition studies on the interaction of concanavalin A with polysaccharides. *Biochemistry* **4:** 876–883.

Gunthorpe, M. E., C. S. Sikes, and A. P. Wheeler. 1990. Promotion and inhibition of calcium carbonate crystallization *in vitro* by matrix protein from blue crab exoskeleton. *Biol. Bull.* **179:** 191–200.

Hackman, R. H. 1974. The soluble cuticular proteins from three arthropod species: *Scylla serrata* (Decapoda: Portunidae), *Boophilus microplus* (Acarina: Ixodidae) and *Agrianome spinicollis* (Coleoptera: Cerambycidae). *Comp. Biochem. Physiol. B* **49:** 457–464.

Hackman, R. H. 1984. Arthropoda: cuticle: biochemistry. Pp. 583–610 in *Biology of the Integument, Vol. I, Invertebrates*, J. Bereiter-Hahn, A. G. Matoltsy, and K. S. Richards, eds. Springer Verlag, Berlin.

Hackman, R. H., and M. Goldberg. 1976. Comparative chemistry of arthropod cuticular proteins. *Comp. Biochem. Physiol. B* **55:** 201–206.

Harvey, M. A., K. Klueg, P. Sheppard, and A. R. Rudolf. 1995. Structure, expression, and extracellular targeting of PM 27, a skeletal protein associated specifically with growth of the sea urchin larval spicules. *Dev. Biol.* **168:** 549–566.

Hayat, M. A. 1993. *Stains and Cytochemical Methods*, M. A. Hayat, ed. Plenum, New York. 455 pp.

Hsu, S. -M., and E. Soban. 1982. Color modification of diaminobenzidine (DAB) precipitation by metallic ions and its application for double immunochemistry. *J. Histochem. Cytochem.* **30:** 1079–1082.

Hunter, G. K., and H. A. Goldberg. 1993. Nucleation of hydroxyapatite by bone sialoprotein. *Proc. Natl. Acad. Sci. USA* **90:** 8562–8565.

Hunter, G. K., P. V. Hauschka, R. A. Poole, L. C. Rosenberg, and H. A. Goldberg. 1996. Nucleation and inhibition of hydroxyapatite formation by mineralised tissue proteins. *Biochem. J.* **317:** 59–64.

Jensen, C., S. O. Andersen, and P. Roepstorff. 1998. Primary structure of two major proteins from the migratory locust, *Locusta migratoria*, and their identification in polyacrylamide gels by mass spectrometry. *Biochim. Biophys. Acta* **1429:** 151–162.

Knibbs, R. N., I. J. Goldstein, R. M. Ratcliffe, and N. Shibuya. 1991. Characterization of the carbohydrate binding specificity of the leukoagglutinating lectin from *Maackia amurensis*. *J. Biol. Chem.* **266:** 83–88.

Kobata, A., and T. Endo. 1992. Immobilized lectin columns: useful tools for the fractionation and structural analysis of oligosaccharides. *J. Chromatogr.* **597:** 111–122.

Kragh, M., L. Molbak, and S. O. Andersen. 1997. Cuticular proteins from the lobster, *Homarus americanus*. *Comp. Biochem. Physiol. B* **118:** 147–154.

Kumari, S. S., and D. M. Skinner. 1993. Proteins of crustacean exoskeleton: II. Immunological evidence for their relatedness to cuticular proteins of two insects. *J. Exp. Zool.* **265:** 195–210.

Kumari, S. S., and D. M. Skinner. 1995. Proteins of crustacean exoskeleton: III. Glycoproteins in the Bermuda land crab *Gecarcinus lateralis*. *J. Exp. Zool.* **271:** 413–424.

Kumari, S. S., J. H. Willis, and D. M. Skinner. 1995. Proteins of crustacean exoskeleton IV: Partial amino acid sequences of exoskeletal proteins from the Bermuda land crab, *Gecarcinus lateralis*, and comparisons to certain insect proteins. *J. Exp. Zool.* **273:** 389–400.

Laemmli, U. K. 1970. Cleavage of structural proteins during the assembly of the head of bacteriophage T4. *Nature* **227:** 680–685.

Lotan, R., H. W. Siegelman, H. Lis, and N. Sharon. 1974. Subunit structure of soybean agglutinin. *J. Biol. Chem.* **249:** 1219–1224.

Maley, F., R. B. Trimble, A. L. Tarentino, and T. H. Plummer, Jr. 1989. Characterization of glycoproteins and their associated oligosaccharides through the use of endoglycosidases. *Anal. Biochem.* **180:** 195–204.

Marsh, M. E. 1994. Polyanions and biomineralization. Pp. 121–128 in *Biomineralization 93, 7th International Symposium on Biomineralization, Vol. 1: Fundamentals of Biomineralization*, D. Allemand and J.-P. Cuif, eds. *Bulletin de l'Institut océanographique de Monaco, n° spécial* **14 (1)**.

Neville, A. C. 1975. *Biology of the Arthropod Cuticle, Vol. 4/5, Zoophysiology and Ecology*, W. S. Hoar, J. Jacobs, H. Langer, and M. Lindauer, eds. Springer Verlag, Berlin. 448 pp.

Neville, A. C. 1984. Arthropoda: cuticle: organization. Pp. 611–625 in *Biology of the Integument, Vol. I, Invertebrates*, J. Bereiter-Hahn, A. G. Matoltsy, and K. S. Richards, eds. Springer Verlag, Berlin.

Neville, A. C. 1993. *Biology of Fibrous Composites. Development Beyond the Cell Membrane.* Cambridge University Press, Cambridge. 214 pp.

Norup, T., T. Berg, H. Stenholm, S. O. Andersen, and P. Hojrup. 1996. Purification and characterization of five cuticular proteins from the spider *Araneus diadematus*. *Insect Biochem. Mol. Biol.* **26:** 907–915.

Nousiainen, M., K. Rafn, L. Skou, P. Roepstorff, and S. O. Andersen. 1998. Characterisation of exoskeletal proteins form the American lobster, *Homarus americanus*. *Comp. Biochem. Physiol. A* **119:** 189–199.

O'Brien, J. J., S. S. Kumari, and D. M. Skinner. 1991. Proteins of crustacean exoskeletons: I. Similarities and differences among proteins of the four exoskeletal layers of four brachyurans. *Biol. Bull.* **181:** 427–441.

O'Brien, J. J., S. S. Kumari, and D. F. Skinner. 1993. Differential localization of specific proteins in the exoskeleton of the Bermuda land crab. Pp. 79–111 in *The Crustacean Integument. Morphology and Biochemistry*, M. N. Horst and J. A. Freeman, eds. CRC Press, Boca Raton, FL.

Ogata, S., T. Muramatsu, and A. Kobata. 1975. Fractionation of glycopeptides by affinity column chromatography on Concanavalin A-Sepharose. *J. Biochem.* **78:** 687–696.

Roer, R., and R. Dillaman. 1993. Molt-related changes in the integumental structure and function. Pp. 1–37 in *The Crustacean Integument: Morphology and Biochemistry*, M. N. Horst and J. A. Freeman, eds. CRC Press, Boca Raton, FL.

Rohringer, R., and D. W. Holden. 1985. Protein blotting: detection of proteins with colloidal gold, and of glycoproteins and lectins with biotin-conjugated and enzyme probes. *Anal. Biochem.* **144:** 118–127.

Samata, T., and M. Matsuda. 1986. Contaminating peptides widely present in ion-exchanged water, reagents, experimental implements and natural sample. *Comp. Biochem. Physiol.* **84B:** 531–535. (Cited in Albeck *et al.*, 1993.)

Segrest, J. P., and R. L. Jackson. 1972. Molecular weight determination of glycoproteins by polyacrylamide gel electrophoresis in sodium dodecyl sulfate. *Methods Enzymol.* **28:** 54–63.

Shafer, T. H., R. D. Roer, C. G. Miller, and R. M. Dillaman. 1994. Postecdysial changes in the protein glycoprotein composition of the cuticle of the blue crab *Callinectes sapidus*. *J. Crustac. Biol.* **14:** 210–219.

Shafer, T. H., R. D. Roer, C. Midgette-Luther, and T. A. Brookins. 1995. Postecdysial cuticle alteration in the blue crab, *Callinectes sapidus*: synchronous changes in glycoproteins and mineral nucleation. *J. Exp. Zool.* **271:** 171–182.

Sikes, C. S., A. Wierzbicki, and V. J. Fabry. 1994. From atomic to global scales in biomineralization. Pp. 1–48 in *Biomineralization 93, 7th International Symposium on Biomineralization, Vol. 1: Fundamentals of Biomineralization*, D. Allemand and J.-P. Cuif, eds. *Bulletin de l'Institut océanographique de Monaco, n° spécial* **14 (1).**

Skinner, D. M., S. S. Kumari, and J. J. O'Brien. 1992. Proteins of the crustacean exoskeleton. *Am. Zool.* **32:** 470–484.

Smith, P. K., R. I. Krohn, G. T. Hermanson, A. K. Mallia, F. H. Gartner, M. D. Provenzano, E. K. Fujimoto, N. M. Goeke, B. J. Olson, and D. C. Klenk. 1985. Measurement of protein using bicinchoninic acid. *Anal. Biochem.* **150:** 76–85.

Stevenson, J. R. 1985. Dynamics of the integument. Pp. 1–42 in *The Biology of Crustacea, Vol. 9, Integument, Pigments, and Hormonal Processes*, D.E. Bliss and L.H. Mantel, eds. Academic Press, New York.

Tarentino, A. L., C. M. Gomez, and T. H. Plummer. 1985. Deglycosylation of asparagine-linked glycans by peptide: *N*-glycosidase F. *Biochemistry* **24:** 4665–4671.

Vranckx, R., and M. Durliat. 1980. Cuticular proteins analysis from *Astacus leptodactylus*—I. Electrophoretical studies of the soluble cuticular components. *Comp. Biochem. Physiol. B* **65:** 55–64.

Vranckx, R., and M. Durliat. 1986. Cuticular proteins in the crayfish *Astacus leptodactylus*—I. Main components. *Comp. Biochem. Physiol. B* **85:** 255–265.

Welinder, B. S. 1974. The crustacean cuticle—I. Studies on the composition of the cuticle. *Comp. Biochem. Physiol. A* **47:** 779–787.

Wiechelman, K. J., R. D. Braun, and J. D. Fitzpatrick. 1988. Investigation of the bicinchoninic acid protein assay: identification of the group responsible for color formation. *Anal. Biochem.* **175:** 231–237.

Wheeler, A. P., K. W. Rusenko, D. M. Swift, and C. S. Sikes. 1988. Regulation of *in vitro* and *in vivo* $CaCO_3$ crystallization by fractions of oyster shell organic matrix. *Mar. Biol.* **98:** 71–80.

Willis, J. H. 1987. Cuticular proteins: the neglected component. *Arch. Insect Biochem. Physiol.* **6:** 203–215.

Willis, J. H. 1999. Cuticular proteins in insects and crustaceans. *Am. Zool.* **39:** 600–609.

Wray, W., T. Boulikas, V. P. Wray, and P. Hancock. 1981. Silver staining of proteins in polyacrylamide gels. *Anal. Chem.* **118:** 197–203.

Zagalsky, P. F., H. J. Ceccaldi, and R. Daumas. 1970. Comparative study on some decapod crustacean carotenoproteins. *Comp. Biochem. Physiol.* **34:** 579–607.

Reference: *Biol. Bull.* **202:** 74–85. (February 2002)

Specificity of a Model Cnidarian-Dinoflagellate Symbiosis

CARMEN A. BELDA-BAILLIE*, BRETT K. BAILLIE†, AND TADASHI MARUYAMA

Marine Biotechnology Institute Co., Ltd., Kamaishi Laboratories, Heita,
Kamaishi City, Iwate 026-0001, Japan

Abstract. To understand the flexibility of symbiotic associations in coral reefs, we investigated the specificity of the *Aiptasia* (cf. *insignis*)-*Symbiodinium* association in the laboratory by rendering the anemones aposymbiotic and inoculating them with different isolates of *Symbiodinium*. Infective algal symbionts were monitored over 3 months by re-isolation and identification using denaturing-gradient gel electrophoresis and sequence comparison of their amplified 18S rRNA hypervariable V1 + V2 gene region. Despite similarity in their external morphology, the algal isolates differed in their infectivity towards the host. Within days of single-isolate inoculation, aposymbiotic anemones formed associations with fresh or cultured isolates (clade B) from the anemones *Aiptasia* sp. or *A. tagetes*, respectively. They associated to a limited extent with cultured isolates (clade A) from the tridacnids *Tridacna crocea* or *Hippopus hippopus*, and not at all with a cultured isolate (clade C) from the stony coral *Montipora verrucosa*, nor with a free-living isolate (clade A) from subtidal sands. Aposymbiotic anemones inoculated with a mixture of all isolates had only the anemone taxon as their detectable symbionts. Re-inoculation of induced symbioses with a mixture of all isolates and incubation with wild anemones showed that the initial induced symbioses with the anemone taxon were stable. Anemones originally infected with tridacnid isolates either additionally acquired the anemone taxon or had the former outgrown by the latter. These results demonstrate the presence of a host-symbiont recognition mechanism, and possibly competition among potential algal symbionts in the *Aiptasia-Symbiodinium* association. Here we present a method that may be useful in monitoring the algal population dynamics in symbiotic corals in the field, along with an efficient method of rendering *Aiptasia* aposymbiotic for further laboratory investigation of *Aiptasia-Symbiodinium* symbioses.

Introduction

Bleaching of symbiotic invertebrates in coral reefs, such as the reef-building corals, anemones, and giant clams, has increasingly been noted over recent years. This phenomenon, which results from the loss of the dinoflagellate symbionts (= zooxanthellae) or their pigment content, has mostly been associated with increasing water temperature (Brown and Ogden, 1993; Glynn, 1996), solar radiation (Gleason and Wellington, 1993; Shick *et al.*, 1996), or both (Drollet *et al.*, 1995). In some cases, bleaching leads to the death of the animal host; in other cases, the symbiosis and the host recover (Knowlton, 2001).

It is not clear how bleached invertebrate hosts recover. Perhaps at the end of the stressful period, any residual symbionts from bleached or unbleached (Hayes and Bush, 1990) host tissues are able to propagate to repopulate their hosts. It is also likely that bleached hosts acquire algal symbionts from those available in the water column (see Belda-Baillie *et al.*, 1999). The actual mechanism may be a combination of these (see also Jones and Yellowlees, 1997).

Recent use of molecular genetic markers has revealed the genetic diversity present among members of the predominant symbiotic genus *Symbiodinium*, which would otherwise be difficult to distinguish morphologically from one another. Analysis of patterns of restriction fragment length

---

Received 3 August 2000; accepted 16 November 2001.

* To whom correspondence should be addressed. Present address: CSIRO Plant Industry, Cnr Clunies Ross Street & Barry Drive, Black Mountain, Canberra, A.C.T. 2601, Australia. E-mail: carmen.baillie@csiro.au

† Present address: Plant Cell Biology Group, Research School of Biological Sciences, Australian National University, Canberra, A.C.T. 2601, Australia.

polymorphism (RFLP) and sequences of their partial 18S rRNA gene revealed that the symbiotic dinoflagellates of many cnidarians form three distinct clades: A, B, and C. Similar algal symbionts associate with dissimilar hosts (Rowan and Powers, 1991a, b). Furthermore, the dominant Caribbean stony corals *Montastraea annularis* and *M. faveolata* have been found to simultaneously host *Symbiodinium* taxa from clades A, B, and C. These taxa are distributed within the host colonies according to gradients of environmental irradiance (Rowan *et al.*, 1997). Recently, distinct functional differences have also been shown among the clades' ability to synthesize mycosporine-like amino acids under the influence of ultraviolet and photosynthetically active radiation (Banaszak *et al.*, 2000).

An increasing appreciation of the genetic and functional diversity of *Symbiodinium* has stimulated interest in the ability of bleached hosts to accept different taxa of *Symbiodinium* and in whether they form stable symbioses. Attempts to address these and related questions in the anemone and clam symbioses, for example, have been hampered by the limited availability of tools that would easily distinguish and monitor any competition between diverse algal populations inside the animal host (*e.g.*, Kinzie and Chee, 1979; Schoenberg and Trench, 1980; Fitt, 1985; Davy *et al.*, 1997; Schwarz *et al.*, 1999; Belda-Baillie *et al.*, 1999).

In this study, we reexamined symbiosis specificity by comparing the relative infectivity of different isolates of *Symbiodinium* with artificially bleached *Aiptasia* sea anemones. These cnidarian hosts have been widely used as test animals for studies of cnidarian-dinoflagellate interactions. Here we used denaturing-gradient gel electrophoresis (DGGE, Fischer and Lerman, 1979) of the hypervariable V1 + V2 region of the alga's 18S rDNA to distinguish between *Symbiodinium* taxa before and after infection of aposymbiotic anemones. DGGE is a fast and inexpensive means of physically separating sequence variants. Used in combination with PCR primers designed to conserved regions of the 18S rRNA gene from *Symbiodinium* (see Carlos *et al.*, 2000), this method allows the study of communities of algal symbionts within marine invertebrates such as *Aiptasia*. Sequencing of the PCR products separated by DGGE permits identification of members of the symbiont community and analysis of phylogenetic relationships between different taxa. By attaching a high-temperature melting domain of GC-rich sequence to the DNA fragment, the technique can detect nearly 100% of all possible sequence variation (Sheffield *et al.*, 1989). This approach can therefore detect a mixture of taxonomically distinct or closely related *Symbiodinium* within the animal host (see Carlos *et al.*, 2000).

DGGE has been successfully used in profiling complex bacterial communities (Muyzer *et al.*, 1993; Øvreås, 2000) and eukaryotic organisms in aquatic environments (Van Hannen *et al.*, 1998), as well as in estimating the relative densities of uncultured bacterial populations (Watanabe and Harayama, 1998). Carlos *et al.* (2000) recently used a variant of this technique, temperature-gradient gel electrophoresis (Rosenbaum and Riesner, 1987), in assessing the genetic diversity of *Symbiodinium* in individual clam and anemone hosts. The same approach can be used to monitor the field dynamics of algal populations in coral reefs (our unpublished data). In this study, we successfully used DGGE analysis for the first time in the investigation of cnidarian-dinoflagellate interactions, particularly the specificity of the association.

Materials and Methods

Induced bleaching of Aiptasia *anemones*

"Wild" symbiotic *Aiptasia* (cf. *insignis*) (*ca.* 1-cm oral-disc size), descendants of a single specimen originally from a coral reef in Okinawa, were carefully collected from an indoor aquarium containing flowing, sand-filtered seawater from a nearby bay (see GenBank accession AY046885 for our 18S rDNA sequence of this study organism). The aquarium was heated to about 25°C, and lit on a 12 h: 12 h photoperiod with approximately 80 μmol photons $m^{-2}s^{-1}$ of photosynthetically active radiation (PAR) from daylight FL 20S-E fluorescent tubes. Except in the case of the infection trials described below, anemones were not fed. In the indoor aquarium the anemones regularly proliferated under fluorescent lights and in the presence of the sand-filtered seawater.

Individual anemones were placed in 30-ml glass vessels with translucent lids. Each glass vessel contained 25 ml of autoclaved 0.45-μm filtered seawater (FSW). The following day, after all anemones had attached themselves inside the glass vessels, the anemones were placed in an incubator at a temperature of 25.0 ± 0.1°C and PAR of 78–82 μmol photons $m^{-2}s^{-1}$ on a 12 h: 12 h photoperiod. After an acclimation period of 2 weeks, replicate anemones were randomly distributed to one of four treatments with controlled temperature and light as follows: (1) 25°C with 80 μmol photons $m^{-2}s^{-1}$ PAR (light control), (2) 25°C in the dark (dark control), (3) 32°C in the dark (moderate heat stress), and (4) 35°C in the dark (high heat stress). All treatments were applied inside a multichamber incubator (Bio multi incubator model LH-30-8CT). The treatments chosen above were based on preliminary experiments which showed that temperatures below 35°C in the presence of light were ineffective in rendering the anemones aposymbiotic, whereas temperatures of 35°C or above in the presence of light were lethal to the anemones. Throughout the bleaching experiment, the FSW medium was replaced twice a week.

At the beginning of the bleaching experiment and at subsequent regular intervals, the chlorophyll *a* (Chl *a*) content of the anemones was monitored to estimate the decline in density of their algal symbionts. Replicate anemones (*n* = 4) from each treatment were separately rinsed in distilled water and homogenized at 5000 rpm for 60 s by beadbeating with a sterile 6-mm stainless steel ball bearing in a 2-ml tube containing FSW (Biospec mini-beadbeater model 3110BX). The algal fraction was separated from the animal fraction by centrifugation at 1000 × *g* for 5 min. To remove any remaining host tissues, the algal pellet was resuspended in FSW before being recovered by a brief centrifugation (10,000 × *g* for ~1 s). This wash procedure was repeated once more before the algal pellet was again recovered by centrifugation (10,000 × *g* for 1 s) and stored frozen at −20°C. The beadbeating procedure did not result in the release of algal pigments into the homogenate; hence, it was assumed that algal cells remained intact throughout the procedure.

Chl *a* was later extracted from the algal cells by beadbeating for 30 s with about 250 μl of 800-μm glass beads in 90% acetone and incubating at 4°C for 24 h. The sample was then centrifuged (2000 × *g* for 10 min), and the absorbance of the supernatant was read at 750, 664, and 630 nm. Chl *a* concentration was quantified using the equations of Jeffrey and Humphrey (1975). When Chl *a* could no longer be detected spectrophotometrically in the anemones at the final sampling, the anemones were examined under a fluorescence microscope (Olympus SZX12) to verify the absence of red fluorescence emanating from any residual algal symbionts. Finally, the total DNA from whole *Aiptasia* individuals (including any remaining symbiotic algae) was extracted and polymerase chain reaction (PCR) carried out using zooxanthellae-specific primers (described below) to determine if they were completely aposymbiotic.

Induced symbiosis between aposymbiotic anemones and Symbiodinium *isolates*

After the development of an efficient means of rendering the anemones aposymbiotic, more anemones in individual vessels were induced to bleach within 1 month. They were acclimated to normal conditions (25°C, 80 μmol photons $m^{-2}s^{-1}$ PAR) for 2 weeks, and then a few representatives were checked for the complete absence of algal symbionts by examination under a fluorescence microscope.

Meanwhile, log-phase cultures of the following isolates of *Symbiodinium* were harvested and washed in FSW by centrifugation at 1000 × *g* for 5 min: (1) TC2A, a clonal isolate from the tridacnid clam *Tridacna crocea* (see isolate PHQU TC2A from Baillie *et al.*, 1998); (2) HH2A, a clonal isolate from the tridacnid clam *Hippopus hippopus* (see isolate PHSC HH2A from Baillie *et al.*, 1998); (3) HA3-5, a clonal isolate of a free-living isolate from Hawaiian subtidal sands (see Carlos *et al.*, 1999); (4) CS164, a clonal isolate from the anemone *Aiptasia tagetes* (culture purchased from the Commonwealth Scientific and Industrial Research Organisation [CSIRO], Australia); and (5) CS156, a clonal isolate from the stony coral *Montipora verrucosa* (culture purchased from CSIRO). In addition to these five clonal cultures, zooxanthellae from a specimen of *Aiptasia* sp. held in the aquarium were freshly isolated (*Aiptasia* FIZ) using the protocol described above. Analysis of the partial sequences of their 18S rDNA indicates that the isolates TC2A, HH2A, and HA3-5 belong to clade A of the *Symbiodinium* phylogeny (GenBank accession numbers: AF289268, AF289269, AB016572, respectively); CS164 (AF289270) and *Aiptasia* FIZ (AF289267) belong to clade B; and CS156 (AB016594) belongs to clade C (see also Carlos *et al.*, 1999, 2000). TC2A and HH2A further differ from one another by one nucleotide, judging from their internal transcribed spacer regions (ITS-5.8S-ITS2) (our unpublished data).

Except for a control group (*n* = 10 anemones), replicate aposymbiotic anemones were inoculated with one of the six isolates (*n* = 10 anemones for each isolate), while another group (*n* = 10 anemones) was inoculated with a mixture of all six isolates. Algal suspensions of the isolate being studied were squirted over the oral discs of the anemones at a final concentration of about 10^4 cells ml^{-1} anemone medium. To check for algal infection, the inoculated anemones were observed daily for a week at high magnification under a dissecting microscope (OM System). At 2, 4, 8, and 12 weeks after the initial inoculation, any infective symbionts were re-isolated from anemones (*n* = 2) from each treatment and frozen for identification and comparison with the inoculating isolates.

To determine whether the initially induced symbioses were stable, the remaining anemones (*n* = 2) from each treatment were re-inoculated once with a mixture of all the cultured isolates; in addition, each was incubated with a wild symbiotic anemone taken from aquarium stocks. This treatment ensured that the remaining anemones from each treatment had access to a wide range of possible algal symbionts, including the *Symbiodinium* that is regularly released by the wild anemones. After 1 month, the symbionts from anemones (*n* = 2 for each treatment) were re-isolated for identification. The experimental anemones were easily distinguishable from the wild symbiotic anemones by their relatively light color and small size.

Two sets of the infection experiment described above were carried out simultaneously. In the first set, the anemones were fed once a week with freshly hatched *Artemia nauplii*. In the second set, the anemones were unfed. This was to determine the effect of host nutritional status on the infectivity of the algal isolates and the stability of the induced symbioses. In both sets, the FSW medium was changed twice a week, a few hours after the anemones in the first set were fed.

Bleached anemones that appeared to remain aposymbiotic after exposure to algal isolates were examined for the presence of algal cells by means of Chl *a* measurements, fluorescence microscopy, and PCR using zooxanthellae-specific primers (described below) to determine if they were completely aposymbiotic. Anemones were considered to have remained completely bleached only if they lacked Chl *a*, they had no fluorescent algal cells in their tissues, and their total DNA failed to produce a zooxanthellae-specific PCR product.

Extraction of DNA from anemones and from symbiotic and cultured algae

Total DNA from visibly bleached *Aiptasia* individuals (including any symbiotic algae present) was extracted by beadbeating each anemone (5000 rpm for 60 s with a sterile 6-mm stainless steel ball bearing) in a 2-ml tube containing 1.0 ml of proteinase K buffer (10 m*M* Tris; 100 m*M* EDTA, 1.0% SDS). The homogenate was then incubated at 40°C overnight with proteinase K (0.1 mg ml^{-1}), the protein fraction extracted twice with an equivalent volume of buffered phenol, and the phenol removed by extraction twice with an equivalent volume of chloroform. DNA was precipitated by addition of 2.5 volumes of absolute ethanol and 0.1 volume of 3 *M* sodium acetate (pH 6.1), and incubation at −20°C for at least 30 min. Precipitated DNA was recovered by centrifugation at 10,000 × *g* for 15 min, washed with 70% ethanol, and dried in a vacuum centrifuge for 2 min. Dried DNA was dissolved in 100 μl TE buffer (10 m*M* Tris; 1 m*M* EDTA, pH 8.0) and quantified by measuring its absorbance at 260 nm on a DU 640 spectrophotometer (Beckman Instruments, Inc., Fullerton, CA).

For DNA extraction from cultured and symbiotic algae, algal pellets were prepared as described earlier. Each algal pellet was suspended in 1.0 ml of proteinase K buffer, transferred to a 2-ml tube containing about 750 μl of 800-μm glass beads, and lysed at 5000 rpm for 60 s in a mini-beadbeater. DNA was then extracted from the lysate as described above, using the proteinase K method.

Molecular genetic identification of infective Symbiodinium *taxa*

PCR was used with the following zooxanthellae-specific primers (Carlos *et al.*, 2000) to amplify the hypervariable V1 + V2 region of the alga's 18S rRNA gene: z8 (forward) 5′-GTCTCAAAGATTAAGCCATG-3′; zPV2R (reverse) 5′-GCCCGCCGCGCGCGGCGGGCGGGGCGGGGGCACGGGGGGCTCCGTTACCCGTCATTGCC-3′ (annealing region underlined). A 40-bp GC-rich sequence or GC-clamp (Sheffield *et al.*, 1989) was attached to the 5′ end of the reverse primer.

AmpliTaq Gold DNA polymerase (PE Applied Biosystems, Foster City, CA) was used for all PCR amplifications. PCRs (20 μl) contained 10 m*M* Tris-HCl, 50 m*M* KCl, 0.001% (w/v) gelatin, 1.5 m*M* $MgCl_2$, 150 μ*M* of each dNTP, 0.5 U of AmpliTaq Gold, 8 pmol of forward primer, 8 pmol of reverse primer, and between 1 and 10 ng of DNA. Amplification reactions were run in a TP240 thermal cycler (Takara Biomedicals, Japan) using the following thermal program: 94°C for 12 min; 40 cycles of 94°C for 30 s, 50°C for 30 s, 68°C for 2 min; and 72 C for 15 min. These reaction conditions were used to amplify any zooxanthellae 18S rDNA present in the total DNA from bleached anemones and also from the DNA extracted from algal pellets. The presence of the PCR product (*ca.* 370 bp) was confirmed by electrophoresis on a 1.5% agarose gel.

To resolve different amplified 18S rDNAs derived from different *Symbiodinium* taxa within the anemone host, 5 μl of the PCR products was loaded on a parallel DGGE gel using the Bio-Rad Dcode universal mutation detection system. The PCR products were resolved on a 6% acrylamide gel (acrylamide/bis 37.5:1) using a 0%–100% denaturing gradient (0–7 *M* urea and 40% v/v formamide) at 58°C, and run at 150 V for 5 h. The gel was later stained in SYBR Green II (Molecular Probes) for 20 min and viewed on a UV transilluminator. Each vertical lane on the gel represents a "population profile," or a pattern of bands with each band representing a different taxon of *Symbiodinium*. Distinct bands containing the DNA fragment were excised, immersed in 100 μl TE buffer, and shaken at 30°C overnight. Eluted DNA was precipitated in absolute ethanol with 0.3 *M* sodium acetate, washed in 70% ethanol, dried in a vacuum centrifuge, and redissolved in 20 μl TE buffer. The purified DNA fragment was then re-amplified using the same set of primers and PCR conditions. The nucleotide sequences of the amplified products were determined using the ABI PRISM dye terminator cycle sequencing ready reaction kit (PE Applied Biosystems) and the nested sequencing primers z9 (forward): 5′-ATGCATGTCTCAGTATAAGC-3′; zSV2R (reverse): 5′-CTCCGTTACCCGTCATTGCC-3′ (Carlos *et al.*, 2000). The sequencing reaction products were read on a 377 DNA sequencer (PE Applied Biosystems).

To identify the algal symbionts from the infected anemone hosts, the nucleotide sequences of their DGGE bands and those of *Symbiodinium* clade representatives from the Genbank database were aligned using the multiple sequence alignment program Clustal W version 1.7 (Thompson *et al.*, 1994). The 18S rDNA V1 + V2 sequences, excluding ambiguous regions (gaps, insertions, flanking primer regions), consisted of 292 aligned sites. To confirm the clade affiliation of the algal symbionts, phylogenetic reconstruction based on the neighbor-joining distance method (Saitou and Nei, 1987) was carried out using Clustal W version 1.7 with a Kimura two-parameter distance matrix. Clade reliability was estimated by 1000 times bootstrap resampling of the aligned data set. This method was used to establish clade affiliations, since phylogenetic reconstruction based on 18S rDNA sequence has been shown by Carlos *et al.* (1999) to result in the reconstruction of *Symbiodinium* phylogenies that are consistent with the clade A, B, and C groups derived from RFLP data. In addition to the 18S rDNA sequence, phylogenetic reconstruction based on the internal transcribed spacer region (Baillie *et al.*, 2000b) and partial RUBISCO sequence (our unpublished data) also recovers phylogenies consistent with clades derived from RFLP data.

Electron microscopy observations of the external morphology of Symbiodinium *isolates*

Log-phase algal cultures of the different strains of *Symbiodinium* were harvested, washed, and resuspended in FSW as described above. One volume of each algal suspension was fixed for 2 h at room temperature with three volumes of 3.3% glutaraldehyde in 0.067 *M* Na-cacodylate buffer (pH 7.2) containing 1.33% NaCl. The final concentrations of glutaraldehyde, NaCl, and cacodylate were 2.5%, 1.0%, and 0.05 *M*, respectively. The fixed cells were serially dehydrated in ethanol (30%, 50%, 75%, 90%, 95%, 100%, and 100%), and transferred into an isoamylalcohol:ethanol mixture (1:1) and then into 100% isoamylalcohol. The cells were dried in a critical-point dryer, sputter-coated with Pt and Pd, and mounted on a specimen stub with double-sided tape. The cells were then observed under a Hitachi S-2500 scanning electron microscope.

Results

Induced bleaching of Aiptasia *anemones*

Figure 1 shows the Chl *a* content of the anemones over time, representing the temporal change in algal density in the different treatments. By day 10, all anemones had lost some Chl *a* or algal symbionts, with those at 35°C in darkness having the least amount of Chl *a* and looking the palest of all. By day 20, all anemones had lost more Chl *a* or algal symbionts and looked much paler, while those at 35°C in darkness had no detectable Chl *a* and appeared completely white. When examined under a fluorescence microscope, these bleached anemones (incubated at 35°C in the dark) had no detectable algal symbionts. When total DNA from bleached anemones was used in PCR using zooxanthellae-specific primers, no algal 18S rDNA could be amplified. These data demonstrate that anemones treated at 35°C in the absence of light for 20 days were free from algal symbionts. The bleaching treatment apparently did not harm the anemones, as indicated by their normal feeding response and continued asexual reproduction through pedal laceration.

Infectivity of different Symbiodinium *isolates*

A few minutes after inoculation, the algae could be seen in the anemone's translucent gastrodermal cavity. Although some motile *Symbiodinium* were present in the inocula, we did not observe motile forms actively swimming into the anemones. Anemones, however, showed feeding behavior immediately upon inoculation, using their tentacles to transfer algae into their oral discs. The algae became immobilized upon touching the anemones' tentacles. It was likely that infection by successful isolates (*i.e.*, the presence of coccoid algal cells inside the host tissues) occurred within a day of inoculation, because by day 2 algal symbionts could be seen spread throughout the transparent tissues around the oral disc and tentacles of the anemones (Table 1).

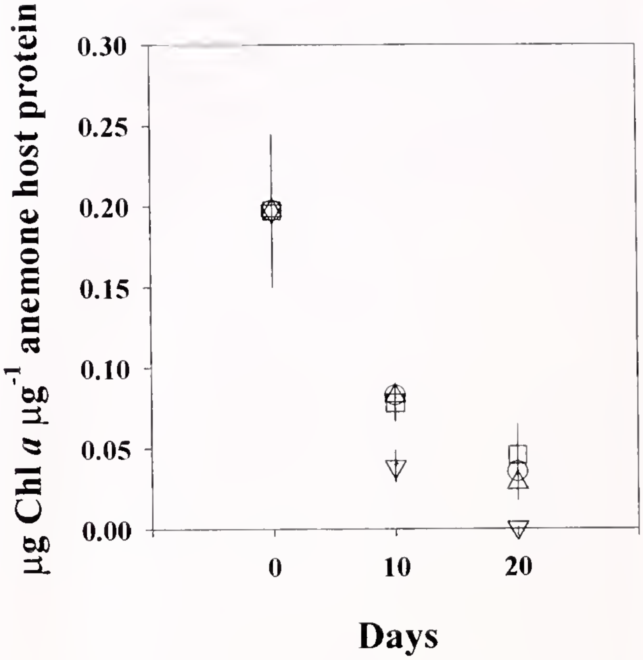

Figure 1. Mean chlorophyll *a* (Chl *a*) content (= algal density) (± SE, $n = 4$) of symbiotic *Aiptasia* anemones exposed to different light and temperature conditions to induce bleaching. (○ = 25°C in light; □ = 25°C in darkness; △ = 32°C in darkness; ▽ = 35°C in darkness.)

After 3 months, uninoculated control anemones remained aposymbiotic (as determined by microscopic observation, Chl *a* measurement, and PCR analysis). Those inoculated with a clade C isolate (CS156) or a clade A isolate (free-living HA3-5) also remained aposymbiotic. This was despite the continued presence for months of motile *Symbiodinium* in the water column and, mostly, on the bottom of the glass vessels (even after cleaning and regular replacement of seawater). Such motile *Symbiodinium* were probably residual algae that could not be removed during cleaning of the vials.

Other anemones became visibly brown within 2–3 weeks. As seen by the naked eye and under the fluorescence microscope, of the anemones inoculated with clade A isolates from tridacnids (isolates TC2A and HH2A), the HH2A anemones were infected with less-dense algal populations than the TC2A anemones. Because of limited time and experimental animals, no attempt was made to quantify the

Table 1

Infectivity over time of different Symbiodinium *isolate on aposymbiotic* Aiptasia *anemones*

		Weeks following inoculation				
Algal strain (clade)	Original source of isolate	1	2	4	8	12
Control (none)	—	–	–	–	–	–
CS156 (C)	*Montipora verrucosa* (coral)	–	–		–	–
HA3-5 (A)	Free-living in subtidal sand	–	–	–	–	–
Hh2a (A)	*Hippopus hippopus* (tridacnid)	$+^{\text{day4}}$	+	+	+	++
Tc2a (A)	*Tridacna crocea* (tridacnid)	$+^{\text{day3}}$	+	++	++	+++
CS164 (B)	*Aiptasia tagetes* (anemone)	$+^{\text{day2}}$	++	+++	+++	+++
Aiptasia FIZ (B)	*Aiptasia* sp. (anemone)	$+^{\text{day2}}$	++	+++	+++	+++
Mixture of above	All of above	$+^{\text{day2}}$	++	+++	+++	+++

[−] = no infection; [day#] = observed time of initial infection; [+] = extent of infection.

relative growth of the algal populations in different treatments. Anemones inoculated with the clade B isolate (CS164) or *Aiptasia* FIZ (clade B algae) from anemones were successfully infected, with dense algal populations in the hosts' tentacles and basal columns. Those inoculated with a mixture of all isolates were also successfully infected. Infectivity of the different algal isolates, as determined by microscopic observation, was the same whether the previously bleached hosts were fed or unfed.

Comparison of the external morphology of different Symbiodinium *isolates*

The coccoid forms of *Symbiodinium* isolates seen under a scanning electron microscope appeared similar, except for size (data not shown). The same was true for all motile forms. No motile forms were observed among symbionts that were freshly isolated from *Aiptasia*. It is difficult, if not impossible, to distinguish one isolate from the other based on their external morphology (*cf.*, Trench and Blank 1987, LaJeunesse, 2001).

Stability of induced symbioses over time and upon re-inoculation

Figure 2 shows the population profiles of the *Symbiodinium* isolates used for inoculating the anemones, the algal populations present in the anemones 1 to 3 months after initial inoculation, and the algal populations 1 month after re-inoculation with a mixture of algal isolates and incubation with wild symbiotic anemones. DGGE analysis of the clonal cultures and FIZ revealed a single band for each of these isolates, and further revealed PCR products that had different DNA sequences. The differences among the 18S rRNA gene copies in the clonal cultures and *Aiptasia* FIZ are therefore negligible, and DGGE analysis was able to resolve differences between the 18S rRNA gene sequences of the *Symbiodinium* clades used in this study. The identical 18S rDNA V1 + V2 sequences of the two clade A isolates from clams are reflected in the same mobility of their single bands. Although difficult to see from the figure (Fig. 2), mixtures of the two different clade A sequences (HA3-5 and

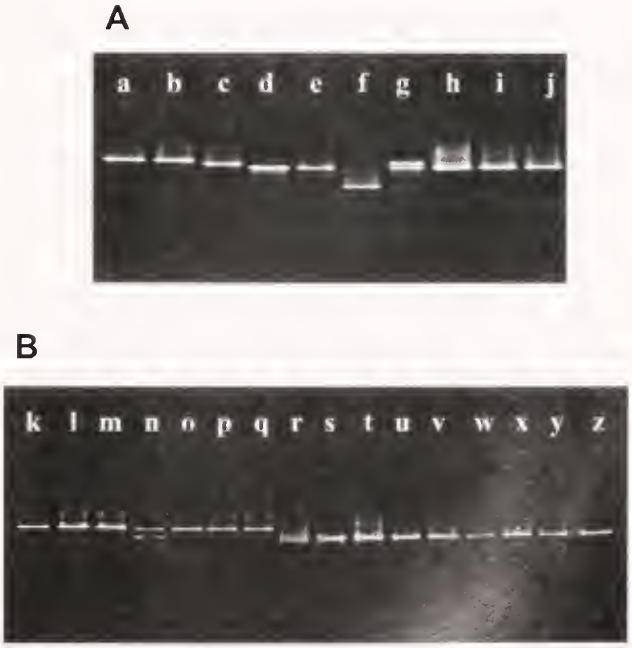

Figure 2. Denaturing-gradient gel electrophoresis (DGGE) profiles of inoculating *Symbiodinium* isolates and re-isolated algal symbionts based on their amplified 18S rDNA V1 + V2 region. Panels A and B represent separate DGGE gels. Panel A: lanes a–g are the respective DGGE profiles of inoculating *Symbiodinium* isolates, namely, Tc2a (clade A), Hh2a (clade A), HA3-5 (clade A), CS164 (clade B), *Aiptasia* FIZ (clade B), CS156 (clade C), and Mixture (clades A-B-C); lanes h–j are the respective DGGE profiles of the symbionts re-isolated from anemones 1 and 3 months after initial inoculation with a mixture of strains, and 1 month after re-inoculation with the mixture. Panel B: lanes k–n respectively represent the original TC2A inoculum, symbionts re-isolated from anemones 1 month after initial TC2A inoculation, symbionts re-isolated from anemones 3 months after initial TC2A inoculation, and symbionts re-isolated from anemones 1 month after Mixture-re-inoculation. This pattern is repeated across the gel for HH2A (o–r), CS164 (s–v), and *Aiptasia* FIZ inoculation (w–z).

the clam isolates) can be separated by DGGE. The identical DNA sequences of the two clade B isolates from anemones (CS164 and *Aiptasia* FIZ) are also reflected in their same mobility under DGGE. The mixed inoculum had a four-band profile, reflecting the presence of two sequences in clade A, one in clade B, and one in clade C.

After 1 to 3 months of initial mixed-isolate inoculation, and a month after re-inoculation with mixed strains (including expelled symbionts from wild anemones), only clade B symbionts could be detected in the anemone hosts. After 1 to 3 months of inoculation, the clade A clonal isolate TC2A had an identical DGGE profile and amplicon sequence to that of the re-isolated symbionts from TC2A-inoculated anemones. After re-inoculation with a mixture of isolates, however, DGGE profiles revealed a second taxon—a clade B anemone symbiont— in the anemones. The clade A clonal isolate HH2A was also identical to re-isolated symbionts from anemones after 1 to 3 months of inoculation with HH2A. But after re-inoculation with a mixture of isolates, this clam taxon was outgrown, or possibly displaced, by a clade B anemone symbiont. The re-isolated symbionts from anemones initially inoculated with cultured or FIZ isolates from *Aiptasia* spp. remained identical to the original inoculum over time and after re-inoculation with mixed isolates. The nutritional status of the hosts affected their final size, with the unfed ones being much smaller than the fed ones, but had no discernible effect on the stability of the induced symbioses (data not shown).

The clade affiliation of the inoculating isolates and infective *Symbiodinium* taxa was confirmed by phylogenetic reconstruction with known *Symbiodinium* clade representatives (data not shown; see Carlos *et al.*, 1999, 2000). In Figure 3, the 18S rDNA V1 + V2 sequences of the inoculating and infective taxa in the previously aposymbiotic anemones are compared. Anemones initially infected with the HH2A (clade A) isolate from a clam appeared to have eventually lost this taxon; they acquired an anemone taxon (clade B) following re-inoculation. Anemones initially infected with the TC2A (clade A) isolate from a clam maintained this taxon, but acquired a second taxon from anemones (clade B) after re-inoculation. Anemones initially infected with cultured (CS164) or fresh (FIZ) anemone isolates (clade B) retained these taxa over time and after re-inoculation. Those inoculated with a mixture of all isolates had only the anemone taxon (clade B) as their detectable symbionts.

Discussion

This study demonstrates the specific nature of the association between *Aiptasia* (cf. *insignis*) and *Symbiodinium*. Some algal isolates were able to infect aposymbiotic anemones while others were not, even in the absence of competing taxa. In particular, symbiosis seemed to be favored between the *Aiptasia* hosts and algal isolates from identical or related anemones. Schoenberg and Trench (1980) found much earlier that aposymbiotic *A. tagetes* were more successfully infected by homologous isolates of *Symbiodinium* (from same host species) than by heterologous isolates (from different host species), some of which were unable to infect the anemones at all, even after 6 months of inoculation. The aposymbiotic planulae of the temperate anemone *Anthopleura elegantissima* were able to form an association with fresh isolates from a conspecific adult, but not with cultured *S. californium*, a species reported to occur in *A. elegantissima* (Banaszak *et al.*, 1993; see Schwarz *et al.*, 1999). In this study, *Aiptasia* hosts also associated to a limited extent with algal isolates from tridacnid clams. Indeed, a number of different marine invertebrates that host *Symbiodinium* were also reported to form heterologous associations under controlled conditions (see Kinzie, 1974; Kinzie and Chee, 1979; Schoenberg and Trench, 1980; Colley and Trench, 1983; Davy *et al.*, 1997). The results presented here provide further support for the presence of some host-symbiont recognition mechanism between the anemone host and its potential dinoflagellate symbionts (Kinzie, 1974; Kinzie and Chee, 1979; Schoenberg and Trench, 1980; Trench *et al.*, 1981; Colley and Trench, 1983; Davy *et al.*, 1997).

An all-or-none process of recognition suggested by Schoenberg and Trench (1980) for zooxanthellate symbioses may account for the observed preference of association between the *Aiptasia* hosts and some algal taxa over at least the short term. Also, in the *Hydra-Chlorella* symbiosis (reviewed by Schoenberg and Trench, 1980), it has been suggested that recognition follows nonspecific phagocytosis of a zoochlorella by a host digestive cell. Retention or expulsion of the alga is determined by interactions between the host vacuole's inside-surface receptors and the algal surface antigens that vary between algal isolates. In the coral *Fungia scutaria-Symbiodinium* association, dinoflagellates that entered the gastric cavity of aposymbiotic coral planulae were also observed to be phagocytosed by the host's endodermal cells (Schwarz *et al.*, 1999).

Davy *et al.* (1997) found that uptake of zooxanthellae from *Anthopleura ballii* into *Cereus pedunculatus* was lower than that for other zooxanthellae. They proposed that discrimination based on the surface characteristics of the algae might explain this phenomena. Although some workers have used morphological characteristics to describe several zooxanthellae species (see Trench and Blank, 1987; LaJeunesse, 2001), our SEM observations of the isolates in the present study showed that they have similar external morphology. There appears to be no observable correlation between symbiont morphology (as seen with SEM) and infectivity (see also Schoenberg and Trench, 1980). As others have proposed, it is possible that the recognition

```
                      48
Hh2a inoculum         CATGTCTCAGTATAAGCTTTTACACGGCGAAACTGCGAATGGCTCATTAAAGCAGTTATAATTTATTTGATGG
"Hh2a" re-isolate     -----------------AG-C-A-T--T--------------------------------G------------
Tc2a inoculum         -----------------TT-T-C-C--C--------------------------------A------------
"Tc2a" re-isolate #1  -----------------TT-T-C-C--C--------------------------------A------------
"Tc2a" re-isolate #2  -----------------AG-C-A-T--T--------------------------------G------------
CS164 inoculum        -----------------AG-C-A-T--T--------------------------------G------------
"CS164" re-isolate    -----------------AG-C-A-T--T--------------------------------G------------
FIZ inoculum          -----------------AG-C-A-T--T--------------------------------G------------
"FIZ" re-isolate      -----------------AG-C-A-T--T--------------------------------G------------
"Mixture" re-isolate  -----------------AG-C-A-T--T--------------------------------G------------

Hh2a inoculum         TCACTGCTACATGGATAACTGTGGTAATTCTAGAGCTAATACATGCACCAAAACCCAACTTCGCAGAAGGGTT
"Hh2a" re-isolate     -TG--------------------------------------------T-C--G---G----T-----------
Tc2a inoculum         -CA--------------------------------------------C-A--A---A----C-----------
"Tc2a" re-isolate #1  -CA--------------------------------------------C-A--A---A----C-----------
"Tc2a" re-isolate #2  -TG--------------------------------------------T-C--G---G----T-----------
CS164 inoculum        -TG--------------------------------------------T-C--G---G----T-----------
"CS164" re-isolate    -TG--------------------------------------------T-C--G---G----T-----------
FIZ inoculum          -TG--------------------------------------------T-C--G---G----T-----------
"FIZ" re-isolate      -TG--------------------------------------------T-C--G---G----T-----------
"Mixture" re-isolate  -TG--------------------------------------------T-C--G---G----T-----------

Hh2a inoculum         GTATTTATTAGATACAGAACCAACGCAGGCTCCGCCTGGT  TGTGGTGATTCATGATAACTCGATGAATCGT
"Hh2a" re-isolate     --G----------C----------C---------------CA--------------------T--C-------
Tc2a inoculum         --A----------A----------G---------------  --------------------C--T-------
"Tc2a" re-isolate #1  --A----------A----------G---------------  --------------------C--T-------
"Tc2a" re-isolate #2  --G----------C----------C---------------CA--------------------T--C-------
CS164 inoculum        --G----------C----------C---------------CA--------------------T--C-------
"CS164" re-isolate    --G----------C----------C---------------CA--------------------T--C-------
FIZ inoculum          --G----------C----------C---------------CA--------------------T--C-------
"FIZ" re-isolate      --G----------C----------C---------------CA--------------------T--C-------
"Mixture" re-isolate  --G----------C----------C---------------CA--------------------T--C-------
                                                                                              339
Hh2a inoculum         GTGGCTTGGCCGACGATGCATCTTTCAAGTTTCTGACCTATCAGCTTCCGACGGTAGGGTATGGGCCTACCGT
"Hh2a" re-isolate     -C---C-T-----------G--A---------------------------------------T----------
Tc2a inoculum         -T---T-G-----------A--T---------------------------------------G----------
"Tc2a" re-isolate #1  -T---T-G-----------A--T---------------------------------------G----------
"Tc2a" re-isolate #2  -C---C-T-----------G--A---------------------------------------T----------
CS164 inoculum        -C---C-T-----------G--A---------------------------------------T----------
"CS164" re-isolate    -C---C-T-----------G--A---------------------------------------T----------
FIZ inoculum          -C---C-T-----------G--A---------------------------------------T----------
"FIZ" re-isolate      -C---C-T-----------G--A---------------------------------------T----------
"Mixture" re-isolate  -C---C-T-----------G--A---------------------------------------T----------
```

Figure 3. Comparison of the 18S rDNA V1 + V2 sequences of inoculating and infective *Symbiodinium* strains following denaturing-gradient gel electrophoresis. "HH2A" re-isolate refers to re-isolated symbionts from HH2A-inoculated anemones after re-inoculation with a mixture of *Symbiodinium* strains and incubation with symbiotic wild anemones; "TC2A" re-isolate refers to re-isolated symbionts from TC2A-inoculated anemones after re-inoculation with a mixture of isolates; and so on. (FIZ = freshly-isolated zooxanthellae from *Aiptasia* sp., [–] = conserved nucleotide, [ ] = missing nucleotide, number = nucleotide position on the 18S rRNA gene.)

between the anemone host and its algal symbionts occurs at the molecular level (for a review see Trench, 1997).

Previous studies by Lin *et al.* (2000) on the *Aiptasia pulchella-Symbiodinium* symbiosis have demonstrated that glycoproteins on the algal cell wall are crucial factors in the establishment of the association (see also Markell and Trench, 1993). It is possible that such surface glycoproteins or related molecules mediate recognition between *Aiptasia* and its potential symbionts (see Lin *et al.*, 2000). Failure of the clade C and free-living *Symbiodinium* isolates to infect *Aiptasia* suggests that they lack the appropriate recognition factors. On the other hand, the clam and clade B isolates appear to possess cell wall components suitable for host-symbiont recognition. Our future studies will investigate the presence of distinguishable surface epitopes on the cell walls of the *Symbiodinium* isolates used in this study.

This study also suggests that after initial recognition, infective taxa proliferate at different rates, with the homologous isolates (CS164 and FIZ from anemones) establishing higher symbiont densities than the heterologous isolates (TC2a and HH2a from clams). A similar observation was made by Davy *et al.* (1997) during the initial 8 weeks following infection of *Cereus pedunculatus* with homologous and heterologous zooxanthellae (see also Schoenberg and Trench, 1980). This effect may have been due to lower growth rates, higher levels of expulsion, or higher levels of digestion of the clade A taxa. Whatever the reason, it is interesting that although the clade A taxa have the same 18S rDNA sequence, their densities within infected anemones were different after 12 weeks. Since these clam isolates are almost certainly conspecific, this supports the idea that there is significant intraspecific genetic (and hence phenotypic) variation in these clade A symbionts from giant clams (see Belda-Baillie *et al.*, 1999; Baillie *et al.*, 2000 a, b).

After inoculation with a mixture of all *Symbiodinium* isolates, all anemones were found to host the clade B symbionts (CS164, *Aiptasia* FIZ, or both). In all but one case (that of TC2A), only the clade B symbionts were detected. This observation demonstrates another difference between these two clade A taxa from giant clams. Given the success of the anemone (clade B) isolates in outgrowing or displacing the HH2A symbionts and in co-inhabiting with the previously established TC2A symbionts, we can rank the isolates according to their ability to form an association with *Aiptasia* (and according to symbiont density after 12 weeks): HA3-5 and CS156 < HH2A < TC2A << CS164, *Aiptasia* FIZ.

The outgrowing or possible displacement of HH2A symbionts by the clade B symbionts could be a result of competitive interactions. In that case the clade B symbionts may be better adapted to growth within the same niche (the anemone) and are able to outcompete the clade A taxon. Alternatively, the same result might be seen if the host is able to distinguish between the two taxa, and the clade A taxon is preferentially digested or expelled even after forming an association with HH2A for many weeks. If the latter case is true, then recognition may occur during, as well as after, initial uptake. It also implies that there may be a range of cell-surface epitopes that a single host could recognize as "self" (see the review by Trench, 1997). On balance, the simplest explanation for the outgrowing or displacement of HH2A symbionts is competition for resources within the anemone host by two "recognized" symbionts. Efficient competitors are expected to maintain high specific growth rates and eventually, according to the principle of competitive exclusion, exclude less efficient taxa (see also Fitt, 1985).

The coexistence of the TC2A and clade B symbionts in the same anemones might be another form of competition between two symbiont taxa. It is arguable whether such an association with both taxa might persist indefinitely. The fact that TC2A was still present may reflect its ability to grow faster than the HH2A isolate when inside the anemone. It is also possible that different taxa may coexist over long periods in the same host by exploiting different niches or resources within that host (see Baillie *et al.*, 1998; Belda-Baillie *et al.*, 1999; Carlos *et al.*, 2000). Anemones, however, may offer algal symbionts fewer microhabitat variations than other hosts, such as the giant clams (see Carlos *et al.*, 2000). If different taxa coexist in the same niche, then diversity may be maintained according to Hutchinson's (1961) concept of diversity under nonequilibrium conditions (for a discussion, see Carlos *et al.*, 2000).

Distinct functional differences between clades A, B, and C *Symbiodinium* have recently been demonstrated (Banaszak *et al.*, 2000). All the A clades tested synthesized mycosporine-like amino acids under the influence of UV and PAR, but the B and C clades did not. In the present study, the limited number of clade representatives available for comparison precludes interpretation of any apparent discrimination between different clades (*i.e.*, selection of clade B over others). However, Schoenberg and Trench (1980) found the growth of infective algal symbionts to be directly related to their isoenzyme similarity coefficient relative to the native algal symbiont in the test host *Aiptasia tagetes,* but there was no correlation between infectivity of algal symbionts and the phylogenetic relatedness of the original hosts to the infected anemones.

In the present study, the aposymbiotic anemones were able to establish symbiosis with algal isolates from tridacnids (*Tridacna, Hippopus*), but not with an algal isolate from a stony coral (*Montipora verrucosa*). This is consistent with previous studies in which isolates from tridacnids were shown to successfully infect aposymbiotic *Aiptasia* (Kinzie and Chee, 1979). These observations suggest that the normally extracellular symbionts of giant clams (Norton *et al.*, 1992) are capable of an intracellular mode of existence in cnidarian hosts (see also Carlos *et al.*, 2000). It was expected, however, that the TC2A isolate from *T. crocea* would eventually have been outcompeted by the FIZ or CS164 isolate from *Aiptasia*, given our observation that only a clade B taxon was present in anemones that have been maintained with *T. crocea* in aquaria. Rowan and Powers (1991a) also found only clade B taxa in *Aiptasia pulchella* and *A. pallida* maintained in the laboratory, and in *Anthopleura elegantissima* collected from the field.

Our study used *Aiptasia* individuals arising from a single individual (*i.e.*, individuals with the same genotype), and thus we cannot say whether different host individuals would have the same preferences for symbionts. Nevertheless, the fact that *Aiptasia-Symbiodinium* associations can harbor clade B algae such as *Symbiodinium pulchrorum* (host = *Aiptasia pulchella*), *S. burmudense* (host = *A. tagetes*), and *Symbiodinium* sp. CS164 (host = *A. tagetes*) supports the idea that some *Aiptasia* species have an affinity for the clade B taxa. Previous analysis of the 18S rDNA sequence from our *Aiptasia* FIZ indicates that it is *S. pulchrorum* (Carlos *et al.*, 2000). On balance, it seems likely that the genotype of *Aiptasia* used in our study may be typical of the other *Aiptasia* spp. studied so far (inasmuch as it seems to have an affinity for the clade B symbionts). However, further study will be needed to determine if other *Aiptasia* genotypes have different symbiont specificities, as has been seen in the gorgonian *Plexaura kuna* (for example, see Goulet and Coffroth, 1997).

It is likely that similar specificity occurs in the anemones' close relatives, the reef-building corals. Schwarz *et al.* (1999) found that the aposymbiotic planular larvae of the scleractinian coral *Fungia scutaria* can be experimentally infected by *Symbiodinium* from clades A, B, and C (from *Cassiopeia xamachana*, *Aiptasia pallida*, and *F. scutaria*, respectively). However, the stability of the induced symbioses and competition between algal symbionts were not investigated. The prevalence of polymorphic symbioses in any given coral reef community (Rowan and Powers, 1991a; Carlos *et al.*, 1999) and the regular expulsion of algal symbionts (Steele, 1975; Hoegh-Guldberg *et al.*, 1987; Stimson and Kinzie, 1991; McCloskey *et al.*, 1996; Maruyama and Heslinga, 1997) suggest a common pool of diverse algal symbionts available for infection (see also Baillie *et al.*, 2000b). However, the specificity of the *Aiptasia-Symbiodinium* association and others in coral reefs suggests that, under normal environment conditions, existing symbiotic associations may be the most favored and stable of all possible partnerships, including those in which symbiont acquisition occurs through maternal inheritance. Nevertheless, the flexible nature of these symbiotic associations may be an adaptational advantage in changing environmental conditions (Buddemeier and Fautin, 1993; Rowan and Knowlton, 1995; Davy *et al.*, 1997).

It is curious that the only free-living *Symbiodinium* reported to date (Carlos *et al.*, 1999), the HA3-5 clade A isolate from Hawaiian subtidal sand, was unable to infect aposymbiotic *Aiptasia* anemones. Phylogenetic studies have shown that this isolate is closely related to the algal symbionts of some foraminiferans (Carlos *et al.*, 1999). However, HA3-5 has not as yet been shown to form associations with any marine invertebrates, so this isolate may be exclusively free-living. If this is indeed the case, there may be other free-living taxa in coral reefs that are genetically, though perhaps not morphologically, distinct from free-living stages of symbiotic algae. Whether the free-living stage of symbiotic taxa of *Symbiodinium* serves only as a dispersal mechanism remains to be seen. Further investigation of free-living *Symbiodinium* will improve our understanding of dinoflagellate population dynamics on coral reefs.

The decline in the algal Chl *a* content in the control anemones (25°C, with or without light) can be attributed to starvation and possibly to decreased shading relative to conditions in the aquarium. In the aquarium, the wild anemones had access to fresh particulates from flow-through seawater, and they were stocked at high densities. It is noteworthy that in rendering the anemones aposymbiotic, dark incubation for one month at elevated temperature was a quick and efficient means of removing algal symbionts, without the use of any chemicals and without apparent harm to the animal host. Elevated temperature (Iglesias-Prieto *et al.*, 1992; Warner *et al.*, 1996) must have acted synergistically with the absence of light to impair the photosynthetic mechanism of the algal symbionts, leading to their quick escape or removal. We believe that this technique for *Aiptasia* is a significant improvement over previously published protocols that required dark incubation for 2 to 3 years to completely remove the anemones' symbionts (Kinzie and Chee, 1979), or use for months of the photosynthesis inhibitor DCMU (3-[3,4-dichlorophenyl]-1,1-dimethylurea), which has been previously shown to be not completely effective (Schoenberg and Trench, 1980). Treatment at 35°C in the dark may not be suitable for inducing bleaching of other marine invertebrates, however. For example, the temperatures used in our study may be lethal to temperate hosts. In addition, a study of the temperate sea anemone *Anthopleura elegantissima* demonstrated that high temperature (20°C) decreased zoochlorellae density and had little effect on zooxanthellae (Saunders and Muller-Parker, 1997). Nevertheless, we believe that the method we used in this study will facilitate symbiosis research with *Aiptasia* sp. The application of a similar technique to other model zooxanthellae-associations, such as giant clams, will require further study and optimization.

This study also underscores the utility of appropriate molecular genetic tools in understanding the dynamics of invertebrate-dinoflagellate associations on coral reefs. In previous studies on the specificity of anemone-dinoflagellate symbioses (Schoenberg and Trench, 1980; Buddemeier and Fautin, 1993; Rowan and Knowlton 1995; Davy *et al.*, 1997; Schwarz *et al.*, 1999), limited research tools precluded any investigation of competition between symbionts within the host. Even the use of a combination of allozyme and random amplified polymorphic DNA analyses in monitoring the progress of giant clams inoculated with different isolates only highlighted the limitation of these techniques in detecting taxonomic differences between *Symbiodinium* taxa (Belda-Baillie *et al.*, 1999). The present study has shown that DGGE of the variable regions of the small-subunit ribosomal gene (or other suitable genetic markers; see also LaJeunesse and Trench, 2000) is an appropriate tool for such studies. Although only DNA fragments up to 500 bp can be separated (Muyzer *et al.*, 1996), the technique is sufficient to identify the DGGE band and should simplify investigations of many important aspects of host-symbiont interactions on coral reefs.

Acknowledgments

We thank Ms. Nakako Hayashi for her assistance with DNA sequencing, Mr. Hiroshi Urata for his assistance with the SEM analysis, Ms. Mika Atsumi for preparing the culture media, and Ms. Rie Aburaki for her help in maintaining the experiments. The cultures of *Symbiodinium* isolates TC2A and HH2A were generously donated by Prof. Edgardo D. Gomez of the University of the Philippines Marine Science Institute. This work was conducted as part of the Industrial Science and Technology Frontier Program, with financial support from the Japanese Ministry of International Trade and Industry.

Literature Cited

Baillie, B. K., V. Monje, V. Silvestre, M. Sison, and C. A. Belda-Baillie. 1998. Allozyme electrophoresis as a tool for distinguishing different zooxanthellae symbiotic with giant clams. *Proc. R. Soc. Lond. B* **265:** 1949–1956.

Baillie, B. K., C. A. Belda-Baillie, V. Silvestre, M. Sison, A. V. Gomez, E. D. Gomez, and V. Monje. 2000a. Genetic variation in *Symbiodinium* isolates from giant clams based on random-amplified-polymorphic DNA (RAPD) patterns. *Mar. Biol.* **136:** 829–836.

Baillie, B. K., C. A. Belda-Baillie, and T. Maruyama. 2000b. Conspecificity and Indo-Pacific distribution of *Symbiodinium* genotypes (Dinophyceae) from giant clams. *J. Phycol.* **36:** 1153–1161.

Banaszak, A. T., R. Iglesias-Prieto, and R. K. Trench. 1993. *Scrippsiella velellae* sp. nov. (Peridiniales) and *Gloeodinium viscum* sp. nov (Phytodiniales): dinoflagellate symbionts of two hydrozoans (Cnidaria). *J. Phycol.* **29:** 517–528.

Banaszak, A. T., T. C. LaJeunesse, and R. K. Trench. 2000. The synthesis of mycosporine-like amino acids (MAAs) by cultured, symbiotic dinoflagellates. *J. Exp. Mar. Biol. Ecol.* **249:** 219--233.

Belda-Baillie, C. A., M. Sison, V. Silvestre, K. Villamor, V. Monje, E. D. Gomez, and B. K. Baillie. 1999. Evidence for changing symbiotic algae in juvenile tridacnids. *J. Exp. Mar. Biol. Ecol.* **241:** 207–221.

Brown, B. E., and J. E. Ogden. 1993. Coral bleaching. *Sci. Am.* **268:** 44–50.

Buddemeier, R. W., and D. G. Fautin. 1993. Coral bleaching as an adaptive mechanism. *Bioscience* **43:** 320–326.

Carlos, A. A., B. K. Baillie, M. Kawachi, and T. Maruyama. 1999. Phylogenetic position of *Symbiodinium* (Dinophyceae) isolates from tridacnids (Bivalvia), cardiids (Bivalvia), a sponge (Porifera), a soft coral (Anthozoa), and a free-living strain. *J. Phycol.* **35:** 1054–1062.

Carlos, A. A., B. K. Baillie, and T. Maruyama. 2000. Diversity of dinoflagellate symbionts (zooxanthellae) in a host individual. *Mar. Ecol. Prog. Ser.* **195:** 93–100.

Colley, N. J., and R. K. Trench. 1983. Selectivity in phagocytosis and persistence of symbiotic algae by the scyphistoma stage of the jellyfish *Cassiopeia xamachana. Proc. R. Soc. Lond. Ser B* **219:** 61–82.

Davy, S. K., I. A. N. Lucas, and J. R. Turner. 1997. Uptake and persistence of homologous and heterologous zooxanthellae in the temperate sea anemone *Cereus pendunculatus* (Pennant). *Biol. Bull.* **192:** 208–216.

Drollet, J. H., M. Faucon, and P. M. V. Martin. 1995. Elevated sea-water temperature and solar UV-B flux associated with two successive coral mass bleaching events in Tahiti. *Mar. Freshw. Res.* **46:** 1153–1157.

Fischer, S. G., and L. S. Lerman. 1979. Length-independent separation of DNA restriction fragments in two-dimensional gel electrophoresis. *Cell* **16:** 191–200.

Fitt, W. K. 1985. Effect of different strains of the zooxanthella *Symbiodinium microadriaticum* on growth and survival of their coelenterate and molluscan hosts. *Proc. Fifth Int. Coral Reef Symp.* **6:** 131–136.

Gleason, D. F., and G. M. Wellington. 1993. Ultraviolet radiation and coral bleaching. *Nature* **365:** 836–838.

Glynn, P. W. 1996. Coral reef bleaching: facts, hypotheses and implications. *Global Change Biol.* **2:** 495–509.

Goulet, T. L., and M. A. Colfroth. 1997. A within colony comparison of zooxanthella genotypes in the Carribean gorgonian *Plexaura kuna. Proc. Eighth Int. Coral Reef Symp.* **2:** 1331–1334.

Hayes, R. L., and P. G. Bush. 1990. Microscopic observation of recovery in the reef-building scleractinian coral, *Montastrea annularis*, after bleaching on a Cayman reef. *Coral Reefs* **8:** 203–209.

Hoegh-Guldberg, O., L. R. McCloskey, and L. Muscatine. 1987. Expulsion of zooxanthellae by symbiotic cnidarians from the Red Sea. *Coral Reefs* **5:** 201–204.

Hutchinson, G. E. 1961. The paradox of the plankton. *Am. Nat.* **95:** 137–145.

Iglesias-Prieto, R. J. L., W. A. Matta, W. A. Robins, and R. K. Trench. 1992. Photosynthetic response to elevated temperature in the symbiotic dinoflagellate *Symbiodinium microadriaticum* in culture. *Proc. Natl. Acad. Sci. USA* **89:** 10302–10305.

Jeffrey, S. W., and G. F. Humphrey. 1975. New spectrophotometric equations for determining Chlorophylls a, b, c1, and c2 in higher plants, algae and natural phytoplankton. *Biochem. Physiol.* **167:** 191–194

Jones, R. J., and D. Yellowlees. 1997. Regulation and control of intracellular algae (= zooxanthellae) in hard corals. *Proc. R. Soc. Lond. B* **352:** 457–468.

Kinzie, R. A. 1974. Experimental infection of aposymbiotic gorgonian polyps with zooxanthellae. *J. Exp. Mar. Biol. Ecol.* **15:** 335–345.

Kinzie, R. A., III, and G. S. Chee. 1979. The effect of different zooxanthellae on the growth of experimentally reinfected hosts. *Biol. Bull.* **156:** 315–327.

Knowlton, N. 2001. The future of coral reefs. *Proc. Natl. Acad. Sci. USA* **98:** 5419–5425.

LaJeunesse, T. C. 2001. Investigating the biodiversity, ecology and phylogeny of endosymbiotic dinoflagellates of the genus *Symbiodinium* using the internal transcribed spacer region: in search of a "species" level marker. *J. Phycol.* **37:** 866–880.

LaJeunesse, T. C., and R. K. Trench. 2000. Biogeography of two species of *Symbiodinium* (Freudenthal) inhabiting the intertidal sea anemone *Anthopleura elegantissima* (Brandt). *Biol. Bull.* **199:** 126–134.

Lin, K-L., J-T. Wang, and L-S. Fang. 2000. Participation of glycoproteins on zooxanthellal cell walls in the establishment of a symbiotic relationship with the sea anemone, *Aiptasia pulchella*. *Zool. Stud.* **39:** 172–178.

Markell, D. A., and R. K. Trench. 1993. Macromolecules exuded by symbiotic dinoflagellates in culture: amino acid and sugar composition. *J. Phycol.* **29:** 64–68.

Maruyama, T., and G. A. Heslinga. 1997. Fecal discharge of zooxanthellae in the giant clam *Tridacna derasa*, with reference to their *in situ* growth rate. *Mar. Biol.* **127:** 473–477.

McCloskey, L. R., T. G. Cove, and E. A. Verde. 1996. Symbiont expulsion from the anemone *Anthopleura elegantissima* (Brandt) (Cnidaria: Anthozoa). *J. Exp. Mar. Biol. Ecol.* **195:** 173–186.

Muyzer, G., E. C. De Waal, and A.G. Uitterlinden. 1993. Profiling of complex microbial populations by denaturing-gradient gel electrophoresis analysis of polymerase chain reaction-amplified genes coding for 16S rRNA. *Appl. Environ. Microbiol.* **59:** 695–700.

Muyzer, G., S. Hottentrager, A. Teske, and C. Wawer. 1996. Denaturing gradient gel electrophoresis of PCR-amplified 16S rDNA—a new molecular approach to analyse the genetic diversity of mixed microbial communities. Chapter 3.4.4, pp. 1–23 in *Molecular Microbial Ecology Manual*, A. D. C. Akkermon, J. D. van Elsas, and F. J. de Bruijn, eds. Kluwer Academic, Dordrecht.

Norton, J. H., M. A. Shepherd, H. M. Long, and W. K. Fitt. 1992. The zooxanthellal tubular system in the giant clam. *Biol. Bull.* **183:** 503–506.

Ovreås, L. 2000. Population and community level approaches for analysing microbial diversity in natural environments. *Ecol. Lett.* **3:** 236–251.

Rosenbaum, V., and D. Riesner. 1987. Temperature-gradient gel electrophoresis. Thermodynamic analysis of nucleic acids and proteins in purified form and in cellular extracts. *Biophys. Chem.* **26:** 235–246.

Rowan, R., and N. Knowlton. 1995. Intraspecific diversity and ecological zonation in coral-algal symbiosis. *Proc. Natl. Acad. Sci. USA* **92:** 2850–2853.

Rowan, R., and D. A. Powers. 1991a. A molecular genetic classification of zooxanthellae and the evolution of animal-algal symbioses. *Science* **251:** 1348–1351.

Rowan, R., and D. A. Powers. 1991b. Molecular genetic identification of symbiotic dinoflagellates (zooxanthellae). *Mar. Ecol. Prog. Ser.* **71:** 65–73.

Rowan, R., N. Knowlton, A. Baker, and J. Jara. 1997. Landscape ecology of algal symbionts creates variation in episodes of coral bleaching. *Nature* **388:** 265–269.

Saitou, N., and M. Nei. 1987. The neighbour-joining method: a new method for reconstructing phylogenetic trees. *Mol. Biol. Evol.* **4:** 406–425.

Saunders, B. K., and G. Muller-Parker. 1997. The effects of temperature and light on two algal populations in the temperate sea anemone *Anthopleura elegantissima* (Brandt, 1835). *J. Exp. Mar. Biol. Ecol.* **211:** 213–224.

Schoenberg, D. A., and R. K. Trench. 1980. Genetic variation in *Symbiodinium* (= *Gymnodinium*) *microadriaticum* Freudenthal, and specificity in its symbiosis with marine invertebrates. III. Specificity and infectivity of *Symbiodinium microadriaticum*. *Proc. R. Soc. Lond. B* **207:** 445–460.

Schwarz, J. A., D. A. Krupp, and V. M. Weis. 1999. Late larval development and onset of symbiosis in the scleractinian coral *Fungia scutaria*. *Biol. Bull.* **196:** 70–79.

Sheffield, V. C., D. R. Cox, L. S. Lerman, and R. M. Myers. 1989. Attachment of a 40-base-pair G+C-rich sequence (GC-clamp) to genomic DNA fragments by the polymerase chain reaction results in improved detection of single-base changes. *Proc. Natl. Acad. Sci. USA* **86:** 232–236.

Shick, J. M., M. P. Lesser, and P. L. Jokiel. 1996. Effects of ultraviolet radiation on corals and other coral reef organisms. *Global Change Biol.* **2:** 527–545.

Steele, R. D. 1975. Stages in the life history of a symbiotic zooxanthella in pellets extruded by its host *Aiptasia tagetes* (Duch. and Mich.) (Coelenterata, Anthozoa). *Biol. Bull.* **149:** 590–600.

Stimson, J., and R. A. Kinzie. 1991. The temporal pattern and rate of release of zooxanthellae from the reef coral *Pocillopora damicornis* (Linnaeus) under nitrogen-enrichment and control conditions. *J. Exp. Mar. Biol. Ecol.* **153:** 63–74.

Thompson, J. D., D. G. Higgins, and T. J. Gibson. 1994. CLUSTAL W: Improving the sensitivity of progressive multiple sequence alignment through sequence weighting, positions-specific gap penalties, and weight matrix choice. *Nucleic Acids Res.* **22:** 4673–4680.

Trench, R. K. 1997. Diversity of symbiotic dinoflagellates and the evolution of microalgal-invertebrate symbioses. *Proc. Eighth Int. Coral Reef Symp.* **2:** 1275–1286.

Trench, R. K., and R. J. Blank. 1987. *Symbiodinium microadriaticum* Freudenthal, *S. goreauii* sp. nov., *S. kawagutii* sp. nov., and *S. pilosum* sp. nov.: gymnodinioid dinoflagellate symbionts of marine invertebrates. *J. Phycol.* **23:** 469–481.

Trench, R. K., N. J. Colley, and W. K. Fitt. 1981. Recognition phenomena in symbioses between marine invertebrates and 'Zooxanthellae'; uptake, sequestration and persistence. *Ber. Dtsch. Bot. Ges.* **94:** 529–545.

Van Hannen, E. J., M. P. van Agterveld, H. J. Gons, and H. J. Laanbroek. 1998. Revealing genetic diversity of eukaryotic microorganisms in aquatic environments by denaturing-gradient gel electrophoresis. *J. Phycol.* **34:** 206–213.

Warner, M. E., W. K. Fitt, and G. W. Schmidt. 1996. The effects of elevated temperature on the photosynthetic efficiency of zooxanthellae *in hospite* from four different species of reef coral: a novel approach. *Plant Cell Environ.* **19:** 291–299.

Watanabe, K., and S. Harayama. 1998. Rapid estimation of population densities of uncultured bacteria in the environment. *Microb. Environ.* **13:** 123–127.

Reference: *Biol. Bull.* **202:** 86–95. (February 2002)

Morphological Plasticity in the Tropical Sponge *Anthosigmella varians*: Responses to Predators and Wave Energy

MALCOLM S. HILL* AND APRIL L. HILL

Biology Department, Fairfield University, Fairfield, Connecticut 06430

Abstract. The goal of the research presented here was to examine phenotypic plasticity exhibited by three morphotypes of the common Caribbean sponge *Anthosigmella varians* (Duchassaing & Michelotti). We were interested in examining the biotic (and, to a lesser extent, abiotic) factors responsible for branch production in this species. We also tested the hypothesis that the skeleton may serve an antipredator function in this sponge, focusing on vertebrate fish predators (*i.e.*, angelfish) in this work. In transplant and caging experiments, unprotected forma *varians* replicates were immediately consumed by angelfish, while caged replicates persisted on the reef for several months. These findings support the hypothesis that predators (and not wave energy) restrict forma *varians* to lagoonal habitats. Branch production was not observed in *A. varians* forma *incrustans* when sponges were protected from predators or placed in predator-free, low-wave-energy environments. It is not clear from our work whether forma *incrustans* is capable of producing branches (*i.e.*, whether branch production is a plastic trait in this morph). Additional field experiments demonstrated that *A. varians* forma *varians* increased spicule concentrations, compared to uninjured sponges, in response to artificial predation events, and *A. varians* forma *rigida* reduced spicule concentrations, compared to uncaged controls, when protected from predators. These findings indicate that spicule concentration is a plastic morphological trait that can be induced by damage, and that *A. varians* may be able to reduce spicule concentrations when environmental conditions change (*e.g.*, in the absence of predators). The potential significance of inducible defenses and structural anti-predator defenses in sponges is discussed in relation to recent work on sponge chemical defenses.

Introduction

Morphological antipredator defenses, whether constitutive or induced, are common and effective strategies for marine organisms with hard body coverings (Harvell, 1984; Lively, 1986; Vermeij, 1987; Trussell, 1996). For soft-bodied marine organisms (*e.g.*, seaweeds and many invertebrates), morphological options to defend against predation are typically limited. Because of this, marine ecologists have focused attention over the past two decades on chemical defensive strategies adopted by organisms that appear physically vulnerable to attack. For example, our understanding of general principles of chemical ecology has increased greatly because of detailed work done with seaweed chemical defenses (*e.g.*, Fenical, 1982, 1997; Faulkner, 1984, 1998; Hay and Fenical, 1988; Schnitzler *et al.*, 2001).

Chemical ecologists have successfully extended this work to marine invertebrates, and studies have demonstrated the defensive importance of secondary metabolites in several invertebrate taxa (*e.g.*, Bakus, 1981; Coll and Samarco, 1988; Duffy and Paul, 1992; Paul, 1992; Pawlik *et al.*, 1995). Much of this work has focused on coral reefs, where predation rates are typically high (Bakus, 1964, 1966; Huston, 1985). Among coral reef invertebrates, sponges have received a great deal of recent attention because these common soft-bodied organisms have impressive capabilities for producing secondary metabolites (see review in Pawlik, 1997). It seems clear that chemical defenses in sponges have been an extremely common and successful evolutionary strategy for dealing with high rates of predation found on coral reefs. For instance, Pawlik *et al.* (1995)

Received 29 March 2001; accepted 20 September 2001.

* To whom correspondence should be addressed. E-mail: mhill@fair1.fairfield.edu

found that out of 71 species examined, 44 sponges had deterrent effects on the non-spongivorous fish *Thalassoma bifasciatum*. Although the focus has been on vertebrate predators, invertebrates are also important sponge predators (Guida, 1976; Pawlik, 1983), and Waddell and Pawlik (2000a, b) recently demonstrated that crude extracts from several species of Caribbean sponge deterred predation by two species of sea star and the hermit crab *Paguristes punticeps*.

It should be noted that neither *T. bifasciatum* nor *P. punticeps* is known to consume sponges in the wild (Pawlik *et al.*, 1995; Waddell and Pawlik, 2000a). Determining whether chemicals have deterrent properties is technically difficult, but it is clear that tests should be performed with organisms that consume sponges, because chemical defenses are not equally effective against all consumers (*e.g.*, Pennings *et al.*, 1994; Cronin *et al.*, 1997; Ridenhour *et al.*, 1999). For example, the specialized fish predator *Chaetodon melannotus* feeds on octocorals that can produce highly toxic compounds (Alino *et al.*, 1992). Indeed, *C. melannotus* uses the "toxic" compounds produced by its octocoral prey as a cue when locating prey (Alino *et al.*, 1992). In feeding assays, these compounds would probably be avoided by generalist predators like *T. bifasciatum*, thus providing misleading ecological information about chemical defense in octocorals if results are extrapolated to all potential predators. Whether the most conspicuous and abundant spongivores—primarily angelfish (Randall and Hartman, 1968; Hourigan *et al.*, 1989; Wulff, 1994; Hill, 1998)—are affected by crude extracts from sponges remains an important unanswered question.

In their classic study of spongivorous fish, Randall and Hartman (1968) proposed that sponges use spicules, noxious chemicals, and tough fibrous components in defense against predation. Despite the sharp, needlelike structure of many spicules and the relative indigestibility of spongin, these two traits have recently been described as serving little or no antipredator function in Caribbean sponges (Pawlik *et al.*, 1995; Chanas and Pawlik, 1995, 1996; Waddell and Pawlik, 2000a, b). The data supporting these claims are based on several feeding assays in which consumers are presented with spicules or slices of freeze-dried skeleton embedded in a squid-carrageenan matrix (*e.g.*, Chanas and Pawlik, 1996). However, much of the defensive functionality of the skeleton may be destroyed when spicules lose their natural orientation, or when strips of skeleton are disconnected from the supporting skeletal matrix.

Although Pawlik and colleagues have dismissed any antipredator role for the sponge skeleton (Chanas and Pawlik, 1996; Waddell and Pawlik, 2000a, b), structural components have been shown to serve defensive roles in other soft-bodied reef invertebrates capable of chemical defense (*e.g.*, Harvell and Fenical, 1989). West (1997, 1998) showed that sclerite production was induced in response to simulated predator damage in the common gorgonian coral *Briareum asbestinum*. Furthermore, *B. asbestinum* is able to modulate spicule morphology depending on the context or position of simulated attacks (West, 1997). It is not clear whether a similar situation exists in sponges. However, several testable predictions follow from the hypothesis that skeletal structures serve defensive purposes in sponges. Common reef sponges that are chemically undefended (*e.g.*, *Anthosigmella varians*, *Mycale laevis*, and *Niphates erecta* [Pawlik *et al.*, 1995]) and experience low rates of predation would be predicted to have skeletal structures that deter spongivores. Although Chanas and Pawlik (1995, 1996) found that the skeleton of some sponges was not a deterrent to *T. bifasciatum*, optimally foraging spongivores may have a different response. Another prediction (based on the assumption that the modification or elaboration of skeletal structures is an energetically expensive process (*e.g.*, Palumbi, 1984, 1986)) is that a positive correlation should exist between sponge spicule or spongin concentrations, and predator presence or attack frequency. In this study, we tested the prediction that skeletal structures respond plastically to predation in the tropical sponge *Anthosigmella varians* (Duchassaing & Michelotti), focusing on the effects of angelfish, a major group of spongivores (Randall and Hartman, 1968).

Furthermore, we examined some of the factors responsible for branch production in *A. varians*. *Anthosigmella varians* is a common sponge that exhibits discontinuous morphological variation on Caribbean reefs (Fig. 1; see also Wiedenmayer, 1977; Vicente, 1978; Hill, 1999). Many of the major distinguishing morphological characteristics are detailed in Table 1. Wiedenmayer (1977) separated the encrusting morph (*A. varians* forma *incrustans*) from the amorphous, irregularly lobate, branching form (*A. varians* forma *varians*). Forma *incrustans* is conspicuous on fore- and back-reefs and can cover large areas of reef substrate (Table 1; Vicente, 1978; Hill, 1999). Forma *varians* is typically found in shallow, lagoonal areas; it covers smaller patches of substrate, but some branches can extend up to 40 cm into the water column. Hill (1999) reported a third morph (*A. varians* forma *rigida*) that produced forma *varians*-like branches but had a stiff skeletal construction. Forma *rigida* and forma *incrustans* occur sympatrically on shallow reefs, whereas forma *varians* is found only in areas without predators (Table 1). Hill (1999) proposed that the thick cortex found in forma *rigida* was a response to, and defense against, sponge predators. Vicente (1978) hypothesized that forma *varians* was restricted to shallow, lagoonal environments because it is incapable of tolerating habitats with high wave energy. In previous work with *A. varians*, we found that sponges with spongin-fortified skeletons coexisted with predators, but sponges with low levels of spongin were restricted to predator-free habitats (Hill, 1999).

We had two major goals with the research reported here. The first was to test whether the *A. varians* skeleton responds to predation in the direction predicted if structural components serve a defensive function. The second goal was to test Vicente's (1978) hypothesis that *A. varians* forma *varians* is restricted to low-wave-energy environments (*e.g.*, lagoons, bays) because their branches would be destroyed on the open reef.

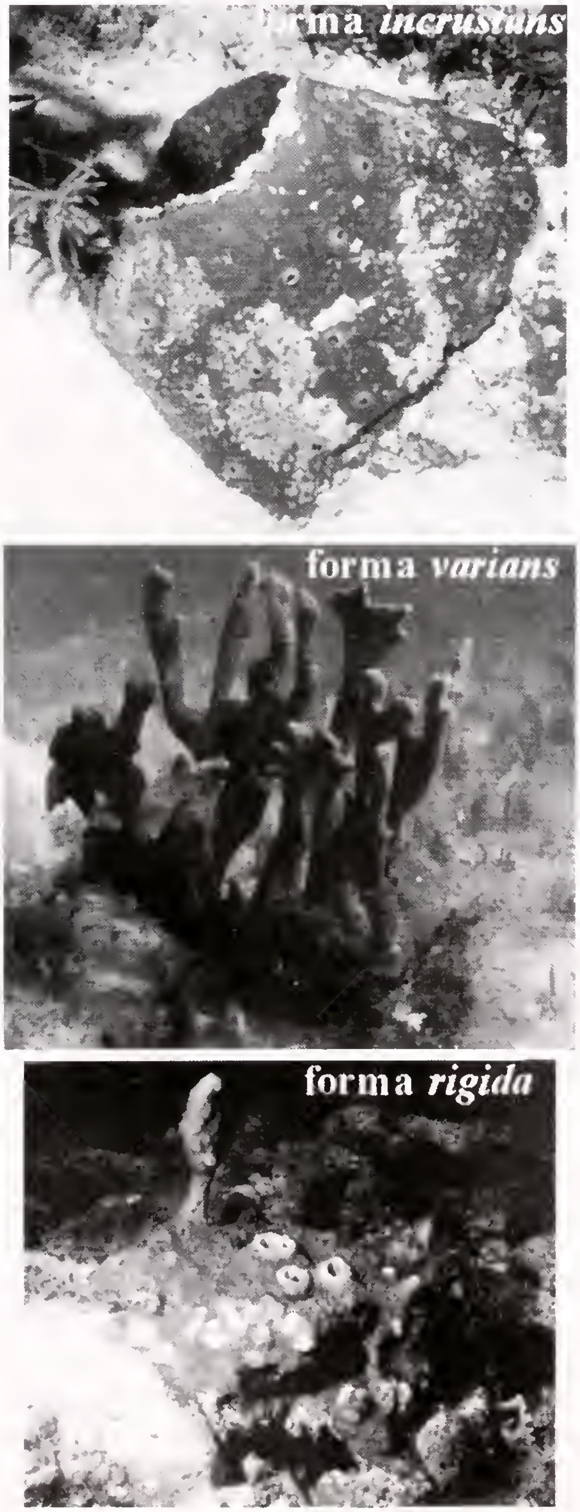

Materials and Methods

Predator exclusion and wave energy

Using a combination of transplantation and caging, *Anthosigmella varians* forma *varians* individuals were placed on Alligator reef in the Florida Keys (24°51′N; 80°37′W) at a depth of 10 m. The first aim of this experiment was to determine whether forma *varians* could exist in branching form in the presence of spongivores. The second aim was to test Vicente's (1978) hypothesis that forma *varians* is unable to persist on the open reef in an environment with relatively high wave energy. The Alligator site was chosen because it has substantial angelfish populations, and because it faces the open ocean, thus experiencing greater water motion (waves and currents) than the Florida Bay.

We cut 5-cm-long branches from 40 different sponges growing in waters adjacent to Long Key (24°50′N; 80°49′W). We made every effort to collect sponges that were separated from one another by at least 15 m to minimize the possibility of collecting genetically identical individuals. These explants were attached, upright, to 8 × 8 × 0.5 cm $CaCO_3$ blocks with monofilament, and were grown for about 90 days in Buttonwood Sound at a depth of 1 m near the Key Largo Marine Research Laboratory (KLMRL), Key Largo, Florida. Once sponges had covered a large portion of the block (≈75% of available surface area) and demonstrated signs of boring (calcareous chips on the sponge surface), we placed the 40 blocks on the reef in an area frequented by spongivores. A suite of predators consume sponges, but the major vertebrate spongivores on Caribbean reefs are angelfish (Randall and Hartman, 1968; Hourigan *et al.*, 1989; Wulff, 1994). Blue, queen, gray, and french angelfish were observed at the Alligator site (Hill 1999), and our experiments were located within a gray angelfish territory.

Blocks were attached with flagging tape to wooden planks anchored to the substratum, and cages (n = 20) were placed over half of the blocks. The other 20 replicates were exposed to predators. Exclosures were made of plastic caging material (Vexar) with a mesh size of 5 cm (see Fig. 2).

Figure 1. *Anthosigmella varians*. (Top) *A. varians* forma *incrustans* is located on Caribbean fore reefs. It assumes an encrusting morphology and bores into calcium carbonate structures. This individual is growing over a colony of *Montastrea cavernosa*, and the debris on the surface of the sponge is evidence of boring. (Middle) *A. varians* forma *varians* is found in shallow, lagoonal habitats. It produces sinuous branches that can exceed 40 cm in height. (Bottom) *A. varians* forma *rigida* produces forma *varians*-like branches from a mounding base and has a thick cortex that produces a rigid skeleton. It is sympatric with forma *incrustans*.

Table 1

Some major morphological and ecological differences observed among the three Anthosigmella varians *morphotypes in the Florida Keys*

Character	forma *incrustans*	forma *varians*	forma *rigida*
Distribution of sponges	Reef	Bay/near island	Shallow reef
Depth (m)	8–27	1–3	8–13
Branches	Absent	Present	Present
Branch length (cm)	n/a	10	4
Area of attachment (cm^2)	1430	68	36
Tissue strength (N)	5	2	>10
Cortex thickness (mm)	1	Absent	6
Spicule concentration ($mg\ cm^{-3}$)	52	112	168
Subtylostyle length (μm)	355	375	375
Subtylostyle width (μm)	8	12	8
Anthosigma shape	Single bend	Two or more bends	Single bend

Values represent approximate averages (modified from Hill (1999)). Predators are found on the reef (in forma *incrustans* and forma *rigida* habitats), but are rare or absent in the nearshore environments or in Florida Bay (*i.e.*, in forma *varians* habitats).

The effects of predators were obvious within the first week, but the experiment ran for 125 days to determine whether any of the transplanted sponges adopted an encrusting morphology. At the conclusion of 125 days, changes in branch height were measured and compared using a one-tailed *t* test (Zar, 1984).

Given that *A. varians* forma *rigida* populations were sparse, we conducted a predator exclusion study on only 10 individuals from this morphotype. Those individuals were collected from Alligator and Tennessee (24°44′N; 80°47′W) reefs, and we made every effort to collect genetically distinct sponges by sampling sponges separated by more than 10 m. These sponges were affixed to ceramic tiles (15 cm × 15 cm) by monofilament. The experiment was run on Tennessee reef at a depth of 8 m, and a number of angelfish were observed at this site (Hill, 1998). As with the Alligator site, this site is exposed to open-ocean water motion. Five replicates were caged, the other five were exposed to predators. After 11 months, changes in spicule concentrations were compared. We measured spicule concentrations by excising a piece of sponge and measuring dimensions so that we could determine volumes. Thus, all spicule densities were standardized to a known sponge volume. Spicules were cleaned of sponge material with nitric acid and washed with double distilled H_2O. We measured spicule mass after drying spicules at 60°C for 48 h, and compared average spicule concentrations (milligrams of spicule per cubic centimeter of sponge) between treatments using a one-tailed *t* test (Zar, 1984). The *a priori* reason for predicting that spicule concentration would decrease (and hence our use of one-tailed *t* tests) was based on work by Palumbi (1986) showing that lower spicule densities were correlated with weaker sponge tissue.

To determine the influence of predators on branch production in *A. varians* forma *incrustans*, we placed exclosures made of plastic caging material (Vexar) with a mesh size of 5 cm over 13 individuals at a depth of 18 m on Tennessee reef. Cages were attached to the substratum using masonry nails and plastic cable ties. In some cases the cage did not cover the entire sponge (Fig. 2b). Nine additional, topless cages (which allowed predator access to the sponge) were placed over sponges to serve as controls for any cage artifacts. Sponges were monitored for about 450 days for production of branches, and cages were cleaned of fouling algae with a frequency of every month or less. We tested for differences in water flow between treatments by measuring the rate of dissolution of plaster-of-paris clods (Wellington, 1982). To achieve equal sample sizes in our statistical tests, we deployed clods within all 9 of the topless cages and within 9 of the 13 predator exclosures. Clods were removed after 2 d. To assess the effect of lower wave energy on morphology, 8 forma *incrustans* individuals were transplanted to Florida Bay at a depth of 1 m (adjacent to the KLMRL). Samples ($\approx 100\ cm^2$) were collected with a hammer and chisel from sponges on Tennessee reef. Specimens were attached to cinder blocks with monofilament within 4 h, and transplants were monitored for more than 8 months for the production of branches.

Artificial predation

We conducted an artificial predation experiment to see if this would cause forma *varians* to increase spicule concentration during simulated predation events. Using the protocol described in the section on forma *varians* above, 60 branches ($\approx$4–5 cm in height) were collected from different forma *varians* sponges near Long Key, and attached to calcareous blocks. The experiment was conducted at 1-m depth in Buttonwood Sound. Thirty sponges were clipped with a pair of scissors each day for 43 days to

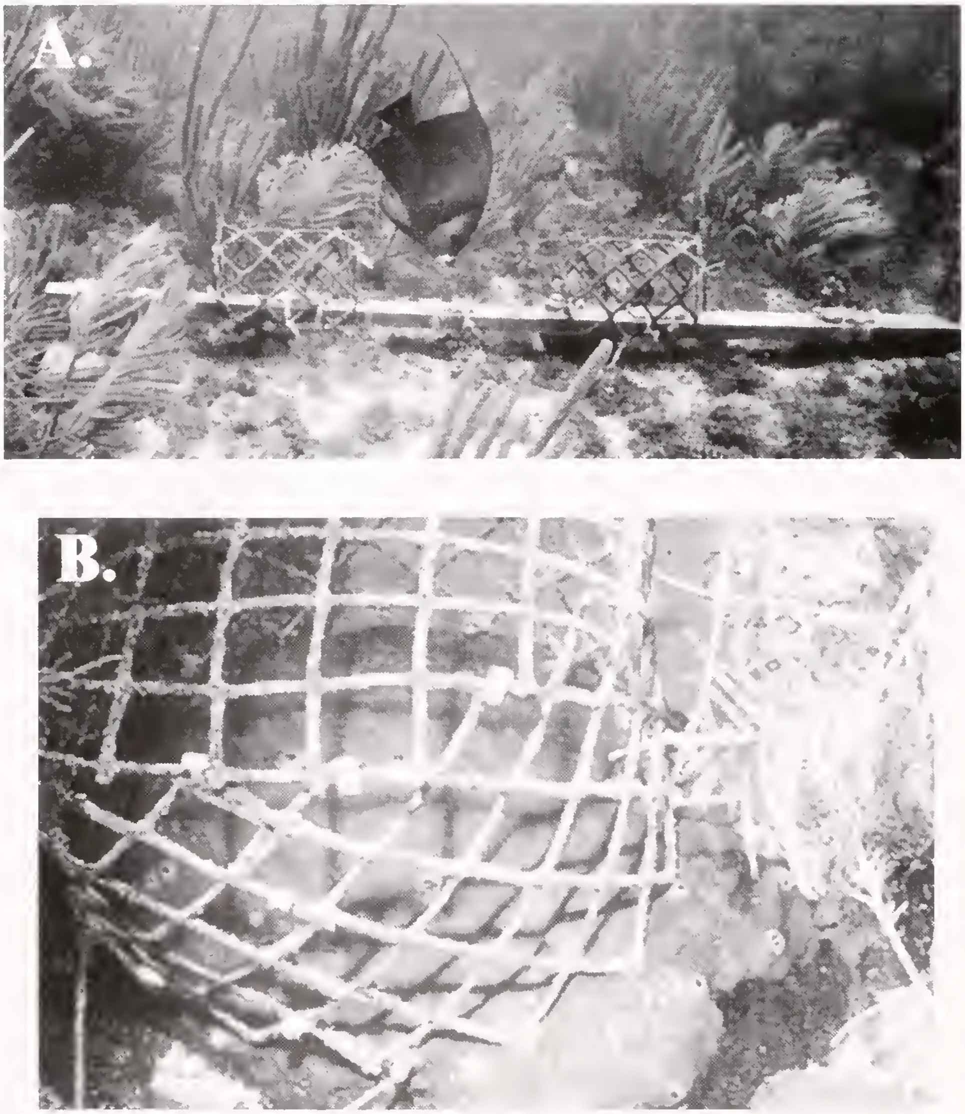

Figure 2. Experimental setups in the field. The material used to create these exclosures (Vexar) was used in all caging experiments. (A) The gray angelfish shown in this picture immediately began to consume exposed sponges after replicates were placed on the reef, and almost all pretransplant height was lost in the first week. The gray angelfish was one of a pair that had a territory in this area. Other angelfish (french, blue, and queen) and a Hawksbill turtle were seen in this area during the experiment. (B) An exclosure placed over a particularly large forma *incrustans* individual. Cages were effective at keeping predators out, but in replicates where the cage did not cover the entire sponge, fish could still bite exposed parts of the sponge (see marks outside of cage on lower right).

simulate wounds from a feeding event; another 30 sponges were left uninjured. Random regions along the length of the sponge branch were clipped each day, and different regions were injured between clippings. Although our simulated predation events differed qualitatively from natural angelfish bites, our objective was to determine whether *A. varians* was capable of modifying spicule concentrations after injury. At the end of the experiment, the entire branch from each replicate was frozen and transported to the laboratory for spicule analysis. For spicule concentration measurements, sections of known volume were taken from areas that appeared to have been injured for replicates in the artificial predation treatment, and from randomly chosen areas in the control replicates. Averages were compared as described above. The *a priori* reason for predicting increased spicule concentrations in the artificial predation treatment (and hence our use of one-tailed t tests) was based on work by Palumbi (1986) showing that spicule density and tissue stiffness and strength were positively correlated.

Results

Predator exclusion and wave energy

Transplanting *Anthosigmella varians* forma *varians* onto the reef produced dramatic results. A suite of spongivores was attracted to transplanted forma *varians*, and uncaged replicates were consumed rapidly (attacks began within 5 min; Fig. 2a). Angelfish removed virtually all above-substratum sponge tissue within the first week. Even though predators were quickly identified as a powerful selective force, we were interested in determining whether transplanted forma *varians* would adopt the morphology typical of forma *incrustans*. They did not, and some sponges ($n = 4$) increased height (*i.e.*, put energy into upward growth as opposed to encrustation) during the experiment. After several visits during the first week of the experiment, we visited the site about every 30 days to clean cages and monitor growth. This included visits before and after the passage of Tropical Storm Gordon (1994). The storm was responsible for the loss of one experimental unit containing several replicates (our buoy was attached to this structure), but appeared to have no effect on the replicates that remained (Fig. 3a). Other replicates were lost when the flagging tape failed to hold blocks to the wooden panels (these losses were not caused by the storm). At the end of this experiment, survivorship was high in the caged treatment, but was less than half in the uncaged treatment (Fig. 3b). Individuals exposed to predators (*i.e.*, uncaged) lost all pretransplantation height (largely within the first week of the experiment), and this was significantly different from the caged treatment ($t = 7.98$, d.f. $= 14$, $P \ll 0.001$). As can be seen in Figure 3b, the only survivors from the uncaged treatment were found within calcareous blocks (*A. varians* is a bioeroder).

Forma *rigida* had significantly lower spicule concentrations in the predator-exclusion treatment compared to the uncaged control ($t = 1.96$; d.f. $= 8$, $P < 0.05$; Fig. 4). Individuals from the uncaged control had spicule concentrations that were statistically indistinguishable from those at the beginning of the experiment (Hill, 1999). Furthermore, we noticed gross morphological changes (*e.g.*, adoption of an encrusting morph and a spongier texture) in replicates from the caged treatment.

Two cages in the experiment involving forma *incrustans* could not be located midway through the experiment, but none of the 11 remaining caged forma *incrustans* individuals produced branches over the 450 days of monitoring. Judging from the dissolution of plaster-of-paris clods, exclosures apparently had no significant effect on water flow compared to uncaged controls ($t = 1.4$; d.f. $= 16$; $P > 0.15$). It was clear that spongivores were prevented from biting the caged portion of the sponge since evidence of predation was only observed on uncaged portions of the sponge (Fig. 2b). In addition, none of the 8 transplanted forma *incrustans* individuals produced branches when placed in Florida Bay. Individuals transplanted into the bay lost zooxanthellar symbionts within 12 days, but recovered normal pigmentation when placed in the shade (Hill and Wilcox, 1998). This had no effect on survivorship since individuals persisted for another 8 months until a pulse of fresh water during the winter killed all replicates (W. Fitt, Key Largo Marine Research Laboratory, pers. comm.).

Artificial predation

During the artificial predation experiment involving forma *varians*, clipping resulted in significant increases in spicule concentrations compared to unmolested controls ($t = 2.14$; d.f. $= 36$; $P < 0.05$; Fig. 4). Injured areas were noticeably white (presumably because of increased spongin concentrations), and could be clearly demarcated from uninjured tissue. Twenty-two replicates were destroyed by snorkelers (10 from the unclipped treatment) and were not included in the analysis.

Discussion

The purpose of this research was to explore environmental factors that may be responsible for some of the observed morphological variablity in *Anthosigmella varians*. Transplant and caging experiments involving forma *varians* demonstrated that this morph is highly vulnerable to fish predation (Fig. 2a). When the uncaged replicates were placed on the reef, angelfish immediately began consuming them, and the exposed sponges lost all of their pretransplant height within the first week of the experiment (Fig. 3). Pawlik (1998) also found that forma *varians* was consumed by a suite of spongivores when transplanted to the reef. Even in the presence of predators, however, forma *varians* was capable of surviving for several months by boring into limestone blocks, but these sponges suffered higher mortality than the replicates in the caged treatment (Fig. 3b). The fact that forma *varians* can persist in an unmodified form on the open reef when protected from predators refutes Vicente's (1978) hypothesis that wave energy is responsible for the discontinuous distribution of forma *incrustans* and forma *varians*. The transplanted sponges were exposed to tropical-storm-strength wave action, yet four of the caged replicates gained height during the course of the experiment, suggesting favorable environmental conditions for growth. This experiment, and Pawlik's (1998) data, indicates that predators, and not wave energy, are the primary selective agent restricting forma *varians* to shallow, lagoonal habitats.

Branch production was not observed in experiments with forma *incrustans*. Excluding predators *in situ* had no effect on morphology, nor did transplanting forma *incrustans* into Florida Bay. There are at least three explanations for the lack of phenotypic change observed in experiments involving this morphotype. First, encrustation may be a fixed (*i.e.*,

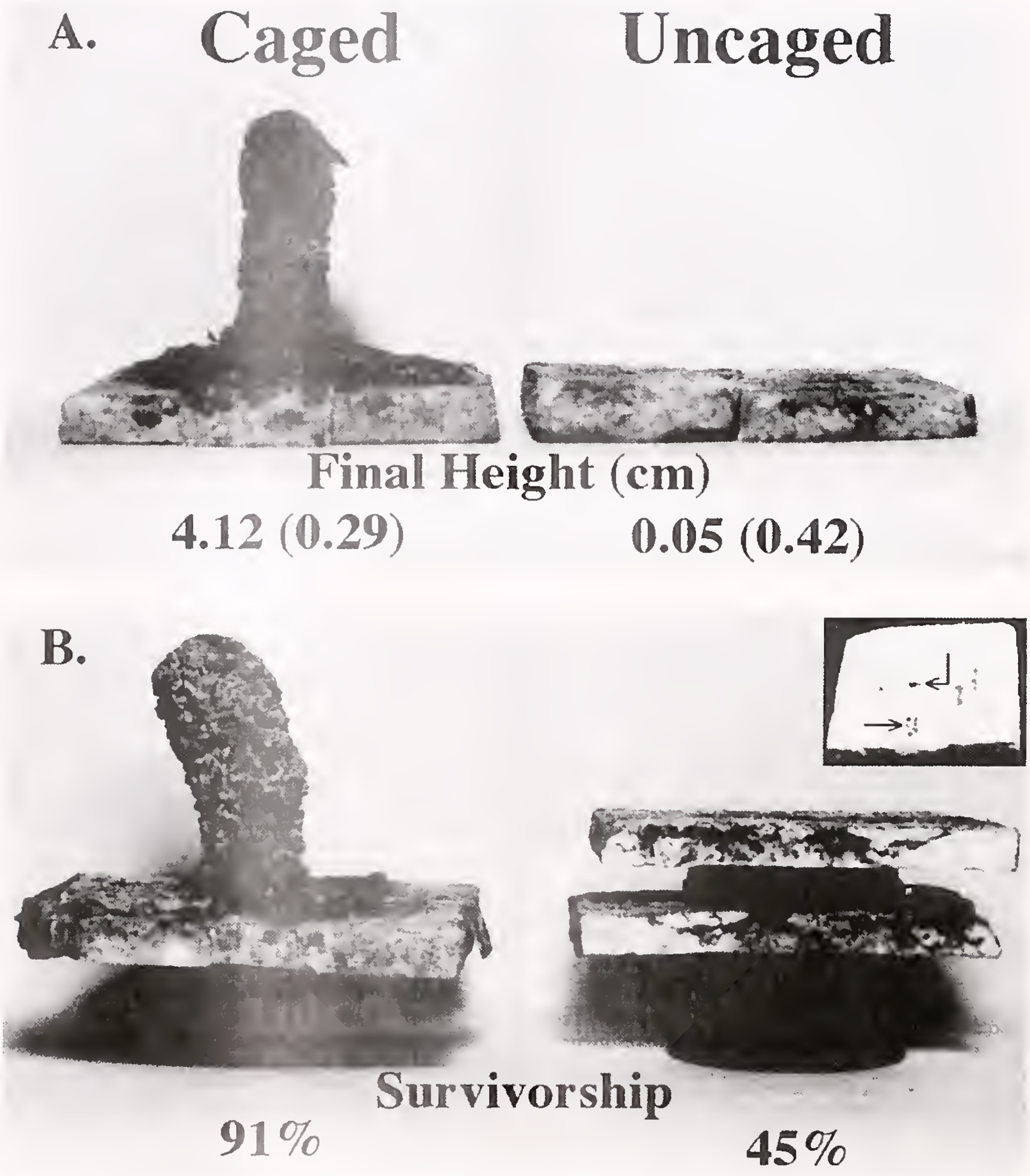

Figure 3. Data from transplant and caging experiments involving *Anthosigmella varians* forma *varians*. (A) Side view of caged (on left) and uncaged replicates. Average final heights (± SE) were significantly different ($t = 7.98$, d.f. $= 14$, $P < 0.001$) between caged ($n = 11$) and uncaged ($n = 5$) treatments. Uncaged replicates lost all of their pretransplant height, while two of the caged replicates gained in height over the course of the experiment. (B) Large differences in the survivorship of sponges from the two treatments were recorded. Although surviving caged sponges (left) were clearly visible, surviving sponges exposed to predation were visible only when the block they had attached to was broken open. Two halves of a block from an uncaged replicate (separated by a black plastic divider) are shown on the right. The inset shows the block before it was broken in half, and oscular openings can be seen on the surface (arrows). The spaces visible within the block on the right were created by boring activities of forma *varians*.

developmentally canalized) trait. Second, in many of the caged replicates, it was impossible to place exclosures over the entire sponge; thus, portions of the sponge were exposed to predators. There may be enough integration within an individual sponge to communicate predation in one part of the body to other parts of the sponge. Finally, it is possible that not enough time had elapsed to allow phenotypic modulation. If encrustation is a response to a stressful environment (wave energy and predation intensity are both higher on the reef), then it is predicted that an organism will delay expression of a vulnerable trait, provided that it is plastic, long after the threat from a stress is gone (Palumbi, 1984;

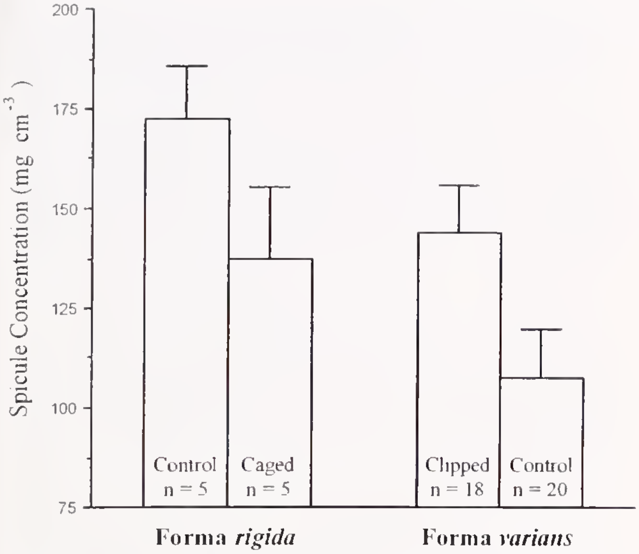

Figure 4. Average spicule concentration (± SE) as measured in experiments involving *Anthosigmella varians* forma *varians* and forma *rigida*. Sample sizes are shown in the figure. The bars on the left show results from the caging experiment involving forma *rigida*. Predator exclusion resulted in significant decreases in spicule concentrations compared to uncaged controls (t = 1.96; d.f. = 8, $P < 0.05$). The two bars on the right show the effects of artificial predation on spicule concentration in forma *varians*. Spicule concentrations increased significantly (t = 2.14; d.f. = 36; $P < 0.05$) in the clipped treatment compared to the unclipped control.

Sih, 1992). Longer periods of time might be necessary to observe branch production in forma *incrustans*. Indeed, given that the transplant experiment involving forma *incrustans* was halted prematurely by a freshwater intrusion, these experiments need to be repeated and allowed to run for a longer time. However, it is also possible that forma *incrustans* is a distinct, cryptic species that is incapable of branch production. We are currently exploring this possibility through analysis of DNA sequences from each of the morphotypes.

Hill (1999) suggested that the spicule- and spongin-rich cortex found in forma *incrustans* and forma *rigida* is an antipredator defense. He found that the tissue strength of forma *rigida* exceeded 10 N and forma *incrustans* was approximately equal to 5 N, whereas forma *varians* was near 2 N (Table 1). He also found that spongivores rapidly consumed the choanoderm of forma *rigida* when the cortex was removed. To assess the possibility that the cortex is an antipredator defense, we measured changes in spicule concentration as a proxy for tissue strength, given that there is a positive correlation between tissue stiffness and spicule concentration (Palumbi, 1986). We found that forma *varians* could increase spicule content in response to simulated predation events, and that forma *rigida* could reduce spicule content when protected from predation (Fig. 4). Although flow effects were not measured in the experiments involving forma *rigida*, cages similar to these have been found to have no significant effect on flow (Hill, 1998). However, statements about the causes of the observed decreases in spicule density must be properly qualified. Nonetheless, skeletal plasticity appears to be a property of both forma *varians* and forma *rigida*. In future experiments, we are interested in determining whether spongin production also increases in areas of damage. The increase in spicule concentration observed in the artificial predation experiment may represent a generalized response to damage, but any damaged tissue would have to be repaired after a predatory attack, so the morphologic response we observed may serve an important antipredator function. This is clearly an area that requires additional experiments.

We propose that the large cortex in both forma *incrustans* and forma *rigida* represents an inducible defense. Four factors have been identified as prerequisites for the evolution of inducible defenses (Havel, 1987; Sih, 1987; Harvell, 1990; Tollrian and Harvell, 1999). First, inducing agents must have a temporally or spatially variable impact. Second, reliable cues concerning the inducer must be present so that a resistant morphology can be adopted. Third, induced defenses must be effective against inducers. Finally, it is hypothesized that inducible defenses must be costly, but costs are offset by fitness gains achieved in the defended state.

The *A. varians* system meets the first prerequisite since the reef has two discrete patches for predation risk: high-risk on the fore-reef, and low-risk in lagoonal habitats. Forma *varians* is located in an environment where predators are absent, whereas the other morphs exist in an environment where the selective pressure of inducers (*i.e.*, spongivores) is strong. Our artificial predation experiment demonstrated that mechanical stimulation could serve as a cue to increase spicule concentration (Fig. 4), thus meeting the second condition for the evolution of inducible defenses. Additional experiments are necessary to address the third and fourth prerequisites for the evolution of inducible defenses in *A. varians*. Forma *varians* appears to lack defenses against angelfish (Figs. 2 and 3), but we have evidence that forma *varians* increases spicule concentrations in response to simulated attacks (Fig. 4). Anecdotal evidence indicates that the cortex of forma *rigida* and forma *incrustans* protects the choanosome (Hill, 1999). Although the idea was not tested in this study, we suggest that the production of a thick cortex (Table 1) represents a physiological cost since less biomass can be devoted to feeding, storage, or reproduction (the cortex has no choanocytic chambers). Observed decreases in spicule concentrations in the caging experiment involving forma *rigida* support the hypothesis that maintenance of a spicule-dense cortex is costly (Fig. 4). *Anthosigmella varians* appears to be a model system in which to determine whether morphology can serve a defensive function, and whether that defense can be induced.

Although the importance of chemical defense in sponges should not be underestimated, there are several reasons to continue to look for evidence of morphological defense in sponges. First, 31% of Caribbean sponges that have been examined to date are chemically undefended (Pawlik *et al.*, 1995). Many of these sponges are abundant on reefs but are not common items in the diets of spongivores (Randall and Hartman, 1968). Furthermore, according to Randall and Hartman's (1968) rankings, five of the top seven sponges most commonly eaten by fish belong to the category designated as unpalatable by Pawlik *et al.* (1995), indicating that the defenses Pawlik and colleagues identified are not very effective against spongivores. Anecdotal evidence also indicates that skeletal structures may protect sponges from predation. During one dive, we observed more than five angelfish (gray, french, and blue) rapidly consuming the interior portions of a damaged *Geodia neptuni* sponge (the sponge appeared to have been bitten by a Hawksbill turtle). It seems that *G. neptuni* is normally capable of fending off fish predators given that *Geodia* spp. were rarely encountered in the stomach contents of spongivorous fish (Randall and Hartman, 1968). It should be noted that although *Geodia* spp. apparently lack chemical defenses against fish (Pawlik *et al.*, 1995), they have an impressive cortex that might serve as a morphological defense. *Anthosigmella varians* may also use the cortex to protect itself from predators because when *A. varians* forma *rigida* and forma *incrustans* are cut open, angelfish rapidly consume the choanoderm (Hill, 1999).

There is common agreement that sponges face strong selective pressure from spongivores. Whether skeletal structures can serve as antipredator defenses remains an open question. The defensive function of the sponge skeleton deserves greater attention, and should be expanded to include the possibility of synergisms between structural and chemical defenses, as has been demonstrated by Hay *et al.* (1994) for seaweeds. In sponges, spicules may serve to abrade digestive surfaces, thus facilitating the intake of sponge-derived secondary compounds. In addition, spicules may increase handling time of food items, thus influencing optimal foraging behaviors of spongivores. Additional field experiments directed at identifying costs associated with the *A. varians* cortex, and determining the potential effectiveness of the cortex as an antipredator defense, are necessary. *A. varians* clearly provides a unique combination of traits to explore the adaptive significance of phenotypic variation, and may provide insights into general evolutionary responses on coral reefs.

Acknowledgments

W. Fitt and the Key Largo Marine Research Laboratory provided outstanding logistical support in the field. This is contribution number 23 from the KLMRL. Several of the field experiments in this study are part of a Ph.D. dissertation completed at the University of Houston (MSH). B. Badgley, G. Chilcoat, J. Fleck, and especially J. Villinski and T. Wilcox provided assistance with the fieldwork. Helpful comments on earlier drafts were provided by R. Chambers, D. Gleason, S. Phelan, S. Rakowitz, and T. Wilcox. Support from the PADI Foundation, Fairfield University, and the Lerner Gray Fund for Marine Research is gratefully acknowledged.

Literature Cited

Alino P. M., J. C. Coll, and P. W. Sammarco. 1992. Toxic prey discrimination in a highly specialized predator *Chaetodon melannotus* (Block et Schneider): visual vs. chemical cues. *J. Exp. Mar. Biol. Ecol.* **164:** 209–220.

Bakus, G. J. 1964. The effects of fish grazing on invertebrate evolution in shallow tropical waters. *Occas. Pap. Allan Hancock Fdn.* **27:** 1–29.

Bakus, G. J. 1966. Some relationships of fishes to benthic organisms on coral reefs. *Nature* **210:** 280–284.

Bakus, G. J. 1981. Chemical defense mechanisms on the Great Barrier Reef, Australia. *Science* **211:** 497–499.

Chanas, B., and J. R. Pawlik. 1995. Defenses of Caribbean sponges against predatory reef fish. II. Spicules, tissue toughness, and nutritional quality. *Mar. Ecol. Prog. Ser.* **127:** 195–211.

Chanas, B., and J. R. Pawlik. 1996. Does the skeleton of a sponge provide defense against predatory reef fish? *Oecologia* **107:** 225–231.

Coll, J. C., and P. W. Sammarco. 1988. The role of secondary metabolites in the chemical ecology of marine invertebrates: a meeting ground for biologists and chemists. *Proc. Sixth Int. Coral Reef Symp. Townsville, Australia* **1:** 167–174.

Cronin, G., V. J. Paul, and W. Fenical. 1997. Are tropical herbivores more resistant than temperate herbivores to seaweed chemical defenses? Diterpenoid metabolites from *Dictyota acutiloba* as feeding deterrents for tropical versus temperate fishes and urchins. *J. Chem. Ecol.* **23:** 289–294.

Duffy, J. E., and V. J. Paul. 1992. Prey nutritional quality and the effectiveness of chemical defenses against tropical reef fishes. *Oecologia* **90:** 333–339.

Faulkner, D. J. 1984. Marine natural products: metabolites of marine algae and herbivorous marine mollusks. *Nat. Prod. Rep.* **1:** 251–280.

Faulkner, D. J. 1998. Marine natural products. *Nat. Prod. Rep.* **15:** 113–158.

Fenical, W. 1982. Natural products chemistry in the marine environment. *Science* **215:** 923–928.

Fenical, W. 1997. New pharmaceuticals from marine organisms. *Trends Biotech.* **15:** 339–342.

Guida, V. G. 1976. Sponge predation in the oyster reef community as demonstrated with *Cliona celata* Grant. *J. Exp. Mar. Biol. Ecol.* **25:** 109–122.

Harvell, C. D. 1984. Predator-induced defenses in a marine bryozoan. *Science* **224:** 1357–1359.

Harvell, C. D. 1990. The ecology and evolution of inducible defenses. *Q. Rev. Biol.* **65:** 323–340.

Harvell, C. D., and W. Fenical 1989. Chemical and structural defenses of Caribbean gorgonians (*Pseudopterogorgia* spp.): intercolony localization of defense. *Limnol. Oceanogr.* **34:** 382–394.

Havel, J. E. 1987. Predator-induced defenses: a review. Pp. 263–278 in *Predation: Direct and Indirect Impacts on Aquatic Communities*, W. Charles Kerfoot and Andrew Sih, eds. University Press of New England, Hanover, NH.

Hay, M. E., and W. Fenical. 1988. Marine plant-herbivore interactions: the ecology of chemical defense. *Annu. Rev. Ecol. Syst.* **19:** 111–145.

Hay, M. E., Q. E. Kappel, and W. Fenical. 1994. Synergisms in plant defenses against herbivores: interactions of chemistry, calcification, and plant quality. *Ecology* **75:** 1714–1726.

Hill, M. S. 1998. Spongivory on Caribbean reefs releases corals from competition from sponges. *Oecologia* **117:** 143–150.

Hill, M. S. 1999. Morphological and genetic examination of phenotypic variability plasticity in the tropical sponge *Anthosigmella varians*. Proceedings of the 5th International Sponge Symposium "Origin & Outlook." J. N. A. Hooper, ed. *Mem. Queensl. Mus.* **44:** 239–248.

Hill, M. S., and T. P. Wilcox. 1998. Unusual mode of symbiont repopulation after bleaching in *Anthosigmella varians:* acquisition of different zooxanthellae strains. *Symbiosis* **25:** 279–289.

Hourigan, T. F., F. G. Stanton, P. J. Motta, C. D. Kelley, and B. Carlson. 1989. The feeding ecology of three species of Caribbean angelfishes (family Pomacanthidae). *Environ. Biol. Fishes* **24:** 105–116.

Huston, M. A. 1985. Patterns of species diversity on coral reefs. *Annu. Rev. Ecol. Syst.* **16:** 149–177.

Lively, C. M. 1986. Canalization versus developmental conversion in a spatially variable environment. *Am. Nat.* **128:** 561–572.

Palumbi, S. R. 1984. Tactics of acclimation: morphological changes of sponges in an unpredictable environment. *Science* **225:** 1478–1480.

Palumbi, S. R. 1986. How body plans limit acclimation: responses of a demosponge to wave force. *Ecology* **67:** 208–214.

Paul, V. J. 1992. Chemical defenses of benthic marine invertebrates. Pp. 164–188 in *Ecological Roles of Marine Natural Products*, V. J. Paul, ed. Comstock Publishing, Ithaca, NY.

Pawlik, J. R. 1983. A sponge-eating worm from Bermuda: *Branchiosyllis oculata* (Polychaeta, Syllidae). *Mar. Ecol.* **4:** 65–79.

Pawlik, J. R. 1997. Fish predation on Caribbean reef sponges: an emerging perspective of chemical defenses. *Proc. 8th Int. Coral Reef Symp. Panama* **2:** 1255–1258.

Pawlik, J. R. 1998. Coral reef sponges: do predatory fishes affect their distributions? *Limnol. Oceanogr.* **43:** 1396–1399.

Pawlik, J. R., B. Chanas, R. J. Toonen, and W. Fenical. 1995. Defenses of Caribbean sponges against predatory reef fish. I. Chemical deterrency. *Mar. Ecol. Prog. Ser.* **127:** 183–194.

Pennings, S. C., S. R. Pablo, V. J. Paul, and J. E. Duffy. 1994. Effects of sponge secondary metabolites in different diets on feeding by three groups of consumers. *J. Exp. Mar. Biol. Ecol.* **180:** 137–149.

Randall, J. E., and W. D. Hartman. 1968. Sponge-feeding fishes of the West Indies. *Mar. Biol.* **1:** 216–225.

Ridenhour, B. J., E. D. Brodie Jr., and E. D. Brodie III. 1999. Repeated injections of TTX do not affect TTX resistance or growth in the garter snake *Thamnophis sirtalis*. *Copeia* **1999:** 531–535.

Schnitzler, I., G. Pohnert, M. Hay, and W. Boland. 2001. Chemical defense of brown algae (*Dictyopteris* spp.) against the herbivorous amphipod *Ampithoe longimana*. *Oecologia* **126:** 515–521.

Sih, A. 1987. Predators and prey lifestyles: an evolutionary and ecological overview. Pp. 203–224 in *Predation: Direct and Indirect Impacts on Aquatic Communities*, W. Charles Kerfoot and Andrew Sih, eds. University of New England Press, Hanover, NH.

Sih, A. 1992. Prey uncertainty and the balancing of antipredator and feeding needs. *Am. Nat.* **139:** 1052–1069.

Tollrian, R., and C. D. Harvell. 1999. *The Ecology and Evolution of Inducible Defenses*. Princeton University Press, Princeton, NJ.

Trussell, G. C. 1996. Phenotypic plasticity in an intertidal snail: the role of a common crab predator. *Evolution* **50:** 448–454.

Vermeij, G. J. 1987. *Evolution and Escalation: An Ecological History of Life*. Princeton University Press, Princeton, NJ.

Vicente, V. P. 1978. An ecological evaluation of the West Indian demosponge *Anthosigmella varians* (Hadromerida: Spirastrellidae). *Bull. Mar. Sci.* **28:** 771–777.

Waddell, B., and J. R. Pawlik. 2000a. Defenses of Caribbean sponges against invertebrate predators: I. Assays with hermit crabs. *Mar. Ecol. Prog. Ser.* **195:** 125–132.

Waddell, B., and J. R. Pawlik. 2000b. Defenses of Caribbean sponges against invertebrate predators: II. Assays with sea stars. *Mar. Ecol. Prog. Ser.* **195:** 132–144.

Wellington, G. M. 1982. An experimental analysis of the effects of light and zooplankton on coral zonation. *Oecologia* **52:** 311–320.

West, J. M. 1997. Plasticity in the sclerites of a gorgonian coral: tests of water motion, light level, and damage cues. *Biol. Bull.* **192:** 279–289.

West, J. M. 1998. The dual role of sclerites in a gorgonian coral: conflicting functions of support and defence. *Evol. Ecol.* **12:** 803–821.

Wiedenmayer, F. 1977. *Shallow-Water-Sponges of the Western Bahamas*. Birkhauser Verlag, Basel.

Wulff, J. L. 1994. Sponge feeding by Caribbean angelfishes, trunkfishes, and filefishes. Pp. 265–271 in *Sponges in Time and Space*, R. W. M. van Soest, J. van Kempen, and J. Braekman, eds. Balkema, Rotterdam.

Zar, J. H. 1984. *Biostatistical Analysis*. Prentice Hall, Englewood Cliffs, NJ.

THE BIOLOGICAL BULLETIN
(www.biolbull.org)
2002 SUBSCRIPTION FORM
(VOLUMES 202-203, 6 ISSUES)

All subscriptions run on the calendar year; price includes both print and online journals.

(please print)

NAME: ____________________

INSTITUTION: ____________________

ADDRESS: ____________________

CITY: ____________________ STATE: ____________________

POSTAL CODE: ____________________ COUNTRY: ____________________

TELEPHONE: ____________________ FAX: ____________________

E-MAIL ADDRESS: ____________________

☐ **Please send me a 2002 subscription to *The Biological Bulletin* at the rate indicated below:**

☐ Individual: $105.00 (6 ISSUES) ☐ Institutional: $260.00 (6 ISSUES)

☐ Individual: $ 52.50 (3 ISSUES) ☐ Institutional: $130.00 (3 ISSUES)

Check one: ☐ February, April, June or ☐ August, October, December

☐ **Please send me the following back issue(s):** ____________________

☐ Individual: at $20.00 (PER ISSUE) ☐ Institutional: at $45.00 (PER ISSUE)

Delivery Options

_____ Surface Delivery (Surface delivery is included in the subscription price.)

_____ Air delivery (Please add the correct amount to your payment.)

☐ U.S. and Canada: $25.00 ☐ Mexico: $60.00 ☐ All other locations: $100.00

Payment Options

_____ Enclosed is my check or U.S. money order for $ ______ made payable to The Marine Biological Laboratory

_____ Please send me an invoice. (Note: Payment must be received before subscription commences.)

_____ Please charge my ☐ VISA, ☐ MasterCard ☐ Discover Card $________

Account No.: ____________________ **Exp. Date:** ____________________

Signature: ____________________ **Date:** ____________________

Return this form with your check or credit card information to:

Marine Biological Laboratory
Subscription Office ◆ The Biological Bulletin ◆7 MBL Street ◆ Woods Hole, MA 02543-1015

Ultimate Fluorescence Machine

Are you continuously searching for higher contrast, increased transmission and maximum system stability for multi-channel studies? Look no further than **Axioplan 2 imaging** – the ultimate fluorescence machine.

Innovation is the key to success. ICS infinity optics and the shortest possible light paths ensure the highest transmission.

Newly designed filter cubes **'push and click'** into position for stability and precision. Contrast is dramatically improved by the unique **'Light Trap'** (patent pending) which captures stray light and deflects it away from the imaging path. The overall result has to be seen to be believed – ask for a demonstration.

Carl Zeiss MicroImaging, Inc.
One Zeiss Drive
Thornwood, NY 10594

800.233.2343
micro@zeiss.com
www.zeiss.com/micro

ZEISS

Volume 202

THE BIOLOGICAL BULLETIN

Number 2

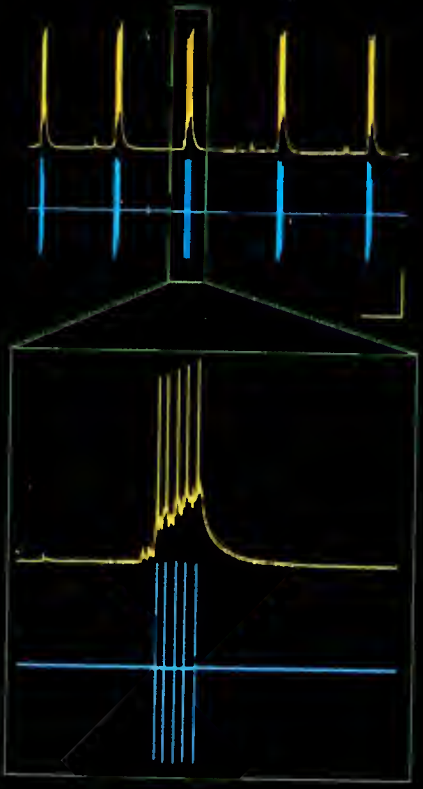

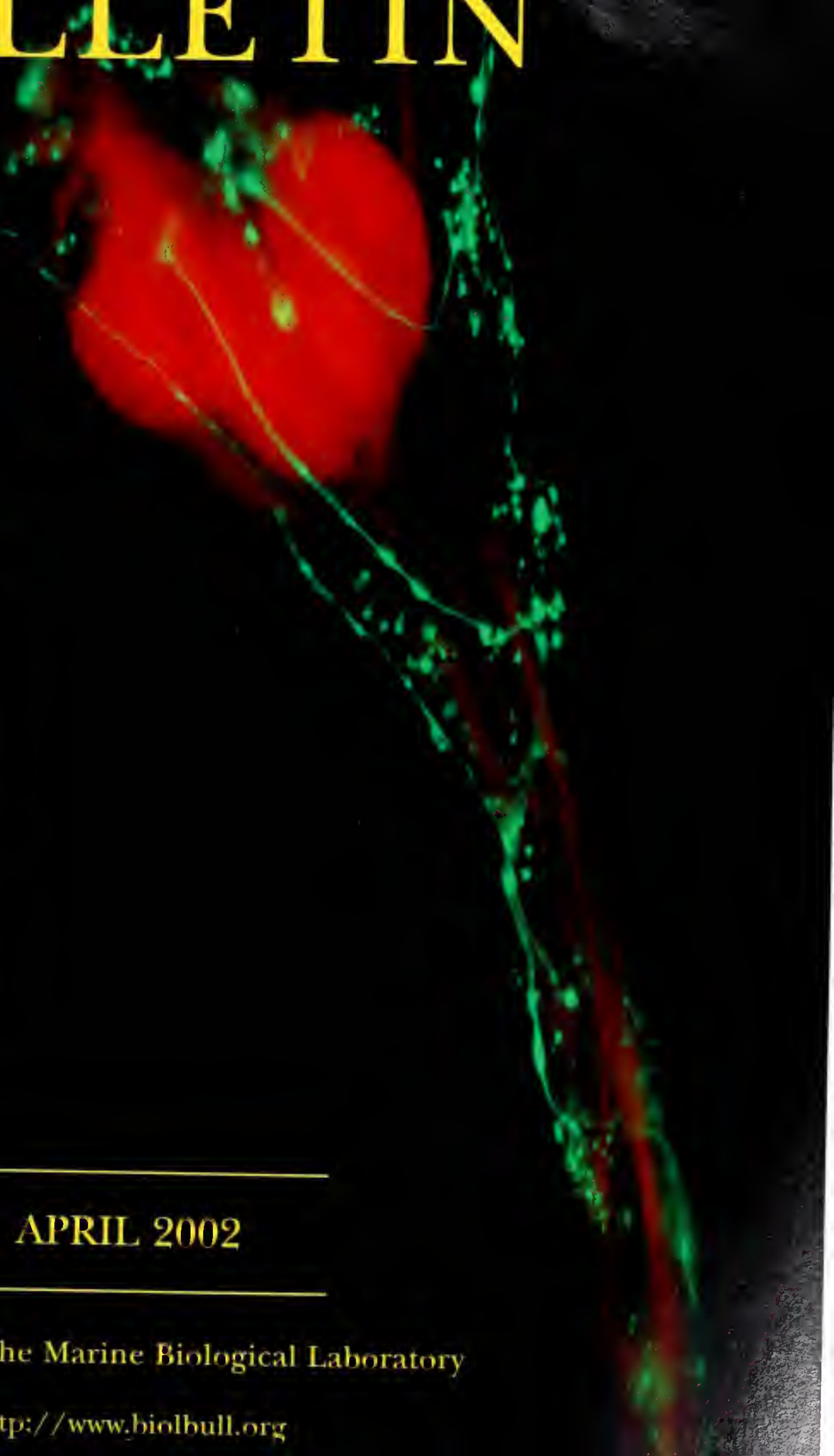

APRIL 2002

Published by the Marine Biological Laboratory

http://www.biolbull.org

THE BIOLOGICAL BULLETIN

ONLINE

The Marine Biological Laboratory is pleased to announce that the full text of *The Biological Bulletin* is available online at

http://www.biolbull.org

The Biological Bulletin publishes outstanding experimental research on the full range of biological topics and organisms, from the fields of Neurobiology, Behavior, Physiology, Ecology, Evolution, Development and Reproduction, Cell Biology, Biomechanics, Symbiosis, and Systematics.

Published since 1897 by the Marine Biological Laboratory (MBL) in Woods Hole, Massachusetts, *The Biological Bulletin* is one of America's oldest peer-reviewed scientific journals.

The journal is aimed at a general readership, and especially invites articles about those novel phenomena and contexts characteristic of intersecting fields.

The Biological Bulletin Online contains the full content of each issue of the journal, including all figures and tables, beginning with the February 2001 issue (Volume 200, Number 1). The full text is searchable by keyword, and the cited references include hyperlinks to Medline. PDF files are available beginning in February 1990 (Volume 178, Number 1), some abstracts are available beginning with the October 1976 issue (Volume 151, Number 2), and some Tables of Contents are online beginning with the October 1965 issue (Volume 129, Number 2).

Each issue will be placed online approximately on the date it is mailed to subscribers; therefore the online site will be available prior to receipt of your paper copy. Online readers may want to sign up for the eTOC (electronic Table of Contents) service, which will deliver each new issue's table of contents *via* e-mail. The web site also provides access to information about the journal (such as Instructions to Authors, the Editorial Board, and subscription information), as well as access to the Marine Biological Laboratory's web site and other *Biological Bulletin* electronic publications.

The free trial period for access to *The Biological Bulletin* online has ended. Individuals and institutions who are subscribers to the journal in print or are members of the Marine Biological Laboratory Corporation may now activate their online subscriptions. All other access (*e.g.*, to Abstracts, eTOCs, searching, Instructions to Authors) remains freely available. Online access is included in the print subscription price.

For more information about subscribing or activating your online subscription, visit <www.biolbull.org/subscriptions>.

---

http://www.biolbull.org

OLYMPUS
LUMPlanFl
20x/0.95 W
∞/0
The objective is not to touch the objective.

The BX51WI. A single 20x water immersion objective. A high N.A. of 0.95. A W.D. of 2.0mm. An intermediate magnification changer. Switch between low and high magnifications. Objective is untouched. Vibrations eliminated. Electrodes unmoved. It's a new movement in microscopy. **How Original. How Olympus.** Visit us at olympusamerica.com or call 1-800-446-5967.

OLYMPUS®
FOCUS ON LIFE

BIOLOGICAL BULLETIN PUBLICATIONS

is pleased to announce the publication
of three new online resources:

R.E. Stevens. 1972. Studies on the Development of the Sea Urchin, *Strongylocentrotus droebachiensis*
I. Ecology and normal development. *Biol. Bull.* **142:** 132-144.
PDF at **http://www.mbl.edu/BiologicalBulletin/classic.ref.html**
A crucial resource for anyone interested in working with this organism.

"Anesthetic, Relaxant, and Narcotizing Agents for Aquatic Invertebrates."
At **http://www.mbl.edu/BiologicalBulletin/compendia.html**
This peer-reviewed compendium provides information on narcotizing and relaxant methods for marine species
that are valuable in aquaculture and in biomedical and ecological research.
For further information contact the editor: William D. Cohen at bbp@mbl.edu

"Notes on Methods for the Narcotization, Killing, Fixation, and Preservation of Marine Organisms."
Compiled by Henry D. Russell, April 1963. Systematics-Ecology Program,
Marine Biological Laboratory, Woods Hole, MA.
At **http://www.mbl.edu/BiologicalBulletin/classic.ref.html**
A historic study collection of methods of preparation and preservation of the marine organisms of the Cape Cod region.

Cover

The heart of adult decapod crustaceans contracts rhythmically, but the beat is driven exclusively by rhythmic barrages of action potentials produced by the cardiac ganglion. This ganglion, located on the inside of the dorsal wall of the heart, fires autonomously, and its activity continues even when it has been isolated from the myocardium and pinned out in a dish; in contrast, a heart with its ganglion removed is quiescent. The cardiac ganglion in most decapod crustaceans is a small network, composed of only nine neurons; it has been studied intensively for the past 50 years as a model neural pacemaker and pattern generator. In this issue of *The Biological Bulletin* (p. 108), Ian M. Cooke (University of Hawaii) reviews the structure, function, and experimental utility of the crustacean cardiac ganglion.

The images on the cover illustrate morphological and physiological aspects of the cardiac ganglion of the blue crab, *Callinectes sapidus*. Three large motor neurons in the anterior portion of the ganglion were filled with neurobiotin and labeled with rhodamine 600 avidin. Further, immunohistochemistry with a primary antiserum raised to tyrosine hydroxylase revealed a pair of fibers (green) that branch and have varicose terminations in the region of the motor neurons. These fibers are one of two pairs of axons that carry excitatory impulses from the central nervous system to the cardiac ganglion. The tyrosine hydroxylase-like immunoreactivity indicates that the fibers are catecholaminergic and probably contain dopamine.

The cover also illustrates rhythmic bursts of action potentials recorded intracellularly from one of the large anterior motor neurons (top record; yellow), and extracellularly from a motor nerve to the heart (top record; blue). One of these bursts (framed in green) is expanded in the bottom records, which show that the impulses recorded intracellularly from any of the five motor neurons correspond exactly to those recorded extracellularly from the nerve. Thus the activity of these motor neurons is precisely synchronized. [Calibration bars: upper records = 16 mV (intracellular recording), 2.5 s; lower (expanded) records = 10 mV, 400 ms.]

The cover illustration was prepared by Timothy J. Fort, Institute of Neurobiology, University of Puerto Rico. The experiments of T. J. Fort and M. W. Miller are mentioned in this issue in the review by I. M. Cooke (see pp. 111 and 125, and Fig. 7E).

THE
BIOLOGICAL BULLETIN
APRIL 2002

Marine Biological Laboratory
Woods Hole Oceanographic Institution
Library

MAY 0 3 2002

Woods Hole, MA 02543

Editor	Michael J. Greenberg	The Whitney Laboratory, University of Florida
Associate Editors	Louis E. Burnett	Grice Marine Biological Laboratory, College of Charleston
	R. Andrew Cameron	California Institute of Technology
	Charles D. Derby	Georgia State University
	Michael LaBarbera	University of Chicago
Section Editor	Shinya Inoué, *Imaging and Microscopy*	Marine Biological Laboratory
Online Editors	James A. Blake, *Keys to Marine Invertebrates of the Woods Hole Region*	ENSR Marine & Coastal Center, Woods Hole
	William D. Cohen, *Marine Models Electronic Record and Compendia*	Hunter College, City University of New York
Editorial Board	Peter B. Armstrong	University of California, Davis
	Ernest S. Chang	Bodega Marine Lab., University of California, Davis
	Thomas H. Dietz	Louisiana State University
	Richard B. Emlet	Oregon Institute of Marine Biology, Univ. of Oregon
	David Epel	Hopkins Marine Station, Stanford University
	Kenneth M. Halanych	Woods Hole Oceanographic Institution
	Gregory Hinkle	Cereon Genomics, Cambridge, Massachusetts
	Nancy Knowlton	Scripps Inst. Oceanography & Smithsonian Tropical Res. Inst.
	Makoto Kobayashi	Hiroshima University of Economics, Japan
	Esther M. Leise	University of North Carolina Greensboro
	Donal T. Manahan	University of Southern California
	Margaret McFall-Ngai	Kewalo Marine Laboratory, University of Hawaii
	Mark W. Miller	Institute of Neurobiology, University of Puerto Rico
	Tatsuo Motokawa	Tokyo Institute of Technology, Japan
	Yoshitaka Nagahama	National Institute for Basic Biology, Japan
	Sherry D. Painter	Marine Biomed. Inst., Univ. of Texas Medical Branch
	J. Herbert Waite	University of California, Santa Barbara
	Richard K. Zimmer	University of California, Los Angeles
Editorial Office	Pamela Clapp Hinkle	Managing Editor
	Victoria R. Gibson	Staff Editor
	Carol Schachinger	Editorial Associate
	Wendy Child	Subscription & Advertising Administrator

Published by
MARINE BIOLOGICAL LABORATORY
WOODS HOLE, MASSACHUSETTS

http://www.biolbull.org

Exceptional Clusters,
Superior Tech Support
Microway's Reputation is Your Guarantee

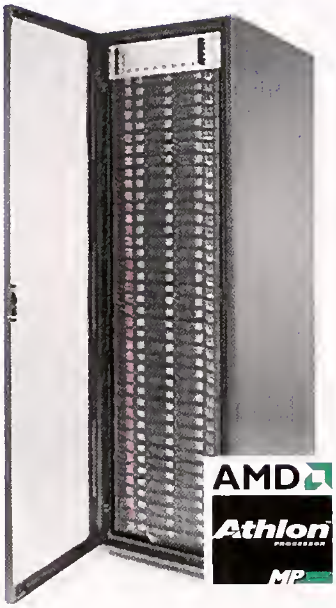

AMD Athlon MP

Harness Dual Athlon Power with a Microway® Scalable 25 Node 50 Processor Cluster Using Dual Athlon MP 2000+ and Myrinet Interconnect, Yielding Peak Throughput of 166 Gigaflops.

Microway® Screamer™ Dual Alpha 21264DP 833 MHz, 16 MB Cache in RuggedRack™ Chassis with RRR™ Redundant Power Supply

Athlon, Xeon, and Alpha Clusters

Since 1982, Microway has designed and manufactured state of the art, cost effective solution for the High Performance Technical Computing community. Our custom Linux clusters an servers are chosen by people at universities, government research labs, biotechs, and financia institutions worldwide. Microway understands that on-time delivery, out-of-the-box reliabilit and excellent ongoing technical support are critical to our users. You can have confidence tha our solutions employ the latest in processor, connectivity, cluster management, and RAI technologies. Visit microway.com to see our latest products and customer testimonials.

Over 17,000 Satisfied Customers Since 1982 Include:

CORPORATIONS AND NON PROFITS
Allied Signal
AT&T
BAE Systems
Carnegie Institute of Washington
Cisco Systems
Cray Research
Disney Studios
EMC Corporation
Exxon
Federal Aviation Administration
Fidelity Investments
Food and Drug Administration
General Electric
General Motors
Grumman Aerospace
Hughes Aircraft
Intel
IBM
Johnson & Johnson
Lion Bioscience
Lockheed Martin
Merrill Lynch
Millennium Pharmaceuticals
Morgan Stanley
Myricom
Nikon
Raytheon Missile Systems
Smithsonian Institution
United Nations
World Bank

RESEARCH LABORATORIES
Ames Laboratory
Argonne
Berkeley Lab
Brookhaven
Lawrence Livermore
Los Alamos
MBL - Woods Hole
Jet Propulsion Lab
NASA
NIH
NIST
NOAA
NSF
Naval Air Warfare Center
Naval Postgraduate School
Naval Research Lab
Naval Surface Warfare Center
Naval Underseas Warfare Center
Oakridge National Laboratory
Sandia National Laboratory
SETI Project
US Air Force
US Army
US Army Corps of Engineers
US Dept. of Defense
US Geological Survey

UNIVERSITIES
Arizona State
Brown
BU
Cal State
Carnegie Mellon
Case Western Reserve
Colorado School of Mines
Colorado State
Columbia
Cornell
Dartmouth
Duke
Duquesne
Harvard
Johns Hopkins
McGill
Kent State
Miami
Michigan State
New Mexico
Northwestern
Princeton
Purdue
Rockefeller
Rutgers
South Carolina
Stanford
SUNY
Syracuse
Tufts
Vanderbilt
Washington (St. Louis)
Yale

TECHNICAL UNIVERSITIES
Cal Tech
Georgia Tech
MIT
New Jersey Tech
New Mexico Tech
Rensselaer (RPI)
Texas Tech
Worcester Poly Tech

UNIVERSITY O
Alaska
Arkansas
California (Berkeley, UCLA, UCSD, UCSF)
Chicago
Connecticut
Colorado
Florida
Hawaii
Illinois
Kentucky
Maine
Maryland
Massachusetts
Mississippi
Missouri
New York
North Carolina
Pennsylvania
Texas
Utah
Virginia
Vermont
Washington
Wisconsin

Expert Integration ~ Cost Effective Solutions

"Our committee chose Microway over other vendors because of their reputation in the HPC community for delivering high quality, fully integrated clusters. Our decision was based also on their extensive technical expertise with Myrinet, demonstrated financial stability and ability to quickly deliver the 210 node cluster we required."

— Jake Ward, Director, Department of Industrial Cooperation, University of Maine at Orono

Microway®
Technology you can count on℠

Call us: 508-746-7341
For a technical salesperson who speaks your language
Visit us: www.microway.com

CONTENTS

Volume 202, No. 2: April 2002

RESEARCH NOTES

Miner, Benjamin G., Jonathan D. Cowart, and Larry R. McEdward
Egg energetics for the facultative planktotroph *Clypeaster rosaceus* (Echinodermata: Echinoidea), revisited 97

Hertzler, Philip L.
Twin meiosis 2 spindles form after suppression of polar body 1 formation in oocytes of the marine shrimp *Sicyonia ingentis* 100

Elphick, Maurice R.
Evolution of cannabinoid receptors in vertebrates: identification of a CB_2 gene in the puffer fish *Fugu rubripes* 104

REVIEW

Cooke, Ian M.
Reliable, responsive pacemaking and pattern generation with minimal cell numbers: the crustacean cardiac ganglion 108

NEUROBIOLOGY AND BEHAVIOR

Pechenik, Jan A., Wei Li, and David E. Cochrane
Timing is everything: the effects of putative dopamine antagonists on metamorphosis vary with larval age and experimental duration in the prosobranch gastropod *Crepidula fornicata* 137

ECOLOGY AND EVOLUTION

Voight, Janet R.
Morphometric analysis of male reproductive features of octopodids (Mollusca: Cephalopoda) 148

Van Winkle, David H., and Neil W. Blackstone
Variation in growth and competitive ability between sexually and clonally produced hydroids 156

McCartney, Michael A., and H. A. Lessios
Quantitative analysis of gametic incompatibility between closely related species of neotropical sea urchins 166

SYSTEMATICS

Cameron, Christopher B.
The anatomy, life habits, and later development of a new species of enteropneust, *Harrimania planktophilus* (Hemichordata: Harrimaniidae) from Barkley Sound 182

PHYSIOLOGY AND BIOMECHANICS

Cameron, Christopher B.
Particle retention and flow in the pharynx of the enteropneust worm *Harrimania planktophilus:* The filter-feeding pharynx may have evolved before the chordates 200

THE BIOLOGICAL BULLETIN

THE BIOLOGICAL BULLETIN is published six times a year by the Marine Biological Laboratory, 7 MBL Street, Woods Hole, Massachusetts 02543.

Subscriptions and similar matter should be addressed to Subscription Administrator, THE BIOLOGICAL BULLETIN, Marine Biological Laboratory, 7 MBL Street, Woods Hole, Massachusetts 02543. Subscription includes both print and online journals. Subscription per year (six issues, two volumes): $260 for libraries; $105 for individuals. Subscription per volume (three issues): $130 for libraries; $52.50 for individuals. Back and single issues (subject to availability): $45 for libraries; $20 for individuals.

Communications relative to manuscripts should be sent to Michael J. Greenberg, Editor-in-Chief, or Pamela Clapp Hinkle, Managing Editor, at the Marine Biological Laboratory, 7 MBL Street, Woods Hole, Massachusetts 02543. Telephone: (508) 289-7428. FAX: 508-289-7922. E-mail: pclapp@mbl.edu.

http://www.biolbull.org

THE BIOLOGICAL BULLETIN is indexed in bibliographic services including *Index Medicus* and MEDLINE, *Chemical Abstracts*, *Current Contents*, *Elsevier BIOBASE/Current Awareness in Biological Sciences*, and *Geo Abstracts*.

Printed on acid free paper,
effective with Volume 180, Issue 1, 1991.

POSTMASTER: Send address changes to THE BIOLOGICAL BULLETIN, Marine Biological Laboratory,
7 MBL Street, Woods Hole, MA 02543.

Copyright © 2002, by the Marine Biological Laboratory

Periodicals postage paid at Woods Hole, MA, and additional mailing offices.
ISSN 0006-3185

INSTRUCTIONS TO AUTHORS

The Biological Bulletin accepts outstanding original research reports of general interest to biologists throughout the world. Papers are usually of intermediate length (10–40 manuscript pages). A limited number of solicited review papers may be accepted after formal review. A paper will usually appear within four months after its acceptance.

Very short, especially topical papers (less than 9 manuscript pages including tables, figures, and bibliography) will be published in a separate section entitled "Research Notes." A Research Note in *The Biological Bulletin* follows the format of similar notes in *Nature*. It should open with a summary paragraph of 150 to 200 words comprising the introduction and the conclusions. The rest of the text should continue on without subheadings, and there should be no more than 30 references. References should be referred to in the text by number, and listed in the Literature Cited section in the order that they appear in the text. Unlike references in *Nature*, references in the Research Notes section should conform in punctuation and arrangement to the style of recent issues of *The Biological Bulletin*. Materials and Methods should be incorporated into appropriate figure legends. See the article by Lohmann *et al.* (October 1990, Vol. **179:** 214–218) for sample style. A Research Note will usually appear within two months after its acceptance.

The Editorial Board requests that regular manuscripts conform to the requirements set below; those manuscripts that do not conform will be returned to authors for correction before review.

1. ***Manuscripts.*** Manuscripts, including figures, should be submitted in quadruplicate, with the originals clearly marked. (Xerox copies of photographs are not acceptable for review purposes.) If possible, please include an electronic copy of the text of the manuscript. Label the disk with the name of the first author and the name and version of the wordprocessing software used to create the file. If the file was not created in some version of Microsoft Word, save the text in rich text format (rtf). The submission letter accompanying the manuscript should include a telephone number, a FAX number, and (if possible) an E-mail address for the corresponding author. The original manuscript must be typed in no smaller than 12 pitch or 10 point, using double spacing (*including* figure legends, footnotes, bibliography, etc.) on one side of 16- or 20-lb. bond paper, 8 by 11 inches. Please, no right justification. Manuscripts should be proofread carefully and errors corrected legibly in black ink. Pages should be numbered consecutively. Margins on all sides should be at least 1 inch (2.5 cm). Manuscripts should conform to the *Council of Biology Editors Style Manual*, 5th Edition (Council of Biology Editors, 1983) and to American spelling. Unusual abbreviations should be kept to a minimum and should be spelled out on first reference as well as defined in a footnote on the title page. Manuscripts should be divided into the following components: Title page, Abstract (of no more than 200 words), Introduction, Materials and Methods, Results, Discussion, Acknowledgments, Literature Cited, Tables, and Figure Legends. In addition, authors should supply a list of words and phrases under which the article should be indexed.

2. ***Title page.*** The title page consists of a condensed title or running head of no more than 35 letters and spaces, the manuscript title, authors' names and appropriate addresses, and footnotes listing present addresses, acknowledgments or contribution numbers, and explanation of unusual abbreviations.

3. ***Figures.*** The dimensions of the printed page, 7 by 9 inches, should be kept in mind in preparing figures for publication. We recommend that figures be about 1 times the linear dimensions of the final printing desired, and that the ratio of the largest to the smallest letter or number and of the thickest to the thinnest line not exceed 1:1.5. Explanatory matter generally should be included in legends, although axes should always be identified on the illustration itself. Figures should be prepared for reproduction as either line cuts or halftones. Figures to be reproduced as line cuts should be unmounted glossy photographic reproductions or drawn in black ink on white paper, good-quality tracing cloth or plastic, or blue-lined coordinate paper. Those to be reproduced as halftones should be mounted on board, with both designating numbers or letters and scale bars affixed directly to the figures. All figures should be numbered in consecutive order, with no distinction between text and plate figures and cited, in order, in the text. The author's name and an arrow indicating orientation should appear on the reverse side of all figures.

Digital art: The Biological Bulletin will accept figures submitted in electronic form; however, digital art must conform to the following guidelines. Authors who create digital images are wholly responsible for the quality of their material, including color and halftone accuracy.

Format. Acceptable graphic formats are TIFF and EPS. Color submissions must be in EPS format, saved in CMKY mode.

Software. Preferred software is Adobe Illustrator or Adobe Photoshop for the Mac and Adobe Photoshop for Windows. Specific instructions for artwork created with various software programs are available on the Web at the Digital Art Information Site maintained by Cadmus Professional Communications at http://cpc.cadmus.com/dal/

Resolution. The minimum requirements for resolution are 1200 DPI for line art and 300 for halftones.

Size. All digital artwork must be submitted at its actual printed size so that no scaling is necessary.

Multipanel figures. Figures consisting of individual parts (*e.g.,* panels A, B, C) must be assembled into final format and submitted as one file.

Hard copy. Files must be accompanied by hard copy for use in case the electronic version is unusable.

Disk identification. Disks must be clearly labeled with the following information: author name and manuscript number; format (PC or Macintosh); name and version of software used.

Color: The Biological Bulletin will publish color figures and plates, but must bill authors for the actual additional cost of printing in color. The process is expensive, so authors with more than one color image should—consistent with editorial concerns, especially citation of figures in order—combine them into a single plate to reduce the expense. On request, when supplied with a copy of a color illustration, the editorial staff will provide a pre-publication estimate of the printing cost.

4. ***Tables, footnotes, figure legends, etc.*** Authors should follow the style in a recent issue of *The Biological Bulletin* in preparing table headings, figure legends, and the like. Because of the high cost of setting tabular material in type, authors are asked to limit such material as much as possible. Tables, with their headings and footnotes, should be typed on separate sheets, numbered with consecutive Roman numerals, and placed after the Literature Cited. Figure legends should contain enough information to make the figure intelligible separate from the text. Legends should be typed double spaced, with consecutive Arabic numbers, on a separate sheet at the end of the paper. Footnotes should be limited to authors' current addresses, acknowledgments or contribution numbers, and explanation of unusual abbreviations. All such footnotes should appear on the title page. Footnotes are not normally permitted in the body of the text.

5. ***Literature cited.*** In the text, literature should be cited by the Harvard system, with papers by more than two authors cited as Jones *et al.,* 1980. Personal communications and material in preparation or in press should be cited in the text only, with author's initials and institutions, unless the material has been formally accepted and a volume number can be supplied. The list of references following the text should be headed Literature Cited, and must be typed double spaced on separate pages, conforming in punctuation and arrangement to the style of recent issues of *The Biological Bulletin.* Citations should include complete titles and inclusive pagination. Journal abbreviations should normally follow those of the U. S. A. Standards Institute (USASI), as adopted by Biological Abstracts and Chemical Abstracts, with the minor differences set out below. The most generally useful list of biological journal titles is that published each year by Biological Abstracts (biosis List of Serials; the most recent issue). Foreign authors, and others who are accustomed to using The World List of Scientific Periodicals, may find a booklet published by the Biological Council of the U.K. (obtainable from the Institute of Biology, 41 Queen's Gate, London, S.W.7, England, U.K.) useful, since it sets out the World List abbreviations for most biological journals with notes of the USASI abbreviations where these differ. Chemical Abstracts publishes quarterly supplements of additional abbreviations. The following points of reference style for The Biological Bulletin differ from USASI (or modified World List) usage:

A. Journal abbreviations, and book titles, all underlined (for *italics*)

B. All components of abbreviations with initial capitals (not as European usage in World List *e.g., J. Cell. Comp. Physiol.* NOT *J. cell. comp. Physiol.*)

C. *All* abbreviated components must be followed by a period, whole word components *must not* (*i.e., J. Cancer Res.*)

D. Space between all components (*e.g., J. Cell. Comp. Physiol.,* not *J.Cell.Comp.Physiol.*)

E. Unusual words in journal titles should be spelled out in full, rather than employing new abbreviations invented by the author. For example, use *Rit Vísindafjélags Islendinga* without abbreviation.

F. All single word journal titles in full (*e.g., Veliger, Ecology, Brain*).

G. The order of abbreviated components should be the same as the word order of the complete title (*i.e.*, *Proc.* and *Trans.* placed where they appear, not transposed as in some BIOLOGICAL ABSTRACTS listings).

H. A few well-known international journals in their preferred forms rather than WORLD LIST or USASI usage (*e.g.*, *Nature, Science, Evolution* NOT *Nature, Lond., Science, N.Y.; Evolution, Lancaster, Pa.*)

6. ***Reprints, page proofs, and charges.*** Authors may purchase reprints in lots of 100. Forms for placing reprint orders are sent with page proofs. Reprints normally will be delivered about 2 to 3 months after the issue date. Authors (or delegates for foreign authors) will receive page proofs of articles shortly before publication. They will be charged the current cost of printers' time for corrections to these (other than corrections of printers' or editors' errors). Other than these charges for authors' alterations, *The Biological Bulletin* does not have page charges.

Reference: *Biol. Bull.* **202:** 97–99. (April 2002)

Egg Energetics for the Facultative Planktotroph *Clypeaster rosaceus* (Echinodermata: Echinoidea), Revisited

BENJAMIN G. MINER*, JONATHAN D. COWART, AND LARRY R. McEDWARD†

Department of Zoology, University of Florida, Gainesville, FL 32611

The sand dollar Clypeaster rosaceus *has an unusual reproductive strategy known as facultative planktotrophy. The egg energy previously reported by Emlet (1) for* C. rosaceus *is low, and because it is used to estimate values of an important parameter in marine invertebrate life-history models* (s), *we remeasured the egg energy content. Our measurement of egg energy content was approximately 2-fold greater than Emlet's (0.11 ± 0.014 SD joules (J) egg^{-1}* vs. *0.047 ± 0.007 SD J egg^{-1}) with no difference in egg diameter (274 ± 4.38 SD μm* vs. *280 ± 7.67 SD μm). This result is unlikely to be due to temporal or spatial variation among populations of* C. rosaceus. *Given the improved technique used to measure egg energy content, an egg energy density (J ml^{-1}) more consistent with other observations, and the improved fit of egg size* vs. *egg energy regressions for echinoderm planktotrophs, we conclude that our estimate is more accurate. In addition, we detected small annual variation (10%) in egg energy content between females sampled during 2000 and 2001.*

Facultative planktotrophy is intermediate between the two common types of echinoid larval development: planktotrophy and lecithotrophy (1). Planktotrophic larvae develop from small, energy-poor eggs and require exogenous food to complete development and metamorphosis. In contrast, lecithotrophic larvae develop from large, energy-rich eggs and can complete development without feeding. Although rare, facultative planktotrophs such as *Clypeaster rosaceus* may represent an important transition in the evolution of marine invertebrate life-history strategies (2, 3).

Models of the evolution of larval strategies in marine invertebrates characterize reproductive strategies in terms of the level of egg provisioning (*s*) (4). These models evaluate the trade-off between fecundity and mortality as a function of *s*, and assume that selection acts on this character. It is therefore important to estimate values of *s* for numerous species to compare the natural distribution of *s* with model results. An informative method for calculating values of *s* requires comparing egg energy content against a reference species that is near the boundary between planktotrophy and lecithotrophy (5). *Clypeaster rosaceus* has a level of egg provisioning close to, though greater than, the minimum necessary for lecithotrophic development (1) and can therefore be used as a reference species to calculate values of *s*.

Emlet (1) reported the eggs of *C. rosaceus* to be 280 ± 7.67 SD μm in diameter and to contain 0.020 ± 0.003 SD joules of energy per egg (J egg^{-1}). This value of egg energy is low, relative to egg size, compared to other species of planktotrophic echinoderms—*C. rosaceus* has the lowest estimated egg energy density (1.79 J ml^{-1}) of all echinoid species for which there are data (minimum value = 2.41 J ml^{-1}; mean = 6.10 J ml^{-1}; maximum = 11.71 J ml^{-1}). Additionally, the egg of the echinoid *Encope michelini* is smaller than that of *C. rosaceus* (175 μm *vs.* 280 μm), but its energy content is greater (6) (0.046 J egg^{-1} *vs.* 0.020 J egg^{-1}). Yet *E. michelini* is an obligate planktotroph (7). Considering the importance of *C. rosaceus* in estimating values of *s* in marine invertebrate life-history models, it is important to verify the published estimate of egg energy (1).

The egg energy content we estimated for *C. rosaceus* ranged from 0.104 to 0.120 J egg^{-1} in 2000 and from 0.076 to 0.120 J egg^{-1} in 2001, with a mean for all eight females of 0.11 ± 0.014 SD J egg^{-1} (Table 1). This mean value (0.11 J egg^{-1}) is much greater than that previously reported (1) (0.020 ± 0.003 SD J egg^{-1}). However, it has been brought to our attention that improper units were published

---

Received 15 October 2001; accepted 4 February 2002.

* To whom correspondence should be addressed. E-mail: miner@zoo.ufl.edu

† Deceased.

in Emlet (1). The correct units are actually micrograms of carbon (R. B. Emlet, pers. comm.), not micrograms of organic matter as originally reported. Therefore, the actual egg energy measured by Emlet was 0.047 ± 0.007 SD J egg^{-1}. Despite this error, our egg energy measurement is still approximately 2-fold greater than the previous one, with no difference in egg size (274 ± 4.38 SD μm and 280 ± 7.67 SD μm). There are two possible explanations for this discrepancy: geographical and temporal differences in egg energy content among populations, or inaccurate measurements of egg energy content.

This study used adult *C. rosaceus* from a different population and different years than Emlet (1); the Florida Keys (east Caribbean) in 2000 and 2001, and Panama (west Caribbean) in 1983, respectively. Although we sampled different populations, no other studies comparing intraspecific variation in egg energy content report differences as great as the discrepancy between Emlet's measurements and ours (8–10). Additionally, equivalent (≥2-fold) interspecific variation in egg energy content is correlated with large increases in egg size (11–17). Furthermore, we detected only a small temporal difference in egg energy between 2000 and 2001 (0.110 ± 0.006 SD J egg^{-1} and 0.098 ± 0.016 SD J egg^{-1}).

We used improved methods, directly counting a small number of eggs for each replicate (exactly 20 eggs) and measuring egg energy content for 5 females in 2000 and 3 females in 2001. Also, our value of egg energy density for *C. rosaceus* (9.8 J ml^{-1}) is within the range of other planktotrophic species of echinoids, and improves McEdward and Morgan's (17) regression of egg size *vs.* egg energy (Fig. 1). We conclude that the value of 0.11 J egg^{-1} should be used to estimate parameters for future models, and for re-examining existing models (2, 3).

Table 1

Mean diameter, volume, and energy of eggs from five (2000) and three (2001) females of Clypeaster rosaceus.

Year	Female	Mean Egg Diameter (μm)	Mean Egg Volume (ml)	Mean Egg Energy (J)
2000	1	267.3	0.0100	0.104
	2	272.9	0.0107	0.108
	3	276.1	0.0110	0.107
	4	276.5	0.0110	0.110
	5	278.5	0.0113	0.120
2001	1	268.9	0.0102	0.120
	2	270.7	0.0104	0.099
	3	278.6	0.0113	0.076
	Mean	274 ± 4.38 SD	0.01 ± 0.0005 SD	0.11 ± 0.014 SD

Mean egg diameter for each female was calculated from 20 eggs, and egg volume was calculated from the female mean egg diameter. Mean egg energy content for each female was calculated from 5 replicate measurements.

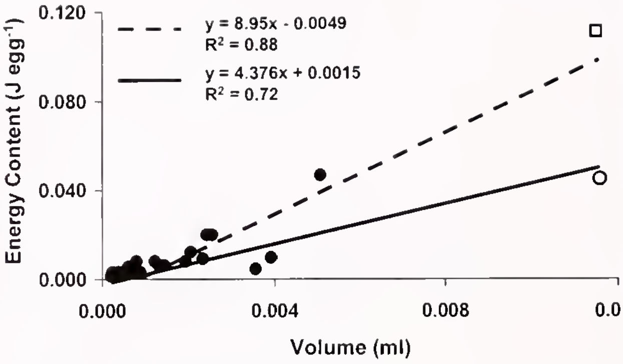

Figure 1. Linear regressions of egg size (volume) *vs.* egg energy content for planktotrophic echinoderms. The open circle represents Emlet's estimate of *Clypeaster rosaceus*, and the open square represents our estimate. Each regression was calculated with data from McEdward and Morgan (17) for 21 species of planktotrophic echinoderms (solid circles) and one of the *C. rosaceus* egg energy estimates. The solid line represents the regression with Emlet's estimate and the dotted line with our estimate.

Collections. Adult *Clypeaster rosaceus* were collected at a depth of 3–7 m during September 2000 and October 2001 at Long Key Channel, Florida. They were maintained in aquaria with recirculating seawater (18–20 °C).

Egg volume and biochemical measurements. Bioenergetic measurements were made on 13 October 2000 and 21 October 2001. Vigorous shaking of adults induced spawning. Eggs from 5 females in 2000 and 3 females in 2001 were collected in separate 100-ml glass beakers containing 0.45-μm Millipore-filtered seawater (MPFSW). After being rinsed three times with MPFSW, the eggs were fertilized (>98% fertilization), which reduces breakage during counting. The diameter (*d*) of 20 fertilized eggs from each female was measured with an ocular micrometer on a light microscope (magnification 20×). Egg volume was calculated using the formula (1/6) πd^3. Egg energy content was measured by the dichromate oxidation method of Parsons *et al.* (18) as modified by McEdward and Carson (9) with glucose as the standard (0–150 μg carbon). Total egg energy content was measured on five replicate batches of 20 eggs per female. Eggs were placed in separate acid-washed (0.3% acid dichromate) 13 × 100-mm glass test tubes, and almost all seawater was removed using a micropipette. Each replicate was incubated in concentrated (70%) phosphoric acid (1 ml, 15 min, 105 °C) to remove residual chloride and then oxidized with potassium dichromate (0.3%) in concentrated sulfuric acid (2 ml, 15 min, 105 °C). Samples were diluted (3.5 ml distilled water) and measured spectrophotometrically (440 nm, 1-cm path length). Energy content was calculated against the weight of glucose (μg) yielding equivalent reduction in dichromate oxidation and was reported as joules per egg (J egg^{-1}) using the conversion 1 μg C = 3.90×10^{-2} J (9).

Acknowledgments

We thank Richard Emlet, John Lawrence, John Pearse, Melissa Wilson, and two anonymous reviewers for comments that improved this manuscript. In addition, we thank Kevin McCarthy and the Keys Marine Laboratory staff for help with animal collection. Funding was provided by NSF grant OCE 9819593.

Literature Cited

1. **Emlet, R. B. 1986.** Facultative planktotrophy in the tropical echinoid *Clypeaster rosaceus* (Linnaeus) and a comparison with obligate

planktotrophy in *Clypeaster subdepressus* (Gray) (Clypeasteroida: Echinoidea). *J. Exp. Mar. Biol. Ecol.* **95:** 183–202.

2. **McEdward, L. R. 1997.** Reproductive strategies of marine benthic invertebrates revisited: facultative feeding by planktotrophic larvae. *Am. Nat.* **150:** 48–72.
3. **Levitan, D. R. 2000.** Optimal egg size in marine invertebrates: theory and phylogentic analysis of the critical relationship between egg size and development time in echinoids. *Am. Nat.* **156:** 175–192.
4. **McEdward, L. R. 2000.** Adaptive evolution of larvae and life cycles. *Cell Dev. Biol.* **11:** 403–409.
5. **McEdward, L. R., and D. A. Janies. 1997.** Relationships among development, ecology, and morphology in the evolution of echinoderm larvae and life cycles. *Biol. J. Linn. Soc.* **60:** 381–400.
6. **George, S. B., C. M. Young, and L. Fenaux. 1997.** Proximate composition of eggs and larvae of the sand dollar *Encope michelini* (Agassiz): the advantage of higher investment in planktotrophic eggs. *Invertebr. Reprod. Dev.* **32:** 11–19.
7. **Eckert, G. L. 1995.** A novel larval feeding strategy of the tropical sand dollar, *Encope michelini* (Agassiz): adaptation to food limitation and an evolutionary link between planktotrophy and lecithotrophy. *J. Exp. Mar. Biol. Ecol.* **187:** 103–128.
8. **Thompson, R. J. 1983.** The relationship between food ration and reproductive effort in the green sea urchin, *Strongylocentrotus droebachiensis*. *Oecologia* **56:** 50–57.
9. **McEdward, L. R., and S. F. Carson. 1987.** Variation in egg organic content and its relationship with egg size in the starfish *Solaster stimpsoni*. *Mar. Ecol. Prog. Ser.* **37:** 159–169.
10. **George, S. B., C. Cellario, and L. Fenaux. 1990.** Population differences in egg quality of *Arbacia lixula* (Echinodermata: Echinoidea): proximate composition of eggs and larval development. *J. Exp. Mar. Biol. Ecol.* **141:** 107–118.
11. **Strathmann, R. R., and K. Vedder. 1977.** Size and organic content of echinoderms and other invertebrates as related to developmental strategies and egg eating. *Mar. Biol.* **39:** 305–309.
12. **McEdward, L. R., and L. K. Coulter. 1987.** Egg volume and energetic content are not correlated among sibling offspring of starfish: implications for life-history theory. *Evolution* **41:** 914–917.
13. **McEdward, L. R., and F. S. Chia. 1991.** Size and energy content of eggs from echinoderms with pelagic lecithotrophic development. *J. Exp. Mar. Biol. Ecol.* **147:** 95–102.
14. **Bridges, T. S. 1993.** Reproductive investment in four developmental morphs of *Streblospio* (Polychaeta: Spionidae). *Biol. Bull.* **184:** 144–152.
15. **Jaeckle, W. B. 1995.** Variation in the size, energy content, and biochemical composition of invertebrate eggs: correlates to the mode of larval development. Pp. 49–77 in *Ecology of Marine Invertebrate Larvae*, L. R. McEdward, ed. CRC Press, Boca Raton, FL.
16. **Bridges, T. S., and S. Heppell. 1996.** Fitness consequences of maternal effects in *Streblospio benedicti* (Annelida: Polychaeta). *Am. Zool.* **36:** 132–146.
17. **McEdward, L. R., and K. H. Morgan. 2001.** Interspecific relationships between egg size and the level of parental investment per offspring in echinoderms. *Biol. Bull.* **200:** 33–50.
18. **Parsons, T. R., Y. Maita, and C. M. Lalli. 1984.** *A Manual of Chemical and Biological Methods for Seawater Analysis.* Pergamon Press, New York.

Reference: *Biol. Bull.* **202:** 100–103. (April 2002)

Twin Meiosis 2 Spindles Form After Suppression of Polar Body 1 Formation in Oocytes of the Marine Shrimp *Sicyonia ingentis*

PHILIP L. HERTZLER

Department of Biology, Central Michigan University, 100 W. Preston Rd.,
Mt. Pleasant, Michigan 48859

The production of triploid shellfish has proven beneficial to the aquaculture industry since triploid organisms have reduced gonadal development, resulting in improved product quality and growth characteristics (1). Triploidization has been achieved for several molluscan species (2, 3, 4, 5, 6). In contrast, little is known about the effects of ploidy manipulation in decapod crustaceans. Triploidy has been induced in Penaeus chinensis *and other penaeid shrimp using heat shock or cold shock, cytochalasin B, and 6-dimethylaminopurine (7, 8, 9, 10, 11). Triploidy was induced by suppression of polar body 2 in the shrimp* Litopenaeus vannemei *using cold shock, but resulted in poor survival for unknown reasons (11). One difficulty of ploidy manipulation in* L. vannemei *is the rapid sequence of meiotic events, since the polar bodies are produced at 8 and 15 min post-spawning at 28°C (12). In addition, the actual behavior of chromosomes and spindles was not addressed. Here I report that in the penaeoidean shrimp* Sicyonia ingentis, *inhibition of polar body 2 resulted in embryos that failed to undergo embryonic cleavage, while inhibition of polar body 1 produced oocytes with "twin" meiosis 2 spindles followed by the simultaneous formation of two "second" polar bodies.*

I performed a dose response study to determine the minimum level of cytochalasin D (CD) needed to inhibit cytokinesis in zygotes of *Sicyonia ingentis*. Embryonic cleavage was sensitive to CD concentrations of 0.1 *μM* or greater, and could be completely inhibited at 0.5–0.8 *μM* (Fig. 1). Inhibition of polar body formation required at least 1 *μM* CD, but percent inhibition of polar bodies was difficult to judge, since they could only be seen if present along the edge of the egg. One hundred percent suppression of polar bodies did not occur, so a qualitative judgement of inhibition was made if few were observed relative to controls. In later experiments, qualitative evidence of first polar body (PB1) suppression was provided if eggs were observed with two second polar bodies (PB2). No inhibition of cleavage or polar body formation was seen in controls that received no treatment or treatment with the carrier dimethyl sulfoxide (DMSO) only.

Oocytes of *S. ingentis* are spawned at metaphase of meiosis 1. At 21°C, PB1 forms at 30–35 min post-spawning (PS), the hatching envelope forms at 40–45 min PS, PB2 formation occurs at 50–55 min PS, and first cleavage occurs about 90 min PS (13, 14). Thus, after meiotic maturation, PB1 lies outside of the hatching envelope while PB2 lies within it (see Fig. 2E). PB2 formation was inhibited by treatment of oocytes with 1 *μM* CD from 40–55 min PS, after formation of PB1. In No Treatment and DMSO controls, eggs extruded both polar bodies, formed hatching envelopes, and went through normal cleavage (Fig. 2A). In the 40–55 min CD treatment, PB1 formed but not PB2, hatching envelopes elevated about 15 min later than the control groups, and cleavage was completely inhibited (Fig. 2B). Cleared regions of cytoplasm were observed within these eggs. When control-group embryos were stained using Sytox green, nuclei were present in the blastomeres (Fig. 2C). In the CD-treatment group, the uncleaved embryo contained many nuclei (Fig. 2D), indicating that the CD treatment from 40–55 min PS did not prevent microtubule-based chromosome segregation. Based on the data from two trials, a comparison of the No Treatment controls with the DMSO controls during PB2 suppression showed no significant difference in percent cleavage, indicating that the

---

Received 8 November 2001; accepted 5 February 2002.

E-mail: Philip.L.Hertzler@cmich.edu

Abbreviations: CD, cytochalasin D; DMSO, dimethyl sulfoxide; PB1, polar body 1; PB2, polar body 2; PS, post-spawning.

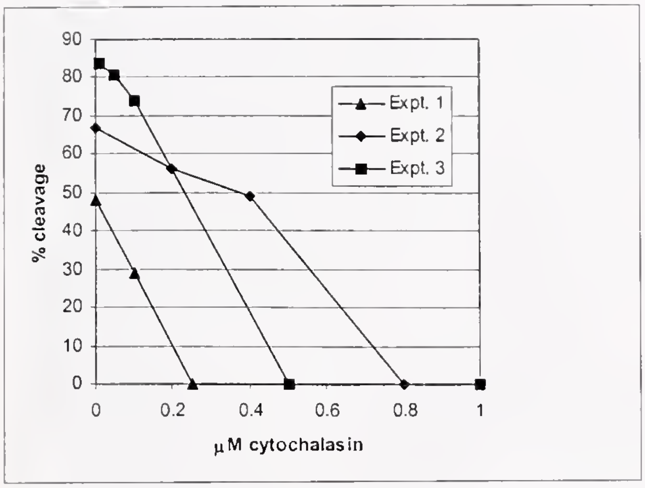

Figure 1. Dose response of inhibition of cleavage to treatment with cytochalasin D (CD). Gravid specimens of *Sicyonia ingentis* were collected by otter trawl one mile south of Palos Verdes, California, from the R/V *Vantuna*, operated by Occidental College. Animals were spawned as described previously (16). Cytochalasin D was obtained from Sigma (Cat. #C8273) and dissolved in dimethyl sulfoxide (DMSO) to make a stock solution of 1 m*M*. In three separate experiments, eggs were spawned into artificial seawater (ASW) then transferred to ASW containing 0–1 μ*M* CD at 15 min post-spawning (PS). In each group, 300 eggs were scored for % cleavage. Cleavage was completely inhibited with 0.5–0.8 μ*M* CD, whereas evidence of polar body suppression required at least 1 μ*M* CD.

DMSO had no effect, whereas CD treatment completely inhibited embryonic cleavage (Table 1).

PB1 formation was inhibited by treating oocytes with 1 μ*M* CD from 15–35 min PS, then washing out the CD with artificial seawater. In No Treatment and DMSO controls, polar bodies formed normally, with PB1 outside the hatching envelope and PB2 inside of it (Fig. 2E). In the 15–35 min CD treatment, two "second" polar bodies formed simultaneously in some eggs, both positioned inside the hatching envelope (Fig. 2F). Oocytes treated from 15–35 min with CD and stained with anti-tubulin antibodies revealed that "twin" meiosis 2 spindles were present in the cortex (Fig. 2G). Two maternal chromosome sets were expelled in the two polar bodies, while two maternal chromosome sets were retained in the egg and decondensed into two female pronuclei (Fig. 2H). Based on the data from two experiments, percent cleavage in DMSO controls showed no significant difference from No Treatment controls, and the CD treatment from 15–35 min showed no significant difference from No Treatment controls (Table 1). Normal cleavage divisions continued in the CD-treatment group.

Each method of polar body suppression should theoretically produce triploid zygotes. In *Sicyonia*, normal embryonic cleavage follows from suppression of PB1 but not PB2. The responses to polar body suppression in marine invertebrates have been best studied in oysters (2, 3, 6). In *Crassostrea gigas,* inhibition of PB1 with cytochalasin B resulted in a number of possible chromosome segregation patterns, including united bipolar, tripolar, and separated bipolar (3). Tripolar spindles have been demonstrated in such treatments by anti-tubulin staining (4). The "twin" meiosis 2 spindles described here correspond to the "separated bipolar" spindle pattern inferred from observations of chromosome staining in *C. gigas*. This report describes the first direct observation of the "separated bipolar" pattern by tubulin immunofluorescence localization. Tripolar spindles or other unusual patterns were not observed as a result of ploidy manipulation in *S. ingentis,* so the occurrence of aneuploidy following PB1 suppression may be less of a problem than it is for oysters (2, 3). However, the studies in oysters used cytochalasin B instead of cytochalasin D, so they may not be directly comparable. The separated bipolar meiosis 2 spindles in PB1-blocked oocytes appear to be of the same size and orientation as normal meiosis 2 spindles, and they progress through the cell cycle at the same time. Therefore, following meiosis 1, both centrosomes retain the ability to duplicate and form meiosis 2 spindle poles.

In response to PB1 suppression, only one "second" polar body forms in *C. gigas* (2), but in *S. ingentis* two polar bodies formed simultaneously. The simultaneous formation of two polar bodies occurs naturally in the androgenetic clam *Corbicula leana* following meiosis 1, which eliminates all maternal chromosomes; development is then directed by the incorporated diploid sperm nucleus (15). A specialized microtubular structure causes this process in *C. leana*. In contrast, the two polar bodies formed after PB1 suppression in *S. ingentis* apparently utilize the same spindle mechanics as does normal meiosis 2. Maternal centro-

Table 1

Effect of cytochalasin D (CD) treatment during polar body suppression on first cleavage

Experiment (Treatment Time)	% Cleavage No Treatment (NT)	DMSO Carrier	1 μ*M* CD
Polar body 2 suppression (40–55 min):			
Trial 1	45	39	0
Trial 2	84	73	0
Mean, *n*, SD	64, 6, 21.9	59.8, 5, 20.0	
t test*		NT *vs.* DMSO	
P		0.731	
Polar body 1 suppression (15–35 min):			
Trial 1	89	92	91 (300)
Trial 2	85	83	71 (300)
Mean, *n*, SD	87, 6, 3.2	87.5, 6, 5.8	81, 6, 11.6
t test*		NT *vs.* DMSO	NT *vs.* CD
P		0.905	0.259

* Independent *t* test performed on pooled data.

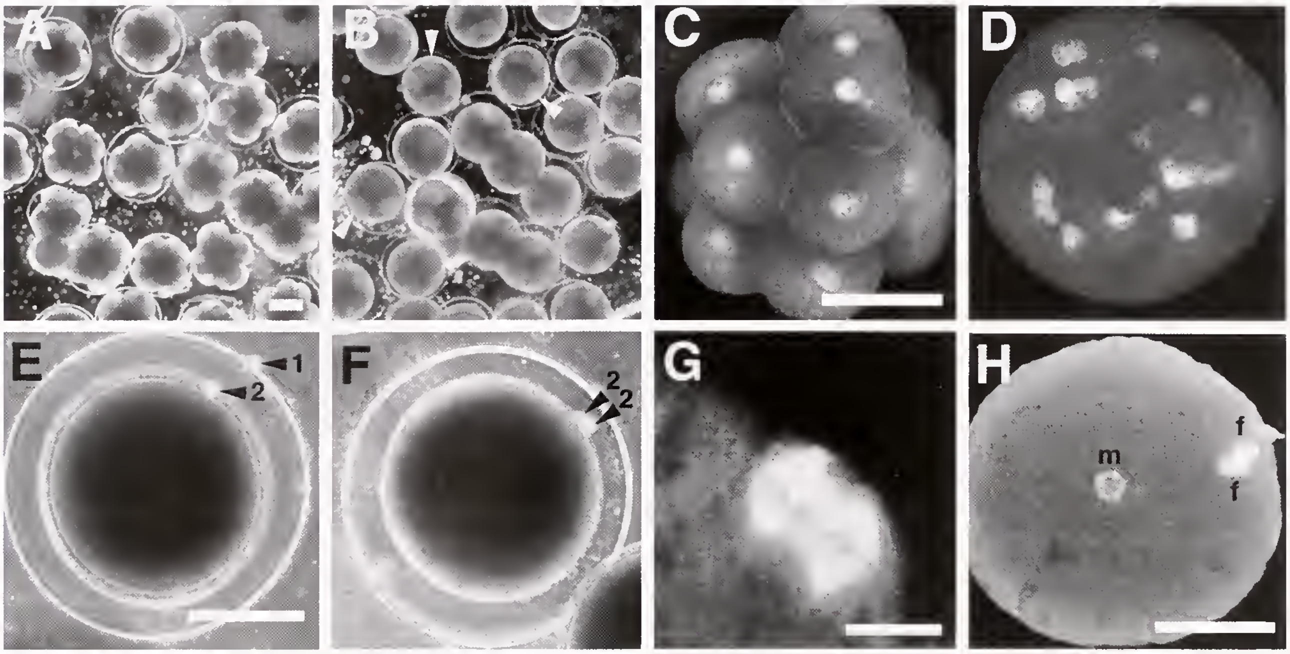

Figure 2. Effects of cytochalasin D (CD) treatments. For inhibition of polar body 2 (PB2) formation, eggs were transferred at 40 min post-spawning (PS) to 1 μM (0.5 mg/l) CD in artificial seawater containing 50 μM 3-amino-1,2,4-triazole (ATA-ASW), to facilitate removal of the hatching envelope for staining (17). At 55 min PS, eggs were washed 4 times with 0.1% DMSO in ATA-ASW. For suppression of polar body 1 (PB1) formation, eggs were transferred at 15 min PS to 1 μM CD in ATA-ASW. At 35 min PS, CD-treated eggs were washed 4 times with 0.1% DMSO in ATA-ASW. Control groups (0.1% DMSO carrier control and No Treatment control) were subjected to identical physical manipulations as CD-treated eggs. CD-treated eggs and control groups were fixed with 4% paraformaldehyde in ASW and examined by phase-contrast microscopy. Other samples were fixed in 90% methanol/50 mM EGTA, pH 8.0, and stained with β-tubulin monoclonal antibody E7 as described previously (14). Nuclei and chromosomes were stained with Sytox green (Molecular Probes, Inc.) for confocal microscopy. (A) DMSO control from 40–55 min PS, dark-field image of embryos at the 16-cell stage, 3-h PS. (B) CD treatment from 40–55 min PS, dark-field image of embryos at 3-h PS. Arrows indicate cleared regions of cytoplasm. (C) DMSO control from 40–55 min PS, embryo at 3-h PS, stained with Sytox green. The image is a composite of optical slices through one-half of the embryo. (D) CD treatment from 40–55 min PS, embryo at 3-h PS, stained with Sytox green. The image is a composite of optical slices through the entire embryo. (E) Phase-contrast image of DMSO control from 15–40 min PS, egg at 60 min PS. Note the positions of PB1 and PB2 (arrowheads) relative to the hatching envelope. (F) Phase-contrast image of CD treatment from 15–40 min PS, egg at 60 min PS. Two "second" polar bodies (arrowheads) have formed beneath the hatching envelope. (G) Confocal fluorescence image of "twin" meiosis 2 spindles in PB1-suppressed egg, revealed by anti-β-tubulin immunofluorescence. (H) Composite of optical sections of PB1-suppressed egg, stained with Sytox green. A single male pronucleus (m) and two female pronuclei (f) are present. Scale bars = 100 μm in A–F and H, and 20 μm in G.

some function, pronuclear formation, pronuclear migration, and embryonic mitoses and cytokinesis seem to occur normally following PB1 suppression. Further work is needed to determine if these embryos develop to the nauplius larval stage and if they are indeed triploid. The diploid number of *S. ingentis* is known to be 64 (10), so ploidy analysis could be performed to answer this question.

Why does PB1 suppression in *S. ingentis* allow embryonic cleavage while PB2 suppression does not? The time of exposure to CD was less for PB2 suppression than for PB1 suppression, and the number of washes was the same, yet cleavage was blocked. The difference may be due to the presence of the hatching envelope during the treatment time for PB2 suppression. The hatching envelope formed more slowly in CD-treated eggs, suggesting that the vesicle secretion needed for this process requires microfilaments. Perhaps the newly formed hatching envelope also retards the loss of CD during the washing steps, creating a higher concentration of CD within the microenvironment of the perivitelline space and thereby inhibiting embryonic cleavage.

The results show that paired meiosis 2 spindles form following PB1 suppression in penaeoidean shrimp, and normal meiotic spindle function follows, so that triploid induction may be possible by this method. Polar body extrusion occurs rapidly in tropical shrimp species; for example, in *L.*

vannamei, the polar bodies form at 8 and 15 min PS. Triploidy induction may be more feasible in cold-water penaeoidean species such as *S. ingentis,* where the events of meiotic maturation occur more slowly (at 35 and 45 min), allowing time for CD treatment and wash steps. The technique may also be possible in warm-water species if performed at the minimum temperature for successful development.

Acknowledgments

I am grateful to Dr. Gary Martin, Occidental College, for his generosity in sharing laboratory space and time, to the crew of the R/V *Vantuna* for assistance in animal collection, and to Jhonatan Sepulveda Villet and Dan Kiernan, Central Michigan University, for technical assistance. The β-tubulin monoclonal antibody E7 developed by Michael Klymkowsky was obtained from the Developmental Studies Hybridoma Bank developed under the auspices of the NICHD and maintained by The University of Iowa, Department of Biological Sciences, Iowa City, IA 52242. Thanks to Felix Famoye, Dept. of Mathematics, Central Michigan University, for help with statistical analysis and to two anonymous reviewers for suggestions on improving the manuscript. This work was supported by a State of Michigan/Central Michigan University Research Excellence Funds award and funds from the Department of Biology and the College of Science and Technology at Central Michigan University.

Literature Cited

1. **Allen, S. K., S. L. Downing, and K. K. Chew. 1989.** *Hatchery Manual for Producing Triploid Oysters.* Washington Sea Grant Program, University of Washington Press, Seattle, WA.
2. **Guo, X., K. Cooper, W. K. Hershberger, and K. K. Chew. 1992a.** Genetic consequences of blocking polar body I with cytochalasin B in fertilized eggs of the Pacific oyster, *Crassostrea gigas*: I. Ploidy of resultant embryos. *Biol. Bull.* **183:** 381–386.
3. **Guo, X., W. K. Hershberger, K. Cooper, and K. K. Chew. 1992b.** Genetic consequences of blocking polar body I with cytochalasin B in fertilized eggs of the Pacific oyster, *Crassostrea gigas*: II. Segregation of chromosomes. *Biol. Bull.* **183:** 387–393.
4. **Longo, F. J., L. Mathews, and D. Hedgecock. 1993.** Morphogenesis of maternal and paternal genomes in fertilized oyster eggs (*Crassostrea gigas*): effects of cytochalasin B at different periods during meiotic maturation. *Biol. Bull.* **185:** 197–214.
5. **Que, H., X. Guo, F. Zhang, and S. K. Allen, Jr. 1997.** Chromosome segregation in fertilized eggs from triploid Pacific oysters, *Crassostrea gigas* (Thunberg), following inhibition of polar body I. *Biol. Bull.* **193:** 14–19.
6. **Gerard, A., C. Ledu, P. Phelipot, and Y. Naciri-Graven. 1999.** The induction of MI and MII triploids in the Pacific oyster *Crassostrea gigas* with 6-DMAP or CB. *Aquaculture* **174:** 229–242.
7. **Xiang, J., L. Zhou, R. Liu, J. Zhu, F. Li, and X. Liu. 1992.** Induction of the tetraploids of the Chinese shrimp, *Penaeus chinensis.* Pp. 841–846 in *Proceedings of the Asia Pacific Conference on Agricultural Biotechnology.* Beijing, China, 20–24 Aug. 1992. China Science and Technology Press, Beijing.
8. **Dai, J., Z. Bao, Q. Zhang, and J. Lin. 1993.** An observation of gynogenesis induced by ^{49}Co gamma rays in Chinese prawn *Penaeus chinensis. J. Ocean Univ. Qingdao* **23:** 151–155.
9. **Bao, Z., Q. Zhang, H. Wang, and J. Dai. 1994.** Cytochalasin B induced triploidy in *Penaeus chinensis. Acta Oceanologica Sinica* **13:** 261–267.
10. **Zhang, X., L. Zhou, and J. Xiang. 2001.** Studies on the chromosome of marine shrimps with special reference to different techniques. P. 712 in *Abstracts of the Annual International Meeting of the World Aquaculture Society,* Lake Buena Vista, FL.
11. **Fast, A. W., and J. Wyban. 2001.** Polyploidy in shrimp: advanced technology for improved performance, genetic and environmental security. *Global Aquacult. Advocate* **4:** 16–17.
12. **Dumas, S., and R. Ramos. 1999.** Triploidy induction in the Pacific white shrimp *Litopenaeus vannemei* (Boone). *Aquac. Res.* **30:** 621–624.
13. **Lindsay, L. L., P. L. Hertzler, and W. H. Clark, Jr. 1992.** Extracellular Mg^{2+} induces an intracellular Ca^{2+} wave during oocyte activation in the marine shrimp *Sicyonia ingentis. Dev. Biol.* **152:** 94–102.
14. **Hertzler, P. L., and W. H. Clark, Jr. 1993.** The late events of fertilisation in the penaeoidean shrimp *Sicyonia ingentis. Zygote* **1:** 287–296.
15. **Komaru, A., K. Ookubo, and M. Kiyomoto. 2000.** All meiotic chromosomes and both centrosomes at spindle pole in the zygotes discarded as two polar bodies in clam *Corbicula leana*: unusual polar body formation observed by antitubulin immunofluorescence. *Dev. Genes Evol.* **210:** 263–269.
16. **Pillai, M. C., F. J. Griffin, and W. H. Clark, Jr. 1988.** Induced spawning of the decapod crustacean *Sicyonia ingentis. Biol. Bull.* **174:** 181–185.
17. **Lynn, J. W., P. S. Glas, J. D. Green, P. L. Hertzler, and W. H. Clark, Jr. 1992.** Manipulations of shrimp embryos: a viable technique for the removal of the hatching envelope. *J. World Aquacult. Soc.* **24:** 1–5.

Reference: *Biol. Bull.* **202:** 104–107. (April 2002)

Evolution of Cannabinoid Receptors in Vertebrates: Identification of a CB_2 Gene in the Puffer Fish *Fugu rubripes*

MAURICE R. ELPHICK

School of Biological Sciences, Queen Mary, University of London, London E1 4NS, UK

Δ^9-tetrahydrocannabinol, the psychoactive ingredient of cannabis, exerts effects in humans by binding to the G-protein-coupled cannabinoid receptors CB_1 and CB_2, which are expressed in the nervous and immune systems, respectively. Genes encoding CB_1 receptors have also been discovered in non-mammalian vertebrates, including the puffer fish Fugu rubripes. *Here the identification of a* Fugu *gene that encodes an ortholog of mammalian CB_2 receptors is reported. This is the first CB_2 gene to be identified in a non-mammalian vertebrate, and it indicates that the gene duplication event that gave rise to CB_1 and CB_2 receptors occurred before the divergence of teleosts and tetrapods. Moreover, non-mammalian vertebrate species can now be considered as potential model systems in which the physiological roles of the CB_2 receptor can be investigated.*

Following the discovery of cannabinoid receptors in mammals (1, 2, 3), endogenous ligands for these receptors ("endocannabinoids") have also been identified; these ligands include arachidonylethanolamide ("anandamide") and 2-arachidonylglycerol (2-AG) (4, 5, 6). Endocannabinoids mediate retrograde signaling at synapses in the brain by diffusing from postsynaptic sites of synthesis to act on presynaptic CB_1 receptors, which results in an inhibition of "classical" neurotransmitter release (7, 8, 9, 10, 11, 12). The physiological roles of CB_2 are less well understood than those of CB_1, although analysis of CB_2-knockout mice indicates that the CB_2 receptor mediates immunomodulatory actions of cannabinoids in mammals (13). The emergence of a cannabinoid signaling system has aroused interest in the physiological roles of endocannabinoids and in the potential of cannabinoids to be therapeutic agents in humans (14).

With the discovery of endocannabinoid signaling mechanisms in mammals, the evolution of cannabinoid receptors has become of interest because non-mammalian species provide important models for analysis of gene function. Orthologs of mammalian CB_1 and CB_2 genes do not, however, appear to be present in protostomian invertebrate species, such as *Drosophila melanogaster* and *Caenorhabditis elegans,* for which complete genome sequences are known (see ref. 7). Thus these cannabinoid receptor genes may have evolved in the deuterostomian, chordate, or vertebrate clades of the animal kingdom. To date, orthologs of mammalian CB_1 or CB_2 receptors have also not been identified in any invertebrate deuterostomes (*e.g.*, cephalochordates, urochordates, hemichordates, and echinoderms); but complete genome sequences have not yet been obtained for species representative of these phyla. CB_1-type genes have, however, been identified in several vertebrate species, including a bird (15), an amphibian (16), and the puffer fish *Fugu rubripes,* which has two CB_1-like genes (FCB_{1A}, FCB_{1B}) (17). These discoveries indicate that the CB_1-type cannabinoid receptor can be traced back at least as far as the common ancestor of teleosts (bony fish) and tetrapod vertebrates (amphibians, reptiles, birds, and mammals). In contrast, CB_2-type receptor genes have so far been identified only in mammalian species. Yamaguchi *et al.* (17) attempted to clone a CB_2-type gene in *Fugu rubripes,* using a probe for human CB_2 (HCB2), but reported that "hybridization with HCB2 failed to identify a *Fugu* homologue." With the recent announcement that 99% of the genome of *Fugu rubripes* has been sequenced (*Nature,* 414, 1 November 2001, page 8; see also ref. 18), it has become possible to search again for a CB_2-type gene in this species using techniques for genome sequence analysis.

To search the *Fugu* genome for a CB_2 gene, the Basic Local Alignment Search Tool (BLAST; 19) was employed,

Received 21 December 2001; accepted 28 February 2002.

To whom correspondence should be addressed: E-mail: M.R.Elphick@qmul.ac.uk

```
                                                                                             :
   Fugu CB2 ------------------------------------------------------------------------MYKVFLCRVS  10
  Human CB2 ---------------------------------------------------------------------------MEECWVT   7
  Mouse CB2 ---------------------------------------------------------------------------MEGCRET   7
  Fugu CB1B MKLALHRIAGATMAALTTEVQYLGSNDASYEDPQADAALMKSRFNFEKPYSAS--SSLHRLIPGNKELIYSGLSTILPTNAS  80
  Fugu CB1A MKSVLDGVADTTFRTITSGLQYLGSNDANYDDPLNDAAFKTGFSLQK-PLSAFRSNSFPNKVPADEELIFFGIPF-FPTNST  80
Taricha CB1 MKSILDGLADTTFRTITTDLLYMGSNDVQYEDTKGEMASKLGYFPQKLPLSSFRRDHSPDKMTIGDDNLLSFYPL-DQFNVT  81
Z-finch CB1 MKSILDGLADTTFRTITTDLLYVGSNDIQYEDMKGDMASKLGYYPQKFPLSSFRGDPFQEKMTGGDDSLLSIIPS-EQVNIT  81
  Human CB1 MKSILDGLADTTFRTITTDLLYVGSNDIQYEDIKGDMASKLGYFPQKFPLTSFRGSPFQEKMTAGDNPQL--VPA-DQVNIT  79
    Rat CB1 MKSILDGLADTTFRTITTDLLYVGSNDIQYEDIKGDMASKLGYFPQKFPLTSFRGSPFQEKMTAGDNSPL--VPAGDTTNIT  80
  Mouse CB1 MKSILDGLADTTFRTITTDLLYVGSNDIQYEDIKGDMASKLGYFPQKFPLTSFRGSPFQEKMTAGDNSPL--VPAGDTTNIT  80
    Cat CB1 MKSILDGLADTTFRTITTDLLYVGSNDIQYEDIKGDMASKLGYFPQKFPLTSFRGSPFQEKMTAGDNSQL--VPA-DQVNIT  79

                             .     :     :*:*   ::  :  :.   * :: :**  ** :*  :  ** :*** **.***
   Fugu CB2 AKMCSFTDN-------RSCKN--LG---CFMVLVEAEKKAIGTICLLAGPITLMENAIVLGVIASTATLRKRPSYLFIGSLA  80
  Human CB2 EIANGSKDG-------LDSNP--MK---DYMILSGPQKTAVAVLCTLLGLLSALENVAVLYLILSSHQLRRKPSYLFIGSLA  77
  Mouse CB2 EVTNGSNGG-------LEFNP--MK---EYMILSSGQQIAVAVLCTLMGLLSALENMAVLYIILSSRRLRRKPSYLFISSLA  77
  Fugu CB1B DFPLSNGSG-----EATQCGEDIVDNMECFMILTPAQQLVIVILAITLGTFTVLENFVVLCVILHSHTLRSRPSYHFIGSLA 157
  Fugu CB1A DLFGNRNTTRDEN--SIQCGENFMD-MECFMILTPSQQLAVAVLSLTLGTFTVLENLVVLCVIFQSRTLRCRPSYHFIGSLA 159
Taricha CB1 EFFNRSVSTFKENDDNLKCGENFMD-MECFMILTASQQLIIAVLSLTLGTFTVLENFLVLCVILQSRTLRCRPSYHFIGSLA 162
Z-finch CB1 EFYNKSLSTFKDNEENIQCGENFMD-MECFMILNPSQQLAIAVLSLTLGTFTVLENLLVLCVILHSRSLRCRPSYHFIGSLA 162
  Human CB1 EFYNKSLSSFKENEENIQCGENFMD-IECFMVLNPSQQLAIAVLSLTLGTFTVLENLLVLCVILHSRSLRCRPSYHFIGSLA 160
    Rat CB1 EFYNKSLSSFKENEENIQCGENFMD-MECFMILNPSQQLAIAVLSLTLGTFTVLENLLVLCVILHSRSLRCRPSYHFIGSLA 161
  Mouse CB1 EFYNKSLSSFKENEDNIQCGENFMD-MECFMILNPSQQLAIAVLSLTLGTFTVLENLLVLCVILHSRSLRCRPSYHFIGSLA 161
    Cat CB1 EFYNKSLSSYKENEENIQCGENFMD-MECFMILNPSQQLAIAVLSLTLGTFTVLENLLVLCVILHSRSLRCRPSYHFIGSLA 160

             **.:.* .*. .*: **:::  **   :*:*:..*  :*::*****:***:***:.:  . :*: ::*: :.:::: ::* 
   Fugu CB2 LADVFASCFFTTSFLDFHLFRRSDSATAYLFKLGGVTMAFSSSVGSLLLTALDRYLCIYQASSYKVLLTRRRALLSLLILWL 162
  Human CB2 GADFLASVVFACSFVNFHVFHGVDSKAVFLLKIGSVTMTFTASVGSLLLTAIDRYLCLRYPPSYKALLTRGRGLVTLGIMWV 159
  Mouse CB2 GADFLASVIFACNFVIFHVFHGVDSNAIFLLKIGSVTMTFTASVGSLLLTAVDRYLCLCYPPTYKALVTRGRALVALCVMWV 159
  Fugu CB1B VADLIGSIIFVYSFLDFHVLHRKDSPSIFLFKLAGVIASFTASVGSLFLTAIDRYVSIHRPMAYKRIITKTKAVIAFSVMWA 239
  Fugu CB1A VADLLGSVIFVYSFLDFHVFHKKDSPNVFLFKLGGVTASFTASVGSLFLTAIDRYISIHRPLAYRRIVTRTKAVIAFCMMWT 241
Taricha CB1 VADLLGSVIFVYSFLDFHVFHRKDSSNVFLFKLGGVTASFTASVGSLFLTAIDRYISIHRPLAYKRIVTRTKAVIAFCVMWT 244
Z-finch CB1 VADLLGSVIFVYSFVDFHVFHRKDSPNVFLFKLGGVTASFTASVGSLFLTAIDRYISIHRPLAYKRIVTRPKAVVAFCVMWT 244
  Human CB1 VADLLGSVIFVYSFIDFHVFHRKDSRNVFLFKLGGVTASFTASVGSLFLTAIDRYISIHRPLAYKRIVTRPKAVVAFCLMWT 242
    Rat CB1 VADLLGSVIFVYSFVDFHVFHRKDSPNVFLFKLGGVTASFTASVGSLFLTAIDRYISIHRPLAYKRIVTRPKAVVAFCLMWT 243
  Mouse CB1 VADLLGSVIFVYSFVDFHVFHRKDSPNVFLFKLGGVTASFTASVGSLFLTAIDRYISIHRPLAYKRIVTRPKAVVAFCLMWT 243
    Cat CB1 VADLLGSVIFVYSFVDFHVFHRKDSPNVFLFKLGGVTASFTASVGSLFLTAIDRYISIHRPLAYKKIVTRPKAVVAFCLMWT 242

             :  .: ***:** *       **::** *   **  *  .  .*.  *: :*  :***:* * . :
   Fugu CB2 TTIFISFLPLMGWRCPTDLNPACSELFPYINPDYLACWTSFILVLLALILGAYALILWKAHRHEASMTS---------FQGS 235
  Human CB2 LSALVSYLPLMGWTCCPRP---CSELFPLIPNDYLLSWLLFIAFLFSGIIYTYGHVLWKAHQHVASLSG---------HQDR 229
  Mouse CB2 LSALISYLPLMGWTCCPSP---CSELFPLIPNDYLLGWLLFIAILFSGIIYTYGYVLWKAHRHVATLAE---------HQDR 229
  Fugu CB1B ISIEFSLLPLLGWNCKRLHS-VCSDIFPLIDEKYLMFWIGMTTVLLLFIIYAYMFILWKSHHHAVRMLSRSSQRSIIVYTSE 320
  Fugu CB1A ISIIIAVLPLLGWNCKRLNS-VCSDIFPLIDENYLMFWIGVTSVLVLFIIYAYIYILWKAHHHAVRMLSRTSQKSLVVYSAE 322
Taricha CB1 IAIIIAVLPLLGWNCKKLKS-VCSDIFPLIDENYLMFWIGVTSILLLFIVYAYVYILWKAHSHAVRMLQRGTQKSIIIHTSE 325
Z-finch CB1 IAIVIAVLPLLGWNCKKLNS-VCSDIFPLIDETYLMFWIGVTSILLLFIVYAYMYILWKAHSHAVRMLQRGTQKSIIIQSTE 325
  Human CB1 IAIVIAVLPLLGWNCEKLQS-VCSDIFPHIDETYLMFWIGVTSVLLLFIVYAYMYILWKAHSHAVRMIQRGTQKSIIIHTSE 323
    Rat CB1 IAIVIAVLPLLGWNCKKLQS-VCSDIFPLIDETYLMFWIGVTSVLLLFIVYAYMYILWKAHSHAVRMIQRGTQKSIIIHTSE 324
  Mouse CB1 IAIVIAVLPLLGWNCKKLQS-VCSDIFPLIDETYLMFWIGVTSVLLLFIVYAYMYILWKAHSHAVRMIQRGTQKSIIIHTSE 324
    Cat CB1 IAIVIAVLPLLGWNCKKLQS-VCSDIFPLIDETYLMFWIGVTSVLLLFIVYAYMYILWKAHIHAVRMIQRGTQKSIIIHTSE 323

                      : *:*:***:*: *:*  *: ** * *::*  .:    :    :  ***** ***::* :**::**:*. ::
   Fugu CB2 ----VRTGHARMRMDIRLARTFGLILLILVGCWLPALSFMLADV-FRQLTPAQRKAFAFCSTLCLVNSAVNPLLYALRCREL 312
  Human CB2 ----QVPGMARMRLDVRLAKTLGLVLAVLLICWFPVLALMAHSL-ATTLSDQVKKAFAFCSMLCLINSMVNPVIYALRSGEI 306
  Mouse CB2 ----QVPGIARMRLDVRLAKTLGLVLAVLLICWFPALALMGHSL-VTTLSDQVKEAFAFCSMLCLVNSMVNPIIYALRSGEI 306
  Fugu CB1B GTKVQTVRPEQARMDLRLAKTLVLILVALIICWGPLLAIMVYDL-FGRVNDFIKTVFAFCSMLCLLNSTINPVIYAMRSKDL 401
  Fugu CB1A GTKVQTTRPEQTRMDIRLAKTLVLILAVLVICWGPLLAIMVYDL-FWKMDDNIKTVFAFCSMLCLLNSTVNPIIYALRSRDL 403
Taricha CB1 DGKVQITRPEQTRMDIRLAKTLVLILVVLIICWGPLLAIMVYDV-FGKMNNPIKTVFAFCSMLCLMDSTVNPIIYALRSQDL 406
Z-finch CB1 DGKVQITRPDQTRMDIRLAKTLVLILVVLIICWGPLLAIMVYDV-FGKMNKLIKTIFAFCSMLCLLNSTVNPIIYALRSKDL 406
  Human CB1 DGKVQVTRPDQARMDIRLAKTLVLILVVLIICWGPLLAIMVYDV-FGKMNKLIKTVFAFCSMLCLLNSTVNPIIYALRSKDL 404
    Rat CB1 DGKVQVTRPDQARMDIRLAKTLVLILVVLIICWGPLLAIMVYDV-FGKMNKLIKTVFAFCSMLCLLNSTVNPIIYALRSKDL 405
  Mouse CB1 DGKVQVTRPDQARMDIRLAKTLVLILVVLIICWGPLLAIMVYDV-FGKMNKLIKTVFAFCSMLCLLNSTVNPIIYALRSKDL 405
    Cat CB1 DGKVQVTRPDQARMDIRLAKTLVLILVVLIICWGPLLAIMVYDV-FGKMNKLIKTVFAFCSMLCLLNSTVNPIIYALRSKDL 404

            * :            :            .       .          .   .
   Fugu CB2 RLALLQLLAKLCDTGRCRPSSADLSPGFPSTEENT-TNPYLKDEVPGTRSIRLNSVSEI-VNNQQMNIG------------- 379
  Human CB2 RSSAHHCLAHWKKCVRG------LGS--EAKEEAP-RSSVTETEADGKITPWPDSRDLD-LSDC------------------ 360
  Mouse CB2 RSAAQHCLIGWKKYLQG------LGP--EGKEEGP-RSSVTETEADVKTT-------------------------------- 347
  Fugu CB1B RRAFVNICHMCRGTTQSLDSSA-ESDWNSRSVRSTGGRAGKDRSVGGKPQVKVAQVTVSGVTASSPAEAV------------ 470
  Fugu CB1A RHAFLSSCHACRGSAQQLDNSL-ESDCQNRNVN---ISANRAAESCVKTTVKIAKVTMS-VSTETSAEAV------------ 468
Taricha CB1 RHAFLEQCPPCEGTSQPLDNSM-ESDCQHRHGNNA-GNVHRAAENCIKSTVKIAKVTMS-VSTETSGEAV------------ 473
Z-finch CB1 RHAFRSMFPTCEGTAQPLDNSM-ESDCQHKHANNA-GNVHRAAESCIKSTVKIAKVTMS-VSTDTTAEAL------------ 473
  Human CB1 RHAFRSMFPSCEGTAQPLDNSMGDSDCLHKHANNA-ASVHRAAESCIKSTVKIAKVTMS-VSTDTSAEAL------------ 472
    Rat CB1 RHAFRSMFPSCEGTAQPLDNSMGDSDCLHKHANNT-ASMHRAAESCIKSTVKIAKVTMS-VSTDTSAEAL------------ 473
  Mouse CB1 RHAFRSMFPSCEGTAQPLDNSMGDSDCLHKHANNT-ASMHRAAESCIKSTVKIAKVTMS-VSTDTSAEAL------------ 473
    Cat CB1 RHAFRSMFPSCEGTAQPLDNSMGDSDCLHKHANNT-ANVHRAAENCIKNTVQIAKVTIS-VSTNTSAKAL------------ 472
```

Figure 1. Alignment of the predicted amino-acid sequence of the *Fugu* CB$_2$ receptor with other cannabinoid receptors including human CB$_2$ (3), mouse CB$_2$ (23), Fugu CB$_{1B}$ (17), Fugu CB$_{1A}$ (17), newt *Taricha granulosa* CB$_1$ (16), zebra finch (z-finch) *Taeniopygia guttata* CB$_1$ (15), human CB$_1$ (24), rat CB$_1$ (2), mouse CB$_1$ (25), and cat CB$_1$ (D. Gebremedhin *et al.*, unpubl.; accession number AAB53440). The sequences were aligned using ClustalX (1.8) multiple alignment program (20). The symbol * indicates the positions of residues that are identical in all of the sequences; the symbols: and . indicate the positions of strongly and weakly conserved residues, respectively.

using the *Fugu* BLAST server at http://fugu.hgmp.mrc.ac.uk/blast/. With the human CB_2 receptor protein sequence as the search query, three clones were identified (T012234, T017853, and T002576) that shared 49%, 45%, and 43% amino-acid identity with human CB_2, respectively, with corresponding BLAST E-values of 4e-78, 6e-78, and 1e-67. Further analysis of T017853 and T002576 revealed that these contained the DNA sequences of the previously discovered *Fugu* CB_{1A} and CB_{1B} genes, respectively (17). Having eliminated these CB_1-type genes, the sequence of T012234 was examined in more detail. BLAST analysis of the putative cannabinoid receptor-encoding region of T012234 using the BLAST server at http://www.ncbi.nlm.nih.gov/BLAST/ (nr database) revealed that this sequence displayed more similarity with the human CB_2 receptor (50% amino-acid identity) than with the human CB_1 receptor (47% amino-acid identity). This suggested that clone T012234 may contain the sequence of a *Fugu* CB_2 gene. To determine the complete sequence of the protein-encoding region of the putative CB_2 gene, the DNA sequence of T012234 was translated in all three possible frames for both the forward (+) and reverse (−) strands using the transeq program at http://www.ebi.ac.uk/emboss/transeq/. This revealed that the putative *Fugu* CB_2 gene was in the −2 frame of clone T012234 and enabled identification of the probable positions of the 5′ start codon and the 3′ stop codon. Based on this analysis, the putative *Fugu* CB_2-like receptor protein has a predicted length of 379 amino-acid residues, which is within the range for CB_2 receptors in mammals (*e.g.*, mouse, 347; human, 360; rat, 410). To establish whether the *Fugu* CB_2-like protein is an ortholog of mammalian CB_2 receptors, it was aligned with human CB_2, mouse CB_2, and CB_1 receptor sequences from several vertebrate species including *Fugu* (CB_{1A} and CB_{1B}), the amphibian *Taricha granulosa*, the zebra finch *Taeniopygia guttata*, human, rat, mouse, and cat (Fig. 1) using the ClustalX multiple alignment program (20). Phylogenetic trees of the aligned sequences were then constructed using the neighbor-joining method (21); human lysophospholipid receptors were used as an outgroup because these receptors are more closely related to cannabinoid receptors than other G-protein-coupled receptors in mammals (see ref. 7). Trees were constructed using the unedited aligned sequences (Fig. 2) or using truncated sequences lacking the N-terminal and C-terminal regions, where there is sequence divergence (not shown). The branching structure of the two trees was identical, with bootstrap values of 980–1000 for all of the major branches. Analysis of the tree shown in Figure 2 reveals that cannabinoid receptors fall into two distinct clades, a CB_1 clade and a CB_2 clade; and, importantly, the *Fugu* CB_2-like sequence is positioned in the CB_2 clade, indicating orthology to mammalian CB_2 receptors.

Based on the data available (99% of the *Fugu* genome sequence), only one CB_2-type gene occurs in the *Fugu* genome. This is of interest because in *Fugu* and in other teleosts there often are two orthologs for each single-copy gene in mammals (22). For example, *Fugu* contains two CB_1 genes (CB_{1A} and CB_{1B}) whereas mammalian genomes contain only one. The existence of two genes in teleosts for each single-copy gene in mammals is thought to reflect a genome duplication that occurred in the ancestor of teleost fish 300 to 450 million years ago (22). Presumably, however, the duplicates of some genes have subsequently been lost, and this probably explains the existence of only one CB_2 gene in *Fugu*. Whether other teleosts such as the zebrafish *Danio rerio* have the same number and distribution of CB_1 and CB_2 genes remains to be determined, but to date neither CB_1 nor CB_2 genes have been sequenced in *Danio*. With the ongoing sequencing of the *Danio* genome, a comprehensive search will probably be practical soon.

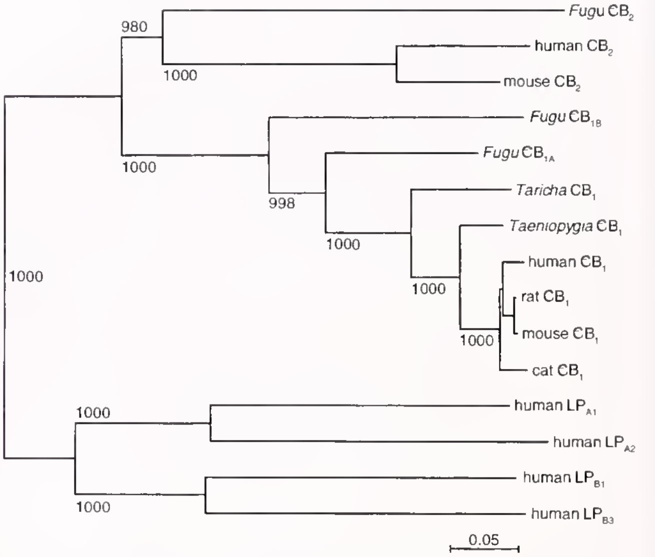

Figure 2. Phylogenetic tree of CB_1-type and CB_2-type cannabinoid receptors with human lysophospholipid receptors as an outgroup (LP_{A1}, LP_{A2}, LP_{B1}, LP_{B3}). The tree was constructed using the neighbor-joining method (21) with bootstrapping (1000 bootstrap trials) and then viewed in NJ Plot. The tree shows that the *Fugu* CB_2-like receptor forms a clade with human CB_2 and mouse CB_2 and is therefore an ortholog of mammalian CB_2 receptors.

The CB_2 gene in *Fugu* is the first CB_2 gene to be identified in a non-mammalian species. The discovery of this gene indicates that the gene duplication event that gave rise to CB_1 and CB_2 receptors occurred before teleosts and tetrapods diverged from a common ancestor. Thus, CB_2-type cannabinoid receptors, like CB_1 receptors, are likely to be also present in non-mammalian tetrapod vertebrates (amphibians, reptiles, birds). Non-mammalian vertebrate species may provide useful model systems with which to explore the physiological roles of the CB_2 receptor. In particular, because the CB_2 receptor appears to be principally involved in immunoregulation in mammals, it may have a related role in the more "primitive" immune systems of fish and other non-mammalian vertebrates.

Acknowledgments

I am grateful to Greg Elgar (Fugu Genomics Project, MRC Human Genome Mapping Project Resource Centre, Wellcome Trust Genome Campus, Hinxton, Cambridge, UK) for permission to publish this analysis of *Fugu* genomic sequence data obtained by the International Fugu Genome Consortium. I am also grateful to Michaela Egertová (Queen Mary, University of London) and three anonymous referees for constructive criticism of the manuscript.

Literature Cited

1. **Devane, W. A., F. A. I. Dysarz, M. R. Johnson, L. S. Melvin, and A. C. Howlett. 1988.** Determination and characterization of a cannabinoid receptor in rat brain. *Mol. Pharmacol.* **34:** 605–613.
2. **Matsuda, L. A., S. J. Lolait, M. J. Brownstein, A. C. Young, and T. I. Bonner. 1990.** Structure of a cannabinoid receptor and functional expression of the cloned cDNA. *Nature* **346:** 561–564.
3. **Munro, S., K. L. Thomas and M. Abu-Shaar. 1993.** Molecular characterization of a peripheral receptor for cannabinoids. *Nature* **365:** 61–65.
4. **Devane, W. A., L. Hanus, A. Breuer, R. G. Pertwee, L. A. Stevenson, G. Griffin, D. Gibson, A. Mandelbaum, A. Etinger, and R. Mechoulam. 1992.** Isolation and structure of a brain constituent that binds to the cannabinoid receptor. *Science* **258:** 1946–1948.
5. **Mechoulam, R., S. Ben-Shabat, L. Hanus, M. Ligumsky, N. E. Kaminski, A. R. Schatz, A. Gopher, S. Almog, B. R. Martin, D. R. Compton, R. G. Pertwee, G. Griffin, M. Bayewitch, J. Barg, and Z. V. I. Vogel. 1995.** Identification of an endogenous 2-monoglyceride, present in canine gut that binds to cannabinoid receptors. *Biochem. Pharmacol.* **50:** 83–90.
6. **Sugiura, T., S. Kondo, A. Sukagawa, S. Nakane, A. Shinoda, K. Itoh, A. Yamashita, and K. Waku. 1995.** 2-arachidonoylglycerol: a possible endogenous cannabinoid receptor ligand in brain. *Biochem. Biophys. Res. Commun.* **215:** 89–97.
7. **Elphick, M. R., and M. Egertová. 2001.** The neurobiology and evolution of cannabinoid signalling. *Philos. Trans. R. Soc. Lond. B* **356:** 381–408.
8. **Egertová, M., D. K. Giang, B. F. Cravatt, and M. R. Elphick. 1998.** A new perspective on cannabinoid signalling: complementary localization of fatty acid amide hydrolase and the CB_1 receptor in rat brain. *Proc. R. Soc. Lond. B* **265:** 2081–2085.
9. **Kreitzer, A. C., and W. G. Regehr. 2001.** Retrograde inhibition of presynaptic calcium influx by endogenous cannabinoids at excitatory synapses onto Purkinje cells. *Neuron* **29:** 717–727.
10. **Ohno-Shosaku, T., T. Maejima, and M. Kano. 2001.** Endogenous cannabinoids mediate retrograde signals from depolarized postsynaptic neurons to presynaptic terminals. *Neuron* **29:** 729–738.
11. **Wilson, R. I., and R. A. Nicoll. 2001.** Endogenous cannabinoids mediate retrograde signalling at hippocampal synapses. *Nature* **410:** 588–592.
12. **Wilson, R. I., G. Kunos, and R. A. Nicoll. 2001.** Presynaptic specificity of endocannabinoid signaling in the hippocampus. *Neuron* **31:** 453–462.
13. **Buckley, N. E., K. L. McCoy, E. Mezey, T. Bonner, A. Zimmer, C. C. Felder, M. Glass, and A. Zimmer. 2000.** Immunomodulation by cannabinoids is absent in mice deficient for the cannabinoid CB2 receptor. *Eur. J. Pharmacol.* **396:** 2–3.
14. **British Medical Association. 1997.** *Therapeutic Uses of Cannabis.* Harwood Academic Publishers, Amsterdam.
15. **Soderstrom, K., and F. Johnson. 2001.** Zebra finch CB1 cannabinoid receptor: pharmacology and *in vivo* and *in vitro* effects of activation. *J. Pharmacol. Exp. Ther.* **297:** 189–197.
16. **Soderstrom, K., M. Leid, F. L. Moore, and T. F. Murray. 2000.** Behavioural, pharmacological and molecular characterization of an amphibian cannabinoid receptor. *J. Neurochem.* **75:** 413–423.
17. **Yamaguchi, F., A. D. Macrae, and S. Brenner. 1996.** Molecular cloning of two cannabinoid type 1-like receptor genes from the puffer fish *Fugu rubripes*. *Genomics* **35:** 603–605.
18. **Elgar, G., M. S. Clark, S. Meek, S. Smith, S. Warner, Y. J. Edwards, N. Bouchireb, A. Cottage, G. S. Yeo, Y. Umrania, G. Williams, and S. Brenner. 1999.** Generation and analysis of 25 Mb of genomic DNA from the pufferfish *Fugu rubripes* by sequence scanning. *Genome Res.* **10:** 960–971.
19. **Altschul, S. F., W. Gish, W. Miller, E. W. Myers, and D. J. Lipman. 1990.** Basic local alignment search tool. *J. Mol. Biol.* **215:** 403–410.
20. **Thompson, J. D., T. J. Gibson, F. Plewniak, F. Jeanmougin, and D. G. Higgins. 1997.** The ClustalX windows interface: flexible strategies for multiple sequence alignment aided by quality analysis tools. *Nucleic Acids Res.* **24:** 4876–4882.
21. **Saitou, N., and M. Nei. 1987.** The neighbor-joining method: a method for reconstructing phylogenetic trees. *Mol. Biol. Evol.* **4:** 406–425.
22. **Taylor, J. S., Y. Van de Peer, I. Braasch, and A. Meyer. 2001.** Comparative genomics provides evidence for an ancient genome duplication event in fish. *Philos. Trans. R. Soc. Lond. B* **356:** 1661–1679.
23. **Shire, D., B. Calandra, M. Rinaldi-Carmona, D. Oustric, B. Pessegue, O. Bonnin-Cabanne, G. Le Fur, D. Caput, and P. Ferrara. 1996.** Molecular cloning, expression and function of the murine CB2 peripheral cannabinoid receptor. *Biochim. Biophys. Acta* **1307:** 132–136.
24. **Gérard, C. M., C. Mollereau, G. Vassart, and M. Parmentier. 1991.** Molecular cloning of a human cannabinoid receptor which is also expressed in testis. *J. Biochem.* **279:** 129–134.
25. **Chakrabarti, A., E. S. Onaivi, and G. Chaudhuri. 1995.** Cloning and sequencing of a cDNA encoding the mouse brain-type cannabinoid receptor protein. *DNA Seq.* **5:** 385–388.

Reference: *Biol. Bull.* **202:** 108–136. (April 2002)

Reliable, Responsive Pacemaking and Pattern Generation With Minimal Cell Numbers: the Crustacean Cardiac Ganglion

IAN M. COOKE

Department of Zoology and Békésy Laboratory of Neurobiology, University of Hawaii,
1993 East-West Road, Honolulu, Hawaii 96822

Abstract. Investigations of the electrophysiology of crustacean cardiac ganglia over the last half-century are reviewed for their contributions to elucidating the cellular mechanisms and interactions by which a small (as few as nine cells) neuronal network accomplishes extremely reliable, rhythmical, patterned activation of muscular activity—in this case, beating of the neurogenic heart. This ganglion is thus a model for pacemaking and central pattern generation. Favorable anatomy has permitted voltage- and space-clamp analyses of voltage-dependent ionic currents that endow each neuron with the intrinsic ability to respond with rhythmical, patterned impulse activity to nonpatterned stimulation. The crustacean soma and initial axon segment do not support impulse generation but integrate input from stretch-sensitive dendrites and electrotonic and chemically mediated synapses on axonal processes in neuropils. The soma and initial axon produce a depolarization-activated, calcium-mediated, sustained potential, the "driver potential," so-called because it drives a train of impulses at the "trigger zone" of the axon. Extreme reliability results from redundancy and the electrotonic coupling and synaptic interaction among all the neurons. Complex modulation by central nervous system inputs and by neurohormones to adjust heart pumping to physiological demands has long been demonstrated, but much remains to be learned about the cellular and molecular mechanisms of action. The continuing relevance of the crustacean cardiac ganglion as a relatively simple model for pacemaking and central pattern generation is confirmed by the rapidly widening documentation of intrinsic potentials such as plateau potentials in neurons of all major animal groups. The suite of ionic currents (a slowly inactivating calcium current and various potassium currents, with variations) observed for the crustacean cardiac ganglion have been implicated in or proven to underlie a majority of the intrinsic potentials of neurons involved in pattern generation.

A Physiologically Responsive, Reliable Heart Pacemaker and Muscle Activator Built From Nine Neurons

The crustacean cardiac ganglion (CG) is composed of from 6 to 16 neurons, 9 in most decapods, that autonomously provide rhythmically recurring barrages of action potentials to activate the heart muscle. In Malacostraca, the heart is neurogenic and in adults dependent for its beating on the impulses from the ganglion. The CG, consisting of the neurons and their processes, wrapped in glial and connective tissue, forms an elongated, discrete branching trunk in or on the heart. It can be dissected from the heart and will continue to show spontaneous, rhythmical bursting. As an accessible and robust *in vitro* preparation, the CG joins a list of crustacean preparations that have provided insights into fundamental neurophysiological mechanisms, in this case the mechanisms by which small neuronal networks can generate rhythmical, patterned output (reviews: Wiens, 1982; Marder and Calabrese, 1996). Possibly the most important contribution was the demonstration that individual neurons are endowed with an intrinsic burst-organizing mechanism that results in a patterned output to any appropriate excitatory drive, and the detailed analysis of the ionic mechanisms involved. Further, the CG demonstrated that interconnections among a small number of neurons with

Received 2 July 2001; accepted 11 January 2002.

E-mail: ian@pbrc.hawaii.edu.

Abbreviations: CG, cardiac ganglion; DP, driver potential; PO, pericardial organ.

such a capability can ensure coordinated, patterned, rhythmic, highly fault-tolerant output from the ensemble. Patterned or bursting impulses are, of course, the essential effective activator of responses of other neurons or muscles or secretory cells. The recognition of patterning mechanisms intrinsic to individual neurons has simplified the analysis of neuronal network pattern generation, freeing it from seeking reliance on properties emergent from a network.

This review seeks to provide a reader with an overview of the studies on the CG in the context of crustacean heart function, with emphasis on the electrophysiological studies of the isolated CG. The ionic mechanisms observed have proven broadly applicable to explaining intrinsic burst generation or pattern generation by neurons in both invertebrate and vertebrate nervous systems (see further below). As early investigators noted (Welsh and Maynard, 1951), the CG has the essential properties of a brain: apparently autonomous spontaneity and the ability to sense relevant environmental changes (degree of heart filling, hormones) and integrate them with intrinsic pattern-generating properties to provide an appropriately adjusted motor output.

The unique suitability of the CG for analyzing cellular mechanisms for pattern generation and rhythmicity derives from particularities of crustacean neuronal functional anatomy, specifically the segregation of the major impulse-generating mechanism (voltage-dependent Na^+ conductance) to axons so that the soma and initial axon segment are not actively invaded by impulses ("spikes"). In the more elongate CG of lobsters, the well-separated distribution of the neuronal somata makes possible the physical separation of the impulse-generating axon or axons from the more subtle electrical responses of the non-impulse-generating soma, initial axon segments, and associated collaterals. One of these is a graded, regenerative, Ca^{2+}-mediated response to depolarization, lasting 200 ms or longer, which provides drive for generation of the burst of impulses by the axon and hence is referred to as a driver potential (DP). As reviewed below, the characteristics of DPs, which, in isolated CG, are initiated in response to spontaneously occurring pacemaker depolarization or to synaptic excitation, provide a basis for interpreting many of the responses of intact hearts as well as the isolated CG to both physiological and experimentally imposed modulatory influences (see also Cooke, 1988, 2002).

Anatomy

Morphological observations

Alexandrowicz (1932) provided an anatomical description of the innervation of decapod hearts that was based on vital methylene blue staining; this description has provided a structural underpinning for many subsequent observations of function (Fig. 1). Similar studies of the heart of stomatopods (1934) and of an isopod (1952) followed (see also Suzuki, 1934). Alexandrowicz described three neuronal elements innervating decapod hearts: the intrinsic neurons (cardiac ganglion); the extrinsic fibers—one inhibitory and two acceleratory axons—arriving *via* three segmental nerves on each side from thoracic ganglia (combined into the dorsal nerves in decapods) to reach the heart and CG; and nerves innervating the suspensory ligaments, ostia, and arterial valves (Fig. 1B, C, D). He called attention to the neurogenic nature of the crustacean hearts, reporting the immediate cessation of contractions after nerves between the ganglion and muscle were cut. He also observed that the most anterior extrinsic nerve pair in stomatopods was inhibitory and the sequentially more posterior two pairs were excitatory, and correctly surmised that these have similar roles in decapods (Wiersma and Novitski, 1942, crayfish; Smith, 1947, crabs; Maynard, 1953, lobsters). Alexandrowicz provided important additional observations relevant to regulation of crustacean hearts: the anatomical description of the pericardial organs (POs) of crabs and their macruran homolog, the ligamental plexuses. These are neurohemal structures that release neurohormones having cardioregulator and other functions into hemolymph returning to the heart (Alexandrowicz, 1953; Alexandrowicz and Carlisle, 1953).

Comparison of the circulatory systems across the orders of Crustacea supports a consensus that evolution from a pulsatile dorsal vessel toward a compact heart accompanies more active lifestyles to provide for more efficient circulation (Wilkens, 1999; for a comprehensive review, see Maynard, 1960). In the primitive branchiopods (*e.g., Daphnia* sp., *Triops longicaudatus*), no neurons have been found in or on the heart, and the heartbeat is thus myogenic (Yamagishi *et al.,* 1997). In the CG of the stomatopod *Squilla* (Alexandrowicz, 1934), 14 or 15 neurons are distributed along a ganglionic trunk that lies on the external dorsal surface of the heart and can be as long as 8 cm. In decapods, the CG lies on the inner dorsal wall of the heart (Fig. 1A, C). Although crayfish have 16 intrinsic neurons, in most decapods examined the number has been reduced to 9. There is a clear distinction in size and function. The most posterior four neurons are smaller and, having axonal terminations within neuropil in the ganglionic trunk, are therefore interneurons. The more anterior five neurons are larger and, because they provide axons that leave the ganglion to innervate heart muscle fibers, are motorneurons (Fig. 1B, E). Each of the neurons has dendritic or collateral processes extending out of the ganglionic trunk to ramify onto nearby muscle fibers that are responsive to stretch. In lobsters the somata are widely spaced along a linear (*e.g., Panulirus,* Fig. 1C) or Y-shaped (*e.g., Homarus,* Fig. 1A) ganglionic trunk spanning nearly a centimeter in a 0.5-kg animal; in crabs of edible size the neurons are usually compacted into anterior and posterior clusters separated by several millimeters of ganglionic trunk (Figs. 1E, 8D).

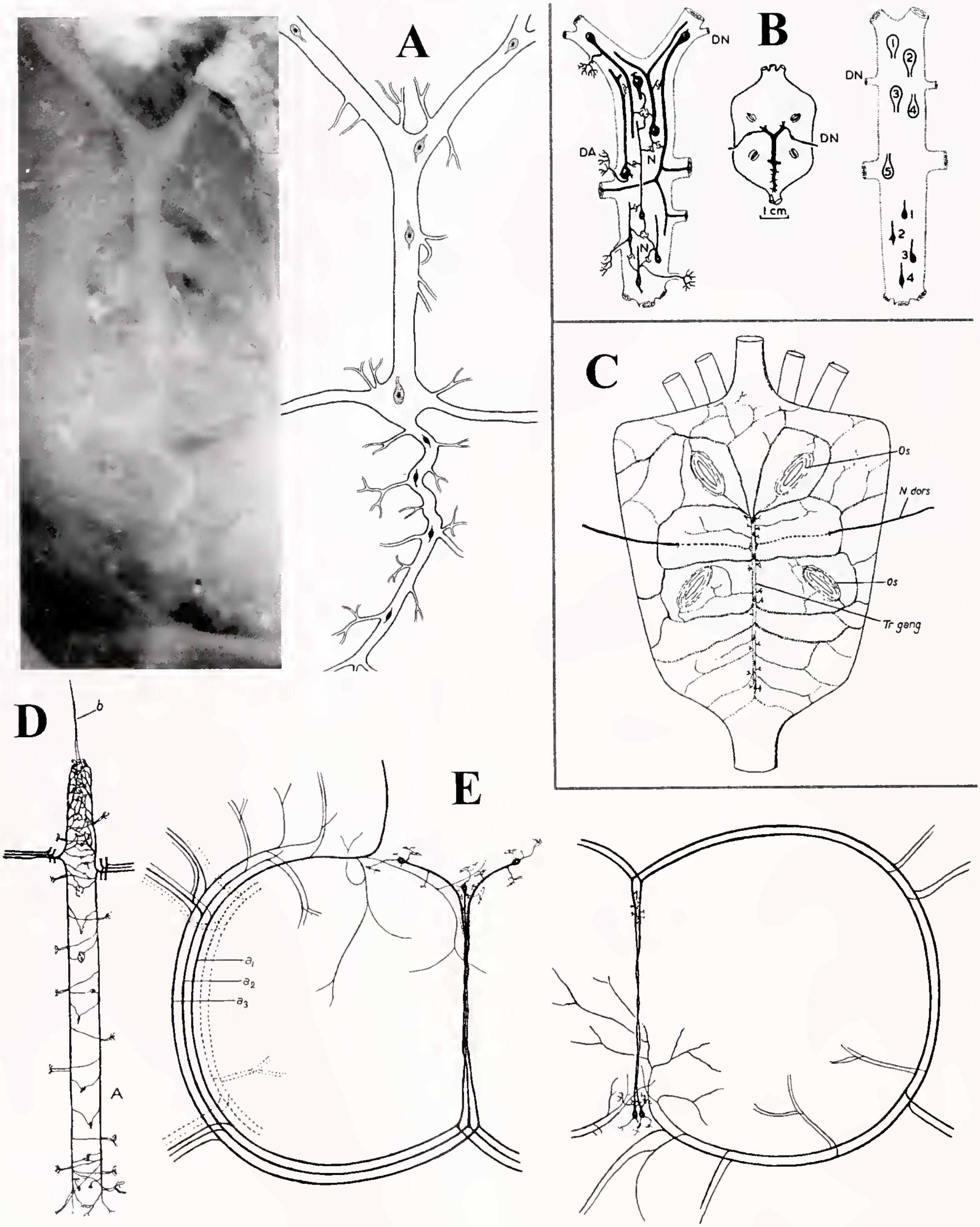
A
B
DN
DA
N
N
DN
1 cm
DN
1
2
3
4
5
1
2
3
4
C
Os
N dors
Os
Tr gang
D
b
A
E
a1
a2
a3

Electrophysiological anatomy

One of the first conclusions to come from electrophysiological recording from lobster CG (Welsh and Maynard, 1951; Maynard, 1955; see also Matsui, 1955) was that not only the rhythmicity but also the pattern of impulses within the bursts of activity is extraordinarily stable (Figs. 2C, E; 6A, B; 9E, F). In *Homarus americanus*, for example, output of isolated CG consists of a 200- to 300-ms burst of tightly grouped efferent impulses that recur spontaneously at rates similar to observed heartbeat rates (50–60/min for lobsters). Further confirmation of the consistency of burst patterning came with analysis of the patterning by Hartline (1967), who used an array of five or more pairs of extracellular electrodes placed along the trunk and major nerves of the *Homarus* ganglion to identify each impulse with its axon by mapping the site of impulse initiation and its conduction route (Fig. 2A, B, D). It was clear that a particular one of the posterior cells (usually 8 or 7, numbering cells from anterior to posterior) consistently fired first in a burst, and that the firing of large cells commenced with the arrival of the first small-cell impulse, propagated along its anterior-traveling axon, at neuropil in which synapses on large-cell collateral processes occur. Thus the most posterior large cell (5) fired first, followed successively by more-anterior cells. The sites of impulse initiation observed in such studies confirmed conclusions reached from intracellular recording from the large cells (early work reviewed by Hagiwara, 1961) that impulses do not invade the somata, but rather are initiated at a site that can be more than a millimeter distant along the axon. Cells having more than one axon—for example, Cell 3 situated at the junction of the Y in *Homarus*—initiate impulses in each axon independently (Fig. 2D). As mentioned above, within each burst, the patterning of impulses of each axon remains highly constant, each unit showing repetitive firing (Fig. 2C). In *Homarus*, the first 3 to 4 impulses of large-cell axons occur at high frequency (90–120/s) and then continue for 3 or more at a slower rate (10–20/s, Hartline, 1967); small-cell axons fire as many as 15 impulses starting at rates of ~80/s and declining during the burst toward 20–30/s. A similar analysis showing minor differences in detail from *Homarus* is available for *Panulirus interruptus* (Friesen, 1975a, b).

Studies of functional anatomy in crab CG (Tazaki and Cooke, 1979a, 1983a, in *Portunus sanguinolentus*; Fort and Miller, 2001, in *Callinectes sapidus*) show an important variation on this organization, namely that large-cell axons, rather than each firing in a consistent individual pattern within each burst, show synchronization of their impulse firing (Fig. 6A). Synchronization also occurs among the rostral neurons of the *Squilla* ganglion (Watanabe and Takeda, 1963).

Axons of the posterior four small cells in the lobster and crab CG remain within the ganglionic trunk and provide excitatory, chemically mediated synaptic input to the large cells. This input initiates burst activity of the large cells, and thus the small cells are considered pacemaker interneurons or premotor neurons. The large-cell axons, while providing synaptic input to each other and perhaps also to the small cells, produce the bursts of motor impulses responsible for heart muscle contraction. Synchronization of ganglionic activity is not only mediated by synaptic drive, but the general excitability of the network is shared among all of the neurons by means of electrotonic coupling capable of passing slow changes in potential. Synaptic and electrotonic interactions are discussed below.

Two further properties of the individual CG neurons are also critical: each has stretch-sensitive dendrites ramifying into heart muscle that account for the ability of intact hearts to adjust heart rate and strength of beating to the degree of filling of the heart; and each has the intrinsic ability to produce a patterned burst of impulses in response to a simple stimulus.

Figure 1. Anatomy of the crustacean cardiac ganglion. Anterior up. (A) Fresh dissection of a *Homarus americanus* cardiac ganglion exposed on the inner dorsal surface of the heart (length of field ~1.3 cm); diagram shows the approximate position of the nine intrinsic neurons (for nomenclature see Fig. 2D). Extrinsic regulator nerves (dorsal nerves) enter laterally just anterior to the most anterior neurons. (Cooke, 1962, fig. 1-1.) (B) Cardiac ganglion (diagrammatic). Left, *Homarus*: relations of the cell bodies, neuropils (N), and dendritic arborizations (DA). Full course of axons is not shown. DN, dorsal nerve. Right, *Panulirus*: positions of cell bodies and direction of major axons. Inset, *Homarus* ganglion trunk *in situ* in heart. Length:width ratio much reduced in all diagrams. (Maynard, 1955, fig. 1.) (C) Alexandrowicz' semi-diagrammatic representation of the nervous system in the dorsal wall of the heart of *Palinurus vulgaris*. *Tr gang*, ganglionic trunk, with its nerve-cells: *N dors*, dorsal nerve piercing the heart-wall; *Os*, ostium. Alexandrowicz' drawings compiled repetitive observations of fresh dissections during methylene blue vital staining. (Alexandrowicz, 1932, Text-fig. 1.) (D) Diagram showing the course of the fibers of System I [inhibitors] of the dorsal nerves in *Palinurus*. Only one fiber on each side is represented. *b*, fibers of unknown destination arising from fibers of System I. (Alexandrowicz, 1932, Text-fig. 19A.) See also Fig. 7F. (E) Diagram illustrating the course of the axons of three anterior cells (left half) and two posterior cells (right half) in *Cancer pagurus*. In dotted line are drawn parts of the axons of posterior cells. (Modified from Alexandrowicz, 1932, Text-figs. 8, 9.) (Figures in C, D, and E from Alexandrowicz, 1932, are by permission of Company of Biologists, Ltd.)

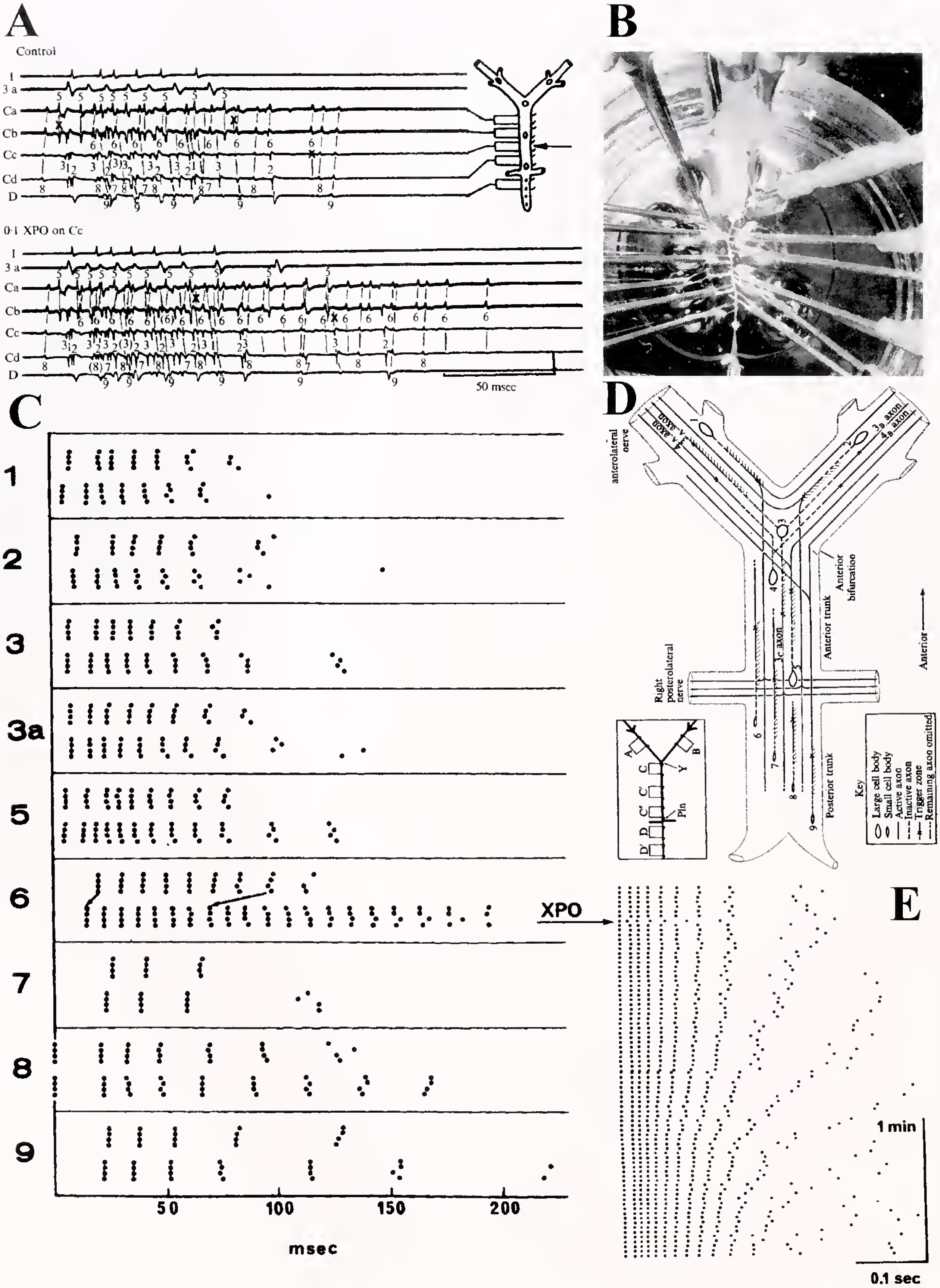
A
Control
1
3 a
Ca
Cb
Cc
Cd
D
0·1 XPO on Cc
50 msec
B
C
1
2
3
3a
5
6
7
8
9
50
100
150
200
msec
XPO
D
anterolateral nerve
3a axon
4a axon
Anterior bifurcation
Anterior trunk
Right posterolateral nerve
Posterior trunk
Anterior
A
B
C
Y
C'
C''
Pin
D
D'
Key
Large cell body
Small cell body
Active axon
Inactive axon
Trigger zone
Remaining axon omitted
E
1 min
0.1 sec

An Intrinsic Burst-Forming Mechanism: the Driver Potential

Possibly first discussed as an *intrinsic* potential by Watanabe (1958) in lobster CG, and further described in studies of the *Squilla* (stomatopod) CG (Watanabe *et al.*, 1967a, b), driver potentials are relatively slow, sustained, regenerative depolarizations that may arise from a gradual pacemaker potential or be evoked by a depolarization, such as an excitatory synaptic potential (or an applied depolarizing stimulus) (Fig. 3). They provide the depolarizing drive for initiating repetitive impulses at an axonal "trigger zone." Because DPs arise in the soma and proximal axon or axons—regions lacking impulse-generating conductances and, particularly in lobster CG, physically well separated from spiking axon—they can be studied in relative isolation. Their properties account for much of the collective behavior of the network, including rhythmicity, reciprocity between burst rate and duration, and phase resetting in response to imposed extra stimuli.

Driver potentials arise in the non-spiking soma and proximal axon

Direct evidence for the localization of DPs is provided by simultaneous intracellular recording from a neuronal soma and its axon at a distance of several millimeters (Fig. 3A): the soma recording shows a sustained, slow depolarization (*i.e.*, the DP) with attenuated sharp deflections that are synchronous with the overshooting impulses arising from a flat baseline recorded from the axon (Watanabe *et al.*, 1967b, *Squilla oratorio*; Tazaki, 1970, *Eriocheir japonicus*; Tazaki, 1973, *Panulirus japonicus*; Tazaki and Cooke, 1983a, *Portunus sanguinolentus*). The localization of DPs to the soma and non-impulse-supporting initial axon was also shown in *Homarus* by intracellular recording during or after ligaturing at distances between 200 μm and more than a millimeter from the soma (Tazaki and Cooke, 1983b) (Fig. 3B). For more distant ligatures, electrotonically decremented impulses, as recorded from the soma, were superimposed on the DP, indicating that the ligatured segment included an axonal trigger zone. It is worth noting that more complex deflections, suggestive of synaptic potentials, were sometimes present in recordings from ganglion segments that include a single soma. This suggests the possibility that the processes of other neurons present in such a segment can contribute synaptic input. Any rapid deflections disappeared with only minimal change in the form of the underlying DP when tetrodotoxin (TTX) was added to the perfusing saline (Tazaki, 1971a). Treatment of ganglia with TTX made it possible to observe DPs in the absence of any impulse-mediated activity by simultaneous intracellular recording in up to three large cells (Tazaki and Cooke, 1979b, in *Portunus*) (Fig. 3D, two cells). Stimulation with a depolarizing current pulse in any one cell simultaneously initiated DPs in all; the amplitudes and form differed slightly, but remained characteristic in each cell, hence indicating that the DP represented an active response of each neuron, but one that was brought to threshold by the spread of the depolarizing

Figure 2. Electrophysiological anatomy: responses to localized neurohormone application. (A) The site of origin of impulses, their route of propagation and recurrence are analyzed by simultaneous recordings from seven pairs of electrodes (selected from 11, see B) placed on an isolated *Homarus* cardiac ganglion. Numbers identify impulses of corresponding cell axons (3 = 3c) as indicated in D. X indicates site of impulse initiation; bar over cell number indicates distally initiated impulse; brackets indicate uncertainty in identification or timing. The lower records show the response to application at the position indicated by the arrow of a droplet (~10 μl) under the mineral oil of pericardial organ extract (XPO, POs from two *Cancer borealis*, 0.5 mg dry weight in 1 ml, heated to 100°C). (B) Photograph of a *Homarus* ganglion with electrodes positioned for extracellular recording as in A. The ganglion is lifted out of saline into mineral oil for recording. (C) "Dot pattern" analysis of the records. For each of eight bursts (four control; four experimental), including the two from A, firing times for each unit are indicated as a horizontal line of dots. Beneath the first burst pattern for a unit, the succeeding three burst patterns for that unit are positioned relative to the pacemaker impulse in Cell 8. Note the typical consistency in firing pattern of a unit within the four bursts. The arrow indicates the change of firing position of the last stable Cell 6 impulse during the response. The effect of the XPO application has been to increase the frequency and number of impulses of Cell 6 selectively and to contract its firing pattern. (D) Diagram of locations, axon courses, and locations of anatomical regions for the nine intrinsic neurons. Active axon (refer to key) is axon carrying a regenerative impulse. The shaded portion between soma and trigger zone represents a region of pharmacological sensitivity. Note that Cells 3 and 4 have more than one independent axon. Width of ganglion exaggerated relative to length (total length about 1 cm in 0.5-kg animals). Inset: Designations given to locations along the ganglion used in identifying electrode and drug placements. (E) Effect on impulse firing pattern of application of XPO to the proximal axon of Cell 5. Axon 5 impulses brighten the oscilloscope beam, which is triggered by the first impulse of each burst and swept horizontally while also being continuously slowly displaced downward. Application was made after the seventh burst (arrow and electrical artifact). The average firing frequency of Cell 5 was increased 38%, but coordinated by addition of impulse firing within bursts without a change of burst rate (dot rows remain evenly spaced). (A, C, fig. 2; D, fig. 1; E, fig. 4 from Cooke and Hartline, 1975; by permission of Company of Biologists, Ltd. B, Cooke and Hartline, unpublished.)

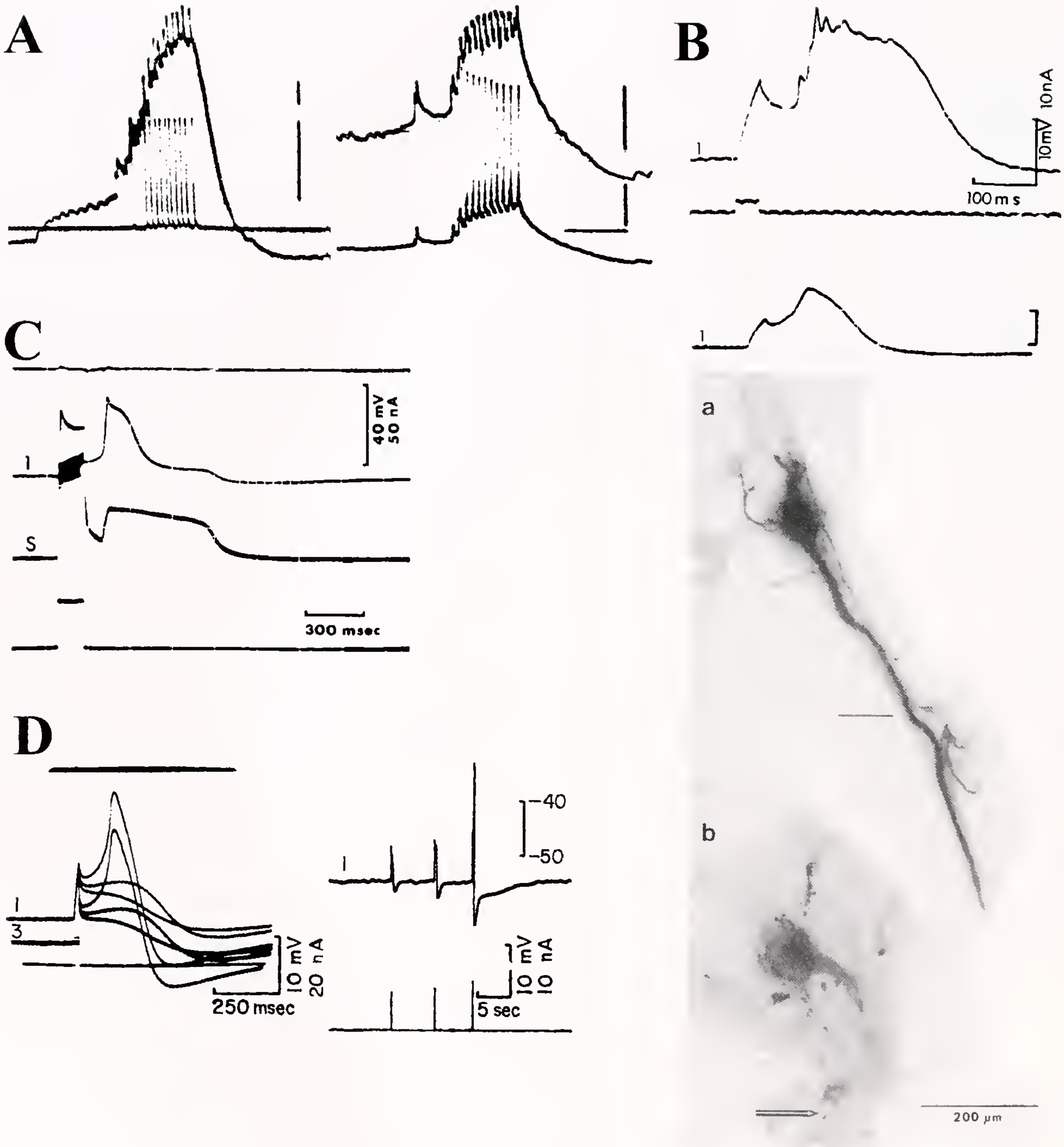

Figure 3. Localization of the driver potential to the soma and proximal axon. (A) Spontaneous bursts of spikes recorded simultaneously from two regions of a large neuron of the crab *Eriocheir japonicus*. Left frame: upper trace, axon; lower trace, soma; distance between them, 2.5 mm. Right frame: upper trace, soma; lower trace, axon; distance, 0.3 mm. Calibration: 10 mV, 100 ms. Note lack of underlying depolarization in distal axon, presence in axon near soma, attenuated impulses in soma. (Tazaki, 1970, fig. 1.) (B) Depolarization-evoked responses of neurons ligatured at different distances (*Homarus*). Upper frame: intracellular recording from Cell 1 ligatured 1.6 mm from the soma (a, below); response to a depolarizing current pulse passed through the recording electrode evokes a driver potential on which are superimposed more rapid, small deflections, interpreted as electronically decremented impulses of the axon and possible other elements present in the ganglion segment. Resting potential, −54 mV. Lower frame: response recorded from Cell 1 ligatured 200 µm from the soma (b, below); a driver potential without superimposed deflections is observed. Calibration mark, 10 mV, 10 nA. Resting potential, −50 mV. Photomicrographs (reversed image) of the neurons after Lucifer yellow

stimulus *via* pervasive electrotonic coupling among all neurons of the ganglion.

The form of their driver potential shapes the pattern of impulses of each neuron

Large cells. The DPs as recorded intracellularly from large cells of crabs or lobsters show little difference in form whether examined in TTX or after isolation of a soma by ligaturing. If the neuron is relatively undamaged (as evidenced by high input resistance and a resting potential ~−50 mV), depolarization to a threshold (~−45 mV) initiates a regenerative response requiring 10 or more ms to reach a maximum ~20 mV depolarized from resting potential (Fig. 3D). The depolarization shows a rounded peak with a gradually declining shoulder, followed by a more rapid repolarization that gives way to hyperpolarizing afterpotentials. These have a relatively rapidly decaying phase lasting up to 1 s, followed by a slowly decaying phase lasting tens of seconds. Although they are regenerative, DPs are not all-or-none responses; rather their size is related to the amplitude and rate of rise of the depolarizing stimulus. More importantly, threshold and amplitude are related to the rate of repetition: given a constant stimulus, threshold becomes lower and amplitude and duration become larger with increasing time since the previous response. A maximal response requires a pause of more than 10 s. It will be obvious that at typical heart rates of 50–60/min, DPs are not at maximal amplitude but are evoked in a range over which changes in heart rate will result in decreased or increased amplitudes (Fig. 5A). Possible cellular mechanisms governing these relations are discussed below.

Small cells. An intracellular recording from a small cell, simultaneously with a large cell, in a *Portunus* CG treated with TTX (Tazaki and Cooke, 1983c) reveals clear differences in the form of DPs of large and small cells (Fig. 3C). The DP in the small cell is lower in amplitude but has a long (~400 ms), sustained, slowly declining plateau. The initiation of the small-cell DP by depolarizing current also causes a DP in the anterior large cell; this has the larger but less sustained form described above. The electrotonically spread continuing plateau of the small-cell DP is apparent in the large-cell recording. As mentioned previously, the bursts of the small cells are longer and show a well-sustained frequency of firing. Thus, the differing form of the DPs of small and large cells accounts for the differing pattern of impulses produced during bursts by the axons of small and large cells (Fig. 6A).

The ability of slow potentials such as DPs to generate trains of impulses from the axonal trigger zone implies that the ionic mechanisms involved in impulse initiation are not subject to rapid inactivation by depolarization. Intracellular recordings from axons, as mentioned above, show typical overshooting, all-or-none impulses with a rapid rise and fall. When intracellular penetrations were attempted, damage to the target neuron was often signaled by appearance in an extracellular recording of repetitive firing not organized into the coordinated bursting of the remaining cells of the ganglion, confirming the ability of axons to respond to sustained depolarization with minimal adaptation.

Voltage-Clamp Analyses of Ionic Currents Giving Rise to Driver Potentials

Characterization of four kinds of current in ligatured somata

The characteristics and ionic conductances responsible for DPs have been examined in most detail in the *Homarus* CG (Tazaki and Cooke, 1983c, 1986, 1990), in which the separation of the neurons permitted the isolation of ganglion segments with a single large-cell soma by ligaturing the ganglionic trunk. Studies with two-electrode voltage clamping show that DP characteristics involve the interplay between an inward Ca^{2+}-mediated current (I_{Ca}) and three outward K^+-mediated currents: a transient current (I_A), a slowly-inactivating K^+ current (I_K), and a Ca-dependent K^+ current (I_{KCa}) (Tazaki and Cooke, 1986, 1990). Space-

---

injection (glycerin-cleared whole mount photographed under dark-field UV illumination immediately after dye injection; scales, 200 μm). Ligature in a was just beyond stained end of axon; at arrow in b. Note fine processes and a major axon collateral proximal to the ligature in a. (Modified from Tazaki and Cooke, 1983b, Figs. 6, 7; by permission of Springer-Verlag GmbH & Co. KG.) (C) A driver potential response of a small cell in a *Portunus sanguinolentus* ganglion perfused with $3 \times 10^{-7} M$ TTX and 50 mM TEA. A depolarizing current pulse applied through the recording electrode in the small cell evokes a driver potential in both the small cell (S) and anterior Cell 1. The driver potential in cell 1 is followed by a low-amplitude potential representing the electrotonically conducted, longer-duration response of the small cell. Resting potentials, −48 mV. (Tazaki and Cooke, 1983c, fig. 8.) (D) Graded driver-potential responses. At the left, three superimposed sweeps show responses recorded intracellularly from Cells 1 and 3 (and absence of responses in extracellular electrode, top trace, $3 \times 10^{-7} M$ TTX in perfusate), to different intensities of 20-ms depolarizing current pulses applied *via* a bridge in Cell 3. Lowest trace is a current monitor. At the right, Cell 1 responses to the same current pulses recorded simultaneously on the penwriter, current monitor below. Responses are graded with current intensity below a threshold; above the threshold, responses are constant (not shown). Slow afterpotentials are observed only following above-threshold responses. Resting potentials, −55 mV. (Tazaki and Cooke, 1979b, fig. 3.)

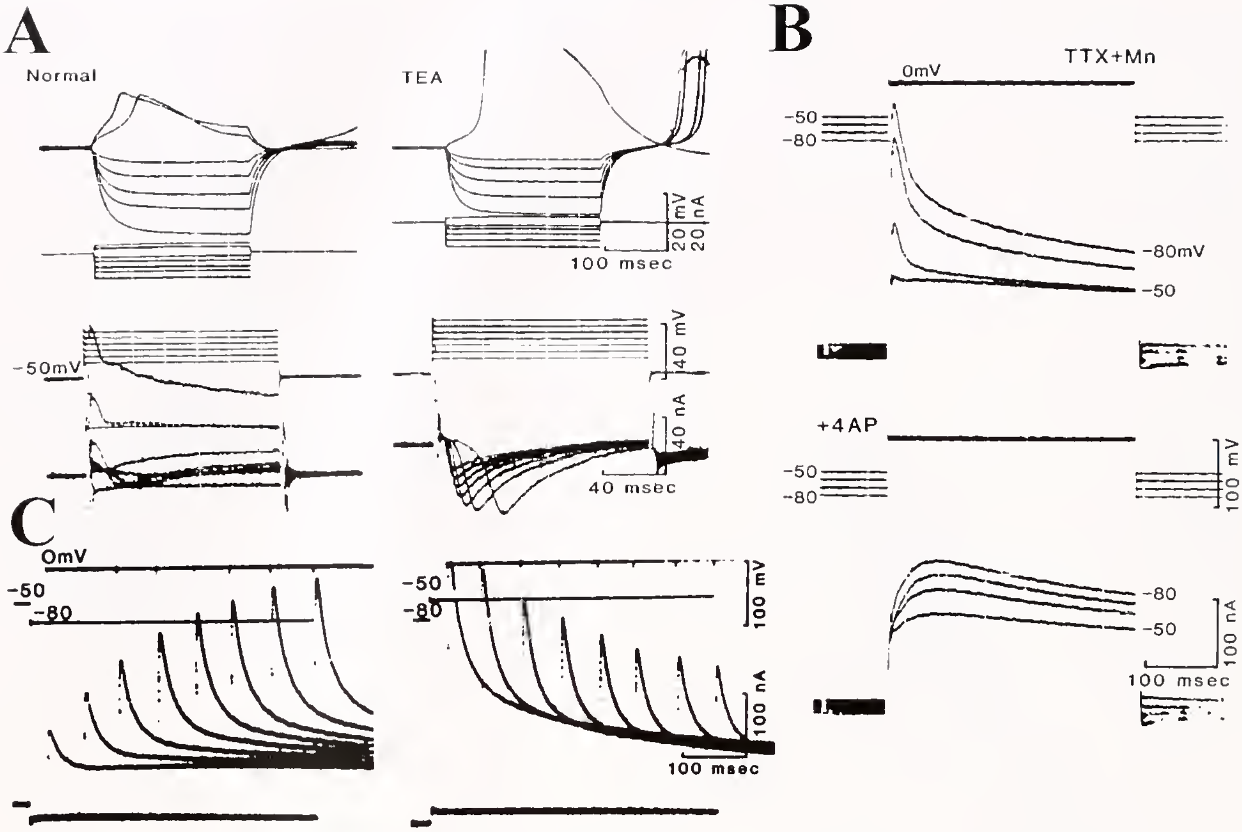

Figure 4. Voltage clamp analyses of ligatured *Homarus* cardiac ganglion large cells. (A) Responses of Cell 1 ligatured 200 μm from the soma and penetrated with separate recording and current-passing electrodes (upper traces, voltage; lower traces, current). Upper frames: responses to current clamps. Note the slowly increasing response to hyperpolarizing current. Depolarizing current produces driver potentials; in TEA (50 m*M*) their peak reaches 0 mV (as recorded from response to a brief pulse, not shown), and their duration is increased. Driver potentials are generated on cessation of hyperpolarizing current. Lower frames: membrane current responses (superimposed oscilloscope sweeps) to voltage clamps from −50 mV to successively more depolarized commands (left, −40 to −15 mV; right, −10 mV). In normal saline, inward current is indicated by downward notches, but outward currents dominate. A hyperpolarizing command (to −85 mV) indicates extent of leakage current. In TEA, outward current is largely inhibited, revealing inward current having nearly maximal amplitude but long latency at the smallest command. Resting potential, −50 mV. (B) Transient outward current (I_A) is selectively inhibited by 4-aminopyridine (4AP), leaving slowly inactivating outward current (I_K). Frames showing superimposed membrane current responses to voltage clamps from different V_h (−50 to −80 mV) to 0 mV in TTX (3×10^{-7} *M*) and Mn (4 m*M*) (above) or in TTX, Mn, and 4AP (4 m*M*) (below). Note the inhibition of the initial outward current peak in 4AP. Cell ligatured at 1.5 mm (resting potential, −45 mV). (C) Effect of conditioning clamps on I_A. In each frame, eight sweeps are superimposed; for each, the conditioning clamp remains on longer before evoking outward current by clamping to 0 mV. Left frame: effect of hyperpolarizing conditioning clamp from V_h = −50 to −80 mV. Rate and amount of I_A augmentation increase with increased hyperpolarization (not shown). Right frame: effect of subthreshold depolarizing conditioning clamp from V_h = −80 to −50 mV. The rate and magnitude of the decrease in I_A increase with increasing depolarization (not shown). Rate of onset and decay of individual responses is not affected by subthreshold potential changes. TTX (3×10^{-7} *M*) present throughout; cell ligatured at 1 mm (resting potential, −45 mV). (A, fig. 10, Tazaki and Cooke, 1983c; B, fig. 8 (modified), C, fig. 9 (modified), Tazaki and Cooke, 1986.)

clamp could be ensured in the *Homarus* ganglion by ligaturing. Without detailing the evidence, a brief summary of the conclusions from voltage-clamp analyses follows (see also Figs. 4 and 5 and legends). The depolarizing current that generates DPs arises from voltage-gated increased conductance to Ca^{2+} and the resulting inward Ca^{2+} current (I_{Ca}) (Figs. 4A, 5B). The amplitude of the DP is determined by the extent of Ca^{2+} channels available for activation. An examination of the effect of the holding potential (V_h) of the large-cell on the amplitude of I_{Ca} shows a maximum for a potential (−60 mV) close to the most hyperpolarized value observed during the afterpotential following a burst. Peak current is reduced to half or less at more hyperpolarized V_h. The amplitude of the DP is normally limited by the nearly

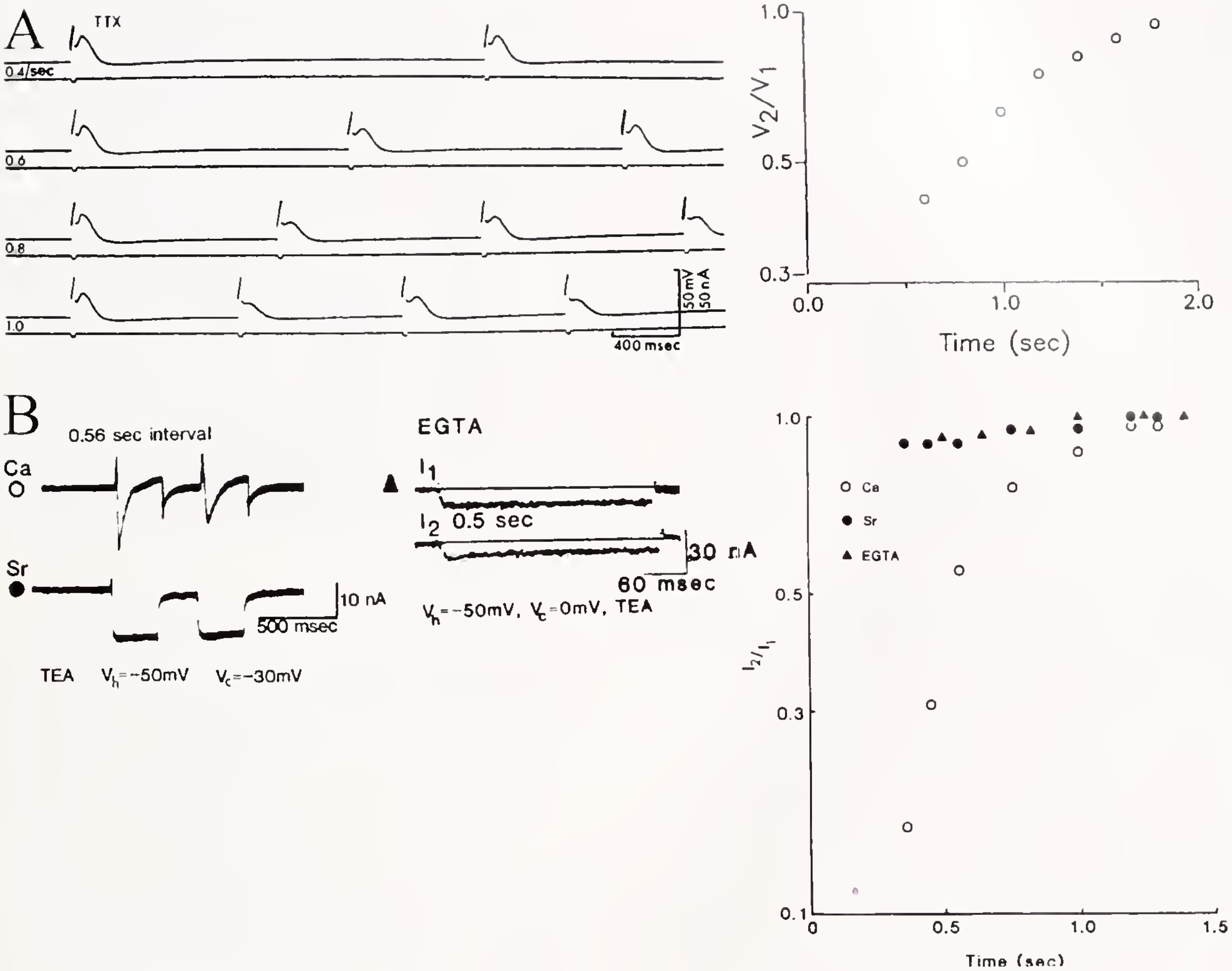

Figure 5. Characteristics of Ca^{2+} current influence driver potential form (*Homarus* large-cell somata, isolated by ligaturing). (A) Change of driver potential form with change of stimulus rate. Brief (25 ms) depolarizing current pulses (3 nA, depolarization downward, bottom trace of each pair) passed through an intracellular electrode elicit regenerative responses recorded with a second intracellular electrode in Cell 2 (resting potential, −55 mV). TTX ($3 \times 10^{-7} M$) is included in the superfused saline. Stimulus rate indicated for each pair of traces (moving photographic paper records from oscilloscope); first response follows an unstimulated interval of ≥30 s. Plot of the amplitude of the second response relative to the first (fully recovered) response *vs.* interval. At stimulus rates corresponding to rates of spontaneous bursting, driver potential responses are graded in amplitude. (B) Recovery of I_{Ca} from inactivation. Net inward current in response to an identical second clamp step given at varied intervals is compared with that to the first, given after ≥30 s rest. Left traces: examples of responses of the same isolated soma in standard and in Sr-substituted saline. Right traces: responses of another soma that had been injected with EGTA. Note that in contrast to the control records, the second responses in the absence of an increase in $[Ca^{2+}]_i$ are nearly equal to the first and show little decline of inward current during clamp steps. Semilogarithmic plot of normalized second response amplitude *vs.* interval for the somata providing the records shown above. Initial recovery in Ca saline occurs with $\tau \sim 640$ ms; complete recovery requires several seconds. (A, fig. 1. B, fig. 14, Tazaki and Cooke, 1990.)

simultaneous development, in response to depolarization, of the I_K conductance. If I_K is blocked with tetraethyl ammonium (TEA), I_{Ca} can produce overshooting potentials (Fig. 4A). Repolarization, and thus the duration of DPs, is the result of the interplay of I_K, inactivation of I_{Ca} primarily from intracellular accumulation of Ca^{2+} (Fig. 5B, D), and development of the Ca^{2+}-dependent I_{KCa}.

The voltage-clamping data are consistent with the major role of Ca^{2+} in mediating the DP depolarization (Figs. 4A, 5). However, a possible role of Na^+ in contributing to inward current remains unclear, with conflicting observations of the effects of its reduction or removal from the saline (Tazaki and Cooke, 1979c; Berlind, 1985, 1993). The differences may be attributable to the manner of substitution for Na^+ and to other differences in the experimental conditions.

The more rapidly decaying phase of the hyperpolarizing afterpotential following a CG driver potential (Fig. 3D) represents the deactivation of I_K with repolarization, while the slowly declining phase of the afterpotential probably reflects the sequestering or extrusion of Ca^{2+} to reduce I_{KCa}. A refractory period for initiation of DPs is imposed by a combination of the inactivation of I_{Ca} by intracellular accumulation of Ca^{2+} as well as the increased K^+ conductance from the Ca^{2+}-activation of I_{KCa}. When Na^+-mediated impulses are present (in non-TTX-treated preparations), a hyperpolarizing current from activation of electrogenic ion transport also contributes to the afterhyperpolarization (Livengood and Kusano, 1972; Livengood, 1983). With time, the threshold for response to a depolarizing stimulus decreases (1) due to progressive reduction of the ability to activate transient K^+ conductance (I_A) with decline of the afterhyperpolarization or pacemaker depolarization (or both); and (2) with progressing Ca^{2+} extrusion or sequestration, reduction of the I_{KCa} conductance and of the Ca^{2+}-mediated inactivation of I_{Ca} due to previous activity (Fig. 5B).

Driver potentials and similar intrinsic patterning potentials have proven to be a more labile response than generation of action potentials. This is easily explained by the relatively smaller current densities involved and the closely balanced interplay of conductances that govern their form. In crustaceans, for example, I_{Ca} observed under voltage-clamping conditions can be inactivated by raised intracellular Ca^{2+}. Thus it is not surprising that crustacean DP generation fails if neural damage causes Ca^{2+} entry from the saline, decreases input resistance, depolarizes the cell membrane (thereby increasing I_K), and increases leakage conductance. That DPs represent a delicate balance in the interplay of inward and outward currents is confirmed by observing the spontaneous initiation of DPs in previously quiescent preparations and the augmentation of their amplitude and duration after addition of TEA to inhibit I_K (Tazaki and Cooke, 1979c; Berlind, 1993) (see below for further discussion of spontaneity).

Changes of DP amplitude and duration with repetition rate are determined by characteristics of I_{Ca}

Analysis of the pharmacologically isolated Ca^{2+} current in ligatured somata suggests that its characteristics dominate the determination of DP amplitude and duration during repetitive activation. Figure 5 combines observations (from Tazaki and Cooke, 1990) on DP amplitude *vs.* DP repetition rate (A), and rates of recovery of I_{Ca} for the second of two stimuli (B). These follow closely parallel time courses; the slightly faster recovery of I_{Ca} studied with a pair of pulses is explained by a cumulative inactivation of I_{Ca} that occurs with repetitive activation. The role of intracellular Ca^{2+} accumulation as the main agent of inactivation is evidenced by the lack of inward current inactivation when Sr^{2+} substitutes for Ca^{2+} or the soma is injected with EGTA (Fig. 5B).

The accumulation of intracellular Ca^{2+} also activates I_{KCa}. This current is of small magnitude relative to I_{Ca} and I_K, and it influences primarily the rate of repolarization after a DP, or of a pacemaker depolarization during the equivalent of interburst intervals (Tazaki and Cooke, 1986).

Rhythmicity of Cardiac Ganglion Electrical Activity

The importance for survival of the animal of a reliable, rhythmic heartbeat cannot be exaggerated. The isolated cardiac ganglion, as the pacemaker and activator of heart contraction, has proven capable of sustaining robust, rhythmical motorneuron bursting when challenged with a variety of insults and perturbations.

Behavior of the cardiac ganglion as an oscillator

A number of studies demonstrate that small sustained currents passed into a large CG soma can alter the coordinated burst rate of the entire ganglion, while brief pulses of hyperpolarizing or depolarizing current can reset the bursting phase (Fig. 6A) (Watanabe and Bullock, 1960; Watanabe *et al.*, 1967b, in *Squilla*; Tazaki, 1972, in *Eriocheir*; Mayeri, 1973a, b, in *Homarus*; Matsui *et al.*, 1977, in *Panulirus*; Tazaki and Cooke, 1979a, and Benson, 1980, in *Portunus*). The coordinated response of the entire ganglion to such perturbation of a single neuron is ensured by the combination of electrotonic and probably reciprocal excitatory synaptic interactions among all the cells. The characteristics of I_{Ca} that determine the threshold and amplitude were discussed above and help to explain the reciprocity observed between burst rate (or interburst interval) and duration.

Autonomous rhythmicity: stretch responsiveness and pacemaker potentials

The basis of the spontaneity exhibited by isolated CG preparations is considered in this section. A question arises from the observation that an intact heart, if not still suspended by its elastic ligaments or stretched by internal perfusion, rapidly becomes quiescent. *In situ*, expansion and filling of the heart, mediated by the suspensory ligaments, probably aided under some conditions by contraction of alary muscles, stimulates heart contraction. The response to stretch or filling is undoubtedly mediated by the dendritic and collateral processes of the CG cells that ramify on heart muscle near the ganglion. Alexandrowicz (1932) pointed out that the terminations of these processes differed from the more peripheral neuromuscular junctions and noted their

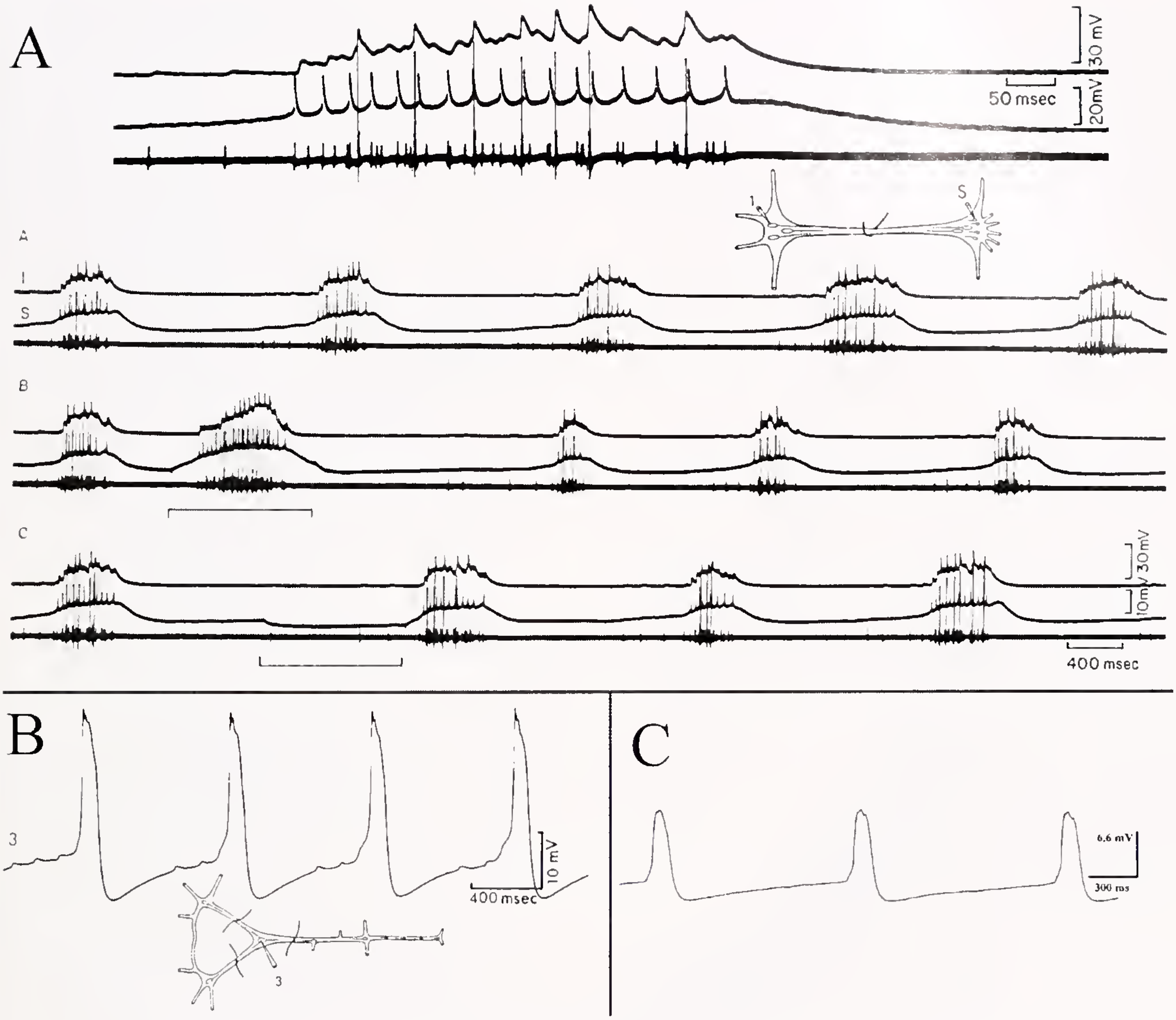

Figure 6. Spontaneous bursting characteristics. (A) Spontaneous bursting of the isolated *Portunus sanguinolentus* ganglion recorded intracellularly from a small cell (S), from an anterior large cell (1), and extracellularly (see inset). In the burst shown at expanded time-base (top), the correspondence between rapid depolarizations in the small cell, a small impulse in the extracellular record and, following a delay, a synaptic potential in the large cell may be observed. Very large spikes in the extracellular record (retouched) represent the synchronous firing of large cell axons and are seen as decremented impulses in the large soma. Records below show A, spontaneous bursting; B, the effect of passing depolarizing current (0.8 nA, upward bar) or C, hyperpolarizing current (0.8 nA *via* a bridge into the small cell). In B, note the premature initiation of a driver potential and burst in the large cell after extensive synaptic driving by the small cell, and the compensatory following delay and reduced burst durations. In C, note delay of the time of bursting until cessation of the current, followed by immediate resumption of normal bursting form and rate. (Tazaki and Cooke, 1979a, figs. 5B, 11.) (B) Spontaneous bursting in an isolated *Homarus* ganglion segment containing a single large-cell soma. The trace is a penwriter record from Cell 3 isolated by three ligatures at distances of *ca.* 1.5 mm from the soma (see diagram). The activity takes the form of pacemaker potentials giving rise to driver potentials with superimposed impulses. The source of the small deflections on the pacemaker potential is undetermined. Maximum hyperpolarization, −55 mV. (Tazaki and Cooke, 1983c, fig. 9.) (C) Spontaneous activity of Cell 1 isolated from *Carcinus maenas* for 1 day in culture (resting $V_m = -34$ mV). Trace shows small deflections riding on top of the driver potential that appear to be aborted spikes. (Saver *et al.*, 1999, fig. 9A.)

responsiveness to stretch. For an isolated heart, the plots of heart rate *vs.* perfusion pressure and the extent of contraction *vs.* perfusion pressure can be superimposed, and they increase along a hyperbolic curve (Maynard, 1960; see also Kuramoto and Ebara, 1984a, 1985). A possible role of hypoxia in governing heart rate has been proposed

(Wilkens, 1993). Although it is likely that stretch depolarizes the neuronal processes, as is well documented for crustacean stretch receptors (*e.g.*, Eyzaguirre and Kuffler, 1955), direct recordings of CG neuron responses to stretch of heart muscle appear not to have been obtained. In decapod hearts opened ventrally to expose the CG (Fig. 1A), contractions of the quiescent heart muscle can be elicited by probing sites in which CG dendrites are embedded (Alexandrowicz, 1932; Cooke, 1962; Hartline, 1967). Electrophysiological monitoring of the CG confirmed the absence of activity in the quiescent *Homarus* heart (Hartline, 1967).

The CG, after removal from the heart, exhibits the spontaneous, continuous, rhythmically recurring bursts of impulse activity described above. Intracellular recordings from the small, posterior neurons have consistently shown a slowly depolarizing pacemaker potential that develops after the post-burst hyperpolarization and leads to the initiation of the next burst (Fig. 6A) (Tameyasu, 1976; Tazaki and Cooke, 1979a, 1983c). In *Homarus*, a pacemaker potential is not usually seen in undamaged large cells, the DP and burst being initiated in them by synaptic driving mediated by impulses of the small-cell axons.

The question raised by the contrast in behavior of unstretched hearts and isolated ganglia is whether stretch-induced depolarization of dendrites and collateral processes normally induces bursting activity of the ganglion, while in isolated ganglia, the pacemaker potentials that functionally replace this stretch response in fact represent an injury current. It is possible that differences in the prominence of pacemaker potentials in recordings from large cells, even in the same species on the same equipment in the same laboratory (*e.g.*, Tazaki and Cooke, 1979a; Benson, 1980; Berlind, 1982), represent differences in techniques of ganglion isolation or of intracellular electrode penetration. During the hyperpolarization following bursts and the interburst interval, the gradual reduction in conductance to K^+ or in hyperpolarizing electrogenic active transport (Livengood and Kusano, 1972; Livengood, 1983) can lead to net depolarization as the balance of currents unmasks an outward injury or "leak" current mediated by nonspecific ionic conductances. The greater prominence of pacemaker potentials in small cells, and thus their role in initiating bursting, may be related merely to their smaller size. Observations thus far available provide no evidence for the participation of a hyperpolarization-activated cationic current, such as I_h, associated with pacemaker depolarization in several vertebrate pattern-generating neurons (reviews: Kaupp and Seifert, 2001; Santaro and Tibbs, 1999). Such a conductance would be expected to cause "sag" in the voltage responses to hyperpolarizing current. The opposite—increasing hyperpolarization indicating a decrease in conductance—occurs, as seen in Figure 4A.

Experiments in which segments of the ganglion that include single large cells are isolated have shown that such cells "spontaneously" produce rhythmical DPs (with superimposed impulse trains, if a trigger zone remains) when a pacemaker (injury?) current provides depolarizing drive (*e.g.*, Connor, 1969; Berlind, 1982; Tazaki and Cooke, 1983a, c). Cell 3 of *Homarus* has more often shown recurrent DPs after ligaturing than have Cells 1 or 2 (Fig. 6B), perhaps because it has three axons and requires three ligatures rather than one, which results in greater injury current. In cells that do not show a pacemaker (or injury) current, rhythmical activity appears if a sustained depolarizing current is passed into the neuron, or, often, if TEA is added to reduce residual K^+ current (Berlind, 1982). Recently, rhythmic "bursting" has been recorded from large cells isolated into primary culture from a crab (*Carcinus maenas*) CG (Saver *et al.*, 1999) (Fig. 6C). The observations on reduced preparations demonstrate that each of the large cells, at least, is intrinsically capable of generating rhythmic, patterned bursts given a nonspecific excitatory drive (*e.g.*, depolarization by injury current).

Synaptic Interactions

Excitatory chemically-mediated synapses

Studies such as those described earlier (*Electrophysiological anatomy*) confirmed that impulses of the posterior small-cell axons, which do not exit the ganglion, initiate activity of the large motor neurons and can thus be considered to have a pacemaker function (see also Mayeri, 1973a). Impulses of specific small-cell axons can be correlated with excitatory postsynaptic potentials (EPSPs) recorded intracellularly from large-cell somata (Fig. 6A) (Hagiwara and Bullock, 1957; Hartline and Cooke, 1969; Connor, 1969; Tazaki, 1971b; Friesen, 1975a, b, c; Tameyasu, 1987). In spiny lobsters, the most anterior of the small cells (Cell 6) provides a large initial EPSP, followed by one or more of reduced amplitude (antifacilitation); after a pause equivalent to the interburst interval, the next EPSP is augmented (Friesen, 1975c; Tameyasu, 1987). Synaptic interaction between large cells has been described in *Homarus* (Hartline, 1979). The observation that the bursts from small cells increase in rate and shorten when large-cell impulses (but not DPs) are eliminated by TTX applied anteriorly demonstrates an influence of large-cell activity on the small cells (Berlind, 1989). Synaptic potentials have not been observable in the intracellular recordings available from small cells. It may be that synapses occur at too great an electrotonic distance from the soma to be recorded. The possibility that non-impulse-mediated transmission occurs, as shown in the stomatogastric ganglion (Graubard *et al.*, 1983), has not been explored. Impulse-mediated EPSPs have been recorded in the large CG cells of several crab species (review: Hagiwara, 1961; Tazaki, 1967; Tazaki and Cooke, 1979a, 1983c; Berlind, 1982).

In the CG, as in crustacean ganglia generally, synaptic interactions occur in complex neuropils formed by collateral processes and branches from axons (Alexandrowicz, 1932, 1934, 1952; Ohsawa, 1972; Aizu, 1975; Hawkins and Howse, 1978; Mirolli *et al.*, 1987; Morganelli and Sherman, 1987). By injecting procion rubine and horseradish peroxidase (markers that can be distinguished by electron microscopy) into two of the large cells, Mirolli *et al.* (1987) demonstrated that synapses occur in all combinations among small and large cells in neuropil of the crab (*Portunus sanguinolentus*) ganglion (Fig. 8A). Electron microscopy of neuropil in *Homarus* showed symmetrical synapses (Morganelli and Sherman, 1987). In both studies, all synapses among CG cells had clear-cored vesicles, similar to those reported by others at excitatory neuromuscular synapses (Atwood, 1976). Synaptic contacts are also contributed within the neuropils by the inhibitory and excitatory extrinsic regulator fibers. These have morphologically different vesicles and, in turn, differ in morphology from those of the intrinsic cell synapses.

The identity of the synaptic transmitter or transmitters among the CG neurons remains under discussion. The small-cell synaptic effect on large cells is rapid and therefore must be mediated by a fast, ionotropic transmitter-receptor interaction. Current evidence now strongly supports glutamate as the intraganglionic transmitter. Applied glutamate depolarizes large CG neurons of *Homarus* by increasing conductance to monovalent cations (Cooke, 1966). Under voltage clamp (but not space clamp), glutamate increased conductance and produced an inward current that had a reversal potential of ~ -15 mV and was dependent nearly equally on K^+ and Na^+. Quisqualate was an even more potent agonist than glutamate, while L-aspartate was as potent as glutamate (Hashemzadeh-Gargari and Freschi, 1992).

Immunolabeling for glutamate-like reactivity in *Panulirus argus* (Fig. 7A, B) has shown a compound presumed to be glutamate in each of the CG cells and their axons. It has also revealed extensive terminations of the small cells in neuropil and in networks surrounding the large-cell somata and proximal neurites (Delgado *et al.*, 2001). Similar termination of labeled processes in the posterior of the ganglion near small cells is not reported. The demonstration of glutamate-like immunoreactivity in the axons and their terminations on the heart muscle supports the electrophysiological evidence for glutamate as a transmitter at the neuromuscular junctions (Benson, 1981). Additional evidence is the detection, by high-pressure liquid chromatography, of glutamate in extracted CG of the isopod *Bathynomus doederleini* and, in lower amounts, in heart muscle (Yazawa *et al.*, 1998). Modulation of CG activity by the extrinsic fibers and neurohormones is further discussed below.

Electrotonic coupling

An important element ensuring the coordinated bursting of the motor axons from the CG is the presence of electrotonic coupling among all of the neurons (Watanabe, 1958; Hagiwara *et al.*, 1959; Watanabe and Takeda, 1963; for small cells in crab CG, see Tazaki and Cooke, 1979a). The coupling passes slowly changing potentials effectively, but not rapidly changing ones such as impulses (the case of synchronization of large-cell impulse firing in the crabs *Portunus* and *Callinectes* was mentioned above). The coupling results in the effective spread of both pacemaker and driver potentials (or of imposed current) among the nine neurons, helping to ensure coordination of their bursting activity (Figs. 3C, D; 6A). Although electrophysiological recording demonstrates effective electrotonic coupling between large and small cells, dye coupling has not been demonstrated. Lucifer yellow injection into any of the large cells in *Portunus* resulted in the appearance of dye in all of the other large cells, but not in any of the small cells (Fig. 8D) (Tazaki and Cooke, 1983a). Similarly, injection of neurobiotin into any of the large cells of the *Panulirus* CG resulted in its appearance in all large cells, but not in any small cells (Delgado *et al.*, 2001). A search for images suggesting gap or tight junctions in neuropil has failed to detect them (*e.g.*, Mirolli *et al.*, 1987, in *Portunus*; Morganelli and Sherman, 1987, *Homarus*). Areas of membrane close apposition are observed among fine processes in neuropil and may serve as electrotonic junctions (Fig. 8A). The location of electrotonic connections on the small collateral processes would account for the low-pass filtering of electrotonic transmission observed electrophysiologically. These studies found that axo-axonic close appositions occur between the small-cell axons (Fig. 8B, C). Such appositions have also been described in CG of *Panulirus* (Ohsawa, 1972) and *Squilla* (Irisawa and Hama, 1965; Watanabe *et al.*, 1967a). In all of these species, the axo-axonic close appositions occur only between axons of small cells or pacemaker neurons.

Mechanisms for Modulation of Heart Function in Response to Physiological Demands

Crustacean heart muscle is similar to other crustacean muscle in being striated and innervated by multiple distributed boutons of the motor axons of most or all of the five CG motorneurons (Fig. 7B; Anderson and Smith, 1971; Kuramoto and Kuwasawa, 1980). Heart muscle fibers are electronically coupled end-to-end, unlike other muscle in the animal (*e.g.*, Anderson and Cooke, 1971). Neural activation of heart muscle shares most of the characteristics of neuromuscular physiology observed in other crustacean muscles: repetitive impulses produce EPSPs that facilitate extensively, and there is spatial as well as temporal summation of responses to impulses arriving from different

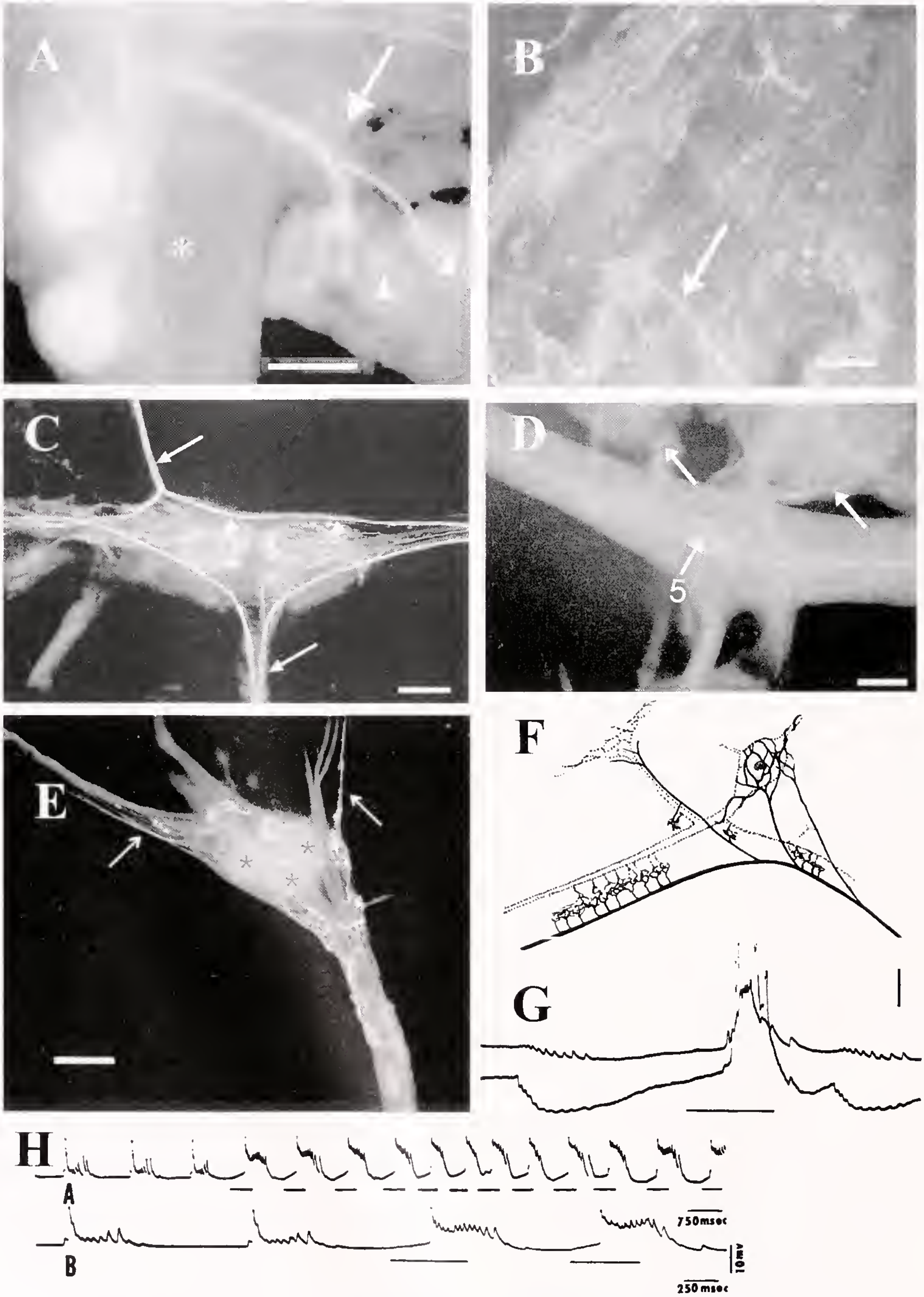

Figure 7. Chemically mediated synaptic interaction and effects of extrinsic regulator fibers. (A) Glutamate-like immunoreactivity in large cells of *Panulirus argus* cardiac ganglion. Fluorescence was present in the somata and neurites, but some major axons within the ganglion did not exhibit high levels of staining (asterisk marks site of an axon visible in neurobiotin fill, not shown). Calibration: 100 μm. (Delgado *et al.*, 2001, fig. 7B.)

motorneurons (van der Kloot, 1970; Anderson and Cooke, 1971; Kuramoto and Kuwasawa, 1980; Benson, 1981; Florey and Rathmayer, 1990; Brown, 1964a, b; for a summary and references to recording from crustacean and other arthropod hearts, see table 1 in Anderson and Cooke, 1971). The strength of contraction depends mainly on the degree to which the facilitated and summed EPSPs produce a sustained depolarization of the muscle (Orkand, 1962). Hence, the heart rate and strength of heart contractions are exquisitely sensitive to the rate, intraburst frequency, and also the patterning of impulses of each of the CG motorneurons. The effects of modulators on heart function can be largely explained by their effects on CG output.

Extrinsic fibers from the CNS

Numerous studies of semi-intact preparations have demonstrated the effects of electrically stimulating the extrinsic fibers to the heart (see Maynard, 1961, for references to early studies). Implanted electrodes and heart monitoring in lobsters (*Homarus*) have shown that the extrinsic nerves modify heart rate appropriately in relation to behavioral demands. For example, exercising on a treadmill accelerated the heart rate; bradycardia accompanied startle responses (Guirguis and Wilkens, 1995). In crayfish and lobsters the inhibitor and the two accelerator extrinsic nerves can be stimulated separately before they combine to enter the heart to reach the CG as the dorsal nerve (Fig. 1B, C). If the regulatory nerves are stimulated together, inhibition predominates.

Responses to stimulation of inhibitory fibers. The effectiveness of stimulation of the inhibitor depends on the rate of stimulation over a range of ~3–40 stimuli per second (review: Maynard, 1961; Cooke, 1962, in *Homarus*), with rapid, complete arrest for tens of seconds observed for rates of 20/s or higher. Inhibition is generally followed by a rebound acceleration of heart rate.

Stimulation of the extrinsic regulator nerve during intracellular recording from large CG neuronal somata produces postsynaptic potentials following, one for one, the stimuli to the axon, and repetitive stimulation causes the expected slowing of bursting (Fig. 7G). Inhibitory stimulation tends to move the membrane potential toward the most hyperpolarized levels observable during spontaneous bursting (Otani and Bullock, 1959; Shimahara, 1969a; Matsui *et al.*, 1973; Watanabe *et al.*, 1968, in *Squilla*). As first seen at the neuromuscular junction (Fatt and Katz, 1953), the reversal potential for the inhibitory conductance is close to the prevailing membrane potential and involves primarily an increase in conductance to Cl^- (Shimahara, 1969a). As for peripheral inhibition, γ-amino butyric acid (GABA) is a candidate for the inhibitory transmitter. In support of the earlier study (Shimahara, 1969a), voltage-clamping of large cells of *Homarus* indicated that GABA application increases conductance to Cl^- (Kerrison and Freschi, 1992).

A study of GABA-like immunoreactivity in *Panulirus* CG (Delgado *et al.*, 2001) found labeling in a single fiber entering the ganglion in the dorsal nerve from each side. These formed extensive processes in neuropil throughout

(B) Glutamate-like immunoreactive fibers could be followed over the surfaces of some muscles, where they often coursed in pairs (arrow) or triplets prior to diverging and producing a fairly uniform innervation of the muscle fibers. Calibration: 40 μm. (Courtesy J. Delgado.) (C) GABA-like immunoreactivity. A single fiber approaches the ganglion from each side *via* the dorsal nerve, bifurcates just before (lower arrow) or after (upper arrow) entering the trunk, giving rise to one large-caliber fiber directed toward the more rostral portions of the ganglion (left) and another directed caudally. Fine branches of both large GABA-immunoreactive fibers produced two spherical baskets of varicose fibers (arrowheads). Calibration: 100 μm. (Delgado *et al.*, 2001, fig. 2B.) Compare Fig. 1D. (D) Two GABA-like immunoreactive fibers that could be traced to their entry *via* their respective dorsal nerve in the anterior portion of the ganglion are seen to give rise to a spherical network of varicose fibers surrounding Cell 5. Additional branches exit the ganglion laterally (arrows) to adhering muscle bundles (compare Fig. 7F). Calibration: 100 μm. (Delgado *et al.*, 2001, fig. 3C.) (E) Tyrosine-hydroxylase-like immunoreactivity (TH-li) in crab (*Callinectes sapidus*) cardiac ganglion; the three motor neurons of the anterior end were filled with neurobiotin and labeled with rhodamine-avidin. A single TH-li fiber entered *via* each dorsal nerve (arrows) and gave rise to sparse varicose networks in the region of the motorneurons. Calibration: 100 μm. (Courtesy of T. Fort and M. W. Miller.) (F) Alexandrowicz' drawing of contacts by a dorsal nerve System 1 fiber with a large cell. A basket of processes surrounds the soma, processes accompany a dendrite, extensive contact occurs with collaterals in neuropil, and a branch extends onto heart muscle. (Alexandrowicz, 1932, Text-fig. 20; by permission of Company of Biologists, Ltd.) Compare Fig. 7D. (G) Intracellularly recorded responses to spontaneous activity of the extrinsic inhibitory fibers recorded in *Panulirus japonicus* cardiac ganglion. KCl electrodes intracellular to Cells 5 (upper) and 2 (lower trace). Trains of inhibitory postsynaptic potentials (IPSPs) corresponding between both cells are seen before and after the intrinsic burst. Net hyperpolarizations of the soma membrane with depolarizing IPSPs in the upper cell correspond to large net hyperpolarizations with hyperpolarizing IPSPs in the lower cell. Calibration: 5 mV, 500 ms. (Matsui *et al.*, 1973, fig. 2; reprinted with permission from Elsevier Science.) (H) Effects of repetitive stimulation of an acceleratory extrinsic regulator fiber on spontaneous burst activity, recorded intracellularly from a large cell of *Panulirus japonicus* cardiac ganglion. A, 30 Hz; B, 50 Hz during periods marked by the bars. (Shimahara, 1969b, fig. 2.)

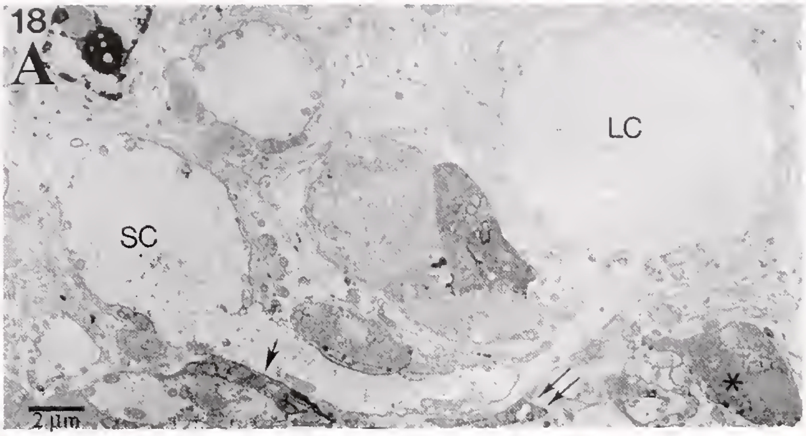
18
A
LC
SC
*
2 µm

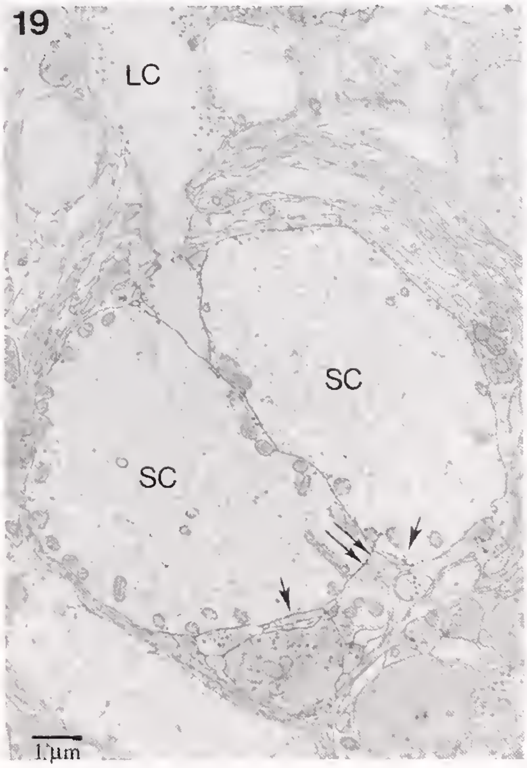
19
LC
SC
SC
SC
1 µm

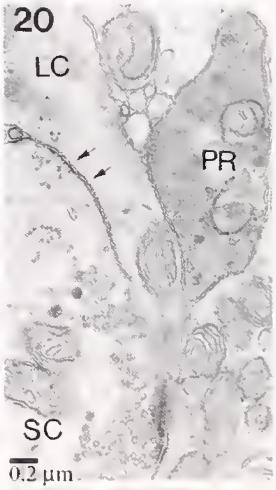
20
LC
PR
SC
0.2 µm

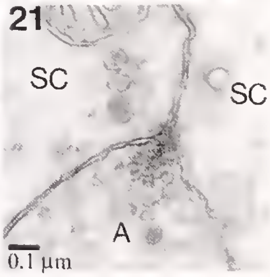
21
SC
SC
A
0.1 µm

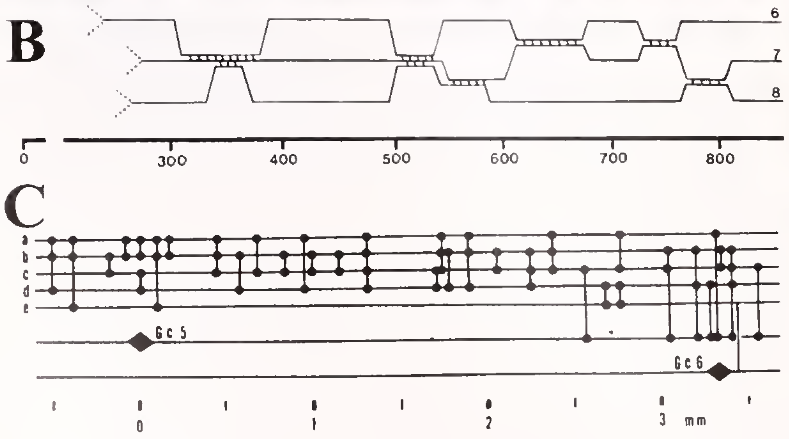
B
6
7
8
0
300
400
500
600
700
800
C
a
b
c
d
e
Gc 5
Gc 6
0
1
2
3 mm

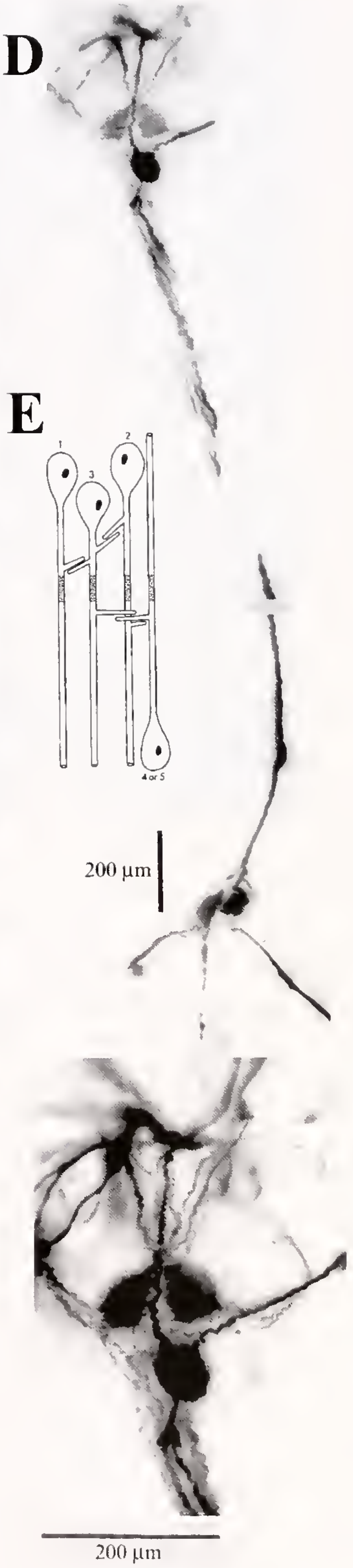
D
E
1
2
3
4 or 5
200 µm
200 µm

the ganglion, including a pericellular network around large-cell somata (Fig. 7C, D). Processes also were seen to ramify into the heart together with the large-cell dendrites presumed to be mediating stretch sensitivity. This morphology strikingly matches the description by Alexandrowicz (1932) of the System I fibers that he proposed were inhibitory (Figs. 1D, 7F).

In electron microscopy studies (Morganelli and Sherman, 1987, *Homarus*; Mirolli *et al.*, 1987, *Portunus*), synapses that were found extensively in neuropils throughout the CG had terminals with vesicles similar to those associated with inhibitory synapses on crustacean muscle (Atwood, 1976). These anatomical observations provide a structural basis for the observation that inhibitory regulatory fibers are more effective than excitatory ones (Maynard, 1961), as well as for the greater prominence of postsynaptic effects of inhibition as observed from CG somata recording.

Responses to stimulation of accelerator fibers. In his 1932 study, Alexandrowicz described a pair of smaller fibers ("System II") accompanying the larger fiber ("System I," now confirmed as inhibitory) in the dorsal nerve (Fig. 1B) bringing extrinsic innervation to the CG. He suggested that these represented the acceleratory inputs. They show sparse terminations in the ganglion and send processes into the cardiac muscle.

Effects of stimulation of the accelerator fibers have been difficult to characterize because the effectiveness of stimulation appears to fatigue rapidly, especially for stimulation of the more posterior of the two fibers. Bouts of stimulation resulted in slowly developing depolarization recorded in large CG neurons of *Panulirus* (Fig. 7H) (Shimahara, 1969b; see also Terzuolo and Bullock, 1958). Similar responses were seen in *Squilla* (Watanabe *et al.*, 1969) and in the isopod *Ligia exotica* (Sakurai and Yamagishi, 1998).

A recent advance toward resolving the nature of the transmitters for the accelerator fibers is the observation of immunoreactivity to an antibody raised against tyrosine hydroxylase in one of the two fibers reaching the CG from the CNS on each side in *Callinectes* (Fig. 7E) (Fort and Miller, 2001). Tyrosine hydroxylase catalyzes the addition of a hydroxyl to tyrosine to form dopamine. Together with earlier observations of the presence of a catecholamine in CG tissue (Ocorr and Berlind, 1983) and the excitatory effects of dopamine on the CG (see further below), the observations implicate dopamine as the transmitter for one of the accelerator fibers. Which of the two fibers shows the immunoreactivity is still unresolved.

Among many agents that have acceleratory effects on the CG, possibly the strongest candidate transmitter for the second fiber is acetylcholine (Freschi and Livengood, 1989; Sullivan and Miller, 1990; see further below). 5-Hydroxytryptamine (5HT) has been eliminated as a transmitter, at least for the more anterior of the accelerator fibers in *Homarus*. Response to 5HT could be blocked by previous application of D-lysergic acid diethylamide (LSD) without blocking the effects of nerve stimulation (Cooke, 1966). Responses to stimulation of the more posterior accelerator nerve were weak or absent, and hence no conclusion about inhibition by LSD was possible. Glutamate is unlikely, as

Figure 8. Morphology of synaptic and electrotonic contacts. (A) Contacts among neurons of *Portunus sanguinolentus* cardiac ganglion: Electron micrographs from Mirolli *et al.*, 1987. (18) Contact between the collateral process of a small-cell axon (SC) and that of an anterior large cell (LC). SC and LC processes are distinguishable by the density and distribution of their cytoskeletal elements. A process from a different anterior LC injected with procion rubine (PR) contacts the SC collateral process (arrow), and another (double arrows) contacts the collateral process of the LC. Asterisk marks another part of the PR-labeled process. (19) Contacts between two SC axons and between them and the collateral process of a LC. Other processes (arrows) are also in contact with the two SC axons. (20) Higher magnification of the contact between the LC and SC collateral processes shown in 18. Note the absence of glia at the region of contact. Arrows point to possible membrane close appositions between the two collaterals and that of the LC and a PR-stained process. (21) Synapse between a process with vesicles typical of intrinsic cell processes and two small axons (SC). (B) Schematic drawing of the chain of contacts made by three small-cell axons of the *P. sanguinolentus* ganglion as reconstructed from a complete series cut for light microscopy. The horizontal scale shows the distance (μm) of the contacts found in this series from a reference section in the anterior end of the trunk. (Mirolli *et al.*, 1987, fig. 17.) (C) Schematic representation of the side-junctions [close contacts] (vertical lines) between axons in the stomatopod (*Squilla oratorio*) cardiac ganglion in a section of the ganglion with ganglion cell (Gc) 5 and Gc 6. Lines a–e represent axons passing in the main trunk. (Watanabe *et al.*, 1967a, fig. 1; reproduced by copyright permission of The Rockefeller University Press.) (D) Reversed photomicrographs of a *P. sanguinolentus* cardiac ganglion injected with Lucifer yellow. The trunk was ligatured (central undyed portion), then Cell 3 in the anterior and Cell 4 in the posterior portion were intracellularly injected. In the photomontage of the entire ganglion, Cells 1 and 2 in the anterior cell group (top) and 5 in the posterior group are dimly visible as a result of dye transfer. Dye fails to diffuse within 100 μm of the ligature. Below: Detail of anterior cell group, overexposed to show web of fine processes near somata and parallel-running anteriorly directed processes. The four posterior small neurons are never visualized in such preparations. (Tazaki and Cooke, 1983a, fig. 1a, b; by permission of Springer-Verlag GmbH & Co. KG.) (E) Schematic showing sites of initiation of the synchronous motorneuron impulses (stippling) in the *P. sanguinolentus* ganglion (I. M. Cooke, unpublished.)

no glutamate-like immunoreactivity was detected in the dorsal nerves of *Panulirus* (Delgado *et al.*, 2001).

Neurohormonal modulation

Neurohormones of the pericardial organs. Alexandrowicz (1953) recognized that the webbings of neural tissue spanning the openings of the branchial sinuses in crabs were neurohemal structures and named them pericardial organs (POs). Given their location in the path of hemolymph returning from the gills and about to enter the heart, functions in modulating heart and circulatory performance were anticipated and soon established (Alexandrowicz and Carlisle, 1953). Homologous structures of lobsters are the ligamental nerve plexuses, now referred to as POs (Alexandrowicz, 1932, 1953; reviews: Cooke and Sullivan, 1982; Chaigneau, 1983). Neurohormones found in POs include the amines 5HT, dopamine (predominant in crabs), and octopamine (predominant in lobsters, Sullivan *et al.*, 1977). Peptides that have been identified include proctolin (Sullivan, 1979), crustacean cardioactive peptide (Stangier *et al.*, 1987; review, Dircksen, 1994) in crabs, and one or more FMRFamide-related peptides (Trimmer *et al.*, 1987; Mercier *et al.*, 1993). Most of these are also found elsewhere in the nervous system but have effects on central pattern generators and at neuromuscular junctions at concentrations consistent with their role as circulating neurohormones.

Neurohormonal effects on the heart. It would not be possible here to review the extensive literature from at least 80 years of experiments on the effects of tissue extracts, putative neurotransmitters, hormones, and pharmacological agents on crustacean hearts. More recent studies examining effects of PO extracts and hormones on nearly intact and *in situ* hearts suggest that each has subtly differing sites and modes of action in altering heart performance (Florey and Rathmeyer, 1978; Kuramoto and Ebara, 1984a, b, 1988, 1991; Krajniak, 1991; Yazawa and Kuwasawa, 1992; Mercier and Russenes, 1992; Wilkens and Mercier, 1993; Wilkens *et al.*, 1996; Saver and Wilkens, 1998; Saver *et al.*, 1998). Hormones may have differential actions on the valves governing hemolymph distribution to different parts of the animal *via* the several arteries (Kuramoto *et al.*, 1992), on alary muscles contributing to distension and refilling of the heart, on tension development by heart muscle, and on the neuromuscular junctions as well as on the CG. A broad generalization that is increasingly supported as further experiments are done is that each of the neurohormones orchestrates a subtly different coordinated response of the circulatory, respiratory, and probably other systems to homeostatic demands—as, for example, to anoxia, osmotic stress, trauma, and the like. In general, the PO neurohormones produce slowly developing and long-lasting increases in heart rate and strength of contraction.

Neurohormonal effects on the cardiac ganglion. Many, but clearly not all, of the effects of PO neurohormones on intact heart preparations can be accounted for by the effects observable on the efferent output from isolated CG. These hormones act on isolated CG preparations, generally increasing burst rate and usually increasing the frequency and number of impulses as well as the duration of the bursts. In an effort to distinguish sites and mechanisms of action within the CG, a localized droplet of hormone-containing saline was applied to a lobster CG held on an array of electrodes in oil (Fig. 2B) (Cooke and Hartline, 1975). Defining excitation of a neuron as an increase in the *average* firing frequency of one of its axons, the study found that sensitivity to neurohormones was greatest at the impulse-initiating zone and confined to the nonspiking, integrative, DP-generating, initial axon segment of each of the neurons; the somata themselves were not sensitive.

The droplet technique and the limited region of cell sensitivity made it possible to observe how neurohormone stimulation of a single cell altered the performance of the otherwise undisturbed cardiac ganglion (see Fig. 2 and legend). Stimulation of individual axons that more than doubled their average firing rate was accommodated into the bursting pattern by correspondingly much greater increases in the rate at which those axons fired within the burst (as in Fig. 2C). Analysis of the impulses of individual axons revealed that those not exposed to the hormone in their sensitive region retained a relatively unchanged *average* firing frequency. The overall burst rate was altered only if an application changed the average firing frequency of the acting pacemaker (small-cell) axon. The robustness of the integrating ganglion as a rhythmic heartbeat activator was emphasized by these observations: despite major perturbation of individual axon frequency, the rhythmical output of tightly grouped motor impulses was never disrupted.

The difference in effects of the neurohormones when the substances are applied regionally to primarily act on sensitive regions of small cells or large cells adds additional evidence for differences in the intrinsic properties of these cells and, particularly, in the nature of their DPs (proctolin: Miller and Sullivan, 1981; Sullivan and Miller, 1984; octopamine: Benson, 1984; dopamine: Miller *et al.*, 1984; Berlind, 1998 [see Fig. 9E], 2001a, b; 5HT: Kuramoto and Ebara, 1988; Kuramoto and Yamagishi, 1990; Berlind, 1998). An example is provided by observations on the effects of proctolin applied to the isolated *Homarus* CG (Miller and Sullivan, 1981; Sullivan and Miller, 1984). Application to small cells increased the duration and firing frequency of small-cell axons, implying an underlying increase in the duration and amplitude of the small-cell DPs. This effect was rapid (5–10 s), and it could be rapidly reversed. Application of proctolin limited to large-cell sensitive regions (Fig. 9A) caused a slowly developing increase in burst frequency accompanying a depolarization of up to

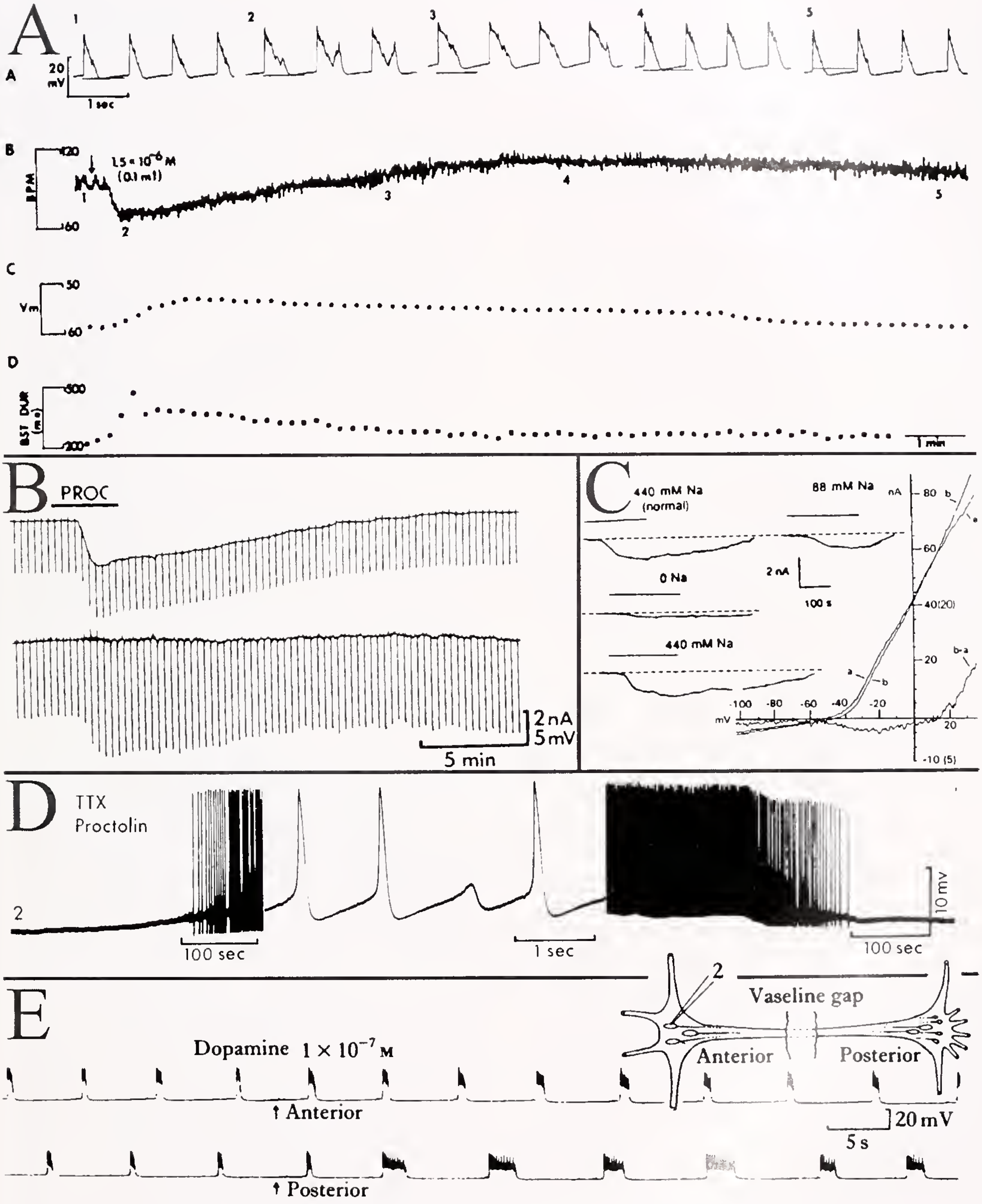

Figure 9. Neurohormonal effects on the isolated cardiac ganglion. (A–D) Responses to proctolin. (A) (A) Intracellular recording from motorneuron 1 ($V_m = -59$ mV) demonstrates the time-dependent proctolin effects. Samples of burst activity (1–5) were taken at the times indicated on the continuous plot of instantaneous burst frequency (B). A total of 14 min is shown. Time 1 is control. Within 10 s of application of a pulse of proctolin (1.5×10^{-6} *M*, 100 μl), burst frequency began to decline, (B) reaching a minimum of 65 per min after about 25 s. Concurrently, the ganglion exhibited a period of double bursting (Time 2). Considering each doublet as a

8 mV. By contrast with responses of the small cells, the response to a brief pulse of proctolin developed over minutes and lasted for tens of minutes.

For proctolin, there are observations suggesting its membrane-level mode of action. When proctolin was applied to *Homarus* large cells isolated by ligaturing and TTX treatment (Fig. 9C), the resulting depolarization could induce rhythmic driver potentials in previously quiescent cells (Sullivan and Miller, 1984). Tests of the cell input resistance (Fig. 9B) showed that proctolin increased resistance, and ionic substitution experiments indicated that this represented primarily a decrease in residual K^+ conductance. Removal of Na^+ decreased the magnitude of proctolin depolarization, which these authors interpreted as confirming that depolarization normally resulted from increased effectiveness of a "leak" conductance, for which Na^+ was the dominant ion in depolarizing the membrane. Similar observations (Fig. 9C) were made by Freschi (1989), but interpreted as representing activation of a Na^+ current.

The actions of crustacean cardioactive peptide and the FMRFamide-related peptides on isolated cardiac ganglia seem not to have been reported.

Are there intrinsic neuromodulators in the cardiac ganglion? There appear to be neurohumoral modulatory effects that arise within the CG and that supplement the actions of the fast-acting synapses. This possibility is raised by observations of the effects of acetylcholine, a catecholamine, and nitric oxide (NO) and by indications that these agents are present in the ganglia. Involvement of ACh is implied by the staining of neuropil showing the presence of acetylcholinesterase (E. Maynard, 1971); the ability of CG tissue to synthesize ACh (Sullivan and Miller, 1990); and sensitivity of the ganglia to ACh, with evidence for both nicotinic and muscarinic receptors (Freschi and Livengood, 1989). Responses of the CG to perfused ACh closely resemble those described above for proctolin (Freschi and Livengood, 1989; Sullivan and Miller, 1990). Synthesis of catecholamines by the CG and catecholamine fluorescence in large cells of *Homarus* have been reported (Ocorr and Berlind, 1983). However, tyrosine-hydroxylase-like immunoreactivity was not observed in cells of the *Callinectes* CG (Fig. 7E) (Fort and Miller, 2001). Large, dense-cored granules are present together with the predominant clear-cored vesicles in some neuropil synaptic profiles, suggesting that a catecholamine could be co-localized with another transmitter (Morganelli and Sherman, 1987). The CG is responsive to low concentrations of dopamine and octopamine, as mentioned above. The complexities of the responses to pharmacological agonists and antagonists of monoamine receptors of vertebrates when tested on the *Homarus* CG leave open the possibility of intrinsic neuromodulators (Berlind, 2001a, b). Recently, nitric oxide synthase has been

single burst, there was a coincident peak in burst duration (D). (C) Maximum V_m of Cell 1: the membrane potential underwent a slow depolarization that began about 15 s after application and became maximal after 1.5 min. Maximum frequency was obtained ~7 min after application of proctolin (Time 4). Burst frequency exceeded the control rate for the ensuing 7 min, returning to the control frequency concurrently with motorneuron repolarization (Time 5). (D) Burst duration: a peak during the period of double bursting corresponded with the time of minimal burst rate. (Sullivan and Miller, 1984, fig. 2; reprinted by permission of Wiley-Liss, Inc., a subsidiary of John Wiley & Sons, Inc.) (B) Manual voltage-clamp records demonstrate that proctolin effects a net inward current and an increase in the membrane input resistance. Transected Cell 2 ($V_m = -40$ mV) in saline containing TTX (3×10^{-7} *M*) and cadmium (4×10^{-4} *M*). The slow depolarizing response was continuously canceled by passage of inward current through a second electrode (top record). Additional constant-current hyperpolarizing test pulses applied throughout the response produced voltage deflections of increased magnitude (lower record), indicating an increase of the membrane input resistance [in this example by 50%]. (Sullivan and Miller, 1984, fig. 9B; reprinted by permission of Wiley-Liss, Inc., a subsidiary of John Wiley & Sons, Inc.) (C) Current-voltage plot of responses to slow (ramp, −140 to +40 mV in 44 s) changes of voltage under two-electrode voltage clamp of a ligated anterior large cell of the *Homarus* cardiac ganglion before (curve a) and in the presence of proctolin (1 μM, curve b). Curve b–a is the subtracted or proctolin-induced current. Records show reversible reduction in inward current observed (holding voltage at resting potential) during 1-μM proctolin perfusion (bars) in saline having reduced Na^+. (Freschi, 1989, fig. 4A, B; reprinted with permission from Elsevier Science.) (D) Intracellularly recorded responses of an anterior *Homarus* cardiac ganglion cell to proctolin. Spontaneity of the ganglion has ceased as a result of inclusion of 3×10^{-7} *M* TTX in the perfusate. At the start of the record, a 0.1-ml pulse of 10^{-7} *M* proctolin was introduced to the continuing perfusion stream (1 ml/min). Gradual depolarization (3 mV from −50 mV) leads to a sustained series of driver potentials (seen at increased chart speed in the center part of the record) and eventual return to quiescence. During the response, input resistance increased 30%. The duration of the record shown is 10.5 min. (K. Tazaki in Cooke, 1988, fig. 5; reprinted with permission from Elsevier Science.) (E) Dopamine effects on spontaneous bursting of the isolated crab (*Portunus sanguinolentus*) ganglion. All traces were recorded from a cell body at the anterior end of the ganglion, but any of the five large neurons would have shown a similar pattern of activity and an identical record of action potentials. The pair of traces shows the response to application of a 50-μl pulse of 10^{-7} *M* dopamine (arrows) to the anterior end of the ganglion (top trace of each pair) only or to the posterior end (lower trace) only. For all applications, burst duration is increased, but responses are greater for applications to the posterior region including the small cells. (Miller *et al.*, 1984, fig. 5; by permission of Company of Biologists, Ltd.)

localized in all nine neurons of a crab (*Cancer productus*) CG (Labenia *et al.*, 1998). This finding may suggest a role for amines and NO in modulating CG bursting activity *via* metabotropic receptors rather than via ionotropic receptors such as those of the fast excitatory synapses. A further question is whether the extrinsic regulatory fibers play a role in governing such neuromodulation.

Cellular mechanisms of neuronal modulation. Effects of the neurohormonal modulators have in common that they develop over tens of seconds and may last for tens of minutes in response to brief exposure. This time-course indicates a mode of action involving second-messenger-mediated modulation of ionic conductances. In support of this type of action, pericardial organ extracts were found to increase cAMP levels in *Homarus* cardiac ganglia, and pharmacological manipulations that increased cAMP mimicked the effect of PO extracts (Lemos and Berlind, 1981). Manipulations expected to increase NO levels increased cGMP levels and inhibited activity of the CG, while decreasing NO synthase activity decreased cGMP levels and increased burst frequency (Labenia *et al.*, 1998). The localization of neuronal regions sensitive to the neurohormonal modulators on the proximal axon segments (Cooke and Hartline, 1975) is consistent with the suggestion that these modulate conductances controlling the pacemaker (or leak) potentials, DPs, or both.

The Relation of Driver Potentials to Other Intrinsic Potentials

The recognition from study of the lobster CG (Watanabe, 1958) that the capability for patterned or bursting impulse activity is an intrinsic property of an individual neuron has now been extended to include a number of types of vertebrate neurons as well as neurons from nearly all major invertebrate groups. A sampling of the studies describing intrinsic DP-like properties underlying patterning include—besides other crustacean systems (see below)—insects (Hancox and Pitman, 1991); molluscs (Kramer and Zucker, 1985; Hurwitz and Susswein, 1996; Perrins and Weiss, 1998); annelids (Arbas and Calabrese, 1987); and vertebrates (reviews, Cooke and Stuenkel, 1985; Llinás, 1988; Kiehn and Eken, 1998). The list of vertebrate neurons includes Purkinje cells (Llinás and Sugimori, 1980); thalmic neurons (Dêschenes *et al.*, 1982; Llinás and Jahnsen, 1982); hypothalamic neurons (Legendre *et al.*, 1982); neurons responsible for lamprey swimming (Grillner *et al.*, 1991); neurons involved in respiratory rhythm generation (Rekling and Feldman, 1998); motorneurons (Hounsgaard and Kiehn, 1989, review; Hultborn, 1999); and subthalamic nucleus neurons (Beurrier *et al.*, 1999). The sustaining relevance of the studies on the CG lies in the remarkable similarity of the underlying ionic mechanisms observed in a major proportion of the pattern-forming neurons that have been analyzed.

Plateau potentials

Neurons of the decapod stomatogastric ganglion display an important variant of the intrinsic properties seen in the DPs of the CG neurons. Certain of the stomatogastric neurons exhibit plateau potentials (*e.g.*, Russell and Hartline, 1978, 1982; Dickinson and Nagy, 1983; Harris-Warrick *et al.*, 1992a; review, Hartline and Graubard, 1992; for voltage-clamp data see Golowasch and Marder, 1992; Zhang and Harris-Warrick, 1995). The term reflects their well-sustained, stable depolarized level (see Hartline, 1997, for diagnostic characteristics). A major embellishment is the control of the neuron's capability to produce plateau potentials by neurotransmitters, neuromodulators, or neurohormones (Russell and Hartline, 1984; Nusbaum *et al.*, 2001). Such modification provides different output patterning (*i.e.*, command of different behaviors) by the ganglion (reviews in Harris-Warrick *et al.*, 1992b). Modulation is also found in other crustacean pattern generators (*e.g.*, the crab ventilatory system, DiCaprio, 1997) and in vertebrate motorneurons (Hounsgaard and Kiehn, 1989; review, Hultborn, 1999) and subthalamic nucleus neurons (Beurrier *et al.*, 1999). A further embellishment on the stereotyped DP is the possibility of controlling plateau duration. Plateau potentials, like DPs (Tazaki and Cooke, 1979b), can be, and often are, terminated by hyperpolarizing current such as produced by an inhibitory synaptic potential. As with DPs, plateau potentials initiate and pattern the action potentials produced by the neuron.

Reviewing common characteristics detailed for the DPs of the CG above that have been associated with the presence of intrinsic pattern-forming capability as found in neurons from a diversity of animals and neurons, they include the following:

- Appropriate depolarization (*e.g.*, a pacemaker, synaptic potential, or imposed depolarizing current) initiates a regenerative, slowly rising, sustained (tenths of seconds to tens of seconds), depolarizing (to above impulse threshold) potential, in a majority, resulting from activation of a slowly inactivating or non-inactivating I_{Ca}. Application of TTX to silence impulse initiation as well as impulse-mediated synaptic input reveals the form of these potentials. However, DP- or plateau-like potentials involving Na^+-inward current rather than, or as well as, I_{Ca} have been described ([for CG, see above], *e.g.*, Angstadt and Choo, 1996, leech Retzius neurons; Kim and McCormick, 1998, ferret perigeniculate neurons; Su *et al.*, 2001, rat hippocampal CA1 pyramidal cells).
- The amplitude and duration of the depolarization is shaped by the suite of K^+ conductances present and by the inactivation mechanisms of the inward currents. These include both voltage- and Ca^{2+}-dependent components. The depolarization can be terminated by

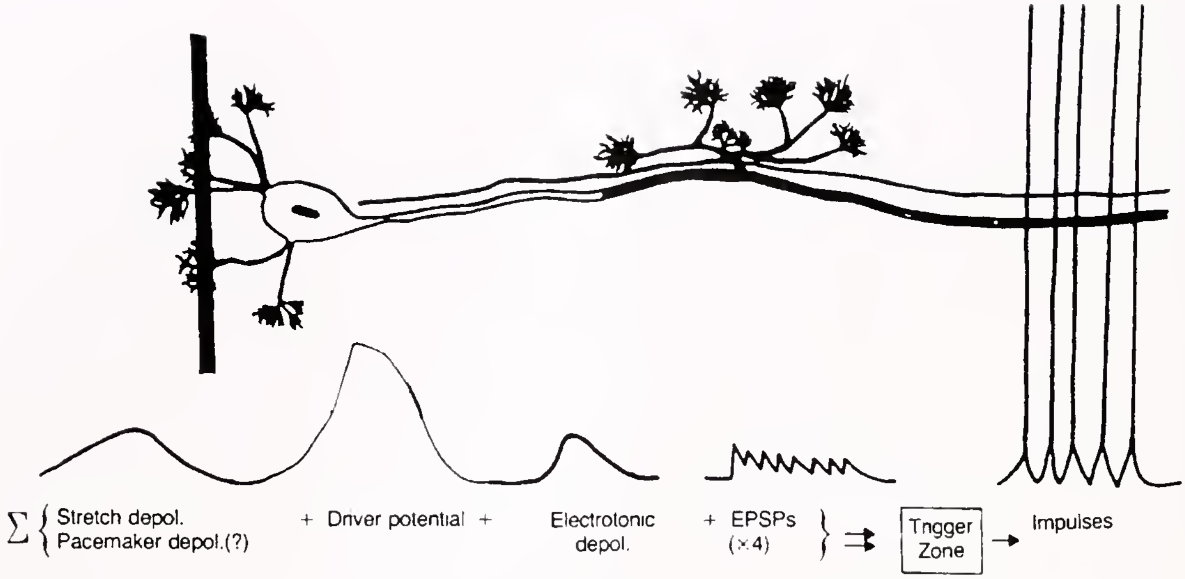

Figure 10. Anatomical segregation of function in cardiac ganglion neurons. Diagram depicting the supposed integrative region of the soma and proximal axon, which is not capable of impulse initiation. In that region, pacemaker depolarizations (if present), inputs of stretch-sensitive dendrites, and electrotonic and chemical synaptic inputs (on axon collateral processes) all sum with the regenerative, non-propagating driver potential to produce a flow of current through the membrane of the more distal axonal trigger zone. The current initiates and influences the temporal patterning of the action potentials that propagate distally. (Benson and Cooke, 1984, fig. 6; reprinted with permission from Elsevier Science.)

hyperpolarizing current (from inhibitory synaptic input or imposed current).

- The pattern-forming potentials often exhibit a relatively refractory period that may include an afterhyperpolarization. The afterpolarization may activate currents (see below) contributing toward a slow pacemaker depolarization that in turn initiates the intrinsic potential, thus contributing to rhythmic pattern generation.

Rhythmicity

Intrinsic pattern-forming characteristics combined with a pacemaking mechanism or source of sustained depolarizing drive result in rhythmic bursting or pattern formation, as exhibited in the isolated CG. One of the ionic mechanisms giving rise to pacemaker potentials is hyperpolarization-activated cationic current, now generally referred to as I_h, which has been implicated in many of the vertebrate neurons studied (reviews: Santoro and Tibbs, 1999; Lüthi and McCormick, 1998; Kaupp and Seifert, 2001). As mentioned above, I_h has not been observed in the CG motorneurons. It has been reported in a crab stomatogastric motorneuron (Kiehn and Harris-Warrick, 1992). I_h is modulated by agents that alter cyclic nucleotides such as 5HT and other amines and peptides, suggesting a mechanism by which neuromodulators influence rhythmic pattern generators.

Another current that may contribute to pacemaking is slowly inactivating or persistent Na^+ current (I_{NaP}) (*e.g.*, Hsiao *et al.*, 1998; Brumberg *et al.*, 2000). By contrast, in subthalamic neurons, activation of I_{NaP} changes burst firing to single-spike activity (Beurrier *et al.*, 2000). Activation or enhancement of an I_{NaP}-like current has been proposed as a mechanism of action of neuromodulators of the crustacean CG, as discussed above (Freschi, 1989; Freschi and Livengood, 1989).

Recapitulation and Conclusions

Economy in neuronal cell numbers is achieved in arthropods by a cellular architecture that permits each cell to serve several functions. Thus, CG cells are stretch receptors, integrative interneurons, and, in the case of the large cells, motorneurons as well; they may also be endowed with the capability for spontaneity and pacemaking. The sensory and integrative functions occur in a region—the soma and initial axon segment and its collateral processes—segregated from the impulse-propagating distal axon (Fig. 10). A trigger zone converts the integrated signal to conducted, all-or-none, Na^+-mediated impulses whose frequency and pattern reflect the form of the integrated depolarizing potential generated in the initial axon segment. The presence of a combination of ionic conductances in the integrating zone that give rise to the regenerative but graded driver potential (or in other ganglia, plateau potential) enables the neuron to produce a specific form of patterned impulses that can be largely independent of the excitatory input. A combination of three factors—a voltage-gated Ca^{2+} conductance that is inactivated by the resulting entry of Ca^{2+}, fast and slowly inactivating voltage-dependent K^+ conductances, and finally a K^+ conductance initiated by the rise of internal Ca^{2+}—imposes a refractory period. The depth and duration of this refractory period reflects the level of previous activity. The removal or sequestering of Ca^{2+} reduces K^+ conductance, allowing increased influence of depolarizing currents (stretch, pacemaker, leak, or synaptic), and removes I_{Ca} inactivation, thus reducing threshold for the DP. Together the behaviors of these ionic conductances account for rhythmic recurrence of DPs and bursting, given general excitatory drive. The conductances also shape the amplitude and duration of DPs as a function of the rate of recurrence; they account for the reciprocity between burst rate and duration, and for the advanced or delayed phasing of the burst cycle when perturbed.

The CG shows remarkable reliability in providing rhythmic bursts of motor impulses in the face of a variety of imposed experimental perturbations and insults, and theoreticians have used it to model fault-tolerant networking (*e.g.*, Sivan *et al.*, 1999). In the CG, reliability surely arises from the intrinsic ability for rhythmic burst formation of each neuron combined with the extensive interconnection among all the neurons that ensures coordination of their activity. Electrotonic coupling links all cells of the ganglion and passes slowly changing potentials such as stretch-induced or pacemaker potentials and DPs, and these can continue to recur synchronously and rhythmically when impulse propagation has been eliminated with TTX. Each of the cells provides fast, chemically mediated excitatory synaptic input to, probably, all other cells. While these synapses are known to be impulse-mediated, the possibility that some are also active in the absence of impulses has not been examined.

Although the similarity among the nine neurons (in the case of most decapods) perhaps provides reliability by means of redundancy, each exhibits consistent differences in the detailed pattern of its impulse bursts. In the isolated CG, small cells have prominent pacemaker depolarizations and a DP of low amplitude and long duration. This form of DP thus generates a long burst of impulses at relatively steady frequency which mediates a sustained barrage of excitatory input to the motorneurons. Large cells exhibit a larger amplitude and a shorter DP, and they produce a burst having an initial high frequency of impulse firing, efficacious in rapidly depolarizing and initiating contraction in the heart muscle fibers. Other more subtle differences among the CG neurons are also documented. Additional differences become evident in considering the modulation of ganglion output by the several neurohormones secreted from the pericardial organs. Each neurohormone produces a different change of CG output and, further, has differing effects on small and large cells. The anatomical segregation of function within neurons is again observed with the restriction of responsiveness to neurohormones to the nonspiking initial axon segment.

The apparent simplicity of the CG has proven somewhat illusory. The above review will make obvious that there are many unresolved questions. To list a few:

- How is stretch (heart filling) transduced and integrated to influence the activity of the CG neurons? The existence and importance of stretch receptiveness is well documented and presumably provides the ability of the CG to monitor and adjust its activity to the results of its actions as well as to other external influences and thus function as an autonomous control system.
- Are there specific currents providing depolarizing pacemaker drive?
- Does non-impulse-mediated synaptic chemical transmission occur among CG neurons as, for example, in the stomatogastric ganglion (Graubard *et al.*, 1983)?
- Where and how do putative neuromodulators intrinsic to the CG such as ACh and NO act?
- What is the identity of the transmitter or transmitters released from the other extrinsic regulator fiber?
- Which conductances are involved in CG modulation by the various known and proposed neurohormones or neuromodulators?
- Which possible second messenger systems participate in modulation of CG activity, how extensive are they, and what roles do they play?

New immunoreagents invite further studies exploiting the resolving capabilities of confocal microscopy for localization of receptors and enzyme systems in the CG. The availability of voltage-clamping analyses of the ionic currents, analyses of impulse-mediated synaptic interactions, and dye-fills that provide anatomical detail invite application of modeling, as in the case of the stomatogastric ganglion, to discover missing components in the available information. Demonstration that it is feasible to isolate CG neurons in primary culture and that they retain their ability to produce rhythmical bursts and respond to neurohormones (Saver *et al.*, 1999) opens the possibility for examining some of these questions free of the complexities presented by the interactions among the neurons in even this small, "simple" ganglion.

A candidate for the most significant contribution to neurobiology of studies on crustacean cardiac ganglia would be the unambiguous demonstration that a single neuron can be endowed with the intrinsic capability of providing an output of distinctively patterned impulses in response to nonpatterned, general excitation or single stimuli. Detailed analyses of the electrophysiological underpinning of this capability are important components of the demonstration. These observations have suggested new, much simpler explanations for the generation of complex neuronal patterns, including mechanisms by which neurohormonal and other modulators can alter these patterns and the behaviors they direct.

Acknowledgments

Professor John H. Welsh requires acknowledgement as a generative force in proposing physiological studies of crustacean cardiac ganglia and their neurohumoral modulation to receptive students (Donald Maynard, D. K. Hartline, and the author). Work in the author's laboratory reflects the intellectual input, technical skill, and hard work of many collaborators: D. K. Hartline, A. Berlind, M. E. Anderson, K. Tazaki, J. Benson, M. W. Miller, M. Mirolli, S. Talbot, R. E. Sullivan. Martha W. Goldstone, B. Haylett, and S. Grau provided valuable technical assistance. The work was supported by grants from the National Science Foundation (GB4315, GB8201, BS81-07289) and the National Institutes of Health (NS-11808), and by grants to the Békésy Laboratory of Neurobiology by the Ida Russell Cades Fund of the University of Hawaii Foundation.

T. Fort and M. W. Miller kindly provided an unpublished figure (Fig. 7E). I thank D. K. Hartline for suggestions on the manuscript; C. Kosaki and H. Roop for assistance in preparing the reference list, and E. Garcia for help with the figures.

Permission to reproduce the figures was kindly provided by the authors and the journal copyright holders.

Literature Cited

Aizu, S. 1975. Fine structure of cardiac ganglion trunk in prawn, *Penaeus japonicus* Bates. *Tissue Cell* **7:** 433–452.

Alexandrowicz, J. S. 1932. Innervation of the heart of the Crustacea. I Decapoda. *Q. J. Microsc. Sci.* **75:** 182–249.

Alexandrowicz, J. S. 1934. The innervation of the heart of Crustacea. II Stomatopoda. *Q. J. Microsc. Sci.* **76:** 511–548.

Alexandrowicz, J. S. 1952. Innervation of the heart of *Ligia oceanica*. *J. Mar. Biol. Assoc. UK* **31:** 85–96.

Alexandrowicz, J. S. 1953. Nervous organs in the pericardial cavity of the decapod Crustacea. *J. Mar. Biol. Assoc. UK* **31:** 563–580.

Alexandrowicz, J. S., and D. B. Carlisle. 1953. Some experiments on the function of the pericardial organs in Crustacea. *J. Mar. Biol. Assoc. UK* **32:** 175–192.

Anderson, M. E., and I. M. Cooke. 1971. Neural activation of the heart of the lobster *Homarus americanus*. *J. Exp. Biol.* **55:** 449–468.

Anderson, M. E., and D. S. Smith. 1971. Electrophysiological and structural studies on the heart muscle of the lobster *Homarus americanus*. *Tissue Cell* **3:** 191–205.

Angstadt, J. D., and J. J. Choo. 1996. Sodium-dependent plateau potentials in cultured Retzius cells of the medicinal leech. *J. Neurophysiol.* **76:** 1491–1502.

Arbas, E. A., and R. L. Calabrese. 1987. Ionic conductances underlying the activity of interneurons that control heartbeat in the medicinal leech. *J. Neurosci.* **7:** 3945–3952.

Atwood, H. L. 1976. Organization and synaptic physiology of crustacean neuromuscular systems. *Prog. Neurobiol.* **7:** 291–391.

Benson, J. A. 1980. Burst reset and frequency control of the neuronal oscillators in the cardiac ganglion of the crab, *Portunus sanguinolentus*. *J. Exp. Biol.* **87:** 285–313.

Benson, J. A. 1981. Synaptic and regenerative responses of cardiac muscle fibers in the crab, *Portunus sanguinolentus*. *J. Comp. Physiol. A* **143:** 349–356.

Benson, J. A. 1984. Octopamine alters rhythmic activity in the isolated cardiac ganglion of the crab, *Portunus sanguinolentus*. *Neurosci. Lett.* **44:** 59–64.

Benson, J. A., and I. M. Cooke. 1984. Driver potentials and the organization of rhythmic bursting in crustacean ganglia. *Trends Neurosci.* **7:** 85–91.

Berlind, A. 1982. Spontaneous and repetitive driver potentials in crab cardiac ganglion neurons. *J. Comp. Physiol. A* **149:** 263–276.

Berlind, A. 1985. Endogenous burst-organizing potentials in two classes of neurons in the lobster cardiac ganglion respond differently to alterations in divalent ion concentration. *J. Comp. Physiol. A* **157:** 845–856.

Berlind, A. 1989. Feedback from motor neurones to pacemaker neurones in lobster cardiac ganglion contributes to regulation of burst frequency. *J. Exp. Biol.* **141:** 277–294.

Berlind, A. 1993. Heterogeneity of motorneuron driver potential properties along the anterior-posterior axis of the lobster cardiac ganglion. *Brain Res.* **609:** 51–58.

Berlind, A. 1998. Dopamine and 5-hydroxytryptamine actions on the cardiac ganglion of the lobster, *Homarus americanus*. *J. Comp. Physiol. A* **182:** 363–376.

Berlind, A. 2001a. Monoamine pharmacology of the lobster cardiac ganglion. *Comp. Biochem. Physiol. C* **128:** 377–390.

Berlind, A. 2001b. Effects of haloperidol and phentolamine on the crustacean cardiac ganglion. *Comp. Biochem. Physiol. C* **130:** 85–95.

Beurrier, C., P. Congar, B. Bioulac, and C. Hammond. 1999. Subthalamic nucleus neurons switch from single-spike activity to burst-firing mode. *J. Neurosci.* **19:** 599–609.

Beurrier, C., B. Bioulac, and C. Hammond. 2000. Slowly inactivating sodium current (I_{NaP}) underlies single-spike activity in rat subthalamic neurons. *J. Neurophysiol.* **83:** 1951–1957.

Brown, H. F. 1964a. Electrophysiological investigations of the heart of *Squilla mantis*. I. The ganglionic nerve trunk. *J. Exp. Biol.* **41:** 689–700.

Brown, H. F. 1964b. Electrophysiological investigations of the heart of *Squilla mantis*. II. The heart muscle. *J. Exp. Biol.* **41:** 701–722.

Brumberg, J. C., L. G. Nowak, and D. A. McCormick. 2000. Ionic mechanisms underlying repetitive high-frequency burst firing in supragranular cortical neurons. *J. Neurosci.* **20:** 4829–4843.

Chaigneau, J. 1983. Neurohemal organs in *Crustacea*. Pp. 53–89 in *Neurohemal Organs of Arthropods: Their Development, Evolution, Structures, and Functions*, A. P. Gupta, ed. Charles C. Thomas, Springfield, IL.

Connor, J. A. 1969. Burst activity and cellular interaction in the pacemaker ganglion of the lobster heart. *J. Exp. Biol.* **50:** 275–295.

Cooke, I. M. 1962. The neurohumoral regulation of the crustacean heart. Ph.D. dissertation, Harvard University.

Cooke, I. M. 1966. The sites of action of pericardial organ extract and 5-hydroxytryptamine in the decapod crustacean heart. *Am. Zool.* **6:** 107–121.

Cooke, I. M. 1988. Studies on the crustacean cardiac ganglion. *Comp. Biochem. Physiol. C* **91:** 205–218.

Cooke I. M. 2002. Physiology of the crustacean cardiac ganglion. In *The Crustacean Nervous System*, Vol. 2, K. Wiese, ed. Springer-Verlag, Berlin. In press.

Cooke, I. M., and D. K. Hartline. 1975. Neurohormonal alteration of integrative properties of the cardiac ganglion of the lobster *Homarus americanus*. *J. Exp. Biol.* **63:** 33–52.

Cooke, I. M., and E. L. Stuenkel. 1985. Electrophysiology of invertebrate neurosecretory cells. Pp. 115–164 in *The Electrophysiology of the*

Secretory Cell, A. M. Poisner and J. M. Trifaró, eds. Elsevier, Amsterdam.

Cooke, I. M., and R. E. Sullivan. 1982. Hormones and neurosecretion. Pp. 205–290 in *The Biology of Crustacea, Vol. 3,* D. Bliss, H. Atwood, and D. Sandeman, eds. Academic Press, New York.

Delgado, J., E. Oyola, and M. W. Miller. 2001. Localization of GABA- and glutamate-like immunoreactivity in the cardiac ganglion of the lobster *Panulirus argus. J. Neurocytol.* **29:** 605–619.

Dêschenes, M., J. P. Roy, and M. Steriade. 1982. Thalamic bursting mechanisms: an inward slow current revealed by membrane hyperpolarization. *Brain Res.* **239:** 289–293.

DiCaprio, R. A. 1997. Plateau potentials in motor neurons in the ventilatory system of the crab. *J. Exp. Biol.* **200:** 1725–1736.

Dickinson, P. S., and F. Nagy. 1983. Control of a central pattern generator by an identified modulatory interneurone in Crustacea. II. Induction and modification of plateau properties in pyloric neurones. *J. Exp. Biol.* **105:** 59–82.

Dircksen, H. 1994. Distribution and physiology of crustacean cardioactive peptide in arthropods. Pp. 139–148 in *Perspectives in Comparative Endocrinology.* National Research Council of Canada, Ottowa.

Eyzaguirre, C., and S. W. Kuffler. 1955. Processes of excitation in the dendrites and in the soma of single isolated sensory nerve cells of the lobster and crayfish. *J. Gen. Physiol.* **39:** 87–119.

Fatt, P., and B. Katz. 1953. The effect of inhibitory nerve impulses on a crustacean muscle fibre. *J. Physiol. (Lond.)* **121:** 374–389.

Florey, E., and M. Rathmayer. 1978. The effects of octopamine and other amines on the heart and on neuromuscular transmission in decapod crustaceans: further evidence for a role as neurohormone. *Comp. Biochem. Physiol. C* **61:** 229–237.

Florey, E., and M. Rathmayer. 1990. Facilitation and potentiation of transmitter release at neuromuscular synapses in the heart of *Squilla mantis*: functional and theoretical implications. Pp. 330–337 in *Frontiers in Crustacean Neurobiology, Advances in Life Sciences,* K. Wiese, W.-D. Krenz, J. Tautz, H. Reichert, and B. Mulloney, eds. Birkhäuser Verlag, Basel.

Fort, T. J., and M. W. Miller. 2001. Functional organization of the cardiac system of the blue crab *Callinectes sapidus*: gabaergic and catecholaminergic regulatory fibers. *Soc. Neurosci. Abstr.* **27:** 2500.

Freschi, J. E. 1989. Proctolin activates a slow, voltage-dependent sodium current in motoneurons of the lobster cardiac ganglion. *Neurosci. Lett.* **106:** 105–111.

Freschi, J. E., and D. R. Livengood. 1989. Membrane current underlying muscarinic cholinergic excitation of motoneurons in lobster cardiac ganglion. *J. Neurophysiol.* **62:** 984–995.

Friesen, W. O. 1975a. Physiological anatomy and burst pattern in the cardiac ganglion of the spiny lobster *Panulirus interruptus. J. Comp. Physiol.* **101:** 173–189.

Friesen, W. O. 1975b. Synaptic interactions in the cardiac ganglion of the spiny lobster *Panulirus interruptus. J. Comp. Physiol.* **101:** 191–205.

Friesen, W. O. 1975c. Antifacilitation and facilitation in the cardiac ganglion of the spiny lobster *Panulirus interruptus. J. Comp. Physiol.* **101:** 207–224.

Golowasch, J., and E. Marder. 1992. Ionic currents of the lateral pyloric neuron of the stomatogastric ganglion of the crab. *J. Neurophysiol.* **67:** 318–331.

Graubard, K., J. A. Raper, and D. K. Hartline. 1983. Graded synaptic transmission between identified spiking neurons. *J. Neurophysiol.* **50:** 508–521.

Grillner, S., P. Wallén, and L. Brodin. 1991. Neuronal network generating locomotor behavior in lamprey: circuitry, transmitters, membrane properties, and simulation. *Annu. Rev. Neurosci.* **14:** 169–199.

Guirguis, M. S., and J. L. Wilkens. 1995. The role of the cardioregulatory nerves in mediating heart rate responses to locomotion, reduced stroke volume, and neurohormones in *Homarus americanus. Biol. Bull.* **188:** 179–185.

Hagiwara, S. 1961. Nervous activities of the heart in Crustacea. *Ergeb. Biol.* **24:** 287–311.

Hagiwara, S., and T. H. Bullock. 1957. Intracellular potentials in pacemaker and integrative neurons of the lobster cardiac ganglion. *J. Cell. Comp. Physiol.* **50:** 25–47.

Hagiwara, S., A. Watanabe, and N. Saito. 1959. Potential changes in syncytial neurons of lobster cardiac ganglion. *J. Neurophysiol.* **22:** 554–572.

Hancox, J. C., and R. C. Pitman. 1991. Plateau potentials drive axonal impulse bursts in insect motoneurons. *Proc. R. Soc. Lond.* **B244:** 33–38.

Harris-Warrick, R. M., E. Marder, A. I. Selverston, and M. Moulins, eds. 1992a. *Dynamic Biological Networks: The Stomatogastric Nervous System.* MIT Press, Cambridge, MA. 328 pp.

Harris-Warrick, R. M., F. Nagy, and M. P. Nusbaum. 1992b. Neuromodulation of stomatogastric networks by identified neurons and transmitters. Pp. 87–138 in *Dynamic Biological Networks: The Stomatogastric Nervous System,* R. M. Harris-Warrick, E. Marder, A. I Selverston, and M. Moulins, eds. MIT Press, Cambridge, MA.

Hartline, D. K. 1967. Impulse identification and axon mapping of the nine neurons in the cardiac ganglion of the lobster, *Homarus americanus. J. Exp. Biol.* **47:** 327–340.

Hartline, D. K. 1979. Integrative neurophysiology of the lobster cardiac ganglion. *Am. Zool.* **19:** 53–65.

Hartline, D. K. 1997. Plateau potential. Pp. 1656–1657 in *The Encyclopedia of Neuroscience,* G. Adelman and B. H. Smith, eds. Elsevier Science, Amsterdam.

Hartline, D. K., and I. M. Cooke. 1969. Postsynaptic membrane response predicted from presynaptic input pattern in lobster cardiac ganglion. *Science* **164:** 1080–1082.

Hartline, D. K., and K. Graubard. 1992. Cellular and synaptic properties in the crustacean stomatogastric nervous system. Pp. 31–86 in *Dynamic Biological Networks: The Stomatogastric Nervous System,* R. M. Harris-Warrick, E. Marder, A. I. Selverston, and M. Moulins, eds. MIT Press, Cambridge, MA.

Hashemzadeh-Gargari, H., and J. Freschi. 1992. The effects of glutamate agonists on voltage-clamped motoneurons of the lobster cardiac ganglion. *J. Exp. Biol.* **169:** 53–63.

Hawkins, W. E., and H. D. Howse. 1978. A light and electron microscopic study of the cardiac ganglion of the blue crab *Callinectes sapidus* Rathbun. *Trans. Am. Microsc. Soc.* **97:** 363–380.

Hounsgaard, J., and O. Kiehn. 1989. Serotonin-induced bistability of turtle motoneurons caused by a nifedipine-sensitive calcium plateau potential. *J. Physiol. (Lond.)* **414:** 265–282.

Hsiao, C. F., C. A. Del Negro, P. R. Trueblood, and S. H. Chandler. 1998. Ionic basis for serotonin-induced bistable membrane properties in guinea pig trigeminal motoneurons. *J. Neurophysiol.* **79:** 2847–2856.

Hultborn, H. 1999. Plateau potentials and their role in regulating motoneuronal firing. *Prog. Brain Res.* **123:** 39–48.

Hurwitz, I., and A. J. Susswein. 1996. B64, a newly identified central pattern generator element producing a phase switch from protraction to retraction in buccal motor programs of *Aplysia californica. J. Neurophysiol.* **75:** 1327–1344.

Irisawa, A., and K. Hama. 1965. Contact of adjacent nerve fibers in the cardiac nerve of mantis shrimp. *Jpn. J. Physiol.* **15:** 323–330.

Kaupp, U. B., and R. Seifert. 2001. Molecular diversity of pacemaker ion channels. *Annu. Rev. Physiol.* **63:** 235–257.

Kerrison, J., and J. E. Freschi. 1992. The effects of γ-aminobutyric acid on voltage-clamped motoneurons of the lobster cardiac ganglion. *Comp. Biochem. Physiol. C* **101:** 227–233.

Kiehn, O., and T. Eken. 1998. Functional role of plateau potentials in vertebrate motor neurons. *Curr. Opin. Neurobiol.* **8:** 746–752.

Kiehn, O., and R. M. Harris-Warrick. 1992. 5-HT modulation of hyperpolarization-activated inward current and calcium-dependent outward current in a crustacean motor neuron. *J. Neurophysiol.* **68:** 496–508.

Kim, U., and D. A. McCormick. 1998. Functional and ionic properties of a slow afterhyperpolarization in ferret perigeniculate neurons *in vitro*. *J. Neurophysiol.* **80:** 1222–1235.

Krajniak, K. G. 1991. The identification and structure-activity relations of a cardioactive FMRFamide-related peptide from the blue crab, *Callinectes sapidus*. *Peptides* **12:** 1295–1302.

Kramer, R. H., and R. S. Zucker. 1985. Calcium-dependent inward current in *Aplysia* bursting pacemaker neurones. *J. Physiol. (Lond.)* **363:** 107–130.

Kuramoto, T., and A. Ebara. 1984a. Effects of perfusion pressure on the isolated heart of the lobster, *Panulirus japonicus*. *J. Exp. Biol.* **109:** 121–140.

Kuramoto, T., and A. Ebara. 1984b. Neurohormonal modulation of the cardiac outflow through the cardioarterial valve in the lobster. *J. Exp. Biol.* **111:** 123–130.

Kuramoto, T., and A. Ebara. 1985. Effects of perfusion pressure on the bursting neurones in the intact or segmented cardiac ganglion of the lobster, *Panulirus japonicus*. *J. Neurosci. Res.* **13:** 569–580.

Kuramoto, T., and A. Ebara. 1988. Combined effects of 5-hydroxytryptamine and filling pressure on the isolated heart of the lobster, *Panulirus japonicus*. *J. Comp. Physiol. B* **158:** 403–412.

Kuramoto, T., and A. Ebara. 1991. Combined effects of octopamine and filling pressure on the isolated heart of the lobster, *Panulirus japonicus*. *J. Comp. Physiol. B* **161:** 339–347.

Kuramoto, T., and K. Kuwasawa. 1980. Ganglionic activation of the myocardium of the lobster, *Panulirus japonicus*. *J. Comp. Physiol.* **139:** 67–76.

Kuramoto, T., and H. Yamagishi. 1990. Physiological anatomy, burst formation, and burst frequency of the cardiac ganglion of crustaceans. *Physiol. Zool.* **63:** 102–116.

Kuramoto, T., E. Hirose, and M. Tani. 1992. Neuromuscular transmission and hormonal modulation in the cardioarterial valve of the lobster, *Homarus americanus*. Pp. 62–69 in *Phylogenetic Models in Functional Coupling of the CNS and the Cardiovascular System*, R. B. Hill, K. Kuwasawa, B. R. McMahon, and T. Kuramoto, eds. Karger, Basel.

Labenia, J., N. L. Scholz, M. F. Goy, and K. Graubard. 1998. NO/cGMP modulates the crustacean cardiac ganglion. *Soc. Neurosci. Abstr.* **24:** 360.

Legendre, P., I. M. Cooke, and J. D. Vincent. 1982. Regenerative responses of long duration recorded intracellularly from dispersed cell cultures of fetal mouse hypothalamus. *J. Neurophysiol.* **48:** 1121–1141.

Lemos, J. R., and A. Berlind. 1981. Cyclic adenosine monophosphate mediation of peptide neurohormone effects on the lobster cardiac ganglion. *J. Exp. Biol.* **90:** 307–326.

Livengood, D. R. 1983. Coupling ratio of the Na-K pump in the lobster cardiac ganglion. *J. Gen. Physiol.* **82:** 853–874.

Livengood, D. R., and K. Kusano. 1972. Evidence for an electrogenic sodium pump in follower cells of the lobster cardiac ganglion. *J. Neurophysiol.* **35:** 170–186.

Llinás, R. R. 1988. The intrinsic electrophysiological properties of mammalian neurons: insights into central nervous system function. *Science* **242:** 1654–1664.

Llinás, R., and H. Jahnsen. 1982. Electrophysiology of mammalian thalamic neurones *in vitro*. *Nature* **297:** 406–408.

Llinás, R., and M. Sugimori. 1980. Electrophysiological properties of *in vitro* Purkinje cell dendrites in mammalian cerebellar slices. *J. Physiol. (Lond.)* **305:** 197–213.

Lüthi, A., and D. A. McCormick. 1998. H-Current: properties of a neuronal and network pacemaker. *Neuron* **21:** 9–12.

Marder, E., and R. L. Calabrese. 1996. Principles of rhythmic motor pattern generation. *Physiol. Rev.* **76:** 687–717.

Matsui, K. 1955. Spontaneous discharges of the isolated ganglionic trunk of the lobster heart (*Panulirus japonicus*). *Sci. Rep. Tokyo Kyoiku Daigaku B* **7:** 257–268.

Matsui, K., N. Ai, and K. Kuwasawa. 1973. Spontaneous inhibitory post-synaptic potentials in the cardiac ganglion preparation of the lobster *Panulirus japonicus*. *Comp. Biochem. Physiol. A* **44:** 953–965.

Matsui, K., K. Kuwasawa, and T. Kuramoto. 1977. Periodic bursts in large cell preparations of the lobster cardiac ganglion (*Panulirus japonicus*). *Comp. Biochem. Physiol. A* **56:** 313–324.

Mayeri, E. M. 1973a. Functional organization of the cardiac ganglion of the lobster, *Homarus americanus*. *J. Gen. Physiol.* **62:** 448–472.

Mayeri, E. M. 1973b. A relaxation oscillator description of the burst generating mechanism in the cardiac ganglion of the lobster, *Homarus americanus*. *J. Gen. Physiol.* **62:** 473–488.

Maynard, D. M. 1953. Activity in a crustacean ganglion. I. Cardio-inhibition and acceleration in *Panulirus argus*. *Biol. Bull.* **104:** 156–170.

Maynard, D. M. 1955. Activity in a crustacean ganglion II. Pattern and interaction in burst formation. *Biol. Bull.* **109:** 420–436.

Maynard, D. M. 1960. Circulation and heart function. Pp. 161–226 in *The Physiology of Crustacea*, T. H. Waterman, ed. Academic Press, New York.

Maynard, D. M. 1961. Cardiac inhibition in decapod Crustacea. Pp. 144–178 in *Nervous Inhibition*, E. Florey, ed. Pergamon Press, New York.

Maynard, E. 1971. Microscopic localization of cholinesterases in the nervous systems of lobsters, *Panulirus argus* and *Homarus americanus*. *Tissue Cell* **3:** 215–230.

Mercier, A. J., and R. T. Russenes. 1992. Modulation of crayfish hearts by FMRFamide-related peptides. *Biol. Bull.* **182:** 333–340.

Mercier, A. J., I. Orchard, V. TeBrugge, and M. Skerrett. 1993. Isolation of two FMRFamide-related peptides from crayfish pericardial organs. *Peptides* **14:** 137–143.

Miller, M. W., and R. E. Sullivan. 1981. Some effects of proctolin on the cardiac ganglion of the Maine lobster, *Homarus americanus* (Milne Edwards). *J. Neurobiol.* **12:** 629–639.

Miller, M. W., J. A. Benson, and A. Berlind. 1984. Excitatory effects of dopamine on the cardiac ganglia of the crabs *Portunus sanguinolentus* and *Podophthalmus vigil*. *J. Exp. Biol.* **108:** 97–118.

Mirolli, M., I. M. Cooke, S. R. Talbott, and M. W. Miller. 1987. Structure and localization of synaptic complexes in the cardiac ganglion of a portunid crab. *J. Neurocytol.* **16:** 115–130.

Morganelli, P. M., and R. G. Sherman. 1987. Nerve terminals and synapses in the cardiac ganglion of the adult lobster *Homarus americanus*. *J. Morphol.* **191:** 177–191.

Nusbaum, M. P., D. M. Blitz, A. M. Swensen, D. Wood, and E. Marder. 2001. The roles of co-transmission in neural network modulation. *Trends Neurosci.* **24:** 146–154.

Ocorr, K. A., and A. Berlind. 1983. The identification and localization of a catecholamine in the motor neurons of the lobster cardiac ganglion. *J. Neurobiol.* **14:** 51–59.

Ohsawa, K. 1972. Morphological organization and fine structures of the cardiac ganglion of the lobster, *Panulirus japonicus*. *Sci. Rep. Tokyo Kyoiku Daigaku B* **15:** 1–24.

Orkand, R. K. 1962. The relation between membrane potential and contraction in single crayfish muscle fibres. *J. Physiol. (Lond.)* **161:** 143–159.

Otani, T., and T. H. Bullock. 1959. Effects of presetting the membrane potential of the soma of spontaneous and integrating ganglion cells. *Physiol. Zool.* **32:** 104–114.

Perrins, R., and K. R. Weiss. 1998. Compartmentalization of information processing in an *Aplysia* feeding circuit interneuron through membrane properties and synaptic interactions. *J. Neurosci.* **18:** 3977–3989.

Rekling, J. C., and J. L. Feldman. 1998. Prebötzinger complex and pacemaker neurons: hypothesized site and kernel for respiratory rhythm generation. *Annu. Rev. Physiol.* **60:** 385–405.

Russell, D. F., and D. K. Hartline. 1978. Bursting neural networks: a reexamination. *Science* **200:** 453–456.

Russell, D. F., and D. K. Hartline. 1982. Slow active potentials and bursting motor patterns in pyloric network of the lobsters, *Panulirus interruptus*. *J. Neurophysiol.* **48:** 914–937.

Russell, D. F., and D. K. Hartline. 1984. Synaptic regulation of properties and burst oscillations of neurons in the gastric mill system of spiny lobster, *Panulirus interruptus*. *J. Neurophysiol.* **52:** 54–73.

Sakurai, A., and H. Yamagishi. 1998. Identification of two cardioacceleratory neurons in the isopod crustacean, *Ligia exotica* and their effects on cardiac ganglion cells. *J. Comp. Physiol. A* **182:** 145–152.

Santoro, B., and G. R. Tibbs. 1999. The HCN gene family: molecular basis of the hyperpolarization-activation pacemaker channels. *Ann. NY Acad. Sci.* **868:** 741–764.

Saver, M. A., and J. L. Wilkens. 1998. Comparison of the effects of five hormones on intact and open heart cardiac ganglionic output and myocardial contractility in the shore crab *Carcinus maenas*. *Comp. Biochem. Physiol. A* **120:** 301–310.

Saver, M. A., J. L. Wilkens, and C. N. Airriess. 1998. Proctolin affects the activity of the cardiac ganglion, myocardium, and cardioarterial valves in *Carcinus maenas* hearts. *J. Comp. Physiol. B* **168:** 473–482.

Saver, M. A., J. L. Wilkins, and N. I. Syed. 1999. *In situ* and *in vitro* identification and characterization of cardiac ganglion neurons in the crab, *Carcinus maenas*. *J. Neurophysiol.* **81:** 2964–2976.

Shimahara, T. 1969a. The inhibitory post-synaptic potential in the cardiac ganglion cell of the lobster, *Panulirus japonicus*. *Sci. Rep. Tokyo Kyoiku Daigaku B* **14:** 9–26.

Shimahara, T. 1969b. The effect of the acceleratory nerve on the electrical activity of the lobster cardiac ganglion. *Zool. Mag.* **78:** 351–355.

Sivan, E., H. Parnas, and D. Dolev. 1999. Fault tolerance in the cardiac ganglion of the lobster. *Biol. Cybern.* **81:** 11–23.

Smith, R. I. 1947. The action of electrical stimulation and of certain drugs on cardiac nerves of the crab, *Cancer irroratus*. *Biol. Bull.* **93:** 72–88.

Stangier, J., C. Hilbich, K. Beyreuther, and R. Keller. 1987. A novel cardioactive peptide (CCAP) from pericardial organs of the shore crab *Carcinus maenas*. *Proc. Natl. Acad. Sci. USA* **84:** 575–579.

Su, H., G. Alroy, E. D. Kirson, and Y. Yaari. 2001. Extracellular calcium modulates persistent sodium current-dependent burst-firing in hippocampal pyramidal neurons. *J. Neurosci.* **21:** 4173–4182.

Sullivan, R. E. 1979. A proctolin-like peptide in crab pericardial organs. *J. Exp. Zool.* **210:** 543–552.

Sullivan, R. E., and M. W. Miller. 1984. Dual effects of proctolin on the rhythmic burst activity of the cardiac ganglion. *J. Neurobiol.* **15:** 173–196.

Sullivan, R. E., and M. W. Miller. 1990. Cholinergic activation of the lobster cardiac ganglion. *J. Neurobiol.* **21:** 639–650.

Sullivan, R. E., B. J. Friend, and D. L. Barker. 1977. Structure and function of spiny lobster ligamental nerve plexuses: evidence for synthesis, storage and secretion of biogenic amines. *J. Neurobiol.* **8:** 581–605.

Suzuki, S. 1934. Ganglion cells in the heart of *Ligia exotica* (Roux). *Sci. Repts. Tohoku Imp. Univ. Fourth Ser.* **9:** 214–218. [Cited in Maynard, 1960.]

Tameyasu, T. 1976. Intracellular potentials in the small cells and cellular interaction in the cardiac ganglion of the lobster, *Panulirus japonicus*. *Comp. Biochem. Physiol.* **54A:** 191–196.

Tameyasu, T. 1987. The mechanism of the burst formation in the cardiac ganglion of the lobster (*Panulirus japonicus*): a re-examination. *J. Comp. Physiol. A* **161:** 389–398.

Tazaki, K. 1967. Intracellular potential changes in the cardiac ganglion cell of the crab, *Eriocheir japonicus*. *Sci. Rep. Tokyo Kyoiku Daigaku* **B12:** 191–210.

Tazaki, K. 1970. Slow potential changes during the burst in the cardiac ganglion of the crab, *Eriocheir japonicus*. *Annot. Zool. Jpn.* **43:** 63–69.

Tazaki, K. 1971a. The effects of tetrodotoxin on the slow potential and spikes in the cardiac ganglion of a crab, *Eriocheir japonicus*. *Jpn. J. Physiol.* **21:** 529–536.

Tazaki, K. 1971b. Small synaptic potentials in burst activity of large neurons in the lobster cardiac ganglion. *Jpn. J. Physiol.* **21:** 645–658.

Tazaki, K. 1972. The burst activity of different cell regions and intercellular co-ordination in the cardiac ganglion of the crab, *Eriocheir japonicus*. *J. Exp. Biol.* **57:** 713–726.

Tazaki, K. 1973. Impulse activity and pattern of large and small neurones in the cardiac ganglion of the lobster, *Panulirus japonicus*. *J. Exp. Biol.* **58:** 473–486.

Tazaki, K., and I. M. Cooke. 1979a. Spontaneous electrical activity and interaction of large and small cells in the cardiac ganglion of the crab, *Portunus sanguinolentus*. *J. Neurophysiol.* **42:** 975–999.

Tazaki, K., and I. M. Cooke. 1979b. Isolation and characterization of slow, depolarizing responses of cardiac ganglion neurons in the crab, *Portunus sanguinolentus*. *J. Neurophysiol.* **42:** 1000–1021.

Tazaki, K., and I. M. Cooke. 1979c. The ionic bases of slow depolarizing responses of cardiac ganglion neurons in the crab, *Portunus sanguinolentus*. *J. Neurophysiol.* **42:** 1022–1047.

Tazaki, K., and I. M. Cooke. 1983a. Topographical localization of function in the cardiac ganglion of the crab, *Portunus sanguinolentus*. *J. Comp. Physiol. A* **151:** 311–328.

Tazaki, K., and I. M. Cooke. 1983b. Separation of neuronal sites of driver potential and impulse generation by ligaturing in the cardiac ganglion of the lobster, *Homarus americanus*. *J. Comp. Physiol. A* **151:** 329–346.

Tazaki, K., and I. M. Cooke. 1983c. Neuronal mechanisms underlying rhythmic bursts in crustacean cardiac ganglia. *Symp. Soc. Exp. Biol.* **37:** 129–157.

Tazaki, K., and I. M. Cooke. 1986. Currents under voltage clamp of burst-forming neurons of the cardiac ganglion of the lobster (*Homarus americanus*). *J. Neurophysiol.* **56:** 1739–1762.

Tazaki, K., and I. M. Cooke. 1990. Characterization of Ca current underlying burst formation in lobster cardiac ganglion motorneurons. *J. Neurophysiol.* **63:** 370–384.

Terzuolo, C. A., and T. H. Bullock. 1958. Acceleration and inhibition in crustacean ganglion cells. *Arch. Ital. Biol.* **96:** 117–134.

Trimmer, B. A., L. A. Kobierski, and E. A. Kravitz. 1987. Purification and characterization of FMRFamide-like immunoreactive substances from the lobster nervous system: isolation and sequence analysis of two closely related peptides. *J. Comp. Neurol.* **266:** 16–26.

van der Kloot, W. 1970. The electrophysiology of muscle fibers in the hearts of decapod crustaceans. *J. Exp. Zool.* **174:** 367–380.

Watanabe, A. 1958. The interaction of electrical activity among neurons of lobster cardiac ganglion. *Jpn. J. Physiol.* **8:** 305–318.

Watanabe, A., and T. H. Bullock. 1960. Modulation of activity of one neuron by subthreshold slow potentials in another in lobster cardiac ganglion. *J. Gen. Physiol.* **43:** 1031–1045.

Watanabe, A., and K. Takeda. 1963. The spread of excitation among neurons in the heart ganglion of the stomatopod, *Squilla oratoria*. *J. Gen. Physiol.* **46:** 773.

Watanabe, A., S. Obara, T. Akiyama, and K. Yumoto. 1967a. Electrical properties of the pacemaker neurons in the heart ganglion of a stomatopod, *Squilla oratoria*. *J. Gen. Physiol.* **50:** 813–838.

Watanabe, A., S. Obara, and T. Akiyama. 1967b. Pacemaker potentials for the periodic burst discharge in the heart ganglion of a stomatopod. *Squilla oratoria. J. Gen. Physiol.* **50:** 839–862.

Watanabe, A., S. Obara, and T. Akiyama. 1968. Inhibitory synapses on pacemaker neurons in the heart ganglion of a stomatopod, *Squilla oratoria. J. Gen. Physiol.* **52:** 908–924.

Watanabe, A., S. Obara, and T. Akiyama. 1969. Acceleratory synapses on pacemaker neurons in the heart ganglion of a stomatopod, *Squilla oratoria. J. Gen. Physiol.* **54:** 212–231.

Welsh, J. H., and D. M. Maynard. 1951. Electrical activity of a simple ganglion. *Fedr. Proc.* **10:** 145.

Wiens, T. J. 1982. Small systems of neurons: control of rhythmic and reflex activities. Pp. 193–240 in *The Biology of Crustacea, Vol. 4*, D. Bliss, D. Sandeman, and H. Atwood, eds. Academic Press, New York.

Wiersma, C. A., and E. Novitski. 1942. The mechanism of the nervous regulation of the crayfish heart. *J. Exp. Biol.* **19:** 255–265.

Wilkens, J. L. 1993. Re-evaluation of the stretch sensitivity hypothesis of crustacean hearts: Hypoxia, not lack of stretch, causes reduction in heart rate of isolated hearts. *J. Exp. Biol.* **176:** 223–232.

Wilkens, J. L. 1999. Evolution of the cardiovascular system in Crustacea. *Am. Zool.* **39:** 199–214.

Wilkens, J. L., and A. J. Mercier. 1993. Peptidergic modulation of cardiac performance in isolated hearts from the shore crab, *Carcinus maenas. Physiol. Zool.* **66:** 237–256.

Wilkens, J. L., T. Kuramoto, and B. R. McMahon. 1996. The effects of six pericardial hormones and hypoxia on the semi-isolated heart and sternal arterial valve of the lobster *Homarus americanus. Comp. Biochem. Physiol. C* **114:** 57–65.

Yamagishi, H., H. Ando, and T. Makioka. 1997. Myogenic heartbeat in the primitive crustacean *Triops longicaudatus. Biol. Bull.* **193:** 350–358.

Yazawa, T., and K. Kuwasawa. 1992. Intrinsic and extrinsic neural and neurohumoral control of the decapod heart. *Experientia* **48:** 834–840.

Yazawa, T., K. Tanaka, M. Yasumatsu, M. Otokawa, Y. Aihara, K. Ohsuga, and K. Kuwasawa. 1998. A pharmacological and HPLC analysis of the excitatory transmitter of the cardiac ganglion in the heart of the isopod crustacean *Bathynomus doederleini. Can. J. Physiol. Pharmacol.* **76:** 599–604.

Zhang, B., and R. M. Harris-Warrick. 1995. Calcium-dependent plateau potentials in a crab stomatogastric ganglion motor neuron. I. Calcium current and its modulation by serotonin. *J. Neurophysiol.* **74:** 1929–1937.

Reference: *Biol. Bull.* **202:** 137–147. (April 2002)

Timing Is Everything: The Effects of Putative Dopamine Antagonists on Metamorphosis Vary With Larval Age and Experimental Duration in the Prosobranch Gastropod *Crepidula fornicata*

JAN A. PECHENIK*, WEI LI, AND DAVID E. COCHRANE

Biology Department, Tufts University, Medford, Massachusetts 02155

Abstract. The signal transduction pathway through which excess potassium ion stimulates the larvae of many marine invertebrates to metamorphose is incompletely understood. Recent evidence suggests that dopamine plays important roles in the metamorphic pathway of *Crepidula fornicata*. Therefore, we asked whether blocking dopamine receptors might prevent excess potassium ion from stimulating metamorphosis in this species. Surprisingly, the effects of the three putative dopamine antagonists tested (all at 10 μM) varied with exposure duration and the age of competent larvae. Chlorpromazine, a nonspecific dopamine antagonist known to have a number of other pharmacological effects, blocked the inductive action of excess potassium ion during the initial 5–8-h exposure periods in most assays, particularly for younger or smaller competent larvae. However, chlorpromazine in the absence of excess potassium ion also stimulated metamorphosis, particularly over the next 18 h, and worked faster on older competent larvae than on younger competent larvae. The specific D_1 antagonist R(+)-Sch-23309 had similar effects, blocking potassium-stimulated metamorphosis in short-term exposures and stimulating metamorphosis in longer exposures, particularly for older competent larvae. Although the specific D_2 antagonist spiperone (SPIP) blocked the inductive effects of excess potassium ion in only 1 of 6 assays during the first 6 h of exposure, it blocked metamorphosis in 2 of the assays during 24-h exposures. Our results indicate that dopamine receptors are involved in the pathway through which excess potassium ion stimulates metamorphosis in *C. fornicata*. In addition, the largely latent inductive effects of chlorpromazine, an inhibitor of nitric oxide synthase, suggest that endogenous nitric oxide may play a natural role in inhibiting metamorphosis in this species. Overall, our results would then suggest that exposing larvae of *C. fornicata* to excess K^+ leads to a shutdown of nitric oxide synthesis *via* a dopaminergic pathway, a pathway that can be blocked by some dopamine antagonists. Alternatively, chlorpromazine might eventually be stimulating metamorphosis by elevating endogenous cyclic nucleotide (*e.g.*, cAMP) concentrations, again acting downstream from the steps acted on directly by excess K^+.

Introduction

As with most other marine gastropods, *Crepidula fornicata* has an obligate planktonic larval stage. After swimming and feeding in the plankton for at least several weeks, the veliger larvae become competent to metamorphose (Pechenik, 1990); that is, they become capable of metamorphosing in response to specific external cues such as adult pheromone and microbial films (Pechenik, 1980; Pechenik and Heyman, 1987; McGee and Targett, 1989; Pechenik and Gee, 1993). In the absence of such external cues, the larval form can be maintained for at least an additional 10 days (Pechenik and Lima, 1984; Zimmerman and Pechenik, 1991). Eventually the larvae metamorphose "spontaneously" in frequently cleaned glassware, in the apparent absence of external cues (Pechenik, 1984; Pechenik and Lima, 1984; Pechenik *et al.*, 1996a).

The signal transduction pathway that leads from perception of the external cue to metamorphosis is incompletely understood in this species, and indeed in any marine invertebrate species (Todd *et al.*, 1991; Pechenik *et al.*, 1995;

Received 13 August 2001; accepted 11 January 2002.

* To whom correspondence should be addressed. E-mail: jan.pechenik@tufts.edu

Clare, 1996; Woollacott and Hadfield, 1996; Pechenik and Qian, 1998; Carpizo-Ituarte and Hadfield, 1998; Holm *et al.*, 1998; Leise and Hadfield, 2000; Leise *et al.*, 2001). Recently, Pires *et al.* (2000b) found that artificially depleting the concentration of endogenous dopamine and its precursor L-DOPA to about 50% of initial concentrations inhibited larvae of *Crepidula fornicata* from metamorphosing in response to adult-conditioned seawater, suggesting that catecholamines play an important role in regulating metamorphosis in this species. Similarly, dopamine and other catecholamines seem to function in the metamorphic pathway of the opisthobranch gastropod *Phestilla sibogae* (Pires *et al.*, 2000a). In those experiments with *P. sibogae*, increasing the endogenous dopamine concentration of competent larvae by 20–50 times significantly increased the sensitivity of larvae to natural inducer (an extract of the coral *Porites compressa*).

In this study we sought direct evidence for the involvement of dopamine receptors in the metamorphic pathway of *Crepidula fornicata*. Such studies first require the ability to reliably identify when larvae become physiologically competent to metamorphose, and the ability to subsequently induce all competent larvae to metamorphose. Although competent larvae of *C. fornicata* can be induced to metamorphose using seawater conditioned by adults (Pechenik, 1980; Pechenik and Heyman, 1987; McGee and Targett, 1989), the results are quite variable from one experiment to the next. When larvae fail to respond to the adult-conditioned seawater, is it because the larvae were not yet competent to respond, or is it because the adults simply did not produce enough cue to induce a response? We cannot distinguish between these possibilities because the adult cue is still only partially defined (McGee and Targett, 1989). Exposure concentrations cannot be standardized in such a situation, and the extent of physiological competence within larval populations cannot be accurately quantified (Pechenik and Heyman, 1987).

However, metamorphosis can be reliably induced in *C. fornicata* artificially, by incubating larvae for 5–6 h in seawater in which the concentration of K^+ has been raised by 15–20 m*M* (Pechenik and Heyman, 1987; Pechenik and Gee, 1993; Pires *et al.*, 2000b). The larvae become competent to respond to excess K^+ only about 12–24 h before they become competent to respond to natural inducer, following 2–3 weeks of development as pre-competent larvae (Pechenik and Gee, 1993). This is not the case for all species: the larvae of at least some other marine invertebrate species become responsive to excess K^+ well after they become responsive to natural cues (Pechenik *et al.*, 1995; Pechenik and Qian, 1998). Exposing larvae to excess K^+ provides a reliable way to monitor the onset of metamorphic competence within laboratory populations of *C. fornicata*.

Moreover, metamorphosis in *C. fornicata*—signaled by loss of the larval swimming organ, the velum—is comparably rapid in response to natural inducer and excess K^+, typically requiring less than 6 h in both cases (Pechenik and Gee, 1993). Finally, triggering metamorphosis of *C. fornicata* with excess K^+ has no detrimental effect on rates of juvenile growth, feeding, or respiration (Eyster and Pechenik, 1988).

In this study, we used excess K^+ as a convenient tool to explore aspects of signal transduction in the metamorphic pathway of *C. fornicata*. In particular, we examined the ability of several specific and nonspecific putative dopamine antagonists to block the ability of excess K^+ to stimulate metamorphosis. Although dopamine receptor types have not yet been characterized in this species, dopamine is known to play several important roles in molluscan physiology, and its various effects can be blocked by a variety of mammalian dopamine receptor antagonists in a number of other gastropod species (*e.g.*, Juel, 1981; Swann *et al.*, 1982; Kim and Woodruff, 1995; Emaduddin and Takeuchi, 1996; Green *et al.*, 1996; Spencer *et al.*, 1996).

Our study differs from most previous studies exploring the effects of neuroactive and pharmacological agents on gastropod metamorphosis in that instead of using larvae of the same age in each experiment (*e.g.*, Bryan and Qian, 1998; Holm *et al.*, 1998; Carpizo-Ituarte and Hadfield, 1998) or subsampling larvae at intervals only from precompetence to the onset of competence (*e.g.*, Pechenik and Qian, 1998; Pires *et al.*, 2000a), we subsampled from the same batches of competent larvae over time. In so doing, we encountered the surprising and potentially revealing result that the effects of particular treatments changed dramatically as competent larvae aged. Moreover, instead of ending our experiments at 6 h, we continued them for an additional 18 h, encountering the equally remarkable result that some treatments had the opposite effect at 24 h as they had at 6 h. We believe this to be the first published demonstration of such phenomena for larval invertebrates. The results suggest new hypotheses about how metamorphosis is controlled in this species.

Materials and Methods

Obtaining competent larvae

Four experiments were conducted, each using larvae released from a different female. Several stacks of adults were collected from Nahant, Massachusetts, at low tide and held in the laboratory on a diet of the naked flagellate *Dunaliella tertiolecta* (clone DUN) for 2–6 days until larvae were released. For each of our four main experiments, about 3000 larvae were then reared in 4-l glass jars in 0.45-μm filtered seawater from Nahant (salinity about 30‰) on a diet of the naked flagellate *Isochrysis galbana* (clone T-ISO). This diet supports rapid growth of these larvae with low mortality (*e.g.*, Pechenik, 1984; Pechenik and Gee, 1993). The water and phytoplankton suspensions were changed every other day, and the glassware was cleaned between water changes. After 10–12 days, larvae were subsampled periodically (three replicates of 10 larvae each) and tested for metamorphic competence by raising the K^+ concentration of seawater by 20 m*M* for 6 h (Pechenik and Heyman, 1987; Pechenik and Gee, 1993). Assays in the first three experiments were initiated once at least 80% of the tested larvae were competent to metamorphose, as described below. In the last experiment (Experiment IV) we initiated our tests when only about 30% of larvae were competent to metamorphose. This was done deliberately, so as to initiate assays when most larvae in the culture were just beginning to acquire metamorphic competence.

Testing the effects of putative dopamine antagonists and a nitric oxide synthase inhibitor

Our experiments focused on the nonspecific (Green *et al.*, 1996) dopamine antagonist chlorpromazine; chlorpromazine has a number of other documented actions, including the inhibition of nitric oxide synthase (see Discussion). A smaller number of studies also included the selective D_2 antagonist spiperone (SPIP) and the D_1 antagonist R+ (R(+)- Sch-23309). Because nitric oxide may be a natural inhibitor of metamorphosis in another gastropod (*Ilyanassa obsoleta*; Leise *et al.*, 2001), we also tested the effects of the nitric oxide synthase inhibitor L-NAME (*N*-nitro-L-arginine methyl ester) in two experiments.

Chlorpromazine was initially tested at concentrations of 5, 10, 20, and 40 μM in seawater. For subsequent experiments the chemical was applied only at 10 μM, because that concentration produced a maximal response with minimal larval mortality (see below). The two other dopamine antagonists were tested only at 10 μM, and L-NAME was tested at 10 and 20 μM. The concentrations of chlorpromazine, SPIP, and R(+)-Sch-23309 that we used are similar to those used in the studies of Croll *et al.* (1997) with *Lymnaea stagnalis* and of Green *et al.* (1996) with *Helisoma trivolvis*. Micromolar concentrations of L-NAME (injected) stimulated metamorphosis in *Ilyanassa obsoleta* (Leise *et al.*, 2001).

Exposure protocol

In all experiments, larvae of *C. fornicata* were exposed to test solutions in sets of four replicates with 8–12 larvae (usually 10) per replicate. When subsampling larvae for different assays within an experiment, we selected the largest larvae, discarding any that were unusually large. Filtered seawater served as the negative control. A positive control, to assess the percentage of larvae that were competent to metamorphosis on the day of each experiment, consisted of seawater whose K^+ concentration had been elevated by 20 m*M* (Pechenik and Heyman, 1987; Pechenik and Gee, 1993). Other larvae were exposed either to the test solutions alone (chlorpromazine, SPIP, R+) or to the test solutions in the presence of excess K^+ (20 m*M*). In this way, the ability of the tested substances to block the effects of excess K^+ on metamorphosis was assessed.

Table 1

Summary of experiments conducted on the metamorphosis of Crepidula fornicata

Experiment	Date of experiment	Larval age (days)	Mean shell length (μm) ± SD (*n*)
Ia	17 April 2000	16	882.6 ± 71.8 (12)
Ib	20 April 2000	19	923.6 ± 76.8 (15)
Ic	23 April 2000	22	955.8 ± 91.7 (14)
Id	25 April 2000	24	960.0 ± 79.2 (12)
Ie	26 April 2000	25	852.3 ± 84.5 (12)
If	30 April 2000	29	959.6 ± 114.5 (12)
II	1 May 2001	17	1073.2 ± 155.4 (13)
IIIa	12 May 2001	16	951.7 ± 64.7 (15)
IIIb	16 May 2001	20	995.6 ± 85.1 (16)
IIIc	21 May 2001	25	1101.0 ± 126.6 (15)*
IIId	26 May 2001	29	1092.1 ± 118.6 (15)*
IVa	6 July 2001	18	908.4 ± 83.2 (15)
IVb	10 July 2001	22	864.8 ± 81.8 (13)
IVc	15 July 2001	27	1034.3 ± 123.3 (18)*
IVd	18 July 2001	30	1099.0 ± 98.7 (20)*
IVe	21 July 2001	33	1079.3 ± 89.8 (14)*

Each numeral represents a series of experiments conducted with larvae from the same batch, released by one female. *Indicates mean shell lengths that are significantly larger than the initial mean shell length ("a" measurements) within each experiment (Dunnett's multiple comparisons test, $P < 0.05$).

The percentage of larvae metamorphosing in each solution was assessed after 6–8 h of exposure (usually 6 h). Percent metamorphosis was also assessed after 24 h. Mean shell lengths of larvae used in each experiment were determined by subsampling at least 12 larvae and measuring them at 50×; those larvae were not used in the experiments, to guard against the possibility that the handling might stimulate metamorphosis. Metamorphosis was signaled by loss of the ciliated larval swimming organ, the velum, as assessed with a dissecting microscope at 50×.

Within each large (numbered) experiment, the exposures were repeated up to 5 times by subsampling from the same batch of larvae over 13–15 days, to determine whether the responses changed as the competent larvae aged. Individual larvae were tested only once. Experimental details, including larval age and mean shell length at each exposure, are given in Table 1.

Time course of the response to chlorpromazine

The response of *C. fornicata* larvae to chlorpromazine was evaluated in one experiment (Experiment Id) at nine time intervals over 12 h, using four replicates of larvae, 10 larvae per replicate.

Data analysis

Percentage data were arcsine transformed before analysis (Sokal and Rohlf, 1981). Mean responses were compared by one-way analysis of variance (ANOVA) unless variances did not pass Bartlett's test of homogeneity, in which case means were compared using nonparametric ANOVA (Kruskal-Wallis *KW* statistic). When significant differences among means were found, treatment means were compared against control means using Bonferroni's method for multiple comparisons.

Mean shell lengths of larvae used in experiments were compared using one-way ANOVA on untransformed data, followed by Bonferroni's method for multiple comparisons (sample means against mean shell length at the first assay within an experiment).

All analyses were conducted using the programs Prism or Instat (both from GraphPad, Inc.).

Results

The effects of chlorpromazine on larvae of *Crepidula fornicata* were consistent among the four experiments (each using larvae from a different female), but varied in interesting and unexpected ways with exposure time and larval age within experiments. With only one exception, at least 50% of larvae metamorphosed within 5–6 h when subjected to 20 m*M* excess K^+ (Fig. 1a). The lower initial response in Experiment IV was an intended outcome of our experimental design, as we wished to begin testing the responses of larvae that were just becoming competent to metamorphose; by the third assay in that experiment, over 90% of larvae were competent to metamorphose. In one experiment (Experiment IIIa), larvae took 2–3 h longer to respond to the excess K^+ than in previous studies, so that initial responses were recorded at 8 h rather than at 6 h. Fewer than 3% of larvae metamorphosed during the first 5–8 h in seawater controls (Fig. 1a); indeed, fewer than 10% of larvae had metamorphosed in seawater controls by the end of 24 h (Fig. 1b). Significantly more larvae ($P < 0.01$) metamorphosed in response to excess K+ than in control seawater in all experiments (one-way ANOVA followed by Bonferroni comparisons between means).

In 11 out of 14 assays, chlorpromazine effectively blocked the inductive action of excess K^+ during the initial 5–8 h exposure periods (Fig. 1a, as indicated by the numeral "2" above the relevant bars). Chlorpromazine failed to block the stimulatory effect of excess K^+ only for some of the oldest or largest larvae tested. Optimal blocking of metamorphosis was achieved at a concentration of 10 μM chlorpromazine; a concentration of 5 μM chlorpromazine did not prevent excess K^+ from inducing metamorphosis (data not shown), and higher concentrations killed the larvae.

As larvae aged within Experiments I and IV, however, chlorpromazine itself stimulated substantial metamorphosis within the same 5–8-h exposure periods, and at least in some assays, apparently became less effective in blocking stimulation by excess K^+. For the larvae used in Experiment I, for example, only about 10% of the larvae that were subsampled on 17 May 2000 (Experiment Ia) metamorphosed in 10 μM chlorpromazine within the first 6 h of exposure. But when larvae from the same batch were subsampled and tested 13 days later (Experiment If), 35% of larvae tested at the same chlorpromazine concentration metamorphosed in the same amount of time, and chlorpromazine did not inhibit the action of excess K^+ at all (Fig. 1a). In some assays, however, chlorpromazine stimulated metamorphosis of older larvae while simultaneously suppressing the inductive effects of excess K^+ (see Experiment III, for example, Fig. 1a).

Furthermore, over the subsequent 18 h or so that larvae were exposed, chlorpromazine alone stimulated metamorphosis in all experiments, even for the youngest and smallest larvae tested (see Table 1), relative to the incidence of metamorphosis occurring in control seawater (Fig. 1b, indicated by the numeral "1" above the relevant bars). In fact, about as many larvae metamorphosed in response to chlorpromazine by the end of 12 h as had metamorphosed in response to excess K^+ in the first 6–7 h (Fig. 2). By the end of 24 h chlorpromazine had stimulated at least 80% of larvae to metamorphose in 11 of 12 assays, even when simultaneously blocking stimulation by excess K^+ as in Experiments IIIb and IIIc (Fig. 1b). In addition, chlorpromazine in 24-h assays generally failed to block the stimulatory effects of excess K^+ significantly.

The effects of the D_1 antagonist R+ were similar to those of chlorpromazine and varied with larval age and exposure duration. As with chlorpromazine, R+ inhibited the stimulatory effects of excess K^+ for younger competent larvae during 5–6-h exposures, but stimulated metamorphosis of older competent larvae in the same amount of time. This is seen most clearly in the comparison between Experiments IVa and IVb *versus* Experiment IVd (Fig. 3a). And, as with chlorpromazine (Fig. 1b), R+ alone stimulated substantial numbers of larvae to metamorphose over 24 h in all but one assay (Fig. 3b, significant effects indicated by the numeral "1" above the relevant bars). In Experiment IV, however, R+ effectively suppressed the effects of excess K^+ on younger and smaller competent larvae for the entire 24-h period (Fig. 3b).

In marked contrast, SPIP by itself did not stimulate metamorphosis above control levels during any 6–8-h exposure, and it blocked the stimulatory effect of excess K^+ significantly in only one experiment; even then, more than 45% of the larvae metamorphosed (Experiment IIIa, Fig. 4a). During 24-h exposures, SPIP had a mildly stimulatory effect on metamorphosis in four assays, spread across all four experiments (Ie, II, IIIa, IVd), but the incidence of metamorphosis was always significantly below ($P < 0.01$) that induced

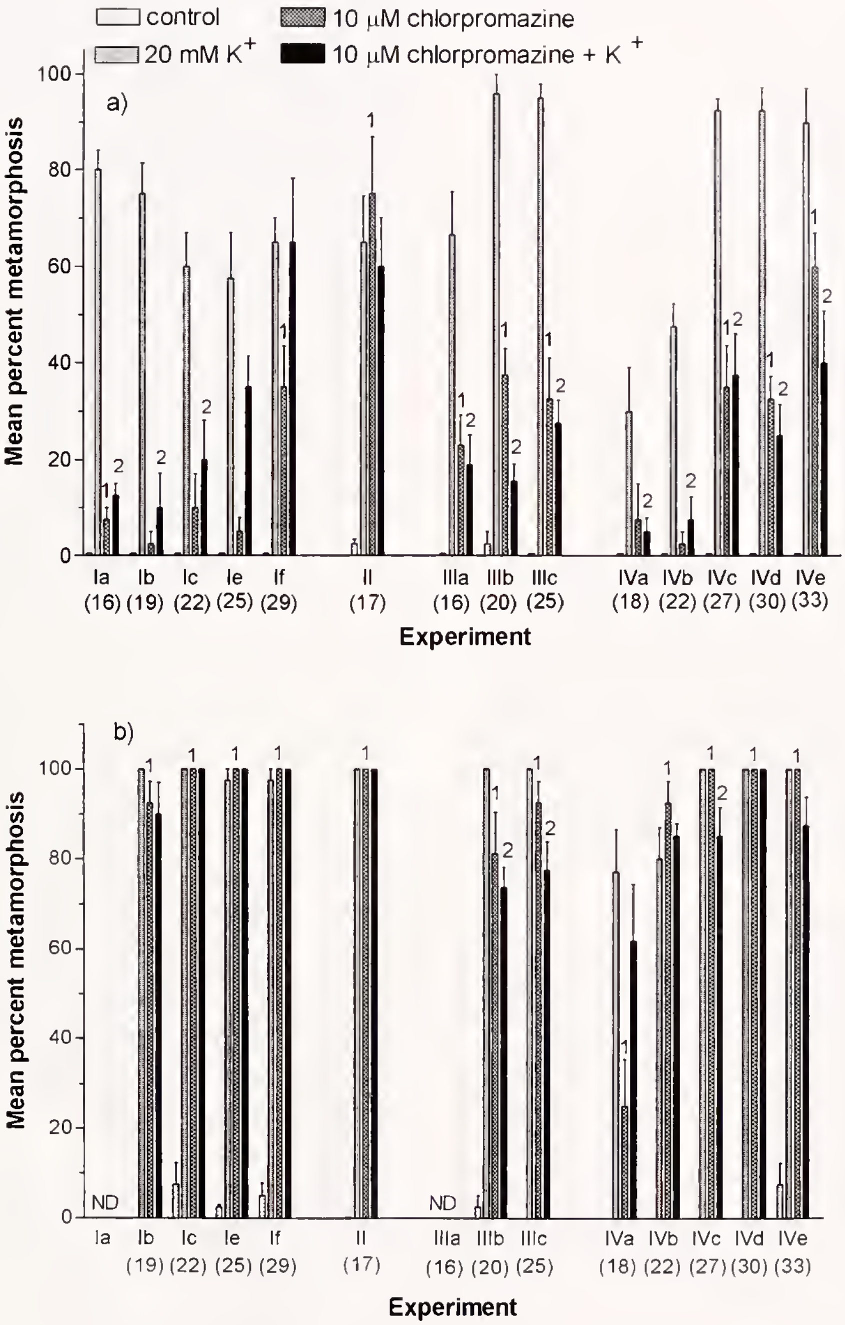

Figure 1. The influence of larval age and exposure duration on the effects that chlorpromazine has on metamorphosis in larvae of *Crepidula fornicata*. Excess K^+ was used as a convenient and reliable method for inducing metamorphosis. (a) Data for the first 6–8 h of exposure. (b) Data for the first 24 h of exposure. Larvae were obtained from a different female for each of the four experiments. Each bar represents the mean response (+ 1 SD) of larvae in 4 replicates, 10–12 larvae per replicate. "1" indicates a significant difference in the means of chlorpromazine and control outcomes ($P < 0.05$); *i.e.*, that chlorpromazine stimulated metamorphosis significantly above control levels. "2" indicates a significant difference in the means of excess K^+ and (chlorpromazine + excess K^+) outcomes; *i.e.*, that chlorpromazine significantly blocked the stimulatory effects of excess K^+. ND = No Data. The numbers in parentheses below the *x*-axis give the ages of the larvae when tested, in days. The dates of each assay, along with mean shell lengths of the larvae tested, are given in Table 1.

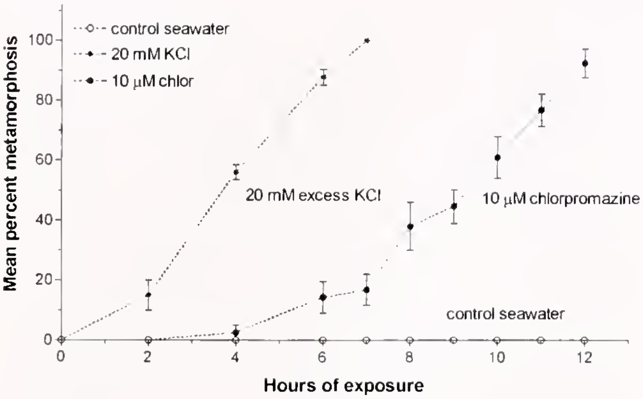

Figure 2. The time-course of larval responsiveness to chlorpromazine and excess K^+. Each point represents the mean response of larvae in four replicates, 10 larvae per replicate.

by excess K^+ (Fig. 4b). Surprisingly, however, SPIP significantly blocked the stimulatory effects of excess K^+ in two experiments over 24-h monitoring periods (Experiments IIIa and IVa, Fig. 4b).

Fewer than 10% of competent larvae within any replicate metamorphosed when exposed to the nitric oxide synthase inhibitor L-NAME at concentrations of 10 or 20 μM over 24 h; in 14 out of 16 replicates, no larvae metamorphosed in response to this chemical (Experiments If and IIa, data not shown).

Discussion

It is always difficult to fully interpret the results of studies in which intact, microscopic animals are immersed in baths of pharmacological agents (Pawlik, 1990). In our studies, problems include not knowing exactly where agents act, or when (or whether) they reach target tissues; the possibility that particular agents will have multiple (and perhaps simultaneous) effects within individual organisms; and uncertainty as to whether substances will operate in the target animal in the same way as they have been demonstrated to operate in the model organism or tissue preparations in which effects have been well-defined. However, the results of these experiments seem clear and convincing, even though our interpretation of those results may be controversial or incomplete. Chlorpromazine, a nonspecific dopamine antagonist, blocked the stimulatory action of excess K^+ clearly and dramatically for competent larvae of *Crepidula fornicata* during the first 6–8 h of exposure, particularly for the younger competent larvae within an experiment, and the specific D_1 antagonist R+ had a similar effect (indicated by the numeral "2" above the relevant bars of Figs. 1a and 3a). The results suggest that D_1 receptors are involved in the signal transduction pathway stimulated by excess K^+ in this species. Because natural cues probably act directly on external sensory receptors at the beginning of the metamorphic pathway (*e.g.*, Baloun and Morse, 1984; Hadfield *et al.*, 2000), upstream from wherever the excess K^+ is acting, we predict that—in short-term assays—chlorpromazine and R+ will also be found to block metamorphosis stimulated by natural cue in this species.

On the other hand, the specific D_2 antagonist SPIP blocked the inductive effect of excess K^+ in only 1 of 6 short-term assays, and even then by only about 30% (Experiment IIIa, Fig. 4a). Possibly the SPIP was simply not reaching the active site within the larvae quickly enough to block the stimulatory effect of excess K^+ during 6-h exposures. If so, a 1–2-h pre-exposure to SPIP might have been more effective at inhibiting metamorphosis in response to an increase in ambient K^+ concentration. This seems likely: although SPIP blocked the stimulatory effect of excess K^+ in only one experiment during 5–6-h exposures (Fig. 4a), it blocked the effect of excess K^+ significantly in two experiments by the end of 24-h exposures (Fig. 4b). Because SPIP is more lipophilic than the other two chemicals that we tested (the other two chemicals are water soluble, but SPIP is not), it should cross cell membranes more readily and have easier access to sites that are not so readily accessible to R+ or chlorpromazine; its limited ability to block the effects of excess K^+ in our studies suggests that it is acting at sites much farther downstream in the signal transduction pathway than the sites acted on by the other two chemicals. That the stimulatory effect of SPIP was slow to develop in these experiments is consistent with this suggestion. Our results with SPIP therefore suggest that D_2 receptors are also involved in the signal transduction pathway of *C. fornicata*. Overall, our data indicate that dopamine receptors may operate at several steps in the signal transduction pathway and lend support to the recent indications (Pires *et al.*, 2000b) that dopamine and perhaps other catecholamines play important roles in regulating metamorphosis in this species.

On the other hand, Pires *et al.* (2000b) found that artificially depleting the concentration of endogenous dopamine and its precursor L-DOPA to about 50% of initial concentrations in larvae of *C. fornicata* did not inhibit them from metamorphosing in response to excess K^+, even though it did inhibit the response to adult-conditioned seawater. We offer two explanations for this apparent discrepancy. One possibility is that neuronal concentrations of catecholamines may have been greatly reduced in some tissues but not significantly reduced in others; dopamine and L-DOPA concentrations were determined by Pires *et al.* (2000b) from pools of 30–40 whole larvae, so that it was not possible to tell whether dopamine and L-DOPA concentrations were reduced to the same extent in all tissues. Another possibility is that adult-conditioned seawater may be a weaker stimulus than excess K^+, causing a weaker depolarization and therefore less dopamine to be released. If so, excess K^+—but not adult-conditioned seawater—might still be able to cause the

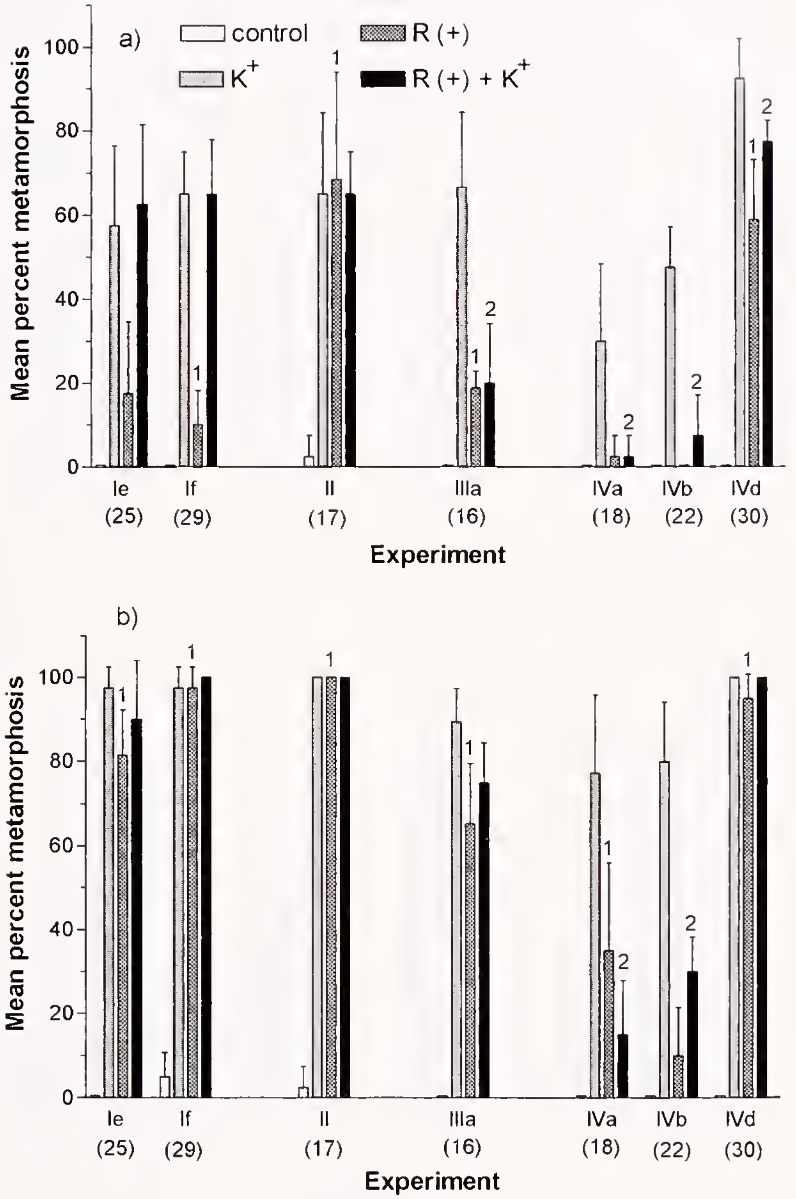

Figure 3. The influence of larval age on the effectiveness of the D_1 antagonist R+ in suppressing metamorphosis and in inducing *Crepidula fornicata* larvae to metamorphose within the first 5–6 h (a) and first 24 h (b) of exposure. Each bar represents the mean response (+ 1 SD) of larvae in four replicates, 10–12 larvae per replicate. "1" indicates a significant difference in the means of R+ and control outcomes ($P < 0.05$); *i.e.*, that R+ stimulated metamorphosis significantly above control levels. "2" indicates a significant difference in the means of excess K^+ and (R+ plus excess K^+) outcomes; *i.e.*, that R+ significantly blocked the stimulatory effects of excess K^+. The numbers in parentheses below the *x*-axis give the ages of the larvae when tested, in days. The dates of each experiment are given in Table 1.

release of sufficient dopamine to induce metamorphosis even when cellular dopamine concentrations are artificially reduced.

It is also clear from our data that chlorpromazine, while acting to block the stimulatory action of excess K^+ on metamorphosis, was itself a stimulus to metamorphosis, particularly for older competent larvae and in the longer (24-h) assays. Chlorpromazine has several additional effects in other model systems that may explain this aspect of our data. Of particular interest is that, in addition to its role as a dopamine D_2 antagonist, chlorpromazine inhibits nitric oxide synthase (NOS). Froggett and Leise (1999) present evidence that endogenous NO inhibits metamorphosis in the prosobranch gastropod *Ilyanassa obsoleta*. They found that although serotonin (5-HT) injections stimulated larvae of that species to metamorphose, the stimulatory effect of

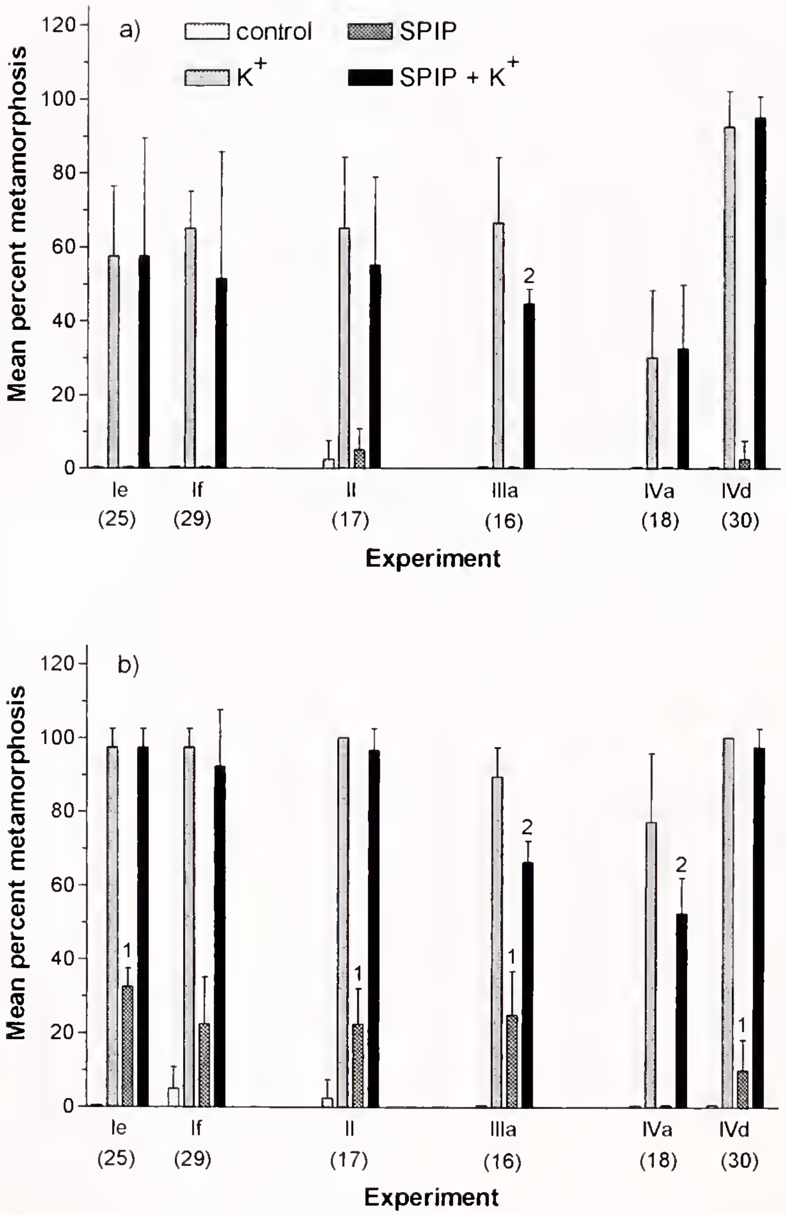

Figure 4. The influence of larval age on the effectiveness of the specific D_2 antagonist SPIP (spiperone) in suppressing metamorphosis and in inducing *Crepidula fornicata* larvae to metamorphose within the first 6–8 h (a) and first 24 h (b) of exposure. Each bar represents the mean response (+ 1 SD) of larvae in four replicates, 10–12 larvae per replicate. "1" indicates a significant difference in the means of SPIP and control outcomes ($P < 0.05$). "2" indicates a significant difference in the means of excess K^+ and (SPIP + excess K^+) outcomes. The numbers in parentheses below the *x*-axis give the ages of the larvae when tested, in days. The dates of each experiment are given in Table 1.

serotonin was blocked by bath application of the NO donors SIN-1 and SNAP (Froggett and Leise, 1999; Leise *et al.*, 2001). Also, they were able to induce metamorphosis by artificially reducing endogenous NO concentrations using the NOS inhibitor L-NAME (Froggett and Leise, 1999; Leise *et al.*, 2001). Similarly, endogenous NO apparently represses metamorphosis in two ascidian species (Bishop *et al.*, 2001) and the sea urchin *Lytechinus pictus* (Bishop and Brandhorst, 2001). This could explain the latent stimulatory effect of chlorpromazine on larvae in our experiments if metamorphosis in *C. fornicata* is also under insect-like inhibitory control (Pechenik and Qian, 1998), and assuming that chlorpromazine takes longer than K^+ to reach its target. It cannot, however, explain the latent stimulatory effect of R+, unless that chemical also has (unexplored) multiple effects in this system. Chlorpromazine can act as a histamine H_1 antagonist in some systems (Martinez and Coleman, 1990; Oken, 1995) and may also elevate intracellular concentrations of cyclic AMP or cGMP (by inhibiting calmodulin-stimulated cyclic nucleotide phosphodiesterase; Alfonso *et al.*, 1995), offering further possibilities for future exploration. Elevated concentrations of cAMP play roles in the signal transduction pathway of insect (Smith, 1995; Gilbert *et al.*, 1997) and barnacle metamorphosis (*Balanus amphitrite*: Clare, 1996; Yamamoto *et al.*, 1998), although apparently not in the metamorphic pathway of the polychaete *Hydroides elegans* (Holm *et al.*, 1998). Finally, chlorpromazine depletes serotonin in the central nervous system of *Lymnaea stagnalis*, but only after exposures of much greater duration than those used in the present study (Croll *et al.*, 1997). Thus it is also possible, though less likely, that chlorpromazine in our experiments stimulated metamorphosis through an effect on serotonin concentration.

Competent larvae of *C. fornicata* become sensitive to excess K^+ about 12–24 h sooner than they become responsive to adult-conditioned seawater, suggesting that excess K^+ acts at a point (or points) somewhat farther downstream from where the natural cue acts (Pechenik and Gee, 1993; see also Hadfield *et al.*, 2000). We cannot exclude the possibility that the excess K^+ may also depolarize the same sensory receptor or receptors eventually acted upon by the natural chemical stimulus; the sensory neurons might become sensitive to excess K^+ before the number of receptors on those neurons is sufficient to allow depolarization by natural chemical stimuli. Regardless of exactly where and at how many points excess K^+ acts, our working hypothesis is that exposing larvae of *C. fornicata* to excess K^+ leads to a shutdown of NO synthesis *via* a dopaminergic pathway—a pathway that can be blocked by some dopamine antagonists. Our results also suggest that chlorpromazine has an additional effect deeper in the metamorphic pathway of this species, downstream from the dopamine receptor block, possibly shutting down NO synthesis directly. The failure of the NOS inhibitor L-NAME to stimulate metamorphosis in our experiments could be an artifact of bath application; Froggett and Leise (1999) stimulated metamorphosis in *Ilyanassa obsoleta* through injection rather than bath application.

Alternatively, chlorpromazine might instead (or in addition) be stimulating metamorphosis in this species by elevating concentrations of calmodulin-dependent cyclic nucleotide phosphodiesterase. Either of these secondary roles could explain why chlorpromazine can act both to inhibit the stimulatory effects of excess K^+ and to stimulate metamorphosis on its own.

It is also clear that the responsiveness of *C. fornicata* larvae to chlorpromazine and R+ changed over time in our experiments, probably reflecting age-related changes in larval physiology. Such age-related changes in response were seen even in Experiment I, in which the mean shell length of larvae tested in the different assays did not increase significantly over time (Table 1, Fig. 1). Previous studies with this species indicate that neither absolute size nor absolute age are good indicators of physiological state (Pechenik and Heyman, 1987; Pechenik *et al.*, 1996b). It is also possible that the different results of assays within an experiment reflect physiological differences between faster and slower-growing larvae, since for each assay we deliberately selected the largest individuals available within a culture (although avoiding any unusually large larvae). Assuming that the different responses are in fact age-related, our results may have some bearing on the phenomenon of "spontaneous metamorphosis" (Crisp, 1974; Pechenik, 1984, 1990). If metamorphosis of competent larvae is prevented, in the absence of an appropriate external cue, by the presence of an endogenous inhibitor such as NO, then spontaneous metamorphosis may reflect an eventual end to the endogenous production of that inhibitor (Chia, 1978; Pechenik and Qian, 1998). A gradual decline in inhibitor titer might explain the age-related effects of chlorpromazine on metamorphosis documented in this study: chlorpromazine, acting as an inhibitor of NOS, would have a more rapid effect on metamorphosis of older competent larvae, as seen in the present study, if NO titers were declining naturally as the larvae aged. More detailed work on the effects of NO donors and NOS inhibitors in competent larvae of *C. fornicata*, following the protocols of Froggett and Leise (1999), could be productive, along with additional studies on the potential role of cAMP (and cGMP) in the signal transduction pathway.

It is worth pointing out that the complexity of our results arises from the apparently novel way that we conducted these experiments. If we had tested larvae at one age—for example when at least 60% of larvae subsampled from a culture were first competent to metamorphose—and if we had monitored our assays only at 24 h, our results would probably have been more straightforward. In general, we would have found that the putative dopamine antagonists that we tested did not block the effects of excess K^+, and we would have failed to find substantial support for the involvement of dopamine receptors in the metamorphic pathway, or at least that portion of the pathway activated by excess K^+. On the other hand, had we sampled only at 5–6 h, our results would have been far more erratic and difficult to interpret, both in the ability of the pharmacological agents to block the effects of excess K^+ and in their ability to stimulate metamorphosis directly (Figs. 1a, 3a). Only by monitoring changes in the responses of competent larvae subsampled from individual cultures over time were we able to determine that the ability of chlorpromazine and R+ to block the stimulatory effects of excess K^+ diminished as competent larvae aged, and that the stimulatory effects of the pharmacological agents themselves increased as the larvae aged and as experimental duration was prolonged. Perhaps the most interesting contribution of the present study is its demonstration that the effects of pharmacological agents on metamorphosis can change dramatically as competent larvae age, and as experimental duration is changed: timing is everything. It might be worth revisiting other marine invertebrate models in this light.

Acknowledgments

We thank Drs. Tony Pires, David Macmillan, and Charles Derby, and two anonymous reviewers, for their detailed comments and helpful suggestions on a draft of the manuscript.

Literature Cited

Alfonso, A., M. Estevez, M. C. Louzao, M. R. Vieytes, and L. M. Botana. 1995. Determination of phosphodiesterase activity in rat mast cells using the fluorescent cAMP analogue anthraniloyl cAMP. *Cell. Signal.* **7:** 513–518.

Baloun A. J., and D. E. Morse. 1984. Ionic control of settlement and metamorphosis in larval *Haliotis rufescens* (Gastropoda). *Biol. Bull.* **167:** 124–138.

Bishop, C. D., and B. P. Brandhorst. 2001. NO/cGMP signaling and HSP90 activity represses metamorphosis in the sea urchin *Lytechinus pictus. Biol. Bull.* **201:** 394–404.

Bishop, C. D., W. R. Bates, and B. P. Brandhorst. 2001. Regulation of metamorphosis in ascidians involves NO/cGMP signaling and HSP90. *J. Exp. Zool.* **289:** 374–384.

Bryan, P. J., and P.-Y. Qian. 1998. Induction of larval attachment and metamorphosis in the abalone *Haliotis diversicolor* (Reeve). *J. Exp. Mar. Biol. Ecol.* **223:** 39–51.

Carpizo-Ituarte, E., and M. G. Hadfield. 1998. Stimulation of metamorphosis in the polychaete *Hydroides elegans* Haswell (Serpulidae). *Biol. Bull.* **194:** 14–24.

Chia, F.-S. 1978. Perspectives: settlement and metamorphosis of marine invertebrate larvae. Pp. 283–285 in *Settlement and Metamorphosis of Marine Invertebrate Larvae,* F. S. Chia and M. E. Rice, eds. Elsevier/North Holland, Amsterdam.

Clare, A. S. 1996. Signal transduction in barnacle settlement: calcium re-visited. *Biofouling* **10:** 141–159.

Crisp, D. J. 1974. Factors influencing the settlement of marine invertebrate larvae. Pp. 177–265 in *Chemoreception in Marine Organisms,* P. T. Grant and A. M. Mackie, eds. Academic Press, New York.

Croll, R. P., M. W. Baker, M. Khabarova, E. E. Voronezhskaya, and D. A. Sakharov. 1997. Serotonin depletion after prolonged chlorpromazine treatment in a simpler model system. *Gen. Pharmacol.* **29:** 91–96.

Emaduddin, M., and H. Takeuchi. 1996. Lineweaver-Burk analysis for the blocking effects of mammalian dopamine receptor antagonists on dopamine-induced currents in *Achatina* giant neurones. *Gen. Pharmacol.* **27:** 1209–1213.

Eyster, L. S., and J. A. Pechenik. 1988. Comparison of growth, respiration, and feeding of juvenile *Crepidula fornicata* L. following natural or potassium chloride triggered metamorphosis. *J. Exp. Mar. Biol. Ecol.* **118:** 269–280.

Froggett, S. J., and E. M. Leise. 1999. Metamorphosis in the marine snail *Ilyanassa obsoleta,* yes or NO? *Biol. Bull.* **196:** 57–62.

Gilbert, L. I., Q. Song, and R. Rybczynski. 1997. Control of ecdysteroidogenesis: activation and inhibition of prothoracic gland activity. *Invertebr. Neurosci.* **3:** 205–216.

Green, K. A., S. J. Harris, and G. A. Cottrell. 1996. Dopamine directly activates a ligand-gated channel in snail neurones. *Pflueg. Arch. Eur. J. Physiol.* **431:** 639–644.

Hadfield, M. G., E. A. Meleshkevitch, and D. Y. Boudko. 2000. The apical sensory organ of a gastropod veliger is a receptor for settlement cues. *Biol. Bull.* **198:** 67–76.

Holm, E. R., B. T. Nedved, E. Carpizo-Ituarte, and M. G. Hadfield. 1998. Metamorphic-signal transduction in *Hydroides elegans* (Polychaeta: Serpulidae) is not mediated by a G protein. *Biol. Bull.* **195:** 21–29.

Juel, C. 1981. Presynaptic modulation of synaptic transmission in *Helix pomatia*: the effects of serotonin and dopamine antagonists. *Neuropharmacology* **20:** 323–326.

Kim, Y.-K., and M. L. Woodruff. 1995. Antagonists of both D_1 and D_2 mammalian dopamine receptors block the effects of dopamine on *Helix aspersa* neurons. *J. Biochem. Mol. Biol.* **28:** 221–226.

Leise, E. M., and M. G. Hadfield. 2000. An inducer of molluscan metamorphosis transforms activity patterns in a larval nervous system. *Biol. Bull.* **199:** 241–250.

Leise, E. M., K. Thavaradhara, N. R. Durham, and B. E. Turner. 2001. Serotonin and nitric oxide regulate metamorphosis in the marine snail *Ilyanassa obsoleta. Am. Zool.* **41:** 258–267.

Martinez, F., and J. W. Coleman. 1990. A comparison of the effects of chlorpromazine and more selective histamine and 5-hydroxytryptamine antagonists on human IgG synthesis *in vitro. Int. J. Immunopharmacol.* **12:** 185–191.

McGee, B. L., and N. M. Targett. 1989. Larval habitat selection in *Crepidula* (L.) and its effect on adult distribution patterns. *J. Exp. Mar. Biol. Ecol.* **131:** 195–214.

Oken, R J. 1995. Antihistamines, a possible risk factor for Alzheimer's disease. *Med. Hypotheses* **44:** 47–48.

Pawlik, J. R. 1990. Natural and artificial induction of metamorphosis of *Phragmatopoma lapidosa californica* (Polychaeta: Sabellariidae), with a critical look at the effects of bioactive compounds on marine invertebrate larvae. *Bull. Mar. Sci.* **46:** 512–536.

Pechenik, J. A. 1980. Growth and energy balance during the larval lives of three prosobranch gastropods. *J. Exp. Mar. Biol. Ecol.* **44:** 1–28.

Pechenik, J. A. 1984. The relationship between temperature, growth rate, and duration of planktonic life for larvae of the gastropod *Crepidula fornicata* (L.). *J. Exp. Mar. Biol. Ecol.* **74:** 241–257.

Pechenik, J. A., 1990. Delayed metamorphosis by larvae of benthic marine invertebrates: Does it occur? Is there a price to pay? *Ophelia* **32:** 63–94.

Pechenik, J. A., and C. C. Gee. 1993. Onset of metamorphic competence in larvae of the gastropod *Crepidula fornicata* (L.), judged by a natural and an artificial cue. *J. Exp. Mar. Biol. Ecol.* **167:** 59–72.

Pechenik, J. A., and W. D. Heyman. 1987. Using KCl to determine size at competence for larvae of the marine gastropod *Crepidula fornicata* (L.). *J. Exp. Mar. Biol. Ecol.* **112:** 27–38.

Pechenik, J. A., and G. M. Lima. 1984. Relationship between growth, differentiation, and length of larval life for individually reared larvae of the marine gastropod, *Crepidula fornicata. Biol. Bull.* **166:** 537–549.

Pechenik, J. A., and P.-Y. Qian. 1998. Onset and maintenance of metamorphic competence in the marine polychaete *Hydroides elegans* Haswell in response to three chemical cues. *J. Exp. Mar. Biol. Ecol.* **226:** 51–74.

Pechenik, J. A., M. G. Hadfield, and L. S. Eyster. 1995. Assessing whether larvae of the opisthobranch gastropod *Phestilla sibogae* Bergh become responsive to three chemical cues at the same age. *J. Exp. Mar. Biol. Ecol.* **191:** 1–17.

Pechenik, J. A., M. S. Estrella, and K. Hammer. 1996a. Food limitation stimulates metamorphosis of competent larvae and alters postmetamorphic growth rate in the marine prosobranch gastropod *Crepidula fornicata. Mar. Biol.* **127:** 267–275.

Pechenik, J. A., K. Hammer, and C. Weiss. 1996b. The effect of starvation on acquisition of competence and postmetamorphic performance in the marine prosobranch gastropod *Crepidula fornicata. J. Exp. Mar. Biol. Ecol.* **199:** 137–152.

Pires, A., R. P. Croll, and M. G. Hadfield. 2000a. Catecholamines modulate metamorphosis in the opisthobranch gastropod *Phestilla sibogae. Biol. Bull.* **198:** 319–331.

Pires, A., T. R. Guilbault, J. V. Mitten, and J. A. Skiendzielewski. 2000b. Catecholamines in larvae and juveniles of the prosobranch gastropod, *Crepidula fornicata. Comp. Biochem. Physiol. C* **127:** 37–47.

Smith, W. A. 1995. Regulation and consequences of cellular changes in the prothoracic glands of *Manduca sexta* during the last larval instar: a review. *Arch. Insect Biochem. Physiol.* **30:** 271–293.

Sokal, R. R., and F. J. Rohlf. 1981. *Biometry: The Principles and Practice of Statistics in Biological Research,* 2nd ed. W.H. Freeman, New York.

Spencer, G. E., K. Lukowiak, and N. I. Syed. 1996. Dopamine regulation of neurite outgrowth from identified *Lymnaea* neurons in culture. *Cell. Mol. Neurobiol.* **16:** 577–589.

Swann, J. W., C. N. Sinback, M. G. Pierson, and D. O. Carpenter. 1982. Dopamine produces muscle contractions and modulates motoneuron-induced contractions in *Aplysia californica* gill. *Cell. Mol. Neurobiol.* **2:** 291–308.

Todd C. D., M. G. Bentley, and J. N. Havenhand. 1991. Larval metamorphosis of the opisthobranch mollusc *Adalaria proxima* (Gastropoda: Nudibranchia): the effects of choline and elevated potassium ion concentration. *J. Mar. Biol. Assoc. UK* **71:** 53–72.

Woollacott, R. M., and M. G. Hadfield. 1996. Induction of metamorphosis in larvae of a sponge. *Invertebr. Biol.* **115:** 257–262.

Yamamoto, H., A. Tachibana, W. Saikawa, M. Nagano, K. Matsumura, and N. Fusetani. 1998. Effects of calmodulin inhibitors on cyprid larvae of the barnacle, *Balanus amphitrite. J. Exp. Zool.* **280:** 8–17.

Zimmerman, K. M., and J. A. Pechenik. 1991. How do temperature and salinity affect relative rates of growth, morphological differentiation, and time to metamorphic competence in larvae of the marine gastropod *Crepidula plana*? *Biol. Bull.* **180:** 372–386.

Reference: *Biol. Bull.* **202:** 148–155. (April 2002)

Morphometric Analysis of Male Reproductive Features of Octopodids (Mollusca: Cephalopoda)

JANET R. VOIGHT

Department of Zoology, The Field Museum, 1400 S. Lake Shore Dr., Chicago, Illinois 60605

Abstract. Taxonomic accounts of octopodids frequently describe the spermatophore, the penis that releases the spermatophore from the internal organs, and the ligula and calamus that transfer it to a female. To explore relationships among these male features and body size, this study applies principal components analysis to data from 43 species of the family Octopodidae, or benthic octopuses. Covariation in penis and mantle length opposed by covariation in ligula and calamus lengths forms primary shape variation. Secondary shape variation is due to opposing variation between ligula and calamus lengths. Primary shape variation is greatest among shallow-water species. The calami and ligulae of diurnal and crepuscular shallow-water species are short compared to those of nocturnal shallow-water species. Because these structures contain heterogeneous collagen arrays and lack camouflaging chromatophore organs, they are white. Diurnal and crepuscular octopus species may minimize their lengths due to selection imposed by visual predators. Secondary shape variation is greater in deep-sea and high-latitude octopuses. Members of Voss's Eledoninae (except *Eledone*) and Graneledoninae and two species of *Benthoctopus* have exceptionally long calami and comparatively short ligulae; these lengths vary among members of the Bathypolypodinae. Variation in spermatophore length is independent of the structures considered.

Introduction

Male octopuses package sperm into spermatophores as it moves from the testis to the wholly internal penis, or terminal organ. To initiate sperm transfer, the muscular penis, which is continuous with the penial diverticulum, propels a stored spermatophore through the funnel to a groove on the ventral margin of the hectocotylus, one of the third arms (usually the right) that is shorter than the opposite arm. The spermatophore travels the length of the arm to its suckerless tip. At the arm tip, the aboral ligula, which depending on species can occupy from 3% to 38% of the arm length, is closely opposed by the shorter calamus. These structures presumably position the spermatophore in the female's oviduct prior to the release of sperm (see Mann, 1984).

Among the Octopodidae, or benthic octopuses, ligula and calamus morphology is extremely variable (Robson, 1926). Because the ligula and calamus function with the penis to transfer spermatophores at copulation, and thereby increase male fitness, these characters may evolve as a unit rather than independently. Voss (1988), for instance, suggested that the large spermatophores and ligulae and calami of deep-sea taxa are causally linked. This hypothesis had yet to be tested by exploration of covariation among the features that handle spermatophores in mating.

This paper explores variation among spermatophore, penis, calamus, and ligula lengths, as well as mantle length, in 43 species to examine patterns of variation and to reveal morphological diversity in the family. Possible functional and ecological constraints that affect their morphology are discussed.

Materials and Methods

Mantle length, spermatophore length, penis length, ligula length, and calamus length of 135 specimens representing 43 species were compiled from literature reports ($n = 102$) and from 33 preserved specimens (Appendix). Generally, published accounts reported measurement data only as indices, forcing the original measurements to be back-calculated. All measurements were log-transformed to base 10 prior to analysis. Log-transformation equalizes error—whether the result of measurement error, investigator bias, or the use of back-calculated measurements—over the wide

Received 12 September 2001; accepted 28 January 2002.

E-mail: jvoight@fieldmuseum.org

size range considered and minimizes the effect of outliers (Bookstein *et al.*, 1985; Strauss, 1985).

The characters chosen for this analysis are those of spermatophores and features that handle spermatophores during copulation; mantle length is included as the standard indicator of body size. Four other characters—sperm reservoir length, penis (terminal organ) diverticulum length, and the lengths of the third arm pair—had to be excluded from the analysis due to the following concerns. Sperm reservoir length is so tightly associated with total spermatophore length that it cannot function as an independent variable (Voight, 2001). The penis diverticulum is continuous with the penis, or terminal organ, proper. Homologies of the end points of the penis diverticulum were questionable, hence its length measurement was excluded. Because the diverticulum and penis are continuous, and subject to deformation apparently related to preservation (Alvina, 1965), their combined *in situ* anterior-posterior length was measured. Voight (1993) documented that arm length contributes considerable size-free shape variation within the Octopodidae. Preliminary analyses found that length variation in the hectocotylus and the unmodified third arm is strongly linked to overall species morphology; to focus this exploration on reproductive characters, arm lengths were not considered.

The measurement of penis length also presented potential problems. This measurement, from the extreme posterior tip of the penis diverticulum to the most cephalad part of the penis near the mantle aperture, generally parallels the ventral mantle septum and seems comparable with other extremal distances. The penis and diverticulum of some specimens, especially in the *O. aegina* group, can curve away from the mantle septum and, in extreme cases, become recurved (*e.g.*, Sasaki, 1929; Adam, 1960). Use of the linear penis length measurement ignored any curves; as a result, penis length may have been underestimated in some specimens. Calamus and ligula lengths are measured from the distal sucker to the tip of each of the arm modifications (Fig. 1).

The specimens included in the analysis sample the benthic octopodids as completely as possible, considering that the analysis requires matrix manipulations that force specimens without complete data to be deleted. For instance, within *Eledone*, only *E. palari* could be included, because only in this species is the calamus present. Regardless of whether the calamus of *Eledone* is represented in the analysis as missing or as zero, the pertinent specimens must be deleted because the log of zero is undefined. Thirteen currently recognized octopodid genera are included here, although sometimes by only one individual (see Appendix 1). Although *Cistopus* also reportedly lacks a calamus, the calamus in the specimen examined could be reliably measured, in contrast to the specimens of *Eledone* examined. To allow inclusion of a representative of *Euaxoctopus*, spermatophore length reported for one specimen had to be combined with data from another specimen. Although phylogenetic relationships among the Octopodidae remain obscure (Voight, 1997), three informally recognized species groups (*e.g.*, Robson, 1929; Norman and Sweeney, 1997) are treated here.

Members of the *Octopus vulgaris* species group tend to be large, with the dorsal arms and web sector shortest. The ligula and calamus are small and, depending on the species, prominent ocelli may be present. Several members of this group are active during daylight hours (Hanlon, 1988; Hanlon and Messenger, 1996). Members of the *O. aegina* group listed by Norman and Sweeney (1997) tend to be medium in size, with the dorsal arms and web sector dramatically the shortest (Robson, 1929). The penis and its diverticulum can be very long; warts characterize the skin texture, ocelli may be present on the web, and longitudinal lines of color often occur on the arms and mantle (Robson, 1929; Norman and Sweeney, 1997). Species in this group are considered to be crepuscular (Norman and Sweeney, 1997), although *O. burryi* has been identified as nocturnal (Hanlon, 1988). Species of the *O. macropus* group tend to be large with the dorsal arms and web sector the longest, and red and white in color. Activity among these species appears to be exclusively nocturnal (Hanlon, 1988; Norman, 1993a). The *O. (Abdopus)* subgenus of Norman and Finn (2001) includes long-armed Indo-West Pacific species with small mantles and complex skin textures. Members of the subgenus reportedly occur only in the intertidal zone, and some forage during daylight low tides (Norman and Finn, 2001).

To explore morphological variation among the five measurements in 135 specimens, the data matrix was analyzed by principal components analysis (PCA) using a covariance matrix in SySTAT version 9 (SPSS). PCA assesses shape and size variation without *a priori* group determinations. If all characters used in the analysis are assigned uniformly large positive loadings on a component, usually principal component 1 (PC1), that component is considered to represent covariation due to size. Shape variation is attributed to secondary components, with the magnitude and sign of the loadings indicating their relative contribution and relationship to other characters. Plots of specimen scores on the shape components PC2 *versus* PC3 help to visualize the size-free shape similarities and differences among the specimens considered.

Because the reproductive characters considered in this analysis enlarge as males mature rather than as they grow, including less than fully mature males in the analysis would complicate the calculation of the size component. To ensure a strong size component and heighten comparability among species represented by mature males of different sizes, an attempt was made to include only fully mature males. Males were excluded if they had short mantles, penises, ligulae, and spermatophores relative to those of conspecifics.

Evidence of investigator bias was assessed by comparing individual specimen scores within species groups and within species, in the few cases in which different investigators reported data for a single species. Bivariate plots of log-transformed data in Microsoft Excel were used to explore patterns of variation discovered by the PCA. Because these plots did not require that each specimen be represented by all five measurements, all possible specimens were included, except specimens of the Atlantic species of *Eledone* that Voight (2001) found to be unique among the octopodids.

To further test the hypothesis that spermatophore size is causally linked to ligula and calamus length, the greatest width of the spermatophore was considered *post hoc*. This measurement, usually taken at the sperm reservoir, is infrequently reported. Weill (1927) found in fresh specimens that spermatophore width varies with the salinity of surrounding fluid. If the salinity of the fixative affects spermatophore width in preserved specimens, the measurement may be unreliable. This possibility could not be tested because data within a species and information on specimen preservation were too limited. With the limited data available, the relationships between spermatophore width and ligula and calamus lengths were explored by plotting log-transformed spermatophore width data *versus* specimen score on PC3 for 87 specimens.

Table 1

PCA (principal components analysis) component loadings for the five length variables considered

	PC1	PC2	PC3	PC4
Log mantle length	0.229	**0.107**	−0.041	0.068
Log ligula length	0.377	**−0.122**	**−0.095**	−0.006
Log calamus length	0.316	−0.101	**0.100**	0.041
Log penis length	0.309	**0.107**	0.014	0.006
Log spermatophore length	0.360	0.057	0.025	**−0.079**
% of total variation explained	84.9	8.4	3.5	2.1

The extremely long spermatophores of some members of the *Octopus aegina* species group are the primary source of shape variation on PC4 and are not further discussed here. Loadings that contribute to primary shape variation are in bold type.

Results

PCA revealed most variation in the data set to be due to size differences among the specimens considered (Table 1). Shape variation on PC2 was dominated by covariation in penis and mantle lengths in opposition to covariation of ligula and calamus lengths. PC3 revealed shape variation created by opposing variation between ligula and calamus lengths. Spermatophore length contributed minimal shape variation on either PC2 or PC3 (Table 1); it was the major source of shape variation on PC4, due largely to species of the *Octopus aegina* group.

Mean scores on PC2 and PC3 for each species are reported in the Appendix, and individual scores are plotted on Figure 1. Shallow-water species show extreme variation on PC2. With near zero or negative scores on PC3, *Cistopus* and the diurnal and crepuscular groups of *Octopus vulgaris* (with the exception of *O. filosus*) and *O. aegina* (with the exception of *O. polyzenia*), which overlap extensively, have positive PC2 scores that reflect their small ligulae and calami and long mantles and penises. In direct opposition, negative PC2 and near zero PC3 scores of *Ameloctopus litoralis* and *Euaxoctopus pillsburyae* reflect their long ligulae and calami and short mantles and penises. With slightly stronger negative PC3 scores and therefore longer ligulae, *O. australis, O. berrima, Bathypolypus arcticus,* and *Benthoctopus* spp. are also negative on PC2. Most members of the *O. macropus* group score near zero on PC2 and are slightly negative on PC3, although within this group both *O. macropus* and *O. rapanui* have positive PC2 scores.

The deep-sea and high-latitude species Voss (1988) assigned to Eledoninae (excluding species of *Eledone* that could not be included) score positively on PC3, indicative of relatively long calami, and near zero on PC2. The species assigned to Voss's Bathypolypodinae have negative PC2 scores but variable PC3 scores.

Species with negative PC3 scores, and therefore a long ligula relative to calamus, vary widely in their PC2 scores. Most members of the diurnal subgenus *Octopus (Abdopus)* are strongly positive on PC2, although some poorly known taxa in that subgenus overlap with species of the *O. macropus* group. Specimens of *O. australis* and *O. berrima* score negatively on both shape components and, based on the characters considered in this analysis, are comparable to *Bathypolypus*.

As noted above, scores for the diurnal *O. vulgaris* and *O. aegina* species groups overlap, being positive on PC2 and near zero on PC3, except *O. filosus* and *O. polyzenia* (Fig. 1). Species of the nocturnal *O. macropus* group tend to score near zero on PC2 and negative on PC3, except *O. rapanui,* which overlaps the *O. vulgaris* and *O. aegina* groups. The taxa assigned to the Eledoninae of Voss (1988) and specimens of *Graneledone* score strongly and uniformly positive on PC3, but are not unique. Individuals of *Benthoctopus macrophallus, B. piscatorum,* and *O. campbelli* have similar scores on both components.

No evidence of investigator bias was apparent. Bivariate analyses support the covariances discovered among these variables; a single linear relationship explains 86.67% of the variation between spermatophore and penis length among 155 specimens. Between spermatophore and mantle length, a single linear relationship explains 73.4% of the variation among 211 specimens. In contrast, the relationship between ligula and mantle length in 325 specimens explains only 40.0% of the variation; between calamus and mantle length,

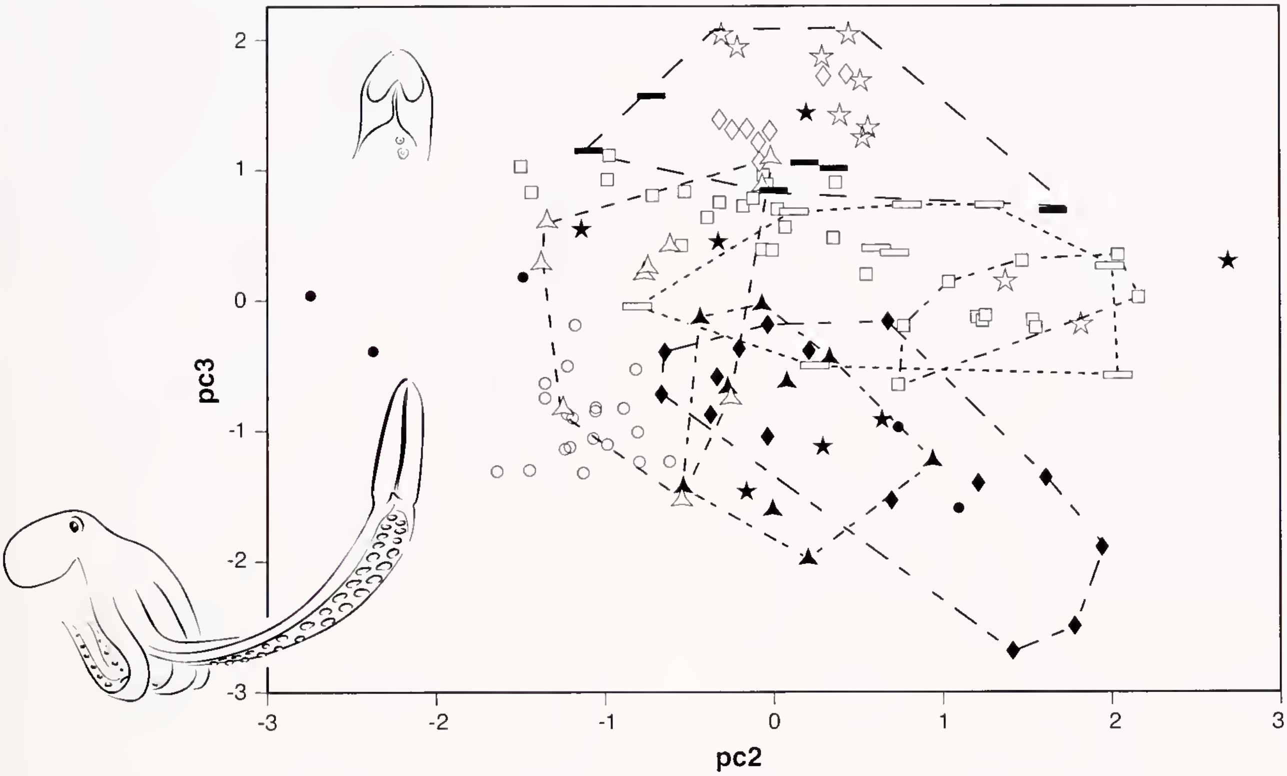

Figure 1. Plotted are individual specimen scores on principal components 2 *versus* principal components 3. Large positive PC2 scores indicate long mantles and penises and short ligulae and calami; large negative PC2 scores represent the converse. Large positive PC3 scores represent comparatively short ligulae and long calami, large negative PC3 scores represent the converse. The inset hectocotylus tips of *Graneledone pacifica* (above), adapted from Voss and Pearcy (1990), and *Octopus dierythraeus* (below), adapted from Norman (1993a), illustrate the differences on PC3. Octopuses with one sucker row cluster at the top of the plot and are outlined by a line of long dashes: included are specimens of *Graneledone pacifica* represented by ☆; those of *Eledone palari* by ◇; those of *Pareledone charcoti, P. harrissoni,* and *Vosseledone charrua* by heavy bars. Members of the *O. vulgaris* group are represented by □; all except *O. filosus* are outlined with a fine dashed line. The *O. aegina* group, with *O. polyzenia* at the far left, is represented by hollow bars, and the complete group is outlined by a dotted line. Overlapping these two groups are two specimens of *O. rapanui*, symbolized by ☆, that were assigned to the *O. macropus* group by Norman and Sweeney (1997). Members of this group (represented by ▲) are outlined with a line of dashes and dots; specimens of *O. macropus* have the two most positive PC2 scores. Specimens of *Octopus (Abdopus)*, represented by ◆, are outlined by a line of alternating dashes. ● indicates long-armed octopuses not assigned to *O. (Abdopus)*: at the far left are two *Ameloctopus litoralis*; the third from the left is *Euaxoctopus pillsburyae*; specimens of *O. defilippi* overlap those of *Octopus (Abdopus)*. Individuals of *O. berrima* and *O. australis*, which are inseparable on this plot, are represented by ○. They, as do many other species, overlap Voss's Bathypolypodinae, indicated by △, and outlined by a dashed line. The far right ★ indicates *Cistopus*, other ★ represent miscellaneous species with scores reported in the Appendix.

the percent of variation explained drops to 36.8% in 297 specimens.

No discernible relationship exists between the PC3 score and spermatophore width in 87 specimens. If species that produced wide spermatophores had long ligulae or calami, the plot would show a U-shape, which it does not. If production of wide spermatophores were associated with either a long ligula or calamus, there would be a significant correlation, which does not exist. There is no pattern with the geographic distribution of the specimens. Deep-sea specimens have either narrow or wide spermatophores, as do those from shallow-water tropical latitudes. Although members of *Graneledone* and Voss's Eledoninae have the highest scores on PC3 and the widest spermatophores, the specimen of *Bathypolypus* included had very wide spermatophores and a negative (−0.75) PC3 score. Most members of *Octopus (Abdopus)* and *Ameloctopus* had remarkably and consistently narrow spermatophores, regardless of their PC3 score.

Discussion

Among the specimens of benthic octopodids considered, mantle and penis lengths covary and oppose variation in ligula and calamus lengths (Table 1). The covariation seen on PC2 in mantle and penis lengths may result from functional constraints. The octopus penis, because it is contained within the mantle, tends to vary in concert with mantle length rather than independent of mantle length. If the maximal lengths of the exceptionally long curved penises of some species of the *Octopus aegina* group had been fully considered in this analysis, they would covary with the very long spermatophores of these species that in this analysis contribute most shape variation to PC4 (Table 1).

Underlying the covariation discussed above is opposing variation between ligula and calamus lengths, which apparently was previously unsuspected. Spermatophore length does not covary with ligula or calamus length, nor does spermatophore width. If, however, during copulation the ligula, the calamus, or both hold the spermatophore at its narrow ejaculatory apparatus, rather than at its widest part, a functional relationship may exist undetected; currently, however, ligula and calamus lengths must be assumed to be free of functional constraints. Variation in these lengths may relate to environmental factors.

Most shallow-water diurnal and crepuscular species, including some species of *Octopus (Abdopus)* and the *O. vulgaris* and *O. aegina* groups, have more positive PC2 scores—and thus shorter ligulae and calami—than do shallow-water nocturnal species from comparable latitudes, such as members of the *O. macropus* group, *Ameloctopus litoralis* and *O. joubini*. The ligula, the calamus, and the groove on the ventral arm that moves the spermatophore to the tip of the hectocotylus lack the chromatophore organs that camouflage cephalopod skin (Racovitza, 1894). Histological sections of these features reveal abundant collagen fibers in a heterogeneous array (J. Thompson, University of North Carolina, pers. comm.). Heterogeneous collagen arrays reflect light (Johnsen and Widder, 1999), to make these structures appear white rather than translucent (S. Johnsen, Duke University, pers. comm.). Their white color may make these structures conspicuous and, especially in diurnal and crepuscular octopuses, vulnerable to visual predators. Although octopuses regenerate lost and damaged arms, including the hectocotylus (Callan, 1939), the fitness cost of damage to the hectocotylus may be high. Males typically hold the hectocotylus in a coiled position, perhaps both to conceal it and to protect its tip (Naef, 1923). Physically minimizing the ligula and calamus in diurnally active octopuses may further reduce the risk of predation and preserve a male's ability to copulate.

The contrast between ligula and calamus lengths of diurnal *versus* nocturnal species parallels the contrast in body patterning complexity in these species, hypothesized to result from selection by visual predators (Hanlon and Messenger, 1996). Diurnal species in complex habitats are hypothesized to have the most complex body patterns because visual predators exert the greatest selection on this group; nocturnal species, and those occurring on more uniform habitats such as sediment, are predicted to show simpler body patterns because visual predators have less effect (Hanlon and Messenger, 1996). Hanlon and Messenger (1996) could not document body patterning complexity among octopuses from deep-sea and high-latitude environments where visual predators are thought to be rare. If ligula and calamus lengths reflect the level of predation by visual predators, octopuses from these areas are predicted to have long ligulae, calami, or both. This study supports this prediction with two opposing patterns.

Long calami characterize most species of Voss's (1988) Eledoninae (except *Eledone*), which are Antarctic and deep-sea in distribution; species of the deep-sea Graneledoninae; specimens of *O. campbelli* (from 52° S); and two specimens of the deep-sea genus *Benthoctopus*. Voss (1988) did not cite calamus length as unifying members of his Eledoninae (exclusive of *Eledone*, which lacks a calamus) and Graneledoninae. Species of *Bathypolypus* and *Benthoctopus*, which compose the Bathypolypodinae, Voss's other subfamily of deep-sea and high-latitude species, are less uniform. Differences in ligula and calamus lengths of these species may reliably reflect their evolutionary histories, notably their polyphyletic origin.

The minute ligula and calamus and large body size help unify the *O. vulgaris* group (Pickford and McConnaughey, 1949); the former two features appear to ally this group with the *O. aegina* group. These groups, in fact, may have been extensively confused in the past. Some members of both groups have ocelli on the web; all species have short dorsal arm pairs and dorsal web sectors and enlarged suckers on the second and third arm pairs of mature males. If the *O. aegina* and *O. vulgaris* groups are closely related, the small ligula and calamus may be ancestral. The differences *O. filosus* shows compared to the other members of *O. vulgaris* suggest, however, that morphology or the relationship between male reproductive organ size and mantle length in this fairly small species is plastic.

Although morphology of copulatory organs may reflect history, variation exists within the widely recognized species groups of *O. vulgaris* and *O. aegina*. *Octopus polyzena* of the *O. aegina* group and *O. filosus* of the *O. vulgaris* group have long ligulae and calami. The ecology of *O. polyzenia* is virtually unknown. Members of *O. filosus* have been most often collected at fish poison stations on Caribbean coral reefs (Voss, 1953; Burgess, 1966). If their high degree of crypsis and use of secluded reef habitats effectively protect them from visual predators as well as from humans, visual predators may impose minimal selection on members of this species. Among species assumed to be nocturnal, the short ligula and calamus of *O. rapanui* place it with diurnal and crepuscular species, rather than with other members of the nocturnal *O. macropus* group. Voss (1979) indicated that this species was only superficially similar to members of the *O. macropus* group; Norman and Sweeney (1997) implicitly disagreed when they assigned it to the group. Additional natural history data on this and other little known species would test the hypothesis that selection by visual predators limits ligula and calamus length in diurnal and crepuscular species.

One taxon that could not be included here, *Grimpella thaumastocheir*, was described by Robson (1928) as having a huge calamus. Although Robson allied this taxon to *Bathypolypus* and *Benthoctopus*, as did Voss (1988), the results reported here show that most members of those genera have a longer ligula than calamus. *Grimpella* therefore appears more similar to *O. campbelli*, another species from cold southern waters (Stranks and Norman, 1993). That both Robson and Voss allied this species with those with longer ligulae, rather than with those with large calami, suggests that neither worker recognized or gave credence to the difference the present analysis emphasizes.

Lu and Stranks (1991) acknowledge that the presence of a calamus makes *E. palari* unique among species of *Eledone*, and they recognize that the calamus is unusually large in that species. They assigned the species to *Eledone* because its male arm tips are hetermorphic, a feature that is otherwise unique to that genus. They clearly assumed that the heteromorphic arm tips were derived from a common ancestor and that the calamus, an octopodid plesiomorphy, was lost in the ancestor of the Atlantic species of the genus. Given the striking similarity between calamus and ligula length in this species and in members of *Pareledone*, the consistency of the geographic and depth distributions of *E. palari* and the circum-Antarctic species of *Pareledone*, the homology of the arm modification merits reinvestigation.

It has been argued that visual predators have strongly impacted cephalopods through their evolution (Packard, 1972, 1988). This study suggests that the influence of visual predators extends to the mechanics of copulation itself. The degree to which the lengths of the calamus and ligula reflect evolutionary history *versus* ecological pressures will remain unknown until we develop a better understanding of the natural history of the organisms.

Acknowledgments

Jodi Sedlock, University of Illinois at Chicago, provided invaluable assistance with the multivariate analysis. Rich Strauss provided insightful comments during this study. The combined expertise of Joe Thompson of The University of North Carolina at Chapel Hill and Sönke Johnsen of Duke University provided unique insight into the pattern seen here. M. Vecchione and R. Toll provided helpful comments on the text; C. Simpson provided the figure. Terry Gosliner of the California Academy of Sciences, Nancy Voss of the University of Miami Marine Laboratories, and George Davis of the Academy of Natural Sciences of Philadelphia allowed me to examine specimens in their care.

Literature Cited

Adam, W. 1960. Cephalopoda from the Gulf of Aqaba. *Bull. of the Sea Fish. Res. Stn. Haifa* **26:** 3–26.

Alvina, L. H. 1965. A study of the morphology and biology of *Octopus hummelinki* Adam, 1936. Master's thesis. University of Miami, FL. 146 pp.

Bookstein, F. L., B. Chernoff, R. L. Elder, J. M. Humphries Jr., G. R. Smith, and R. E. Strauss, Eds. 1985. *Morphometrics in Evolutionary Biology.* Academy of Natural Sciences of Philadelphia Special Publication **15**, Philadelphia, PA. 277 pp.

Burgess, L. A. 1966. A study of the morphology and biology of *Octopus hummelincki* Adam, 1936 (Mollusca: Cephalopoda). *Bull. Mar. Sci.* **16:** 762–813.

Callan, H. G. 1939. The absence of a sex-hormone controlling regeneration of the hectocotylus in *Octopus vulgaris* Lam. *Pubbl. Staz. Zool. Napoli* **18:** 15–19.

Hanlon, R. T. 1988. Behavioral and body patterning characters useful in taxonomy and field identification of cephalopods. *Malacologia* **29:** 247–264.

Hanlon, R. T., and J. B. Messenger. 1996. *Cephalopod Behaviour.* Cambridge University Press, Cambridge.

Johnsen, S., and E. A. Widder. 1999. The physical basis of transparency in biological tissue: ultrastructure and the minimization of light scattering. *J. Theor. Biol.* **199:** 181–198.

Kubodera, T., and T. Okutani. 1994. Eledonine octopods from the Southern Ocean: systematics and distribution. *Antarct. Sci.* **6:** 205–214.

Lu, C. C., and T. N. Stranks. 1991. *Eledone palari*, a new species of octopus (Cephalopoda: Octopodidae) from Australia. *Bull Mar. Sci.* **49:** 73–87.

Mann, T. 1984. *Spermatophores: Development, Structure, Biochemical Attributes and Role in the Transfer of Spermatozoa.* Springer-Verlag, Berlin.

Naef, Adolf. 1923. *Fauna und Flora des Golfes von Neapel und der angrenzenden Meeres. Vol. 1. Cephalopoda.* Monograph 35, Zoological Station, Naples. English translation: *Fauna and Flora of the Bay of Naples.* 1972. A. Mercado, trans. Israel Program for Scientific Translations, Jerusalem.

Norman, M. D. 1991. *Octopus cyanea* Gray, 1849 (Mollusca: Cephalopoda) in Australian waters. *Bull Mar. Sci.* **49:** 20–38.

Norman, M. D. 1992. *Ameloctopus litoralis*, gen. et sp. nov. (Cephalopoda: Octopodidae), a new shallow-water octopus from tropical Australian waters. *Invertebr. Taxon.* **6:** 567– 582.

Norman, M. D. 1993a. Four new octopus species of the *Octopus macropus* group (Cephalopoda: Octopodidae) from the Great Barrier Reef, Australia. *Mem. Mus. Vic.* **53:** 267–308.

Norman, M. D. 1993b. Ocellate octopuses (Cephalopoda: Octopodidae) of the Great Barrier Reef, Australia: description of two new species and redescription of *Octopus polyzenia* Gray, 1849. *Mem. Mus. Vic.* **53:** 309–344.

Norman, M. D. 1993c. *Octopus ornatus* Gould, 1852 (Cephalopoda: Octopodidae) in Australian waters: morphology, distribution, and life history. *Proc. Biol. Soc. Wash.* **106:** 645–660.

Norman, M. D., and J. Finn. 2001. Revision of the *Octopus horridus* species-group, including erection of a new subgenus and description of two member species from the Great Barrier Reef, Australia. *Invertebr. Taxon.* **15:** 13–35.

Norman, M. D., and M. J. Sweeney. 1997. The shallow-water octopuses (Cephalopoda: Octopodidae) of the Philippines. *Invertebr. Taxon.* **11:** 89–140.

Packard, A. 1972. Cephalopods and fish: the limits of convergence. *Biol. Rev.* **47:** 241–307.

Packard, A. 1988. Visual tactics and evolutionary strategies. Pp. 89–103 in *Cephalopods Present and Past*, J. Wiedmann and J. Kullmann, eds. Second International Cephalopod Symposium, Tübingen. E. Schweizerbart'sche Verlagsbuchhandlung, Stuttgart, Germany.

Palacio, F. J. 1978. *Vosseledone charrua*: A new Patagonian cephalopod (Octopodidae) with notes on related genera. *Bull. Mar. Sci.* **28:** 282–296.

Pickford, G. E. 1945. Le poulpe Américain: A study of the littoral Octopoda of the western Atlantic. *Trans. Connecticut Acad. Arts Sci.* **36:** 701–777.

Pickford, G. E. 1946. A review of the littoral Octopoda from central and western Atlantic stations in the collections of the British Museum. *Ann. Mag. Nat. Hist.* **13:** 412–429.

Pickford, G. E., and B. H. McConnaughey. 1949. The *Octopus bimaculatus* problem: A study in sibling species. *Bull. Bingham Oceanogr. Collect. Yale Univ.* **12:** 1–66.

Racovitza, E.-G. 1894. Notes de Biologie. *Arch. Zool. Exp. Gen.* **2:** 21–49.

Robson, G. C. 1926. On the hectocotylus of the Cephalopoda—a reconsideration. *Proc. Malacol. Soc. Lond.* **17:** 117–122.

Robson, G. C. 1928. On *Grimpella*, a new genus of Octopoda, with remarks on the classification of the Octopodidae. *Ann. Mag. Nat. Hist.* **2:** 108–114.

Robson, G. C. 1929. *A Monograph of the Recent Cephalopoda. Vol 1. Octopodinae.* British Museum of Natural History, London.

Sasaki, M. 1929. A monograph of dibranchiate cephalopods of the Japanese and adjacent waters. *J. Fac. Agric. Hokkaido Univ.* **20** (Suppl.): 1–357.

Stranks, T. N., and M. D. Norman. 1993. Review of the *Octopus australis* complex from Australia and New Zealand, with description of a new species (Mollusca: Cephalopoda). *Mem. Mus. Vic.* **53:** 345–373.

Strauss, R. E. 1985. Evolutionary allometry and variation in body form in the South American catfish genus *Corydoras* (Callichthyidae). *Syst. Zool.* **34:** 381–396.

Tait, R. W. 1982. A taxonomic revision of *Octopus australis* Hoyle, 1885 (Octopodidae: Cephalopoda), with a redescription of the species. *Mem. Natl. Mus. Vic.* **43:** 15–24.

Villanueva, R., P. Sánchez, and M. A. Compagno Roeleveld. 1991. *Octopus magnificus* (Cephalopoda: Octopodidae), a new species of large octopod from the southeastern Atlantic. *Bull. Mar. Sci.* **49:** 39–56.

Voight, J. R. 1993. The association between distribution and octopodid morphology: implications for classification. *Zool. J. Linn. Soc.* **108:** 209–223.

Voight, J. R. 1997. Cladistic analysis of the order Octopoda based on anatomical characters. *J. Molluscan Stud.* **63:** 311–325.

Voight, J. R. 2001. The relationship between sperm reservoir and spermatophore length in benthic octopuses (Cephalopoda: Octopodidae). *J. Mar. Biol. Assoc. UK* **81:** 983–986.

Voss, G. L. 1951. Further description of *Octopus burryi* Voss with a note on its distribution. *Bull. Mar. Sci. Gulf Caribb.* **1:** 231–240.

Voss, G. L. 1953. Observations on a living specimen of *Octopus hummelincki* Adam. *Nautilus* **66:** 73–76.

Voss, G. L. 1964. *Octopus defilippi* Verany, 1851, an addition to the cephalopod fauna of the western Atlantic. *Bull. Mar. Sci. Gulf Caribb.* **14:** 554–560.

Voss, G. L. 1968. Octopods from the R/V *Pillsbury* southwestern Caribbean cruise, 1966, with a description of a new species, *Octopus zonatus*. *Bull. Mar. Sci.* **18:** 645–659.

Voss, G. L. 1975. *Euaxoctopus pillsburyae*, new species, (Mollusca: Cephalopoda) from the southern Caribbean and Surinam. *Bull. Mar. Sci.* **25:** 346–352.

Voss, G. L. 1979. *Octopus rapanui*, new species, from Easter Island (Cephalopoda: Octopoda). *Proc. Biol. Soc. Wash.* **92:** 360–367.

Voss, G. L. 1988. Evolution and phylogenetic relationships of deep-sea octopods (Cirrata and Incirrata). Pp. 253–276 in *The Mollusca. Vol. 12. Paleontology and Neontology of the Cephalopods*, M. R. Clarke and E. R. Trueman, eds. Academic Press, San Diego, CA.

Voss, G. L., and W. G. Pearcy. 1990. Deep-water octopods (Mollusca; Cephalopoda) of the Northeastern Pacific. *Proc. Calif. Acad. Sci.* **47:** 47–94.

Weill, R. 1927. La structure, la valeur systématique et le fonctionnement du spermatophore de *Sepiola atlantica* D'Orb. *Bull. Biol. Fr. Belg.* **61:** 59–92.

Appendix

Listed here are species by species group, with each species' mean PC2 and PC3 scores reported in parentheses, the mantle length of each specimen considered and the sources of the data and specimens that contributed to this analysis. Specimen depositories are ANSP, Academy of Natural Sciences, Philadelphia; CAS, California Academy of Sciences; FMNH, Field Museum of Natural History; UMML, University of Miami Marine Laboratories.

Species group of *Octopus vulgaris*: *Octopus vulgaris* (1.447; −0.143); 61, 90, 101, 49, 45 (Pickford, 1945, 1946). *O. veligero* (1.037; 0.126); 84; UA. *O. filosus* (−0.324; 0.707); 10, 11, 12, 13, 13.5, 14, 15 (n = 2), 16, 16.5 (n = 2), 17, 18, 22, 24.5, 27, 28, 29, 34, 37 (Alvina, 1965). *O. cyanea* (1.381; 0.017); 49.8 (n = 2), 103.9 (n = 2), 105.6, 127.1 (n = 2) (Norman, 1991)

Species group of *Octopus aegina*: *O. aegina* (0.457; −0.069); 31.9, 42.3 CAS 077992; CAS 077993. *O. polyzena* (−0.818; −0.050); 26.3 (Norman, 1993b). *O. exannulatus* (1.23; 0.064); 37.2, 41.7, 45.4 (Norman, 1993b); 38.7; 42.3 CAS 077990. *O. mototi* (0.377; 0.548); 66.2, 70.5 (Norman, 1993b). *O. burryi* (0.117; 0.657); 39 (Voss, 1951).

Species group of *Octopus macropus*: *O. macropus* (0.929; −1.208); 115 (Pickford, 1945). *O. alpheus* (0.094; −0.360); 61.9, 63.9, 74.2 (Norman, 1993a). *O. aspilosomatis* (−0.255; 0.783); 37.3, 42.2, 83.2 (Norman, 1993a). *O. rapanui* (1.557; 0.029); 113, 115 (Voss, 1979). *O. ornatus* (−0.182; −1.686); 103.5, 104.2 (Norman, 1993c). *O. graptus* (0.055; −0.587); 157.9 (Norman, 1993a).

Species assigned to the Eledoninae of Voss 1988:

Pareledone charcoti (−0.134; 0.777); 55.5, 71.6 (Kubodera and Okutani, 1994); 34.8 UMML 31.2561. *Pareledone harrissoni* (1.637; 0.673); 96 (Kubodera and Okutani, 1994). *Megaleledone* sp. (0.195; 1.060); 67.8 UMML 31.2562. *Vosseledene charrua* (−0.166; 1.28); 49, 50 (Palacio, 1978). *Eledone palari* (−0.025; 1.373); 32.1; 34.4; 37; 37.9 (*n* = 2), 38.3; 38.7; 39.6 (Lu and Stranks, 1991). *Graneledone pacifica* (0.268; 1.679); 85 (Voss and Pearcy, 1990); 77.9, 83.2, 86.9, 94.4, 98.4, 106.3, 116.4 FMNH uncat.; FMNH 278061; FMNH 278062; FMNH 281001; FMNH 281002; CAS 031474; CAS 061434.

Species assigned to the Bathypolypodinae of Voss 1988: *Bathypolypus arcticus* (−1.259; −0.807); 56.8 FMNH 278080. *B. piscatorum* (−0.059; 0.890); 125.1 FMNH 281720. *B. yaquinae* (−1.068; 0.358); 29.1, 31 (*n* = 2), 33.4 FMNH 278308; FMNH 278309; FMNH 278311. *B. macrophallus* (−0.018; 1.130); 83 (Voss and Pearcy, 1990). *Benthoctopus* sp. a (−0.557; −1.505); 48.8 FMNH 278066. *Benthoctopus* sp. b (−0.256; −0.718); 45 CAS 018763.

Octopus (Abdopus): *O. (A.) aculeatus* (−0.213; −0.503); 35.3, 41.4 (Australia) (Norman and Finn, 2001). *O. (A.) cf. aculeatus* (1.081; −1.361); 25.5, 29.3, 40.5, 45.9, 47.6, 57.8 (Thailand) CAS 077987; CAS 078001; CAS 078002 (*n* = 4). *O. (A.) capricornicus* (1.480; −1.948); 40, 42.1 (Norman and Finn, 2001). *O. (A.)* n sp. (−0.581; −0.602); 38.3, 40.7, 44.4, 45.4, 45.6, CAS 077999 (*n* = 3); CAS 078000 (*n* = 2).

Long-armed octopuses: *Ameloctopus litoralis* (−2.556; −0.164); 14, 15.9 (Norman, 1992). *O. defilippi* (0.914; −1.296); 25.5, 39 (Voss, 1964). *Euaxoctopus pillsburyae* (−1.486; 0.171); 24 (Voss, 1975).

***Octopus australis* and *berrima*:** *O. australis* (−1.22; −1.001); 27.1, 40.5, 45.2, 46.5, 57.6, 58.2, 60.4, 67.1, 68.7 (Stranks and Norman, 1993). *O. berrima* (−1.043; −0.964); 31.3, 32.6, 36.3, 58.9, 63.5, 79.6 (Stranks and Norman, 1993). *O. berrima*, as *O. australis* (−0.993; −0.804); 45 (*n* = 2), 54, 56, 67 (Tait, 1982).

Miscellaneous species with uncertain affiliation: *Octopus briareus* (−0.336; 0.445); 46 (Pickford, 1945). *O. joubini* (0.233; −0.193); 17, 36 (Pickford, 1945). *Enteroctopus magnificus* (0.274; −1.136); 285 (Villanueva *et al.*, 1991). *O. zonatus* (−1.148; 0.564); 19 (Voss, 1968). *O. campbelli* (0.184; 1.443); 34.1 (Stranks and Norman, 1993). *Cistopus* sp. (2.685; 0.303); 47.8 ANSP 6394. *Vulcanoctopus hydrothermalis* (−0.625; 0.450); 43.9 FMNH 287365.

Reference: *Biol. Bull.* **202:** 156–165. (April 2002)

Variation in Growth and Competitive Ability Between Sexually and Clonally Produced Hydroids

DAVID H. VAN WINKLE* AND NEIL W. BLACKSTONE

Department of Biological Sciences, Northern Illinois University, DeKalb, Illinois 60115

Abstract. In controlled laboratory experiments, colonies of *Podocoryna carnea* typically overgrow and kill colonies of *Hydractinia symbiolongicarpus*. Generally, these experiments have used colonies grown from tissue explants (clonal replicates) surgically removed from mature colonies taken from natural populations. In contrast, experiments involving interspecific bouts between small, sexually produced colonies reveal that both the characteristics and outcomes of competition differ from previous studies. During competition between small sexually produced colonies, *H. symbiolongicarpus* exhibits directional growth toward *P. carnea* and produces nematocyte-rich hyperplastic stolons more readily than *P. carnea* does. Nevertheless, *P. carnea* can still overcome *H. symbiolongicarpus* if it initially grows away from the contact zone and subsequently flanks *H. symbiolongicarpus*. Overall, sexually produced colonies of *H. symbiolongicarpus* destroyed their *P. carnea* counterparts in more than 35% of competitive bouts, whereas *P. carnea* dominated their *H. symbiolongicarpus* counterparts in all similar encounters between clonally produced colonies. In natural populations, competition between small sexually produced colonies of *H. symbiolongicarpus* may predominate, and these results support the hypothesis that this species is adapted to competition early in colony development. More generally, studies of competition between sexually produced colonies should complement similar studies of clonally produced colonies.

Introduction

Colonial animals can be described morphologically as a collection of iterated modules or ramets interconnected by a common vascular network. The arrangement of modules and vascular connections defines two contrasting colonial morphologies and associated life histories (*e.g.*, Larwood and Rosen, 1979; Jackson *et al.*, 1985; Buss and Blackstone, 1991). Briefly, "sheets" exhibit a robust morphology, having tightly packed modules interconnected by short vascular stolons. Specialized to particular habitats, sheets are typically good competitors and persistent over time. In contrast, "runners" tend to have a haphazard distribution of modules, and they are typically transient generalists that are competitively inferior to sheets but can potentially escape competitive encounters through copious asexual or sexual propagation. Within these extremes, many colonial organisms display varying degrees of morphological plasticity in response to environmental conditions, which probably enables them to adapt to heterogenous environments (*e.g.*, de Kroon and Hutchings, 1995; Umeki, 1995; Stuefer, 1996; Kleijn and Van Groenendael, 1999; Muko *et al.*, 2000; Equiza *et al.*, 2001).

The colonial hydroids *Podocoryna carnea* and *Hydractinia symbiolongicarpus* (Cnidaria: Hydrozoa) occur sympatrically. Both encrust gastropod shells of paguriid hermit crabs in North American nearshore waters of the Atlantic Ocean. Although genotypic and phenotypic variation does occur, each is more or less representative of the extremes of the classic runner-sheet dichotomy. Specifically, *P. carnea* is runner-like and *H. symbiolongicarpus* is sheet-like (*e.g.*, McFadden, 1986; Blackstone and Buss, 1991; Buss and Blackstone, 1991; Van Winkle *et al.*, 2000). The former has sparse, unevenly spaced modules, whereas the latter develops a tight network of evenly spaced modules and grows over available space more slowly. Additionally, the ectoderm fuses between stolons of *H. symbiolongicarpus* within 2 weeks after metamorphosis from planula larvae. This stolonal "mat" (Hauenschild, 1954, 1956) expands from the colony's center to encompass existing peripheral stolons and slowly deposits a thick, chitin-like understory, which markedly increases the sheet-like appearance of these colonies.

Received 14 August 2001; accepted 12 December 2001.

* To whom correspondence should be addressed. E-mail: rip@niu.edu

Although *H. symbiolongicarpus* and *P. carnea* display contrasting life-history characteristics consistent with runner and sheet generalizations, such is not the case with competitive ability. Previous work using clonally produced colonies has shown that *P. carnea* is almost invariably the competitive dominant to *H. symbiolongicarpus* under laboratory conditions (McFadden, 1986; Van Winkle *et al.*, 2000). Additionally, *P. carnea* covers available space faster and responds more aggressively to foreign tissue (Tardent and Bührer, 1982; Buss *et al.*, 1984; McFadden *et al.*, 1984; McFadden, 1986; Lange *et al.*, 1992; Van Winkle *et al.*, 2000). A unique aspect of cnidarian biology can explain these disparities: competition in hydroids is mediated by cnidarian-specific cells (nematocytes) actively deployed from hyperplastic stolons. These specialized stolons develop only from previously existing stolons or from a particular type of mat tissue termed astogenetic mat (Buss and Grosberg, 1990), and they represent an example of an inducible defense (*c.f.*, Frank, 1993; Harvell, 1990). Thus, competitive ability in hydroids is largely determined by colony morphology, and runner-like colonies have consistently been shown to be superior competitors, presumably due to their extensive peripheral stolons (McFadden *et al.*, 1984; Buss and Grosberg, 1990; Yund, 1991).

Regardless of its competitive inferiority, *H. symbiolongicarpus* is far more abundant than its competitor on small gastropod shells occupied by *Pagurus longicarpus* (Yund *et al.*, 1987; Buss and Yund, 1988; Yund and Parker, 1989), and colonies eventually cover the entire shell surface, thus excluding further larval recruitment. Although *P. carnea* can be found on small, rough-surfaced shells (e.g., *Nassarius trivittatus*) amidst shells covered by the more common *H. symbiolongicarpus*, these colonies are small, rarely covering the shell surface entirely (Buss and Yund, 1988). In natural populations of *H. symbiolongicarpus*, competition is probably more common among small, newly established colonies shortly after the metamorphosis of larvae generated by sexual reproduction than among older, well-established colonies (Yund *et al.*, 1987). Thus, competitive encounters among young, sexually produced hydroid colonies in nature and those experimentally induced among clones of unknown age may be qualitatively different. Nevertheless, studies of both intraspecific and interspecific competition in these hydroids have been limited exclusively to clonal replicates usually taken from well-established colonies of unknown age in natural populations (Hauenschild, 1954, 1956; Braverman and Schrandt, 1966; Tardent and Bührer, 1982; McFadden, 1986; Müller *et al.*, 1987; Plickert *et al.*, 1987; Lange *et al.*, 1989; Buss, 1990; Buss and Grosberg, 1990; Blackstone and Buss, 1991; Yund, 1991; Grosberg *et al.*, 1996; Van Winkle *et al.*, 2000).

Considerable recent work regarding age-specific variation in growth, morphology, and competitive ability has focused on plants (*e.g.*, Lundberg *et al.*, 1996; Bertschy, 1998; Moora and Zobel, 1998), which are similar to colonial animals in developmental mode and morphology (*i.e.*, modular organization). Colonial hydroids also seem to display age-specific differences in growth and morphology, and these differences could affect competitive ability at different stages of colony development. Clonally produced colonies (clonal replicates) of *H. symbiolongicarpus* exhibit important morphological and physiological differences relative to newly established (hereafter termed sexually produced) colonies. First, the development of stolonal mat is delayed for up to 2 weeks in sexually produced colonies, whereas clonally produced colonies always exhibit these mats. Second, sexually produced colonies initially produce many more peripheral stolons than clonal replicates do, and the morphological shift associated with stolonal mat formation is accompanied by a decrease in the rate of flow of gastrovascular fluid to peripheral stolon tips (Blackstone, 1996). In contrast, the flow rate to stolon tips gradually increases after metamorphosis in *P. carnea* (Blackstone, 1996), which tends to grow more sheet-like only after sexual maturity, never becoming as sheet-like as *H. symbiolongicarpus*. Due to the qualitative differences between early growth in sexually produced and clonally produced colonies, it is plausible that such colonies may also display age-specific differences in competitive ability.

We examined interspecific competition between *H. symbiolongicarpus* and *P. carnea* during early post-metamorphic development of sexually produced colonies and likewise between clonally produced colonies. We sought to characterize competitive ability in two ways. First, the outcome of single colony interspecific competition for space was determined both among F1 sexually produced colonies and among the parental clonal replicates. Second, in these interactions we characterized directional growth before and after colony interaction by using colony area and geometric center of mass. Overall growth toward a competitor may indicate a controlled and purposeful attack response, whereas overall growth away from a competitor may indicate an escape response. We found considerable variation between sexually and clonally produced colonies; thus our results complement earlier studies of competition between clonally produced colonies and perhaps suggest why *H. symbiolongicarpus* predominates on gastropod shells inhabited by paguriid hermit crabs.

Materials and Methods

Competition in sexually produced colonies

Wild-type colonies of *Hydractinia symbiolongicarpus* and *Podocoryna carnea* were maintained as described previously (Van Winkle *et al.*, 2000). A single cross of wild-type parental colonies was used to generate F1 planula larvae of each species. We used only a single cross of each species because a broad distribution of runner- and sheet-like morphologies is represented among full siblings (Blackstone, 1996), and the crosses used produced a typical distribution of forms. Thus, broad variation in competitive ability of F1 full sibs was expected for each species.

Mature male and female colonies of each species were placed in covered glass dishes in an incubator at 20.5 °C and induced to release gametes or medusae by exposure to artificial, full-spectrum lighting following an overnight period of total darkness. Parental colonies were separated from gametes or medusae after this period. Colonies of *P. carnea* were induced to release medusae 3 days prior to the induced spawning of *H. symbiolongicarpus* gametes because the latter lack the medusoid phase and thus require less time to generate mature planulae. Medusae were fed brine shrimp and placed in fresh seawater daily during this time and for 2 days thereafter. On the 3rd, 4th, and 5th days, medusae spawned gametes, and fertilized eggs were collected and isolated in a dish containing fresh seawater. Also on the night of the 3rd day, colonies of *H. symbiolongicarpus* were induced to release gametes as described. On the following morning, fertilized eggs of *H. symbiolongicarpus* were transferred to a dish containing fresh seawater. All F1 larvae of both species were fully mature by the 9th day after medusoid release of *P. carnea* parental colonies. Planulae were induced to metamorphose using 50 m*M* CsCl in seawater for 3 h (Spindler and Müller, 1972; Blackstone, 1996). Single metamorphosing larvae of each species were randomly paired and placed about 4 mm apart near the center of 30 round (18-mm) glass coverslips in petri dishes; these were left undisturbed in total darkness for 48 h. Once attached to the glass surfaces, all newly metamorphosed primary-polyp pairs were digitally imaged, placed in floating racks in 120-l aquaria, and hand-fed brine shrimp nauplii daily until each grew large enough to consistently capture its own food. Primary polyps of each species were easily distinguished by their appearance. Thirteen coverslips were excluded due to degeneration or the inability to feed of one primary polyp. Of the 13, 12 were excluded due to the degeneration of a *P. carnea* primary polyp, and one was excluded due to the degeneration of a *H. symbiolongicarpus* primary polyp.

Second images of the remaining colony pairs ($n = 17$) were captured at the time of inter-colony contact and third images at 14 d after first contact. The 14-d time interval was chosen based on previous observations of interspecific competition; that is, "snapshots" of competition were most meaningful as far along in the interaction as possible while both colonies were still alive and growing. Three of the competitive interactions were resolved (one of the pair was killed by the other) before 14-d images were captured (remaining, $n = 14$). All three sequential images were captured at equal magnification and orientation, such that colony spatial relationships were preserved in each image sequence.

Competition in clonally produced colonies

Tissue explants of mature, field-collected colonies were used to generate clonal replicates. These were treated identically to sexually produced colonies in all respects except for the manner in which they were initiated. Eight clonal replicates of each of the two parents of sexually produced colonies of each species were used as clonally produced colonies, yielding a total of 32 colonies and allowing four unique interspecific pairwise combinations replicated four times ($n = 16$). Single-polyp tissue explants were placed about 4 mm apart near the center of 18-mm round glass coverslips. Explants were held in place with nylon threads until attachment occurred, whereupon the threads were removed. Initial colony images were captured upon attachment of both colonies to the growing surface. Of the 16 colonies of *H. symbiolongicarpus*, 3 died prior to first contact ($n = 13$), and 2 were killed during competition prior to 14 days post-contact (remaining, $n = 11$).

Data collection and analysis

Images of all competing colonies were analyzed using Optimas 6.1 image analysis software (Media Cybernetics). From all images, geometric center of mass (hereafter termed "position") was calculated based on total area covered as measured by the outer perimeter of each colony. The outer perimeter was digitally traced according to the actual contours of the colony, not as a polygon. The resulting data were in the form of a single point in Cartesian space for each colony, where all positive x and y values numerically balanced with their corresponding $-x$ and $-y$ values; therefore, each point represented the overall average of two-dimensional space controlled by a colony at a given time. Overlapping areas were considered to be mutually controlled. Since the three sequential images of each bout were captured at equal magnification and orientation, relative changes in position could be followed for each species on each coverslip.

These data were analyzed in two ways. Multivariate analysis of variance (MANOVA) was used to test whether the relationship among colony positions—as given by x and y coordinates—changed between the time of contact and 14 days post-contact. Thus, MANOVA tested for a significant change in the overall relationship of four response variables (position x and y coordinates of each species) using time as a predictor. While each response variable was technically two repeated measures grouped by coverslip, it was impossible to simultaneously test four repeated response variables using time as the predictor, due to the lack of error variance in such a model. Analysis of colony position relationships prior to contact was meaningless using this method of analysis, because colonies of each species begin growth from a predefined position. Nevertheless, MANOVA provided a clear and intuitive exploratory analysis of an overall post-contact colony response. The initial distance between competing colonies varied slightly on each coverslip due to larval or explant placement error. To allow for realistic comparisons of relative changes in colony position coordinates among coverslips, the initial distances between competitor positions were adjusted to a common value equal to the average distance between primary polyps or explants among all coverslips. The remaining data were standardized proportionately to reflect these changes.

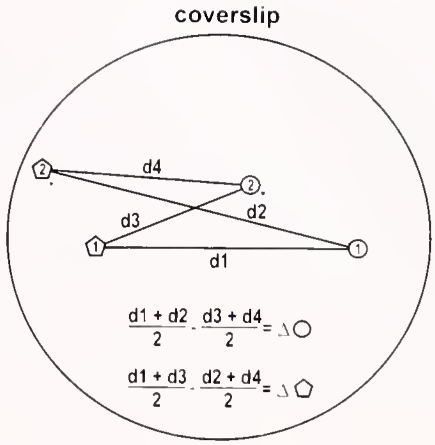
coverslip
2
d4
2
d3
d2
1
d1
1
$\frac{d1 + d2}{2} - \frac{d3 + d4}{2} = \Delta$○
$\frac{d1 + d3}{2} - \frac{d2 + d4}{2} = \Delta$⬠

Figure 1. Schemata of changes (dashed arrows) in colony position over a single time interval for *Podocoryna carnea* (pentagons) and *Hydractinia symbiolongicarpus* (circles) growing on coverslips. The relative change in geometric center of mass (termed "position") of a particular colony from the start (labeled "1") to the end (labeled "2") of each interval was determined by calculating the difference in the distance of that colony from both the start and end positions of its competitors, as shown.

An alternate and more precise method of analysis using paired *t* tests was devised to determine whether relative position changed over each interval for each species. This method simultaneously accounted for the potential interdependency of within-subject colony interactions and the effects of repeated measures on the same subject (*i.e.*, coverslip). The three images of each coverslip (primary polyps, contact, and 14 days post-contact) contained two time intervals over which colony position changed: (1) the change from initiation (positions of primary polyps or explants) to contact and (2) the change from contact to 14 days post-contact. As stated previously, the initial distance between competing colonies varied slightly on each coverslip due to error in larval or explant placement. All unique initial distances between competitor positions were adjusted to a common value as described above. However, inter-colony positions at the beginning of the second interval (*i.e.*, at the time of contact) varied among coverslips, rendering comparisons among coverslips after contact meaningless. To correct for this, coordinate data obtained from contact images were transformed in Cartesian space (using basic algebraic and trigonometric functions) such that the orientation of colony positions was identical to the common standardized positions at the beginning of the first interval; *i.e.*, colony positions at the beginning of the second interval were mathematically juxtaposed to be identical to positions at the beginning of the first interval. Since positions of both competitors changed simultaneously during each interval, the start and end positions of each colony were used to determine the relative position change of competitors. This was accomplished by using four distances between competing colony positions from images representing both the start and end of each interval (1 and 2 above): (a) the distance ($d1$) between competitor positions from the first image, (b) the distance ($d2$) between the positions of *H. symbiolongicarpus* from the first image and *P. carnea* from the second image, (c) the distance ($d3$) between the positions of *P. carnea* from the first image and *H. symbiolongicarpus* from the second image, and (d) the distance ($d4$) between colony positions from the second image. The following formulas were used to determine the difference between initial and final colony positions relative to one another (Fig. 1):

$$\frac{d1 + d2}{2} - \frac{d3 + d4}{2} = \Delta\text{colony 1}$$

and

$$\frac{d1 + d3}{2} - \frac{d2 + d4}{2} = \Delta\text{colony 2}$$

or

$$(\text{initial distance} - \text{final distance} = \Delta\ \text{position})$$

Positive values indicated overall position change toward and negative values indicated change away from the "average" position of a competitor. The initial and final distances of each colony relative to its competitor were analyzed among coverslips using paired *t* tests, with significant deviations from zero indicating position change toward (positive mean) or away from (negative mean) a competitor. In addition to providing information on changes in both direction and magnitude, the paired *t* test is also robust, having few assumptions of the data (Sokal and Rohlf, 1995).

The outcome of competition was determined when one colony killed and overgrew the other. The number of winning *versus* the number of losing *H. symbiolongicarpus* colonies was compared between sexually and clonally produced colonies using likelihood-ratio chi-square.

Larval size

Larvae of each species were generated using the methods described above. The size of larvae was quantified in two ways. First, images of 10 randomly chosen larvae from each of 2 wild-type parental crosses of both species were captured at identical magnification and used to determine the cross sectional area of each using Optimas software. Images were captured when larvae were fully developed and relaxed (about 3 d after fertilization). Larval area was compared between species using a nested analysis with area nested within cross and cross nested within species. Second, 100 larvae from two crosses of *H. symbiolongicarpus* and 118 larvae from two crosses of *P. carnea* were each homogenized in 0.5 ml of 0.05% sodium dodecyl sulfate and assayed for total protein using the BCA (bicinchoninic acid) total protein assay with triple-sample replication (Smith *et al.*, 1985). Larvae from the two crosses were pooled to increase the sample size and hence the accuracy of the assay. Because the number of larvae used in the assay differed between species, numbers were standardized prior to comparison.

Results

Competition in sexually produced colonies

Of the 30 *Podocoryna carnea* and *Hydractinia symbiolongicarpus* primary polyps established on coverslips, 12 *P. carnea* and 1 *H. symbiolongicarpus* primary polyp died. This corresponds to a survivorship of 60% of *P. carnea* and 97% of *H. symbiolongicarpus* colony initiates.

The relationship of the four response variables (position x and y coordinates of each species) using time as the predictor changed between the time of contact and 14 days post-contact (Fig. 2A; MANOVA, $F = 4.96$; df = 4, 26; $P = 0.0041$). Univariate analysis of variance (ANOVA) of each response variable, using time as the predictor, revealed that only the position change of *H. symbiolongicarpus* colonies along the x-axis was significant (ANOVA, $F = 13.54$, df = 1, 29, $P = 0.0009$). There was a near-significant position change of *P. carnea* colonies along the y-axis (ANOVA, $F = 3.40$, df = 1, 29, $P = 0.0753$).

Paired comparisons support the results obtained using MANOVA. Relative inter-colony position did not significantly change prior to contact (interval 1) in colonies of either species (Fig. 3A), although *P. carnea* position showed a near-significant change away from competitors (for *H. symbiolongicarpus*: $t = 0.84$, $P = 0.4150$; for *P. carnea*: $t = -2.06$, $P = 0.0556$). After contact (interval 2; Fig. 3B), *P. carnea* position showed a near-significant change away from *H. symbiolongicarpus* ($t = -2.06$, $P = 0.0603$), and there was a highly significant change in *H. symbiolongicarpus* colony position toward *P. carnea* after contact ($t = 3.88$, $P = 0.0019$).

Overall, sexually produced colonies of *H. symbiolongicarpus* defeated and overgrew their counterparts in 6 of the 17 bouts. Qualitatively, *H. symbiolongicarpus* winners immediately responded to contact by directional growth of nematocyte-filled hyperplastic stolons toward competitors; these stolons, which often overgrew and destroyed the sparsely arranged stolonal network of *P. carnea* colonies (Fig. 4), were often produced from existing mat tissue at or near the point of contact. In some cases, *H. symbiolongicarpus* winners generated defensive dactilozooids. Shortly after contact, many *H. symbiolongicarpus* winners produced stolonal mat from existing hyperplastic stolons in the region of overlap (Fig. 4C, D). *H. symbiolongicarpus* losers often grew directionally and produced hyperplastic stolons but were simply unable to overcome their *P. carnea* counterparts. Likewise, *P. carnea* winners did not appear to grow differently than losers. Unlike clonally produced colonies in previous studies, sexually produced *P. carnea* colonies did not produce hyperplastic stolons or dactilozooids upon contact, and they did not display directional growth.

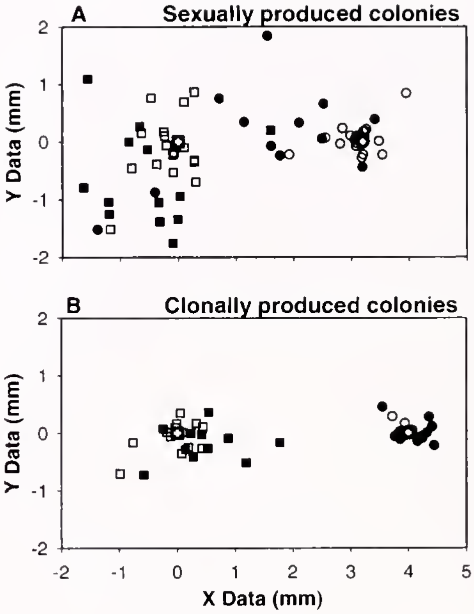

Figure 2. Colony positions in Cartesian space at each of the three times that images were captured (initiation = symbols with crosses, contact = open symbols, and 14 days post-contact = filled symbols) for sexually produced colonies (A) and clonally produced colonies (B) of *Podocoryna carnea* (squares) and *Hydractinia symbiolongicarpus* (circles). The initial distances between competitor positions were adjusted to a common value equal to the average distance between primary polyps or explants among all coverslips. Treated as separate response variables, the remaining data were standardized proportionately to reflect these changes. The x and y coordinates of these data were analyzed for each experiment using MANOVA to detect whether these relationships changed during contact to 14 days post-contact.

Competition in clonally produced colonies

The relationship of the four response variables (position x and y coordinates of each species) using time as the predictor did not differ between the time of contact and 14 days post-contact (Fig. 2B; $F = 2.09$; df = 4, 19; $P = 0.1218$). Univariate ANOVA, using time as the predictor, revealed that only the position change of *P. carnea* colonies along the x-axis was significant (ANOVA, $F = 5.35$, df = 1, 22, $P = 0.0305$).

Relative inter-colony position did not significantly

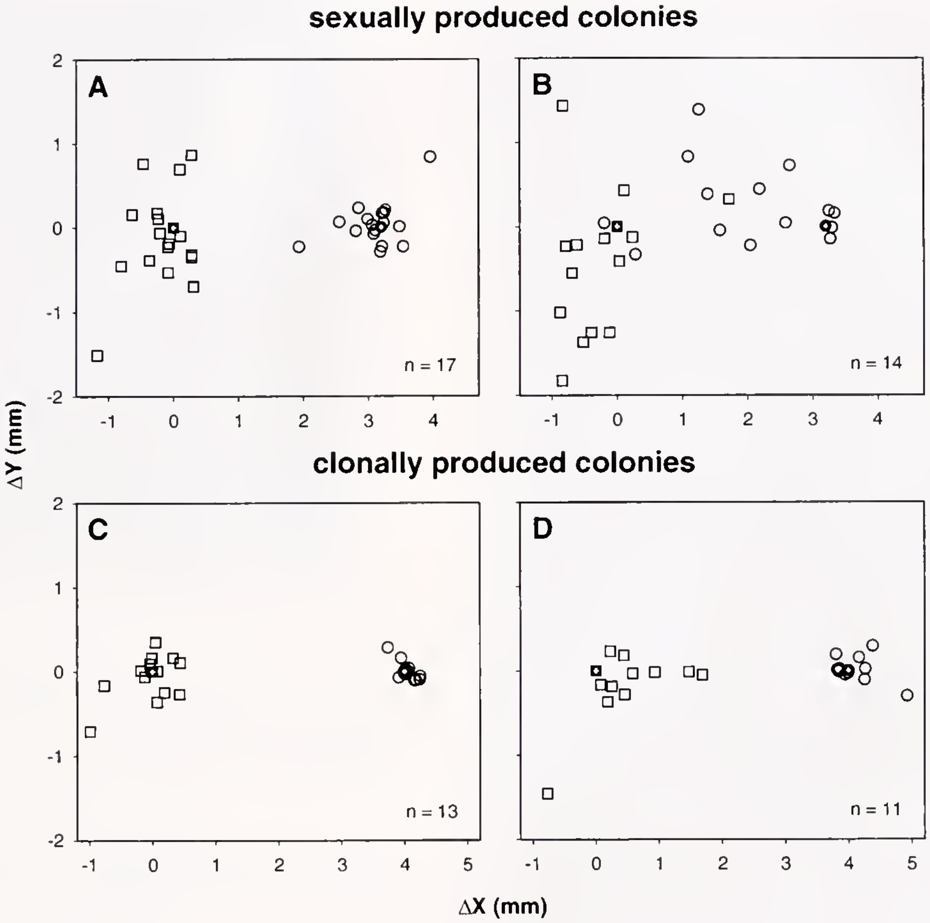

Figure 3. The position change (open symbols) of all colonies from a common starting position (filled symbols) of *Podocoryna carnea* (squares) and *Hydractinia symbiolongicarpus* (circles) over initial-contact (A, C) and contact–14 d post-contact (B, D) intervals in sexually (A, B) and clonally produced (C, D) colonies. For each colony on a coverslip, the difference between initial and final positions relative to a competitor was analyzed over both intervals using paired *t* tests, with significant deviations from zero indicating the position change toward or away from a competitor.

change prior to contact (Fig. 3C) among colonies of either species (paired *t* tests; $t = -1.11$, $P = 0.2906$ for *H. symbiolongicarpus* and $t = -0.38$, $P = 0.7081$ for *P. carnea*). After contact, *P. carnea* colony position change was toward *H. symbiolongicarpus* (Fig. 3D; $t = 2.26$, $P = 0.0474$), but there was no significant change in *H. symbiolongicarpus* colony position relative to *P. carnea* ($t = -1.15$, $P = 0.2785$; Fig. 2).

Overall, *P. carnea* clonally produced colonies destroyed and overgrew their counterparts in all competitive bouts. A likelihood-ratio chi-square reveals that the outcome of competition was significantly different between clonally and sexually produced colonies ($G = 7.9497$, $P = 0.0048$). As previous studies have shown, clonally produced colonies of *P. carnea* covered available space more quickly than *H. symbiolongicarpus*, and the former consistently produced hyperplastic stolons upon contact whereas the latter did not. Minimal directional growth was observed in *P. carnea* after contact, but this growth was qualitatively different from that of *H. symbiolongicarpus* sexually produced colonies (see Discussion).

Larval size

Larvae differed significantly with respect to cross-sectional area between the species (Fig. 5; nested ANOVA, $F = 275.79$, df = 1, 2, $P = 0.0036$). Larvae of *H. symbiolongicarpus* were 38% larger (average area = 0.062 mm^2) than *P. carnea* larvae (average area = 0.038 mm^2). The physical size of *H. symbiolongicarpus* larvae was consistent with past findings (Weis and Buss, 1987). Because larvae cross-sectional area did not differ significantly between crosses within species (nested ANOVA, $F = 0.39$, df = 2, 36, $P = 0.6772$), pooling of larvae generated from the separate parental crosses was validated. The average total protein content was roughly 34% higher in *H. symbio-*

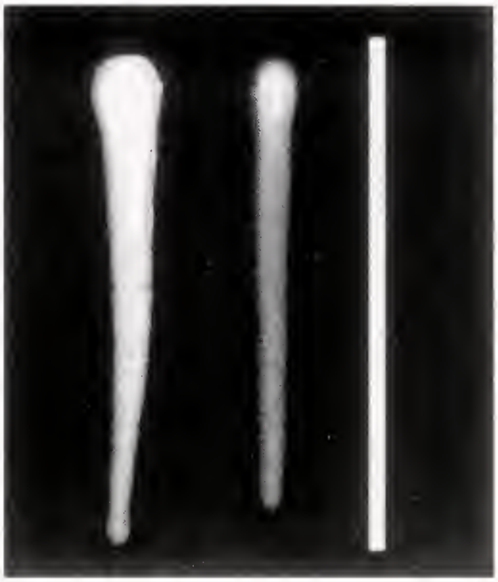

Figure 5. Mature planulae larvae of *Hydractinia symbiolongicarpus* (at left) and *Podocoryna carnea*. Larvae of the former are significantly larger (nested ANOVA using the cross-within-species effect as the error term, $F = 275.79$, df = 1, 2, $P = 0.0039$). Relative larval size was also estimated using the BCA total protein assay. Results revealed that *H. symbiolongicarpus* larvae contain about 34% more protein on average than *P. carnea* larvae. Scale bar = approx. 1 mm.

longicarpus larvae (mean value of 6.49 μg/larva) than in *P. carnea* larvae (4.30 μg/larva).

Discussion

Previous experimentation using clonally produced colonies has suggested that general life-history patterns of runners and sheets may not apply to these hydroids; that is, the runner-like *Podocoryna carnea* dominates the sheet-like *Hydractinia symbiolongicarpus* (McFadden, 1986; Van Winkle *et al.*, 2000). The data presented here support these studies: clonally produced colonies of *P. carnea* always overwhelmed those of *H. symbiolongicarpus*. Conversely, sexually produced colonies of *H. symbiolongicarpus* were able to defeat and overgrow *P. carnea* in more than 35% of competitive interactions. Hitherto unknown competitive behavior was observed in sexually produced colonies of *H.*

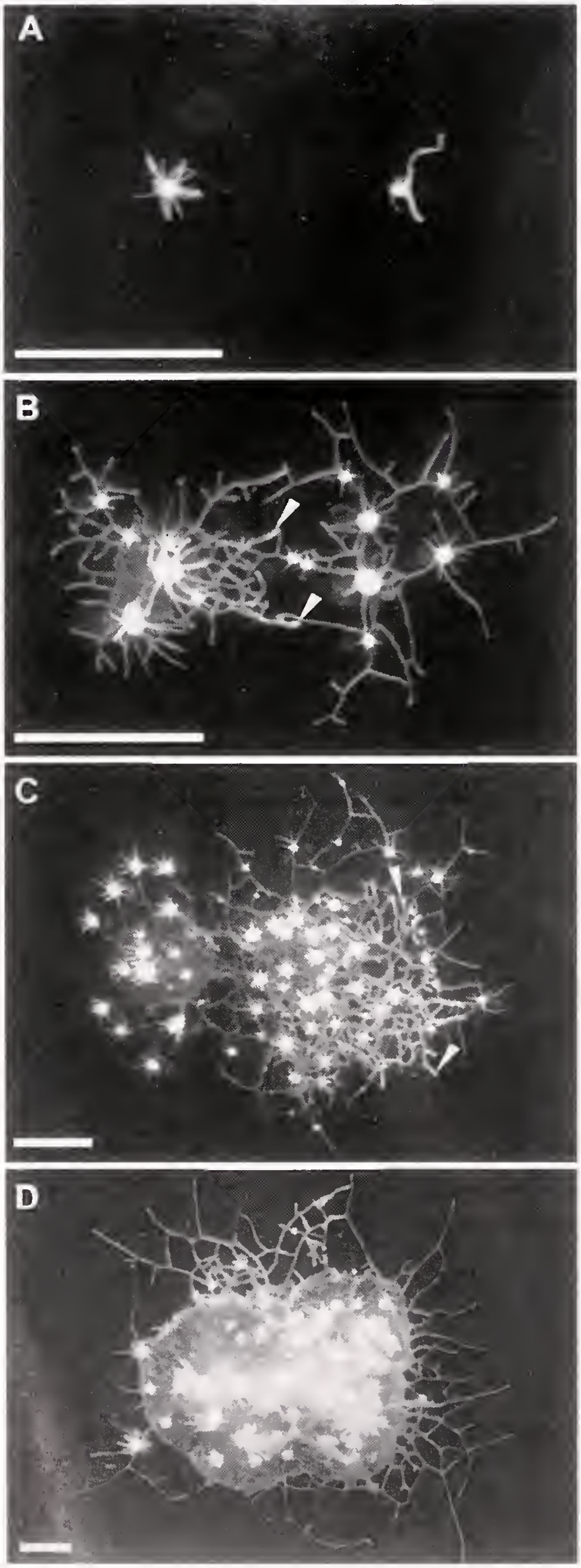

Figure 4. Image sequence of sexually produced competing colonies. Both species initially adopt a runner-like appearance as primary polyps (A). *Hydractinia symbiolongicarpus* (at left) begins directional growth toward *Podocoryna carnea* upon contact (B), after which the former responds by growing nematocyst-filled hyperplastic stolons in the direction of the stimulus. Many *H. symbiolongicarpus* colonies formed hyperplastic stolons (arrows) that grew directly over and destroyed the foreign tissue (B, C), ultimately forming an ectodermal mat and polyps over the newly acquired space (D). (A) Primary polyps; (B) 2 d post-contact; (C) 7 d post-contact; (D) 14 d post-contact. Scale bars = approx. 2 mm.

symbiolongicarpus, which showed a highly significant tendency to grow directionally toward *P. carnea* after contact. Furthermore, most sexually produced *H. symbiolongicarpus* colonies responded to contact by rapidly generating runner-like hyperplastic stolons from the point of contact that were able to grow directly over *P. carnea* colonies, which usually lacked hyperplastic stolons during this time. This concentrated projection of hyperplastic stolons progressed until the underlying *P. carnea* tissue was destroyed, after which the ectoderm between hyperplastic stolons fused to form a mat. In contrast, the clones produced from parental colonies of both species displayed growth patterns similar to those found in previous studies (Tardent and Bührer, 1982; Buss *et al.*, 1984; McFadden *et al.*, 1984; McFadden, 1986; Lange *et al.*, 1992; Van Winkle *et al.*, 2000).

Sexually produced colonies of *H. symbiolongicarpus* showed morphological as well as physiological features not observed in clonally produced colonies. These differences suggest that growth and development differ qualitatively between the two. First, nearly all sexually produced *H. symbiolongicarpus* colonies were able to directionally produce hyperplastic stolons, whereas clonally produced colonies did not produce such stolons or grow directionally. Previous studies also report ineffective or little to no hyperplastic stolon production in clonally produced colonies of *H. symbiolongicarpus* during interspecific bouts (McFadden, 1986; Lange *et al.*, 1992). Unlike *P. carnea* clones, the capacity of clonally produced *H. symbiolongicarpus* colonies to generate hyperplastic stolons is highly variable and dependent on colony morphology at the time of contact (McFadden *et al.*, 1984; Buss and Grosberg, 1990; Yund, 1991). In most cases, *H. symbiolongicarpus* is able to generate hyperplastic stolons only from previously existing stolons (Buss *et al.*, 1984; Lange *et al.*, 1989; Yund, 1991; Grosberg *et al.*, 1996); however, a particular form of underdeveloped mat tissue ("astogenetic" mat) has the capacity to produce hyperplastic stolons (Buss and Grosberg, 1990). In this study, sexually produced colonies of *H. symbiolongicarpus* initially grew like runners but produced stolonal mat within 2 weeks, thereby giving them their characteristic sheet-like morphology. In contrast, clonal explants of *H. symbiolongicarpus* produced mat tissue immediately upon attachment to the substratum, as observed in previous studies (McFadden *et al.*, 1984; Blackstone, 1996; Van Winkle *et al.*, 2000). The mat tissue of clonally produced colonies did not develop hyperplastic stolons after contact, suggesting that an astogenetic mat may be an age-specific feature.

Second, *H. symbiolongicarpus* primary polyps pump gastrovascular fluid to peripheral stolons at a higher rate than those same colonies after mat production, whereas gastrovascular flow rate gradually increases throughout early postmetamorphic development of *P. carnea* colonies (Blackstone, 1996). Such variation in gastrovascular flow rate may be an important factor mediating colony growth and morphology in hydroids (Dudgeon and Buss, 1996; Van Winkle and Blackstone, 1997; Dudgeon *et al.*, 1999); that is, higher flow rates are associated with more runner-like morphologies. These morphological and physiological differences suggest that sexually produced *H. symbiolongicarpus* colonies initially adopt a runner-like morphology, which may facilitate their enhanced directional and aggressive growth responses during competition with clonally produced colonies.

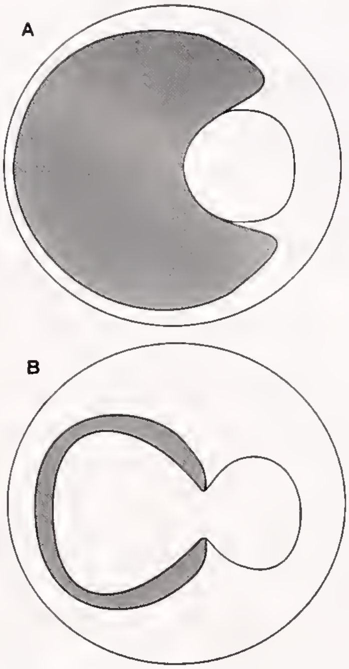

Figure 6. Schemata showing directional growth patterns between clonally produced colonies (A) and sexually produced colonies (B). *Podocoryna carnea* (gray) clonally produced colonies could not grow directly over their slower advancing *Hydractinia symbiolongicarpus* (white) competitors and tended to flank them. *H. symbiolongicarpus* sexually produced colonies tended to project hyperplastic stolons directly over *P. carnea* colonies soon after contact, whereas clonally produced *H. symbiolongicarpus* colonies did not.

To a lesser degree than their counterparts, sexually produced colonies of *P. carnea* exhibited differences from clonally produced colonies, which more readily and abundantly produced hyperplastic stolons upon contact. The directional growth observed in clonal replicates—and to some extent in sexually produced colonies—most likely represents opportunistic growth into unoccupied areas; that is, clonally produced *P. carnea* colonies were often able to flank (but not overgrow) their slower-advancing counterparts, which translated into an overall shift in center of mass toward competitors (Fig. 6A). This was not the case in sexually produced *H. symbiolongicarpus* colonies, which tended to grow hyperplastic stolons from the edge of the ectodermal mat directly into and over the sparsely arranged stolons of *P. carnea* competitors (Fig. 6B). *P. carnea* is not able to grow over living *H. symbiolongicarpus* tissue, presumably due to the space-filling morphology of the stolonal mat. Consequently, *H. symbiolongicarpus* colonies can survive for extended periods under these circumstances, given that they are able to feed (McFadden, 1986; Buss and Grosberg, 1990; Van Winkle *et al.*, 2000). The ability to generate hyperplastic stolons immediately after contact seems to be an important factor in determining competitive outcome for both species. This was exemplified by the relative success of sexually produced colonies of *H. symbiolongicarpus* and clonally produced colonies of *P. carnea* in this study, both of which generated hyperplastic stolons more readily than their corresponding competitors.

Ultimately, the source of every clonally produced colony is a sexually produced colony. Yet critical morphological and physiological aspects of colony development not seen in clonally produced colonies can be observed in very young *H. symbiolongicarpus* colonies in particular. Sexually produced colonies of *H. symbiolongicarpus* initially grow like runners, producing both peripheral stolons and presumably astogenetic mat tissue, which suggests age-specific growth that is possible only during a limited time of post-metamorphic colony development. At present, it is impossible to determine the absolute age of the field-collected clones used in this and preceding studies. Thus, the relationship of colony age and competitive ability in *H. symbiolongicarpus* remains to be quantified using sexually produced colonies. The production of stolonal mat (as opposed to astogenetic stolonal mat) and the deposition of the chitinous understory may divert colony resources from the development and maintenance of morphologies related to competitive ability. Alternatively, a suite of additional factors (*e.g.*, colony size, resource availability, cost of reproduction, somatic maintenance, senescence) may all contribute to the apparent reduction in runner-like growth and competitive ability observed in this species over time (*c.f.*, Braverman and Schrandt, 1966).

The data presented here reveal that during early ontogeny, *H. symbiolongicarpus* is capable of a pattern of growth and development unprecedented in past studies using clonal replicates. There may be a selective advantage of runner-like growth and enhanced competitive ability during early colony development: in natural populations, the probability of new larval recruitment to gastropod shells decreases with the size and age of resident colonies due to exclusion, and the frequency of competition is thus likewise expected to decrease (Yund *et al.*, 1987; Yund and Parker, 1989). The data presented in this study support the hypothesis that *H. symbiolongicarpus* is adapted to competition during early colony development. Additionally, the same factors that lead to differential larval settlement over the shell surface (*e.g.*, hermit crab feeding behavior; Yund *et al.*, 1987) are likely to also produce food gradients over the shell surface (*c.f.*, Koehl and Strickler, 1981; LaBarbera, 1984). The directional and runner-like growth potential of young *H. symbiolongicarpus* colonies leading to the occupation and defense of these nutrient-rich zones may thus provide a significant advantage owing to increased growth rates in early ontogeny. The observed growth and relative success of sexually produced *H. symbiolongicarpus* colonies may in part explain why this species is considerably more abundant than *P. carnea* on small gastropod shells inhabited by paguriid hermit crabs. Overall, variation in competitive ability and growth habit between sexually and clonally produced colonies of *H. symbiolongicarpus*—and to lesser extent between those of *P. carnea*—suggest that future assessments of competitive ability in colonial organisms (and in colonial hydroids specifically) include the use of sexually produced colonies.

Acknowledgments

Comments were provided by R. B. King, J. Miller, B. Johnson-wint, and C. von Ende. Support was provided by the National Science Foundation (IBN-0090580).

Literature Cited

Bertschy, K. A. 1998. *The Influence of Age-specific Survivorship and Growth on Pumpkinseed,* Lepomis gibbosus, *Life Histories.* Canadian Theses Series. National Library of Canada, Ottawa.

Blackstone, N. W. 1996. Gastrovascular flow and colony development in two colonial hydroids. *Biol. Bull.* **190:** 56–68.

Blackstone, N. W., and L. W. Buss. 1991. Shape variation in hydractiniid hydroids. *Biol. Bull.* **180:** 394–405.

Braverman, M. H., and R. G. Schrandt. 1966. Colony development of a polymorphic marine hydroid as a problem in pattern formation. Pp. 169–198 in *The Cnidaria and Their Evolution,* W. J. Rees, ed. Academic Press, New York.

Buss, L. W. 1990. Competition within and between encrusting colonial invertebrates. *Trends Ecol. Evol.* **5:** 352–356.

Buss, L. W., and N. W. Blackstone. 1991. An experimental exploration of Waddington's epigenetic landscape. *Philos. Trans. R. Soc. Lond. B* **332:** 49–58.

Buss, L. W., and R. K. Grosberg. 1990. Morphogenetic basis for phenotypic differences in hydroid competitive behaviour. *Nature* **343:** 63–66.

Buss, L. W., and P. O. Yund. 1988. A comparison of recent and historical populations of the colonial hydroid *Hydractinia. Ecology* **69:** 646–654.

Buss, L. W., C. S. McFadden, and D. R. Keene. 1984. Biology of hydractiniid hydroids. 2. Histocompatibility effector system/competitive mechanism mediated by nematocyst discharge. *Biol. Bull.* **167:** 139–158.

de Kroon, H., and M. J. Hutchings. 1995. Morphological plasticity in clonal plants: the foraging concept reconsidered. *J. Ecol.* **83:** 143–152.

Dudgeon, S. R., and L. W. Buss. 1996. Growing with the flow: on the maintenance and malleability of colony form in the hydroid *Hydractinia. Am. Nat.* **147:** 667–691.

Dudgeon, S., A. Wagner, J. R. Vaisnys, and L. W. Buss. 1999. Dynamics of gastrovascular circulation in the hydrozoan *Podocoryne carnea*: the one-polyp case. *Biol. Bull.* **196:** 1–17.

Equiza, M., J. Miravé, and J. Tognetti. 2001. Morphological, anatomical and physiological responses related to differential shoot vs. root growth inhibition at low temperature in spring and winter wheat. *Ann. Bot.* **87:** 67–76.

Frank, S. A. 1993. A model of inducible defense. *Evolution* **47:** 325–327.

Grosberg, R. K., D. R. Levitan, and B. B. Cameron. 1996. Evolutionary genetics of allorecognition in the colonial hydroid *Hydractinia symbiolongicarpus. Evolution* **50:** 2221–2240.

Harvell, C. D. 1990. The ecology and evolution of inducible defenses. *Q. Rev. Biol.* **65:** 323–340.

Hauenschild, C. 1954. Genetische und entwicklungphysiologische Untersuchungen über Intersexualität und Gewebeverträglichkeit bei *Hydractinia echinata* Flemm. (Hydroz. Bougainvill.). *Wilhelm Roux' Arch. Entwicklungsmech. Org.* **147:** 1–41.

Hauenschild, C. 1956. Über die Vererbung einer Gewebeverträglichkeitseigenschaft bei dem Hydroidpolypen *Hydractinia echinata. Z. Naturforsch. C* **11b:** 132–138.

Jackson, J. B. C., L. W. Buss, and R. E. Cook. 1985. *Population Biology and Evolution of Clonal Organisms.* Yale University Press, New Haven, CT.

Kleijn, D., and J. M. Van Groenendael. 1999. The exploitation of heterogeneity by a clonal plant in habitats with contrasting productivity levels. *J. Ecol.* **87:** 873–885.

Koehl, M. A. R., and J. R. Strickler. 1981. Copepod feeding currents: food capture at low Reynolds number. *Limnol. Oceanogr.* **26:** 1062–1073.

LaBarbera, M. 1984. Feeding currents and particle capture mechanisms in suspension feeding animals. *Am. Zool.* **24:** 71–84.

Lange, R. G., G. Plickert, and W. A. Müller. 1989. Histocompatibility in a lower invertebrate, *Hydractinia echinata:* analysis of the mechanism of rejection. *J. Exp. Zool.* **249:** 284–292.

Lange, R. G., M. H. Dick, and W. A. Müller. 1992. Specificity and early ontogeny of historecognition in the hydroid *Hydractinia. J. Exp. Zool.* **262:** 307–316.

Larwood, G., and B. R. Rosen. 1979. *Biology and Systematics of Clonal Organisms.* Academic Press, London.

Lundberg, S., P. Nilsson, and T. Fagerstrom. 1996. Seed dormancy and frequency dependent selection due to sib competition: the effect of age specific gene expression. *J. Theor. Biol.* **183:** 1–9.

McFadden, C. S. 1986. Laboratory evidence for a size refuge in competitive interactions between the hydroids *Hydractinia echinata* (Flemming) and *Podocoryne carnea* (Sars). *Biol. Bull.* **171:** 161–174.

McFadden, C. S., M. J. McFarland, and L. W. Buss. 1984. Biology of hydractiniid hydroids. 1. Colony ontogeny in *Hydractinia echinata* (Flemming). *Biol. Bull.* **166:** 54–67.

Moora, M., and M. Zobel. 1998. Can arbuscular mycorrhiza change the effect of root competition between conspecific plants of different ages? *Can. J. Bot.* **76:** 613–619.

Muko, S., K. Kawasaki, and K. Sakai. 2000. Morphological plasticity in the coral *Porites sillimaniani* and its adaptive significance. *Bull. Mar. Sci.* **66:** 225–239.

Müller, W. A., A. Hauch, and G. Plickert. 1987. Morphogenetic factors in hydroids. 1. Stolon tip activation and inhibition. *J. Exp. Zool.* **243:** 111–124.

Plickert, A., A. Heringer, and B. Hiller. 1987. Analysis of spacing in a periodic pattern. *Dev. Biol.* **120:** 399–411.

Smith, P. K., R. I. Krohn, G. T. Hermanson, A. K. Mallia, E. H. Gartner, M. D. Provenzano, E. K. Fujimoto, N. M. Goeke, B. J. Olson, and D. C. Klenk. 1985. Measurement of protein using bicinchoninic acid. *Anal. Biochem.* **150:** 76–85.

Sokal, R. R., and F. J. Rohlf. 1995. *Biometry,* 3rd ed. Freeman, San Francisco.

Spindler, A. N., and W. A. Müller. 1972. Induction of metamorphosis by bacteria and by lithium pulse in the larvae of *Hydractinia echinata* (Hydrozoa). *Wilhelm Roux' Arch. Entwicklungsmech. Org.* **169:** 271–280.

Stuefer, J. F. 1996. Potential and limitations of current concepts regarding the response of clonal plants to environmental heterogeneity. *Vegetatio* **127:** 55–71.

Tardent, P., and M. Bührer. 1982. Intraspecific incompatibilities in the metagenetical *Podocoryne carnea* M. Sars (Cnidaria, Hydrozoa). Pp. 295–308 in *Embryonic Development, Part B: Cellular Aspects,* M. M. Burger and R. Weber, eds. Alan R. Liss, New York.

Umeki, K. 1995. Importance of crown position and morphological plasticity in competitive interactions in a population of *Xanthium canadense. Ann. Bot.* **75:** 259–265.

Van Winkle, D. H., and N. W. Blackstone. 1997. Video microscopical measures of gastrovascular flow in colonial hydroids. *Invertebr. Biol.* **116:** 6–16.

Van Winkle, D. H., K. Longnecker, and N. W. Blackstone. 2000. The effects of hermit crabs on hydractiniid hydroids. *Mar. Ecol.* **21:** 55–67.

Weis, V. M., and L. W. Buss. 1987. Biology of hydractiniid hydroids. 5. Ultrastructure of metamorphosis in *Hydractinia echinata. Postilla* **200:** 1–24.

Yund, P. O. 1991. Natural selection on hydroid colony morphology by intraspecific competition. *Evolution* **45:** 1564–1573.

Yund, P. O., and H. Parker. 1989. Population structure of the colonial marine hydroid *Hydractinia* sp. nov. C in the Gulf of Maine. *J. Exp. Mar. Biol.* **125:** 63–82.

Yund, P. O., C. W. Cunningham, and L. W. Buss. 1987. Recruitment and postrecruitment interactions in a colonial hydroid. *Ecology* **68:** 971–982.

Reference: *Biol. Bull.* **202:** 166–181. (April 2002)

Quantitative Analysis of Gametic Incompatibility Between Closely Related Species of Neotropical Sea Urchins

MICHAEL A. McCARTNEY[1] AND H. A. LESSIOS

Smithsonian Tropical Research Institute, Apartado 2072, Balboa, Republic of Panama

Abstract. Species of the sea urchin genus *Echinometra* found on the two coasts of Panamá are recently diverged and only partially isolated by incomplete barriers to interspecific fertilization. This study confirms previous work that revealed incompatibility between the eggs of the Atlantic *E. lucunter* and the sperm of the other two neotropical species, whereas eggs of its sympatric congener *E. viridis* and allopatric *E. vanbrunti* are largely compatible with heterospecific sperm. Here we quantify fertilization using a range of sperm dilutions. We demonstrate a much stronger block to cross-species fertilization of *E. lucunter* eggs than was previously shown at fixed sperm concentrations, and mild incompatibility of the other two species' eggs where previous crosses between species were not distinguishable from within-species controls. Additionally, we present evidence for intraspecific variation in egg receptivity towards heterospecific sperm. Our findings here again discount the "reinforcement model" as a viable explanation for the pattern of prezygotic isolation. Gamete incompatibility in these *Echinometra* has appeared recently—within the last 1.5 million years—but is weaker in sympatry than in allopatry. Accidents of history may help explain why incompatibility of eggs emerged in one species and not in others. Compensatory sexual selection on sperm in this species could follow, and promote divergence of proteins mediating sperm-egg recognition.

Introduction

How reproductive isolation evolves between species of marine invertebrates that shed their eggs and sperm into the sea is a matter of considerable interest (Palumbi, 1992, 1994). Apart from asynchrony of gamete release and possible chemical communication between individuals, courtship and mating behaviors that could isolate species are largely absent in free-spawning organisms. When spawning seasons of coexisting closely related species overlap (Lessios, 1985) or when more than one species participates in a mass spawning event (*e.g.*, Babcock *et al.*, 1986; McCuen, 1988; Pearse *et al.*, 1988), incompatibility between gametes may be the most likely prezygotic reproductive barrier. Cross-species *in vitro* fertilizations are then an effective method for obtaining quantitative data on the strength of blocks to fertilization. Such data are crucial for judging the contribution of gamete incompatibility to the maintenance of reproductive isolation between free-spawning species, and may also provide clues to how fertilization barriers evolve.

Gamete compatibility between species has been studied in hydroids (Buss and Yund, 1989), corals (Knowlton *et al.*, 1997; Miller and Babcock, 1997; Szmant *et al.*, 1997), polychaetes (Pawlik, 1988; Marsden, 1992; Pernet, 1999), oysters (Banks *et al.*, 1994), abalones (Leighton and Lewis, 1982), sea urchins (Branham, 1972; Summers and Hylander, 1975; Strathmann, 1981; Lessios and Cunningham, 1990; Minor *et al.*, 1991; Palumbi and Metz, 1991; Metz *et al.*, 1994, 1998a; Aslan and Uehara, 1997), and sea stars (Byrne and Anderson, 1994). Although complete reciprocal incompatibility between species is often observed and a complete lack of incompatibility is rare (Pernet, 1999), these are not the most common outcomes. Most fertilization barriers are "partial"—the percent of eggs fertilized by heterospecific sperm is not zero but is some fraction of the percent fertilized by sperm of conspecifics.

Often, incompatibility between gametes of recognized species is also asymmetric; percent fertilization of the eggs

Received 19 July 2001; accepted 4 February 2002.

[1] Current address: Department of Biological Sciences and Center for Marine Science, University of North Carolina at Wilmington, 5600 Marvin Moss Lane, Wilmington, NC 28409; E-mail: McCartneyM@uncwil.edu

of one species of a pair is lower than in the reciprocal cross (Vacquier *et al.*, 1995). Asymmetric incompatibility has been found between species of hydroids (Buss and Yund, 1989), polychaetes (Pawlik, 1988), oysters (Banks *et al.*, 1994), abalones (Leighton and Lewis, 1982), and is particularly common in sea urchins (Branham, 1972; Strathmann, 1981; Lessios and Cunningham, 1990; Minor *et al.*, 1991; Metz *et al.*, 1994; Aslan and Uehara, 1997). Why fertilization barriers should often be asymmetric and incomplete is not known and is worthy of further study.

The three species of *Echinometra* sea urchins found on the two coasts of the Americas provide an excellent case in which to examine partial, asymmetric gametic isolation. First, the phylogeny of these species and the timing of their speciation relative to the closure of the Isthmus are known (McCartney *et al.*, 2000). Hence, we can determine whether fertilization barriers are stronger in species separated earlier than in species more recently split, and we can address whether the evolution of these barriers is accelerated in sympatric species compared to species living in different oceans. *Echinometra vanbrunti* ranges along the Pacific coast of America from the Gulf of California to Peru. *Echinometra lucunter* occurs from Bermuda south to Brazil and east to the Atlantic coast of tropical Africa. *Echinometra viridis* is restricted to the Caribbean, where it co-occurs with *E. lucunter*, and although *E. viridis* is usually found in deeper water, the spawning seasons of the two sympatric species overlap (Lessios, 1981b). *E. viridis* is morphologically most distinct from the other two species (Mortensen, 1928-1951; Lessios, 1981a), yet mitochondrial DNA (mtDNA) sequences show it to be a sister species to the sympatric *E. lucunter*, with the allopatric *E. vanbrunti* having split off earlier (McCartney *et al.*, 2000). Thus, it is probable that closure of the Isthmus of Panama 3.1 million years ago (MYA) (Coates and Obando, 1996) split *E. vanbrunti* from the common ancestor of the two Atlantic species, whose mtDNA divergence places their speciation at *ca.* 1.5 MYA (McCartney *et al.*, 2000).

An earlier study (Lessios and Cunningham, 1990) demonstrated asymmetric gamete compatibility of one species towards the other two. Both heterospecific crosses involving eggs of *E. lucunter* females showed a greatly lowered percent fertilization compared to homospecific controls. In contrast, fertilization in both of the reciprocal crosses between *E. lucunter* and the other two species, as well as in the *E. viridis* male × *E. vanbrunti* female crosses, was no lower than in homospecific crosses. Fertilization in the *E. vanbrunti* male × *E. viridis* female cross was slightly reduced relative to controls. Finally, incompatibility between the sympatric species was less than that between the allopatric *E. lucunter* and *E. vanbrunti*. This finding runs contrary to predictions from the "speciation by reinforcement" model (Dobzhansky, 1940; Butlin, 1989; Liou and Price, 1994). The model envisions that populations that have acquired a degree of reproductive isolation in allopatry, will, when they become sympatric, develop pre-zygotic isolation to avoid gamete wastage in inferior hybrids. Reinforcement should therefore yield greater gamete incompatibility between *Echinometra* species that currently live in the same ocean than between those that have been allopatric for the last 3 MY.

Each of the above conclusions was reached in experiments that combined gametes at a single concentration. McClary (1992) suggested that a different pattern might have emerged if concentrations of sperm had been varied. Though there were reasons to consider this suggestion unlikely (Lessios and Cunningham, 1993), we here report a determination of percent fertilization at various sperm concentrations. We construct "fertilization curves" estimated using a series of sperm dilutions, then examine the degree to which the added sensitivity of these experiments permits a better understanding of the mechanisms by which sympatric and allopatric species have developed prezygotic isolation.

Materials and Methods

Gametic compatibility experiments

Sea urchins were collected from the Caribbean coast of Panamá near Portobelo (*Echinometra lucunter* and *E. viridis*), and from the Pacific coast of Panamá at Isla Taboguilla (*E. vanbrunti*) between August and October 1996, and again in June 1997. These are months during which all three species are reproductively active (Lessios, 1981b). Animals were induced to spawn by intracoelomic injection of 0.5 *M* KCl.

Females releasing eggs were inverted so that their gonopores were immersed in a 50-ml beaker partially filled with 0.22-μm-filtered seawater (FSW). Eggs were resuspended, poured through doubled gauze to trap debris, and then washed once by aspiration and replacement of the FSW. The eggs were settled in a volumetric centrifuge tube to estimate their volume, and their concentration was adjusted to 2 ml of eggs in 100 ml of FSW. Counts of eggs from three females per species indicated that 2% suspensions contained, on average, 58 eggs of *E. lucunter*, 50 eggs of *E. viridis*, and 104 eggs of *E. vanbrunti* per microliter. Eggs were stored at room temperature for no more than 6 h prior to their use.

Sperm was drawn directly off male gonopores after injection of KCl solution. Undiluted ("dry") sperm was stored in capped microcentrifuge tubes for less than 1 h at room temperature. Preliminary experiments indicated that dry sperm maintained full fertilizing potency for at least 1 h.

A polypropylene microplate (Whatman #7701-5200) with 96 wells of 2-ml capacity each was used to conduct the fertilization experiments. Each well was filled with 0.2 ml FSW. A starting suspension of sperm was prepared by diluting 5 μl dry sperm in 25 ml FSW for homospecific crosses and 5μl of sperm into 2.5 ml FSW for crosses in which *E. lucunter* eggs were exposed to heterospecific sperm. These starting concentrations were chosen so that subsequent dilutions would bracket those necessary to produce the descending portion of the fertilization curves. Equal amounts (200 μl each) of the starting suspension and FSW were mixed together, and 200 μl of this diluted suspension was again transferred to 200 μl FSW. This process was repeated to prepare 12 serial 2-fold dilutions. Egg suspension (200 μl) was mixed into each well in succession, starting with the well containing the most concentrated sperm suspension. Each sperm dilution series was prepared from a fresh dilution of dry sperm. A portion of the original sperm suspension was saved for later spectrophotometric estimates of sperm concentration. The microplate was capped, then gently rotated on an orbital shaker at 30°C for 90 min. This amount of time was previously determined to ensure that all fertilized eggs had passed through at least two cleavage divisions. Incubations were stopped after 90 min by fixing with 400 μl of 5.5% formaldehyde in FSW. In preliminary experiments, washing of the eggs to rid them of excess sperm had no effect on the yield of fertilized eggs at fixed sperm concentrations in homospecific crosses, so it was not considered necessary to remove the sperm during the experiments.

All animals spawned were used in fertilizations on a single day, then discarded. Each female was used in a single experiment involving crosses with conspecific males, and with males of either one or both of the other two *Echinometra* species. A total of 181 crosses on eight trial dates were performed. To score percent fertilization, a drop of fixed suspension was placed on a slide, and a haphazardly selected track through the suspension was scanned under a compound microscope. At least 100 eggs were scored as either cleaving or not cleaving. Cleavage was selected as a convenient index of fertilization in lieu of raised fertilization membranes because fertilization membranes are difficult to see in these species of *Echinometra*. Previous work (Lessios and Cunningham, 1990) has shown that although percent of cleaving eggs is in some crosses lower than percent of eggs with raised fertilization membranes, this reduction is slight and introduces no bias in comparisons between homospecific and heterospecific crosses.

Sperm concentration was quantified spectrophotometrically (Vacquier and Payne, 1973). First, a standard curve was constructed. Three males of *E. lucunter* and two males each of *E. vanbrunti* and *E. viridis* were spawned, and a dilution series consisting of 10 serial 2-fold dilutions in FSW was prepared for each male. Each sperm dilution was fixed in an equal volume of 5.5% formaldehyde in FSW, and its absorbance at 340 nm (A_{340}) was determined against a blank of 2.25% formaldehyde in FSW. We made triplicate hemacytometer counts of the number of spermatazoa in each dilution, then determined the correspondence between optical absorbance and sperm concentration using linear regression. Separate regressions for each species showed no consistent differences in slope, so a common curve with slope equal to the average was used. This standard curve was used to convert A_{340} readings taken from the males used in each of the experimental trials to numbers of sperm per microliter.

Data analyses

The nonlinear, sigmoid relation between number of sea urchin eggs fertilized and sperm concentration presents a problem for quantifying and statistically comparing gamete compatibility. One solution is to fit the data to an explicit nonlinear fertilization kinetics model (Vogel *et al.*, 1982; Levitan, 1996, 1998). An alternative approach is to first linearize the response using an appropriate transformation. We preferred the latter approach, because it does not assume that cross-species fertilizations adhere to the kinetic model developed for crosses performed within species. This approach also permits the application of linear statistical models. We used a standard transformation that has been successfully applied to other sigmoid responses, such as toxicity. This is the logit transformation (Finney, 1964; Hewlett and Plackett, 1979). The proportion of eggs fertilized (P) was transformed to its logit as follows: logit (P) = ln ($P/1 - P$). Linear regression of logit (P) values was then performed on log-transformed sperm concentration for each of the 181 crosses.

As a measure of egg-sperm compatibility over the range of sperm concentrations tested, we calculated the F_{50}, or the sperm concentration at which 50% of the eggs were fertilized (see Levitan, 1996, 1998). F_{50} values were calculated from the linear regression by determining the sperm concentration at which logit (0.5) = 0 (Figs. 1B, 2B, 3B). To compare F_{50} values across experimental trials, we took two approaches, each of which relied on different assumptions. In the first approach, we treated each F_{50} estimate as a unique value, independent of all others. This would be true if gamete compatibility were an emergent property of a given egg-sperm combination and not reflective of sperm or egg "qualities" (*e.g.*, swimming speed, viability) that would influence multiple crosses.

For this analysis, we grouped the log F_{50} values calculated from individual crosses by the species of female used in the cross. We then compared the mean log F_{50} values among the three male species tested on each species of female. Results of a Kolmogorov-Smirnov test indicated that distributions of log F_{50} values were not significantly different from an ideal normal distribution with the same mean and variance. The distributions were then tested for heteroscedasticity across the three species of sperm donor by using Bartlett's test. In two of the three species of females, variances were not significantly different between species of male, and ANOVA was performed using log F_{50} as the response variable and species of male as the main effect. In the case of *E. lucunter* females, unequal variances were found ($F = 7.590$, $P < 0.001$), so the log F_{50} values were compared using Welch's (1951) approximate ANOVA. Multiple comparisons among mean log F_{50} values for each class of cross were conducted using the Games and Howell (1976) test at the 5% significance level. ANOVA and multiple comparisons were performed using StatView 5.0.1 (SAS Institute, 1999).

For the second approach, we assumed that percent fertilization of eggs of a given female by one male is not independent of percent fertilization of that female by a second male. In other words, we assumed that unknown qualities of the eggs of a female could influence their compatibility with any male tested; a similar argument applies to the sperm of a male used in more than one egg-sperm combination. To take such lack of independence into account, we analyzed the data using a randomized complete blocks design in ANOVA. Each of the three species of females was analyzed separately. It was also necessary to separately analyze each of three types of crossing designs to maintain a balanced statistical design. In all of the trials, eggs from a single female were mixed with sperm from a single male (no experiment involved mixtures of sperm of multiple males), but slightly different crossing designs were used to make efficient use of ripe animals available on a given day. In type I crosses, one female was tested with several conspecific males and several males of one of the other two *Echinometra* species. In type II crosses, one female was tested with several conspecific males and several males of the remaining *Echinometra* species. In type III crosses, one female was tested with a single male from each of the three species. The dependent variable was log-transformed F_{50}. Females were treated as blocks in the analysis, and species of male was treated as the main effect. Multiple comparisons among species of male were conducted using the Games and Howell (1976) procedure.

As a final method for comparing compatibility, we fit our data to the nonlinear sea urchin fertilization kinetics model developed by Vogel *et al.* (1982). Untransformed proportion of eggs fertilized (P) was fit to the following equation:

$$P = 1 - \exp\left(\frac{-\beta S_0}{\beta_0 E_0}\left(1 - e^{-\beta_0 E_0 \tau}\right)\right)$$

where S_0 = number of sperm/μl, E_0 = number of eggs/μl, τ = sperm/egg contact time (set to equal 90 min) and β and β_0 are parameters obtained from nonlinear regression of P on S_0 (the ratio β/β_0 is roughly interpretable as the proportion of the egg surface area that is fertilizable (Vogel *et al.*, 1982). Because the eggs of the three species are different sizes, the number of eggs per microliter of seawater was estimated from counts made separately for each species. As measured by Lessios (1990), *E. viridis* has the largest eggs (3.97×10^5 μm^3 volume), *E. lucunter* has eggs intermediate in size (3.40×10^5 μm^3), and *E. vanbrunti* has the smallest eggs (1.94×10^5 μm^3). Values of β and β_0 were estimated separately for each of the 181 trials and are not given, but are available from the first author. Fits to this equation were performed using the Gauss-Newton least squares iterative method provided in JMP 2.0 (SAS Institute, 1989). The F_{50} value was calculated by solving the resulting nonlinear regression equation for S_0 at $P = 0.5$. Values of F_{50} obtained from fits to the Vogel *et al.* (1982) model were analyzed statistically in the same manner as were the log F_{50} values obtained from linear regression described above.

We found great variation among *E. lucunter* females in F_{50} values calculated from heterospecific crosses (Figs. 4 and 7, Appendix). To determine whether this was due to differences among females in egg "quality"—that is, whether it reflected a capacity to be fertilized by sperm of conspecific males—we performed the following analyses. We used the results from the 13 *E. lucunter* females that were each tested with one different male of each of the three species. We calculated the correlation (Kendall's τ) between the F_{50} values estimated for each of the possible pairwise comparisons among males: *E. lucunter* males with *E. viridis* males, *E. lucunter* males with *E. vanbrunti* males, and *E. viridis* males with *E. vanbrunti* males. Significant values of Kendall's τ in the former two comparisons would indicate that differences in fertilizability of eggs by heterospecific sperm arise due to differences in egg quality; significant values in the latter comparison would indicate that fertilizability of eggs by sperm of the allopatric species covaried with fertilizability by sperm of the sympatric species.

Results

Relation between sperm concentration and optical absorbance

The standard curve relating A_{340} to sperm concentration yielded a highly significant linear regression ($F = 651.08$; $df = 1,46$; $P < 0.001$; $R^2 = 0.935$). The regression equation ($f(x) = 1.84 \times 10^{-5}x + 0.014$), when solved for x at $A_{340} = 1$, produced an extinction factor of 5.35×10^4 sperm/μl per A_{340} unit. We used this value to convert optical density measurements to sperm concentrations in all of our fertilization experiments. Our calibration was very close to those published. Branham (1972) reported extinction factors of 5.37×10^4 for *E. mathei* and 4.94×10^4 for *E. oblonga*. Using methods similar to ours, Tyler *et al.* (1956) and Minor *et al.* (1991) estimated that two species of *Strongylocentrotus* and *Lytechinus variegatus* produced dry sperm with concentrations ranging between 2 and 9.5×10^7 sperm/μl. The eight *Echinometra* males used in our study produced dry sperm with a similar average concentration—3.04×10^7 sperm/μl.

Fertilization curves

Fertilization of eggs in all homospecific and some heterospecific crosses rose sharply with increasing sperm concentration, producing characteristic sigmoid curves (Figs. 1, 2 and 3). Curve fitting to the fertilization kinetics model of Vogel *et al.* (1982) was generally good (Figs. 1A, 2A, 3A), as was the fit of the linear regressions on logit-transformed data (Figs. 1B, 2B, 3B). Crosses in which eggs of *E. lucunter* females were fertilized by sperm of either of the other two species produced curves that shifted greatly towards higher sperm concentrations (Fig. 1A, 1B). As Figure 1B shows, sperm of this *E. viridis* male needed to be more than 250 times more concentrated than that of *E. lucunter* to fertilize half the eggs of this *E. lucunter* female. Sperm of the *E. vanbrunti* male shown had to be about 2000 times more concentrated than that of *E. lucunter* to achieve the same effect. Other *E. lucunter* females showed even stronger incompatibilities towards heterospecific sperm (Appendix).

Incompatibility of eggs from the other two species with heterospecific sperm was more moderate, or lacking altogether. For example, to fertilize half the eggs of the *E. viridis* female shown in Figure 2B, *E. lucunter* sperm needed to be only three times more concentrated and *E. vanbrunti* sperm only about 25 times more concentrated than *E. viridis* sperm. Eggs of *E. vanbrunti* showed an even milder barrier to cross-species fertilization, or none at all. For example, the *E. vanbrunti* female shown in Figure 3 displayed no detectable gamete incompatibility towards the other two species. Fertilization of her eggs was actually highest when they were exposed to sperm of *E. viridis*, and fertilization by *E. lucunter* and by *E. vanbrunti* sperm was nearly indistinguishable.

Linear regression analysis

The logit-transformed fertilization data showed good fit to log sperm concentrations, with r^2 values from linear regression often exceeding 0.90 (Appendix). Of the 181 crosses analyzed, only 6 crosses did not yield significant regressions. In four of these cases, this occurred because several sperm dilutions were too dilute to yield detectable fertilization, resulting in a regression based on few values and in increased error in estimation. The two other cases involved highly incompatible crosses (between *E. vanbrunti* sperm and *E. lucunter* eggs) that showed poor dependence of percent fertilization on sperm concentration.

Comparison of F_{50} *values*

To compare the results obtained across multiple females, F_{50} values were estimated for all crosses. The F_{50} values were then placed into nine groups representing the nine cross classes (with each class of cross defined as one species of male crossed with one species of female: Figs. 4, 5, and 6). Fertilization of *E. lucunter* eggs required considerably more heterospecific than conspecific sperm. The mean F_{50} values were 65 times higher for *E. viridis* sperm and over 1700 times higher for *E. vanbrunti* sperm than was the F_{50} value estimated for conspecific sperm crossed with *E. lucunter* eggs (Fig. 4, Table 1).

E. viridis females showed much more modest heterospecific incompatibility. Compared with conspecific sperm, just over twice as much *E. lucunter* sperm and about 18 times as much *E. vanbrunti* sperm fertilized half the *E. viridis* eggs (*Fig.* 5, Table 1). *E. vanbrunti* females were only slightly less fertilizable by heterospecific sperm (Fig. 6; Table 1). Just over 2.5 times as much *E. lucunter* as conspecific sperm fertilized half the eggs of this species. Only two *E. viridis* males were tested against *E. vanbrunti* eggs, but neither of them was incompatible.

Welch's ANOVA showed highly significant differences among male species tested with *E. lucunter* females ($W = 125.41$, $P < 0.001$), and multiple comparisons showed significant differences between means in all three species of sperm donor (Games-Howell test). ANOVA also showed significant differences among male species tested on *E. viridis* females ($F = 15.96$, $df = 2,43$; $P < 0.001$). In this case, multiple comparisons revealed differences between *E. viridis* and *E. vanbrunti* males, but *E. viridis* and *E. lucunter* males were not distinguishable. ANOVA also showed marginally significant differences among species of sperm donor tested on *E. vanbrunti* females ($F = 3.425$; $df = 2, 30$; $P = 0.046$). In this case, significant differences were apparent between *E. lucunter* and *E. vanbrunti* males; the other two comparisons were not possible because there were only two (*E. viridis* male × *E. vanbrunti* female) crosses.

A potential problem with the above analysis is that males and females were used in more than one fertilization experiment, so a randomized complete blocks analysis was used to allow for any non-independence. The results closely matched those from one-way ANOVA. Highly significant differences in fertilization of *E. lucunter* eggs were present between species of males, but these differences were less clear with eggs of *E. viridis* and *E. vanbrunti*. The seven *E. lucunter* females involved in crosses with multiple *E. viridis* and *E. lucunter* males had significantly fewer eggs fertilized by *E. viridis* than by *E. lucunter* sperm ($F = 140.29$, $P < 0.001$). For the two *E. lucunter* females involved in crosses with multiple *E. vanbrunti* and *E. lucunter* males, significantly fewer eggs were fertilized by *E. vanbrunti* than by *E. lucunter* males ($F = 142.0$, $P < 0.001$). And for the 13 *E. lucunter* females, each crossed with a single male of each species, highly significant differences existed among species of males ($F = 48.01$, $P < 0.001$). Multiple comparisons

①

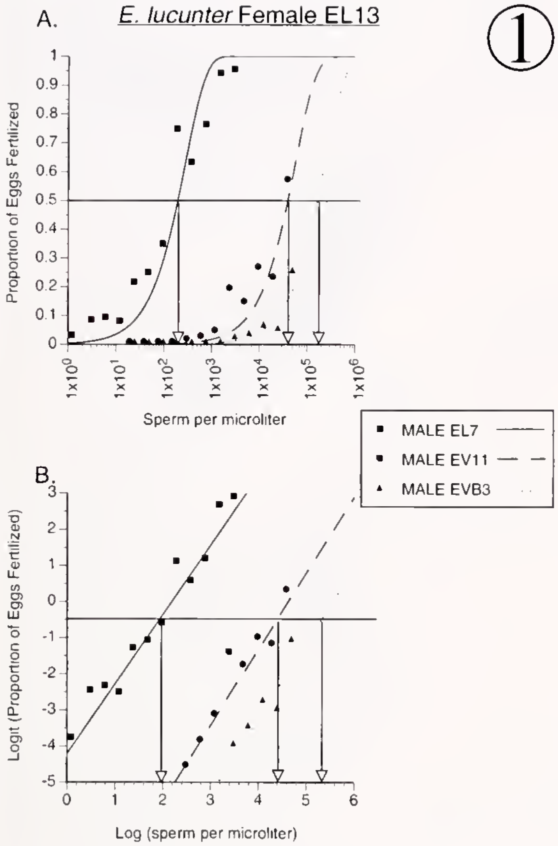

②

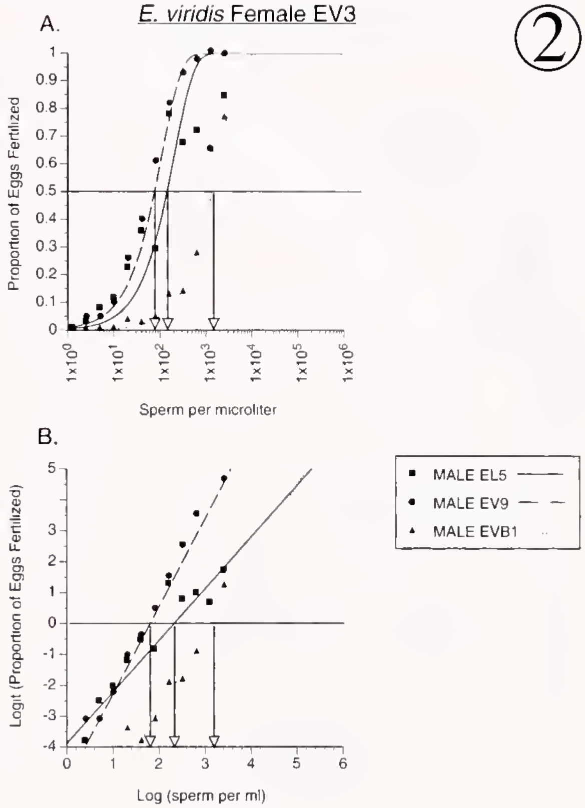

③

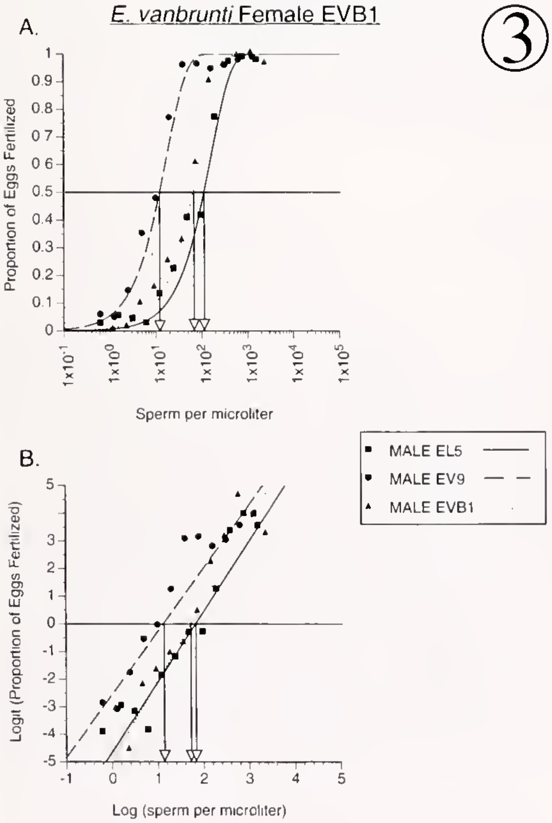

Figures 1–3. Representative results from *Echinometra* fertilization experiments performed at a series of sperm dilutions. Top panels (A) show the proportion of eggs fertilized (*P*) as a function of log sperm concentration (number of sperm/μl); curves are least-squares fits to the fertilization kinetics model of Vogel *et al.* (1982). Bottom panels (B) show logit (*P*) plotted against log sperm concentration; lines are from linear regression. Solid lines = *E. lucunter* (EL) males, dashed lines = *E. viridis* (EV) males, dotted lines = *E. vanbrunti* (EVB) males. The female involved in the crosses is indicated above the top panel. Data from other experiments are shown in the appendix.

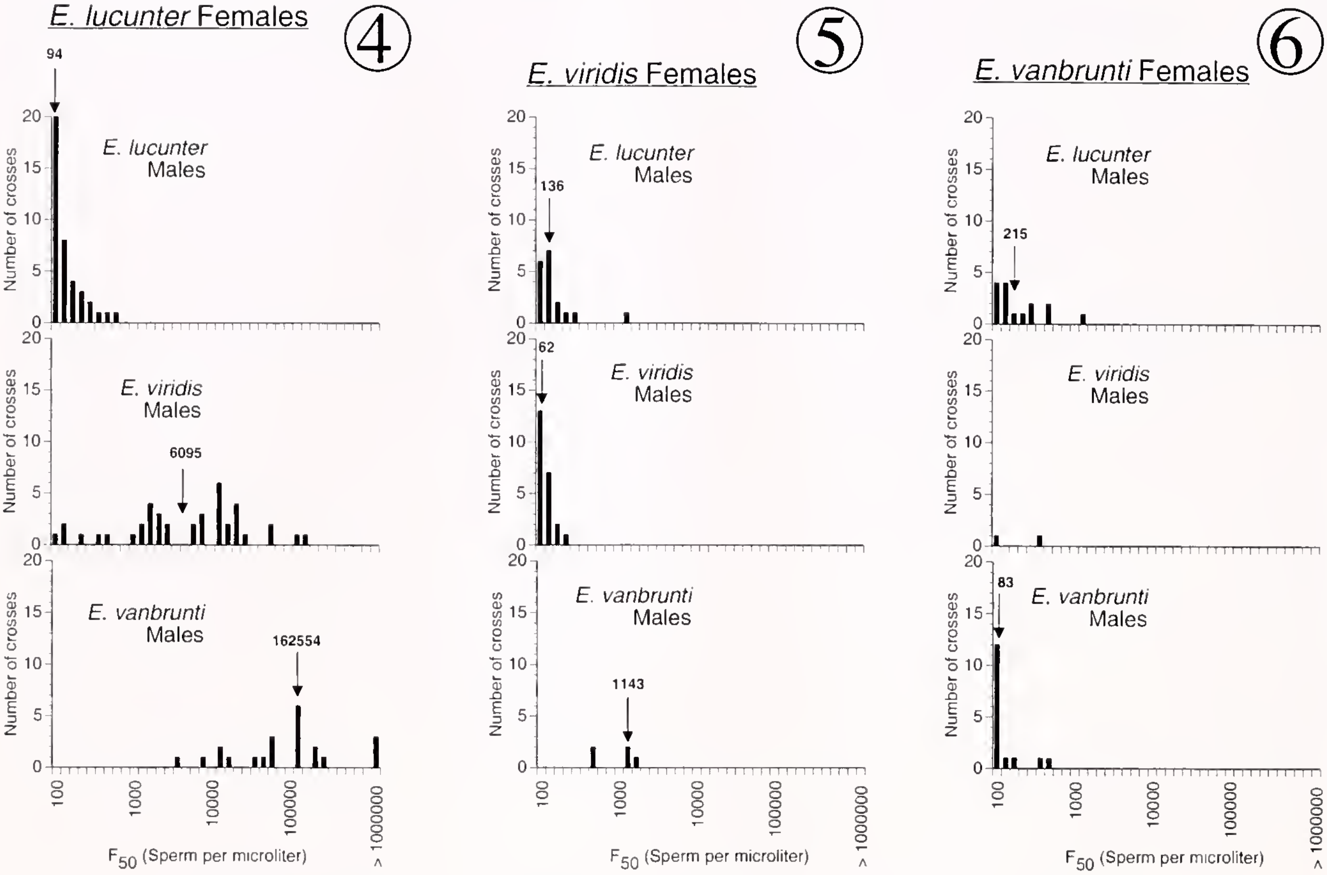

Figures 4–6. Distributions of F_{50} values derived from linear regressions of logit-transformed data from *Echinometra* fertilization experiments. Bars indicate the number of crosses in which F_{50} values fell between the class limits labeled on the X-axis (note the logarithmic scale to the labels). Arrows mark the back-transformed value of the mean log F_{50}. The number of crosses in each cross category was 40 *E. lucunter* female × *E. lucunter* male, 40 *E. lucunter* female × *E. viridis* male, 22 *E. lucunter* female × *E. vanbrunti* male; 18 *E. viridis* female × *E. lucunter* male, 23 *E. viridis* female × *E. viridis* male, 5 *E. viridis* female × *E. vanbrunti* male; 15 *E. vanbrunti* female × *E. lucunter* male, 2 *E. vanbrunti* female × *E. viridis* male, and 16 *E. vanbrunti* female × *E. vanbrunti* male.

ranked compatibility of the males with *E. lucunter* eggs in the order *E. lucunter* > *E. viridis* = *E. vanbrunti*. In contrast, the five *E. viridis* females crossed with multiple males showed no significant difference between F_{50} values estimated for *E. lucunter* and *E. viridis* males ($F = 1.329$, $P > 0.05$). The three *E. viridis* crossed with a single male of each species showed significant differences between male species ($F = 30.40$, $P < 0.01$). But as in the one-way analysis, multiple comparisons discriminated between *E. viridis* and *E. vanbrunti* males, but not between *E. viridis* and *E. lucunter* males. Results with *E. vanbrunti* females were mixed: significantly fewer eggs were fertilized by *E. lucunter* than *E. vanbrunti* males in crosses with multiple males ($F = 37.26$, $P < 0.001$), whereas crosses with a single male of all three species revealed no differences among male-species ($F = 0.919$, $P > 0.05$).

Compatibility estimated using the fertilization kinetics model

Estimates of F_{50} from nonlinear fits to the fertilization kinetics model of Vogel *et al.* (1982) were highly correlated with the F_{50} values from linear regression (correlation between log F_{50} values = $r = 0.970$, $P < 0.001$). Differences between heterospecific and homospecific values tended to be smaller using the Vogel method, particularly in highly incompatible crosses (see Figs. 1, 2, and 3; Appendix). Mean F_{50} values calculated from the Vogel model estimated that 60 times as much *E. viridis* sperm and 735 times as much *E. vanbrunti* sperm as conspecific sperm was required to achieve 50% fertilization of *E. lucunter* eggs. About 1.5 times as much *E. lucunter* sperm and about 12 times as much *E. vanbrunti* sperm

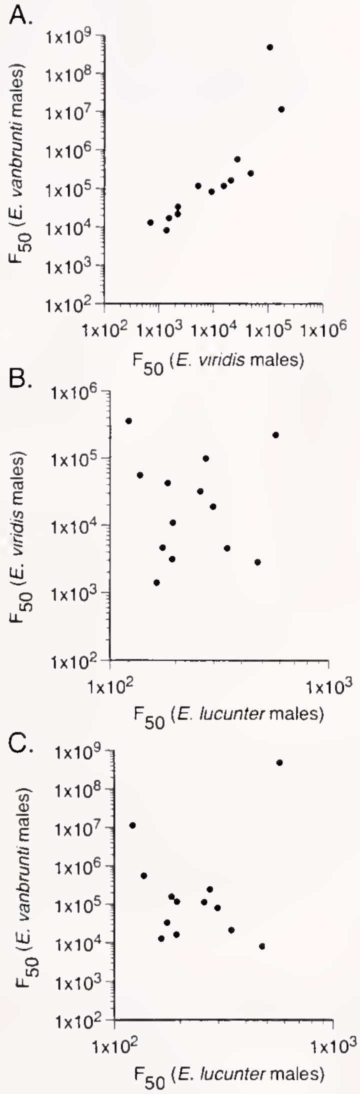

Figure 7. Correlation of F_{50} values from *Echinometra* fertilization experiments. Data shown are for 13 crosses of *E. lucunter* females, each of which was tested with a single male of each of the three species. Points are F_{50} values measured in the cross with a male of one species (ordinate) plotted against the F_{50} values measured in the cross with a male of the other species (abscissa).

fertilized half the *E. viridis* eggs. Just over twice as much *E. lucunter* as conspecific sperm fertilized half the eggs of *E. vanbrunti* (Table 2).

Correlation among F$_{50}$ *values*

Females of *E. lucunter* differed by as much as 2 orders of magnitude in their receptivity towards heterospecific sperm (Fig. 4; Appendix). Differences in receptivity towards conspecific sperm do not explain these differences; that is, they do not arise from differences in gamete "quality." In 13 cases, fertilization trials combined the eggs of a single *E. lucunter* female with one male of each of the three species. No correlation existed between the F_{50} value calculated (from linear regression) for the homospecific cross and for the cross with either *E. viridis* (Fig. 7A: Kendall's $\tau = -0.077$, $P > 0.05$) or *E. vanbrunti* (Fig. 7B: $\tau = -0.154$, $P > 0.05$) males. Similarly, no correlation was found in the same comparisons for F_{50} values calculated using nonlinear regressions ($\tau = 0.154$, $P > 0.05$ for both comparisons). Significant, positive correlations would have indicated that females that required more heterospecific sperm for fertilization also required more conspecific sperm. This would implicate gamete quality differences as responsible, but none were apparent. In contrast, significant positive correlations were found for these same 13 trials between F_{50} values of *E. viridis* and those of *E. vanbrunti* males, when calculated using both linear (Fig. 7C: $\tau = 0.872$, $P < 0.001$) and nonlinear regression ($\tau = 0.795$, $P < 0.001$). These results show that females with eggs that were less discriminating towards sperm of one heterospecific were also less discriminating towards sperm of the other.

Discussion

Patterns of gametic incompatibility

The neotropical species of *Echinometra* each show partial cross-species gametic incompatibility, but to very different degrees. The eggs of *E. lucunter* are strongly incompatible with the sperm of its two most closely related species. Incompatibility can be defined as the ratio of the mean F_{50} values (the heterospecific value divided by the homospecific value: see Tables 1 and 2). With this approach, incompatibility between *E. lucunter* eggs and *E. viridis* sperm is estimated to range from 60-fold (using the F_{50} values estimated by fitting the Vogel *et al.* (1982) model) to 65-fold (using fits to linear regressions). Incompatibility between *E. lucunter* eggs and *E. vanbrunti* sperm ranges from > 700 to > 1700-fold. This is a much stronger block than was found by Lessios and Cunningham (1990). If, from this previous study, incompatibility is defined as the inverse of the ratio of percent cleaving eggs in homospecific:heterospecific crosses, incompatibility of *E. lucunter* eggs with *E. viridis* sperm would be estimated at 5.2-fold, and with *E. vanbrunti* sperm only 11-fold. Hence, the present approach of using sperm dilution curves detects much greater quantitative differences in gamete compatibility, but the rankings among the species are the same.

Compatibility differences between homospecific and heterospecific gametes are much more moderate for eggs of the other two species. In the present study, we estimate compatibility of *E. viridis* eggs with *E. lucunter* sperm to be just 1.4–2.2 times lower, and with *E. vanbrunti* sperm 12–18 times lower than with conspecific sperm. *E. vanbrunti* eggs are only 2.2–2.6 times less compatible with *E. lucunter* than with conspecific sperm, and appear—from the two crosses

Table 1

Summary comparison of F_{50} *values among the nine possible crosses of* Echinometra *species.*

Female	Male	n	$\bar{F}_{50}$	F_{50} ratio	L_1	L_2
E. lucunter	*E. lucunter*	40	94	—	65	137
E. lucunter	*E. viridis*	22	6095	64.8	3359	11,059
E. lucunter	*E. vanbrunti*	40	162,554	1729	56,032	471,585
E. viridis	*E. lucunter*	18	136	2.19	85	216
E. viridis	*E. viridis*	23	62	—	39	100
E. viridis	*E. vanbrunti*	5	1143	18.4	737	1770
E. vanbrunti	*E. lucunter*	15	215	2.59	133	351
E. vanbrunti	*E. viridis*	2	81	0.98	NA	NA
E. vanbrunti	*E. vanbrunti*	16	83	—	52	132

F_{50} estimated by linear regression, as described in the text; n = number of crosses; $\bar{F}_{50}$ = mean F_{50}; F_{50} ratio = F_{50} (heterospecific cross)/F_{50} (homospecific cross); L_1 and L_2 = 95% confidence limits for $\bar{F}_{50}$; means and confidence limits are back-transformed from their logs.

performed here and from the results of Lessios and Cunningham (1990)—to show no incompatibility with *E. viridis* sperm. So, although *E. lucunter* eggs have evolved a strong barrier to cross-species fertilization, weaker or undetectable barriers are present in eggs of the other two species. This result is in large part identical to that found in Lessios and Cunningham (1990), with the exception that the weak incompatibilities in *E. viridis* and *E. vanbrunti* were previously not detectable (the somewhat stronger incompatibility between *E. viridis* eggs and *E. vanbrunti* sperm was detected). Thus, testing sperm dilution series is a more sensitive method for identifying small fertility differences that are not apparent at single sperm concentrations. The question is whether unidirectional differences of small magnitude, such as those involving *E. viridis* and *E. vanbrunti* eggs, have any biological meaning. In the absence of any other isolating mechanism, it is unlikely that they alone could serve to keep two sympatric species from fusing.

A new approach to quantifying gametic incompatibility

In the present study, fitting by linear regression of logit-transformed data was a more accurate method than was fitting to the Vogel *et al.* (1982) fertilization kinetics model. Fits to the latter model were poor in some heterospecific crosses, particularly those in which incompatibility was strong. This casts doubts on the general utility of the Vogel model for estimating gamete compatibility between species. Vogel *et al.* aimed their approach at homospecific fertilization and built their model from a kinetic study. When sperm and eggs of different species are involved, the probability of fertilization is likely to be affected by factors that their kinetic model cannot take into account, such as compatibility of gamete recognition molecules. As a more general alternative, loaded with fewer assumptions, we recommend the use of the linear regression approach adopted in our paper.

When using a single metric to compare fertilization curves, one must consider whether the chosen metric is biologically meaningful. For example, an F_{50} estimate obtained solely through extrapolation (in crosses in which 50% fertilization was never achieved) would be of questionable significance, and an alternative (say an F_{10} or F_{20} value) would be preferable. We chose to use F_{50} for the following reasons. First, it worked well for a majority of our

Table 2

Comparison of F_{50} *values estimated from the nonlinear model of Vogel* et al. *(1982) for the nine possible crosses of* Echinometra *species*

Female	Male	n	$\bar{F}_{50}$	F_{50} ratio	L_1	L_2
E. lucunter	*E. lucunter*	40	118	—	78	181
E. lucunter	*E. viridis*	22	7030	59.5	4165	11,867
E. lucunter	*E. vanbrunti*	40	86,696	735	54,465	138,000
E. viridis	*E. lucunter*	18	153	1.45	90	261
E. viridis	*E. viridis*	23	105	—	71	156
E. viridis	*E. vanbrunti*	5	1288	12.3	458	3621
E. vanbrunti	*E. lucunter*	15	160	2.28	102	253
E. vanbrunti	*E. viridis*	2	55	0.78	NA	NA
E. vanbrunti	*E. vanbrunti*	16	70	—	41	121

n = number of crosses; $\bar{F}_{50}$ = mean F_{50}; F_{50} ratio = F_{50} (heterospecific cross)/F_{50} (homospecific cross); L_1 and L_2 = 95% confidence limits for $\bar{F}_{50}$; means and confidence limits are back-transformed from their logs.

crosses. In our data set, most (156 of 181 or 85%) of the crosses produced a maximum of ≥50% fertilization of eggs, so extrapolation beyond the tested concentrations was not necessary. For the remaining 25 crosses in which maximum fertilization was less than 50% (maximum fertilization averaged 35% for these crosses), extrapolation of the curve was necessary to obtain an F_{50}. There was a difference in the fit of data to the regressions in these two groups of crosses. The r^2 value from linear regression was 0.917 for crosses in which ≥50% was achieved, and r^2 equaled 0.847 for crosses from which F_{50} had to be extrapolated. Hence while there is a suggestion of a trend towards lower accuracy with these most incompatible crosses, extrapolation itself would not have created excessive additional error.

Our second reason for using F_{50} is that calculating F_{10} or F_{20} values from the fertilization curves would have introduced even greater inaccuracy. In the more compatible crosses, 10% or 20% fertilization was reached with extremely dilute sperm whose concentration is more difficult to estimate accurately and is less reproducible. Also, F_{10} and F_{20} values lie farther away from the bivariate mean of regression, which introduces additional error. Confidence intervals around F_{10} or F_{20} estimates (not shown) were wider than were those surrounding F_{50} for the great majority of our crosses.

The evolution of gamete incompatibility in sea urchins

The results from the present study indicate that incompatibility of sea urchin eggs does not steadily evolve at equal rates as species diverge. Based on mtDNA sequence comparisons, *E. lucunter* and *E. viridis* are sister species that separated about 1.5 MYA. This occurred after closure of the Isthmus of Panamá, which split *E. vanbrunti* from the *E. lucunter/E. viridis* ancestor some 3.1 MYA (McCartney *et al.*, 2000). A scenario in which gametic incompatibility closely tracked time and genetic divergence would predict the following. First, we would expect eggs of *E. viridis* to show incompatibility with sperm of *E. lucunter* equal to that in the reciprocal cross. Second, eggs of *E. vanbrunti* would show the greatest block towards sperm of the other two species. Instead, the primary fertilization barrier in the eggs appears to have evolved in a single lineage leading to *E. lucunter* (see also Lessios and Cunningham (1990) and Lessios (1998)), during the last 1.5 million years (McCartney *et al.*, 2000).

The barrier that eggs evolve to fertilization by heterospecific sperm does not appear to develop continuously as species diverge. Yet once such a barrier emerges, it does appear to strengthen with time. With *E. lucunter* eggs, *E. viridis* sperm is more compatible than is *E. vanbrunti* sperm, just as would be predicted from divergence estimates based on mtDNA. In contrast, if incompatibility were the product of reinforcement (Dobzhansky, 1937; Butlin, 1989; Liou and Price, 1994), it would be expected that selection against hybrids would lead to greater incompatibilities in the sympatric species pair than in the allopatric pair. *E. viridis* eggs are fertilized to a greater extent by *E. lucunter* than by *E. vanbrunti* sperm, again the ranking predicted by genetic distances, but not by the reinforcement model. Compatibility in other sea urchin species is due to the interaction of gamete recognition molecules on both eggs and sperm (*e.g.*, Minor *et al.*, 1991; Metz and Palumbi, 1996). Our data suggest that, in the American *Echinometra*, differences in sperm-egg recognition molecules do accumulate over time as species diverge.

Asymmetric gamete incompatibility like that observed here has often been found between species pairs of sea urchins and other free-spawning marine invertebrates. As Lessios and Cunningham (1990) and Palumbi (1994) point out, such cases are reminiscent of asymmetric behavioral isolation observed between closely related, allopatric *Drosophila* species (Kaneshiro, 1976, 1983). Why such a similar pattern should be shared between such different mechanisms for reproductive isolation is worthy of consideration. Borrowing from a hypothesis originally suggested by Muller (1942), Kaneshiro (1980) suggests that behavioral isolation evolves as a byproduct of disruptive or directional selection in allopatry, and its asymmetry is due to drift and founder effects in one but not both of the descendent populations. In an analogous fashion, asymmetric barriers to fertilization could emerge as an accident of history, such as a bottleneck in one of the two sister species, then become exaggerated as selection within the bottlenecked population promoted coevolutionary changes of sperm and eggs.

Asymmetric gametic compatibility between sympatric species, such as the one observed between *E. lucunter* and *E. viridis*, has been found several times. Putative morphospecies of *Echinometra mathei* that coexist in Okinawa show highly asymmetric gamete incompatibility (Aslan and Uehara, 1997). A high percentage of eggs of *Strongylocentrotus droebachiensis* are fertilized by sperm of its sympatric (but bathymetrically displaced) congener *S. pallidus*, but the reciprocal cross of *S. pallidus* eggs and *S. droebachiensis* sperm produces very low percent fertilization (Strathmann, 1981). Oyster species in the genus *Crassostrea* that co-occur in Japan show an asymmetric block to fertilization (Banks *et al.*, 1994). Percent fertilization of eggs from white abalones (*Haliotis sorenseni*) by sperm of another California species, *H. rufescens*, is close to 100%, but is much lower in the reciprocal cross (Leighton and Lewis, 1982). In one case, asymmetric incompatibility exists between sympatric species that are distantly related. Close to 100% of the eggs of the Hawaiian sea urchin *Colobocentrotus atratus* can be fertilized by sperm of the sea urchins *Echinometra mathei*, *Pseudoboletia indiana*, and *Tripneustes gratilla* (the latter two of which are in a different family). In contrast, the same concentration of *C. atratus* sperm fertilizes a much smaller percentage of eggs in the reciprocal crosses (Branham, 1972).

As in other cases where species are sympatric, it is tempting to propose an adaptive hypothesis to explain why *E. lucunter* should have "choosier" eggs than *E. viridis*. Lessios and Cunningham (1990) examined the hypothesis of natural selection against hybridization that differs in intensity between the two species. *E. lucunter* inhabits a narrow band from the water surface down to a depth of about 1 m. *E. viridis* individuals are often found within this zone as well, but they are more abundant in deeper coral reef, where *E. lucunter* is absent (McPherson, 1969; Lessios *et al.*, 1984). Spawning seasons for the two species overlap (Lessios, 1981b, 1985), and neither species shows a lunar cycle (Lessios, 1991). Since sperm from one male can fertilize the eggs of many females, the infiltration of *E. viridis* into the *E. lucunter* zone may create a hazard to a large fraction of spawning *E. lucunter* females, and if hybrids are less viable, may strongly select for discrimination by its eggs. The zone of overlap, however, represents a small fraction of the *E. viridis* population, which would therefore be under much weaker selection to avoid hybridization. Under this hypothesis, discrimination against *E. vanbrunti* sperm would be a byproduct of discrimination against *E. viridis* sperm. However, as Lessios and Cunningham indicate, this "reinforcement" model predicting higher discrimination by *E. lucunter* eggs would also predict that *E. lucunter* eggs should protect themselves more effectively against sperm of the sympatric *E. viridis* than against sperm of the allopatric *E. vanbrunti*. This is not the case.

We found that different females of *E. lucunter* show great variation in their discrimination against heterospecific sperm. Recognition of heterospecifics that varies within species implies variation at compatibility loci in females. Such variation plays a crucial role in some models for the evolution of prezygotic isolation between species (Nei *et al.*, 1983; Wu, 1985). These models invoke relaxed selection on females for compatibility with conspecific male variants and suggest that drift and mutational input may determine the fate of female compatibility alleles (Wu, 1985). An important prerequisite for these models is that female alleles are neutral with respect to their effect on female reproductive success. Our data are consistent with this, given that large differences in cross-species compatibility are not associated with fertility differences within species.

An incomplete barrier to fertilization of the strength described here could only partially account for the apparent lack of hybridization between sympatric *E. lucunter* and *E. viridis* in nature, shown by fixed differences in two isozymic loci (Lessios, 1979). It may be that habitat preferences work in concert with gametic incompatibility to severely lower the production of hybrid embryos; but a postzygotic isolation mechanism not yet discovered is necessary to account for the complete lack of introgression between the sympatric species (Lessios and Cunningham, 1990).

Conclusion

Other studies have shown that fertilization barriers between free-spawning marine invertebrates can evolve rapidly (Palumbi and Metz, 1991; Metz *et al.*, 1998b; Hellberg and Vacquier, 1999). Indeed, the gametic incompatibility between *E. lucunter* and *E. viridis* must have appeared within the last 1.5 million years (McCartney *et al.*, 2000). However, the emergence of incompatibility must still represent an unlikely evolutionary event. In large part, the proteins mediating fertilization are subject to strong stabilizing selection, and many of them are greatly conserved (Vacquier, 1998). Hence, it is not surprising that gamete incompatibility in the neotropical *Echinometra* has not evolved in a continuous fashion, resulting in a complete barrier to genetic exchange. Rather the process has been lineage-specific and has produced asymmetric reproductive isolation. It may be that historical accidents such as population bottlenecks play an important role in the initial emergence of gamete incompatibility and explain why it does not always evolve. One likely scenario in the present case would be that accidental changes in gamete recognition molecules on eggs initiate the process. These changes could then drive compensatory sexual selection on cognate molecules in sperm and fuel their divergence. This scenario would predict greater divergence of proteins mediating sperm-egg recognition and binding in *E. lucunter* compared to its neotropical congeners.

Acknowledgments

We are grateful to Gwen Keller for assistance in performing many of the fertilization experiments, to Vic Vacquier for his technical advice, to Don Levitan for suggestions and assistance in fitting the fertilization kinetics models, and to two anonymous reviewers for many helpful comments. Financial support was provided by an NSF/Sloan Foundation Postdoctoral Fellowship in Molecular Evolution to MAM and by a grant to HAL and MAM from the Smithsonian Scholarly Studies Program.

Literature Cited

Aslan, L. M., and T. Uehara. 1997. Hybridization and F1 backcrosses between two closely related tropical species of sea urchins (genus *Echinometra*) in Okinawa. *Invertebr. Reprod. Dev.* **31:** 319–324.

Babcock, R. C., G. D. Bull, P. L. Harrison, A. J. Heyward, J. K. Oliver, C. C. Wallace, and B. L. Willis. 1986. Synchronous spawnings of 105 scleractinian coral species on the Great Barrier Reef. *Mar. Biol.* **90:** 379–394.

Banks, M. A., D. J. McGoldrick, W. Borgeson, and D. Hedgecock. 1994. Gametic incompatibility and genetic divergence of Pacific and Kumamoto oysters, *Crassostrea gigas* and *C. sikamea*. *Mar. Biol.* **121:** 127–135.

Branham, J. M. 1972. Comparative fertility of gametes from six species of sea urchins. *Biol. Bull.* **142:** 385–396.

Buss, L. W., and P. O. Yund. 1989. A sibling species group of *Hydractinia* in the northeastern United States. *J. Mar. Biol. Assoc. UK* **69:** 857–874.

Butlin, R. 1989. Reinforcement of pre-mating isolation. Pp. 158–179 in *Speciation and its Consequences*. D. Otte and J. A. Endler, eds. Sinauer, Sunderland, MA.

Byrne, M., and M. J. Anderson. 1994. Hybridization of sympatric *Patiriella* species in New South Wales. *Evolution* **48:** 564–576.

Coates, A. G., and J. A. Obando. 1996. The geologic evolution of the Central American Isthmus. Pp. 21–56 in *Evolution and Environment in Tropical America*, J. B. C. Jackson, A. G. Coates, and A. Budd, eds. University of Chicago Press, Chicago.

Dobzhansky, T. 1937. *Genetics and the Origin of Species*, Columbia University Press, New York.

Dobzhansky, T. 1940. Speciation as a stage in evolutionary divergence. *Am. Nat.* **74:** 312–321.

Finney, D. J. 1964. *Statistical Method in Biological Assay*, Griffin, London.

Games, P. A., and J. F. Howell. 1976. Pairwise multiple comparison procedures with unequal *n*'s and/or variances: a Monte Carlo study. *J. Educ. Stat.* **1:** 113–125.

Hellberg, M. E., and V. D. Vacquier. 1999. Rapid evolution of fertilization selectivity and lysin cDNA sequences in teguline gastropods. *Mol. Biol. Evol.* **16:** 839–848.

Hewlett, P. S., and R. L. Plackett. 1979. *The Interpretation of Quantal Responses in Biology*. University Park Press, Baltimore.

Kaneshiro, K. 1976. Ethological isolation and phylogeny in the planitibia subgroup of Hawaiian *Drosophila*. *Evolution* **30:** 740–745.

Kaneshiro, K. 1980. Sexual isolation, speciation, and the the direction of evolution. *Evolution* **34:** 437–444.

Kaneshiro, K. Y. 1983. Sexual selection and direction of evolution in the biosystematics of Hawaiian Drosophilidae. *Annu. Rev. Entomol.* **28:** 161–178.

Knowlton, N., J. Maté, H. Guzmán, and R. Rowan. 1997. Direct evidence for reproductive isolation among the three species of the *Montastraea annularis* complex in Central America (Panamá and Honduras). *Mar. Biol.* **127:** 705–711.

Leighton, D. L., and C. A. Lewis. 1982. Experimental hybridization in abalone. *Int. J. Invertebr. Reprod. Dev.* **5:** 273–282.

Lessios, H. A. 1979. Use of Panamanian sea urchins to test the molecular clock. *Nature* **280:** 599–601.

Lessios, H. A. 1981a. Divergence in allopatry: molecular and morphological differentiation between sea urchins separated by the Isthmus of Panama. *Evolution* 35: 618–634.

Lessios, H. A. 1981b. Reproductive periodicity of the echinoids *Diadema* and *Echinometra* on the two coasts of Panama. *J. Exp. Mar. Biol. Ecol.* **50:** 47–61.

Lessios, H. A. 1985. Annual reproductive periodicity in eight echinoid species on the Caribbean coast of Panama *in Echinodermata: Proceedings of the Fifth International Echinoderm Conference*, Galway. B. F. Keegan and B. D. O'Connor, eds. A. A. Balkema, Rotterdam.

Lessios, H. A. 1990. Adaptation and phylogeny as determinants of egg size in echinoderms from the two sides of the Isthmus of Panama. *Am. Nat.* **135:** 1–13.

Lessios, H. A. 1991. Presence and absence of monthly reproductive rhythms among eight Caribbean echinoids off the coast of Panama. *J. Exp. Mar. Biol. Ecol.* **153:** 27–47.

Lessios, H. A. 1998. The first stage of speciation as seen in organisms separated by the Isthmus of Panama. Pp. 186–201 in *Endless Forms: Species and Speciation*. D. Howard and S. Berlocher, eds. Oxford University Press, Oxford.

Lessios, H. A., and C. W. Cunningham. 1990. Gametic incompatibility between species of the sea urchin *Echinometra* on the two sides of the Isthmus of Panama. *Evolution* **44:** 933–941.

Lessios, H. A., and C. W. Cunningham. 1993. The evolution of gametic incompatibility in neotropical *Echinometra*: a reply to McClary. *Evolution* **47:** 1883–1885.

Lessios, H. A., J. D. Cubit, D. R. Robertson, M. J. Shulman, M. R. Parker, S. D. Garrity, and S. C. Levings. 1984. Mass mortality of *Diadema antillarum* on the Caribbean coast of Panama. *Coral Reefs* **3:** 173–182.

Levitan, D. R. 1996. Effects of gamete traits on fertilization in the sea and the evolution of sexual dimorphism. *Nature* **382:** 153–155.

Levitan, D. R. 1998. Does Bateman's principle apply to broadcast-spawning organisms? Egg traits influence *in situ* fertilization rates among congeneric sea urchins. *Evolution* **53:** 1043–1056.

Liou, L. W., and T. D. Price. 1994. Speciation by reinforcement of premating isolation. *Evolution* **48:** 1451–1459.

Marsden, J. 1992. Reproductive isolation in two forms of the serpulid polychaete, *Spirobranchus polycerus* (Schmarda) in Barbados. *Bull. Mar. Sci.* **51:** 14–18.

McCartney, M. A., G. Keller, and H. A. Lessios. 2000. Dispersal barriers in tropical oceans and speciation of Atlantic and eastern Pacific *Echinometra* sea urchins. *Mol. Ecol.* **9:** 1391–1400.

McClary, D. 1992. Gamete compatibility or incompatibility? A comment on Lessios and Cunningham (1990). *Evolution* **46:** 1579–1580.

McCuen, F. S. 1988. Spawning behaviors of northeast Pacific sea cucumbers (Holothuroidea: Echinodermata). *Mar. Biol.* **98:** 565–585.

McPherson, B. F. 1969. Studies on the biology of the tropical sea urchins *Echinometra lucunter* and *E. viridis*. *Bull. Mar. Sci.* **19:** 194–213.

Metz, E. C., and S. R. Palumbi. 1996. Positive selection and sequence rearrangements generate extensive polymorphism in the gamete recognition protein bindin. *Mol. Biol Evol.* **13:** 397–406.

Metz, E. C., R. E. Kane, H. Yanagimachi, and S. R. Palumbi. 1994. Fertilization between closely related sea urchins is blocked by incompatibilities during sperm-egg attachment and early stages of fusion. *Biol. Bull.* **187:** 23–34.

Metz, E. C., G. Gomez-Gutierrez, and V. D. Vacquier. 1998a. Mitochondrial DNA and bindin gene sequence evolution among allopatric species of the sea urchin genus *Arbacia*. *Mol. Biol. Evol.* **15:** 185–195.

Metz, E. C., R. Robles-Sikisaka, and V. D. Vacquier. 1998b. Nonsynonymous substitution in abalone sperm fertilization gene exceeds substitution in introns and mitochondrial DNA. *Proc. Natl. Acad. Sci. USA* **95:** 10676–10681.

Miller, K., and R. Babcock. 1997. Conflicting morphological and reproductive species boundaries in the coral genus *Platygyra*. *Biol. Bull.* **192:** 98–110.

Minor, J. E., D. R. Fromson, R. J. Britten, and E. H. Davidson. 1991. Comparison of the bindin proteins of *Strongylocentrotus franciscanus*, *S. purpuratus*, and *Lytechinus variegatus:* sequences involved in the species specificity of fertilization. *Mol. Biol. Evol.* **8:** 781–795.

Mortensen, T. 1928–1951. *A Monograph of the Echinoidea*. C. A. Reitzel, Copenhagen.

Muller, H. J. 1942. Isolating mechanisms, evolution and temperature. *Biological Symposia* **6:** 71–125.

Nei, M., T. Maruyama, and C.-I. Wu. 1983. Models of evolution of reproductive isolation. *Genetics* **103:** 557–579.

Palumbi, S. R. 1992. Marine speciation on a small planet. *Trends Ecol. Evol.* **7:** 114–118.

Palumbi, S. R. 1994. Genetic divergence, reproductive isolation, and marine speciation. *Annu. Rev. Ecol. Syst.* **25:** 547–572.

Palumbi, S. R., and E. C. Metz. 1991. Strong reproductive isolation between closely related tropical sea urchins (genus *Echinometra*). *Mol. Biol. Evol.* **8:** 227–239.

Pawlik, J. 1988. Larval settlement and metamorphosis of sabellariid polychaetes, with special reference to *Phragmatopoma lapidosa*, a reef-building species, and *Sabellaria floridensis*, a non-gregarious species. *Bull. Mar. Sci.* **43:** 41–60.

Pearse, J. S., D. J. McClary, M. A. Sewell, W. C. Austin, A. Perez-Ruzafa, and M. Byrne. 1988. Simultaneous spawning of six species of echinoderms in Barkley Sound, British Columbia. *Invertebr. Reprod. Dev.* **14:** 279–288.

Pernet, B. 1999. Gamete interactions and genetic differentiation among three sympatric polychaetes. *Evolution* **53:** 435–446.

SAS Institute. 1989. *JMP, Version 2.0.* Cary, NC.

SAS Institute. 1999. *StatView, Version 5.0.1.* Cary, NC.

Strathmann, R. R. 1981. On barriers to hybridization between *Strongylocentrotus droebachiensis* (O. F. Muller) and *S. pallidus* (G. O. Sars). *J. Exp. Mar. Biol. Ecol.* **55:** 39–47.

Summers, R. G., and B. L. Hylander. 1975. Species-specificity of acrosome reaction and primary gamete binding in echinoids. *Exp. Cell Res.* **96:** 63–68.

Szmant, A., E. Weil, M. Miller, and D. Colón. 1997. Hybridization within the species complex of the scleractinian coral *Montastrea annularis*. *Mar. Biol.* **129:** 561–572.

Tyler, A., A. Monroy, and C. B. Metz. 1956. Fertilization of fertilized sea urchin eggs. *Biol. Bull.* **110:** 184–195.

Vacquier, V. D. 1998. Evolution of gamete recognition proteins. *Science* **281:** 1995–1998.

Vacquier, V. D., and J. E. Payne. 1973. Methods for quantitating sea urchin sperm-egg binding. *Exp. Cell Res.* **82:** 227–235.

Vacquier, V. D., W. J. Swanson, and M. E. Hellberg. 1995. What have we learned about sea urchin sperm bindin? *Dev. Growth Differ.* **37:** 1–10.

Vogel, H., G. Czihak, P. Chang, and W. Wolf. 1982. Fertilization kinetics of sea urchin eggs. *Math. Biosci.* **58:** 189–216.

Welch, B. L. 1951. On the comparison of several mean values: an alternative approach. *Biometrika* **38:**330–336.

Wu, C.-I. 1985. A stochastic simulation study on speciation by sexual selection. *Evolution* **39:** 66–82.

Appendix

Summary of fertilization data. n = number of sperm dilutions tested; R^2 = coefficient of determination; F(reg) = F ratio testing significance of regression coefficient: $***P < 0.001$, $**P < 0.01$, $*P < 0.05$, ns = not significant.

					Linear regression			Nonlinear regression F_{50}
#	Date	Female	Male	n	R^2	F (reg)	F_{50} (linear)	(nonlinear)
1	8/13/96	EL1	EL1	10	0.957	178.1***	74	86
2	8/13/96	EL1	EL2	9	0.867	45.93***	16	32
3	8/13/96	EL1	EV1	12	0.922	118.2***	520	905
4	8/13/96	EL1	EV2	12	0.891	82.38***	675	1270
5	8/13/96	EL1	EV3	12	0.917	110.1***	967	1183
6	8/13/96	EL1	EV4	8	0.844	32.53***	2875	2461
7	8/13/96	EL2	EL1	10	0.870	53.80***	67	62
8	8/13/96	EL2	EL2	10	0.755	24.67***	19	40
9	8/13/96	EL2	EV1	12	0.890	80.49***	155	312
10	8/13/96	EL2	EV2	12	0.869	66.37***	159	237
11	8/13/96	EL2	EV3	12	0.705	24.01***	52	140
12	8/13/96	EL2	EV4	12	0.815	44.18***	320	305
13	8/13/96	EV1	EL1	10	0.975	310.5***	78	120
14	8/13/96	EV1	EL2	10	0.889	64.71***	114	151
15	8/13/96	EV1	EV1	9	0.823	32.59***	148	168
16	8/13/96	EV1	EV2	10	0.951	157.0***	105	133
17	8/13/96	EV1	EV3	10	0.875	55.91***	53	94
18	8/13/96	EV1	EV4	9	0.943	117.7***	30	48
19	8/20/96	EL3	EL3	11	0.972	317.8***	79	107
20	8/20/96	EL3	EL4	12	0.943	164.4***	64	119
21	8/20/96	EL3	EV5	5	0.983	177.6***	14764	17750
22	8/20/96	EL3	EV6	5	0.853	17.47*	8438	7968
23	8/20/96	EL3	EV7	12	0.883	75.26***	1901	3659
24	8/20/96	EL3	EV8	10	0.960	194.0***	7721	9646
25	8/20/96	EL4	EL3	11	0.891	73.68***	90	204
26	8/20/96	EL4	EV5	7	0.905	47.87***	19571	19336
27	8/20/96	EL4	EV6	12	0.897	87.47***	11395	11855
28	8/20/96	EL4	EV7	9	0.947	126.4***	8454	10138
29	8/20/96	EV2	EL3	7	0.734	13.80*	97	116
30	8/20/96	EV2	EL4	11	0.970	291.6***	181	313

Appendix (*Continued*)

					Linear regression			Nonlinear regression
#	Date	Female	Male	n	R^2	F (reg)	F_{50} (linear)	F_{50} (nonlinear)
31	8/20/96	EV2	EV5	12	0.935	146.1***	49	75
32	8/20/96	EV2	EV6	11	0.875	63.13***	142	219
33	8/20/96	EV2	EV7	8	0.983	360.4***	127	174
34	8/20/96	EV2	EV8	12	0.973	365.2***	56	79
35	8/29/96	EL5	EL5	7	0.817	22.32**	533	664
36	8/29/96	EL5	EV9	12	0.909	100.3***	2231	2323
37	8/29/96	EL5	EVB1	12	0.880	73.47***	5294	7181
38	8/29/96	EL6	EL5	8	0.953	124.1***	137	143
39	8/29/96	EL6	EV9	12	0.884	76.58***	283550	100147
40	8/29/96	EL6	EVB1	10	0.898	71.14***	7530070	324044
41	8/29/96	EL7	EL5	9	0.922	83.02***	184	159
42	8/29/96	EL7	EV9	12	0.927	127.2***	1108	1301
43	8/29/96	EL7	EVB1	12	0.957	223.7***	8437	11619
44	8/29/96	EL8	EL5	8	0.885	46.33***	645	1030
45	8/29/96	EL8	EV9	11	0.933	127.1***	174077	82327
46	8/29/96	EL8	EVB1	6	0.613	6.358ns	315066738	513944
47	8/29/96	EL9	EL5	10	0.908	79.11***	206	443
48	8/29/96	EL9	EV9	8	0.956	132.7***	33471	40535
49	8/29/96	EL9	EVB1	5	0.901	27.35*	105567	112169
50	8/29/96	EV3	EL5	11	0.886	70.04***	217	200
51	8/29/96	EV3	EV9	10	0.989	728.5***	64	107
52	8/29/96	EV3	EVB1	8	0.931	80.96***	1409	1876
53	8/29/96	EVB1	EL5	12	0.918	112.0***	67	76
54	8/29/96	EVB1	EV9	12	0.909	100.4***	13	8
55	8/29/96	EVB1	EVB1	10	0.902	73.85***	53	43
56	9/3/96	EL10	EL6	9	0.971	235.5***	310	442
57	9/3/96	EL10	EV10	10	0.709	19.56**	77923	51024
58	9/3/96	EL10	EVB2	10	0.914	85.12***	163104	73180
59	9/3/96	EL11	EL6	10	0.970	259.4***	387	430
60	9/3/96	EL11	EV10	10	0.978	369.9***	3581	5822
61	9/3/96	EL11	EVB2	9	0.941	113.1***	14156	22449
62	9/3/96	EV4	EL6	9	0.919	80.2***	491	1090
63	9/3/96	EV4	EV10	10	0.974	307.5***	142	222
64	9/3/96	EV4	EVB2	7	0.967	147.4***	1424	2307
65	9/3/96	EVB2	EL6	6	0.897	35.18**	373	278
66	9/3/96	EVB2	EV10	6	0.798	15.82*	505	378
67	9/3/96	EVB2	EVB2	6	0.974	155.8***	536	376
68	9/10/96	EL12	EL7	1	0.977	396.0***	218	297
69	9/10/96	EL12	EV11	11	0.982	510.7***	8503	12683
70	9/10/96	EL12	EVB3	10	0.886	62.19***	77716	65298
71	9/10/96	EL13	EL7	12	0.957	228.0***	154	233
72	9/10/96	EL13	EV11	8	0.914	64.09***	43940	49352
73	9/10/96	EL13	EVB3	5	0.816	13.33*	373349	212238
74	9/10/96	EL14	EL7	12	0.964	275.2***	217	231
75	9/10/96	EL14	EV11	12	0.905	95.31***	2442	2806
76	9/10/96	EL14	EVB3	10	0.864	50.98***	10857	16817
77	9/10/96	EL15	EL7	9	0.934	99.15***	291	323
78	9/10/96	EL15	EV11	10	0.963	209.1***	24955	24195
79	9/10/96	EL15	EVB3	7	0.960	120.3***	76890	64534
80	9/10/96	EL16	EL7	8	0.975	234.8***	334	547
81	9/10/96	EL16	EV11	5	0.973	108.9**	14813	19479
82	9/10/96	EL16	EVB3	3	0.998	579.2***	54651	88914
83	9/10/96	EL17	EL7	11	0.863	57.06***	196	115
84	9/10/96	EL17	EV11	12	0.917	110.8***	3612	3512
85	9/10/96	EL17	EVB3	10	0.938	122.7***	22039	29284
86	9/10/96	EV5	EL7	10	0.898	70.59***	305	42
87	9/10/96	EV5	EV11	10	0.953	165.59***	22	1227
88	9/10/96	EV5	EVB3	10	0.871	54.05***	692	382

Appendix *(Continued)*

					Linear regression			Nonlinear regression
#	Date	Female	Male	*n*	R^2	*F* (reg)	F_{50} (linear)	F_{50} (nonlinear)
89	9/10/96	EVB3	EL7	10	0.897	70.03***	1057	742
90	9/10/96	EVB3	EVB3	9	0.973	258.2***	608	504
91	9/19/96	EL18	EVB3	5	0.859	18.33*	159890	229668
92	9/19/96	EV6	EVB3	6	0.924	49.07**	2091	3764
93	9/19/96	EV7	EVB3	8	0.960	144.3***	671	857
94	9/19/96	EVB4	EVB3	11	0.960	220.7***	273	178
95	10/3/96	EL19	EL8	12	0.801	40.29***	146	191
96	10/3/96	EL19	EL9	5	0.953	61.45**	452	1568
97	10/3/96	EL19	EL10	5	0.973	108.1**	133	77
98	10/3/96	EL19	EL11	5	0.845	16.42*	720	3361
99	10/3/96	EL19	EVB4	7	0.925	62.00***	346555	223114
100	10/3/96	EL19	EVB5	5	0.661	5.874ns	14271563	204606
101	10/3/96	EL19	EVB6	6	0.650	7.438*	427516	270235
102	10/3/96	EL19	EVB7	7	0.889	40.27**	128093	106011
103	10/3/96	EL20	EL8	5	0.805	12.43*	102	122
104	10/3/96	EL20	EL9	5	0.830	14.69*	118	57
105	10/3/96	EL20	EL10	5	0.944	51.41**	473	916
106	10/3/96	EL20	EL11	5	0.916	32.94**	68	51
107	10/3/96	EL20	EVB4	6	0.958	92.14***	76713	103441
108	10/3/96	EL20	EVB5	7	0.885	38.50**	147808	112384
109	10/3/96	EL20	EVB6	5	0.888	24.00*	184934	145387
110	10/3/96	EL20	EVB7	8	0.932	83.13***	62560	84298
111	10/3/96	EVB5	EL8	8	0.921	69.86***	82	53
112	10/3/96	EVB5	EL9	9	0.961	176.23***	170	101
113	10/3/96	EVB5	EL10	8	0.916	65.96***	38	41
114	10/3/96	EVB5	EL11	8	0.936	89.13***	100	89
115	10/3/96	EVB5	EVB4	5	0.930	39.99**	37	30
116	10/3/96	EVB5	EVB5	6	0.972	140.79***	43	32
117	10/3/96	EVB5	EVB6	8	0.944	102.8***	41	30
118	10/3/96	EVB5	EVB7	8	0.952	121.1***	28	22
119	10/3/96	EVB6	EL8	8	0.927	77.11***	169	93
120	10/3/96	EVB6	EL9	10	0.977	345.1***	290	228
121	10/3/96	EVB6	EL10	9	0.931	94.96***	110	83
122	10/3/96	EVB6	EL11	10	0.966	229.6***	157	93
123	10/3/96	EVB6	EVB4	7	0.979	236.8***	39	31
124	10/3/96	EVB6	EVB5	7	0.850	28.46**	91	62
125	10/3/96	EVB6	EVB6	6	0.904	37.67**	73	64
126	10/3/96	EVB6	EVB7	6	0.978	179.3***	114	89
127	10/3/96	EVB7	EL8	8	0.954	126.8***	447	314
128	10/3/96	EVB7	EL9	10	0.908	79.69***	627	406
129	10/3/96	EVB7	EL10	9	0.962	178.0***	446	351
130	10/3/96	EVB7	EL11	9	0.969	220.4***	695	532
131	10/3/96	EVB7	EVB4	5	0.919	34.14**	49	46
132	10/3/96	EVB7	EVB5	6	0.943	66.61**	88	75
133	10/3/96	EVB7	EVB6	7	0.948	92.22***	100	72
134	10/3/96	EVB7	EVB7	7	0.892	41.37**	47	31
135	6/28/97	EL21	EL12	6	0.693	9.039*	70	60
136	6/28/97	EL21	EL13	4	0.944	34.25*	9	17
137	6/28/97	EL21	EL14	5	0.971	103.7**	51	55
138	6/28/97	EL21	EL15	5	0.914	32.26**	7	14
139	6/28/97	EL21	EV12	6	0.917	44.29**	4853	5885
140	6/28/97	EL21	EV13	7	0.874	34.85**	4187	5509
141	6/28/97	EL21	EV14	4	0.962	51.67*	25784	26663
142	6/28/97	EL21	EV15	8	0.971	205.4***	11555	16463
143	6/28/97	EL22	EL12	7	0.915	54.31***	40	33
144	6/28/97	EL22	EL13	5	0.933	41.79**	13	15
145	6/28/97	EL22	EL14	5	0.864	19.19*	39	22
146	6/28/97	EL22	EL15	3	0.999	1573*	74	82

Appendix (*Continued*)

					Linear regression			Nonlinear regression
#	Date	Female	Male	n	R^2	F (reg)	F_{50} (linear)	F_{50} (nonlinear)
147	6/28/97	EL22	EV12	6	0.821	18.35*	13791	19123
148	6/28/97	EL22	EV13	5	0.823	14.03*	3340	3902
149	6/28/97	EL22	EV14	4	0.533	2.285ns	31424	47940
150	6/28/97	EL22	EV15	6	0.884	30.51**	32570	41095
151	6/28/97	EL23	EL12	7	0.969	157.6***	16	26
152	6/28/97	EL23	EL13	5	0.958	69.71**	10	10
153	6/28/97	EL23	EL14	5	0.880	22.03*	55	41
154	6/28/97	EL23	EL15	5	0.980	152.4***	57	67
155	6/28/97	EL23	EV12	8	0.948	109.5***	7275	8390
156	6/28/97	EL23	EV13	6	0.965	112.6***	2165	2272
157	6/28/97	EL23	EV14	6	0.903	37.61**	71798	41261
158	6/28/97	EL23	EV15	7	0.886	38.93**	38868	43075
159	6/28/97	EV8	EL13	4	0.822	9.261ns	141	144
160	6/28/97	EV8	EL14	4	0.965	56.31*	52	93
161	6/28/97	EV8	EL15	4	0.939	31.25*	154	97
162	6/28/97	EV8	EV12	7	0.989	488.4***	18	37
163	6/28/97	EV8	EV13	5	0.966	85.97**	36	76
164	6/28/97	EV8	EV14	4	0.989	193.6**	44	76
165	6/28/97	EV8	EV15	5	0.943	49.76**	266	395
166	6/28/97	EV9	EL12	5	0.972	107.2**	111	159
167	6/28/97	EV9	EL13	5	0.756	9.32*	170	119
168	6/28/97	EV9	EL14	4	0.985	132.9**	37	56
169	6/28/97	EV9	EL15	3	0.940	15.81ns	269	138
170	6/28/97	EV9	EV12	7	0.939	77.75***	2	5
171	6/28/97	EV9	EV13	5	0.900	27.03*	14	40
172	6/28/97	EV9	EV14	5	0.714	7.52ns	143	244
173	6/28/97	EV9	EV15	4	0.968	61.43*	229	213
174	6/28/97	EV10	EL12	5	0.977	129.3**	113	162
175	6/28/97	EV10	EL13	5	0.866	19.39*	27	23
176	6/28/97	EV10	EL14	4	0.701	4.71ns	41	21
177	6/28/97	EV10	EL15	3	0.907	9.840ns	1906	2705
178	6/28/97	EV10	EV12	7	0.895	42.83**	44	169
179	6/28/97	EV10	EV13	6	0.929	52.69**	48	111
180	6/28/97	EV10	EV14	3	0.973	36.14ns	150	334
181	6/28/97	EV10	EV15	4	0.902	18.49*	384	275

Reference: *Biol. Bull.* **202:** 182–191. (April 2002)

The Anatomy, Life Habits, and Later Development of a New Species of Enteropneust, *Harrimania planktophilus* (Hemichordata: Harrimaniidae) From Barkley Sound

CHRISTOPHER B. CAMERON

Department of Biological Sciences, CW 405 Biological Sciences Building, University of Alberta, Edmonton, Alberta T6G 2E9, Canada

Abstract. A new species of enteropneust, *Harrimania planktophilus*, lives intertidally and subtidally in mixed sediments in Barkley Sound, British Columbia, Canada. *H. planktophilus* has a long proboscis skeleton extending into the pharyngeal region. The collar (mesosome) has complete dorsal and ventral mesenteries. The trunk (metasome) has four distinct regions that can be recognized externally: the branchial region, esophageal region, hepatic region, and an undifferentiated intestinal region leading to the anus. The dorsal pharynx is large and has long gill slits without synapticles. Posterior to the gills is a constriction followed by a short esophageal region and a long gonadal region. The paired dorsolateral gonads extend almost to the end of the trunk. Eggs in the ovaries appear amber yellow, and the testes appear slightly paler. The trunk terminates at an anus with a well-developed sphincter muscle. *H. planktophilus* forms long sinuous burrows that are semipermanent and shared. Females deposit a tubular egg mass in a burrow in which the embryos develop directly into juveniles. Gastrulation appears to be by invagination, followed by a ciliated stage that has a telotrochal swimming band, suggesting that the ancestor to *H. planktophilus* developed *via* a tornaria larva. The juveniles emerge from the egg membrane with a ventral post-anal tail and assume an interstitial burrowing life habit. The post-anal tail, mode of development, small size and correlated simplification in body plan suggest that *H. planktophilus* is closely related to *Saccoglossus*, and together these worms may be sister taxa to the colonial Pterobranchia. A taxonomic key is provided to the enteropneust genera, and to the species of *Harrimania*.

Introduction

The deuterostome phylum Hemichordata is composed of three extant classes: the Enteropneusta are solitary worms, the Pterobranchia are colonial tube-dwelling suspension feeders, and the Planktosphaeroidea are known only from their larvae. The enteropneusts and pterobranchs differ sufficiently in size and modes of reproduction and feeding that some investigators have considered the phylum Hemichordata to be polyphyletic (Jeffries, 1986; Nielsen, 1994). A recent molecular study strongly supports hemichordate monophyly and suggests an entirely new hypothesis for the evolution of the hemichordates (Cameron *et al.*, 2000). That study proposes that the pterobranchs are a sister taxon to the enteropneust family Harrimaniidae, and that this clade is a sister taxon to the enteropneust family Ptychoderidae (*i.e.*, enteropneust paraphyly). If this phylogeny is correct, then detailed studies of the morphology and development of the harrimaniid worms should yield important insights into the biology and evolution of the ancestral hemichordate and the colonial pterobranchs.

Thirteen genera are currently recognized from four families of Enteropneusta: the Ptychoderidae, including the familiar *Balanoglossus*; the monotypic hydrothermal vent Saxipendiidae (Franzén *et al.*, 1985; Woodwick and Sensenbaugh, 1985); the Spengeliidae; and the Harrimaniidae, including the genera *Protoglossus*, *Saccoglossus*, *Xenopleura*, *Stereobalanus*, and *Harrimania*. Harrimaniids are the most morphologically simple of the Enteropneusta; they lack hepatic sacs, synapticles joining adjacent gill bars, and

Received 9 November 2000; accepted 23 January 2002.

Current address: Department of Biology, University of Victoria, Victoria, BC V8W 2Y2, Canada. E-mail: jetsam@uvic.ca

nerve roots extending from the collar cord; about 20 species have been described from the family. To date, developmental observations of the family Harrimaniidae have been restricted to *Saccoglossus* (Davis, 1908; Burdon-Jones, 1952; Colwin and Colwin, 1953). *Saccoglossus pusillus* (Davis, 1908) is the only harrimaniid from the West Coast of North America for which developmental information exists.

Ricketts *et al.* (1985; originally published in 1939) remains the most comprehensive review of the Enteropneusta from the Pacific Coast of North America. The present status of the Enteropneusta from this region is briefly summarized here. From the family Harrimaniidae, *Saccoglossus* (formerly *Dolichoglossus*) *pusillus* (Ritter) (in Davis, 1908; Horst, 1930) is described from San Pedro and San Diego, California. In an earlier work, Ritter (1902) indicates that this same animal is abundant in Puget Sound. Recently, the *Saccoglossus* from Puget Sound was described by King *et al.* (1994), who found it conspecific with *S. bromophenolosus* (formerly identified as *S. kowalevskii*) from the Northeast Coast of the United States. Two other apparently undescribed species of *Saccoglossus* occur on the Pacific Coast; one is common subtidally in Barkley Sound, British Columbia (Cameron and Mackie, 1996; Cameron *et al.*, 1999), and the other is from the Santa Maria Basin (Woodwick, 1996). Molecular tools should help us to distinguish the morphologically similar species of this North American genus. *Stereobalanus* sp. has been discovered from the Santa Maria Basin (Woodwick, 1996), and *Harrimania maculosa* (Ritter, 1900) is described from Alaska.

Two undescribed species of *Schizocardium* (family Spengeliidae) have been found on the coast of California: the first is from Mugu Lagoon (Ricketts *et al.*, 1985) (now a military base) and Newport Bay (Ricketts *et al.*, 1985) (which now has a highly modified and heavily populated shoreline), and the second is from the Santa Maria Basin (Woodwick, 1996). From the family Ptychoderidae, Ritter (1902) mentioned, but did not describe, *Balanoglossus occidentalis* from San Pedro, California. Other species of *Balanoglossus* have been collected from the Santa Maria Basin (Woodwick, 1996) and from the northeast coastline of the Sea of Cortez (author's collection). *Glossobalanus berkeleyi* (Willey, 1931), originally described from Nanaimo, British Columbia, is no longer present in Nanaimo Bay, but is found in Puget Sound, Washington (author's records). Ptychoderidae is the morphologically most complex of the enteropneust families, and the life cycle of its species usually includes a tornaria larva. Two species of tornaria larvae have been described from western North America (see Ritter and Davis, 1904), but the corresponding adult worms are unknown.

The purpose of the study reported here was to describe *Harrimania planktophilus*, a newly discovered member of the Harrimaniidae from the West Coast of North America. The description includes—in addition to details of habitat and morphology—observations on the mode of development of *H. planktophilus*. Features of this development support the recent hypothesis (Cameron *et al.*, 2000) that the Harrimaniid worms are sister taxa to the colonial class Pterobranchia; the evidence also suggests that these taxa evolved from a worm-like ancestor with indirect development. See the appendix for a key to the families and genera of the Enteropneusta and the species of the genus *Harrimania*.

Materials and Methods

Harrimania planktophilus (Figs. 1 through 5) was collected from the intertidal sand flat at Cape Beale (48° 47′ 30″ N, 125° 12′ 56″ W) in Barkley Sound, Vancouver Island, Canada. Six worms were collected during February 1997, and another twenty-one were collected over the summer of 1999. All worms were transported to the Bamfield Marine Station, where they were kept in specimen bowls containing their natural sediment under a flow of fresh seawater. One or two worms at a time were removed from their bowls for histology. These animals were allowed to defecate their gut contents, and the external surface was cleaned of sediment. The cleaned worms were relaxed in 7% $MgCl_2$, then fixed in Bouin's solution, and dehydrated in a graded series of ethanol. Once in 100% ethanol, the animals were dissected into small pieces, transferred to xylene, and infiltrated with paraffin wax. Sections were cut on an American Optical Corporation 820 Spencer microtome, stained with either Delafield's hematoxylin or eriochrome-cyanin, and viewed and photographed with an Olympus OM-4T 35-mm camera mounted on an Olympus BH2 compound microscope.

I was unable to study unfertilized eggs, fertilization, and early cleavage stages preceding the late blastula stage. Blastulae were obtained on 19 February 1997 from a single egg mass maintained in an aquarium; about 70 embryos were in this tubular mass. Twenty of these embryos were removed and reared in finger bowls containing fresh seawater that was changed daily, but mortality was high. Consequently, the remaining 50 embryos were allowed to develop in the jelly mass, in the sediment, but an individual was removed periodically to document development. The temperature of the seawater during the observation period varied between 10 °C and 11 °C. The various stages were measured, photographed, described, and drawn.

Taxonomic Treatment

Harrimania Ritter 1900

Harrimania Ritter 1900: 112.

TYPE SPECIES: *Harrimania maculosa* Ritter 1900: 112–115.

Harrimania planktophilus new species

Figs. 1, 2, 3, 4.

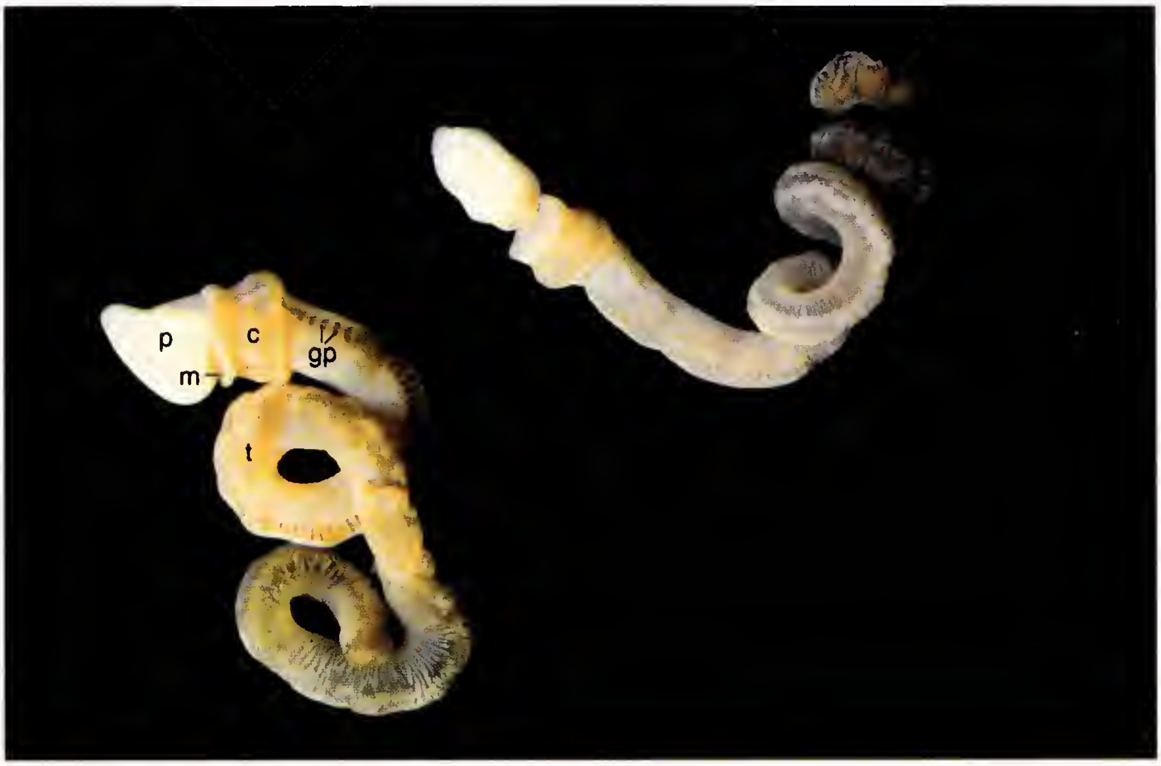

Figure 1. *Harrimania planktophilus*. Total length of a relaxed and uncoiled animal is approximately 32 mm. c, collar; gp, gill pores; m, mouth; p, proboscis; t, trunk.

Description

External

Harrimania planktophilus is, in general, muscular and active. It is robust and can be collected intact, unlike many other species of enteropneust, which are fragile and easily broken. *H. planktophilus* (Fig. 1) is small compared with other enteropneusts. The longest individual was 6 cm in length when extended in the bottom of a specimen bowl, and the average specimen was approximately 3.5 cm. The proboscis is conical, is longer than broad, and about twice as long as the collar (Fig. 1, 2). It bears a middorsal groove that extends two-thirds the length of the proboscis from the posterior margin. In some animals, the proboscis skeleton is pigmented black and can easily be seen through the proboscis epithelium. The collar is shorter than it is wide, with a distinctive circumbuccal groove about halfway between anterior lip and posterior marginal ridge. The posterior marginal ridge of the collar is accompanied by a fine crease. Anteriorly the collar lip (see fig. 4, in Cameron, 2002) is muscular and contractile, altering the circumference and shape of the mouth. An epidermal pit is always present at the dorsal midline where the collar meets the trunk, and its perimeter is rust colored. The trunk can be separated into four regions: a long anterior branchial region; an esophageal region with a reddish esophageal organ; a short transparent region, followed by a darkly pigmented hepatic region (there are no liver sacs); and an intestinal region that has a terminal anus with a sphincter muscle. In gravid males and females the gonads are a pair of large, irregular masses, located dorsolaterally and extending from the posterior pharyngeal region to the anus. The pharyngeal region has many ($36.2 \pm$ SD 9.7; $n = 6$) pairs of large, muscular gill pores (Figs. 1, 5) that open to the outside in paired dorsolateral grooves. A strong exhalent water current was observed in animals acclimated to cold (5–7 °C) seawater. Under these conditions, the pores are expanded, and through the pores can be seen the tongue bars in the wall of the pharynx. In about 1 of 10 animals, the skeletal bars are black, rather than the more common collagenous opaque white. The pharyngeal region is 5 times the length of the extended proboscis. The esophageal region has a large bilobed muscular organ that is pigmented dark red, and posterior to this is a darkly stained hepatic region, and then a meandering gut that can be seen through the translucent body wall. The following measurements are from an average adult living specimen: length of proboscis, 2 mm; length of collar, 1 mm; length of pharynx, 9 mm; length of esophagus to anus, 20 mm; total, 32 mm.

Color (Ridgway, 1912): cream-colored proboscis (pl XVI, f-19); capucine orange collar (pl III, d-13); pale yellow-orange trunk (pl III, f-15), except for the esophageal

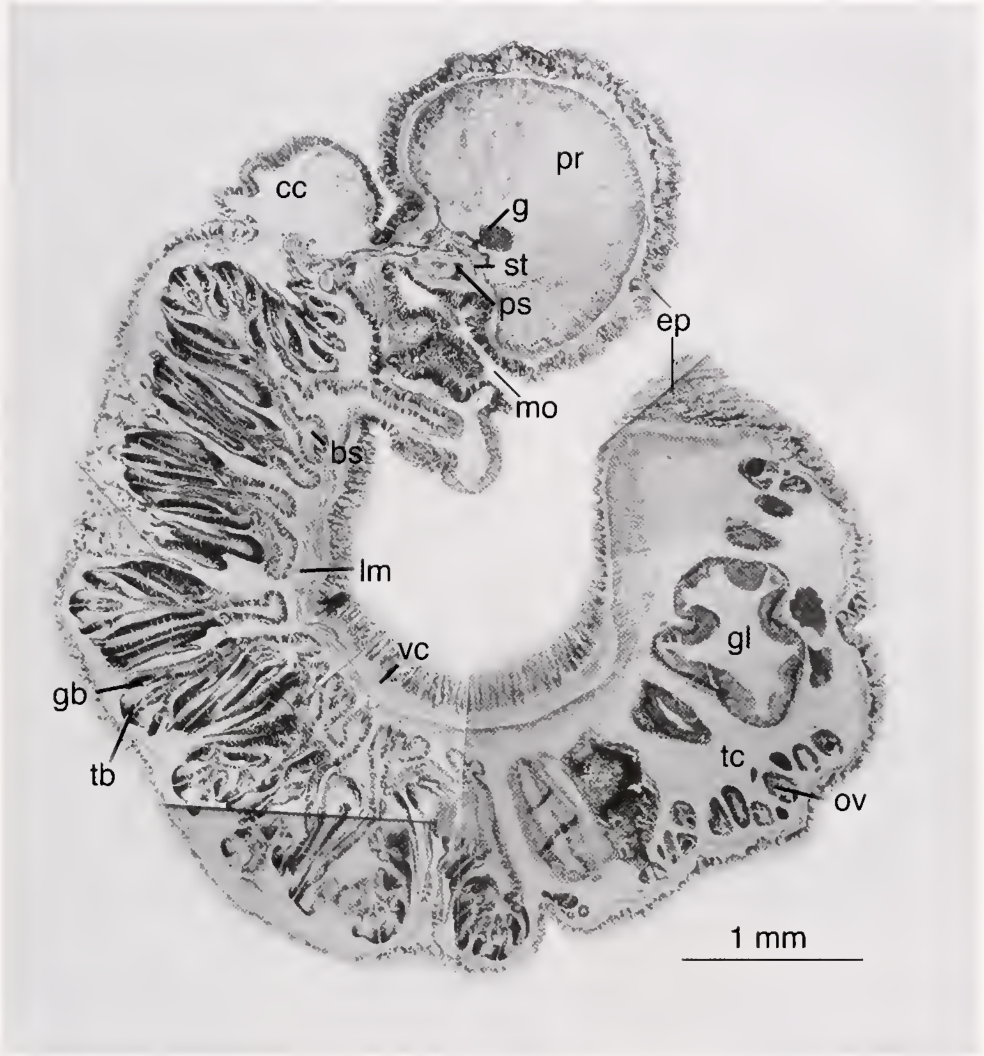

Figure 2. Light micrograph of a longitudinal section of *Harrimania planktophilus*. bs, branchial sac (= atrium); cc, collar coelom; ep, epithelium; g, glomerulus; gb, primary or gill bar; gl, gut lumen; lm, longitudinal muscles; mo, mouth; ov, ovaries; pr, proboscis; ps, proboscis skeleton; st, stomochord; tb secondary or tongue bar; tc, trunk coelom (or metacoel); vc, ventral cord.

organ, which is brick red (pl XIII, k-5), and the hepatic region, which is brownish olive (pl XXX, m-19). The eggs are amber yellow (pl XVI, b-21), and the male gonads are slightly paler.

Anatomical and histological characters

Proboscis. The epithelium of the proboscis is simple and columnar, with multiciliated cells and with glandular cells having basal nuclei. The nervous layer of the ectoderm is about equal in thickness to the underlying circular muscle layer, and thickening slightly under the dorsal proboscis groove. The longitudinal muscle fibers, in transverse section, are arranged in radiating plates, as in *Ptychodera* and *Stereobalanus* (Woodwick, 1996); there are fewer than 50 plates, with spaces between them, and they narrow near the center of the proboscis where the coelom is small or absent (Fig. 3A). There is no ventral proboscis mesentery; instead, a plate of connective tissue underlies the ventral stomochord and extends ventrally, nearly halfway to the epidermis, wedging itself between two radial muscle plates. This connective tissue is contiguous with the posterior portion of the proboscis stomochord (Fig. 3G) and becomes continuous with the proboscis skeleton posteriorly. The stomochord, which lacks the vermiform process of *Schizocardium* (Horst, 1939), is composed of columnar cells arranged radially around a central ciliated lumen, each cell with a large vacuole distally and a proximal nucleus. The ciliated lumen opens into the dorsal midline of the buccal collar, just

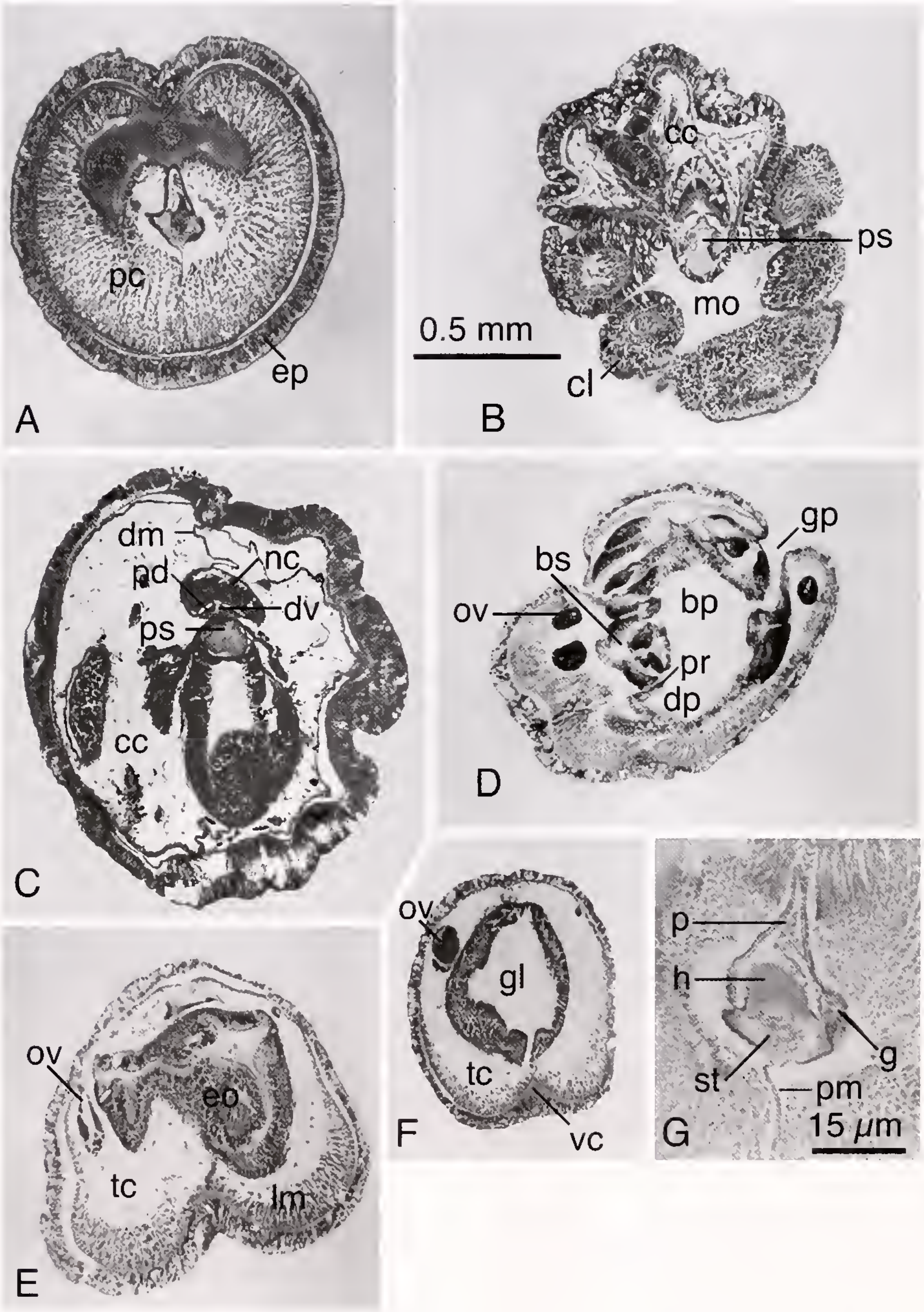
pc
ep
A
cc
ps
mo
0.5 mm
cl
B
dm
nc
pd
dv
ps
cc
C
gp
bs
ov
bp
pr
dp
D
ov
eo
tc
lm
E
ov
gl
tc
vc
F
p
h
g
st
pm
15 μm
G

Figure 3. Light micrographs of transverse sections of *Harrimania planktophilus*. (A) Proboscis. (B) Proboscis stalk and anterior collar lip. (C) Collar. (D) Pharyngeal region of the trunk. (E) Esophageal region. (F) Intestinal region. (G) The stomochord is flanked by the heart-kidney coelomic complex, and has a central lumen. bp, branchial pharynx; bs, branchial sac (= atrium); cc, collar coelom; cl, collar lip; dm, dorsal mesentery; dp, digestive pharynx; dv, dorsal vessel; eo, esophageal organ; ep, epithelium; g, glomerulus; gl, gut lumen; gp, gill pore; h, heart; lm, longitudinal muscles; mo, mouth; nc, nerve cord; ov, ovaries; p, pericardial sac; pc, proboscis coelom (protocoel); pd, perihaemal diverticula; pm, proboscis mesentery; pr, parabranchial ridge; ps, proboscis skeleton; st, stomochord; tc, trunk coelom (metacoel); vc, ventral cord.

posterior to the position where the two proboscis skeleton crura bifurcate from the skeletal body. An extensive U-shaped glomerulus is situated on the wall of the heart and at the anterior tip of the stomochord. The pericardium, in transverse section, is a small wedge-shaped sac that extends dorsally from the heart, nearly halfway to the epidermis, between two longitudinal muscle plates (Fig. 3G).

The proboscis coelom is small to absent, is never divided completely, and extends posteriorly on the ventral and dorsal sides of the stomochord. Ventrally the coelom ends in a blind sac; dorsally it extends extremely posteriorly into the stalk and opens to the outside through a single proboscis pore just left of the dorsal midline of the proboscis stalk and almost into the anterior neuropore.

Collar. In some specimens, an anterior neuropore is located at the midline of the proboscis stalk where it meets the collar. A posterior neuropore is always present at the dorsal midline where the collar meets the trunk. Over the length of the collar nerve cord, one or two small lacunae may reside lateral to the midline. Giant nerve cells are absent. A dorsal mesentery is present throughout the length of the collar cord (Fig. 3C). Ventral to the collar cord, the perihaemal coelomic diverticula are well developed and extend from the trunk coelom for two-thirds the length of the collar; the mesentery between the diverticula is well defined. Anteriorly the diverticula become confluent, reduced in size, and enveloped in collagenous tissue that is continuous with the proboscis skeleton. In the collar, the dorsal blood vessel lies in the mesentery formed by the adjacent medial walls of the perihaemal diverticula (Fig. 3C). The collar coelom extends far anteriorly into the proboscis neck (Fig. 3B). Peribuccal spaces are apparently absent. The body of the proboscis skeleton (Fig. 3B) reaches beyond the middle of the collar before bifurcating into two crura that extend into the pharyngeal region. The stomochord consists of two distinct parts. The anterior pouch-shaped part has a central ciliated lumen that opens into the buccal cavity (Fig. 3G), as it does in all Hemichordata. The anterior part is continuous with a posterior gutter-shaped part, which projects posteriorly from the pore of the stomochord lumen, farther along the roof of the buccal cavity, before ending as two open troughs. The stomochord of *H. planktophilus* is thus similar in design to that of *Harrimania maculosa* (Ritter, 1900), but not as extensive.

Trunk. Poorly developed parabranchial ridges (Fig. 3D), formed by the ventral edge of the gill bars projecting into the pharynx (see fig. 2 in Cameron, 2002), separate the dorsal branchial pharynx from the ventral digestive pharynx (Fig. 3D). The gill slit skeletal bars are commonly opaque, but in 1 of every 10 animals, they are pigmented black. Peripharyngeal diverticula extend into the tongue bars only. No synapticles join the gill bars with the tongue bars (see figs. 1, 2 in Cameron, 2002). The atrial canal (branchial sac) (Fig. 3D, and see fig. 2 in Cameron, 2002) is U-shaped, heavily ciliated, and leads from the pharyngeal gill slits to the outside *via* the ciliated gill pore. An epibranchial ridge is absent. *Harrimania planktophilus* is dioecious. Gonads, which are restricted to the posterior two-thirds of the trunk perivisceral coelom, begin in the pharyngeal region and extend into the intestinal region (Figs. 2, 3D). Gonadal pores occur dorsolaterally. Immediately behind the pharynx, the esophageal epithelium thickens laterally (Fig. 3E) and forms two opposing lobes, called here the esophageal organ; the lumen is correspondingly reduced in size, as compared with that of the intestine. The intestine meanders *en route* to the anus; it is lined with a simple epithelium, and hepatic sacs are absent. Two longitudinal muscles are broad and well-developed ventrolaterally, and narrow dorsally (Fig. 3E). Circular muscle is absent in this part of the body. The subepidermal nerve layer is thickened on the dorsal midline and even more so on the ventral midline (Fig. 3F). Thus, the midventral cord may be the main conductive channel in the trunk, as it is in a sympatrically occurring and apparently undescribed *Saccoglossus* sp. (Cameron and Mackie, 1996).

Diagnosis

The adult animal is distinguished by having a single proboscis pore, a glomerulus that extends frontally over the stomochord (Fig. 3G), and a proboscis skeleton that extends into the pharyngeal trunk. The stomochord begins in the buccal collar as a middorsal ridge; the ridge is maintained on the lateral sides by the proboscis skeletal crura. The opening of the stomochord canal is positioned just posterior to where the two crura meet to form the skeletal body. The collar has a complete dorsal mesentery (Fig. 3C). Animals may have as many as 54 pairs of gill pores. Gonads overlap with only a few of the most posterior gill pores, and the eggs are pigmented yellow.

Development

Embryos were found in aquaria at early blastula to mid-blastula stage and, therefore, information about gamete structure, egg maturation, events of fertilization, early cleavage stages, and blastulation is lacking. The coeloblastula (Fig. 4A) is 75 μm in diameter and heavily pigmented lemon yellow. It develops in a fertilization membrane 83 μm across that has a thin (1.5 μm) sticky jelly layer, thus development of the animal was often obscured by debris and sand adhering to the jelly coat. Gastrulation appears to proceed by invagination of the posterior (vegetal) pole, resulting in a hemispherical shape that persists for about 12 h (Fig. 4B). The wide archenteron greatly reduces the blastocoel. The blastopore begins to constrict, changing the shape of the gastrula, once again into a sphere (Fig. 4C). Over a period of 24 h the blastopore shrinks, finally persisting as a teardrop shape. There are no external cilia.

The development of cilia initiated rotation within the

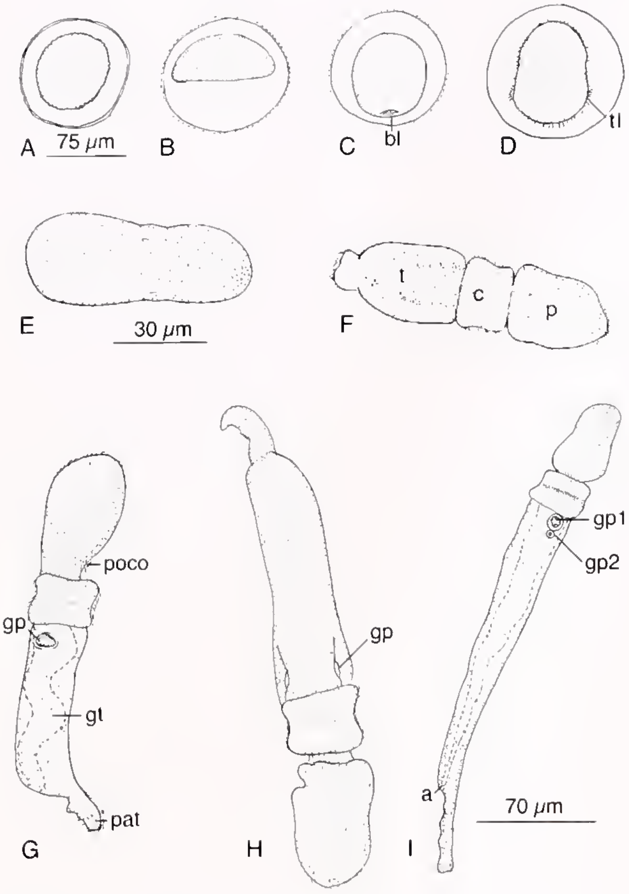

Figure 4. Diagram of the later development of *Harrimania planktophilus*. (A) Blastula. (B) Gastrulation showing obliteration of the blastocoel. (C) Unciliated gastrula. (D) Ciliated embryo with a diffuse ciliated telotrochal band. (E) Newly hatched juvenile. (F) Juvenile with distinct body regions. (G) Juvenile at the first gill pore stage, lateral view. (H) Juvenile at the first gill pore stage, dorsal view. (I) Juvenile at the second gill pore stage, lateral view. a, anus; bl, blastopore; c, collar; gp, gill pore; gp1, first gill pore; gp2, second gill pore; gt, gut; p, proboscis; pat, post-anal tail; poco, pre-oral ciliary organ; t, trunk; tl, telotroch.

embryonic chorion 42 h after the embryos were discovered (Fig. 4D). In addition to rotating, the "larvae" propel themselves in the apical direction. A dimple is all that remains of the closed blastopore. The spherical larvae are 72 μm in diameter. A wide telotrochal band forms on the otherwise uniformly ciliated ball; there is no ciliated apical tuft. Elongation by the constriction of a midventral groove is followed by the hatching of a 90-μm-long, benthic pre-juvenile stage (Fig. 4E). As with the rest of the development, hatching is asynchronous. Of 20 individuals that were extracted from the burrow egg mass and reared in culture, only a single animal hatched. Of about 50 embryos left in the burrow, 14 survived development into juveniles. The fate of the remaining eggs is uncertain, but predation cannot be ruled out because sympatrically occurring species were present in the sediment. Often the jelly layer is shed shortly before the embryo hatches from the transparent chorion.

Elongation and differentiation of the body into a distinct proboscis, collar, and trunk was complete by day 8 for the remaining few animals in culture (Fig. 4F). The lengths of these body regions were 55.0 μm, 18.5 μm, and 75.0 μm, respectively. The animal could locomote on a plastic dish one body length every 2 s. Forward locomotion is guided by a ciliated muscular proboscis. Posterior locomotion is equally efficient and accomplished by a reversal in ciliary beat. Ciliation is most apparent on the proboscis tip, the collar, and the end of the tail. The pre-oral ciliary organ developed later, after about 12 days. The posterior ventral tail becomes post-anal with the completion of the alimentary canal. The tail extends from the ventral trunk and is heavily ciliated and glandular. The tail can adhere to sediments, plastic, and glass. Like the adults, the juveniles move away from light.

The first pair of gill clefts (perforating the pharyngeal epithelium) and gill pores (perforating the ectoderm) are large and appeared on day 15 (Fig. 4G). The circular clefts are lined with long cilia and lack any sign of a skeleton. When the juvenile is viewed perpendicular to its body axis, ciliary waves are seen to pass in a clockwise direction on the left side of the body and counterclockwise on the right side of the body. In other words, the metachronal ciliary beat, around the rim of each pair of clefts, is in a bilaterally symmetrical pattern. At day 17, the juveniles had a second pair of gill pores and a ventral post-anal tail (Fig. 4I). Eventually a gill skeleton develops around the perimeter of the gill cleft, elongating it into a dorsoventrally elongated gill slit (data not shown).

Biology

Harrimania planktophilus is an active infaunal burrower. Individuals were found in two locations in Barkley Sound, subtidally in the Ross Islets (49° 52′N, 125° 10′W) and in the low intertidal of a protected beach adjacent to the eastern slope of Cape Beale (48° 47′ 30″ N, 125° 12′ 56″ W). At Cape Beale, *H. planktophilus* was collected at the extreme low tides that occur during the morning hours in spring and summer, and during the evening in fall and winter (Canadian Tidal Tables). *H. planktophilus* was typically found in a mixture of biogenic calcium carbonate debris and sorted sands with a low concentration of organics. The carbonate fraction of the Cape Beale deposits in the lower tidal range typically contains more than 30% barnacle plates together with fragments of gastropods and, in lower abundance, echinoids, bryozoa, and foraminifera.

H. planktophilus creates sinuous interconnected tunnel systems that do not seem to approach the epibenthos. They are strongly photonegative and lack the odor of bromophenols. In aquaria, more than one animal would frequent a

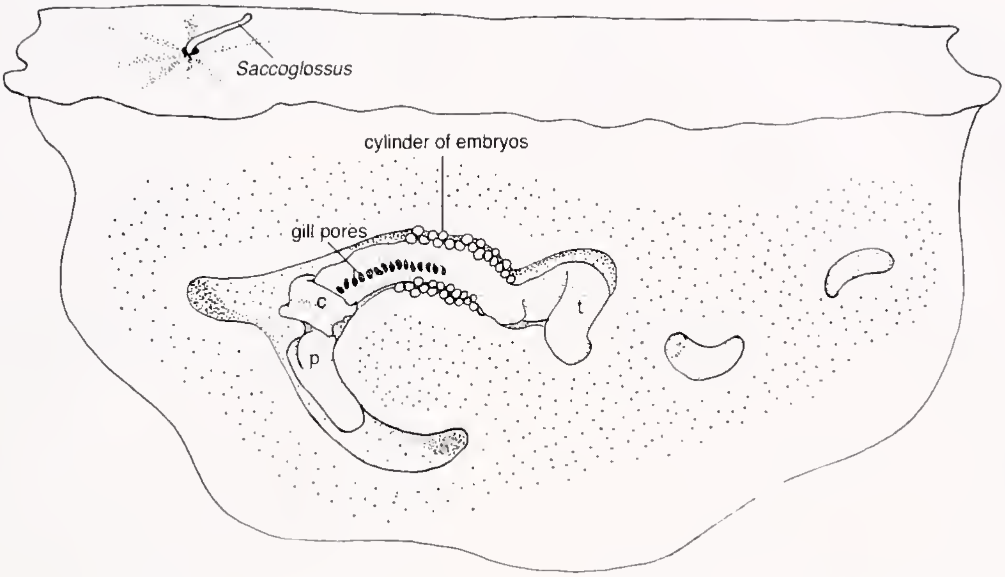

Figure 5. Diagram of *Harrimania planktophilus in situ* with a cylindrical mass of embryos. A tentatively undescribed species of enteropneust, *Saccoglossus* (a surface deposit feeder), is sympatric with *H. planktophilus* at Cape Beale. c, collar; p, proboscis; t, trunk.

single burrow system. Embryos are deposited in the burrow; the egg mass is cylindrical and has a hollow center, through which adult worms and water currents may pass (Fig. 5). Embryos stick to each other with a thin, sticky jelly coat. The face of the embryonic chorion directed towards the lumen of the burrow is clean, whereas the face directed towards the burrow wall is coated with sediment and detritus.

H. planktophilus ingests sediments that it traps in mucus on its proboscis (Fig. 5) and transports back to the mouth with cilia. It also feeds on organic matter in interstitial pore water, employing its pharyngeal cilia to propel water into its mouth and out of its gill pores (Cameron, 2002). Although debris acquired from pore water may constitute a small amount of the total gut content, it may have a significant nutritional role.

Etymology

The species name is Latin and means "plankton loving," reflecting the animal's ability to suspension feed on plankton in interstitial pore water.

Holotype

Adult female: British Columbia, Vancouver Island, Barkley Sound, Cape Beale protected beach, north side adjacent to the "gap," 48° 47′ 30″ N, 125° 12′ 56″ W, 20 September 1999, C. B. Cameron.

Sectioned specimen deposited at the Royal British Columbia Museum (RBCM); holotype number 001-00109-001.

Paratypes

Two specimens of undetermined sex deposited at the RBCM; paratype number 001-00109-002.

Evidence the Genus *Harrimania* is Monophyletic

There are three families of Enteropneusta—four if *Saxipendium coronatum*, the deep-sea hydrothermal vent enteropneust (Woodwick and Sensenbaugh, 1985), constitutes a family of its own. *Harrimania planktophilus* belongs to the family Harrimaniidae, of which there are about 20 described species from the genera *Saccoglossus, Protoglossus, Stereobalanus, Xenopleura*, and *Harrimania*. Harrimaniids have no liver sacs, no synapticles joining the primary and secondary gill bars, and no nerve roots in the collar cord mesentery. *Harrimania* is distinguished from *Saccoglossus* by having a short proboscis (Figs. 1, 2), and from *Xenopleura* by having large pharyngeal pores (Fig. 1). *Harrimania* is distinguished from *Protoglossus* by having a more developed gill skeleton. *Harrimania* is distinguished from *Stereobalanus* by lacking a pair of genital wings and gill pores fused to a common dorsal slit (Ritter, 1900).

Two other species of *Harrimania* are known: *H. maculosa* (Ritter, 1900) and *H. kupfferi* (Spengel, 1901, in Horst, 1939); both have, like *Stereobalanus*, paired proboscis pores. *H. maculosa* is commonly found intertidally in Alaska at Kodiak, Prince William Sound, Orca, and Valdez. This thick, dark brown acorn worm is about 12 cm long and emits a strong bromophenol odor (Ritter, 1900). It does not burrow as do most enteropneusts, but lies under stones after the fashion of some holothurians. In all of these respects *H. maculosa* is unlike the species described here, *H. planktophilus*. Perhaps the most distinctive feature of *H. maculosa* is its two-part stomochord. *H. maculosa* always has two proboscis pores, and has an epibranchial ridge (Ritter, 1900).

H. kupfferi is from Scandinavia (Öresund near Hellebaek, Kattegatt, east of Laessö Island) and Greenland (Horst, 1939). *H. kupfferi* is 8-9 cm long, with a pale-colored proboscis and collar, reddish gonads, and a brown trunk. It differs from *H. planktophilus* in that its glomerulus halves do not connect frontally. The crura of the proboscis skeleton are not as extensive, extending to the posterior end of the collar, whereas in *H. maculosa* and *H. planktophilus* they extend into the trunk. *H. kupfferi* has no mesentery separating the dorsal and ventral collar coelomic cavities, and the dorsal pharynx, with up to 40 gill pores, is smaller than the ventral pharynx (Horst, 1939). In contrast, the dorsal pharynx of *H. planktophilus* is larger than the ventral pharynx (Fig. 3D) and has as many as 54 pairs of gill pores.

Phylogenetic Relationships

The presence of a telotrochal swimming band (Fig. 4D) during the development of *Harrimania planktophilus* suggests that the harrimaniids had an ancestor that developed indirectly. Within the family Harrimaniidae, *Harrimania* is a sister taxon to *Stereobalanus* (Reinhard, 1942) a conclusion based on the shared presence of paired protocoel ducts and pores. Molecular sequence data suggest that the harrimaniid worms are more closely related to the colonial class Pterobranchia (including the genera *Rhabdopleura* and *Cephalodiscus*), which also have paired protocoel ducts and pores, than they are to the ptychoderid worms (*Balanoglossus* and *Ptychodera*) (Cameron *et al.*, 2000). The evolution of the pterobranchs from a harrimaniid ancestor may have involved a reduction in body size and a switch to coloniality. Harrimaniids and pterobranchs, when compared to ptychoderid enteropneusts, show a reduction and disappearance of coelomic diverticula, gonads, and gill slits. The pterobranchs show the most extreme reduction in the size and complexity of these structures. The ventral post-anal tail of juvenile *H. planktophilus* (Fig. 4G–I) may be homologous to the stalk that joins pterobranch zooids. The phylogenetic position (Cameron *et al.*, 2000) and ontogeny of *H. planktophilus* support the idea that the harrimaniid worms are intermediate in form between a complex and indirectly developing worm-like ancestral body plan, and the simple and directly developing body plan of the colonial class Pterobranchia. See the appendix for a key to the families and genera of the Enteropneusta and the species of the genus *Harrimania*.

Acknowledgments

Dr. A. R. Palmer provided support (NSERC Operating Grant A7245 [A.R.P.]) for this project. I gratefully acknowledge Dr. A. Martel for providing his microscope, Dr. R. Marx for help with translating the taxonomy text for *H. kupfferi*, and the staff of the Bamfield Marine Station for providing facilities.

Literature Cited

Burdon-Jones, C. 1952. Development and biology of the larvae of *Saccoglossus horsti* (Enteropneusta). *Proc. R. Soc. Lond. B. Biol. Sci.* **236:** 553–589.

Cameron, C. B. 2002. Particle retention and flow in the pharynx of the enteropneust worm *Harrimania planktophilus*: the filter-feeding pharynx may have evolved before the chordates. *Biol. Bull.* **202:** 192–200.

Cameron, C. B., and G. O. Mackie. 1996. Conduction pathways in the nervous system of *Saccoglossus* sp. (Enteropneusta). *Can. J. Zool.* **74:** 15–19.

Cameron, C. B., G. O. Mackie, J. F. F. Powell, and N. M. Sherwood. 1999. Gonadotropin-releasing hormone in mulberry cells of *Saccoglossus* (Hemichordata: Enteropneusta). *Gen. Comp. Endocrinol.* **114:** 2–10.

Cameron, C. B., J. R. Garey, and B. J. Swalla. 2000. Evolution of the chordate body plan: new insights from phylogenetic analyses of deuterostome phyla. *Proc. Natl. Acad. Sci. USA* **97:** 4469–4474.

Caullery, M., and F. Mesnil. 1904. Contribution à l'étude des Entéropneustes. *Protobalanus (n.g.) koehleri. Zool. Jahrb. Anat.* **20:** 227.

Colwin, A. L., and L. H. Colwin. 1953. The normal embryology of *Saccoglossus kowalevskii* (Enteropneusta). *J. Morphol.* **92:** 401–453.

Davis, B. 1908. The early life history of *Dolichoglossus pusillus*. *Univ. Calif. Publ. Zool.* **4:** 187–226.

Delle Chiaje, S. 1829. Memorie sulla storia e notomia degli animali senza vertebre del Regno di Neapel. *Napoli* **4:** 1–72.

Eschscholtz, F. 1825. Bericht über die zoologische Ausbeute der Reise von Kronstadt bis St. Peter und Paul. *Oken's Isis* **6:** 64–67.

Franzén, Å., K. H. Woodwick, and T. Sensenbaugh. 1985. Spermiogenesis and ultrastructure of spermatozoa in *Saxipendium coronatum* (Hemichordata, Enteropneusta), with consideration of their relation to reproduction and dispersal. *Zoomorphology (Berl.)* **105 (5):** 302–307.

Gilchrist, J. 1925. *Xenopleura vivipara*, g. et sp. n. (Enteropneusta). *Q. J. Microsc. Sci.* **69:** 555–573.

Horst, C. J. van der. 1930. Observations of some Enteropneusta. Papers from Dr. Th. Mortensen's Pacific expedition, 1914–1916, H. *Vidensk. Medd. Dan. Naturhist. Foren.* **87:** 135–200.

Horst, C. J. van der. 1939. Hemichordata. *Kl. Ordn. Tierreichs* **4:** 1–737.

Jeffries, R. P. S. 1986. *The Ancestry of the Vertebrates*. British Museum, London.

King, G. M., C. Giray, and I. Kornfield. 1994. A new hemichordate, *Saccoglossus bromophenolosus* (Hemichordata: Enteropneusta: Harrimaniidae), from North America. *Proc. Biol. Soc. Wash.* **107:** 383–390.

Nielsen, C. 1994. *Animal Evolution: Interrelationships of the Living Phyla*. Oxford University Press, Oxford. 467 pp.

Punnett, R. C. 1903. The Enteropneusta. *The Fauna and Geography of the Maldive and Laccadive Archipelagoes*, J. S. Gardner, ed. Vol. 2, part 2. Cambridge Univ. Press, Cambridge.

Reinhard, E. G. 1942. *Stereobalanus canadensis*, a little known Enteropneusta from the coast of Maine. *J. Wash. Acad. Sci.* **32:** 309–311.

Ricketts, E. F., J. Calvin, J. W. Hedgpeth, and D. W. Phillips. 1985. *Between Pacific Tides*. 5th ed. Stanford University Press, Stanford. 652 pp.

Ridgway, R. 1912. *Color Standards and Color Nomenclature*. Washington, DC. Published by the author.

Ritter, W. E. 1900. Papers from the Harriman Alaska Expedition. II. *Harrimania maculosa*, a new genus and species of Enteropneusta from Alaska, with special regard to the character of its notochord. *Proc. Wash. Acad. Sci.* **2:** 111–132.

Ritter, W. E. 1902. The movements of the Enteropneusta and the mechanisms by which they are accomplished. *Biol. Bull.* **3:** 255–261.

Ritter, W. E., and B. M. Davis. 1904. Studies on the ecology, morphology, and speciology of the young of some Enteropneusta of western North America. *Univ. Calif. Publ. Zool.* **1:** 171–210.

Schimkewitsch, W. M. 1892. *Über die Beziehungen zwischen den Enteropneusta und Acrania.* Verlag der St.-Petersburger Naturforschergesellschaft, St. Petersburg.

Spengel, J. W. 1893. Die Enteropneusten des Golfes von Neapel. *Fauna und Flora des Golfes von Neapel.* Monograph 18. Friedländer, Berlin.

Spengel, J. W. 1901. Die Benennung der Enteropneusten-Gattungen. *Zool. Jahrb. Abt. Syst.* **15:** 209–218.

Willey, A. 1898. On *Ptychodera flava* Eschscholtz. *Q. J. Microsc. Sci.* **40:** 7–9.

Willey, A. 1931. *Glossobalanus berkeleyi,* a new enteropneust from the West Coast. *Trans. R. Soc. Canada* **5:** 19–28.

Woodwick, K. H. 1996. Hemichordata: Enteropneusta. Pp. 251–259 in *Taxonomic Atlas of the Benthic Fauna of the Santa Maria Basin and the Western Santa Barbara Channel.* Vol. 14. J. A. Blake, P. H. Scott, and A. Lissner, eds. Santa Barbara Museum of Natural History, Santa Barbara, CA.

Woodwick, K. H., and T. Sensenbaugh. 1985. *Saxipendium coronatum,* new genus, new species (Hemichordata: Enteropneusta): the unusual spaghetti worms of the Galápagos Rift hydrothermal vents. *Proc. Biol. Soc. Wash.* **98:** 351–365.

Appendix

Keys to the families and genera of the Enteropneusta, and to the species of the genus Harrimania

A. Stomochord with a vermiform process; pericardium and glomerulus with paired anterior diverticula more or less developed	**Spengeliidae**
(a) Liver sacs and synapticles present; gill slits almost equaling the pharynx in depth, so that the ventral, non-pharyngeal part of the pharynx is reduced to a mere groove; nerve roots absent; pericardial diverticula long	*Schizocardium,* Spengel (1893)
(b) Liver sacs absent; ventral part of pharynx well developed; pericardial diverticula short	
(i) Synapticles and nerve roots absent,	
(*α*) Peribuccal spaces	*Willeyia,* Punnett (1903)
(*β*) Without peribuccal spaces	*Glandiceps,* Spengel (1893)
(ii) Synapticles present; nerve roots present or absent; genital region with dermal pits	*Spengelia,* Willey (1898)
B. Stomochord with no vermiform process; pericardium simple; ventral part of pharynx large, and sometimes more or less separated from the branchial part	
(a) Liver sacs, synapticles, and nerve roots present	**Ptychoderidae**
(i) Genital wings well developed	
(*α*) Atrium opening by long slits	*Ptychodera,* Eschscholtz (1825)
(*β*) Atrium opening by small pores	*Balanoglossus,* Delle Chiaje (1829)
(ii) Genital wings hardly developed	*Glossobalanus,* Spengel (1893)
(b) Liver sacs, synapticles, and nerve roots absent	**Harrimaniidae**
(i) With many atria	
(*α*) Proboscis long; one proboscis pore	
(1) burrowing	*Saccoglossus,* Schimkewitsch (1892)
(2) non-burrowing	*Saxipendium,* Woodwick & Sensenbaugh (1985)
(*β*) Proboscis short	
(1) one proboscis pore; viviparous	*Xenopleura,* Gilchrist (1925)
(2) usually two proboscis pores	
(a) Two pairs of genital wings	*Stereobalanus,* Spengel (1901)
(b) No genital wings	*Harrimania,* Ritter (1900)
(I) Proboscis skeleton extending into trunk, with collar mesenteries	
- Extensive branchial ridge and collar stomochord	*H. maculosa,* Ritter (1900)
- Reduced branchial ridge and reduced collar stomochord	*H. planktophilus,* Cameron
(II) Proboscis skeleton not extending into trunk, without collar mesenteries	*H. kupfferi,* Spengel (1901)
(ii) Without atria	*Protoglossus,* Caullery & Mesnil (1904)

Reference: *Biol. Bull.* **202:** 192–200. (April 2002)

Particle Retention and Flow in the Pharynx of the Enteropneust Worm *Harrimania planktophilus*: The Filter-Feeding Pharynx May Have Evolved Before the Chordates

CHRISTOPHER B. CAMERON

Department of Biological Sciences, CW 405 Biological Sciences Building, University of Alberta, Edmonton, Alberta T6G 2E9, Canada

Abstract. An investigation of the feeding behavior of the acorn worm *Harrimania planktophilus* suggests a novel form of enteropneust feeding with significant phylogenetic implications. *H. planktophilus* is a holoinfaunal worm that feeds on deposited sediments, and filter feeds on suspended particles in interstitial pore water. To visualize the particle retention behavior involved in filter feeding, adult animals were held in chilled seawater under low light and fed food coloring and fluorescent particles. The behavior was recorded by videography. Most particles ingested were drawn into the mouth by an incurrent flow created by cilia on the pharyngeal bars and without the aid of mucus. Particles that passed freely through the gill pores averaged 3.04 μm, whereas particles retained in the gut and defecated in the feces averaged 13.9 μm. Food coloring entered the mouth and was pumped through the pharynx at a rate of 0.5–2.0 mm/s. There is no evidence of an endostyle or mucus-net capture mechanism in *H. planktophilus*, but instead particles are filtered and manipulated by a dense covering of cilia on the pharyngeal gill bars. This study suggests that the filter-feeding pharynx is not an innovation of the chordates, but evolved prior to the evolutionary divergence of the hemichordate-echinoderm clade from the chordates.

Introduction

The enteropneust worms and bryozoan-like pterobranchs constitute the small deuterostome phylum Hemichordata, which is generally regarded as an early offshoot from the chordate line of evolution (Ruppert and Barnes, 1994). Such a group might be expected to hold clues concerning early chordate pharyngeal evolution, but pharyngotremy and the feeding behavior of hemichordates have been little studied since the work of Barrington (1940; Barrington and Thorpe, 1963). What little work has been done on enteropneust feeding behavior has primarily focused on deposit feeding. The Enteropneusta have long been considered classical mucociliary feeders, collecting their food particles on the proboscis with mucous secretions, and transporting them on the surface of multiciliated cells to the mouth (Barrington, 1940; Knight-Jones, 1953; Burdon-Jones, 1962; Thomas, 1972). In addition to deposit feeding, some evidence of filter feeding in the Enteropneusta has also emerged from the research of Barrington (1940; *Glossobalanus minutus*), Knight-Jones (1953; *Saccoglossus horsti*), and Burdon-Jones (1962; *Balanoglossus gigas*). Barrington (1940) studied the path of carmine particles as they moved in and around the collar lip of *Glossobalanus minutus*. The majority of particles were transported with the aid of mucus, but some were pulled into the mouth with a ciliary current, suggesting that *G. minutus* is able to acquire food by filter feeding. Flow velocities and particle-size measurements were not reported in that feeding experiment, so the effectiveness of the feeding mechanism, including the size selectivity of suspended particles, could not be estimated. Respiratory currents were also observed to enter the mouth of burrowing *Saccoglossus horsti*, apparently to assist sediment-laden mucus to enter the mouth (Knight-Jones, 1953).

Balanoglossus gigas, the largest of the enteropneusts, grows to lengths exceeding 2 m (Horst, 1939), and creates deep burrow systems with many connections to the surface

Received 9 November 2000; accepted 23 January 2002.

Current address: Department of Biology, University of Victoria, Victoria, BC V8W 2Y2, Canada. E-mail: jetsam@uvic.ca

(Burdon-Jones, 1962). When graphite suspensions were released at the margin of the collar lip of *B. gigas*, the particles were swiftly drawn into the dorsal branchial pharynx, with no indication that mucus was playing a role in transport. Particles were trapped in the branchial pharynx, and transported ventrally to two grooves on the parabranchial ridges, which separate the dorsal branchial pharynx from the ventral digestive pharynx. The parabranchial ridges rolled the graphite into mucus produced by the pharyngeal epithelium, forming a loose cord. This cord was then transported ventrally to the digestive pharynx, and then posteriorly to the esophagus, hepatic region, and eventually the intestine. This branchial sieving mechanism was very efficient and prevented particles of 1 to 2 μm from passing out through the branchial pores (Burdon-Jones, 1962). Notwithstanding these observations in support of filter feeding, this mechanism was regarded as secondary to deposit feeding (Knight-Jones, 1953; Burdon-Jones, 1962) or of minor importance (Thomas, 1972).

Among deuterostomes, gill slits occur in fossil echinoderms (Jeffries, 1986), hemichordates, and chordates. In enteropneusts they are generally believed to dispose of excess water that is transported into the pharynx with ingested sediment (Barrington, 1940; Knight-Jones, 1953; Burdon-Jones, 1962; Barrington and Thorpe, 1963), and are also assumed to be gas-exchange surfaces (Ruppert and Barnes, 1994). The chordate pharynx, on the other hand, collects and concentrates suspended food (ascidians and amphioxus), and provides a means of locomotion for salps and doliolids (Bone, 1998). The pharynx of lamprey ammocete larvae functions much like that of amphioxus, and the vertebrate pharynx functions as a surface for gas exchange (although filter feeding has been reinvented in some taxa). In higher vertebrates, the gill bars have been modified to form the jaws and the hyoid arches (Radinsky, 1987).

Given the unquestionable shared form of the hemichordate pharynx with that of fossil echinoderms and protochordates, I decided to investigate the potential for filter feeding in the enteropneust worm *Harrimania planktophilus*. My goals were (i) to confirm my preliminary observations suggesting filter feeding by this enteropneust (Cameron, 2002), (ii) to quantify the size range of particles that the pharynx can filter from seawater, and (iii) to examine the pharynx microscopically to better understand the movement of water and particles through it. The results of this study challenge the long-held view that the filter-feeding pharynx is a synapomorphy of the chordates, and suggest that it may have been present in the common ancestor to the hemichordates, echinoderms, and chordates.

Materials and Methods

Harrimania planktophilus was collected from the intertidal sand flats at Cape Beale (48° 47′ 30″ N, 125° 12′ 56″ W) Barkley Sound, Vancouver Island, Canada. Twenty-one worms were collected over the summer of 1999 and transported to the Bamfield Marine Station, where they were kept in specimen bowls containing their natural sediment under a flow of fresh seawater. One or two worms at a time were removed from their bowls for videomicrography, light microscopy, or scanning electron microscopy. The feeding behavior of *H. planktophilus* was recorded as follows. Animals were first placed in finger bowls without sediment, and then allowed to cool on ice until the water temperature was between 5 and 7 °C. Cooling was the most effective way to relax the muscular and mucus secretory responses of the animals, which are otherwise stressed from being removed from the sediment. An ice bath was also the most effective means of keeping the water cool during videorecording. *H. planktophilus* is strongly photonegative, and animals were therefore filmed with the lowest light levels consistent with maintaining a visible image. Orange, red, and blue filters were placed between the fiber-optic light source and the animal, but this did not appear to reduce its photosensitivity. To make images of the water current through the mouth and pharynx of *H. planktophilus*, a number of particles suspended in seawater were tried, including carbon dust, starch, Sephadex beads, carmine red, and fluorescent particles (Dayglo Color Corp.). Dyes in seawater solution were also tried, including diluted milk, methylene blue, fluorescein, and blue food coloring. *H. planktophilus* responded most positively to the orange fluorescent particles (Dayglo Color Corp.) and blue food coloring in seawater. The orange fluorescent particles were positively charged and had a size range of 1.6–30 μm, with 20% at 6 μm. The size of the particles cleared and captured by *H. planktophilus* was determined by direct measurement of the particles that passed freely through the gill slits, and that were bound into fecal material. Feeding trials were taped and measurements taken with a JVC 3-CCD color video camera mounted on a Wild dissecting microscope. Still pictures in Figures 2 and 3 were captured with imaging software (Optimus Corporation).

From these data, the Reynolds number was estimated as:

$$Re = \frac{lU}{\nu}.$$

where l is the inside diameter of the pharynx (in meters), U is the flow velocity (m s^{-1}) of the dyestream front as it entered the mouth, and ν is the kinematic viscosity of seawater ($= 1.047 \times 10^{-6}$ m^2 s^{-1} @ 20 °C) (Vogel, 1981).

In preparation for light microscopy, animals were allowed to defecate their gut contents and were cleaned externally of sediment. They were then relaxed in 7% $MgCl_2$, fixed in Bouin's solution, and dehydrated through a graded series of ethanol dilutions. Once in 100% ethanol, these specimens were dissected into small pieces, transferred to

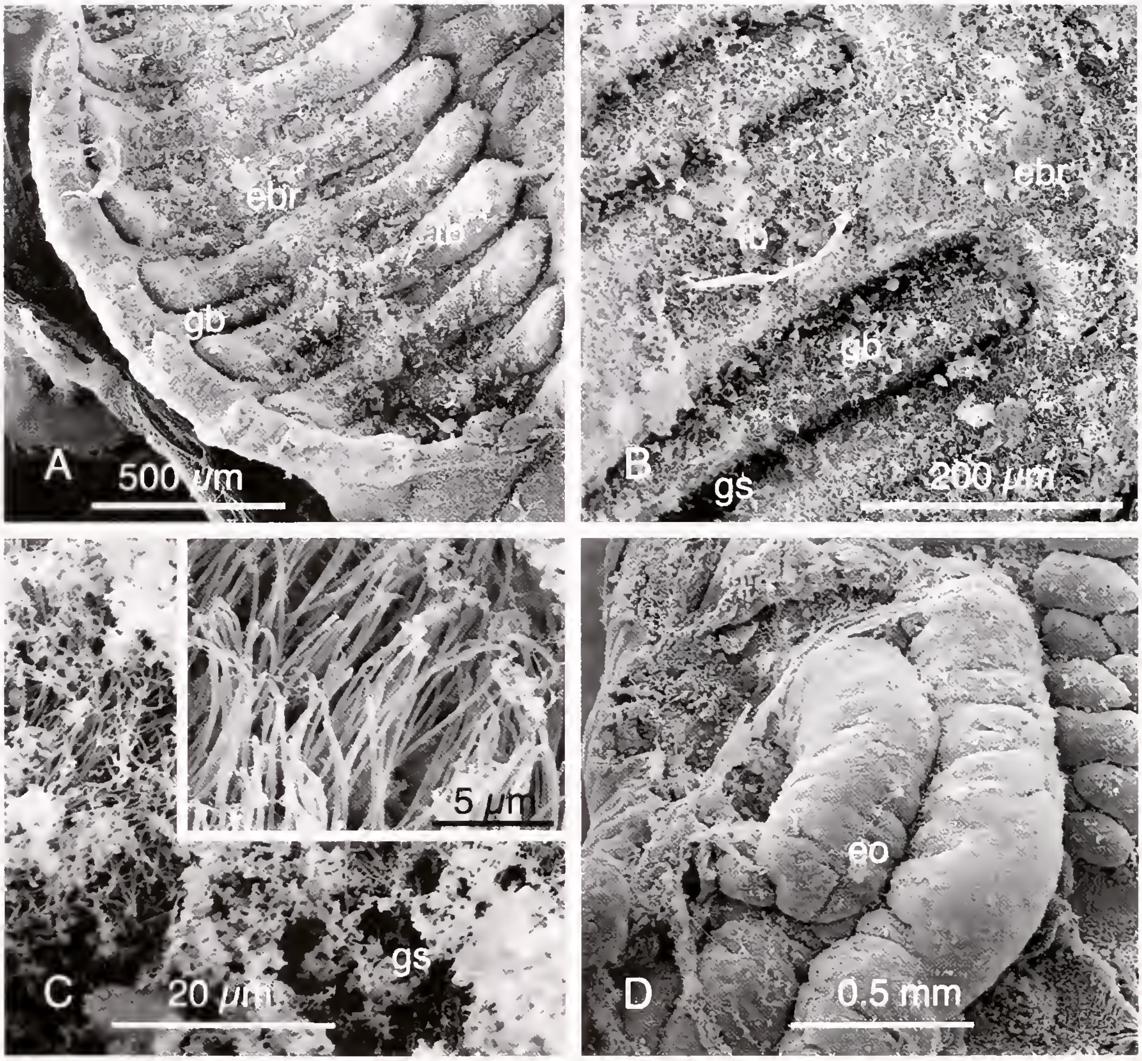

Figure 1. Scanning electron microscope images of sectioned material of *Harrimania planktophilus*. (A) The dorsal branchial pharynx, showing the primary bars, tongue bars, and gill slits. (B) The gill bars and slits in the dorsal branchial pharynx. (C) Cilia and mucus on a gill bar. (C inset) High-magnification image of cilia on a tongue bar. (D) The esophageal organ concentrates food in passage from the pharynx to the hepatic region of the gut. ebr, epibranchial region; eo, esophageal organ; gb, primary or gill bar; tb, secondary or tongue bar; gs, gill slit.

xylene, and then infiltrated with paraffin wax. Sections were cut on an American Optical Corporation 820 Spencer microtome and stained with either Delafield's hematoxylin or eriochrome-cyanin, and viewed and photographed with an Olympus OM-4T 35-mm camera mounted on an Olympus BH2 compound microscope.

For scanning electron microscopy, pieces of tissue were dissected from a relaxed animal so that the dorsal pharynx was exposed. The specimen was then fixed in 2.5% glutaraldehyde in 0.2 *M* Millonig's phosphate buffer at pH 7.4 for 1.5 h and postfixed in 1% osmium tetroxide in 0.2 *M* Millonig's buffer for 1 h. The specimen was then dehydrated through a graded series of ethanol solutions, followed by critical point drying. After sputter coating with colloidal gold, the specimen was examined with a Hitachi S-3500N scanning electron microscope.

Results

Histology and microstructure

Sections were cut through the pharynx and particular attention was given to the dorsal branchial pharynx (Figs. 1A, 2, and see fig. 1B in Cameron, 2002), where the feeding current was presumed to be maintained in *Balanoglossus gigas* (Burdon-Jones, 1962). Long cilia were observed on the lateral side of the primary and secondary gill bars (Fig. 1C inset), and at the pharyngeal edge of the brachial sac.

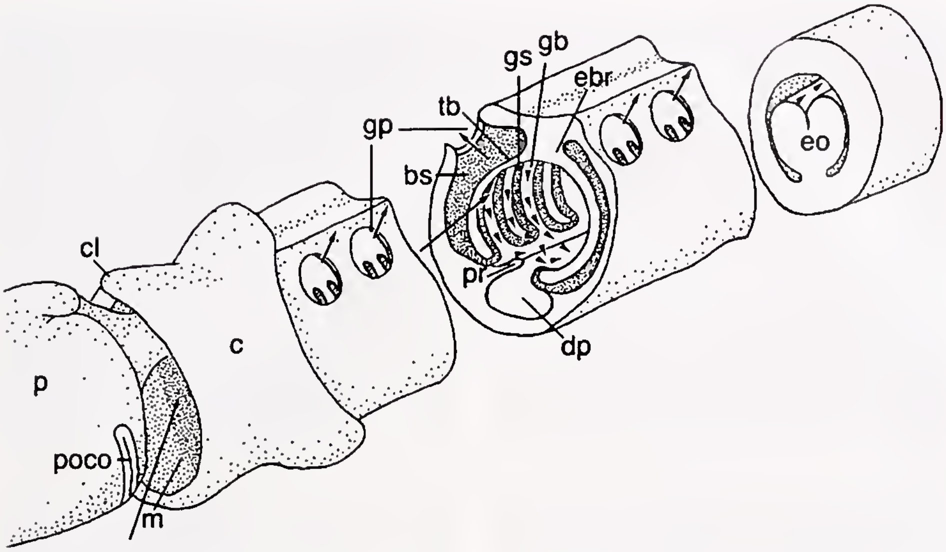

Figure 2. Organization of the filter-feeding morphology of *Harrimania planktophilus*. Anterior is at the left of the figure. Particle-laden seawater (long arrows) enters the mouth on a current that is generated by cilia. Particles (arrowheads) are trapped in dense cilia that line the gill slits; transported ventrally down the gill bars, and carried over the parabranchial ridge to the digestive (ventral) pharynx. Once in the digestive pharynx, particles are transported posterior to the esophagus organ and intestine (not shown). Filtered seawater (short arrows) exits the pharynx through the gill slits, flows into the branchial sac, and reaches the outside through a gill pore. bs, branchial sac; c, collar; cl, collar lip; dp, digestive pharynx; ebr, epibranchial region; eo, esophagus organ; gb, gill bar; gp, gill pore; gs, gill slit; m, mouth; p, proboscis; poco, pre-oral ciliary organ; pr, parabranchial ridge; tb, tongue bar.

Pharyngeal cilia did not show evidence of modified tips (Fig. 1C inset). Scanning electron micrographs revealed no synapticles bridging the tongue bars to the primary gill bars, and consequently the tongue bars project far into the pharynx lumen (Fig. 1A). The pharyngeal region of *H. planktophilus* is 5 times the length of the extended proboscis, and has 36.2 ± 9.7 ($n = 6$) pairs of large gill slits that connect to muscular gill pores. The gill pores are located in paired dorsolateral grooves on the outside of the body (see Cameron, 2002, fig. 1). In some animals the gill skeleton is pigmented dark black, rather than the more common collagenous-opaque white color, allowing it to be easily visualized through the body wall. The esophagus region has a large bilobed thickening of the ventrolateral gut muscle, here called the esophageal organ (Fig. 1D). In live animals the esophageal organ is brick red, as observed through the body wall. This organ may be involved in squeezing excess water from the food before the latter is transported to the digestive gut. Just posterior to the esophageal organ, the gut is darkly pigmented and sinuous. The gut straightens before reaching the anal sphincter.

Observations of flow

Fluid velocity through the mouth was estimated from video recordings of blue food coloring (Fig. 3) that was introduced around the mouth with a handheld pipette (Fig. 3B). The average rate of flow into the mouth and through the pharynx is 0.5–2.0 mm/s. The Reynolds number is approximately between 0.2 and 1.0 in the pharynx (~0.5 mm diameter), and therefore water flow is laminar (the breakover point for purely laminar flow is $Re = 1.0$ (Vogel, 1981)). *H. planktophilus* was observed to regulate its feeding flow in three ways: (1) by contracting the gill pore sphincter muscles; (2) by plugging the mouth, either by withdrawing the proboscis or constricting the collar lip around the neck; and (3) by ciliary arrest in the branchial pharynx. The feeding flow through the mouth of *H. planktophilus* was stopped by ciliary arrest when the animal began to burrow or when it had a pharynx full of particles. Under these conditions, the mouth and gill pores would be wide open, yet a feeding current could not be observed. A muscular sphincter, derived from the longitudinal trunk musculature, curves around each pore (Horst, 1939). When the worm bent its body to turn right, the gill pores on the inside (right) side closed and water exited only from the left pores, and *vice versa*.

Particle retention

Suspended fluorescent particles enter the mouth (Fig. 4) and pass through the collar region and into the dorsal (branchial) pharynx (Figs. 1A, 2, and see fig. 3D in Cameron, 2002) on a current created by the pharyngeal cilia. The

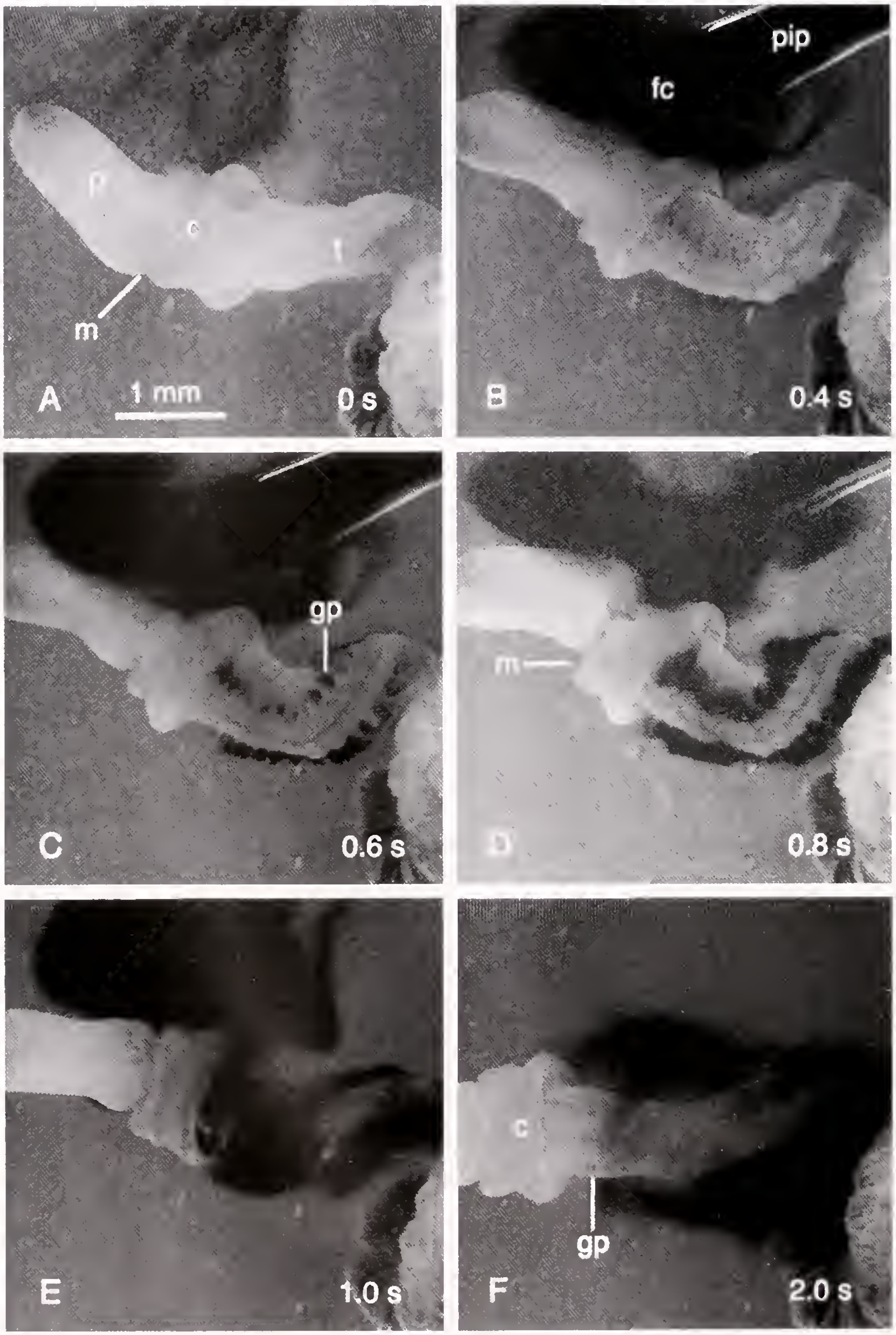

Figure 3. Photographs captured from a videotape, showing the flow of food coloring into the mouth and out of the gill pores of *Harrimania planktophilus*. Scale bar is indicated in A, time in tenths of seconds is indicated in frames A–F. c, collar; fc, food coloring; gp, gill pore; m, mouth; p, proboscis; pip, pipette tip; t, trunk.

particles are then filtered from the water by cilia on the primary gill bars and tongue bars (Figs. 1A, 1B, 1C inset, and 2). Excess water is pumped from the pharynx through the gill slits, into the branchial sac, and through the gill pore to the outside (Fig. 2). Particles that are trapped in the branchial pharynx are transported ventrally down the gill bars and over the parabranchial ridges (Fig. 2) to the digestive pharynx. Once in the digestive pharynx, the particles

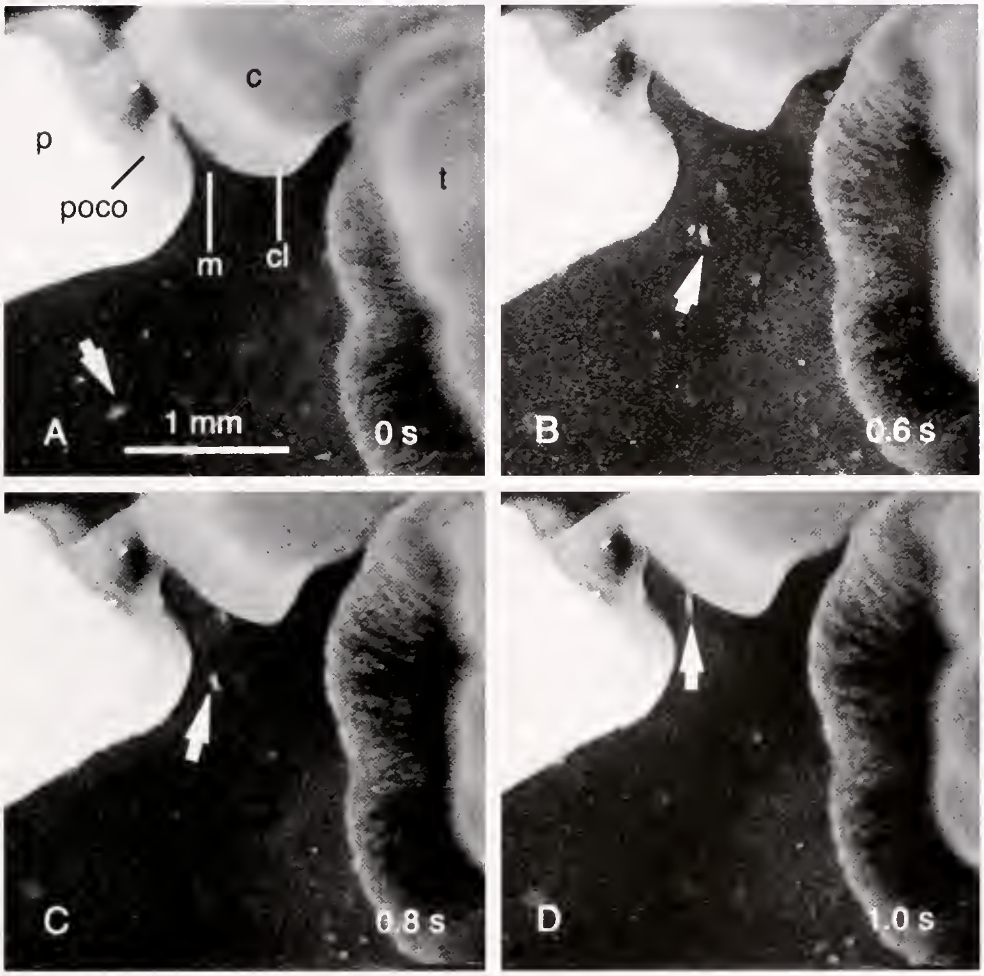

Figure 4. Photographs captured from a videotape of suspended particles moving towards the mouth of *Harrimania planktophilus*. Scale bar is indicated in A, time in tenths of seconds is indicated in frames A-D. c, collar; cl, collar lip; m, mouth; p, proboscis; poco, pre-oral ciliary organ; t, trunk. Arrows indicate the movement of a single particle in suspension as it is drawn towards the mouth on a feeding current.

are transported posteriorly to the esophagus organ and intestine. Mucus was observed in the pharynx (Fig. 1B, C), where it possibly aided in the trapping and transport of particles. Enteropneusts that were fed particles in suspension for more than a few minutes would slow their feeding rates and eventually stop feeding altogether because the pharynx would become plugged with particles. In other words, the branchial pharynx can capture particles at a rate that exceeds the processing efficiency of the gut. The "bottle neck" in the particle filtration system is at the esophagus organ (Fig. 1D) and in the intestine. Fluorescent particles passed through the gut in about 5 h in a 3-cm-long worm.

The size of particles that passed freely through the gill slits (Fig. 2) and gill pores of 6 worms measured 3.04 μm ± SD 1.52 μm ($n = 61$), the maximum particle size was 5.8 μm, and the minimum was 0.2 μm. Particles collected from the feces had a mean size of 13.9 ± SD 8.6 μm ($n = 48$) with a minimum size of 0.2 μm and a maximum of 28.4 μm. Particles in the feces were compacted in the gut and packaged in a mucous matrix, resulting in a tubular fecal casting. Particles had to be teased from the fecal casting for measuring and therefore the large size range may have been overestimated if particles stuck together, or underestimated if larger particles fragmented while the feces were being manipulated. Therefore particle sizes measured in the feces may not be a precise indicator of those that entered the mouth. Despite the problems with particle size estimations, *H. planktophilus* appears capable of ingesting particles ranging from 0.2 μm to 28.4 μm, and the largest size to pass through the gill slits, branchial sac, and gill pore was 5.8 μm. These data suggest that *H. planktophilus* is a facultative filter feeder that exploits a wide size range of particles available in sedimentary pore water.

In addition to being a suspension feeder, *H. planktophilus* is a deposit feeder. Food in the form of sediment, detritus, and interstitial plankton is trapped in mucus on the proboscis and transported posteriorly over its surface toward the mouth. The preoral ciliary organ (POCO) (Figs. 2, 4A), a horseshoe-shaped organ located on the posterioventral face of the proboscis, does not have an obvious function in suspension feeding, but effectively sorts particles that are trapped while deposit feeding. The POCO functions to transport food to the ventral midline and into the mouth on mucous strings. Unwanted particles, on the other hand, are transported by the POCO to the dorsal proboscis, where they are rejected over the collar lip on mucous strings. Strangely, not all deposit-fed particles, or all rejected particles, are manipulated by the POCO. It is not known how the POCO distinguishes between food and nonfood particles.

Discussion

Harrimania planktophilus appears to have a feeding behavior similar to that described in protochordates, suggesting that a filter-feeding pharynx evolved before the divergence of the hemichordate-echinoderm clade from the chordates. Long cilia located on the lateral sides of the gill bars probably mediate the pumping behavior and capture most of the particles from suspension, but a fuller experimental study would be necessary to demonstrate this conclusively.

Burdon-Jones (1962) described a ciliary current within the collar and the anterior region of the pharynx of *Balanoglosus gigas*. Particles entering the pharynx of dissected animals are initially trapped by the dorsal, branchial pharynx and then transported ventrally to the digestive pharynx *en route* to the gut. The observations of particle movement in the present study were made through the body wall and closely resemble those reported by Burdon-Jones (1962). In neither case was there any indication of a mucous net associated with the pharynx as there is in the invertebrate chordates. Instead, heavily ciliated gill bars appear to secrete the mucus. Except for the long cilia mentioned above, cilia in the pharynx were unspecialized, and none exceeded about 8 μm in length. Such cilia are evidently sufficient for pumping and filtration of food-laden water.

The observations above agree with those of Burdon-Jones (1962), who found particles of 1–2 μm retained by the gill slits of *B. gigas*. *H. planktophilus* retained particles as small as 0.2 μm and as large as 28.4 μm in the pharynx, suggesting that the filtering adaptation makes use of microbial as well as interstitial plankton production. *H. planktophilus*, like appendicularians and amphioxus (Ruppert *et al.*, 2000), can feed on a wide size range of particles, exceeding that of the ascidians *Ascidiella aspersa, Molgula manhattensis, Clavelina lepadiformis*, and *Ciona intestinalis* (Randlov and Riisgård, 1979).

Recent experiments reveal that key developmental genes are expressed in the epithelia of differentiating gills of the ascidians and of the enteropneust *Ptychodera flava* (Ogasawara *et al.*, 1999), suggesting that the gill slits of enteropneusts are homologous to those of chordates. A test of this idea might be to look for the expression of members of this gene family in the pharyngeal pores of macrodasyid gastrotrichs (Ruppert and Barnes, 1994) to see if the gene is responsible for pores or openings in the pharynx in general, rather than having an expression that is specific to deuterostome gill pores. The evidence that the gill slits of enteropneusts and chordates are homologous is based on their shared location, developmental origin, and, at least in *H. planktophilus*, their shared function. How then do the gill skeletal arches and the endostyle fit into this picture?

The enteropneust and cephalochordate pharynx share serially paired gill slits in the pharynx that are framed on either side by collagenous gill arches, and parted down the middle by a secondary gill (or tongue) bar. In ptychoderid enteropneusts (but not in *Harrimania*), synapticles, or collagenous bridges, join the primary bars with the secondary bars. The cephalochordate pharynx differs from that of the Enteropneusta in that it possesses an endostyle on the ventral midline. Horst (1939) considered the ventral digestive gut of enteropneusts to be homologous to the chordate endostyle, but recent evidence indicates an endostyle-like organ in the *dorsal* pharynx of the enteropneust *Schizocardium brasiliense* (Ruppert *et al.*, 1999). Further support for the dorsoventral inversion hypothesis may be found in the direction of particle movement in the pharynx of *H. planktophilus*. The food is gathered on the gill bars and transported from dorsal to ventral (in chordates, particles move from ventral to dorsal), and then transported posteriorly to the gut in a mucous food cord. The direction of food transport in *H. planktophilus* suggests that the enteropneusts are inverted dorsoventrally with respect to the chordates, and this notion is supported by molecular evidence (Arendt and Nübler-Jung, 1994). If true, such an inversion means that the gill bars could not be considered homologous with those of amphioxus, because they would also be inverted dorsoventrally and therefore contradict the conformational consistency required to assign homology. The coelomic diverticula in the gill bars and tongue bars is different in the two groups, suggesting that the gills of the common ancestor may have lacked primary and secondary gill bars. This idea is consistent with the absence of gill skeletal structures in adult pterobranchs, the adult enteropneust *Protoglossus*, urochordates, and developmental stages of all other chordates. Clearly, more comparative research is needed before we can be confident about gill-arch homologies among the deuterostomes.

The enteropneust pharynx should not be considered less specialized than that of the chordate pharynx on the basis that it lacks an endostyle organ that produces a mucous net. The pharynx of *H. planktophilus* is effective at capturing a wide range of particle sizes, and although it does not have a mucous net, mucus is produced abundantly by the surface of the enteropneust body and surely plays a role in capture and transport of ingested material. The enteropneust pharynx may represent an intermediate stage in the evolution of the chordate pharynx; that is, first came the filter-feeding gill slits, and later came the capacity to make a mucous net. It is not clear whether the mucous net was present in the ancestral deuterostome animal and lost in the lineage to the enteropneust worms, or absent in the common ancestor and gained in the lineage to the chordates. The lack of the chordate-like endostyle and mucous net in *H. planktophilus* may be due to the undue stress that the net would receive from sediment acquired while deposit feeding. In any case, *H. planktophilus* is an effective filter feeder, even in apparent absence of a mucous net and endostyle.

H. planktophilus is perhaps unique among the filter-feeding protochordates because it lives entirely beneath the sediment. In aquaria, the burrows of this worm do not approach the sediment surface. Initially, these filter-feeding experiments were tried with worms *in situ*, but the difficulty in viewing particles entering the mouth made it impossible to establish whether particles found in the gut of exhumed worms were ingested *via* deposit feeding or suspension feeding. Most investigations that quantify filter feeding have been concerned with epifaunal organisms (including sessile, tube-dwelling, and free-living organisms) or infaunal forms that have part of their body or tube in direct contact with the epibenthos (examples include the bivalve *Mya arenaria* and the polychaete *Chaetopterus*) (Wildish and Kristmanson, 1997). *H. planktophilus* apparently exploits nutrients from interstitial pore water, a world occupied by protozoans, diatoms, foraminifera, flatworms, gastrotrichs, nematodes, copepods, molluscs, tardigrades, and bacteria that thrives at the boundary of the reduced oxygen layer (Levinton, 1995). *H. planktophilus* is a very active enteropneust and responds negatively to low light levels. When it is removed from its burrow, its gut is full of sediment. Sediment obtained from deposits probably accounts for the bulk of the gut's content, but food filtered from pore water may be most important nutritionally (Barrington, 1940). Many deposit feeders display adaptations that improve their efficiency in sediment processing and food absorption (Lopez and Levinton, 1987), and the filtration of nutrient-rich pore water, such as observed in *H. planktophilus*, may be more common than formerly realized.

Harrimania planktophilus is a facultative filter feeder, and a detailed comparison between a wide range of hemichordates will undoubtedly reveal further evolutionary innovations of the branchial pharynx. Several species seem to be especially good candidates for filter feeders, including the swimming enteropneust *Glandiceps hacksii* (Spengel, 1909); the deep-sea rock-pendulum worm *Saxipendium coronatum*, which lives atop rocky outcrops and extends its proboscis into the water column (Woodwick and Sensenbaugh, 1985); *Harrimania maculosa*, which lives on the underside of rocks in Alaska (Ritter, 1900); and species of *Schizocardium* because of their well-developed branchial pharynx (Ruppert *et al.*, 1999). Much remains to be learned about the form, function, and origin of the filtering pharynx of deuterostomes.

Clearly the evolution of slits in the pharynx is one of the most important events in the evolution of the deuterostomes. Protochordates and *H. planktophilus* have a filter-feeding pharynx. Given the occurrence of homologous pharyngeal slits (but possibly not gill arches) in enteropneusts and chordates, and given the sister group relationship between hemichordates and echinoderms (Cameron *et al.*, 2000), it is not surprising that echinoderm paleontologists have found fossil carpoid echinoderms with pharyngeal slits (Jeffries, 1986). The most parsimonious conclusion is that the carpoid pharynx was also a filter-feeding pharynx. This study suggests that the filter-feeding pharynx may not be a synapomorphy of the chordates, but a defining feature of the deuterostomes.

Acknowledgments

I thank Dr. A. R. Palmer for his generosity (NSERC Operating Grant A7245 [A.R.P.]), and E. E. Ruppert for providing critical comments on the manuscript. The staff of the Bamfield Marine Station are gratefully acknowledged for their assistance during my stay at the facility.

Literature Cited

Arendt, D., and K. Nübler-Jung. 1994. Inversion of dorsal ventral axis? *Nature* **371:** 26.

Barrington, E. J. W. 1940. Observations on feeding and digestion in *Glossobalanus minutus. Q. J. Microsc. Sci.* **82:** 227–260.

Barrington, E. J. W., and A. Thorpe. 1963. Comparative observations on iodine binding by *Saccoglossus horsti* Brambell and Goodhart, and by the tunic of *Ciona intestinalis* (L). *Gen. Comp. Endocrinol.* **3:** 166–175.

Bone, Q. 1998. Locomotion, locomotor muscles, and buoyancy. Pp. 35–54 in *The Biology of Pelagic Tunicates*, Q. Bone, ed. Oxford University Press, Oxford.

Burdon-Jones, C. 1962. The feeding mechanism of *Balanoglossus gigas. Bol. Fac. Filos. Ciênc. Letr. Univ. S. Paulo*, No 261. *Zoologia* **24:** 255–280.

Cameron, C. B. 2002. The anatomy, life habits, and later development of a new species of enteropneust, *Harrimania planktophilus* (Hemichordata: Harrimaniidae) from Barkley Sound. *Biol. Bull.* **202:** 182–191.

Cameron, C. B., J. R. Garey, and B. J. Swalla. 2000. Evolution of the chordate body plan: new insights from phylogenetic analyses of deuterostome phyla. *Proc. Natl. Acad. Sci. USA* **97:** 4469–4474.

Horst, C. J. van der. 1939. Hemichordata. *Kl. Ordn. Tierreichs* **4:** 1–737.

Jeffries, R. P. S. 1986. *The Ancestry of the Vertebrates.* British Museum, London.

Knight-Jones, E. W. 1953. Feeding in *Saccoglossus* (Enteropneusta). *Proc. Zool. Soc. Lond.* **123:** 637–658.

Levinton, J. S. 1995. *Marine Biology: Function. Biodiversity. Ecology.* Oxford University Press, Oxford.

Lopez, G. R., and J. S. Levinton. 1987. Ecology of deposit-feeding animals in marine sediments. *Q. Rev. Biol.* **62:** 235–260.

Ogasawara, M., H. Wada, H. Peters, and N. Satoh. 1999. Developmental expression of Pax 1/9 genes in urochordate and hemichordate gills: insight into function and evolution of the pharyngeal epithelium. *Development* **126:** 2539–2550.

Radinsky, L. B. 1987. *The Evolution of Vertebrate Design.* University of Chicago Press, Chicago.

Randløv, A., and H. U. Riisgård. 1979. Efficiency of particle retention and filtration rate in four species of ascidians. *Mar. Ecol. Prog. Ser.* **1:** 55–59.

Ritter, W. E. 1900. Papers from the Harriman Alaska Expedition. II. *Harrimania maculosa*, a new genus and species of Enteropneusta from Alaska, with special regard to the character of its notochord. *Proc. Wash. Acad. Sci.* **2:** 111–132.

Ruppert, E. E., and R. D. Barnes. 1994. *Invertebrate Zoology.* Saunders College Publishing, Fort Worth, TX.

Ruppert, E. E., C. B. Cameron, and J. E. Frick. 1999. Endostyle-like features of the dorsal epibranchial ridge of an enteropneust and the hypothesis of dorsal-ventral axis inversion in chordates. *Invertebr. Biol.* **118:** 202–212.

Ruppert, E. E., T. R. Nash, and A. J. Smith. 2000. The size range of suspended particles trapped and ingested by the filter-feeding lancelet *Branchiostoma floridae* (Cephalochordata: Acrania). *J. Mar. Biol. Assoc. UK* **80:** 329–332.

Spengel, J. W. 1909. Pelagisches Vorkommen von Enteropneusten. *Zool. Anz.* **34:** 54–59.

Thomas, I. M. 1972. Action of the gut in *Saccoglossus otagoensis* (Hemichordata: Enteropneusta). *N. Z. J. Mar. Freshw. Res.* **6:** 560–569.

Vogel, S. 1981. *Life in Moving Fluids. The Physical Biology of Flow.* Willard Grant Press, Boston, MA.

Wildish, D., and D. Kristmanson. 1997. *Benthic Suspension Feeders and Flow.* Cambridge University Press, Cambridge.

Woodwick, K. H., and T. Sensenbaugh. 1985. *Saxipendium coronatum*, new genus, new species (Hemichordata: Enteropneusta): the unusual spaghetti worms of the Galapagos Rift hydrothermal vents. *Proc. Biol. Soc. Wash.* **98:** 351–365.

MARINE RESOURCES CENTER

MARINE BIOLOGICAL LABORATORY • WOODS HOLE, MA 02543 • (508)289-7700
WWW.MBL.EDU/SERVICES/MRC/INDEX.HTML

zebrafish facilities

Animal and Tissue Supply for Education & Research

- 150 aquatic species available for shipment via online catalog: <http://www.mbl.edu/animals/index.html>; phone: (508)289-7375; or e-mail: specimens@mbl.edu
- zebrafish colony containing limited mutant strains
- custom dissection and furnishing of specific organ and tissue samples

MRC Services Available

- basic water quality analysis
- veterinary services (clinical, histopathologic, microbial services, health certificates, etc.)
- aquatic systems design (mechanical, biological, engineering, etc.)
- educational tours and collecting trips aboard the R/V Gemma

Using the MRC for Your Research

- capability for advanced animal husbandry (temperature, light control, etc.)
- availability of year-round, developmental life stages
- adaptability of tank system design for live marine animal experimentation

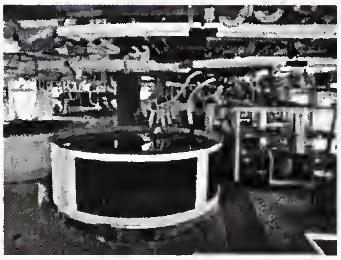

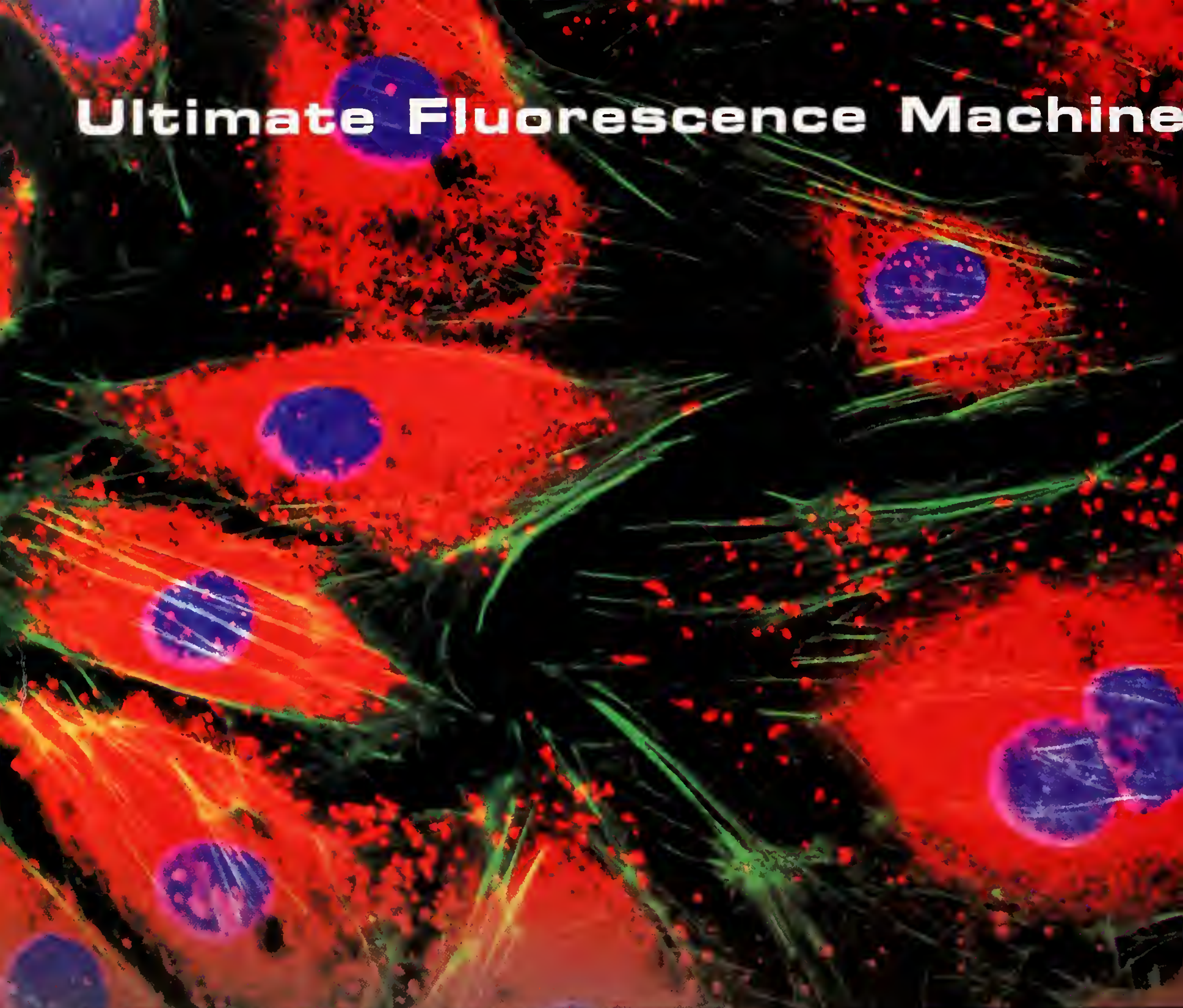

Are you continuously searching for higher contrast, increased transmission and maximum system stability for multi-channel studies? Look no further than **Axioplan 2 imaging** – the ultimate fluorescence machine.

Innovation is the key to success. ICS infinity optics and the shortest possible light paths ensure the highest transmission.

Newly designed filter cubes **'push and click'** into position for stability and precision. Contrast is dramatically improved by the unique **'Light Trap'** (patent pending) which captures stray light and deflects it away from the imaging path. The overall result has to be seen to be believed – ask for a demonstration.

Carl Zeiss MicroImaging, Inc.
One Zeiss Drive
Thornwood, NY 10594

800.233.2343
micro@zeiss.com
www.zeiss.com/micro

ZEISS

Volume 202

Number 3

THE BIOLOGICAL BULLETIN

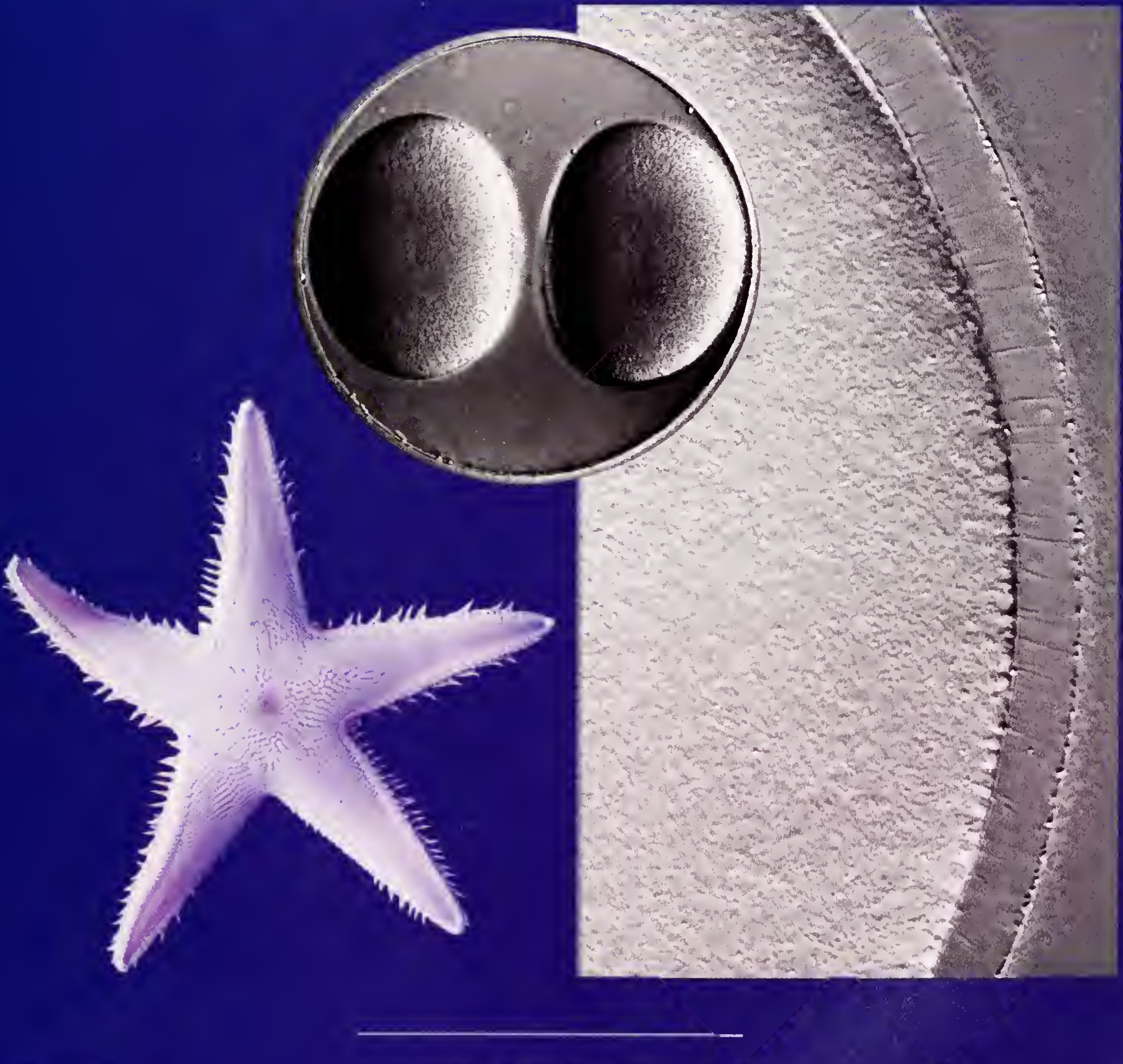

JUNE 2002

Published by the Marine Biological Laboratory

http://www.biolbull.org

THE BIOLOGICAL BULLETIN
ONLINE

The Marine Biological Laboratory is pleased to announce that the full text of *The Biological Bulletin* is available online at

http://www.biolbull.org

The Biological Bulletin publishes outstanding experimental research on the full range of biological topics and organisms, from the fields of Neurobiology, Behavior, Physiology, Ecology, Evolution, Development and Reproduction, Cell Biology, Biomechanics, Symbiosis, and Systematics.

Published since 1897 by the Marine Biological Laboratory (MBL) in Woods Hole, Massachusetts, *The Biological Bulletin* is one of America's oldest peer-reviewed scientific journals.

The journal is aimed at a general readership, and especially invites articles about those novel phenomena and contexts characteristic of intersecting fields.

The Biological Bulletin Online contains the full content of each issue of the journal, including all figures and tables, beginning with the February 2001 issue (Volume 200, Number 1). The full text is searchable by keyword, and the cited references include hyperlinks to Medline. PDF files are available beginning in February 1990 (Volume 178, Number 1), some abstracts are available beginning with the October 1976 issue (Volume 151, Number 2), and some Tables Contents are online beginning with the October 1965 issue (Volume 129, Number 2

Each issue will be placed online approximately on the date it is mailed to subscribers; therefore the online site will be available prior to receipt of your paper copy Online readers may want to sign up for the eTOC (electronic Table of Contents) service, which will deliver each new issue's table of contents *via* e-mail. The web site also provides access to information about the journal (such as Instructions to Authors, the Editorial Board, and subscription information), as well as access to the Marine Biological Laboratory's web site and other *Biological Bulletin* electronic publications.

The free trial period for access to *The Biological Bulletin* online has ended. Individuals and institutions who are subscribers to the journal in print or are members of the Marine Biological Laboratory Corporation may now activate their online subscriptions. All other access (*e.g.*, to Abstracts, eTOCs, searching, Instructions to Authors) remains freely available. Online access is included in the print subscription price.

For more information about subscribing or activating your online subscription, visit <www.biolbull.org/subscriptions>.

---

http://www.biolbull.org

OLYMPUS
XLUMPlanFl
20x/0.95 W
∞/0
The objective is not to touch the objective.

The BX51WI. A single 20x water immersion objective. A high N.A. of 0.95. A W.D. of 2.0mm. An intermediate magnification changer. Switch between low and high magnifications. Objective is untouched. Vibrations eliminated. Electrodes unmoved. It's a new movement in microscopy. **How Original. How Olympus.** Visit us at olympusamerica.com or call 1-800-446-5967.

OLYMPUS®
FOCUS ON LIFE

Cover

Early in the development of multicellular animals, information that determines the specific fate of cells and their progeny is distributed unequally at each cell division. As cleavage and the specification of embryonic territories proceeds, the location of each blastomere with respect to its neighbors must be fixed, ensuring normal development of the embryo. In mammals, the positions of the blastomeres are fixed by desmosomes. But specification begins early in many invertebrates, and long before desmosomes are formed; thus, other mechanisms are needed to fix the relative position of the blastomeres in these species.

In this issue of *The Biological Bulletin*, Shin-ichi Nemoto and his colleagues report on a novel mechanism that fixes the relative positions of blastomeres in developing embryos of the starfish *Astropecten scoparius* (see Matsunaga *et al.*, p. 213). After fertilization and elevation of the fertilization envelope the centrally positioned egg cleaves; and the daughter cells move peripherally, away from each other and toward the envelope, to which they adhere. Moreover, during subsequent cleavages, through the blastula stage, the blastomeres—mothers and daughters—remain firmly anchored in place on the fertilization envelope, as on a scaffold. This critical binding to the envelope is due to specialized microvilli that already exist on the surface of the unfertilized egg. After the fertilization envelope is raised, each microvillus extends and becomes a thin filamentous process that adheres to the inner layer of the envelope. The authors call this structure a "fixing process."

The stabilizing mechanism observed in *Astropecten scoparius* seems, at first, to be different from that in sea urchins, where the blastomeres are held in position by a hyaline layer lacking in starfish. However, Nemoto and colleagues provide evidence from immuno-electron microscopy that the material constituting the echinoid hyaline layer may be a homolog of the inner layer of the asteroid fertilization envelope—a satisfying, and unifying, conclusion.

Three important components of this story are illustrated on the cover: the starfish (about 15 cm from tip to tip, on average); the 2-cell stage (about 250 μm in diameter); and of course the fixing processes, which extend (for about 32 μm) from the surface of the fertilized egg to the inside of the fertilization envelope.

The cover images were provided by Shin-ichi Nemoto and Miwa Tamura, Ochanomizu University, Tokyo, Japan. Cover design by Beth Liles, MBL.

THE
BIOLOGICAL BULLETIN
JUNE 2002

Editor	Michael J. Greenberg	The Whitney Laboratory, University of Florida
Associate Editors	Louis E. Burnett	Grice Marine Laboratory, College of Charleston
	R. Andrew Cameron	California Institute of Technology
	Charles D. Derby	Georgia State University
	Michael LaBarbera	University of Chicago
Section Editor	Shinya Inoué, *Imaging and Microscopy*	Marine Biological Laboratory
Online Editors	James A. Blake, *Keys to Marine Invertebrates of the Woods Hole Region*	ENSR Marine & Coastal Center, Woods Hole
	William D. Cohen, *Marine Models Electronic Record and Compendia*	Hunter College, City University of New York
Editorial Board	Peter B. Armstrong	University of California, Davis
	Ernest S. Chang	Bodega Marine Lab., University of California, Davis
	Thomas H. Dietz	Louisiana State University
	Richard B. Emlet	Oregon Institute of Marine Biology, Univ. of Oregon
	David Epel	Hopkins Marine Station, Stanford University
	Kenneth M. Halanych	Woods Hole Oceanographic Institution
	Gregory Hinkle	Cereon Genomics, Cambridge, Massachusetts
	Nancy Knowlton	Scripps Inst. Oceanography & Smithsonian Tropical Res. Inst.
	Makoto Kobayashi	Hiroshima University of Economics, Japan
	Esther M. Leise	University of North Carolina Greensboro
	Donal T. Manahan	University of Southern California
	Margaret McFall-Ngai	Kewalo Marine Laboratory, University of Hawaii
	Mark W. Miller	Institute of Neurobiology, University of Puerto Rico
	Tatsuo Motokawa	Tokyo Institute of Technology, Japan
	Yoshitaka Nagahama	National Institute for Basic Biology, Japan
	Sherry D. Painter	Marine Biomed. Inst., Univ. of Texas Medical Branch
	J. Herbert Waite	University of California, Santa Barbara
	Richard K. Zimmer	University of California, Los Angeles
Editorial Office	Pamela Clapp Hinkle	Managing Editor
	Victoria R. Gibson	Staff Editor
	Carol Schachinger	Editorial Associate
	Wendy Child	Subscription & Advertising Administrator

Published by
Marine Biological Laboratory
Woods Hole, Massachusetts

http://www.biolbull.org

Marine Biological Laboratory / Woods Hole Oceanographic Institution
Library
JUN 27 2002
Woods Hole, MA 02543

Exceptional Clusters, Superior Tech Support

Microway's Reputation is Your Guarantee!

Athlon, Xeon, and Alpha Clusters

Since 1982, Microway has designed and manufactured state of the art, cost effective solutions for the High Performance Technical Computing community. Our custom Linux clusters and servers are chosen by people at universities, government research labs, biotechs, and financial institutions worldwide. Microway understands that on-time delivery, out-of-the-box reliability, and excellent ongoing technical support are critical to our users. You can have confidence that our solutions employ the latest in processor, connectivity, cluster management, and RAID technologies. Visit microway.com to see our latest products and customer testimonials.

AMD
Athlon
MP

Harness Dual Athlon Power with a Microway® Scalable 25 Node 50 Processor Cluster Using Dual Athlon MP 2000+ and Myrinet Interconnect, Yielding Peak Throughput of 166 Gigaflops.

Microway® Screamer™ Dual Alpha 21264DP 833 MHz, 16 MB Cache in RuggedRack™ Chassis with RRR™ Redundant Power Supply

Over 17,000 Satisfied Customers Since 1982 Include:

CORPORATIONS AND NON PROFITS

Allied Signal
AT&T
BAE Systems
Carnegie Institute of Washington
Cisco Systems
Cray Research
Disney Studios
EMC Corporation
Exxon
Federal Aviation Administration
Fidelity Investments
Food and Drug Administration
General Electric
General Motors
Grumman Aerospace
Hughes Aircraft
Intel
IBM
Johnson & Johnson
Lion Bioscience
Lockheed Martin
Merrill Lynch
Millennium Pharmaceuticals
Morgan Stanley
Myricom
Nikon
Raytheon Missile Systems
Smithsonian Institution
United Nations
World Bank

RESEARCH LABORATORIES

Ames Laboratory
Argonne
Berkeley Lab
Brookhaven
Lawrence Livermore
Los Alamos
MBL - Woods Hole
Jet Propulsion Lab
NASA
NIH
NIST
NDAA
NSF
Naval Air Warfare Center
Naval Postgraduate School
Naval Research Lab
Naval Surface Warfare Center
Naval Underseas Warfare Center
Oakridge National Laboratory
Sandia National Laboratory
SETI Project
US Air Force
US Army
US Army Corps of Engineers
US Dept. of Defense
US Geological Survey

UNIVERSITIES

Arizona State
Brown
BU
Cal State
Carnegie Mellon
Case Western Reserve
Colorado School of Mines
Colorado State
Columbia
Cornell
Dartmouth
Duke
Duquesne
Harvard
Johns Hopkins
McGill
Kent State
Miami
Michigan State
New Mexico
Northwestern
Princeton
Purdue
Rockefeller
Rutgers
South Carolina
Stanford
SUNY
Syracuse
Tufts
Vanderbilt
Washington (St. Louis)
Yale

TECHNICAL UNIVERSITIES

Cal Tech
Georgia Tech
MIT
New Jersey Tech
New Mexico Tech
Rensselaer (RPI)
Texas Tech
Worcester Poly Tech

UNIVERSITY OF

Alaska
Arkansas
California (Berkeley, UCLA, UCSD, UCSF)
Chicago
Connecticut
Colorado
Florida
Hawaii
Illinois
Kentucky
Maine
Maryland
Massachusetts
Mississippi
Missouri
New York
North Carolina
Pennsylvania
Texas
Utah
Virginia
Vermont
Washington
Wisconsin

Expert Integration ~ Cost Effective Solutions

> **"Our committee chose Microway over other vendors because of their reputation in the HPC community for delivering high quality, fully integrated clusters. Our decision was based also on their extensive technical expertise with Myrinet, demonstrated financial stability and ability to quickly deliver the 210 node cluster we required."**
>
> ***— Jake Ward, Director, Department of Industrial Cooperation, University of Maine at Orono***

Microway®
Technology you can count on℠

Call us: 508-746-7341
For a technical salesperson who speaks your language
Visit us: www.microway.com

CONTENTS

VOLUME 202, NO. 3: JUNE 2002

RESEARCH NOTE

Hall, Jonathon M., Christopher C. Parrish, and Raymond J. Thompson
Eicosapentaenoic acid regulates scallop (*Placopecten magellanicus*) membrane fluidity in response to cold 201

PHYSIOLOGY AND BIOMECHANICS

Yu, Xiaoli, Ernest S. Chang, and Donald L. Mykles
Characterization of limb autotomy factor–proecdysis (LAF_{pro}), isolated from limb regenerates, that suspends molting in the land crab *Gecarcinus lateralis* 204

DEVELOPMENT AND REPRODUCTION

Matsunaga, Maki, Isao Uemura, Miwa Tamura, and Shin-ichi Nemoto
Role of specialized microvilli and the fertilization envelope in the spatial positioning of blastomeres in early development of embryos of the starfish *Astropecten scoparius* 213

NEUROBIOLOGY AND BEHAVIOR

Keskinen, Essi, Yasuharu Takaku, V. Benno Meyer-Rochow, and Takahiko Hariyama
Postembryonic eye growth in the seashore isopod *Ligia exotica* (Crustacea, Isopoda) 223

SYSTEMATICS

Lapègue, S., I. Boutet, A. Leitão, S. Heurtebise, P. Garcia, C. Thiriot-Quiévreux, and P. Boudry
Trans-Atlantic distribution of a mangrove oyster species revealed by 16S mtDNA and karyological analyses . . . 232

THE LIMITS TO SELF-ORGANIZATION IN BIOLOGICAL SYSTEMS

Blazis, Diana E. J.
Introduction 245
Anderson, Carl
Self-organization in relation to several similar concepts: are the boundaries to self-organization indistinct? 247
Cole, Blaine J.
Evolution of self-organized systems 256
Deneubourg, J. L., A. Lioni, and C. Detrain
Dynamics of aggregation and emergence of cooperation 262
Detrain, Claire, and Jean-Louis Deneubourg
Complexity of environment and parsimony of decision rules in insect societies 268
Gerard, Jean-François, Eric Bideau, Marie-Line Maublanc, Patrice Loisel, and Carole Marchal
Herd size in large herbivores: encoded in the individual or emergent? 275
Hemelrijk, C. K.
Self-organization and natural selection in the evolution of complex despotic societies 283
Jeanne, Robert L., and Andrew M. Bouwma
Scaling in nests of a social wasp: a property of the social group 289
Parrish, Julia K., Steven V. Viscido, and Daniel Grünbaum
Self-organized fish schools: an examination of emergent properties 296
Roces, Flavio
Individual complexity and self-organization in foraging by leaf-cutting ants 306
Seeley, Thomas D.
When is self-organization used in biological systems? . . . 314

PUBLISHED BY TITLE ONLY 319
LIST OF PARTICIPANTS 320

* * *

Index for Volume 202 321

THE BIOLOGICAL BULLETIN

THE BIOLOGICAL BULLETIN is published six times a year by the Marine Biological Laboratory, 7 MBL Street, Woods Hole, Massachusetts 02543.

Subscriptions and similar matter should be addressed to Subscription Administrator, THE BIOLOGICAL BULLETIN, Marine Biological Laboratory, 7 MBL Street, Woods Hole, Massachusetts 02543. Subscription includes both print and online journals. Subscription per year (six issues, two volumes): $260 for libraries; $105 for individuals. Subscription per volume (three issues): $130 for libraries; $52.50 for individuals. Back and single issues (subject to availability): $45 for libraries; $20 for individuals.

Communications relative to manuscripts should be sent to Michael J. Greenberg, Editor-in-Chief, or Pamela Clapp Hinkle, Managing Editor, at the Marine Biological Laboratory, 7 MBL Street, Woods Hole, Massachusetts 02543. Telephone: (508) 289-7428. FAX: 508-289-7922. E-mail: pclapp@mbl.edu.

http://www.biolbull.org

THE BIOLOGICAL BULLETIN is indexed in bibliographic services including *Index Medicus* and MEDLINE, *Chemical Abstracts, Current Contents, Elsevier BIOBASE/Current Awareness in Biological Sciences*, and *Geo Abstracts*.

Printed on acid free paper,
effective with Volume 180, Issue 1, 1991.

POSTMASTER: Send address changes to THE BIOLOGICAL BULLETIN, Marine Biological Laboratory,
7 MBL Street, Woods Hole, MA 02543.

Copyright © 2002, by the Marine Biological Laboratory

Periodicals postage paid at Woods Hole, MA, and additional mailing offices.
ISSN 0006-3185

INSTRUCTIONS TO AUTHORS

The Biological Bulletin accepts outstanding original research reports of general interest to biologists throughout the world. Papers are usually of intermediate length (10–40 manuscript pages). A limited number of solicited review papers may be accepted after formal review. A paper will usually appear within four months after its acceptance.

Very short, especially topical papers (less than 9 manuscript pages including tables, figures, and bibliography) will be published in a separate section entitled "Research Notes." A Research Note in *The Biological Bulletin* follows the format of similar notes in *Nature*. It should open with a summary paragraph of 150 to 200 words comprising the introduction and the conclusions. The rest of the text should continue on without subheadings, and there should be no more than 30 references. References should be referred to in the text by number, and listed in the Literature Cited section in the order that they appear in the text. Unlike references in *Nature*, references in the Research Notes section should conform in punctuation and arrangement to the style of recent issues of *The Biological Bulletin*. Materials and Methods should be incorporated into appropriate figure legends. See the article by Lohmann *et al.* (October 1990, Vol. **179:** 214–218) for sample style. A Research Note will usually appear within two months after its acceptance.

The Editorial Board requests that regular manuscripts conform to the requirements set below; those manuscripts that do not conform will be returned to authors for correction before review.

1. ***Manuscripts.*** Manuscripts, including figures, should be submitted in quadruplicate, with the originals clearly marked. (Xerox copies of photographs are not acceptable for review purposes.) If possible, please include an electronic copy of the text of the manuscript. Label the disk with the name of the first author and the name and version of the wordprocessing software used to create the file. If the file was not created in some version of Microsoft Word, save the text in rich text format (rtf). The submission letter accompanying the manuscript should include a telephone number, a FAX number, and (if possible) an E-mail address for the corresponding author. The original manuscript must be typed in no smaller than 12 pitch or 10 point, using double spacing (*including* figure legends, footnotes, bibliography, etc.) on one side of 16- or 20-lb. bond paper, 8 by 11 inches. Please, no right justification. Manuscripts should be proofread carefully and errors corrected legibly in black ink. Pages should be numbered consecutively. Margins on all sides should be at least 1 inch (2.5 cm). Manuscripts should conform to the *Council of Biology Editors Style Manual*, 5th Edition (Council of Biology Editors, 1983) and to American spelling. Unusual abbreviations should be kept to a minimum and should be spelled out on first reference as well as defined in a footnote on the title page. Manuscripts should be divided into the following components: Title page, Abstract (of no more than 200 words), Introduction, Materials and Methods, Results, Discussion, Acknowledgments, Literature Cited, Tables, and Figure Legends. In addition, authors should supply a list of words and phrases under which the article should be indexed.

2. ***Title page.*** The title page consists of a condensed title or running head of no more than 35 letters and spaces, the manuscript title, authors' names and appropriate addresses, and footnotes listing present addresses, acknowledgments or contribution numbers, and explanation of unusual abbreviations.

3. ***Figures.*** The dimensions of the printed page, 7 by 9 inches, should be kept in mind in preparing figures for publication. We recommend that figures be about 1 times the linear dimensions of the final printing desired, and that the ratio of the largest to the smallest letter or number and of the thickest to the thinnest line not exceed 1:1.5. Explanatory matter generally should be included in legends, although axes should always be identified on the illustration itself. Figures should be prepared for reproduction as either line cuts or halftones. Figures to be reproduced as line cuts should be unmounted glossy photographic reproductions or drawn in black ink on white paper, good-quality tracing cloth or plastic, or blue-lined coordinate paper. Those to be reproduced as halftones should be mounted on board, with both designating numbers or letters and scale bars affixed directly to the figures. All figures should be numbered in consecutive order, with no distinction between text and plate figures and cited, in order, in the text. The author's name and an arrow indicating orientation should appear on the reverse side of all figures.

Digital art: The Biological Bulletin will accept figures submitted in electronic form; however, digital art must conform to the following guidelines. Authors who create digital images are wholly responsible for the quality of their material, including color and halftone accuracy.

Format. Acceptable graphic formats are TIFF and EPS. Color submissions must be in EPS format, saved in CMKY mode.

Software. Preferred software is Adobe Illustrator or Adobe Photoshop for the Mac and Adobe Photoshop for Windows. Specific instructions for artwork created with various software programs are available on the Web at the Digital Art Information Site maintained by Cadmus Professional Communications at http://cpc.cadmus.com/dal/

Resolution. The minimum requirements for resolution are 1200 DPI for line art and 300 for halftones.

Size. All digital artwork must be submitted at its actual printed size so that no scaling is necessary.

Multipanel figures. Figures consisting of individual parts (*e.g.*, panels A, B, C) must be assembled into final format and submitted as one file.

Hard copy. Files must be accompanied by hard copy for use in case the electronic version is unusable.

Disk identification. Disks must be clearly labeled with the following information: author name and manuscript number; format (PC or Macintosh); name and version of software used.

Color: The Biological Bulletin will publish color figures and plates, but must bill authors for the actual additional cost of printing in color. The process is expensive, so authors with more than one color image should—consistent with editorial concerns, especially citation of figures in order—combine them into a single plate to reduce the expense. On request, when supplied with a copy of a color illustration, the editorial staff will provide a pre-publication estimate of the printing cost.

4. ***Tables, footnotes, figure legends, etc.*** Authors should follow the style in a recent issue of *The Biological Bulletin* in preparing table headings, figure legends, and the like. Because of the high cost of setting tabular material in type, authors are asked to limit such material as much as possible. Tables, with their headings and footnotes, should be typed on separate sheets, numbered with consecutive Roman numerals, and placed after the Literature Cited. Figure legends should contain enough information to make the figure intelligible separate from the text. Legends should be typed double spaced, with consecutive Arabic numbers, on a separate sheet at the end of the paper. Footnotes should be limited to authors' current addresses, acknowledgments or contribution numbers, and explanation of unusual abbreviations. All such footnotes should appear on the title page. Footnotes are not normally permitted in the body of the text.

5. ***Literature cited.*** In the text, literature should be cited by the Harvard system, with papers by more than two authors cited as Jones *et al.*, 1980. Personal communications and material in preparation or in press should be cited in the text only, with author's initials and institutions, unless the material has been formally accepted and a volume number can be supplied. The list of references following the text should be headed Literature Cited, and must be typed double spaced on separate pages, conforming in punctuation and arrangement to the style of recent issues of *The Biological Bulletin*. Citations should include complete titles and inclusive pagination. Journal abbreviations should normally follow those of the U. S. A. Standards Institute (USASI), as adopted by BIOLOGICAL ABSTRACTS and CHEMICAL ABSTRACTS, with the minor differences set out below. The most generally useful list of biological journal titles is that published each year by BIOLOGICAL ABSTRACTS (BIOSIS List of Serials; the most recent issue). Foreign authors, and others who are accustomed to using THE WORLD LIST OF SCIENTIFIC PERIODICALS, may find a booklet published by the Biological Council of the U.K. (obtainable from the Institute of Biology, 41 Queen's Gate, London, S.W.7, England, U.K.) useful, since it sets out the WORLD LIST abbreviations for most biological journals with notes of the USASI abbreviations where these differ. CHEMICAL ABSTRACTS publishes quarterly supplements of additional abbreviations. The following points of reference style for THE BIOLOGICAL BULLETIN differ from USASI (or modified WORLD LIST) usage:

A. Journal abbreviations, and book titles, all underlined (for *italics*)

B. All components of abbreviations with initial capitals (not as European usage in WORLD LIST *e.g., J. Cell. Comp. Physiol.* NOT *J. cell. comp. Physiol.*)

C. *All* abbreviated components must be followed by a period, whole word components *must not* (*i.e., J. Cancer Res.*)

D. Space between all components (*e.g., J. Cell. Comp. Physiol.*, not *J.Cell.Comp.Physiol.*)

E. Unusual words in journal titles should be spelled out in full, rather than employing new abbreviations invented by the author. For example, use *Rit Vísindafjélags Islendinga* without abbreviation.

F. All single word journal titles in full (*e.g., Veliger, Ecology, Brain*).

G. The order of abbreviated components should be the same as the word order of the complete title (*i.e., Proc.* and *Trans.* placed where they appear, not transposed as in some BIOLOGICAL ABSTRACTS listings).

H. A few well-known international journals in their preferred forms rather than WORLD LIST or USASI usage (*e.g., Nature, Science, Evolution* NOT *Nature, Lond., Science, N.Y.; Evolution, Lancaster, Pa.*)

6. ***Reprints, page proofs, and charges.*** Authors may purchase reprints in lots of 100. Forms for placing reprint orders are sent with page proofs. Reprints normally will be delivered about 2 to 3 months after the issue date. Authors (or delegates for foreign authors) will receive page proofs of articles shortly before publication. They will be charged the current cost of printers' time for corrections to these (other than corrections of printers' or editors' errors). Other than these charges for authors' alterations, *The Biological Bulletin* does not have page charges.

CONTENTS
for Volume 202

No. 1: February 2002

SYSTEMATICS OF SEA MONSTERS

Carr, S. M., H. D. Marshall, K. A. Johnstone, L. M. Pynn, and G. B. Stenson
How to tell a sea monster: molecular discrimination of large marine animals of the North Atlantic 1

DEVELOPMENT AND REPRODUCTION

Page, Louise R.
Apical sensory organ in larvae of the patellogastropod *Tectura scutum* 6

Masseau, Isabelle, Pierre Bannon, Michel Anctil, and François Dubé
Localization and quantification of gonad serotonin during gametogenesis of the surf clam *Spisula solidissima* 23

Williams, Mark Elliott, and Matthew Graeme Bentley
Fertilization success in marine invertebrates: the influence of gamete age 34

Gross, Paul S., and Robert E. Knowlton
Morphological variations among larval-postlarval intermediates produced by eyestalk ablation in the snapping shrimp *Alpheus heterochaelis* Say 43

NEUROBIOLOGY AND BEHAVIOR

Stuart, Ann E., Harold E. Mekeel, and Elizabeth Kempter
Uptake of the neurotransmitter histamine into the eyes of larvae of the barnacle (*Balanus amphitrite*) 53

CELL BIOLOGY

Compère, Philippe, Marie-France Jaspar-Versali, and Gerhard Goffinet
Glycoproteins from the cuticle of the Atlantic shore crab *Carcinus maenas:* I. Electrophoresis and western-blot analysis by use of lectins 61

SYMBIOSIS AND PARASITOLOGY

Belda-Baillie, Carman A., Brett K. Baillie, and Tadashi Maruyama
Specificity of a model cnidarian-dinoflagellate symbiosis 74

ECOLOGY AND EVOLUTION

Hill, Malcolm S., and April L. Hill
Morphological plasticity in the tropical sponge *Anthosigmella varians:* responses to predators and wave energy 86

No. 2: April 2002

RESEARCH NOTES

Miner, Benjamin G., Jonathan D. Cowart, and Larry R. McEdward
Egg energetics for the facultative planktotroph *Clypeaster rosaceus* (Echinodermata: Echinoidea), revisited 97

Hertzler, Philip L.
Twin meiosis 2 spindles form after suppression of polar body 1 formation in oocytes of the marine shrimp *Sicyonia ingentis* 100

Elphick, Maurice R.
Evolution of cannabinoid receptors in vertebrates: identification of a CB_2 gene in the puffer fish *Fugu rubripes* 104

REVIEW

Cooke, Ian M.
Reliable, responsive pacemaking and pattern generation with minimal cell numbers: the crustacean cardiac ganglion 108

NEUROBIOLOGY AND BEHAVIOR

Pechenik, Jan A., Wei Li, and David E. Cochrane
Timing is everything: the effects of putative dopamine antagonists on metamorphosis vary with larval age and experimental duration in the prosobranch gastropod *Crepidula fornicata* 137

ECOLOGY AND EVOLUTION

Voight, Janet R.
Morphometric analysis of male reproductive features of octopodids (Mollusca: Cephalopoda) 148
Van Winkle, David H., and Neil W. Blackstone
Variation in growth and competitive ability between sexually and clonally produced hydroids 156
McCartney, Michael A., and H. A. Lessios
Quantitative analysis of gametic incompatibility between closely related species of neotropical sea urchins 166

SYSTEMATICS

Cameron, Christopher B.
The anatomy, life habits, and later development of a new species of enteropneust, *Harrimania planktophilus* (Hemichordata: Harrimaniidae) from Barkley Sound 182

PHYSIOLOGY AND BIOMECHANICS

Cameron, Christopher B.
Particle retention and flow in the pharynx of the enteropneust worm *Harrimania planktophilus:* The filter-feeding pharynx may have evolved before the chordates 192

No. 3: June 2002

RESEARCH NOTE

Hall, Jonathon M., Christopher C. Parrish, and Raymond J. Thompson
Eicosapentaenoic acid regulates scallop (*Placopecten magellanicus*) membrane fluidity in response to cold 201

PHYSIOLOGY AND BIOMECHANICS

Yu, Xiaoli, Ernest S. Chang, and Donald L. Mykles
Characterization of limb autotomy factor–proecdysis (LAF_{pro}), isolated from limb regenerates, that suspends molting in the land crab *Gecarcinus lateralis*. 204

DEVELOPMENT AND REPRODUCTION

Matsunaga, Maki, Isao Uemura, Miwa Tamura, and Shin-ichi Nemoto
Role of specialized microvilli and the fertilization envelope in the spatial positioning of blastomeres in early development of embryos of the starfish *Astropecten scoparius* 213

NEUROBIOLOGY AND BEHAVIOR

Keskinen, Essi, Yasuharu Takaku, V. Benno Meyer-Rochow, and Takahiko Hariyama
Postembryonic eye growth in the seashore isopod *Ligia exotica* (Crustacea, Isopoda) 223

SYSTEMATICS

Lapègue, S., I. Boutet, A. Leitão, S. Heurtebise, P. Garcia, C. Thiriot-Quiévreux, and P. Boudry
Trans-Atlantic distribution of a mangrove oyster species revealed by 16S mtDNA and karyological analyses 232

THE LIMITS TO SELF-ORGANIZATION IN BIOLOGICAL SYSTEMS

Blazis, Diana E. J.
Introduction 245
Anderson, Carl
Self-organization in relation to several similar concepts: are the boundaries to self-organization indistinct? 247
Cole, Blaine J.
Evolution of self-organized systems 256
Deneubourg, J. L., A. Lioni, and C. Detrain
Dynamics of aggregation and emergence of cooperation 262
Detrain, Claire, and Jean-Louis Deneubourg
Complexity of environment and parsimony of decision rules in insect societies 268
Gerard, Jean-François, Eric Bideau, Marie-Line Maublanc, Patrice Loisel, and Carole Marchal
Herd size in large herbivores: encoded in the individual or emergent?. 275
Hemelrijk, C. K.
Self-organization and natural selection in the evolution of complex despotic societies 283
Jeanne, Robert L., and Andrew M. Bouwma
Scaling in nests of a social wasp: a property of the social group. 289
Parrish, Julia K., Steven V. Viscido, and Daniel Grünbaum
Self-organized fish schools: an examination of emergent properties 296
Roces, Flavio
Individual complexity and self-organization in foraging by leaf-cutting ants 306
Seeley, Thomas D.
When is self-organization used in biological systems? . . . 314

Published by Title Only 319
List of Participants 320

* * *

Index for Volume 202 321

Reference: *Biol. Bull.* **202:** 201–203. (June 2002)

Eicosapentaenoic Acid Regulates Scallop (*Placopecten magellanicus*) Membrane Fluidity in Response to Cold

JONATHON M. HALL[1], CHRISTOPHER C. PARRISH[2], AND RAYMOND J. THOMPSON

Ocean Sciences Centre, Memorial University of Newfoundland, St. John's,
Newfoundland, Canada A1C 5S7

The lipid core of a biological membrane requires a certain degree of structural rigidity, but it must also be sufficiently fluid to permit lateral movement of the constituent lipids and embedded proteins. Ectotherms can counteract the ordering effects of reduced temperature by changing the structure of their membranes, a process known as homeoviscous adaptation (1). Although the content of unsaturated fatty acids in the membranes of ectothermic animals is generally known to increase in response to cold (2), no clear and direct relationship between unsaturated fatty acids and membrane fluidity has been established in marine organisms. For example, phospholipid molecular species containing docosahexaenoic acid (22:6ω3) are believed to be important in controlling finfish membrane fluidity (3–6), but a direct correlation between 22:6ω3 and membrane fluidity has not been found (4, 5, 7, 8). In contrast, we show here a simple but very strong relationship between fluidity and a single polyunsaturated fatty acid, eicosapentaenoic acid (20:5ω3), in gill membranes from a marine bivalve mollusc, the sea scallop Placopecten magellanicus.

Phospholipids are the main structural elements of biological membranes, and their physical characteristics are key determinants of membrane structure and function. Many vital cell activities that depend on the optimal functioning of membranes are therefore sensitive to the chemistry of the membrane lipids (9) and to environmental conditions, such as temperature and pressure, that perturb the phase behavior and dynamics of lipids in membranes (10). Under extreme or variable conditions, organisms can exploit the tremendous chemical diversity among membrane lipids to defend the physical properties of the membrane (10). Thus in ectotherms, where changes in temperature cause important membrane perturbations, the usual adaptive response includes a modification of lipid composition (11).

Sessile animals living in Newfoundland waters must maintain membrane structure and function in the face of extreme cold in deep waters (as low as −1.4°C) or seasonally highly variable conditions in surface waters (as much as 22°C in 6 months) (12). In the present study, we exposed sea scallops to a 10°C decrease in temperature for up to 3 weeks and then examined the relationship between the fatty acid composition of branchial phospholipids and membrane fluidity.

Vesicles were prepared from the gills of scallops acclimated to temperatures of 15 and 5°C. After three weeks of thermal acclimation, the structural order of the phospholipids was measured by electron spin resonance (ESR) spectroscopy at five temperatures (0–20°C) that span the physiological range of *Placopecten magellanicus* (Fig. 1). The vesicles prepared from gills of 5°C-acclimated scallops were significantly (ANCOVA, $P = 0.03$) less ordered than vesicles from 15°C-acclimated scallops. Temperature acclimation had shifted the order parameter curve 1–2°C toward lower assay temperatures, giving a homeoviscous efficacy (13) of 14%. Such a partial adjustment towards an ideal or complete homeoviscous response has also been found in crabs (14) and crayfish (15). In these invertebrates, the costs of perfect compensation may be too high, or the benefits too low. On the other hand, the ESR measurements in this study were made with the spin probe 5-doxyl stearic acid, reflecting the homeoviscous response in the outer region of the purified lipid bilayer. It is possible that the response deeper in the bilayer, in the actual region of alkenyl chain unsaturation, would have been greater (16).

Received 30 November 2001; accepted 22 March 2002.

[1] Present address: Department of Physiology and Experimental Medicine, The George Washington University Medical Center, Ross Hall Room 402, 2300 Eye Street, NW, Washington, DC 20037.

[2] To whom correspondence should be addressed. E-mail: cparrish@mun.ca

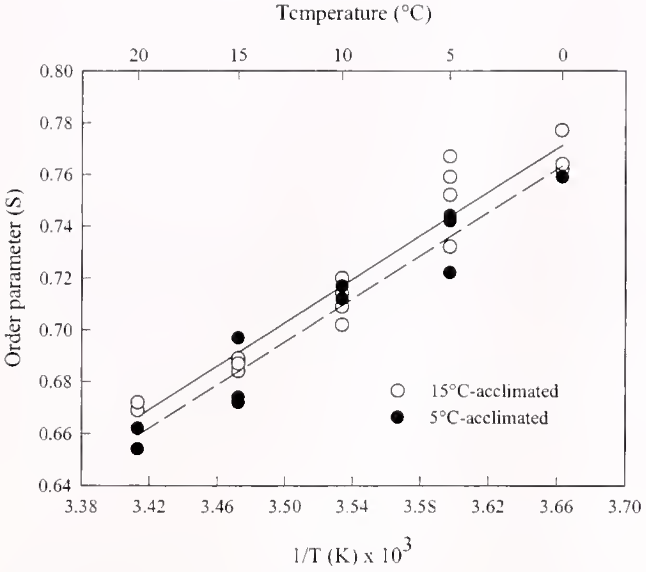

Figure 1. Temperature dependence of the structural order of phospholipids in vesicles prepared from scallop gills. The order parameter (S) was measured by electron spin resonance (ESR) using 5-doxyl stearic acid incorporated into the hydrated phospholipid vesicles. Gills were obtained from scallops acclimated in the laboratory for three weeks to 5°C ($n = 3$) and 15°C ($n = 4$). Each data point represents a single animal. The solid regression line represents 15°C acclimation, the broken line 5°C acclimation. *Methods:* Twenty-eight sea scallops of 8–12 cm shell height were collected in Placentia Bay, Newfoundland, and held at 14–15°C for 4 weeks. They were fed four times weekly a diet of two microalgae, *Isochrysis galbana* (T-Iso) and *Nanochloropsis* sp. In *I. galbana*, the major long-chain polyunsaturated fatty acid was 22:6ω3, accounting for 8.6% ± 0.4% of total fatty acids, while in *Nanochlaropsis* the major fatty acid was 20:5ω3, accounting for 34% ± 1 %. (Shorthand notation for fatty acids gives the ratio of carbon atoms to double bonds and the position of the first double bond relative to the terminal methyl group.) Four scallops were randomly selected, and their gills were sampled at 15°C; the remaining animals were then transferred directly to temperature-controlled aquaria (80 l) and maintained at 5 ± 0.5°C for up to 21 days. Four randomly selected scallops were sampled periodically from day 1 to day 21 of the experiment. The gills were excised, the phospholipids were extracted and purified according to Bligh and Dyer (28), and the fatty acid composition was determined by gas chromatography (22). Phospholipids were separated from the neutral lipids by silica column chromatography, the neutral fraction being eluted with chloroform: methanol: formic acid (9.9:0.1:0.1 by vol.) and the polar fraction with methanol (22). The spin label 5-doxyl stearic acid (29) was incorporated into the phospholipids at <1 mol%, and vesicles were prepared by sonication in Tris-HCl (6, 30). Labeled vesicles were drawn into a capillary tube, which was sealed, then centrifuged, and finally inserted into a quartz tube for ESR spectroscopy in a Bruker ESP-300 spectrometer. Spectra were obtained from 0 to 20°C at 5°C intervals, and the samples were maintained in the instrument at each temperature for 15 min before measurement. The outer and inner hyperfine splitting values were used to calculate the order parameter (16), which was interpreted to be inversely proportional to membrane fluidity. Values of the order parameter obtained for different acclimation groups were compared statistically by analysis of covariance (ANCOVA).

Membrane order in gills of thermally acclimated scallops was strongly and negatively correlated ($r = -0.714$, $P < 0.001$) with the proportion of 20:5ω3 in gill phospholipids (Fig. 2). This finding is consistent with a role for 20:5ω3 in regulating gill phospholipid structure, demonstrating one important function of this essential metabolite (17, 18), which is also believed to be an essential nutrient in scallops, because they are unable to synthesize it from precursors (19–21). The relationship between 20:5ω3 and low acclimation temperature explains, at least in part, the high proportions of this polyunsaturated fatty acid found in bivalves living permanently at sub-zero temperatures in Newfoundland waters (22).

In contrast to 20:5ω3, the proportion of 22:6ω3 was not significantly correlated with membrane gill phospholipid order. This suggests that 22:6ω3 in scallop gills may have a function other than regulating membrane fluidity, whereas finfish seem to rely mainly on changes in 22:6ω3 levels to regulate bilayer order (3, 6, 17, 23). Although the melting point of 20:5ω3 is 10°C lower (24) than that of 22:6ω3, the biological importance of 20:5ω3 is usually associated with its role as a precursor of biologically active metabolites, including prostaglandins (25, 26). The possible dual function of this fatty acid in scallop gill membranes would explain the paradoxical increase in membrane order during the first 6 days of exposure to cold (Fig. 2), since 20:5ω3 in scallops may also serve as a substrate for prostaglandin biosynthesis as a stress response to the acute drop in temperature. Gill tissues isolated from marine bivalves are known to synthesize prostaglandins in response to hypos-

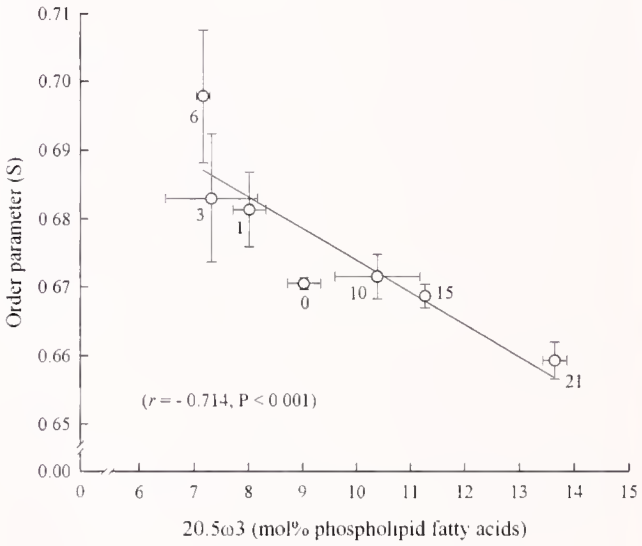

Figure 2. Relative changes in membrane fluidity as a function of the proportion of eicosapentaenoic acid (20:5ω3) in gill phospholipids of scallops during acclimation from 15 to 5°C. Data are mean ± SEM for 3–4 individuals. Membrane fluidity is expressed as an order parameter (S) using 5-doxyl stearic acid incorporated into hydrated phospholipid vesicles prepared from excised gills. Order parameter measurements were made in duplicate at an assay temperature of 20°C, and 50% of the variance in the measurements was accounted for by 20:5ω3. The numbers associated with the data points represent the time, in days, after the temperature change from 15 to 5°C.

motic stress (27), but little is known about the modes of action of these compounds in marine invertebrates (26).

Acknowledgments

This work was supported by Natural Sciences and Engineering Research Council grants to R.J.T. and C.C.P and a MUN graduate fellowship to J.M.H. We thank L.K. Thompson of the Chemistry Department of Memorial University for use of the ESR spectrometer.

Literature Cited

1. **Sinensky, M. 1974.** Homeoviscous adaptation—a homeostatic process that regulates the viscosity of membrane lipids in *Escherichia coli*. *Proc. Natl. Acad. Sci. USA* **71:** 522–525.
2. **Hazel, J. R. 1988.** Homeoviscous adaptation in animal cell membranes. Pp. 149–188 in *Physiological Regulation of Membrane Fluidity*, R. C. Aloia, C. C. Curtain, and L. M. Gordon, eds. A. R. Liss, New York.
3. **Hazel, J. R., E. E. Williams, R. Livermore, and N. Mozingo. 1991.** Thermal adaptation in biological membranes: functional significance of changes in phospholipid molecular species composition. *Lipids* **26:** 277–282.
4. **Dey, I., C. Buda, T. Wiik, J. E. Halver, and T. Farkas. 1993.** Molecular and structural composition of phospholipid membranes in livers of marine and freshwater fish in relation to temperature. *Proc. Natl. Acad. Sci. USA* **90:** 7498–7502.
5. **Buda, C., I. Dey, N. Balogh, L. I. Horvath, K. Maderspach, M. Juhasz, Y. K. Yeo, and T. Farkas. 1994.** Structural order of membranes and composition of phospholipids in fish brain cells during thermal acclimatization. *Proc. Natl. Acad. Sci. USA* **91:** 8234–8238.
6. **Fodor, E., R. Jones, C. Buda, K. Kitajka, I. Dey., and T. Farkas. 1995.** Molecular architecture and biophysical properties of phospholipids during thermal adaptation in fish: an experimental and model study. *Lipids* **30:** 1119–1126.
7. **Farkas, T., I. Dey, C. Buda, and J. E. Halver. 1994.** Role of phospholipid molecular species in maintaining lipid membrane structure in response to temperature. *Biophys. Chem.* **50:** 147–155.
8. **Bowden, L. A., C. J. Restall, and A. F. Rowley. 1996.** The influence of environmental temperature on membrane fluidity, fatty acid composition and lipoxygenase product generation in head kidney leucocytes of the rainbow trout, *Oncorhynchus mykiss*. *Comp. Biochem. Physiol.* **115B:** 375–382.
9. **Spector, A. A., and M. A. Yorek. 1985.** Membrane lipid composition and cellular function. *J. Lipid Res.* **26:** 1015–1035.
10. **Hazel, J. R., and E. E. Williams. 1990.** The role of alterations in membrane lipid composition in enabling physiological adaptation of organisms to their physical environment. *Prog. Lipid Res.* **29:** 167–227.
11. **Hazel, J. R. 1995.** Thermal adaptation in biological membranes: is homeoviscous adaptation the explanation? *Annu. Rev. Physiol.* **57:** 19–42.
12. **deYoung B., and B. Sanderson. 1995.** The circulation and hydrography of Conception Bay, Newfoundland. *Atmos.-Ocean* **33:** 135–162.
13. **Cossins, A. R. 1994.** Homeoviscous adaptation of biological membranes and its functional significance. Pp. 63–76 in *Temperature Adaptation of Biological Membranes*, A. R. Cossins, ed. Portland Press, London.
14. **Cuculescu, M., D. Hyde, and K. Bowler. 1995.** Temperature acclimation of marine crabs: changes in plasma membrane fluidity and lipid composition. *J. Therm. Biol.* **20:** 207–222.
15. **Lehti-Koivunen, S. M., and L. A. Kivivuori. 1998.** Fluidity of neuronal membranes of crayfish (*Astacus astacus* L.) acclimated to 5°C and 20°C. *Comp. Biochem. Physiol.* **119A:** 773–779.
16. **Kamada, T., and S. Otsuji. 1983.** Lower levels of erthrocyte membrane fluidity in diabetic patients: a spin label study. *Diabetes* **32:** 585–591.
17. **Bell, M. V., R. J. Henderson, and J. R. Sargent. 1986.** The role of polyunsaturated fatty acids in fish. *Comp. Biochem. Physiol.* **83B:** 711–719.
18. **Gurr, M. I., and J. L. Harwood. 1991.** *Lipid Biochemistry: an Introduction*. 4th ed. Chapman-Hall, London.
19. **Whyte, J. N. C., N. Bourne, and C. A. Hodgson. 1989.** Influence of algal diets on biochemical composition and energy reserves in *Patinopecten yessoensis* (Jay) larvae. *Aquaculture* **78:** 333–347.
20. **Marty, Y., F. Delaunay, J. Moal, and J.-F. Samain. 1992.** Changes in the fatty acid composition of *Pecten maximus* (L.) during larval development. *J. Exp. Mar. Biol. Ecol.* **163:** 221–234.
21. **Delaunay, F., Y. Marty, J. Moal, and J.-F. Samain. 1993.** The effect of monospecific algal diets on growth and fatty acid composition of *Pecten maximus* (L.) larvae. *J. Exp. Mar. Biol. Ecol.* **173:** 163–179.
22. **Parrish, C. C., Z. Yang, A. Lau, and R. J. Thompson. 1996.** Lipid composition of *Yoldia hyperborea* (Protobranchia), *Nephthys ciliata* (Nephthyidae) and *Artacama proboscidea* (Terebellidae) living at subzero temperatures. *Comp. Biochem. Physiol.* **114B:** 59–67.
23. **Behar, D., U. Cogan, S. Viola, and S. Mokaday. 1989.** Dietary fish oil augments the function and fluidity of the intestinal brush-border membrane of the carp. *Lipids* **24:** 737–742.
24. **Fasman, G. D., ed. 1975.** *CRC Handbook of Biochemistry and Molecular Biology. Lipids, Carbohydrates, Steroids*. 3rd ed. CRC Press, Cleveland.
25. **Stanley-Samuelson, D. W. 1994.** The biological significance of prostaglandins and related eicosanoids in invertebrates. *Am. Zool.* **34:** 589–598.
26. **Stanley, D. W., and R. W. Howard. 1998.** The biology of prostaglandins and related eicosanoids in invertebrates: cellular, organismal and ecological actions. *Am. Zool.* **38:** 369–381.
27. **Freas, W., and S. Grollman. 1980.** Ionic and osmotic influences on prostaglandin release from the gill tissue of a marine bivalve, *Modiolus demissus*. *J. Exp. Biol.* **84:** 169–185.
28. **Bligh, E. G., and W. J. Dyer. 1959.** A rapid method of total lipid extraction and purification. *Can. J. Biochem. Physiol.* **37:** 911–917.
29. **Schreier, S., C. F. Polnaszek, and I. C. P. Smith. 1978.** Spin labels in membranes: problems in practice. *Biochim. Biophys. Acta* **515:** 375–436.
30. **Williams, E. E., and G. N. Somero. 1996.** Seasonal-, tidal-cycle- and microhabitat-related variation in membrane order of phospholipid vesicles from gills of the intertidal mussel *Mytilus californianus*. *J. Exp. Biol.* **199:** 1587–1596.

Reference: *Biol. Bull.* **202:** 204–212. (June 2002)

Characterization of Limb Autotomy Factor–Proecdysis (LAF_{pro}), Isolated From Limb Regenerates, That Suspends Molting in the Land Crab *Gecarcinus lateralis*

XIAOLI YU[1], ERNEST S. CHANG[2], AND DONALD L. MYKLES[1,*]

[1]*Department of Biology, Cell and Molecular Biology Program, and Program in Molecular, Cellular and Integrative Neurosciences, Colorado State University, Fort Collins, Colorado 80523; and* [2]*University of California, Davis, Bodega Marine Laboratory, Bodega Bay, California 94923*

Abstract. Molting and limb regeneration are tightly coupled processes, both of which are regulated by ecdysteroid hormone synthesized and secreted by the Y-organs. Regeneration of lost appendages can affect the timing and duration of the proecdysial, or premolt, stage of the molt cycle. Autotomy of all eight walking legs induces precocious molts in various decapod crustacean species. In the land crab *Gecarcinus lateralis*, autotomy of a partially regenerated limb bud before a critical period during proecdysis (regeneration index <17) delays molting so that a secondary limb bud (2° LB) forms and the animal molts with a complete set of walking legs. It is hypothesized that 2° LBs secrete a factor, termed limb autotomy factor–proecdysis (LAF_{pro}), that inhibits molting by suppressing the Y-organs from secreting ecdysone. Molting was induced by autotomy of eight walking legs; autotomy of primary (1°) LBs reduced the level of ecdysteroid hormone in the hemolymph 73% by one week after limb bud autotomy (LBA). Injection of extracts from 2° LBs, but not 1° LBs, inhibited 1° LB growth in proecdysial animals, thus having the same effect on molting as LBA. The inhibitory activity in 2° LB extracts was stable after boiling in water for 15 min, but was destroyed by boiling 15 min in 0.1 N acetic acid or incubation with proteinase K. These results support the hypothesis that LAF_{pro} is a peptide that resembles a molt-inhibiting hormone.

Introduction

In response to injury, decapod crustaceans autotomize walking legs and claws, which are regenerated before the next molt (reviewed in Skinner, 1985; Hopkins, 1993, 2001). Limb regeneration is composed of two phases. The basal growth phase, which can occur at any time during the molt cycle, involves primarily cell proliferation and differentiation, and it results in the formation of basal papillae. The proecdysial growth phase, which is restricted to the proecdysial or premolt period (mostly stage D_0), involves tissue growth and is under hormonal control (Holland and Skinner, 1976; Hopkins, 1993, 2001). In the fiddler crab, exposure to the molting hormone 20-hydroxyecdysone (20E) is essential for the proecdysial growth phase (Hopkins, 1989). In addition, a limb growth inhibitory factor (LGIF) has been shown to inhibit rapid proecdysial growth of limb bud in the land crab (Hopkins *et al.*, 1979). Limb regeneration is measured by the regeneration index [*R* index = length of limb regenerate × 100/carapace width (Bliss *et al.*, 1966)]; in land crabs, the *R* index increases from 0 to a maximum of 22–24 about one week before ecdysis (Skinner and Graham, 1970, 1972; Holland and Skinner, 1976).

Molting in decapod crustaceans is controlled by the X-organ/sinus gland complex, which is located within the eyestalks and secretes a neuropeptide, molt-inhibiting hormone (MIH), that inhibits ecdysone production by a pair of

---

Received 10 October 2001; accepted 12 March 2002.

* To whom correspondence should be addressed. E-mail: don@lamar.ColoState.edu

Abbreviations: CHH, crustacean hyperglycemic hormone; 20E, 20-hydroxyecdysone; LAF_{an}, limb autotomy factor–anecdysis; LAF_{pro}, limb autotomy factor–proecdysis; LB, limb bud; LBA, limb bud autotomy; LGIF, limb growth inhibitory factor; MIH, molt-inhibiting hormone; MLA, multiple limb autotomy.

Y-organs located in the cephalothorax (reviewed in Skinner, 1985; Hopkins, 1992; Chang *et al.*, 1993; Laufer *et al.*, 1993). Neuropeptides possessing MIH activity have been isolated from a number of crustacean species (reviewed in Chang *et al.*, 1993; Chang, 2001; De Kleijn and Van Herp, 1995; Lacombe *et al.*, 1999). MIH acts by inhibiting steroidogenesis through a high-affinity receptor in the Y-organ cell membrane (Webster, 1993) coupled to a second-messenger cascade involving cAMP and cGMP (Sedlmeier and Fenrich, 1993; Saïdi *et al.*, 1994; Spaziani *et al.*, 1999). Molting, therefore, is induced by a reduction in MIH in the hemolymph; the Y-organs, which are no longer repressed, synthesize and secrete ecdysone. Ecdysone is then hydroxylated to the active molting hormone, 20E, by 20-monooxygenase activity in peripheral tissues, such as digestive gland, testis, epidermis, and muscle (Soumoff and Skinner, 1988).

Precocious molts can be induced by eyestalk ablation, which reduces circulating MIH and results in an immediate rise in hemolymph ecdysteroids (reviewed in Skinner, 1985). Precocious molts are also induced by autotomy from five to eight walking legs; adults of the land crab *Gecarcinus lateralis* molt 6–8 weeks after multiple limb autotomy (MLA) (Skinner and Graham, 1970, 1972; Holland and Skinner, 1976; reviewed in Skinner, 1985 and Mykles, 2001). Autotomy of one or more of the primary (1°) limb regenerates (limb bud autotomy, or LBA) before a critical period interrupts proecdysis until secondary (2°) limb buds differentiate and grow to the approximate size of those lost (Holland and Skinner, 1976). On the basis of these observations, Skinner (Skinner, 1985; Skinner *et al.*, 1992) proposed that limb buds (LBs) produce two factors that control proecdysial events. Limb autotomy factor–anecdysis, or LAF_{an}, produced by 1° LBs when at least five legs are autotomized, stimulates anecdysial animals to enter proecdysis. Limb autotomy factor–proecdysis, or LAF_{pro}, produced by 2° LBs in proecdysial animals when at least one 1° LB is autotomized, inhibits proecdysial processes.

The existence of LAF_{pro} challenges the central paradigm in crustacean endocrinology that all proecdysial processes are coordinated by the eyestalk neurosecretory centers. Proecdysis is also suspended by LBA in eyestalk-ligated animals (Holland and Skinner, 1976), indicating that the action of LAF_{pro} is not mediated by MIH or other factors secreted by the X-organ/sinus gland. The mode of action of LAF_{pro} is unknown. As a MIH-like factor it may act on Y-organs by inhibiting the secretion of ecdysone. It may also act on peripheral organs (*e.g.*, epidermis, 1° LB, claw muscle) by inhibiting the action of 20E or by inhibiting the conversion of ecdysone to 20E by monooxygenase.

Here we report the initial characterization of a factor from 2° LBs, the putative LAF_{pro}, that suspends molting in *G. lateralis*. The effects of LBA on 1° LB growth and hemolymph hormone levels were determined. The stability of the molt inhibitory activity in 2° LB extracts to boiling, acetic acid, and proteinase K was also determined. Our results suggest that LAF_{pro} is a MIH-like peptide.

Materials and Methods

Animals

Adults of the land crab *Gecarcinus lateralis* were collected in Bermuda or Puerto Rico and maintained as described (Koenders *et al.*, 2002). All eight walking legs were autotomized (multiple limb autotomy, or MLA) to induce limb regeneration and molting (Skinner and Graham, 1970, 1972). The molt stage was monitored by measuring the growth of the limb bud at the location of the second walking leg on the right side (R2). The regeneration (*R*) index, which is the ratio of the LB length to carapace width expressed as a percentage, varies from zero after autotomy to 22–24 by late proecdysis (stage D_1; Holland and Skinner, 1976). Limb regenerates that formed after MLA are referred to as 1° LBs, whereas those formed after autotomy of one or more 1° LBs (limb bud autotomy, or LBA) are designated as 2° LBs.

Preparation of limb bud extracts

Seven 1° LBs were autotomized from each animal at *R* index 13–15; the R2 regenerate was left for determining the effect of LBA on 1° LB growth. Secondary LBs were autotomized at *R* index 8–10 while growth of the R2 1° LB was still inhibited. Limb buds were frozen immediately in liquid nitrogen and stored at −80°C.

Six or seven LBs from each animal were homogenized in 2 ml of ice-cold deionized water with a Polytron homogenizer (Brinkmann Instruments, Westbury, NY) at medium speed until the tissue was completely homogenized (about 30 s). The *R* indices of the 1° LBs were between 13 and 15 (average wet weight: 38.85 mg/LB) and of the 2° LBs were between 8 and 10 (average wet weight: 7.43 mg/LB). The homogenates were centrifuged at 5000 × *g* at 4 °C for 15 min. The supernatant fraction was divided between three 1.5-ml Eppendorf tubes, lyophilized with a Speed-Vac centrifuge, and stored at −20 °C.

To assess the temperature stability of LAF_{pro}, lyophilized pellets containing three 2° LB equivalents were dissolved in 200 μl deionized water or 0.1 N acetic acid (pH 2.9), incubated in a boiling water bath for 15 min, and centrifuged at 5000 × *g* for 15 min. Supernatant fractions were lyophilized and stored at −20 °C; they were dissolved in 120 μl deionized water just before use. To assess the stability of LAF_{pro} to proteolytic digestion, supernatant fractions from extracts boiled in deionized water were incubated with proteinase K (Boehringer Mannheim; 0.5 μg/μl) at 50 °C for 1.5 h, lyophilized, and stored at −20 °C; they were dissolved in 120 μl deionized water just before use. The rationale for heating the extract before proteinase

K treatment was to remove contaminating proteins (LAF_{pro} was resistant to high temperatures) and therefore increase the effectiveness of the enzyme by reducing the amount of potential substrates. Secondary LB extracts from the same animal without the treatments served as positive controls.

Bioassay for inhibitory activity

The bioassay used proecdysial animals with eight 1° LBs (*R* index 13–16) that were growing at a constant rate (about one *R* index unit per day). Each animal received a series of three 40-μl injections of LB extract at 2-day intervals through the arthrodial membrane at the base of a walking leg. Initial experiments examined the effects of extracts from 1° or 2° LBs. Lyophilized pellets containing 6–7 LB equivalents were dissolved in 120 μl deionized water and used for an injection series. For the heat-, acetic acid-, and proteinase K-treated 2° LB extracts, three LB equivalents in 120 μl deionized water were used for an injection series, as it was found that one LB equivalent per injection was as effective in inhibiting 1° LB growth as two LB equivalents. The growth of the R2 1° LB was monitored before, during, and after the injection series at 2-day intervals.

Measurement of ecdysteroid by radioimmunoassay

Samples (100 μl) of hemolymph were combined with 300 μl methanol and stored at −20 °C for later analysis. Suspensions were centrifuged at 10,000 × *g* for 3–5 min to remove precipitated protein. Supernatant fractions were measured for ecdysteroid by radioimmunoassay as described by Chang and O'Connor (1979). Briefly, duplicate 100-μl samples were lyophilized and dissolved in 100 μl ^{3}H-ecdysone (8000 cpm/100 μl 0.1 *M* sodium borate, pH 8.4). Ecdysone antiserum (Horn *et al.*, 1976) (100 μl 1:1000 dilution in 6% normal rabbit serum, 0.002% methiolate, and 0.1 *M* sodium borate, pH 8.4) was added to each tube and incubated at room temperature for 2–4 h. After incubation, antibody was precipitated with 200 μl saturated (100%) ammonium sulfate in 0.1 *M* sodium borate (pH 8.4) and centrifuged at 4800 × *g* at 4 °C for 15 min. The pellets were washed with 400 μl 50% saturated ammonium sulfate, centrifuged at 4800 × *g* at 4 °C for 15 min, dissolved in 25 μl deionized water, and mixed with 600 μl CytoScint scintillation cocktail (ICN Biomedicals, Inc.). Radioactivity was quantified with a Beckman LS7000 liquid scintillation counter.

Statistical analysis

Data are presented as mean ± 1 standard deviation (SD). The Student's *t* test was used to determine the significance of the means between control and experimental treatments, except for the data presented in Figure 6, in which the Wilcoxon matched-pairs signed-ranks test was used.

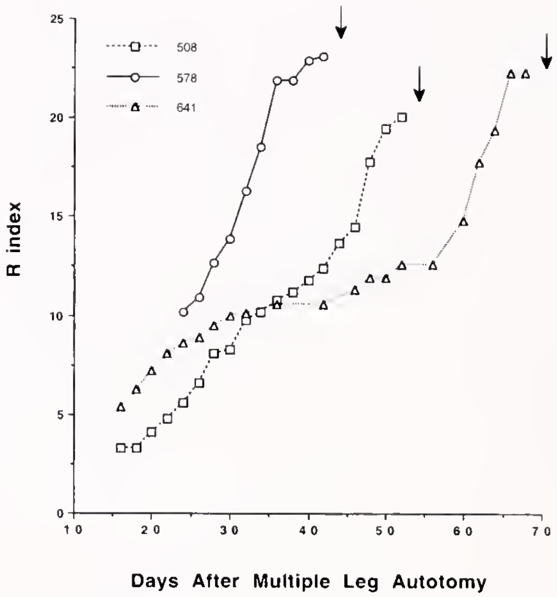

Figure 1. Primary limb bud growth and molting in *Gecarcinus lateralis* without interruption by limb bud autotomy. Animals were induced to autotomize eight walking legs on Day 0 (multiple leg autotomy, or MLA). The length of the 1° LB at the second position on the right side (R2) was measured every 2 days until molting; *R* indices were calculated as described in Materials and Methods. Three adult males (#508, #578, and #641) were selected to represent the range of responses to MLA. In most cases it took 30–45 days for animals to reach an *R* index of 15 after MLA (#508, #578). In some cases, this period could be as long as 60 days (#641). Ecdysis (arrows) occurred at 45 days (#578), 55 days (#508), and 70 days (#641) post-MLA.

Results

Effects of leg or limb bud autotomy on molting

Multiple leg autotomy induced precocious molting. The 1° LB at the second position on the right side (R2) was measured every other day after formation of basal papillae (*R* index 4–8). It usually took 30 to 45 days for animals to reach an *R* index of 15; the *R* index reached a maximum of 22–24 about 1 week before ecdysis. There was considerable individual variation in LB growth. Figure 1 shows the measurements from three individuals to represent the range of responses observed. Some animals responded quickly, with rapid LB growth rates and subsequent ecdysis 5 to 6 weeks after MLA (Fig. 1, animal #578). Other animals responded more slowly and molted about 10 weeks after MLA (Fig. 1, animal #641). Other animals had intermediate responses (Fig. 1, animal #508).

As shown previously (Holland and Skinner, 1976), LBA before a critical period (*R* index < 17) suspended LB growth and delayed molting. The measurements from one individual are shown in Figure 2 and are typical of the response of proecdysial crabs to LBA. The R2 1° LB stopped growing when the other seven 1° LBs were autotomized. The 2° LB

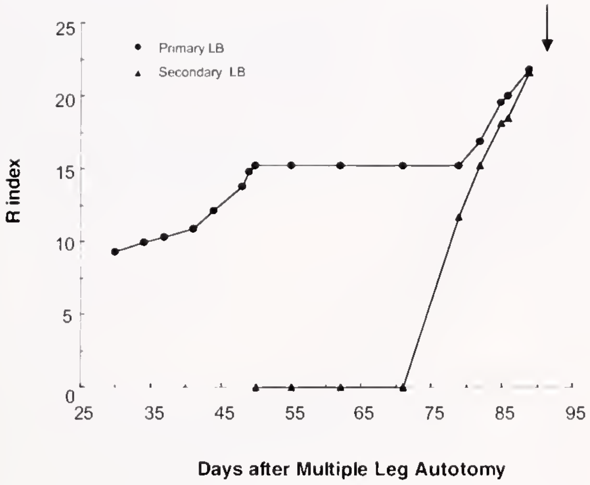

Figure 2. Limb bud autotomy suspends molting. All eight walking legs were autotomized from an adult male at Day 0, and the growth of the R2 1° LB was measured (●). On Day 50 (*R* index 15), all but the R2 1° LB were autotomized, and the growth of the L2 2° LB was measured (▲). LBA suspended proecdysis until the 2° LBs differentiated and grew to about the same size as the R2 1° LB that remained. The animal molted 91 days post-MLA (arrow), delaying ecdysis about 4 weeks.

at the second position on the left side (L2) was used to monitor 2° LB growth. Primary LB growth remained inhibited until the L2 2° LB reached a size similar to that of the autotomized 1° LB; subsequently, both 1° and 2° LBs grew continuously (Fig. 2). A consequence of LBA was that molting was delayed several weeks; for the data from the animal shown in Figure 2, molting was delayed about 30 days.

Autotomy of 2° LBs prolonged molting even further. In the experiment shown in Figure 3, seven 1° LBs were autotomized at *R* index 12.5 twenty-five days after MLA. On Day 70, all seven 2° LBs were autotomized; tertiary (3°) LBs differentiated and grew. Growth of the 1° LB remained inhibited until the L2 3° LB attained the size of the 1° LB. It took longer for the 3° LB to grow to a size similar to that of the 2° LB that was autotomized at the same location.

Effects of limb bud autotomy on hemolymph ecdysteroid

LBA reduced ecdysteroid levels in the hemolymph of animals induced to molt by MLA. In a control group in which molting was not interrupted by LBA, ecdysteroid levels increased continuously during proecdysis (Fig. 4, filled circles). In another group of animals, LBs were autotomized at *R* index 13–16, and hemolymph was sampled either during inhibition or after resumption of 1° LB growth (Fig. 4, filled and open triangles, respectively). The average ecdysteroid concentration in inhibited animals (130.3 ± 16.2 ng/ml; $n = 24$) was 45% that of the control animals (287.7 ± 28.3 ng/ml; $n = 30$) within the same range of *R* indices (between 14 and 18 in Fig. 4). However, due to the large amount of variation between individuals, the means were not significantly different. The ecdysteroid levels of animals after resumption of 1° LB growth fell within those of the control group.

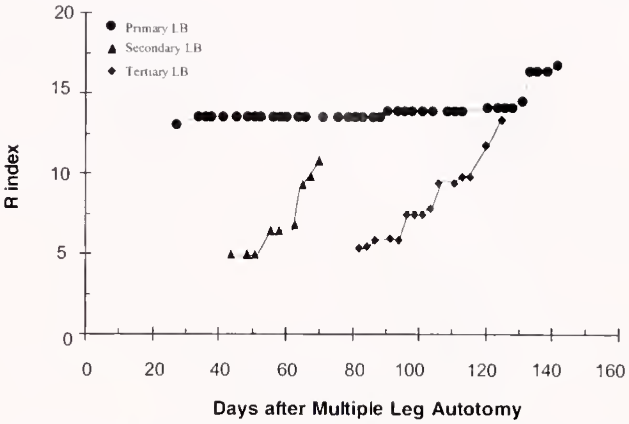

Figure 3. Autotomy of secondary limb buds prolongs proecdysis. Eight walking legs were autotomized from an adult male at Day 0, and the growth of the R2 1° LB was measured (●). On Day 27 (*R* index 12.5), seven 1° LBs were autotomized, and the growth of the L2 2° LB was measured (▲). On Day 70 all seven of the 2° LBs were autotomized, and the growth of the L2 3° LB was measured (◆). Growth of the R2 1° LB was suspended until the 3° LBs grew to a size similar to that of the 1° LB. The crab died 145 days post-MLA, before molting.

Since ecdysteroid titers varied between individuals, sam-

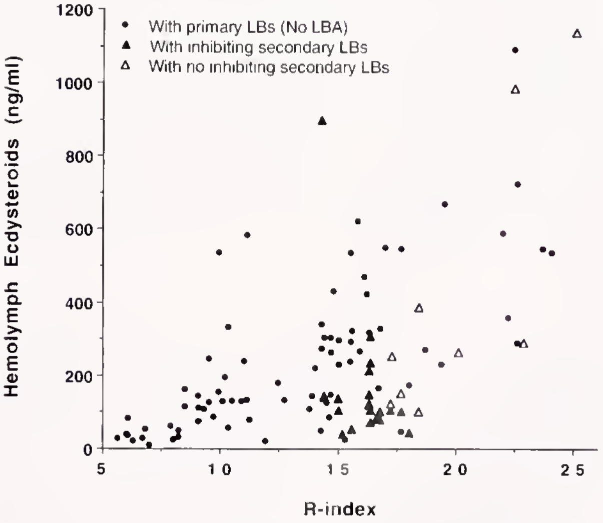

Figure 4. Effect of limb bud autotomy on hemolymph ecdysteroid concentrations during proecdysis. Molting was induced by autotomy of all eight walking legs, and 1° LB growth was monitored (*R* index). Samples were taken from three groups of animals: a control group in which proecdysis was not interrupted by LBA (●); a group subjected to LBA at *R* index 13–16 with 2° LBs (*R* index 8–10) inhibiting 1° LB growth (▲); and a group subjected to LBA at *R* index 13–16 with 2° LBs (*R* index >16) no longer inhibiting 1° LB growth (△). In most cases, hemolymph ecdysteroid was lower in animals in which 2° LBs inhibited 1° LB growth.

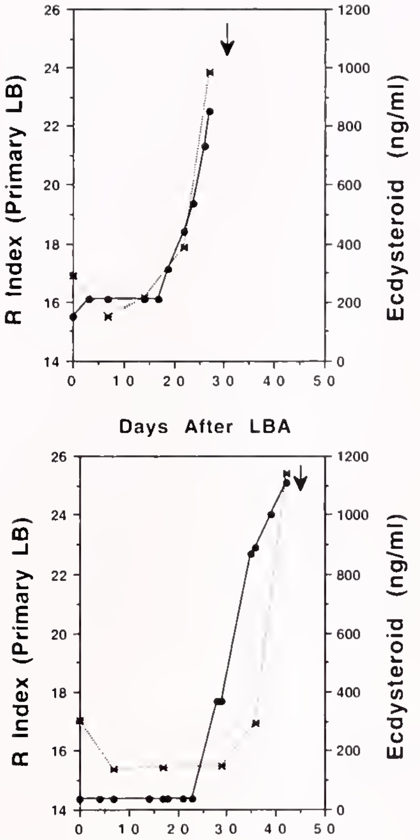

Figure 5. Effect of limb bud autotomy on hemolymph ecdysteroid concentrations in two individual crabs during proecdysis. Eight walking legs were autotomized, and the growth of the R2 1° LB was measured and expressed as *R* index (●). On Day 0, all but the R2 1° LB were autotomized, and hemolymph samples were taken at various intervals post-LBA. The ecdysteroid concentration (X) dropped within one week after LBA and remained low until the L2 2° LB approached the size of the contralateral 1° LB. There was no consistent relationship between resumption of 1° LB growth and ecdysteroid levels. For animal #805 (lower panel), the 1° LB resumed growth at Day 29 post-LBA, even though ecdysteroid level did not increase until Day 36. For animal #771 (upper panel), hemolymph ecdysteroid began to increase at Day 14, but 1° LB growth did not resume until Day 19. Arrows indicate when ecdysis occurred.

ples were taken from the same individuals on the day of LBA and the days following LBA. In Figure 5, hemolymph ecdysteroid concentrations and 1° LB growth (*R* index) from two animals (#805 and #771) are presented. LBA resulted in an immediate cessation of 1° LB growth, and ecdysteroid levels decreased about 52% by one week post-LBA. Levels remained low until 1° LB growth resumed, and the animals eventually molted. However, resumption of 1° LB growth did not always follow an increase in ecdysteroid concentration. For animal #805 (Fig. 5, upper panel), the 1° LB resumed growth by Day 29 post-LBA, even though ecdysteroid level did not increase until Day 36. For animal #771, however, hemolymph ecdysteroid began to increase by Day 14, but 1° LB growth did not resume until Day 19 (Fig. 5, lower panel). Ecdysteroid reached a maximum concentration of more than 1000 ng/ml just before ecdysis. Data from a group of animals in which hemolymph samples were taken on the day of LBA and one week after LBA are summarized in Figure 6. The level was reduced 73% at one week post-LBA; the means are significantly different ($P < 0.043$, using the Wilcoxon matched-pairs signed-ranks test).

Effects of primary and secondary limb bud extracts on molting

Proecdysial animals (*R* index 13–15) with continuously growing 1° LBs were selected for determining the effects of LB extracts on molting. An injection series consisted of injections of either 1° or 2° LB extracts (two LB equivalents/injection) at 2-day intervals, for a total of three injections per animal. Twelve proecdysial crabs were injected with 2° LB extracts; the data from three animals are shown in Figure 7 (open symbols) to represent the range of responses observed. Secondary LB extracts inhibited the growth of 1° LB during the injection series. This effect was usually sustained 2–4 days after the last injection before 1° LB growth resumed (Fig. 7, animals #124 and #386). In contrast, injection of 1° LB extracts had no effect on 1° LB growth. The data from one animal (Fig. 7; #331) is representative of the results from ten proecdysial animals that were injected with 1° LB extracts.

To quantify the effects of LB extracts, the 1° LB growth rates were determined for the 1-week intervals before and after the first injection of the series (Fig. 8). Secondary LB extracts significantly inhibited 1° LB growth by 68%, from 1.08 *R* index/day before injection to 0.35 *R* index/day dur-

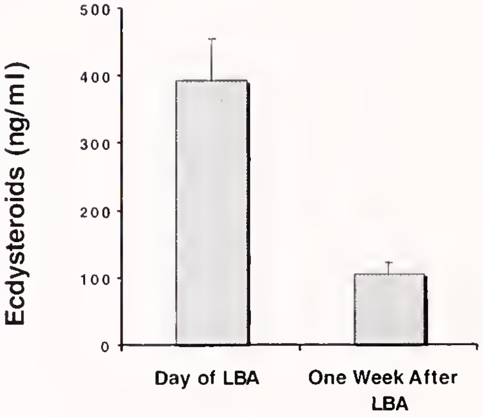

Figure 6. Hemolymph ecdysteroid concentrations before and after limb bud autotomy. Eight walking legs were autotomized, and the growth of the R2 1° LB was measured. On Day 0, a hemolymph sample was taken, followed by autotomy of all 1° LBs except the R2 1° LB; on Day 7, a second hemolymph sample was taken. LBA reduced significantly the mean ecdysteroid level 73% by one week post-LBA ($P < 0.043$; $n = 5$). Error bars are ± 1 SD.

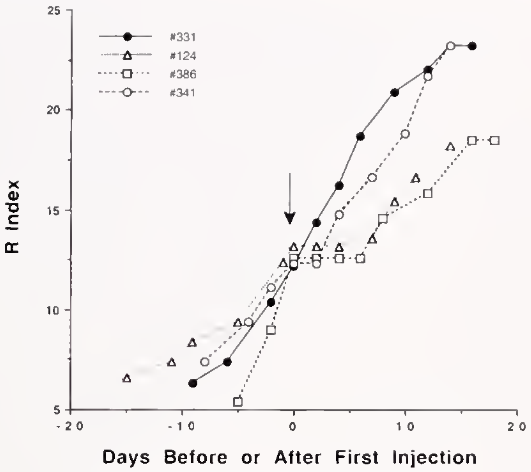

Figure 7. Effects of injection of limb bud extracts on 1° limb bud growth. Proecdysial animals (R index 13–15) were injected with extracts of either 1° LBs (●) or 2° LBs (open symbols) three times at 2-day intervals beginning at Day 0 (arrow). Each injection contained two LB equivalents (see Materials and Methods). The effect of injections was determined by monitoring the R index of the R2 1° LB. The injection of 2° LB extracts inhibited 1° LB growth (animals #124, #386, and #341), whereas injection of 1° LB extract had no effect (#331).

ing injection ($P < 0.005$; $n = 12$). The 1° LB growth rates of animals injected with 1° LB extracts were the same before and during the injection series ($P < 0.86$; $n = 10$). For animals that were allowed to complete proecdysis and molt, injection of 2° LB extract delayed ecdysis about 6 days. The interval between the first injection to ecdysis was 16 to 18 days for three animals injected with 1° LB extract and 22 to 24 days for three animals injected with 2° LB extract.

Characterization of limb autotomy factor–proecdysis

The reduction in hemolymph ecdysteroid concentration after LBA suggested that LAF_{pro}, like MIH, inhibits ecdysteroid secretion by the Y-organs. Consequently, we determined whether LAF_{pro} shared physical and chemical properties with MIH. MIH is a neuropeptide that is resistant to boiling in deionized water or acids, but is inactivated by proteases (Ranga Rao, 1965; Freeman and Costlow, 1979; Webster, 1986; Webster and Keller, 1986; Chang *et al.*, 1990).

To determine the properties of LAF_{pro}, 2° LB extracts were either boiled in deionized water, boiled in 0.1 N acetic acid, or incubated with proteinase K. An injection series consisted of three injections at 2-day intervals; each injection contained one LB equivalent (because we found that one LB equivalent was as effective as two, we used one LB equivalent to conserve material). The growth of the R2 1° LB was measured for the week before and the week after the first injection. The thermal stability of LAF_{pro} was determined by heating 2° LB extracts in a boiling water bath for 15 min. The denatured protein was removed by centrifugation, and the supernatant fraction was injected into proecdysial animals. The boiled extract significantly inhibited 1° LB growth by 68%, indicating that the factor was heat-stable (Fig. 9). In a second set of experiments, the injection of extracts boiled in 0.1 N acetic acid had no effect on 1° LB growth, while the positive control (2° LB extracts from the same animal boiled 15 min in deionized water) inhibited growth (Fig. 9). In a third set of experiments, incubation of 2° LB extracts with proteinase K also destroyed LAF_{pro} activity, as injection of treated extracts did not inhibit 1° LB growth (Fig. 9). Positive controls, in which untreated 2° LB extracts from the same animals were injected, inhibited 1° LB growth (data not shown).

Discussion

Since LB growth in decapod crustaceans is restricted to the proecdysial stage, limb regeneration must be coordinated and integrated with other physiological processes for an animal to molt successfully. In various decapod species, multiple leg autotomy (MLA) acts as a potent inducer of precocious molting, probably due to the need to restore functional appendages as quickly as possible (Skinner and Graham, 1970, 1972; Holland and Skinner, 1976; see Skinner, 1985, for additional references). Limb bud autotomy (LBA) can delay molting so that animals will molt with a

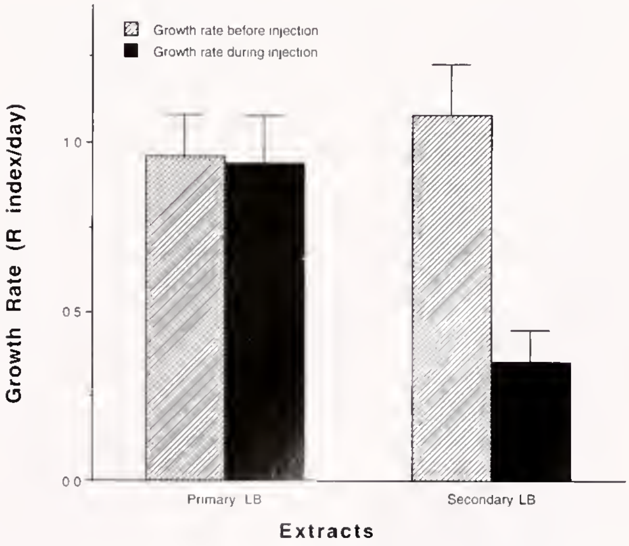

Figure 8. Injection of 2° limb bud extracts inhibits 1° LB growth. Proecdysial animals were injected with extracts of either 1° or 2° LBs, and the effect of injections was determined by monitoring the R index of the R2 1° LB. The graph compares the mean 1° LB growth rates the week before and the week after the first injection. Secondary LB extract significantly inhibited 1° LB growth ($P < 0.05$; $n = 12$). Primary LB extract did not have any significant effect on 1° LB growth ($P < 0.86$, $n = 10$). Error bars are ± 1 SD.

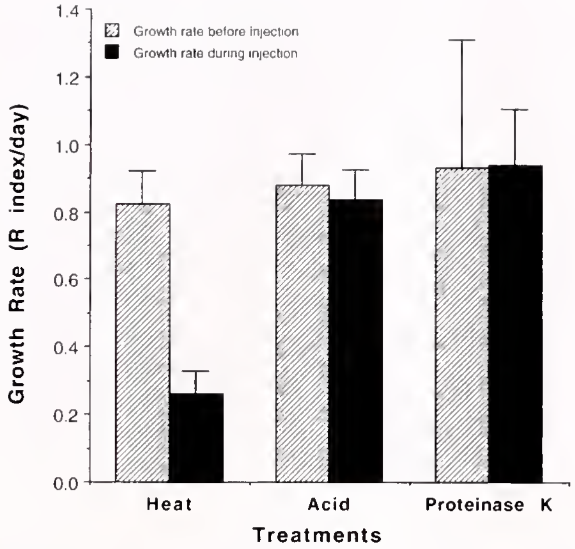

Figure 9. Characterization of LAF$_{pro}$ activity in 2° limb bud extracts. Extracts of 2° LBs were first either boiled in deionized water, boiled in 0.1 N acetic acid, or incubated with proteinase K; they were injected into proecdysial animals (R index 13–15; see Materials and Methods). The effects of injections were determined by comparing the mean 1° LB growth rates during the week before and the week after the first injection. Each injection contained one LB equivalent. Extracts boiled in deionized water retained inhibitory activity; growth rate was inhibited 68% ($P < 0.05, n = 10$). However, boiling in 0.1 N acetic acid or incubation with proteinase K destroyed the inhibitory activity; growth rates were not significantly different ($P < 0.37, n = 8$ for acetic acid and $P < 1.78, n = 7$ for proteinase K). Error bars are ± 1 SD.

full complement of appendages (Holland and Skinner, 1976; Weis, 1976; McConaugha, 1991). In *Gecarcinus lateralis*, Holland and Skinner (1976) showed that autotomy of one or more LBs before a critical stage in proecdysis (R index < 17) delays ecdysis several weeks so that 2° LBs are regenerated before the next molt. LBA causes slowing (autotomy at R index 7–10) or complete cessation (autotomy at R index 10–16) of growth of any remaining 1° LBs, as measured by R index and DNA synthesis, until 2° LBs differentiate and grow to about the same size as the 1° LBs that remain (Holland and Skinner, 1976). We obtained similar results in this study (Fig. 2). Furthermore, we showed that proecdysis is prolonged further by autotomy of 2° LBs (Fig. 3). Growth of the 3° LBs is slower than that of the 2° LBs, which suggests that repetitive regeneration places increasing energetic demands on an animal. Such demands can limit the number or size of regenerates or reduce the size increment at ecdysis (Chittleborough, 1975; Kuris and Mager, 1975; McConaugha, 1991).

The hormone 20E plays a central role in regulating molting. Thus, it is not surprising that LBA lowers hemolymph ecdysteroid levels. The changes in ecdysteroid concentration over the molt cycle follow the same general pattern in all decapod species. Beginning at proecdysis, decreased secretion of MIH results in derepression of the Y-organs. Ecdysteroid levels increase during proecdysis to a maximum in stage D_3, drop precipitously at stage D_4, and remain at low levels through metecdysis and anecdysis (reviewed in Skinner, 1985). Circulating ecdysteroid drops in response to LBA and remains low during basal regeneration; ecdysteroid titers begin to increase during the subsequent growth of the 2° LB (Figs. 5, 6; McCarthy and Skinner, 1977). Primary LBs removed later in proecdysis (R index > 17) are not regenerated, and the animal molts without the full complement of appendages (Holland and Skinner, 1976). In this case hemolymph ecdysteroid levels remain elevated (Fig. 4). This may result from reduced release of LAF$_{pro}$ from 2° LBs. Alternatively, if LAF$_{pro}$ release is sustained at R index >17, then elevated ecdysteroid may result from reduced sensitivity of Y-organs to LAF$_{pro}$. This is analogous to the reduced sensitivity of Y-organs to MIH during late proecdysis when there is maximal ecdysone production and high levels of ecdysteroid in hemolymph (Blais *et al.*, 1994).

Primary and 2° LBs respond differently to the same concentration of ecdysteroid, which suggests that limb regeneration is not regulated simply by ecdysteroid levels. It probably involves interactions between ecdysteroid and peptide factors on tissues that may have different sensitivities to these factors. Low ecdysteroid allows formation of basal papillae, since injection of exogenous ecdysone inhibits LB differentiation (Hopkins *et al.*, 1979). Higher levels are required for sustained proecdysial LB growth (Hopkins, 1989). LBA causes a decline in ecdysteroid, but the levels are still higher than those of anecdysial and early proecdysial animals (Figs. 4–6). At these levels following LBA, 2° LBs differentiate and grow, whereas 1° LBs stop growing. This differential sensitivity may be due to a higher expression of ecdysteroid receptors in 2° LBs, thus causing the 2° LBs to respond as if the ecdysteroid concentration were higher. In *Uca pugilator*, ecdysteroid receptor mRNA levels increase in 1° LBs during the proecdysial growth phase, but receptor expression was not examined in 2° LBs (Chung *et al.*, 1998). Furthermore, resumption of LB growth is not always preceded with increases in hemolymph ecdysteroid (Fig. 5), suggesting that other factors are involved. One possible factor is a limb growth-inhibiting factor (LGIF), which may be secreted by eyestalk neurosecretory centers to slow LB growth in *G. lateralis* (Hopkins *et al.*, 1979).

Secondary LBs contain a factor that inhibits proecdysial growth of limb buds and delays molting (Figs. 7, 8). We believe this factor is LAF$_{pro}$, the existence of which was originally proposed by Skinner (1985). Extracts of 2° LBs were injected into proecdysial animals before (R index 13–15) or near (R index 16–17) the critical period. Previous work by Holland and Skinner (1976) suggested that animals near the critical period would be less responsive to the extract. As expected, growth of 1° LBs slowed in the animals near the critical period (data not shown), but was completely blocked in animals at *R* index 13–15. Limb bud growth resumed 3–5 days after the final injection. Since injection of 1° LB extracts did not inhibit LB growth, it is unlikely that the cessation of LB growth by 2° LB extracts was a consequence of the injection procedure or a general toxic reaction.

Initial characterization of LAF_{pro} indicates that it is a novel molt-inhibitory factor. It is a small peptide, as it is not denatured when boiled in deionized water and it is degraded by proteinase K (Fig. 9). However, LAF_{pro} is inactivated in 0.1 N acetic acid, whereas other inhibitory peptides, such as MIH and LGIF, are acid-stable (Ranga Rao, 1965; Freeman and Costlow, 1979; Hopkins *et al.*, 1979; Webster, 1986; Webster and Keller, 1986; Chang *et al.*, 1990). MIH is a neuropeptide of about 8.5 kDa (71–78 amino acid residues, depending on species) that inhibits synthesis and secretion of ecdysone by the Y-organs (reviewed in Chang *et al.*, 1993; Chang, 2001; De Kleijn and Van Herp, 1995; Lacombe *et al.*, 1999). LGIF (M_r approximately 1 kDa) inhibits LB growth in *G. lateralis* at concentrations that have no effect on molting, and thus it appears to be distinct from MIH (Hopkins *et al.*, 1979).

Although LAF_{pro} appears to be a small peptide related to MIH, its identity remains incomplete until the inhibitory factor is purified and sequenced. Those efforts are underway. The site of LAF_{pro} synthesis is also unknown, but the factor may be synthesized in neurons in the thoracic ganglion or nerve roots and transported *via* axonal processes to the 2° LBs. This is supported by the recent discovery of crustacean hyperglycemic hormone (CHH)/MIH-immunoreactive neurons in the thoracic second roots in lobster (Chang *et al.*, 1999). Cells containing CHH-like peptides are also found in the pericardial organ and gastrointestinal tract of *Carcinus maenas* (Chung *et al.*, 1999; Webster *et al.*, 2000; Dircksen *et al.*, 2001). In lobster, hemolymph levels of CHH/MIH drop 20 days after eyestalk ablation, although significant amounts are detected as long as one year without eyestalks (Chang *et al.*, 1998). These data indicate that extra-eyestalk sites for neuropeptide synthesis and secretion are common and are biologically important. Perhaps the most compelling evidence for an extra-LB site of LAF_{pro} synthesis is that LBA has an immediate inhibition on 1° LB growth before any 2° LBs differentiate (Fig. 2; Holland and Skinner, 1976). The tissue target (or targets) of LAF_{pro} also needs to be identified. All the data are consistent with the view that LAF_{pro} acts directly on the Y-organs by inhibiting ecdysone synthesis and secretion. The neurosecretory centers in the eyestalks are not involved, since LBA inhibits 1° LB growth and lowers hemolymph ecdysteroid in eyestalk-ablated animals (Holland and Skinner, 1976; McCarthy and Skinner, 1977). We have begun experiments to determine whether LAF_{pro} blocks ecdysone secretion by land crab Y-organs *in vitro*. Our working model is that severing the thoracic nerve by LBA results in LAF_{pro} transport from neurosecretory cells in the central nervous system and release of LAF_{pro} into the hemolymph at the autotomy plane (reviewed in Mykles, 2001). LAF_{pro} suppresses ecdysone secretion by Y-organs, thus inhibiting 1° LB growth and other proecdysial processes that are ecdysteroid-dependent.

Acknowledgments

This research was supported by the National Science Foundation (IBN-9723576 and IBN-9904528). We thank Bill Mitchell (Bermuda Aquarium and Zoo), Hector C. Horta (Puerto Rico Department of Natural Resources), Hector J. Horta, and Vicki and Christopher Mykles for collecting land crabs; Courtney Rocheleau, Phillip Mendoza, and Laura Baker (Colorado State University) for animal care and technical assistance; and Eva Mulder and Sharon Chang (Bodega Marine Laboratory) for technical assistance. The authors acknowledge Dr. Dorothy M. Skinner, whose pioneering work served as inspiration to this research.

Literature Cited

Blais, C., M. Sefiani, J.-Y. Toullec, and D. Soyez. 1994. *In vitro* production of ecdysteroids by Y-organs of *Penaeus vannamei* (Crustacea, Decapoda). Correlation with hemolymph titers. *Invertebr. Reprod. Dev.* **26:** 3–11.

Bliss, D. E., S. M. E. Wang, and E. A. Martinez. 1966. Water balance in the land crab, *Gecarcinus lateralis*, during the intermolt cycle. *Am. Zool.* **6:** 197–212.

Chang, E. S. 2001. Crustacean hyperglycemic hormone family: old paradigms and new perspectives. *Am. Zool.* **41:** 380–388.

Chang, E. S., and J. D. O'Connor. 1979. Arthropod molting hormones. Pp. 797–814 in *Methods of Hormone Radioimmunoassay*, B. M. Jaffe and H. R. Behrman, eds. Academic Press, New York.

Chang, E. S., G. D. Prestwich, and M. J. Bruce. 1990. Amino acid sequence of a peptide with both molt-inhibiting and hyperglycemic activities in the lobster, *Homarus americanus*. *Biochem. Biophys. Res. Commun.* **171:** 818–826.

Chang, E. S., M. J. Bruce, and S. L. Tamone. 1993. Regulation of crustacean molting: a multi-hormonal system. *Am. Zool.* **33:** 324–329.

Chang, E. S., R. Keller, and S. A. Chang. 1998. Quantification of crustacean hyperglycemic hormone by ELISA in hemolymph of the lobster, *Homarus americanus*, following various stresses. *Gen. Comp. Endocrinol.* **111:** 359–366.

Chang, E. S., S. A. Chang, B. S. Beltz, and E. A. Kravitz. 1999. Crustacean hyperglycemic hormone in the lobster nervous system: localization and release from cells in the subesophageal ganglion and thoracic second roots. *J. Comp. Neurol.* **414:** 50–56.

Chittleborough, R. G. 1975. Environmental factors affecting growth and survival of juvenile western rock lobsters *Panulirus longipes* (Milne-Edwards). *Aust. J. Mar. Freshw. Res.* **26:** 177–196.

Chung, A. C. K., D. S. Durica, and P. M. Hopkins. 1998. Tissue-specific patterns and steady-state concentrations of ecdysteroid receptor and retinoid-X-receptor mRNA during the molt cycle of the fiddler crab, *Uca pugilator*. *Gen. Comp. Endocrinol.* **109:** 375–389.

Chung, J. S., H. Dircksen, and S. G. Webster. 1999. A remarkable, precisely timed release of hyperglycemic hormone from endocrine cells in the gut is associated with ecdysis in the crab *Carcinus maenas*. *Proc. Natl. Acad. Sci. USA* **96:** 13,103–13,107.

De Kleijn, D. P. V., and F. Van Herp. 1995. Molecular biology of neurohormone precursors in the eyestalk of Crustacea. *Comp. Biochem. Physiol.* **112B:** 573–579.

Dircksen, H., D. Böcking, U. Heyn, C. Mandel, J. S. Chung, G. Baggerman, P. Verhaert, S. Daufeldt, T. Plösch, P. P. Jaros, E. Waelkens, R. Keller, and S. G. Webster. 2001. Crustacean hyperglycaemic hormone (CHH)-like peptides and CHH-precursor-related peptides from pericardial organ neurosecretory cells in the shore crab, *Carcinus maenas,* are putatively spliced and modified products of multiple genes. *Biochem. J.* **356:** 159–170.

Freeman, J. A., and J. D. Costlow. 1979. Hormonal control of apolysis in barnacle mantle tissue epidermis, *in vitro. J. Exp. Zool.* **210:** 333–346.

Holland, C. A., and D. M. Skinner. 1976. Interactions between molting and regeneration in the land crab. *Biol. Bull.* **150:** 222–240.

Hopkins, P. M. 1989. Ecdysteroids and regeneration in the fiddler crab *Uca pugilator. J. Exp. Zool.* **252:** 293–299.

Hopkins, P. M. 1992. Hormonal control of the molt cycle in the fiddler crab *Uca pugilator. Am. Zool.* **32:** 450–458.

Hopkins, P. M. 1993. Regeneration of walking legs in the fiddler crab *Uca pugilator. Am. Zool.* **33:** 348–356.

Hopkins, P. M. 2001. Limb regeneration in the fiddler crab *Uca pugilator*: hormonal and growth factor control. *Am. Zool.* **41:** 389–398.

Hopkins, P. M., D. E. Bliss, S. W. Sheehan, and J. R. Boyer. 1979. Limb growth-controlling factors in the crab *Gecarcinus lateralis,* with special reference to the limb growth-inhibiting factor. *Gen. Comp. Endocrinol.* **39:** 192–207.

Horn, D. H. S., J. S. Wilkie, B. A. Sage, and J. D. O'Connor. 1976. A high affinity antiserum specific for the ecdysone nucleus. *J. Insect Physiol.* **22:** 901–905.

Koenders, A., X. L. Yu, E. S. Chang, and D. L. Mykles. 2002. Ubiquitin and actin expression in claw muscles of land crab, *Gecarcinus lateralis,* and American lobster, *Homarus americanus*: differential expression of ubiquitin in two slow muscle fiber types during molt-induced atrophy. *J. Exp. Zool.* **292:** 618–632.

Kuris, A. M., and M. Mager. 1975. Effect of limb regeneration on size increase at molt of the shore crabs *Hemigrapsus oregonensis* and *Pachygrapsus crassipes. J. Exp. Zool.* **193:** 353–360.

Lacombe, C., P. Grève, and G. Martin. 1999. Overview on the subgrouping of the crustacean hyperglycemic hormone family. *Neuropeptides* **33:** 71–80.

Laufer, H., J. S. B. Ahl, and A. Sagi. 1993. The role of juvenile hormones in crustacean reproduction. *Am. Zool.* **33:** 365–374.

McCarthy, J. F., and D. M. Skinner. 1977. Interruption of proecdysis by autotomy of partially regenerated limbs in the land crab, *Gecarcinus lateralis. Dev. Biol.* **61:** 299–310.

McConaugha, J. R. 1991. Limb regeneration in juveniles of the mud crab *Rhithropanopeus harrisii* following removal of developing limb buds. *J. Exp. Zool.* **257:** 64–69.

Mykles, D. L. 2001. Interactions between limb regeneration and molting in decapod crustaceans. *Am. Zool.* **41:** 399–406.

Ranga Rao, K. 1965. Isolation and partial characterization of the molt-inhibiting hormone of the crustacean eyestalk. *Experientia* **21:** 593–594.

Saïdi, B., N. De Bessé, S. G. Webster, D. Sedlmeier, and F. Lachaise. 1994. Involvement of cAMP and cGMP in the mode of action of molt-inhibiting hormone (MIH), a neuropeptide which inhibits steroidogenesis in a crab. *Mol. Cell. Endocrinol.* **102:** 53–61.

Sedlmeier, D., and R. Fenrich. 1993. Regulation of ecdysteroid biosynthesis in crayfish Y-organs: I. Role of cyclic nucleotides. *J. Exp. Zool.* **265:** 448–453.

Skinner, D. M. 1985. Molting and regeneration. Pp. 43–146 in *The Biology of Crustacea,* D. E. Bliss and L. H. Mantel, eds. Academic Press, New York.

Skinner, D. M., and D. E. Graham. 1970. Molting in land crabs: stimulation by leg removal. *Science* **169:** 383–385.

Skinner, D. M., and D. E. Graham. 1972. Loss of limbs as a stimulus to ecdysis in Brachyura (true crabs). *Biol. Bull.* **143:** 222–233.

Skinner, D. M., S. S. Kumari, and J. J. O'Brien. 1992. Proteins of the crustacean exoskeleton. *Am. Zool.* **32:** 470–484.

Soumoff, C., and D. M. Skinner. 1988. Ecdysone 20-monooxygenase activity in land crabs. *Comp. Biochem. Physiol.* **91C:** 139–144.

Spaziani, E., M. P. Mattson, W. N. L. Wang, and H. E. McDougall. 1999. Signaling pathways for ecdysteroid hormone synthesis in crustacean Y-organs. *Am. Zool.* **39:** 496–512.

Webster, S. G. 1986. Neurohormonal control of ecdysteroid biosynthesis by *Carcinus maenas* Y-organs *in vitro,* and preliminary characterization of the putative molt-inhibiting hormone (MIH). *Gen. Comp. Endocrinol.* **61:** 237–247.

Webster, S. G. 1993. High-affinity binding of putative moult-inhibiting hormone (MIH) and crustacean hyperglycaemic hormone (CHH) to membrane-bound receptors on the Y-organ of the shore crab *Carcinus maenus. Proc. R. Soc. Lond.* **251:** 53–59.

Webster, S. G., and R. Keller. 1986. Purification, characterisation and amino acid composition of the putative moult-inhibiting hormone (MIH) of *Carcinus maenas* (Crustacea, Decapoda). *J. Comp. Physiol.* **156:** 617–624.

Webster, S. G., H. Dircksen, and J. S. Chung. 2000. Endocrine cells in the gut of the shore crab *Carcinus maenas* immunoreactive to crustacean hyperglycaemic hormone and its precursor-related peptide. *Cell Tissue Res.* **300:** 193–205.

Weis, J. S. 1976. Regeneration in the fiddler crab, *Uca pugilator,* after injury or removal of limb buds. *J. Exp. Zool.* **197:** 21–30.

Reference: *Biol. Bull.* **202:** 213–222. (June 2002)

Role of Specialized Microvilli and the Fertilization Envelope in the Spatial Positioning of Blastomeres in Early Development of Embryos of the Starfish *Astropecten scoparius*

MAKI MATSUNAGA[1], ISAO UEMURA[2], MIWA TAMURA[1], AND SHIN-ICHI NEMOTO[1,*]

[1]*Department of Biology, Faculty of Science, Ochanomizu University, Otsuka, Bunkyo, Tokyo 112-8610, Japan; and* [2]*Department of Biology, Faculty of Science, Tokyo Metropolitan University, Minami-Oosawa, Hachioji, Tokyo 192-0397, Japan*

Abstract. In the eggs of a wide range of animal species, various factors that determine the blastomeres' presumptive fate are known to locate unevenly within the egg. In the embryos of these animals, cleavage occurs not just to increase cell numbers, but also to distribute the factors to the respective blastomeres, resulting in cell specialization at the later stages. In the early cleavage stages, before the establishment of a device such as desmosomes to directly join the blastomeres, some other means is needed to keep the blastomeres together and maintain the relative positions among them. In this study, we found that the embryos of the starfish *Astropecten scoparius* lack the hyaline layer seen in sea urchin embryos and that blastomeres adhere to the fertilization envelope (FE) *via* filamentous cellular projections (fixing processes). Electron microscopy revealed the fixing processes to be specialized microvilli formed, after the elevation of the FE, by the elongation of short microvilli that pre-exist in unfertilized eggs. After the first cleavage, the two blastomeres separate from each other and finally attach to the FE. In the subsequent cleavages, the blastomeres undergo repeated cell division without separating from the FE. Between the blastomeres and the FE, only shortened fixing processes were observed. Destruction of the fixing processes caused release of the blastomeres from the FE and disturbance of the relative positions of the blastomeres, resulting in abnormal development of the embryos. These observations suggest that the fixing process is a device to keep the egg placed centrally in the FE up to the first cleavage, and after the first cleavage and beyond to anchor the blastomeres to the FE so that the FE can be used as a scaffold for morphogenesis. Electron microscopy also suggests that the inner layer of the FE, which is derived from the contents of cortical granules, reinforces the adhesion of the fixing processes to the FE. Immuno-electron microscopy, using an antibody against sea urchin hyaline layer, showed that the inner layer of the FE of starfish eggs and the hyaline layer of sea urchin eggs, which are both derived from cortical granules, contain some common elements.

Introduction

In mammals, "compaction" of the embryo occurs at the 8-cell stage, leading to binding of the blastomeres together (Tarkowski and Wroblewska, 1967; Hillman *et al.*, 1972; Fleming *et al.*, 1989). The presumptive fate of the blastomeres is first determined at this stage. In these embryos there is accordingly a close relationship between the formation of a binding device for the blastomeres and their differentiation.

In most invertebrate embryos, however, the presumptive fate of each blastomere is determined at a much earlier stage than the formation of intercellular binding devices such as desmosomes (*cf.* Kuraishi and Osanai, 1989; Kiyomoto and Shirai, 1993a, 1993b). It is known that a number of morphogenetic determinants, which play a role in the determination of the blastomeres' presumptive fate, are located unevenly within the egg of these animals (Boveri, 1910; Hörstadius, 1935; Anderson and Nusslein-Volhard, 1984). In those embryos, cell division occurs not just to increase cell numbers, but also to distribute the various determinants

Received 25 June 2001; accepted 4 March 2002.

* To whom correspondence should be addressed. E-mail: snemo@cc.ocha.ac.jp

to the respective blastomeres and induce cell specialization. If the distribution of the determinants is upset, or some of the blastomeres are removed, and the spatial positions of blastomeres are changed, normal development of the embryo is disturbed (Chabry, 1887; Hörstadius, 1935; Gilbert, 1994). Animal development provides examples of many ways to maintain the relative positions among blastomeres in the period before the formation of intercellular binding devices. For example, in the embryos of jellyfish (Dan and Dan, 1947) and hydra (Martin *et al.*, 1997), species that lack an investing layer, spinning processes or ladderlike membrane structures are formed, respectively, between blastomeres. In sea urchins, a hyaline layer is formed on the surface of the egg immediately after fertilization (Endo, 1961), and this layer holds the outer surface of the embryo in place by means of microvilli (Dan and Ono, 1952; Endo, 1961). If the embryo is exposed to antibodies against the hyaline layer, normal morphogenesis is inhibited (Adelson and Humphreys, 1988). In sea urchin embryos, therefore, the relative positions among the blastomeres are maintained by the hyaline layer and microvilli (Burgess and Schroeder, 1977; Adelson and Humphreys, 1988). In the embryos of starfish, which belong to the same class of Echinodermata as sea urchins, a hyaline layer is not formed in the early cleavage stages (Matsunaga *et al.*, 2000), so some other means must exist to unite the blastomeres. In the embryos of the starfish *Astropecten scoparius*, we observed the individual blastomeres lining up along the inner surface of the fertilization envelope and found threadlike structures (fixing processes) connecting the blastomeres to the fertilization envelope. Normal morphogenesis was prevented if the connection between the blastomeres and the fertilization envelope was severed, suggesting that the fertilization envelope and the fixing process play an important role in maintaining the relative positions of the blastomeres in *A. scoparius* embryos. In this study, we examined the shape, character, and function of these fixing processes.

Materials and Methods

Handling of gametes

The starfish *Astropecten scoparius* was collected from Tateyama Bay in Chiba Prefecture, Japan. Isolated ovaries were treated with calcium-free seawater for 20–30 min, and then ovulation was induced by returning them to filtered normal seawater (NSW), yielding immature oocytes without the follicular envelope (Nemoto *et al.*, 1980). "Dry sperm" taken from isolated testes were diluted with NSW just before use. Maturation division of oocytes was induced with 2 μM of 1-methyladenine (1-MeAde; Sigma-Aldrich, St. Louis, MO) dissolved in NSW (Kanatani, 1969). At 20 °C, germinal vesicle breakdown (GVBD) and extrusion of the first and second polar bodies occurred, respectively, at about 25, 60, and 90 min after treatment with 1-MeAde. The maturing oocytes were fertilized 40 min after treatment with 1-MeAde. The fertilized oocytes and embryos were rinsed once with NSW and then cultured at 20 °C. The average diameters of the oocytes and the fertilization envelope were 210 and 300 μm, respectively.

Light microscopy

Oocytes, eggs, and embryos were flattened to a 180-μm thickness and examined under a differential interference-contrast microscope (Axiophoto; Zeiss, Oberkochen, Germany). Microphotographs were taken with Neopan 400 Presto film (Fuji Photo Film, Tokyo, Japan).

Transmission electron microscopy

Two fixing methods were used in this study. A quick-freeze and freeze-substitution method was mainly used for examination of cytoskeletons, and chemical fixation was used for examination of other structures.

Chemical fixation. Oocytes and embryos were first fixed in 2% glutaraldehyde (TAAB, Berkshire, England) dissolved in NSW for 2 h at room temperature, then in Karnovsky's fixative (Karnovsky, 1965) for 2 h at room temperature, followed by 10 h at 4 °C. After being rinsed several times with 0.1 M sodium-cacodylate buffer (pH 7.2), they were then fixed in 1% osmium tetroxide (Polyscience, Warrington, PA) dissolved in 0.1 M sodium cacodylate for 60 min on ice (Steinbeck *et al.*, 1993). The fixed specimens were rinsed twice with distilled water (DW) and then dehydrated with ethanol.

Quick-freeze and freeze-substitution fixation. Oocytes were first treated with 15% butanediol (Wako Pure Chemical, Tokyo, Japan) diluted with NSW for 20 min on ice (Reimer and Crawford, 1997), and then they were collected with a hand-driven centrifuge. A 20-μl aliquot of the specimen was placed on an electron microscopy grid. Excess NSW was drawn off with a piece of filter paper, and the specimens were frozen by immersion for 10 s in liquid propane that had itself been cooled with liquid nitrogen. The frozen materials were placed in 4% osmium tetroxide/acetone cooled to −90 °C. Five days later, the specimens were first brought up to −20 °C and then to 4 °C for 2 h each. They were finally placed at room temperature (Burke *et al.*, 1998) and dehydrated using acetone.

Embedding and examination. The dehydrated specimens were embedded in epoxy resin (Kushida, 1980), and ultrathin sections (90 nm in thickness) were produced using an ultramicrotome (MT-XL, RMC Inc., Tucson, AZ). The sections were stained with uranyl nitrate and lead acetate for 2 min each and examined under a JEOL 1010 transmission electron microscope (JEOL, Tokyo, Japan).

Immuno-electron microscopy

Ultrathin sections made from the chemically fixed specimens underwent 5 min of etching with 3% sodium meta-

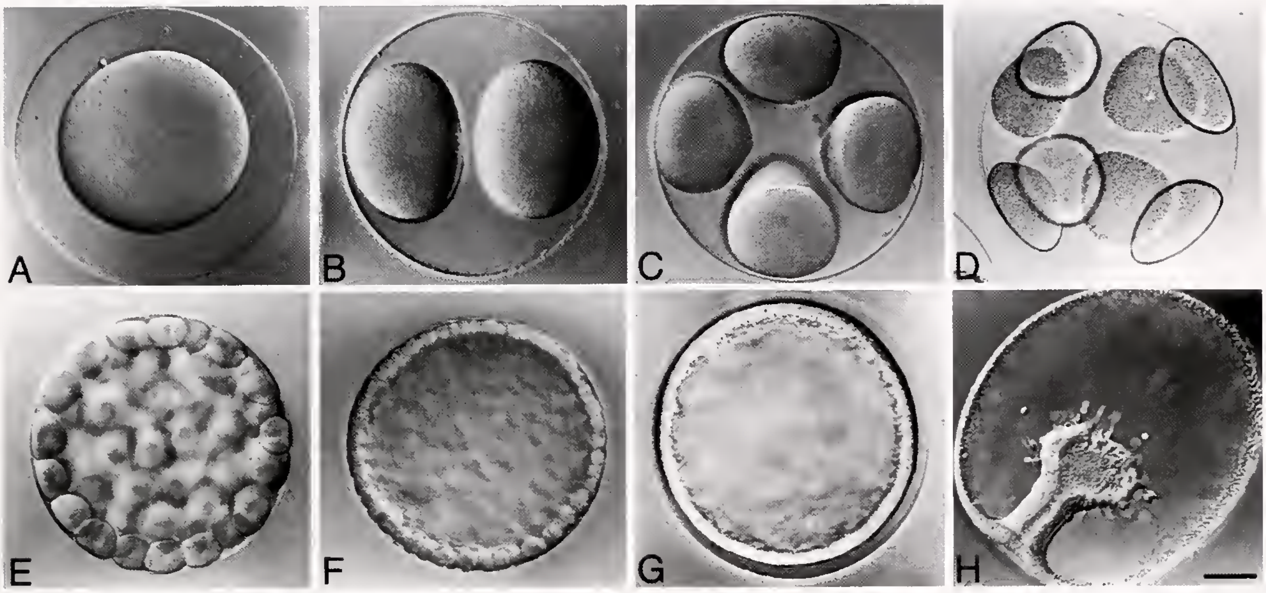

Figure 1. Development of *Astropecten scoparius* embryos derived from oocytes fertilized 40 min after treatment with 1-MeAde. (A) Just after the completion of meiotic division (2 h 10 min after 1-MeAde treatment). A second polar body is seen at the upper left of the egg. (B) The 2-cell stage just before the second cleavage (2 h 40 min). The two blastomeres moved toward and adhered to the fertilization envelope, producing space between them. (C) The 4-cell stage just before third cleavage (3 h 10 min). The blastomeres are separated from each other along the fertilization envelope in a direction perpendicular to the cleavage plane. (D) The 8-cell stage just after cleavage (3 h 40 min). The blastomeres adhere to the fertilization envelope, and adjacent blastomeres have become widely separated. (E) The 2^6-cell stage (6 h 10 min). The blastomeres continued to undergo cell division without separating from the fertilization envelope, and eventually lined up along the inside surface of the fertilization envelope. (F) The 2^8-cell stage (7 h 10 min). A blastula consisting of a single cell layer. (G) A rotating blastula just before hatching (12 h 40 min). A space is seen between the fertilization envelope and the embryo. (H) A gastrula (24 h 40 min). Scale bar: 50 μm.

periodate. After being rinsed with DW, they were treated with an antibody raised against sea urchin hyaline layer (Yazaki, 1968) diluted in 0.2% Tween 80 for 5 min at room temperature. After another rinse with DW, the sections were treated with an anti-rabbit IgG antibody (Sigma-Aldrich) bound to protein A-colloidal gold (20 nm in diameter), diluted 1/40 in 0.2% Tween 80, for 5 min (Morris and Ciraolo, 1997). These sections were not stained with lead acetate or uranyl nitrate.

Results

Cleavage and development of fertilized eggs

Oocytes fertilized immediately following germinal vesicle breakdown (GVBD) extruded a second polar body 1½ h after treatment with 1-MeAde, completing their maturation division (Fig. 1A). As with the embryos of other starfish species, elevation of the fertilization envelope continued for about 2 h after fertilization. The first cleavage occurred some 40 min after the formation of the second polar body. After the first cleavage, the two blastomeres moved in a direction perpendicular to the cleavage plane, as if to separate from each other. Some 15–20 min after the first cleavage, the two blastomeres impressed themselves into the fertilization envelope at the surface of their mitotic poles (Fig. 1B). As the area of contact between the blastomeres and the fertilization envelope became progressively larger, the blastomeres changed their shape to ellipsoids with the long axis in the animal-vegetal pole direction, producing space between them. The second cleavage occurred some 30 min after the first. After this cleavage, as after the first, space was produced between the blastomeres (Fig. 1C). The cleavage plane for the third cleavage was formed at right angles to the first and second cleavage planes. After this division also, the blastomeres did not separate from the fertilization envelope (Fig. 1D). The blastomeres at this stage adhered to the fertilization envelope over a wide area and had become flattened. Adjacent blastomeres had become widely separated from each other. A hyaline layer could not be distinguished. At the 16-cell stage and beyond, blastomeres continued to undergo cell division without separating from the fertilization envelope, and they lined up along its inside surface (Fig. 1E). As a result, the embryo did not go through the cell-mass, "morula" shape, but became a blastula consisting of a single cell layer (Fig. 1F). When hatching commenced, a space developed between the fertilization envelope and the embryo, and the embryo began to spin around (Fig. 1G). Gastrulation began about 3 h

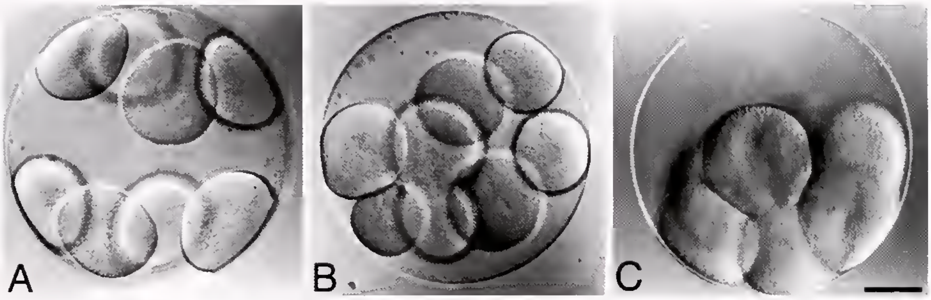

Figure 2. Effect of acidified seawater (pH 4) treatment for 1 min at the 8-cell stage on the alignment of blastomeres. (A) Just before the treatment (3 h after fertilization). Blastomeres show a flattened shape, attaching to the fertilization envelope. (B) One minute after the treatment. Blastomeres changed from ellipsoid to spherical, and the area of the cell surface in contact with the fertilization envelope became smaller. (C) After brief centrifugation. Blastomeres are gathered to the centrifugal end inside the fertilization envelope. Scale bar: 50 μm.

after hatching. The embryos developed to mid-gastrulae 10 h after hatching (Fig. 1H). Development beyond this stage was described by Oguro *et al.* (1976).

Morphogenesis of embryos that have lost attachment between blastomeres and the fertilization envelope

When embryos at the 8-cell stage (3 h postfertilization) were subjected to a 1-min pulse treatment with acidified seawater adjusted to pH 4 with HCl, blastomeres changed from a flattened shape to a globular one, and the area of the cell surface in contact with the fertilization envelope became smaller (compare Fig. 2A with Fig. 2B). Blastomeres also became globular when the fertilization envelope was removed. When embryos treated with acidified seawater were returned to NSW and then gently spun with a hand-driven centrifuge, blastomeres were gathered at the centrifugal end inside the fertilization envelope (Fig. 2C). In untreated embryos, however, the arrangement of the blastomeres was not disturbed even by such centrifugation. These results indicate that the attachments between the fertilization envelope and the blastomeres are severed by treatment with acidified seawater.

Even after embryos pulse-treated with acidified seawater were returned to NSW, the blastomeres did not restore their connection with the fertilization envelope but remained globular, not returning to their normal flattened shape. At 24 h postfertilization, at which time control embryos had formed gastrulae, the embryos treated with acidified seawater alone were morphologically abnormal, many with distorted shapes or abnormal archenterons, and some embryos had multiple archenterons (Fig. 3A, B). The effects of treatment with acidified seawater were especially marked if conducted between 3 and 4.5 h postfertilization (8- to 64-cell stage). No morphological abnormalities were seen in embryos treated with acidified seawater 6.5 h postfertilization (2^9-cell stage) (Fig. 3C), and normal gastrulae were formed 24 h postfertilization (Fig. 3D). The effect of acidified seawater treatment was no longer observed when it was done with embryos 6.5 h postfertilization and beyond. These results indicate that in the early stages of cleavage, blastomeres in *A. scoparius* embryos maintain their spatial positions relative to each other by means of the fertilization envelope.

The mechanism of anchoring blastomeres to the fertilization envelope

The above observations suggest the existence of some means that attaches blastomeres to the fertilization envelope. Within a minute postinsemination, when the fertilization envelope could be identified, a number of particles were observed in the perivitelline space (perivitelline-space particles) (Fig. 4A). A few minutes after insemination, many thin processes connecting the fertilization envelope and the egg proper could be seen (Fig. 4B, arrow). These processes will hereafter be referred to as fixing processes. These fixing processes elongated rapidly with elevation of the fertilization envelope and were located over the entire surface of the egg. The perivitelline-space particles moved along the fixing processes towards the fertilization envelope (Fig. 4B, arrowheads), reaching it by several minutes after insemination, by which time very few could be seen in the perivitelline space (Fig. 4C). The perivitelline-space particles adhering to the fertilization envelope eventually disappeared, leaving a smooth inner surface (Fig. 4C). Around this time, the basal part of the process assumed the shape of a cone (Fig. 4C, white arrowheads). After the first cleavage, fixing processes could still be seen between the blastomeres and the fertilization envelope but not on the surface of the cleavage furrow (Fig. 4D; *cf.* Fig. 5A). The length of the fixing processes varied with the distance between the egg surface and the fertilization envelope; the longest, some 60 μm, was seen in the vicinity of the cleavage furrow (Fig. 4D). Near the boundary between the areas of the blastomeres touching the fertilization envelope, fixing processes were short and straight, with no bending being seen. Short

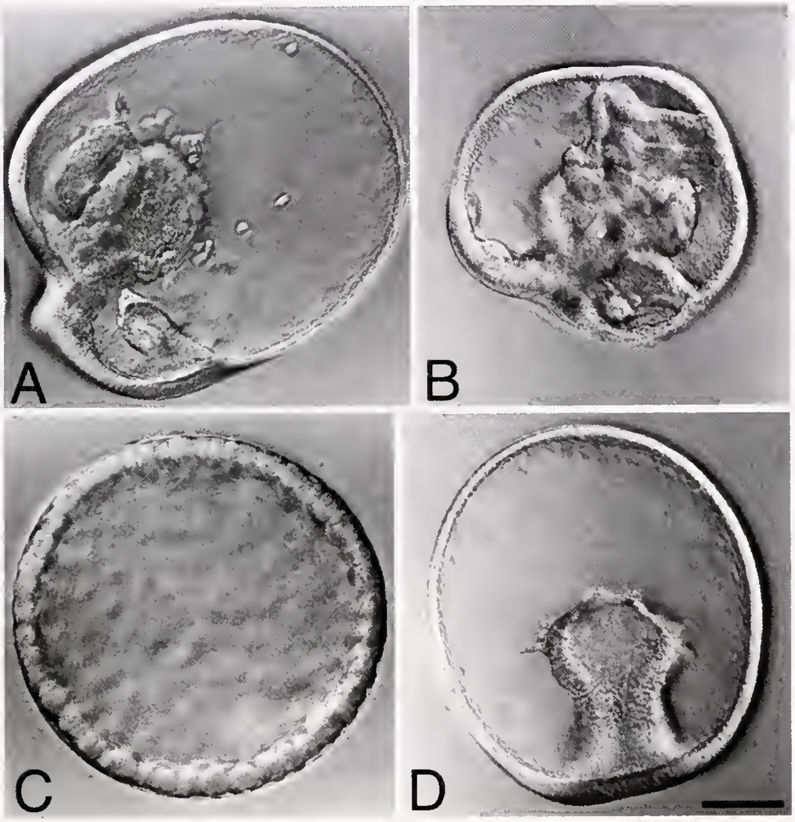

Figure 3. Development of embryos treated with acidified seawater. (A, B) Embryos cultured in normal seawater for 21 h after 1-min pulse treatment with acidified seawater at the 8-cell stage (3 h after fertilization). (A) An embryo with multiple archenterons. (B) An embryo showing abnormal morphology. (C) An embryo just after acidified-seawater treatment at the 2^9-cell stage (6.5 h after fertilization). No marked changes in morphology are observed (*cf.* Fig.1F). (D) An embryo from the same batch of embryos as in C, cultured for 17.5 h in normal seawater after the treatment, showing normal morphology of gastrula. Scale bar: 50 μm.

fixing processes were also observed in embryos at later stages of development (Fig. 5A, white arrowheads).

In embryos at the 8-cell stage, blastomeres still adhered to the fertilization envelope over a wide area and were ellipsoid (Fig. 5A; *cf.* Fig. 2A). Fixing processes (white arrowheads), near the boundary between the areas of the blastomeres touching the fertilization envelope, were thin and straight. After a 1-min pulse treatment with acidified seawater (Fig. 5B), fixing processes were badly damaged and became deformed and thicker (arrowheads) than those of embryos before treatment; they looked as if they had lost their rigidity. Blastomeres separated from the fertilization envelope and became roughly spherical. These observations suggest that the fixing processes are the way that blastomeres are anchored to the fertilization envelope.

Transmission electron microscopic examination of fixing processes

Microvilli, some 700 nm in length, were identified embedded in the vitelline coat on the surface of both immature (Fig. 6A) and maturing unfertilized oocytes (Fig. 6B). At 30 s postfertilization, the tips of the microvilli were connected to the vitelline coat that was transforming into the fertilization envelope (Fig. 6C, arrows). Subsequently, the microvilli elongated with the elevating of the fertilization envelope (Fig. 6D, E). The fixing processes seen under light microscopy (Figs. 4 and 5) are therefore considered to be specialized microvilli. These specialized microvilli sprout from all over the surface of the egg. At early cleavage stages, short fixing processes some 500 nm in length were seen on the surface of the blastomeres adhering to the fertilization envelope (Fig. 6F), and the tips of those processes were connected with the fertilization envelope (arrows). No extracellular matrix surrounding the embryo, such as a hyaline layer, was observed (Fig. 6D–F). Some membranous structures (white asterisk) were sometimes seen in the space between the blastomeres and the fertilization envelope.

In the specimens prepared by the quick-freeze and freeze-substitution method, bundles of fibers could be identified within microvilli in immature oocytes (Fig. 6A). After oocyte maturation, these fiber bundles extended in the direc-

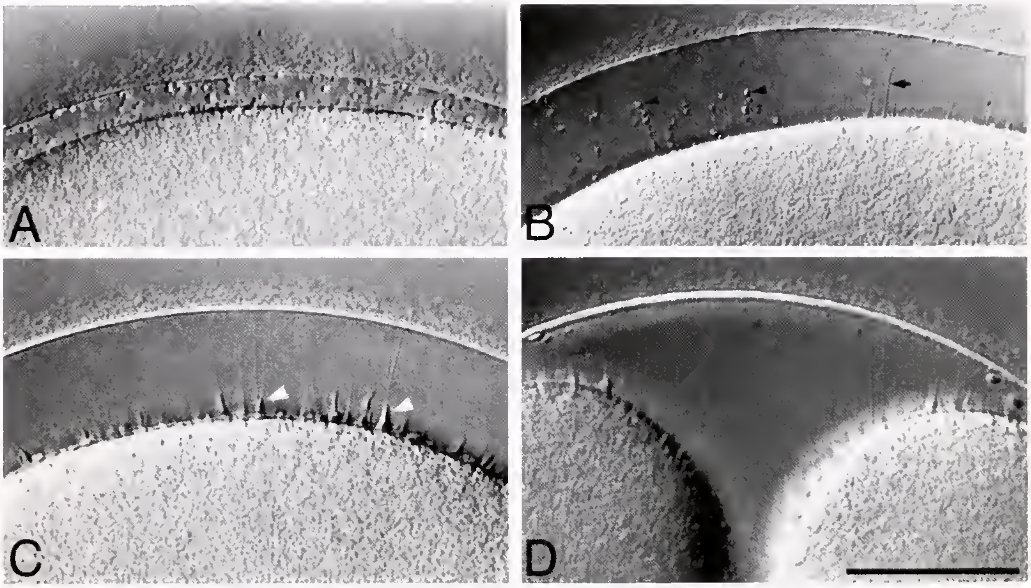

Figure 4. Surface change of eggs immediately after fertilization (inseminated 40 min after 1-MeAde treatment). (A) Forty seconds after insemination. A number of particles are observed in the perivitelline space (perivitelline-space particles). (B) Two minutes after insemination. Note thin processes (fixing processes; arrow) connecting the fertilization envelope and the egg. Perivitelline-space particles (arrowheads) moved along the fixing processes towards the fertilization envelope. (C) Three minutes after insemination. Note the prominent cone-like shape at the bases of the fixing processes (white arrowheads). Very few perivitelline-space particles could be seen in the perivitelline space. (D) The 2-cell stage (3 h after insemination). Fixing processes were elongated in the vicinity of the cleavage furrow and were shortened near the boundary between the areas of the blastomeres touching the fertilization envelope. Scale bar: 50 μm.

tion of the cytoplasm (Fig. 6B, white arrow), reaching a length of 2 μm. The diameter of these fibers was 5–6 nm, so they can be considered microfilaments. Crossing the microfilament bundle, repeated bands were observed (Fig. 6B, black arrowheads).

We could not examine microfilaments in the fixing processes by transmission electron microscopy, because the fixing processes were not preserved by the quick-freeze and freeze-substitution fixation that effectively preserves microfilaments. To get information on these microfilaments, we examined the effects of cytochalasin D on the fixing processes. When the cytochalasin was applied to fertilized eggs, intact fixing processes disappeared within several minutes of treatment, and only fragmented fixing processes were observed in the perivitelline space (Fig. 7A). In embryos pulse-treated with the cytochalasin at early cleavage stages, the fixation of blastomeres on the fertilization envelope were severely damaged, and the blastomeres changed shape from flattened to globular (compare Fig. 7B with Figs. 1D and 2A). These results suggest the presence of microfilaments in the fixing processes.

Immuno-electron microscopic examination of the perivitelline-space particles

In unfertilized maturing oocytes, granular structures with fairly high electron density could be seen along the cortex (Fig. 8A, asterisks). On fertilization, these granules opened

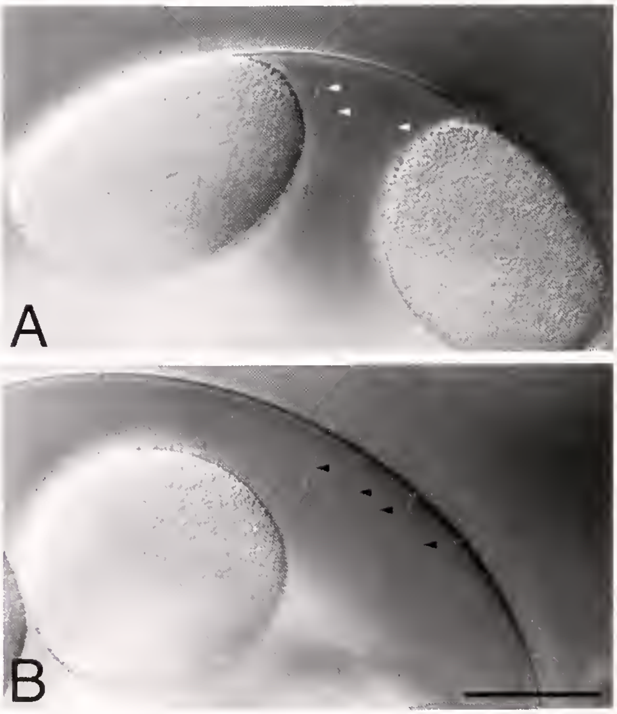

Figure 5. Changes of fixing processes after treatment of 8-cell stage embryos with acidified seawater. (A) An egg before the treatment. Fixing processes are straight and thin (white arrowheads). (B) Two minutes after the treatment. Fixing processes became thicker and were badly damaged (black arrowheads), and the blastomeres changed their shape from ellipsoid to spherical. Scale bar: 50 μm.

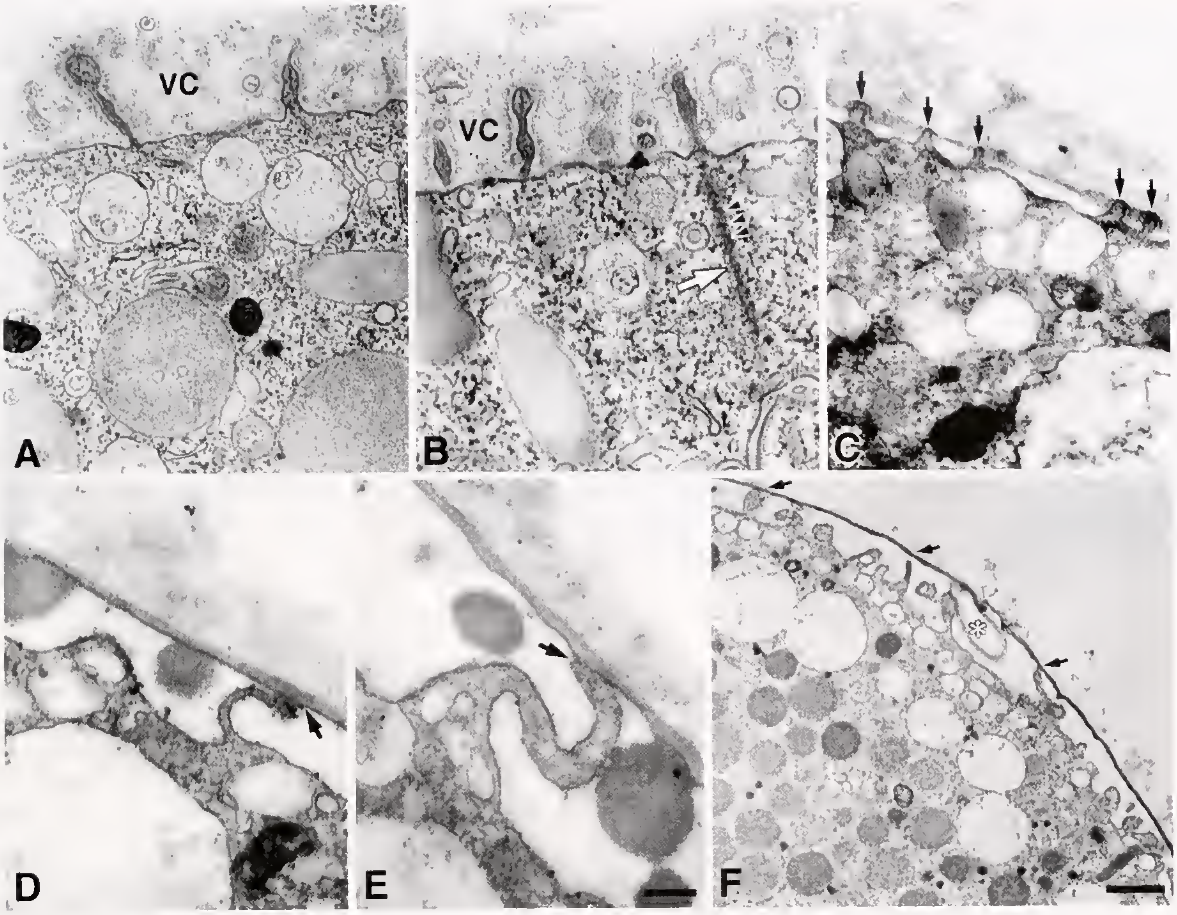

Figure 6. Transmission electron microscopy of microvilli and fixing processes. (A, B) Quick-freeze and freeze-substitution fixation. (C-F) Chemical fixation. (A) An immature oocyte. Microvilli were identified embedded in the vitelline coat (VC) on the surface of the oocyte. Note bundles of fibers within microvilli. (B) A maturing oocyte 40 min after 1-MeAde treatment. Fiber bundles inside microvilli extend into the cytoplasm (white arrow). On the fiber bundles, some repeated strips are observed (black arrowheads). (C) Thirty seconds after insemination (40 min after 1-MeAde treatment). The tips of microvilli (arrows) were connected to the vitelline coat that was transforming into the fertilization envelope. (D) One minute after insemination. Microvilli were lengthening with the elevation of the fertilization envelope, thereby transforming themselves into the fixing processes. A fixing process attached to the electron-dense innermost layer of the fertilization envelope (arrow). (E) Two minutes after insemination. The length of microvilli increased compared to that in D. A fixing process attached to the electron-dense innermost layer of the fertilization envelope (arrow). (F) The 8-cell stage. Short fixing processes were observed on the blastomere surface adherent to the fertilization envelope. The tips of the processes were connected with the fertilization envelope (arrows). Scale bars: 500 nm (A–E), and 2 μm (F).

onto the cell surface and discharged the contents into the perivitelline space (Fig. 8B–D; *cf.* Fig. 6D, E), resulting in their disappearance from the cytoplasm (Fig. 6F). These granules are therefore considered to be cortical granules. Following exocytosis of the cortical granules, electron-dense particles appeared in the perivitelline space, indicating that the particles correspond to the perivitelline-space particles observed under light microscopy (Fig. 4A, B) and are derived from the cortical granules. To confirm this, immuno-electron microscopy was performed using an antibody against the sea urchin egg's hyaline layer (Yazaki, 1968), which is known to derive from the cortical granules (Endo, 1961). As shown in Figure 8A, gold particles are present inside the cortical granules (asterisks) in unfertilized oocytes. After fertilization, gold particles could be seen specifically in the cortical granule contents that were just being discharged outside the egg (Fig. 8B, asterisk). After their discharge into the perivitelline space (Fig. 8C, asterisk), the cortical granule contents, recognizable by the gold particles, reached the fertilization envelope (Fig. 8D, asterisk). As can be clearly seen in Figures 6 and 8, there is no hyaline layer over the egg surface, and gold particles cannot be identified outside the cell surface (Fig. 8C, D). As the perivitelline-space particles began to arrive at the fertilization envelope, a layer with fairly high electron density appeared on the inner part of the fertilization envelope, to

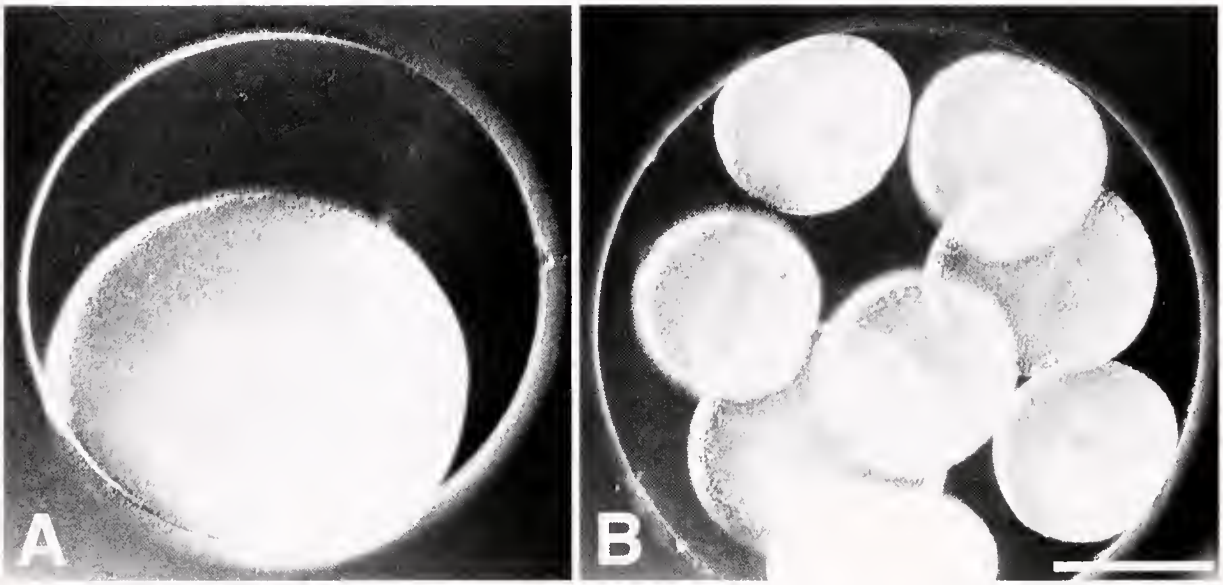

Figure 7. Effects of cytochalasin D on the fixing processes. Eggs were fertilized at 40 min after 1-MeAde treatment. (A) Ten minutes after application of 3 μM cytochalasin D (Sigma-Aldrich, St. Louis, MO), which is applied to the fertilized eggs at 90 min after fertilization. (B) Fertilized eggs were pulse-treated with the cytochalasin (3 μM) for 10 min after the third cleavage. Each blastomere lost its contact with the fertilization membrane, and transformed its flattened shape into a globular one. Scale bar: 100 μm.

which the tips of the fixing processes were joined (Fig. 6D, G). Near the cleavage furrows (Fig. 9), the inner layer was occasionally seen detached from the fertilization envelope and was linked with a number of fixing processes (arrows).

Discussion

In the early cleavage stages before the establishment of some mechanism, such as desmosomes, to directly bind blastomeres, animal embryos devise various means to keep the blastomeres together and maintain their spatial positions relative to each other. In sea urchin eggs, a hyaline layer is formed by the exocytosis of cortical granules immediately after fertilization (Endo, 1961). Microvilli are embedded into the hyaline layer, thus fixing the surface of fertilized eggs to the hyaline layer. Each blastomere produced by cleavage is therefore held in place by the hyaline layer (Dan and Ono, 1952) by means of microvilli, thereby maintaining the three-dimensional spatial relationship among the blastomeres. In sea urchin embryos, even if the fertilization envelope is removed, normal morphogenesis continues as long as the hyaline layer remains (Showman and Foerder, 1979).

In this study, we found that in *Astropecten scoparius* embryos, which lack a hyaline layer, the relative positions among blastomeres are maintained by the fertilization envelope and the cytoplasmic threads (fixing processes) attached to it. As can be seen in Figure 6, fixing processes are altered microvilli. On fertilization, the tips of the microvilli buried in the vitelline coat are attached to the fertilization envelope, and the microvilli rapidly lengthen with elevation of the fertilization envelope. Because fixing processes are located all over the cell surface, the balance of their tensions may keep the egg placed in the center of the fertilization envelope at the one-cell stage before the first cleavage. Hiramoto (1954, 1955) predicted the presence of a certain structure that connects the egg proper and the fertilization envelope in sea urchin zygotes, but its true nature is unknown.

After maturation division begins in *A. scoparius* oocytes, microfilament bundles within the microvilli lengthen, protruding some distance into the cytoplasm from the bases of the microvilli in unfertilized oocytes. Such lengthening following maturation division can be thought to be preparation for rapid elongation of microvilli postfertilization. Repeated bands were observed crossing the microfilament bundles (Fig. 6B, black arrowheads). The interval between the strips is some 60 nm. These bands may be formed of a kind of fascins, a family of actin-bundling proteins, although the band interval is wider than that reported in other types of cells (11 nm) (see Edwards and Bryan, 1995, for review).

After the first cleavage, the fixing processes near the cleavage furrow can be as long as 60 μm. This rivals the length of the acrosomes of the sea cucumber *Dendrochirotida thyone* (Tilney and Inoue, 1982)—a well-known example of the long actin fibers in gametes. In embryos after the second cleavage, fixing processes are short around the contact region between the blastomeres and the fertilization envelope (Fig. 6F). On the surface of the blastomeres in

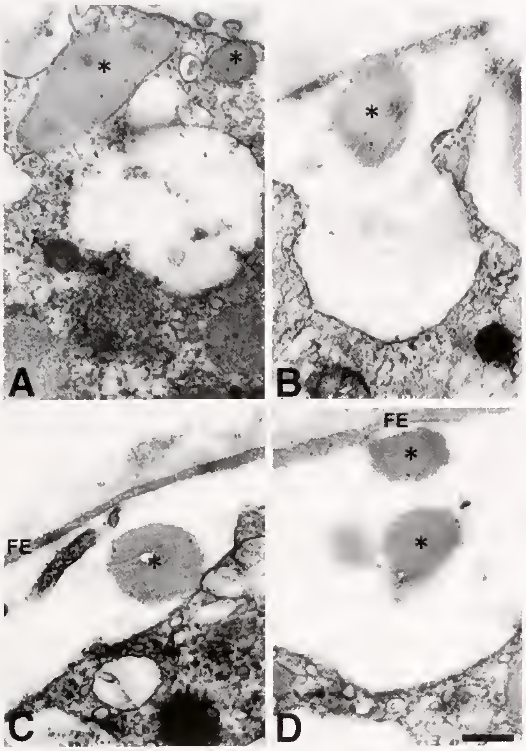

Figure 8. Immuno-electron microscopy of perivitelline-space particles using an antibody raised against sea urchin hyaline layer in chemically fixed specimens. (A) A maturing unfertilized oocyte. Cortical granules (asterisks), which were seen along the cortex, were decorated with gold particles. (B) Thirty seconds after insemination at 40 min after 1-MeAde treatment. Gold particles specifically decorated the cortical granule contents (asterisk) being discharged into the perivitelline space. (C) Five minutes after insemination. A perivitelline-space particle (asterisk) was decorated with gold particles. (D) Ten minutes after insemination. The fertilization envelope (FE) became decorated with gold particles after the perivitelline-space particles (asterisks) reached the envelope. Scale bar: 500 nm.

contact with the fertilization envelope, fixing processes are so short that they are difficult to detect by light microscopy (see Figs. 4D and 5A). Such short processes are thought to be the product of reduction of the long fixing processes seen before the first cleavage, although the mechanism of the reduction is not known.

Before the first cleavage, perivitelline-space particles reach the fertilization envelope and form its inner layer (Fig. 8D). As can be seen in Figures 6 and 8, this inner layer is derived from substances contained in the cortical granules, and the tips of the fixing processes are attached to the layer. Near the cleavage furrows, the inner layer, with fixing processes attached, could sometimes be seen detached from the fertilization envelope (Fig. 9), suggesting that the inner layer, derived from cortical granule contents, reinforces the attachment of the fixing processes to the fertilization envelope.

Treatment with acidified seawater breaks the attachments between the blastomeres and the fertilization envelope. The effects of acidified seawater are not seen on embryos more than 6.5 h postfertilization, indicating that after that time, the fixing processes play a lesser role in holding the blastomeres in place. Intercellular binding devices such as desmosomes are probably fulfilling this role at this stage (*cf.* Dan-Sohkawa *et al.,* 1986). It is not known when the connections between fixing processes and the fertilization envelope are broken, but around the time of hatching the embryo is able to spin around inside the fertilization envelope, so the attachments have been severed by this time at the latest.

The spatial relationship between blastomeres is maintained by the hyaline layer and microvilli in sea urchin embryos, and in *A. scoparius* embryos, which lack a hyaline layer, by the fertilization envelope and microvilli. The morphology and location of the hyaline layer and the fertilization envelope are different, but each contains substances derived from cortical granules. It is of great interest that, as shown in the immuno-electron microscopic findings (Fig. 8), they contain some common elements. This way of using the fertilization envelope as a scaffold for morphogenesis, which has been seen in *A. scoparius* embryos, may be a

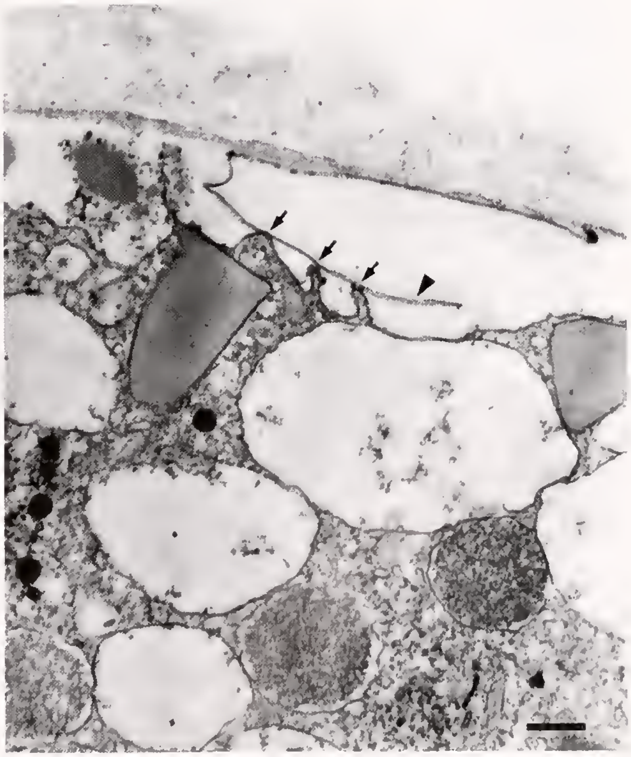

Figure 9. Detachment of fixing processes from the fertilization envelope during cleavages. Transmission electron micrograph of the specimen chemically fixed at the third cleavage. Near the cleavage furrow, the innermost layer of the fertilization envelope (arrow), to which fixing processes (arrowheads) were becoming attached, was ripped off from the fertilization envelope proper. The cleavage furrow was on the left side of the blastomere. Scale bar: 500 nm.

common mechanism for starfish embryos that lack a hyaline layer in early cleavage stages.

Acknowledgments

We thank Dr. I. Yazaki, Tokyo Metropolitan University, for the kind gift of an antibody against the hyaline layer of sea urchin eggs, and Dr. Y. Nakajima, Keio University, for valuable advice and kind help in preparing specimens fixed by the quick-freeze and freeze-substitution method. Our thanks are also due to Mr. M. Yamaguchi and Dr. M. Kiyomoto, Tateyama Marine Laboratory, Ochanomizu University, for technical assistance and providing facilities.

Literature Cited

Adelson, D. L., and T. Humphreys. 1988. Sea urchin morphogenesis and cell-hyaline adhesion are perturbed by a monoclonal antibody specific for hyaline. *Development* **104:** 391–402.

Anderson, K. V., and C. Nüsslein-Volhard. 1984. Information for the dorsal-ventral pattern of the *Drosophila* embryo is stored as maternal mRNA. *Nature* **311:** 223–227.

Boveri, T. 1910. Über die Teilung centrifugierter Eier von *Ascaris megalocephala. Wilhelm Roux' Arch. Entwicklungsmech. Org.* **30:** 101–125.

Burgess, D. R., and T. E. Schroeder. 1977. Polarized bundles of actin filaments within microvilli of fertilized sea urchin eggs. *J. Cell Biol.* **74:** 1032–1037.

Burke, R. D., M. Lail, and Y. Nakajima. 1998. The apical lamina and its role in cell adhesion in sea urchin embryos. *Cell Adhes. Commun.* **5:** 97–108.

Chabry, L. M. 1887. Contribution a l'embryologie normale tératologique des ascidies simples. *J. Anat. Phys. (Paris)* **23:** 163–321.

Dan, K., and J. C. Dan. 1947. Behavior of the cell surface during cleavage. VIII. On the cleavage of medusan eggs. *Biol. Bull.* **93:** 163–188.

Dan, K., and T. Ono. 1952. Cyto-embryological studies of sea urchins. I. The means of fixation of the mutual positions among the blastomeres of sea urchin larvae. *Biol. Bull.* **102:** 58–73.

Dan-Sohkawa, M., H. Yamanaka, and K. Watanabe. 1986. Reconstruction of bipinnaria larvae from dissociated embryonic cells of the starfish *Asterina pectinifera. J. Embryol. Exp. Morphol.* **94:** 47–60.

Edwards, R. A., and J. Bryan. 1995. Fascins, a family of actin bundling proteins. *Cell Motil. Cytoskelet.* **32:** 1–9.

Endo, Y. 1961. Changes in the cortical layer of sea urchin eggs at fertilization as studied with the electron microscope. *Exp. Cell Res.* **25:** 383–397.

Fleming, T. P., J. McConnell, M. H. Johnson, and B. R. Stevenson. 1989. Development of tight junctions de novo in the mouse early embryo: control of assembly of the tight junction-specific protein, ZO-1. *J. Cell Biol.* **108:** 1407–1418.

Gilbert, S. F. 1994. *Developmental Biology.* 4th ed. Sinauer Associates, Sunderland, MA. Pp. 493–530.

Hillman, N., M. I. Sherman, and C. Graham. 1972. The effect of spatial arrangement on cell determination during mouse development. *J. Embryol. Exp. Morphol.* **28:** 263–278.

Hiramoto, Y. 1954. Nature of the perivitelline space in sea urchin eggs. I. *Jpn. J. Zool.* **11:** 227–243.

Hiramoto, Y. 1955. Nature of the perivitelline space in sea urchin eggs. II. *Jpn. J. Zool.* **11:** 333–334.

Hörstadius, S. 1935. Über die Determination im Verlaufe der Eiasche bei Seeigeln. *Pubbl. Stn. Zool. Napoli* **14:** 251–479.

Kanatani, H. 1969. Induction of spawning and oocyte maturation by 1-methyl-adenine in starfishes. *Exp. Cell Res.* **57:** 333–337.

Karnovsky, M. J. 1965. A formaldehyde-glutaldehyde fixative of high osmolarity for use in electron microscopy. *J. Cell Biol.* **27:** 137A.

Kiyomoto, M., and H. Shirai. 1993a. Reconstruction of starfish egg by electric cell fusion: A new method of detecting the cytoplasmic determinant for archenteron formation. *Dev. Growth Differ.* **35:** 107–114.

Kiyomoto, M., and H. Shirai. 1993b. The determinant for archenteron in starfish: co-culture of an animal egg fragment-derived cell cluster and selected blastomere. *Dev. Growth Differ.* **35:** 99–105.

Kuraishi, R., and K. Osanai. 1989. Structural and functional polarity of blastomeres. *Dev. Biol.* **136:** 304–310.

Kushida, H. 1980. An improved embedding method using ERL 4206 and Quetol 653. *J. Electron Microsc.* **29:** 193–194.

Martin, V. J., C. L. Littlefield, W. E. Archer, and H. R. Bode. 1997. Embryogenesis in hydra. *Biol. Bull.* **192:** 345–363.

Matsunaga, M., I. Uemura, M. Tamura, and S. Nemoto. 2000. Role of the fertilization envelope and specialized microvilli in morphogenesis of starfish embryos. *Zygote* **8** (Suppl.): 65.

Morris, R. E., and G. M. Ciraolo. 1997. A universal post-embedding protocol for immunogold labeling of osmium-fixed, epoxy resin-embedded tissue. *J. Electron Microsc.* **46:** 315–319.

Nemoto, S., M. Yoneda, and I. Uemura. 1980. Marked decrease in the rigidity of starfish oocytes induced by 1-methyladenine. *Dev. Growth Differ.* **22:** 315–324.

Oguro, C., M. Komatsu, and Y. T. Kano. 1976. Development and metamorphosis of the sea-star, *Astropecten scoparius* Valenciennes. *Biol. Bull.* **151:** 560–573.

Reimer, C. L., and B. J. Crawford. 1997. Isolation and characterization of an endodermally derived, proteoglycan-like extracellular matrix molecule that may be involved in larval starfish digestive tract morphogenesis. *Dev. Growth Differ.* **39:** 381–397.

Showman, R. M., and C. A. Foerder. 1979. Removal of the fertilization membrane of sea urchin embryos employing aminotriazole. *Exp. Cell Res.* **120:** 253–255.

Steinbeck, M. J., A. U. Khan, and M. J. Karnovsky. 1993. Extracellular production of singlet oxygen by stimulated macrophages quantified using 9, 10-diphenylanthracene and perylene in a polystyrene film. *J. Biol. Chem.* **268:** 15649–15654.

Tarkowski, A. K., and J. Wroblewska. 1967. Development of blastomeres of mouse eggs isolated at the 4- and 8-cell stage. *J. Embryol. Exp. Morphol.* **181:** 155–180.

Tilney, L. G., and S. Inoue. 1982. Acrosomal reaction of *Thyone* sperm. II. The kinetics and possible mechanism of acrosomal process elongation. *J. Cell Biol.* **93:** 820–827.

Yazaki, I. 1968. Immunological analysis of the calcium precipitable protein of sea urchin eggs. I) hyaline layer substance. *Embryologia* **10:** 131–141.

Reference: *Biol. Bull.* **202:** 223–231. (June 2002)

Postembryonic Eye Growth in the Seashore Isopod *Ligia exotica* (Crustacea, Isopoda)

ESSI KESKINEN[1], YASUHARU TAKAKU[2], V. BENNO MEYER-ROCHOW[3,*],
AND TAKAHIKO HARIYAMA[4]

[1]*Department of Biology, University of Oulu, P.O. Box 3000, SF-90014 Oulu, Finland;* [2]*Department of Developmental Genetics, National Institute of Genetics, Mishima 411-8540, Japan;* [3]*Department of Biology, School of Engineering and Science, International University Bremen, D-28725 Bremen, Germany; and* [4]*Department of Biology, Hamamatsu University School of Medicine, 1-20-1 Handayama, Hamamatsu 431-3192, Japan*

Abstract. The eye of *Ligia exotica* is of the apposition type and has open rhabdoms. The facets are hexagonal, and the dioptric apparatus consists of a flat cornea and a spherical crystalline cone placed in the center of two large cone cells. Each ommatidium has seven regular retinula cells and one eccentric cell; a basement membrane forms the proximal boundary of the retina. With increases in body size from 0.6 to almost 4.0 cm, facet numbers and ommatidial diameters increased from 800 to 1500 and 35 μm to 100 μm, respectively; eye length and width grew from 1.2 to 3.2 and 0.9 to 2.5 mm, respectively; and length of dioptric apparatus and width of retinal layer changed from 70 μm to 180 μm and about 70 μm to 120 μm. Visual angles and interommatidial angles of centrally located ommatidia remained constant at about 30 and 6.9 degrees, respectively. An almost perfect linear relationship was found when eye length was plotted against the product between the square root of the total number of ommatidia and the ommatidial diameter. No difference between males and females was observed in any of the relationships, but the results suggest that, compared with smaller specimens, larger ones possess increased absolute sensitivity in single ommatidia, increased sensitivity to point sources, and overall larger angular visual fields for the eye in its totality. This means that larger individuals of *L. exotica* (which are also faster) have an advantage over smaller individuals at night, but that smaller individuals may cope better with bright lights. Vision in *L. exotica* seems useful not only in detecting potential danger, but also in locating and approaching cliffs from a distance of 2–4 m when swimming in seawater.

Introduction

The eyes of the semiterrestrial isopod *Ligia exotica* have previously been the subjects of investigations into circadian changes (Hariyama *et al.*, 1986), ultraviolet responses (Hariyama *et al.*, 1993), and acceptance angles (Hariyama *et al.*, 2001). Because *L. exotica*, like most crustaceans, has indeterminate growth, changes in eye size (possibly shape as well), facet numbers, and ommatidial dimensions must occur as individuals undergo successive molting. The existence of such growth-related changes in eye morphology suggests that at least some aspects of the way individuals of *L. exotica* see the world around them could depend on body size, age and, if males and females were of different size, even sex. Thus, one goal of this study was to examine the morphology of the eyes of a wide range of differently sized male and female *L. exotica*.

A second goal of this study was to examine postembryonic changes (and their functional consequences) in the eyes of crustaceans in general and isopods in particular. Only one paper known to us lists ommatidial numbers in relation to an approximately 10-fold increase in body size in an isopod (Meyer-Rochow, 1982). Although Barlow (1952) provided details on the influence of the dimensions in apposition compound eyes on acuity and resolution and Horridge (1978) later added to these observations, few researchers of crustacean compound eyes, as documented by Meyer-Rochow and Reid (1996), ever mentioned the size or age of their experimental animals.

Received 3 July 2001; accepted 5 March 2002.

* To whom correspondence should be addressed. E-mail: B.Meyer-Rochow@iu-bremen.de

Investigations of postembryonic eye growth in crustaceans (*e.g., Gammarus chevreuxi:* Bélehrádek and Huxley, 1930; *Panulirus longipes:* Meyer-Rochow, 1975; *Homarus gammarus:* Shelton *et al.*, 1981; *Procambarus clarkii:* Tokarski and Hafner, 1984; *Neomysis integer* and *Thysanoessa raschii:* Nilsson *et al.*, 1986; *Hemigrapsus sanguineus:* Eguchi *et al.*, 1989; Anomura: Fincham, 1988; *Petrolisthes elongatus:* Meyer-Rochow *et al.*, 1990, *Carcinus maenas* and *Hyas araneus:* Harzsch and Dawirs, 1996) show that crustacean compound eyes grow neither isometrically nor allometrically, but that certain eye components may follow their own separate growth patterns. In some cases, this leads to a change from one functional eye type to another, for instance, from the apposition to the superposition system in the rock lobster *Panulirus longipes* (Meyer-Rochow, 1975), the mysid *Neomysis integer*, and the euphausiid *Thysanoessa raschii* (Nilsson *et al.*, 1986). By examining certain aspects of postembryonic eye growth in *L. exotica*, we aim to better understand the role of vision in this species and the patterns governing size and age-related phenomena of vision in crustaceans generally.

Materials and Methods

Animals

Numerous individuals of *Ligia exotica*, representing a wide range of sizes, were collected by hand along the seashore of Shiogama (Miyagi Prefecture, Japan) at low tide around noon. On the same day, the captured specimens were taken to the laboratory in plastic containers and transferred to spacious tanks (100 × 40 × 40 cm). In the laboratory, the animals were maintained at a constant temperature of 24 °C under regular, cyclic light/dark conditions (L/D = 12/12 h) for about one week. During that time, they were fed commercially available dry pellets of insect food.

Measurements

The total number of ommatidia was determined from light micrographs and scanning electron micrographs of 24 eyes of differently sized animals (13 males and 11 females). Care was taken that only animals with seven pairs of legs were used in this investigation, since larvae of this species (usually reared under a female's abdomen in the marsupium, but occasionally dropping out or escaping from it) have only six pairs of legs. To count all the ommatidia of the curved and asymmetrically shaped eyes, each specimen was photographed from at least four angles. Debris particles on the eye's surface (Fig. 1C, white arrows) enabled us to identify individual ommatidia and thus allowed us to recognize the borders between adjacent micrographs. Ommatidia were counted from either the left or the right eye and in one case from both eyes.

Lengths and widths along the two principal axes of the compound eyes were determined from light micrographs of 13 male and 9 female specimens; the diameters of individual ommatidia from the dorsal non-rim area of the eyes were also measured. Eyes of 26 males and 13 females, frozen through rapid immersion in liquid nitrogen and then split with a razor blade, served as material for scanning electron microscopy (SEM). From the micrographs, facet diameters, lengths of dioptric structures, retinal widths, and interommatidial angles were measured. For each of these four features, depending on the condition of the specimen and the quality of the photographs, three to seven measurements per individual were taken. SAS statistical and graph software (SAS Institute Inc., Cary, NC) was used in curve constructions, calculations, and statistical analyses.

Specimen preparation

Out of several hundred individuals collected, 111 were randomly chosen (56 males and 55 females of various sizes) for this part of the study. Following confirmation of the sex through external inspection, each animal was weighed on an electric balance. To determine an animal's size (Fig. 1), four measurements were taken with a pair of dividers and a ruler calibrated to 1 mm: antennal length, uropod length, body length (excluding antennae and uropods), and total specimen length (including antennae and uropods). Any further observations, principally involving the eyes (see below), were carried out on material from these measured individuals.

For light microscopy, specimens were decapitated in the prefixative solution (2% paraformaldehyde and 2% glutaraldehyde in 0.1 *M* sodium cacodylate at pH 7.4) with a sharp razor blade. The surface of the compound eye was observed immediately thereafter under a light microscope (Nikon FX) by epi (= orthodromic) illumination. The light microscope (Zeiss Axiovar 100) was also used to pre-examine samples prepared for scanning electron microscopy and thick sections made with a cryostat. Semithin sections were stained in an aqueous solution of 1% toluidine blue.

For SEM, the eyes were surgically removed from the head while the latter was immersed in 0.1 *M* phosphate buffer (pH 7.2). The severed eyes were then fixed for 2 h in 2.5% glutaraldehyde in 0.1 *M* sodium cacodylate (pH 7.2). After the preparations were rinsed three times for 10 min in 0.1 *M* phosphate buffer, they were dehydrated in a graded series of ethanol and transferred into isoamyl acetate. The preparations were then dried with a critical point drying apparatus, attached to a metal plate, and ion-coated. To observe aspects of the longitudinal organization of the retina, some of the samples, after fixation, were frozen with liquid nitrogen, split longitudinally with a razor blade to expose the cleaved tissue layers, and dried and ion-coated with white-gold vapor (Eico ion coater IB-3) like the rest of the SEM samples. Observations were carried out under a Hitachi S-430 scanning electron microscope, operated at an accelerating voltage of 20 kV.

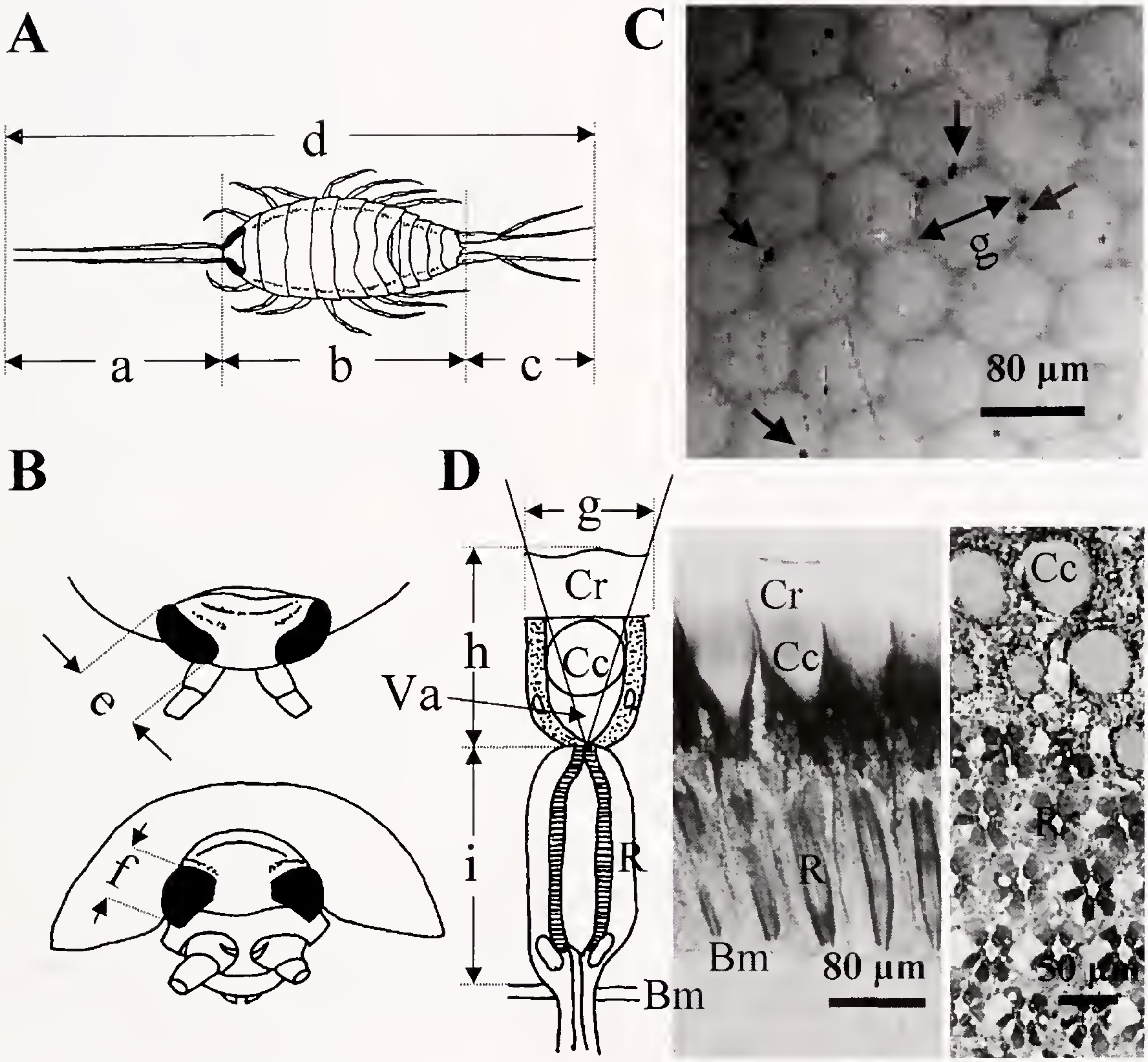

Figure 1. (A) Schematic drawing of *Ligia exotica* with the four lengths monitored indicated by small letters: (a) length of antennae, (b) length of body excluding antennae and uropods, (c) length of uropods alone, and (d) total body length. (B) Head region with eyes in black, viewed from above and showing horizontal (= anteroposterior) extent of eye measurable as e, and head region seen from the front with dorsoventral extent of the eye measurable as f. (C) Scanning electron micrograph of the outer surface of the compound eye of *L. exotica*, showing facets with hexagonal outlines. Ommatidial diameter was defined as the corner-to-corner distance (g), while debris on the cornea (white arrows) served as landmarks, assisting in identifying specific places on the eye. (D) Schematic drawing (left) and photomicrograph (right) of longitudinally sectioned ommatidia. Diameter of a facet was measured as g at the cornea (Cr), length of the dioptric apparatus, h, with the spherical crystalline cone (Cc) at its center, was defined as the distance from the corneal surface to the distal tip of the rhabdom, and the length of the retina, i, covered the distance between distal tip of the rhabdom (R) and basement (Bm). The angle Va defined the visual angle of an ommatidium.

Results

All individuals of *Ligia exotica* examined, irrespective of size, possessed apposition-type compound eyes with a hexagonal ommatidial lattice. The eyes were always sessile and occupied almost the entire lateral region of the head (Fig. 1A, B). The eyes were uniformly black; the ommatidial arrangement showed no obvious morphological differences, except for the marginal row of ommatidia all around the edge of the eye, in which smaller and seemingly immature ommatidia prevailed.

First we determined the relationship between individual weights and sizes. Size was used in preference to age, since (a) food quality and quantity as well as other environmental factors can affect the speed of growth in crustaceans, and (b)

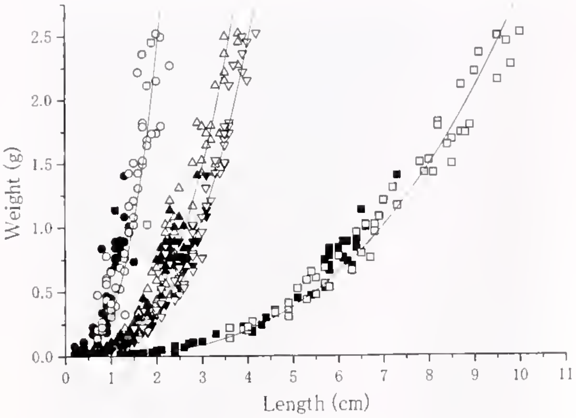

Figure 2. Relationship, obeying the function $y = kX^3$, between body weight (ordinate) and length of uropods (circles), antennae (triangles pointing upward), total body length (squares), and body length excluding antennae and uropods (triangles pointing downward) in male and female individuals of *Ligia exotica* (open and filled symbols, respectively). The values for k in the four relationships were calculated as 0.321, 0.062, 0.0038, and 0.045; the respective chi-square (χ^2) values were 0.104, 0.039, 0.016, and 0.011.

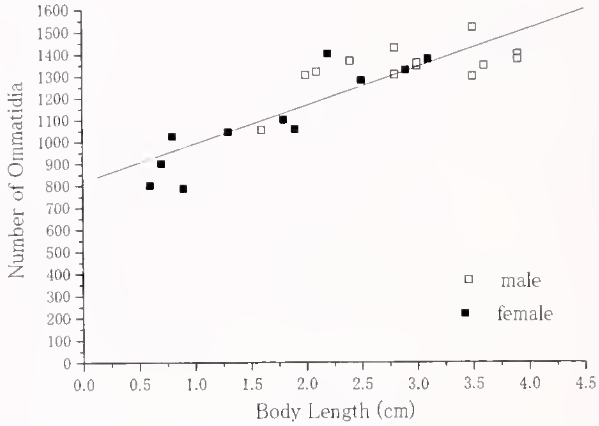

Figure 3. Relationship between number of ommatidia per single eye and body length in male and female *Ligia exotica*, obeying the formula $y = 174.3X + 816.4$ (SD = 104; $R = 0.87$).

we have no way of telling how old an individual really is and how many times it may have molted prior to capture. Lengths of the antennae, uropods, and bodies (with and without antennae and uropods) all increased with body weight (Fig. 2) and fitted the equation $y = kX^3$ (where y = weight, k = constant, and X = length). The largest individuals encountered were males of about 2.75 g in weight and about 11 cm in total body length (*i.e.*, measured with antennae and uropods). Females, being somewhat shorter and reaching a maximum total length of 7.5 cm and a weight of about 1.5 g (Fig. 2), appear to form a subpopulation of smaller individuals within the greater population of *L. exotica*. However, the shape and slope of the graph of the females' weight/size relationship were comparable to those of the males, provided we disregarded the upper (only males) and lower (only females) reaches. The smallest males weighed 0.14 g and measured 4.6 cm in total body length. Since the best correlation (*i.e.*, smallest variation) existed between weight and body length (defined as the length of an animal *excluding* antennae and uropods), we used body length alone (and not *total* body length) in all relationships regarding eye measurements and specimens of different sizes (see below).

The total number of ommatidia increased with an individual's increasing body length (Fig. 3). The smallest individuals (body lengths of *ca.* 0.75 cm) had about 800 ommatidia, whereas the largest specimens (body lengths *ca.* 4 cm) had about 1500. The increase in facet number between smallest and largest individuals was thus nearly two-fold, while body length increased at least five-fold. No statistical difference was detected between the curves of males and females; both had a correlation coefficient for the least-squares fit of the data points of $R = 0.87$.

The extent of the horizontal and vertical spread of the eye was measured along the eye's two principal axes (Fig. 1B). The length of the eye along its horizontal (anteroposterior) extent and across its vertical (dorsoventral) range increased linearly with body size (Fig. 4). No obvious differences between the growth curves of male and female eyes were noticed, but eye growth in the anteroposterior direction slightly outpaced that of the dorsoventral direction. Thus, the general shape of the eye (but not its overall size) changed rather little throughout the animal's life.

The diameter of an individual ommatidium, measured either from the surface of the eye as facet diameter or from cross sections of the eye at corneal levels, increased nearly linearly with eye size and, when plotted against the body

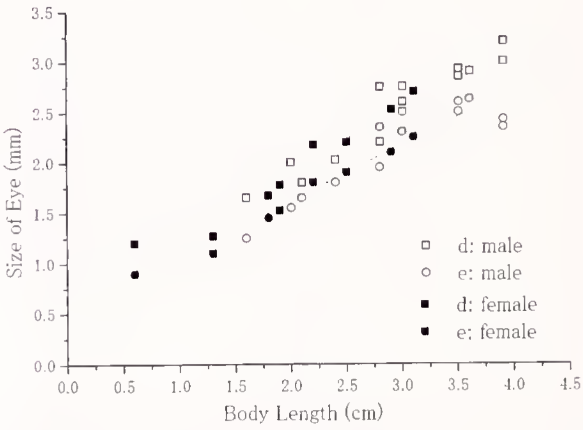

Figure 4. Length (anteroposterior: d) and width (dorsoventral: e) increases of the eye of *Ligia exotica* males and females in relation to body size. The equation $y = 0.65X + 0.62$ (SD = 0.144) describes the length relationship, while $y = 0.56X + 0.5$ (SD = 0.16; $R = 0.95$) describes the width relationship.

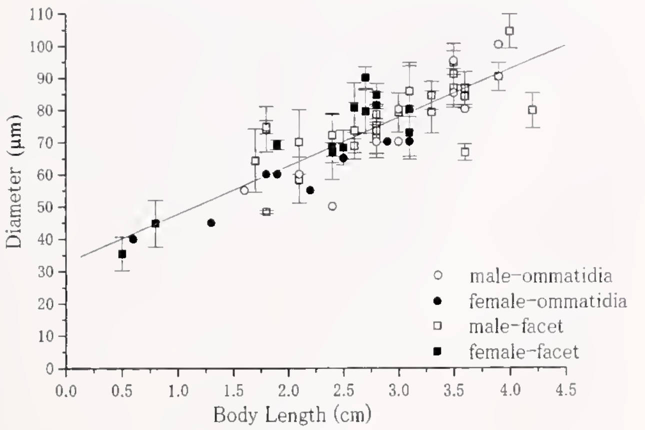

Figure 5. Relationship, obeying $y = 15X + 32.7$ (SD = 7.7; $R = 0.85$) between body length and ommatidial diameters, the latter either determined directly from scanning electron micrographs (single values) or as the average of 3–7 measurements taken from each longitidinally sectioned eye (values with standard deviation bars) of male and female specimens.

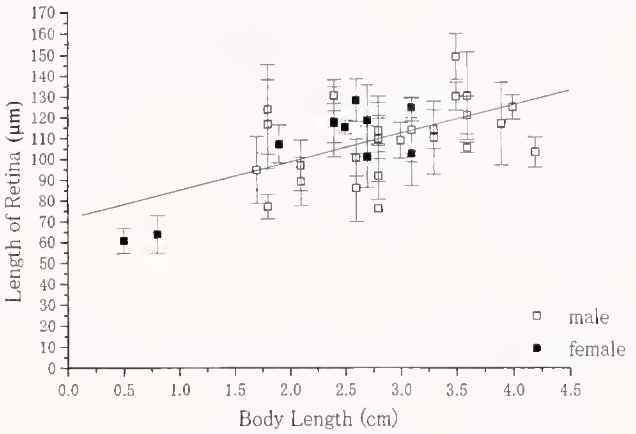

Figure 7. Relationship, obeying $y = 13.5X + 71.5$ (SD = 15.3), between body length and ommatidial length of retina, determined as the average of 3–7 measurements taken from each longitudinally sectioned eye of male and female specimens.

length of an animal, with growth of the whole animal as well (Fig. 5). The smallest and the largest specimens examined exhibited facet diameters of 35 µm and 105 µm, respectively. Once again, there were no differences between male and female individuals. The length of the dioptric structures (h in Fig. 1D) for both male and female individuals increased linearly in relation to body length of an animal (Fig. 6). The width of the retinal layer, measured as retina length per ommatidium in the eye of both males and females, also increased in relation to greater individual body size (Fig. 7), but with more variability ($R = 0.586$) than some other structures of the eye, for example, the layer of the dioptric elements mentioned earlier (see above).

True interommatidial angles cannot be obtained in *L. exotica*, because rhabdomeres are frequently skewed and the axes of ommatidial groups of retinula cells are not always parallel to the axes of the dioptric structures. Since the spacing of the facets is an important parameter in vision, two alternative angles, which are probably independent from each other, were measured. Dioptric systems of neighboring ommatidia, involving only cornea and cone cells, were usually straight. It was thus possible to measure the inclination of the axes through the dioptric structures of neighbouring ommatidia in 11 females and 16 males, ranging from 1 to 6 cm in body length. The interommatidial angle obtained in this way was 6.91° ± 0.95 and showed no appreciable difference across the size range of animals or between male and female. The second approach we used to examine interfacetal constancy involved what we termed *the visual angle*. This angle is *not* identical to the interommatidial angle, but it provides an estimate of the optical "catchment" of each dioptric apparatus on purely geometric grounds. It was measured on longitudinal sections as the figure formed by the two lines leading from the outer edges of the cornea to a common point at the proximal end of the crystalline cone (*cf.* Fig. 1D). Corneal surfaces and crystalline cone cells were arranged at right angles to each other, and facet diameters in both males and females increased in relation to body size. The dioptric elements in the ommatidia, however, also increased in size and became thicker and longer. Since the ratio between diameter and length remained more or less constant as *L. exotica* grew, the visual angles, representing optical catchment per ommatidium, also remained basically the same (*i.e.*, 30°) for different body lengths (Fig. 8).

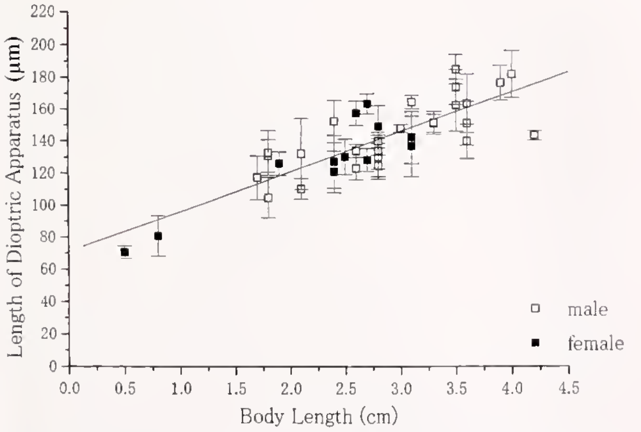

Figure 6. Relationship, obeying $y = 24.8X + 71$ (SD = 13.55; $R = 0.831$) between body length and length of dioptric apparatus, determined as the average of 3–7 measurements taken from each longitudinally sectioned eye of male and female specimens.

Discussion

In contrast to the embryological morphogenesis of the crustacean compound eye (Fincham, 1984, 1988; Hafner

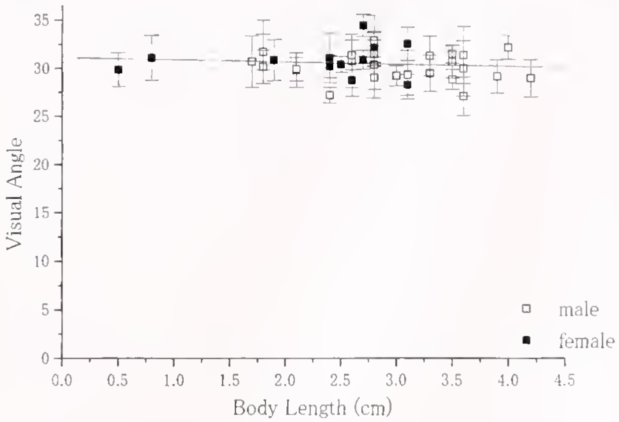

Figure 8. Relationship, obeying $y = -0.25X + 31.1$ (SD = 1.53) between body length and visual angle, determined as the average of 3–7 measurements taken from each micrograph of longitudinally sectioned eye of male and female specimens.

and Tokarski, 1998), postembryonic eye differentiation presents a far less uniform picture. The variety of patterns seen in different crustaceans reflects the wide range of tasks a compound eye has to carry out. Cases are known in which larvae possess eyes, but adults are eyeless and have lost their photoreceptors (*e.g., Troglocaris anophthalmus:* Christian Juberthie, CNRS, Laboratoire souterrain, pers. comm., and Juberthie-Jupeau, 1972; *Alvinocaris markensis:* Chamberlain, 2000); or in which juvenile individuals feature apposition eyes, but adults have superposition eyes (*e.g., Panulirus longipes:* Meyer-Rochow, 1975; mysids and euphausiids: Nilsson *et al.,* 1986); or in which the dioptric elements are lost and the retina changes from the imaging type to a nonimaging one (bresiliid shrimps: Gaten *et al.,* 1998). Obviously, such changes must have an effect on the more central components of the visual system; however, apart from a study of the optic ganglia of two brachyuran species by Harzsch and Dawirs (1996), no other detailed information on the events in the eyestalk ganglia during postembryonic compound eye maturation is available, and specifically for *L. exotica,* only a basic study of the optic neuropils (Sharma, 1982) has been published.

Not surprisingly, in view of the rather similar ecological requirements and behavior of the different size classes of *L. exotica,* postembryonic eye development in this species is less dramatic than that of the crustaceans mentioned in the preceding paragraph. The eye and most of its components grow isometrically, although the slopes of the growth curves for different structures, as our observations have shown, need not be identical. Through the addition of ommatidia following molts, interommatidial angles of the central region of the eye frequently decrease (*e.g., Hemigrapsus sanguineus*: Eguchi *et al.,* 1989; *Carcinus maenas* and *Hyas araneus:* Harzsch and Dawirs, 1996), allowing the animal to develop greater resolving power in that part of the eye. On the other hand, interommatidial angles can remain constant (*Petrolisthes elongatus*: Meyer-Rochow *et al.,* 1990) or may even increase with the addition of extra ommatidia (*Argulus foliaceus*: Madsen, 1964), depending on where in or around the eye the proliferation zone or zones exist. In *L. exotica,* ommatidia closest to the edge, all around the eye, displayed smaller and more irregular facet outlines than those of the central region. Ultrastructurally they also differed, but we have just begun to investigate whether a distinct proliferation zone is responsible for the recruitment of these marginal ommatidia and to what extent they can transform themselves into the more regular type. We noticed that the increase in ommatidia with age was neither strictly linear, as in the amphipod *Gammarus chevreuxi* (Bělehrádek and Huxley, 1930), nor exponential, as in *Petrolisthes elongatus*: Meyer-Rochow *et al.,* 1990). Because the number of the ommatidia in *L. exotica* appears to be correlated with the area of the compound eye (rather than simply with the size of the animal), we calculated the product of the square root of the total number of ommatidia and the average ommatidial diameter, plotting the values against the maximum length of the eye. The result is an almost perfect linear relationship (Fig. 9), suggesting that image quality (resolution) remains constant as the eye increases in size. When the growth relationship is expressed in this way, it becomes independent of an individual's age or molt status, which is an advantage because age and size in crustaceans cannot easily be connected (Shelton *et al.,* 1981).

L. exotica is an alert and agile species, and—as anyone who has tried to catch live specimens on a beach, whether during the day or under twilight conditions, would testify—it has keen eyesight. Electrophysiological recordings from adult animals, in air, confirm that acuity is impressive and that the acceptance angle of a single receptor cell is

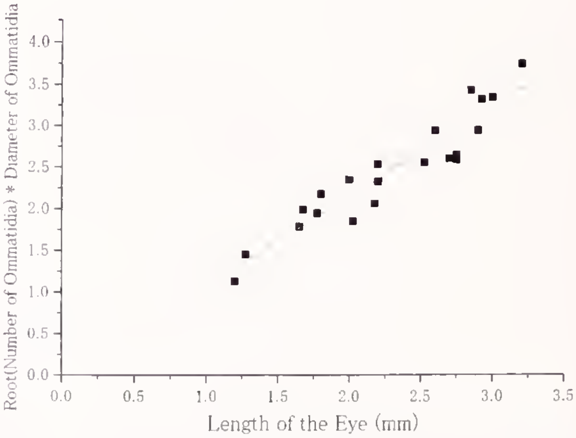

Figure 9. Plotting the product of the square root of total number of ommatidia and ommatidial diameter against eye length results in an almost perfect linear relationship, following the equation $y = 1.0X - 7.7$.

about 2°, even at night when sensitivity increases 10-fold (Hariyama *et al.*, 2001). Apparently, however, *L. exotica*, not only can see in air, but also can use vision underwater, for example, in attempts to reach coastal rocks or the shore from distances of 0.5–1.0 m (Taylor and Carefoot, 1990). Since this species undoubtedly had aquatic ancestors, and crustaceans are known to be able to use underwater visual landmarks (Cannicci *et al.*, 2000), we have to consider the possibility that some of the eye's functions as well as its structural characteristics (Richter, 1999) are rooted in *L. exotica's* behavior in the aquatic environment.

L. exotica can feed and survive submerged in seawater for at least 14 days, but small as well as large individuals immediately seek to reach the shore after being blown into the sea by a gust of wind or after accidentally jumping into the water as part of an escape maneuver (Taylor and Carefoot, 1990). At night, in total darkness, Taylor and Carefoot (1990) did not notice any swimming orientation that differed from randomness; most of the individuals tossed into the water sank to the bottom, where they would slowly crawl up the slope, presumably making use of leg proprioceptive inputs (Nalbach *et al.*, 1989). During the day, however, waterborne individuals tended to swim at the surface, and the chief factors influencing their directional surface-swims appeared to be "angle of sun and darkness of bottom or wall" (Taylor and Carefoot, 1990). Yet the same researchers pointed out that orientation to the sun "was of secondary importance" and that differentiation between lighter and darker features apparently provided the principal navigational cues.

In addition to spatial resolution and sensitivity, another important photoreceptor property that, according to Frank (1999), needs to be considered in "any comprehensive analysis of the visual system of organisms" is flicker fusion frequency (= temporal resolution). The latter is generally high in terrestrial and rapidly moving, daytime-active species and lower in aquatic organisms. Flicker fusion frequency (FFF) is not known in *L. exotica*, but Ruck and Jahn (1954) measured an average FFF of 120 in adults of the closely related *L. occidentalis*. Resembling that of the bumblebee eye (Meyer-Rochow, 1981), such a relatively high FFF value is not unusual for flying insects, but it is unusual for crustaceans (*cf.* Frank, 1999); it is probably related to the great speed with which all *Ligia* spp. scuttle around on the beach. Autrum (1950) showed that fast-moving arthropods require higher FFFs than slow-moving ones; and Srinivasan and Bernard (1975) showed that at angular velocities above a critical value, the temporal properties of an eye begin to determine spatial resolution to a greater extent than the optics of the eye do. Figures for running speeds of *L. exotica* individuals of different sizes are unavailable, but swimming speeds have been measured: animals 10–15 mm in body length are capable of velocities corresponding to about 3 body lengths/s, but individuals of 40–50 mm are faster and cover 4–5 body lengths/s (Taylor and Carefoot, 1990). On that basis, we tentatively conclude that, unlike bigger specimens of *Ligia*, small ones do not need a high FFF value. We see confirmation for this notion in the ommatidial organization of the eye of the smaller specimens, which seemingly favors spatial resolution.

Since the shape of the eye in *L. exotica* stays roughly the same, density and contours of individual ommatidia are kept constant, and both interommatidial and visual angles persist unchanged throughout an individual's life; hence the resolving power of the eye should also remain rather stable, even if the FFF were to rise as the animal grows and becomes faster. With no significant change to the overall form of the compound eye in *Ligia*, we would expect the overall visual field of an eye to remain about the same throughout life. In small specimens, the visual fields of photoreceptor cells are, however, difficult to measure, and only recordings from larger individuals have been successful (Hariyama *et al.*, 2001). But because their facets are fewer as well as smaller, the eyes of younger specimens are likely to be less sensitive to point sources as well as extended sources of light (Land, 1981). Bigger specimens, with their more numerous facets and wider ommatidia, thus ought to have an advantage when it comes to exploiting dimmer environments. The ability to distinguish minor differences in contrast fits well with the observation by Taylor and Carefoot (1990) that bigger specimens of *L. exotica* will swim longer (25 s *versus* 16 s) and faster than smaller ones. Thus, larger *L. exotica* individuals can detect (and attain) a goal from a greater distance (as far as 3 m according to Taylor and Carefoot, 1990) than can smaller ones with less sensitive eyes.

The inability to see a rock or a cliff in the distance could actually be an advantage for a smaller individual because its swimming speed and endurance would be insufficient to allow it to reach such a far-off goal. A similar situation is seen in the intertidal halfcrab *Petrolisthes elongatus*, a species whose postembryonic eye-growth patterns resemble those in *L. exotica* (Meyer-Rochow *et al.*, 1990). When crabs of this species are robbed of their shelters, they immediately look for a new shelter. Larger individuals preferentially crawl towards boulders at greater distances, whereas smaller individuals seek out nearby ones, even if the sizes of the near and far boulders subtend the same degree of arc within the visual field of the crabs (Meyer-Rochow and Meha, 1994). Because the smaller crabs tire faster and are slower, an ability to visually perceive attractive boulders in the far distance (distance perception in the ant *Myrmecia nigriceps* was found to be 80 cm: Eriksson, 1985) would be wasted on them and, in fact, could leave them exposed to predators for dangerously long periods if they attempted to reach the distant target.

On the other hand, prolonged exposures to bright lights are generally much better tolerated by arthropods with smaller and strongly curved eyes (Kelber, 2000). Compared with the larger eyes of fully grown individuals, the smaller eyes and narrower ommatidia in small *L. exotica* admit considerably less light to the photoreceptive membranes, thus reducing the risk of light-induced photoreceptor damage (Meyer-Rochow, 1994; Meyer-Rochow *et al.*, 2002). By requiring more (or brighter) light than large specimens to see, small individuals are predisposed to exploit the daytime hours. Although larger adults are also active during that part of the day, they are more cautious and more inclined to hide than the youngsters. At night the situation is reversed: the largest individuals with the most sensitive eyes are out and active, presumably relying on their improved vision to detect disturbances and the approach of danger even in semidarkness.

L. exotica is not the only peracarid crustacean that behaves in this way. The aquatic isopod *Idotea baltica* shows a growing preference with age for a dark background and night feeding (Merilaita and Jormalainen, 2000). Similarly, small juvenile shore talitrids are active under bright conditions but become increasingly dark-active as they age and grow (Rüppell, 1967). Even in the terrestrial isopod *Scyphax ornatus*, it is the adults that make lengthy foraging excursions at night (Quilter and Lewis, 1989). One might argue that it is not vision but humidity that governs activity periods and the place on the beach where shore crustaceans assemble. If, however, that were the case in *L. exotica* and the talitrids, cited above, smaller individuals—in greater danger of desiccation than larger ones—should come out predominantly at night, while bigger individuals should be more active during the day. Clearly, the need for moisture alone cannot explain the size-related exposure differences; a link with the anatomical organization of the eye and its functional limitations seems a considerably stronger explanation.

Acknowledgments

This work was supported in part by a Grant-in-Aid to T.H. for Scientific Research on Priority Areas (A) (12048204) and a grant to V.B. M-R. from the Oskar Öflunds Stiftelse.

Literature Cited

Autrum, H. 1950. Die Belichtungspotentiale und das Sehen der Insekten (Untersuchungen an *Calliphora* und *Dixippus*). *Z. Vgl. Physiol.* **32:** 176–227.

Barlow, H. B. 1952. Size of ommatidia in apposition eyes. *J. Exp. Biol.* **29:** 667–674.

Bélehrádek, J., and J. S. Huxley. 1930. The rate of eye-growth and its variation in *Gammarus chevreuxi*. *J. Exp. Biol.* **7:** 37–40.

Cannicci, S., C. Barelli, and M. Vannini. 2000. Homing in the swimming crab *Thalamita crenata*: a mechanism based on underwater landmark memory. *Anim. Behav.* **60:** 203–210.

Chamberlain, S. C. 2000. Vision in hydrothermal vent shrimp. *Philos. Trans. R. Soc. Lond. B* **355:** 1151–1154.

Eguchi, E., K. Arikawa, S. Ishibashi, T. Suzuki, and V. B. Meyer-Rochow. 1989. Growth-related biometrical and biochemical studies of the compound eye of the crab *Hemigrapsus sanguineus*. *Zool. Sci.* **6:** 241–250.

Eriksson, E. S. 1985. Attack behaviour and distance perception in the Australian bulldog ant *Myrmecia nigriceps*. *J. Exp. Biol.* **119:** 115–131.

Fincham, A. A. 1984. Ontogeny and optics of the eyes of the common prawn *Palaemon serratus* (Pennant, 1777). *Zool. J. Linn. Soc.* **81:** 89–113.

Fincham, A. A. 1988. Ontogeny of anomuran eyes. *Symp. Zool. Soc. Lond.* **59:** 123–155.

Frank, T. M. 1999. Comparative study of temporal resolution in the visual systems of mesopelagic crustaceans. *Biol. Bull.* **196:** 137–144.

Gaten, E., P. J. Herring, P. M. J. Shelton, and M. L. Johnson. 1998. Comparative morphology of the eyes of postlarval bresiliid shrimps from the region of hydrothermal vents. *Biol. Bull.* **194:** 267–280.

Hafner, G. S., and T. R. Tokarski. 1998. Morphogenesis and pattern formation in the retina of the crayfish *Procambarus clarkii*. *Cell Tissue Res.* **293:** 535–550.

Hariyama, T., V. B. Meyer-Rochow, and E. Eguchi. 1986. Diurnal changes in structure and function of the compound eye of *Ligia exotica* (Crustacea, Isopoda). *J. Exp. Biol.* **123:** 1–26.

Hariyama, T., Y. Tsukahara, and V. B. Meyer-Rochow. 1993. Spectral responses, including a UV-sensitive cell type, in the eye of the isopod *Ligia exotica*. *Naturwissenschaften* **80:** 233–235.

Hariyama, T., V. B. Meyer-Rochow, T. Kawauchi, Y. Takaku, and Y. Tsukahara. 2001. Diurnal changes in retinal cell sensitivities and receptive fields (two-dimensional angular sensitivity functions) in the apposition eyes of *Ligia exotica* (Crustacea, Isopoda). *J. Exp. Biol.* **204:** 239–248.

Harzsch, S., and R. R. Dawirs. 1996. Maturation of the compound eyes and eyestalk ganglia during larval development of brachyuran crustaceans *Hyas araneus* L. (Decapoda, Majidae) and *Carcinus maenas* L. (Decapoda, Portunidae). *Zoology* **99:** 189–204.

Horridge, G. A. 1978. The separation of visual axes in apposition compound eyes. *Philos. Trans. R. Soc. Lond. B* **285:** 3–59.

Juberthie-Jupeau, L. 1972. L'alimentation des cinq premiers stades de *Troglocaris anophthalmus*—donnés biologiques et histologiques. *Ann. Speleol.* **27:** 221–227.

Kelber, A. 2000. Eyes up. *New Sci.* **166:** 93.

Land, M. F. 1981. Optics and vision in invertebrates. Pp. 471–492 in *Vision in Invertebrates: Handbook of Sensory Physiology*, Vol. VII/6B, H. Autrum, ed. Springer, New York.

Madsen, N. 1964. The anatomy of *Argulus foliaceus* Linné. *Lunds Universitets Årsskrift N.F. Avd. II* **59:** 1–32.

Merilaita, S., and V. Jormalainen. 2000. Different roles of feeding and protection in diel microhabitat choice of sexes in *Idotea baltica*. *Oecologia* **122:** 445–451.

Meyer-Rochow, V. B. 1975. Larval and adult eye of the Western rock lobster *Panulirus longipes*. *Cell Tissue Res.* **162:** 439–457.

Meyer-Rochow, V. B. 1981. Electrophysiology and histology of the eye of the bumblebee *Bombus hortorum* (L.) (Hymenoptera: Apidae). *J. R. Soc. N. Z.* **11:** 123–153.

Meyer-Rochow, V. B. 1982. The divided eye of the isopod *Glyptonotus antarcticus*: effects of unilateral dark adaptation and temperature elevation. *Proc. R. Soc. Lond. B* **215:** 433–450.

Meyer-Rochow, V. B. 1994. Light-induced damage to photoreceptors of spiny lobsters and other crustaceans. *Crustaceana* **67:** 97–111.

Meyer-Rochow, V. B., and W. P. Meha. 1994. Tidal rhythm and the role of vision in shelter-seeking behavior of the half-crab *Petrolisthes elongatus* (Crustacea; Anomura; Porcellanidae). *J. R. Soc. N. Z.* **24:** 423–427.

Meyer-Rochow, V. B., and W. A. Reid. 1996. Does age matter in studying the crustacean eye? *J. Comp. Physiol. B* **166:** 319–324.

Meyer-Rochow, V. B., D. Towers, and I. Ziedins. 1990. Growth patterns in the eye of the halfcrab *Petrolisthes elongatus* Milne-Edwards. (Crustacea; Decapoda; Anomura). *Exp. Biol.* **48:** 329–340.

Meyer-Rochow, V. B., T. Kashiwagi, and E. Eguchi. 2002. Selective photoreceptor damage in four species of insects induced by experimental exposures to UV-irradiation. *Micron* **33:** 23–31.

Nalbach, H.-O., J. Zeil, and L. Forzin. 1989. Multisensory control of eye-stalk orientation in space: crabs from different habitats rely on different senses. *J. Comp. Physiol. A* **165:** 643–649.

Nilsson, D. E., E. Hallberg, and R. Elofsson. 1986. The ontogenetic development of refracting superposition eyes in crustaceans: transformation of optical design. *Tissue Cell* **18:** 509–519.

Quilter, C. G., and R. D. Lewis. 1989. Clock control of foraging in the isopod *Scyphax ornatus* Dana. *N. Z. J. Zool.* **16:** 373–382.

Richter, S. 1999. The structure of the ommatidia of the Malacostraca (Crustacea)—a phylogenetic approach. *Verh. Naturwiss. Ver. Hamburg NF* **38:** 161–204.

Ruck, P., and T. L. Jahn. 1954. Electrical studies on the compound eye of *Ligia occidentalis*. *J. Gen. Physiol.* **37:** 825–849.

Rüppell, G. 1967. Tagesrhythmische und langfristige Faunenverschiebungen im marinen Supralitoral. *Z. Morphol. Ökol. Tiere* **60:** 338–375.

Sharma, S. P. 1982. Microanatomical studies on the optic neuropiles of an isopod, *Ligia exotica* Roux (Crustacea). *Folia Morphol.* **30:** 70–75.

Shelton, P. M. J., R. G. J. Shelton, and P. R. Richards. 1981. Eye development in relation to moult stage in the European lobster *Homarus gammarus* (L.). *J. Cons. Int. Explor. Mer.* **39:** 239–243.

Srinivasan, M. V., and G. D. Bernard. 1975. The effect of motion on visual acuity of the compound eye: a theoretical analysis. *Vision. Res.* **15:** 515–525.

Taylor, B., and T. Carefoot. 1990. Underwater survival, orientation, and locomotory ability in the semiterrestrial Japanese "funamushi" *Ligia exotica* (Roux). Pp. 121–130 in *Third International Symposium on Biology of Terrestrial Isopods*, University of Poitiers Publ., Poitiers, France.

Tokarski, T. R., and G. S. Hafner. 1984. Regional morphological variations within the crayfish eye. *Cell Tissue Res.* **235:** 387–392.

Reference: *Biol. Bull.* **202:** 232–242. (June 2002)

Trans-Atlantic Distribution of a Mangrove Oyster Species Revealed by 16S mtDNA and Karyological Analyses

S. LAPÈGUE[1,*], I. BOUTET[1,2,†], A. LEITÃO[3], S. HEURTEBISE[1], P. GARCIA[2],
C. THIRIOT-QUIÉVREUX[3], AND P. BOUDRY[1]

[1]*IFREMER, Laboratoire de Génétique et Pathologie, B.P. 133, 17390 La Tremblade, France;*
[2]*Laboratoire de Biologie et Environnement Marins, Institut de la Mer et du Littoral,*
Avenue Lazaret, Port des Minimes, 17000 La Rochelle, France; and [3]*Observatoire*
Océanologique, UPMC-CNRS-INSU, B.P. 28, 06230 Villefranche-sur-mer, France

Abstract. Three species of mangrove oysters, *Crassostrea rhizophorae, C. brasiliana,* and *C. gasar,* have been described along the Atlantic shores of South America and Africa. Because the distribution of these molluscs is of great biological and commercial interest, their taxonomy and distribution deserve further clarification. Therefore, 15 populations were sampled from both continents. Their 16S mitochondrial polymorphism was studied by sequencing and PCR-RFLP analysis. Two haplotypes were identified. Haplotype a was the only one observed in Africa, but it was also observed in South America together with haplotype b. Because *C. gasar* is the only mangrove oyster identified on the west coast of Africa, haplotype a was attributed to this species, which has thus been shown to occur in South America. Haplotype b is attributed to *C. rhizophorae.* The karyotypes of specimens of *C. gasar,* from Africa and from South America, were very similar, and both species were observed at the same location in Brazil. The occurrence of *C. gasar* in South America adds a third species—in addition to *C. rhizophorae* and *C. brasiliana*—to the list of species present along these coasts. The predominant surface circulation patterns in this part of the Atlantic Ocean favor the hypothesis that *C. gasar* was transported from Africa to America. Finally, a phylogenetic tree built with seven 16S sequences from *Crassostrea* and *Saccostrea* species showed that *C. gasar* is intermediate between the American *Crassostrea* species (*C. virginica* and *C. rhizophorae*) and the Asian species (*C. gigas* and *C. ariakensis*).

Introduction

Mangrove ecosystems are widely distributed; they cover 100,000–200,000 km^2 of the world's tropical estuarine zones where sea and rivers mix (Blasco *et al.,* 1998). The mangrove trees characterize these ecosystems and constitute a natural habitat for mangrove oysters; the aerial prop roots of the trees provide the oyster larvae with a convenient place to settle in the intertidal zone. Because mangrove oysters live naturally on mangrove roots, which are called rhizophores, the latter term was used in the taxonomic name of a South American mangrove oyster, *Crassostrea rhizophorae* (Guilding, 1828). In fact, numerous species of mangrove oysters have been described, all in the genus *Crassostrea*; but the taxonomic identification is difficult and uncertain, so their geographical ranges are also often poorly known.

These problems and uncertainties are well illustrated by the mangrove oysters of South America and Africa. The taxonomic status of the oysters growing along the Atlantic coast of South America has been widely investigated morphologically, ecologically, physiologically, and genetically. Some authors have regarded the subtidal rocky shore form of *C. rhizophorae* (Guilding, 1828) as distinct, mainly because of its large size (*e.g.,* Nascimento, 1991), and have applied to it the binomen *C. brasiliana* (Lamarck, 1819).

Received 30 May 2001; accepted 3 April 2002.

[*] To whom correspondence should be addressed. E-mail: slapegue@ifremer.fr

[†] Current address: Laboratoire des Sciences de l'Environnement Marin (LEMAR), UMR CNRS 6539, Institut Universitaire Européen de la Mer, Université de Bretagne Occidentale, 29280 Plouzané, France.

But because size is considered unreliable as a taxonomic character, *C. brasiliana* was held by Rios (1994) to be synonymous with the generally smaller *C. rhizophorae*. However, large differences in growth rates and larval morphology have been described between *C. rhizophorae* and *C. brasiliana* populations, suggesting that they may indeed be distinct biological species (Absher, 1989). Moreover, their geographic range appears to be different: *C. brasiliana* occurs on the Caribbean coast of South America, whereas *C. rhizophorae* is more common and is found from Florida to Brazil (Littlewood, 1991). Finally, the occurrence of two distinct species along the South American coasts was clearly demonstrated recently by an allozyme study (Ignacio *et al.*, 2000). *C. rhizophorae* is now extensively cultivated throughout the various countries of the Caribbean Sea, as well as in the West Indies, and is considered to be a commercially important species (Arakawa, 1990). Moreover, *C. rhizophorae* is also being produced in New Guinea (FAO, 1999).

Oysters from the coasts of Africa have been less extensively studied than those from South America (Marozova *et al.*, 1991). Although *C. cucculatta* (Born) is the only species described from the eastern coast of Africa (and Madagascar), two species names are used for oysters growing along the western coast: *C. gasar* (Adanson) and *C. tulipa* (Lamarck). *C. gasar* has been reported in Mauritania (Gowthorpe, 1993), Senegal and Gambia (Diop, 1993), Ivory Coast (Egnankou, 1993), Nigeria (Isebor and Et Awosika, 1993), and Cameroon (Zogning, 1993). Two different names were given in Togo: "*Gryphea*" or *C. gasar* (Akpagana, 1993); and in Congo: *Gryphea gasar* (*Crassostrea tulipa*, Lamarck) (Makaya, 1993). The *C. tulipa* species name is also mentioned in Liberia (Yoo and Ryu, 1984) and in Sierra Leone (Kamara, 1982). As *C. tulipa* is now considered a synonym of *C. gasar* (Marozova *et al.*, 1991), we will use this name for samples collected from the south Atlantic African coast. *C. gasar* is a commercially important bivalve in Africa (Nicklès, 1950)—for example, in Nigeria (Ajana, 1979) and Senegal (Cormier-Salem, 1987)—and its potential for more intensive aquacultural production has been studied (Cormier-Salem, 1987; Marozova *et al.*, 1991).

A typical feature of oysters from the genus *Crassostrea* is the extreme variability of the shell (Galtsoff, 1964). Moreover, this variability also extends to the soft tissues (Lawrence, 1995). Therefore, oysters are often difficult to differentiate on the basis of their morphology. Consequently, other methods, such as karyological and molecular analyses, must be applied to distinguish the different mangrove oyster species. A study of seven species of cupped oyster showed that the karyotype of *C. gasar* is clearly isolated from two other groups, one composed of *C. gigas*, *C. angulata*, and *C. sikamea*, and the other of *C. virginica*, *C. ariakensis*, and *Saccostrea commercialis* (Leitão *et al.*, 1999). The karyotype of *C. rhizophorae* has also been previously reported in specimens from Mexico (Rodriguez-Romero *et al.*, 1979; Ladron de Guevara *et al.*, 1996) and from Venezuela (Marquez, 1992), and it appears to be different from those of the species described by Leitão *et al.* (1999).

Molecular methods can usefully complement morphological and karyological studies in determining the status of oyster taxa. For example, such methods have already been used to infer the phylogenetic relationships among species of cupped oysters (Littlewood, 1994), to discriminate between closely related Asian *Crassostrea* species (Banks *et al.*, 1993; Hedgecock *et al.*, 1999), to better understand the close relationship between *C. gigas* and *C. angulata* (Boudry *et al.*, 1998; O'Foighil *et al.*, 1998), and to distinguish among sympatric species of the rock oyster *Saccostrea* in Thailand (Day *et al.*, 2000). However, little molecular taxonomy has been done on mangrove oysters: a few genetic studies (allozyme data) have been carried out on *C. rhizophorae* (Hedgecock and Okazaki, 1984; Ignacio *et al.*, 2000), but nothing has been published previously about *C. gasar*.

In this study, the methods of molecular biology and karyology were used to ascertain the taxonomic status of the mangrove species present along the shores of the south Atlantic, and to determine the phylogenetic position of the African species in the *Crassostrea* clade. To these ends, we studied African mangrove oyster samples, described as *C. gasar* or *C. rhizophorae* (W.B. Dambo, Rivers State University of Science and Technology, Nigeria, pers. comm.), and American mangrove oysters, presumed to be *C. rhizophorae* or *C. brasiliana*. In particular, we analyzed the 16S mitochondrial fragment that had already been studied in other species of the genus *Crassostrea* by O'Foighil *et al.* (1995), and also in *Saccostrea* (K.K.Y. Lam and B. Morton, Swire Institute of Marine Science, The University of Hong Kong, China, unpubl. data) and *Ostrea* (Jozefowicz and O'Foighil, 1998). With these data, we could analyze the genetic relationship between *C. gasar* and the other species. We also examined the karyotype of the presumed *C. rhizophorae* samples from French Guiana and compared them with the karyotype of *C. gasar* from Senegal.

Materials and Methods

Sampling

Ethanol-fixed samples or live mangrove oysters were obtained from wild populations of south Atlantic coasts (see Fig. 1 for locations). Putative *C. rhizophorae* were collected along the Atlantic coast of South America: from Martinique in 1997 (MAS), French Guiana in 1997 (SIN), and Brazil. From this last location, two samplings were made, the first in 1997 (PAR1) on two islands (Ilha Rosa and Ilha das Gambas) inside Paranagua Bay, and the second sampling in 1998 at the harbor of Guaraqueçaba on the border of the

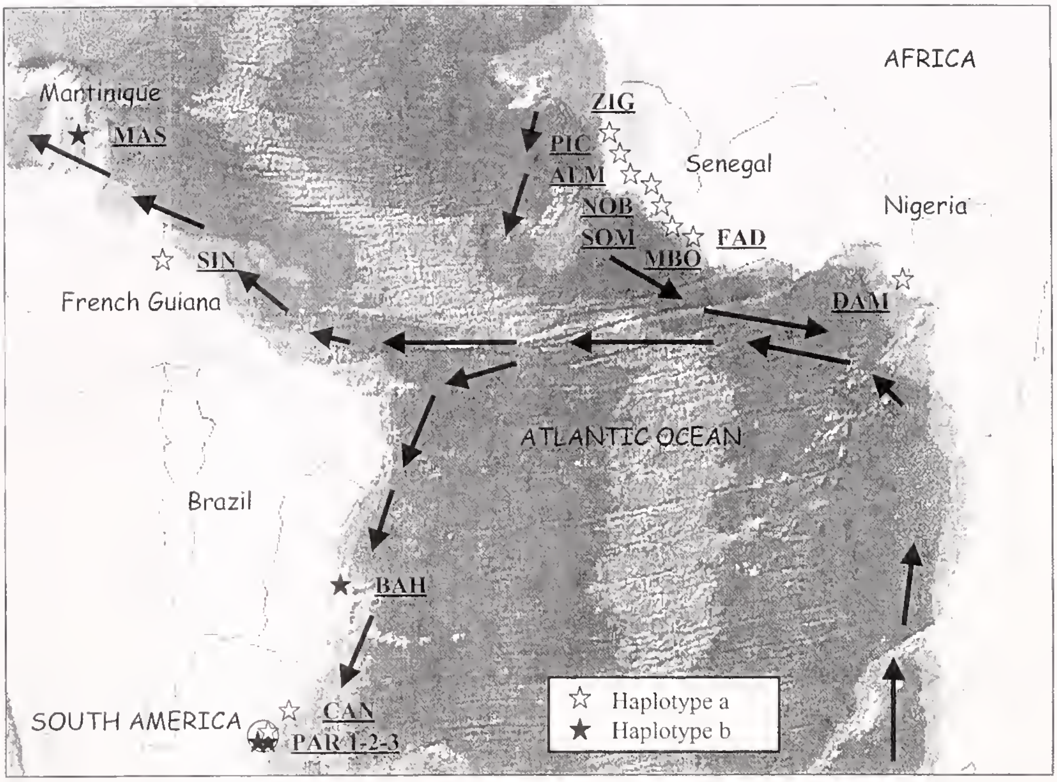

Figure 1. Population collection sites and their taxonomic status based on 16S gene analysis. The arrows indicate the predominant surface circulation patterns in this part of the Atlantic Ocean. See legend of Table 1 for details on the three PAR samples.

same bay. In this second sample, two groups (PAR2 and PAR3) were selected on the basis of their size: PAR2 specimens described as "fast growers," and PAR3 specimens described as "slow growers." Two other samples from Brazil were collected in 1999: in the Cananéia Bay (CAN), and near Salvador do Bahia (BAH). Putative *C. gasar* samples were provided in 1999 from locations along the Senegalese coasts (ZIG, NOB, PIC, ALM, SOM, MBO, FAD), and specimens were taken from the Niger estuary (DAM), described as *C. rhizophorae* in Nigeria in 2000. Generally, the samples were collected on either mangrove roots or rocks; but in the Paraguana Bay, they were all sampled on rocks, and in French Guiana on mangrove roots. Table 1 summarizes the characteristics of these samples. Two animals from each of the populations SIN and NOB were chosen for karyological analysis, as they were initially thought to represent *C. rhizophorae* and *C. gasar* respectively.

Mitochondrial DNA analysis

DNA extraction of gill fragments was performed either by a Chelex-based method, as described in Estoup *et al.* (1996), or by a phenol/chloroform method, as described by Moore (1993). We amplified the 16S mitochondrial fragment (16SrDNA: the large subunit rRNA-coding gene) with primers described by Banks *et al.* (1993), according to the protocol detailed in Boudry *et al.* (1998).

A first set of samples (two individuals from each of nine populations, as indicated in Table 1) was studied by sequencing the mitochondrial 16S fragment. The PCR products were then purified with a high pure PCR product purification kit (Boehringer-Mannheim, Germany), and manually sequenced with an oligonucleotide tailing kit (Boehringer-Mannheim, Germany) and γ33P radiolabeled deoxynucleotide triphosphate (dNTP). The sequencing reaction, consisting of 35 cycles (30 s, 95°C, denaturating; 30 s, 55°C, annealing; 1 min, 72°C, elongation), was performed according to the manufacturer's instructions.

The samples sequences—together with some sequences already obtained for *C. virginica, C. gigas, C. ariakensis* (O' Foighil *et al.*, 1995), *S. commercialis* and *S. mordax* (K.K.Y. Lam and B. Morton, Swire Institute of Marine Science, The University of Hong Kong, China, unpubl. data, accession numbers AF353099 AF353100), and *O. edulis* (Jozefowicz and O'Foighil, 1998)—were aligned with the software CLUSTALW (Thompson *et al.*, 1994). Parsimony analysis was implemented with PHYLIP (Felsenstein, 1989) using the program DNAPARS. Boot-

Table 1

Characteristics of the populations of Crassostrea *sampled*

Population name	Putative species	Location	Number of individuals	DNA sequence	PCR-RFLP haplotype
ZIG	*C. gasar*	Zinguichor, Senegal	2	A	a
NOB	*C. gasar*	Kafountine, Senegal	2	A	a
PIC	*C. gasar*	Senegal	2	A	a
ALM	*C. gasar*	Almadies, Senegal	2	A	a
SOM	*C. gasar*	Somone, Senegal	12		a
MBO	*C. gasar*	M'Bour, Senegal	6		a
FAD	*C. gasar*	Joal, Senegal	6		a
DAM	*C. rhizophorae*	Niger estuary, Nigeria	12		a
SIN	*C. rhizophorae*	Mont Sinery, French Guiana	2	A	a
MAS	*C. rhizophorae*	Martinique	2	B	b
PAR1*	*C. rhizophorae*	Paranagua Bay, Brazil	2	A	a
PAR2*	*C. rhizophorae*	Paranagua Bay, Brazil	2	B	b
PAR3*	*C. rhizophorae*	Paranagua Bay, Brazil	2	B	b
BAH	*C. rhizophorae*	Salvador do Bahia, Brazil	6		b
CAN	*C. rhizophorae* or *C. brasiliana*	Cananéia	6		a

* The three samples PAR were collected in the same area, the Paranagua Bay in Brazil. However, PAR1 was collected in 1997 on two islands inside the bay, and PAR2 and PAR3 in 1998 in a harbor on the border on the bay. Furthermore, the latest two samples differ in size. See Figure 1 for the location of the samples.

strap analysis with 100 replicates was performed by the SEQBOOT and CONSENSE programs from the PHYLIP package. Pairwise sequence divergences between species were estimated by the DNADIST program from PHYLIP according to Kimura's two-parameter model (Kimura, 1980).

With a second set of samples, the same mitochondrial fragment was studied by PCR-RFLP using the appropriate *Taq*I restriction enzyme at 65°C; the particular enzyme selected was determined by the sequence information we obtained. Restriction reactions were performed in a 20-μl volume composed of PCR product, 1× reaction buffer, and 2–5 units of endonuclease for 2 h. The digested results were resolved after electrophoresis on 1% agarose gels in 1× TBE (Tris–boric acid–EDTA), and stained with ethidium bromide.

Karyological analysis

Chromosome preparations were carried out according to Leitão *et al.* (1999). After acclimation in the hatchery of La Tremblade, France, oysters were incubated in a solution of colchicine (0.005%) in seawater. Dissected gills were treated in sodium citrate (0.9%), and then fixed in four successive baths of a freshly prepared mixture of absolute ethanol and acetic acid (3:1). Slides were prepared by an air-drying technique (Thiriot-Quiévreux and Ayraud, 1982) and finally stained with Giemsa 4%, pH 6.8. Ten metaphases from each supposed species were selected, and karyotypes were constructed. Chromosome measurements were then performed with a digitizer tablet (Summa Sketch II) interfaced with a Macintosh computer. Data analysis was performed with an Excel (Microsoft) macro program. Terminology relating to centromere position follows that of Levan *et al.* (1964) and takes into account the confidence limits of the centromeric index means. Nucleolus organizer regions (NORs) were silver-stained directly on unstained slides using the technique of Howell and Black (1982).

Results

Mitochondrial DNA sequence analysis

A PCR fragment of 570 base-pairs from the 16S mitochondrial ribosomal gene was obtained and sequenced for 18 individuals from nine South American and African Atlantic coast samples of mangrove oysters (Table 1). Only two different sequences were obtained; they are denoted by capital letters A and B in Table 1. These were registered in the DDBJ/EMBL/GenBank databases under accession numbers AJ312937 and AJ312938. These two sequences differ in length (473 and 465 bases-pairs) due to 14 insertion or deletion sites. In addition, 45 substitution sites (30 transitions and 15 transversions) were observed. Their divergence, based on Kimura's two-parameter model, was 11.34% (Table 2).

The alignment in Figure 2 is the result of comparing mitochondrial 16S sequences A and B with those obtained for *C. gigas*, *C. virginica*, and *C. ariakensis* by O'Foighil *et al.* (1995), and those obtained for *S. mordax*, *S. commercialis* (accession numbers AF353099 and AF353100), and *O. edulis* by Jozefowicz and O'Foighil (1998); *O. edulis*

Table 2

Pairwise sequence divergences, according to Kimura's two-parameter model (Kimura, 1980), among the seven species studied for the 480 nucleotide mt 16S rDNA fragment

Species*	1	2	3	4	5	6	7
1. Sequence A (*C. gasar*)	0						
2. Sequence B (*C. rhizophorae*)	*0.1132*	0					
3. *C. virginica*	*0.1288*	**0.0357**	0				
4. *C. gigas*	*0.1772*	0.1653	0.1657	0			
5. *C. ariakensis*	*0.1805*	0.1923	0.1835	**0.0575**	0		
6. *S. commercialis*	0.2380	0.2185	0.2221	0.1905	0.1758	0	
7. *S. mordax*	0.2403	0.2318	0.2187	0.1965	0.1834	0.1021	0
8. *O. edulis*	0.2314	0.2126	0.2028	0.1823	0.1706	0.1575	0.1716

O. edulis serves as an outgroup. Two pairwise comparisons yielding low genetic distance estimates are presented in boldface. Species in parentheses are those associated to the sequences described in this report.

* Genera: C., *Crassostrea*; S., *Saccostrea*; O., *Ostrea*.

was considered as an outgroup. The sequence divergences are given in Table 2. Apart from the *O. edulis* outgroup, four groups of sequences can clearly be distinguished on the tree presented in Figure 3: (1) *C. gigas* and *C. ariakensis*, (2) *C. virginica* and sequence B, (3) *S. mordax* and *S. commercialis*, and (4) sequence A. The first three groups are congruent with the three clades of cupped oysters described in O'Foighil and Taylor (2000). Inside the first two groups, divergence is relatively low: 5.75% between *C. gigas* and *C. ariakensis*, and 3.57% between *C. virginica* and sequence B. Inside the *Saccostrea* group, the divergence is higher: 10.21% between *S. mordax* and *S. commercialis*. In this context, sequence A—which displays an 11% divergence with the American *Crassostrea* oysters (group 2), and 17% with the Asian *Crassostrea* oysters (group 1)—can be considered as closer to the American *Crassostrea* oysters. However, whether sequence A is intermediate between the Asian and American *Crassostrea* oysters, or falls within the American *Crassostrea* oysters, is difficult to determine.

Geographic distribution of PCR-RFLP haplotypes

In the PCR-RFLP analysis, using the *Taq*I endonuclease, the two haplotypes (denoted by lower-case letters a and b, corresponding to the sequences A and B, respectively) were rapidly identified. Haplotype b was found only on the South American coast, whereas haplotype a was found on both the African and South American coasts: in French Guiana (SIN) and in two locations in Brazil (PAR1 and CAN) (Table 1, Fig. 1). All locations were monomorphic for one or the other haplotype, but both haplotypes were found within Paranagua Bay among samples PAR1, PAR2, and PAR3.

Karyological analysis

A diploid complement of 20 chromosomes, which is commonly observed in oysters (Nakamura, 1985), was confirmed in the samples. Means of the relative chromosome length and centromeric indexes (Table 3) are given for the individuals from Senegal (sample NOB), presumed to be *C. gasar*, and French Guiana (sample SIN), initially identified as *C. rhizophorae*. The African oyster presented a karyotype (Fig. 4A) of six metacentric and four submetacentric pairs (numbers 2, 8, 9, and 10), while the American (Fig. 4B) showed six metacentric and four submetacentric-subtelocentric pairs (numbers 3, 7, 9, and 10). The position of the large submetacentric pair differed in the African (pair 2) and the American (pair 3) samples, as did a small submetacentric pair (pair 8 in the African samples and pair 7 in the American samples). But taking into account the confidence limits of the relative length means, pairs 2 and 3 of the African oyster may be confounded, as may pairs 7 and 8 (see Table 3). This means that these karyotypes are very similar overall. Furthermore, silver-stained NORs were located on the largest submetacentric chromosome pairs in both samples, and these most probably have the same position in the two karyotypes (Fig. 4, C and D).

Discussion

The molecular and karyological data reported here extend previous morphological, ecological, and allozyme studies on the taxonomic status and distribution of mangrove oysters from Africa and the east coast of South Africa. Our most striking and important result, however, is that one of the species occurs on both sides of the South Atlantic. This finding compels us to reassess the number of species of South American mangrove oysters, and to consider the mode and direction of the dispersal that must have led to this transoceanic distribution.

In the present study, all the African samples, initially identified as *C. gasar*, were found to be monomorphic for haplotype a, corresponding to sequence A. In contrast,

```
                          10        20        30        40        50
                           |         |         |         |         |
Sequence A        TTGATTTTTAGTAGTACCTGCCCAGTGCG-TATTATCTTGTTAACGGCCGCCTTAGCGTG
Sequence B        ...........C.................A.....AG.C..C..................
C. virginica      ----------.C.................AC.A..AG.C..C....
C. gigas          ----------.C.AT..............AA..AT.AC...A..........C.......
C. ariakensis     ----------.C.AT..............AA..AT.AC...A..........C
S. commercialis   ----------.C..T.............A-----..A....A..........C..
S. mordax         ----------.C..T..............TC---..A....A..........C
O. edulis         ----------.C.AT..............A.CAA.AG.C..A..........C

                          70        80        90       100       110       120
                           |         |         |         |         |         |
Sequence A        AGGGTGCTAAGGTAGCGAAATTCCTTGCCTTTTAATTGTAGGCCAGCATGAATGGTTTGA
Sequence B        .................................G.....G....................
C. virginica      .................................G.....G....T...............
C. gigas          .................................G.....G....T.............A.
C. ariakensis     .................................G..........T.............A.
S. commercialis   .......C....................................T..........A....
S. mordax         .......C....................................T..........A....
O. edulis         ............................................T.............

                         130       140       150       160       170       180
                           |         |         |         |         |         |
Sequence A        CGAGGGCCTCACTGTCTCTTAGTTC-TATGTTGAAATTGTAGTGTAGGTGAAGATACCTT
Sequence B        .......T.TG........CGA..T-.T.A......................A.......
C. virginica      .......T.TG.........GA..T-.T.A......................A.......
C. gigas          ......TT.G.........A.A..T-.T.A...........C..A...............
C. ariakensis     ......TT.A..........GA..T-A.AA...........C..A...............
S. commercialis   ......T.AAG.........GC..TGAGCAGC.......G.C..A...............
S. mordax         ........ATT.........GCC.TA.GAAGT.......G...AA...............
O. edulis         .......T.A.........AG-..TG..A..CT......G...AA.............

                         190       200       210       220       230       240
                           |         |         |         |         |         |
Sequence A        CATAAAAAAGTAAGACAAAAAGACCCCGTGCAACTTTGAAAA-TTAAGCTAGATTAAATG
Sequence B        .....G.....T......G.......................-C...--CGA.....TAA
C. virginica      .....G.....T......G.......................GC......GA.....TAA
C. gigas          ...TT......T......G..A....................T.A.C--.TT...C.GGA
C. ariakensis     ...T.......C......T..A....................T.A.C--.TT...C.GAA
S. commercialis   ....T......T......G.............G....T....A..T.--.TT.....GGA
S. mordax         T..T.......T......G.............G....T....GA.CC--.TT.....GA.
O. edulis         T..........C......G..................T...-G.C..--CTTG..T.GGA

                         250       260       270       280       290       300
                           |         |         |         |         |         |
Sequence A        GCAAAAGATTTTTAGGTGGGCGCCAAAAGAGGAAACTATAACCTC-TG-------CTGT-
Sequence B        CT...........G...........T......A...--T.......-..------T...G
C. virginica      .T...........G...........T......T...A.T.......-..------T..AA
C. gigas          .T.......................T.G.A..C..-G.C......TTC--------..AA
C. ariakensis     .TG......................T.G.A..T..-A.C......TTC--------..AA
S. commercialis   TTGT.....................T.GGA..T...ACT......TC.---TA--T.TGT
S. mordax         AGGT.-...................T.GGA..T...A.T......TC..TGTAATT.TGT
O. edulis         .TTTC....................T.TTA..T..TA-T......T------AG--.-GT

                         310       320       330       340       350       360
                           |         |         |         |         |         |
Sequence A        TTAAGCTAATTCTTAC-TGGAGTTGACCTGACTTAAGTCGATCAAAGGAGAAGTTACGCC
Sequence B        ...CA--......G..A.A..T.-..........TG........................
C. virginica      ...CAGA......A..-.A..T............C.........T...............
C. gigas          .A.CT--..C....T.-.A..T......C..T.AT.T.......T...............
C. ariakensis     CATTT--.GT....T.-C...C......C..T.AT.T.......T...............
S. commercialis   .A..A--GCAA..GT.-...T..A....C.G.-A.GTC......T...............
S. mordax         ..GT.--.CAA..CT.-.A.TA.A....C.GTGA.ATC......T...............
O. edulis         ACG.T--..AA...T.-AA.TA.A....C...-A.T........T...............

                         370       380       390       400       410       420
                           |         |         |         |         |         |
Sequence A        GGGGATAACAGGCCAATTCTTTAGTAAAGCTCGTATTAACTAAAGGGCTTGGCACCTCGA
Sequence B        .................C...........T..............................
C. virginica      .................C..C........T..............................
C. gigas          .............T...C........G..T.......GG........A............
C. ariakensis     .............T...C........G..........GG........A...
S. commercialis   .............TT..CTA......G..........GG....TA..A...
S. mordax         .............TT..C.A......G..........GG....T...A...
O. edulis         .............T...C.AC.....G..AA......GG...GT...A...

                         430       440       450       460
                           |         |         |         |
Sequence A        TGTTGAATCAGGGATTATAGCTTCAAGGCGTAGATGCTTT
Sequence B        .......................T..........A.....
C. virginica      .......................T..........A.....
C. gigas          ...............A..................G...
C. ariakensis     ...............G..................G...
S. commercialis   ........T.A....G..A...T..........G.....
S. mordax         ........T.....CA...A...T..........A...
O. edulis         ...............G...C..CT..........A...
```

Figure 2. Alignment of the sequences A and B, and of published sequences for *Crassostrea virginica, C. gigas,* and *C. ariakensis* (O'Foighil *et al.*, 1995), *Saccostrea commercialis, S. mordax* (Lam and Morton, AF353100), and *Ostrea edulis* (Jozefowicz and O'Foighil, 1998). The four nucleotides in bold at position 141–144 correspond to a polymorphic restriction site for the *Taq*I enzyme.

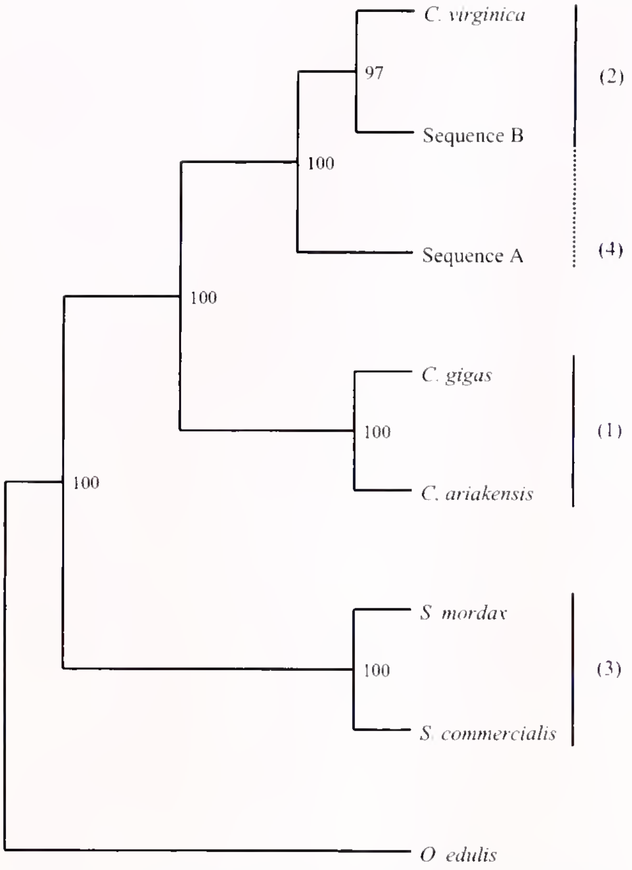

Figure 3. A phylogenetic tree based on a parsimony analysis of 480 nucleotide sequences of the 16S gene according to Kimura's model (Kimura, 1980). Numbers on the branches indicate bootstrap values. Four groups of species were identified (1,2,3, and 4).

although almost all of the South American samples were first identified as *C. rhizophorae*, the 16S sequence and RFLP analyses confirm the presence of at least two mangrove oyster species (haplotypes a and b, corresponding to sequences A and B). That these two types can be considered as two different species is supported by the nucleotide divergence (11%) between them, which is large when compared with the divergence calculated between *C. gigas* and *C. ariakensis* on the same fragment (5%). On the basis of our results from the African samples, we propose that haplotype a and sequence A from along American coasts are attributable to the identified African species *C. gasar*. The other species present along the American coasts (sequence B and its corresponding PCR-RFLP haplotype b) can be referred to as *C. rhizophorae* with more confidence. Hence, its close relationship with *C. virginica* (3.5% divergence) is strong evidence of its taxonomic status. The karyological observations support this species distribution. The karyotype of the French Guiana samples (presumed to be *C. rhizophorae*) showed six metacentric and four submetacentric-subtelocentric pairs. This picture is clearly different from the karyotypes previously described for *C. rhizophorae*; that is, five metacentric and five submetacentric pairs (Rodriguez-Romero *et al.*, 1979; Ladron de Guevara *et al.*, 1996) or eight metacentric and two submetacentric chromosomes (Marquez, 1992). However, when the French Guiana samples are compared with the African *C. gasar* samples, both karyotypes are very similar in the number and position of the metacentric and submetacentric pairs and the location of silver-stained NORs. The very slight differences in the centromere position of submetacentric-subtelocentric pairs in our American sample should not be taken as an interspecific chromosomal character, because karyotypes of cupped oysters differ in such characteristics (Leitão *et al.*, 1999). Therefore, on the basis of our karyological observations, individuals from the French Guiana and Senegal samples are likely to be the same species, as was revealed by molecular analysis.

That populations separated by the Atlantic Ocean—and supposedly members of distinct species—are now revealed as being in the same species calls into question the actual number of species that occur on the eastern coast of South America. Recently, Ignacio *et al.* (2000) demonstrated, on the basis of allozyme data, that two distinct biological species, *C. brasiliana* and *C. rhizophorae*, occur along the coast of Brazil. To this short list, our study now adds *C. gasar*, which was found at three locations along the Atlantic coast of South America, one in French Guiana, and two in Brazil, in two bays 70 km apart. Now we must ask whether *C. brasiliana* and *C. gasar* are the same species. Unfortunately, a direct comparison between the *C. brasiliana* and *C. gasar* specimens could not be performed, but the question might be answered if we were to consider the interesting ecological preferences characterized by Ignacio *et al.* (2000). His specimens of *C. rhizophorae* oysters were small and attached in the intertidal zone, either to mangrove (*Rhizophorae mangle*) roots, or to rocks in the intertidal zone. Conversely, *C. brasiliana* oysters were larger and attached to rocks in the subtidal zone. In comparison, *C. rhizophorae* typically settles on the mangrove roots, but occasionally also on rocks (Nascimento *et al.*, 1991; Rios, 1994). Finally, in Nigeria (Africa), *C. gasar* favors the subtidal zone, although it can, in the dry season, occur a little above the level of low tide (Ajana, 1980). These preferences do not resolve species relationships, and in our South American study, we could not correlate either the size of the oysters or their habitat with their taxonomic status.

Our genetic study, based on the mitochondrial and nuclear genomes, clearly demonstrates that a common mangrove species is present in South America and Africa. But did this species originate in South America or Africa? And when, and by what means, did the dispersal occur? The identical mtDNA sequences of American and African *C. gasar* oysters show that these two population groups have a

Table 3

Chromosome measurements derived from 10 cells of each sample

Chrom. pair no.	Mean RL	Conf. L.	RL max	RL min	Mean CI	Conf. L.	CI max	CI min	Type*
			NOB sample: putative *Crassostrea gasar*						
1	11.36	0.48	11.84	10.89	43.64	2.34	45.99	41.30	m
2	11.19	0.53	**11.72**	**10.67**	27.52	1.67	29.19	25.84	sm
3	11.04	0.29	**11.33**	**10.75**	45.62	1.77	47.39	43.85	m
4	10.62	0.54	11.16	10.08	37.80	1.65	39.45	36.14	m/sm
5	10.54	0.36	10.90	10.18	46.95	1.75	48.70	45.20	m
6	9.97	0.31	10.28	9.66	45.77	1.66	47.43	44.10	m
7	9.64	0.39	**10.03**	**9.25**	45.21	2.53	47.75	42.68	m
8	9.54	0.45	**9.99**	**9.08**	30.78	2.45	33.23	28.33	sm
9	8.82	0.43	9.25	8.39	28.65	2.15	30.80	26.49	sm
10	7.28	0.40	7.68	6.88	27.89	2.70	30.59	25.19	sm
			SIN sample: putative *Crassostrea rhizophorae*						
1	12.08	0.40	12.48	11.68	44.51	1.76	46.26	42.75	m
2	11.83	0.48	12.31	11.35	42.57	2.52	45.09	40.05	m
3	10.86	0.36	11.22	10.50	26.02	2.37	28.39	23.66	sm/st
4	10.73	0.41	11.15	10.32	44.15	2.95	47.10	41.21	m
5	10.58	0.60	11.18	9.98	37.00	2.22	39.22	34.78	m/sm
6	9.87	0.29	10.16	9.58	42.65	2.16	44.81	40.50	m
7	9.76	0.42	**10.18**	**9.33**	24.98	1.35	26.33	23.63	sm/st
8	9.15	0.56	**9.71**	**8.59**	43.57	1.39	44.96	42.19	m
9	8.76	0.27	9.04	8.49	24.29	1.00	25.29	23.29	sm/st
10	6.37	0.53	6.90	5.84	26.07	2.23	28.30	23.85	sm/st

CI: centromeric index, Conf. L.: confidence limit of means, RL: relative length, m: metacentric, sm: submetacentric, st: subtelocentric. The boldface values correspond to the confidence limits of the relative length means of chromosome pairs that allow pairs 2 and 3 to be confounded, and likewise pairs 7 and 8.

* The morphological type of chromosome is given according to the CI max and CI min; m/sm means that the type of the chromosome pair is on the edge of the two classes—metacentric and submetacentric (see classification in Levan *et al.*, 1964).

relatively recent common origin. O'Foighil *et al.* (1998) analyzed sequences of the cytochrome oxidase I gene and dated the genetic divergence between *C. gigas* and *C. angulata* at 1 to 2 million years. When the 16S ribosomal gene was analyzed, the divergence between the two taxa was estimated to be 0.46% (Huvet, 2000; unpubl. data provided by O'Foighil). If we assume that mutation rates at the cytochrome oxidase I gene are similar among *Crassostrea* species, then the African and American populations of *C. gasar* were established less than 1 to 2 million years ago. To assess the level of polymorphism of the 16S ribosomal gene in *C. gasar*, a larger sample size would be necessary. For example, Small and Chapman (1997) used a PCR-RFLP approach (10 restriction enzymes) on 410 individuals from the Atlantic coasts and the Gulf of Mexico to study intraspecific variation in the 16S ribosomal gene of *C. virginica*. They found 11 haplotypes, of which one was highly frequent (95 %). Thus, the level of genetic divergence between the American and African *C. gasar* populations could probably be better estimated if more polymorphic markers were available.

The relatively recent divergence between the American and African populations of *C. gasar* supports the hypothesis that man was an agent of the dispersal. Many recent transfers and worldwide introductions of oysters for aquacultural purposes have been reported (Carlton and Mann, 1996). Furthermore, events of introduction in historic time have been demonstrated on the basis of genetic markers (O'Foighil *et al.*, 1998; Boudry *et al.*, 1998). In the case of *C. gasar*, shipping between South America and the west coast of Africa may have transferred these oysters from one coast to the other. Note, however, that no *C. rhizophorae* samples were found in Senegal or Nigeria. Although the west African coast must be more extensively sampled to confirm this result, it does imply that, unlike *C. gasar*, *C. rhizophorae* either was not transported to or did not persist on the African coast.

Natural transport may also be responsible for the present geographic range of *C. gasar*. Larval dispersal might have been possible, even over such a long distance (at least 3000 km), because the larval stage of most *Crassostrea* species lasts about 3 weeks. However, the transport of adult oysters on drifting objects, a common phenomenon in the marine environment, may be a mode of dispersal with a larger potential range than that achievable by swimming larvae (Johannesson, 1988; O'Foighil, 1989). For example, dis-

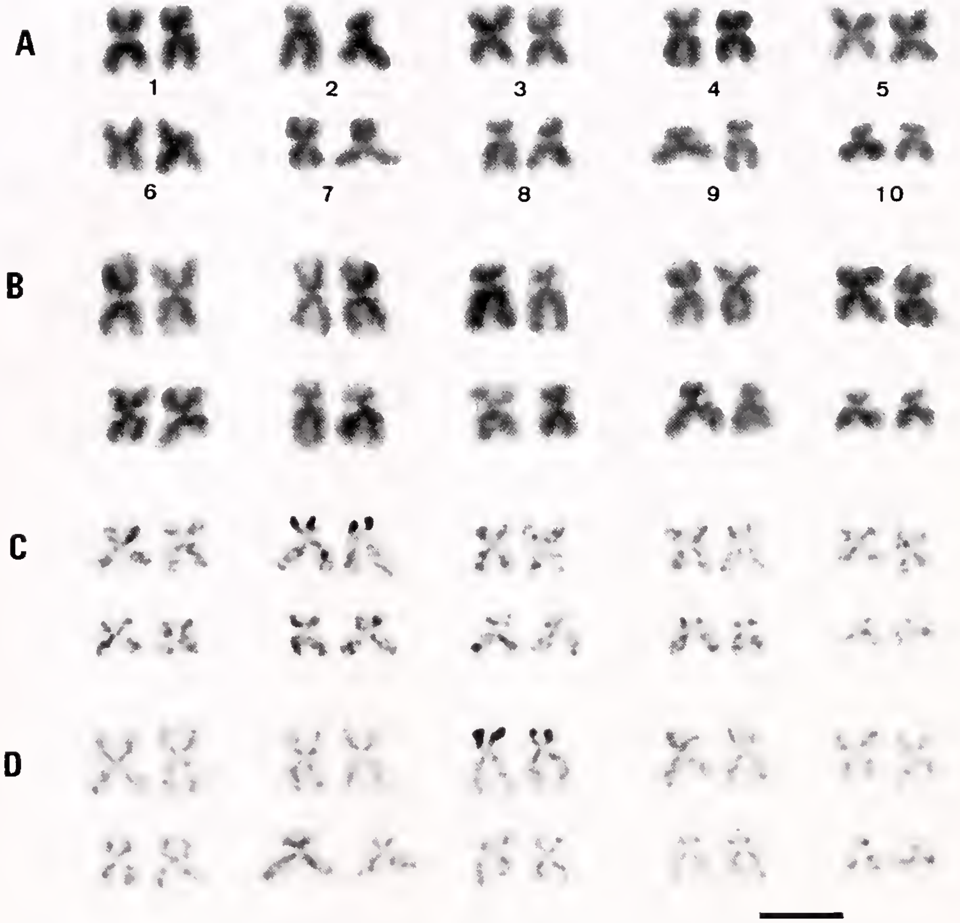

Figure 4. (A) Giemsa-stained karyotype of African *Crassostrea gasar,* (B) Giemsa-stained karyotype of putative *C. rhizophorae* from French Guiana, (C) NOR-stained karyotype of African *C. gasar,* (D) NOR-stained karyotype of putative *C. rhizophorae* from French Guiana. Scale bar = 5 μm.

persal by rafting was the most likely explanation for trans-Pacific range extension by the flat oyster *Ostrea chilensis* from New Zealand to Chile (O'Foighil *et al.,* 1999). The predominant surface circulation patterns in this part of the Atlantic Ocean (Fig. 1) favor the hypothesis that *C. gasar* was transported from Africa to America, as also hypothesized by Lessios *et al.* (1999) to explain the close genetic similarity of specimens of *Eucidaris tribuloides* from the Caribbean Sea and Brazil to those from the Gulf of Guinea.

Focusing on the Paraguana Bay (Brazil) where two species were found, PAR1 exhibited the *C. gasar* haplotype, but PAR2 and PAR3, both located in the same bay about 30 km away, exhibited the *C. rhizophorae* haplotype. One can ask whether these species are completely or incompletely reproductively isolated, and whether they have different habitats. A more intensive survey could provide an answer by revealing whether individuals from these species inhabit the same site, and whether hybrids occur in the wild. Based on the rRNA large subunit DNA sequences, and those known between other species in the genus (see Table 2), the genetic distance between *C. gasar* and *C. rhizophorae* is sufficiently large (88.7% similarity) that they are unlikely to produce viable hybrids. Indeed, the genetic distance between *C. gigas* and *C. virginica,* two species for which viable hybrids could not be obtained (Allen *et al.,* 1993), is of similar value (84.5% similarity).

Acknowledgments

We thank M. Antonio, F. Blouin, F. Cornette, W.B. Dambo, H.D. Diadhiou, P. Favrenière, N. Jan, P. Noble, P. Phelipot, Y. Pichot, A. Pinheiro, J.-L. Seugnet, and A. Thébault for providing oyster samples; B. Verdon for technical help; and L. Petit de la Villeon for his research on surface circulation patterns in the South Atlantic. Part of this work was supported by the Région Poitou-Charentes (Convention 99 RPC-A-201). We are grateful to D. Moraga, A. Tanguy, D. O'Foighil, and another anonymous reviewer for their help in improving the manuscript, as well as to H. McCombie for English editing.

Literature Cited

Absher, T. M. 1989. Populações naturais de ostras do gênero *Crassostrea* do litoral do Paraná—desenvoltimento larval, recrutamento e crescimento. Ph.D. thesis. Oceanography Institute, Universadade de São Paulo, São Paulo, Brazil.

Ajana, A. M. 1979. Preliminary investigation into some factors affecting the settlement of the larvae of the mangrove oyster *Crassostrea gasar* (Adanson) in the Lagos lagoon. *Malacologia* **18:** 271–275.

Ajana, A. M. 1980. Fishery of the mangrove oyster, *Crassostrea gasar,* Adanson (1757), in the Lagos area, Nigeria. *Aquaculture* **21:** 129–137.

Akpagana, K. 1993. L'écosystème des mangroves et des formations affiliées du Sud-Est du Togo. Pp. 108–119 in *Conservation et utilisation rationnelle des forêts de Mangrove de l'Amérique latine et de l'Afrique,* Vol. 2. E. S. Diop, ed. UNESCO-COMAR, Paris.

Allen, S. K., Jr., P. M. Gaffney, J. Scarpa, and D. Bushek. 1993. Inviable hybrids of *Crassostrea virginica* (Gmelin) with *C. rivularis* (Gould) and *C. gigas* (Thunberg). *Aquaculture* **113:** 269–289.

Arakawa, K. Y. 1990. Commercially important species of oysters in the world. *Mar. Behav. Physiol.* **17:** 1–13.

Banks, M. A., D. Hedgecock, and C. Waters. 1993. Discrimination between closely related Pacific oyster species (*Crassostrea*) *via* mitochondrial DNA sequences coding for large subunit rRNA. *Mol. Mar. Biol. Biotechnol.* **2:** 129–136.

Blasco, F., T. Gauquelin, M. Rasolofoharinoro, J. Denis, M. Aizpuru, and V. Caldairou. 1998. Recent advances in mangrove studies using remote sensing data. *Mar. Freshw. Res.* **49:** 287–296.

Boudry, P., S. Heurtebise, B. Collet, F. Cornette, and A. Gérard. 1998. Differentiation between populations of the Portuguese oyster, *Crassostrea angulata* (Lamarck) and the Pacific oyster, *Crassostrea gigas* (Thunberg), revealed by mtDNA RFLP analysis. *J. Exp. Mar. Biol. Ecol.* **226:** 279–291.

Carlton, J. T., and R. Mann. 1996. Transfers and world-wide introductions. Pp. 691–706 in *The Eastern Oyster* Crassostrea virginica, V.S. Kennedy, R.I.E. Newell, and A.F. Eble, eds. Maryland Sea Grant, College Park, MD.

Cormier-Salem, M. C. 1987. La cueillette des huîtres en Casamance. Place de cette pratique dans le système d'exploitation Diola. *Document scientifique du Centre de recherche océanographiques de Dakar-Tiaroye* **106:** 104 pp.

Day, A. J., A. J. S. Hawkins, and P. Visootiviseth. 2000. The use of allozymes and shell morphology to distinguish among sympatric species of the rock oyster *Saccostrea* in Thailand. *Aquaculture* **187:** 51–72.

Diop, E. S. 1993. Les mangroves du Sénégal et de la Gambie. Pp. 22–40 in *Conservation et utilisation rationnelle des forêts de Mangrove de l'Amérique latine et de l'Afrique,* Vol. 2. E. S. Diop, ed. UNESCO-COMAR, Paris.

Egnankou, M. W. 1993. Les mangroves de Côte d'Ivoire. Pp. 83–93 in *Conservation et utilisation rationnelle des forêts de Mangrove de l'Amérique latine et de l'Afrique,* Vol. 2. E. S. Diop, ed. UNESCO-COMAR, Paris.

Estoup, A., C. R. Largiader, E. Perrot, and D. Chourrout. 1996. Rapid one-tube DNA extraction for reliable PCR detection of fish polymorphic markers and transgenes. *Mol. Mar. Biol. Biotechnol.* **5:** 295–298.

Felsenstein, J. 1989. PHYLIP—Phylogeny Inference Package (Version 3.2). *Cladistics* **5:** 164–166.

FAO. 1999. *Aquaculture Production Statistics, 1988–1997.* FAO Fishery Circular 815, Revision 11, p. 82, Food and Agriculture Organization of the United Nations, Rome.

Galtsoff, P. S. 1964. The American oyster *Crassostrea virginica* Gmelin. *U.S. Fish and Wildl. Serv. Fish. Bull.* **64:** 479 pp.

Gowthorpe, P. 1993. Les mangroves de la Mauritanie. Pp. 3–21 in *Conservation et utilisation rationnelle des forêts de Mangrove de l'Amérique latine et de l'Afrique;* Vol. 2. E. S. Diop, ed. UNESCO-COMAR, Paris.

Hedgecock, D., and N. B. Okazaki. 1984. Genetic diversity within and between populations of American oysters (*Crassostrea*). *Malacologia* **25:** 535–549.

Hedgecock, D., G. Li, M. A. Banks, and Z. Kain. 1999. Occurrence of the Kumamoto oyster *Crassostrea sikamea* in the Ariake Sea, Japan. *Mar. Biol.* **133:** 65–68.

Howell, W. M., and D. A. Black. 1982. Controlled silver-staining of nucleolus organizer regions with a protective colloidal developer: a 1-step method. *Experientia* **36:** 1014–1015.

Huvet, A. 2000. Ressources génétiques et phylogéographie des huîtres creuses *Crassostrea gigas* et *C. angulata*: variabilité, différenciation et adaptation des populations naturelles et introduites. Ph.D. thesis. Université de Tours, France. 202 pp.

Ignacio, B. L., T. M. Absher, C. Lazoski, and A. M. Solé-Cava. 2000. Genetic evidence of the presence of two species of *Crassostrea* (Bivalvia: Ostreidae) on the coast of Brazil. *Mar. Biol.* **136:** 987–991.

Isebor, C. E., and L. F. Et Awosika. 1993. Les ressources de la mangrove au Nigeria: son état et sa mise en valeur. Pp. 169–188 in *Conservation et utilisation rationnelle des forêts de Mangrove de l'Amérique latine et de l'Afrique;* Vol. 2. E. S. Diop, ed. UNESCO-COMAR, Paris.

Johannesson, K. 1988. The paradox of Rockall: Why is a brooding gastropod (*Littorina saxatilis*) more widespread than one having a planktonic larval stage (*L. littorea*)? *Mar. Biol.* **99:** 507–513.

Jozefowicz, C. J., and D. O. O'Foighil. 1998. Phylogenetic analysis of southern hemisphere flat oysters based on partial mitochondrial 16S rDNA gene sequences. *Mol. Phylogenet. Evol.* **10:** 426–435.

Kamara, A. B. 1982. Preliminary studies to culture mangrove oysters, *Crassostrea tulipa,* in Sierra Leone. *Aquaculture* **27:** 285–294.

Kimura, M. 1980. A simple method for estimating evolutionary rates of base substitutions through comparative studies of nucleotide sequences. *J. Mol. Evol.* **16:** 111–120.

Ladron de Guevara, B., F. Winkler, F. Rodriguez-Romero, and C. Palma-Rojas. 1996. Comparative karyology of four American oyster species. *Veliger* **39:** 260–266.

Lawrence, D. R. 1995. Diagnosis of the genus *Crassostrea* (Bivalvia, Ostreidae). *Malacologia* **36:** 185–202.

Leitão, A., P. Boudry, J.-P. Labat, and C. Thiriot-Quiévreux. 1999. Comparative karyological study of cupped oyster species. *Malacologia* **41:** 175–186.

Lessios, H. A., B. D. Kessing, D. R. Robertson, and G. Paulay. 1999. Phylogeography of the pantropical sea urchin *Eucidaris* in relation to land barriers and ocean currents. *Evolution* **53:** 806–817.

Levan, A., K. Fredga, and A. A. Sandberg. 1964. Nomenclature for centromere position in chromosomes. *Hereditas* **52:** 201–220.

Littlewood, D. T. 1991. Oyster cultivation in the Caribbean with an emphasis on mangrove oysters in Jamaica. *World Aquacult.* **22:** 70–73.

Littlewood, D. T. 1994. Molecular phylogenetics of cupped oysters based on partial 28S rRNA gene sequences. *Mol. Phylogenet. Evol.* **3:** 221–229.

Makaya, J.-F. 1993. La mangrove au Congo: son état actuel. Pp. 208–213 in *Conservation et utilisation rationnelle des forêts de Mangrove de l'Amérique latine et de l'Afrique,* Vol. 2. E. S. Diop, ed. UNESCO-COMAR, Paris.

Marozova, A. L., K. D. Leung-Tack, V. I. Kholodov, V. V. Trousevich, S. Camara, V. K. Maskevski, F. X. Ibrahimov, and P. D. Lamakin. 1991. *L'ostréiculture en milieux de mangroves (Etude de cas en Guinée et au Sénégal),* I.E. Timchenko and S. Konate, eds. Série documentaire **7**, COMAR, France. 148 pp.

Marquez, E. G. 1992. Comparación de cariotipos entre las ostras *Crassostrea virginica* (Gmelin), *C. rhizophorae* (Guilding) y *Pinctada imbricata* (Röding). *Caribb. J. Sci.* **28:** 51–55.

Moore, D. 1993. Preparation of genomic DNA from mammalian tissue. Pp. 1–2 in *Current Protocols in Molecular Biology*, Vol. 1, F.M. Ausubel, ed. John Wiley, New York.

Nakamura, H. 1985. A review of molluscan cytogenetic information based on CISMOCH-Computerized index system for molluscan chromosomes. Bivalvia, Polyplacophora and Cephalopoda. *Venus Jpn. J. Malacol.* **44:** 193–225.

Nascimento, I. A. 1991. *Crassostrea rhizophorae* (Guilding) and *C. brasiliana* (Lamarck) in South and Central America. Pp. 125–134 in *Estuarine and Marine Bivalve Mollusk Culture*, W. Menzel, ed. CRC Press, Boca Raton, FL.

Nicklès, M. 1950. Mollusques testaces marins de la côte occidentale d'Afrique, *Manuels Ouest-Africains* **2:** 1–269.

O'Foighil, D. 1989. Planktotrophic larval development is associated with a restricted geographic range in *Lasea*, a genus of brooding, hermaphrodite bivalves. *Mar. Biol.* **103:** 349–358.

O'Foighil, D., and D. J. Taylor. 2000. Evolution of parental care and ovulation behavior in oysters. *Mol. Phylogenet. Evol.* **15:** 301–313.

O'Foighil, D., P. Gaffney, and T. J. Hilbish. 1995. Differences in mitochondrial 16S ribosomal gene sequences allow discrimination among American [*Crassostrea virginica* (Gmelin)] and Asian [*C. gigas* (Thunberg) *C. ariakensis* (Wakiya)] oyster species. *J. Exp. Mar. Biol. Ecol.* **192:** 211–220.

O'Foighil, D., P. Gaffney, A. E. Wilbur, and T. J. Hilbish. 1998. Mitochondrial cytochrome oxidase I gene sequences support an Asian origin for the Portuguese oyster *Crassostrea angulata*. *Mar. Biol.* **131:** 497–503.

O'Foighil, D., B. A. Marshall, T. J. Hilbish, and M. A. Pino. 1999. Trans-Pacific range extension by rafting is inferred for the flat oyster *Ostrea chilensis*. *Biol. Bull.* **196:** 122–126.

Rios, E. C. 1994. *Seashells of Brazil*. Fundaçao Universidade do Rio Grande, Rio Grande, Brazil.

Rodriguez-Romero, F., M. Uribe-Alcocer, A. Laguarda-Figueras, and M. E. Diopotex-Chong. 1979. The karyotype of *Crassostrea rhizophorae* (Guilding). *Venus Jpn. J. Malacol.* **38:** 135–140.

Small, M. P., and R. W. Chapman. 1997. Intraspecific variation in the 16S ribosomal gene of *Crassostrea virginica*. *Mol. Biol. Biotechnol.* **3:** 189–196.

Thiriot-Quiévreux, C., and N. Ayraud. 1982. Les caryotypes de quelques espèces de Bivalves et de Gastéropodes marins. *Mar. Biol.* **70:** 165–172.

Thompson, J. D., D. G. Higgins, and T. J. Gibson. 1994. CLUSTAL W: improving the sensitivity of progressive multiple sequence alignment through sequence weighting, position-specific gap penalties and weight matrix choice. *Nucleic Acids Res.* **22:** 4673– 4680.

Yoo, S. K., and H. K. Ryu. 1984. Comparative morphological characteristics of mangrove oysters. *Bull. Korean Fish. Soc.* **174:** 321–326.

Zogning, A. 1993. Les mangroves du Cameroun. Pp. 189–196 in *Conservation et utilisation rationnelle des forêts de Mangrove de l'Amérique latine et de l'Afrique*, Vol. 2. E. S. Diop, ed. UNESCO-COMAR, Paris.

THE LIMITS TO SELF-ORGANIZATION IN BIOLOGICAL SYSTEMS

Proceedings
of a workshop
sponsored by
THE CENTER FOR ADVANCED STUDIES
IN THE SPACE LIFE SCIENCES
AT THE MBL

11 to 13 May 2001

J. Erik Jonsson Center
of the National Academy of Sciences,
Woods Hole, Massachusetts

Funded by THE NATIONAL AERONAUTICS AND SPACE ADMINISTRATION under Cooperative Agreement NCC 2-896. Reprints of this symposium can be obtained from the Center for Advanced Studies in the Space Life Sciences, 7 MBL Street, Woods Hole, MA 02543.

CONTENTS

The Limits to Self-Organization in Biological Systems

Blazis, Diana E. J.
Introduction 245
Anderson, Carl
Self-organization in relation to several similar concepts: are the boundaries to self-organization indistinct? 247
Cole, Blaine J.
Evolution of self-organized systems 256
Deneubourg, J. L., A. Lioni, and C. Detrain
Dynamics of aggregation and emergence of cooperation 262
Detrain, Claire, and Jean-Louis Deneubourg
Complexity of environment and parsimony of decision rules in insect societies 268
Gerard, Jean-François, Eric Bideau, Marie-Line Maublanc, Patrice Loisel, and Carole Marchal
Herd size in large herbivores: encoded in the individual or emergent? 275
Hemelrijk, C. K.
Self-organization and natural selection in the evolution of complex despotic societies 283
Jeanne, Robert L., and Andrew M. Bouwma
Scaling in nests of a social wasp: a property of the social group 289
Parrish, Julia K., Steven V. Viscido, and Daniel Grünbaum
Self-organized fish schools: an examination of emergent properties 296
Roces, Flavio
Individual complexity and self-organization in foraging by leaf-cutting ants 306
Seeley, Thomas D.
When is self-organization used in biological systems? . . . 314
Published by Title Only 319
List of Participants 320

Reference: *Biol. Bull.* **202:** 245–246. (June 2002)

Introduction

DIANA E. J. BLAZIS

The Center for Advanced Studies in the Space Life Sciences, Marine Biological Laboratory, Woods Hole, Massachusetts 02543

This workshop, entitled "The Limitations of Self-Organization in Biological Systems," was sponsored by the Center for Advanced Studies in the Space Life Sciences, at the Marine Biological Laboratory. The focus of the workshop was on self-organization, which is defined as "a process [through] which pattern at the global level of a system emerges solely from numerous, [local] interactions among lower level components of the system" (Camazine *et al.*, 2001). This broad definition, which has its roots in physics, drove the workshop's examination of the concept, its utility, its limitations as a principle for understanding patterns that appear in biological systems during such activities as schooling in fish, foraging in bees, and nest-building in termites.

Scott Camazine (Pennsylvania State University), chair of the workshop, collaborated with other workshop participants in posing a series of questions intended to frame the discussion. I describe some of the questions below and point to the papers in this volume that address them.

What is self-organization? When is self-organization used?

During the workshop, substantial discussion focused on the definition of self-organization and when it operates. Anderson (this volume) presents a theoretical exploration of self-organization and related concepts. Key characteristics of self-organization include positive and negative feedback loops, multiple interactions, stochasticity and randomness. These processes lead to so-called "emergent behaviors," multistability, and robustness. Many in the group, such as Cole (this volume) observed that self-organization occurs widely among biological systems, and at many levels.

Systems that generate these characteristics of self-organization include Turing patterns, postulated in 1952 by Alan Turing in the context of physical and chemical systems. Stationary patterns arise *via* reaction-diffusion mechanisms, *e.g.*, when mixtures of chemicals react with one another while drifting at different rates through a medium. Reaction-diffusion systems were considered throughout the workshop as mechanisms that can account for pattern formation in inorganic systems (such as the Belousov-Zhabotinsky reaction) and organic systems (zebra stripes, termite nests, and more). As Theraulaz *et al.* discussed at the workshop and demonstrated recently (Theraulaz *et al.*, 2002), a theoretical model constructed using assumptions based on reaction-diffusion mechanisms can account for a well-defined behavior in social insects: the formation of cemeteries by ants.

Seeley (this volume) suggests that particular circumstances favor the self-organized system. Specifically, a biological system composed of a large number of subunits that lack the mechanisms of communication and computation required for centralized control is likely to be self-organized, regardless of the complexity of the individual subunits.

One theme of workshop discussion concerned the interaction between self-organization and individual behaviors. Deneubourg *et al.* (1999) have argued that self-organization and individual complexity need not be mutually exclusive. Levels of organization can interact. Roces (this volume) discusses collective foraging in leaf-cutting ants. These ants cut vegetation into small fragments that constitute the precursor for the colony's food: the fragments are processed by symbiotic fungi in the nest's fungus garden. When desirable food sources are discovered by individual ants, they are harvested and cut into especially small pieces, which causes intense recruitment of additional ants to harvesting activity. Thus a greater number of ants carry smaller loads, which are returned more rapidly to the nest, stimulating even further recruitment and, eventually, maximal harvesting.

What are the perturbations (e.g., environmental or internal stressors, growth or damage during development) that potentially affect self-organization? How do biological systems take advantage of and compensate for these perturbations?

Social organisms took front stage as the group grappled with this set of questions. Ants again are heuristic model organisms. For example, Detrain *et al.* (this volume) use ant societies to examine the effects of environmental factors on collective patterns; they suggest that changes in the environment can generate diverse foraging patterns. Jeanne and Bouwma (this volume) show that an internal stressor—the size of the group—affects nest-building in social wasps. They demonstrate that the morphology of the nest varies quantitatively and qualitatively with nest size and propose that this relationship arises as a consequence of self-organizing processes. Deneubourg *et al.* (this volume) show that multiple patterns of aggregation in social insects can emerge from changes in a single parameter: in their example, resting time. Self-organization also appears to be important in determining herd size in large mammalian herbivores, such as roe deer or kangaroo; the process of herd formation is described both theoretically and with field observations by Gerard *et al.* (this volume).

Does self-organization interact with evolution to produce behavioral complexity?

The consensus of the group was that natural selection and self-organization are complementary mechanisms. Cole (this volume) argues that biological self-organized systems are expressions of the hierarchical character of biological systems and are, therefore, both the products of, and subject to, natural selection. However, some self-organized patterns, for example, the wave fronts of migrating herds, are not affected by natural selection because, he suggests, there is no obvious genetic connection between the global behavior (the wave front) and the actions of individual animals. Hemelrijk (this volume) also explores the interaction of natural selection with self-organized systems. Using simulations that combine representations of individual selection, self-organization, and group selection, Hemelrijk documents the evolution of despotic societies from egalitarian ones. She supports these theoretical results with examples from insect and non-human primate societies.

Teasing apart the roles of evolution, self-organization, and individual behavior in biological pattern formation is a task that requires a common framework, as demonstrated by Parrish and colleagues (this volume). An important question emerging is whether spatial patterns are biologically significant or are epiphenoma (a theme also echoed by Cole [this volume]).

Throughout the workshop, participants warned against naïve attempts to emulate the activity of natural systems in the generation of spatial and temporal patterns. Self-organized systems can be remarkably inefficient; those emulating such systems may need to turn to central controllers to improve performance. Moreover, as participant Carl Anderson noted, self-organized systems can respond nonadaptively to environmental conditions, as for example, when ants develop group circling behaviors instead of effective foraging patterns. Throughout, participants such as Walter Tschinkel and Tom Seeley cautioned against overreliance on the notion that subunits or individual social insects are necessarily "simple." Tschinkel noted that it is important to "identify the behaviors, interactions, signals and cues" that the subunits actually use. Moreover, different mechanisms can give rise to the same phenotype or pattern. Thus the predictive power of a mechanism or mechanisms must be used to develop testable hypotheses about the function of complex systems.

The Center for Advanced Studies in the Space Life Sciences (CASSLS) was established in 1995 through a cooperative agreement between the Marine Biological Laboratory and the Life Sciences Division of the National Aeronautics and Space Administration. The Center acts as an interface between NASA and the basic science community, promoting interactions and discussion in areas that are of mutual interest.

Literature Cited

Anderson, C. 2002. Self-organization in relation to several similar concepts: are the boundaries to self-organization indistinct? *Biol. Bull.* **202:** 247–255.

Camazine, S., J. L. Deneubourg, N. R. Franks, J. Sneyd, E. Bonabeau, and G. Theraulaz. 2001. *Self-organization in Biological Systems.* Princeton University Press, Princeton.

Cole, B. J. 2002. Evolution of self-organized systems. *Biol. Bull.* **202:** 256–261.

Deneubourg, J., S. Camazine, and C. Detrain. 1999. Self-organization or individual complexity: a false dilemma or a true complementarity. Pp. 401–407 in *Information Processing in Social Insects.* C. Detrain *et al.*, eds. Birkhäuser Verlag, Basel.

Deneubourg, J. L., A. Lioni, and C. Detrain. 2002. Dynamics of aggregation and emergence of cooperation. *Biol. Bull.* **202:** 262–267.

Detrain, C., and J.-L. Deneubourg. 2002. Complexity of environment and parsimony of decision rules in insect societies. *Biol. Bull.* **202:** 268–274.

Gerard, J.-F., E. Bideau, M.-L. Maublanc, P. Loisel, and C. Marchal. 2002. Herd size in large herbivores: encoded in the individual or emergent? *Biol. Bull.* **202:** 275–282.

Hemelrijk, C. K. 2002. Self-organization and natural selection in the evolution of complex despotic societies. *Biol. Bull.* **202:** 283–288.

Jeanne, R. L., and A. M. Bouwma. 2002. Scaling in nests of a social wasp: a property of the social group. *Biol. Bull.* **202:** 289–295.

Parrish, J. K., S. V. Viscido, and D. Grünbaum. 2002. Self-organized fish schools: an examination of emergent properties. *Biol. Bull.* **202:** 296–305.

Roces, F. 2002. Individual complexity and self-organization in foraging by leaf-cutting ants. *Biol. Bull.* **202:** 306–313.

Seeley, T. D. 2002. When is self-organization used in biological systems? *Biol. Bull.* **202:** 314–318.

Theraulaz G., E. Bonabeau, S. C. Nicolis, R. V. Solé, V. Fourcassié, S. Blanco, R. Fournier, J. L. Joly, P. Fernández, A. Grimal, P. Dalle, and J. L. Deneubourg. 2002. Turing-like patterns in ant colonies. *Proc. Natl. Acad. Sci.* (In press).

Reference: *Biol. Bull.* **202:** 247–255. (June 2002)

Self-Organization in Relation to Several Similar Concepts: Are the Boundaries to Self-Organization Indistinct?

CARL ANDERSON*

LS Biologie I, Universität Regensburg, Universitätsstrasse 31, D-93040 Regensburg, Germany

Abstract. Self-organization is a concept and phenomenon whereby system-level patterns spontaneously arise solely from interactions among subunits of the system. Focusing on self-organization at the organismal level, I ask the question: are the boundaries to self-organization indistinct? After reviewing a number of published definitions of self-organization, I explore the conceptual boundaries among self-organization and two similar concepts, stigmergy and self-assembly. I highlight borderline cases that may blur the distinction among these and suggest that they may indeed be conceptually indistinct and difficult to separate in practice. Consequently, I propose a classification scheme based upon three aspects: whether the stimuli to which individuals respond are quantitative or qualitative, whether positive feedback is involved, and whether interindividual interactions are direct or indirect (stigmergic). In addition, I consider several other issues about self-organization, including (1) could a self-organized system use global information? (2) what is the role of the degree of correlation of activity among individuals? and (3) what is the role of positive feedback?

Introduction

Ernst Mayr, that grand old father of evolutionary biology, claims that "classifications are necessary wherever one has to deal with diversity" (Mayr, 1982: p. 147). In this essay, I consider the diversity around the concept of self-organization—a phenomenon in which system-level patterns spontaneously arise solely from interactions among subunits of the system—and ask the question, are the boundaries to self-organization indistinct? In particular, I focus on the conceptual boundaries among self-organization and two similar concepts, stigmergy and self-assembly. In an ideal, perfectly ordered world, we would possess strict definitions and criteria by which different examples could be categorized unambiguously—this would, for example, provide a rigorous and objective way of identifying the same phenomena and emergent properties occurring in very different systems, such as a purely physical system and a biological one. However, as I discuss, and illustrate with deliberately chosen borderline cases, this does not seem possible with self-organization. Instead, I attempt a classification scheme to deal with this diversity based upon three aspects of the systems: whether the stimuli to which individuals respond are quantitative or qualitative; whether or not positive feedback is involved; and whether interindividual interactions are direct or indirect.

This does not solve the issue, but does serve to highlight the diversity of combinations of key properties that give rise to self-organized behavior in such systems. I also take this opportunity to discuss a few other related issues about self-organization: could a self-organized system use global information? what is the role of the degree of correlation of activity among individuals? and what is the role of positive feedback?

In this essay, I concentrate on self-organization at the organismal level, that is, in systems of (eu)social and gregarious animals. I do this not because I view their self-organization as fundamentally different from self-organization in purely physical and chemical systems (such as sand

---

* Present address: School of Industrial and Systems Engineering, Georgia Institute of Technology, Atlanta, GA 30332-0205.

This paper was originally presented at a workshop titled *The Limits to Self-Organization in Biological Systems.* The workshop, which was held at the J. Erik Jonsson Center of the National Academy of Sciences, Woods Hole, Massachusetts, from 11–13 May 2001, was sponsored by the Center for Advanced Studies in the Space Life Sciences at the Marine Biological Laboratory, and funded by the National Aeronautics and Space Administration under Cooperative Agreement NCC 2-896.

Table 1

Various definitions of self-organization (arranged chronologically)

Self-organization is considered to be

1. indicative of a machine that is "determinate and yet able to undergo spontaneous changes of internal organisation" (Ashby, 1947: p. 125)
2. "a set of dynamical mechanisms whereby structures appear at the global level of a system from interactions among its lower level components" (Nicolis and Prigogine, 1977, cited in Bonabeau *et al.*, 1997)
3. "associated with the spontaneous emergence of long-range spatial and/or temporal coherence among the variables of the (organized) system" (Nicolis, 1986: p. 7)
4. "the spontaneous emergence of coherence or structure without externally applied coercion or control" (Ho and Saunders, 1986: p. 233)
5. "a system is self-organizing if it acquires a spatial, temporal or functional structure without specific interference from the outside. By 'specific' we mean that the structure or functioning is not impressed on the system, but that the system is acted upon from the outside in a nonspecific fashion" (Haken, 1988: p. 11)
6. "the ability of systems comprising many units and subject to constraints, to organize themselves in various spatial, temporal or spatiotemporal activities. These emerging properties are pertinent to the system as a whole and cannot be seen in units which comprise the system" (Babloyantz, 1991: p. ix)
7. "the creation of macroscopical patterns by the action of forces distributed in a much more homogeneous way than the structures that arise. Hence, this kind of transformation implies a spontaneous breaking of symmetry" (Beloussov, 1993)
8. "the spontaneous emergence of nonequilibrium structural organization on a macroscopic level due to collective interactions between a large number of simple, usually microscopic, objects" (Coveney and Highfield, 1995: p. 432)
9. "a process where the organization (constraint, redundancy) of a system spontaneously increases, i.e. without this increase being controlled by the environment or an encompassing or otherwise external system" (Heylighen, 1997)
10. "a process in which pattern at the global level of a system emerges solely from numerous interactions among the lower-level components of the system. Moreover, the rules specifying interactions among the system's components are executed using only local information, without reference to the global pattern" (Camazine *et al.*, 2001: p. 8)

dunes and the Beloussov-Zhabotinsky reaction)—although animals do have the added potential to vary the individual-level rules they employ, and thus may represent another level of complexity of individual-level behavior and collective-level patterns—but because study of organismal self-organization is relatively new and lags behind the decades of progress made in these other fields. Before we proceed with the above issues, it is crucial to consider the question of what precisely is self-organization.

What Is Self-Organization?

Consider the collective movement of a school of fish. The school snakes through the water like a single entity, turning in unison, waves of activity flashing across the shoal. This group-level behavior is not encoded within each individual, nor is there a leader or small group of individuals directing the movement of the school. It is a process whereby individual fish react to movements of their immediate neighbors, and, as a result of such local interactions, the group-level pattern of activity emerges spontaneously (Reynolds, 1987; Huth and Wissel, 1992; Camazine *et al.*, 2001; Parrish *et al.*, 2002)—in short, the school is self-organized.

Self-organization, or at least use of the term self-organizing system, dates back to at least 1947 (Ashby, 1947). However, the general concept stems much further back in history, at least since Aristotle's *Metaphysica*. It is perhaps surprising then that rigorous study of self-organization has its roots in physics and chemistry (but often inspired by biological systems), yet only relatively recently have biologists taken up the challenge to understand biological self-organization, at least at the organismal level (Bonabeau *et al.*, 1997, 1999; Camazine *et al.*, 2001; Anderson, 2002).

What precisely, however, is self-organization, and do we have an adequate definition of it? Table 1 lists 10 definitions of self-organization from the literature (mostly from physics). Summarizing across all these definitions, what picture emerges? A key aspect is the creation of a macroscopic, group-level "pattern." Such a pattern may consist of a spatio-temporal physical structure or behavior. And this pattern is "emergent" (another term difficult to define satisfactorily); that is, it cannot be deduced from even a full knowledge of the lower-level components and the nature of the interactions among them—the stock phrase is that "the whole is more than the sum of its parts" (Aristotle, *Metaphysica*, 10f-1045a). This emergence implies that there is some nonadditive, nonlinear interaction involved, and thereby implicates the role of positive feedback (but see later). What is crucial too is that there are multiple lower-level components and hence multiple interactions, or possibly even a single individual but many repeated interactions (phase transitions often occur such that the emergent patterns arise only above a certain critical number or density of interactions or components). Also, Table 1 shows that the authors of the definitions consider that the group-level properties must arise solely from within the system, not generated from interference or other external guiding forces, such as templates (Camazine *et al.*, 2001; Anderson, 2002). This is not to say, however, that the environment has no role to play. Self-organized systems often exhibit what is termed multistability, so that the system may sometimes switch between different semi-stable patterns, but without any changes in the lower-level behavioral characteristics (Ünsal, 1993). Importantly, the system may switch because of intrinsic factors, such as random fluctuations within the system, or extrinsic factors, such as small changes in the environment with which the system interacts (Deneubourg *et al.*, 1989; Camazine *et al.*, 2001).

To sum up, self-organization supposedly contains a number of "key ingredients": (1) positive feedback as one of the forces driving change in the system (usually nonstabilizing change, that is, change in the same direction as a perturbation; see later); (2) negative feedback as a stabilizing force (that is, driving change in the opposing direction to a perturbation); (3) stochasticity and randomness generating diversity upon which the feedback works, and (4) multiple interactions (Bonabeau *et al.*, 1997, 1999; Camazine *et al.*, 2001).

The "characteristics" or signatures of self-organization include, but are not restricted to, (1) creation of emergent group-level spatiotemporal structures or behaviors, and (2) multistability and symmetry breaking, such that even only small changes in individual behavior can lead to large changes in collective behavior (even multistationarity), and small changes in the environment, without changes in individual behavior, can lead to different collective states (Ünsal, 1993; Bonabeau *et al.*, 1997; Camazine *et al.*, 2001).

If I have labored the above points, it is because a comparison between self-organization and similar mechanisms requires an understanding of what self-organization is perceived to be even if we lack a satisfactory all-encompassing definition. As background for the comparison, two points should be considered.

Could a self-organized system use global information?

Could a self-organized system in fact use some global information? The following example, albeit simple and debatable, is instructive (I must acknowledge J. L. Deneubourg for his insights and discussion of this example). Bumblebees, *Bombus* spp., actively regulate the climate in their nests. When nest air temperature becomes too high, bees fan their wings to draw in and circulate fresh air, thereby cooling the nest (O'Donnell and Foster, 2001; Weidenmüller, 2001; Weidenmüller *et al.*, 2002). If the temperature becomes too low, they may commence brood incubation, releasing heat from their shivering muscles. At certain temperatures the two behaviors may co-occur (Vogt, 1986; O'Donnell and Foster, 2001).

Each bee appears to have her own temperature threshold, and when the temperature exceeds that threshold she may or may not start to fan (Weidenmüller, 2001; C. Anderson *et al.*, unpubl. ms.). Thus, in this sense, bees make individual decisions on the basis of the air temperature around them, and hence the decision is local. However, the air is reasonably homogeneously mixed, and so in another sense is the equivalent of a *global* signal, the same temperature experienced by all the bees. I would argue that the dynamics of nest air temperature is the global pattern, determined by which bees and how many are fanning or incubating over time. This is, of course, a simple temporal pattern. (There is a strong analogy here with the Beloussov-Zhabotinsky reaction [*e.g.*, Goodwin, 1994; Ball, 1999]; if the reactants for this autocatalytic process are left to develop in a petri dish, wonderful spiral and circular patterns arise. However, if homogeneously mixed, the solution oscillates between red and blue. The mixing of air would seem to be constraining the complexity of the temperature dynamics in a similar manner. Might it generally be true that the degree of "locality" of interactions somehow determines the spatial scale of a self-organized pattern—more local meaning a finer pattern—in the same way that diffusion rate has such a crucial role in other pattern formation processes, such as reaction-diffusion?)

The temperature profile is generated by the action of individuals interacting with each other indirectly through the medium of the air. Moreover, the air acts as a sort of filter, screening off the individual level to produce only the net effect of all individuals fanning and incubating. Overall, I would argue that this is a system with local decisions: bees do not need to know what every other bee is doing and they do not interact directly, but they do affect others *indirectly* by their actions upon the stimulus. Because bees' decisions to fan are probabilistic, we cannot deduce the precise dynamics from knowledge of a bee's proximate rule. To my mind, this could be considered an example of quantitative stigmergy (see below) with a homogeneously mixed stimulus and without positive feedback.

What is the role of the degree of correlation of activity among individuals?

I suggest—merely as a working hypothesis that could be tested—that there must be a critical window of correlation of activity among individuals in order for self-organization to occur. That is, above some upper threshold and below some lower threshold, self-organization breaks down, and the emergent properties no longer exist.

By correlation of activity I mean a combination of the strength and likelihood that the behavior, location, movement, etc., of individual A affects and so causes a similar change in those properties of individual B. This is best illustrated by a simple example. Imagine a reasonably polarized school of fish. Each fish reacts to some predator or to the movements of a few of its nearest neighbors. Fish react solely in terms of a change of heading, either in order to swim away from a predator or to avoid crashing into neighbors. Finally, consider a parameter $0 \leq r \leq 1$, which determines the degree of correlation of activity among individuals: if fish *i* moves, Prob(*i*'s neighbors move) = *r*. (The parallel with a product moment correlation coefficient should thus be clear.) Thus, if *r* is high, movement of one individual causes a change in most or all of its neighbors, and if *r* is very low, the movements of fish A cause little or no change in the school. I hypothesize that there are two thresholds, r_l and r_u (where $0 \leq r_l < r_u \leq 1$), that define the range within which self-organization exists.

My reasoning is thus: suppose that $r = 1$ (as if each fish were connected to its neighbors by a rigid rod). Any fish that turns causes a change in its neighbors, and therefore their neighbors, and so on across the school. A group-level pattern, polarity (or more precisely, the exact initial configuration), is maintained as the school moves. However, the pattern is not self-organized; the behavior is not emergent, it is simply additive—tell me how fish A will turn and I can predict precisely the behavior of non-neighbor fish Z. (There is of course the problem that different fish—for example, those trying to flee predators coming from different directions—could conflict with each other.) Such a rigidly constrained system would not have sufficient "slack" to allow group-level adaptive behavior, such as the fountain effect, hourglass, or other anti-predator strategies that are observed in real fish schools (Partridge, 1982; Camazine *et al.*, 2001). Consider the other extreme, $r = 0$: each fish has no effect upon its neighbors, and no spatiotemporal structure could exist. Overall, it is tempting to consider $1 - r$ as similar to λ, Langton's (1986) parameter associated with behavioral complexity in dynamic systems and in particular "the edge of chaos." This is the region at which these systems act as complex adaptive systems (Lewin, 1993; Bonabeau, 1998), and therefore are more likely to be selected for.

The above example is highly simplified; in particular, the crucial region of parameter space is likely to be a function of a number of other factors too. For instance, is there also a crucial range of the number of neighbors each individual interacts with? (An alternative way to express this is to ask whether there is a crucial range of "average system connectedness," *sensu* Moritz and Southwick [1992].) For example, Huth and Wissel's (1992) simulation of fish schools demonstrates that tight, coherent schooling behavior requires that each fish interacts with more than two neighbors. As hinted earlier, the locality of those interactions (*i.e.*, whether immediate neighbors or individuals farther away in the school) may also play a crucial role. Finally, the strength of response (and hence feedback) may have crucial limits. These working hypotheses should be testable.

Quantitative *versus* Qualitative Stigmergy

I suggest that the definitions of self-organization (Table 1) could encompass two other similar pattern-formation mechanisms found in biological systems: qualitative stigmergy and self-assembly. Stigmergy, a term first coined by termite researcher Pierre Paul Grassé (1895–1985), is a "class of mechanisms that mediate animal-animal interactions" through work in progress (Theraulaz and Bonabeau, 1999). The work (for example, a half-built pillar in a termite mound) acts as a stimulus to respond, that is, do more work by adding further material to the pillar. Importantly, the result of this stimulus-response sequence is that it alters the stimulus for subsequent individuals. (Note that these are *indirect* interactions among individuals.) In some cases, the stimulus varies in a *quantitative* manner, altering the probability of eliciting the same response from other individuals (thus, the bumblebees would qualify here). Termite mound construction is one such example because workers add pheromone-containing saliva to the soil pellets they place on the growing structure. The local pheromone concentration affects where subsequent individuals will place their pellets—new individuals tend to place their pellets in an area where there is already a high pheromone concentration (Deneubourg, 1977), thus creating a positive feedback (probably absent from the bumblebee case). The response, to place or not to place a pellet, is always the same, and it is the intensity of a single stimulus, the pheromone concentration, that determines whether an individual will respond or not. This mechanism is termed quantitative stigmergy, is characterized by positive feedback and phase transitions (a.k.a. instabilities and mulistationarity; Solé and Goodwin, 2000; Camazine *et al.*, 2001), and is considered to be "an ingredient of self-organization [that] mediates interactions among workers" (Camazine *et al.*, 2001: p. 58).

The second mechanism, qualitative stigmergy, is similar to quantitative stigmergy in that it involves a series of stimulus-responses. In this situation, however, the stimuli differ from each other *qualitatively* and may elicit different responses. Qualitative stimuli include the shape of a structure. A proposed example, nest construction in *Polistes* wasps, is shown in Figure 1 (Bonabeau *et al.*, 1999; Theraulaz and Bonabeau, 1999; Camazine *et al.*, 2001). Builders add new cells to the margin of the nest, and in this particular case there are 12 places, 12 stimulating configurations (S_i's), where they can build a new cell. However, there are different classes of stimuli here that will require a slightly different building procedure. That is, there are 7 locations (S_1's) where there is already a single wall present and individuals must construct 5 new walls to complete a new hexagonal cell; there are 4 locations (S_2's) with 2 walls already present, thus requiring 4 new walls. Finally, there is a single location (S_3) with 3 adjacent walls, thus requiring just 3 new walls. It is clear, at least from a human perspec-

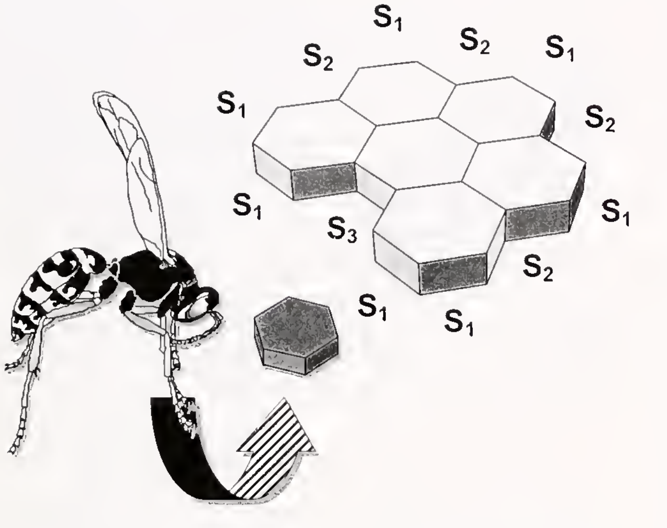

Figure 1. In qualitative stigmergy, an individual responds to qualitatively different stimuli, which involve qualitatively different responses. Thus, to create a new hexagonal cell on the margin of this comb, the *Polistes* wasp must respond by adding 5 new walls (at one of the locations indicated by stimuli, S_1's), 4 new walls (at the S_2's) or just 3 walls (at S_3). Qualitative stigmergy is not considered to be a self-organized process. Figure drawing by Guy Theraulaz, used with permission.

tive (Karsai, 1999), that different stimuli (S_i) elicit qualitatively different responses (R_i) from the builders. Qualitative stigmergy (reviewed in Bonabeau *et al.*, 1999; Camazine *et al.*, 2001), although similar in many ways to quantitative stigmergy, is not characterized by positive feedback and is not considered an ingredient of self-organization (Camazine *et al.*, 2001).

Although these two mechanisms are conceptually very different, I question how easy it is in practice to distinguish between them. Is the boundary between them indistinct? For instance, in *Polistes* nest construction, the probability of constructing a new cell in a certain location is dependent upon the number of adjacent walls (3 walls: probability = 0.55; 2 walls = 0.05; 1 wall = 0; from Camazine *et al.*, 2001: 425; see also Bonabeau *et al.*, 1999). (This is excepting the very earliest stages of construction when only a few cells are present; Downing and Jeanne, 1990; Karsai and Theraulaz, 1995.) These are interpreted as three qualitatively different configurations, but how can we be sure that they do not represent a nonlinear relationship to a quantitative variable? Would we still categorize the response as qualitative if the construction probabilities were directly proportional to the number of adjacent walls (or data resembled fig. 3 of Karsai and Pénzes, 1993)? Karsai and Pénzes (2000) recently suggested that age of cells (a quantitative variable) might be a better explanatory variable of *Polistes* nest construction than the number of adjacent walls (a qualitative variable). Thus, their study, and earlier works (Pénzes and Karsai, 1993; Karsai and Penzés, 1993; Karsai, 1999), interprets the same phenomenon, nest construction in social wasps, solely from a quantitative stigmergic viewpoint. Viewing the qualitative *versus* quantitative question from the other direction, in the formation of an ant cemetery, the number of corpses in a pile is believed to be a *quantitative* variable, and self-organization plays a role (G. Theraulaz *et al.*, unpubl. ms.). But what if an ant regards a group of two or more ants as a processed "pile," and perceives a single dead ant as something qualitatively different—perhaps as an unprocessed ant that just happened to die on that spot?

My point is that for us—animals sometimes several orders of magnitude larger than the organisms we study—it may be difficult to decide what represents qualitatively or quantitatively different configurations and responses. What appears to be a randomly deposited soil pellet to our eyes may represent a particular qualitative configuration to a termite. A confounding problem is that behavioral data are often noisy. Furthermore, nature probably has few pure self-organization systems; that is, situations that involve no other pattern-formation mechanism. Given these problems, such issues may be difficult to tease out without detailed, tedious, and time-consuming observations and experiments. We must invest some thought into considering what key features and critical tests will allow us to distinguish between qualitative and quantitative stimuli and responses.

Qualitative Stigmergy *versus* Self-Assembly

In this section, I propose that the distinction between qualitative stigmergy and self-assemblages may not be clear-cut. Self-assemblages are "physical structures formed by individuals linking themselves to one another" (Anderson *et al.*, 2002). In insect societies, various examples of self-assemblages exist. For instance, an army ant bivouac is an adaptive structure composed of many workers linked together and is therefore a self-assemblage. Other examples include living ant-bridges (*Oecophylla* and *Eciton*), bee-curtains (see below), and floating ant-rafts that allow colonies to survive nest flooding (*Solenopsis*). Self-assemblages are reviewed in Anderson *et al.* (2002) and are a product of the process of self-assembly (see Sendova-Franks and Franks, 1999).

The way that self-assemblages form involves a new individual moving over the surface of the growing structure and attaching itself. As the individual moves over the surface, it is likely to encounter different stimulating configurations of individuals already part of the structure. Once it attaches itself, it has created a modified structure that probably affects the attachment of subsequent individuals (Fig. 2). Qualitative stigmergy and self-assembly have many common features: movement of an individual over a structure; individuals that presumably encounter different stimulating configurations; qualitatively different responses (attaching at the end of the chain is a different response than

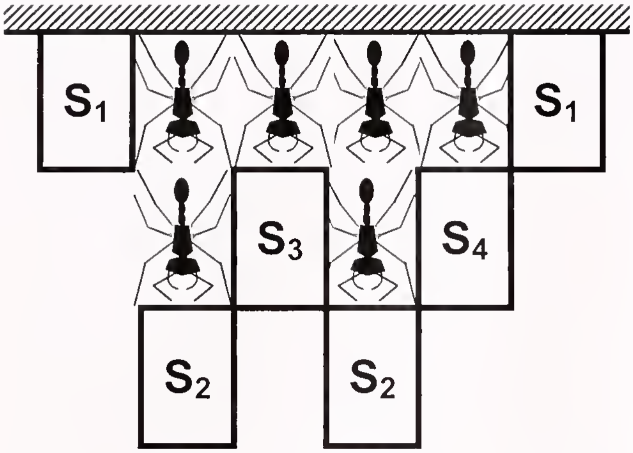

Figure 2. An individual must make a choice when joining a self-assemblage. In this highly stylized view of the beginnings of an army ant bivouac (hanging from an attachment point, hatched section), there are four qualitatively different attachment positions, or stimuli (S_1–S_4). If these different stimuli are associated with different probabilities of joining at this site, then there is a very strong similarity with qualitative stigmergy.

attaching oneself in a "hole" on the surface); and responses that produce a new and probably qualitatively different structure.

In qualitative stigmergy, individuals place new material, in this case wood pulp, onto a structure, the nest, creating a new, qualitatively different structure. The distinction between the material being placed, pulp, and the individuals doing the placing, the worker wasps, is clear. However, in self-assemblages there is not this clear distinction; in a sense, self-assemblages involve individuals that are both the workers, while searching for an attachment site, and the material, once they have attached. In my opinion, this difference between qualitative stigmergy and self-assemblages is unimportant because the same feedbacks seem to be operating in both mechanisms. Are they regarded as distinct merely because qualitative stigmergy involves inanimate stimulating structures whereas self-assemblages involve animate ones?

Self-Assembly *versus* Self-Organization

The way that self-assemblages form, self-assembly, is a mechanism in which the global pattern, in this case a physical structure such as a chain of ants, presumably depends entirely upon local and probably simple interactions among neighboring individuals, without reference to the global pattern. Compare this to the definitions of self-organization (Table 1 and earlier section) and a strong similarity between self-assembly and self-organization is evident (but see Sendova-Franks and Franks, 1999). For instance, it is extremely unlikely that an army ant joining a bivouac has any sense of the global structure it is joining. For one thing, workers of some army ants species are totally blind—for example, *Eciton burchelli*, which produces what perhaps are the most striking and impressive bivouacs—and rely on local pheromone trails and other chemical and tactile signals rather than visual cues (Franks, 1989; Gotwald, 1995). It is, of course, possible that in some self-assemblages a signal or cue such as total pheromone concentration might correlate with the number of individuals composing the current structure and could give a new individual some information about the global pattern. However, my feeling is that this is probably not the case in most situations, and that—as in self-organization—local information and local interactions are the major mechanisms involved.

What Is the Role of Positive Feedback?

If the above similarity were not enough, another major aspect of self-organization that may link and perhaps blur the distinction between self-organization and self-assembly is positive feedback. Positive feedback is considered a key ingredient but not a crucial component of self-organization: "*most* self-organizing systems use positive feedback" [my italics] (Camazine *et al.*, 2001: p. 15). In this section, I argue first that positive feedback could occur in self-assemblage formation; and second, that some examples of biological self-organization may contain little or no positive feedback. I propose that these are further reasons why self-organization and self-assembly may be conceptually indistinct.

Could self-assemblages involve positive feedback?

Positive feedback is a mechanism that promotes change in a system; moreover, it drives change in the same direction as a perturbation. For instance, in many ant species, a scout ant that has found a source of food lays down a pheromone trail as it returns to the nest. This provides a source of information for other individuals, allowing them to follow the trail and find the food. In turn, as new recruits reach the food and return to the nest, each laying a trail, the trail gets progressively stronger, making it more likely that other recruits will both follow the trail and reinforce it with additional pheromone (*e.g.*, Hölldobler and Wilson, 1990). (Incidentally, the pheromone trails here are another example of quantitative stigmergy.) Thus, from a small "perturbation" such as a single pheromone trail across the ground, a strong trail can develop (Camazine *et al.*, 2001; Deneubourg *et al.*, 2002; Detrain and Deneubourg, 2002).

I argue that positive feedback could be involved in self-assemblage formation. Imagine several chains of *Eciton* ants hanging from a rock, as in Figure 2. A new ant wanders over the chains and attaches itself at some position. If it is more likely to attach itself to the end of the longest chain—the lowest available attachment position—then this creates a positive feedback mechanism: longer chains attract more ants, and so grow faster and longer, thus attracting more

Table 2

A classification scheme of the different examples on the basis of three variables: (1) whether interindividual interactions are direct or indirect (stigmergic), (2) whether or not positive feedback is involved, and (3) whether the stimuli to which individuals respond are quantitative or qualitative. All examples are discussed in the text

Nature of stimulus	Positive feedback involved?	Nature of interindividual interactions	Example
Quantitative	Yes	Direct	(A) Self-organization: fish schools
		Indirect	(B) Self-organization involving quantitative stigmergy: termite nest construction
	No	Direct	(C) Honeybee swarm thermoregulation
		Indirect	(D) Bumblebee thermoregulation
Qualitative	Yes	Direct	(E) Self-assembly: defense posturing in *Apis dorsata*
		Indirect	(F) Not possible?
	No	Direct	(G) Self-assembly: *Eciton* chain formation?
		Indirect	(H) Qualitative stigmergy: *Polistes* nest construction

ants, and so on. In Figure 2, this would mean that the individual responds with greater probability to qualitative stimulus S_2 than S_1, S_3, or S_4.

Positive feedback mechanisms are certainly involved in relation to the probability that an individual will join a growing structure. For example, in weaver ants (*Oecophylla*), which form chains between branches, the probability of joining a group is positively correlated with the size of the group (Lioni *et al.*, 2001). This is presumably adaptive for the colony in that it helps form a collective choice so that there is just a single quick-growing cluster rather than several competing and slow-growing clusters. For this section, however, the key issue is whether positive feedback could operate *within* the structure, that is, once a new individual is wandering over the surface of (and perhaps in) the growing structure. I feel that such positive feedback could occur in self-assemblages, which could further blur the distinction between self-assemblages and self-organization.

Do some examples of self-organization lack positive feedback?

Although a "key ingredient," positive feedback is not part of the self-organization definitions (Table 1). Consequently, in some examples of self-organization the positive feedbacks, if they do occur, are not obvious. Self-organized thermoregulation in honeybee (*Apis mellifera*) swarms is one such example. Bees move between the surface and core of the swarm cluster in an attempt to regulate their own temperature. Overall, there is an adaptive global pattern: the temperature profile of the cluster, which buffers changes in ambient conditions (Heinrich, 1981; Watmough and Camazine, 1995; Sumpter and Broomhead, 2000). Similarly, in two species of Asian bees, *A. dorsata* and *A. florea*, individuals link together to form a living curtain, a self-assemblage, over the comb (Michener, 1974; Anderson *et al.*, 2002). Individuals actively regulate their temperature, and that of the comb below, by altering their interindividual spacing. When temperature rises they push against their neighbors, increasing the interneighbor distance, thereby allowing air to move more freely through the curtain and cool the nest. Cooling may also be enhanced by individuals fanning their wings and thus increasing airflow (Morse and Laigo, 1969; Michener, 1974; see also Anderson and Franks, 2001). In contrast, at cold ambient temperatures, individuals pull against their neighbors to reduce airflow and increase temperatures. Like these Asian species, honeybee swarms also fan their wings for cooling and move closer together for warming.

Why does the honeybee case class as self-organization (*e.g.*, Camazine *et al.*, 2001) and a self-assemblage (Anderson *et al.*, 2002), but the bees forming a living curtain in an *A. dorsata* colony only class as a self-assemblage (Anderson *et al.*, 2002)? Both seem to utilize very similar mechanisms.

Conclusions

In considering all the previous examples, I have primarily focused on three aspects: (1) whether the stimuli to which individuals respond are quantitative or qualitative, (2) whether positive feedback is involved, and (3) whether interindividual interactions are direct or indirect (stigmergic). From these three binary variables, there are eight possible combinations (Table 2).

It is likely that many researchers would view fish schools (case A) and termite nest construction (case B)—both examples with quantitative stimuli and positive feedback—as self-organized (Bonabeau *et al.*, 1997; Camazine *et al.*, 2001). Honeybee swarm thermoregulation (case C), however, lacking the "key ingredient" of positive feedback, has merely the "flavor" of self-organization, yet is still considered self-organized (Camazine *et al.*, 2001: esp. p. 58). I have proposed that nest thermoregulation in bumblebees (case D) has this same flavor of self-organization yet involves global information.

It has been previously suggested that qualitative stigmergy (case H) is not a self-organized process (Bonabeau *et al.*, 1997, 1999; Camazine *et al.*, 2001). However, I would like to suggest that, by itself, the criterion of qualitative stimuli may be insufficient grounds for declaring that a system is not self-organized. Might a self-organized system involve qualitative stimuli, positive feedback, and direct interindividual interactions? Consider defensive posturing in the giant Asian honeybee, *Apis dorsata* (case E), the species mentioned earlier that forms a living curtain of bees over the comb. When attacked, the outermost bees of this self-assemblage perform a jerky abdominal shaking, behavior that spreads across the surface as a wave (Kastberger and Biswas, 1998; see also Kastberger *et al.*, 1998), sometimes even as spirals, as observed in many other "excitable media" such as heart tissue during cardiac arrhythmia (*e.g.*, Davidenko *et al.*, 1992; Goodwin, 1994; Ball, 1999). A responding bee performs a single wing stroke (of 80–160 ms duration), an abdominal thrust (an additional 200–250 ms), and remains still for a period (200 ms) (Kastberger and Biswas, 1998). A bee performing this sequence of behaviors stimulates its neighbors to "jerk," which in turn affects their neighbors, and so on. Thus, this behavior spreads across the surface in a positively reinforced manner coupled with a crucial refractory period (remain still for 200 ms). (Such refractory periods are vital for traveling waves of activity—as in nerve cells, the Beloussov-Zhabotinsky reaction, activity cycles in ants, etc.—because they prevent back-propagation; that is, the wave travels forward only [*e.g.*, Goodwin, 1994; Ball, 1999].) A bee can be classified as defense posturing or not, and thus the stimulus is most likely qualitative. Lastly, interactions are clearly direct, neighbor to neighbor. What is observed, however, at the global level—traveling and spiraling waves—is generated entirely from within the system and emergent. At least from the definitions in Table 1, it would classify as self-organized.

I cannot envision a situation in which both positive feedback and indirect interactions could be realized with a qualitative stimulus (case F). I will, therefore, *tentatively* suggest that this scenario is not possible, but would welcome suggestions from readers. Finally, with my conceptual scenario of self-assemblage formation (described earlier), I suggest that a situation with direct interactions, qualitative stimuli, and no positive feedback is possible (case G) and would probably qualify as self-organized under the definitions of Table 1. However, as Anderson *et al.* (2002) stress, we are very ignorant about the proximate mechanism involved in self-assemblage formation.

Where does this leave us? I have endeavored to show that the distinction between a number of mechanisms—principally self-organization, qualitative stigmergy, and self-assembly—may, in certain cases, be indistinct. This is not necessarily a problem, as borderline cases can be very illuminating (Anderson and Franks, 2001); only by attempting to push the limits of a concept are we likely to find where the boundaries truly lie. The identification of key variables—direct *versus* indirect interindividual interactions, positive feedback, and quantitative *versus* qualitative stimuli—helps to distinguish among these indistinct cases and also highlights the observed diversity of functional organization (Table 2). It does not, however, solve the problem of what precisely is, and is not, self-organization. I believe that we are unlikely to suceed in formulating a single, well-defined, and satisfactory definition of self-organization. (The concept of "complexity" is similar: you know it when you see it, but there is no consensus on its definition.) Rather than worry about semantics, we should focus on studying these fascinating phenomena, in particular, striving to identify their underlying proximate mechanisms.

Acknowledgments

I thank the organizers of the NASA-sponsored workshop for giving me the opportunity to both present some of this work and to discuss these ideas with the delegates. I also thank the European Science Foundation's Theoretical Biology of Adaptation Programme for funding a visit to Guy Theraulaz's group in Toulouse where I first conceived some of these issues. Finally, thanks go to Guy Theraulaz and especially Jean-Louis Deneubourg for stimulating discussions and their insights on self-organization and also to Scott Camazine, Jenna Jadin, István Karsai, and two anonymous referees for comments on the manuscript.

Literature Cited

Anderson, C. 2002. Self-organized behavior: case studies. (Review of: S. Camazine, J. L. Deneubourg, N. R. Franks, J. Sneyd, G. Theraulaz and E. Bonabeau. 2001. *Self-organization in Biological Systems.* Princeton University Press.) *Complexity* **7:** 14–15.

Anderson, C., and N. R. Franks. 2001. Teams in animal societies. *Behav. Ecol.* **12:** 534–540.

Anderson, C., G. Theraulaz, and J. L. Deneubourg. 2002. Self-assemblages in insect societies. *Insectes Soc.* **49(2):** (In press).

Ashby, W. R. 1947. Principles of the self-organizing dynamic system. *J. Gen. Psychol.* **37:** 125–128.

Babloyantz, A. 1991. Introduction. Pp. ix-xv in *Self-organization, Emerging Properties, and Learning,* A. Babloyantz, ed. NATO ASI Series B, Vol. 260. Plenum, New York.

Ball, P. 1999. *The Self-made Tapestry.* Oxford University Press, Oxford.

Beloussov, L. V. 1993. Generation of morphological patterns: mechanical ways to create regular structures in embryonic development. Pp. 149–168 in *Thinking About Biology,* W. D. Stein and F. J. Varela, eds. Santa Fe Institute Studies in the Sciences of Complexity, Lect. Notes Vol. III, Addison-Wesley, Reading, MA.

Bonabeau, E. 1998. Social insect colonies as complex adaptive systems. *Ecosystems* **1:** 437–443.

Bonabeau, E., G. Theraulaz, J. L. Deneubourg, S. Aron, and S. Camazine. 1997. Self-organization in social insects. *Trends Ecol. Evol.* **12:** 188–193.

Bonabeau, E., M. Dorigo, and G. Theraulaz. 1999. *Swarm Intelli-*

gence: from Natural to Artificial Systems. Santa Fe Institute on the Sciences of Complexity, Oxford University Press, New York.

Camazine, S., J. L. Deneubourg, N. R. Franks, J. Sneyd, G. Theraulaz, and E. Bonabeau. 2001. *Self-organization in Biological Systems.* Princeton University Press, Princeton, NJ.

Coveney, P., and R. Highfield. 1995. *Frontiers of Complexity.* Fawcett Columbine, New York.

Davidenko, J. M., A. V. Pertsov, R. Salomonsz, W. Baxter, and J. Jalife. 1992. Stationary and drifting spiral waves of excitation in isolated cardiac muscle. *Nature* **355:** 349–351.

Deneubourg, J. L. 1977. Application de l'ordre par fluctuations a la description de certaines étapes de la construction du nid chez les termites. *Insectes Soc.* **24:** 117–130.

Deneubourg, J. L., S. Goss, N. R. Franks, and J. M. Pasteels. 1989. The blind leading the blind: modelling chemically mediated army ant raids. *J. Insect Behav.* **2:** 719–725.

Deneubourg, J. L., A. Lioni, and C. Detrain. 2002. Dynamics of aggregation and emergence of cooperation. *Biol. Bull.* **202:** 262–267.

Detrain, C., and J.-L. Deneubourg. 2002. Complexity of environment and parsimony of decision rules in insect societies. *Biol. Bull.* **202:** 268–274.

Downing, H. A., and R. L. Jeanne. 1990. The regulation of complex behaviour in the paper wasp, *Polistes fuscatus* (Insecta, Hymenoptera, Vespidae). *Anim. Behav.* **39:** 105–124.

Franks, N. R. 1989. Army ants: a collective intelligence. *Am. Sci.* **77:** 138–145.

Goodwin, B. 1994. *How the Leopard Changed its Spots.* Phoenix, London.

Gotwald, W. H. 1995. *Army Ants: the Biology of Social Predation.* Cornell University Press, New York.

Haken, H. 1988. *Information and Self-organization.* Springer, Berlin.

Heinrich, B. 1981. The mechanisms and energetics of honey bee swarm temperature regulation. *J. Exp. Biol.* **91:** 25–55.

Heylighen, F. 1997. Self-organization. [Online]. *Principia Cybernetica Web.* Available: http://pespmc1.vub.ac.be/SELFORG.html [2002, April 8].

Ho, M. W., and P. T. Saunders. 1986. Evolution: natural selection or self-organization? Pp. 231–242 in *Disequilibrium and Self Organization,* C. W. Kilmister, ed. D. Reidel, Dordrecht, Netherlands.

Hölldobler, B., and E. O. Wilson. 1990. *The Ants.* Harvard University Press, Cambridge.

Huth, A., and C. Wissel. 1992. The simulation of the movement of fish schools. *J. Theor. Biol.* **156:** 365–385.

Karsai, I. 1999. Decentralized control behavior in paper wasps: an overview of the stigmergy approach. *Artif. Life* **5:** 117–136.

Karsai, I., and Z. Pénzes. 1993. Comb building in social wasps: self-organization and stigmergic script. *J. Theor. Biol.* **161:** 505–525.

Karsai, I., and Z. Pénzes. 2000. Optimality of cell arrangement and rules of thumb of cell initiation in *Polistes dominulus*: a modeling approach. *Behav. Ecol.* **11:** 387–395.

Karsai, I., and G. Theraulaz. 1995. Nest building in a social wasp: postures and constraints (Hymenoptera: Vespidae). *Sociobiology* **26:** 83–113.

Kastberger, G., and S. Biswas. 1998. The alarm cascade in the giant honeybee colony. P. 245 in *Social Insects at the Turn of the Millenium,* M. Schwarz and K. Hogendoorn, eds. Proceedings of the XIII International Congress of IUSSI, Adelaide Australia, 29 December 1998–3 January 1999. XIII Congress of IUSSI, Adelaide.

Kastberger, G., G. Raspotnig, S. Biswas, and O. Winder. 1998. Evidence of Nasonov scenting in colony defence of the giant honeybee *Apis dorsata. Ethology* **104:** 27–37.

Langton, C. G. 1986. Studying artificial life with cellular automata. *Physica* **22D:** 120–149.

Lewin, R. 1993. *Complexity: Life on the Edge of Chaos.* Phoenix, London.

Lioni, A., C. Sauwens, G. Theraulaz, and J. L. Deneubourg. 2001. Chain formation in *Oecophylla longinoda. J. Insect Behav.* **14:** 679–696.

Mayr, E. 1982. *The Growth of Biological Thought.* Harvard University Press, Cambridge.

Michener, C. D. 1974. *The Social Behavior of the Bees.* Harvard University Press, Cambridge.

Moritz, R. F. A., and E. E. Southwick. 1992. *Bees as Superorganisms.* Springer, Berlin.

Morse, R. A., and F. M. Laigo. 1969. *Apis dorsata* in the Philippines. *Monogr. Philippine Assoc. Entomol.* **1:** 1–96.

Nicolis, G. 1986. *Dynamics of Hierarchical Systems.* Springer, Berlin.

Nicolis, G., and I. Prigogine. 1977. *Self-organization in Non-equilibrium Systems.* Wiley, New York.

O'Donnell, S., and R. L. Foster. 2001. Thresholds of response in nest thermoregulation by worker bumble bees, *Bombus bifarius nearticus* (Hymenoptera: Apidae). *Ethology* **107:** 387–399.

Parrish, J. K., S. Viscido, and D. Grünbaum. 2002. Self-organized fish schools: an examination of emergent properties. *Biol. Bull.* **202:** 296–305.

Partridge, B. L. 1982. The structure and function of fish schools. *Sci. Am.* **246:** 114–123.

Pénzes, Z., and I. Karsai. 1993. Round shape combs produced by stigmergic scripts in social wasps. Pp. 896–905 in *Self Organization and Life: From Simple Rules to Global Complexity,* Proceedings of the Second European Conference on Artificial Life, Brussels, 24–26 May. MIT Press, Cambridge.

Reynolds, C. 1987. Flocks, herds, and schools. *Comput. Graphics* **21:** 25–34.

Sendova-Franks, A., and N. R. Franks. 1999. Self-assembly, self-organization and division of labour. *Philos. Trans. R. Soc. Lond. B* **354:** 1395–1405.

Solé, R., and B. Goodwin. 2000. *Signs of Life.* Basic Books, New York.

Sumpter, D. J. T., and D. S. Broomhead. 2000. Shape and dynamics of thermoregulating honey bee clusters. *J. Theor. Biol.* **204:** 1–14.

Theraulaz, G., and E. Bonabeau. 1999. A brief history of stigmergy. *Artif. Life* **5:** 97–116.

Ünsal, C. 1993. Self-organization in large populations of mobile robots. Master's thesis, Virginia State University, Petersburg, VA.

Vogt, F. D. 1986. Thermoregulation in bumblebee colonies. I. Thermoregulatory *versus* brood-maintenance behaviors during acute changes in ambient temperature. *Physiol. Zool.* **59:** 55–59.

Watmough, J., and S. Camazine. 1995. Self-organized thermoregulation of honey bee clusters. *J. Theor. Biol.* **176:** 391–402.

Weidenmüller, A. 2001. From individual behavior to collective structure: pollen collection and nest climate control in social bees. Ph.D. thesis, Julius-Maximilians-Universität, Würzburg, Germany.

Weidenmüller, A., C. Kleinedam, and J. Tautz. 2002. Collective control of nest climate parameters in bumble bee colonies. *Anim. Behav.* (In press).

Reference: *Biol. Bull.* **202:** 256–261. (June 2002)

Evolution of Self-Organized Systems

BLAINE J. COLE

Department of Biology and Biochemistry, University of Houston, Houston, Texas 77204-5001

Abstract. In this paper I ask questions about the evolution of self-organized activity cycles that are found in some ant colonies. I use a computer model that generates periodic activity patterns in interacting subunits and explore the parameters of this model using a genetic algorithm in which selecting on one aspect of the system produces the distinctive self-organized pattern. The general point that I explore, using the example of activity cycles, is that the observation of a self-organized pattern does not mean that the pattern is an adaptation. Self-organized patterns can represent nonadaptive correlated responses to selection, exaptations or even selectively disadvantageous traits. Evolution of self-organized patterns requires genetic feedback between the self-organized output and the subunits that produce the pattern. Without this necessary feedback, a self-organized system does not evolve.

Introduction

Many features of biological complexity result from self-organization. Biological systems are, in general, global patterns produced by local interactions. The biological structures that seem closest to the ideal of directed organization are proteins that arise from a coding sequence of DNA. Even here, the complex folded structure of a protein is not simply coded in the DNA sequence. Protein structure is the result of genetic and epigenetic processes that produce a single or a few appropriate folded structures from the huge number of stable and thermodynamically equivalent structures. Their structure is not specified uniquely by some central pattern generator, the DNA sequence, but requires interactions among all of the molecular machinery of the cell, including DNA, RNA, and other proteins (Voet and Voet, 1995).

The adult body plan of an organism is a self-organized system produced by the complex interactions among cells and tissues mediated by differential gene expression, local chemical communication among cells, and local regulation that constitute development. The development of an organism is not simply coded by the DNA sequence, but is again a process that is produced by a complex, self-organized system with genetic and epigenetic components (Goodwin 1994; Solé and Goodwin, 2000).

Because social insect colonies are intermediate in their degree of integration between a single soma and a collection of unconnected individuals, they have been favorite subjects for studies of self-organization (see, *e.g.*, Camazine *et al.*, 2001). This same intermediate position in the levels of genetic integration also makes social insects favorite subjects for studies on levels of selection, cooperation, and conflict. The purpose of this paper is to look at an example of selection operating on colony functions to change interactions among workers in such a way as to alter the self-organized activity patterns of the colony.

One of the appealing aspects of the study of self-organized systems is that we do not need anything specific from biology to understand the existence of self-organization. Self-organization occurs for reasons that have to do with the organization of the interacting elements. When we recognize that the same ripple patterns that can exist in sand dunes also exist in biological patterns, some of us feel a profound sense of connection between the physical processes and the biological ones. However, it is undeniable that biological self-organized systems have a capacity that nonbiological self-organized systems usually do not have. Inheritance produces temporal continuity that causes a sort of memory in the system. The difference between the essentially nonbiological self-organized systems and the self-organized systems that most biologists are interested in is

---

This paper was originally presented at a workshop titled *The Limits to Self-Organization in Biological Systems*. The workshop, which was held at the J. Erik Jonsson Center of the National Academy of Sciences, Woods Hole, Massachusetts, from 11–13 May 2001, was sponsored by the Center for Advanced Studies in the Space Life Sciences at the Marine Biological Laboratory, and funded by the National Aeronautics and Space Administration under Cooperative Agreement NCC 2-896.

that sand grains have no system of inheritance. The sand grains do not produce more sand grains that behave in similar ways, or more importantly, with slight modifications. The pattern of ripples in the sand can be changed only by changing the external conditions or by making a qualitative change to the material of which the sand is composed. In biological systems, inheritance allows individual "sand grains" to persist with slightly altered rules for interaction.

Biological self-organized systems should be interesting to those who study self-organization because the inheritance that is intrinsic to biological systems gives them a level of complexity that is unique. Biological self-organized systems should be of interest to evolutionary biologists for two reasons. The first is that self-organized systems produce phenotypes that are subject to selection or other evolutionary processes. Secondly, evolutionary processes may operate on the inherited elements of self-organized systems. These elements may be the subunits (*e.g.*, cells or organisms), but more interestingly, they may be the interactions among subunits. Systematic, microscopic changes in interactions can produce sudden macroscopic phase-shifts in the behavior of self-organized systems, and thus in the phenotype of a organism. This is a characteristic of complex systems in general (*e.g.*, Bak *et al.*, 1988; Kauffman, 1993; Goodwin, 1994; Solé and Goodwin, 2000), but natural selection is a mechanism that produces these systematic microscopic changes. A corollary is that selection on one aspect of a biological self-organized system can produce dramatic changes in some other aspect of the phenotype. This duality between levels of organization of the output of a self-organized system and the interacting components mirrors the duality in levels of selection, or indeed between phenotype and genotype. A standard caveat from evolutionary biology that I develop in this paper is that we must be careful when we impute adaptation to the observation of self-organization, even a self-organized system that is subject to selection.

Evolution in a Self-Organized System

In this paper I examine the model consequences of selection operating on a complex interacting system. The consequence is the emergence of a self-organized property that is independent of selection operating on the system. The system that I describe is that of activity cycles in ant colonies. I use models of ant activity in which colonies can vary in size and in how the worker ants interact with one another. Using a genetic algorithm, I allow the population to evolve in colony size and in the types of interactions. Fitness is assigned to colonies on the basis of a trait that is independent of the degree of periodicity in the colonies, that is, independent of the expression of the self-organized phenotype.

The point that I want to make in this section is that selection on a complex system can result in self-organized patterns even when these patterns have no selective consequence themselves. When we observe self-organized systems, we are under no compulsion to assume that the pattern represents an adaptation. The general point that changes, even when produced by selection, do not represent adaptations has been made for such diverse examples as the variety of patterns of the sutures of ammonite shells (Gould, 1977) and the changes in allele frequency due to genetic hitchhiking (Hedrick, 1982). Specifically, I examine an instance of a self-organized trait that occurs as a correlated response to selection.

The metaphor that I use to make these points is ant colony activity cycles. The activity within colonies of certain species of ants is characterized by short-term cycles (Franks *et al.*, 1990; Hemerik *et al.*, 1990; Cole, 1991a, c, 1992; Tofts *et al.*, 1992; Cole and Cheshire, 1995; Cole and Trampus, 1999; Boi *et al.*, 1999). These activity patterns, while by no means perfectly periodic, have a substantial periodic component. The periodicity is not a property of individual worker ants since they have activity patterns that are either random or chaotic (Cole, 1991b, 1994). As larger numbers of worker ants are added to an experimental aggregate, the magnitude of the largest periodic component increases (Fig. 1a; Cole and Cheshire, 1995). The periodic activity of colonies represents a self-organized temporal pattern. There is a spatial component to this pattern as well, since activity spreads in a traveling wave throughout the colony (Cole and Trampus, 1999; Boi *et al.*, 1999).

Models of ant colony activity were first developed by Solé *et al.* (1992) and expanded and modified by Miramontes *et al.* (1993), Cole and Cheshire (1995), Solé and Miramontes (1995), Solé and Delgado (1996), Delgado and Solé (1997a, b, 2000). These models are mobile cellular automata (MCA) or fluid neural network (FNN) models in which an automaton (a worker ant) becomes active spontaneously and, when active, may move through the gridded nest. The level of activity declines spontaneously at a constant rate, until a threshold level is reached. Neighboring ants may also influence each other's activity depending on the types of interactions that are allowed—that is, depending on the rule set for interactions. For example, we may allow an active ant to influence the activity of a neighboring active ant, or we may allow an inactive ant to influence the activity of a neighboring active ant. The influence of an active ant is to increase the activity of neighbors, and the influence of an inactive ant is to reduce the activity of neighbors. In this simplest model, we allow the ants to be in one of two states, active or inactive. Active ants have an activity level above a threshold, and inactive ants have an activity level below this threshold. The activity of each ant in subsequent time steps is computed according to an algorithm that describes how the activity of the ant changes through time on its own, and the effect of the interactions of

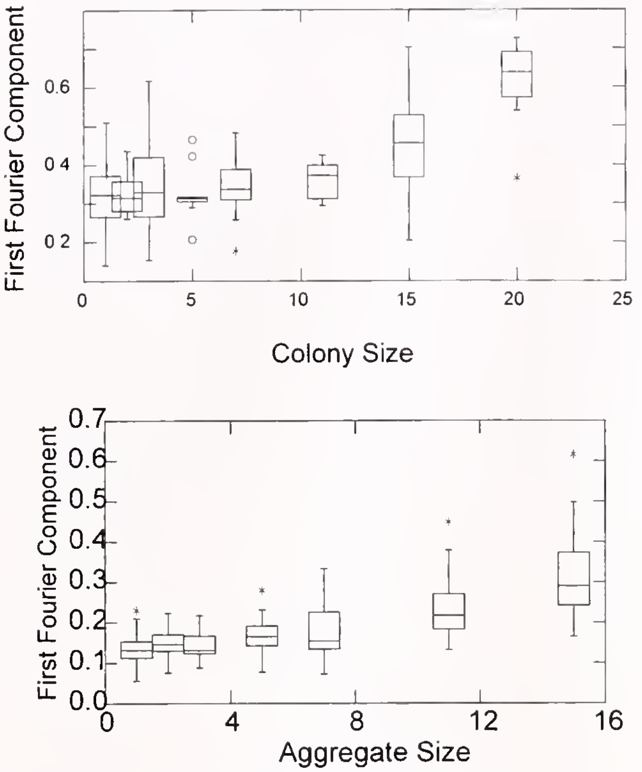

Figure 1. (A) Data from activity records of the ant *Leptothorax allardycei*. The number of individuals is given on the abscissa and the power in the first fourier component of the activity record is given on the ordinate. Activity records are at least four hours long. (B) Magnitude of the first fourier component in simulations of the MCA model described in the text for varying numbers of automata. These figures are adapted from data described by Cole and Cheshire (1995). (© Copyright 2002, The University of Chicago Press. All rights reserved. Used with permission.)

each of its neighbors. The details of the model can be found elsewhere (Solé *et al.*, 1992; Cole and Cheshire, 1995). The rule sets are coded by a matrix that dictates how active or inactive ants influence the activity of their active or inactive neighbors. Since we have two activity states for the ants, there are four terms in this matrix. The first term is the effect that an active ant has on another active ant. A value of 1 indicates that the interaction is allowed, and a value of 0 indicates that the interaction is forbidden. It is convenient to speak of $J_1 = 1$ rules, to indicate that active ants are allowed to influence the activity of other active ants. For example, $J_4 = 0$ rules would indicate that inactive ants are forbidden to influence the activity of inactive ants.

Since the four terms of the interaction matrix can be either 0 or 1, there are 16 rule sets that apply to this model. Earlier work (Cole and Cheshire, 1995) showed that if the model follows the rule $J_1 = 1$, then as larger numbers of workers are added to the system, the degree of periodicity of the simulated outcome increases in the same way that experimental results do (Fig. 1b). In other words, $J_1 = 1$ rule sets are necessary and sufficient to generate periodic activity; the other rules are not critical. Since we are speaking of social behavior, we might regard this as a social facilitation term.

Having $J_1 = 1$ means that active ants stimulate other active ants; in other words, there is a autocatalytic term. Since ants are allowed to move only one space step per time step, there is also an implicit time delay in the system as a whole. Active ants cannot influence ants more than one spatial step away. The activity pattern of the colony is due to a reaction-diffusion system (Murray, 1989) that exhibits self-organized activity cycles that occur as waves propagating throughout the colony.

However, the fact that these patterns can be produced does not mean that they represent an adaptation. The next step is to produce a model of the evolution of activity patterns and colony size in ants. I start with the assumption that activity cycles themselves have no functional or selective consequence. When I make this assumption in the model, I am not claiming that activity cycles have no functional consequence, I am just exploring the consequence of making that assumption. Delgado and Solé (2000) use the same models to consider possible increases in colony efficiency that may result from periodicity in activity. What I assume does have selective value is the rate with which an ant can traverse the colony. I take as a reasonable assumption that the longer the time that is required for an ant to move between specified locations in the nest (for example, from one side of the nest to the other), the longer the time required for food or information to travel through the nest. Provided food is carried by ants or information is propagated by physical contact, these are reasonable assumptions. The assumption that I am making is that colonies in which food or information or workers themselves travel more quickly from place to place have higher fitness. The fitness of a colony that has a particular rule set will be the reciprocal of the time required for transiting the nest.

The strategy is to take a model population of "ant colonies" and follow the changes in the rule sets used by colonies. Initially, all colonies are composed of three workers with $J_1 = J_2 = J_3 = J_4 = 0$; workers are not allowed to influence the activity of any other workers. In each time step, fitness is assigned by noting the transit time of workers within colonies that use particular interaction rules. Fitness varies with the size of the colony and the rule set that the colony is using. Fitness assignments were made by performing 10 simulations for each of the 16 rule sets using 3, 5, 7, 11, 15, 20, 25, 30, 35, 40, 45, 50, 55, 60, and 65 workers (since the same grid size is used, this results in increasing density). In each simulation a single transit time was measured. A fourth order polynomial was fitted to the relation of transit time and colony size to interpolate the nonlinear relationships. The polynomial was then used to calculate transit time, or 1/fitness for a particular combination of rule

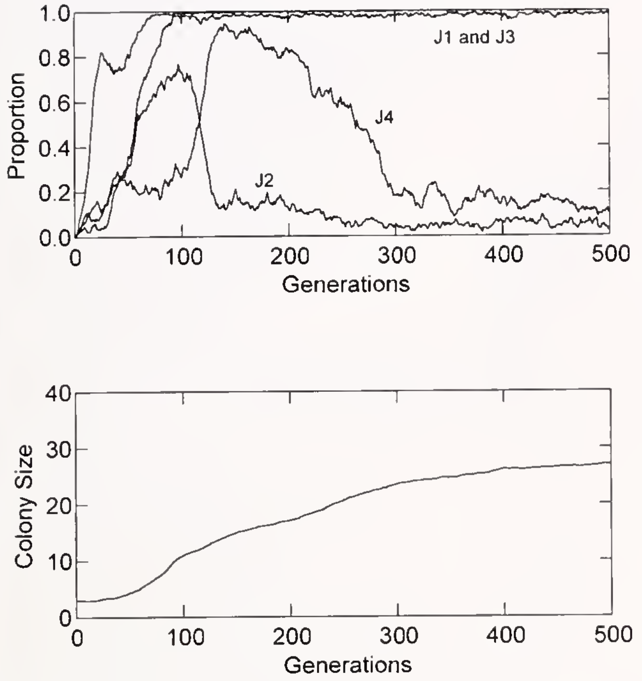

Figure 2. The outcome of selection for various rule sets in the genetic algorithm described in the text. (A) The proportion of colonies that obey the $J1 = 1$, $J2 = 1$, $J3 = 1$ or $J4 = 1$ rule through time, starting with a colony size of three workers with all workers obeying the rule $J1 = J2 = J3 = J4 = 0$. $J3 = 1$ becomes fixed in the population first, followed rapidly by $J1 = 1$. Both the $J2 = 1$ and the $J4 = 1$ rule transiently reach high proportions before declining in frequency. The $J1 = 1$ and $J3 = 1$ rules do not remain fixed due to recurrent mutation. (B) The average colony size of the 1000 colonies composing the population.

set and colony size. The mutation rate, going up or down in colony size (in one-worker increments) or changing one of the rules (from 0 to 1 or back) was 0.01. The population of 1000 colonies was repopulated by random replication of colonies with probabilities based on a colony's relative fitness.

The outcome of this genetic algorithm is shown in Figure 2a. Both rules $J_3 = 1$ and $J_1 = 1$ rapidly go to near fixation in the population. Other rules are transiently selected for because colony size is changing as well (Fig. 2b). Selection on transit time produced a rule set that generates self-organized activity cycles. These self-organized patterns are themselves not the outcome of selection; they have no effect on function or fitness, and yet they appear due to selection on transit time. They are a correlated response to selection.

A second consequence of this selection is that it produces activity patterns of greater complexity. For each rule set, I measured the complexity of the activity record as the average mutual information per pair of ants (Langton, 1992; Solé and Miramontes, 1995). The mutual information in a pair of activity records is the sum of the entropy in each ant's activity record minus the entropy in the joint activity record: entropy of ant 1 + entropy of ant 2 − joint entropy. Entropy is, $\Sigma p_i \log_2 p_i$, summing over the proportion, p_i, of time that the aggregate spends in each of the $n + 1$ activity states (n = number of ants). If the ants behave independently, joint entropy equals the sum of the individual entropies and the mutual information is zero. If the ants remain in one behavioral state, then the sum of the entropies is low and the mutual information is low as well. For each aggregate I calculated the mutual information per pair of ants and analyzed their average values. The average mutual information per pair of ants is shown in Figure 3 for various rule sets. When selection operates on the speed of movement through the nest, the correlated effect is to increase the complexity of activity patterns. In this simulation, colony size and the rule sets coevolve to place the activity pattern near the peak of complexity, or in the region that Langton (1992) calls "edge of chaos."

Discussion

As with any complex trait, the observation of a self-organized pattern says little about the functional consequence of the pattern. In the model results, the self-organized structure is neither advantageous nor disadvantageous; it is simply nonadaptive. However, the self-organized trait could be disadvantageous if we measure the effect that increasing expression has on fitness, provided this effect is less than the increase in fitness gained through selection on the other trait. We might measure the effect that activity cycles have on fitness and detect a negative relationship. Provided the negative effects of activity cycles are more than balanced by the positive effects on transit time, particular rule sets that generate periodic activity could be at a selective advantage.

Finally, it is possible that a self-organized pattern could be produced as a correlated response but then be acted upon by selection in the future. Under a new set of circumstances, the self-organized pattern may have a positive effect. This would be an exaptation in the sense of Gould and Vrba (1982). Selection on the self-organized pattern may modify it to become more effective at producing these positive consequences; however, the self-organized pattern could not be regarded as an adaptation. Subsequent modifications to the system to produce additional changes should be regarded as secondary adaptations, although it would still be fair to regard the pattern itself as an exaptation. We could imagine, for example, that cycles of activity are produced in ant colonies by selection operating on the level of activity of individual worker ants. The existence of activity cycles may then be co-opted to improve certain colony functions according to the mechanism suggested by Delgado and Solé (2000).

Self-organized systems happen, but that may not mean anything. Logically, the possibilities are that they have no selective consequence (they are nonadaptive), they contrib-

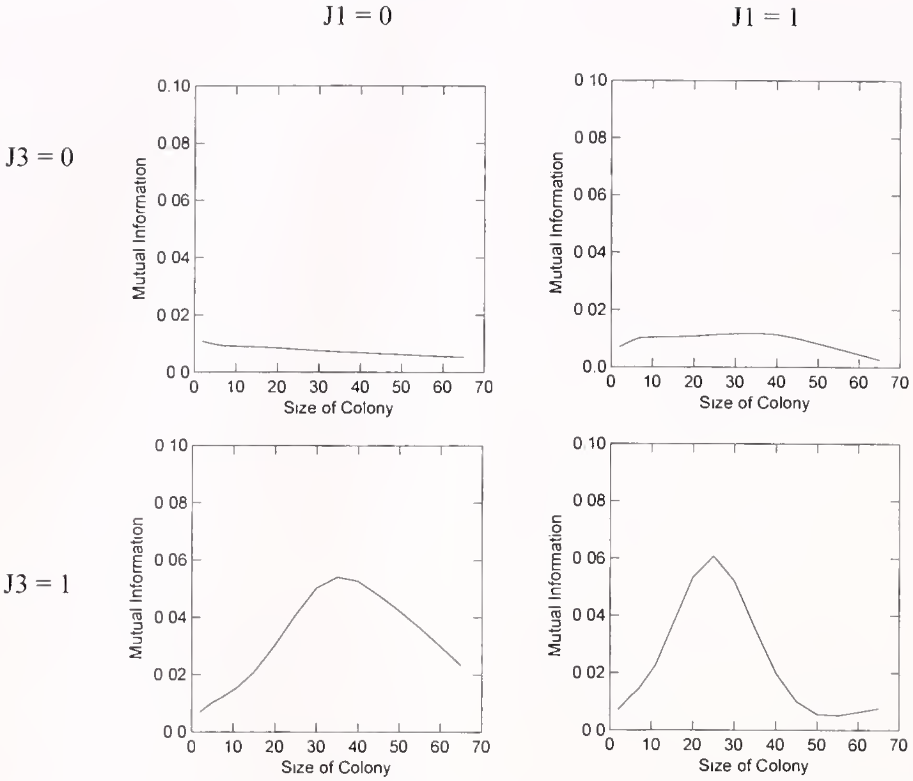

Figure 3. The mutual information content of activity patterns for various rule sets and colony sizes. The different *J1* rules are found across columns and the *J3* rules are shown on the rows. These two rules are the only two that influence the degree of complexity of the activity patterns; other rule sets yield flat curves. The results are based on the average mutual information per pair of ants in 10 simulations for each of the colony sizes given in the text. The lines are a locally weighted scatterplot smooth (tension = 0.3).

ute to the fitness of an organism (are an adaptation), they contribute to the fitness of an organism as a consequence of a cooptation of the effect of self-organization (an exaptation), or they represent a trait at a selective disadvantage that is produced because of indirect selection.

The key distinction concerning the evolution of self-organized systems is whether they are anything different from ripples of sand on a sand dune. The key difference is inheritance. To the extent that the rules for a biological self-organized system can be inherited, they are more interesting than ripples of sand because they are subject to evolutionary change. This requirement places limits on the places where self-organization can evolve. If the fitness of the subunits in the interaction cannot be influenced by the self-organized pattern, then the pattern cannot evolve.

The self-organized pattern is produced by a feed-forward mechanism from the subunits to the pattern. In order for the self-organized system to evolve, there must also be feedback between the self-organized pattern that emerges from the interaction and the units of action. There is clearly a genetic feedback between the elements that produce an organism (the cells, for example) and the self-organized phenotype of the organism. In most cases the subunits composing the whole have near genetic identity. Hamilton (1964, 1970) and Price (1970) showed us how to think about the evolution of self-organized systems, such as social insect colonies, that do not have genetic identity, but genetic relatedness.

In the hierarchical organization of biological systems, there are limits to this progression. Take, for example, the self-organized wave fronts of migrating wildebeest herds (Gueron and Levin, 1993). These large herds characteristically form movement fronts with a wavelike structure that has a wavelength of kilometers, even though the local interactions among the wildebeest are occurring over the scale of meters. This is a self-organized structure where there is probably no genetic feedback between the emergent output and the actions of the subunits. It is unlikely that these self-organized patterns can evolve. Evolutionary processes operating at lower levels can change the rules of interaction that may lead to different forms of the wave front, but the form of the wave front is not evolving, in the sense that there are no evolutionary forces acting on the form of this wavefront. In a similar way, self-organized patterns of ecosystems that may emerge from interactions among the component species may not evolve either. If the self-organized pattern itself has no influence on the reproduction of those that have inheritance, the self-organized pattern may change, but it does not evolve.

Acknowledgments

I thank Scott Camazine and Diana Blazis for organizing the conference, and Diane Wiernasz and two anonymous reviewers for helpful comments and suggestions on this manuscript.

Literature Cited

Bak, P., C. Tang, and K. Wiesenfield. 1988. Self-organized criticality. *Phys. Rev. A* **38:** 364.

Boi, S., I. Couzin, N. Del-Buono, N. R. Franks, and N. Britton. 1999. Coupled oscillators and activity waves in ant colonies. *Proc. R. Soc. Lond. B* **1417:** 371–378.

Camazine, S., J.-L. Deneubourg, N. R. Franks, J. Sneyd, G. Theraulaz, and E. Bonabeau. 2001. *Self-Organization in Biological Systems.* Princeton University Press, Princeton, NJ.

Cole, B. J. 1991a. Short-term activity cycles in ants: generation of periodicity by worker interaction. *Am. Nat.* **137:** 244–259.

Cole, B. J. 1991b. Is animal behavior chaotic? Evidence from the activity of ants. *Proc. R. Soc. Lond. B* **244:** 253–259.

Cole, B. J. 1991c. Short-term activity cycles in ants: a phase response curve and phase resetting in worker activity. *J. Insect Behav.* **4:** 129–137.

Cole, B. J. 1992. Short-term activity cycles in ants: age-related changes in tempo and colony synchrony. *Behav. Ecol. Sociobiol.* **31:** 181–187.

Cole, B. J. 1994. Chaos and behavior: the perspective of nonlinear dynamics. Pp. 423–443 in *Behavioral Mechanisms in Evolutionary Ecology,* L. Real, ed. University of Chicago Press, Chicago.

Cole, B. J., and D. Cheshire. 1995. Mobile cellular automata models of ant behavior: movement activity of *Leptothorax allardycei. Am. Nat.* **148:** 1–15.

Cole, B. J., and F. I. Trampus. 1999. Activity cycles in ant colonies: worker interactions and decentralized control. Pp. 289–308 in *Information Processing in Social Insects,* Claire Detrain, J. L. Deneubourg, and J. M. Pasteels, eds. Birkhauser Verlag, Basel.

Delgado, J., and R. V. Solé. 1997a. Noise induced transitions in fluid neural networks. *Phys. Lett. A* **229:** 183–189.

Delgado, J., and R. V. Solé. 1997b. Collective-induced computation. *Phys. Rev. E* **55:** 2338–2344.

Delgado, J., and R. V. Solé. 2000. Self-synchronization and task fulfillment in ant colonies. *J. Theor. Biol.* **205:** 433–441.

Franks, N. S., R. Bryant, R. Griffiths, and L. Hemerik. 1990. Synchronization of the behavior within nests of the ant *Leptothorax acervorum* (Fabricius). I. Discovering the phenomenon and its relation to the level of starvation. *Bull. Math. Biol.* **52:** 597–612.

Goodwin, B. C. 1994. *How the Leopard Changed Its Spots.* C. Scribner's Sons, New York.

Gould, S. J. 1977. *Ontogeny and Phylogeny.* Belknap Press of Harvard University Press, Cambridge, MA.

Gould, S. J., and E. S. Vrba. 1982. Exaptation—a missing term in the science of form. *Paleobiology* **8:** 4–15.

Gueron, S., and S. A. Levin. 1993. Self-organization of front patterns in large wildebeest herds. *J. Theor. Biol.* **165:** 541–552.

Hamilton, W. D. 1964. The genetical evolution of social behaviour. I. *J. Theor. Biol.* **7:** 1–16.

Hamilton, W. D. 1970. Selfish and spiteful behaviour in an evolutionary model. *Nature* **228:** 1218–1220.

Hedrick, P. W. 1982. Genetic hitchhiking: a new factor in evolution? *BioScience* **32:** 845–853.

Hemerik, L., N. F. Britton, and N. R. Franks. 1990. Synchronization of the behavior within nests of the ant *Leptothorax acervorum* (Fabricius). II. Modeling the phenomenon and predictions from the model. *Bull. Math. Biol.* **52:** 613–662.

Kauffman, S. A. 1993. *The Origins of Order.* Oxford University Press, New York.

Langton, C. G. 1992. Life at the edge of chaos. Pp. 41–92 in *Artificial life II, SFI Studies in the Sciences of Complexity,* Vol. 10, C. G. Langton, C. Taylor, J. D. Farmer, and S. Rasmussen, eds. Addison-Wesley, Redwood City, CA.

Miramontes, O., R. Solé, and B. C. Goodwin. 1993. Collective behaviour on random-activated mobile cellular automata. *Physica D* **63:** 145–160.

Murray, J. D. 1989. *Mathematical Biology.* Springer-Verlag, New York.

Price, G. R. 1970. Selection and covariance. *Nature* **227:** 520–521.

Solé, R., O. Miramontes, and B. C. Goodwin. 1992. Collective oscillations and chaos in the dynamics of ant societies. *J. Theor. Biol.* **159:** 469.

Solé, R. V., and J. Delgado. 1996. Universal computation in fluid neural networks. *Complexity* **2:** 49–56.

Solé, R. V., and B. C. Goodwin. 2000. *Signs of Life.* Basic Books, New York.

Solé, R. V., and O. Miramontes. 1995. Information at the edge of chaos in fluid neural networks. *Physica D* **80:** 171–180.

Solé, R. V., O. Miramontes, and B. C. Goodwin. 1993. Oscillations and chaos in ant societies. *J. Theor. Biol.* **161:** 343–357.

Tofts, C., M. Hatcher, and N. R. Franks. 1992. The autosynchronization of the ant *Leptothorax acervorum* (Fabricius): theory, testability and experiment. *J. Theor. Biol.* **157:** 71–82.

Voet, D., and J. Voet. 1995. *Biochemistry,* 2nd ed. John Wiley and Sons, New York. 1361 pp.

Reference: *Biol. Bull.* **202:** 262–267. (June 2002)

Dynamics of Aggregation and Emergence of Cooperation

J. L. DENEUBOURG*, A. LIONI, AND C. DETRAIN
Université Libre de Bruxelles, Unit of Social Ecology, CP 231, B-1050 Brussels, Belgium

Abstract. Aggregation is one of the most basic social phenomena, and many activities of social insects are linked to it. For instance, the selection of a valuable site and the spatial organization of the population are very often by-products of amplifications based on the local density of nestmates. The patterns of aggregation are very diverse, ranging from the gathering of all animals in a unique site to their splitting between several ones. One might question how these multiple patterns emerge. Do ants actively initiate the formation of such patterns by modulating the emission of an attracting signal such as the trail pheromone? Alternatively, do patterns result from quantitative changes in the duration of interaction between animals once they have reached the gathering site, without any active modulation of the communications? To discuss these questions, we present two empirical studies: the gregarious behavior of cockroaches (*Blatella*) and self-assembly in the weaver ant (*Oecophylla*).

Through experimental and theoretical studies, we show how a single behavior—the resting time—leads to a collective choice in both species. This behavior is a response to the density of conspecifics and can also be modulated by heterogeneities in the environment. In weaver ants, it allows the colony to focus the formation of chains in a given area among several potential sites. In cockroaches, it allows the gathering of individuals in particular shelters, depending on the proximity between strains. These results are discussed with emphasis on the role of aggregation processes in the emergence of cooperativity and task allocation.

Introduction

In animal societies, collective decisions and patterns emerge from a variety of interactions among individuals. Self-organization is the theory of how minimal complexity at the individual level can generate much greater complexity at the collective one. The rules specifying the interactions among the system's components are executed using only local information, that is, without reference to the global pattern. Thus collective decisions that can be made using rules of thumb that require only a limited cognitive ability and a limited knowledge of the environment might be characterized in terms of the multiplicity of parameters as well as by heterogeneity and unpredictability (Camazine *et al.*, 2001).

Most self-organized decisions and patterns arise as a result of a competition between different sources of information that are then amplified through different forms of positive feedback. In contrast, negative feedback often arises "automatically" as a result of the system's constraints (*e.g.*, limits on the supply of food, the space for settlement, and the number of available workers). An example of such processes is the competition between trail recruitments to multiple food sources in social insects or gregarious arthropods (social caterpillars or spiders) where the modulation of communication is essential (Deneubourg and Goss, 1989; Camazine *et al.*, 1990, 2001; Camazine and Sneyd, 1991; Seeley *et al.*, 1991; Seeley, 1995; Fitzgerald, 1995; Detrain *et al.*, 1999; Saffre *et al.*, 1999). For instance, the ability of a bee or an ant to modulate its dancing or trail-laying behaviors, in relation to its perception of the profitability of a particular source, is sufficient for a collective and adapted decision to be made.

We generally observe a high diversity of collective patterns at both intraspecific and interspecific levels. But how is this diversity produced in self-organized systems? Do individuals need specific behavioral algorithms and a modulation of their communication for each situation? Or do

---

* To whom correspondence should be addressed. E-mail: jldeneub@ulb.ac.be

This paper was originally presented at a workshop titled *The Limits to Self-Organization in Biological Systems.* The workshop, which was held at the J. Erik Jonsson Center of the National Academy of Sciences, Woods Hole, Massachusetts, from 11–13 May 2001, was sponsored by the Center for Advanced Studies in the Space Life Sciences at the Marine Biological Laboratory, and funded by the National Aeronautics and Space Administration under Cooperative Agreement NCC 2-896.

they just modulate some generic rules without changing their individual interactions? Can we find a convergence of similar and simple mechanisms for different species and for different collective tasks? These are fundamental questions, not only for better understanding mechanisms of organization, but also for making the link between the proximal and ultimate view of social evolution (Krebs and Davies, 1997).

To discuss these questions, we choose to focus on a very widespread phenomenon, that of aggregation. It is of particular interest because it is a prerequisite for the development of other forms of cooperation and is involved in many tasks performed by an insect society. In addition, the gathering of individuals at the same place is significant because it is often the consequence of a collective choice.

Through two empirical studies—on the gregarious behavior of cockroaches (*Blattela germanica*) and on self-assembly in weaver ants (*Oecophylla*)—we show (1) how collective decisions are a by-product of the mechanisms involved in aggregation; and (2) how different collective patterns, with different functions, arise from the same generic rules, based on the individual response (mainly the resting time) to local signals including the presence of conspecifics (positive feedback). Though we do not deny the possible modulation of a signal depending on the environment, we demonstrate here that such modulation is neither observed nor necessary for the emergence of aggregation patterns.

Self-Assembly in *Oecophylla*

Ants of the genus *Oecophylla* (Ledoux, 1950; Hölldobler and Wilson, 1978, 1990; Lioni *et al.*, 2001; Lioni and Deneubourg, unpubl. data) are characterized by their capacity to hang on to each other to form chains. This allows the bridging of an empty space, for example between two branches (see Hölldobler and Wilson, 1990, pp. 618–629). These self-assembled structures are a particular type of aggregation. In nature the challenge of such an activity is to avoid the formation of multiple small and inefficient chains. What are the mechanisms that allow the colony to focus its activity at a particular and useful site?

To address this question, we set up an experimental apparatus using a binary choice (Fig. 1a), and we observed how the probability of an ant entering (P_{ei}) or leaving (P_{li}) a chain depends on the size of the chain (Fig. 1b). We found that

$$P_{ei} = a + \frac{bX_i}{1 + cX_i} \qquad (1)$$

$$P_{li} = \frac{dX_i}{1 + eX_i^h} \qquad (2)$$

where X_i is the number of ants in the chain *i*.

The fitting of the experimental values gives the following parameter values: $a = 0.55$; $b = 0.11$; $c = 0.28$ ($r = 0.89$; $P < 0.001$); $d = 0.33$; $e = 0.48$; $h = 1.3$ ($r = 0.92$; $P < 0.001$).

The function P_{ei} expresses the idea that the probability for an ant to join the chain grows with the number of nestmates already present (X) and reaches a plateau value equal to $a + bX_i$; a is the value of spontaneous hanging when $X_i = 0$. The probability for an ant to leave the chain (P_{li}) decreases with X_i. Considering T_p as the total population in the nest, we also observed a linear dependence between the arrival flow ϕ_p and the population remaining in the nest ($T_p - (X_1 + X_2)$).

At the beginning of the experiment, we observe a similar increase in the number of ants in both chains. A slight asymmetry between the populations appears, after 10 min, and is amplified during the rest of the experiments. After 20 min there is a strong asymmetry, which results in the survival of one chain with a high number of ants (Fig. 2). The asymmetry is not due to a higher flow of arrivals from the nest to the strongest chain (this flow remains equal on both branches); it is due only to the process of the ants entering and leaving the chains.

Positive feedback mechanisms expressed by equations (1) and (2) generate a nonlinear growth that focuses activity on a single and functional chain instead of on several small and inefficient ones.

Furthermore, these probabilities (P_{ei}) and (P_{li}) can be triggered by the presence of a visual stimulus or by the geometry of the environment (*e.g.*, a dead-end). The symmetry of the set-up can be broken by placing a visual stimulus under one branch (black bar, 1 cm width, placed 6 cm below one branch). In this situation the growth and the persistence of the chain above the stimulus are favored (Fig. 3). There is still an equal flow of arrivals on both branches, and the same logic applies as in the symmetrical setup. The visual stimulus quantitatively changes the individual response by slightly increasing P_e and decreasing P_1, thereby increasing the resting time in the chain. As a result, the visual stimulus can be reached by the ants, and the chain is used as a bridge.

To summarize, this example shows that a slight modulation of the resting time, which corresponds to $1/P_1$, can generate different patterns and allow the colony to focus its activity. The individual response is based on the local density of nestmates and can be triggered by any favorable configuration, such as the presence of leaves in a tree. It is important to note that this decision is reached without any need for an active modulation of the communication.

Cockroach Aggregation and Strain Odor Recognition

Cockroaches in the species *Blattella germanica* exhibit gregarious behavior in shelters during their resting period. The shelters are an important resource for these insects, and the gregarious behavior facilitates cooperation (Dambach and Goehlen, 1999). Binary choice tests were carried out

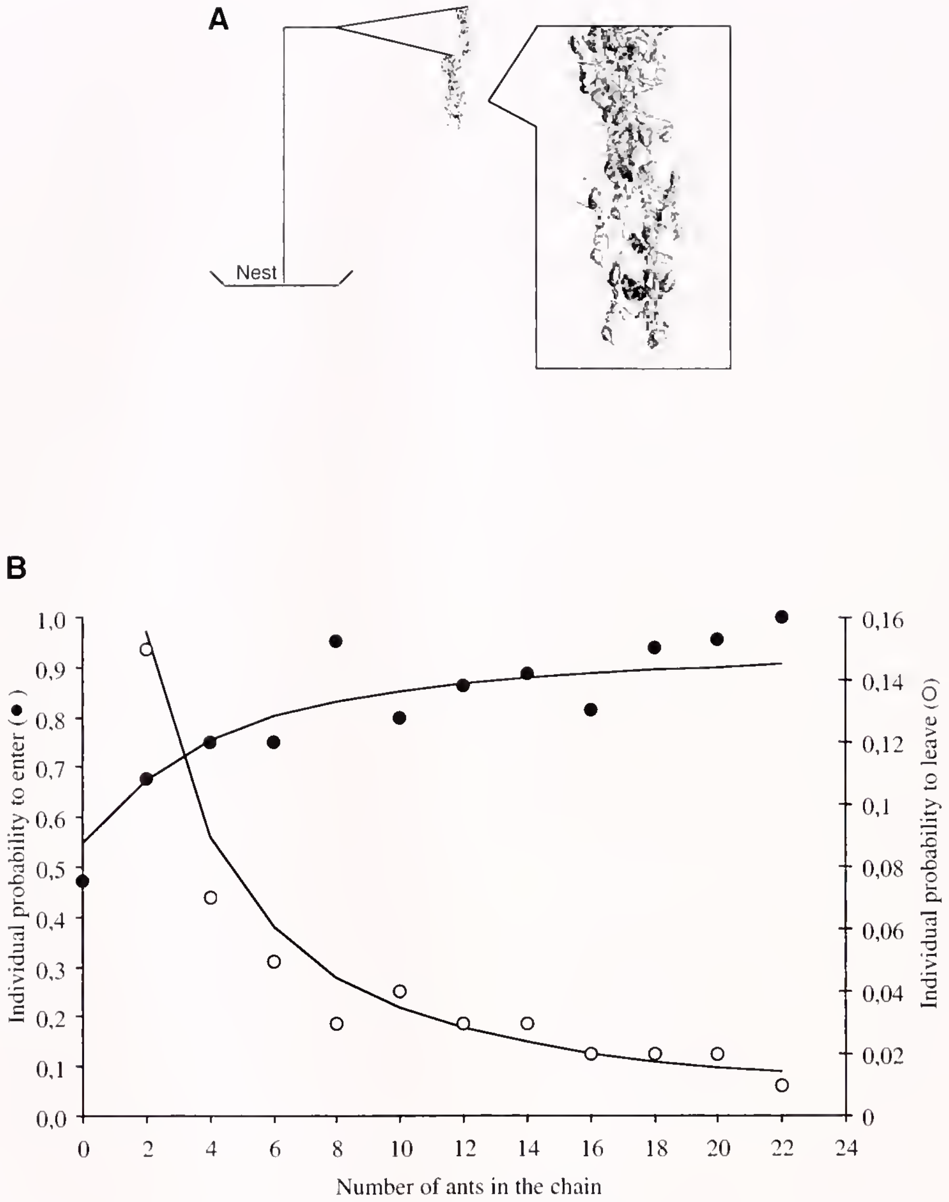

Figure 1. (A) Binary choice experimental set-up used to study chain competition in weaver ants. (B) Individual probabilities to enter a chain depending on its size (●) and to leave a chain depending on its size (○).

between two large and identical shelters each with a carrying capacity (S) large enough to contain the whole population. Tested groups of larvae show a strong tendency to aggregate on a unique, randomly selected, resting site (Fig. 4; Rivault and Cloarec, 1998). This collective choice results from a random walk and hence random discovery of the shelter by larvae and a probability P_i to leave the shelter i (P_i = 1/resting time). Due to inter-attraction between individuals, this probability decreases with the number of conspecifics (X_i) in the shelter i and is ruled by an empirical equation very similar to that proposed for *Oecophylla* (Rivault *et al.*, 1999; Ame *et al.*, Université Libre de Bruxelles, unpubl. data):

$$P_i = \frac{a}{1 + bX_i^2} \qquad (3)$$

with $a = 0.01$, $b = 0.16$. The characteristics of the shelter affect the resting time of the individuals, which for an isolated animal is $\cong 1/a$. The expression $(1 + bX_i^2)$ describes how the presence of other conspecifics increase the resting time. A theoretical model suggests that these basic mechanisms account for the clustering of insects (Rivault *et al.*, 1999; Ame *et al.*, unpubl. data). This model also predicts that other collective patterns can emerge, keeping the same individual rules.

For instance, a group of cockroaches is able to select a

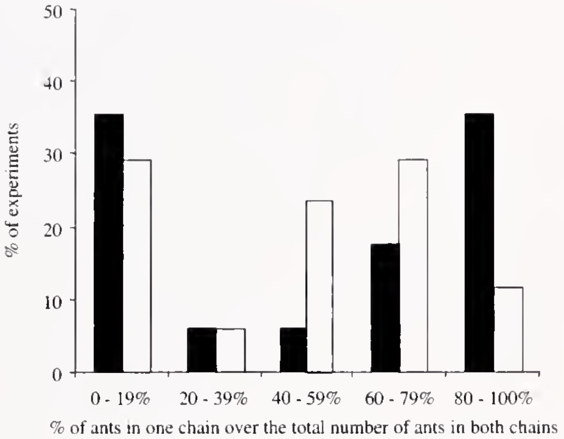

Figure 2. Distributions of the proportion of ants in one chain on the total number of ants in each chain at times 2 (☐) and 20 min (■) ($N = 19$).

single shelter only if the number of shelters is small or its population is large. This result shows that different patterns of aggregation may be spontaneously adopted based only on changes in the environment.

In natural situations, the shelters are not identical, and they are characterized by different parameters, which are more or less easily detected and integrated by an individual. Any parameter of the shelter that increases the individual resting time favors the formation of the cluster in this shelter. Because of the competition between shelters, most of the larvae will aggregate in the site that has the highest resting time. Furthermore, the interactions between individuals increase the probability of an individual staying on the site that produces the largest resting time and benefit *per capita*.

Individual tests show that the larvae prefer the odor of their own strain to that of another (Rivault *et al.*, 1999). However, in mixed groups with individuals from two strains, experiments show that the final aggregation is not different for mixed or pure groups (Rivault and Cloarec, 1998). In simulations, it is rather easy to take these interactions between strains into account:

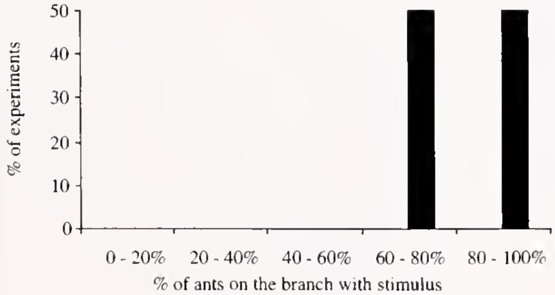

Figure 3. Distributions of the proportion of ants in the chain above the stimulus, on the total number of ants in each chain at 10 min ($N = 6$).

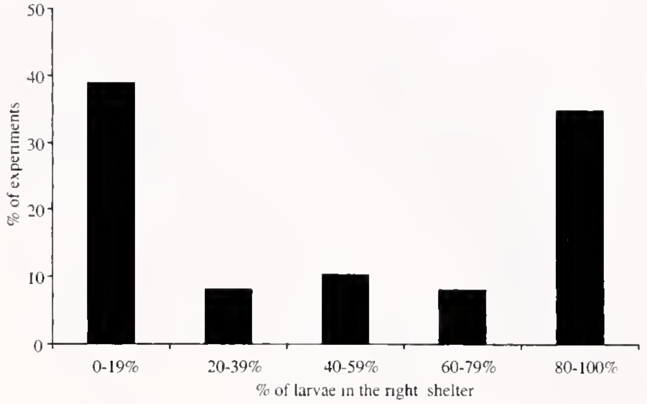

Figure 4. Experimental distribution of the proportion of cockroach larvae present in shelter 1 ($n = 49$). Number of larvae in each tested group = 20.

$$P_{1i} = \frac{a}{1 + b(X_{1i} + \beta X_{2i})^2} \tag{4}$$

$$P_{2i} = \frac{a}{1 + b(X_{2i} + \beta X_{1i})^2} \tag{5}$$

where P_1 (P_2) are the probabilities for an individual of strain 1 (2) to leave the shelter i, X_{1i} and X_{2i} are respectively the number of individuals of strain 1 and 2 in this shelter i. β is the inter-attraction between both strains: if $\beta = 1$, there is no difference between the strains; and if $\beta = 0$, there is no inter-attraction between the strains. Simulations show that even with a very low attractivity between strains (β is low), there is no difference between the gregarious patterns of mixed and pure groups.

However, the model also predicts that the two strains are able to segregate when the resting sites are overcrowded ($S \cong$ total population). Each cluster is characterized by a majority of larvae from the same strain. In this case, group closure is an emergent component of the dynamics, in that the segregation is obtained without aggressive parameters or any other form of repulsion between strains. The smaller the shelter and the greater the difference between the two strains (β small), the more easily the segregation emerges. If the two strains are similar enough ($\beta > 0.5$), the segregation is never observed. To summarize, the crowding in the shelter and the degree to which individuals recognize each other (proximity between strains given by β) affect the dynamics of aggregation and lead to opposite patterns.

Conclusion and Perspectives

Both examples given in this paper illustrate how one parameter (here the resting time) can produce different patterns of aggregation independent of any active signaling by animals. In cockroaches, the amplification is modulated only by the time spent in a shelter, which is enough to produce the patterns. The resting time is increased by the presence of conspecifics and is used as a key for assessing the quality of the site. In *Oecophylla*, the same mechanisms act to focus the colonial activity in a particular area.

In cockroaches, the unique modulated parameter contrasts with the different patterns. The shift between aggregation and segregation is obtained without any behavioral modification, such as the introduction of aggressive behavior. In *Oecophylla*, these mechanisms regulate the location of the chain and prevent the formation of numerous and inefficient ones. Moreover, experimental and theoretical results show that, through such mechanisms, the colony can adjust the number of chains: a small colony will not form more than one chain, but a large colony will be able to produce several functional chains (Lioni and Deneubourg, unpubl. data).

Our conviction is that these self-organized processes are numerous despite the fact that the individual or group benefits will differ and will occur in different situations. The mechanisms involved in the aggregation and segregation of the cockroaches—amplification of the resting time and chemical recognition—could have their equivalent in different spatial organization of items by insect societies (Camazine, 1991; Deneubourg *et al.*, 1991; Franks and Sendova-Franks, 1992) and of workers from different castes or from different matrilines or patrilines. For gregarious and eusocial insects, communication relies essentially on chemical signals and amplification mechanisms (Camazine *et al.*, 2001). Phenotypic recognition that is mainly chemically based (Vander Meer and Morel, 1998; Rivault *et al.*, 1998, 1999; Lenoir *et al.*, 1999) can be modulated by genetic background and environment and can be associated with division of labor (Bonavita-Cougourdan and Clement, 1994; Wagner *et al.*, 1998).

In the context of self-organization and transition between different social organizations, aggregation, and its resulting increase in density, is a prerequisite for the emergence of higher forms of cooperation. The density could be involved in, or even lead, the process of the social differentiation. The interplay between amplification mechanisms (*e.g.*, growth or learning) and the competition in a cluster could be enough to produce the social differentiation that has been described for very different species, such as social spiders (Rypstra, 1993), sea urchins (Grosjean *et al.*, 1996), and ant queens (Fewell and Page, 1999); for a model, see Bonabeau *et al.* (1998).

Considering specifically the eusocial species, one of the key questions is the emergence of division of labor. Though there is no doubt that some genetic or physiological aspects must be taken into account (Page and Erber, 2002), we can assume that division of labor is also the result of self-organized mechanisms where amplification is essential (Beshers and Fewell, 2001). Eusocieties express a strong correlation between the colony size and the level of individual specialization (Anderson and McShea, 2001): the bigger the colony, the higher the specialization. As we have shown in the weaver ant (the number of chains depends on the colony size) and the cockroach (aggregation and segregation depend on the available place on a site), aggregation can lead to segregation into a few clusters, depending on the total population of the group. Thus, depending on their location, the individuals constituting a cluster will have different probabilities of being involved in one or another task. For example, a cluster located close to the nest entrance will have a higher probability of interacting with the foragers and being involved in collective recruitment. In contrast, a cluster located close to the food reserves will be stimulated to perform the tasks of sorting and management. To summarize, task allocation and individual specialization will be shaped by the dynamics of aggregation and segregation, and in return these specialized activities will shape the spatial organization within the nest.

The consequence of such a generic logic could then be one of the keys to understanding the transition between different forms of cooperativity, and therefore different degrees of sociality. For instance, it could help to explain how animal species have shifted, through evolution, from solitary to some simple forms of social life. Furthermore, it also brings new ideas on how a solitary species might be manipulated to become gregarious, or how a gregarious species might be manipulated to exhibit more complex forms of cooperation and social specialization (see, *e.g.*, the experimental shift from solitary to social organization in the spider *Coelotes terrestris*, Gunderman *et al.*, 1993). In this context, it is important to notice that even solitary species use amplification mechanisms based on the chemical marking of resting sites or on trail orientation (see, *e.g.*, for spiders, Saffre *et al.*, 1997; B. Krafft, Université de Nancy, pers. comm.).

Our theoretical results on cockroaches show that a slight inter-attraction between the marking of different individuals may induce the formation of a cluster (see also Saffre *et al.*, 1999). We could hypothesize that, for some species, this marking gives the opportunity to shift from solitary to gregarious behavior: the greater this phenotypic recognition, the easier the shift towards gregariousness. Because genetic proximity is one way to increase phenotypic recognition, the clustering of individuals having a similar genotype should be easier, and the synergy between amplification and genetic proximity should facilitate the emergence of cooperation. Therefore, we consider haplodiploidy to be one element that favors the evolution of cooperativity and sociality, but not the keystone of the process.

Finally, positive feedbacks and their synergy with genetic proximity and phenotypic recognition are essential to resolving cooperation problems and conflict situations. This could explain why these aggregative mechanisms are so widespread in group living systems.

Acknowledgments

Many thanks to J. M. Amé, Ph. Rasse, and C. Rivault (University of Rennes) for their interest and work on this topics. Jean-Louis Deneubourg and Claire Detrain are research associates of the Belgian National Foundation for Scientific Research. This work was financially supported by grant number 2.4510.01 for Joint Basic Research. Jean-Louis Deneubourg thanks Les Instituts Solvay and the Santa Fe Institute, and the members of the working group "Social Insects."

Literature Cited

Anderson, C., and D. W. McShea. 2001. Individual versus social complexity. *Biol. Rev. (Camb.)* **76:** 211–237.

Beshers, S. N., and J. H. Fewell. 2001. Models of division of labor in social insects. *Annu. Rev. Entomol.* **46:** 413–440.

Bonabeau, E., J.-L. Deneubourg, and G. Theraulaz. 1998. Within brood competition and the optimal partitioning of parental investment. *Am. Nat.* **152:** 419–427.

Bonavita-Cougourdan, A., and J. L. Clement. 1994. Complexité du message chimique cuticulaire chez les fourmis: le modèle *Camponotus vagus* (Scop.) (Hymenoptera, Formicidae). *Memorabilia Zool.* **48:** 23–37.

Camazine, S. 1991. Self-organizing pattern formation on the combs of honey bee colonies. *Behav. Ecol. Sociobiol.* **28:** 61–76.

Camazine, S., and J. Sneyd. 1991. A model of collective nectar source selection by honey bees: self-organization through simple rules. *J. Theor. Biol.* **149:** 547–571.

Camazine, S., J. Sneyd, M. J. Jenkins, and J. D. Murray. 1990. A mathematical model of self-organized pattern formation on the combs of honeybee colonies. *J. Theor. Biol.* **147:** 553–571.

Camazine, S., J. L. Deneubourg, N. Franks, J. Sneyd, E. Bonabeau, and G. Theraulaz. 2001. *Self-Organization in Biological Systems.* Princeton University Press, Princeton, NJ.

Dambach, M., and B. Goehlen. 1999. Aggregation density and longevity correlate with humidity in first-instar nymphs of the cockroach (*Blattella germanica* L. Dictyoptera). *J. Insect Physiol.* **45:** 423–429.

Deneubourg, J. L., and S. Goss. 1989. Collective patterns and decision-making. *Ethol. Ecol. Evol.* **1:** 295–311.

Deneubourg, J. L., S. Goss, N. Franks, A. Sendova-Franks, C. Detrain, and L. Chrétien. 1991. The dynamics of collective sorting: robot-like ants and ant-like robots. Pp. 356–365 in *From Animals to Animals: Proceedings of the First International Conference on Simulation of Adaptive Behavior,* J.-A. Meyer and S. Wilson, eds. MIT Press, Cambridge, MA.

Detrain, C., J. L. Deneubourg, and J. M. Pasteels. 1999. Decision-making in foraging by social insects. Pp. 331–354 in *Information Processing in Social Insects,* C. Detrain, J. L. Deneubourg, and J. M. Pasteels, eds. Birkhauser, Basel.

Fewell, J. H., and R. E. Page, Jr. 1999. The emergence of division of labour in forced associations of normally solitary ant queens. *Evol. Ecol. Res.* **1:** 537–548.

Fitzgerald, T. D. 1995. *The Tent Caterpillars.* Cornell University Press, Ithaca, NY.

Franks, N. R., and A. B. Sendova-Franks. 1992. Brood sorting by ants: distributing the workload over the work-surface. *Behav. Ecol. Sociobiol.* **30:** 109–123.

Grosjean, Ph., Ch. Spirlet, and M. Jangoux. 1996. Experimental study of growth in the echinoid *Paracentrotus lividus* (Lamarck, 1816) (Echinodermata). *J. Exp. Mar. Biol. Ecol.* **201:** 173–184.

Gunderman, J. L., A. Horel, and B. Krafft. 1993. Experimental manipulations of social tendencies in the subsocial spider *Coelotes terrestris. Insectes Soc.* **40:** 229–239.

Hölldobler, B., and E. O. Wilson. 1978. The multiple recruitment systems of the African Weaver ant *Oecophylla longinoda* (Latreille) (Hymenoptera: Formicidae). *Behav. Ecol. Sociobiol.* **3:** 19–60.

Hölldobler, B., and E. O. Wilson. 1990. *The Ants.* Harvard University Press, Cambridge, MA.

Krebs, J. R., and N. B. Davies. 1997. *Behavioural Ecology: An Evolutionary Approach.* Blackwell Scientific, Oxford.

Ledoux, A. 1950. Recherche sur la biologie de la fourmi fileuse (*Oecophylla longinoda* Latr.). *Ann. Sci. Nat. Zool.* Hème série, **13:** 313–409.

Lenoir A., D. Fresneau, C. Errard, and A. Hefetz. 1999. Individual and colonial identity in ants: the emergence of the social representation concept. Pp. 219–237 in *Information Processing in Social Insects,* C. Detrain, J. L. Deneubourg and J. M. Pasteels, eds. Birkhauser, Basel.

Lioni, A., C. Sauwens, G. Theraulaz, and J. L. Deneubourg. 2001. Chain formation in *Oecophylla longinoda. J. Insect Behav.* **15:** 679–696.

Page R. E., and J. Erber. 2002. Levels of behavioral organization and level of division of labour. *Naturwissenschaften* **89:** 91–106.

Rivault, C., and A. Cloarec. 1998. Cockroach aggregation: discrimination between strain odours in *Blattella germanica* (L). *Anim. Behav.* **55:** 177–184.

Rivault, C., A. Cloarec, and L. Streng. 1998. Cuticular extracts inducing aggregation in the German cockroach, *Blattela germanica* (L). *J. Insect Physiol.* **44:** 909–918.

Rivault, C., G. Theraulaz, A. Cloarec, and J. L. Deneubourg. 1999. Auto-organisation et reconnaissance coloniale: le modèle de l'agrégation de la blatte. Pp. 11–18 in *Actes Colloque Insectes Sociaux,* Vol. 12, J. P. Lachaud and V. Fourcassie, eds. L'Union Internationale pour l'Etude des Insectes Sociaux, Section Francaise, Paris.

Rypstra, A. L. 1993. Prey size, social competition, and the development of reproductive division of labor in social spider groups. *Am. Nat.* **142:** 868–880.

Saffre, F., B. Krafft, and J. L. Deneubourg. 1997. What are the mechanisms involved in the emergence of cooperativity? The "spider" model. Pp. 85–90 in *Auto-organisation et Comportement,* G. Theraulaz and F. Spitz, eds. Hermès, Paris.

Saffre, F., R. Furey, B. Krafft, and J. L. Deneubourg. 1999. Collective decision-making in social spiders: dragline-mediated amplification process acts as a recruitment mechanism. *J. Theor. Biol.* **198:** 507–517.

Seeley, T. D. 1995. *The Wisdom of the Hive.* Harvard University Press, Cambridge, MA.

Seeley, T. D., S. Camazine, and J. Sneyd. 1991. Collective decision-making in honey bees: how colonies choose among nectar sources. *Behav. Ecol. Sociobiol.* **28:** 277–290.

Vander Meer, R. K., and L. Morel. 1998. Nestmate recognition in ants. Pp. 79–103 in *Pheromone Communication in Social Insects: Ants, Wasps, Bees and Termites,* R. K. Vander Meer and K. E. Espelie, eds. Westview Press, Boulder, CO.

Wagner, D., M. J. F. Brown, P. Broun, W. Cuevas, L. E. Moses, D. L. Chao, and D. M. Gordon. 1998. Task-related differences in the cuticular hydrocarbon composition of harvester ants, *Pogonomyrmex barbatus. J. Chem. Ecol.* **24:** 2021–2037.

Reference: *Biol. Bull.* **202:** 268–274. (June 2002)

Complexity of Environment and Parsimony of Decision Rules in Insect Societies

CLAIRE DETRAIN* AND JEAN-LOUIS DENEUBOURG

Unit of Social Ecology (CP 160/12), Université Libre de Bruxelles, Av F. Roosevelt 50 B-1050, Brussels, Belgium

Abstract. This paper shows how colonies of social insects process information and solve problems in a complex environment, while keeping some parsimony at the level of the individuals' decision rules. Two studies on ant foraging reveal the diversity of adaptive colony-level patterns that can be generated through self-organization, based on the same individual-level recruitment rules. Regarding prey scavenging, the "ability to retrieve the prey" rule accounts for changes in foraging patterns, with increasing prey size, that show all stages intermediate between an individual and a mass exploitation of food resources. Regarding liquid food foraging, the "ability to ingest a desired volume" rule enables a colony to adjust the number of tending ants to the honeydew production of aphids. In both cases, decision rules are based on intelligent criteria that intrinsically integrate information on multiple variables that are relevant to the ants. Furthermore, the environment can contribute directly to the emergence of collective patterns, independently of any individual behavioral changes. Each environmental factor, including abiotic ones, that alters the dynamics of information transfer in group-living animals should be reconsidered not simply as a constraint but also as a part of the decision-making process and as a agent that shapes the collective pattern.

Introduction

The Darwinian fitness of animals depends on their ability to assess their environment and to decide accordingly which behavior is the most appropriate. Ideally, group foragers—including social insects—should measure all relevant parameters and process information related to environmental resources and colony needs in order to optimize their foraging decisions. (For an optimization approach to foraging in vertebrates see, for example, Krebs and Davies, 1991; Giraldeau and Caraco, 2000; in social insects, see Oster and Wilson, 1978; Schmid-Hempel *et al.*, 1985.) However, in an ever-changing environment, there may be an advantage to making rapid decisions instead of perfectly informed ones based on multiple time-consuming assessments. Furthermore, one can hypothesize that mechanisms have been selected that enable animal societies to adaptively respond to a complex environment, despite some simplicity of decision rules at the individual level. Self-organization is a means to generate such diversity, flexibility, and complexity of collective responses from interacting individuals that follow simple behavioral rules based on local information (Camazine *et al.*, 2001).

The present essay illustrates how self-organized insect societies adjust their collective response and track the complexity and the diversity of the environment while showing some parsimony of decision rules at the individual level. The following related questions will be addressed in the context of ants' foraging. How many different patterns can be produced with the same behavioral rules? How do ant societies cope with the complexity of their environment? Is decision making based on assessments of multiple parameters or of only a few relevant criteria? Can the environment generate some of the diversity in collective foraging patterns, without behavioral change by the individuals?

---

* To whom correspondence should be addressed. E-mail: cdetrain@ulb.ac.be

This paper was originally presented at a workshop titled *The Limits to Self-Organization in Biological Systems*. The workshop, which was held at the J. Erik Jonsson Center of the National Academy of Sciences, Woods Hole, Massachusetts, from 11–13 May 2001, was sponsored by the Center for Advanced Studies in the Space Life Sciences at the Marine Biological Laboratory, and funded by the National Aeronautics and Space Administration under Cooperative Agreement NCC 2-896.

Diversity of Foraging Patterns and Parsimony of Recruitment Decision Rules

Ant societies exhibit a high diversity of foraging patterns that allow them to exploit resources efficiently, meet internal needs, and face environmental constraints. Ant scouts are widely recognized as the primary agents that determine the foraging choices of the whole colony since they decide whether or not to lay a trail, and they modulate the intensity of their recruiting behavior according to food characteristics (for a review see Hölldobler and Wilson, 1990; Traniello and Robson, 1995; Detrain *et al.*, 1999). Though essential for understanding the link between individual and collective behaviors, decision-making processes related to information transfer have scarcely been investigated through specifically designed research protocols (see Roces, 2002). Two studies on foraging, for prey or liquid food sources, illustrate how the same decision rule, when operating under different conditions, can give rise to different foraging patterns in ant societies.

The first study (Detrain and Deneubourg, 1997) was carried out on the dimorphic ant *Pheidole pallidula*, characterized by two morphologically distinct castes of workers (minor and major). Members of this species scavenge on various sizes of insect prey and exhibit different foraging patterns ranging from an individual retrieval of small prey to a mass exploitation of large prey by a well-defined foraging trail. We demonstrated that the resistance of prey to traction, and its associated retrievability, governs the decision of the forager to recruit nestmates. Indeed, by simply preventing ants from moving a small prey away (*e.g.*, fruit flies pinned down on the substrate or placed under a net), one can artificially increase the recruitment trail intensity to a value similar to that observed for a large prey item (*e.g.*, a cockroach). This simple decision rule based on prey retrievability generates all the major scavenging patterns of the ant species, as shown by the following algorithm (Fig. 1). Success in prey carrying stimulates the forager to move on and lay only a weak trail on its way back to the nest; this results in the individual exploitation of small prey. When these small food items are numerous and aggregated, weak but frequent reinforcements of the trail lead to a slow and progressive monopolization of the source. Failure to retrieve the prey item is followed by an intense trail-laying that mobilizes additional foragers to the discovery site. Recruited ants can then either retrieve the prey collectively or, if still unsuccessful, dissect it on the spot and suck the hemolymph. Majors, which show a higher response threshold to recruitment stimuli, are mobilized only to large prey items when the trail is strongly reinforced and highly concentrated. The powerful mandibles of those large-headed foragers then facilitate the cutting of the prey. In sum, the same decision rule generates several foraging strategies that differ in their level of cooperation between workers and leads to the emergence of the scavenging strategy best suited to the circumstances.

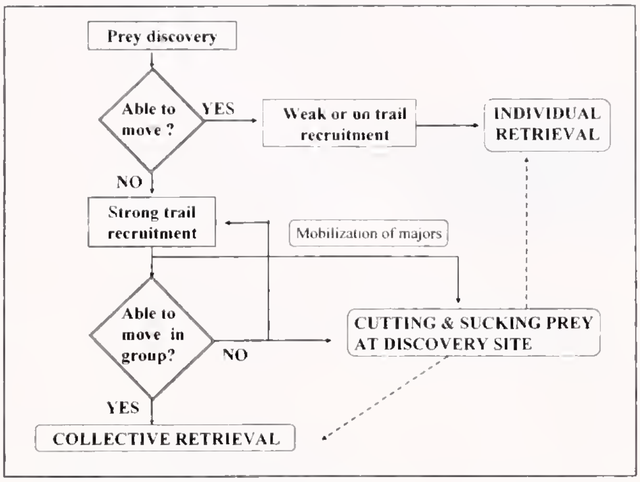

Figure 1. Algorithm and decision-making process followed by the ants during prey scavenging. Redrawn from Detrain and Deneubourg, 1997.

In the second study (Mailleux *et al.*, 2000), the foraging strategies of ants exploiting sugary liquid sources such as aphid honeydew were investigated by comparing the behavior of *Lasius niger* scouts at sucrose droplets of different volumes. When the food volume delivered exceeds the capacity of a worker ant's crop, nearly all scouts (90%) lay a recruitment trail. When a smaller droplet is offered, several scouts return to the nest without laying a trail. The percentage of trail-layers decreases with the droplet size, but the number of chemical marks emitted by each trail-laying ant does not change. The key criterion the scout uses to start laying a recruitment trail is her ability to ingest a desired volume, independently of the time spent drinking. This volume is not a fixed value shared by all scouts but varies from one ant to another. Desired volumes act as thresholds that are normally distributed (see also Page *et al.*, 1998; Beshers and Fewell, 2001). The "ability to ingest a desired volume" rule accounts for the collective regulation of foraging to the amount of food available, as shown by the following algorithm (Fig. 2). If the ant is able to ingest its desired volume, it lays a trail and recruits nestmates. If it cannot obtain its desired volume due to small droplet size, food depletion, or crowding at the food site, it searches for additional droplets in the foraging area. If unsuccessful, it goes back to the nest without laying a trail. This "desired volume" decision rule allows the colony to adjust the number of tending ants to the honeydew production of aphid colonies. Hence, information about the droplet size is not represented at the individual level but rather at a group level, through the fraction of trail-layers among returning ants.

These two studies of ant foraging reveal that, in the absence of centralized control, collective problem-solving

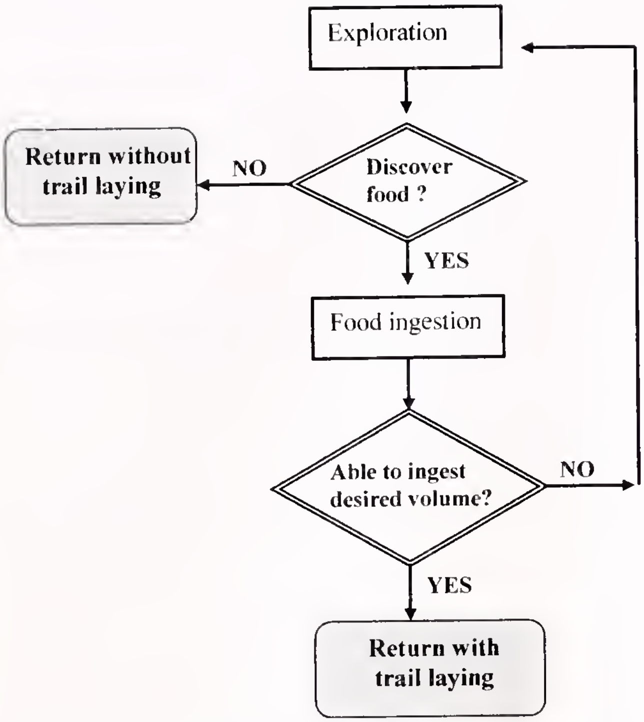
Exploration
Discover food ?
NO
Return without trail laying
YES
Food ingestion
Able to ingest desired volume?
NO
YES
Return with trail laying

Figure 2. Algorithm and decision-making processes followed by the ants when exploiting liquid food sources. Drawn from results of Mailleux *et al.*, 2000.

and foraging strategies can emerge through simple rules for information transfer between individuals. Moreover, in multiple-source situations, the same behavioral rule can produce different group-level patterns of exploitation: these range from a scattering of foragers over all food items to a focus on one or a few food sources (Nicolis and Deneubourg, 1999).

The Concept of Intelligent Decision Criteria

One way for insect societies to cope with the complexity of their environment is the use of intelligent decision criteria at the individual level. Intelligent decision criteria do not require the ant to make some complex and precise assessment of all environmental parameters; instead, they rely on cues that automatically integrate several variables (inside or outside the nest). Since potential cues vary in their value as indicators, one might expect that, through evolution, only very good cues—those with a high, reliable, and functional informative content—have been retained as decision criteria. In other words, the "intelligence" of a decision criterion results not simply from the use of cues that intrinsically catch a part of the environmental complexity, but also from the selection of the best cue—that is, the one most pertinent for the activity of the ants. Both recruitment strategies described in the previous section are based on such intelligent decision criteria.

As regards scavenging, prey retrievability is a seemingly crude estimator of prey size. Nevertheless, it is a highly functional decision criterion because it integrates information not only about the size, the shape, and the weight of the prey, but also about environmental factors that alter its retrievability. Such factors would include the surface roughness and slope of the soil and the density of the vegetation (Fig. 3A). This decision criterion is also a means for each forager to assess the current force of cooperating carriers and the possible need to recruit additional helpers.

The "desired volume" criterion plays an essential role in the regulation of foraging and in the adjustment of the number of recruiting ants to the productivity profile of aphid colonies (Mailleux, 2001). Monte Carlo simulations based on this simple behavioral rule also predict the existence of an optimum number of foragers that maximizes trail recruitment for a given honeydew production (Fig. 4, see caption

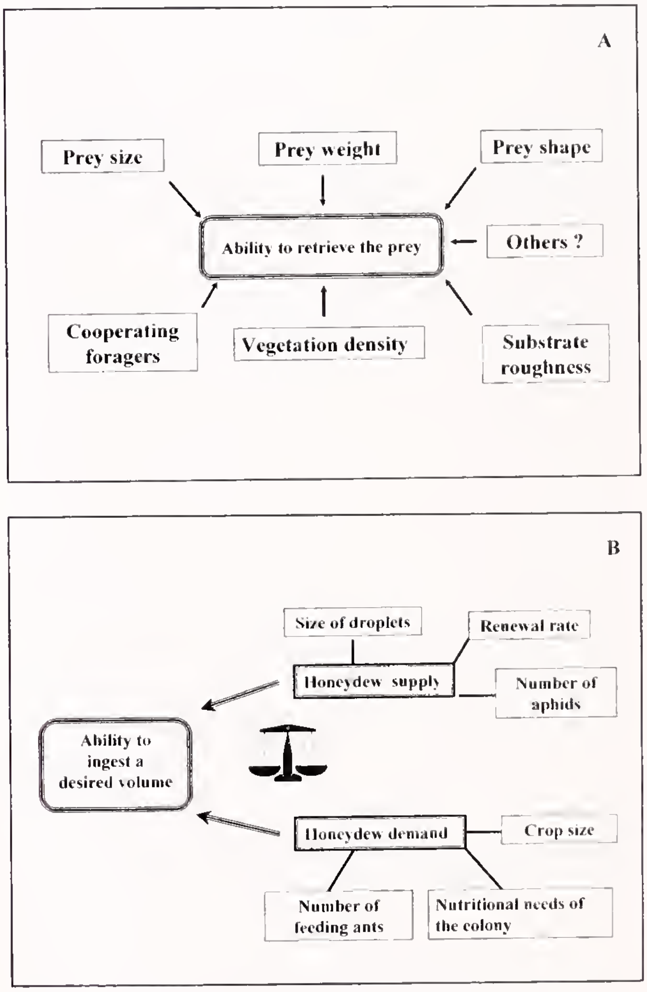
A
Prey size
Prey weight
Prey shape
Ability to retrieve the prey
Others ?
Cooperating foragers
Vegetation density
Substrate roughness
B
Size of droplets
Renewal rate
Honeydew supply
Number of aphids
Ability to ingest a desired volume
Honeydew demand
Crop size
Number of feeding ants
Nutritional needs of the colony

Figure 3. Examples of intelligent decision criteria used by ants to recruit. Such decision criteria automatically integrate multiple parameters from the environment and the colony in the case of prey scavenging (A) and honeydew exploitation (B).

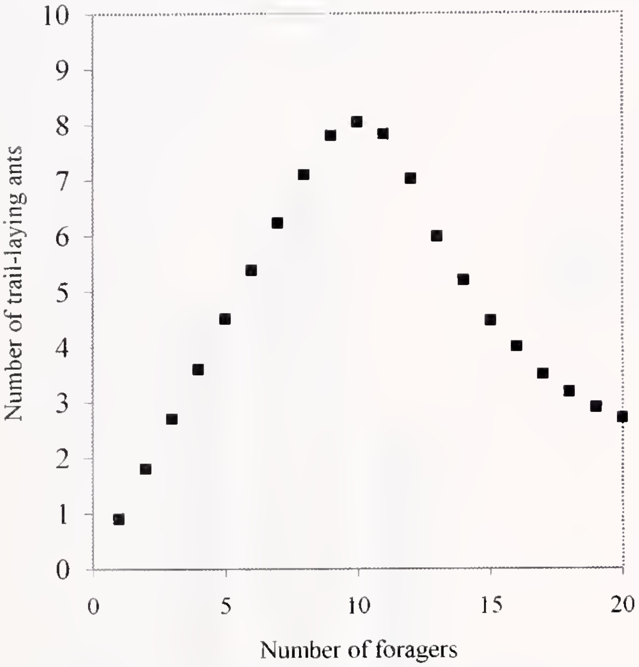

Figure 4. Regulation of the number of trail-laying ants as a function of the number of foragers attending aphids. The curve was drawn for a total production of 10 μl honeydew by 400 aphids, each emitting 0.025 μl of droplet. Results from 2000 Monte Carlo simulations. After Mailleux, 2001. The model assumes that an ant ingests, per second, a volume $\Delta V = 10^{-2}$ μl. The probability that an ant will stop ingesting food and leave a source follows a stimulus-response function described in Mailleux *et al.*, 2000. When one source is exhausted, some ants have to leave it even though they have not reached their desired volume. The probabilities for those "unsatisfied" ants (1) to discover an additional source per unit time is equal to 1/20 s^{-1} and (2) to leave the foraging area without laying a trail per unit time is equal to 1/85 s^{-1}. Satisfied ants that succeed in ingesting their desired volume lay the same amount of trail pheromone whatever the number of visited sources or the ingested volume.

for details about the model). This can be explained by the decrease in the probability of trail-laying when foragers no longer succeed in ingesting their desired volumes due to temporary depletion of or overcrowding at the food sources. Functionally, it means that the global trail intensity increases with the foraging force as long as the supply of honeydew exceeds the demand of the foragers. Conversely, when the demand of the foragers exceeds the supply of honeydew, fewer workers will lay a trail. Hence, the "desired volume" is another intelligent decision rule that takes into account the balance between supply and demand (Fig. 3B). This simple decision criterion indirectly assesses several environmental factors related to honeydew production, such as the number of aphids and the size or renewal rate of emitted droplets. It also implicitly integrates characteristics of the ant colony, such as its nutritive needs, the number of feeding ants, and the ant species' body size and its related crop load.

The existence of intelligent decision criteria that functionally integrate multiple parameters should be generic for all insect societies. Concerning honeybees, Seeley (1995) emphasizes the importance of cues that incidentally convey reliable information within the hive. One of these cues that influence recruiting behavior is the time spent by a returning forager searching in the hive for a nestmate willing to receive her load of nectar or water (Lindauer, 1971; Seeley, 1989). Similarly, in social wasps, the queuing delay that a forager experiences waiting to be unloaded by a builder conveys information on the colony's need for the materials (pulp or water) (Jeanne, 1999). These temporal cues are highly informative by-products of the colony's collection (supply) and consumption (demand) of resources. It is highly probable that intelligent decision criteria have been selected preferentially among cues, like time-based ones, that intrinsically alter the dynamics of a group response based on amplification processes. (For the impact of time delays on collective patterns in ants, see Goss *et al.*, 1989; Detrain *et al.*, 1999.) Through evolution, the reliance of recruitment modulation on such time parameters might have enhanced their already existing effect on the dynamics and hence on the efficiency of the colony response.

That intelligent decision criteria should also occur outside the context of foraging is suggested by studies in ants on nest emigration (Mallon and Franks, 2000), brood rearing (Cassill and Tschinkel, 1999), nest excavation (Rasse and Deneubourg, 2001), and colony fights (Lumsden and Hölldobler, 1983). As proposed by Seeley (1995) concerning the use of cues in honeybee foraging, information transfer based on intelligent decision criteria may evolve more readily than that involving numerous signals coding for each parameter. Indeed, this communication process involves the tuning of only one or a few adaptive decision rules based on preexisting stimuli.

Contribution of the Environment to the Emergence of Self-Organized Patterns

Environmental factors, such as the distribution and abundance of food resources (see Bernstein 1975; Rissing and Wheeler, 1976; Hölldobler, 1976; Hahn and Maschwitz, 1985), the presence of competitors (see Hölldobler, 1976; Acosta *et al.*, 1995), and the existence of predators (see Nonacs and Dill, 1988), act upon the collective patterns of ant colonies. One can question whether these collective patterns arise through changes in the behavior of the ants or as the direct result of the environment's properties. Evidence of direct contributions of the environment comes from the diversity of foraging patterns that emerge even though individual ants behave similarly. Franks *et al.* (1991) demonstrate how the distribution and abundance of food acts upon the recruitment dynamics of army ants and contributes to the emergence of species-specific raiding patterns. Colonies of *Eciton hamatum* have a dendritic raiding

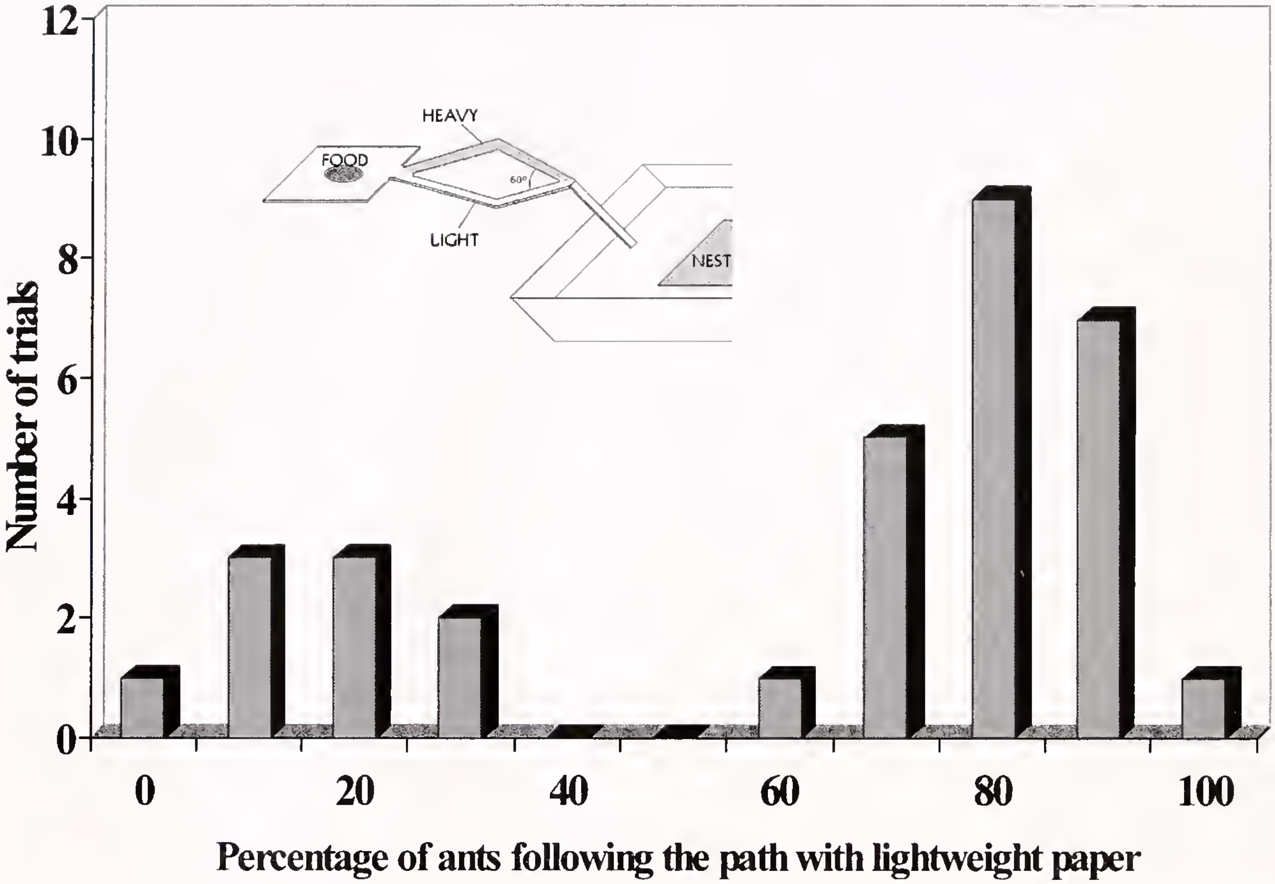

Figure 5. Influence of the substrate on collective choice of a foraging path. The number of trials ($n = 32$) is given as a function of path selection expressed as the percentage of all of the ants traversing the bridge that chose the lightweight paper (x-axis). After Detrain *et al.*, 2001, Fig. 1. © Springer-Verlag. Used with permission.

pattern and attack wasp nests that are rare but large packets of prey. Conversely, colonies of *E. burchelli* have large cohesive raids and prey mainly on common solitary arthropods. One can elicit the splitting of an *E. burchelli* raid into sub-swarms (close to the *E. hamatum* pattern) simply by manipulating the distribution of its prey, gathering them into a few discrete, dense packets. Theoretical studies and empirical knowledge also strongly suggest that an adaptive plasticity and diversity of responses can arise from the same behavioral rule applied in different environments (for a review, see Camazine *et al.*, 2001). Hence, different foraging patterns can arise independently of any modulation of trail recruitment since they can be simple by-products of the biotic environment.

Even the abiotic environment can directly contribute to an ant colony's decision making. Traditionally, the impact of the abiotic environment on foraging patterns has been linked to changes in the behavior of individual ants, as in the case of ambient temperature (Traniello *et al.*, 1984; Marsh, 1985), which influences the activity level, running speed, and searching behavior of individual workers. Here we cast new light on abiotic factors such as the substrate, which can determine the collective choices of ant colonies without altering or acting as a constraint to behavior at the individual level (Detrain *et al.*, 2001). A nest of *Lasius niger* is given access to a foraging area and a food source *via* a diamond-shaped bridge, the two branches of which are identical except for the weight of the paper covering their surface. Though paper is an artificial substrate, it allows us to investigate the impact of a chosen abiotic factor on the ants' foraging decisions. After the discovery of the food source, the path covered with the light-weight paper is followed by more than half of foragers in the majority of the trials (72%, $n = 32$, Fig. 5). Surprisingly, this collective preference for one foraging path cannot be linked to any substrate-related change in the individual behaviors of scouting or recruiting ants. Scouts make a similar number of U-turns and walk at the same speed on both paths. Furthermore, after food discovery, similar percentages of ants are engaged in trail-laying and emit the same average numbers of chemical marks whatever the substrate of their foraging path. Clear-cut choices of a foraging path appear to be driven by the substrate itself independently of any behavioral changes at the individual level. Evidently, physicochemical differences between the two papers alter the accessibility of the trail pheromone to foragers and hence the dynamics of information transfer by chemical trails. Monte Carlo simulations confirm that these differences underlie the ants' collective choices. Note that collective choices are not unanimous (in about 28% of the trials, the heavy substrate was chosen): these "unexpected" choices are signatures of a self-organized process in which "errors" or less likely decisions of the first foragers are amplified by positive feedbacks such as trail recruitment. Hence, the abiotic environment can directly contribute to collective decision-making by determining, through its physicochemical properties, the dynamics of information transfer by chemical trails. This is likely to apply to other information-laden signals such as vibrations produced by stridulating ants, where the recruitment range might depend on the resonance properties of the substrate (Baroni-Urbani *et al.*, 1988). Similarly, for nest construction, the air stream could shape the structures built by termites (regularly spaced pillars or walls) independently of any individual change in building behavior (Bonabeau *et al.*, 1998). Even in vertebrates, some studies suggest that the environment could determine the spatial patterns of animals without altering their individual behavior (see Gérard *et al.*, 2002). Hence, the role of the environment should be reconsidered not simply as a constraint but as a part of the decision-making process, as a shaping agent of collective patterns.

Conclusion

How animals acquire and integrate multiple and complex information from their environment deserves closer analysis. Among social insects, the individual has limited cognitive abilities, assesses only local environmental parameters, and cannot compare its experience to that of all its nestmates. Such limitations of the individual contrast with the diversity of collective responses that efficiently track environmental opportunities and challenges. Self-organization allows insect societies to fill the gap between these two levels of complexity. Global behaviors are generated through competing amplification processes and limiting factors in which individuals follow a few simple decision rules. Rules based on intelligent decision criteria have been selected, since these enable individuals to automatically integrate multiple sources of information that are relevant to a behavioral strategy. The concept of intelligent decision criteria should be more widely investigated for many activities, not only in group-living animals but also in solitary ones, with the aim of understanding how animals cope with the complexity of their world. In the future, new intelligent criteria could be identified mainly among those parameters such as energy or time that are now seen essentially as optimization criteria (see Roces, 2002). This essay also stresses the direct contribution of the environment to problem-solving. By altering the dynamics of information transfer, some environmental parameters can be responsible, together with simple decision rules, for the emergence of adaptive collective behaviors in self-organized systems as different as insect societies and vertebrate groups.

Acknowledgments

We thank T. Seeley and two anonymous referees for their highly constructive comments to improve the manuscript. We gratefully acknowledge C. Devigne, A. Hérédia, A. C. Mailleux, C. Natan, S. Portha, and G. Sempo for valuable discussion of some of the ideas contained herein. C. Detrain and J. L. Deneubourg are research associates of the Belgian National Foundation for Scientific Research. This work was financially supported by grant number 2.4510.01 for Belgian Joint Basic Research.

Literature Cited

Acosta, F. J., F. L. Lopez, and J. M. Serrano. 1995. Dispersed versus central-place foraging: intra- and intercolonial competition in the strategy of trunk trail arrangement of a harvester ant. *Am. Nat.* **145:** 389–411.

Baroni-Urbani, C., M. W. Buser, and E. Schillinger. 1988. Substrate vibration during recruitment in ant social organization. *Insectes Soc.* **35:** 241–250.

Bernstein, R. 1975. Foraging strategies of ants in response to variable food density. *Ecology* **56:** 213–219.

Beshers, S. N., and J. H. Fewell. 2001. Models of division of labor in social insects. *Annu. Rev. Entomol.* **46:** 413–440.

Bonabeau, E., G. Theraulaz, J. L. Deneubourg, N. R. Franks, O. Rafelsberger, J. L. Joly, and S. Blanco. 1998. A model for the emergence of pillars, walls and royal chambre in termite nests. *Philos. Trans. R. Soc. Lond. B* **353:** 1561–1576.

Camazine, S., J. L. Deneubourg, N. R. Franks, J. Sneyd, E. Bonabeau, and G. Theraulaz. 2001. *Self-organization in Biological Systems.* Princeton University Press, Princeton.

Cassill, D. L., and W. R. Tschinkel. 1999. Information flow during social feeding in ant societies. Pp. 69–82 in *Information Processing in Social Insects*, C. Detrain, J. L. Deneubourg, and J. M. Pasteels, eds. Birkhauser Verlag, Basel.

Detrain, C., and J. L. Deneubourg. 1997. Scavenging by *Pheidole pallidula*: a key for understanding decision-making systems in ants. *Anim. Behav.* **53:** 537–547.

Detrain, C., J. L. Deneubourg, and J. M. Pasteels. 1999. Decision-making in foraging by social insects. Pp. 331–354 in *Information Processing in Social Insects*, C. Detrain, J. L. Deneubourg, and J. M. Pasteels, eds. Birkhauser Verlag, Basel.

Detrain, C., C. Natan, and J. L. Deneubourg. 2001. The influence of the physical environment on the self-organised foraging patterns of ants. *Naturwissenschaften* **88:** 171–174.

Franks, N., N. Gomez, S. Goss, and J. L. Deneubourg. 1991. The blind leading the blind in army ant raid patterns: testing a model of self-organization. *J. Insect Behav.* **4:** 583–607.

Gérard, J.-F., E. Bideau, M.-L. Maublanc, P. Loisel, and C. Marchal. 2002. The herd size in large herbivores: encoded in the individual or emergent? *Biol. Bull.* **202:** 275–282.

Giraldeau L. A., and T. Caraco. 2000. *Social Foraging Theory.* Princeton University Press, Princeton.

Goss, S., S. Aron, J. L. Deneubourg, and J. M. Pasteels. 1989. Self-organized short-cuts in the Argentine ant. *Naturwissenschaften* **76:** 579–581.

Hahn, M., and U. Maschwitz. 1985. Foraging strategies and recruitment behaviour in the European harvester ant *Messor rufitarsis. Oecologia* **68:** 45–51.

Hölldobler, B. 1976. Recruitment behavior, home range orientation and territoriality in harvester ants, *Pogonomyrmex. Behav. Ecol. Sociobiol.* **1:** 3–44.

Hölldobler, B., and E. O. Wilson. 1990. *The Ants.* Springer Verlag, Berlin.

Jeanne, R. L. 1999. Group size, productivity and information flow in social wasps. Pp. 3–30 in *Information Processing in Social Insects,* C. Detrain, J. L. Deneubourg, and J. M. Pasteels, eds. Birkhauser Verlag, Basel.

Krebs, J. R., and N. B. Davies. 1991. *Behavioural Ecology: An Evolutionary Approach.* Blackwell Scientific Publications, Oxford, UK.

Lindauer, M. 1971. *Communication Among Social Bees.* Harvard University Press Cambridge, MA.

Lumsden, C. J., and B. Hölldobler. 1983. Ritualized combat and intercolony communication in ants *J. Theor. Biol.* **100:** 81–98.

Mailleux, A. C. 2001. Les règles de comportement à l'origine des stratégies alimentaires chez *Lasius niger.* Ph.D. thesis, Université Libre de Bruxelles.

Mailleux, A. C., J. L. Deneubourg, and C. Detrain. 2000. How do ants assess food volume? *Anim. Behav.* **59:** 1061–1069.

Mallon, E. B., and N. R. Franks. 2000. Ants estimate area using Buffon's needle. *Proc. R. Soc. Lond. B.* **267:** 765–770.

Marsh, A. C. 1985. Microclimatic factors influencing foraging patterns and success of the thermophilic desert ant, *Ocymyrmex barbiger. Insectes Soc.* **32:** 286–296.

Nicolis, S., and J. L. Deneubourg. 1999. Emerging patterns and food recruitment in ants: an analytical study. *J. Theor. Biol.* **198:** 575–592.

Nonacs, P., and L. M. Dill. 1988. Foraging response of the ant *Lasius pallitarsis* to food sources with associated mortality risk. *Insects Soc.* **35:** 293–303.

Oster, G. F., and E. O. Wilson. 1978. *Caste and Ecology in Social Insects.* Princeton University Press, Princeton.

Page, R. E., J. Erber, and M. K. Fondrk. 1998. Effect of genotype on response thresholds to sucrose and foraging behavior of honey bees (*Apis mellifera* L.). *J. Comp. Physiol. A* **182:** 489–500.

Rasse P., and J. L. Deneubourg. 2001. Dynamics of nest excavation and nest size regulation of *Lasius niger. J. Insect Behav.* **14:** 433–449.

Rissing, S. W., and J. Wheeler. 1976. Foraging responses of *Veromessor pergandei* to changes in seed production. *Pan Pac. Entomol.* **52:** 63–72.

Roces, F. 2002. Individual complexity and self-organization in foraging by leaf-cutting ants. *Biol. Bull.* **202:** 306–313.

Schmid-Hempel, P., A. Kacelnik, and A. Houston. 1985. Honeybees maximize efficiency by not filling their crop. *Behav. Ecol. Sociobiol.* **17:** 61–66.

Seeley, T. 1989. Social foraging in honeybees: how nectar's foragers assess their colony nutritional status. *Behav. Ecol. Sociobiol.* **24:** 181–199.

Seeley, T. 1995. *The Wisdom of the Hive.* Harvard University Press, Cambridge, MA.

Traniello, J. F., and S. K. Robson. 1995. Trail and territorial communication in social insects. Pp. 241–246 in *The Chemical Ecology of Insects* vol. 2, W. J. Bell and R. Cardé, eds. Chapman and Hall, London.

Traniello, J. F., M. S. Fujita, and R. V. Bowen. 1984. Ant foraging behavior: ambient temperature affects prey selection. *Behav. Ecol. Sociobiol.* **15:** 65–68.

Reference: *Biol. Bull.* **202:** 275–282. (June 2002)

Herd Size in Large Herbivores: Encoded in the Individual or Emergent?

JEAN-FRANÇOIS GERARD[1,*], ERIC BIDEAU[1], MARIE-LINE MAUBLANC[1], PATRICE LOISEL[2], AND CAROLE MARCHAL[1]

[1]*Institut de Recherche sur les Grands Mammifères, INRA, BP 27, 31326 Castanet Tolosan Cedex, France; and* [2]*Laboratoire d'Analyse des Systèmes et Biométrie, INRA, 2 Place Viala, 34060 Montpellier Cedex 1, France*

Abstract. In large mammalian herbivores, the increase of group size with habitat openness was first assumed to be an adaptive response, encoded in the individual. However, it could, alternatively, be an emergent property: if groups were nonpermanent units, often fusing and splitting up, then any increase of the distance at which animals perceive one another could increase the rate of group fusion and thus mean group size. Dynamical models and empirical data support this second hypothesis. This is not to say that adaptive modifications of mean herd size cannot occur. However, this changes the way in which we can envisage the history of gregariousness in large herbivores during the Tertiary.

Introduction

Large mammalian herbivores, such as ruminants or kangaroos, make up groups that are easily recognizable in the field: they consist of individuals located a short distance from one another and most often engaged in a common activity, for example, feeding, traveling, or resting. The size of these groups is very variable and has been a matter of study for ethologists and ecologists for about 40 years.

Two general trends were early identified. First, within a species, group size tends to increase with population density (Spinage, 1969; Johnson, 1983; Wirtz and Lörscher, 1983; Table 1). Second, herd size increases with habitat openness: whereas groups are small in forested habitats, they are much larger in grassland and other open landscapes. This second trend was initially reported in African antelope taken as a whole, considering the typical habitat and herd size of each species (Estes, 1974; Jarman, 1974). It was then recorded within species using habitats of varying openness (Leuthold, 1970: Evans, 1979; LaGory, 1986; Hillman, 1987; Table 2; Fig. 1).

These two general trends were rapidly explained in two diverging ways. As early as 1964, Caughley hypothesized that groups of large herbivores were nonpermanent units that often fused and split up. On this basis, the author suggested that any increase in population density should increase the rate of group meeting, and thus the average group size. This purely mechanistic proposal is equivalent to saying that group size is an emergent property, resulting from multiple fusion and fragmentation events, and that it is sensitive to variations of population density.

In contrast to Caughley's proposal, the variation of group size with habitat openness was assumed to be a biological adaptation, encoded in the individual. A central argument, developed by Estes (1974) and Jarman (1974), was that in closed habitat, a herbivore can easily reduce the probability of being detected by predators by being discreet and, especially, by living in small groups. By contrast, in open habitat, it is more difficult to escape notice. Being surrounded by many conspecifics should then ensure the best protection against predators because, in the event of an attack, there is a high probability that the victim will be another group member ("selfish avoidance of predators by aggregation"; Hamilton, 1971). As a consequence, natural

---

* To whom correspondence should be addressed. E-mail: jfgerard@toulouse.inra.fr

This paper was originally presented at a workshop titled *The Limits to Self-Organization in Biological Systems*. The workshop, which was held at the J. Erik Jonsson Center of the National Academy of Sciences, Woods Hole, Massachusetts, from 11–13 May 2001, was sponsored by the Center for Advanced Studies in the Space Life Sciences at the Marine Biological Laboratory, and funded by the National Aeronautics and Space Administration under Cooperative Agreement NCC 2-896.

Table 1

*Variation of group size with population density in different species of large herbivores (*Macropus *spp. are kangaroos, which are marsupials; the other species are ruminants—*i.e., *eutherians)*

	Study period	Habitat	Pop. density (ind./100 ha)	Group size Mean	SD	Range	*n*	Reference
Wallaroo	Year	Pasture and woodland (2)	8	1.8	1.2	1–7	233	Taylor (1982, 1983)
Macropus robustus			55	2.2	1.7	1–>12	1610	
Grey kangaroo	Year	Open woodland (2)	10	3.1	1.6	1–9	86	Southwell (1984a)
Macropus giganteus			37	4.2	2.8	1–13	220	
			91	8.5	8.3	1–65	348	
Sika deer	January	Forest (1)	60	5.5	3.9	1–?	85	Borkowski (2000)
Cervus nippon			120	6.8	4.3	1–?	158	
Fallow deer	Winter	Forest (1)	25	4.4	3.0	1–16	297	Vincent (unpubl. data)
Dama dama			31	4.6	3.1	1–20	432	
			73	5.7	4.4	1–37	473	
Dorcas gazelle	Summer	Desert (2)	0.3	2.2	1.2	1–5	9	Lawes and Nanni (1993)
Gazella dorcas			2	3.2	2.0	1–5	18	
Pyrenean chamois	Year	Pasture and cliff (2)	5	5.0	8.4	1–77	301	Richard-Hansen *et al.* (1992 and unpubl. data)
Rupicapra pyrenaica			30	7.6	10.3	1–139	1886	
Alpine ibex	Year	Pasture and cliff (1)	1	1.8	0.7	1–?	9	Toïgo *et al.* (1996)
Capra ibex			3	2.8	2.0	1–?	117	
			7	4.5	3.7	1–?	49	

(1) A single study area supporting different population densities year to year.
(2) Different study areas supporting similar habitats but different population densities.

selection should have retained individuals preferring to be within small groups when in closed habitat, and within large groups when in open landscape.

Because they relate to the effect of two different ecological factors, these contrasting hypotheses seem to have been implicitly considered as compatible, and the opposition

Table 2

*Variation of group size with habitat openness in different species of large herbivores (*Macropus giganteus *is a kangaroo, which is a marsupial; the other species are ruminants—*i.e., *eutherians)*

	Study period	Habitat	Pop. density (ind./100 ha)	Group size Mean	SD	Range	*n*	Reference
Grey kangaroo	Winter	Closed shrubland	13	1.8	1.1	1–5	71	Southwell (1984a)
Macropus giganteus		Open woodland	12	3.5	1.7	1–9	24	
Moose	August	Forest	1.4*	1.6	?	1–6	146	Peek *et al.* (1974)
Alces alces		Alpine tundra		2.6	?	1–12	178	
White-tailed deer	Year	Forest	50*	1.9	?	1–?	197	Hirth (1977)
Odocoileus virginianus		Intermediate		2.5	?	1–?	872	
		Grassland		4.3	?	1–51	1667	
Axis deer	Year	Forest	5*	3.8	3.0	1–23	362	Barrette (1991 and pers. comm.)
Axis axis		Edge		8.3	8.2	1–100	555	
		Grassland		12.1	14.2	1–160	1889	
Fallow deer	Winter	Forest	6*	4.7	3.5	1–27	317	Schaal (1982)
Dama dama		Harvested maize field		15.8	12.7	1–55	349	
Grant's gazelle	Year	Bush	?	6.5	?	1–37	393	Walther (1972)
Gazella granti		Intermediate	?	12.5	?	1–120	125	
		Open plain	?	37.7	?	1–428	221	
Mouflon sheep	Year	Forest	?	2.1	?	1–14	?	Maisels (1993)
Ovis gmelini		Moor and woodland	?	4.4	4.1	1–61	1178	Maublanc (unpubl. data)

* Population density estimated for the whole set of habitats.

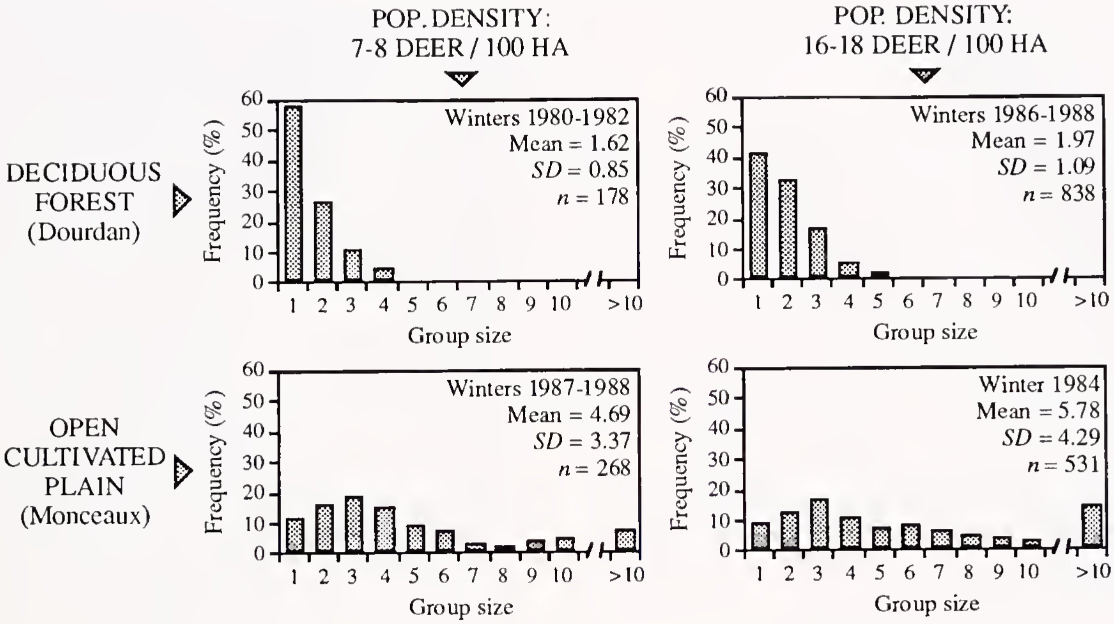

Figure 1. Relative frequencies of roe deer (*Capreolus capreolus*) group sizes recorded in winter in two study areas, and for two levels of population density supported by the two areas some years apart (n: number of groups sighted, solitary animals included; after Gerard *et al.* 1995, with permission of the *Revue d'Ecologie Terre et Vie*). Group size increases with both population density (Mann-Whitney U test: in forest, $P < 0.0001$; in open plain, $P = 0.001$) and habitat openness (at low density, $P < 0.0001$; at high density, $P < 0.0001$).

between emergence and individual encoding long passed unnoticed. Moreover, the plausibility of the two hypotheses remained unquestioned for a long time. The situation has changed owing to theoretical and empirical works carried out during the 1980s and 1990s.

Models Assuming Optimum-Size-Seeking

An important step was made when Sibly (1983) had the idea to develop and examine the properties of a dynamical model of group formation formalizing the idea that individuals exhibited preferences for group sizes shaped by natural selection.

The basic assumptions of this model are the following. First, there is a relationship between fitness and group size such that fitness is maximized for a given size (according to the rationale of Estes and Jarman, the optimal size should be small in closed habitat and large in open habitat). Second, the individuals behave as if they know which group size, in the actual environment, will give them better fitness than another: in the course of encounters, each individual leaves a group for another as soon as the size of the latter will enhance its fitness.

Although these assumptions seem to prescribe the group size that should be obtained, Sibly's model exhibits emergent properties that are rather puzzling.

1. Mean group size at equilibrium is, unexpectedly, generally larger than the optimum size. The reason for this is not very difficult to understand. Suppose that a solitary animal encounters a group of optimal size s^*. None of the group members will leave, but the solitary individual will join the group, provided being within a group of size $s^* + 1$ entails a better fitness than being alone. Groups still greater can form in the same way, provided their members keep a fitness higher than that of a solitary individual.

2. At equilibrium, no group shows a size lower than the optimum size, and the standard deviation of group sizes is always extremely limited (≤ 0.5). This is inconsistent with the group size distributions actually observed in large herbivores, where small groups are rarely lacking, even when average herd size is large, and the standard deviation of group sizes can be very great, especially when the mean is large (Table 1, Table 2, and Fig. 1).

3. Mean group size at equilibrium depends on the initial group size distribution. However, it does not depend on population density. The absence of effect of population density contrasts with the effect recorded in the populations of large herbivores.

4. Groups no longer fuse or split up once the equilibrium is reached: they become permanent units. This is inconsistent with the high lability of groups revealed in an increasing number of large herbivore species since the beginning of the 1980s (Murray, 1981; Schaal, 1982; Southwell, 1984b; Fichter, 1987; Hillman, 1987; Putman, 1988; Barrette, 1991; Estes, 1991; Le Pendu *et al.*, 1995, 2000). Further-

more, this shows that Sibly's model is incompatible with the hypothesis proposed by Caughley for the increase of group size with population density.

Sibly's model was further developed during the 1980s and 1990s, by introducing altruism towards relatives and/or the possibility for group members to limit the increase of the size of their group by repelling joiners (see Giraldeau and Caraco, 2000, for a review). Indeed, the initial model ignored kin selection. Moreover, by joining a group whose size is larger than or equal to the optimal size, an individual enhanced its fitness but lowered the fitness of the group members, so that the latter could be assumed to repel the joiner. Some of these modifications of the initial model improve the first property described above in that they lead, at equilibrium, to a mean group size that tends to be closer to the optimal size. However, they do not improve the other properties of the model. So, they remain both inconsistent with the data recorded in large herbivores and incompatible with Caughley's hypothesis.

Fusion-Fission Models

According to Caughley (1964), an increase in population density should increase the mean size of groups that frequently fuse and split up, by enhancing the rate of group encounter and thus fusion. Following the same rationale, it could be hypothesized that any increase of habitat openness, and thus of the distance at which groups can perceive one another, should increase the rate of group fusion, and thus mean group size (Gerard *et al.*, 1993). This should at least be the case, provided group fusion results from an attraction between groups. Clearly, if group fusion results from simple "collisions," then the distance at which animals can perceive one another should be without influence.

The plausibility of this hypothesis was confirmed in the mid-1990s, when Bonabeau and Dagorn (1995), Gueron and Levin (1995), and two of the authors of the present paper (Gerard and Loisel, 1995) developed new dynamical models of group formation. These models contrasted with Sibly's model in that groups were assumed to fuse and split up without any group size being preferred by the individuals. They were in fact generalizations of a previous model by Cohen (1971), in which "casual groups" were assumed to increase or decrease by a single individual (see also Okubo, 1986: pp. 45–49).

The model by Bonabeau and Dagorn (1995) is probably the simplest. First, the groups (solitary individuals included) that compose the population are assumed to move at random. Second, two groups arriving within the same portion of space systematically merge, then behave as a single group. Third, at each time step, a fraction p of the individuals leave the groups they are in by temporarily becoming solitary.

In its basic version, the model by Gueron and Levin (1995) differs from the latter in two aspects. First, two groups arriving in view of each other merge with a probability that is independent of their sizes, but not necessarily equal to 1. Second, the groups are assumed to split into two (and not only to lose single individuals) with a probability βs, where β is a constant and s, the group size. Here, β can be interpreted as the probability with which any individual adopts a trajectory differing from that of the other group members and is possibly followed by some of them. In practice, the size distribution of splitting groups is assumed to be uniform.

The assumptions of our model (Gerard and Loisel, 1995) are more complicated than those considered by Bonabeau and Dagorn, and Gueron and Levin. First, as is more or less implicit in the two latter models, each individual is assumed to be able to detect any conspecific present inside an area α, characterizing habitat openness. Second, each individual oscillates in a probabilistic way between a "social" state and an "individualistic" state. When in the social state, an animal joins every perceived conspecific, then behaves in such a way as to stay with it. By contrast, when in the individualistic state, an animal moves without taking conspecifics into account. As a consequence, groups fuse through attraction and split up. When two individuals (or groups of individuals) in the social state perceive one another, the individuals merge and form a single group. When an individual (or a group of individuals) in the social state perceives an animal in the individualistic state, it joins it. In this case, the resulting group actually includes a leader, which is the animal in the individualistic state. However, if, within a group of this kind, a second individual turns out to be individualistic, then the group includes two leaders moving independently of each other; as a consequence, the other group members distribute themselves at random (with probability 1/2) near the two leaders, and the group splits up. The probability ε of shifting from the social state to the individualistic state and the probability μ of the reverse shifting are fixed, so that the individual's behavior is independent of habitat openness, population density, and group size.

Though they rely on different assumptions, the Bonabeau and Dagorn model (1995), the Gueron and Levin model (1995), and our model exhibit remarkably similar emergent properties.

1. The first property that the three models have in common is that the group size distributions obtained at equilibrium resemble those ordinarily recorded in large herbivore populations: the group frequency exhibits a single maximum for isolated individuals or a small group size, then monotonously decreases with group size; moreover, the standard deviation of group sizes tends to be large when the mean is large.
2. Whatever the model, the group size distribution obtained at equilibrium for any given values of the parameters

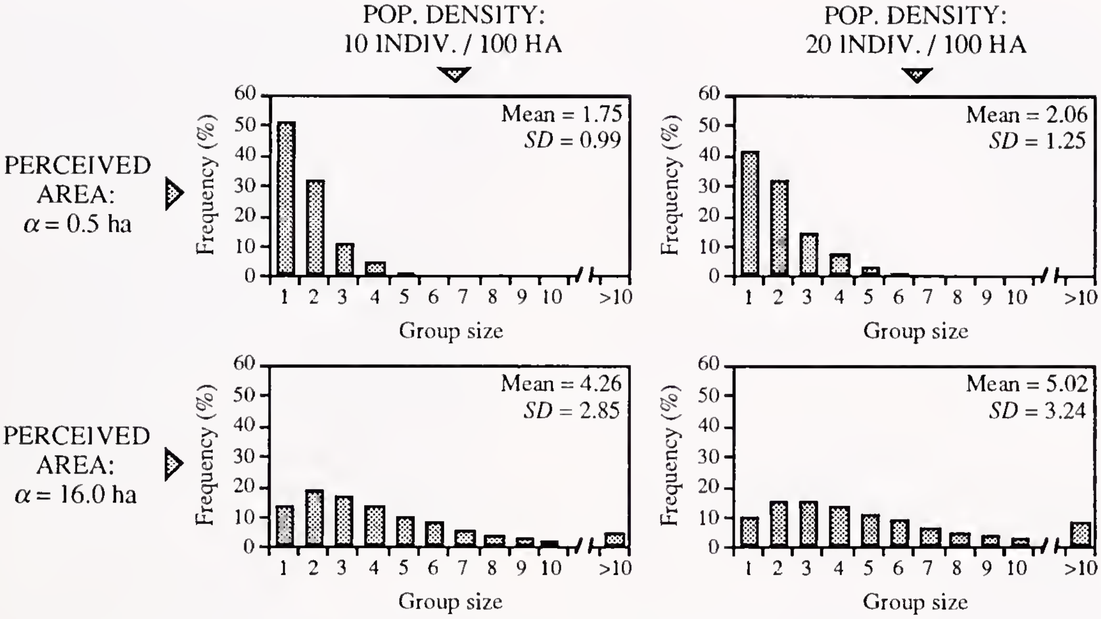

Figure 2. Relative frequencies of group sizes obtained at equilibrium with the model of Gerard and Loisel (1995), for two values of population density and two values of the area perceived by the individual (after Gerard *et al.*, 1997, with permission of Hermes editions). In every case, the probabilities of individual state shifting are $\mu = 0.9$ and $\varepsilon = 0.1$.

is independent of the initial group size distribution, provided population density is left unchanged.

3. Whatever the model and the values of its parameters, any increase of population density entails, at equilibrium, not only an increase of mean group size, as suggested by Caughley, but also an increase of group density (*i.e.*, the number of groups per unit area).

4. Whatever the model and the values of its other parameters, any increase of the distance at which groups can perceive one another increases mean group size at equilibrium (see Fig. 2 for an illustration with our model). Actually, in the three models, multiplying the area perceived by the individuals by a factor *k* has exactly the same effect on mean group size as multiplying the population density by the same factor (Gerard and Loisel, 1995; Gueron and Levin, 1995; Appendix).

Checking Assumptions and Predictions

The fusion-fission models just described thus exhibited realistic, emergent properties. In addition, they showed that the same mechanism could be both at the origin of the increase of group size with population density and of the increase of group size with habitat openness. What remained to be checked were the main basic assumptions of the models, as well as predictions that could be deduced from their emergent properties. This is what we have begun to do in a population of roe deer (*Capreolus capreolus*) living in an open cultivated plain in Northern France (Marchal, 1998; Marchal *et al.*, 1998). The data were recorded between November and April, observability being maximum at this season owing to the high proportion of plowed fields and the low height of crops in the cultivated fields (mainly winter cereal and rapeseed).

First, we checked that roe deer groups, like those of many other herbivores, were nonpermanent units. To that aim, we monitored 73 groups during 3 h or more. The proportion of these groups that had not broken up or fused with another group since the beginning of their observation decreased rapidly and regularly through time: after 2 h 38 min of observation, half had their composition altered by at least one fusion or fission event (Marchal *et al.*, 1998).

We then checked that group fusion generally involved inter-attraction, and thus perception at distance. Among the 103 fusion events observed, 3% were simple "collisions": they occurred when two groups met at a wood's corner, without having previously perceived each other (as shown by the absence of any behavior directed towards the members of the other group before the encounter, and the reactions exhibited on the encounter). In some other cases (21%), fusion followed a human disturbance. However, in 76% of the instances, fusion did result from an attraction between groups whose members indisputably perceived one another: the deer of at least one of two groups looked at the members of the other group and approached them over a distance often exceeding 100 m (Marchal *et al.*, 1998).

We also examined the causes of splitting up. Among the

Peek, J. M., R. E. LeResche, and D. R. Stevens. 1974. Dynamics of moose aggregations in Alaska, Minnesota, and Montana. *J. Mammal.* **55:** 126–137.

Putman, R. J. 1988. *The Natural History of Deer.* Christopher Helm, London.

Richard-Hansen, C., G. Gonzalez, and J.-F. Gerard. 1992. Structure sociale de l'isard (*Rupicapra pyrenaica*) dans trois sites pyrénéens. *Gibier Faune Sauvage* **9:** 137–149.

Schaal, A. 1982. Influence de l'environnement sur les composantes du groupe social chez le daim *Cervus (Dama) dama* L. *Rev. Ecol. Terre Vie* **36:** 161–174.

Sibly, R. M. 1983. Optimal group size is unstable. *Anim. Behav.* **31:** 947–948.

Southwell, C. J. 1984a. Variability in grouping in the Eastern grey kangaroo, *Macropus giganteus*. I. Group density and group size. *Aust. Wildl. Res.* **11:** 423–435.

Southwell, C. J. 1984b. Variability in grouping in the Eastern grey kangaroo, *Macropus giganteus*. II. Dynamics of group formation. *Aust. Wildl. Res.* **11:** 437–449.

Spinage, C. A. 1969. Territoriality and social organization of the Uganda defassa waterbuck *Kobus defassa ugandae*. *J. Zool. Lond.* **159:** 329–361.

Taylor, R. J. 1982. Group size in the Eastern grey kangaroo, *Macropus giganteus*, and the wallaroo, *Macropus robustus*. *Aust. Wildl. Res.* **9:** 229–237.

Taylor, R. J. 1983. Association of social classes of the wallaroo, *Macropus robustus* (Marsupialia: Macropodidae). *Aust. Wildl. Res.* **10:** 39–45.

Toïgo, C., J.-M. Gaillard, and J. Michallet. 1996. La taille des groupes: un bioindicateur de l'effectif des populations de bouquetin des Alpes (*Capra ibex ibex*)? *Mammalia* **60:** 463–472.

Walther, F. R. 1972. Social grouping in Grant's gazelle (*Gazella granti* Brooke 1827) in the Serengeti national park. *Z. Tierpsychol.* **31:** 348–403.

Wirtz, P., and J. Lörscher. 1983. Group sizes of antelopes in an East African national park. *Behaviour* **84:** 135–156.

Appendix

Mean group size at equilibrium in the model by Bonabeau and Dagorn

We here correct an error made by Bonabeau and Dagorn (1995) when deriving the mean group size from their fusion-fission model. We further show that once the correction is made, increasing the population density or the area perceived by the individuals by a multiplicative factor k has exactly the same effect on mean group size.

Analytical expression of mean group size

In the model by Bonabeau and Dagorn, space is divided into N sites, the whole population included n individuals ($n \ll N$), and the individuals simultaneously present within any given site are considered as the members of a single group. At each discrete time step, a fraction p of the n individuals of the population leave the group they are in as solitary animals, and are reinjected at random into the N sites. In addition, each group moves towards a randomly selected site, and the groups (and solitary individuals) entering the same site aggregate to form a single group.

As a consequence of these assumptions, the expected number of groups (*i.e.*, the number of sites occupied) N^+ varies between two successive time steps according to:

$$N^+(t+1) \approx N^+(t) + pn - \frac{[N^+(t) + pn][N^+(t) + pn - 1]}{2} \frac{1}{N}.$$

The denominator of the right part of the equation is N, and not N^2 as written by Bonabeau and Dagorn (1995). At equilibrium, $N^+(t+1) = N^+(t)$, so that the expected number of groups is approximately

$$N^+(t) = N^+_{\mathrm{eq}} \approx \sqrt{2Npn},$$

and the mean size of groups

$$\langle s \rangle = \frac{n}{N^+_{\mathrm{eq}}} \approx \sqrt{\frac{n}{2pN}}.$$

Mean group size therefore varies with $\sqrt{n/N}$, and not with $\sqrt{n}/N$ as found by Bonabeau and Dagorn. Furthermore, once corrected, the analytical expressions of the number and mean size of groups at equilibrium become strictly equivalent to those obtained by Gueron and Levin (1995) with their own model.

Effect of population density and habitat openness

In the model of Bonabeau and Dagorn, groups entering the same site aggregate into a single group. So, a site can be considered as an area in which any individual perceives its conspecifics. If A designates the area available to the whole population, then the area of each site is $\alpha = A/N$. It follows that the mean size of groups at equilibrium is

$$\langle s \rangle = \sqrt{\frac{\alpha d}{2p}}$$

where $d = n/A$ is the population density. It then appears that multiplying the area perceived by the individuals (α) or the population density (d) by a factor k has exactly the same effect on the mean size of groups at equilibrium. The same is true with the model by Gueron and Levin (1995) and ours (Gerard and Loisel, 1995: appendix B).

Reference: *Biol. Bull.* **202:** 283–288. (June 2002)

Self-Organization and Natural Selection in the Evolution of Complex Despotic Societies

C. K. HEMELRIJK

Department of Information Technology and Anthropological Institute and Museum, University of Zurich, Switzerland

Abstract. Differences between related species are usually explained as separate adaptations produced by individual selection. I discuss in this paper how related species, which differ in many respects, may evolve by a combination of individual selection, self-organization, and group-selection, requiring an evolutionary adaptation of only a single trait. In line with the supposed evolution of despotic species of macaques, we take as a starting point an ancestral species that is egalitarian and mildly aggressive. We suppose it to live in an environment with abundant food and we put the case that, if food becomes scarce and more clumped, natural selection at the level of the individual will favor individuals with a more intense aggression (implying, for instance, biting and fierce fighting).

Using an individual-centered model, called DomWorld, I show what happens when the intensity of aggression increases. In DomWorld, group life is represented by artificial individuals that live in a homogeneous world. Individuals are extremely simple: all they do is flock together and, upon meeting one another, they may perform dominance interactions in which the effects of winning and losing are self-reinforcing. When the intensity of aggression in the model is increased, a complex feedback between the hierarchy and spatial structure results; *via* self-organization, this feedback causes the egalitarian society to change into a despotic one. The many differences between the two types of artificial society closely correspond to those between despotic and egalitarian macaques in the real world. Given that, in the model, the organization changes as a side effect of the change of one single trait proper to an egalitarian society, in the real world a despotic society may also have arisen as a side effect of the mutation of a single trait of an egalitarian species.

If groups with different intensities of aggression evolve in this way, they will also have different gradients of hierarchy. When food is scarce, groups with the steepest hierarchy may have the best chance to survive, because at least a small number of individuals in such a group may succeed in producing offspring, whereas in egalitarian societies every individual is at risk of being insufficiently fed to reproduce. Therefore, intrademic group selection (selection within an interbreeding group) may have contributed to the evolution of despotic societies.

Introduction

The assumption that evolution occurs through a single evolutionary process is no longer tenable (*e.g.*, see Plotkin and Odling-Smee, 1981), and multiple-level selection theories have slowly become more accepted (*e.g.*, Hogeweg, 1994; Maynard Smith and Szathmary, 1995; Mitteldorf and Wilson, 2000). Multiple-level selection processes may include some, or all, of the following factors: the multi-level character of biological systems and natural selection operating on them (Lewontin, 1970; Hogeweg, 1994; Sober and Wilson, 1998), self-organization and its consequences for evolution (Boerlijst and Hogeweg, 1991), and nonlinear genotype-phenotype mappings (Kauffman, 1993; Huynen and Hogeweg, 1994; Kauffman, 1995).

Within this framework of multiple-level selection theories, I present in this paper an example of the way in which a certain type of society may evolve. In studies of animal behavior, a distinction is usually made between two types of societies—egalitarian and despotic. In her studies of birds, Vehrencamp (1983) distinguishes between these two on the

E-mail: hemelrij@ifi.unizh.ch

This paper was originally presented at a workshop titled *The Limits to Self-Organization in Biological Systems*. The workshop, which was held at the J. Erik Jonsson Center of the National Academy of Sciences, Woods Hole, Massachusetts, from 11–13 May 2001, was sponsored by the Center for Advanced Studies in the Space Life Sciences at the Marine Biological Laboratory, and funded by the National Aeronautics and Space Administration under Cooperative Agreement NCC 2–896.

Peek, J. M., R. E. LeResche, and D. R. Stevens. 1974. Dynamics of moose aggregations in Alaska, Minnesota, and Montana. *J. Mammal.* **55:** 126–137.

Putman, R. J. 1988. *The Natural History of Deer.* Christopher Helm, London.

Richard-Hansen, C., G. Gonzalez, and J.-F. Gerard. 1992. Structure sociale de l'isard (*Rupicapra pyrenaica*) dans trois sites pyrénéens. *Gibier Faune Sauvage* **9:** 137–149.

Schaal, A. 1982. Influence de l'environnement sur les composantes du groupe social chez le daim *Cervus (Dama) dama* L. *Rev. Ecol. Terre Vie* **36:** 161–174.

Sibly, R. M. 1983. Optimal group size is unstable. *Anim. Behav.* **31:** 947–948.

Southwell, C. J. 1984a. Variability in grouping in the Eastern grey kangaroo, *Macropus giganteus*. I. Group density and group size. *Aust. Wildl. Res.* **11:** 423–435.

Southwell, C. J. 1984b. Variability in grouping in the Eastern grey kangaroo, *Macropus giganteus*. II. Dynamics of group formation. *Aust. Wildl. Res.* **11:** 437–449.

Spinage, C. A. 1969. Territoriality and social organization of the Uganda defassa waterbuck *Kobus defassa ugandae*. *J. Zool. Lond.* **159:** 329–361.

Taylor, R. J. 1982. Group size in the Eastern grey kangaroo, *Macropus giganteus*, and the wallaroo, *Macropus robustus*. *Aust. Wildl. Res.* **9:** 229–237.

Taylor, R. J. 1983. Association of social classes of the wallaroo, *Macropus robustus* (Marsupialia: Macropodidae). *Aust. Wildl. Res.* **10:** 39–45.

Toïgo, C., J.-M. Gaillard, and J. Michallet. 1996. La taille des groupes: un bioindicateur de l'effectif des populations de bouquetin des Alpes (*Capra ibex ibex*)? *Mammalia* **60:** 463–472.

Walther, F. R. 1972. Social grouping in Grant's gazelle (*Gazella granti* Brooke 1827) in the Serengeti national park. *Z. Tierpsychol.* **31:** 348–403.

Wirtz, P., and J. Lörscher. 1983. Group sizes of antelopes in an East African national park. *Behaviour* **84:** 135–156.

Appendix

Mean group size at equilibrium in the model by Bonabeau and Dagorn

We here correct an error made by Bonabeau and Dagorn (1995) when deriving the mean group size from their fusion-fission model. We further show that once the correction is made, increasing the population density or the area perceived by the individuals by a multiplicative factor k has exactly the same effect on mean group size.

Analytical expression of mean group size

In the model by Bonabeau and Dagorn, space is divided into N sites, the whole population included n individuals ($n \ll N$), and the individuals simultaneously present within any given site are considered as the members of a single group. At each discrete time step, a fraction p of the n individuals of the population leave the group they are in as solitary animals, and are reinjected at random into the N sites. In addition, each group moves towards a randomly selected site, and the groups (and solitary individuals) entering the same site aggregate to form a single group.

As a consequence of these assumptions, the expected number of groups (*i.e.*, the number of sites occupied) N^+ varies between two successive time steps according to:

$$N^+(t+1) \approx N^+(t) + pn - \frac{[N^+(t) + pn][N^+(t) + pn - 1]}{2} \frac{1}{N}.$$

The denominator of the right part of the equation is N, and not N^2 as written by Bonabeau and Dagorn (1995). At equilibrium, $N^+(t+1) = N^+(t)$, so that the expected number of groups is approximately

$$N^+(t) = N^+_{\text{eq}} \approx \sqrt{2Npn},$$

and the mean size of groups

$$\langle s \rangle = \frac{n}{N^+_{\text{eq}}} \approx \sqrt{\frac{n}{2pN}}.$$

Mean group size therefore varies with $\sqrt{n/N}$, and not with $\sqrt{n}/N$ as found by Bonabeau and Dagorn. Furthermore, once corrected, the analytical expressions of the number and mean size of groups at equilibrium become strictly equivalent to those obtained by Gueron and Levin (1995) with their own model.

Effect of population density and habitat openness

In the model of Bonabeau and Dagorn, groups entering the same site aggregate into a single group. So, a site can be considered as an area in which any individual perceives its conspecifics. If A designates the area available to the whole population, then the area of each site is $\alpha = A/N$. It follows that the mean size of groups at equilibrium is

$$\langle s \rangle = \sqrt{\frac{\alpha d}{2p}}$$

where $d = n/A$ is the population density. It then appears that multiplying the area perceived by the individuals (α) or the population density (d) by a factor k has exactly the same effect on the mean size of groups at equilibrium. The same is true with the model by Gueron and Levin (1995) and ours (Gerard and Loisel, 1995: appendix B).

Reference: *Biol. Bull.* **202:** 283–288. (June 2002)

Self-Organization and Natural Selection in the Evolution of Complex Despotic Societies

C. K. HEMELRIJK

Department of Information Technology and Anthropological Institute and Museum, University of Zurich, Switzerland

Abstract. Differences between related species are usually explained as separate adaptations produced by individual selection. I discuss in this paper how related species, which differ in many respects, may evolve by a combination of individual selection, self-organization, and group-selection, requiring an evolutionary adaptation of only a single trait. In line with the supposed evolution of despotic species of macaques, we take as a starting point an ancestral species that is egalitarian and mildly aggressive. We suppose it to live in an environment with abundant food and we put the case that, if food becomes scarce and more clumped, natural selection at the level of the individual will favor individuals with a more intense aggression (implying, for instance, biting and fierce fighting).

Using an individual-centered model, called DomWorld, I show what happens when the intensity of aggression increases. In DomWorld, group life is represented by artificial individuals that live in a homogeneous world. Individuals are extremely simple: all they do is flock together and, upon meeting one another, they may perform dominance interactions in which the effects of winning and losing are self-reinforcing. When the intensity of aggression in the model is increased, a complex feedback between the hierarchy and spatial structure results; *via* self-organization, this feedback causes the egalitarian society to change into a despotic one. The many differences between the two types of artificial society closely correspond to those between despotic and egalitarian macaques in the real world. Given that, in the model, the organization changes as a side effect of the change of one single trait proper to an egalitarian society, in the real world a despotic society may also have arisen as a side effect of the mutation of a single trait of an egalitarian species.

If groups with different intensities of aggression evolve in this way, they will also have different gradients of hierarchy. When food is scarce, groups with the steepest hierarchy may have the best chance to survive, because at least a small number of individuals in such a group may succeed in producing offspring, whereas in egalitarian societies every individual is at risk of being insufficiently fed to reproduce. Therefore, intrademic group selection (selection within an interbreeding group) may have contributed to the evolution of despotic societies.

Introduction

The assumption that evolution occurs through a single evolutionary process is no longer tenable (*e.g.*, see Plotkin and Odling-Smee, 1981), and multiple-level selection theories have slowly become more accepted (*e.g.*, Hogeweg, 1994; Maynard Smith and Szathmary, 1995; Mitteldorf and Wilson, 2000). Multiple-level selection processes may include some, or all, of the following factors: the multi-level character of biological systems and natural selection operating on them (Lewontin, 1970; Hogeweg, 1994; Sober and Wilson, 1998), self-organization and its consequences for evolution (Boerlijst and Hogeweg, 1991), and nonlinear genotype-phenotype mappings (Kauffman, 1993; Huynen and Hogeweg, 1994; Kauffman, 1995).

Within this framework of multiple-level selection theories, I present in this paper an example of the way in which a certain type of society may evolve. In studies of animal behavior, a distinction is usually made between two types of societies—egalitarian and despotic. In her studies of birds, Vehrencamp (1983) distinguishes between these two on the

E-mail: hemetrij@ifi.unizh.ch

This paper was originally presented at a workshop titled *The Limits to Self-Organization in Biological Systems*. The workshop, which was held at the J. Erik Jonsson Center of the National Academy of Sciences, Woods Hole, Massachusetts, from 11–13 May 2001, was sponsored by the Center for Advanced Studies in the Space Life Sciences at the Marine Biological Laboratory, and funded by the National Aeronautics and Space Administration under Cooperative Agreement NCC 2-896.

basis of reproductive success. In egalitarian societies, the reproductive success of all female group members is more or less the same, whereas in despotic ones there is a great variation in the reproductive success of individual females. When the terms egalitarian and despotic are used for other taxa, such as primates, these terms denote their so-called dominance style rather than their reproductive success (Hand, 1986). Dominance style depends on the gradient of the hierarchy (van Schaik, 1989): despotism signifies that the dominance hierarchy is steep (which means that there is a great difference in the success in fighting between individuals); egalitarianism implies that the hierarchy is weakly developed. Furthermore, in primates, particularly of the genus macaques, these societies differ in a number of other characteristics: in despotic societies aggression is more unidirectional, social behavior is correlated more strongly with dominance, grouping is less cohesive (de Waal and Luttrell, 1989; Thierry, 1990), mate choice is more selective, and male migration is more frequent (Caldecott, 1986). Whereas each of these differences between related species is usually explained as a separate adaptation shaped by individual selection, I propose to show in this paper how a despotic species may evolve from an egalitarian one by a combination of individual selection, self-organization, and group-selection, involving an evolutionary adaptation in one single trait only.

How individual selection and self-organization may operate, I will explain with the help of an individual-centered model of a group-living species, called "DomWorld" (Hemelrijk, 1999a,b, 2000). How group selection may favor the survival of groups with the steepest hierarchy above groups with weaker gradients of the hierarchy, I will explain with the help of an ecological model at an evolutionary time-scale designed by Ulbrich *et al.* (1996).

The Model DomWorld (Dominance World)

A summary of DomWorld may suffice (for a more complete description, see Hemelrijk (1999b, 2000)). The model is based on only a small number of essentials of social life. It represents a homogeneous virtual world inhabited by agents that are provided with only two tendencies: to group (right half of Fig. 1) and to perform dominance interactions (left part of Fig. 1). Why agents actually do group (whether this is to avoid predators or because resources are clumped) is not specified and irrelevant to the model. The same holds for dominance interactions. They reflect competition for resources (such as food and mates), but these resources are not specified.

When an individual is activated and it does not see another agent close by (within its personal space, see PersSpace in Fig. 1), then grouping rules come into effect. It starts looking for others at greater and greater distances (Near View = 24 and Max View = 50 units). If even then no one else is in sight, it turns over a SearchAngle (Fig. 1) in order to rejoin its group. In this way individuals tend to remain in a group.

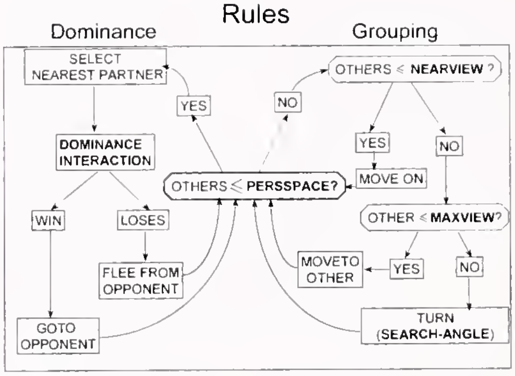

Figure 1. Flow chart for the behavioral rules of agents.

If, however, an agent sees another agent close by, within its personal space (PersSpace = 2 or 4), a dominance interaction takes place. The likelihood that an agent initiates an aggressive interaction increases with its chance to defeat its opponent (Hemelrijk, 2000). The agent's capacity to be victorious (reflected in its dominance value) depends on chance, on its current dominance value (which initially is the same for all individuals), and on the self-reinforcing effect of the outcome (winning a fight increases the probability of winning the next one and losing decreases it). This is known as the "winner and loser" effect and has been empirically established in many animal species (*e.g.*, see Chase, 1985). After victory, the dominance value of the victorious agent increases and that of its defeated opponent is reduced by the same amount. When, unexpectedly, an agent defeats a higher ranking opponent, the dominance values of both opponents are changed by a greater amount than when an agent conquers, as expected, a lower ranking opponent (this result conforms to detailed behavioral studies on bumblebees by Honk and Hogeweg, 1981). In this way the model allows for rank reversals. After a fight, the winner chases the opponent, and the defeated agent flees.

Groups usually consist of 8 to 10 individuals. The behavior of the agents is analyzed by means of behavioral units and statistical methods similar to those used for observing real animals.

Natural Selection and Self-Organization

Group life of primates (including macaques) is generally supposed to have evolved as a protection against predators (van Schaik and van Hooff, 1983; van Schaik, 1989). Egalitarian primate societies, at least those of macaques, are thought to precede despotic ones evolutionarily (Matsumura, 1999; Thierry *et al.*, 2000). Correspondingly, let us suppose that a group-living egalitarian species lives in an environment in which food is abundant, and therefore its competition is low and its aggression mild (consisting of, for instance, threats and

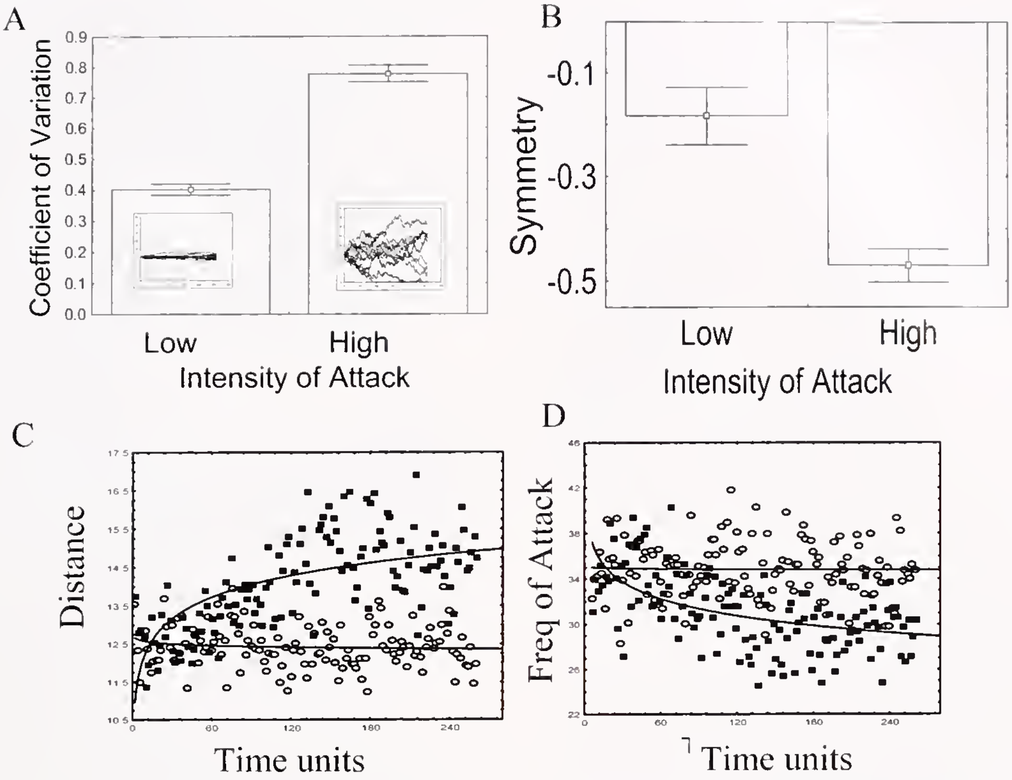

Figure 2. Effects of different intensities of aggression. (A) Gradient of the hierarchy as measured by the coefficient of variation of dominance values. (B) Symmetry of aggression measured as a τ_{Kr}-correlation between an actor- and receiver-matrix of aggression. (C) Average distance among all individuals over time. (D) Average frequency of aggression over time. Open circles: low intensity of aggression, closed boxes: high intensity of aggression.

slapping). Now suppose that some populations of this species are forced to invade an environment with resources that are more clumped and where food is scarce: what do we expect to happen? Natural selection then favors individuals gifted with more intense aggression (manifesting itself, for example, by biting), because they are more able to get hold of the food. In the course of evolutionary time, a population with higher intensity of aggression may thus evolve. What are the consequences of such increasing intensity of aggression if applied to a model that simply reflects grouping and competition, such as DomWorld (Hemelrijk, 1999b)? First, at a high intensity of aggression, the hierarchy is steep (as measured by the high value of the coefficient of variation of the dominance values, see Fig. 2A), because each interaction is fiercer and therefore has a greater impact. Simultaneously, we see that aggression is less symmetrical (Fig. 2B): the correlation between aggression directed against and received from certain partners measured by a τ_{Kr}-correlation between the actor- and receiver-matrix of aggression (see Hemelrijk, 1990a, b) is more negative. Symmetry of aggression decreases, because, if the hierarchy is steep, it is a greater risk for low-ranking individuals to attack higher ranking agents (and less risky the other way around). Perhaps unexpectedly, the average distance among individuals is larger, because groups spread out over time more at a high intensity of aggression than at a low one (Fig. 2C and (1) in Fig. 3) due to the increasing steepness of the hierarchy, which turns some individuals into permanent losers that flee from everyone else. As a consequence, the encounter frequency diminishes and thus aggression declines (Fig. 2D and (2) in Fig. 3). (This decrease of aggression is also observed in real

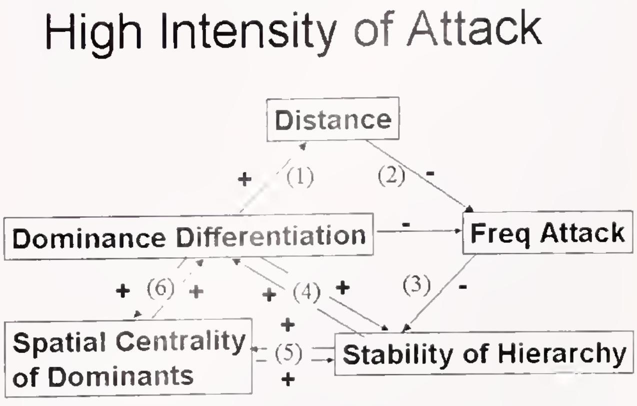

Figure 3. Summary of spatial-social structuring among artificial individuals (for explanation see text).

animals when unfamiliar individuals are put in a group together, but the decline of aggression has so far never been attributed to a widening of the group.) A consequence of the decline of aggression is that the hierarchy becomes more stable ((3) in Fig. 3). Further, because low-ranking individuals flee from everyone else, they end up at the periphery of the group; this automatically leaves the dominants in the center ((5) in Fig. 3). This spatial structure develops in spite of a total lack of any preference of the individuals to be in the center. Yet such a preference (a so-called centripetal instinct) is assumed in the "selfish herd" theory by Hamilton (1971). It is supposed to have been evolved because individuals are better protected in the center, where they are shielded on all sides from possible predators. However, the model shows that even without such a centripetal instinct, whenever the hierarchy is steep, we must expect a spatial structure with dominants in the center.

Spatial centrality, in turn, stabilizes the hierarchy and supports its differentiation ((5) and (6) in Fig. 3). This arises because the spatial structure causes individuals to be close to partners of similar dominance rank; therefore, if incidentally a dominance-reversal occurs, it is usually between individuals that are similar in dominance, and thus the extent to which dominance values are changed is only a minor one. In this way, the spatial structure strengthens the hierarchy ((5) and (6) in Fig. 3). This becomes evident when we eliminate spatial centrality. We can do this by decreasing the SearchAngle. If the SearchAngle for returning to the group is made smaller, so that individuals return more slowly and the group therefore spreads out more and more, no spatial structure develops. In this case (for the same number of dominance interactions), the hierarchy becomes weaker (*i.e.*, dominance values differentiate less) than in cohesive groups (Hemelrijk, 1999a). The steeper hierarchy in cohesive groups is thus partly due to a feedback reinforcement of the hierarchical development under the influence of spatial structure.

We may also include the sexes in the model; for instance, by making two classes of individuals that differ in initial dominance value and intensity of aggression (both are made higher for "males" than for "females"). Unexpectedly, it turns out that at a high intensity of aggression, female dominance over males is greater than at a low one. This arises because a stronger differentiation of the hierarchy causes some females to reach high dominance and some males to become very low in rank. Consequently, some females become dominant over some males. This is of interest, because in comparative studies between egalitarian macaques (with mild aggression) and despotic ones (with fierce aggression), Thierry (1990) notes that despotic adult females remain dominant over fast-growing adolescents longer than females in egalitarian species do (which is in accordance with DomWorld). He attributes this to a stronger coalitionary tendency among kin-related individuals in despotic species than in egalitarian ones. DomWorld, however, shows that greater female dominance may also arise as a direct consequence of a steeper hierarchy. Further, at a high intensity of aggression the lowest ranking males in the model are of a lower rank than they are at a low intensity. It is known that in real primates, the lowest males migrate to other groups; supposing migration were possible in the model, we would surely expect a higher frequency of migration for a higher intensity of aggression. This indeed is exactly what Caldecott (1986) describes for real macaques, where migration is higher among despotic than among egalitarian species.

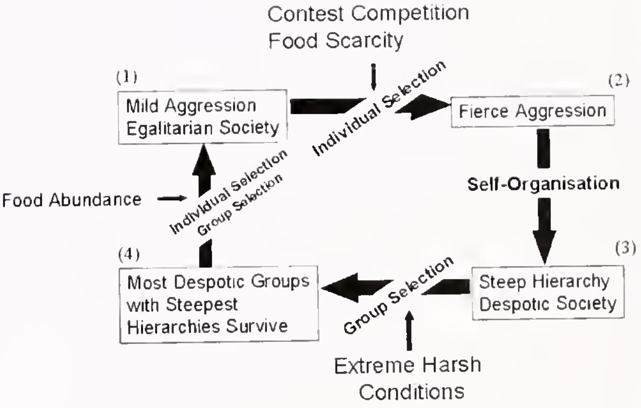

Figure 4. Sketch of the evolution of a despotic society. (1) Food is abundant, aggression is mild, society is egalitarian. (2) Food is scarce: aggression has become intense *via* individual selection. (3) Grouping and fierce aggression have led to a steep dominance hierarchy *via* self-organization due to social-spatial structuring. (4) Food availability has decreased even further and only the most despotic societies survive.

In general, it appears that all differences between egalitarian and despotic societies in DomWorld resemble those found between real groups of egalitarian and despotic macaques as far as they have actually been measured. Since, in the model, such differences (those regarding cohesion, bidirectionality of aggression, and correlations of behavior with dominance, see Hemelrijk, 1999b) arise from a change in one trait only (intensity of aggression), we may take it that also in the real world a single mutation (in the form of an increase of intensity of aggression due to food shortage) may have caused an egalitarian ancestor to beget a fledgling species that is in many characteristics despotic. Thus individual selection on intensity of aggression may lead, *via* self-organization, to a switch from an egalitarian to a despotic society (Fig. 4).

Group Selection

Suppose that in this way groups have evolved with high intensity of aggression, and suppose there is a certain variation among groups in their average intensity of aggression and therefore in the gradient of their hierarchy. Then, what do we expect to happen if environmental conditions worsen even more? In that case group selection may further increase despotism in a way similar to that shown in a model study of social spiders by Ulbrich *et al.* (1996). Their individual-based model represents, among other things, colony survival, reproductive behavior, the kind of competition for food ("contest" or "scramble" competition), and feeding behavior. If food is clumped, it leads to contest competition, whereby dominants get more than subordinates; if it is scattered and unpredictable, everyone gets about the same (so-called scramble competition, see Nicholson, 1967). Results show that during levels of food scarcity, colonies where there is contest competition survive longer than colonies in which competition is of the scrambling type. This is a consequence of the steeper dominance hierarchy and, therefore, greater variety in body-size of members, which allows a small number of dominant individuals to eat all the food so that at least some of the females are sufficiently nourished to reach reproductive age. In this way, because some individuals in more intensely despotic groups are likely to survive and reproduce, the group itself may survive (although the number of its members decreases during periods of diminished food availability). In contrast, in groups with a weaker hierarchy, food will be distributed more evenly and no single individual may reach reproductive success (see also Rypstra, 1993). Thus, severe shortage of food in clumped patches may result in group selection in favor of the most despotic societies ((3) to (4) in Fig. 4).

Note that in macaques, adult males usually migrate from their natal group to other groups. Therefore, the degree of despotism in macaques is defined on the basis of the dominance hierarchy among the females. Also, the survival and extinction of "the group" implies the core group of females only, because they are the resident sex. Among such female resident core-groups, we may expect that when food is scarce, group selection will lead to better survival of those groups that have a steeper hierarchy (in accordance with the findings in social spiders).

Discussion

Changing only one trait—intensity of aggression—in the model leads to a great number of phenotypic differences at the level of the individual and of the group. Thus, by changing the intensity of aggression in DomWorld, as suggested by the hypothesis for egalitarian and despotic macaques (McKenna, 1979; Thierry, 1985a, b, 1990), we may switch from an egalitarian society to a despotic one. Intensity of aggression is not the only variable, however, that can produce such a cascade of effects. If we increase cohesion under one and the same level of intensity of aggression (which must lie somewhere between medium and high values), the society becomes more despotic in all its characteristics (Hemelrijk, 1999a). The question of whether stronger cohesion of groups is also accompanied by greater despotism in real primates must be studied empirically.

Thus, the model shows how self-organization causes nonlinearity in the connection between the behavioral rules and the observed behavior (which respectively correspond to the genotype and the phenotype). These results of DomWorld may also be relevant to results of a selection experiment with fish by Ruzzante and Doyle (1991, 1993). After two generations of selection for speed of growth, an increase in growth speed among fish fed on clumped food (leading to intense competition) was accompanied by three effects: a decrease in aggressiveness, an increase in density of schooling, and an increase in social tolerance. According to the authors, selection for fast growth results in a high threshold for aggression, and this threshold also genetically influences the other two features of social behavior—cohesion and social tolerance. These findings resemble those from DomWorld; but in DomWorld only the intensity of aggression is changed "genetically," and all other changes of social behavior are mere side effects. Such parsimonious explanations may be relevant to many species of despotic animals that have been studied and possibly even to plants, where a kind of despotism is also described (for a study on a hemiparasite, see Prati *et al.*, 1997).

Groups with different degrees of intensity of aggression may be liable to group selection similar to that suggested for spiders by Ulbrich *et al.* (1996). Group selection has always been a controversial issue. The only studies in which any evidence has been produced (Bradley, 1999) concern invertebrates (namely, a species of virus, social spider, and ant). However, designating group selection as a useful explanation for behavior of (nonhuman) primates is usually avoided (Bradley, 1999). Yet, primates utter alarm calls that, though they are at the expense of the fitness of the individual that uses them, may serve to protect group members (both kin and non-kin). When alarm-calls are more beneficial for the group than they are costly for the individual, they will evolve by group selection, as explained by differential selection among groups for the same trait—so-called intrademic group selection (Wilson, 2001). Computer models show how such an intrademic group selection favors altruistic traits, particularly under harsh conditions (Mitteldorf and Wilson, 2000; Pepper and Smuts, 2000).

Similarly, I suggest that group selection may operate on a non-altruistic trait, namely intensity of aggression, in primate societies in which there is sharp contest competition for food (during harsh conditions). Such stronger competition leads to a more asymmetrical distribution of food intake, and by guaranteeing that at least some individuals of a group reproduce, aids group survival (of the core group of the resident sex).

Note that in the other transition, from despotic societies to egalitarian ones (see Fig. 4), progressively milder aggression would be favored by selection on the level of the individual and the group, because less energy is wasted on conflicts. In this case, selection at the level of the group and the individual will be weak, and self-organization will not be operative. Thus, a different number of processes are at work depending on the direction of the transition between egalitarian and despotic societies.

The different ways in which selection may act (namely, on self-organized patterns, and on the level of the individual and the group) illustrate how we may envision a multiple-level selection theory for the creation of a despotic society. Although, for the sake of clarity in the sketch I have given above, I have made individual selection, self-organization, and group selection function one after the other, in reality they operate mostly simultaneously in different proportions (Lewontin, 1970).

Acknowledgments

I thank Rolf Pfeifer and Bob Martin for continuous support. I am grateful to Scott Camazine for inviting me to the workshop on "The Limits to Self-organization in Biological Systems," and to Bernard Schmidt and Jens Krause for making me aware of similarities between DomWorld and plant and fish communities. This work is partly supported by a grant from the A. H. Schultz foundation.

Literature Cited

Boerlijst, M. C., and P. Hogeweg. 1991. Self-structuring and selection: spiral waves as a substrate for evolution. Pp. 255–276 in *Artificial Life II*, C. G. Langton, C. Taylor, J. D. Farmer, and S. Rasmussen, eds. Addison-Wesley, Redwood City, CA.

Bradley, B. J. 1999. Levels of selection, altruism and primate behavior. *Q. Rev. Biol.* **74:** 171–194.

Caldecott, J. O. 1986. Mating patterns, societies and ecogeography of macaques. *Anim. Behav.* **34:** 208–220.

Chase, I. D. 1985. The sequential analysis of aggressive acts during hierarchy formation: an application of the 'jigsaw' puzzle approach. *Anim. Behav.* **33:** 86–100.

de Waal, F. B. M., and L. M. Luttrell. 1989. Towards a comparative socioecology of the genus *Macaca*: different dominance styles in rhesus and stumptail monkeys. *Am. J. Primatol.* **19:** 83–109.

Hamilton, W. D. 1971. Geometry for the selfish herd. *J. Theor. Biol.* **31:** 295–311.

Hand, J. L. 1986. Resolution of social conflicts: dominance, egalitarianism, spheres of dominance, and game theory. *Q. Rev. Biol.* **61:** 201–220.

Hemelrijk, C. K. 1990a. A matrix partial correlation test used in investigations of reciprocity and other social interaction patterns at a group level. *J. Theor. Biol.* **143:** 405–420.

Hemelrijk, C. K. 1990b. Models of, and tests for, reciprocity, unidirectional and other social interaction patterns at a group level. *Anim. Behav.* **39:** 1013–1029.

Hemelrijk, C. K. 1999a. Effects of cohesiveness on intersexual dominance relationships and spatial structure among group-living virtual entities. Pp. 524–534 in *Advances in Artificial Life. Fifth European Conference on Artificial Life*, Vol. 1674, D. Floreano, J-D. Nicoud, and F. Mondada, eds. Springer Verlag, Berlin.

Hemelrijk, C. K. 1999b. An individual-oriented model on the emergence of despotic and egalitarian societies. *Proc. R. Soc. Lond. B* **266:** 361–369.

Hemelrijk, C. K. 2000. Towards the integration of social dominance and spatial structure. *Anim. Behav.* **59:** 1035–1048.

Hogeweg, P. 1994. Multi-level evolution: replicators and the evolution of diversity. *Physica D* **75:** 275–291.

Honk, C. v., and P. Hogeweg. 1981. The ontogeny of the social structure in a captive *Bombus terrestris* colony. *Behav. Ecol. Sociobiol.* **9:** 111–119.

Huynen, M. A., and P. Hogeweg. 1994. Pattern generation in molecular evolution: exploitation of the variation in RNA landscapes. *J. Mol. Evol.* **39:** 71–79.

Kauffman, S. 1995. *At Home in the Universe. The Search for Laws of Complexity.* Penguin Group, London.

Kauffman, S. A. 1993. *The Origins of Order: Self-organisation and Selection in Evolution.* Oxford University Press, New York.

Lewontin, R. C. 1970. The units of selection. *Annu. Rev. Ecol. Syst.* **1:** 1–18.

Matsumura, S. 1999. The evolution of 'Egalitarian' and 'Despotic' social systems among macaques. *Primates* **40:** 23–31.

Maynard Smith, J., and E. Szathmary. 1995. *The Major Transitions in Evolution.* W. H. Freeman, New York.

McKenna, J. J. 1979. The evolution of allomothering behavior among Colobine monkeys: function and opportunism in evolution. *Am. Anthropol.* **81:** 818–840.

Mitteldorf, J. and D. S. Wilson. 2000. Population viscosity and the evolution of altruism. *J. Theor. Biol.* **204:** 481–496.

Nicholson, A. J. 1967. Self-adjustment of populations to change. *Cold Spring Harbor Symp. Quant. Biol.* **22:** 153–173.

Pepper, J. W., and B. B. Smuts. 2000. The evolution of cooperation in an ecological context: an agent-based model. Pp. 45–76 in *Dynamics in Human and Primate Societies: Agent-based Modeling of Social and Spatial Processes*, T. Kohler and G. Gumerman, eds. Oxford University Press, New York.

Plotkin, H. C., and F. J. Odling-Smee. 1981. A multiple-level model of evolution and its implications for sociobiology. *Behav. Brain Sci.* **4:** 225–268.

Prati, D., D. Matthies, and B. Schmid. 1997. Reciprocal parasitization in *Rhinanthus serotinus*: a model system of physiological integration in clonal plants. *Oikos* **78:** 221–229.

Ruzzante, D. E., and R. W. Doyle. 1991. Rapid behavioral changes in medaka caused by selection for competitive and noncompetitive growth. *Evolution* **45:** 1936–1946.

Ruzzante, D. E., and R. W. Doyle. 1993. Evolution of social behaviour in a resource rich, structured environment: selection experiments with medaka. *Evolution* **47:** 456–470.

Rypstra, A. L. 1993. Prey size, social competition, and the development of reproductive division of labor in social spider groups. *Am. Nat.* **142:** 868–880.

Sober, E., and D. S. Wilson. 1998. *Unto Others.* Harvard University Press, Cambridge.

Thierry, B. 1985a. Patterns of agonistic interactions in three species of macaque (*Macaca mulatta, M. fascicularis, M. tonkeana*). *Aggress. Behav.* **11:** 223–233.

Thierry, B. 1985b. Social development in three species of macaque (*Macaca mulatta, M. fascicularis, M. tonkeana*). *Behav. Process* **11:** 89–95.

Thierry, B. 1990. Feedback loop between kinship and dominance: the macaque model. *J. Theor. Biol.* **145:** 511–521.

Thierry, B., A. N. Iwaniuk, and S. M. Pellis. 2000. The influence of phylogeny on the social behaviour of macaques (Primates: Cercopithecidae, genus *Macaca*). *Ethology* **106:** 713–728.

Ulbrich, K., J. R. Henschel, F. Jeltsch, and C. Wissel. 1996. Modelling individual variability in a social spider colony (*Stegodyphus dumicola*: Eresidae) in relation to food abundance and its allocation. Proc. 13th Int. Congr. Arachnol., Geneva, 3–8 Sept. 1995. *Rev. Suisse Zool.* vol. hors serie: 661–670.

van Schaik, C. P. 1989. The ecology of social relationships amongst female primates. Pp. 195–218 in *Comparative Socioecology, the Behavioural Ecology of Humans and Other Mammals*, V. Standen and G. R. A. Foley, eds. Blackwell, Oxford.

van Schaik, C. P., and J. A. R. A. M. van Hooff. 1983. On the ultimate causes of primate social systems. *Behaviour* **85:** 91–117.

Vehrencamp, S. L. 1983. A model for the evolution of despotic versus egalitarian societies. *Anim. Behav.* **31:** 667–682.

Wilson, D. S. 2001. Cooperation and altruism. Pp. 222–231 in *Evolutionary Ecology: Concepts and Case Studies*, C. W. Fox, D. A. Roff, and D. J. Fairbairn, eds. Oxford University Press, Oxford.

Reference: *Biol. Bull.* **202:** 289–295. (June 2002)

Scaling in Nests of a Social Wasp: A Property of the Social Group

ROBERT L. JEANNE* AND ANDREW M. BOUWMA

Department of Entomology, University of Wisconsin, 1630 Linden Drive, Madison, Wisconsin 53706

Abstract. The numbers of brood cells in nests built by founding swarms of the Neotropical social wasp *Polybia occidentalis* closely correlate with the numbers of wasps in the swarms. We analyzed nests of different sizes to determine how they scale with respect to the allocation of brood cells among combs. Three patterns were evident: compared to smaller nests, larger nests have (1) more combs and (2) larger combs; and (3) among nests containing the same number of combs, the last two combs diverge in relative size as nest size increases. Taken together, these results suggest that members of a swarm somehow "know" the size of the swarm they are in. This information feeds back to individual builders, which quantitatively modulate their responses to stigmergic cues in ways that result in the nest-size-scaled allocation of brood cells among combs. The patterns also suggest that swarms fine-tune the final size of their nests by making corrections as they build.

Introduction

The process of nest construction by a social wasp colony does not differ fundamentally from nest construction by a solitary wasp. In each case individuals construct the nest by executing a series of discrete innate building acts. Each act adds to the nest one new load of material, oriented in response to cues intrinsic and extrinsic to the nest. As far as we know, in no social insect species do individual workers specialize only in certain kinds of building activity over their lifetimes. That is, every individual in the colony possesses the full repertory of acts required to build the nest. Thus, even the most complex nests of colonial species could, in principle, be constructed by a solitary individual working alone, given enough time. To the extent that this is true of the social wasps, it argues that the broad, species-typical form of the nest does not depend on properties of the group or on processes such as self-organization, but is simply the result of the additive contributions of individual actions by individual actors. In this view, the construction process is directed by a mechanism in which builders respond to stimuli arising from the structure of the nest. Interactions among builders are only indirect, mediated by the structure they are cooperating to build, a mechanism referred to as stigmergy (Grassé, 1959; Theraulaz and Bonabeau, 1995; Camazine *et al.*, 2001).

But are there any patterns in the nest of a social species that are under the more direct influence of the social group? Here we provide evidence that the answer is yes. We show for a swarm-founding social wasp, *Polybia occidentalis* (Olivier), that nests of different sizes scale in ways that point to a quantitative modulation of the building rules in response to feedback about the size of the swarm.

Nest Construction in *Polybia*

Polybia occidentalis is a Neotropical wasp whose nesting behavior has been described in some detail (Forsyth, 1978; Jeanne, 1986, 1996). Colony-founding swarms comprise a small number of queens and a large number of workers. As a swarm arrives at the nest site it has chosen, a few workers immediately begin constructing the first downward-oriented, hexagonal cells. These are attached directly to the substrate, typically a twig. As more cells are added radially, the developing comb takes on a discoid form, extending freely from both sides of the twig. As the comb grows, there is space for increasing numbers of workers to become

---

* To whom correspondence should be addressed. E-mail: jeanne@entomology.wisc.edu

This paper was originally presented at a workshop titled *The Limits to Self-Organization in Biological Systems*. The workshop, which was held at the J. Erik Jonsson Center of the National Academy of Sciences, Woods Hole, Massachusetts, from 11–13 May 2001, was sponsored by the Center for Advanced Studies in the Space Life Sciences at the Marine Biological Laboratory, and funded by the National Aeronautics and Space Administration under Cooperative Agreement NCC 2-896.

engaged in building. Meanwhile, the queens begin laying eggs in the cells.

When the first comb reaches a certain size, the builders' behavior makes a qualitative shift (*qualitative stigmergy*; Camazine *et al.*, 2001). Instead of adding more cells to the edges of the comb, workers begin extending the outer walls of the peripheral cells downward and outward to initiate the envelope, starting at the back and sides of the comb. As this sheet grows, it is warped toward the center to form a domelike covering about 2 cm below the comb (Fig. 1A). The envelope is not completely closed, however; a 1-cm opening is left in the front to provide an entrance to the comb. Then in the reverse qualitative shift, the second comb is immediately begun, the walls of its cells being drawn downward from the lower surface of the envelope just completed. This comb is expanded from the center (bottom) of the supporting envelope outward toward its margins (Fig. 1B). A new envelope is constructed over it in the same manner as the first. Then the next comb is begun in the same way. The alternation between construction of combs and envelopes continues until the nest is large enough to house the adult wasps of the swarm and the brood they will rear. The entire construction process typically takes a week to 10 days. The nest remains at this size for many weeks or months; thereafter, enlargement occurs episodically (Wenzel, 1993; AMB, unpubl. data).

Thus the nests of *P. occidentalis* are modular, each module consisting of a comb and its envelope. Swarms work in complete modules: each comb + envelope module is constructed to its final size before the next one is begun, and it is rare for a founding swarm, once it starts a new comb, to leave it half-finished or uncovered (RLJ and AMB, pers. obs.).

P. occidentalis swarms vary widely in size, yet each is able to construct its nest with a number of cells that correlates closely with the number of wasps in the founding group (Forsyth, 1978; Jeanne and Nordheim, 1996). A similar pattern is seen among founding groups of *Polistes* (Wenzel, 1996). The size of the nest built by the swarm may well optimize the trade-off of opposing costs such that colony output is maximized. On the one hand, if the swarm builds too few cells, it will not have the space to house the brood it is capable of rearing, and the subsequent rate of colony growth will be limited. On the other hand, if the nest is much larger than required to house the brood population, forager mortality may be high due to the extra foraging demands for nest material, leaving too few workers to rear the brood efficiently (O'Donnell and Jeanne, 1992).

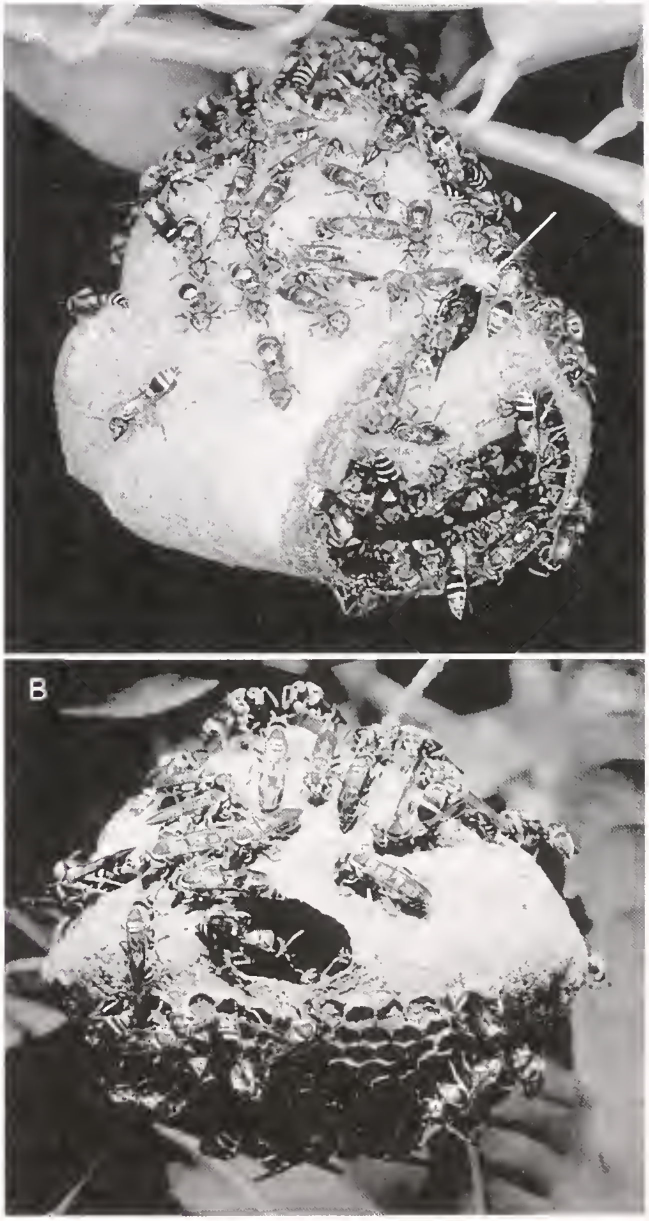

Figure 1. Nests of *Polybia occidentalis* under construction. (A) Envelope construction. The envelope covering comb 3, whose cells are visible inside, is nearing completion. The rim of dark material is recently added carton, still wet. As more material is added to the envelope edge, the opening will be constricted to form the new entrance to the nest, just below the current entrance (line). The greatest width of the nest is about 6.5 cm. (B) Comb construction, frontal view. The nest entrance, center, opens into the space between comb 2 and its envelope, which forms the bottom of the nest. Comb 3, its cells exposed on the lower surface of the envelope covering comb 2, is expanding outward with the addition of new cells. When the cells reach the angled edge of the envelope, their outer walls will be extended downward and outward to initiate envelope 3, beginning at the back of the nest. Note the campanulate shape of the nest. The greatest width of the nest is about 5 cm.

The form the nest takes is a function of two sets of decision processes engaged in by individual builders in the colony. One is the decision by a worker as to what kind of building act to engage in. *P. occidentalis* workers perform three primary kinds of building acts: brood-cell-wall construction, envelope construction, and surface thickening for reinforcement of the upper nest walls (Jeanne, 1986). The second set of processes has to do with the orientation of the material being added to the nest during a particular kind of

Table 1

Descriptive statistics for the Polybia occidentalis *colonies used in the study*

Component	Mean	Median	SD	Range	*n*
Adults	476	355	399	24–1,802	80
Nest cells	1,360	1,050	1,154	109–7,152	85
Nest combs	3.9	4	1.2	2–8	85

All colonies were initiated by absconding swarms. Data were collected after 25 days of pre-emergence-stage development.

building act. The most important orienting cues are stigmergic, that is, come from the nest itself (Grassé, 1959; Camazine *et al.*, 2001), and it is the innate response to these that determines the species-typical nest form. Gravity is an important external orienting cue.

We investigated the influence of group size on workers' responses to the stigmergic orienting cues that determine the allocation of cells among combs. We did this indirectly by measuring nests built by different sizes of swarms in Guanacaste, Costa Rica. (For details about the site and methods, see Jeanne and Nordheim [1996] and Bouwma *et al.* [2000].) Combs were numbered sequentially from the top of the nest, in order of construction. We define the size of the i^{th} comb in terms of the number of brood cells, C_i, it contained, and the size of the nest in terms of the total number of brood cells, C_t, in all combs.

The 85 nests used in the study covered a 65-fold range in size, while the number of combs per nest, m, ranged from 2 to 8 (Table 1). For the analyses of patterns in scaling, nests of 2–5 combs were used ($n = 78$); the sample size of nests of 6–8 combs was too small to analyze ($n = 7$). Three patterns were evident in the scaling of nests. We describe these in order of their salience.

Larger nests have more combs

Not surprisingly, larger nests contained more combs than did smaller ones, although there was considerable overlap in size between nests of m and $m + 1$ combs (Fig. 2). The distribution of the number of combs, m, in the nest as a function of nest size, C_t, fits a power function with the equation

$$m = 0.335C_t^{0.351}.$$

This relationship implies that each new comb was larger than the preceding one. This is seen more clearly in a plot of the number of cells in each successive comb (Fig. 3). The data fit the first-order linear regression equation

$$C_i = -156.6 + 192.4i,$$

where i is the ordinal number of the i^{th} comb in the nest. Thus, each new comb, i, had on average 192 more cells than the preceding one, $i - 1$. Because the number of cells in a comb is proportional to the comb's area, while the comb's diameter increases as the square root of its area, the constant absolute increase in cell number from comb to comb gives the nest a campanulate shape (Fig. 1B).

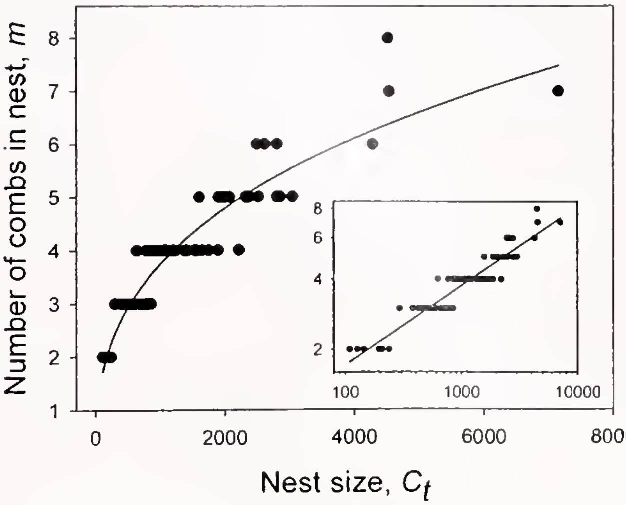

Figure 2. Number of combs in swarm-constructed nests of *Polybia occidentalis* as a function of the total number of cells in the nest. The fitted regression is the power function, $m = 0.335C_t^{0.351}$ ($r^2 = 0.89$, $n = 85$ nests). Inset shows same data plotted on log-log axes with a fitted linear regression. Linear regression equation: Log $m = -0.45 + 0.34\log C_t$ ($r^2 = 0.90$).

Larger nests have larger combs

The second pattern is that combs of larger nests were larger than the corresponding combs of smaller nests (Fig. 4). This pattern held both within the set of nests with the

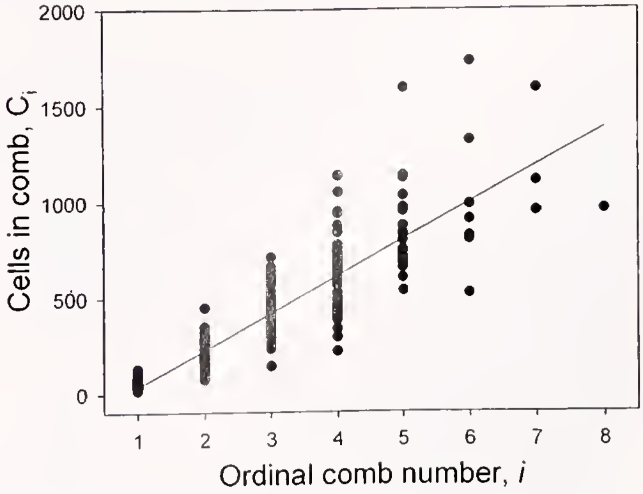

Figure 3. Comb size by ordinal comb number. The equation for the regression line is $C_i = -156.6 + 192.4i$ ($r^2 = 0.80$, $n = 85$ nests).

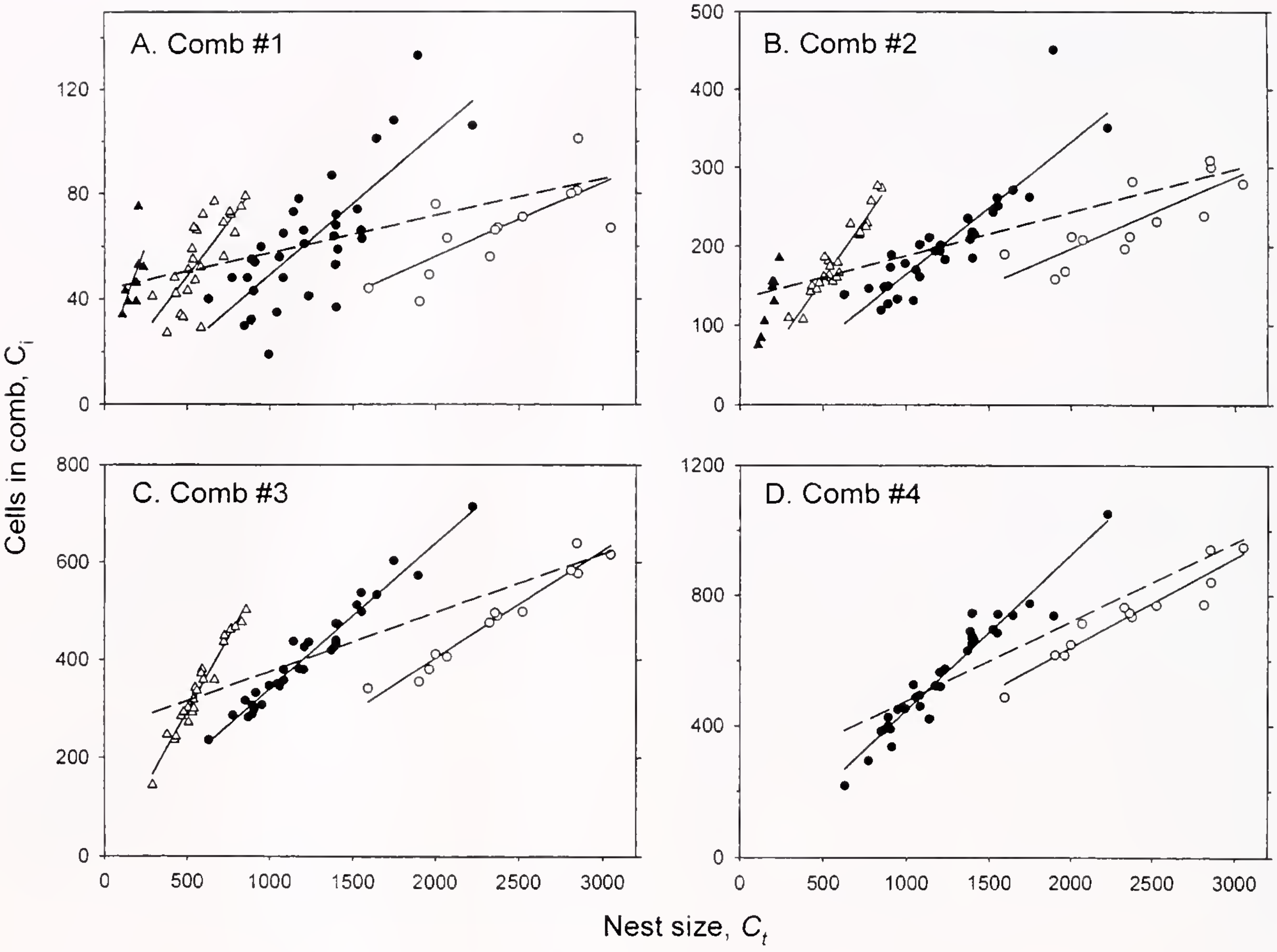

Figure 4. Distributions of sizes of individual combs as a function of overall nest size. Each graph plots sizes of combs of the indicated ordinal comb number. (A) Comb 1; (B) Comb 2; (C) Comb 3; (D) Comb 4. Within a graph, each plot is of nests of the same total comb number, m: solid triangles: $m = 2$ (*i.e.*, 2-comb nests); open triangles: $m = 3$; solid circles: $m = 4$; open circles: $m = 5$. For all regression lines shown, $P < 0.001$ (regression for comb 1 in 2-comb nests: $P = 0.11$). Solid lines represent linear regression equations for nests of the same comb number, m: (A) $m = 2$: $y = 16.76 + 0.17x$, $r^2 = 0.37$; $m = 3$: $y = 6.87 + 0.08x$, $r^2 = 0.58$; $m = 4$: $y = -5.07 + 0.05x$, $r^2 = 0.60$; $m = 5$: $y = -0.08 + 0.03x$, $r^2 = 0.55$. (B) $m = 2$: $y = -16.76 + 0.83x$, $r^2 = 0.93$; $m = 3$: $y = 7.71 + 0.30x$, $r^2 = 0.91$; $m = 4$: $y = -3.91 + 0.17x$, $r^2 = 0.77$; $m = 5$: $y = 15.31 + 0.09x$, $r^2 = 0.66$. (C) $m = 3$: $y = -14.58 + 0.62x$, $r^2 = 0.96$; $m = 4$: $y = 42.55 + 0.30x$, $r^2 = 0.96$; $m = 5$: $y = -38.64 + 0.22x$, $r^2 = 0.95$. (D) $m = 4$: $y = -33.57 + 0.48x$, $r^2 = 0.93$; $m = 5$: $y = 84.35 + 0.28x$, $r^2 = 0.90$. Dashed lines represent fitted linear regression equations for all data in each graph (*i.e.*, comb i for all nests): (A) Comb 1: $y = 43.5 + 0.01x$, $r^2 = .25$, $n = 78$. (B) Comb 2: $y = 133.1 + 0.05x$, $r^2 = 0.43$, $n = 78$. (C) Comb 3: $y = 254.5 + 0.12x$, $r^2 = 0.58$, $n = 70$. (D) Comb 4: $y = 230.2 + 0.24x$, $r^2 = 0.73$, $n = 46$. Note that the scale of the y axis increases in the graphs from A through D.

same number of combs, m, (Fig. 4, solid regression lines) as well as across the set of all nests of 2–5 combs (Fig. 4, dashed regression lines).

Among nests of m *combs, the last two combs diverge in relative size as nest size increases*

The third pattern is the least clear-cut, but is worth noting nonetheless. Within each set of nests of a given number of combs (m), the proportions of cells in combs m vs. $m - 1$ tended to diverge as nest size increased (Fig. 5). Although the slope of only one regression differed significantly from zero (comb 3 of 4-comb nests) and the slopes of the regression lines for the last and the next-to-last combs differed significantly from each other only for 4-comb nests, for all four sets the slope of the regression of cells in comb m on total cells in the nest was positive, but that of comb $m - 1$ was negative.

The number of combs in the nest depends on how individual builders respond to the choice, "Now that the envelope is complete over comb i, do I initiate cells of comb i +

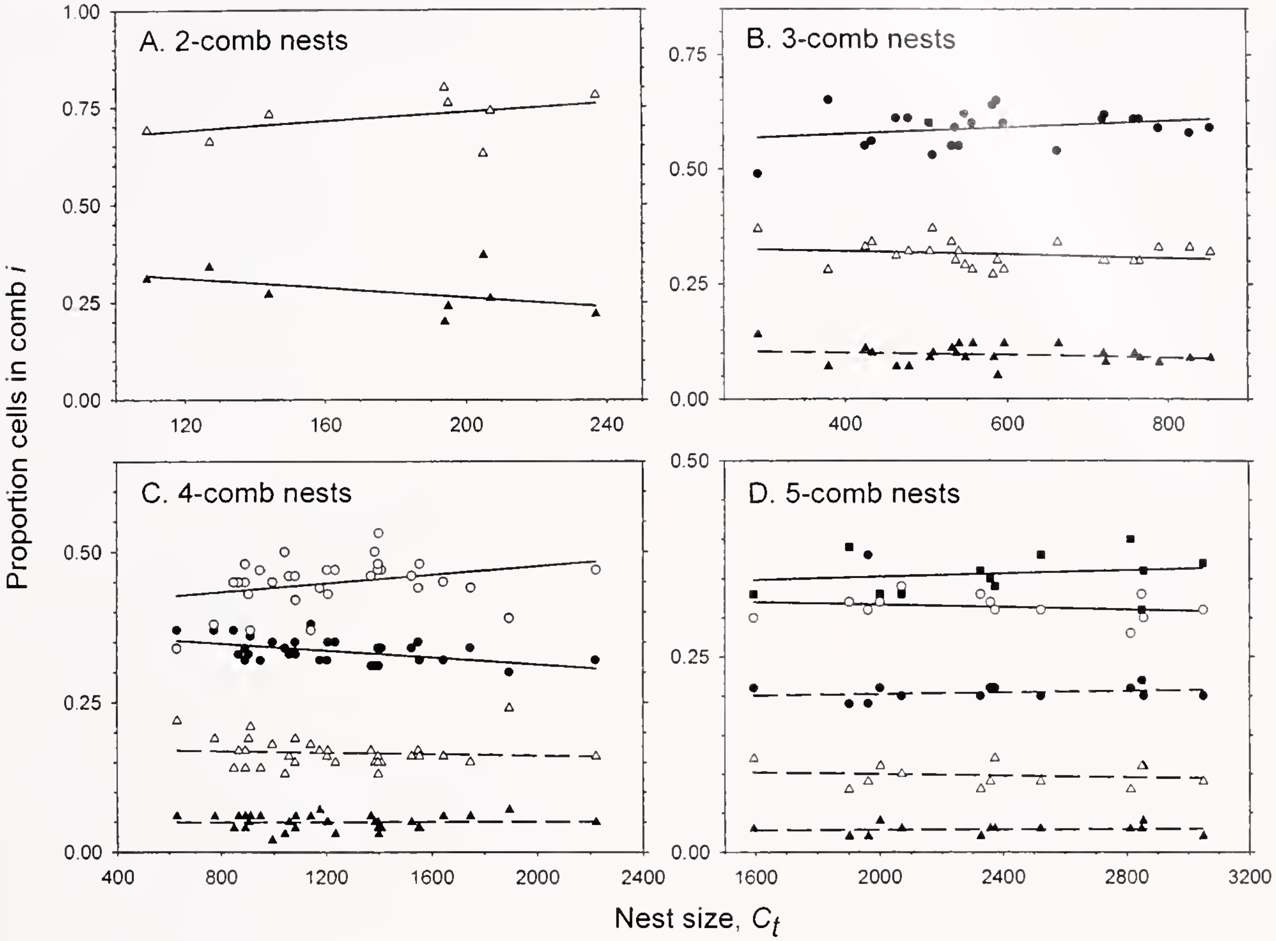

Figure 5. Proportion of cells in the nest in each comb, i, as a function of nest size, by nests of a given comb number. (A) 2-comb nests; (B) 3-comb nests; (C) 4-comb nests; (D) 5-comb nests. Solid triangles: $i =$ (comb) 1; open triangles: $i = 2$; solid circles: $i = 3$; open circles: $i = 4$; solid squares: $i = 5$. Lines are fitted linear regression equations: (A) $i = 1$: $y = 0.38 - 0.0006x$; $i = 2$: $y = 0.62 + 0.0006x$. (B) $i = 1$: $0.11 - 0.00003x$; $i = 2$: $y = 0.34 - 0.00004$; $i = 3$: $y = 0.55 + 0.00007x$. (C) $i = 1$: $y = 0.05 + 0.0000008x$; $i = 2$: $y = 0.17 - 0.000007x$; $i = 3$: $y = 0.37 - 0.00003x$; $i = 4$: $y = 0.40 + 0.00004x$. (D) $i = 1$: $y = 0.03 + 0.000001x$; $i = 2$: $y = 0.11 - 0.000005x$; $i = 3$: $y = 0.19 + 0.000005x$; $i = 4$: $y = 0.33 - 0.000008x$; $i = 5$: $y = 0.33 + 0.00001x$.

I or do I quit?" Given the correlations between swarm size and nest size (Jeanne and Nordheim, 1996) and between nest size and number of combs reported here, the conclusion that group size influences this decision is inescapable. As a rule, once a founding swarm initiates a new comb, it completes it and covers it. However, the occasional observation of a few unfinished cells exposed on the lower envelope of a completed nest hints at variation among individuals with respect to their threshold of response to the cue (or cues) that stimulates initiation of a new comb.

The size of a comb under construction is determined by the switch from expanding the comb to constructing its envelope. The later this decision is made, the larger the comb. It is clear from our data (Fig. 4) that the switch is made later by swarms building larger nests. Since combs $i > 1$ are built on the envelope of the preceding comb, part of the input into the decision to switch may be stigmergic. As these combs are expanded from the center of the domed envelope, each successive cell is built on a surface whose angle is increasingly divergent from horizontal. The cue that the switching rule uses may include this angle. Comb $i = 1$, on the other hand, is just a shelf of cells extending into space, providing far less in the way of potential stigmergic cues as to when to switch to construction of the envelope. Yet this comb also increases in size with nest size (Fig. 4A), suggesting that a larger swarm builds a larger first comb using no information other than the size of its own group.

The third pattern gets at the question of when, during the course of constructing the nest, the final nest size is set. Does the swarm "know" from the start of construction how large a nest it will build, or does it make corrections as it goes? Three observations suggest that the latter is the case. First, whereas the correlation between the size of combs 1 and 2 is relatively strong ($r = .83$; $n = 85$), the correlation of comb 1 with later combs progressively weakens. The ability of comb 1 to predict the overall nest size is not very good ($r = .46$). Second, the amount of variance in comb size that is explained by nest size increases with comb number, i (Fig. 4, r^2 values increase, A–D). Third, there is substantial overlap in size among nests of m and $m + 1$ combs, especially for nests of $m > 2$ combs (Fig. 2; Figs. 5B–D), suggesting that swarms adjust final nest size by deciding whether to add a final module. The overlap is probably due to variation in the sizes of the first few combs built by swarms of similar size. Consider, for example, two swarms, each of which will ultimately build a nest of 2000 cells. Nests of this size may have four or five combs (Fig. 2). If swarm A builds combs 1–4 smaller than average, it will build a 5th comb, but this final comb will not need to be much bigger than comb 4 to achieve the total of 2000 cells in the nest (see Fig. 5D). On the contrary, if swarm B builds combs 1–3 larger than average, then it will get the 2000 cells by adding one more comb, but that comb will have to be disproportionately larger (see Fig. 5C). The nest of swarm A is toward the low end of the size distribution of 5-comb nests, while that of swarm B is toward the high end of the size range of 4-comb nests. The combs of nest B will average 25% larger than those of nest A. As Figure 5 shows, however, most of this average difference in proportions tends to be absorbed by the last comb.

Taken together, these observations suggest that swarms fine-tune the final size of their nests in the later stages of construction. Thus, although comb 1 aims roughly in the direction of the ultimate nest size, the trajectory toward the final nest size is guided en route, rather than ballistically following from comb 1.

Conclusions

The construction of a nest by a social insect colony involves the performance of a set of behavior patterns that vary in species-specificity and evolutionary age (Wenzel, 1996). Some may be invariant across higher taxa. The use of the mandibles to manipulate nest material, for example, is universal among social Hymenoptera and Isoptera and apparently pre-dates the evolution of sociality in both groups. The rules by which nest material is applied in response to stigmergic cues from the nest also vary in their taxonomic breadth.

At one extreme, tactile feedback *via* the antennae is used to center construction of a shared cell wall between opposite walls of two adjacent brood cells and to determine the size of the cells (West-Eberhard, 1969). This is an example of the use of the body as a template to produce the regular hexagonal pattern of the comb. This building rule probably varies little if at all among species of social wasp, except in the interesting case of the Vespinae, where the queen builds worker-sized cells, and the workers (which are smaller) build both worker- and queen-sized cells.

At the other extreme are species-specific rules—those that result in the nest architecture characteristic of a species. In our view, there is little evidence that the resulting patterns in nest structure at any of these levels are emergent properties of a self-organizing process. Rather, they appear to be largely the products of quantitative and qualitative stigmergy (Camazine *et al.*, 2001).

At the intraspecific level, however, things may work differently. The evidence we have presented clearly indicates that *Polybia occidentalis* swarms are able to allocate brood cells among combs so that size and number of combs scale with swarm size. What mechanism could give rise to this pattern? Several previous studies have suggested ways that groups of social insects might build their nests to a size that accommodates them. One possibility is that the mass of the swarm itself serves as a template to adjust the size of the nest to the size of the swarm. This appears to play a role in construction of the two-dimensional nests of *Leptothorax* ants (Franks *et al.*, 1992; Camazine *et al.*, 2001). Swarms of *Metapolybia* wasps build nests of single combs on a flat surface. A ring of "guards" is arrayed around the comb as it is constructed (Forsyth, 1978). If the guards are a fixed proportion of the swarm, then expanding the comb to the ring could produce a nest of the right size. But use of such a template cannot explain the scaling patterns seen in *P. occidentalis,* whose three-dimensional nests are extended into open space below a supporting twig, while the bulk of the swarm remains clustered to the side on the twig.

A related idea is that construction stops when the nest is large enough to house the swarm (Camazine *et al.*, 2001). In its simplest form, this mechanism would predict that comb size would be constant across swarm size and that larger swarms would simply build nests with more combs. It does not explain our observation in *P. occidentalis* that the scaling of the nest to swarm size begins with the first comb and continues throughout construction.

A third possible mechanism is that cells are constructed to keep up with the oviposition rate of the laying queens (Deleurance, 1950; Camazine *et al.*, 2001; but see Wenzel, 1996). Again, this mechanism cannot be working in *P. occidentalis,* because cells are built at a rate that well outpaces the collective rate of oviposition by the queens in the swarm (RLJ and AMB, pers. obs.).

A fourth possibility is that self-organization plays a role. However, there is no evidence that the scaling of the nest proportions by a particular swarm is an emergent pattern arising at the colony level from interactions among workers, nor is there any apparent involvement of positive feedback in the process.

None of these mechanisms adequately explains our results. Likewise, stigmergic cues, although important, are clearly insufficient alone to account for the swarm-size-dependent patterns we see among nests. Instead, we suggest the following mechanism. All three of the scaling patterns we describe for *P. occidentalis* indicate that information about group size flows from the group to the individual builders. We suggest that the quantitative rules governing the details of nest size and proportions in response to stigmergic cues are plastic and are modulated by group size. Although nothing is yet known about the building rules or stigmergic cues used by *P. occidentalis*, the following hypothetical example illustrates how this mechanism might work. The size of a comb may be determined by a rule according to which a builder decides between adding another new cell at the periphery of the comb being constructed and beginning the envelope for that comb. The quantitative set point for such a rule apparently differs according to whether the builder is in a large or a small swarm. A possible stigmergic cue in this case is the angle of the surface of the envelope on which the cells are being built. The first cells in the comb are built in the center of the envelope, that is, where the envelope's curved surface is tangent to a horizontal plane, or 0°. Because the envelope is domed, as the comb expands radially across the surface of the envelope, each new cell is built at a steeper angle from the horizontal than the previous cell (Fig. 1B). Thus, the behavioral rule in the context of a small swarm might be, "If the angle at which the current edge of the comb is $\geq 25°$, then begin building the envelope instead of adding another cell." We suggest that in a large swarm, this quantitative set point may be nudged up to, say, 30° in response to information about swarm size fed back to the builder from the group. This change would result in a comb's being larger when being built by a large swarm than when built by a small swarm. Because the envelope subsequently built over the larger comb would also be larger, the increased size would propagate itself throughout the remaining modules of the nest. In other words, we are hypothesizing that information about group size modulates the quantitative set points of the rules of response to stigmergic cues.

In conclusion, we see little evidence that self-organizing processes play a role in nest construction in *Polybia occidentalis*. Rather, construction of the species-typical features of the nest can be understood as quantitative and qualitative stigmergic mechanisms, wherein cues from the nest structure at each stage of construction provide information to the builders as to what building act to perform next, where to perform it, and how to orient the addition of the new material. In accomplishing these tasks, individual workers interact only indirectly, *via* the structure of the nest (Camazine *et al.*, 2001). We have provided evidence that changes in nest proportions accompany changes in swarm size. We argue that these patterns cannot be explained by stigmergy alone, but appear to involve direct communication, no doubt through cues, of information about the size of the group. In response, builders subtly modulate their responsiveness to quantitative stigmergic cues so as to yield the appropriate nest proportions. Although the mechanisms by which group-size information is transferred to, perceived by, and acted upon by individuals are unknown, there is little evidence that a self-organizing process is involved.

Acknowledgments

We thank Kory Kramer and Peter Bouwma for helping to collect data in Costa Rica. Carl Anderson, Jeffrey Baylis, David Curson, Ellen Davis, and members of the Genes, Neurons, and Societies work group at the Santa Fe Institute provided valuable discussion and gave us feedback as our ideas developed. Lee Clippard, Ken Howard, and Cristie Hurd helped improve early drafts of the manuscript. Erik Nordheim provided statistical help. Research supported by NSF grant IBN9514010 to R. L. Jeanne and by the College of Agricultural and Life Sciences, University of Wisconsin, Madison.

Literature Cited

Bouwma, P. E., A. M. Bouwma, and R. L. Jeanne. 2000. Social wasp swarm emigration: males stay behind. *Ethol. Ecol. Evol.* **12:** 35–42.

Camazine, S., J.-L. Deneubourg, N. R. Franks, J. Sneyd, G. Theraulaz, and E. Bonabeau. 2001. *Self-Organization in Biological Systems.* Princeton University Press, Princeton, NJ.

Deleurance, E. Ph. 1950. Sur le mécanisme de la monogynie fonctionelle chez les *Polistes* (Hyménoptères-Vespides). *C. R. Hebd. Seances Acad. Sci. Paris* **230:** 782–784.

Forsyth, A. B. 1978. Studies on the behavioral ecology of polygynous social wasps. Ph.D. dissertation, Harvard University, Cambridge, MA. 226 pp.

Franks, N. R., A. Wilby, B. W. Silverman, and C. Tofts. 1992. Self-organizing nest construction in ants: sophisticated building by blind bulldozing. *Anim. Behav.* **44:** 357–375.

Grassé, P.-P. 1959. La reconstruction du nid et les coordinations inter-individuelles chez *Bellicositermes natalensis* et *Cubitermes* sp. La théorie de la stigmergie: essai d'interprétation du comportement des termites constructeurs. *Insectes Soc.* **6:** 41–83.

Jeanne, R. L. 1986. The organization of work in *Polybia occidentalis:* the costs and benefits of specialization in a social wasp. *Behav. Ecol. Sociobiol.* **19:** 333–341.

Jeanne, R. L. 1996. Regulation of nest construction behaviour in *Polybia occidentalis. Anim. Behav.* **52:** 473–488.

Jeanne, R. L., and E. V. Nordheim. 1996. Productivity in a social wasp: per capita output increases with swarm size. *Behav. Ecol.* **7:** 43–48.

O'Donnell, S., and R. L. Jeanne. 1992. The effects of colony characteristics on life span and foraging behavior of individual wasps (*Polybia occidentalis*, Hymenoptera: Vespidae). *Insectes Soc.* **39:** 73–80.

Theraulaz, G., and E. Bonabeau. 1995. Coordination in distributed building. *Science* **269:** 686–688.

Wenzel, J. W. 1993. Application of the biogenetic law to behavioral ontogeny: a test using nest architecture in paper wasps. *J. Evol. Biol.* **6:** 229–247.

Wenzel, J. W. 1996. Learning, behaviour programs, and higher-level rules in nest construction of *Polistes*. Pp. 58–74 in *Natural History and Evolution of Paper-Wasps*, S. Turillazzi and M. J. West-Eberhard, eds. Oxford University Press, Oxford.

West-Eberhard, M. J. 1969. The social biology of polistine wasps. *Misc. Publ. Mus. Zool. Univ. Mich.* **140:** 1–101.

Reference: *Biol. Bull.* **202:** 296–305. (June 2002)

Self-Organized Fish Schools: An Examination of Emergent Properties

JULIA K. PARRISH[1,2,*], STEVEN V. VISCIDO[2], AND DANIEL GRÜNBAUM[3]

[1] *School of Aquatic and Fishery Sciences, Box 355020, University of Washington, Seattle, Washington 98195-5020;* [2] *Zoology Department, University of Washington; and* [3] *School of Oceanography, University of Washington*

Abstract. Heterogeneous, "aggregated" patterns in the spatial distributions of individuals are almost universal across living organisms, from bacteria to higher vertebrates. Whereas specific features of aggregations are often visually striking to human eyes, a heuristic analysis based on human vision is usually not sufficient to answer fundamental questions about how and why organisms aggregate. What are the individual-level behavioral traits that give rise to these features? When qualitatively similar spatial patterns arise from purely physical mechanisms, are these patterns in organisms biologically significant, or are they simply epiphenomena that are likely characteristics of any set of interacting autonomous individuals? If specific features of spatial aggregations do confer advantages or disadvantages in the fitness of group members, how has evolution operated to shape individual behavior in balancing costs and benefits at the individual and group levels? Mathematical models of social behaviors such as schooling in fishes provide a promising avenue to address some of these questions. However, the literature on schooling models has lacked a common framework to objectively and quantitatively characterize relationships between individual-level behaviors and group-level patterns. In this paper, we briefly survey similarities and differences in behavioral algorithms and aggregation statistics among existing schooling models. We present preliminary results of our efforts to develop a modeling framework that synthesizes much of this previous work, and to identify relationships between behavioral parameters and group-level statistics.

Types of Aggregations

Aggregation occurs in the smallest organisms—bacteria—and the largest—whales—and spans virtually the entire extant diversity of taxon, habitat, trophic level, life-history strategy, degree of mobility, and many other biological characteristics (Parrish and Edelstein-Keshet, 1999; Camazine *et al.*, 2001). Physical aggregation can be regarded as part of a continuum in group integration. At one end of this continuum are territorial animals with little need to engage in information transfer and no need for group structure. At the other end are highly integrated, long-term associations between individuals that know—and perhaps are even related to—other members of the group, and in which members can potentially have high rates of direct and indirect information exchange. Honeybee hives, cetacean pods, and human communities are examples of these highly integrated groups (Wilson, 1975). In these systems, established pathways of long-term communication between known individuals (clones, siblings, reciprocating group members), or at predetermined locations (the hive, the calving grounds, the dinner table), may supplement immediate sensory contact. Thus, the members remain part of the "group" even while they range widely in space. In these dispersed groups, coordinated function can be maintained as long as the necessary information is transferred between group members (*e.g.*, the sensory integration systems of Norris and Schilt, 1988; Schilt and Norris, 1997), though distance between interacting components inevitably affects the evolution and stability of emergent group properties (Hillier and Hanson, 1990; Latané *et al.*, 1995).

---

* To whom correspondence should be addressed. E-mail: jparrish@u.washington.edu

This paper was originally presented at a workshop titled *The Limits to Self-Organization in Biological Systems.* The workshop, which was held at the J. Erik Jonsson Center of the National Academy of Sciences, Woods Hole, Massachusetts, from 11–13 May 2001, was sponsored by the Center for Advanced Studies in the Space Life Sciences at the Marine Biological Laboratory, and funded by the National Aeronautics and Space Administration under Cooperative Agreement NCC 2-896.

Between these extremes of group integration are what could be considered "prototypical" animal aggregations—herds, swarms, flocks, and schools. Within the fishes, over 50% of species school—that is, display synchronous and coordinated movement—at some point in their life histories (Shaw, 1978), and an unknown additional number aggregate more coarsely. Prototypical aggregations exhibit coordinated motion, but group members are generally unrelated and never develop lasting relationships (in the game-theoretic, "tit-for-tat" sense) with other members. Many of these groups are extremely large (*e.g.*, a school of a billion herring). Individuals in such groups interact with a neighborhood of other members, but those may represent a vanishingly small fraction of the group as a whole. This suggests that mechanisms which maximize information transfer among individuals could be evolutionarily beneficial. One example of this is a repeated arrangement within the group, reminiscent of crystal lattices, in which individuals assume preferred positions and orientations relative to their neighbors. Such arrangements could, for example, maximize sensory contact between members in such as way as to reflect ambient conditions, and the organisms' predominant sensory systems, morphology, etc. (Parrish, 1992; Parrish and Edelstein-Keshet, 2000).

We can characterize possible behavioral adaptations in members of these groups on at least two levels: (1) short-term reactions to modify position with respect to immediate neighbors; and (2) behavioral responses that do not necessarily improve position relative to immediate neighbors but that contribute to group-level characteristics that ultimately benefit the individual by benefiting the group. These group-level adaptations are among the most fascinating—and the most difficult to assess—aspects of animal aggregations.

Pattern *versus* Function

Human perception tends to recognize attributes of the whole: an even density profile, polarity, distinct edges, or specific shape. While it is tempting to assume that conspicuous features of biological aggregations are somehow beneficial, the existence of qualitatively similar patterns that arise from physical phenomena shows that this need not be the case. For example, some shapes found in three-dimensional schools (*e.g.*, torus and funnel) are echoed in two-dimensional insect configurations (*e.g.*, wheel), suggesting that such shapes may be adaptive for group members (Fig. 1). However, these patterns could be evolutionarily neutral, or even pathological. Virtually identical shapes can be found in a wide range of inanimate aggregations, from water vapor to planets, in which these patterns arise from simple abiotic interactions between individual components, in the absence of evolutionary dynamics. Key steps in understanding biological aggregations in nature must be to distinguish biologically relevant features from nonadaptive epiphenomena, and to more explicitly and mechanistically describe the links between individual behaviors and group pattern.

Dynamic patterns and movement are necessary characteristics of many biological aggregations, and are perhaps better criteria to distinguish adaptive responses from epiphenomena. For example, fish schools display complex emergent properties such as coordinated motion and directed activity. Compression, hourglass, vacuole, fountain, and flash expansion (Fig. 2; Pitcher and Parrish, 1993) are all maneuvers that minimize predatory risk *only* if all members perform them correctly (*e.g.*, Parrish, 1989). Parabolic formations in tuna schools may allow cooperative hunting advantages (Partridge *et al.*, 1983). These emergent group properties appear to have readily apparent biological interpretations, and physical analogs may be harder to find. However, these dynamic group properties clearly confer more evolutionary advantages under some circumstances than others (*e.g.*, evading small predators that target individuals while becoming targets for large predators that target groups; Parrish, 1993). Furthermore, the key evolutionary question remains: do these behaviors involve trade-offs between short-term gain for the individual and long-term functioning of the group? If so, what is the evolutionary context in which selection for these behaviors occurs?

Traffic Rules

Assuming structure is advantageous, how is it maintained? Laboratory and field attempts to address this question in fish schools have been limited (Partridge and Pitcher, 1980; Aoki *et al.*, 1986; Parrish and Turchin, 1997), in part because obtaining three-dimensional trajectories on specific individuals for a relevant period of time is difficult. Data that do exist are typically from highly artificial conditions (*e.g.*, relatively small schools in highly lit still-water tanks; Parrish and Turchin, 1997). Three-dimensional tracking techniques have not yet advanced to the stage where it is feasible to observe large schools (*i.e.*, over 10), in three dimensions, over long times (*i.e.*, for more than seconds). Despite these difficulties, quantitatively accurate observations of fish behavior within schools will undoubtedly become available in the next few years. However, while those data will provide a means of assessing short-term behavioral responses by fish to neighbors within a group, they will not by themselves provide the strong linkage between individual and group characteristics that we require to understand the mechanics and evolution of schooling behaviors.

Making this linkage requires an additional approach, namely, mathematical or computational models of schooling behavior. These models posit a specific, quantitative set of behavioral interactions—essentially, they create a set of traffic rules—and quantitatively assess the emergent properties of the resulting schools. Ideally, both the inputs (*i.e.*,

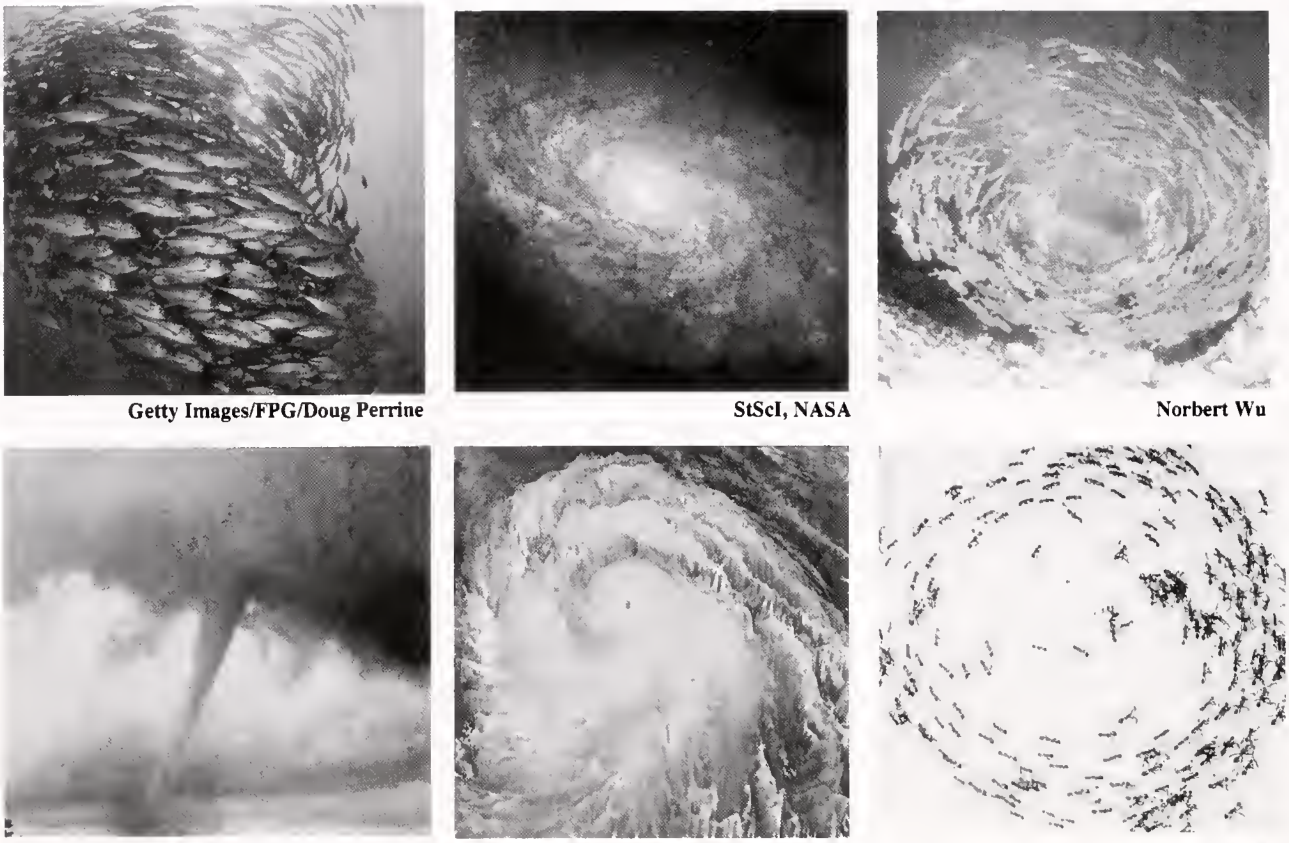

Getty Images/FPG/Doug Perrine
StScI, NASA
Norbert Wu
OAR/ERL/NSSL
NASA
T. C. Schneirla

Figure 1. Three- and two-dimensional expressions of emergent structure in animate and inanimate aggregations—whorl patterns. Left: tornado structure in fish (top) and water vapor (bottom). Middle and right: whorl and toroid in planets, fish, ants, and water vapor, clockwise from top left. Top left reprinted with permission by FPG; bottom left courtesy of National Severe Storm Laboratory; middle top and bottom courtesy of National Aeronautic Space Administration; top right taken by Norbert Wu, www.norbertwu.com © 1999; bottom right taken by T. Schneirla and reprinted with permission by W. H. Freeman & Company.

individuals' responses to neighbors) and model output (group-level characteristics) can be compared to data from real aggregations.

A key purpose of modeling is to distinguish behavioral cause from organizational effect by studying the consequences of various hypothetical social interaction rules. Most simulation models of animal aggregations in the literature assign a set of forces that act on the speed and direction of each individual and are modulated in response to other individuals or the local environment. Typical force components include locomotory (*e.g.*, biomechanical forces such as drag), aggregative (*e.g.*, long-range attraction, short-range repulsion), arrayal (*e.g.*, velocity matching), and random (*e.g.*, individual stochasticity; Grünbaum and Okubo, 1994). The detailed biomechanics of locomotory forces are usually not considered in fish schooling simulations. Instead, most simulations simply associate behavioral movement "decisions" with the movements that result. However, there are exceptions, notably a few modeling studies that specifically address hydrodynamic interactions between members of a school (*e.g.*, Weihs, 1973).

Published modeling studies have for the most part addressed a relatively restricted range of behavioral algorithms. Most analyses focus on variation in one of three categories: behavioral matching, positional preference, and numerical preference.

Behavioral matching (aka allelomimesis: Deneubourg and Goss, 1989) occurs when the individual agents try to match their behavior with other nearby agents. Most often, behavioral matching is modeled by having each agent explicitly match its orientation with that of its nearby neighbors (*e.g.*, a zone of parallel orientation: Aoki, 1982; Huth and Wissel, 1992; Dill *et al.*, 1997; Table 1, Fig. 3). Less often, fish match their speed, either to that of their companions, or to some arbitrarily decided value (*e.g.*, Romey, 1996; Vabø and Nøttestad, 1997).

Positional preference refers to each fish having a preferred position relative to one or more of its companions.

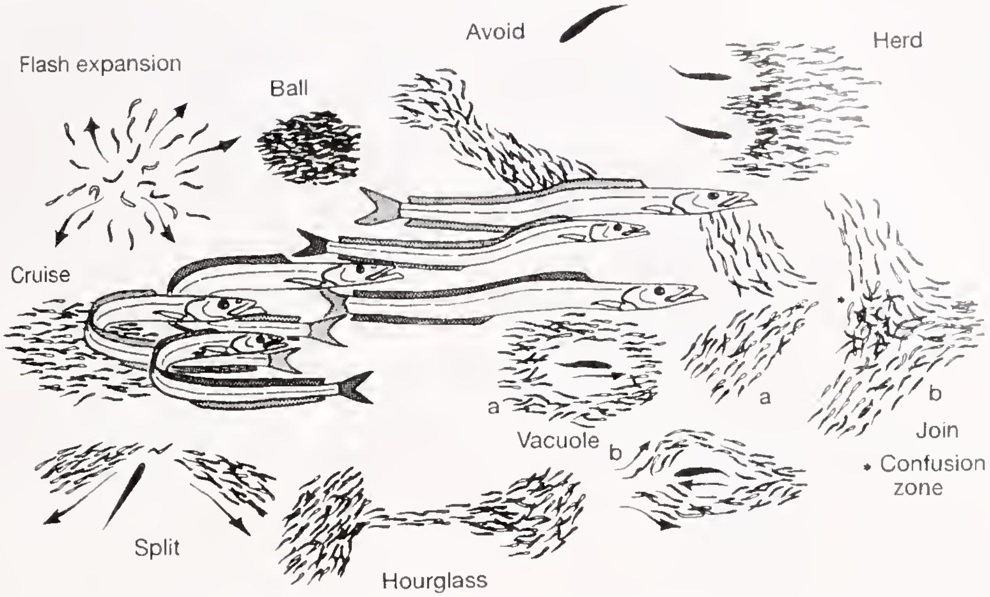

Figure 2. Examples of coordinated movement and directed activity, both emergent properties of fish schools, which are also commonly cited defense tactics against predatory attack. Fig. 12.8. from Pitcher and Parrish 1993. Reprinted with permission from the author and Kluwer Academic Publishers.

Usually, positional preference is formulated as a preferred distance to one or more nearest neighbor(s). Variations on positional preference include assigned distance zones (*e.g.*, repulsion, parallel orientation, attraction, searching) within which neighbors are treated equally (Huth and Wissel, 1992; Stöcker, 1999) or continuous distance weighting (Warburton and Lazarus, 1991; Reuter and Breckling, 1994; Romey, 1996). In some models, other positional parameters influence responses, such as bearing angle to neighbors, or estimated collision time (Dill *et al.*, 1997). The biological underpinning is obvious: that individual group members do not collide, that groups do not dissolve, and that stragglers join. Taken together, behavioral matching and positional preference describe what a fish should do, *e.g.*, move towards or away from neighbors, align with neighbors, search for neighbors (Fig. 3; RPOA dependence, Table 1), and how much consideration it should give any neighbor in the perception field (neighbor scaling rule, Table 1).

Numerical preference refers to the number of neighbors to which a fish pays attention, which we generically refer to as the rule size. Variations include an *a priori* value (*e.g.*, 4: Warburton and Lazarus, 1991) or a conditional value (*e.g.*, choose up to 4 in the nearest zone: Aoki, 1982; choose up to 4, front prioritized: Huth and Wissel, 1992). Many simply have each fish average over all other fish (*e.g.*, all visible: Reuter and Breckling, 1994; Vabø and Nøttestad, 1997; all fish: Romey, 1996).

In general, modeling studies of schooling have been limited in several important respects, which future studies should aim to improve upon. Most models have used a relatively small population (*e.g.*, 8 to 20 fish; Table 1), despite the fact that several studies point out that small numbers of fish may produce artificial results (*e.g.*, Romey, 1996). Most models have operated in two dimensions. Although this may be justified on the basis of computational resources, generalizing from two to three dimensions may not be straightforward. Many models include some stochastic or chaotic elements; however, the degree of replication in modeling studies is generally lower than ideal to characterize the frequency distributions of possible outcomes.

Most simulation studies also assume that all individuals are identical. Romey (1996) has shown that the inclusion of a single fish with different traffic rules will alter schooling (measured as group speed and turning rate). Furthermore, the inclusion of multiple agents with one of two rule sets produces sorting (Romey, 1996), which may translate into emergent properties (*e.g.*, horizontal bands *versus* extended columns of ungulates, Gueron *et al.*, 1996). The possibility that variability within the group may not only affect emergent properties such as coordinated movement and spatial pattern, but may also itself be an emergent property, clearly deserves further consideration in modeling studies.

The parameter space explored by each model is typically only a small subset of possible variations, which ideally would include variations in (at least): initial position and velocity; the strength and type of stochastic components; spatial distribution of repulsion, parallel orientation, and attraction; and degree of variation between individuals in a group (Table 1). Because most studies are not consistent in

Table 1

Summary of fish school simulation parameters and output variables. R/PO/A-sequential zones of repulsion, parallel orientation (variably used), and attraction where "zone" implies equal force within a proscribed area (see Figure 3). Direction matching implies the use of a zone of parallel orientation. All other definitions as in the text. Numbers in parentheses refer to footnotes.

Reference	Population Size	Starting Orientation	Velocity	R/PO/A Dependence	Direction Matching?	Neighbor Scaling	Rule Size
Aoki (1982, 1984)	8, 32	Random position & orientation within bounded area	Random	Zone (1, 2)	Yes	Position, weighted by front priority	Up to 4
Warburton & Lazarus (1991)	2–9	Regular square lattice	Not specified	Linear distance	No	Constant	1–8
Huth & Wissel (1990, 1992, 1994)	8	Random position & orientation in fixed area	Random	Zone (1)	Yes	Constant; Single choice (4)	Up to 4, front prioritized
Reuter & Breckling (1994)	10, 20, 30, 40, 50	Random position, orientation & speed within bounded area	Not clear	Linear distance	Yes	Distance-weighted average ($1/D$; $1/D^2$)	All visible
Romey (1996)	2–10	Random position & orientation within bounded area (5)	Constant	Linear distance	No	Constant	All
Vabø & Nøttestad (1997)	900	Random position & orientation within bounded & fixed areas	Constant	Discrete distance	No	Single choice (7)	All visible
Stöcker (1999)	12, 64	Random position & orientation within bounded area	Constant	Zone (1)	Yes	Constant	Variable (8)

Reference	Random Component (distribution)	Aggregation Indices Individual	Aggregation Indices Group	Aggregation Indices Population
Aoki (1982, 1984)	Gamma (speed); Normal (direction; 3)	Net Individual Displacement	Compactness (1/SD of x, y coordinates)	
Warburton & Lazarus (1991)	Circular normal (direction)	Inter-Individual Distance	Group Center Displacement; Group Shape (max IID^2)/area	
Huth & Wissel (1990, 1992, 1994)	Gamma (speed); Normal (direction)	Nearest Neighbor Distance (neighbors 1–3)	Polarization; Expanse (rms distance to center)	
Reuter & Breckling (1994)	Normal (direction, speed)	Nearest Neighbor Distance	Polarization; Expanse (mean distance to center)	
Romey (1996)	Uniform (direction; 6)		Group Speed; Group Turning Rate	
Vabø & Nøttestad (1997)	Discrete probabilities of choosing less than optimal direction	Instability (maximum individual distance traveled)		Number of Schools
Stöcker (1999)	Uniform (direction; 9)		Polarization; School Direction	Number of Schools; School Size

Note that random components selected from a normal distribution are centered on calculated means as per Figure 3.

(1) Distance-specific zones of repulsion, parallel orientation, attraction, and searching. A blind spot (30–60 deg.) behind.

(2) Beyond the zone of attraction, but within the visual angle (270 deg), attraction based on linear distance.

(3) Outside the sensed area, direction was chosen from a uniform circular distribution (*i.e.*, random walk).

(4) Single Choice = choose only one neighbor with a weighted probability N1, 1/2N2, 1/4N3, 1/8N4.

(5) Individuals can sense entire area (~100 BL).

(6) Every 15 or 30 time steps.

(7) Highest (optimal) attraction value direction (of eight 45 deg increments) chosen.

(8) All neighbors within the parallel orientation zone considered equally. Only closest neighbor within attraction zone considered.

(9) Only applied to single fish with no neighbors (*i.e.*, random walk searching).

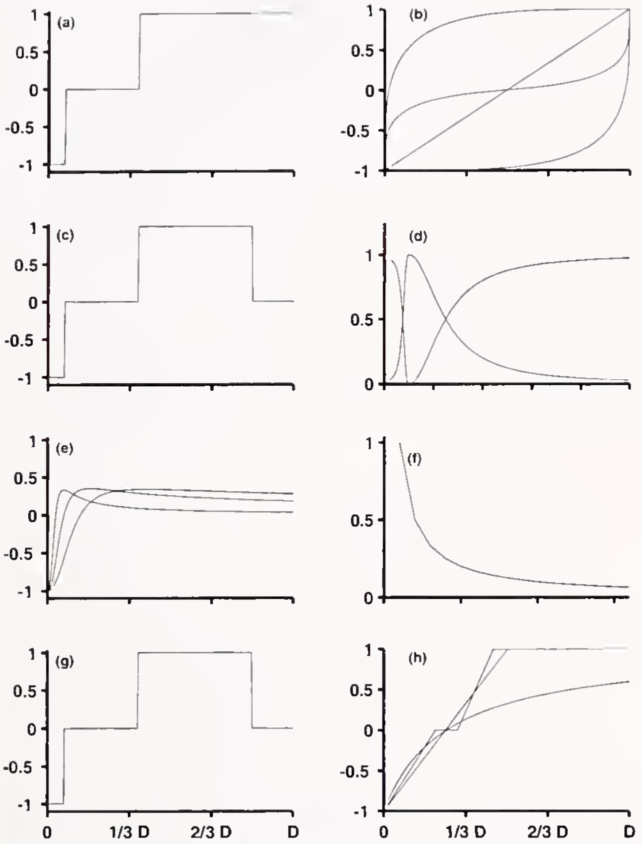

Figure 3. Caricatures of the attraction-repulsion functions used by various authors to simulate schooling in fish (see also Table 1). Repulsion is always negative on the y-axis, whereas attraction is positive. Zones of no repulsion or attraction (*e.g.*, parallel orientation) are at zero. The x-axis is distance from fish of interest, displayed in arbitrary units. (a) Aoki (1982). (b) Warburton and Lazarus (1991). (c) Huth and Wissel (1990, 1992, 1994). (d) Curves showing the relative strengths of repulsion (left), parallel orientation (center), and attraction (right) in Reuter and Breckling (1994). Note that total social force always sums to 1.0 (e) Romey (1996). (f) The attraction strength used by Vabø and Nøttestad (1997). (g) Stöcker (1999). (h) Our simulation.

these aspects (among others), direct comparisons of their results are not possible.

Finally, although most authors quantified school characteristics in their simulations with one or more index of aggregation, there is little or no consensus on which indices are most biologically relevant. Consequently, different studies tend to cite different statistics, again making comparisons difficult. For example, it is difficult to determine whether Romey's (1996) model provides the same amount of polarization as Huth and Wissel's (1992), because the former did not report that particular emergent property. A related but more subtle problem is that no single paper has simultaneously presented indices at the individual, group, and population levels (Table 1). In part this is because the distinction between group and population is meaningless in some models (*i.e.*, all individuals always interact and therefore the entire population is always part of the same group, *e.g.*, Aoki, 1982; Reuter and Breckling, 1994). Even when this is not the case, most studies use initial conditions or behaviors that predispose individuals to start and remain within a single large group. However, there are again notable exceptions, for example, the cellular automata models of Vabø and Nøttestad (1997) and Stöcker (1999); see also Flierl *et al.* (1999).

Inconsistencies between modeling approaches and aggregation indices have led different authors to draw seemingly contradictory conclusions about how individual behaviors affect group-level characteristics. For example, Aoki (1982; 1984) reports that removing the repulsion zone causes school disintegration, whereas Huth and Wissel (1990, 1992, 1994) assert it has little effect on schooling. Huth and Wissel (1990, 1992, 1994) maintain that only a low number of influential neighbors (< = 3) are needed, whereas Warburton and Lazarus (1991) state that increasing the rule size is essential for school stability. Reuter and Breckling (1994) and Romey (1996) found that adding random or individual movement had little effect on schooling, but Warburton and Lazarus (1991) concluded that the incorporation of random movements destroyed schooling. Because these studies lack a common framework for specifying behaviors and summarizing spatial patterns, it is not possible to resolve whether these reflect true biological differences or simply comparisons between apples and oranges.

A Synthetic Simulation Study

We are currently working on a simulation model of fish schooling that explores much of the parameter space covered in previous models. Our model operates in three dimensions, and does not (as yet) include any rules that, *a priori*, program emergent property (*i.e.*, no behavior matching or zone of parallel orientation). Following Grünbaum and Okubo (1994) and others, we model the movement decisions of each fish as a sum of locomotory, social, and random forces. Model fish are based on our quantitative observations of schooling giant danios (*Danio aequipinatus*; unpub. data), with a mass of 1.7 g, a length of 5.3 cm, a maximum speed of 11.2 body lengths [BL]/s, and a maximum acceleration of 11.2 BL/s^2). Locomotory force consists of drag, specified as a drag coefficient (C_D) of 0, 0.01, or 0.02 (based on a range of estimated drag coefficients for streamlined bodies = 0.01–0.001; Videler, 1993). Details of the methodology are presented elsewhere (Viscido *et al.*, unpub. data).

We have thus far used this model to study a range of population from 2 to 128 fish, but report here only results for 128 fish. We examined variation in three aspects of the social force: the attraction/repulsion function, the neighbor scaling rule, and the rule size. Attraction/repulsion was modeled as a linear, piecewise linear, or convex (*sensu*

Table 2

Aggregation indices at the individual, group, or population level used to evaluate traffic rules in our simulation

Index	Computation	Level
Curvature	Mean turning angle per cm traveled	Individual
Fractal Dimension	How "dimensional" the path is	Individual
NGDR	Net displacement divided by gross displacement	Individual
NND	Mean linear distance to nearest neighbor	Individual
Group Size	Number of fish within 5 body lengths of each other	Group
Expanse	Mean quadratic distance to center for each group	Group
Polarization	Mean angle deviation between individual and group heading	Group
Groups	Number of groups in the universe, including stragglers	Population
Stragglers	Number of fish more than 5 body lengths from any other fish	Population
Collisions	Number of collisions per fish per minute (reported as total collisions)	Population
Clark and Evans (1954) Index	Observed NND *vs.* expected NND for a randomly spaced population	Population

Warburton and Lazarus, 1991) function with $F = 0$ centered at 1.9 BL (Fig. 3h). We based this preferred nearest neighbor distance on schooling experiments with real fish from a previous study (Parrish and Turchin, 1997). We used a perception distance of 180 BL (*i.e.*, so individuals could detect neighbors to which they choose not to respond). A neighbor scaling rule weighted the attraction/repulsion force by the distance to each influential neighbor. Weighting was constant (*i.e.*, equal weighting), negative linear, or negative sigmoid. Finally, the number of influential neighbors (rule size) was set at 4, 8, 16, or 24 fish.

Random force was chosen for each timestep from a normal distribution with mean $F = 0$ and standard deviation equivalent to 1/3, 1/6, and 1/18 of the maximum social force an individual fish could experience from another fish. The amount of random force experienced by any individual was a function of the distribution of nearby neighbors. Individuals within a school experienced relatively little social force because most neighbors are at or near the equilibrium (*i.e.*, $F = 0$), thus random forces can be proportionately large. Individuals divorced from the group but close enough to sense it experienced maximum social force (*i.e.*, attraction), and proportionately little random force. In our simulations, median random force as a function of total force ranged from 8%–18% depending on rule size. We computed fish movement as acceleration resulting from the sum of random and social forces, minus drag.

Each parameter combination in our simulations were replicated 15 times, for 1800 time steps (of 1 s) each. We examined our model output with a suite of 11 aggregation indices that encompass individual- to population-level characteristics (Table 2). Statistics were based on time averages taken over the second half of each simulation (900 time steps), to avoid undue influence from initial conditions. We report here the results of systematic comparison within a single rule (*e.g.*, drag off *versus* high drag) where the default conditions were medium random force, no drag, piecewise linear attraction/repulsion, constant neighbor scaling, and a rule size of 16. All numbers in text are means, and all statistics are one-way ANOVAs.

In general, over the range of parameter values we used, asocial forces (drag, randomness) had a less drastic effect on fish schooling behavior than did the various functions composing the social force (Fig. 4). Within the range of random force examined, there was no significant effect on any index of aggregation (Fig. 4). The addition of drag slowed fish down and increased the tortuousity of their paths, with a resulting increase in group size (without drag—46 fish/group, with drag—104 fish/group) and cohesion (without drag—1.5BL, with drag—1.1BL). These larger, slower groups milled rather than moving forward (net to gross displacement ratio [NGDR] dropped from 0.5 to 0.1), which decreased polarization. However, once added, there was no difference between the low and high drag condition (Fig. 4).

Social forces had a significant effect on most measures of schooling. Fish with convex attraction-repulsion (A/R) responses stayed closer together and had more tortuous paths than fish with piecewise linear A/R responses. The result was an increase in collisions (convex—720 collisions; piecewise linear—270 collisions; Fig. 4). Polarization was unaffected; it was equally low (83 deg.) for both functions.

Numerical preference had strong effects, both in terms of the number of influential neighbors and how that influence was scaled. Changing the neighbor scaling rule from equal weighting to a negative sigmoid function effectively increased the influence of close neighbors. Fish moved faster and in straighter paths. Schools became smaller (sigmoid—33 fish/group; constant—104 fish/group) and slightly more polarized (sigmoid—70 deg.; constant—83 deg.), but also more diffuse (sigmoid—1.9BL; constant—1.1BL). As a result, collisions decreased (sigmoid—5 collisions; constant—270 collisions). Using a smaller rule size (4 fish) produced equivalent results to negative sigmoid neighbor scaling. Thus a higher number of influential neighbors increases school size at the expense of internal structure (measured as polarization). Paying attention to more neighbors leads to large groups because it causes a

Index	RandomForce Low *(High)*	Drag High *(Low)*	A/R function Convex *(Piecewise linear)*	Neighbor Scaling Logistic *(Constant)*	Rule Size 4 *(16)*
Curvature	◇	↑	↑	↑	◇
Fractal D	◇	◇	↑	↓	◇
NGDR	◇	◇	↓	↑	↑
NND	◇	◇	↓	↑	↑
Grp Size	◇	◇	◇	↓	↓
Expanse	◇	◇	↓	↑	↓
Polar	◇	◇	◇	↑	↑
# groups	◇	◇	◇	↑	↑
# strag	◇	◇	◇	◇	↑
# crashes	◇	↓	↑	↓	↓
IoA	◇	◇	↓	↑	◇

Figure 4. Results of one-way ANOVAs systematically comparing parameter values within a given traffic rule listed as column headings. Within each traffic rule, arrows indicate a significant difference in the index between the listed condition (*e.g.*, rule size, "4" nearest neighbors) to that of the default set in parentheses (one-way ANOVA, $n = 15$, $P < 0.001$). White diamonds indicate no significant difference. Rows are 11 indices of aggregation. Individual level: path curvature, fractal dimension (higher is more tortuous), net to gross displacement ratio (NGDR: higher is straighter), nearest neighbor distance (NND). Group level: group size (in fish), mean distance to group center (or expanse, in body lengths), polarization (lower is more aligned). Population level: number of groups, number of collisions, number of stragglers, and the Clark and Evans (1954) index. See Table 2 for details on how each index was computed.

"network of overlapping influences" (Warburton and Lazarus, 1991): each group member "pulls on" a different set of companions, causing groups to remain cohesive. Over the range of rule size (RS) examined,

$$\text{Group Size} = 3\ \text{RS} - 7\ (\text{df} = 59,\ r^2 = 0.85).$$

Several other higher order properties emerged during our modeling. There was a clear linear relationship between group speed and polarization, across all rule sizes. Faster groups are more polarized (Fig. 5a). We note that there is no preferred speed, so that this is not an inevitable result of a polarized group, but probably reflects the fact that slower groups are composed of individuals with more tortuous paths. We also have begun to examine substructure within groups. At the level of an individual's immediate neighbors (here defined as N1–6), nearest neighbor distance is virtually identical (Fig. 5b), indicating that at this scale, spacing is quite regular. However, when rule size is very large (24 influential neighbors), this relationship breaks down (Fig. 5b), perhaps indicating an upper limit for rule size.

Although our results are preliminary, they highlight some interesting patterns. First, school cohesion and coordinated movement can be partially achieved by positional and numerical preferences, without the need for behavioral matching. This shows that schools might indeed arise by large numbers of simple, overlapping interactions (Warburton and Lazarus, 1991; Romey, 1996). Our preliminary results also indicate that the shapes of the functions used to characterize both positional and numerical preferences are clearly very important (Fig. 4), and worthy of careful investigation in the future. Finally, our results demonstrate the need to consider many different quantitative indices of aggregation when assessing model results (Fig. 4).

Emergent Evolution

A central issue in modeling studies of aggregation is distinguishing between group- and population-level characteristics that are direct, inevitable consequences of the assumptions built into the model, and those that are truly "emergent properties." In an evolutionary context, the im-

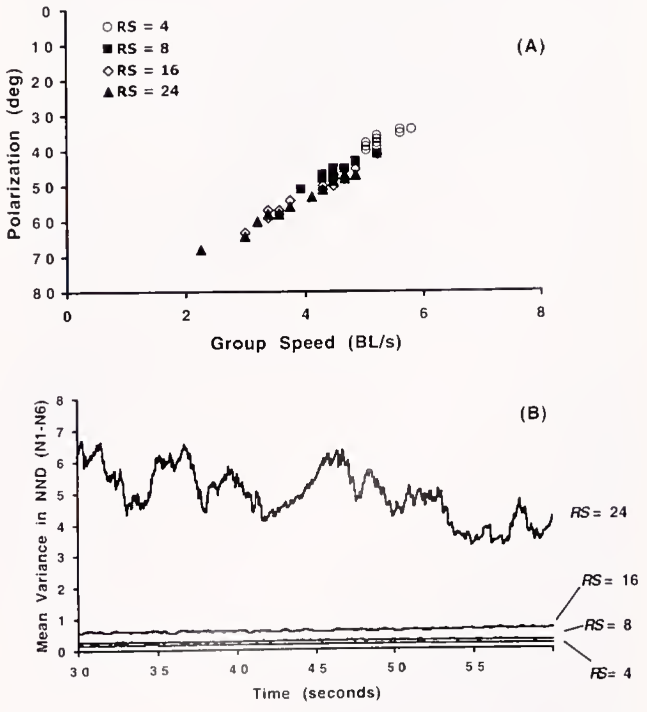

Figure 5. Higher-order index comparisons. (A) Group speed *versus* polarization for rule sizes 4, 8, 16, and 24. (B) Mean variance in the six nearest neighbor distances for individuals in the center of the school, over four rule sizes. Individuals were considered "central" if they were closer to the group center than the median distance to center for the whole group.

portance of this distinction is that emergent properties may be closely tied to indirect behavioral adaptations, which benefit individuals by benefiting the group. To satisfy the definition of emergent properties, the larger system (the group) must possess them, while its components (the individual members) do not (Clark *et al.*, 1997). To a large extent, designating a group characteristic as "emergent" or not is a matter of degree. For instance, models in which individuals actively align their directions to those of neighbors typically produce polarized groups (Huth and Wissel, 1992, 1994; Reuter and Breckling, 1994; Stöcker, 1999), but this is probably too direct an outcome of the assumptions to be considered an emergent property. Dill *et al.* (1997) pose a model in which each fish estimates its time to impact with other fish. In such a system, agents *implicitly* consider their neighbors' orientation, velocity, and position, rather than *explicitly* doing so. Collision avoidance would therefore seem to be a direct outcome and not an emergent property of this model. However, what about the converse: is polarization an emergent property of collision-avoidance behavior?

From a biological perspective, an operational distinction might be to consider whether the group behavior benefits the members *because of their membership*. For example, Grünbaum (1998) used model results to suggest that when individuals simultaneously display gradient-climbing and alignment behaviors in a noisy environment, groups to which they belong more accurately climb environmental gradients, whereas loners can not. If displaying both behaviors is costly to an individual, but it nonetheless benefits by being part of a group in a better environment, this would qualify as emergent under this criterion.

Given the relatively underdeveloped state of schooling behavior models and observations that unify individual, group, and population characteristics, it is unavoidable that studies of the evolutionary "hows and whys" of schooling remain somewhat speculative and oversimplified. Nonetheless, several studies have attempted to incorporate evolutionary ideas into schooling models by allowing iterative improvement of parameters, using an objective function as an analog to "fitness" in the evolutionary sense (Huse and Gjoesaete, 1999; Bonabeau *et al.*, 2000). For instance, Hiramatsu *et al.* (2000) link a standard simulation of schooling (à la Huth and Wissel, 1992) to a genetic algorithm that selects the width of the parallel orientation zone, the size of the blind angle, the number of influential neighbors, and the neighbor scaling rule (front, side, or distance priority, random choice) to maximize fitness. In this case, fitness is modeled as the minimization of four output variables: nearest neighbor distance, polarization, expanse, and fractal dimension. As a result, parallel orientation zone is maximized and blind angle is minimized. A larger question is whether this definition of most fit—that is, least variable—is correct?

Simulation studies like these hinge directly on two questions (1) what is optimal, and (2) what is the relationship between individual and group optimality? Such questions are certain not to have simple or universal answers. It is unlikely that we will soon attain complete, realistic models of an aggregating organism's life history that would allow us to truly represent "fitness" in a population with evolving behaviors. However, we are optimistic about the role of schooling simulations in addressing two central issues raised in this paper. First, we believe model studies will be successful in elucidating the mechanistic relationships between individual-level behavior and the group-level spatial patterns they produce. Second, we expect that the combination of explicit observations of schooling fish, improved simulations of the observed behaviors, and expanded use of statistical indices of aggregation on real and model aggregations will prove sufficient to identify the true behavioral algorithms used by fish.

Acknowledgments

This paper is the result of fruitful interactions with the participants of the CASSLS workshop (*The Limits to Self Organization in Biological Systems*) and the International Ethological Conference symposium (*The Many Facets of Gregariousness*), in particular Jean-Louis Deneubourg, Guy Theraulaz, Charlotte Hemelrijk, and Laurent Dagorn. Kate Litle and Jennifer Weitzman provided invaluable last-minute help. The original manuscript was greatly improved by two anonymous reviewers. This research was supported in part by a National Science Foundation grant to JKP and DG, CCR-9980058.

Literature Cited

Aoki, I. 1982. A simulation study on the schooling mechanism in fish. *Bull. Jpn. Soc. Sci. Fish.* **48:** 1081–1088.

Aoki, I. 1984. Internal dynamics of fish schools in relation to inter-fish distance. *Bull. Jpn. Soc. Sci. Fish.* **50:** 751–758.

Aoki, I., T. Inagaki, and L. van Long. 1986. Measurements of the three-dimensional structure of free-swimming pelagic fish schools in a natural environment. *Bull. Jpn. Soc. Sci. Fish.* **52:** 69–77.

Bonabeau, E., G. Sylvain, D. Snyers, P. Kuntz, and G. Theraulaz. 2000. Three-dimensional architectures grown by simple 'stigmergic' agents. *Biosystems* **56:** 13–32.

Camazine, S., J.-L. Deneubourg, N. R. Franks, J. Sneyd, G. Theraulaz, and E. Bonabeau. 2001. *Self-Organization in Biological Systems.* Princeton University Press, Princeton, NJ.

Clark, P. J., and F. C. Evans. 1954. Distance to nearest neighbor as a measure of spatial relationships in populations. *Ecology* **35:** 445–453.

Clark, M., K. Irwig, and W. Wobke. 1997. Emergent properties of teams of agents in the Tileworld. *Lect. Notes Comput. Sci.* **1209:** 164–176.

Deneubourg, J. L., and S. Goss. 1989. Collective patterns and decision-making. *Ethol. Ecol. Evol.* **1:** 295–311.

Dill, L. M., C. S. Holling, and L. H. Palmer. 1997. Predicting the three-dimensional structure of animal aggregations from functional considerations: the role of information. Pp. 207–224 in *Animal Groups* *in Three Dimensions*, J. K. Parrish and W. M. Hamner, eds. Cambridge University Press, New York.

Flierl, G., D. Grünbaum, S. Levin, and D. Olson. 1999. From individuals to aggregations: the interplay between behavior and physics. *J. Theor. Biol.* **196:** 397–454.

Grünbaum, D. 1998. Schooling as a strategy for taxis in a noisy environment. *Evol. Ecol.* **12:** 503–522.

Grünbaum, D., and A. Okubo. 1994. Modelling social animal aggregations. Pp. 296–325 in *Frontiers in Theoretical Biology: Lecture Notes in Biomathematics*, Vol. 100, S. A. Levin, ed. Springer-Verlag, New York.

Gueron, S., S. A. Levin, and D. I. Rubenstein. 1996. The dynamics of herds: from individuals to aggregations. *J. Theor. Biol.* **182:** 85–98.

Hillier, B., and J. Hanson. 1990. *The Social Logic of Space.* Cambridge University Press, New York.

Hiramatsu, K., S. Shikasho, and K. Mori. 2000. Mathematical modeling of fish schooling of Japanese medaka using basic behavioral patterns. *J. Fac. Agric. Kyushu Univ.* **45:** 237–253.

Huse, G., and H. Gjoesaete. 1999. A neural network approach for predicting stock abundance of the Barents Sea capelin. *Sarsia* **84:** 457–464.

Huth, A., and C. Wissel. 1990. The movement of fish schools: a simulation model. Pp. 578–590 in *Biological Motion: Lecture Notes in Biomathematics*, Vol. 89, W. Alt and G. Hoffman, eds. Springer, Berlin.

Huth, A., and C. Wissel. 1992. The simulation of the movement of fish schools. *J. Theor. Biol.* **156:** 365–385.

Huth, A., and C. Wissel. 1994. The simulation of fish schools in comparison with experimental data. *Ecol. Model.* **75:** 135–145.

Latané, B., J. Liu, A. Nowak, M. Bonavento, and L. Zheng. 1995. Distance matters: physical space and social influence. *Pers. Soc. Psych. Bull.* **21:** 795–805.

Norris, K. S., and C. R. Schilt. 1988. Cooperative societies in three-dimensional space: on the origins of aggregations, flocks, and schools, with special reference to dolphins and fish. *Ethol. Sociobiol.* **9:** 149–179.

Parrish, J. K. 1989. Re-examining the selfish herd: are central fish safer? *Anim. Behav.* **38:** 1048–1053.

Parrish, J. K. 1992. Do predators 'shape' fish schools: interactions between predators and their schooling prey. *Neth. J. Zool.* **42:** 358–370.

Parrish, J. K. 1993. Comparison of the hunting behavior of four piscine predators attacking schooling prey. *Ethology* **95:** 233–246.

Parrish, J. K., and L. Edelstein-Keshet. 1999. Complexity, pattern, and evolutionary trade-offs in animal aggregation. *Science* **284:** 99–101.

Parrish, J. K., and L. Edelstein-Keshet. 2000. Reply to Danchin and Wagner. *Science* **287:** 804–805.

Parrish, J. K., and P. Turchin. 1997. Individual decisions, traffic rules, and emergent pattern in schooling fish. Pp. 126–142 in *Animal Groups in Three Dimensions*, J. K. Parrish and W. M. Hamner, eds. Cambridge University Press, New York.

Partridge, B. L., and T. J. Pitcher. 1980. The sensory basis of fish schools: relative roles of lateral line and vision. *J. Comp. Physiol.* **135:** 315–325.

Partridge, B. L., J. Johansson, and J. Kalisk. 1983. Structure of schools of giant bluefin tuna in Cape Cod Bay. *Environ. Biol. Fishes* **9:** 253–262.

Pitcher, T. J., and J. K. Parrish. 1993. Functions of shoaling behavior in teleosts. Pp. 363–439 in *Behaviour of Teleost Fishes*, 2nd ed. Chapman and Hall, London.

Reuter, H., and B. Breckling. 1994. Self-organization of fish schools: an object-oriented model. *Ecol. Model.* **75:** 147–159.

Romey, W. L. 1996. Individual differences make a difference in the trajectories of simulated schools. *Ecol. Model.* **92:** 65–77.

Schilt, C. R., and K. S. Norris. 1997. Perspectives on sensory integration systems: problems, opportunities, and predictions. Pp. 225–244 in *Animal Groups in Three Dimensions*, J. K. Parrish and W. M. Hammer, eds. Cambridge University Press, Cambridge, UK.

Shaw, E. 1978. Schooling fishes. *Am. Sci.* **66:** 166–175.

Stöcker, S. 1999. Models for tuna school formation. *Math. Biosci.* **156:** 157–190.

Vabø, R., and L. Nøttestad. 1997. An individual-based model of fish school reactions: predicting antipredator behaviour as observed in nature. *Fish. Oceanogr.* **6:** 155–171.

Videler, J. J. 1993. *Fish Swimming.* Chapman & Hall, London. 260p.

Warburton, K., and J. Lazarus. 1991. Tendency-distance models of social cohesion in animal groups. *J. Theor. Biol.* **150:** 473–488.

Weihs, D. 1973. Hydromechanics of fish schooling. *Nature* **241:** 290–291.

Wilson, E. O. 1975. *Sociobiology: The New Synthesis.* Harvard University Press, Cambridge. 672p.

Reference: *Biol. Bull.* **202:** 306–313. (June 2002)

Individual Complexity and Self-Organization in Foraging by Leaf-Cutting Ants

FLAVIO ROCES

Zoologie II, Universität Würzburg, Biozentrum, Am Hubland, D-97074 Würzburg, Germany

Abstract. Leaf-cutting ants cut vegetation into small fragments that they transport to the nest, where a symbiotic fungus cultivated by the ants processes the material. Since the harvested leaf fragments are incorporated into the fungus garden and not directly consumed by the workers, it is expected that foraging workers select plants by responding to those physical or chemical traits that promote maximal fungal growth, irrespective of the potential direct effects of these leaf features on them. In this paper I summarize experimental work focusing on the decision-making processes that occur at the individual level, and discuss to what extent individual complexity contributes to the emergence of collective foraging patterns. Although some basic features of self-organizing systems, such as the existence of regulatory positive and negative feedback loops, are expected to be involved in the collective organization of leaf-cutting ant foraging, I contend that they are combined with complex individual responses that may result from the integration of local information during food collection with an assessment of colony conditions.

Social Foraging in Leaf-Cutting Ants: Self-Organized?

Leaf-cutting ants are the dominant herbivores in the Neotropics. They cut vegetation into small fragments that they transport to the nest, which may contain over a million workers. To support these large colonies, workers search out and harvest plant species that are suitable for the development of the colony's resident symbiotic fungus. Adults obtain more than 90% of their energy requirements during foraging from the plant sap of the cut material (Littledyke and Cherrett, 1976). The fungus garden, which represents the sole food source of the developing brood, appears to be responsible for the ability of the ants to utilize most of the available plant species. Since the harvested leaf fragments are incorporated into the fungus garden and not directly consumed by the workers, it is conceivable that ants and fungus have conflicting requirements for the quality of the plants to be harvested. On the one hand, ant workers may prefer resources that support maximal rates of fungus growth, more or less irrespective of the attractiveness of the plant sap being imbibed during the harvesting process. On the other hand, workers may base decisions about the quality of a given resource on the immediate availability of energy to support their foraging activity. Given these two different demands, the herbivory patterns of leaf-cutting ants can be understood only by investigating the measures used by foraging workers when making decisions and the extent to which the behavior of the individuals is influenced by the state of the symbiotic fungus. For that, emphasis should be put on both the kind of information workers use during foraging and the integration of individual responses that results in the emergence of a collective pattern. Leaf-cutting ants appear to be well suited to analyze this interplay between individual and social aspects of foraging. At the individual level, information is available about the rules used by workers to decide on the size of the leaf fragment to be cut (Roces, 1990a; Wetterer, 1990, 1991a; Burd, 1995, 1996). At the colony level, studies have provided details about plant selection and foraging activity of colonies in the field (*e.g.*, Howard, 1990, 1991; Nichols-Orians and Schultz, 1990).

In trying to understand the contribution of regulated, self-organizing processes to the emergence of collective foraging patterns in colonies of leaf-cutting ants, it is im-

---

E-mail: roces@biozentrum.uni-wuerzburg.de

This paper was originally presented at a workshop titled *The Limits to Self-Organization in Biological Systems*. The workshop, which was held at the J. Erik Jonsson Center of the National Academy of Sciences, Woods Hole, Massachusetts, from 11–13 May 2001, was sponsored by the Center for Advanced Studies in the Space Life Sciences at the Marine Biological Laboratory, and funded by the National Aeronautics and Space Administration under Cooperative Agreement NCC 2-896.

portant first to draw attention to three features of the colony-level foraging patterns that would not, *a priori*, be expected. First, workers show strong preferences for a few plant species but persist in harvesting numerous species that remain, in a consistent way, only slightly preferred (Rockwood, 1976). Second, plants are usually abandoned before they are completely defoliated, even those that are ranked among the most preferred (Cherrett, 1968; Fowler and Stiles, 1980). Third, ants travel long distances on foraging trails to reach plant resources, with individual round-trips lasting several hours; and they bypass conspecific plants of apparently equal quality located much closer to the colony (Cherrett, 1983).

To explain such complex foraging patterns, three hypotheses have been advanced. The optimal foraging hypothesis (Fowler and Stiles, 1980; Rockwood and Hubbell, 1987) suggests that the observed patterns are the result of workers foraging to maximize the rate of resource delivery. According to that reasoning, a distant plant of moderate quality located close to an existing foraging trail may provide a higher return than a nearby plant of much higher quality, but at some distance from a trail. Thus workers may abandon plants being harvested when a new plant offering a higher rate of return is found. The resource conservation hypothesis (Cherrett, 1983) suggests that the ants limit the damage caused to highly preferred or nearby resources, thus conservatively managing resources over the lifespan of their colony. Finally, the nutrient balance hypothesis (Powell and Stradling, 1991; Stradling and Powell, 1992) contends that the harvested resources represent a complementary diet for the symbiotic fungus, so that ants are expected to seek out a variety of plants to provide the fungus with an appropriate mix of nutrients and to avoid high levels of any single toxic secondary plant compound.

As predicted by Howard (1991), it has proven difficult to evaluate the extent to which colony-level foraging patterns are uniquely explained by any one of these hypotheses. Moreover, the mechanisms underlying the short- and long-term dynamics of plant selectivity are completely unknown. Are self-organizing processes able to account for such complexity in pattern formation, without the need to invoke complexity in the decision-making processes at the individual level? In recent years, investigations of self-organization in biological systems have suggested that social insect colonies often work as a decentralized system composed of cooperative, more or less autonomous units distributed in the environment that manage local information and exhibit simple probabilistic stimulus-response behavior (Bonabeau *et al.*, 1997). My present contribution focuses on both the decision-making processes observed in individual leaf-cutting ant workers and the integration of individual behavior into colony function. I shall first describe the kind of information single workers use to make decisions about resource quality, and then discuss the emergence of collective patterns and to what extent regulatory, self-organizing processes may be involved.

Decision Making During Foraging: Individual Complexity

In the field, scout workers from a colony of leaf-cutting ants search for suitable resources and, upon discovery, they decide whether a given resource is worth communicating to other nestmates. Plant selectivity is mainly based on both chemical and physical features of the leaves (Howard, 1987; Nichols-Orians and Schultz, 1990). If the source is attractive, workers may decide to return to the nest, laying a chemical trail, or to cut a fragment and carry it back to the nest. Polymorphic leaf-cutting ant foragers frequently harvest leaf pieces that correspond in mass to that of their own bodies (Lutz, 1929; Cherrett, 1972). This, in part, results from the geometric method of leaf cutting. Since workers anchor on the leaf edge by their hind legs and pivot around them while cutting arcs out of the leaves, the load-size selected may be directly determined by a fixed reach while cutting, dependent on worker body size (Weber, 1972). However, there is evidence that not all workers cut fragments as large as they are able to, which suggests a more flexible mechanism of load-size selection in leaf-cutting ants. For instance, foraging distance was shown to affect load-size selection in *Acromyrmex lundi*—ants cut larger fragments farther from the nest (Roces, 1990a)—but not in *Atta cephalotes* (Wetterer, 1991b). For an ant of a given size, Cherrett (1972), Rudolph and Loudon (1986), Roces and Hölldobler (1994), and Burd (1995) found a negative correlation between leaf area density (leaf mass/leaf area) and the size of the harvested fragment.

To understand these decision rules, it should be emphasized that in species with recruitment communication, foraging behavior includes not only the collection of food but also the transmission of information about its location and quality. Because colony food intake is increased through recruitment communication, even at the expense of reduced foraging performance of the individuals, there may be a trade-off between time spent either in acquiring food or in recruiting nestmates, especially during the initial phase of exploiting a food source. This interplay between food-collection behavior and recruitment behavior was analyzed in leaf-cutting ants under controlled experimental conditions (Roces, 1993; Roces and Núñez, 1993). The question of whether the information about food quality obtained during recruitment communication influences the cutting behavior of recruited workers was addressed in an attempt to integrate individual behavior into colony function. Attention was not centered on the successful scout ant that initiated recruitment, but on the behavior of recruited workers that were confronted with standardized stimuli rather than with the original food source. Their responses to these stimuli were compared after they were informed about food sources of different qualities.

The rationale of the experimental approach was as follows: in independent assays, scout workers of the leaf-cutting ant *Acromyrmex lundi* were first exposed to droplets of scented sugar solution of either 1% or 10% sucrose. Scouts detected these droplets and returned to the colony, leaving a chemical recruiting trail. When the recruited workers arrived, they encountered, not sugar solution, but sheets of Parafilm impregnated with the same scent, containing no sugar. Since all recruited workers found the same standardized material (Parafilm as a pseudo-leaf), differences in cutting behavior between the groups must be the result of the information transmitted by the scout worker that initially found the sugar solution (Roces and Núñez, 1993).

Several behavioral parameters of the recruited workers were observed to depend on the information about food quality they received from a single recruiting scout. Workers recruited by scouts that found 10% sucrose will be referred to as "10%-workers," and those recruited by scouts that found 1% sucrose as "1%-workers", but it should remain clear that both groups encountered a sugar-free pseudo-leaf at the source. The 10%-workers (*i.e.*, those recruited to the better food source) cut smaller fragments of Parafilm, returned to the nest at higher velocities, and displayed more active recruiting behavior (by laying chemical trails) than 1%-workers. In another experiment, recruited workers were confronted with small pieces of paper of a homogeneous size. They still traveled at a faster pace if they had been recruited by 10%-scouts, indicating that the differences in speed found in the previous experiment were *not* caused by differences in loading. More interesting, greater velocity did not compensate for the reduction in fragment size: 10%-workers, despite their higher velocity, showed a lower rate of leaf transport to the nest than 1%-workers (Roces and Núñez, 1993).

These results contradicted the most obvious functional hypotheses and led to a vivid discussion (Kacelnik, 1993; Clark, 1994; Roces, 1994a; Ydenberg and Schmid-Hempel, 1994). Different hypotheses were examined. The "delivery rate maximization hypothesis" would suggest that a behavioral strategy leading to maximum rate of leaf delivery is independent of real or expected sugar content. Since 10%- and 1%-workers behaved in a different manner when cutting the pseudo-leaf, they could not have maximized leaf delivery rate in both treatments. Workers could, however, have been maximizing a compromise between leaf delivery rate and some unknown costs associated with travel speed. If such a cost exists, 10%-workers may pay it (*i.e.*, may run faster) if the value of the food source is greater. Thus they would achieve a higher rate of leaf delivery for a high-quality resource. Indeed, 10%-workers were observed to run faster, but why did they cut smaller fragments? The outlined hypothesis failed to explain these changes in cutting behavior.

An alternative hypothesis, called the "information transfer hypothesis," (Roces and Núñez, 1993) focused on the recruitment strategies of workers, and was based on the original proposition advanced by Núñez (1982) when analyzing partial crop-filling and foraging behavior in honey bees (see also Varjú and Núñez, 1991, 1993; Schmid-Hempel, 1993, for a detailed discussion about honey bee foraging). The idea was that the decision to transfer information about a newly discovered food source motivates a worker to shorten its cutting behavior and to return to the nest sooner to recruit additional nestmates. A worker sacrifices its individual leaf delivery rate, but the colony as a whole increases its harvesting rate due to the recruited workers that joined in the resource-gathering activity (Roces and Núñez, 1993). This hypothesis was consistent with the higher travel speed and the reduced leaf fragment size in 10%-workers. By cutting smaller fragments, 10%-workers saved cutting time; and by increasing speed, they saved travel time. This hypothesis could, in addition, accommodate the more intense trail-marking behavior observed in 10%-workers.

Further support for the information transfer hypothesis was obtained by analyzing the behavior of recruited workers in more detail, addressing the changes in worker responses after the perception of recruitment signals (Roces, 1993). The behavioral responses of recruited workers have rarely been investigated in ants (Beckers *et al.*, 1992), despite the fact that they are responsible for the amplification and establishment of a recruitment process. The experimental approach was similar to that outlined above. Attention was not centered on the successful scout ant that initiated recruitment, but on the behavior of recruited workers that were confronted with standardized stimuli rather than with the original food source. Their responses to these stimuli were compared after they were informed about food sources of different qualities. Scout workers of the leaf-cutting ant *Acromyrmex lundi* were first exposed to droplets of scented sucrose solution of different concentrations. Once at the source, recruited workers encountered, not sugar solution, but standardized paper discs impregnated with the same scent. Paper discs were either untreated or had sugar added in order to increase their quality. Comparison between assays using untreated and sugared discs of the same weight allowed a distinction between workers' responses based on the information they obtained during recruitment (which was similar for workers recruited to a given sucrose solution), and those that resulted from their actual evaluation of the disc quality (untreated or sugared disc). In a subsequent experimental series, paper discs of different masses were offered to analyze the effects of load mass on foraging decisions (Roces, 1993).

The information about resource quality transferred by a single scout ant had several effects on the behavioral responses of recruited workers. The more concentrated the solution found by the initial scout, the faster the recruited workers ran to the source, even though they had no contact with the sucrose solution. After collecting the standardized (untreated) paper discs, the workers also ran faster, the more concentrated the sugar solution initially found by the scout ant. In other words, travel speed of recruited workers to and from the nest depended on the information they received about resource quality. As intuitively expected, disc-laden workers ran more slowly than outbound workers. This reduction in speed, however, could not be attributed to the effects of the load itself, since workers collecting discs of the same weight, but with sugar added, ran as rapidly as outbound, unladen workers.

Workers collecting sugared discs were observed to reinforce the chemical trail on their way to the nest. The percentage of trail-layers was higher when workers were recruited to 10% sugar solution than to 1%, despite the collection of the same kind of discs at the source. These facts indicate that workers' own evaluation of resource quality depended on the perception of recruitment signals. Such differences in responsiveness to the same stimulus (a given sugared disc) can therefore be attributed to variations in the worker's motivational state as a result of the information they received during recruitment (Roces, 1993).

The observed decrease in speed after the collection of a nonsugared disc, which could be intuitively attributed to an effect of the load carried, turned out to be the result of a reduced motivation of workers to carry such a material when they have been informed about a high-quality resource (a given sugar solution). That the load itself had no effect on velocity was demonstrated when workers recruited to the same sugar solutions collected sugared discs of the same weight. In this situation, no reduction in velocity was observed. The reduction in speed suggests, therefore, that workers, through the information received during recruitment, may have expected to find a resource of a given quality, and their expectation was not confirmed by the collection of a nonsugared disc. Even when workers were recruited to a sugar concentration of 50%, to which they ran with the highest speed recorded, they never reinforced the chemical trail after the collection of a standard, nonsugared disc, and their velocity turned out to be lower after collection. Those that found sweet discs of the same weight, however, reinforced the trail, and showed no reduction in speed (Roces, 1993).

These results point out the importance of considering the motivational state of foraging workers when their behavior is under scrutiny. This aspect has been largely disregarded in the literature on insect behavior, despite early observations that flight velocity of outgoing (unladen) honey bees depends on the concentration of the sugar solution they collect (Frisch and Lindauer, 1955). Changes in the workers' motivational state that depend on differences in resource quality are also suggested from measurements in honey bees collecting at different flow rates of sugar solution (Núñez, 1982; Balderrama *et al.*, 1992; Moffatt, 2000) or sugar solutions of different concentrations (Seeley, 1986; Stabentheiner and Hagmüller, 1991).

Why do recruited workers run faster when they have been informed about a richer source? The adaptive value of this response might be assigned to the importance of a rapid transmission of information about a newly discovered food source. Workers arriving earlier to the nest can induce nestmates to follow the trail, for instance *via* tactile stimulation. At the initial phases of trail development, saving time would be of great importance, in order to monopolize a food source as soon as possible. The evaluation of resource quality by recruited workers and, therefore, the probability of reinforcing the chemical trail are, in part, dependent on the information they received; that is, recruits seem to partially rely on the decisions of the first successful ants to amplify a recruitment process. That their decisions appear to be "channeled" by those of the scouts, which may be responsible for the integration of local signals with more general information about resource quality and colony (fungus) conditions, remains to be investigated (see below). This interindividual variability during decision making (see also Jaffé *et al.*, 1985) may be related to both the complexity of food assessment by leaf-cutting ants and the need for rapid responses to monopolize newly discovered sources.

As mentioned above, *Acromyrmex lundi* workers recruited to rich food sources cut smaller fragments than those recruited to poorer ones (Roces and Núñez, 1993), although both groups found the same standard material at the source. This behavior, unexpected from an individual point of view, also indicates that, in the initial phases of trail development, workers rely in part on the decisions made by the first successful scout workers. By cutting smaller fragments, they save time at the source and run back sooner to inform about it through reinforcement of the chemical trail (Roces and Núñez, 1993); this decision-making system ensures a rapid build-up of workers to exploit the discovered source. That this complexity in individual decision making indeed affects the development of colony-level foraging patterns was demonstrated under controlled laboratory conditions by comparing the foraging behavior of satiated and harvesting-deprived workers (Roces and Hölldobler, 1994). Harvesting-deprived workers cut smaller leaf fragments than did satiated workers, a fact that appears counter-intuitive at the individual level. This reduction in fragment size was observed only in the initial phases of a recruitment process, when information about the discovery is worth transferring. And in fact, these responses correlated with the intensity of recruitment: harvesting-deprived workers showed higher recruitment rates than did satiated workers (Roces and Hölldobler, 1994).

Individual Behavior and Colony Function

As discussed above, leaf-cutting ant workers are central-place foragers (Orians and Pearson, 1979), since they deliver resources to the nest. As a consequence, they may be expected to maximize the rate of resource delivery to this central place. For social insects in general, the analysis of worker responses in the framework of optimality theory is particularly complex because the maximizing agent is the colony as a whole and not necessarily each individual worker. Thus, if the foraging performance of the colony is enhanced through recruitment communication, one could expect a trade-off between time spent by the individuals in collecting food and time spent recruiting, even at the expense of a reduction in the foraging performance of the individual. In fact, it has been shown that leaf-cutting ant workers rarely maximize either their individual gross rate of leaf delivery to the nest or their individual energetic efficiency (Roces and Núñez, 1993; Burd, 1996), suggesting that performance is maximized at the colony level.

Interpretation of individual foraging performance, and particularly its extension to assess foraging efficiency at the colony level, is further complicated by the fact that a considerable percentage of leaf-cutting ant workers on an active foraging trail return to the nest unladen (between 13% and 75%, Hodgson, 1955; Cherrett, 1972; Lugo *et al.*, 1973; Lewis *et al.*, 1974b). Although a number of these unladen workers can be involved in trail-clearing (Daguerre, 1945) or transport of plant sap (Stradling, 1978), others seem to be engaged in the reinforcement of the chemical trail or in a combination of recruiting and food transport (Jaffé and Howse, 1979). In addition, worker responses may differ at different times during the beginning of a daily foraging cycle (laboratory experiments: Roces and Hölldobler, 1994; field experiments: Bollazzi and Roces, 2001), or when foraging behavior is scrutinized along established foraging trails (Burd, 2000) where the role of recruitment communication in regulating collective foraging has not been clearly understood.

How are the individual responses integrated to generate a collective response? At the colony level, foraging patterns and the selection of suitable plants are particularly complex. Mature colonies have a number of well-established foraging trails that radiate from the nest. Several trails leading to different plants are usually active during a daily foraging cycle (Cherrett, 1968), with outgoing workers leaving the nest using these different trails more or less simultaneously (Lutz, 1929). It is unclear what kind of environmental cues, colony cues, or both trigger the start of a daily foraging cycle (Lewis *et al.*, 1974a,b). Simultaneous exploitation of different food sources has been observed in large colonies of several social insects. For honey bees and ants, it has been shown that self-organizing processes are involved in the collective choice between two simultaneously available patches that differ in quality (Beckers *et al.*, 1990; Seeley *et al.*, 1991). Such collective decision making works well, even though individual workers manage local information and do not directly compare the two alternatives. Laboratory colonies of leaf-cutting ants, over very short distances of at most 1 meter, rapidly exploit available resources and select the most attractive one (Jaffé and Howse, 1979), with the collective patterns being reproduced by models based on simple decision rules and regulatory feedback mechanisms (Jaffé, 1980). Such "explosive" processes may be relevant under these reduced conditions, but may play a minor role under field conditions. In the field, colonies of leaf-cutting ants were observed to repeatedly attack the same individual plants over days, without completely defoliating them, and then move on to others, returning to the former ones after several days (Fowler and Stiles, 1980). This apparent conservative management of resources is probably brought about by the responses of foraging workers to the differences in the relative quality of the vegetation being harvested. Whether the palatability of the plants changes after leaf-cutting attack, a fact that may account for the dynamics of plant choice, was not clearly demonstrated; and experimental evidence indicates that this is not the case for some species (Vasconcelos, 1997). In addition, leaf-cutting ant workers show trail fidelity, with workers choosing the same trail out of the nest over days (Shepherd, 1982). Taken together, trail fidelity by workers and the long time intervals that mediate the changes in foraging activity along particular trails (in the range of days or weeks) make it unlikely that plant selectivity is based on competing self-organizing foraging processes that occur at the nest, as has been described for a small number of ant species under controlled laboratory conditions (*e.g.*, Beckers *et al.*, 1990). It is more likely that scout workers visiting different food sources at the end of, or close to, existing trails may base their decision on whether to lay chemical trails on both the resource quality actually perceived and on the information about colony needs.

It is still unclear how foraging workers assess (and respond to) the state of the symbiotic fungus. Recent evidence indicates that changes in plant selectivity by workers strongly depend on the effects of the previously collected material on fungal growth, suggesting that foraging workers manage information about the actual state of their symbiotic fungus when selecting a plant outside the nest (see below). Since foraging workers do not directly process the collected leaf fragments, but instead transfer them to a "working chain" inside the nest, their responses are expected to be ultimately controlled by regulatory feedback loops involving information transfer between fungus and gardening workers, and between gardening workers and foragers.

Perspective

Plant material harmful to the fungus may cause foraging workers to cease harvesting of these plants. Once the colony has commenced rejecting a particular plant material, it will continue to refuse it for days or even weeks, a phenomenon called "delayed rejection" (Knapp *et al.*, 1990). As mentioned above, it has been demonstrated that leaf-cutting ants learn to reject plant material that contains chemicals harmful to the fungus (Ridley *et al.*, 1996; North *et al.*, 1997). Ridley *et al.* (1996) provided bait containing a fungicide, which was initially carried into the nest by the foragers. Eventually, workers stopped foraging on the bait, and this rejection was maintained for weeks. Interestingly, these colonies also rejected bait that contained no fungicide, so that the authors hypothesized that if the substrate causes toxic effects on the fungus, the fungus will produce a chemical signal that acts as a negative reinforcement to the ant servicing that particular fungus garden. North *et al.*, (1999) attempted to trace the pathway of this putative fungal signal. Their results suggest that a signal produced by the fungus does not affect the foragers directly, but indirectly *via* nest workers that interact with the fungus. Indeed, some of their results suggest that the information is transferred from smaller fungus-garden workers to the larger foraging workers. This putative chemical signal produced by the fungus has not been identified, and the authors discuss an alternative hypothesis that rejection may occur when ants detect fungal breakdown products from unhealthy or dead fungus. The workers would then associate dead fungus with the flavors of the treated bait. In fact, it is known that leaf-cutting ants learn the odors associated with food (Roces, 1990b, 1994b; Howard *et al.*, 1996).

These considerations show that we are far from understanding the regulation of foraging behavior and the emergence of collective, colony-level responses. Although some basic features of self-organizing systems, such as the existence of regulatory positive and negative feedback loops, are expected to be involved in the collective organization of foraging by leaf-cutting ants (Jaffé and Howse, 1979), individual responses appear to be particularly complex. And this seems also to be the case for the organization of social foraging in fire ants, which was described 40 years ago (Wilson, 1962) and has repeatedly been discussed as an example of decentralized colonial decision making. Even though collective responses ("mass recruitment") are organized by information transmitted from one group of individuals to another, recent evidence indicates that individual ants are able to display a complex array of modulatory communication signals that influence the development of such collective responses (Cassill, 2001).

As recently asserted by Deneubourg *et al.* (1999), self-organization and individual complexity need not be mutually exclusive processes. I propose that, to understand to what extent individual complexity contributes to generating a collective pattern, we should rise to the challenge of integrating theoretical arguments with empirical research, focusing on the precise mechanisms underlying individual decision making and collective responses in large ant colonies. In particular, elucidating how leaf-cutting ants perceive changes in fungal productivity and use this information to alter their own quality criteria for plant selection remains a major challenge in understanding their individual foraging behavior, and ultimately their herbivory patterns.

Acknowledgments

I thank Josué A. Núñez for tireless discussion and helpful comments, Bert Hölldobler for discussion and support, Tom Seeley for comments that improved the manuscript, and the participants of the Woods Hole meeting "The Limits to Self-organization in Biological Systems" for insights and exchange. The experimental work reported here was possible through financial funds provided by the DFG (SFB 567/TP C4).

Literature Cited

Balderrama, N., L. O. Almeida de B, and J. A. Núñez. 1992. Metabolic rate during foraging in the honeybee. *J. Comp. Physiol. B.* **162:** 440–447.

Beckers, R., J. L. Deneubourg, S. Goss, and J. M. Pasteels. 1990. Collective decision making through food recruitment. *Insectes Soc.* **37:** 258–267.

Beckers, R., J. L. Deneubourg, and S. Goss. 1992. Trail laying behaviour during food recruitment in the ant *Lasius niger* (L.). *Insectes Soc.* **39:** 59–72.

Bollazzi, M., and F. Roces. 2001. The control of foraging decisions in leaf-cutting ants: individual vs. collective aspects. P. 20 in *Berlin Meeting of the European Sections of IUSSI*, R. Menzel and E. Rademacher, eds. Free University Berlin, Berlin.

Bonabeau, E., G. Theraulaz, J.-L. Deneubourg, S. Aron, and S. Camazine. 1997. Self-organization in social insects. *TREE* **12:** 188–193.

Burd, M. 1995. Variable load size-ant size matching in leaf-cutting ants, *Atta colombica* (Hymenoptera: Formicidae). *J. Insect Behav.* **8:** 715–722.

Burd, M. 1996. Foraging performance by *Atta colombica*, a leaf-cutting ant. *Am. Nat.* **148:** 597–612.

Burd, M. 2000. Foraging behavior of *Atta cephalotes* (leaf-cutting ants): an examination of two predictions for load selection. *Anim. Behav.* **60:** 781–788.

Cassill, D. 2001. Distributed intelligence: a mechanism for social organization in an unpredictable environment. In *The Limits to Self-organization in Biological Systems* [online], Center for Advanced Studies in the Space Life Sciences at the Marine Biological Laboratory, Woods Hole, MA. Available: http://www.mbl.edu/CASSLS/deby_cassill.htm [11 Feb. 2002]

Cherrett, J. M. 1968. The foraging behaviour of *Atta cephalotes* L. (Hymenoptera: Formicidae). I. Foraging patterns and plant species attacked in tropical rain forest. *J. Anim. Ecol.* **37:** 387–403.

Cherrett, J. M. 1972. Some factors involved in the selection of vegetable substrate by *Atta cephalotes* (L.) (Hymenoptera: Formicidae) in tropical rain forest. *J. Anim. Ecol.* **41:** 647–660.

Cherrett, J. M. 1983. Resource conservation by the leaf-cutting ant *Atta cephalotes* in tropical rain forest. Pp. 253–263 in *Tropical Rain Forest:*

Ecology and Management, S. L. Sutton, T. C. Whitmore, and A. C. Cahdwick, eds. Blackwell Scientific Publications, Oxford.

Clark, C. W. 1994. Leaf-cutting ants may be optimal foragers. *TREE* **9:** 63.

Daguerre, J. B. 1945. Hormigas del género *Atta* Fabricius de la Argentina (Hymenop. Formicidae). *Rev. Soc. Entomol. Argent.* **12:** 438–460.

Deneubourg, J., S. Camazine, and C. Detrain. 1999. Self-organization or individual complexity: a false dilemma or a true complementarity. Pp. 401–407 in *Information Processing in Social Insects*, C. Detrain, J. L. Deneubourg, and J. M. Pasteels, eds. Birkhäuser Verlag, Basel.

Fowler, H. G., and E. W. Stiles. 1980. Conservative resource management by leaf-cutting ants? The role of foraging territories and trails, and environmental patchiness. *Sociobiology* **5:** 25–41.

Frisch, K. V., and M. Lindauer. 1955. Über die Fluggeschwindigkeit der Bienen und über ihre Richtungsweisung bei Seitenwind. *Naturwissenschaften* **42:** 377–385.

Hodgson, L. D. 1955. An ecological study of the behavior of the leaf-cutting ant *Atta cephalotes*. *Ecology* **36:** 293–304.

Howard, J. J. 1987. Leafcutting ant diet selection: the role of nutrients, water, and secondary chemistry. *Ecology* **68:** 503–515.

Howard, J. J. 1990. Infidelity of leafcutting ants to host plants: resource heterogeneity or defense induction? *Oecologia* **82:** 394–401.

Howard, J. J. 1991. Resource quality and cost in the foraging of leaf-cutter ants. Pp. 42–50 in *Ant-plant Interactions*, C. R. Huxley and D. F. Cutler, eds. Oxford University Press, Oxford.

Howard, J. J., M. L. Henneman, G. Cronin, J. A. Fox, and G. Hormiga. 1996. Conditioning of scouts and recruits during foraging by a leaf-cutting ant, *Atta colombica*. *Anim. Behav.* **52:** 299–306.

Jaffé, K. 1980. Theoretical analysis of the communication system for chemical mass recruitment in ants. *J. Theor. Biol.* **84:** 589–609.

Jaffé, K., and P. E. Howse. 1979. The mass recruitment system of the leaf cutting ant, *Atta cephalotes* (L.). *Anim. Behav.* **27:** 930–939.

Jaffé, K., G. Villegas, O. Colmenares, H. Puche, N. A. Zabala, M. I. Alvarez, J. G. Navarro, and E. Pino. 1985. Two different decision-making systems in recruitment to food in ant societies. *Behaviour* **92:** 9–21.

Kacelnik, A. 1993. Leaf-cutting ants tease optimal foraging theorists. *TREE* **8:** 346–348.

Knapp, J. J., P. E. Howse, and A. Kermarrec. 1990. Factors controlling foraging patterns in the leaf-cutting ant *Acromyrmex octospinosus* (Reich). Pp. 382–409 in *Applied Myrmecology—A World Perspective*, R. K. Vander Meer and K. Jaffé, eds. Westview Press, Boulder, CO.

Lewis, T., G. V. Pollard, and G. C. Dibley. 1974a. Micro-environmental factors affecting diel patterns of foraging in the leaf-cutting ant *Atta cephalotes* (L.) (Formicidae: Attini). *J. Anim. Ecol.* **43:** 143–153.

Lewis, T., G. V. Pollard, and G. C. Dibley. 1974b. Rhythmic foraging in the leaf-cutting ant *Atta cephalotes* (L.) (Formicidae: Attini). *J. Anim. Ecol.* **43:** 129–141.

Littledyke, M., and J. M. Cherrett. 1976. Direct ingestion of plant sap from cut leaves by the leaf-cutting ants *Atta cephalotes* (L.) and *Acromyrmex octospinosus* (Reich) (Formicidae, Attini). *Bull. Entomol. Res.* **66:** 205–217.

Lugo, A. E., E. G. Farnworth, D. Pool, and P. Jerez. 1973. The impact of the leaf cutter ant *Atta colombica* on the energy flow of a tropical wet forest. *Ecology* **54:** 1292–1301.

Lutz, F. E. 1929. Observations on leaf-cutting ants. *Am. Mus. Novit.* **388:** 1–21.

Moffatt, L. 2000. Changes in the metabolic rate of the foraging honeybee: effect of the carried weight or of the reward rate? *J. Comp. Physiol. A* **186:** 299–306.

Nichols-Orians, C. M., and J. C. Schultz. 1990. Interactions among leaf toughness, chemistry, and harvesting by attine ants. *Ecol. Entomol.* **15:** 311–320.

North, R. D., C. W. Jackson, and P. E. Howse. 1997. Evolutionary aspects of ant-fungus interactions in leaf-cutting ants. *TREE* **12:** 386–389.

North, R. D., C. W. Jackson, and P. E. Howse. 1999. Communication between the fungus garden and workers of the leaf-cutting ant, *Atta sexdens rubropilosa*, regarding choice of substrate for the fungus. *Physiol. Entomol.* **24:** 127–133.

Núñez, J. A. 1982. Honeybee foraging strategies at a food source in relation to its distance from the hive and the rate of sugar flow. *J. Apic. Res.* **21:** 139–150.

Orians, G. H., and N. E. Pearson. 1979. On the theory of central place foraging. Pp. 155–177 in *Analysis of Ecological Systems*, D. J. Horn, G. R. Stairs, and R. D. Mitchell, eds. Ohio State University Press, Columbus, OH.

Powell, R. J., and D. J. Stradling. 1991. The selection and detoxification of plant material by fungus-growing ants. Pp. 19–41 in *Ant-Plant Interactions*, C. R. Huxley and D. F. Cutler, eds. Oxford University Press, Oxford.

Ridley, P., P. E. Howse, and C. W. Jackson. 1996. Control of the behaviour of leaf-cutting ants by their 'symbiotic' fungus. *Experientia* **52:** 631–635.

Roces, F. 1990a. Leaf-cutting ants cut fragment sizes in relation to the distance from the nest. *Anim. Behav.* **40:** 1181–1183.

Roces, F. 1990b. Olfactory conditioning during the recruitment process in a leaf-cutting ant. *Oecologia* **83:** 261–262.

Roces, F. 1993. Both evaluation of resource quality and speed of recruited leaf-cutting ants (*Acromyrmex lundi*) depend on their motivational state. *Behav. Ecol. Sociobiol.* **33:** 183–189.

Roces, F. 1994a. Cooperation or individualism: how leaf-cutting ants decide on the size of their loads. *Trends Ecol. Evol.* **9:** 230.

Roces, F. 1994b. Odour learning and decision-making during food collection in the leaf-cutting ant *Acromyrmex lundi*. *Insectes Soc.* **41:** 235–239.

Roces, F., and B. Hölldobler. 1994. Leaf density and a trade-off between load-size selection and recruitment behavior in the ant *Atta cephalotes*. *Oecologia* **97:** 1–8.

Roces, F., and J. A. Núñez. 1993. Information about food quality influences load-size selection in recruited leaf-cutting ants. *Anim. Behav.* **45:** 135–143.

Rockwood, L. L. 1976. Plant selection and foraging patterns in two species of leaf-cutting ants (*Atta*). *Ecology* **57:** 48–61.

Rockwood, L. L., and S. P. Hubbell. 1987. Host-plant selection, diet diversity, and optimal foraging in a tropical leafcutting ant. *Oecologia* **74:** 55–61.

Rudolph, S. G., and C. Loudon. 1986. Load size selection by foraging leaf-cutter ants (*Atta cephalotes*). *Ecol. Entomol.* **11:** 401–410.

Schmid-Hempel, P. 1993. On optimality, physiology and honeybees—a reply to Varjú and Núñez. *J. Comp. Physiol. A* **172:** 251–256.

Seeley, T. D. 1986. Social foraging by honeybees: how colonies allocate foragers among patches of flowers. *Behav. Ecol. Sociobiol.* **19:** 343–354.

Seeley, T. D., S. Camazine, and J. Sneyd. 1991. Collective decision-making in honey bees: how colonies choose among nectar sources. *Behav. Ecol. Sociobiol.* **28:** 277–290.

Shepherd, J. D. 1982. Trunk trails and the searching strategy of a leaf-cutter ant, *Atta colombica*. *Behav. Ecol. Sociobiol.* **11:** 77–84.

Stabentheiner, A., and K. Hagmüller. 1991. Sweet food means "hot dancing" in honeybees. *Naturwissenschaften* **78:** 471–473.

Stradling, D. J. 1978. The influence of size on foraging in the ant, *Atta cephalotes*, and the effect of some plant defence mechanisms. *J. Anim. Ecol.* **47:** 173–188.

Stradling, D. J., and R. J. Powell. 1992. Fungiculture and the choice of substrates by attine ants. Pp. 133–143 in *Biology and Evolution of Social Insects*, J. Billen, ed. Leuven University Press, Leuven, Belgium.

Varjú, D., and J. Núñez. 1991. What do foraging honeybees optimize? *J. Comp. Physiol. A* **169:** 729–736.

Varjú, D., and J. Núñez. 1993. Energy balance versus information exchange in foraging honeybees. *J. Comp. Physiol. A* **172:** 257–261.

Vasconcelos, H. L. 1997. Foraging activity of an Amazonian leaf-cutting ant: responses to changes in the availability of woody plants and to previous plant damage. *Oecologia* **112:** 370–378.

Weber, N. A. 1972. *Gardening Ants—The Attines.* The American Philosophical Society, Philadelphia. 146 pp.

Wetterer, J. K. 1990. Load-size determination in the leaf-cutting ant, *Atta cephalotes. Behav. Ecol.* **1:** 95–101.

Wetterer, J. K. 1991a. Allometry and the geometry of leaf-cutting in *Atta cephalotes. Behav. Ecol. Sociobiol.* **29:** 347–351.

Wetterer, J. K. 1991b. Source distance has no effect on load size in the leaf-cutting ant, *Atta cephalotes. Psyche* **98:** 355–359.

Wilson, E. O. 1962. Chemical communication among workers of the fire ant *Solenopsis saevissima* (Fr. Smith). *Anim. Behav.* **10:** 134–164.

Ydenberg, R., and P. Schmid-Hempel. 1994. Modelling social insect foraging. *TREE* **9:** 491–493.

Reference: *Biol. Bull.* **202:** 314–318. (June 2002)

When Is Self-Organization Used in Biological Systems?

THOMAS D. SEELEY

Department of Neurobiology and Behavior, Mudd Hall, Cornell University, Ithaca, NY 14853

Abstract. Self-organization, or decentralized control, is widespread in biological systems, including cells, organisms, and groups. It is not, however, the universal means of organization. I argue that a biological system will be self-organized when it possesses a large number of subunits, and these subunits lack either the communicational abilities or the computational abilities, or both, that are needed to implement centralized control. Such control requires a well informed and highly intelligent supervisor. I stress that the subunits in a self-organized system do not necessarily have low cognitive abilities. A lack of preadaptations for evolving a system-wide communication network can prevent the evolution of centralized control. Hence, sometimes even systems whose subunits possess high cognitive abilities will be self-organized.

Introduction

Self-organization is widespread in biological systems. That is to say, it is common to find biological systems that function without guidance from an external controller, or even from an internal control center. Instead, we often find that biological systems function with mechanisms of decentralized control in which the numerous subunits of the system—the molecules of a cell, the cells of an organism, or the organisms of a group—adjust their activities by themselves on the basis of limited, local information. An apple tree, for example, "wisely" allocates its resources among woody growth, leaves, and fruits without a central manager of its cells. Likewise, an ant colony "intelligently" distributes its work force among such needs as brood rearing, colony defense, and nest construction without an omniscient overseer of its workers. Much of the challenge in understanding the inner workings of living systems arises from their use of decentralized control mechanisms, which are harder for the human mind to grasp than centralized control mechanisms. This is why mathematical models, computer simulations, and the other tools used by investigators of self-organization (Bonabeau *et al.*, 1997; Camazine *et al.*, 2001) are helpful in building a solid understanding of how living things work.

Given that self-organization is widespread in biological systems, the question arises of why this is the case. In this essay, I will share my thoughts on this issue. My views derive partly from what I have learned through studying one of nature's most accessible self-organized systems, the honeybee colony, and partly from what I have learned through reading various works in the fields of biology, economics, and engineering.

The biological systems I will be considering are all ones in which the genetics interests of the system's subunits are largely, if not entirely, congruent; hence the subunits cooperate closely for the effective functioning of the system as a whole. Such systems are what Dawkins (1982) has called *vehicles*: thoroughly integrated entities that have evolved to foster the survival and reproduction of the genes they contain. These systems include single-celled creatures, multicellular organisms, and even some animal societies, such as colonies of honeybees and army ants. Hence, this essay relates to the general issue in biology of how functionally integrated entities arise, or individuation occurs, at various hierarchical levels (Maynard Smith and Szathmáry, 1995; Seeley, 1995; Bonner, 1998; Sober and Wilson, 1998; Keller, 1999; Michod, 1999; Wilson, 1999). In addressing the question of where self-organization occurs in biological

---

E-mail: tds5@cornell.edu

This paper was originally presented at a workshop titled *The Limits to Self-Organization in Biological Systems*. The workshop, which was held at the J. Erik Jonsson Center of the National Academy of Sciences, Woods Hole, Massachusetts, from 11–13 May 2001, was sponsored by the Center for Advanced Studies in the Space Life Sciences at the Marine Biological Laboratory, and funded by the National Aeronautics and Space Administration under Cooperative Agreement NCC 2–896.

systems, we examine an issue that applies across the hierarchical spectrum.

The Importance of Communicational and Computational Abilities

My basic argument is this: a biological system will be self-organized if it consists of a large number of subunits, and these subunits do not possess the communicational and computational abilities needed to implement centralized control, which necessarily involves a well informed and highly intelligent supervisor.

As Friedrich von Hayek (1945) and Herbert Simon (1962) pointed out long ago, centralized control of any large system requires (1) that a tremendous amount of information—usually dispersed among all the subunits of the system—be communicated to a central decision-making body (one subunit or a group of subunits), (2) that this body integrate all this information to decide a course of action, and (3) that it then issue instructions to the other subunits in the system. When we look across the range of functionally integrated entities in nature, we see that some have indeed evolved the sophisticated communicational and computational mechanisms required for some degree of centralized control. In the adult form of many metazoan organisms, for example, we find an elaborate peripheral nervous system that makes possible the rapid transmission of information throughout the organism, and a sophisticated central nervous system that processes the sensory input and decides most of the motor output for the organism. Likewise, in some of the colonial marine invertebrates, particularly the swimming colonies of the Siphonophora, we find a colony-wide network of nerves and a simple brain that together support a rudimentary level of centralized control of the propulsion zooids within a colony (Mackie, 1986). And, obviously, we humans have developed sophisticated communicational and computational technologies that make it possible for certain human groups, notably military and manufacturing units, to function with a high level of centralized, hierarchical control (Bartholdi, 1993).

Besides these biological systems that function with some degree of centralized control, there are many others that operate with little or no central authority. These are self-organizing systems. Their subunits have not evolved either broad communicational networks or powerful computational abilities; thus it is not surprising that they operate without central planning. For instance, no species of social insect has evolved anything like a colony-wide communicational network that would enable information to flow rapidly and efficiently to and from a central manager. Moreover, no individual within a social insect colony is capable of processing huge amounts of information. (Contrary to popular belief, the queen of a colony is not an omniscient individual that issues orders; rather, she is an oversized individual that lays eggs. The biblical King Solomon was correct when he noted, in reference to ant colonies, there is "no guide, overseer, or ruler" [Proverbs 6:7]). Therefore, it is not surprising that social insects with large colonies provide us with striking examples of self-organized systems. Other good examples in biology are multicellular animals during development—that is, before they have assembled their communicational networks (peripheral nervous systems) and central computers (central nervous systems); plants at all levels of evolutionary sophistication (nonvascular and vascular forms); and bacterial colonies (reviewed in Camazine *et al.*, 2001; see also Shapiro and Dworkin, 1998).

Why Is There Self-Organization?

Given that some biological systems have evolved centralized control, it is clear that self-organization is not always the best means of coordinating the subunits in a system. The absence of a central authority leaves a system (of molecules, of cells, or of organisms) prone to opposing actions among its subunits, for they will respond to their different, local conditions rather than to the shared, global situation of the system as a whole. Colonies of social insects frequently experience this problem, such as when an ant colony changes nest sites and some workers carry brood items out of the old site while others carry them back in again (Wilson, 1971, p. 224). Also, when no one is supervising a system, needless redundancies are apt to arise within it. The IBM corporation experienced precisely this problem in the 1980s when it decentralized its operations and costly duplications of activities arose among its divisions (Drucker, 1988). Furthermore, the absence of a centralized authority within a system can limit its ability to find the globally optimal solution to a problem and can even render it vulnerable to getting stuck in a pathological state. A gruesome example of this is the "circular mill" of *Eciton* army ants in Guyana that William Beebe (1921; cited in Anderson and Bartholdi, 2000) described: a circle, measuring some 100 m in diameter and lasting for two days, of ants continuously following each other round and round, and gradually dying from exhaustion. In short, systems with decentralized control can easily lack "the vision thing."

Despite the potential problems of decentralized control (self-organization), many biological systems do rely on it. One can ask whether these systems have been unable to evolve mechanisms of communication and computation sufficient to support centralized control (*i.e.*, centralized control *is* an adaptive peak, but one that is hard to reach) or whether they have experienced selection pressures that favor low communicational abilities or low computational abilities, or both (*i.e.*, centralized control *is not* an adaptive peak). I believe that the first reason explains the widespread existence of self-organization in social insect colonies. The subunits in these colony-level systems, unlike those in organism-level and cell-level systems, do not form stable, physical connections. With the exception of human groups, which possess advanced technologies for communication, all biological systems with powerful communication networks have their subunits arranged in stable configurations with solid connections between the subunits. Such spatial stability and connectivity evidently facilitates the evolution of a system-wide communication network. Thus it appears that colonies of social insects, whose workers typically move about within the nest, lack a crucial preadaptation for evolving sophisticated, colony-wide communication systems.

The second possible reason for decentralized control, that it is more adaptive than centralized control, may apply in situations where the high costs of centralized control are not compensated by high benefits. Certainly there are high costs to having the sophisticated communicational and computational abilities that underlie centralized control. Just consider the high metabolic costs of maintaining the nervous system of a metazoan organism, or the high financial costs of maintaining the industrial engineering department of a manufacturing enterprise. One American food distributor, for example, employs two engineers and one programmer to maintain the work-content models for managing their warehouses, at a cost of $250,000 annually (B. Little, Manhattan Associates, cited in Anderson and Bartholdi, 2000). For centralized control to evolve, such high costs must be outweighed by high benefits. It is not hard to imagine situations where there are actually *low benefits* to having centralized control. One is when a biological system is highly susceptible to the loss of subunits, perhaps through predation or disease. In a system with centralized control, the loss of the central manager can result in a catastrophic failure of the entire system. In contrast, systems with decentralized control are generally robust to the loss of subunits. Anderson and Bartholdi (2000) compare the characteristics of centralized and decentralized control paradigms and discuss the logistical situations in which each type of control is likely to yield high benefits. Their article focuses on manufacturing operations, but because it is inspired by the ways that social insects have solved problems of colony organization, it has much relevance to biological systems.

Self-Organization and the Cognitive Abilities of Subunits

I have presented the view that high communicational and computational abilities in a system's subunits are essential for the evolution of centralized control in large systems, for without such abilities centralized control cannot be implemented. This view implies that biological systems whose subunits lack broad communicational abilities or sophisticated computational (cognitive) abilities, or both, must function with decentralized control. I wish to stress, however, that the subunits in a self-organized system do not necessarily have low cognitive abilities. The subunits might possess cognitive abilities that are high in an absolute sense, but low relative to what is needed to effectively supervise a large system. A human being, for example, is an intelligent subunit in the economy of a nation, but no human possesses the information-processing abilities that are needed to be a successful central planner of a nation's economy. It is also possible that the subunits possess high cognitive abilities, but are in a system that lacks an extensive communication network. Such subunits would be *highly intelligent,* but *poorly informed.* A worker honeybee, for example, is an intelligent creature (see below) that functions in a system that lacks a communication network capable of supporting centralized control.

It is important to consider the issue of the cognitive abilities of the subunits in decentralized (self-organized) systems because it points to a fundamental flaw in many studies of self-organization: the assumption that the subunits in a self-organized system are dumb. This viewpoint is generally expressed in terms of "simple individuals" (*e.g.*, Goss and Deneubourg, 1988; Strickland *et al.*, 1993) following "very simple rules of behavior" (*e.g.*, Camazine *et al.*, 1990; Jenkins *et al.*, 1992; Strickland *et al.*, 1992) or executing "simple stimulus-response acts" (Camazine *et al.*, 2001, p. 488). It is certainly true that many studies have shown that decentralized control can produce complexity at the system level—for example, the intricate nests and foraging operations of social insect colonies—without need for comparable complexity at the individual level (Theraulaz and Bonabeau, 1995; Bonabeau, 1998; Theraulaz *et al.*, 1998; Karsai, 1999). This does not, however, prove that the subunits in the systems studied lack behavioral complexity and high cognitive abilities; it indicates only that the subunits did not show complexity in these studies, most of which involve a deliberate simplification or even a mere simulation of reality.

The implicit assumption of dumb subunits underlying most studies of self-organization could be tested for social insects by looking at individual complexity in relation to colony size. If individual complexity decreases as colony size (and decentralization/self-organization) increases, the dumb subunits paradigm gains credence. However, there is no compelling evidence of an inverse relation between individual complexity and colony size (Anderson and McShea, 2001). The workers of large colonies do show a loss of totipotency, especially with respect to reproductive potential (Crespi and Yanega, 1995; Bourke, 1999), and they do show a loss of structures associated with reproduction (*e.g.*, ovaries in ants); but they do not show signs of reduced behavioral or cognitive complexity. Indeed, one can make a strong argument that the cognitive complexity of individuals needs to be greater in species with large colonies than in those with small colonies, especially when the workers do not have lifelong task specializations (*e.g.*, physical polyethism) but instead perform different tasks at different stages of life (*e.g.*, temporal polyethism). As colony size evolves to higher levels, new ecological opportunities and problems arise that can favor the evolution of additional behaviors, such as recruiting to food sources, activities for fighting diseases, colonial thermoregulation measures, and coordinated ambushing of prey. Also, new, more efficient ways of organizing work can evolve, such as task partitioning (Jeanne, 1986; reviewed by Ratnieks and Anderson, 1999) and teamwork (Anderson and Franks, 2001); and these necessitate the evolution of behavioral mechanisms for coordinating the individuals working together on a task. Bonner (1988) makes similar arguments for systems of cells in the evolution of multicellular organisms: as the size of an assemblage of cells increases, new opportunities and new needs arise for more sophisticated methods of food acquisition, gas exchange, and internal circulation.

My view that self-organized systems can be composed of subunits possessing high cognitive abilities is based on my experience in analyzing the functional organization of honeybee colonies. These are large biological systems that function with decentralized control (Seeley, 1995) and that are composed of subunits—worker bees—whose cognitive sophistication is certainly impressive. One indication of this sophistication is the large number of signals (17) and cues (34) that we know workers are sensitive to inside a hive (reviewed in Seeley, 1998). Another indication is the remarkable behavioral versatility of worker bees and their impressive ability to integrate information when deciding how to behave; they do not follow "very simple rules of behavior" or execute "simple stimulus-response acts." Consider, for example, the actions of a worker bee scouting a nest site, starting when she has discovered a promising tree cavity. She first spends 20–40 minutes inspecting the site, acquiring information about the cavity's volume, the size of its entrance, its height off the ground, its exposure to sun and wind, and still other variables (Seeley, 1977; Seeley and Morse, 1978). In short, she makes a multifactorial evaluation of her find. She then integrates the information that she has acquired about her site to determine its overall desirability as a future dwelling place. Next, she returns to the swarm cluster, where she performs a waggle dance to advertise her site to the other scout bees (Lindauer, 1955). Because the recruitment target is small, just the entrance opening to her site, she adopts a special form of the dance; she produces waggle runs with less directional scatter (thereby indicating the target's direction with greater precision) than she would if she were advertising a spacious patch of flowers (Weidenmüller and Seeley, 1999). Moreover, she skillfully adjusts both the duration and the rate of her production of waggle runs in relation to the desirability of her site (Seeley and Buhrman, 2001), and she gradually reduces the number of waggle runs produced per return to the swarm over sequential returns (Seeley, unpubl.). All of these tunings of her dance behavior are important to the consensus-building process whereby the scouts of a swarm collectively choose its new home. Once the swarm's domicile has been chosen, our scout somehow senses this, ceases waggle dancing, and starts producing a different signal, called *wings-together piping*. This signal stimulates the non-scouts in the swarm to warm themselves to a flight-ready temperature (35°C) in preparation for liftoff (Seeley and Tautz, 2001). Finally, once all the bees in the swarm are suitably warmed, the scout stops piping and starts producing a third signal, called *buzz running*, which triggers the break-up of the cluster (Lindauer, 1955; Esch, 1967).

There can be no doubt that a worker honeybee is a sophisticated piece of biological machinery; one that is exquisitely sensitive to its environment and that makes intricate adjustments of its behavior in adaptation to the ever-changing state of its environment. After all, the sketch just painted of a scout bee's actions does not capture the full complexity of her behavior, and the complexity of a scout bee's behavior is but a small fraction of the full complexity of a worker bee's behavior across her life (when she also functions as a cleaner bee, nurse bee, food-storer bee, forager bee, etc.). Such complexity in the behavior of a worker bee shows us that the subunits in a self-organized system can possess a high level of cognitive sophistication. This fact must be kept in mind by investigators of self-organization in biological systems, especially systems that are animal groups, lest we hold a falsely simplified view of life.

Acknowledgments

I am grateful to the National Science Foundation, National Geographic Society, and U.S. Department of Agriculture, whose financial support has made possible the bee research that underlies many of the ideas expressed in this essay.

Literature Cited

Anderson, C., and J. J. Bartholdi, III. 2000. Centralized versus decentralized control in manufacturing: lessons from social insects. Pp. 92–105 in *Complexity and Complex Systems in Industry*, I. P. McCarthy and T. Rakotobe-Joel, eds. The University of Warwick, Warwick, UK.

Anderson, C., and N. R. Franks. 2001. Teams in animal societies. *Behav. Ecol.* **12:** 534–540.

Anderson, C., and D. W. McShea. 2001. Individual *versus* social complexity, with particular reference to ant colonies. *Biol. Rev.* **76:** 211–237.

Bartholdi, J. J., III. 1993. Interactive program to balance assembly lines. *Int. J. Prod. Res.* **31:** 2447–2461.

Beebe, W. 1921. *Edge of the Jungle*. Henry Holt, New York.

Bonabeau, E. 1998. Social insect colonies as complex adaptive systems. *Ecosystems* **1:** 437–443.

Bonabeau, E., G. Theraulaz, J.-L. Deneubourg, S. Aron, and S. Cam-

azine. 1997. Self-organization in social insects. *Trends Ecol. Evol.* **12:** 188–193.

Bonner, J. T. 1988. *The Evolution of Complexity.* Princeton University Press, Princeton.

Bonner, J. T. 1998. The origins of multicellularity. *Integr. Biol.* **1:** 27–36.

Bourke, A. F. G. 1999. Colony size, social complexity and reproductive conflict in social insects. *J. Evol. Biol.* **12:** 245–257.

Camazine, S., J. Sneyd, M. J. Jenkins, and J. D. Murray. 1990. A mathematical model of self-organized pattern formation on the combs of honeybee colonies. *J. Theor. Biol.* **147:** 553–571.

Camazine, S., J.-L. Deneubourg, N. R. Franks, J. Sneyd, G. Theraulaz, and E. Bonabeau. 2001. *Self-organization in Biological Systems.* Princeton University Press, Princeton, NJ.

Crespi, B. J., and D. Yanega. 1995. The definition of eusociality. *Behav. Ecol. Sociobiol.* **6:** 109–115.

Dawkins, R. 1982. *The Extended Phenotype: The Gene as the Unit of Selection.* Oxford University Press, Oxford.

Drucker, P. F. 1988. The coming of the new organization. *Harvard Bus. Rev.* **66:** 45–53.

Esch, H. 1967. The sounds produced by swarming honey bees. *Z. Vgl. Physiol.* **56:** 408–411.

Goss, S., and J. L. Deneubourg. 1988. Autocatalysis as a source of synchronised rhythmical activity in social insects. *Insectes Soc.* **35:** 310–315.

Hayek, F. A. von. 1945. The use of knowledge in society. *The American Economic Review* **35:** 519–530.

Jeanne, R. L. 1986. The evolution of the organization of work in social insects. *Monit. Zool. Ital.* **20:** 119–133.

Jenkins, M. J., J. Sneyd, S. Camazine, and J. D. Murray. 1992. On a simplified model for pattern formation in honey bee colonies. *J. Math. Biol.* **30:** 281–306.

Karsai, I. 1999. Decentralized control of construction behavior in paper wasps: an overview of the stigmergy approach. *Artif. Life* **5:** 117–136.

Keller, L. 1999. *Levels of Selection in Evolution.* Princeton University Press, Princeton.

Lindauer, M. 1955. Schwarmbienen auf Wohnungssuche. *Z. Vgl. Physiol.* **37:** 263–324.

Mackie, G. O. 1986. From aggregates to integrates: physiological aspects of modularity in colonial animals. *Philos. Trans. R. Soc. Lond. B.* **313:** 175–196.

Maynard Smith, J., and E. Szathmáry. 1995. *The Major Transitions in Evolution.* Oxford University Press, Oxford.

Michod, R. E. 1999. *Darwinian Dynamics: Evolutionary Transitions in Fitness and Individuality.* Princeton University Press, Princeton.

Ratnieks, F. L. W., and C. Anderson. 1999. Task partitioning in insect societies. *Insectes Soc.* **46:** 95–108.

Seeley, T. D. 1977. Measurement of nest cavity volume by the honey bee (*Apis mellifera*). *Behav. Ecol. Sociobiol.* **2:** 201–227.

Seeley, T. D. 1995. *The Wisdom of the Hive: The Social Physiology of Honey Bee Colonies.* Harvard University Press, Cambridge, MA.

Seeley, T. D. 1998. Thoughts on information and integration in honey bee colonies. *Apidologie* **29:** 67–80.

Seeley, T. D., and S. C. Buhrman. 2001. Nest-site selection in honey bees: how well do swarms implement the "best-of-N" decision rule? *Behav. Ecol. Sociobiol.* **49:** 416–427.

Seeley, T. D., and R. A. Morse. 1978. Nest site selection by the honey bee. *Insectes Soc.* **25:** 323–337.

Seeley, T. D., and J. Tautz. 2001. Worker piping in honey bee swarms and its role in preparing for liftoff. *J. Comp. Physiol. A* **187:** 667–676.

Shapiro, A. B., and C. D. Dworkin. 1998. *Bacteria as Multicellular Organisms.* Oxford University Press, Oxford.

Simon, H. A. 1962. The architecture of complexity. *Proc. Am. Philos. Soc.* **106:** 467–482.

Sober, E., and D. S. Wilson. 1998. *Unto Others: The Evolution and Psychology of Unselfish Behavior.* Harvard University Press, Cambridge.

Strickland, T. R., C. M. N. Tofts, and N. R. Franks. 1992. A path choice algorithm for ants. *Naturwissenschaften* **79:** 567–572.

Strickland, T. R., C. Tofts, and N. R. Franks. 1993. Algorithms for ant foraging. *Naturwissenschaften* **80:** 427–430.

Theraulaz, G., and E. Bonabeau. 1995. Coordination in distributed building. *Science* **269:** 686–688.

Theraulaz, G., E. Bonabeau, and J.-L. Deneubourg. 1998. The origin of nest complexity in social insects. *Complexity* **3:** 686–688.

Weidenmüller, A., and T. D. Seeley. 1999. Imprecision in waggle dances of the honey bee (*Apis mellifera*) for nearby food sources: error or adaptation? *Behav. Ecol. Sociobiol.* **46:** 190–199.

Wilson, E. O. 1971. *The Insect Societies.* Harvard University Press, Cambridge, MA.

Wilson, J. 1999. *Biological Individuality.* Cambridge University Press, Cambridge, UK

Reference: *Biol. Bull.* **202:** 319. (June 2002)

Published by Title Only

Camazine, Scott
Is termite nest architecture self-organized?

Cassill, Deby
Distributed intelligence: a mechanism for social organization in an unpredictable environment

Dagorn, Laurent
Self-organization and heterogeneous systems: the example of tropical tuna around floating objects

Moritz, Robin F. A.
Genetic variance and self-organized patterns in social evolution of honeybees

Naug, Dhruba
What role does self-organization play in the ergonomic design of a colony?

Page, Dhruba
Evolution of division of labor

Theraulaz, Guy
Turing-like structures in ant colonies

Tschinkel, Walter
Is ant nest architecture self-organized, and does it matter?

Reference: *Biol. Bull.* **202:** 320. (June 2002)

Participants

Anderson, Carl
Universität Regensburg

Aranow, Abe
NASA Ames Research Center

Ayers, Joe
Northeastern University

Basil, Jennifer
Brooklyn College

Blazis, Diana
Marine Biological Laboratory – CASSLS

Camazine, Scott
Penn State University

Cassill, Deby
University of Arizona

Chiao, Chuan-Chin
Massachusetts General Hospital

Cole, Blaine
University of Houston

Copren, Kirsten
University of California, Davis

Dagorn, Laurent
IRD (Institut de Recherché pour le Développement)

Deneubourg, Jean Louis
Université Libre de Bruxelles

Detrain, Claire
Université Libre de Bruxelles

Fraser, Peter
Aberdeen University

Gérard, Jean-François
IRGM, INRA

Grasso, Frank
Brooklyn College
Boston University Marine Program

Hemelrijk, Charlotte K.
Anthropological Institute and Museum

Hurd, Christine
University of Wisconsin

Jeanne, Robert L.
University of Wisconsin, Madison

Johnson, Brian
Cornell University

MacElroy, Robert
NASA Ames Research Center

Mikheyev, Alexander
Florida State University

Moritz, Robin F.A.
Universität Halle, Germany

Naug, Dhruba
St. Mary's College of Maryland

Page, Robert E., Jr.
University of California, Davis

Parrish, Julia
University of Washington

Reilly, Christian
Stanford University

Roces, Flavio
Theodor Boveri Institut Zoologie II

Seeley, Tom
Cornell University

Théraulaz, Guy
Université Paul Sabatier

Tschinkel, Walter R.
Florida State University

Wright, Geraldine
Ohio State University

INDEX

A

Acorn worm, 182
Activity pattern, 148, 256
Adaptation, 256
Age-specific, 156
Aggregation, 262, 296
Aiptasia, 74
Alpheus heterochaelis, 43
The anatomy, life habits, and later development of a new species of enteropneust, *Harrimania planktophilus* (Hemichordata: Harrimaniidae) from Barkley Sound, 182
Anctil, Michel, see Isabelle Masseau, 23
Anderson, Carl, Self-organization in relation to several similar concepts: are the boundaries to self-organization indistinct?, 247
Anemone, 74
Ant, 256, 268, 306
Apical ganglion, 6
Apical sensory organ in larvae of the patellogastropod *Tectura scutum*, 6
Arenicola, 34
Asterias, 34

B

Baillie, Brett K., see Carmen A. Belda-Baillie, 74
Bannon, Pierre, see Isabelle Masseau, 23
Barnacle larva, 53
Behavior, 223
  feeding, 192
  nesting, 289
Belda-Baillie, Carmen A., Brett K. Baillie, and Tadashi Maruyama, Specificity of a model cnidarian-dinoflagellate symbiosis, 74
Bentley, Matthew Graeme, see Mark Elliott Williams, 34
Bideau, Eric, see Jean-François Gerard, 275
Bivalve mollusc, 201
Blackstone, Neil W., see David H. Van Winkle, 156
Blastomere positioning, 213
Blazis, Diana E., Introduction. The Limits to Self-Organization in Biological Systems, a workshop, 245
Boudry, P., see S. Lapègue, 232
Boutet, I., see S. Lapègue, 232
Bouwma, Andrew M., see Robert L. Jeanne, 289
Bovid, 275

C

Calcium
  current, 108
  potential, 108
Cameron, Christopher B., Particle retention and flow in the pharynx of the enteropneust worm *Harrimania planktophilus:* the filter-feeding pharynx may have evolved before the chordates, 192
Cameron, Christopher B., The anatomy, life habits, and later development of a new species of enteropneust, *Harrimania planktophilus* (Hemichordata: Harrimaniidae) from Barkley Sound, 182
Cannabinoid receptor, 104
Carcinus maenas, 61
Cardiac ganglion, 108
Carr, S. M., H. D. Marshall, K. A. Johnstone, L. M. Pynn, and G. B. Stenson, How to tell a sea monster: molecular discrimination of large marine animals of the North Atlantic, 1
CB_2, 104
Centralized control, 314
Cephalopoda, 148
Chang, Ernest S., see Xiaoli Yu, 204
Characterization of limb autotomy factor–proecdysis (LAF_{pro}), isolated from limb regenerates, that suspends molting in the land crab *Gecarcinus lateralis*, 204
Chordate evolution, 192
Clam, surf, 23
Clonal, 156
Clypeaster rosaceus, 97
Cnidaria, 156
Cochrane, David E., see Jan A. Pechenik, 137
Cole, Blaine J., Evolution of self-organized systems, 256
Colonial, 156
Communication, 306
Compère, Philippe, Marie-France Jaspar-Versali, and Gerhard Goffinet, Glycoproteins from the cuticle of the Atlantic shore crab *Carcinus maenas:* I. Electrophoresis and western-blot analysis by use of lectins, 61
Competition, interspecific, 156
Complexity, 268, 283
Complexity of environment and parsimony of decision rules in insect societies, 268
Control
  centralized, 314
  decentralized, 314
Cooke, Ian M., Reliable, responsive pacemaking and pattern generation with minimal cell numbers: the crustacean cardiac ganglion, 108
Cooperation, 262
Copulatory organs, 148
Cortical granules, 213
Cowart, Jonathan D., see Benjamin G. Miner, 97
Crassostrea
  brasiliana, 232
  gasar, 232
  rizophorae, 232
Crepidula, 137
Crustacea, 100, 108
Crustacean compound eye, 223
Cryptozoology, 1
Cuticle, 61
Cytochalasin, 100

D

Decapod crustacean, 61
Decentralized control, 314
Decision-making, 306
Deer, 275
Deneubourg, J. L., A. Lioni, and C. Detrain, Dynamics of aggregation and emergence of cooperation, 262
Deneubourg, Jean-Louis, see Claire Detrain, 268
Despotic, 283
Detrain, C., see J. L. Deneubourg, 262
Detrain, Claire, and Jean-Louis Deneubourg, Complexity of environment and parsimony of decision rules in insect societies, 268
Development, 182
DGGE, 74
Dinoflagellate, 74
Dopamine receptors, 137
Driver potential, 108
Dubé, François, see Isabelle Masseau, 23
Dynamics of aggregation and emergence of cooperation, 262

E

Echinoderm, 34, 97
Echinoid, 97
Egg energetics, 97
Egg energetics for the facultative planktotroph *Clypeaster rosaceus* (Echinodermata: Echinoidea), revisited, 97
Eicosapentaenoic acid regulates scallop (*Placopecten magellanicus*) membrane fluidity in response to cold, 201
Electrophoresis, 61
Electrotonic transmission, 108
Elphick, Maurice R., Evolution of cannabinoid receptors in vertebrates: identification of a CB_2 gene in the puffer fish *Fugu rubripes*, 104
Embryo, starfish, 213
Enteropneusta, 182, 192
Environment, 268
Evolution, 256, 283, 296
  chordate, 192
Evolution of cannabinoid receptors in vertebrates: identification of a CB_2 gene in the puffer fish *Fugu rubripes*, 104
Evolution of self-organized systems, 256
Eye size, 223

F

Facultative planktotrophy, 97
Feeding behavior, 192
Fertilization, 166
  envelope, 213
  success, 34
Fertilization success in marine invertebrates: the influence of gamete age, 34
Filter feed, 192
Fish lysophospholipid receptor, 104
Fish schooling, 296
Foraging, 268, 306
Forensic DNA sequencing, 1
Fugu rubripes, 104

G

Gamete
  age, 34
  incompatibility, 166
Gametogenesis, 23
Garcia, P., see S. Lapègue, 232
GenBank database, 1
Gerard, Jean-François, Eric Bideau, Marie-Line Maublanc, Patrice Loisel, and Carole Marchal, Herd size in large herbivores: encoded in the individual or emergent?, 275
Gill slit, 192
Glycoprotein, 61
Glycoproteins from the cuticle of the Atlantic shore crab *Carcinus maenas*: I. Electrophoresis and western-blot analysis by use of lectins, 61
Goffinet, Gerhard, see Philippe Compère, 61
Gross, Paul S., and Robert E. Knowlton, Morphological variations among larval-postlarval intermediates produced by eyestalk ablation in the snapping shrimp *Alpheus heterochaelis* Say, 43
Group
  fitness, 296
  formation, 275
  lability, 275
  size, 275
Grünbaum, Daniel, see Julia K. Parrish, 296

H

Hall, Jonathon M., Christopher C. Parrish, and Raymond J. Thompson, Eicosapentaenoic acid regulates scallop (*Placopecten magellanicus*) membrane fluidity in response to cold, 201
Hariyama, Takahiko, see Essi Keskinen, 223
Harrimania, 182
Heart, neurogenic, 108
Hemelrijk, C. K., Self-organization and natural selection in the evolution of complex despotic societies, 283
Hemichordata, 182, 192
Herbivore, 275
Herd size in large herbivores: encoded in the individual or emergent?, 275
Hertzler, Philip L., Twin meiosis 2 spindles form after suppression of polar body 1 formation in oocytes of the marine shrimp *Sicyonia ingentis*, 100
Heurtebise, S., see S. Lapègue, 232
Hill, April L., see Malcolm S. Hill, 86
Hill, Malcolm S., and April L. Hill, Morphological plasticity in the tropical sponge *Anthosigmella varians*: responses to predators and wave energy, 86
Histamine, 53
Hormone, 204
Host-symbiont recognition, 74
How to tell a sea monster: molecular discrimination of large marine animals of the North Atlantic, 1

I

Image analysis, 156
Individual complexity and self-organization in foraging by leaf-cutting ants, 306
Induced defenses, 86, 156
Insects
  social, 289, 314
  pre-social, 262
Intelligent decision criteria, 268
Interspecific competition, 156

J

Jaspar-Versali, Marie-France, see Philippe Compère, 61
Jeanne, Robert L., and Andrew M. Bouwma, Scaling in nests of a social wasp: a property of the social group, 289
Johnstone, K. A., see S. M. Carr, 1

K

Kangaroo, 275
Karyotypes, 232
Kempter, Elizabeth, see Ann E. Stuart, 53
Keskinen, Essi, Yasuharu Takaku, V. Benno Meyer-Rochow, and Takahiko Hariyama, Postembryonic eye growth in the seashore isopod *Ligia exotica* (Crustacea, Isopoda), 223
Knowlton, Robert E., see Paul S. Gross, 43

L

Lapègue, S., I. Boutet, A. Leitão, S. Heurtebise, P. Garcia, C. Thiriot-Quiévreux, and P. Boudry, Trans-Atlantic distribution of a mangrove oyster species revealed by 16S mtDNA and karyological analyses, 232
Larva, 6, 43, 53, 137
Leaf-cutting ants, 306
Lectin probing, 61
Leitão, A., see S. Lapègue, 232
Lessios, H. A., see Michael A. McCartney, 166
Li, Wei, see Jan A. Pechenik, 137
Limb regeneration, 204
The Limits to Self-Organization in Biological Systems, a workshop, 243
Lioni, A., see J. L. Deneubourg, 262
Localization and quantification of gonad serotonin during gametogenesis of the surf clam, *Spisula solidissima*, 23
Loisel, Patrice, see Jean-François Gerard, 275

M

Mangrove oyster, 232
Marchal, Carole, see Jean-François Gerard, 275
Marshall, H. D., see S. M. Carr, 1
Maruyama, Tadashi, see Carmen A. Belda-Baillie, 74
Masseau, Isabelle, Pierre Bannon, Michel Anctil, and François Dubé, Localization and quantification of gonad serotonin during gametogenesis of the surf clam, *Spisula solidissima*, 23
Matsunaga, Maki, Isao Uemura, Miwa Tamura, and Shin-ichi Nemoto, Role of specialized microvilli and the fertilization envelope in the spatial positioning of blastomeres in early development of embryos of the starfish *Astropecten scoparius*, 213
Maublanc, Marie-Line, see Jean-François Gerard, 275
McCartney, Michael A., and H. A. Lessios, Quantitative analysis of gametic incompatibility between closely related species of neotropical sea urchins, 166
McEdward, Larry R., see Benjamin G. Miner, 97
Meiosis, 100
Mekeel, Harold E., see Ann E. Stuart, 53
Metamorphosis, 137
Meyer-Rochow, V. Benno, see Essi Keskinen, 223
Microvilli, 213
Miner, Benjamin G., Jonathan D. Cowart, and Larry R. McEdward, Egg energetics for the facultative planktotroph *Clypeaster rosaceus* (Echinodermata: Echinoidea), revisited, 97
Mitochondrial DNA, 232
Mollusc, 6, 23
Molting, 204
Morphogenesis, 43
Morphological plasticity in the tropical sponge *Anthosigmella varians:* responses to predators and wave energy, 86
Morphological variations among larval-postlarval intermediates produced by eyestalk ablation in the snapping shrimp *Alpheus heterochaelis* Say, 43
Morphology, 148, 156
Morphometric analysis of male reproductive features of octopodids (Mollusca: Cephalopoda), 148
Mykles, Donald L., see Xiaoli Yu, 204

N

Nemoto, Shin-ichi, see Maki Matsunaga, 213
Nereis, 34
Nesting behavior, 289
Neuroendocrine regulation, 108
Neurogenic heart, 108

O

Ocelli, 53
Octopodidae, 148
Oyster, mangrove, 232

P

Page, Louise R., Apical sensory organ in larvae of the patellogastropod *Tectura scutum*, 6
Parrish, Christopher C., see Jonathon M. Hall, 201
Parrish, Julia K., Steven V. Viscido, and Daniel Grünbaum, Self-organized fish schools: an examination of emergent properties, 296
Parsimony of decision rules, 268
Particle capture, 192
Particle retention and flow in the pharynx of the enteropneust worm *Harrimania planktophilus:* the filter-feeding pharynx may have evolved before the chordates, 192
Pechenik, Jan A., Wei Li, and David E. Cochrane, Timing is everything: the effects of putative dopamine antagonists on metamorphosis vary with larval age and experimental duration in the prosobranch gastropod *Crepidula fornicata*, 137
Pharynx, 192
Phenotypic plasticity, 86
Phospholipid, 201
Photoreceptor, 53
Physeter catodon, 1
Plateau potential, 108
Polar body suppression, 100
Polychaete, 34
Polyunsaturated fatty acid, 201
Positive feedback, 247
Postembryonic eye growth in the seashore isopod *Ligia exotica* (Crustacea, Isopoda), 223
Predator, visual, 148
Primates, 283
Prototroch, 6
Pynn, L. M., see S. M. Carr, 1

Q

Quantitative analysis of gametic incompatibility between closely related species of neotropical sea urchins, 166

R

18S rDNA, 74
Regeneration, limb, 204
Reliable, responsive pacemaking and pattern generation with minimal cell numbers: the crustacean cardiac ganglion, 108
Reproductive
  biology, 148
  isolation, 166
Resting time, 262
Rhythmic bursting, 108
Roces, Flavio, Individual complexity and self-organization in foraging by leaf-cutting ants, 306
Role of specialized microvilli and the fertilization envelope in the spatial positioning of blastomeres in early development of embryos of the starfish *Astropecten scoparius*, 213

S

"S" life-history theory, 97
Sand dollar, 97
Scaling, 289
Scaling in nests of a social wasp: a property of the social group, 289
"Sea monster", 1
Sea urchin, 166
Seeley, Thomas D., When is self-organization used in biological systems?, 314
Selection, 148
Self-assembly, 247, 262
Self-organization, 247, 256, 275, 283, 289, 296, 306, 314
Self-organization and natural selection in the evolution of complex despotic societies, 283
Self-organization in relation to several similar concepts: are the boundaries to self-organization indistinct?, 247
Self-organized fish schools: an examination of emergent properties, 296
Sensory neurons, 6
Serotonin, 6, 23
Shrimp, 43, 100
Slow wave, 108
Social organization, 275
Society, 283
Spawning, 23
Speciation, 166
Specificity, 74
Specificity of a model cnidarian-dinoflagellate symbiosis, 74
Spicule, 86
Spisula, 23
Spongivore, 86
Starfish embryo, 213
Stenson, G. B., see S. M. Carr, 1
Stigmergy, 247, 289

Stuart, Ann E., Harold E. Mekeel, and Elizabeth Kempter, Uptake of the neurotransmitter histamine into the eyes of larvae of the barnacle *(Balanus amphitrite)*, 53

Symbiosis, 74

Symbiodinium, 74

T

Takaku, Yasuharu, see Essi Keskinen, 223

Tamura, Miwa, see Maki Matsunaga, 213

Taxonomic key, 182

Temperature, 201

Thiriot-Quiévreux, C., see S. Lapègue, 232

Thompson, Raymond J., see Jonathon M. Hall, 201

Timing is everything: the effects of putative dopamine antagonists on metamorphosis vary with larval age and experimental duration in the prosobranch gastropod *Crepidula fornicata*, 137

Trans-Atlantic distribution of a mangrove oyster species revealed by 16S mtDNA and karyological analyses, 232

Twin meiosis 2 spindles form after suppression of polar body 1 formation in oocytes of the marine shrimp *Sicyonia ingentis*, 100

U

Uemura, Isao, see Maki Matsunaga, 213

Ungulate, 275

Uptake of the neurotransmitter histamine into the eyes of larvae of the barnacle (*Balanus amphitrite*), 53

V

Van Winkle, David H., and Neil W. Blackstone, Variation in growth and competitive ability between sexually and clonally produced hydroids, 156

Variation in growth and competitive ability between sexually and clonally produced hydroids, 156

Veliger, 137

Viscido, Steven V., see Julia K. Parrish, 296

Vision, 223

Visual predator, 148

Voight, Janet R., Morphometric analysis of male reproductive features of octopodids (Mollusca: Cephalopoda), 148

W

Whale, sperm, 1

When is self-organization used in biological systems?, 314

Williams, Mark Elliott, and Matthew Graeme Bentley, Fertilization success in marine invertebrates: the influence of gamete age, 34

Y

Yu, Xiaoli, Ernest S. Chang, and Donald L. Mykles, Characterization of limb autotomy factor–proecdysis ($\mathrm{LAF}_{\mathrm{pro}}$), isolated from limb regenerates, that suspends molting in the land crab *Gecarcinus lateralis*, 204

?081 31

MARINE RESOURCES CENTER

[illegible]

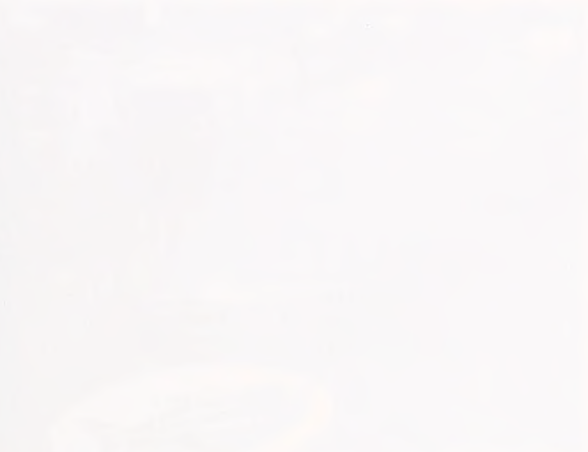

[illegible]

Animal and Tissue Supply for Education & Research

- [illegible]
- [illegible]

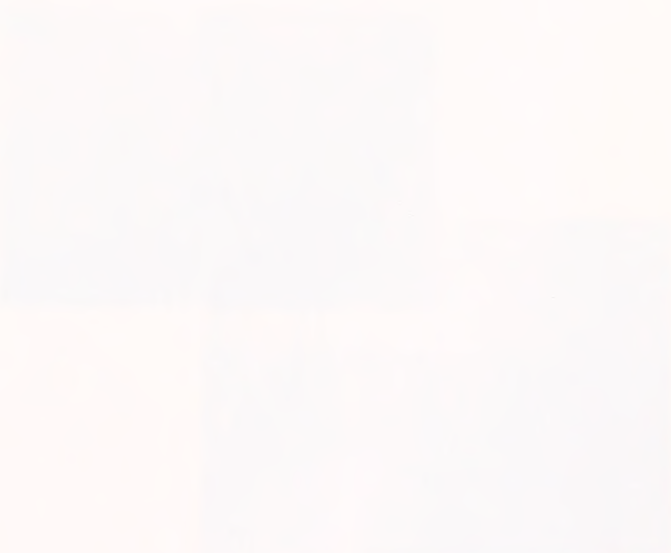

MRC Services Available

- [illegible]
- [illegible]

Using the MRC For Your Research

- [illegible]
- [illegible]
- [illegible]

MARINE RESOURCES CENTER

MARINE BIOLOGICAL LABORATORY • WOODS HOLE, MA 02543 • (508)289-7700
WWW.MBL.EDU/SERVICES/MRC/INDEX.HTML

zebrafish facilities

Animal and Tissue Supply for Education & Research

- 150 aquatic species available for shipment via online catalog: <http://www.mbl.edu/animals/index.html>; phone: (508)289-7375; or e-mail: specimens@mbl.edu
- zebrafish colony containing limited mutant strains
- custom dissection and furnishing of specific organ and tissue samples

MRC Services Available

- basic water quality analysis
- veterinary services (clinical, histopathologic, microbial services, health certificates, etc.)
- aquatic systems design (mechanical, biological, engineering, etc.)
- educational tours and collecting trips aboard the R/V Gemma

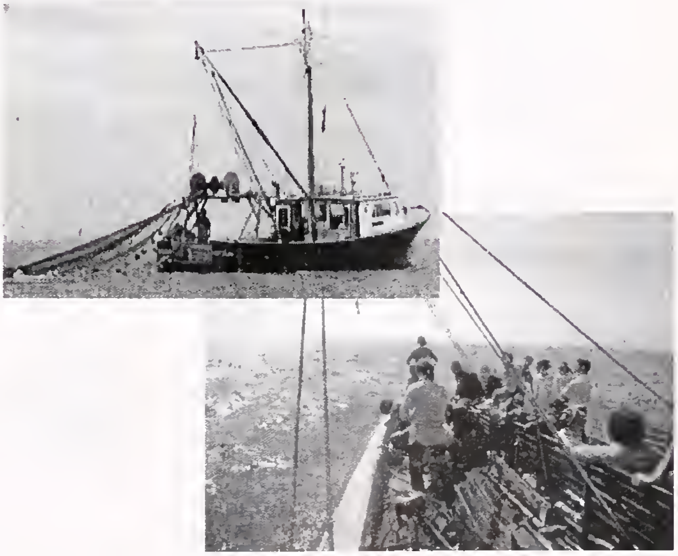

Using the MRC for Your Research

- capability for advanced animal husbandry (temperature, light control, etc.)
- availability of year-round, developmental life stages
- adaptability of tank system design for live marine animal experimentation

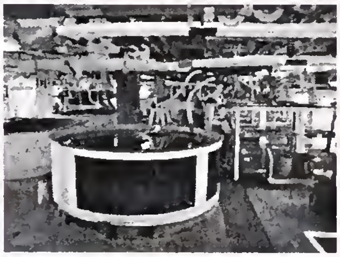

Ultimate Fluorescence Machine

Are you continuously searching for higher contrast, increased transmission and maximum system stability for multi-channel studies? Look no further than **Axioplan 2 imaging** – the ultimate fluorescence machine.

Innovation is the key to success. ICS infinity optics and the shortest possible light paths ensure the highest transmission.

Newly designed filter cubes **'push and click'** into position for stability and precision. Contrast is dramatically improved by the unique **'Light Trap'** (patent pending) which captures stray light and deflects it away from the imaging path. The overall result has to be seen to be believed – ask for a demonstration.

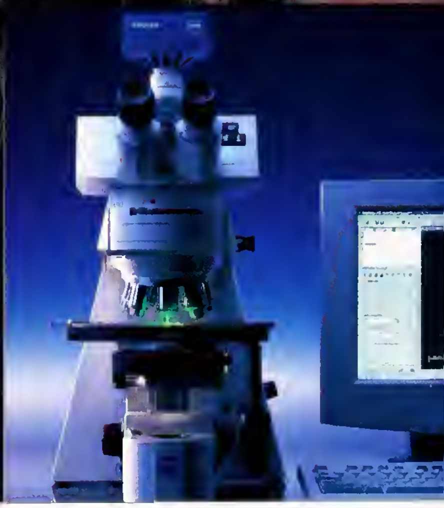

Carl Zeiss MicroImaging, Inc.
One Zeiss Drive
Thornwood, NY 10594

800.233.2343
micro@zeiss.com
www.zeiss.com/micro

ZEISS

MBL/WHOI LIBRARY
WH 1B3A V